

Modern Polyesters: Chemistry and Technology of Polyesters and Copolyesters

Wiley Series in Polymer Science

Series Editor

John Scheirs
ExcelPlas
PO Box 2080
Edithvale, VIC 3196
AUSTRALIA
scheirs.john@pacific.net.au

Modern Fluoropolymers

High Performance Polymers for Diverse Applications

Polymer Recycling

Science, Technology and Applications

Metallocene-based polyolefins

Preparation, Properties and Technology

Polymer–Clay Nanocomposites

Dendrimers and Other
Dendritic Polymers

Modern Styrenic Polymers

Polystyrenes and Related Plastics

Forthcoming titles:

Light Emitting Polymers

Environmentally Degradable Polymers

Modern Polyesters: Chemistry and Technology of Polyesters and Copolyesters

Edited by

JOHN SCHEIRS

ExcelPlas Australia, Edithvale, VIC, Australia

and

TIMOTHY E. LONG

Department of Chemistry, Virginia Tech, Blacksburg, VA, USA

WILEY SERIES IN POLYMER SCIENCE



John Wiley & Sons, Ltd

Copyright © 2003

John Wiley & Sons Ltd, The Atrium, Southern Gate, Chichester,
West Sussex PO19 8SQ, England

Telephone (+44) 1243 779777

Email (for orders and customer service enquiries): cs-books@wiley.co.uk

Visit our Home Page on www.wileyeurope.com or www.wiley.com

All Rights Reserved. No part of this publication may be reproduced, stored in a retrieval system or transmitted in any form or by any means, electronic, mechanical, photocopying, recording, scanning or otherwise, except under the terms of the Copyright, Designs and Patents Act 1988 or under the terms of a licence issued by the Copyright Licensing Agency Ltd, 90 Tottenham Court Road, London W1T 4LP, UK, without the permission in writing of the Publisher. Requests to the Publisher should be addressed to the Permissions Department, John Wiley & Sons Ltd, The Atrium, Southern Gate, Chichester, West Sussex PO19 8SQ, England, or emailed to permreq@wiley.co.uk, or faxed to (+44) 1243 770620.

This publication is designed to provide accurate and authoritative information in regard to the subject matter covered. It is sold on the understanding that the Publisher is not engaged in rendering professional services. If professional advice or other expert assistance is required, the services of a competent professional should be sought.

Other Wiley Editorial Offices

John Wiley & Sons Inc., 111 River Street, Hoboken, NJ 07030, USA

Jossey-Bass, 989 Market Street, San Francisco, CA 94103-1741, USA

Wiley-VCH Verlag GmbH, Boschstr. 12, D-69469 Weinheim, Germany

John Wiley & Sons Australia Ltd, 33 Park Road, Milton, Queensland 4064, Australia

John Wiley & Sons (Asia) Pte Ltd, 2 Clementi Loop #02-01, Jin Xing Distripark, Singapore 129809

John Wiley & Sons Canada Ltd, 22 Worcester Road, Etobicoke, Ontario, Canada M9W 1L1

Wiley also publishes its books in a variety of electronic formats. Some content that appears in print may not be available in electronic books.

Library of Congress Cataloging-in-Publication Data

Modern polyesters / edited by John Scheirs and Timothy E. Long.

p. cm. – (Wiley series in polymer science)

Includes bibliographical references and index.

ISBN 0-471-49856-4 (alk. paper)

1. Polyesters. I. Scheirs, John. II. Long, Timothy E., 1969-III. Series.

TP1180.P6M64 2003

668.4'225 – dc21

2003041171

British Library Cataloguing in Publication Data

A catalogue record for this book is available from the British Library

ISBN 0-471-49856-4

Typeset in 10/12pt Times by Laserwords Private Limited, Chennai, India

Printed and bound in Great Britain by Antony Rowe Ltd, Chippenham, Wiltshire

This book is printed on acid-free paper responsibly manufactured from sustainable forestry in which at least two trees are planted for each one used for paper production.

Contents

Contributors	xxiii
Series Preface	xxvii
Preface	xxix
About the Editors	xxxiii

I HISTORICAL OVERVIEW

1 The Historical Development of Polyesters	3
<i>J. Eric McIntyre</i>	
1 Introduction	3
2 Alkyd and Related Resins	4
3 Fibres from Partially Aromatic Polyesters	6
3.1 Early Work Leading to Poly(ethylene Terephthalate)	6
3.2 Spread of Polyester Fibre Production	10
3.3 Intermediates	12
3.4 Continuous Polymerisation	13
3.5 Solid-phase Polymerisation	13
3.6 End-use Development	14
3.7 High-speed Spinning	15
3.8 Ultra-fine Fibres	16
4 Other Uses for Semi-aromatic Polyesters	16
4.1 Films	16
4.2 Moulding Products	17
4.3 Bottles	17
5 Liquid-crystalline Polyesters	18

6	Polyesters as Components of Elastomers	19
7	Surface-active Agents	20
8	Absorbable Fibres	21
9	Polycarbonates	22
10	Natural Polyesters	23
	10.1 Occurrence	23
	10.2 Poly(β -hydroxyalkanoate)s	23
11	Conclusion	24
	References	24

II POLYMERIZATION AND POLYCONDENSATION

2 Poly(ethylene Terephthalate) Polymerization – Mechanism, Catalysis, Kinetics, Mass Transfer and Reactor Design 31

Thomas Rieckmann and Susanne Völker

Notation	31
1 Introduction	35
2 Chemistry, Reaction Mechanisms, Kinetics and Catalysis	37
2.1 Esterification/Hydrolysis	41
2.2 Transesterification/Glycolysis	48
2.3 Reactions with Co-monomers	50
2.4 Formation of Short Chain Oligomers	52
2.5 Formation of Diethylene Glycol and Dioxane	54
2.6 Thermal Degradation of Diester Groups and Formation of Acetaldehyde	58
2.7 Yellowing	62
2.8 Chemical Recycling	65
2.9 Conclusions	67
3 Phase Equilibria, Molecular Diffusion and Mass Transfer	72
3.1 Phase Equilibria	72
3.2 Diffusion and Mass Transfer in Melt-phase Polycondensation	75
3.2.1 Mass-transfer Models	78
3.2.2 Diffusion Models	79
3.2.3 Specific Surface Area	83
3.3 Diffusion and Mass Transfer in Solid-state Polycondensation	84
3.4 Conclusions	86

4	Polycondensation Processes and Polycondensation Plants	89
4.1	Batch Processes	90
4.1.1	Esterification	90
4.1.2	Polycondensation	93
4.2	Continuous Processes	93
5	Reactor Design for Continuous Melt-phase Polycondensation	98
5.1	Esterification Reactors	99
5.2	Polycondensation Reactors for Low Melt Viscosity	99
5.3	Polycondensation Reactors for High Melt Viscosity	100
6	Future Developments and Scientific Requirements	103
	Acknowledgements	104
	References	104
3	Synthesis and Polymerization of Cyclic Polyester Oligomers	117
	<i>Daniel J. Brunelle</i>	
1	Introduction	117
2	History	119
3	Preparation of Polyester Cyclic Oligomers from Acid Chlorides	120
4	Polyester Cyclic Oligomers via Ring–Chain Equilibration (Depolymerization)	124
5	Mechanism for Formation of Cyclics via Depolymerization	131
6	Polymerization of Oligomeric Ester Cyclics	134
7	Conclusions	139
	References	139
4	Continuous Solid-state Polycondensation of Polyesters	143
	<i>Brent Culbert and Andreas Christel</i>	
1	Introduction	143
2	The Chemical Reactions of PET in the Solid State	147
2.1	Basic Chemistry	147
2.2	Mechanism and Kinetics	151
2.3	Parameters Affecting SSP	154
2.3.1	Temperature	154
2.3.2	Time	154
2.3.3	Particle Size	156

2.3.4	End Group Concentration	156
2.3.5	Crystallinity	157
2.3.6	Gas Type	158
2.3.7	Gas Purity	158
2.3.8	Catalyst	158
2.3.9	Molecular Weight	158
3	Crystallization of PET	158
3.1	Nucleation and Spherulite Growth	161
3.2	Crystal Annealing	164
4	Continuous Solid-state Polycondensation Processing . .	166
4.1	PET-SSP for Bottle Grade	166
4.2	Buhler PET-SSP Bottle-grade Process	167
4.2.1	Crystallization (Primary)	168
4.2.2	Annealing (Secondary Crystallization) . .	168
4.2.3	SSP Reaction	171
4.2.4	Cooling	172
4.2.5	Nitrogen Cleaning Loop	173
4.3	Process Comparison	173
4.4	PET-SSP for Tyre Cord	175
4.5	Other Polyesters	176
4.5.1	SSP of Poly(butylene terephthalate) . . .	176
4.5.2	SSP of Poly(ethylene naphthalate)	177
5	PET Recycling	178
5.1	PET Recycling Market	178
5.2	Material Flow	179
5.3	Solid-state Polycondensation in PET Recycling	179
5.3.1	PET Bottle Recycling: Flake SSP	181
5.3.2	PET Bottle Recycling: SSP After Repelletizing	182
5.3.3	Closed-loop Bottle-to-bottle Recycling .	183
5.3.4	Buhler Bottle-to-bottle Process	184
5.3.5	Food Safety Aspects	186
	References	186
5	Solid-state Polycondensation of Polyester Resins: Fundamentals and Industrial Production	195
	<i>Wolfgang Göltner</i>	
1	Introduction	195
2	Principles	196
2.1	Aspects of Molten-state Polycondensation	197
2.2	Aspects of Solid-state Polycondensation	199
2.3	Physical Aspects	200

2.3.1	The Removal of Side Products	200
2.3.2	Temperature	202
2.3.3	Reactivity	205
2.3.4	Diffusivity	205
2.3.5	Particle Size	206
2.3.6	Polydispersity	210
2.3.7	Crystallinity	210
2.4	Other Polyesters	213
3	Equipment	215
3.1	Batch Process	216
3.2	Continuous Process	218
3.3	SSP of Small Particles and Powders	220
3.4	SSP in the Suspended State	221
4	Practical Aspects of the Reaction Steps	221
4.1	Crystallization and Drying	221
4.2	Solid-state Polycondensation	224
4.2.1	Discontinuous Process	224
4.2.2	Continuous Process	226
4.3	Process Parameters Influencing SSP	227
4.3.1	Particle Size	227
4.3.2	Catalysts	228
4.3.3	Intrinsic Viscosity	229
4.3.4	Carboxylic End Groups	230
4.3.5	Temperature	233
4.3.6	Vacuum and Gas Transport	234
4.3.7	Reaction Time	235
4.3.8	Oligomers and Acetaldehyde	235
5	Economic Considerations	236
6	Solid-state Polycondensation of Other Polyesters	237
7	Conclusions	238
	References	239

III TYPES OF POLYESTERS

6 New Poly(Ethylene Terephthalate) Copolymers 245

David A. Schiraldi

1	Introduction	245
2	Crystallinity and Crystallization Rate Modification	246
2.1	Amorphous Copolyesters of PET	247
2.2	Increased Crystallization Rates and Crystallinity in PET Copolymers	248

3	PET Copolymers with Increased Modulus and Thermal Properties	251
3.1	Semicrystalline Materials	251
3.2	Liquid Crystalline Copolyesters of PET	254
4	Increased Flexibility Copolymers of PET	254
5	Copolymers as a Scaffold for Additional Chemical Reactions	256
6	Other PET Copolymers	257
6.1	Textile-related Copolymers	257
6.2	Surfaced-modified PET	260
6.3	Biodegradable PET Copolymers	260
6.4	Terephthalate Ring Substitutions	261
6.5	Flame-retardant PET	261
7	Summary and Comments	261
	References	262
7	Amorphous and Crystalline Polyesters based on 1,4-Cyclohexanedimethanol	267
	<i>S. Richard Turner, Robert W. Seymour and John R. Dombroski</i>	
	Notation	267
1	Introduction	267
2	1,4-Cyclohexanedimethanol	269
3	1,3- and 1,2-Cyclohexanedimethanol: Other CHDM Isomers	271
3.1	Definitions: PCT, PCTG, PCTA and PETG	271
4	Synthesis of CHDM-based Polyesters	272
5	Poly(1,4-Cyclohexylenedimethylene Terephthalate)	273
5.1	Preparation and Properties	273
5.2	Other Crystalline Polymers Based on PCT or CHDM	276
5.3	Processing of Crystalline PCT-based Polymers	277
5.4	Applications For PCT-based Polymers	277
5.4.1	Injection Molding	277
5.4.2	Extrusion	279
6	GLYCOL-modified PCT Copolyester: Preparation and Properties	279
7	CHDM-modified PET Copolyester: Preparation and Properties	280
8	Dibasic-acid-modified PCT Copolyester: Preparation and Properties	282
9	Modification of CHDM-based Polyesters with Other Glycols and Acids	283

9.1	CHDM-based Copolyesters with Dimethyl 2,6-naphthalenedicarboxylate	284
9.2	Polyesters Prepared with 1,4-Cyclohexanedicarboxylic Acid	285
9.3	CHDM-based Copolyesters with 2,2,4,4-tetramethyl-1,3-cyclobutanediol	287
9.4	CHDM-based Copolyesters with Other Selected Monomers	287
	Acknowledgments	288
	References	288
8	Poly(Butylene Terephthalate)	293
	<i>Robert R. Gallucci and Bimal R. Patel</i>	
1	Introduction	293
2	Polymerization of PBT	294
2.1	Monomers	296
2.1.1	1,4-Butanediol	296
2.1.2	Dimethyl Terephthalate and Terephthalic Acid	297
2.2	Catalysts	297
2.3	Process Chemistry	297
2.4	Commercial Processes	300
3	Properties of PBT	301
3.1	Unfilled PBT	303
3.2	Fiberglass-filled PBT	305
3.3	Mineral-filled PBT	307
4	PBT Polymer Blends	307
4.1	PBT–PET Blends	308
4.2	PBT–Polycarbonate Blends	308
4.3	Impact-modified PBT and PBT–PC Blends . . .	310
4.4	PBT Blends with Styrenic Copolymers	311
5	Flame-retardant Additives	313
6	PBT and Water	315
7	Conclusions	317
	References	317
9	Properties and Applications of Poly(Ethylene 2,6-naphthalene), its Copolyesters and Blends	323
	<i>Doug D. Callander</i>	
1	Introduction	323
2	Manufacture of PEN	324
3	Properties of PEN	325

4	Thermal Transitions of PEN	326
5	Comparison of the Properties of PEN and PET	326
6	Optical Properties of PEN	328
7	Solid-state Polymerization of PEN	328
8	Copolyesters	329
	8.1 Benefits of Naphthalate-modified Copolyesters	329
	8.2 Manufacture of Copolyesters	330
9	Naphthalate-based Blends	330
10	Applications for PEN, its Copolyesters and Blends	331
	10.1 Films	331
	10.2 Fiber and Monofilament	332
	10.3 Containers	332
	10.4 Cosmetic and Pharmaceutical Containers	333
11	Summary	333
	References	333
10	Biaxially Oriented Poly(Ethylene 2,6-naphthalene) Films: Manufacture, Properties and Commercial Applications	335
	<i>Bin Hu, Raphael M. Ottenbrite and Junaid A. Siddiqui</i>	
1	Introduction	335
2	The Manufacturing Process for PEN Films	337
	2.1 Synthesis of Dimethyl-2,6-naphthalene Dicarboxylate	337
	2.2 Preparation Process of PEN Resin	339
	2.2.1 Oligomer and Prepolymer Formation	340
	2.2.2 High-polymer Formation	340
	2.3 Continuous Process for the Manufacture of Biaxially Oriented PEN Film	341
3	Properties of PEN	341
	3.1 Morphology of PEN	344
	3.2 Chemical Stability	344
	3.3 Thermal Properties	346
	3.4 Mechanical Properties	346
	3.5 Gas-barrier Properties	347
	3.6 Electrical Properties	348
	3.7 Optical Properties	349
4	Applications for PEN Films	350
	4.1 Motors and Machine Parts	352
	4.2 Electrical Devices	352
	4.3 Photographic Films	353
	4.4 Cable and Wires Insulation	354
	4.5 Tapes and Belts	354

4.6	Labels	355
4.7	Printing and Embossing Films	356
4.8	Packaging Materials	356
4.9	Medical Uses	357
4.10	Miscellaneous Industrial Applications	357
	References	357

11 Synthesis, Properties and Applications of Poly(Trimethylene Terephthalate) 361

Hoe H. Chuah

1	Introduction	361
2	Polymerization	362
2.1	1,3-Propanediol Monomer	363
2.2	The Polymerization Stage	363
2.3	Side Reactions and Products	367
3	Physical Properties	368
3.1	Intrinsic Viscosity and Molecular Weights	369
3.2	Crystal Structure	370
3.3	Crystal Density	370
3.4	Thermal Properties	371
3.4.1	Melting and Crystallization	371
3.5	Crystallization Kinetics	372
3.6	Non-isothermal Crystallization Kinetics	374
3.7	Heat Capacity and Heat of Fusion	374
3.8	Glass Transition and Dynamic Mechanical Properties	374
3.9	Mechanical and Physical Properties	376
3.10	Melt Rheology	377
4	Fiber Properties	378
4.1	Tensile Properties	378
4.2	Elastic Recovery	379
4.3	Large Strain Deformation and Conformational Changes	381
4.4	Drawing Behavior	383
4.5	Crystal Orientation	384
5	Processing and Applications	385
5.1	Applications	385
5.2	Fiber Processing	386
5.2.1	Partially Oriented and Textured Yarns for Textile Applications	386
5.2.2	Carpets	388

5.3	Dyeing	388
5.4	Injection Molding	389
6	PTT Copolymers	390
7	Health and Safety	391
	References	391

IV FIBERS AND COMPOUNDS

12	Polyester Fibers: Fiber Formation and End-use Applications	401
	<i>Glen Reese</i>	
1	Introduction	401
2	General Applications	402
3	Chemical and Physical Structure	404
3.1	Melt Behavior	404
3.2	Polymer Structure	406
3.3	Fiber Geometry	410
4	Melt Spinning of PET Fibers	410
4.1	Spinning Process Control	416
5	Drawing of Spun Filaments	418
5.1	Commercial Drawing Processes	420
6	Specialized Applications	422
6.1	Light Reflectance	422
6.2	Low Pill Fibers	424
6.3	Deep Dye Fibers	424
6.4	Ionic Dyeability	425
6.5	Antistatic/Antisoil Fibers	426
6.6	High-shrink Fibers	427
6.7	Low-melt Fibers	427
6.8	Bicomponent (Bico) Fibers	427
6.9	Hollow Fibers	429
6.10	Microfibers	429
6.11	Surface Friction and Adhesion	430
6.12	Antiflammability and Other Applications	430
7	The Future of Polyester Fibers	431
	References	432
13	Relationship Between Polyester Quality and Processability: Hands-on Experience	435
	<i>Wolfgang Göltner</i>	
1	Introduction	435
2	Polyesters for Filament and Staple Fiber Applications	438

2.1	Spinnability	438
2.1.1	Solidification, Structure Formation and Deformability	439
2.2	Yarn Break	450
2.2.1	Spinning	452
2.2.2	Drawing	454
2.2.3	Heat Setting	455
3	Polymer Contamination	456
3.1	Oligomeric Contaminants	459
3.2	Technological Aspects	465
3.3	Thermal, Thermo-oxidative and Hydrolytic Degradation	468
3.4	Insoluble Polyesters	471
3.5	Gas Bubbles and Voids	471
3.6	Dyeability	471
4	Films	472
4.1	Surface Properties	474
4.2	Streaks	476
4.3	Processability	477
5	Bottles	477
5.1	Processing	480
5.2	The Quality of Polyester Bottle Polymer	482
5.2.1	Definitions of Color, Haze and Clarity	482
5.2.2	Color	483
5.2.3	Stability	484
5.2.4	Acetaldehyde	485
5.2.5	Barrier Properties	486
6	Other Polyesters	487
7	Conclusions	489
	References	490
14	Additives for the Modification of Poly(ethylene Terephthalate) to Produce Engineering-grade Polymer	495
	<i>John Scheirs</i>	
1	Introduction	495
2	Chain Extenders	497
2.1	Pyromellitic Dianhydride	499
2.2	Phenylenebisoxazoline	502
2.3	Diepoxide Chain Extenders	503
2.4	Tetraepoxide Chain Extenders	504
2.5	Phosphites Chain Extension Promoters	504
2.6	Carbonyl Bis(1-caprolactam)	505

3	Solid-stating Accelerators	505
4	Impact Modifiers (Tougheners)	506
4.1	Reactive Impact Modifiers	507
4.2	Non-reactive Impact Modifiers (Co-modifiers)	510
4.2.1	Core–Shell Elastomers	511
4.3	Theory of Impact Modification of PET	514
5	Nucleating Agents	515
6	Nucleation/Crystallization Promoters	520
7	Anti-hydrolysis Additives	522
8	Reinforcements	524
9	Flame Retardants	526
10	Polymeric Modifiers for PET	528
11	Specialty Additives	529
11.1	Melt Strength Enhancers	529
11.2	Carboxyl Acid Scavengers	530
11.3	Transesterification Inhibitors	530
11.4	Gloss Enhancers	530
11.5	Alloying (Coupling) Agents	531
11.6	Processing Stabilizers	531
12	Technology of Commercial PET Engineering Polymers	532
12.1	Rynite™	532
12.2	Petra™	533
12.3	Impet™	533
13	Compounding Principles for Preparing Engineering-grade PET Resins	534
14	Commercial Glass-filled and Toughened PET Grades	534
15	‘Supertough’ PET	535
16	Automotive Applications for Modified PET	536
	References	537
15	Thermoplastic Polyester Composites	541
	<i>Andrew E. Brink</i>	
1	Introduction	541
2	Poly(ethylene Terephthalate)	542
2.1	Crystallization of Poly(ethylene Terephthalate)	543
2.2	Advantages of Poly(ethylene Terephthalate)	546
3	Comparison of Thermoplastic Polyesters	546
3.1	Poly(butylene Terephthalate)	546
3.2	Poly(1,4-cyclohexylenedimethylene Terephthalate)	547
3.3	Poly(trimethylene Terephthalate)	547

CONTENTS

xvii

4	Composite Properties	549
4.1	Kelly–Tyson Equation	549
4.2	Interfacial Shear Strength – The Importance of Sizing	554
4.3	Carbon Fiber Reinforcements	556
5	New Composite Applications	557
	References	558

V DEPOLYMERIZATION AND DEGRADATION

16 Recycling Polyesters by Chemical Depolymerization . . . 565

David D. Cornell

1	Introduction	565
2	Chemistry	566
3	Background	570
4	Technology for Polyester Depolymerization	572
5	Commercial Application	575
6	Criteria for Commercial Success	576
7	Evaluation of Technologies	576
7.1	Feedstock	577
7.2	Capital	578
8	Results	579
9	Conclusions	586
10	Acknowledgement and disclaimer	587
	References	587

17 Controlled Degradation Polyesters 591

F. Glenn Gallagher

1	Introduction	591
2	Why Degradable Polymers?	591
3	Polymer Degradation	593
4	Degradable Polyester Applications	594
4.1	Medical	594
4.2	Aquatic	595
4.3	Terrestrial	595
4.4	Solid Waste	595
4.4.1	Recycling	597
4.4.2	Landfills	597
4.4.3	Wastewater Treatment Facilities	598
4.4.4	Composting	598
4.4.5	Litter	599

5	Selecting a Polymer for an Application	600
5.1	Understand Application Requirement for a Specific Location	600
5.2	Degradation Testing Protocol including Goal Degradation Product	602
5.3	Lessons from Natural Products	602
6	Degradable Polyesters	604
6.1	Aromatic Polyesters	604
6.2	Aliphatic Polyesters	605
6.3	Copolyesters of Terephthalate to Control Degradation	605
7	Conclusions	606
	References	606
18	Photodegradation of Poly(ethylene Terephthalate) and Poly(ethylene/1,4-Cyclohexylenedimethylene Terephthalate)	609
	<i>David R. Fagerburg and Horst Clauberg</i>	
1	Introduction	609
2	Weather-induced Degradation	610
2.1	Important Climate Variables	610
2.2	Artificial Weathering Devices	612
3	Recent Results for Degradation in PECT	613
3.1	Coloration	613
3.2	Loss of Toughness	617
3.3	Depth Profile of the Damage	618
4	Degradation Mechanisms in PET and PECT	626
5	Summary	638
	References and Notes	638

VI LIQUID CRYSTAL POLYESTERS

19	High-performance Liquid Crystal Polyesters with Controlled Molecular Structure	645
	<i>Toshihide Inoue and Toru Yamanaka</i>	
1	Introduction – Chemical Structures and Liquid Crystallinity	645
2	Experimental	646
2.1	Synthesis of Polyarylates	646

2.2	Preparation of Fibers	646
2.3	Preparation of Specimens	646
3	Measurements	646
3.1	Flexural Modulus	646
3.2	Dynamic Storage Modulus	647
3.3	Anisotropic Melting Temperature and Clearing Point	647
3.4	Melting Temperature and Glass Transition Temperature	647
3.5	Orientation Function of Nematic Domains	647
3.6	Relative Degree of Crystallinity	647
3.7	Morphology	648
3.8	Heat Distortion Temperatures	648
4	Results and Discussion	648
4.1	Moduli of As-spun Fibers	648
4.2	Moduli of Injection Molded Specimens	655
4.3	Heat Resistance	659
4.3.1	Glass Transition Temperature	659
4.3.2	Heat Distortion Temperature	660
5	Conclusions	662
6	Acknowledgement	662
	References	662

20 Thermotropic Liquid Crystal Polymer Reinforced Polyesters 665

Seong H. Kim

1	Introduction	665
2	PHB/PEN/PET Mechanical Blends	666
2.1	The Liquid Crystalline Phase	666
2.2	Thermal behavior	669
2.3	Mechanical properties	671
2.4	Transesterification	673
3	Effect of a catalyst on the compatibility of LCP/PEN Blends	674
3.1	Mechanical property improvement	674
3.2	Dispersion of LCP in PEN	678
3.3	Heterogeneity of the blend	679
4	Thermodynamic miscibility determination of TLCP and polyesters	679
5	Crystallization kinetics of LCP with polyesters	686

5.1	Non-isothermal crystallization dynamics	687
5.2	Isothermal crystallization dynamics	690
6	Conclusions	693
7	Acknowledgements	694
	References	694

VII UNSATURATED POLYESTERS

21	Preparation, Properties and Applications of Unsaturated Polyesters	699
	<i>Keith G. Johnson and Lau S. Yang</i>	
1	Introduction	699
2	Preparation of Unsaturated Polyester Resins	700
2.1	Three Types of Unsaturated Polyester Resin Products	701
3	Properties of Unsaturated Polyester Resins	705
3.1	Chemical Constituents	706
3.2	Additives	706
3.3	Fillers	707
3.4	Reinforcements	707
4	Applications of Unsaturated Polyester Resins	708
4.1	Marine	710
4.2	Construction	710
4.3	Transportation	711
5	Future Developments	712
	References	712
22	PEER Polymers: New Unsaturated Polyesters for Fiber-reinforced Composite Materials	715
	<i>Lau S. Yang</i>	
1	Introduction	715
2	Experimental	716
2.1	Materials	717
2.2	General Procedure for the Preparation of Unsaturated Polyester Resin from a Polyether Polyol	717
2.3	A Typical Example of the Preparation of Cured Polyesters	717
2.4	Other Examples of Cured Polyester Processes	717
2.4.1	System 1	717
2.4.2	System 2	718

CONTENTS	xxi
3 Results and Discussion	718
3.1 Ether Cleavage Reaction Leading to Poly(Ether Ester) Resins	718
3.2 Reaction Conditions and Mechanisms	721
3.3 The Early Product and Strong-acid Catalysis Development	723
3.4 Liquid properties of PEER Resins	725
3.5 Physical properties of Cured PEER Resins . . .	726
4 Applications	727
5 Acknowledgements	729
References	730
Index	733

Contributors

Andrew E. Brink,
Hydrosize Technologies, Inc.,
9201 Dawnshire Road,
Raleigh,
NC 27615, USA

Daniel J. Brunelle,
GE Global Research,
Building K-1, Room 5A26,
One Research Circle,
PO Box 8, Schenectady,
NY 12309, USA

Doug D. Callander,
M & G Polymers USA, LLC,
PO Box 590,
6951 Ridge Road,
Sharon Center,
OH 44274, USA

Andreas Christel,
Department TP51,
Bühler AG,
CH-9240 Uzwil,
Switzerland

Hoe H. Chuah,
Shell Chemical LP,
Westhollow Technology
Center,
3333 Highway 6 South,
Houston,
TX 77082-3101, USA

Horst Clauberg,
Kulicke and Soffa Industries, Inc.,
2101 Blair Mill Rd,
Willow Grove,
PA 19090, USA

David D. Cornell,
D. D. Cornell Associates LLC,
230 Hammond Avenue,
Kingsport,
TN 37660, USA

Brent Culbert,
Department TP51,
Bühler AG,
CH-9240 Uzwil,
Switzerland

John R. Dombroski,
Polymers Technology Department,
Eastman Chemical Company,
Kingsport,
TN 37662, USA

David R. Fagerburg,
Northeast State Technical
Community College,
Blountville,
TN 37617, USA

Robert Gallucci,
Global Color Technology,
General Electric Company
(GE Plastics),
One ColorXpress Way,
Selkirk, NY 12158, USA

F. Glenn Gallagher,
DuPont Experimental Station,
Building E304, Room C320,
Wilmington,
DE 19880-0304, USA

Wolfgang Göltner,
Mönchesweg 18,
D-36251 Bad Hersfeld,
Germany

Bin Hu,
Department of Chemistry,
Virginia Commonwealth University,
Richmond,
VA 23284, USA

Toshihide Inoue,
Chemicals Research Laboratories,
Toray Industries, Inc.,
2-2-1, Nihonbashi-Muromachi
Chuo-ku,
Tokyo 103-8666, Japan

Keith G. Johnson,
Structural Composites, Inc.,
Melbourne,
FL 32903, USA

Seong Hun Kim,
Department of Fibre and Polymer
Engineering,
Centre for Advanced Functional
Polymers,
Hanyang University,
Seoul 133-791,
Korea

J. Eric McIntyre,
3 Rossett Gardens,
Harrogate,
HG2 9PP, UK

Raphael M. Ottenbrite,
Department of Chemistry,
Virginia Commonwealth University,
Richmond,
VA 23284, USA

Bimal R. Patel,
Global Color Technology,
General Electric Company
(GE Plastics),
One ColorXpress Way,
Selkirk, NY 12158, USA

Glen Reese,
KoSa Corporation,
4601 Carmel Vista Lane,
Charlotte,
NC 28226, USA

CONTRIBUTORS

xxv

Thomas Rieckmann,
Department of Chemical Engineering
and Plant Design,
University of Applied
Sciences Cologne,
Betzdorfer Str. 2,
D-50679 Cologne,
Germany

Robert W. Seymour,
Polymers Technology Department,
Eastman Chemical Company,
Kingsport,
TN 37662, USA

John Scheirs,
ExcelPlas Polymer Technology,
PO Box 2080,
Edithvale,
VIC 3196, Australia

David Schiraldi,
Department of
Macromolecular Science, 538 Kent
Hale Smith Building,
2100 Adelbert Road,
Case Western Reserve University,
Cleveland, OH 44106-7202, USA

Junaid A. Siddiqui,
DuPont *i*-Technologies,
14 T.W. Alexander Drive,
Research Triangle Park,
NC 27709, USA

S. Richard Turner,
Polymers Technology Department,
Eastman Chemical Company,
Kingsport,
TN 37662, USA

Lau S. Yang,
Lyondell Chemical Company,
Newtown Square,
PA 19073, USA

Susanne Völker,
42 Engineering,
von-Behring-Str. 9,
D-34260 Kaufungen,
Germany

Toru Yamanaka,
Chemicals Research Laboratories,
Toray Industries, Inc.,
2-2-1, Nihonbashi–Muromachi
Chuo-ku,
Tokyo 103-8666,
Japan

Series Preface

The Wiley Series in Polymer Science aims to cover topics in polymer science where significant advances have been made over the past decade. Key features of the series will be developing areas and new frontiers in polymer science and technology. Emerging fields with strong growth potential for the twenty-first century such as nanotechnology, photopolymers, electro-optic polymers, etc. will be covered. Additionally, those polymer classes in which important new members have appeared in recent years will be revisited to provide a comprehensive update.

Written by foremost experts in the field from industry and academia, these books have particular emphasis on structure–property relationships of polymers and manufacturing technologies, as well as their practical and novel applications. The aim of each book in the series is to provide readers with an in-depth treatment of the state-of-the-art in that field of polymer technology. Collectively, the series will provide a definitive library of the latest advances in the major polymer families, as well as significant new fields of development in polymer science.

This approach will lead to a better understanding and improve the cross-fertilization of ideas between scientists and engineers of many disciplines. The series will be of interest to all polymer scientists and engineers, providing excellent up-to-date coverage of diverse topics in polymer science, and thus will serve as an invaluable ongoing reference collection for any technical library.

John Scheirs
June 1997

Preface

Polyesters are one of the most important classes of polymers in use today. In their simplest form, polyesters are produced by the polycondensation reaction of a glycol (or dialcohol) with a difunctional carboxylic acid (or diacid). Hundreds of polyesters exist due to the myriad of combinations of dialcohols and diacids, although only about a dozen are of commercial significance.

Mankind has been using natural polyesters since ancient times. There are reports of the use of shellac (a natural polyester secreted by the lac insect) by the ancient Egyptians for embalming mummies. Early last century, shellac was still used as a moulding resin for phonographic records. True synthesis of aliphatic polyesters began in the 1930s by Carothers at DuPont in the USA and more significantly with the discovery of aromatic polyesters by Whinfield and Dickson at the Calico Printers Association in the UK. The complete historical development of polyesters is described in Chapter 1.

Polyesters are in widespread use in our modern life, ranging from bottles for carbonated soft drinks and water, to fibres for shirts and other apparel. Polyester also forms the base for photographic film and recording tape. Household tradenames, such as Dacron[®], Fortrel[®], Terylene[®] and Mylar[®], demonstrate the ubiquitous nature of polyesters.

The workhorse polyester is poly(ethylene terephthalate) (PET) which is used for packaging, stretch-blown bottles and for the production of fibre for textile products. The mechanism, catalysis and kinetics of PET polymerization are described in Chapter 2. Newer polymerization techniques involving the ring-opening of cyclic polyester oligomers is providing another route to the production of commercial thermoplastic polyesters (see Chapter 3).

High-molecular-weight polyesters cannot be made by polymerization in the molten state alone – instead, post-polymerization (or polycondensation) is performed in the solid state as chips (usually under vacuum or inert gas) at temperatures somewhat less than the melting point. The solid-state polycondensation of polyesters is covered in detail in Chapters 4 and 5.

Polyester copolymers (or copolyesters) are those polyesters synthesized from more than one glycol and/or more than one dibasic acid. The copolyester chain is less regular than the homopolymer chain and therefore has a reduced tendency to crystallize. Such copolyesters are thus predominately amorphous and have high clarity and toughness (see Chapters 6 and 7).

Poly(butylene terephthalate) (PBT) is a semicrystalline, thermoplastic polyester which is completely analogous to PET except that it has a longer, more flexible butylene chain linkage which imparts a rapid crystallization rate, thus making PBT well suited to injection moulding processes. This polyester is used widely for electrical and electronic components due to its high temperature resistance and good electrical properties (Chapter 8).

Poly(ethylene naphthalate) (PEN) is also completely analogous to PET except that it incorporates a naphthalene group in its main structure as opposed to a phenyl group. The naphthalene unit stiffens the backbone and gives PEN a higher glass transition temperature and improved mechanical properties when compared to PET (see Chapters 9 and 10).

The newest commercial polymer to join the polyester family is poly(trimethylene terephthalate) (PTT) which is being targeted at fibre applications (Chapter 11). It is sold under the Corterra[®] trademark by Shell. After packaging, the single largest use for polyesters is for fibre applications such as clothing, textiles and non-wovens. The technology of polyester fibre formation is described in Chapters 12 and 13.

The slow crystallization rate of PET makes it difficult to injection mould. However, the advances in additive chemistry described in Chapter 14 enables low-cost recycled PET to be upgraded through formulation enhancements to give engineering-grade resins. Glass- and mineral-filled engineering-grade PET composites exhibit enhanced strength, stiffness and heat-resistant properties, thus allowing them to be used in applications replacing such metals as die-cast aluminium or zinc in motor or pump housings and structural steel in furniture such as office chair bases (see Chapter 15).

The recycling of PET is an important environmental topic as well as a commercial opportunity due to its widespread use, abundance and availability in bottles, packaging and fibres. While mechanical recycling of PET is now well established, newer chemical recycling techniques rely on depolymerization routes which cleave the polymer chains into 'new' monomer building blocks (see Chapter 16).

Biodegradable polymers have recently emerged as a viable solution to plastic litter and landfilling problems. The majority of biodegradable polymers are based on aliphatic polyesters. Chapter 17 gives an overview of controlled degradation polyesters and introduces a modified biodegradable PET called BIOMAX[®]. The photodegradation of PET and related copolyesters is described in Chapter 18.

Liquid crystalline aromatic polyesters are a class of thermoplastic polymers that exhibit a highly ordered structure in both the melt and solid states. They can be used to replace such materials as metals, ceramics, composites and other plastics

because of their exceptional strength at extreme temperatures and outstanding resistance to most chemicals, weathering, radiation and burning (see Chapters 19 and 20).

Finally, glass-reinforced unsaturated polyesters are well known as building materials for boats, yachts and cars and generally termed ‘fibre-glass resin’. The preparation, properties and applications of these unsaturated polyesters are summarized in Chapter 21, while the chemistry and properties of a new unsaturated polyester resin for fibre-reinforced composite materials are discussed in Chapter 22.

The future direction of polyester R & D efforts is likely to involve further progress in polyester synthesis given the wide range of potential monomer combinations, new blending technology and the use of advanced functional additives such as nanoclay reinforcements, reactive impact modifiers, anti-hydrolysis agents and chain extenders.

This book provides the reader with comprehensive information about polyester resins with an emphasis on their structure–property relationships. The latest advances in polyesters are described along with current and emerging application areas.

John Scheirs
ExcelPlas Australia, Edithvale, Victoria, Australia

Timothy E. Long
Virginia Tech, Blacksburg, Virginia, USA

About the Editors

Dr John Scheirs has worked extensively with poly(ethylene terephthalate) (PET) and related polyesters. His early work involved studying the UV stability of PET and poly(ethylene naphthalate) (PEN) in France and later he was involved with studying various industrial problems involving polyesters, such as photodegradation, annealing, crystallization behaviour, embrittlement, degradation by aminolysis, differential scanning calorimetry (DSC) analysis, environmental stress cracking, hydrolysis, nucleating agents, transesterification, injection moulding of recycled PET compounds, solid-state polycondensation, desiccant drying of PET and melt stabilization of PET. More recently in the period 1998–2000, he was the technical manager for Coca-Cola Amatil's world-first PET reforming plant which converts post-consumer PET bottles into high-grade, high IV pelletized PET for direct reuse in new bottles and injection and sheet moulding applications. John Scheirs is now the principal consultant with ExcelPlas Polymer Technology where he specializes in polymer recycling, chemistry, formulation, processing and testing.

Dr Timothy E. Long is a professor in the Department of Chemistry and the Macromolecular Science and Engineering Program at Virginia Tech in Blacksburg, VA, USA. Professor Long was employed at Eastman Kodak and Eastman Chemical for 12 years prior to joining the faculty at Virginia Tech in 1999. He has extensive industrial and academic experience in fundamental macromolecular chemistry, with an awareness of the industrial and commercial impact of polyester chemistry and processing, structure–property relationships, and polyester applications. His research interests include polyester ionomers, high-gas-barrier polyesters for packaging, new polyester catalyst development, thermotropic liquid crystalline polyesters, functional poly(lactides), and branched and hyperbranched polyesters. He is the author of over 100 refereed papers and holds 25 patents dealing with various aspects of macromolecular science and engineering.

PART I

Historical Overview

1

The Historical Development of Polyesters

J. E. McINTYRE

3 Rossett Gardens, Harrogate, HG2 9PP, UK

1 INTRODUCTION

Strictly speaking, the term *polyester* ought to refer to a chemical compound containing many ester groups in each molecule. In practice, however, it usually refers to polymeric materials containing ester groups as major structural components of the main chains of the macromolecules of which the polymer is composed, and this is the sense in which it is used here. The term is not now usually applied to polymers that contain ester groups attached to the main chain either directly, as in cellulose triacetate, poly(vinyl acetate) or poly(methyl acrylate), or within short side-chains.

There has in the past been some confusion in the use of the term *alkyd*, which is said to have been derived from *alcohol* plus *acid*. The definition offered by Kienle [1], discussed later, is broad enough to include all polyesters derived essentially from diols and dicarboxylic acids, and consequently linear polyesters were initially included in this class of polymer. On the other hand, Bjorksten *et al.* [2], in their 1956 compilation of published information about polyesters, restrict the term *polyester* to the polycondensation products of dicarboxylic acids with dihydroxy alcohols, and say that 'this definition does not include materials commonly known as alkyds'. At the present time, there are still problems of nomenclature in the fibre field arising from the use of *polyester* as a generic term to cover fibres containing only a very restricted range of chemical groups.

The term *ester* applies not only to products derived from carboxylic acids but also to products derived from other types of organic acid such as phosphonic or

sulphonic acids and from inorganic acids such as phosphoric acid, and thus the term *polyester* also includes polymers containing these inorganic groups. Relatively little work has been carried out in this field, with the very important exception of nucleic acids. Polynucleotides are linear polyesters of phosphoric acid with ribose (ribonucleic acids, RNA) or with 2'-deoxyribose (deoxyribonucleic acids, DNA), and are of very high molecular weight. In both cases, purine and pyrimidine bases are attached to the pentose groups. This field is so different from the general field of polyesters that it will not be considered further here.

2 ALKYD AND RELATED RESINS

The earliest synthetic resin to be used in commerce seems to have been a polyester then termed *ester gum*, which was made by esterifying rosin (essentially an unsaturated monocarboxylic terpenoid acid, abietic acid) with glycerol. When cooked with tung oil (a glycerol ester of 9,11,13-octadecatrienoic acid), this provided varnishes that dried overnight. In this case, the polymer is formed by an addition copolymerisation process, but the product is nevertheless also a polyester.

Alkyd resins were the first polyesters to become of major commercial importance. They were originally defined as reaction products of polyhydric alcohols and resinifying carboxylic acids such as polybasic acids and their anhydrides. This definition is no longer appropriate, since it can be interpreted as including, for example, modern polyester fibres. Alkyds were first introduced into the market by the General Electric Company in the USA, whose trade mark, 'Glyptal', became an alternative name for them [3]. Earlier reports of polyester resins of this type include those from Berzelius (1847) [4], who reported a resin from tartaric acid and glycerol, Berthelot (1853) [5], who obtained a resin from glycerol and camphoric acid (*cis*-1,2,2-trimethyl-1,3-cyclopentane-dicarboxylic acid), and Van Bemmelen (1856) [6], who made glycerides of succinic acid and citric acid. The most important product of this class, i.e. the reaction product of glycerol and phthalic anhydride, was first described in 1901 by Watson Smith [7], who obtained a solid, transparent, strongly refractive resin on heating these two compounds together in a molar ratio of 2:3, and showed that a very similar product was obtained if the molar ratio was varied, even with a large excess of glycerol. He found that at temperatures above about 190 °C under vacuum the reaction mass frothed with an accompanying rise in temperature, leaving a glassy product.

According to Kienle [3], the early development work on alkyd resins was carried out between 1910 and 1915 in the laboratories of the General Electric Company. In particular, in a patent filed in 1912, Callahan [8] showed that the reaction between glycerol and phthalic anhydride should be carried out in two stages – first with the temperature being gradually raised to about 210 °C, and

then at a lower temperature of about 100 °C over a period of many hours, whose duration depends upon the dimensions of the sample. The second stage, which leads to hardening, can be carried out after coating or impregnating the material to be treated. Continuing the first stage to higher temperatures led to formation of a hard, brittle mass filled with cavities, presumably due to a combination of cross-linking (i.e. reaching the gel point) with an evolution of water vapour too rapidly for it to diffuse through the resin. Callahan believed [9] that the cavity formation was due to evolution of glycerol, but his use of a high molar ratio, i.e. 2:1, of phthalic anhydride to glycerol and the low volatility of glycerol render this unlikely. Callahan [9] then described conditions that allowed the second stage to be carried out at 200–210 °C and showed that further hardening could be obtained by continuing to heat at temperatures up to 250 °C. Other GEC patents from that period showed that it was possible to incorporate small amounts of butyric acid [10], or oleic acid [11], or castor oil [12], or both oleic acid and castor oil [13]. These were the first of many developments that extended the range of alkyd resins by giving control over the flexibility or hardness, modifying the rate of cure, and introducing the possibility of additional olefinic curing reactions, at that time referred to as ‘drying’.

The main ingredients for the early alkyd resins, namely phthalic anhydride and glycerol, were already quite readily available at the time of their development. At that time, phthalic anhydride was made by catalytic oxidation of naphthalene with sulphuric acid. However, a considerable boost to the competitiveness of alkyds was the development from about 1917 of a much cheaper process for phthalic anhydride, based on catalytic vapour-phase oxidation of naphthalene.

In 1924, Kienle and Hovey began to study the kinetics of the polyesterification reaction between glycerol and phthalic anhydride. First [3] they demonstrated, among other aspects, that the reaction proceeded solely by esterification, that the initial stages were very rapid and exothermic, and that gelation occurred before esterification was complete. Further papers from Kienle and his co-workers developed a distinction between heat-non-convertible, heat-convertible, and oxygen-convertible (later element-convertible) alkyd resins. These corresponded, respectively, with the non-gelling products of a reaction between bifunctional alcohols and acids (a 2:2 reaction, where the numbers represented the ‘reactivity’ or functionality in ester formation of the compounds), the thermally gelling products of a reaction between reactants of the 2:3 type or higher (Figure 1.1), and the gelling products of a reaction involving unsaturated groups [1, 14]. At that time, products in the first group were not recognised as being potentially useful.

Development of the third class, i.e. unsaturated polyester resins, remained rather slow until the late 1930s, but after commercial production of maleic anhydride by catalytic oxidation of benzene began in 1933, maleic anhydride and fumaric acid rapidly became the most important sources of unsaturated groups in polyesters. The mechanism of ‘drying’ of these resins on their own and with the addition of drying oils (i.e. unsaturated compounds such as linseed oil) was

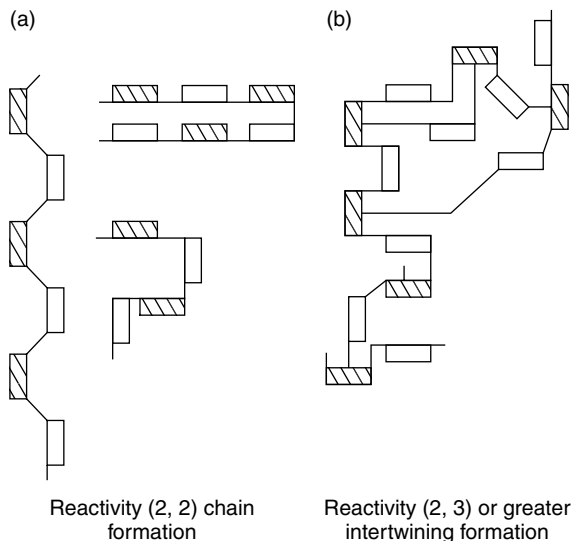


Figure 1.1 Kienle's illustration of polymer formation from (a) two bifunctional reactants and (b) one bifunctional and one trifunctional reactant [1]

investigated and, to some extent, clarified by Bradley and co-workers [15] and Vincent [16] during this period, and their 'convertibility' to insoluble, infusible structures was identified as being due to the double bonds, whose concentration in the precursors had to exceed a certain limit.

During World War II, polyesters containing unsaturated groups, particularly those based on maleic and fumaric esters with various diols, grew greatly in importance as constituents of shaped composite structures, notably in combination with glass fibres to make glass-reinforced polyesters (GRPs). The polyester was dissolved in an unsaturated monomer, commonly styrene, and copolymerisation was brought about by any of the various forms of initiation appropriate to double-bond polymerisation.

3 FIBRES FROM PARTIALLY AROMATIC POLYESTERS

3.1 EARLY WORK LEADING TO POLY(ETHYLENE TEREPHTHALATE)

In February 1928, Wallace H. Carothers (Figure 1.2), then an Instructor at Harvard, joined du Pont at Wilmington to set up a fundamental research group in organic chemistry. One of the first topics he chose was the nature of polymers, which he proposed to study by using synthetic methods. He intended to build up some very large molecules by simple and definite reactions in such a way that



Figure 1.2 Wallace H. Carothers (photograph *circa* 1930)

there could be no doubt as to their structures. If he could build up a molecule containing 300 or 400 carbon atoms and having a definitely known structure, he could study its properties and find out to what extent it resembled those of other polymeric substances already investigated [17]. The reaction between aliphatic alcohols and aliphatic carboxylic acids was one of the most fully understood condensation reactions, with very few complications from side-reactions, and suitable diols and dicarboxylic acids were available, so this was the reaction that Carothers chose for his first attack on the topic. He also noted that a study of this type of reaction should cast light on the structure of glyptals, which were already commercially important [18].

By reacting dicarboxylic acids with 5 % excess of diols, Carothers and Arvin obtained a range of polyesters with molecular weights up to about 4000 [19]. One of the collaborators in this work was J. W. Hill, who constructed a molecular still attached to a mercury diffusion pump that was capable of reducing the pressure in the reaction vessel to 10^{-5} mm of mercury [20]. He made a polyester by reacting

octadecanedioic acid with an excess of propane-1,3-diol at a temperature rising to 180 °C and then, at a reduced pressure of 1 mm, to 200 °C. He then subjected it to further reaction in the molecular still at 200 °C and a pressure below 10⁻⁵ mm, and thus raised the molecular weight to about 12 000 [21]. On April 30, 1930, he found that he could now pull fibres from the molten product, and that when the cooled fibres were subjected to an extensional force, they extended irreversibly at their necks to form oriented fibres of uniformly lower cross-sectional area. Carothers and Hill called this behaviour ‘cold drawing’ [22].

Although the acid used in this work was the 18-carbon linear dicarboxylic acid, the polymer is referred to in Reference [22] as the 3–16 ω -ester, based on the number of methylene groups in the diol and dicarboxylic acid respectively. This terminology has led to occasional confusion about the structure of these first polyester fibres, since later usage would give this polymer a code ‘3G18’, including the carbon atoms in the carbonyl groups. This was the first ‘superpolyester’, or ω -ester, as Carothers named these products of high molecular weight.

Carothers and his research group synthesised many polyesters, nearly all of them aliphatic. His basic patent was filed on July 3, 1931 [23]. This work, together with his work on condensation polymers in general, proved influential in convincing the scientific community that polymers were indeed macromolecules, as maintained by Staudinger, and not assemblies of small molecules in a special state of association. Staudinger himself was initially reluctant to accept that the polyesters were polymers, since he had defined polymers in such a way as to refer solely to products of addition reactions. He thus excluded products of condensation reactions, where small molecules were eliminated as co-products of the reaction [24].

The polyesters made by Carothers and his team proved a dead end in terms of commercial development for the time being, since the majority of them had melting points too low for practical utility, and there were also problems with low hydrolytic stability. Carothers turned to other classes of polymer, including, in 1934, polyamides, which he had previously briefly explored with Hill without any success. This work led to nylon fibres – first with Coffman, to nylon 9, then with Peterson, to nylon 5,10, and then, early in 1935, with Berchet, to nylon 6,6 [17].

The first synthetic fibres to be commercialised, the chlorofibres *Pe-Ce* and *Vinyon* and the polyamides nylon 6,6 and *Perlon L* (nylon 6), all appeared in the mid to late 1930s. In 1940, ICI and Courtaulds formed a jointly owned company in the UK to make and sell nylon 6,6 under licence from du Pont. This was the situation when, in 1940, a research programme began at the laboratories of the Calico Printers Association (CPA) in Accrington, UK, which was aimed at making a polyester from ethylene glycol and terephthalic acid. The programme was initiated by J. R. Whinfield, who had been greatly influenced by a period of training nearly twenty years earlier in the laboratories of C. F. Cross, inventor of viscose, and by reading the papers published by Carothers. Whinfield asked J. T. Dickson (Figure 1.3), who had just joined CPA in 1940 from his Ph.D.



Figure 1.3 J. R. Whinfield (left) and J. T. Dickson (right) re-enact the discovery of fibre-forming poly(ethylene terephthalate) [30] (photograph *circa* 1942)

studies at the University of Edinburgh, to carry out the work. Success came quickly, and the first patent application was filed on July 29, 1941 [25–27].

Early in 1942, the discovery was brought to the attention of the British Ministry of Supply, who arranged for further experimental work to be carried out at the government's Chemical Research Laboratory at Teddington, near London. This work was carried out by D. V. N. Hardy [28], who scaled up production of polymer to a metal autoclave giving a theoretical yield of about 600 g of polymer per batch. He also set up a simple form of continuous-filament melt spinning and drawing, and attained very encouraging tensile properties (specific strength of 4.95 g/denier and extension at break of 11.8 %). In December 1943, ICI was told about the discovery and the development, and was invited to negotiate with CPA to take over further work on the topic [28–30]. At that time, ICI and du Pont had in place an agreement to exchange research results, and accordingly ICI disclosed this information to du Pont in July 1944. When ICI subsequently supplied samples to du Pont in February 1945, du Pont had already made rapid progress, due particularly to their discovery of an improved catalyst. Subsequently, in February 1947, ICI acquired the worldwide rights from CPA on a royalty basis, with the exception of the USA, where du Pont had acquired the patent rights outright

from CPA in August 1946. The US patent was therefore issued to du Pont, with a number of additional examples that are not in the UK patent [31].

According to Ludewig [32], the use of terephthalic acid for the development of polyester fibres was implemented almost at the same time by Schlack and by Whinfield and Dickson. Schlack, who had already been responsible for the development of nylon 6 fibres, directed his attention mainly to polyesters produced from terephthalic acid and 1,4-butanediol. Schlack's patent [32, 33] was not filed until 2 July, 1942, well after that of Whinfield and Dickson. This describes the preparation of crystalline oligomeric poly(1,4-butylene terephthalate) from butane-1,4-diol and terephthaloyl chloride under conditions that should give a degree of polymerisation (DP) of at most 9 (not high enough for fibre formation), and their reaction with aromatic diisocyanates to produce melt-spinnable polyesterurethanes. These products had melting points in the range 201 to 208 °C, which were due to the polyester crystallites, but the polymers were, of course, of a different chemical class from those claimed by Whinfield and Dickson. However, the BIOS report [34] of a British team on wartime textile research in Germany records that Schlack carried out an ester-producing polycondensation that gave a spinnable product which on cold-drawing gave strong fibres. Schlack himself [35] confirmed this later.

In 1953, E. F. Izard of du Pont was awarded the Schoellkopf Medal of the American Chemical Society. The report [36] of this award states that 'work on the development of a hydrolytically stable polyester was started by Dr Izard in 1944, and it led in a comparatively short time to the discovery of polyethylene terephthalate'. The report recognises that 'polyethylene terephthalate was earlier discovered independently in England by J. R. Whinfield'. Izard himself says [37] that the duPont research programme led immediately to the discovery of poly(ethylene terephthalate) (PET), which suggests that detailed information from ICI about the structure of the new fibre had not yet reached him by that time.

3.2 SPREAD OF POLYESTER FIBRE PRODUCTION

In the early days of polyester fibre development, du Pont possessed the Whinfield and Dickson patent in the USA, and while its monopoly lasted no other company could enter that market. ICI possessed licence rights for the rest of the world, and took the view that it could not exploit all of these markets on its own as effectively as if it sub-licensed to other companies in major markets outside of the UK. The first sub-licences were granted to Algemene Kunstzijde Unie (AKU) (*Terlenka*) in the Netherlands, Société Rhodiaceta (*Tergal*) in France, Vereinigte Glanzstoff-Fabriken (*Diolen*) and Farbwerke Hoechst (*Trevira*) in Germany, and Società Rhodiatocce (*Terital*) in Italy. The first plant in France was built at Besançon, a city closely associated with the first production of a manufactured fibre by Chardonnet. ICI itself set up manufacturing facilities in Canada, where a subsidiary, Canadian Industries Ltd (CIL), was already

established and the UK name *Terylene* was adopted. Soon thereafter, licences were granted to Teikoku Jinzo Kenshi (now Teijin) and Toyo Rayon (Toray) in Japan, where both companies used the name *Tetoron* for the product [38].

This widespread sub-licensing by ICI reduced the incentive to develop a patent-free product in most of the major industrialised countries. The US market, however, was potentially so large that inevitably other large companies looked for polyester fibres that fell outside the scope of the patent now owned by du Pont. Only one such product was commercialised within the life of that patent. This was a fibre produced from poly(cyclohexane-1,4-dimethylene terephthalate), patented by Kodak [39]. This polymer was made from dimethyl terephthalate and 1,4-di(hydroxymethyl)cyclohexane, a diol that Kodak synthesised by a two-stage hydrogenation of dimethyl terephthalate, with the first stage being hydrogenation of the ring and the second hydrogenation of the ester groups to hydroxymethyl groups. Both of these hydrogenation products consist of mixtures of two isomers, *cis* and *trans*. The *cis:trans* ratio in the commercial polymer was approximately 2:1. This fibre was marketed in the USA from 1958 under the trade name *Kodel*, and later in Germany by Faserwerke Hüls as *Vestan*. Its properties differed significantly in many respects from those of PET fibres. For example, its melting and glass transition temperatures were considerably higher, and its density was about 12 % lower – a property that helped to offset the higher materials cost by improving the covering power.

Other US companies chose to await expiration of the Whinfield and Dickson patent before entering the market. One of the earliest to become involved was Celanese Corporation, whose joint venture with ICI, named Fiber Industries Inc. (FII; *Fortrel*), began construction of its first PET plant in 1959. Beaunit (*Vycron*) was also an early entrant, initially with a copolymer fibre that was arguably not covered by the basic patent, using polymer from Goodyear.

Thereafter, polyester fibre manufacture spread very rapidly throughout the world. Initially, the technology transfer was mainly from the existing producers, but after expiry of the patents it was provided increasingly by engineering firms, who provided not only specific sections of production plant but also ‘turnkey’ plants with start-up support, thus enabling relatively undeveloped countries to establish fibre production.

Many other semi-aromatic polyesters were evaluated and patented in the period immediately following the invention of PET. Some gave excellent fibres and other shaped products, with property advantages over PET, but in general the intermediates were more expensive and the polymers were not commercialised at that time. Poly(*p*-ethyleneoxybenzoate) (*A-Tell*) production began in 1967 in Japan, but the product struggled to compete. Poly(1,4-butylene terephthalate) (PBT) has proved more successful as a moulding polymer than as a fibre. Recent advances in the synthesis of naphthalene-2,6-dicarboxylic acid and of propane-1,3-diol have encouraged re-evaluation of polyesters based upon them, as described in later chapters in this book.

3.3 INTERMEDIATES

When poly(ethylene terephthalate) fibres were invented, and for the first few years thereafter, terephthalic acid and its esters were only available in small amounts and were correspondingly expensive. Whinfield and Dickson, and also Hardy [28] in the first stages of his scale-up work during the period 1942–1944, made the acid by dehydrogenating dipentene (*dl*- $\Delta^{1:8}$ -*p*-menthadiene) with sulphur to form *p*-cymene (*p*-isopropyltoluene), which they oxidised in two stages, first with dilute nitric acid, and then with alkaline permanganate. The first commercially viable route was through oxidation of *p*-xylene under pressure using dilute nitric acid. The product contained coloured and colour-forming impurities that could not be removed, so it was necessary to esterify it with methanol to form dimethyl terephthalate (DMT), which still required successive recrystallisation and distillation to bring it to an acceptable state of purity. For the first few years of PET production, the polymer was all made by an ester interchange route from DMT.

An alternative route to DMT was introduced in 1953. This was based on air oxidation of *p*-xylene to *p*-toluic acid, which was esterified by methanol to form methyl *p*-toluate, which was oxidised by air to monomethyl terephthalate [40], which in turn was esterified by methanol to make DMT. The two oxidations could be combined so that *p*-xylene and methyl *p*-toluate were oxidised in the same vessel, and so could the two esterifications [41]. The process was due to Katzschnmann of Imhausen, a firm based at Witten and later known as Chemische Werke Witten. This process, known variously by its inventor's name and by various combinations of the names of the companies involved in its development, i.e. Hercules, Imhausen, Witten, and Dynamit Nobel, rapidly replaced the rather unsatisfactory and sometimes hazardous nitric acid oxidation route to DMT.

Meanwhile attempts to find an air oxidation route directly from *p*-xylene to terephthalic acid (TA) continued to founder on the relatively high resistance to oxidation of the *p*-toluic acid which was first formed. This hurdle was overcome by the discovery of bromide-controlled air oxidation in 1955 by the Mid-Century Corporation [42, 43] and ICI, with the same patent application date. The Mid-Century process was bought and developed by Standard Oil of Indiana (Amoco), with some input from ICI. The process adopted used acetic acid as solvent, oxygen as oxidant, a temperature of about 200 °C, and a combination of cobalt, manganese and bromide ions as catalyst. Amoco also incorporated a purification of the TA by recrystallisation, with simultaneous catalytic hydrogenation of impurities, from water at about 250 °C [44]. This process allowed development of a route to polyester from purified terephthalic acid (PTA) by direct esterification, which has since become more widely used than the process using DMT.

Several other novel processes for manufacturing TA have been patented, and some of them have been used commercially, but these two remain the most important.

3.4 CONTINUOUS POLYMERISATION

Du Pont were already working on a process for continuous polymerisation of PET in 1952 and commercialised this in an early plant [45]. However, until 1963 most PET was made by a discontinuous polymerisation process. In 1962, the engineering firm Hans J. Zimmer, as it then was, started to develop an integrated continuous ester interchange and polycondensation process [46]. This process was described in 1965, by which time a plant producing three tons per day of polymer was in operation [47]. The advent of processes for pure TA led to parallel development, started in 1966, of a continuous process in which the first stage was direct esterification of TA, based on Mobil technology. Vickers-Zimmer was one of the leaders in developing methods of handling the final stages of polymerisation, where the molten polymer was highly viscous, yet it was essential to minimise the diffusion path to the polymer surface. Their disc-rising reactor was one of several devices designed to deal with these requirements, and the resulting system was capable of producing polymer of intrinsic viscosity as high as 1.0 [48].

3.5 SOLID-PHASE POLYMERISATION

Since the tensile properties obtainable from synthetic fibres are in general superior the higher the molecular weight of the polymer, there was a considerable incentive to find methods of raising the molecular weight of polyesters beyond those readily obtainable by melt polymerisation. Some of the most valuable potential outlets for PET lay in the field of technical textiles, where uses such as tyre cords would benefit from the higher work to break. The limitations of melt polymerisation were due to the reversibility of the polymerisation reaction, which made the rate of glycol removal rate-determining for the later stages of the reaction, and also to the degradation reactions that became increasingly important at the higher reaction temperatures used to reduce the melt viscosity. Although solid-phase polymerisation involved additional handling stages, it was a potentially attractive means of overcoming these difficulties. It introduced difficulties of its own, since polymerisation rates are higher the smaller the particle size, due to the shorter diffusion path [49, 50], but conversion of molten polymer to chip is much easier than to fine particles. In addition, it is necessary to crystallise the solidified polymer before heating it to polymerisation temperatures in order to avoid coalescence of the particles, although further crystallisation during the polymerisation process permits use of temperatures above the normal melting point of PET [51, 52]. Originally developed for the production of fibres for high-performance technical textiles, solid-phase polymerisation has become particularly useful in the manufacture of PET bottles.

3.6 END-USE DEVELOPMENT

The relatively high modulus of PET fibre played a large part in making it suitable for blending in staple-fibre form with both cotton and wool, thus producing fabrics that in some respects were superior to those made from unblended fibres. Pleat retention was an important property. Some dyers considered the new fibre to be undyeable, but rapid progress was made in producing new dyestuffs and in accelerating the rate of dyeing, first by the use of carriers in the dyebath and then through the introduction of pressure dyeing at temperatures of the order of 130°C. Continuous filament yarns were introduced, and methods of texturing them, initially adapted from those already in use for nylon, were developed. Industrial uses, such as tyre cord, made rapid progress, although problems such as adhesion to rubber had to be solved. Variants, such as basic dyeable, pill-resistant, and high shrinkage products were brought onto the market. PET proved the most versatile of all synthetic fibres, and since its materials cost basis was more favourable than that of its competitors, other than the less versatile polyolefins, it rapidly became much the most important in volume terms. Its main deficiencies are relatively poor recovery from strains greater than about 5 %, and correspondingly poor fatigue resistance.

Marketing by brand name remained important in most sectors until about 1970. A particularly interesting example is the trade name *Crimplene*, which was introduced by ICI in 1959 to describe a bulked continuous-filament polyester yarn made by a process due initially to Nava and Ruffini, who worked at the firm of Cheslene and Crepes in Macclesfield, Cheshire, in the UK. Their patents, filed in 1957–1958 [53, 54], describe a process that consists of false-twisting a continuous-filament yarn, partially heat-setting the yarn without making the crimp permanent, over-feeding the yarn onto a package to produce partial relaxation, and then heat setting, preferably using steam. The earlier patent is directed particularly at nylon yarns, but the later one concentrates on polyester. In the *Crimplene* process as promoted by ICI, the final setting was carried out on a soft wind-up package using steam in an autoclave, typically at about 130°C. Initially commercial progress was slow, but a move in 1962 to fabrics having more attractive surface appearance led to a rapid increase in sales and profits [55, 56]. ICI licensed this process to selected customers, who became known as the ‘Crimplene Club’. *Crimplene* was highly profitable from 1964 to 1971, but then it suddenly became a liability. Towards the end of its profitable life, it had the highest recognition factor of any trademark in the UK, but it had acquired a dowdy image. In August 1971, the USA imposed a surcharge on imports of polyester continuous-filament yarn. This immediately created overcapacity in the rest of the world, and a collapse in prices. Moreover, the process was slow and expensive. Rapid advances in simultaneous draw-texturing processes in the early 1970s led to a new and much cheaper type of textured yarn, and provided a final ‘nail in the coffin’.

3.7 HIGH-SPEED SPINNING

At quite an early stage in the development of polyester and nylon fibres, it was recognised that there might be significant benefits in raising spinning speeds and thus obtaining higher throughput at that stage, particularly if the need for a subsequent orientational drawing process could thus be eliminated. In 1950, du Pont filed two patents disclosing the invention by H. H. Hebler of high-speed spinning processes specifically for polyester yarns [57]. One of them claimed the use of a spinning speed, defined as the speed attained after the yarn had solidified, in the range of from 3000 to 5200 yd/min (2743 to 4755 m/min). The product was found to crimp spontaneously on thermal relaxation to give wool-like resilience, but it is doubtful whether such a process could be commercialised. The other patent claimed the use of a spinning speed of 5200 yd/min (4755 m/min) or above. The highest speed exemplified was 6350 yd/min (5806 m/min). These speeds were said to be obtainable by using a driven bobbin, a high-speed pirn take-up, or an air jet, which could be used as a forwarding and tensioning device for delivering the yarn directly to a staple cutter. This patent clearly envisaged that the products would not require any further orientation by drawing, and illustrated the production of yarns having tenacities in the range 3.2 to 4.6 g/denier and shrinkages in boiling water of 2 to 4 %. The elongations to break, however, were in the range 38 to 72 %, and so the higher-modulus fibres preferred for many outlets were evidently not available by this route. These two patents were rather ahead of their time. The engineering of high-speed wind-ups reliable enough to be used in regular production did not occur until the early 1970s, when machines operating at up to 4000 m/min became generally available through engineering firms such as Barmag and IWK, and wind-ups for still higher speeds followed a little later [58].

Spinning at wind-up speeds such as 3000 to 4000 m/min gave spun yarns that possessed higher orientation and crystallinity than those previously available, and which could also be further crystallised at temperatures lower by about 30 °C than the yarns of very low orientation (LOYs) and crystallinity obtained from the established low-speed spinning processes. They were sufficiently stable to be stored and transported without structural or dimensional changes taking place, and were therefore suitable feedstocks for simultaneous draw-texturing and draw-warping processes. This type of product, known as POY (Partially Oriented Yarn or Pre-Oriented Yarn), rapidly became a major product. At the same time, new devices for texturing POY were developed, of which the most important were friction-twisting devices based on aggregates of intermeshing discs. These displaced existing pin-twisting devices because they gave very much higher rates of false-twist insertion and hence a much increased productivity.

The further step up to 6000 m/min or more led to flat yarns that were sufficiently oriented and crystalline, of sufficiently low extension to break, and of sufficiently high tenacity to be used for many purposes without further drawing.

These FOY (Fully Oriented Yarn) products therefore eliminated the need for separate spinning and drawing stages, although not for all uses. In particular, the highest tenacity and modulus are best approached by a LOY plus high draw ratio route.

3.8 ULTRA-FINE FIBRES

The introduction of ultra-fine fibres was not solely a polyester phenomenon, although polyester was the fibre most involved. Okamoto of Toray, who was a leader in this development, defines an ultra-fine fibre as a fibre of less than 0.7 denier [59]. The word microfibre, which covers essentially the same products, is usually defined as a fibre of less than 1 decitex ($=0.9$ denier). These products were developed in Japan from the late 1960s, primarily to improve the hand of fabrics by reducing the bending and torsional stiffness of their constituent fibres. The earliest products to reach the market were non-woven suede-like fabrics such as Toray's *Ecsaine*. The technology was expensive, since for most products it involved extrusion of bicomponent fibres, either of the 'side-side' type, with subsequent splitting by flexing or other mechanical means, or even more effectively the 'islands-in-the sea' type, where the 'sea' polymer could be dissolved away leaving the 'islands' as extremely fine fibres. The bicomponent fibres could be subjected to normal textile processing before generating the microfibres. Moreover, the interest in improved hand and the recognition of its value in the market led to renewed attention to the direct spinning of fibres of low linear density, mostly of about 1 decitex, although products can be made in a range down to about 0.1 decitex. These products have done much to improve the image of polyester and synthetic fibres in general.

4 OTHER USES FOR SEMI-AROMATIC POLYESTERS

4.1 FILMS

The companies first involved in fibre manufacture recognised the potential value of poly(ethylene terephthalate) in films from a very early stage. *Mylar* (duPont), *Melinex* (ICI), and *Celanar* (Celanese) were among the products that entered the field first. The basic technology of film formation by melt extrusion processes is not confined to polyester film, although there are special processing features due mainly to the relatively high T_m and T_g values of poly(ethylene terephthalate) [60]. Early products were mainly rigid film that took advantage of the high modulus and high thermal deformation temperature. More recently, cast films and thermoformed packaging have become important, and co-extrusion lines have been introduced for the latter type of product.

4.2 MOULDING PRODUCTS

PET was evaluated in its early days as a moulding polymer, particularly for injection moulding. It was not very successful, because of its low crystallisation rate. Even when using a hot mould system, with mould temperatures that maximised the rate of crystallisation, the product morphology was difficult to control and the production rates were low. Attempts were made to increase the crystallisation rate, for example, by incorporating a crystallisation-promoting liquid such as benzophenone together with a small amount of a finely divided nucleating agent [61]. Early products were *Arnite*, from Akzo, and *Rynite*, from du Pont. Poly(1,4-butylene terephthalate) was marketed as a moulding polymer in 1970 by the Celanese Corporation (*Celanex*), followed by numerous other producers [62]. Its rapid crystallisation rate made it much more suitable for moulding than PET, and it proved very successful both unfilled and filled with glass fibre. In 1987, the polymer already used in manufacturing *Kodel* fibre, together with some of its copolymeric variants, was also introduced by Eastman Kodak under the name *Ektar*, later *Thermx PCT*, as a moulding product with higher thermal stability than other polyesters.

4.3 BOTTLES

In 1970, du Pont filed a patent application that proved to be the foundation stone of a major new use for PET. Two US patents resulted in 1973, with one covering 'a hollow, biaxially oriented, thermoplastic article, prepared from PET', and the other claiming a process and apparatus for preparing such an article [63]. The process was based on moulding a hollow cylindrical-shaped preform or parison (a term from the glass industry), which was then subjected to a stretch blow-moulding process involving application of internal air pressure. This led to expansion of the structure to the final dimensions, with development of biaxial orientation. Du Pont chose not to embark on bottle production itself, but instead to license the product to others. The rate of growth of polyester bottle production was very high, particularly in the more industrialised countries, and bottles rapidly became second in importance only to fibres as a market for polyester materials.

An early problem was that the blowing process as originally developed produced rounded bases, and so the bottles could not be stacked upright on shelves. Initially, bottles were equipped with separately moulded base cups, usually made from polyolefin and readily attached by a snap-on or glue-on process. The Continental Group then introduced in the USA a bottle with a shaped multilobal bottom that did not require a base cup, and further designs have followed [64].

Among the controlling factors in the production of bottles from PET are the molecular weight of the polymer and the draw ratio applied. The molecular weight required is in general higher than that of the polymer manufactured for

standard fibre products, and is higher the smaller the bottle size. The draw ratio must exceed the natural draw ratio, which is lower the lower the stretching temperature and the higher the molecular weight [65]. Particularly high draw ratios are needed for products that can maintain their dimensional stability where the pressure within the bottle is high.

Two processes have been developed – the single-stage process due to the Nissei Corporation in Japan, where both injection moulding and bottle blowing are conducted on the same machine, and the two-stage process, where preforms are made on an injection moulding unit and transferred to a stretch blowing unit, not necessarily on the same site, where they must be re-heated before stretching [66]. The need for higher molecular weights has led to increased use of solid-phase polymerisation techniques, which have the further advantage over melt-polymerised polymers that they give much lower acetaldehyde contents in the product [62].

5 LIQUID-CRYSTALLINE POLYESTERS

In 1956, Flory published two papers about the theoretical criteria for formation of a single anisotropic phase in solutions of rigid and semi-flexible polymers [67]. The theory can also be interpreted as applying to polymers where the solvent concentration is zero, in which case any anisotropic phase would become thermotropic. No thermotropic systems based on main-chain rigidity were identified until the mid-1970s, when Jackson and co-workers at Eastman Kodak [68], Schaeffgen and colleagues at duPont [69], and Roviello and Sirigu in Italy [70] identified thermotropic liquid-crystalline polyesters of different structural types. It then emerged that some of the polymers described earlier in patents from the Carborundum Company (Economy and colleagues) [71] were thermotropic liquid-crystalline polyesters, although this property was not identified at the time. Still earlier patents from ICI (Goodman and colleagues) [72] described, among other things, the synthesis of aromatic polyesters that were based upon asymmetrically substituted *p*-phenylene groups and included compositions that gave thermotropic anisotropic phase behaviour, but here too the nature of this phase was not identified.

Aromatic polyesters were particularly good candidates for this new field of thermotropic main-chain polymers, since the relatively low energy of association of the ester groups led to low inter-chain forces. Further research led to the discovery that incorporation of 2,6-naphthylene or of 4,4'-biphenyl groups, in addition to *p*-phenylene groups, as components of aromatic polyesters, introduced a useful new degree of randomness. Particularly useful, and the basis of the commercial products *Vectra* (polymer) and *Vectran* (fibre) from Hoechst-Celanese and Kuraray, are the copolymers formed by polymerisation of mixtures of *p*-acetoxybenzoic acid and 6-acetoxy-2-naphthoic acid. Within a range of

molar compositions from 75/25 to 40/60 they are readily melt-processable [73]. Polyesters of the Carborundum type became the basis of the commercial product *Xydar* (Dart Corporation, later Amoco).

6 POLYESTERS AS COMPONENTS OF ELASTOMERS

The use of polyesters in the development of elastomeric products began in Germany with the *Vulcollan* series of polymers from I. G. Farben (post-war by Farbenfabriken Bayer) [74]. The first products were typically based on hydroxyl-ended polyesters made from adipic acid and a small excess of ethylene glycol, which were then reacted with naphthalenic diisocyanates to lengthen the chains and to cap them with isocyanate groups. These isocyanate-ended polymers were chain-extended by a coupling reaction with water or other reagents, usually difunctional, such as diamines. Cross-linking by formation of biuret groups was then thermally induced to produce the final elastomeric polyester-urethane in the required shape and situation. Many other polyester-diols have since been found to be useful. Other companies that produced products of similar types included Goodyear (*Chemigum*) and ICI (*Vulcaprene*), some of which were made from aliphatic polyesteramides rather than from polymers based solely on ester linkages.

Flexible foams based on polyesterurethanes were introduced in the mid-1950s. There are now three main types, i.e. flexible, rigid and structural. The flexible type was based on aliphatic polyester-diols; rigidity can be increased by using aromatic polyester-diols, by increasing the degree of branching in the polyester, and by increasing the urethane content, and hence the degree of biuret cross-linking.

Elastomeric fibres based upon both polyester-urethane and polyether-urethane structures followed. The early work by Bayer led to the use of highly polar solvents such as dimethyl formamide. Formation of fibres by reactive spinning, where the isocyanate-ended polymer is extruded into an aqueous solution of a chain-coupling agent, was described in 1949 [75] and by dry-spinning a solution of the chain-coupled polymer in 1951 [76]. However, Bayer did not immediately use their technology to produce commercial fibres [77].

Following the introduction in the USA of *Vyrene* (US Rubber) in 1958 and of *Lycra* (du Pont; *Fiber K*, 1959, *Lycra*, 1962), many producers entered the field. In 1964, Bayer started production of *Dorlastan*, a dry-spun elastomeric fibre based on a polyester soft segment and a urethane/urea hard segment produced using diphenylmethane-4,4'-diisocyanate for chain extension and a dihydrazide as coupling agent [78]. Among the other companies involved, two, i.e. Asahi Kasei in Japan and Fillatice (*Lynel*) in Italy, used polycaprolactone as the polyester soft segment. Fujibo in Japan and Fillatice used wet-spinning techniques to make their polyester-based elastomeric fibres [79]. Polyether-based fibres, however, now dominate the market.

The elastomeric possibilities of copolyesters based upon PET (2GT) were studied at an early stage in the development of the fibre. Random copolymers with ester repeating units derived from aliphatic dicarboxylic acids containing a relatively large number of methylene groups, notably 2G9 from azelaic (nonanedioic) acid and 2G10 from sebacic (decanedioic) acid, were found to have values of T_g at or below typical room temperatures when the copolymer contained 40 to 70 mol % of units derived from the aliphatic acid. These polymers could be melt-spun and drawn to give elastic yarns, with extensions to break as high as 300 % and recoveries from 100 % extension as high as 96 %, but with low melting temperatures [80]. Melt-blending 2GT and 2G10 for a limited period of time, so that a block copolymeric structure was produced, gave better elastic properties and higher melting temperatures. In ICI, Coleman showed that block copolymers could be made by replacing part of the ethylene glycol by a substantial wt % of a polyether, polyethylene glycol (polyoxyethylene diol; PEG), with very little depression of the melting point of the polyester, since the depression is a function of the mol % of comonomer [81, 82]. However, Coleman did not extend the proportion of PEG beyond 30 wt %. Charch and Shivers, at du Pont, studied the complete spectrum of compositions, and established that elastic properties were obtained in the range 40 to 70 wt % of PEG, that the best results were obtained using PEG of molecular weight 4000, and that these products gave higher melting temperatures, higher elongations to break, and lower values of short-term stress decay than any of the previous elastomeric polyesters [83].

This work did not lead immediately to commercial elastomers, but its identification of the importance of block copolymeric structures in the field of melt-processable elastomers laid the foundation for later commercialisation of products based largely on the polyester and polyether units containing four-carbon instead of two-carbon sequences. These block copolymers of 4GT with polyoxytetramethylene diol possess superior properties in that the 4GT blocks crystallise much more readily than the 2GT blocks, the molar depression of melting point is lower for 4GT than for 2GT, and the dioxytetramethylene units present in both the polyether and the polyester possess conformational energy properties more suited than dioxyethylene units to loss-free recovery of the original dimensions after distortion. Products based on this technology were introduced as moulding grades from the early 1970s, and included *Hytrel* (du Pont), *Riteflex* (Celanese), and *Arnitel* (Akzo).

7 SURFACE-ACTIVE AGENTS

One of the problems encountered in early polyester fibre processing was that the sizes generally used with other classes of fibre to protect yarns, particularly warp yarns, against damage during weaving were not sufficiently adherent to the yarn. ICI found a surface treatment that would improve the adhesion of sizes to

polyester fibres which involved converting a polyether (polyethylene glycol) to its alkoxide anion and reacting this with the fibre surface. This process formed a di-block polyester/polyether, with the polyester block lying within the fibre and the polyether block lying on the surface, to which it provided hydrophilic properties. The process was not commercially viable, but it was then found that certain multi-block copolyetheresters formed dispersions in water that could be applied to polyester yarns or fabrics by 'pad-bake' techniques. Provided that the polyester blocks were long enough to crystallise, this treatment gave excellent hydrophilic surface properties [84]. These properties were durable towards washing, particularly if the polyester blocks consisted of the same repeating units as the fibre.

This product therefore solved more important problems than the original target, since it improved the washability and resistance to electrostatic charge development of polyester fabrics. It was marketed first by ICI in Europe as *Permalose* and in the USA as *Milease*; other companies produced similar products. Moreover, aqueous dispersions of this type of surface-active agent proved useful as rinse additives for washing hydrophobic fibres in general and became ingredients of consumer-oriented products.

8 ABSORBABLE FIBRES

Two of the deficiencies of the aliphatic polyester fibres made by Carothers were their poor hydrolytic stability and their low melting temperatures. One aliphatic polyester that had already been made many years earlier [85] by polymerisation of glycolide, the cyclic dimer of hydroxyacetic (glycolic) acid, melted at about 225°C, quite high enough for commercial use, but these fibres had even lower hydrolytic stability than the polyesters made by Carothers. In 1963, however, American Cyanamid filed a patent application in the USA that claimed absorbable articles, particularly medical sutures, made from polyhydroxyacetic ester (i.e. polyglycolide) [86]. The Davis and Geck division of American Cyanamid made a virtue of this deficiency by manufacturing polyglycolide fibres, which they named *Dexon*, for use as absorbable sutures. The sutures were strong and flexible enough to be used in place of the sutures then normally in use, most of which remained in the body long after there was any surgical need for them, so that often a further operation was required to remove them. Some, made from catgut or collagen, were slowly and rather uncontrollably absorbed through attack by cellular enzymes. These new absorbable polyester sutures, on the other hand, hydrolysed in the body over a period of days or weeks to form harmless products.

An interesting legal case ensued in the English High Court [87], where Ethicon (Johnson & Johnson) maintained, among other things, that the formation and hydrolytic behaviour of polyglycolide fibres were already known and that it was therefore obvious to use the material as an absorbable suture. The outcome was basically favourable to American Cyanamid.

Meanwhile Ethicon (and others) developed alternative absorbable surgical sutures, based, for example, on copolymers of polyglycolide with poly-L-lactide or poly(trimethylene carbonate), and on polydioxanone, and on poly(ϵ -oxycaproate), and also on copolymers of these with polyglycolide or with each other. These different structures made it possible to provide fibres with different rates of absorption, with different degrees of stiffness or flexibility, and for use in monofilaments, braided multifilaments, and other yarn structures, as required for different surgical operations.

9 POLYCARBONATES

Polycarbonates form a rather specialised class of linear polyesters, since they are formed from a diol, usually an aromatic diol, with a derivative of carbonic acid. The commercially useful products also differ from other types of polyester in that they are generally non-crystalline, melt-processable polymers of high T_g , possessing very high optical clarity and toughness.

One of the earliest reports of a reaction that can now be interpreted as forming a polycarbonate came from Birnbaum and Lurie in 1881 [88]. They reacted resorcinol, phosgene and pyridine, but assigned a cyclic carbonate structure to the product. In 1898, Einhorn [89] repeated this work and also used hydroquinone and catechol. He assigned a polymeric structure to the products from hydroquinone and resorcinol, and a cyclic structure to the product from catechol. Bischoff and van Hedenström [90] confirmed this work by using ester exchange with diphenyl carbonate (DPC) as the synthetic method. Thus, the two main synthetic methods were both used at an early stage. In 1930, Carothers published the results of his syntheses of polycarbonates, mainly from aliphatic diols but including *p*-xylylene glycol, and diethyl carbonate, both directly and through intermediate cyclic carbonates. Most of the polymers were crystalline but of too low a melting point to be useful in their own right, although a poly(*p*-xylylene carbonate) melting at about 180°C was isolated but not examined further [91].

Much the most important polycarbonate in commercial terms is made from 2,2-di(4-hydroxyphenyl)propane, commonly known as bisphenol A. This polymer was discovered and developed by Farbenfabriken Bayer [92]. The synthesis and properties of this and many other polycarbonates were described by Schnell in 1956 [93]. The polymer became available in Germany in 1959, and was given the trade name *Makrolon* by Bayer (in the USA, *Merlon* from Mobay). General Electric (GE) independently developed a melt polymerisation route based on transesterification of a bisphenol with DPC [94]. Their product, *Lexan*, entered the US market in 1960. The solution polymerisation route using phosgene has since been displaced by an interfacial polymerisation.

10 NATURAL POLYESTERS

10.1 OCCURRENCE

Polyesters are found in nature in a wide range of bacteria and also in higher plants. In the case of bacteria, two types of polymer have been identified [95]. One type consists of poly(3-hydroxybutyrate) (PHB), also known as poly(β -hydroxybutyrate), and its copolymers with related repeating units, particularly 3-hydroxyvalerate. These polymers are produced within the bacteria and stored in an inter-cellular granular form for consumption in times of hardship. The other type consists of poly(β -malate) (poly(L-3-carboxy-3-hydroxypropionate)), which has the same carbon skeleton as PHB but which does not appear to be used as a storage reserve. In the case of higher plants, again two types have been identified [96], with both having complex network structures. *Cutin* plays a structural and protective role at the surfaces of plants. It is based mainly upon C_{16} and C_{18} fatty acids that have various degrees of substitution by hydroxyl groups, and in some cases also contain 9,10-epoxy groups. *Suberin* occurs in outer cell walls as a barrier against environmental stress. This material is even more complex, since its aliphatic polyester domains are attached to aromatic domains derived from units such as 3,4-dihydroxycinnamic acid.

Polyesters are also produced naturally in some animals. In particular, shellac is a natural product that was for many years of major commercial importance as a moulding resin (e.g. for phonograph records) and a varnish. It is a constituent of lac, which is secreted by the lac insect of S. E. Asia and exuded by it onto trees. Shellac, which is obtained by purification from lac, is a complex polyester which can be hydrolysed to polyhydroxylic acids such as 9,10,16-trihydroxyhexadecanoic acid [97].

10.2 POLY(β -HYDROXYALKANOATE)S

In 1925, Lemoigne [98] described the isolation of an aliphatic polyester, poly(β -hydroxybutyrate) (PHB), from the cytoplasm of the bacterium *Alcaligenes eutrophus*. This polymer is synthesised by the bacterium for storage as a reserve against times of famine, and can be consumed enzymatically with release of energy whenever such times occur. The proportion of the mass of the bacteria attributable to this polyester can be very high, well over 90 %. Numerous bacterial species of different types, Gram-positive and Gram-negative, aerobic and photosynthetic, have since been shown to synthesise this polymer. The feedstock for the synthesis is normally of carbohydrate origin, for example, glucose, but the bacteria can be induced to transform other organic chemicals, such as

methanol, into the polymer. Lemoigne found that chloroform was the best solvent for extracting the polymer from the bacteria of those he tried. About 20 % (by weight) of the dried bacteria consisted of this material, which he found melted at 157 °C. He concluded that the extracted material was a product of dehydration and polymerisation of β -oxybutyric acid, with the empirical formula $(C_4H_6O_2)_n$. He referred to this as a polylactide, although by modern terminology this would not be correct.

During the period 1960–1962, W. R. Grace and Company filed several patents that claimed methods of extracting poly(β -hydroxybutyric acid) from bacteria and its use for making absorbable prosthetic devices, particularly sutures [99]. The polymer was said to be degraded by esterases in the body. This degradation was too slow to be competitive with existing degradable sutures, so no commercial product appeared.

In the 1970s, ICI introduced this polymer and copolymers in which it was the major constituent as commercial products, initially under the acronym PHB, and a little later under the trade name *Biopol*, which referred specifically to copolymers containing β -oxybutyrate and up to 30 % of β -oxyvalerate repeating units. The copolymer is more flexible and tougher than the homopolymer [100, 101].

11 CONCLUSION

The foregoing summary of the history of polyesters to date illustrates the diversity of chemical structures available and the wide range of uses to which they have been put, although it is far from being exhaustive. There can be no doubt that polyesters will continue to be one of the most important classes of polymer. Predictably, as the supply of cheap fossil-fuel-based chemical primaries declines, biological sources can be persuaded to yield appropriate intermediates and even polyesters themselves.

REFERENCES

Note that the dates given for patent references are the years of publication and/or of grant of the patents, and not the years of application.

1. Kienle, R. H. and Ferguson, C. S., *Ind. Eng. Chem.*, **21**, 349 (1929).
2. Bjorksten, J., Tovey, H., Harker, B. and Henning, J., *Polyesters and their Applications*, Reinhold, New York, and Chapman & Hall, London (1956).
3. Kienle, R. H. and Hovey, A. G., *J. Am. Chem. Soc.*, **51**, 509 (1929).
4. Berzelius, J., *Rapt. Ann. Inst. Geol. Hongrie*, **26** (1847).
5. Berthelot, M. M., *Comptes Rend.*, **37**, 398 (1853).
6. Van Bemmelen, J., *J. prakt. Chem.*, **69**, 84, 93 (1856).
7. Smith, W., *J. Soc. Chem. Ind.*, **20**, 1075 (1901).

8. General Electric Company (Callahan, M. J.), US Patent, 1 108 329 (1914).
9. General Electric Company (Callahan, M. J.), US Patent, 1 108 330 (1914).
10. General Electric Company (Friedburg, L. H.), US Patent, 1 119 592 (1914).
11. General Electric Company (Arsem, W. C.), US Patent, 1 098 777 (1914).
12. General Electric Company (Howell, K. B.), US Patent, 1 098 728 (1914).
13. General Electric Company (Dawson, E. S.), US Patent, 1 141 944 (1915).
14. Kienle, R. H., *Ind. Eng. Chem.*, **22**, 590 (1930).
15. Bradley, T. F., *Ind. Eng. Chem.*, **29**, 440, 579 (1937); **30**, 689 (1938); Bradley, T. F., Kropa, E. L. and Johnston, W. B., *Ind. Eng. Chem.*, **29**, 1270 (1937).
16. Vincent, H. L., *Ind. Eng. Chem.*, **29**, 1267 (1937).
17. Hermes, M. E., *Enough for One Lifetime: Wallace Carothers, Inventor of Nylon*, American Chemical Society, Washington, DC, 1996, p. 92.
18. Letter, W. H. Carothers (Harvard) to Hamilton Bradshaw (du Pont), 9 November 1927, quoted in Reference [17], p. 56.
19. Carothers, W. H. and Arvin, J. A., *J. Am. Chem. Soc.*, **51**, 2560 (1929).
20. Carothers, W. H. and Hill, J. W., *J. Am. Chem. Soc.*, **54**, 1557 (1932).
21. Carothers, W. H. and Hill, J. W., *J. Am. Chem. Soc.*, **54**, 1559 (1932).
22. Carothers, W. H. and Hill, J. W., *J. Am. Chem. Soc.*, **54**, 1579 (1932).
23. E. I. du Pont de Nemours and Company (Carothers, W. H.), US Patent 2 071 250 (1937); US Patent 2 071 251 (1937).
24. Craig, R. A., in *Polyester: 50 Years of Achievement*, Brunnschweiler, D. and Hearle, J. W. S. (Eds), The Textile Institute, Manchester, UK, 1993, pp. 30–33.
25. Calico Printers Association (Whinfield, J. R. and Dickson, J. T.), Br. Patent 578 079 (1946).
26. Whinfield, J. R., *Nature*, **158**, 930 (1946).
27. Whinfield, J. R., *Text. Res. J.*, **23**, 290 (1953).
28. Hardy, D. V. N., *J. Soc. Chem. Ind.*, **67**, 426 (1948).
29. Osborne, W. F., *A History of the Early Development of 'Terylene' Polyester Fibre by Imperial Chemical Industries Limited: November 1943–March 1951*. [Copy in the Library of the Society of Dyers and Colourists, Bradford, UK].
30. Brunnschweiler, D., in *Polyester: 50 Years of Achievement*, Brunnschweiler, D. and Hearle, J. W. S. (Eds), The Textile Institute, Manchester, UK, 1993, pp. 34–37.
31. E. I. du Pont de Nemours and Company (Whinfield, J. R. and Dickson, J. T.), US Patent 2 465 319 (1949).
32. Ludewig, H., *Polyester Fibres: Chemistry and Technology*, Wiley-Interscience, London, 1971, p. 4.
33. Bobingen, A.-G. für Textil-Faser (Schlack, P.), Ger. Patent 922 255 (1955).

34. Alexander, P. and Whewell, C. S., *Some Aspects of Textile Research in Germany*, BIOS Final Report No. 1472, HMSO, London, 1947, p. 33.
35. Schlack, P., *Textil-Praxis*, **8**, 1055 (1953).
36. Anon, *Chem. Eng. News*, **31**, 1754 (1953).
37. Izard, E. F., *Chem. Eng. News*, **32**, 3724 (1954).
38. Steele, R., in *Polyester: 50 Years of Achievement*, Brunnschweiler, D. and Hearle, J. W. S. (Eds), The Textile Institute, Manchester, UK, 1993, pp. 48–51.
39. Kodak (Kibler, C. J., Bell, A. and Smith, J. G.), Br. Patent 818 157 (1959).
40. Imhausen and Company (Katzschmann, E.), Ger. Patent 949 564 (1956).
41. Katzschmann, E., *Chem. Ingr. Technik*, **38**, 1 (1966).
42. Mid-Century Corporation (Saffer, A. and Barker, R. S.), Br. Patent 807 091 (1959); US Patent 2 833 816 (1958); US Patent 3 089 906 (1963).
43. Landau, R. and Saffer, A., *Chem. Eng. Prog.*, **64**, 20 (1968).
44. Standard Oil Company, Br. Patent 994 769 (1965).
45. E. I. du Pont de Nemours and Company (Vodonik, J. L.), US Patent 2 727 882 (1955); US Patent 2 758 915 (1956); US Patent 2 829 153 (1958).
46. Hummel, U. and Oxley, J. H., *ACS Div. Petrol. Chem. Prepr.*, **13**, 461 (1969).
47. Schaller, H., *Chemiefasern*, **12**, 923 (1965).
48. Dietze, M. and Kühne, H., *Chemiefasern*, **19**, 194 (1969).
49. Chen, F. C., Griskey, R. G. and Beyer, G. H., *Am. Inst. Chem. Eng. J.*, **15**, 680 (1969).
50. Chang, T. M., *Polym. Eng. Sci.*, **10**, 364 (1970).
51. Goodyear Tire and Rubber Company (Wilson, W. K.), Ger. OLS 2 041 018 (1971).
52. Mobil Oil Corporation (Maxion, E. J.), US Patent 3 728 309 (1973).
53. Imperial Chemical Industries (Nava, M. and Ruffini, W.), Br. Patent 881,729 (1961).
54. Imperial Chemical Industries (Nava, M.), Br. Patent 921 583 (1963).
55. Dwek, J., in *Polyester: 50 Years of Achievement*, Brunnschweiler, D. and Hearle, J. W. S. (Eds), The Textile Institute, Manchester, UK, 1993, pp. 304–307.
56. Hayman, N. W. and Smith, F. S., Major Advances in Polyester 2GT Technology, 1941–1990. In *Manmade Fibers: Their Origin and Development*, Seymour, R. B. and Porter, R. S. (Eds), Elsevier Applied Science, London, 1993, pp. 369–394.
57. E. I. du Pont de Nemours and Company (Hebeler, H. H.) US Patent 2 604 689 (1952); US Patent 2 604 667 (1952).

58. Schilo, D. and Roth, T., in *Polyester: 50 Years of Achievement*, Brunnschweiler, D. and Hearle, J. W. S. (Eds), The Textile Institute, Manchester, UK, 1993, pp. 70–73.
59. Okamoto, M., in *Polyester: 50 Years of Achievement*, Brunnschweiler, D. and Hearle, J. W. S. (Eds), The Textile Institute, Manchester, UK, 1993, pp. 108–111.
60. Heffelfinger, C. J., *Polym. Eng. Sci.*, **18**, 1163 (1978).
61. Algemene Kunstzijde Unie, Fr. Patent 1 501 269 (1952).
62. East, A. J., Golder, M. and Makhija, S., Polyesters, thermoplastic, in *Kirk-Othmer Encyclopedia of Chemical Technology*, 4th Edn, Vol. 19, Wiley-Interscience, New York, 1996, pp. 609–653.
63. E. I. du Pont de Nemours and Company (Wyeth, N. C. and Roseveare, R. N.), US Patent 3 733 309 (1973); US Patent 3 778 214 (1973).
64. Von Hassell, A., *Plast. Technol.*, **25** (January), 69–76 (1979).
65. Bonnebat, C., Rouillet, G. and de Vries, A. J., *Polym. Eng. Sci.*, **21**, 189 (1981).
66. Jones, K. M., in *Polyester: 50 Years of Achievement*, Brunnschweiler, D. and Hearle, J. W. S. (Eds), The Textile Institute, Manchester, UK, 1993, pp. 266–269.
67. Flory, P. J., *Proc. R. Soc. London, A*, **234**, 60, 73 (1956).
68. Eastman Kodak (Kuhfuss, H. F. and Jackson, W. J.), US Patent 3 778 441 (1973).
69. DuPont (Kleinschuster, J. J., Pletcher, T. C., Schaefgen, J. R. and Luise, R. R.), Ger. OLS 2 520 819 (1975).
70. Roviello, A. and Sirigu, A., *J. Polym. Sci., Polym. Lett. Ed.*, **13**, 455 (1975).
71. The Carborundum Company (Cottis, S. G., Economy, J. and Wohrer, L. C.), Br. Patent 1 303 484 (1973).
72. Imperial Chemical Industries (Goodman, I., McIntyre, J. E. and Aldred, D. H.), Br. Patent 993 272 (1965).
73. Celanese Corporation (Calundann, G. W.), Br. Patent 2 006 242 (1979); US Patent 4 161 470 (1979).
74. Bayer, O., Müller, E., Petersen, S., Piepenbrink, H.-F. and Windemuth, E., *Angew. Chemie*, **62**, 57 (1950).
75. Farbenfabriken Bayer (Windemuth, E.), Ger. Patent 826 641 (1952).
76. Farbenfabriken Bayer (Brenschede, W.), Ger. Patent 888 766 (1953).
77. Oertel, H., in *Synthesefasern*, von Falkai, B. (Ed.), Verlag Chemie, Weinheim, Germany, 1981.
78. Farbenfabriken Bayer (Oertel, H., Rinke, H. and Thoma, W.), Ger. Patent 1 123 467 (1962).
79. Ultee, A. J., History of Spandex Elastomeric Fibers. In *Manmade Fibers: Their Origin and Development*, Seymour, R. B. and Porter, R. S. (Eds), Elsevier Applied Science, Amsterdam, 1992, pp. 278–294.

80. E. I. du Pont de Nemours and Company (Snyder, M. D.), US Patent 2 623 031 (1952); US Patent 2 623 033 (1952).
81. Coleman, D., *J. Polym. Sci.*, **14**, 15 (1954).
82. Imperial Chemical Industries (Coleman, D.), Br. Patent 682 866 (1952).
83. Charch, W. H. and Shivers, J. C., *Text. Res. J.*, **29**, 536 (1959).
84. Imperial Chemical Industries (McIntyre, J. E. and Robertson, M. M.), US Patent 3 416 952 (1968); US Patent 3 557 039 (1970); US Patent 3 619 269 (1971).
85. Bischoff, C. A. and Walden, P., *Ann. Chem.*, **279**, 45 (1893); *Ber.*, **26**, 262 (1893).
86. American Cyanamid Company (Schmitt, E. E. and Polistina, R. A.) US Patent 3 297 033 (1967); Br. Patent 1 043 518 (1966).
87. *Fleet Street Patent Law Report*, August 1974, p. 312.
88. Birnbaum, K. and Lurie, G., *Ber.*, **14**, 1753 (1881).
89. Einhorn, A., *Ann. Chem.*, **300**, 135 (1898).
90. Bischoff, C. A. and van Hedenström, A., *Ber.*, **35**, 3431 (1902).
91. Carothers, W. H. and van Natta, F. J., *J. Am. Chem. Soc.*, **52**, 314 (1930).
92. Bayer A.-G. (Schnell, H., Bottenbruch, L. and Krimm, H.), Belg. Patent 532 543 (1954).
93. Schnell, H., *Angew. Chem.*, **68**, 633 (1956).
94. General Electric Company (Fox, D. W.), US Patent 3 153 008 (1964).
95. Kim, Y. B. and Lenz, R. W., Polyesters from Micro-organisms. In *Advances in Biochemical Engineering/Biotechnology*, Vol. 71, *Biopolyesters*, Babel, W. and Steinbüchel, A. (Eds), Springer-Verlag, Berlin, 2001, pp. 52–79.
96. Kolattukudy, P. E., Polyesters in Higher Plants. In *Advances in Biochemical Engineering/Biotechnology*, Vol. 71, *Biopolyesters*, Babel, W. and Steinbüchel, A. (Eds), Springer-Verlag, Berlin, 2001, pp. 1–51.
97. Barnes, C. E., *Ind. Eng. Chem.*, **30**, 449 (1938).
98. Lemoigne, M., *Ann. Inst. Pasteur (Paris)*, **39**, 144 (1925); **41**, 148 (1927).
99. W. R. Grace and Company (Baptist, J. N.), US Patent 3 036 959 (1962); US Patent 3 044 942 (1962).
100. Holmes, P. A., *Phys. Technol.*, **16**, 32 (1985).
101. Imperial Chemical Industries (Holmes, P. A., Wright, L. F. and Collins, S. H.), Eur. Patent Application 0 052 459 (1982).

PART II

Polymerization and Polycondensation

2

Poly(Ethylene Terephthalate) Polymerization – Mechanism, Catalysis, Kinetics, Mass Transfer and Reactor Design

TH. RIECKMANN

Institute of Chemical Engineering and Plant Design, University of Applied
Sciences Cologne, Cologne, Germany

and

S. VÖLKER

42 Engineering, Kaufungen, Germany

NOTATION

a	specific surface area	(m^2/m^3)
a^*	colour, CIELAB system, green–red	
AA	acetaldehyde	
b^*	colour, CIELAB system, blue–yellow	
bDEG	bound diethylene glycol	
bEG	bound ethylene glycol, diester group	
BHET	bis-hydroxyethyl terephthalate, PET ‘monomer’	

BOPET	biaxial oriented PET film	
bTPA	bound terephthalic acid	
c_{acid}	concentration of R-COOH groups	(mol/m ³)
c_i	concentration of component or functional group i	(mol/m ³)
Ca	capillary number	
CHDM	cyclohexane dimethanol, co-monomer	
Co(Ac) ₃	cobalt acetate, colour improvement	
COOH	carboxyl end groups	
CSTR	continuous stirred tank reactor	
d	disc diameter	(m)
D	polydispersity index	(g/mol/g/mol)
$D_{i,\text{PET}}$	mutual diffusion coefficient	(m ² /min)
$D_{0,i}$	constant in $D_i = D_{0,i} \exp(-E_{a,D}/(RT)) M_n^{0.5}/\eta^{0.5}$	(m ² /min (mol/g) ^{0.5} (Pa s) ^{0.5})
DEG	diethylene glycol, co-monomer	
DMT	dimethyl terephthalate, monomer	
E_a	activation energy	(kJ/mol)
$E_{a,D}$	activation energy of diffusion	(kJ/mol)
EG	ethylene glycol, 1,2-ethanediol, monomer	
Fr	Froude number	
GeO ₂	germanium dioxide, catalyst	
GPC	gel permeation chromatography	
h	polymer film thickness, filling level	(mm, m)
HET	hydroxyethyl terephthalate	
H ₃ PO ₄	phosphoric acid, stabilizer	
IPA	isophthalic acid, co-monomer	
IV	intrinsic viscosity	(dL/g)
J	molar flux across the interface, film theory	(mol/(m ³ s))
k_c	crystallization rate constant	(s ⁻¹)
k_i	reaction rate constant	(1/min; m ³ /mol/min; m ⁶ /mol ² /min, etc.)

$k_{i,j}$	mass transfer coefficient	(m/min)
$k_{i,0}$	coefficient of Arrhenius equation	(1/min; m ³ /mol/min; m ⁶ /mol ² /min, etc.)
$k_{G,i}$	mass transfer coefficient, gas phase	(m/min)
$k_{L,i}$	mass transfer coefficient, liquid phase	(m/min)
K_i	equilibrium constant	
L	distance between discs	(m)
L^*	colour, CIELAB system, black–white	
m_i	ratio of molar volumes of polymer and species i	
M_i	molecular weight of the component i	(g/mol)
\overline{M}_n	number-average molecular weight	(g/mol)
\overline{M}_w	weight-average molecular weight	(g/mol)
n	reaction order	
N	number of disc rings	
N_x	number of moles of x -mer	(mol)
N_0	total number of moles of repeat units	(mol)
NDC	2,6-naphthalene dicarboxylic acid	
p	probability of reaction	
P_i^0	partial pressure of component i	(torr, Pa)
P_n	degree of polycondensation	
\overline{P}_n	average degree of polycondensation	
$\overline{P}_{n,0}$	average initial degree of polycondensation	
PBT	poly(butylene terephthalate)	
PEI	poly(ethylene isophthalate)	
PEN	poly(ethylene naphthalate)	
PET	poly(ethylene terephthalate)	
PTA	purified terephthalic acid	
r	radial position	(m)
R	gas constant, 8.314	(J/mol/K)
R	disc radius	(m)

Re	Reynolds number	
RI	refractive index	
Sb(Ac) ₃	antimony(III) acetate, polycondensation catalyst	
Sb ₂ O ₃	diantimony trioxide, polycondensation catalyst	
SiO ₂	silicon dioxide	
SSP	solid-state polycondensation	
STA	simultaneous thermogravimetry (TGA) and differential thermal analysis (DTA)	
<i>t</i>	time	(s, min, h, d, a)
<i>T</i>	temperature	(°C, K)
<i>T</i>	dimensionless film thickness	
TBT	tetrabutoxytitanium, polycondensation catalyst	
tDEG	terminal diethylene glycol	
tEG	terminal ethylene glycol	
TEP	triethyl phosphate, stabilizer	
TiO ₂	titanium dioxide	
TMP	trimethyl phosphate, stabilizer	
TOC	total oxygen consumption	
TPA	terephthalic acid, monomer	
tTPA	terminal terephthalic acid	
tV	terminal vinyl group	
<i>w_x</i>	weight fraction of <i>x</i> -mer	(kg/kg)
W	water	
<i>x</i>	length	(m)
<i>x</i>	number of repeat units	
<i>x_i</i> [*]	mole fraction	(mol/mol)
<i>z</i>	spatial dimension	
<i>γ_i</i>	activity coefficient of component <i>i</i>	
η	melt viscosity	(Pa s)
θ	angle with respect to horizontal	
ρ	density	(kg/m ³)
σ	surface tension	(N/m)
Φ	dimensionless radius	
Φ _{<i>i</i>}	volume fraction	
χ	dimensionless number	
χ _c	mass fraction crystallinity	(kg/kg)

χ_i	polymer–solvent interaction parameter	(for EG/PET, 1.3)
χ_{\max}	maximum crystallinity (mass fraction)	(kg/kg)
ω	disc rotating speed	(1/s)
Ω	velocity	(rad/s)

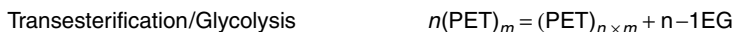
1 INTRODUCTION

Poly(ethylene terephthalate) (PET) is a polymer formed by step-growth polycondensation from ethylene glycol (EG) and terephthalic acid (TPA). The synthesis of PET requires two reaction steps. The first of these is esterification of TPA with EG, forming a so-called *prepolymer* which contains the monomer bis-hydroxyethyl terephthalate (BHET) and short-chain oligomers. The esterification by-product, i.e. water, is removed via a column system. The second reaction step is polycondensation, in which a transesterification reaction takes place in the melt phase. The by-product, EG, is removed from the melt by using high vacuum. High-viscosity PET grades for bottles or technical yarns are typically produced by further polycondensation in an additional solid-state process (SSP) under vacuum or in an inert gas atmosphere, respectively [1].

The formation of prepolymer can also be achieved by transesterification of dimethyl terephthalate (DMT) with EG, releasing the by-product methanol. High-purity DMT is easily obtained by distillation and in the early years of PET production, all processes were based on this feedstock. During the late 1960s, highly purified TPA was produced for the first time on an industrial scale by re-crystallization. Since then, more and more processes have shifted to TPA as the feedstock and today more than 70 % of global PET production is based on TPA. The TPA-based PET production saves approximately 8 % of total capital investment and 15 % of feedstock cost (Figure 2.1).

Two PET grades now dominate the global market, i.e. fibre-grade PET and bottle-grade PET. These standard grades differ mainly in molecular weight or intrinsic viscosity (IV), respectively, optical appearance and the production recipes. The latter differ in the amount and type of co-monomers, stabilizers and metal catalysts, as well as colorants.

Textile fibre-grade PET contains 0.03 to 0.4 wt% of titanium dioxide (TiO_2) as a delustering agent. This grade has a molecular weight (number-average molecular weight, \overline{M}_n) of 15 000 to 20 000 g/mol, which refers to an IV of between 0.55 and 0.67 dL/g. The standard textile fibre-grade has an IV of 0.64 dL/g. PET fibre-grades for technical yarns such as tyre cord are high-modulus low-shrinkage types with very high molecular weights, respectively, with an IV above 0.95 dL/g.

Direct Esterification**Transesterification****Melt-Phase Polycondensation****Solid-State Polycondensation****Figure 2.1** Stoichiometric equations for the synthesis of PET

Bottle-grade PET appears 'glass-clear' in the amorphous state. Special requirements for bottle-grade PET are a brilliant white colour and a composition fulfilling the regulations for food packaging. The average molecular weight ranges from 24 000 to 36 000 g/mol, which refers to an IV of between 0.75 and 1.00 dL/g. The standard bottle grade has an IV of 0.80 dL/g.

Other PET grades are manufactured for packaging films, as well as for the production of video and audio tapes. These PET types are often standard grades with an IV of 0.64 dL/g. To reduce the sticking tendency of the final product, solid additives such as SiO_2 or china clay with specific particle sizes and particle-size distributions are incorporated by master-batch processes. The final product, the so-called BOPET, is a biaxial oriented PET film with high mechanical strength and a thickness between 1 and 180 μm .

The total PET world production capacity amounted to 30 megatonnes per year (Mt/y) in the year 2000. This total production includes 8.5 Mt/y of packaging resins, comprising 93 % of bottle-grade PET and 7 % of film-grade PET. The staple fibre and textile filament capacities have been 9.1 Mt/y and 11.1 Mt/y, respectively, while the industrial yarn capacity has been 1.2 Mt/y. Typical plant capacities are 240–600 t/d for bottle resin production, 100–200 t/d for staple fibres and 100–300 t/d for filament-spinning textile grades. Batch plants for the production of industrial yarns have typical capacities of 20–40 t/d [2].

Although PET has been manufactured for a long time and in large amounts, knowledge about the underlying chemistry and mass transport mechanisms is still incomplete. These aspects will be discussed in detail in the next two sections. The sections following these will deal with the state-of-the-art of PET plants and reactor design. The chapter will conclude with a section discussing future developments and scientific requirements.


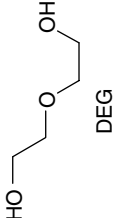
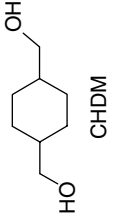
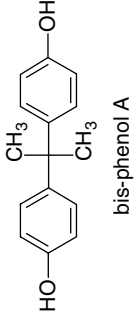
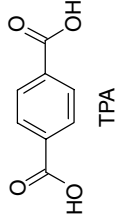
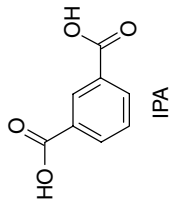
2 CHEMISTRY, REACTION MECHANISMS, KINETICS AND CATALYSIS

The monomers of PET are TPA and EG. The polymer properties may be modified by other dicarboxylic acids and diols which may be incorporated into the polymer as co-monomers. The most important compounds for PET synthesis are presented in Table 2.1.

The formation of PET chains comprises two main reactions, namely (1) esterification of carboxyl end groups with hydroxyl end groups, and (2) transesterification (transalcoholysis) of glycolesters with terminal hydroxyl groups, which is termed polycondensation. The reverse reactions are hydrolysis and glycolysis, respectively. In addition, ester interchange between two ester groups occurs, as well as the reaction of carboxyl end groups with bound ester groups, known as acidolysis. Depending on the concentration of the different reactive species, the medium chain length of the polymer is either increased (synthesis) or decreased (recycling). Additionally, temperature-dependent side reactions occur which influence the product quality significantly. The main quality problems arise from thermal scission of the PET chains with formation of carboxyl end groups and acetaldehyde, as well as from reactions leading to discoloration of the polymer.

Because of the high number of molecules with different chain lengths and compositions present in the polymer, reactions are commonly described as reactions between functional groups. Equal reactivity is assumed for functional groups with the same chemical vicinity, meaning that their reactivity is independent of the chain length of the parent molecule. This concept was initially introduced by Flory [3, 4] and applies without any serious errors if the functional groups are separated by more than three atoms in the chain. If the functional groups in the monomer are separated by only one or two atoms, the reactivities of the monomer and dimer may differ greatly. The difference in reactivity will diminish rapidly, however, as we compare dimer to trimer, trimer to tetramer, and so on. One can assume that the decreasing mobility of the molecules with increasing size of the molecule or with increasing viscosity of the reaction medium in the course of polycondensation causes a decreasing reactivity. However, the reactivity does not depend on the mobility of the molecules as a whole but on the mobility of the functional groups. The number of collisions between reactive centres will not depend largely on the molecule size, since functional groups in large molecules can move over a considerable distance merely by rearrangements of the chain configuration without dislocation of the centre of gravity of the entire molecule. The lower mobility of functional groups in a highly viscous medium is compensated by an increased number of collisions pertaining to each encounter of reactive centres. Schulz [5] studied the relationship between reaction rates and diffusion coefficients of the reactants. He demonstrated that diffusion becomes rate-determining only for very reactive species with reactions

Table 2.1 PET monomers and co-monomers

Diols	 EG	 DEG	 CHDM	 bis-phenol A
Dicarboxylic acids	 TPA	 IPA		

occurring during nearly every encounter of reactive centres. Polycondensation reactions have a moderate reaction rate and the functional groups will diffuse over a longer range and collide with many other groups before they finally react. In this case, the observed reaction rate is independent of the size of the molecules and the viscosity of the medium.

Equations of an Arrhenius type are commonly used for the temperature-dependent rate constants: $k_i = k_{i,0} \exp(-E_{a,i}/RT)$. The kinetics of all participating reactions are still under investigation and are not unambiguously determined [6–8]. The published data depend on the specific experimental conditions and the resulting kinetic parameters vary considerably with the assumed kinetic model and the applied data-fitting procedure. Fradet and Maréchal [9] pointed out that some data in the literature are erroneous due to the incorrect evaluation of experiments with changing volume.

All reactions involved in polymer chain growth are equilibrium reactions and consequently, their reverse reactions lead to chain degradation. The equilibrium constants are rather small and thus, the low-molecular-weight by-products have to be removed efficiently to shift the reaction to the product side. In industrial reactors, the overall esterification, as well as the polycondensation rate, is controlled by mass transport. Limitations of the latter arise mainly from the low solubility of TPA in EG, the diffusion of EG and water in the molten polymer and the mass transfer at the phase boundary between molten polymer and the gas phase. The importance of diffusion for the overall reaction rate has been demonstrated in experiments with thin polymer films [10].

The reversibility of the reactions, on the other hand, allows an efficient redistribution of chain lengths. Based on the principle of equal reactivity, Flory derived a function describing the normal molecular weight distribution for linear polymers formed by random synthesis [3] and for polymeric systems in a dynamic equilibrium, taking into account reversible redistribution reactions [11]. Schulz [12] derived the same relationships for the normal number and weight distributions of polymers from reversible polycondensation in chemical equilibrium under the assumption that the equilibrium constant K_i is independent of the sizes of the equilibrating molecules. Flory finally generalized the normal distribution function by application of statistic-thermodynamical results from the ‘liquid lattice theory’ of Flory and Huggins [13–17].

The normal distribution function, also referred to as the *Flory–Schulz* distribution, relates the fraction of an x -mer (a polymer molecule consisting of x repeat units) in the entire assembly of molecules to its formation probability. It can be defined either as a number distribution function or as a weight distribution function. The number of moles of an x -mer (N_x) is given by the normal number distribution as follows:

$$N_x = N_0(1 - p)^2 p^{x-1} \quad (2.1)$$

with N_0 being the total number of moles of repeat units and p being the probability of reaction (of the formation of any ester bond). If for high average molecular

weights the small contribution of the end groups to the molecular weight is neglected, then the normal weight distribution can be deduced as follows:

$$w_x = x(1 - p)^2 p^{x-1} \quad (2.2)$$

with w_x being the weight fraction of an x -mer.

A given polymer is characterized by its number-average molecular weight (\overline{M}_n), together with its weight-average molecular weight (\overline{M}_w), which can both be obtained by analytical techniques.

$$\overline{M}_n = \frac{\sum N_i M_i}{\sum N_i}; \quad \overline{M}_w = \frac{\sum N_i M_i^2}{\sum N_i M_i} \quad (2.3)$$

where \overline{M}_n depends only on the average degree of polycondensation (\overline{P}_n) and is given for pure PET chains by:

$$\overline{M}_n = 192\overline{P}_n + 62 \text{ (g/mol)}$$

while \overline{M}_w depends on \overline{P}_n and additionally on the actual distribution of x -mers. Therefore, the distribution of x -mers (or chain length distribution) can be characterized by the so-called polydispersity index (D) defined as $\overline{M}_w/\overline{M}_n$. A polymer consisting of only one type of x -mer will have a polydispersity index of 1 whereas a fully equilibrated polymer showing the Flory-Schulz distribution will have a polydispersity index of 2. Values of $D > 2$ will be found for polymers with over-proportional fractions of long-chain molecules.

In industrial reactors, the full equilibration of the chain length distribution is prevented by incomplete mixing, as well as by the residence time distribution, thus resulting in considerable deviations from the equilibrium polydispersity index. These deviations are generally higher for continuous plants than for batch plants and increase with increasing plant capacity as demonstrated in Figure 2.2.

The use of catalysts is essential in PET synthesis to achieve sufficiently high reaction rates although some catalysts will also accelerate side reactions. Esterification, as well as transesterification, are catalyzed by protons or carboxyl groups, respectively. During esterification, the concentration of carboxyl groups is high enough and no additional catalyst is needed. Nevertheless, in some industrial processes, metal catalysts and stabilizers have already been added at this stage of the reaction. During polycondensation, the concentration of carboxyl groups is too low for effectively catalyzing the reaction and the addition of suitable catalysts is indispensable. Antimony compounds are the most common by used polycondensation catalysts although almost every metal in the Periodic Table has been patented as a catalyst for these reactions. Japan is alone in requiring the use of germanium catalysts. However, antimony is not known to be required in

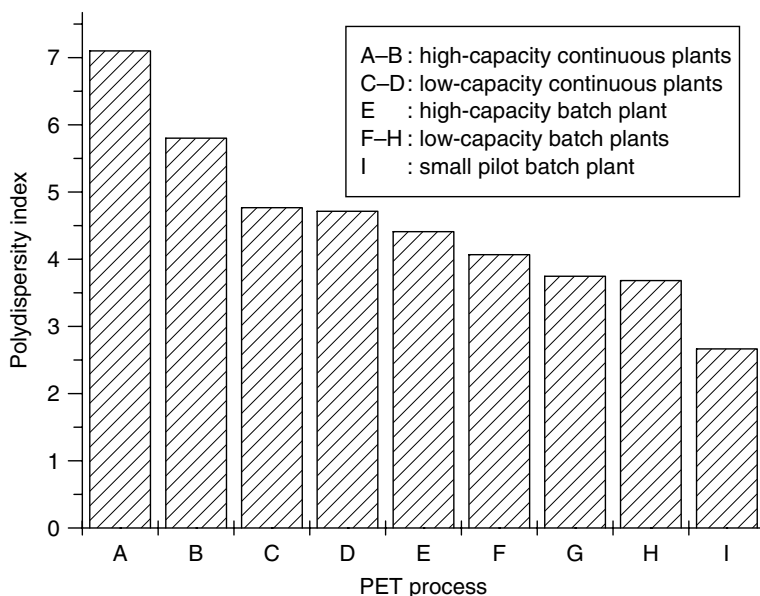


Figure 2.2 Polydispersity index for different PET processes and reactor sizes. GPC conditions: TCM/HFIP (98:2); columns PSS SDV10 (10^5 Å) and SDV5 (500 Å); detection, UV (269 nm) and RI; polystyrene calibration [94]

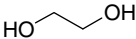
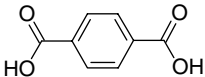
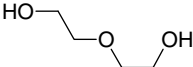
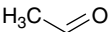
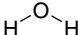
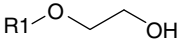
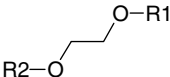
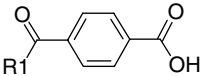
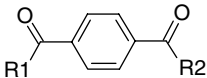
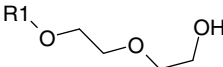
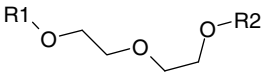
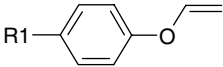
nutrition and can also be poisonous. Antimony catalysts may be substituted by titanium in the near future.

In the next sections, we will discuss the chemical and kinetic details of the main reactions and the product-quality relevant side reactions. This information is the basis for a proper understanding of reactor and process design in PET production. The compounds and functional groups which have to be considered are given in Table 2.2.

2.1 ESTERIFICATION/HYDROLYSIS

Esterification is the first step in PET synthesis but also occurs during melt-phase polycondensation, SSP, and extrusion processes due to the significant formation of carboxyl end groups by polymer degradation. As an equilibrium reaction, esterification is always accompanied by the reverse reaction being hydrolysis. In industrial esterification reactors, esterification and transesterification proceed simultaneously, and thus a complex reaction scheme with parallel and serial equilibrium reactions has to be considered. In addition, the esterification process involves three phases, i.e. solid TPA, a homogeneous liquid phase and the gas phase. The respective phase equilibria will be discussed below in Section 3.1.

Table 2.2 Compounds and functional groups involved in PET synthesis

Symbol ^a	Molecule/functional group	Molecular structure
EG	ethylene glycol	
TPA	terephthalic acid	
DEG	diethylene glycol	
AA	Acetaldehyde	
W	Water	
tEG	EG end group	
bEG	EG repeat unit	
tTPA	TPA end group	
bTPA	TPA repeat unit	
tDEG	DEG end group	
bDEG	DEG repeat unit	
tV	vinyl end group	

^a t, terminal segments; b, bound/repeat segments.

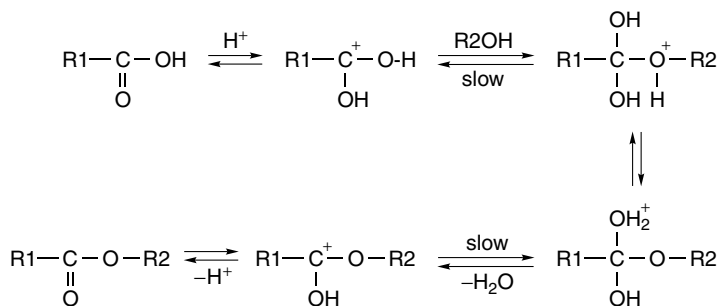


Figure 2.3 A_{AC2} mechanism for esterification/hydrolysis and transesterification/ glycolysis

Esterification, hydrolysis, transesterification and glycolysis have equilibrium constants close to unity and proceed via an A_{AC2} mechanism (Figure 2.3) [9, 18].

The esterification of TPA with EG is a reaction between two bifunctional molecules which leads to a number of reactions occurring simultaneously. To simplify the evaluation of experimental data, model compounds have been used for kinetic and thermodynamic investigations [18–21]. Reimschuessel and co-workers studied esterification by using EG with benzoic acid and TPA with 2-(2-methoxyethoxy) ethanol as model systems [19–21]. The data for the temperature dependency of the equilibrium constants, $K_i = K_i(T)$, given in the original publications are affected by printing errors. The corrected equations are summarized in Table 2.3.

In Figure 2.4, data for the equilibrium constants of esterification/hydrolysis and transesterification/glycolysis from different publications [21–24] are compared. In addition, the equilibrium constant data for the reaction $\text{TPA} + 2\text{EG} \rightleftharpoons \text{BHET} + 2\text{W}$, as calculated by a Gibbs reactor model included in the commercial process simulator *Chemcad*, are also shown. The equilibrium constants for the respective reactions show the same tendency, although the correspondence is not as good as required for a reliable rigorous modelling of the esterification process. The thermodynamic data, as well as the dependency of the equilibrium constants on temperature, indicate that the esterification reactions of the model compounds are moderately endothermic. The transesterification process is a moderately exothermic reaction.

Esterification reactions are acid catalyzed [18–21], and an overall reaction order of 3 (2 with respect to acid and 1 with respect to alcohol) is generally accepted [9]. Thus, the acid behaves both as reactant and as catalyst. It can be assumed that the concentration of acid groups, c_{acid} , is the sum of the concentrations of carboxylic end groups (tTPA) and carboxylic groups of the free acid (TPA).

The use of metal catalysts in esterifications and polyesterifications has been summarized by Fradet and Maréchal [9]. Tetrabutoxytitanium is a very efficient

Table 2.3 Corrected equations for the calculation of temperature-dependent equilibrium constants based on publications of Reimschuessel and co-workers [21]

Reaction	$K_i = \exp\left(\frac{\Delta S_i}{R} - \frac{\Delta H_i}{RT}\right)$	ΔS_i	ΔH_i
$W + tEG \rightleftharpoons tTPA + EG$	$K_H^t = K_C K_H^i$		
	$K_H^t = \frac{2[tTPA][EG]}{[tEG][W]}$		
$tTPA + tEG \rightleftharpoons bEG + W$	K_H^i	$-45.1 \text{ J mol}^{-1} \text{ K}^{-1}$	$-23.7 \text{ kJ mol}^{-1}$
	$K_H^i = \frac{[tTPA][tEG]}{2[bEG][W]}$		
$2tEG \rightleftharpoons bEG + EG$	K_C	$-80.3 \text{ J mol}^{-1} \text{ K}^{-1}$	$-38.1 \text{ kJ mol}^{-1}$
	$K_C = \frac{4[bEG][EG]}{[tEG]^2}$		

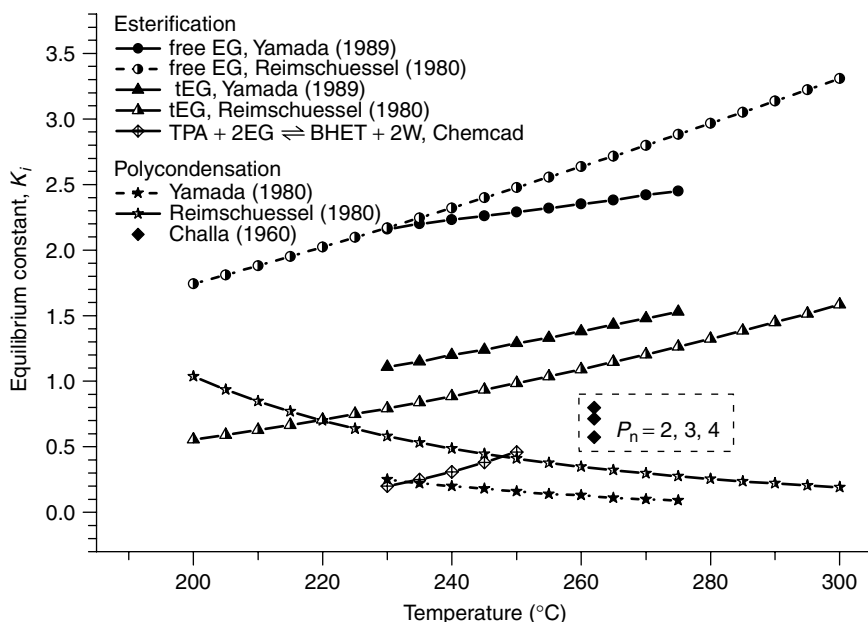


Figure 2.4 Equilibrium constants of esterification and polycondensation as a function of temperature. The data have been published by Yamada and co-workers [23, 24], Reimschuessel [21] and Challa [22], or have been calculated by using the commercial process simulator *Chemcad* (Chemstations)

catalyst, whereas zinc acetate or diantimony trioxide are not. For the esterifications of aromatic carboxylic acids with glycols it has been concluded [25] that the formation of complexes of the metal compound with the acid or of the acid with the metal glycolate having high ligand exchange rates is a prerequisite for a high catalytic activity.

Kinetic measurements have been performed by different working groups for the esterification of TPA with EG and for model systems. The results taken from some important publications are summarized in Table 2.4.

Krumpolc and Málek [26] performed detailed kinetic experiments at 190 °C on the reaction rates of esterifications involving different combinations of TPA, EG and short chain molecules, which are all present in industrial esterification reactors. As shown in Figure 2.5, they found significant variations in the reaction rates for different reactant combinations and concluded that the equal-reactivity hypothesis does not hold for the esterification stage.

Otton and Ratton performed experiments on the esterification of different carboxylic acids [18]. They emphasized the influence of the nature of the carboxylic acid on the reaction rate, which supports the assumption that the equal-reactivity hypothesis does not hold for the esterification of TPA, IPA and oligomers. The

Table 2.4 Kinetic data obtained for esterification/hydrolysis reactions

Reaction ^a				
Year	Author(s)	Reference	tTPA + EG \rightleftharpoons tEG + W	tTPA + tEG \rightleftharpoons bEG + W
1978	Yokoyama <i>et al.</i>	91	—	$n = 2$, no H^+ ; Sb $T = 275\text{--}285$ $E_a = 73.6$
1979	Reimschuessel	20	$n = 3$; H^+ yes $K = 1.262$ $T = 230$	$n = 3$; H^+ yes $K = 0.530$ $T = 230$
1980	Reimschuessel	21	$n = 3$; H^+ yes $K = K(T)$ $T = 202; 215; 226$ $k_{0,\text{no cat}} = 2.55 \times 10^{-5}$ $k_{0,\text{cat}} = 8.672 \times 10^5$ $E_{a,\text{cat}} = 86$	$n = 3$; H^+ yes $K = K(T)$ $T = 202; 215; 226$ $k_{0,\text{no cat}} = 8.426 \times 10^8$ $E_{a,\text{no cat}} = 124$ $k_{0,\text{cat}} = 75.64$ $E_{a,\text{cat}} = 43$
1988	Otton <i>et al.</i>	18	—	$n = 3$; H^+ yes $T = 185\text{--}275$ $E_a = 73.2\text{--}77.4$
1989	Otton <i>et al.</i>	37	—	H^+ no for Li; Na; K; Zn; Mn; Co, $n = 2$ H^+ yes for Ti, $n = 3$ $T = 200\text{--}226$ $E_a = 84\text{--}100$
1989	Yamada	23	$n = 2$; no H^+ , Sb $T = 240\text{--}265$ $k_{\text{ester}} = 1.80 \times 10^9$ $k_{\text{hydrolysis}} = 1.85 \times 10^8$ $E_{a,\text{ester}} = 82.1$ $E_{a,\text{hydrolysis}} = 75.8$	$n = 2$; no H^+ , Sb $T = 240\text{--}265$ $k_{\text{ester}} = 4.57 \times 10^9$ $k_{\text{hydrolysis}} = 7.98 \times 10^7$ $E_{a,\text{ester}} = 93.3$ $E_{a,\text{hydrolysis}} = 76.8$

^a Reaction order (n) is shown for H^+ or various metal catalysis systems; K , equilibrium constant; T , temperature or temperature range ($^{\circ}\text{C}$); k_0 , rate constant, with no catalysis ($\text{m}^3 \text{mol}^{-1} \text{min}^{-1}$); k_0 , rate constant, with catalysis ($\text{m}^6 \text{mol}^{-2} \text{min}^{-1}$); E_a , activation energy (kJ mol^{-1}).

reactivity of a carboxylic acid is affected by steric and electronic conditions and by the possibility of an intramolecular assistance in the course of the reaction. The rate constant of esterification can be correlated to the pK_a of the carboxylic acid, as demonstrated in Figure 2.6.

A survey of the literature shows that the most reliable kinetic data on esterification and hydrolysis have been gained by experiments with model systems. For

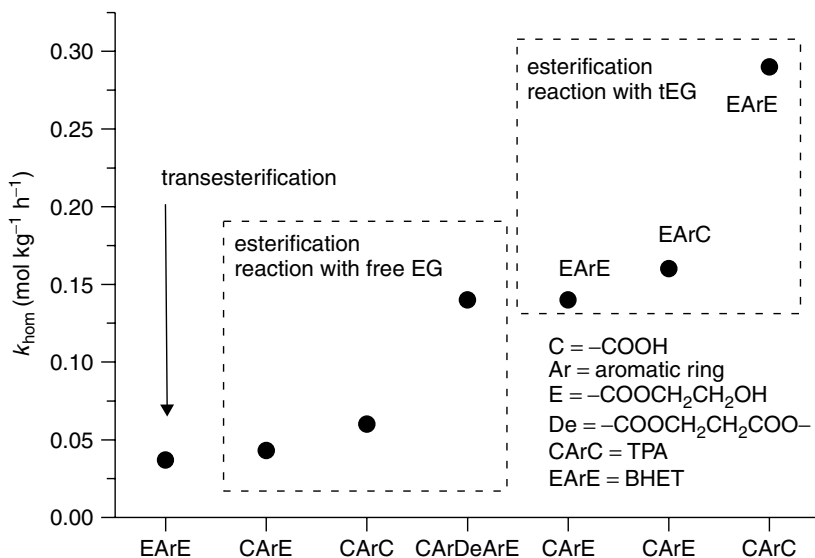


Figure 2.5 Esterification rate constants in the homogeneous phase for different combinations of reacting molecules at 190°C , as published by Krumpolc and Málek [26]

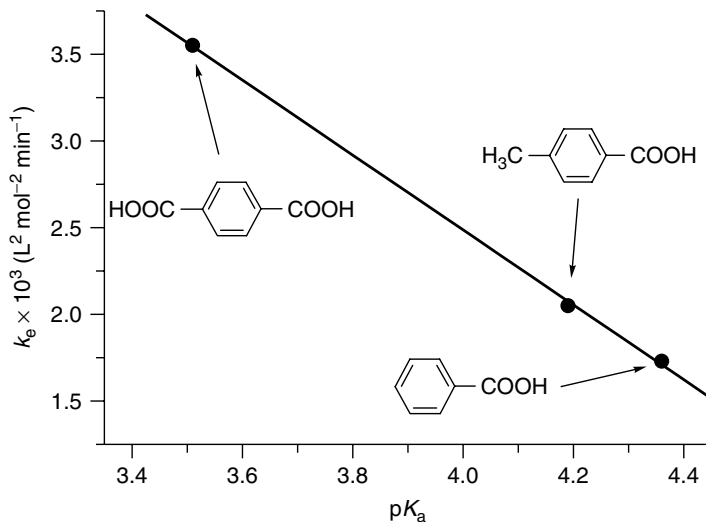


Figure 2.6 Esterification rate constants as a function of pK_a for different carboxylic acids, according to Otton and Ratton [18]

process modelling, kinetic parameters and equilibrium constants are often extrapolated beyond the range of the original experimental conditions. The published values for the equilibrium constants and activation energies show less variation, although the values for the corresponding pre-exponential factors differ by orders of magnitude.

2.2 TRANSESTERIFICATION/GLYCOLYSIS

Transesterification is the main reaction of PET polycondensation in both the melt phase and the solid state. It is the dominant reaction in the second and subsequent stages of PET production, but also occurs to a significant extent during esterification. As mentioned above, polycondensation is an equilibrium reaction and the reverse reaction is glycolysis. The temperature-dependent equilibrium constant of transesterification has already been discussed in Section 2.1. The polycondensation process in the melt phase involves a gas phase and a homogeneous liquid phase, while the SSP process involves a gas phase and two solid phases. The respective phase equilibria, which have to be considered for process modelling, will be discussed below in Section 3.1.

The transesterification and glycolysis reactions proceed via the $A_{AC}2$ mechanism described above in Section 2.1. The reactions are acid catalyzed as demonstrated by Chegolya *et al.* [27], who added TPA to the polycondensation of PET and observed a significant increase of the apparent reaction rate. The industrial polycondensation process is accelerated by the use of metal catalysts, with these being mainly antimony compounds.

Many working groups have published results on catalyst activities and catalysis mechanisms [28–34]. It is generally accepted that compounds of antimony, tin and titanium are the most active catalysts for polycondensation. Catalysts such as manganese or zinc compounds used for transesterification in the DMT process are less active in a PET environment. Hovenkamp [35] found that the latter catalysts are very active in media having both high and low hydroxyl group contents, but are easily poisoned by traces of carboxylic groups. Diantimony trioxide is insensitive to the presence of acidic groups, but its activity is inversely proportional to the hydroxyl group concentration. Otton and co-workers [18, 36–38] performed extensive studies on the catalyzed formation of PET with model systems. They concluded that alkali metals activate the nucleophile by forming the metal alcoholates, whereas Lewis acids like zinc or manganese activate the carbonyl oxygen of the ester group. Antimony or titanium compounds catalyze the polycondensation by ligand-exchange reactions. A detailed investigation on the catalysis mechanism of titanium compounds has been performed by Weingart [39], demonstrating that the titanium atom co-ordinates to the oxygen atom of fast-exchanging alkoxy ligands and that the polycondensation reaction is favoured by the formation of

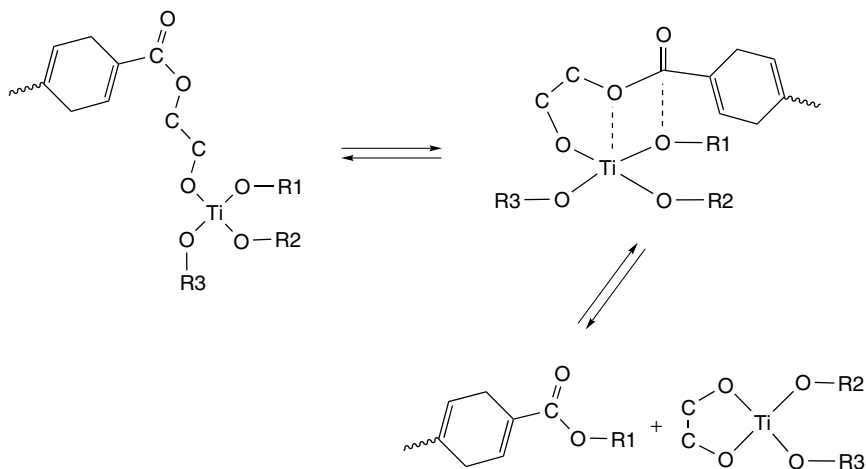


Figure 2.7 Mechanism for the titanium-catalyzed transesterification in PET, as proposed by Weingart [39]

more stable complexes with chelating glycolate. The mechanism proposed by Weingart is illustrated in Figure 2.7.

An extensive review on titanium catalysts for esterification and transesterification has been published by Siling and Laricheva [40].

In 1959 and 1960, Challa published the first results of quantitative experiments on the polycondensation equilibrium in PET [22, 41, 42]. He determined the polycondensation equilibrium constant K at different temperatures and average degrees of polycondensation and found that this parameter depends only slightly on temperature, but increases significantly with increasing degree of polycondensation. The monomer BHET was found not to follow the principle of equal reactivity.

Later, Fontana [43] performed experiments on transesterification and reinterpreted Challa's results. He concluded that the value of the polycondensation equilibrium constant is close to 0.5, being independent of temperature or degree of polycondensation and that the normal Flory–Schulz distribution does hold in the PET system. In Figure 2.8, the polycondensation equilibrium constant K from different sources [22, 43, 44] is shown as a function of the average degree of polycondensation, \bar{P}_n .

Many publications have appeared on the kinetics of transesterification, dealing with either PET or model compounds. A selection of these papers is summarized in Table 2.5. The overall reaction order of polycondensation is 3, being 1 each for ester, alcohol, and catalyst [43]. The reaction rate of polycondensation is generally limited by the rate of removal of EG from the reaction mixture. A

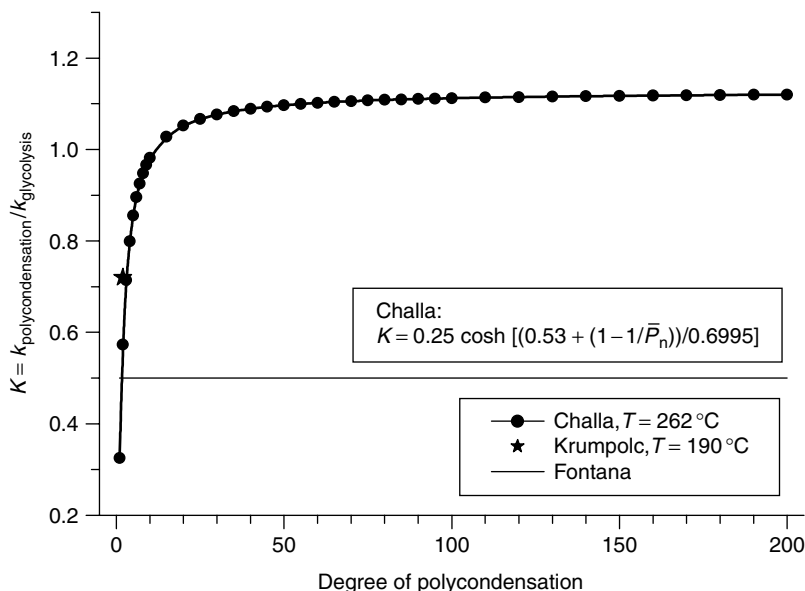


Figure 2.8 The polycondensation constant K as a function of the average degree of polycondensation \bar{P}_n , according to Challa [42], Krumpolc and Málek [44] and Fontana [43]

comprehensive description of the polycondensation process must therefore cover chemical kinetics together with diffusion and mass transfer. This issue will be discussed in detail in Section 3. Hoftyzer [45] emphasized the important effect of esterification and of side reactions, such as thermal degradation, on the overall polycondensation rate. To determine reliable reaction rates for transesterification, careful experimentation and data evaluation are needed.

The published values for the activation energies and pre-exponential factors of transesterification and glycolysis vary significantly. Catalysts and stabilizers influence the overall reaction rate markedly, and investigations using different additives cannot be compared directly. Most investigations are affected by mass transport and without knowledge of the respective mass transport parameters, kinetic results cannot be transferred to other systems.

2.3 REACTIONS WITH CO-MONOMERS

The properties of PET can be modified by the incorporation of co-monomers. Typical examples of these are isophthalic acid (IPA) (influences stress cracking resistance and melting temperature), 2,6-naphthalene dicarboxylic acid (NDC) (improves mechanical properties and reduces gas permeability), cyclohexane

Table 2.5 Kinetic data obtained for transesterification/glycolysis reactions

Year	Author(s)	Reference	Reactions	Catalysis	Definition of equilibrium constant K	Equilibrium constant K	T (°C)	E_a (kJ mol ⁻¹)
1960	Challa	22, 42	2tEG \rightleftharpoons bEG + EG	No	$\frac{4[bEG][EG]}{[tEG]^2}$	$K = K(\overline{P}_n)$ 0.4–1.2 (262 °C)	195–282	96
1968	Fontana	43	2tEG \rightleftharpoons bEG + EG bEG \rightleftharpoons tTPA + tV tV + tEG \rightarrow bEG + AA tTPA + tEG \rightleftharpoons bEG + W	Pb, Zn, Ca, Sb	–	0.5	152–228	–
1968, 1969	Stevenson and co-workers	99, 133	2tEG \rightleftharpoons bEG + EG	Sb ₂ O ₃	–	0.36	275	59, Sb catalyst; 167, no catalyst
1971	Hovenkamp	35	2tEG \rightleftharpoons bEG + EG	Sb ₂ O ₃ , Mn, Zn, Pb, Ca	$\frac{4[bEG][EG]}{[tEG]^2}$	0.8 for model system	197	–
1973	Tomita	134	2tEG \rightarrow bEG + EG bEG \rightarrow tTPA + tV	Zn	Assumption – irreversible	–	270–300	$E_p = 99$; $E_d = 195$
1978	Yokoyama <i>et al.</i>	91, 136, 137	2tEG \rightleftharpoons bEG + EG tTPA + tEG \rightleftharpoons bEG + W tEG \rightarrow tTPA + AA bEG \rightarrow tTPA + tV tV + tEG \rightarrow bEG + AA	Sb ₂ O ₃	–	1 for polycondensation; 4 for esterification; others irreversible	275, 280, 285	77.3, Sb catalyst; 167, no catalyst
1979	Chegolya <i>et al.</i>	27	2tEG \rightleftharpoons bEG + EG	H ⁺ , TPA	$\frac{4[bEG][EG]}{[tEG]^2}$	0.50 (214); 0.49 (234); 0.48 (244)	214, 234, 244	102, polycondensation; 104, glycolysis
1980	Reimschuessel	21	2tEG \rightleftharpoons bEG + EG	H ⁺ , Sb ₂ O ₃	$\frac{4[bEG][EG]}{[tEG]^2}$	$\Delta S = -80.3$ J mol ⁻¹ K ⁻¹ $\Delta H = -38.1$ kJ mol ⁻¹	202, 215, 226	205, no catalyst; 91.4, H ⁺ ; 115, Sb
1989	Yamada	23	tTPA + EG \rightleftharpoons tEG + W tTPA + tEG \rightleftharpoons bbEG + W 2tEG \rightleftharpoons bbEG + EG 2tEG \rightarrow DEGt + W tEG + EG \rightarrow DEG + W	Sb ₂ O ₃	–	–	240–265	11.7, polycondensation; 62.5, glycolysis
2000	Collins <i>et al.</i>	135	Transesterification	No	–	–	270, 280, 290	168 (±18)

dimethanol (CHDM) (influences rate of crystallization and melting temperature), diethylene glycol (DEG) (improves dyeability of fibre grades and lowers melting temperature) and bisphenol A (improves melt stiffness).

Like the monomers, the co-monomers are diols or diacids, and according to their functional groups, their reactions with TPA and EG follow the principal mechanisms outlined above. Very few data have been published on reactions with co-monomers, and it may be assumed that the same mechanisms and catalysis concepts should hold. Nevertheless, it has been observed that co-monomers influence the overall reaction rates significantly. In a typical batch process, the polycondensation time needed to prepare a polymer with an IV of 0.64 dL/g increases by about one third with co-monomer IPA and by about two thirds with co-monomer CHDM, in comparison to homo-PET. This may in part be due to the differing correlations between \overline{P}_n and IV, but additionally a reduced reactivity due to steric and electronic effects or the influence of co-monomers on the mobility of functional groups seems probable.

Yoda [28] investigated the activity of 20 catalysts in the transesterification reaction of PET and poly(ethylene isophthalate) (PEI) and found the same order of reactivity as for the transesterification of DMT with EG. The most effective catalysts were the acetates of Zn, Pb(II) and Hg(II), together with Co(III) acetylacetonate and Sb₂O₃. Titanium catalysts were not included in Yoda's study, but are known to be effective catalysts in PET blending [46].

Kinetic data have not been published for PET containing small amounts of co-monomers. Data for PET blending with different polyesters and polycarbonates [46, 47] indicate activation energies for the transesterification reactions of between 110 and 145 kJ/mol. Wang *et al.* [48] studied the depolymerization of PET with bisphenol A. They considered all possible equilibrium reactions between the ester and alcohol groups and found activation energies of between 110 and 134 kJ/mol for the reactions involving bisphenol A.

2.4 FORMATION OF SHORT CHAIN OLIGOMERS

PET contains about 2–3 % of short chain oligomers, which cause problems in the processing of the polymer. Oligomers can occur as linear or cyclic molecules and can be extracted by suitable solvents. Different compounds have been identified depending on the solvent and the analysis technique used [49–52]. After their extraction from the polymer, oligomers will reform by thermal treatment of the extracted sample [49], and a dynamic equilibrium between polymer and oligomers has been proposed.

Among the oligomers, the cyclic trimer has been postulated to be uniquely stable [53, 54]. This could be due to either a mechanism favouring the formation of trimer (kinetic control) or to the trimer having a lower energy than other oligomers (thermodynamic control), thus decreasing its rate of further reaction.

Lower reactivity of short chain oligomers had already been found by Challa [41], who determined that the reaction rate for the transesterification of BHET was half that for longer molecules. Challa assumed that the reactivities of the dimer and the trimer may also be lower but was not able to verify this hypothesis.

In a recent study, West *et al.* [55] showed that neither the linear nor the cyclic trimer have any higher formation probability during polycondensation than longer PET molecules. However, the reactivity of the monomer HET and of the linear dimer have been found to be significantly lower, and thus they are enriched in the polymer, as demonstrated by careful evaluation of gel permeation chromatograms and electrospray mass spectrometric analysis of PET spinneret sublimate. The low reactivity of HET has been attributed to its unesterified acid group. For the linear dimer, a folded conformation stabilized by hydrogen bonding between the terminal hydroxyl group and the carbonyl group and π -bonding by aromatic rings has been proposed. Molecular modelling analysis confirmed that the folded dimer conformers have an average energy of about 9 kJ/mol lower than the full set of conformations [55].

Peebles *et al.* [50] found that the formation of cyclic oligomers at 290 °C increased with decreasing \overline{M}_n of the polymer, and that the cyclization rate depended linearly on the hydroxyl end group concentration. Therefore, a 'back-biting' mechanism (cyclodepolymerization) has been proposed as a probable mechanism for oligomer formation (Figure 2.9).

Ha and Choun [51] confirmed these findings from the investigation of cyclic oligomer formation at 270 °C. They derived a rate equation for cyclic oligomer formation taking thermal degradation of the polymer into account.

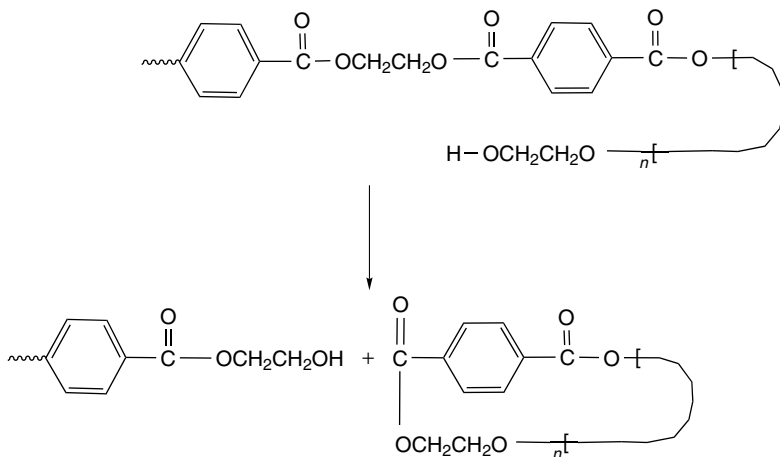


Figure 2.9 'Back-biting' mechanism for the formation of cyclic oligomers

De A. Freire *et al.* [56] investigated the formation of oligomers in PET samples heated to temperatures between 150 and 270 °C. In this temperature range, the concentration of cyclic oligomers remained nearly constant with time, whereas the concentration of linear oligomers increased markedly, probably due to hydrolytic or glycolytic degradation reactions.

In a thorough study on oligomers in recycled PET, Dulio *et al.* [52] found that the oligomer formation depended on the reaction temperature and the type of thermal treatment. During vacuum treatment of solid PET at 150–220 °C, the oligomer concentration decreased with increasing reaction temperature. In contrast, the oligomer concentration increased during melt extrusion at 270–310 °C with increasing reaction temperature or residence time, respectively. In both cases, a broadening of the molecular weight distribution was observed.

According to the experimental findings, the cyclic oligomers may be formed primarily as degradation products during prolonged heating by a 'back-biting' mechanism. Linear and cyclic oligomers are subject to a dynamic equilibrium and cyclization is only favoured in polymers containing few water molecules and hydroxyl groups.

2.5 FORMATION OF DIETHYLENE GLYCOL AND DIOXANE

Etherification of EG to form DEG is an important side reaction in PET synthesis. Most of the DEG is generated during the initial stages of polycondensation in the preheating stage (up to 50 % of total DEG) and in the low-vacuum stage (up to 90 % of total DEG). In the final high-vacuum stage, approximately 10 % of the total DEG is formed [57, 58]. Chen and Chen [59] found that most of the DEG is already formed during the esterification stage.

DEG, together with dioxane, can be regarded as condensation products of EG formed according to the stoichiometric Equations: $2\text{EG} = \text{DEG} + \text{W}$ and $\text{DEG} = \text{dioxane} + \text{W}$. Dioxane has a high vapour pressure and will be removed from the process as the column top product. DEG is less volatile and, as a diol, it can be incorporated into the PET chain as co-monomer. In some fibre grades, a DEG content of up to 1.5–2.5 % is specified to improve the dyeability. Nevertheless, DEG contents should be as low as possible in other PET grades, because DEG decreases the melting point and the thermal stability of the polymer.

Several authors have studied DEG formation, but the formation of dioxane in PET synthesis is rarely considered. Hovenkamp and Munting [60] investigated DEG formation in sealed tubes at 270 °C and found dioxane in amounts of up to 10 % of the DEG value. They suggested an intramolecular mechanism forming dioxane from a terminal DEG group (Figure 2.10).

No kinetic data are available for dioxane formation in a PET environment. Nevertheless, dioxane may become an important side-product when reactions are proceeding with long residence times of EG and DEG. Calculations of the

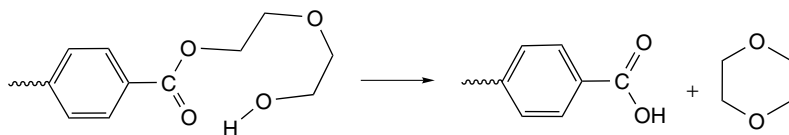


Figure 2.10 Mechanism for the formation of dioxane, as proposed by Hovenkamp and Munting [60]

equilibrium constants for the system water, EG, DEG, and dioxane showed that dioxane is the most stable species in this system. The equilibrium constant for the formation of dioxane from DEG is 72 500 at 310 °C and 143 100 at 180 °C. The reaction is slightly exothermic with a reaction enthalpy of approximately -7.1 kJ/mol. In the above temperature range, the equilibrium constant for the formation of DEG from EG is significantly lower, as shown in Figure 2.11.

With values between 13 and 16, the equilibrium constant is still high enough to regard the formation of DEG from EG to be irreversible in an open industrial system. DEG formation is not only an important side reaction during esterification, polycondensation and glycolysis, but also during distillation of EG and water in the process columns. In particular, the residence time in the bottom reboiler of the last separation column is critical, where the polycondensation catalyst and

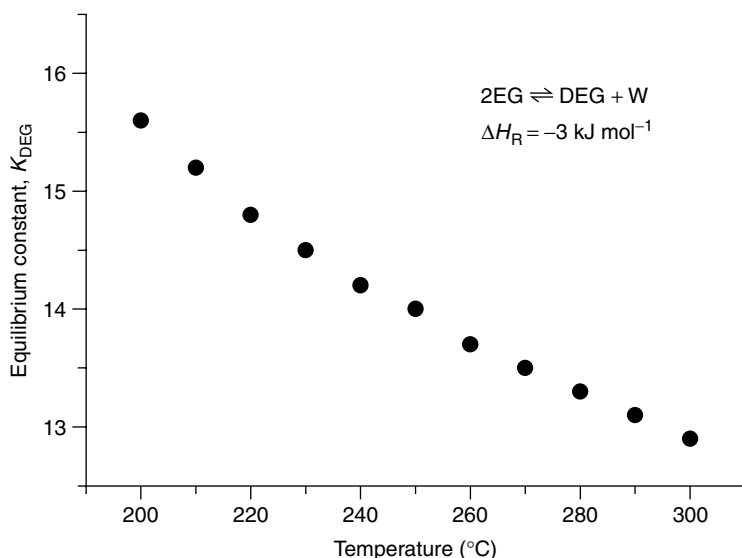


Figure 2.11 Equilibrium constant for the formation of DEG from EG as a function of temperature, calculated by using the Gibbs Reactor model of the commercial process simulator *Chemcad* (Chemstations)

TPA accumulate due to carry-over from the reactors. Long residence times in the distillation unit at elevated temperatures also result in an undesired yellowing of the recovered glycol.

Different mechanisms have been published for the formation of DEG. Hovenkamp and Munting [60] proposed a mechanism of ester + alcohol \rightarrow ether + acid, which is very unusual for a weak organic acid. Buxbaum [61] and Reimschuessel [21] discussed the formation of DEG by the reaction of different reactive intermediates from the thermal degradation of ester groups with hydroxyl groups, before they rearrange into acetaldehyde. More recent publications [24, 38, 57, 59], however, favour the formation of DEG by direct etherification, which is condensation of two hydroxyl groups as $2\text{R-OH} \rightarrow \text{R-O-R} + \text{H}_2\text{O}$. The work of Otton and Ratton [38] and Chen and Chen [59, 62–65] demonstrated that reactions involving different combinations of hydroxyl groups (free or terminal EG) have differing reaction rates and that the reaction between terminal EG and free EG is exceptionally fast. This may be due to an intramolecular assistance by the carbonyl oxygen of the ester group, which is known to accelerate nucleophilic substitution reactions of the $\text{S}_{\text{N}}2$ type [66] (Figure 2.12).

Etherification reactions are known to be acid catalyzed. Hornof has investigated the influence of metal catalysts (acetates of Zn, Pb and Mn) on the formation of ether bonds [57]. He found that all metals catalyzed etherification, with the strong Lewis acid Zn having the highest activity. Model experiments with pure EG showed that at temperatures above approximately 250°C significant amounts of DEG are formed even without added catalyst. Yamada found a catalytic activity of Sb_2O_3 , potassium titanium oxyoxalate and TiO_2 on the dehydration of EG [23, 24, 67]. He set up an unusual kind of rate equation with the catalyst increasing the pre-exponential factor instead of decreasing the activation energy. Chen and Chen [59, 62–65] verified the strong catalytic effect of TPA and demonstrated the catalytic activity of Sb_2O_3 and zinc acetate on DEG formation.

Different working groups have published kinetic data for the DEG formation and the results are summarized in Table 2.6.

The most detailed investigations have been performed by Chen and Chen [59, 62–65]. They considered catalyzed and uncatalyzed reactions between different hydroxyl groups at esterification temperatures ($180\text{--}195^\circ\text{C}$) and at polycondensation temperatures ($270\text{--}290^\circ\text{C}$). Their results are illustrated in Figure 2.13 in the form of Arrhenius plots. The type of catalysis and the reaction equation

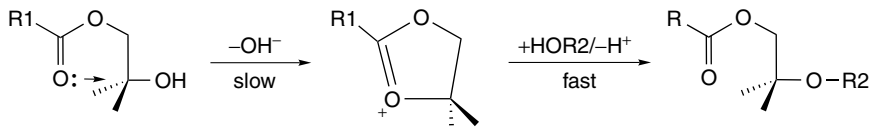


Figure 2.12 Mechanism for the formation of DEG with intramolecular assistance of the ester group

Table 2.6 Kinetic data obtained for the formation of diethylene glycol

Year	Author(s)	Reference	Reactions	Catalysis	$T(^{\circ}\text{C})$	k_0 ($\text{kg mol}^{-1} \text{h}^{-1}$)	E_a (kJ mol^{-1})
1970	Hovenkamp and Munting	60	ester + alcohol \rightarrow ether + acid tDEG \rightarrow tTPA + dioxane	Mn, Sb ₂ O ₃ Not COOH	270	0.00 122 (270 $^{\circ}\text{C}$)	–
1981	Hornof	57	2EG \rightarrow DEG + W	Zn, Pb, Mn Ac Sb ₂ O ₃	280	–	–
1983	Renwen <i>et al.</i>	58	2tEG \rightarrow bDEG + W bEG + tEG \rightarrow tTPA + bDEG tEG \rightarrow tTPA + AA AA + EG \rightarrow DEG AA + tEG \rightarrow tDEG bEG \rightarrow tTPA + tV tV + EG \rightarrow tDEG tV + tEG \rightarrow bDEG tEG + EG \rightarrow tTPA + DEG tEG + tEG \rightarrow tTPA + tDEG bEG + EG \rightarrow tTPA + tDEG bEG + tEG \rightarrow tTPA + bDEG 2tEG \rightarrow bDEG + W tEG + EG \rightarrow tDEG + W 2EG \rightarrow DEG + W tTPA + DEG \rightarrow tDEG + W 2EG \rightarrow DEG + W 2tEG \rightarrow bDEG + W		220–290	0.517 (mol/l) ^{0.1} min ^{–1}	34.3, apparent E_a ; overall reaction order, 0.9
1985	Mössner and Vollmert	138			Ca acetate, Sb ₂ O ₃	280	0.001 24 (280 $^{\circ}\text{C}$)
1989 1992	Yamada	23 67		Sb ₂ O ₃ (1989) TiO ₂ (1992)	250	–	178
1998	Chen and Chen	59		Direct esterification No catalyst added	180, 185, 190, 195 270, 280, 285, 290	3.7×10^{13} 8×10^{10}	181 137
1998	Chen and Chen	62	2EG \rightarrow DEG + W	TPA	175, 180, 185, 190	3.59×10^{13} 3.90×10^{13}	125.5 (DEG) 122.7 (TEG)
1999	Chen and Chen	63	EG + DEG \rightarrow TEG + W 2tEG \rightarrow bDEG + W	Sb ₂ O ₃	270, 280, 285, 290	2.93×10^{10}	91.7 (Sb)
2000	Chen and Chen	64	2tEG \rightarrow bDEG + W tEG + EG \rightarrow tDEG + W 2EG \rightarrow DEG + W	H ⁺	120, 130, 140, 150	4.4×10^{10} 4.2×10^4	96.6 38.0
2000	Chen and Chen	65	2tEG \rightarrow bDEG + W	Zn acetate	270, 280, 285, 290	3.59×10^{13} 9.7×10^{10}	125.5 88.3

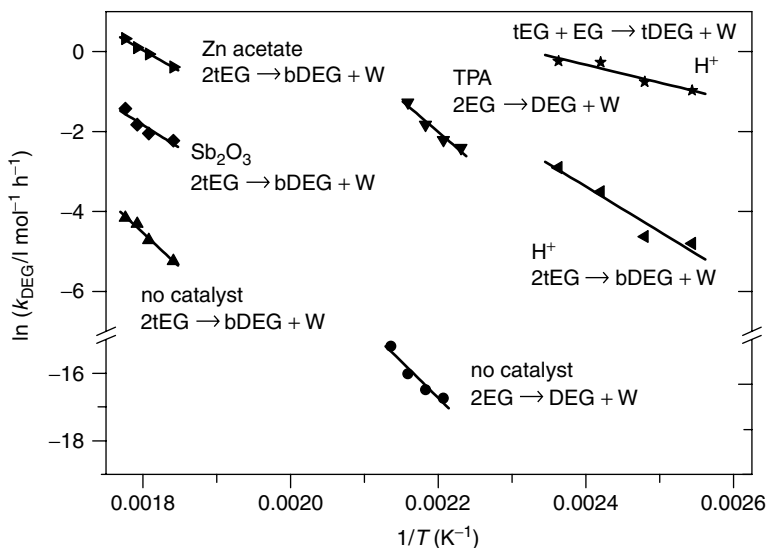


Figure 2.13 Arrhenius plots for the DEG formation at temperatures between 175 and 290 °C, without [59] and with additionally added TPA [62], Sb_2O_3 [63], protons [64] and zinc acetate [65] as catalysts, according to Chen and Chen

are indicated for the respective data points. Activation energies of between 38 and 181 kJ/mol have been calculated, demonstrating that DEG formation is very sensitive to the chemical environment regarding the concentration of different functional groups and the presence of proton and metal catalysts.

2.6 THERMAL DEGRADATION OF DIESTER GROUPS AND FORMATION OF ACETALDEHYDE

Thermal degradation of PET is a major problem at temperatures above the melting point and inevitably occurs in polymer melts during synthesis and processing. The primary degradation reactions have higher activation energies than the polycondensation reactions, and thus become more and more important with increasing reaction temperature. Major consequences for the PET quality are an IV drop, the formation of carboxyl end groups and acetaldehyde, and the yellowing of the polymer. Carboxyl end groups reduce the hydrolytic and thermal stability, and in standard PET grades their concentration should not exceed 25 mmol/kg. Acetaldehyde migrates into the contents of food packaging, so causing flavour problems of the products. For bottle-grade PET, often an acetaldehyde content below 1 ppm is specified. By-products of thermal degradation are light gases, being mainly CO , CO_2 , ethene, methane, and benzene, together with TPA, HET and short-chain oligomers.

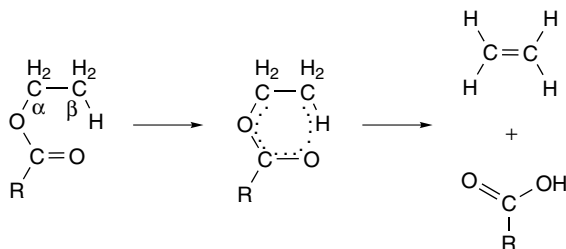


Figure 2.14 Mechanism for the thermal degradation of ester bonds

The first reaction step of thermal degradation is scission of an ester bond. Esters containing at least one β -hydrogen atom decompose pyrolytically to give olefins and acids via a cyclic transition state (Figure 2.14).

The olefinic product is either a terminal vinyl group from scission of a bound ester group or vinyl alcohol from scission of a terminal ester group, which rearranges instantaneously into acetaldehyde. A second route to acetaldehyde is transesterification of terminal vinyl groups, liberating vinyl alcohol, with the content of terminal vinyl groups in a polymer being often referred to as 'potential acetaldehyde'. The acidic product of thermal degradation is a carboxyl end group. If the content of hydroxyl groups in the polymer is low, carboxyl end groups may add in significant amounts to the olefinic double bond, generating an acylal which then decomposes to an anhydride and acetaldehyde. The anhydride group can react with hydroxyl groups, forming one ester and one carboxyl group, or with water, forming two carboxyl groups (Figure 2.15).

As long as significant amounts of hydroxyl groups are present in the polymer, the carboxyl and vinyl groups will be esterified or transesterified, respectively. Thus, the broken ester group will reform and the net effect is the decomposition of a hydroxyl end group into a carboxyl end group and acetaldehyde. A polymer, therefore, can be markedly affected by thermal degradation before this may be detected as an IV change. The molecular weight will begin to fall when most of the hydroxyl end groups have been consumed and carboxyl and vinyl end groups have accumulated.

The thermal degradation of PET is influenced by metal catalysts. Zimmermann and co-workers [29, 68–70] have investigated the influence of various metal catalysts on thermal degradation and suggested a mechanism for the catalyzed reaction. The most active catalysts were Zn, Co, Cd and Ni. Thermal degradation was reduced by the addition of triarylphosphites or triarylphosphates blocking the metal ions. Kao *et al.* [71] found that the acetates of Na and Mg have little activity, whereas the acetates of Co, Cu and Zn accelerate the thermal degradation, with Zn being the most active.

In the presence of oxygen, thermo-oxidative degradation takes place, which is much faster than thermal degradation in an inert atmosphere.

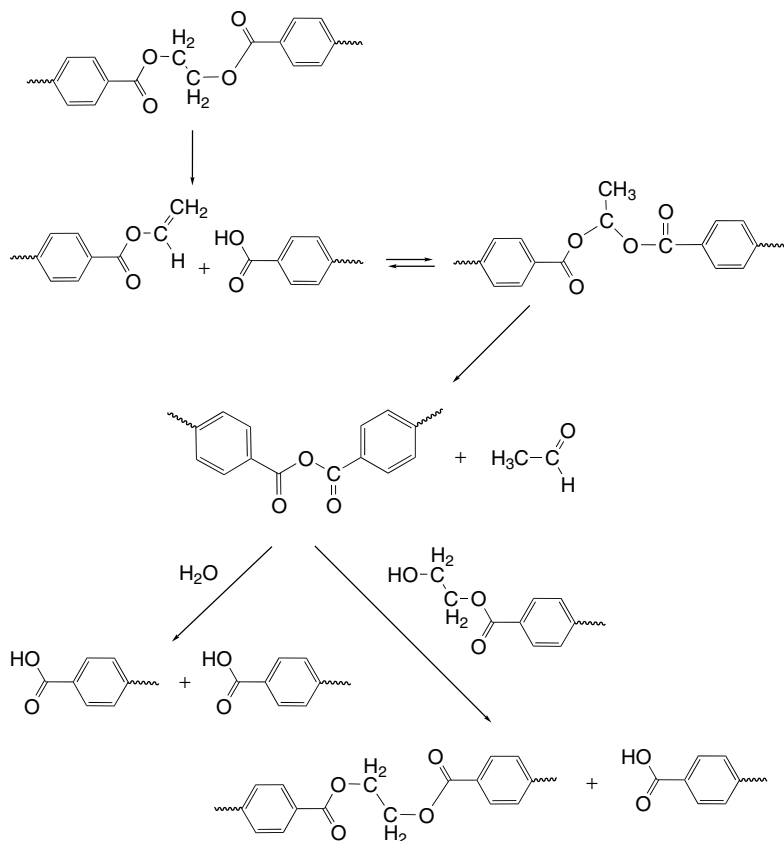


Figure 2.15 Mechanism for the thermal degradation of PET

Free radical mechanisms have been proposed for this reaction [61, 72], and 4,4'-biphenyldicarboxylic acid, 2,4',5-biphenyltricarboxylic acid, and 1,2-bis(4-carboxyphenyl)ethane have been detected as side products [72]. The formation of chromophores is also enhanced by the presence of oxygen, as discussed below in Section 2.7.

Thermal ester degradation is a uni-molecular reaction following first-order kinetics. Most investigations on kinetics have been performed under an inert gas atmosphere when measuring the reaction rate of thermal degradation, but some authors have regarded the thermo-oxidative degradation as well. Key publications on the degradation of PET are summarized in Table 2.7. The reaction rates have been determined by following the formation of acetaldehyde or the formation of carboxyl end groups, the viscosity decrease, or the mass loss of the polymer. Depending on the experimental method, differing results are obtained and the data

Table 2.7 Kinetic data obtained for the thermal and thermo-oxidative degradation of PET

Year	Author(s)	Reference	Reactions and mechanism	Degradation by	Catalysis	T ($^{\circ}\text{C}$)	E_a (kJ mol^{-1})
1953	Marshall and Todd	139	$\text{tEG} \rightarrow \text{tV} + \text{W}$ $\text{bEG} + \text{W} \rightarrow \text{tTPA} + \text{tEG}$ $\text{tV} \rightarrow$ free radical reactions	Pyrolysis, oxidation, hydrolysis	No	280–322	134 (overall)
1968	Buxbaum	61	ester pyrolysis; no free radical reactions	Pyrolysis, oxidation, hydrolysis, radiation	No	280	–
1973	Tomita	134	$\text{bEG} \rightarrow \text{tTPA} + \text{tV}$ $\text{tEG} + \text{tTPA} \rightarrow \text{bEG} + \text{W}$ $\text{tEG} \rightarrow \text{tTPA} + \text{AA}$	Pyrolysis	Zn acetate	270, 280, 290, 300	99 (polycondensation) 195 (depolymerization) 178–192
1973	Zimmermann and Chu	29	Thermal degradation	Pyrolysis	Ca/Sb ; Mn/Ge ; Zn/Sb	280–300	86.1–92.8 (air) 186–188 (N_2) 158 125
1974	Schaaf and Zimmermann	70	$\text{bEG} \rightarrow \text{tTPA} + \text{tV}$	Pyrolysis, oxidation	Sb , Ge , Zn , Mn	200–360	
1978	Yokoyama	91	$\text{bEG} \rightarrow \text{tTPA} + \text{tV}$ $\text{tEG} \rightarrow \text{tTPA} + \text{AA}$	Pyrolysis	Sb_2O_3	275, 280, 285	
1980	Rafler <i>et al.</i>	104	Overall thermal degradation	Pyrolysis	Mn acetate , Sb_2O_3	270	Overall: $k(270^{\circ}\text{C}) = 7.6 \times 10^{-8} \text{ s}^{-1}$
1983	Jenekhe <i>et al.</i>	140	Mass loss measured by TGA; formal kinetics	Pyrolysis	–	$0.3\text{--}10 \text{ K min}^{-1}$, $T_{\text{max}} = 550^{\circ}\text{C}$	200–235, function of heating rate
1983	Dollimore <i>et al.</i>	141	$\text{bEG} \rightarrow \text{tTPA} + \text{tV}$ $\text{tEG} \rightarrow \text{tTPA} + \text{AA}$	Pyrolysis	No catalyst and Sb_2O_3	Non-isothermal, no 0.062 K min^{-1} 265–290	201 (isothermal, no catalyst), $k_0 = 6.4 \times 10^{-11} \text{ s}^{-1}$ 191 (non-isothermal, no catalyst), $k_0 = 8.0 \times 10^{-11} \text{ s}^{-1}$ 117 (overall, air); 159 (overall, vacuum); 84 (COOH , air) 113; (COOH , vacuum)
1984	Jabarin and Lofgren	142	Overall thermal degradation and COOH formation	Pyrolysis, oxidation	No	275–350	

in Table 2.7 show non-uniform values for the activation energies. Generally, the activation energy for thermo-oxidative degradation is distinctly lower than for thermal degradation, as expected. In our opinion, the most reliable data are the results of the group of Zimmermann.

2.7 YELLOWING

The polymer colour is regarded as a *quality* parameter, and low-quality PET grades show yellow colouring. The colour can be measured in a standardized system, and for PET the CIELAB system is often used. The colour value is characterized by a combination of the three parameters L^* , a^* and b^* . The parameter L^* characterizes the brightness of the sample between black (0) and white (100), a^* is the colour co-ordinate for green (−100) and red (+100) and b^* is the colour co-ordinate for blue (−100) and yellow (+100). High-quality PET grades have high L^* values and low b^* values between −1 and +1.

Yellowing of the polymer can be caused by thermal as well as by oxidative degradation and is a severe problem in PET synthesis, especially in the production of bottle grades. Oxidative degradation can be minimized by careful operation under an inert gas atmosphere, but thermal degradation can only be avoided by reducing the reaction temperature – which also reduces the polycondensation rate.

The formation mechanisms and the nature of chromophores in PET are still a matter of discussion. Postulated chromophores are polyenaldehydes from the aldol condensation of acetaldehyde [73] and polyenes from polyvinyl esters [69], as well as quinones [74, 75]. Goodings [73] has proposed aldol condensation as forming polyconjugated species by subsequent reactions of acetaldehyde molecules (Figure 2.16).

The formation of polyenes from vinyl end groups was first postulated by Zimmermann and Leibnitz [69] and requires two reaction steps, i.e. (1) the polymerization of vinyl end groups to polyvinyl esters, and (2) the elimination of carboxylic acids to form the polyenes (Figure 2.17).

Edge *et al.* [74, 75] investigated PET samples degraded at melt temperatures in nitrogen and air by fluorescence, phosphorescence and infrared spectroscopy. They found that formation of coloured species is much faster in air than in nitrogen and concluded, that for short residence times, polyenes are not responsible for yellowing. Chromophores in PET degraded in the presence of oxygen arise

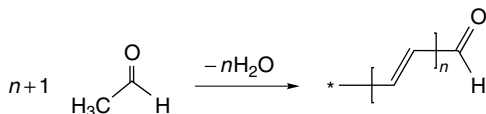


Figure 2.16 Aldol condensation of acetaldehyde

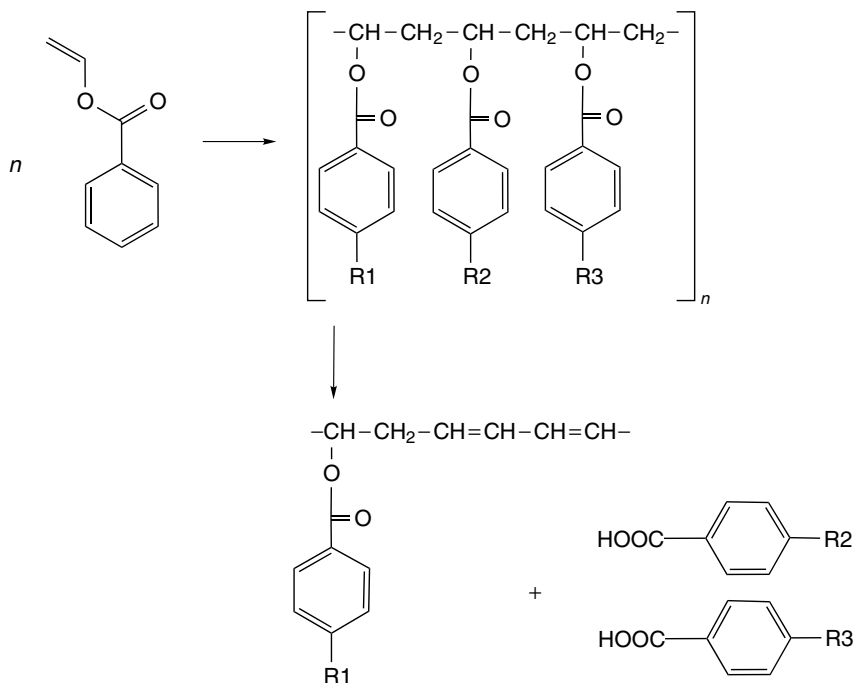


Figure 2.17 Formation of polyenes from vinyl end groups, as proposed by Zimmermann and Leibnitz [69]

from hydroxylation of the terephthalate ring and formation of unsaturated ester and quinoid species. The reaction scheme proposed by Edge *et al.* is depicted in Figure 2.18.

Early investigations by Zimmermann and co-workers [68, 69] showed the influence of different catalysts on the yellowing of PET, and the addition of stabilizers such as triphenylphosphates or triphenylphosphites has been recommended [68]. In a later work, Zimmermann and Chu [29] demonstrated that during thermal degradation of well-mixed polymer melts more acetaldehyde is liberated and less yellowing is observed than in 'stagnant' melts. They ascribed these findings to the enhanced transesterification of vinyl end groups and the increased mass transport of acetaldehyde into the gas phase, both of which would reduce the formation of polyenes.

Chung [34] concluded that the semiconducting properties of a metal species influence discoloration. In contrast to metals belonging to the insulator group, metals belonging to the semiconductor group promote yellowing, perhaps due to catalysis of the polymerization of vinyl esters. The formation of chromophores is enhanced when the metal has a variable valency with a reduction potential near to zero.

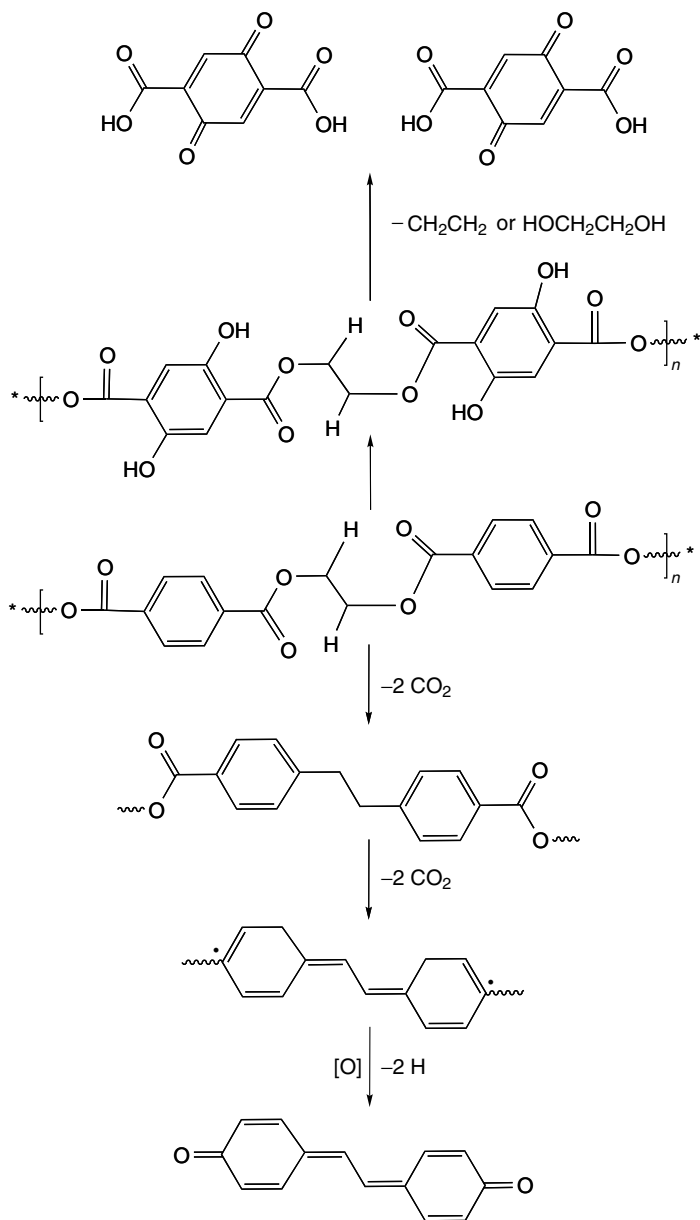


Figure 2.18 Degradation mechanism for PET in the presence of oxygen, as proposed by Edge *et al.* [75]

Weingart and co-workers [39, 76] ascribed the enhanced yellowing observed in PET synthesis with titanium catalysts to the easy formation of titanium vinylates from titanium glycolates. Titanium vinylates can liberate acetaldehyde or introduce vinyl end groups into the PET chains. These workers found that the degree of yellowing is proportional to the catalyst concentration but can be reduced significantly by adding phosphorous compounds as stabilizers. No kinetic data are available for PET yellowing.

2.8 CHEMICAL RECYCLING

Mechanical recycling, comprising washing, sorting and extrusion, is a well-established technology and market for bottle to fibre recycling [77, 78]. Nevertheless, bottle to bottle recycling is preferable due to its higher added value [79, 80].

Recycled PET has to satisfy the requirements for bottle processing (glass transition and melting temperatures, melt viscosity, melt stiffness, rate of crystallization, thermal stability, etc.) as well as approval for food contact (decontamination, colour, haze, etc.). Due to the required high decontamination levels of recycled PET for food-packaging applications, bottle to bottle recycling should be a chemical recycling process comprising chain degradation and re-polycondensation. Such mechanisms cause contaminants to be either degraded or evaporated, thus ensuring reliable decontamination of the recycled PET. The chain degradation can be performed either by hydrolysis [81], glycolysis [82], methanolysis [83] or saponification [84], thus forming monomers and/or oligomers. By reactive extrusion, a polymer with reduced molecular weight is generated [85].

The decontamination capability is the most important objective function in the design of a chemical PET recycling process to recycle polymer for food-packaging applications. The complete and reliable removal of various contaminants has to be proven according to the requirements of governmental regulations. Water-soluble contaminants can be removed by a thorough high-energy wash of the feedstock. Other contaminants can be destroyed during extrusion by thermal decomposition and hydrolysis, respectively.

The reactions, which have to be considered in a process model of chemical PET recycling, are the same as those for PET synthesis – saponification excepted. The rate-determining step in chemical PET recycling is the mass transfer of the low-molecular-weight reactant into the polymer phase. Two mass transfer models can be distinguished, as follows. (1) For depolymerization in the solid state, the coupling of chemical reactions and mass transfer can be described by a fluid/solid mass-transfer model, e.g. by the shrinking core model [86, 87]. (2) During depolymerization in the melt phase, two nearly immiscible phases have to achieve thorough contact, while the more polar low-viscous reactant has to diffuse into the less polar high-viscous polymer melt. Fluid/fluid mass-transfer models, such as the two-film model, can be employed. Table 2.8 summarizes some important publications on kinetics and process models for PET recycling.

Table 2.8 Publications on kinetics and process models for PET recycling

Year	Author(s)	Reference	Reactions	Catalysis	T (°C)	K	k (g PET mol ⁻¹ min ⁻¹)	E_a (kJ mol ⁻¹)	Reaction system
1993	Campanelli <i>et al.</i>	143	Hydrolysis with water, melt phase	No	250 265	1.43 0.664 0.384	0.242 0.352 0.487	56	Batch, stirred vessel
1994	Campanelli <i>et al.</i>	144	Hydrolysis with water, melt phase	Zn acetate	280 250 265	—	0.299 0.425 0.542	48	Batch, stirred vessel
1994	Campanelli <i>et al.</i>	145	Glycolysis with EG, melt phase	Zn acetate, no effect at $T > 245^\circ\text{C}$	280 255 265 275	—	4.87×10^{-2} 6.67×10^{-2} 10.44×10^{-2} (L mol ⁻¹ min ⁻¹)	92	Batch, stirred vessel
1995	Wang <i>et al.</i>	48	Glycolysis with bisphenol A (BPA), initially solid-phase reaction	bEG + BPA \rightleftharpoons tBPA + tEG, plus five other equilibrium reactions involving BPA	190 210 230	—	0.330 1.10 3.25	111	Batch, stirred vessel
1998	Kao <i>et al.</i>	146	Hydrolysis in two liquid phases	H ⁺	235 250 265	7.09 3.99 1.53	—	123	Batch, stirred vessel
1998	Kao <i>et al.</i>	147	Saponification in solid state	NaOH, KOH	10 K/min	—	—	110	DSC, TGA
1999	Chen and Chen	148	Glycolysis, initially in solid state	Zn acetate	190	0.51	—	—	Batch, stirred vessel
2001	Wan <i>et al.</i>	149	Saponification, solid state	KOH	120 140 160	—	3.32×10^{-7} 8.31×10^{-7} 22.4×10^{-7} (L mol ⁻¹ cm ⁻²)	69	Batch, stirred vessel
2001	Rieckmann and Völker	85	Glycolysis Hydrolysis Hydrolysis DEG formation DEG formation AA formation Thermal degradation Transesterification of vinyl end groups	H ⁺ , Sb H ⁺ H ⁺	270 280 290 300	2.0 0.80 0.40	—	74 75 75 125 125 125 158	Extruder, SSP

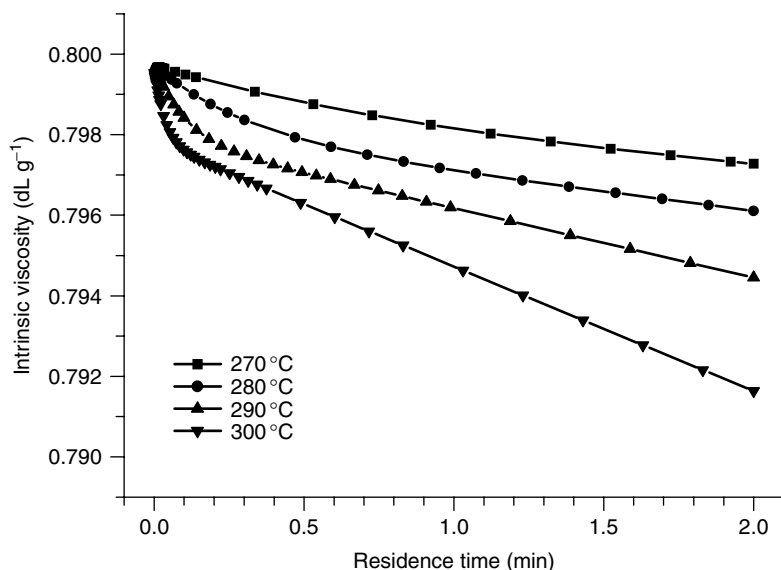


Figure 2.19 Intrinsic viscosity of the polymer melt as a function of extruder residence time and temperature for an initial water content of 3 ppm

Besides the main depolymerization reactions, side reactions should also be considered in the kinetic description of a PET recycling process. This is emphasized by the results obtained from a PET extrusion model [85] shown in Figures 2.19–2.23. The complete set of reactions summarized below in Table 2.10 have been used, but shear effects have not been taken into account. Chain degradation, accompanied by a significant reduction of intrinsic viscosity, occurs even within residence times of a few minutes. Carboxyl end groups, vinyl end groups and acetaldehyde are formed in amounts depending on residence time, temperature and initial moisture content of the PET flakes.

2.9 CONCLUSIONS

Many studies on the modelling of esterification, melt polycondensation, or solid-state polycondensation refer to the reaction scheme and kinetic data published by Ravindranath and co-workers. Therefore, we will examine the data sources they have used over the years. The first paper concerned with reactor modelling of PET production was published by Ravindranath *et al.* in 1981 [88]. The reaction scheme was taken from Ank and Mellichamps [89] and from Dijkman and Duvekot [90]. The kinetics for DEG formation are based on data published by Hovenkamp and Munting [60], while the kinetics for esterification were deduced

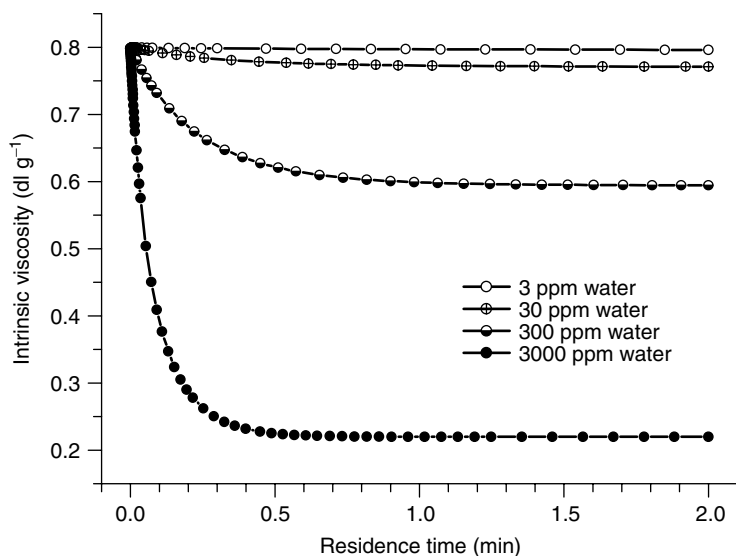


Figure 2.20 Intrinsic viscosity of the polymer melt as a function of extruder residence time and initial water content for a temperature of 280 °C

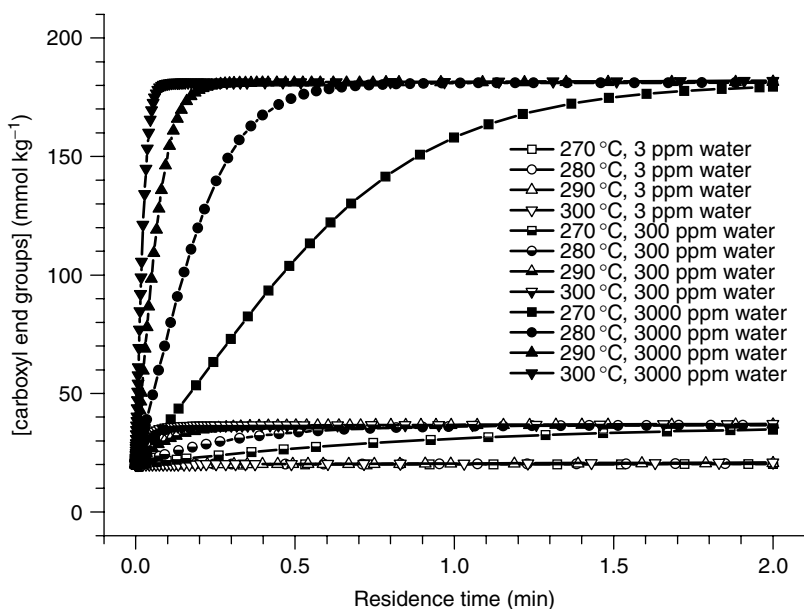


Figure 2.21 Concentration of carboxyl end groups as a function of extruder residence time, temperature and initial water content

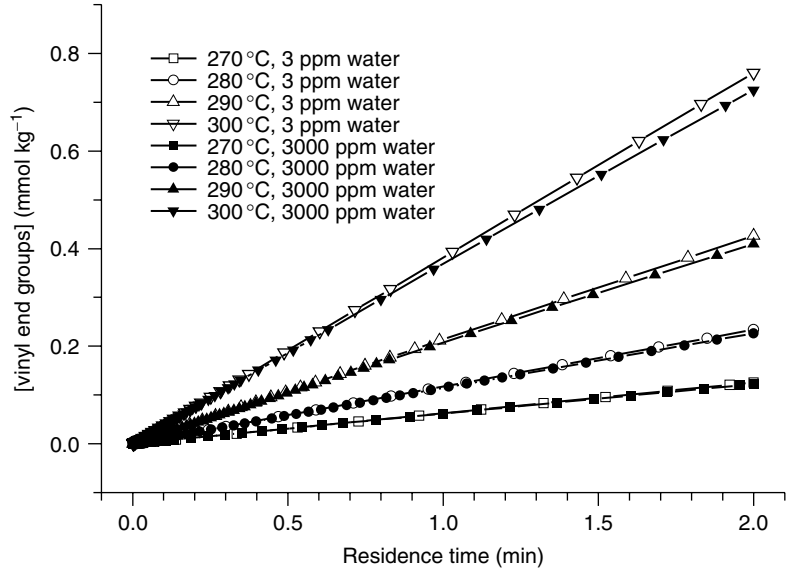


Figure 2.22 Concentration of vinyl end groups as a function of extruder residence time and temperature for initial water contents of 3 and 3000 ppm

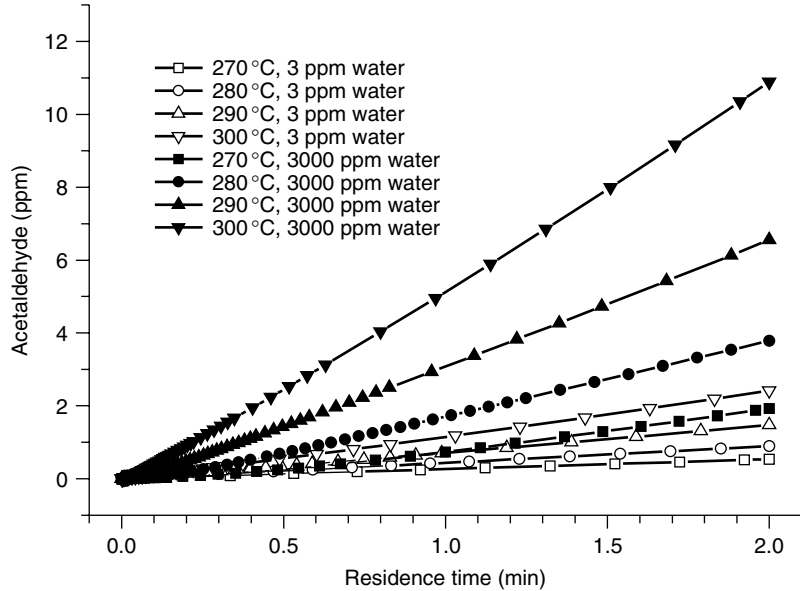


Figure 2.23 Generation of acetaldehyde as a function of extruder residence time and temperature for initial water contents of 3 and 3000 ppm

Table 2.9 Evolution of the kinetic data^a used in process models published by Ravindranath and co-workers

Year and reference	Reactor/reaction	Esterification, free EG	Esterification, tEG	Polycondensation	DEG formation ^b	AA formation ^{b,c}	Diester group degradation ^{b,c}	Polycondensation of vinyl groups ^b
1981 [88]	Semi-batch ester-interchange	2.5 1.0 × 10 ³ 73.6	1.25 1.0 × 10 ³ 73.6	0.5 6.8 × 10 ² 77.3	irrev 2.17 × 10 ⁶ 125	irrev 2.17 × 10 ⁹ 125	—	—
1982 [92]	Continuous transesterification	2.5 1.0 × 10 ³ 73.6	1.25 1.0 × 10 ³ 73.6	0.5 6.8 × 10 ² 77.3	irrev 2.17 × 10 ⁶ 125	irrev 2.17 × 10 ⁹ 125	—	—
1982 [150]	Semi-batch prepolymerization	2.5 1.04 × 10 ³ 73.6	1.25 1.04 × 10 ³ 73.6	0.5 6.8 × 10 ² 77.3	irrev 4.16 × 10 ⁴ 125	irrev 4.16 × 10 ⁷ 125	irrev 3.6 × 10 ⁹ 158	—
1982 [151]	Continuous esterification	$K = K(T)$ H ⁺ catalysis $k_{no\ cat} = 2.55 \times 10^{-5}$ $k_{0,cat} = 8.672 \times 10^5$ $E_{a,cat} = 86$	$K = K(T)$ H ⁺ catalysis $k_{no\ cat} = 8.426 \times 10^8$ $E_{a,no\ cat} = 124$ $k_{cat} = 75.64$ $E_{a,cat} = 43$	$K = K(T)$ Sb catalysis $k_{no\ cat} = 5.038 \times 10^{17}$ $E_{a,no\ cat} = 205$ $k_{cat} = 3.325 \times 10^8$ $E_{a,cat} = 91$	irrev 1.04 × 10 ⁵ 125	irrev 1.04 × 10 ⁸ 125	—	—
1982 [152]	Continuous prepolymerization	2.5 1.04 × 10 ³ 73.6	1.25 1.04 × 10 ³ 73.6	0.5 6.8 × 10 ² 77.3	irrev 4.16 × 10 ⁴ 125	irrev 4.16 × 10 ⁷ 125	irrev 3.6 × 10 ⁹ 158	0.5 6.8 × 10 ² 77.3
1984 [153]	MWD considerations	2.5 2.08 × 10 ³ 73.6	1.25 2.08 × 10 ³ 73.6	0.5 1.36 × 10 ³ 77.3	—	irrev 8.32 × 10 ⁷ 125	irrev 7.2 × 10 ⁹ 158	—
1984 [112]	Continuous finisher	2.5 2.08 × 10 ³ 73.6	1.25 2.08 × 10 ³ 73.6	0.5 1.36 × 10 ³ 77.3	irrev 8.32 × 10 ⁴ 125	irrev 8.32 × 10 ⁷ 125	irrev 7.2 × 10 ⁹ 158	irrev 1.36 × 10 ³ 77.3
1990 [121]	SSP	—	—	0.5, with diffusion control	—	—	—	—

^a Data presented as equilibrium constant K , rate constant k_i (m³ mol⁻¹ min⁻¹) and activation energy E_a (kJ mol⁻¹). Reaction orders: 2, for esterification, polycondensation and polycondensation of tV; 3, for H⁺ catalyzed reactions; 1, for diester group formation and AA degradation.

^b irrev, irreversible.

^c Rate constant k (min⁻¹).

from data published by Yokoyama *et al.* [91]. The kinetic data for polycondensation were 'calculated from the literature'. Data for acetaldehyde formation were also taken from Yokoyama *et al.* [91].

Table 2.9 summarizes the kinetic data which were employed by Ravindranath and co-workers in PET process models. The activation energies for the different reactions have not been changed in a decade. In contrast, the pre-exponential factors of the Arrhenius equations seem to have been fitted to experimental observations according to the different modelled process conditions and reactor designs. It is only in one paper, dealing with a process model for the continuous esterification [92], that the kinetic data published by Reimschuessel and co-workers [19–21] have been used.

The reactions, which should be considered in a rigorous modelling of PET synthesis, PET processing, and PET recycling, are summarized in Table 2.10. This set of reactions covers the main reactions of esterification/hydrolysis and transesterification/glycolysis, together with the side reactions leading to chain degradation and the formation of DEG and acetaldehyde. For the formation of yellowing species, no kinetic data are available, and so this important side reaction cannot be taken into account up until the present time. Regarding the wide variation in published data on mechanisms, catalysis and kinetics for the different reactions, it is obvious that additional and more reliable kinetic data have to be

Table 2.10 Reactions which should be considered in rigorous modeling of PET synthesis, PET processing and PET recycling

Number	Reaction ^a	k_{i+}	k_{i-}	Reaction type ^a
1	tEG + tEG \rightleftharpoons bEG + EG	k_1	k_1/K_1	Transesterification
2	tEG + bTPA \rightarrow tTPA + AA	k_2	–	Acetaldehyde formation
3	tEG + tEG \rightarrow bDEG + W	k_3	–	Etherification, bDEG formation
4	tEG + EG \rightarrow tDEG + W	k_4	–	Etherification, tDEG formation
5	EG + EG \rightarrow DEG + W	k_5	–	Etherification, free DEG formation
6	EG + TPA \rightleftharpoons tEG + tTPA + W	k_6	k_6/K_6	Esterification
7	EG + tTPA \rightleftharpoons tEG + bTPA + W	k_7	k_7/K_7	Esterification
8	tEG + TPA \rightleftharpoons bEG + tTPA + W	k_8	k_8/K_8	Esterification
9	tEG + tTPA \rightleftharpoons bEG + bTPA + W	k_9	k_9/K_9	Esterification
10	2 bTPA + bEG \rightarrow tV + tTPA	k_{10}	–	Degradation of diester groups
11	tV + tEG \rightarrow bEG + AA	k_{11}	–	Transesterification of vinyl end groups

^a t, terminal segments; b, bound/repeat segments.

determined before a predictive model can be established which does not rely on adjusted parameters.

3 PHASE EQUILIBRIA, MOLECULAR DIFFUSION AND MASS TRANSFER

In industrial PET synthesis, two or three phases are involved in every reaction step and mass transport within and between the phases plays a dominant role. The solubility of TPA in the complex mixture within the esterification reactor is critical. Esterification and melt-phase polycondensation take place in the liquid phase and volatile by-products have to be transferred to the gas phase. The effective removal of the volatile by-products from the reaction zone is essential to ensure high reaction rates and low concentrations of undesirable side products. This process includes diffusion of molecules through the bulk phase, as well as mass transfer through the liquid/gas interface. In solid-state polycondensation (SSP), the volatile by-products diffuse through the solid and traverse the solid/gas interface. The situation is further complicated by the co-existence of amorphous and crystalline phases within the solid particles.

The phase equilibria of the most important compounds will be described in the following section. In the sections thereafter, we will treat mass transport in melt-phase polycondensation, as well as in solid-state polycondensation, and discuss the diffusion and mass transfer models that have been used for process simulation.

3.1 PHASE EQUILIBRIA

Terephthalic acid is relatively insoluble in EG or the monomer BHET. Experiments on the solubility of TPA in EG or BHET are difficult to evaluate, because at esterification temperatures the dissolution of TPA cannot be performed without its simultaneous reaction. Kang *et al.* [7] found that TPA is more soluble in EG than in BHET. This is contradicted by the data published by Baranova and Kremer, indicating a higher solubility of TPA in BHET [93] which agree with the principle 'like dissolves like'. Data for the solubility of TPA in EG and BHET at different temperatures are summarized in Figure 2.24.

In typical industrial operations, TPA is not dissolved in EG or BHET but in prepolymer. The latter contains PET oligomers with one to approximately six to eight repeat units and a significant concentration of carboxyl end groups of between 200 and 1100 mmol/kg. It was found [94] that the solubility of TPA in prepolymer is much higher than indicated by the values given in the literature. Nevertheless, the esterification reactor still contains a three-phase system and only the dissolved TPA may react with EG in a homogenous liquid-phase

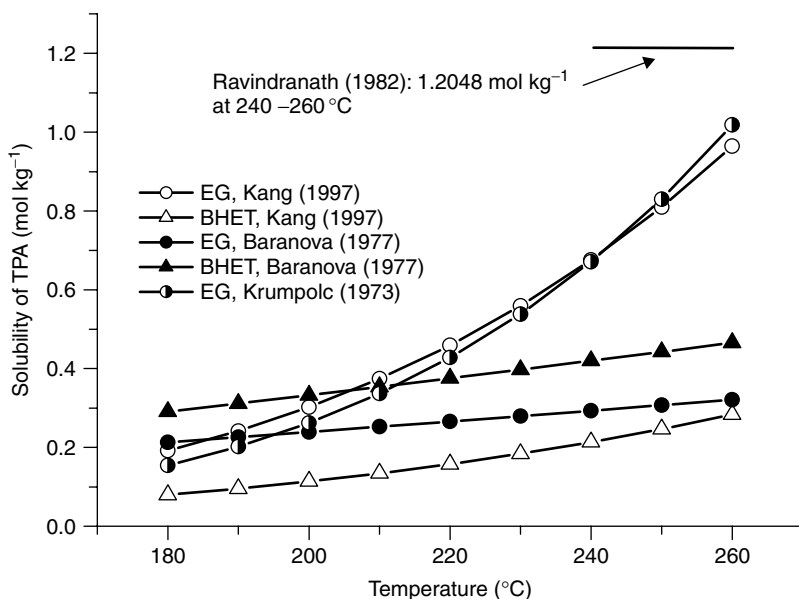


Figure 2.24 Solubility of TPA in EG and BHET at different temperatures, according to Ravindranath and Mashelkar [151], Krumpolc and Málek [26], Baranova and Kremer [93] and Kang *et al.* [7]

esterification. The rate of esterification is much higher than the dissolution rate of TPA. Therefore, the latter is the rate-determining step in the overall esterification process. For a rigorous modelling of the esterification process, reliable data for the solubility of TPA in prepolymer and for the dissolution rate are required.

The vapour pressures of the main volatile compounds involved in esterification and polycondensation are summarized in Figure 2.25. Besides EG and water, these are the etherification products DEG and dioxane, together with acetaldehyde as the main volatile product of thermal PET degradation. Acetaldehyde, water and dioxane all possess a high vapour pressure and diffuse rapidly, and so will evaporate quickly under reaction conditions. EG and DEG have lower vapour pressures but will still evaporate from the reaction mixture easily.

The vapour pressure of BHET is approximately three orders of magnitude lower than that of EG. Nevertheless, evaporation of BHET still occurs in significant amounts under vacuum. In Figure 2.26, the experimentally determined vapour pressure of BHET is compared to the vapour pressure predicted by the Unifac group contribution method [95]. The agreement between the measured and calculated values is quite good. In the open literature, no data are available for the vapour pressure of dimer or trimer and so a prediction by the Unifac method is shown in Figure 2.26. The correspondence between measured and predicted data for BHET indicates that the calculated data for dimer and trimer

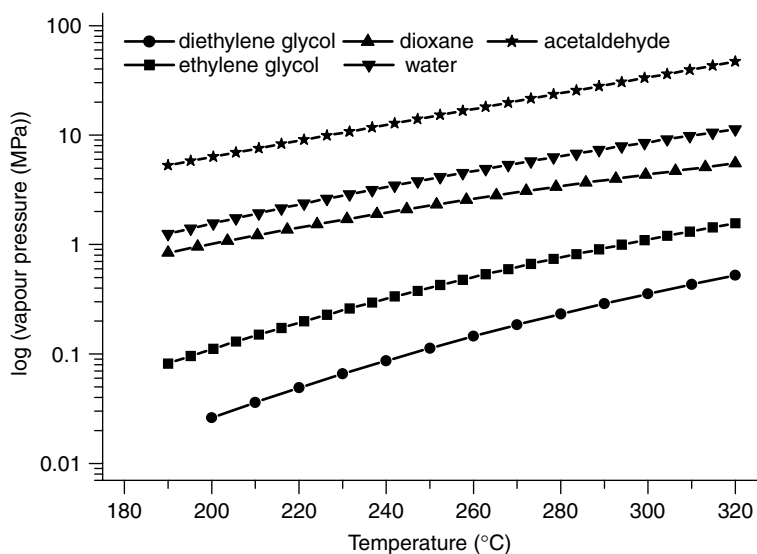


Figure 2.25 Vapour pressures of acetaldehyde, water, dioxane, ethylene glycol and diethylene glycol, where the data have been calculated from the database of the commercial process simulator *Chemcad* (Chemstations)

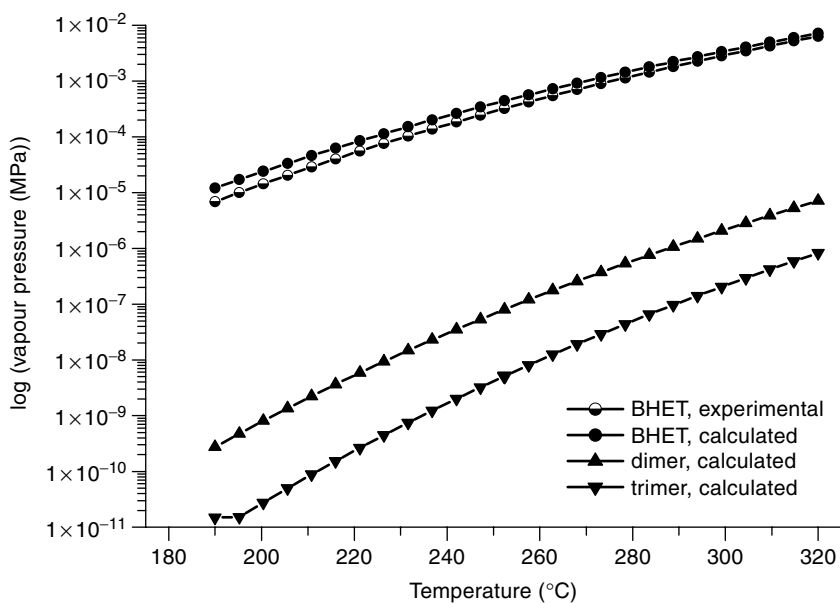


Figure 2.26 Calculated vapour pressures of BHET, dimer and trimer, compared to experimental data obtained for BHET

may be useful. According to these data, the vapour pressure of dimer is much lower than that of BHET and dimer evaporation should be insignificant, which is confirmed by our own experiments [94].

Roult's law is known to fail for vapour–liquid equilibrium calculations in polymeric systems. The *Flory–Huggins* relationship is generally used for this purpose (for details, see 'mass-transfer models' in Section 3.2.1). The polymer–solvent interaction parameter, χ_i , of the Flory–Huggins equation is not known accurately for PET. Cheong and Choi used a value of 1.3 for the system PET/EG for modelling a rotating-disc reactor [113]. For other polymer solvent systems, χ_i was found to be in the range between 0.3 and 0.5 [96].

Solid PET feedstock for the SSP process is semicrystalline, and the crystalline fraction increases during the course of the SSP reaction. The crystallinity of the polymer influences the reaction rates, as well as the diffusivity of the low-molecular-weight compounds. The crystallization rate is often described by the Avrami equation for auto-accelerating reactions: $(1 - \chi_c) = \exp(-k_c t^n)$, with χ_c being the mass fraction crystallinity, k_c the crystallization rate constant and n a function of nucleation growth and type.

Crystallization of PET proceeds in two distinct steps [97], i.e. (1) a fast primary crystallization which can be described by the Avrami equation, and (2) a slow secondary crystallization which can be described by a rate being proportional to the crystallizable amorphous fraction: $d\chi_c/dt = (\chi_{\max} - \chi_c)k_c$, with χ_{\max} being the maximum crystallinity (mass fraction) [98]. Under SSP conditions, the primary crystallization lasts for a few minutes before it is replaced by secondary crystallization. The residence time of the polymer in the reactor is of the order of hours to days and therefore the second rate equation can be applied for modelling the SSP process.

3.2 DIFFUSION AND MASS TRANSFER IN MELT-PHASE POLYCONDENSATION

By the 1960s, it was already well known that the polycondensation rate can be enhanced considerably if the low-molecular-weight by-products are removed at a sufficient rate. Many patent applications for polycondensation reactors describe inventions especially suited for the efficient removal of volatile components. Nevertheless, a good understanding of the interaction of chemical reactions and mass transport was still lacking at that time.

Stevenson [99] conducted the first polycondensation experiments with thin polymer melt films of 0.07–5 mm thickness. The experiments were performed on metal surfaces at temperatures between 265 and 285 °C under vacuum. He varied the kind of metal and observed that the behaviour of the polycondensation rate with decreasing film thickness depended on the metal being used. He concluded that the reaction rate increased only on metals soluble in the polymerizing melts

and ascribed this to an inactivation of the volatile compounds by a reversible interaction with the metal, thus resulting in a shifting of the polycondensation equilibrium.

Hoftyzer and van Krevelen [100] investigated the combination of mass transfer together with chemical reactions in polycondensation, and deduced the rate-determining factors from the description of gas absorption processes. They proposed three possible cases for polycondensation reactions, i.e. (1) the polycondensation takes place in the bulk of the polymer melt and the volatile compound produced has to be removed by a physical desorption process, (2) the polycondensation takes place exclusively in the vicinity of the interface at a rate determined by both reaction and diffusion, and (3) the reaction zone is located close to the interface and mass transport of the reactants to this zone is the rate-determining step.

Schumann [10] investigated stirred and non-stirred PET films between 0.1 and 1.5 mm thickness at temperatures between 280 and 290 °C. This worker rejected Stevenson's interpretation of the metal deactivating the volatile compound (mainly due to lacking experimental thoroughness) and conducted his own experiments. He concluded that the overall rate of polycondensation is determined by mass transport of EG in every film with a thickness of more than 0.2 mm.

In 1973, Bonatz *et al.* [101] finally showed by carefully performed experiments that the first reaction model proposed by Hoftyzer and van Krevelen [100] is correct. Thus, the polycondensation reaction (transesterification of bEG) takes place in the entire melt phase and the removal of EG is the rate-determining step for the overall polycondensation process.

Currently, the accepted interpretation of experimental evidence is that the polycondensation of PET in industrial reactors is dominantly controlled by diffusion of EG in the melt phase [1, 6, 8, 102–110].

In Figure 2.27, the good quality experimental data of Rafler *et al.* [106] for the antimony acetate catalyzed polycondensation under vacuum are shown, demonstrating the dependency of the overall polycondensation rate on the polymer film thickness.

Data for the uncatalyzed polycondensation from STA (simultaneous TGA/DTA) experiments under high-flow inert gas at atmospheric pressure [8] are shown in Figure 2.28. These data also demonstrate the dependency of the overall polycondensation rate on the polymer film thickness.

We will now describe the application of the two principal methods for considering mass transport, namely mass-transfer models and diffusion models, to PET polycondensation. Mass-transfer models group the mass-transfer resistances into one mass-transfer coefficient $k_{i,j}$, with a linear concentration term being added to the material balance of the volatile species. Diffusion models employ Fick's concept for molecular diffusion, i.e. $J = -D_{i,\text{PET}}\partial c_i/\partial x$, with J being the molar flux and $D_{i,j}$ being the mutual diffusion coefficient. In this case, the second derivative of the concentration to x , $D_{i,\text{PET}}\partial^2 c_i/\partial x^2$, is added to the material balance of the volatile species.

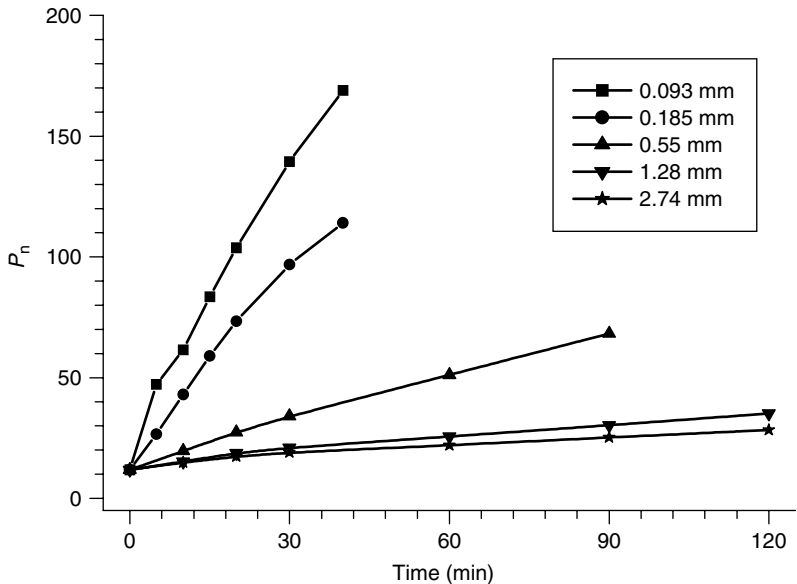


Figure 2.27 Dependency of the overall polycondensation rate on polymer film thickness, according to Rafler *et al.* [106]

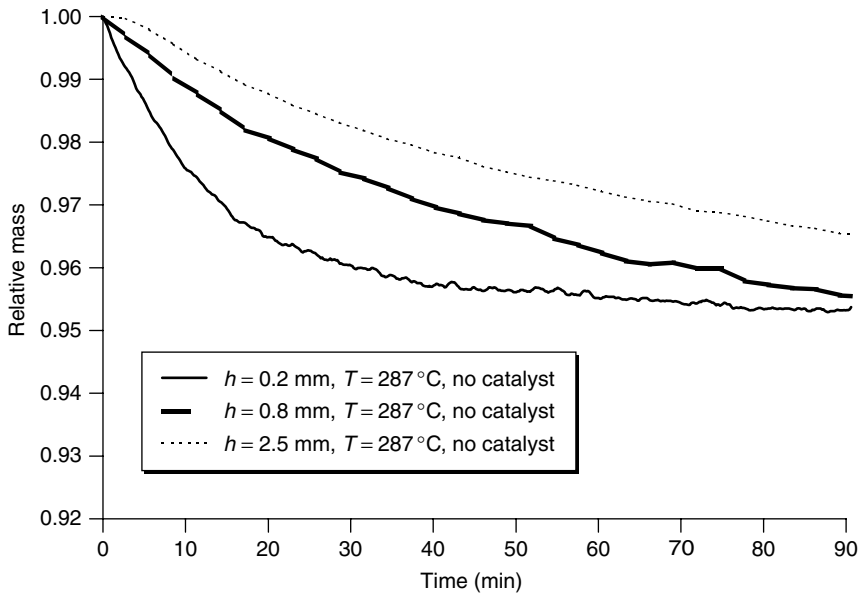


Figure 2.28 Dependency of the reaction progress on film thickness and time: PET esterification product (prepolymer, $\bar{P}_{n,0} = 2-3$), with no catalyst added [8]

3.2.1 Mass-Transfer Models

The volatilization of low-molecular-weight by-products from molten PET can be described by using the classical two-film model or the penetration theory of interfacial transport [95].

Rafler *et al.* [105] applied the two-film model to the mass transfer of different alkane diols in poly(alkylene terephthalate) melts and demonstrated a pressure dependency of the mass-transfer coefficient in experiments at 280 °C in a small 3.6 L stirred reactor. They concluded that the mass-transfer coefficient $k_{l,j}$ is proportional to the reciprocal of the molecular weight of the evaporating molecule.

Laubriet *et al.* [111] modelled the final stage of polycondensation by using the set of reactions and kinetic parameters published by Ravindranath and Mashelkar [112]. They used a mass-transfer term in the material balances for EG, water and DEG adapted from film theory: $J = (k_l a)_i (c_i - c_i^*)$, with c_i^* being the interfacial equilibrium concentration of the volatile species i .

This equilibrium concentration c_i^* , or the corresponding mole fraction x_i^* , of EG, water and DEG in the interface can be calculated from the vapour pressure and the activity coefficient γ_i derived from the Flory–Huggins model [13–17]. Laubriet *et al.* [111] used the following correlations (with T in K and P in mm Hg) for their modelling:

$$\ln P_{\text{EG}}^0 = 49.703 - 8576.7/T - 4.042 \ln(T) \quad (2.4)$$

$$\ln P_{\text{w}}^0 = 18.568 - \frac{4047.606}{T - 33.3} \quad (2.5)$$

$$\ln P_{\text{DEG}}^0 = 17.0326 - \frac{4122.52}{T - 122.5} \quad (2.6)$$

$$x_i^* = \frac{P}{\gamma_i P_i^0} \quad (2.7)$$

$$\gamma_i = \ln \left[1 - \left(1 - \frac{1}{m_i} \right) \Phi_2 \right] + \left(1 - \frac{1}{m_i} \right) \Phi_2 + \chi_i \Phi_2 \quad (2.8)$$

with subscripts i representing EG, water or DEG and subscript 2 representing the polymer, respectively; Φ_2 is the volume fraction of polymer, χ_i the polymer–solvent interaction parameter ($\chi_{\text{PET}} = 1.3$ for EG), and m_i the ratio of molar volumes of polymer and species i . As the mole fraction of i is very small, $\Phi_2 \approx 1$, and Equation (2.8) is reduced to the following [113, 114]:

$$\gamma_i = \frac{1}{m_i} \exp \left(1 - \frac{1}{m_i} + \chi_{\text{PET}} \right) \quad (2.9)$$

Rieckmann *et al.* introduced a mass-transfer concept with a mass-transfer coefficient depending on the average molecular weight of the polymer, the melt

viscosity and the temperature [115]. According to the penetration theory, the mass-transfer coefficient $k_{L,i}$ is proportional to the square root of the diffusion coefficient, $D_{i,PET}$. The *Wilke–Chang* technique (an empirical modification of the Stokes–Einstein relationship) was used where the mutual diffusion coefficient of a species at very low concentrations in a solvent is proportional to $\overline{M}_n^{0.5}$, T and $1/\eta$ of the solvent [95]. This leads to the mass-transfer coefficient being a function of the average molecular weight, the temperature and the melt viscosity of the polymer: $k_{L,i} = k_{L,i}(M_n^{0.25}, T^{0.5}, 1/\eta^{0.5})$. Figure 2.29 shows the dependency of $k_{L,i}$ on the degree of polycondensation obtained by multivariate regression of data from polycondensation experiments with STA analysis at temperatures of 267, 277, 287, 297 and 307 °C, and polymer film thicknesses of 0.2, 0.8 and 2.5 mm. For the calculation of the mass-transfer coefficient, a comprehensive reaction model with kinetic parameters taken from the literature was used. For long-chain polymers, the mass-transfer coefficient indicates an asymptotic behaviour which becomes less dependent on the chain length, as suggested by molecular modelling approaches.

3.2.2 Diffusion Models

The diffusion coefficient of EG in molten PET has been discussed for several decades. Most of the data were gained for polycondensation at a temperature

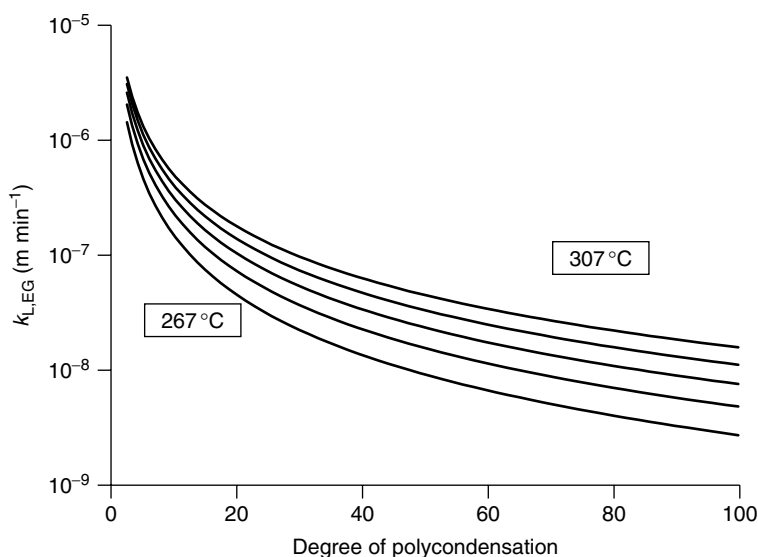


Figure 2.29 Mass-transfer coefficient, $k_{L,EG}$, in molten PET as a function of polycondensation and temperature for the uncatalyzed polycondensation (no additional metal catalyst added) of esterification product ($\overline{P}_{n,0} = 2-3$) at atmospheric pressure [115]

of 270 °C and the published diffusion coefficients differ by approximately three orders of magnitude. Data for the diffusion coefficient of water are sparse and have mostly been estimated [106]. No experiments at all have been performed on the diffusion of DEG or acetaldehyde in PET melts and the diffusion of acetaldehyde is usually modelled as being infinitely fast.

Rafler *et al.* showed in an early work [102] that the diffusion coefficient of EG varies with the overall effective polycondensation rate and they proposed a dependency of the diffusion coefficient on the degree of polycondensation. This dependency is obvious, because the diffusion coefficient is proportional to the reciprocal of the viscosity which increases by four orders of magnitude during polycondensation from approximately 0.001 Pa s (for $\overline{P}_n = 3$) to 67 Pa s (for $\overline{P}_n = 100$) at 280 °C. In later work, Rafler *et al.* [103, 104, 106] abandoned the varying diffusion coefficient and instead added a convective mass-transport term to the material balance of EG and water. The additional model parameter for convection in the polymer melt and the constant diffusion coefficient were evaluated by data fitting.

Zimmerer also supposed in his Ph.D. thesis [110] a dependency of the diffusion coefficient of EG on the melt viscosity. For the uncatalyzed polycondensation of BHET, the diffusion coefficient was found to be one order of magnitude higher than for the catalyzed polycondensation and it was deduced that this is due to the lower melt viscosity in the uncatalyzed case (lower resulting \overline{P}_n). These findings were supported by molecular modelling. The diffusion coefficient of EG in BHET was calculated as $D_{\text{EG,BHET}} = 3.9 \times 10^{-9} \text{ m}^2/\text{s}$, while the diffusion coefficient of EG in PET with $\overline{P}_n = 40$ was calculated as $D_{\text{EG,PET}} < 3 \times 10^{-10} \text{ m}^2/\text{s}$.

Rieckmann and Völker [8] performed polycondensation experiments with varying film thicknesses in an STA study. They investigated a mass-transport concept with diffusion coefficients of EG and water being a function of temperature, average molecular weight of the polymer and melt viscosity. Early experiments showed that the diffusion coefficients do not depend only on temperature as described in the literature and that the temperature dependency is not linear. An application of the Wilke–Chang equation for diffusion coefficients in its original definition was also not successful for describing the mass transport of EG and water in molten PET. With this equation, the influence of the temperature was underrated, while the influence of the melt viscosity was overestimated. Instead, a distinct improvement of the Wilke–Chang model was achieved by introducing an Arrhenius-like temperature dependency, which had also been proposed by Lee *et al.* [109], and molecular modelling. The Wilke–Chang model was further modified by assuming a weaker dependency on melt viscosity and the diffusion coefficients for EG and water were calculated by the equation $D_{i,\text{PET}} = D_{0,i} \exp(-E_{a,D}/RT) \overline{M}_n^{0.5} / \eta^{0.5}$. The results obtained for $D_{\text{EG,PET}}$ are shown in Figure 2.30. In this work, it was assumed that the ratio of the diffusion coefficients of water and EG depends on the ratio of their molecular weights

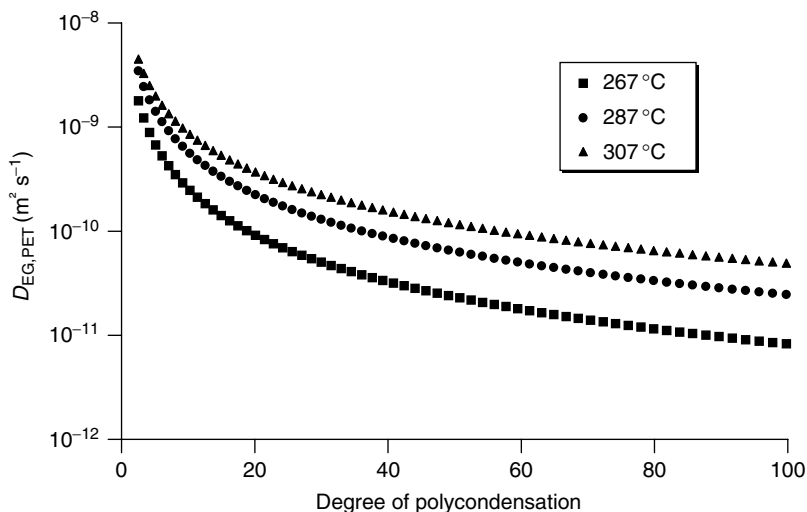


Figure 2.30 Diffusion coefficient, $D_{EG,PET}$, in molten PET films as a function of degree of polycondensation and temperature [8]

and the diffusion coefficient of water was fixed to $D_{W,PET} = 62(g/mol)/18(g/mol) D_{EG,PET}$. The modelling indicated that the diffusion coefficient of water is not a very sensitive parameter.

It was shown that the modified Wilke–Chang model was applicable for experiments which span a range of \bar{P}_n between 3 and 30 and a temperature range between 267 and 307 °C. An important finding was that even at $\bar{P}_n < 30$, the mass transport of EG is the rate-determining step in PET synthesis.

Rieckmann and Völker fitted their kinetic and mass transport data with simultaneous evaluation of experiments under different reaction conditions according to the multivariate regression technique [116]. The multivariate regression enforces the identity of kinetics and diffusivities for all experiments included in the evaluation. With this constraint, model selection is facilitated and the evaluation results in one set of parameters which are valid for all of the conditions investigated. Therefore, kinetic and mass transfer data determined by multivariate regression should provide a more reliable data basis for design and scale-up.

Published data for the diffusion coefficient of EG have progressively decreased from approximate values between 10^{-8} and $10^{-10} m^2/s$ to values between 10^{-9} and $10^{-11} m^2/s$ at 270 °C. This decrease is accompanied by an increasing complexity of the proposed reaction mechanisms and by increasing values for the rate constants, which are less influenced by mass transport. The published data for the diffusion coefficient of EG in PET are summarized in Table 2.11.

Table 2.11 Diffusion coefficients for EG in molten PET at different temperatures

Working group (year)	Reference	$D_{\text{EG, PET}} (T) (\text{m}^2 \text{s}^{-1})$				
		265 °C	270 °C	275 °C	280 °C	290 °C
Hoflyzer and van Krevelen (1971)	100	1×10^{-9}	—	—	—	—
Pell and Davis (1973), $P_n = 50-120$	154	—	1.66×10^{-8}	—	—	—
Rafler <i>et al.</i> (1979)	102	—	2.94×10^{-9}	—	—	—
Rafler <i>et al.</i> (1980)	103	—	8.2×10^{-10}	—	—	—
Rafler, <i>et al.</i> (1985)	105	—	1.0×10^{-9}	—	1.6×10^{-9}	2.2×10^{-9}
Rafler <i>et al.</i> (1987)	106	—	2.8×10^{-9}	—	—	—
D_{water}			1.0×10^{-9}			
Lee <i>et al.</i> (1992)	109	2.58×10^{-11}	7.92×10^{-11}	1.11×10^{-10}	—	—
$E_D = 161 \text{ kJ/mol}$						
Zimmerer (1997)	110	—	3.9×10^{-9}	—	—	—
$P_n < 20$			3.0×10^{-10}			
$P_n = 40$						
Rieckmann and Völker (2001)	8	8.3×10^{-11}	1.1×10^{-10}	1.3×10^{-10}	1.7×10^{-10}	2.6×10^{-10}
$P_n = 20$		2.9×10^{-11}	3.7×10^{-11}	4.7×10^{-11}	6.0×10^{-11}	9.8×10^{-11}
$P_n = 40$						
$E_D = 103 \text{ kJ/mol}$						

3.2.3 Specific Surface Area

The crucial aspect of the interface mass-transfer model, as well as the diffusion model, is the estimation of the specific surface area or the characteristic length. For the modelling of existing equipment, these parameters can easily be fitted by using experimental data. If modelling is performed for the development of new reactor designs or the extensive scale-up of small reactors, then the specific surface area or the characteristic length have to be calculated reliably beforehand, using geometric data only.

The specific surface area of an industrial-sized continuous stirred tank reactor (CSTR) can be calculated from the reactor dimensions. However, it is difficult to estimate the effect of the formation of bubbles and of the stirrer-induced vortex at low melt viscosity. The calculation of the characteristic length of diffusion in a high-viscosity finishing reactor with devices for the generation of thin films with respective high specific surface areas is more complex.

Laubriet *et al.* [111] used a correlation for the specific surface area in disc-ring reactors as proposed by Dietze and Kuhne [117]:

$$a = \frac{N(1.72 - 1.87h/d)}{L(0.085 + 0.955h/d)} \quad (2.10)$$

with N being the number of disc rings, h the filling level, d the disc diameter and L the distance between the discs. This type of correlation cannot be used for scale-up or the estimation of the surface area in different reactor designs without experimental determination of the respective correlation parameters.

More promising are correlations according to the Buckingham-PI theorem [118], such as the correlation published by Vijayraghvan and Gupta [119]:

$$T = 7.99Ca^{2.93}\varphi^{0.15}\Re^{5.23}Cas^{-3.08}\chi^{0.024} \quad (2.11)$$

with T being the dimensionless film thickness ($(\rho g/\eta r\Omega)^{0.5}$), Ca the capillary number ($\eta\Omega r/\sigma$), φ a dimensionless surface tension number depending on fluid properties only, \Re a dimensionless number accounting for the dependency of the film shape on the depth to which the disc is immersed in the fluid, Cas a modified capillary number ($\eta\Omega R/\sigma$), and χ a dimensionless number accounting for the variation in the radial component of the acceleration due to gravity ($\Omega^2 R_0/g - \sin(\theta)$). The model compounds used for the experiments were water ($\sigma = 0.070$ N/m; $\eta = 0.00089$ Pa s; $\rho = 1000$ kg/m³), glycerol ($\sigma = 0.067$ N/m; $\eta = 0.0131$ Pa s; $\rho = 1164$ kg/m³) and vacuum pump oil ($\sigma = 0.03$ N/m; $\eta = 0.7826$ Pa s; $\rho = 910$ kg/m³). In Figure 2.31, the film thickness is shown as a function of the melt viscosity for different radial positions on the discs of a finishing reactor for two liquids with different surface tensions.

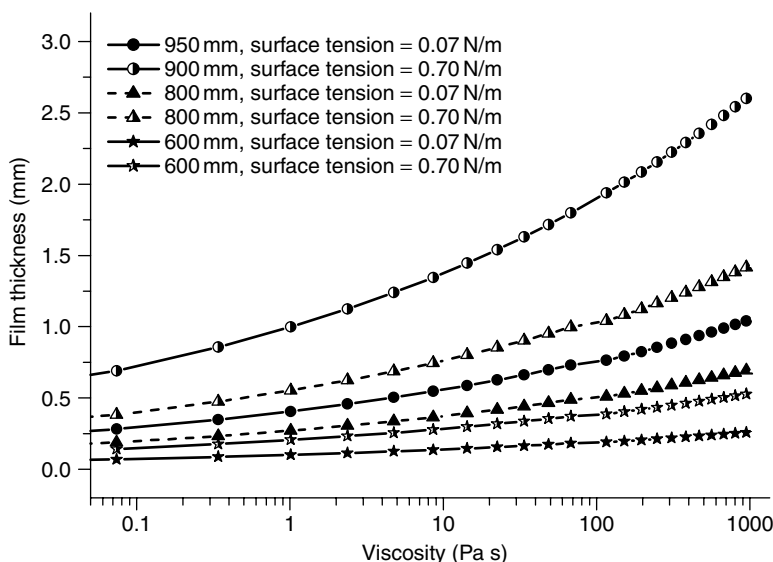


Figure 2.31 Film thickness on the discs of a finishing reactor as a function of melt viscosity for different radial positions: disc radius, 1 m; frequency, 5 min^{-1} ; surface tension, 0.7 and 0.07 N/m. Calculated by using the correlation proposed by Vijayraghvan and Gupta [119]

Cheong and Choi [113] and Soroka and Tallmadge [120] also estimated correlations according to the Buckingham-PI theorem. Both groups used other dimensionless parameter sets to those used by Vijayraghvan and Gupta and the modelling results of these groups did not represent their experimental data too well. The deviations may be due to the fact that neither the melt viscosity nor the surface tension were included in the correlations. Such properties are non-linear functions of the temperature as well as of the molecular weight (and respectively the melt viscosity). Although the surface tension of molten PET is a key parameter for the film thickness, reliable data are still not yet available.

3.3 DIFFUSION AND MASS TRANSFER IN SOLID-STATE POLYCONDENSATION

Depending on the size and shape of the polymer particles, solid-state polycondensation (SSP) is performed at temperatures between 220 and 235 °C, which lie above the glass transition temperature ($\approx 70\text{--}85^\circ\text{C}$) and below the melting point (measured by DSC $\approx 245\text{--}255^\circ\text{C}$) of PET. The temperature range for operation of SSP is rather small because on the one hand, the temperature should be as

high as possible to maximize the reaction rate, but on the other hand has to be sufficiently below the melting point to prevent sticking of the polymer particles.

The chemistry of the solid-state polycondensation process is the same as that of melt-phase polycondensation. Most important are the transesterification/glycolysis and esterification/hydrolysis reactions, particularly, if the polymer has a high water concentration. Due to the low content of hydroxyl end groups, only minor amounts of DEG are formed and the thermal degradation of polymer chains is insignificant at the low temperatures of the SSP process.

Care has to be taken when extrapolating kinetic parameters measured under melt-phase conditions for describing the solid-state reaction. The available kinetic data are not free from mass-transfer influences and the effects of proton and metal catalysis are not thoroughly separated. Therefore, the adaptation of kinetic parameters is often carried out by fixing the activation energies and adjusting the pre-exponential factors to the experimental data.

Two approaches are common in modelling the SSP process. For the first approach, an overall reaction rate is used which describes the polycondensation rate in terms of the increase of intrinsic viscosity with time. Depending on the size and shape of the granules, the reaction temperature, the pressure, and the amount and type of co-monomers, the overall polycondensation rate lies between 0.01 and 0.03 dL/g/h. The reaction rate has to be determined experimentally and can be used for reactor scale-up, but cannot be extrapolated to differing particle geometry and reaction conditions.

The second approach employs a detailed reaction model as well as the diffusion of EG in solid PET [98, 121–123]. Commonly, a Fick diffusion concept is used, equivalent to the description of diffusion in the melt-phase polycondensation. Constant diffusion coefficients lying in the order of $D_{\text{EG, PET}}(220^\circ\text{C}) = 2\text{--}4 \times 10^{-10} \text{ m}^2/\text{s}$ are used, as well as temperature-dependent diffusion coefficients, with an activation energy for the diffusion of approximately 124 kJ/mol.

In SSP, the boundaries for the mass balances are defined by the particle instead of the reactor or the reactor compartment dimensions and the process conditions are accounted for by a boundary condition. The mass transfer at the particle/gas interface is mostly described according to the film theory by using a mass-transfer coefficient.

The papers of Mallon and Ray [98, 123] can be regarded as the state of the art in understanding and modelling solid-state polycondensation. They assumed that chain ends, catalysts and by-products exist solely in the amorphous phase of the polymer. Because of the very low mobility of functional groups in the crystalline phase, the chemical reactions are modelled as occurring only in the amorphous phase. Additionally, the diffusion of by-products is hindered by the presence of crystallites. The diffusivity of small molecules was assumed to be proportional to the amorphous fraction. Figure 2.32 shows the diffusion coefficients for the diffusion of EG and water in solid PET.

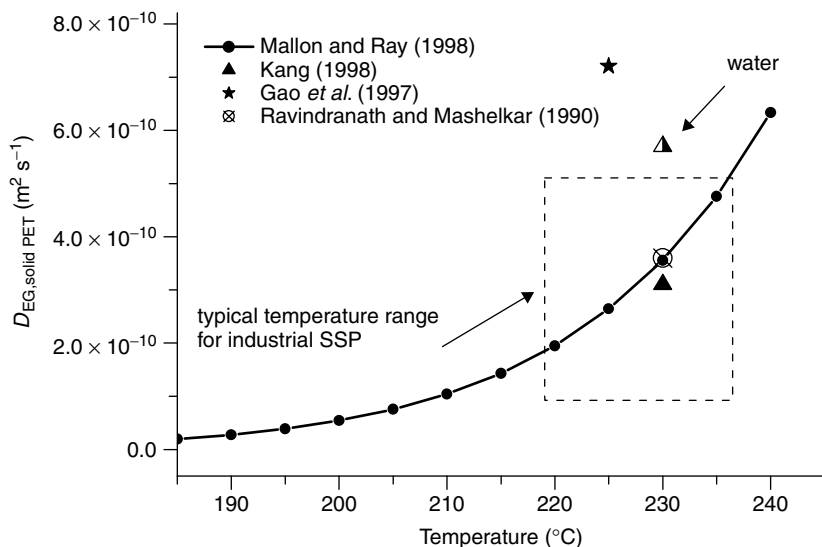


Figure 2.32 Diffusion coefficients for EG and water in solid PET at different temperatures, according to Mallon and Ray [98], Kang [122], Gao *et al.* [155] and Ravindranath and Mashelkar [121]

3.4 CONCLUSIONS

Both the mass-transfer approach as well as the diffusion approach are required to describe the influence of mass transport on the overall polycondensation rate in industrial reactors. For the modelling of continuous stirred tank reactors, the mass-transfer concept can be applied successfully. For the modelling of finishers used for polycondensation at medium to high melt viscosities, the diffusion approach is necessary to describe the mass transport of EG and water in the polymer film on the surface area of the stirrer. Those tube-type reactors, which operate close to plug-flow conditions, allow the mass-transfer model to be applied successfully to describe the mass transport of volatile compounds from the polymer bulk at the bottom of the reactor to the high-vacuum gas phase.

Every process step of PET synthesis, from direct esterification, and respectively transesterification, of DMT, through melt-phase polycondensation to SSP and recycling, has been modelled by different working groups. Some interesting publications are summarized in Table 2.12. The reactions which are necessary to describe the evolution of the degree of polycondensation and the formation of by-products are agreed upon by many working groups although reaction models with reduced complexity are sometimes used. In contrast, the model parameters that are used differ considerably. Published diffusion coefficients vary by orders of magnitude and mass-transfer coefficients are always given in the form of $k_{L,i}a$

Table 2.12 Publications on the modelling of batch and continuous esterification, transesterification, polycondensation, and recycling of PET

Year	Working group	Reference	Mode of operation	Process stage	Type of reactor
1981	Ravindranath and Mashelkar	88	Semi-batch	Ester interchange	Stirred tank reactor
1982	Ravindranath and Mashelkar	92	Continuous	Transesterification	Stirred tank reactor
1982	Ravindranath and Mashelkar	150	Semi-batch	Prepolycondensation	Stirred tank reactor
1982	Ravindranath and Mashelkar	151	Continuous	Esterification	Stirred tank reactor cascade
1982	Ravindranath and Mashelkar	152	Continuous	Prepolycondensation	Stirred tank reactor cascade
1982	Ravindranath and Mashelkar	156	Continuous	Polycondensation, finisher	Tube reactor, disc type
1984	Ravindranath and Mashelkar	112	Continuous	Polycondensation, finisher	Tube reactor, disc type
1990	Ravindranath and Mashelkar	121	Unsteady state	Solid-state polycondensation	Particle

(continued overleaf)

Table 2.12 (*continued*)

Year	Working group	Reference	Mode of operation	Process stage	Type of reactor
1991	Martin and Choi	157	Continuous	Polycondensation, finisher	Tube reactor
1991	Laubriet <i>et al.</i>	111	Continuous	Polycondensation, finisher	Tube reactor, disc type
1995	Cheong and Choi	113	Continuous	Polycondensation, finisher	Tube reactor, disc type
1996	Cheong and Choi	114	Continuous	Polycondensation, finisher	Tube reactor, disc type
1996	Kang <i>et al.</i>	158	Semi-batch	Esterification	Stirred tank reactor
1997	Kang <i>et al.</i>	7	Continuous	Esterification	Stirred tank reactor
1997	Zhi-Lian and Gerkin	155	Unsteady state	Solid-state polycondensation	Particle
1998	Kang	122	Unsteady state	Solid-state polycondensation	Particle
1998	Mallon and Ray	98	Unsteady state	Solid-state polycondensation	Particle
1998	Mallon and Ray	123	Continuous	Solid-state polycondensation	Tube reactor
1999	Samant and Ng	159	Continuous	Esterification, prepolycondensation	Reactive distillation column
2001	Bashkar <i>et al.</i>	160	Continuous	Polycondensation, finisher	Tube reactor, wiped film
2001	Rieckmann and Völker	8	Semi-batch	Polycondensation	Crucible of TGA

and $k_{G,i}a$ due to the difficulty of calculating true surface areas. Published activation energies are more or less consistent but pre-exponential factors are often fitted to experimental or plant data and vary also by many orders of magnitude. Different catalysts are used and their influence on the individual reactions is still not fully quantified. Data for the kinetics of yellowing or for the reactions of co-monomers such as IPA or CHDM are not yet available.

In conclusion, the goal of predictive process modelling has not yet been achieved due to the interference of chemical reactions with mass transport. All polycondensation models and process simulators available in the public domain, such as *Polymer Plus* from AspenTech or *Predici* from CIT, as well as 'in-house' polycondensation models from engineering companies and producers, cannot be used for design or scale-up successfully without the use of fitting parameters.

4 POLYCONDENSATION PROCESSES AND POLYCONDENSATION PLANTS

PET is produced continuously on a large scale as well as in small-sized batch plants. Currently, batch plants are mainly used for specialities and niche products. Batch plant capacities span the range from 20 to 60 t/d. Depending on process conditions, process technology and the desired PET grade, six to ten batches per day are commonly manufactured, each with a capacity of between 1.5 and 9.0 t. Batch plants are often designed as multi-purpose plants in which also PBT, PEN and different co-polyesters are produced.

The increasing demand for PET gave rise to the development of continuously operated large-scale plants. As shown in Figure 2.33, the capacity of continuous PET plants has grown since the late 1960s from 20 t/d to presently 600 t/d in a single line, with the tendency to still higher capacities.

Direct spinning plants for filaments and fibres that are fed by large-scale continuously operated melt polycondensation plants have become the state of the art in downstream fibre processing, although the direct-feed preforming process for bottle production is still under development. The main reasons for this are an increased acetaldehyde content and an undesired colouring of the polymer, with increasing residence time in the melt. For tyre-cord PET grades with very high molecular weights of 40 000 to 50 000 g/mol ($IV > 1.00$ dL/g), colour and acetaldehyde content are not thus important and these fibres can be produced by using special high-melt-viscosity reactors and direct spinning.

To increase the PET molecular weight beyond 20 000 g/mol ($IV = 0.64$ dL/g) for bottle applications, with minimum generation of acetaldehyde and yellowing, a further polycondensation is performed in the solid state at low reaction temperatures of between 220 and 235 °C. The chemistry of the solid-state polycondensation (SSP) process is the same as that for melt-phase polycondensation. Mass-transport limitation and a very low transesterification rate cause the necessary residence time to increase from 60–180 minutes in the melt phase to

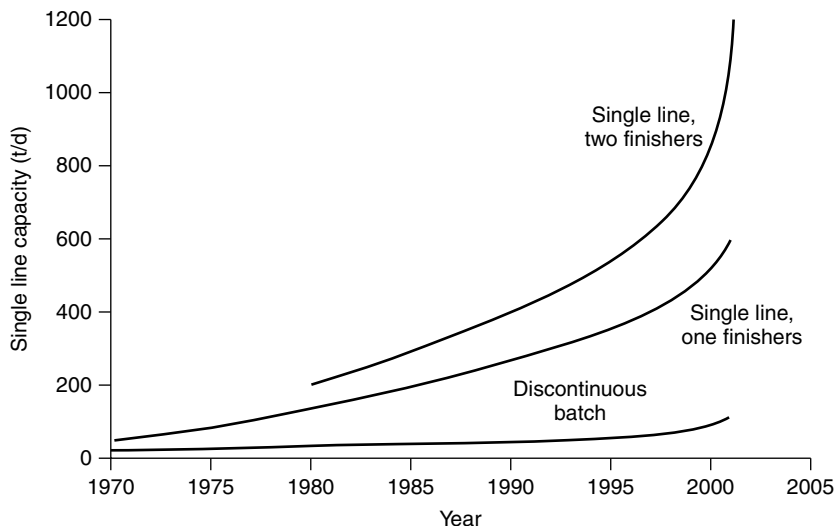


Figure 2.33 Capacity development of continuous and discontinuous PET plants [2]. From manufacturer's literature published by Zimmer AG and reproduced with permission

8–24 hours in the solid state. As the activation energies for the polycondensation and esterification reactions are lower than for the undesired degradation reactions, polycondensation in the solid state is not significantly affected by side reactions. The technology of the SSP process is described in detail in a separate chapter of this present book.

4.1 BATCH PROCESSES

4.1.1 Esterification

Due to different residence times needed for the esterification and the polycondensation steps, the industrial-batch polycondensation process is designed with two main reactors, i.e. one esterification reactor and one or two parallel polycondensation reactors (Figure 2.34).

The monomers TPA and EG are mixed upstream to the esterification reactor in a jacketed slurry preparation unit equipped with a stirrer for highly viscous fluids (e.g. 'Intermig'). The typical molar ratio of EG to TPA lies between 1.1 and 1.3. The esterification temperature and the molar ratio of monomers are the main controlling factors for the average degree of polycondensation of the esterification product (prepolymer), as well as for its content of carboxyl end groups and DEG. The latter mainly occurs as randomly distributed units of the polymer molecules.

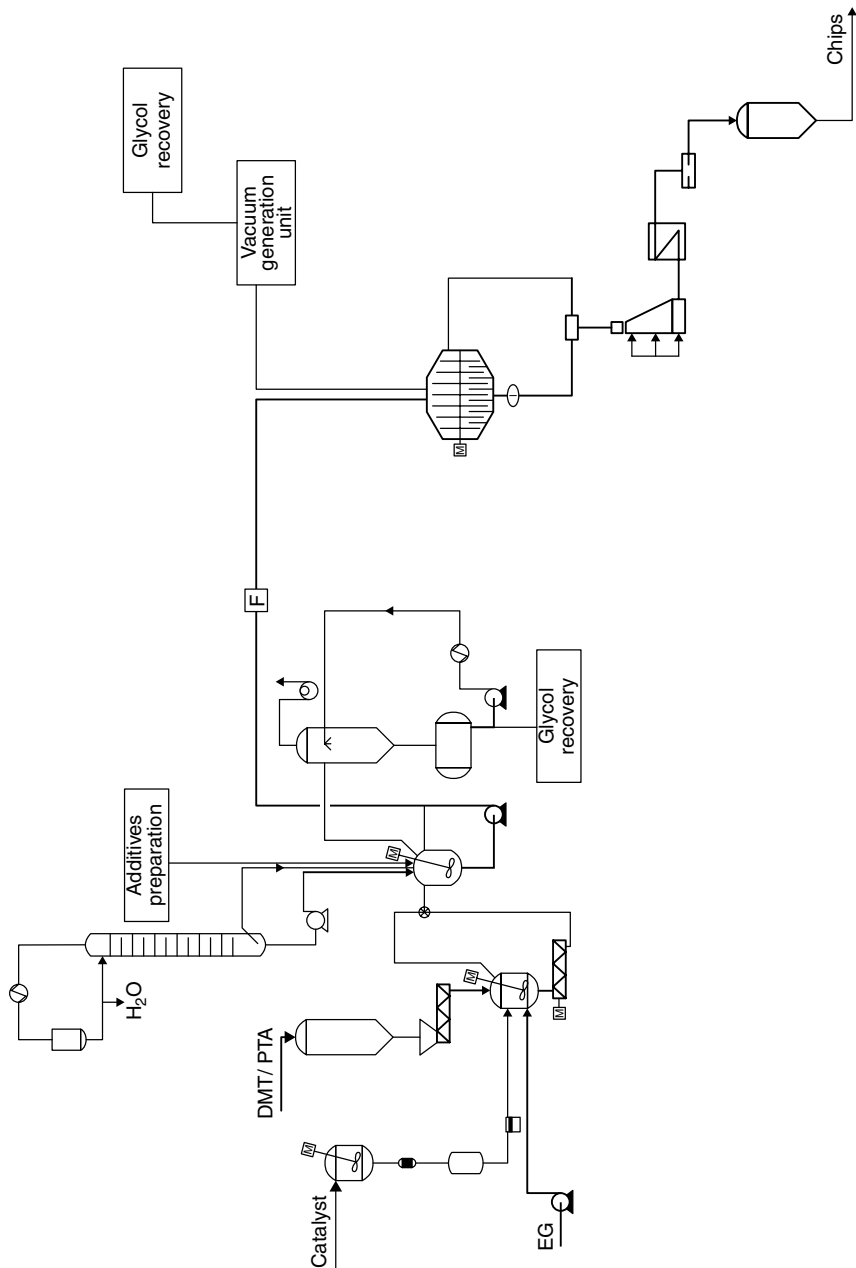


Figure 2.34 Simplified flow sheet of a multi-purpose discontinuous PET plant [2]. From manufacturer's literature published by Zimmer AG and reproduced with permission

The esterification reactor is usually not emptied completely after a batch is finished and a small amount of prepolymer is retained in the reactor. The reason for this is the solubility of TPA in EG and BHET, as discussed earlier in Section 3.1. During operation, the batch-wise prepared slurry is fed continuously into the esterification reactor while the esterification is already proceeding. For a significant part of the process time, the batch esterification reactor is operating semi-continuously.

The esterification by-product, water, is removed via a process column in a continuous steady-state mode of operation. The bottom product of the column, being mainly EG, flows back into the esterification reactor. The condensed top product consists mainly of water with small traces of EG. In cases where a reverse-osmosis unit is connected to the distillate flow line, the residual EG can be separated very efficiently from the water [124]. The combination of a process column with reverse osmosis saves energy cost and capital investment. The total organic carbon (TOC) value of the permeate is sufficiently low to allow its discharge into a river or the sea without any environmental impact.

The esterification of TPA is catalyzed by protons and in standard industrial operations neither an additional esterification catalyst nor a polycondensation catalyst is added to the esterification reactor. Some new 'antimony-free' polycondensation catalysts [125–128] also affect the speed of esterification significantly and it could be advantageous to add them directly into the slurry preparation vessel. Co-monomers, which should be randomly incorporated into the polymer chains, are usually fed into the slurry preparation vessel. How and when additives, catalysts, colorants and co-monomers are added influences the overall reaction rate and therefore affects the product quality.

The esterification temperature ranges between 235 and 265 °C, while the absolute pressure is controlled between ambient pressure and a slight overpressure (0.1–0.4 MPa). Accurate pressure control can be achieved by controlling a small additional nitrogen flow. This serves also as an inert-gas blanket to prevent oxygen from diffusing into the reacting melt which would cause polymer degradation. At the end of the esterification, the temperature is raised to values between 260 and 285 °C and the pressure is often reduced to a moderate vacuum, thus increasing the evaporation of excess EG. The final prepolymer is transported by pumps or nitrogen through a filter unit with 10 to 60 µm mesh size into the pre-heated polycondensation reactor.

The standard esterification reactor is a stirred tank reactor. Due to the required latent heat for the evaporation of EG and water, heating coils are installed in addition to the heating jacket. In some cases, an external heat exchanger, together with a recirculation pump, is necessary to ensure sufficient heat transfer. During esterification, the melt viscosity is low to moderate (ca. 20 to 800 mPa s) and no special stirrer design is required.

4.1.2 Polycondensation

In the polycondensation reactor, the prepolymer reacts, forming longer polymer chains and EG is liberated. To shift the chemical equilibrium to the product side, the by-product EG is removed via vacuum (ca. 1 mbar (100 Pa)). EG vapour jet pumps or mechanical rotary piston pumps are used for vacuum generation. In the first quarter of the polycondensation process, the reaction temperature is increased to values between 270 and 295 °C and the pressure is slowly reduced with time to avoid high carry-over of prepolymer into the vacuum system. The final degree of polycondensation is controlled by either setting the reaction time to a fixed value for operation under standard conditions or by stopping the reaction at a certain melt viscosity which can be correlated to the torque of the stirrer. The melt viscosity at 280 °C increases from approximately 0.8 to 400 Pa s during polycondensation.

Band or anchor stirrers are commonly used to renew the surface of the melt and to provide heat which is transferred into the melt by dissipation of the stirrer energy. The stirrer speed is reduced by a time programme to avoid overheating and reduce power consumption. Recently, a special disc-ring reactor was adapted from the continuous PET process for batch processes with high capacities. This reactor provides a high specific surface area and short diffusion lengths, thus maintaining high polycondensation rates at reduced temperatures (Figure 2.35).

After the polycondensation is finished, the vacuum valve to the polycondensation reactor is closed and the vessel is emptied by nitrogen pressure or gear pumps. When the latter are used for this purpose, the reactor can be discharged under vacuum which avoids glycolytic degradation of the polymer by maintaining a low EG partial pressure. The PET strands are cooled by water or by air and water. After solidification, the strands are cut into small granules. The granule size and shape controls the overall polycondensation rate in the SSP process as well as the time for re-melting in processing extruders.

Figure 2.36 presents some typical process data and the evolution of polymer properties during the synthesis of PET from TPA and EG in a batch plant.

4.2 CONTINUOUS PROCESSES

The continuous polycondensation process consists of four main process units, i.e. (1) slurry preparation vessel, (2) reaction unit, (3) vacuum system, and (4) distillation unit. The molar EG/TPA ratio is adjusted to an appropriate value between 1.05 and 1.15 in the slurry preparation vessel. In most industrial processes, the melt-phase reaction is performed in three up to six (or sometimes even more) continuous reactors in series. Commonly, one or two esterification

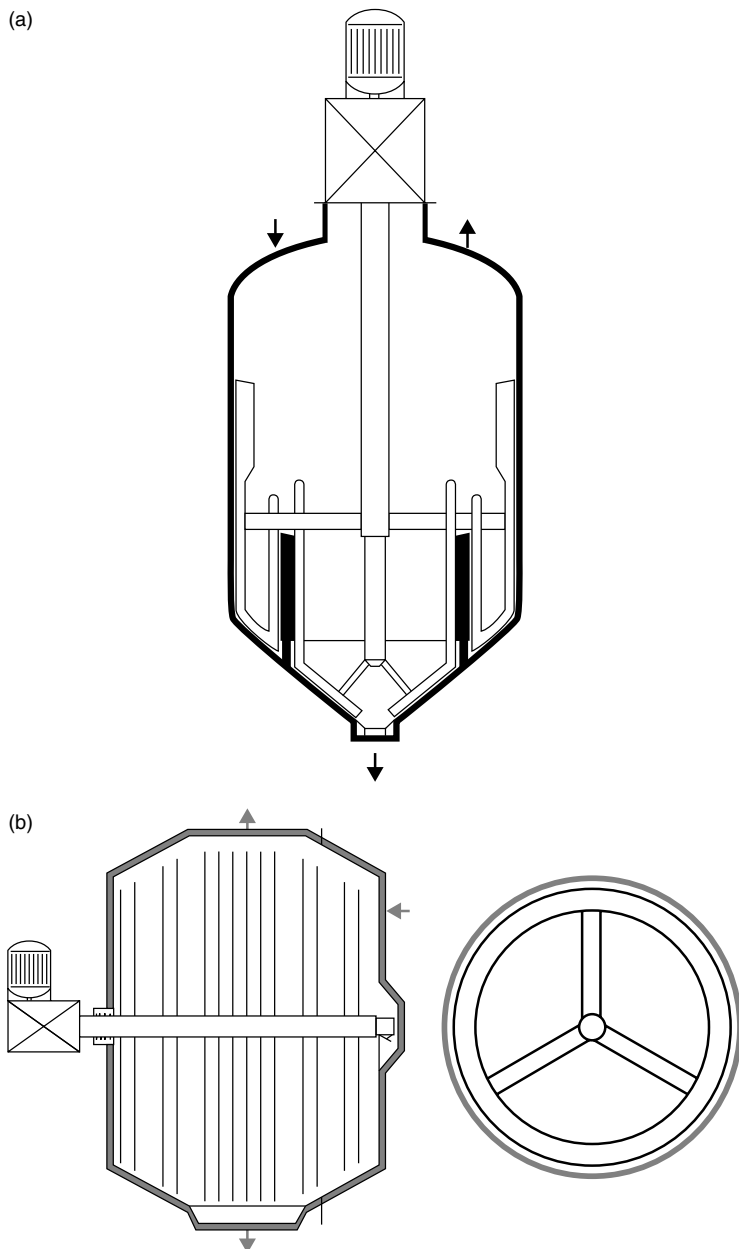


Figure 2.35 Discontinuous polycondensation reactors: (a) conventional design for capacities up to 35 t/d; (b) novel discontinuous disc-ring reactor for capacities up to 100 t/d [2]. From manufacturer's literature published by Zimmer AG and reproduced with permission

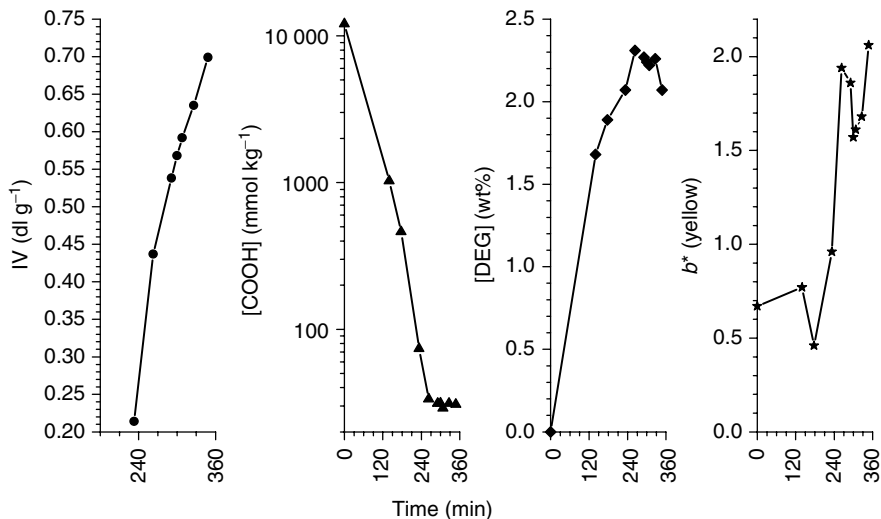


Figure 2.36 Typical process data and polymer properties for a polycondensation batch plant: temperature, 285 °C (maximum); pressure, 1 mm Hg; catalyst, 200 ppm Sb₂O₃ (based on PET) [129]

reactors, one or two prepolycondensation reactors, and one or two high-viscosity reactors, so called ‘finishers’, are used (Figures 2.37 and 2.38).

Typical process conditions and a typical evolution of product properties are summarized in Tables 2.13 and 2.14, respectively.

Stabilizers, additives and colorants are mostly added into the esterification reactor or before the prepolycondensation reactor. The product of the esterification reactor is fed by gravity into the prepolycondensation reactor. From the prepolycondensation stage, the product is pumped by gear pumps through a filter into the finisher. The final polymer is discharged from the finisher by pumping, then cooled and granulated. If required, additives such as TiO₂ for fibre applications or SiO₂ for film-grade PET, are added by using static mixers located between the finisher discharge pump and the granulator.

Most of the generated vapour is condensed in spray condensers which are equipped with circulation pumps and an EG cooler. The vapour that is still uncondensed is withdrawn from the gas phase with the help of a vapour jet which is located down-stream behind the spray condenser and generates the necessary vacuum in the reaction zone. The most critical part of the spray condenser system is the end of the pipe leading the vapour from the prepolycondensation reactors and the finishers into the spray condenser. The transition from a hot to a cold environment causes deposition of solid material onto the cold walls which has to be removed manually or by means of a mechanical scraper.

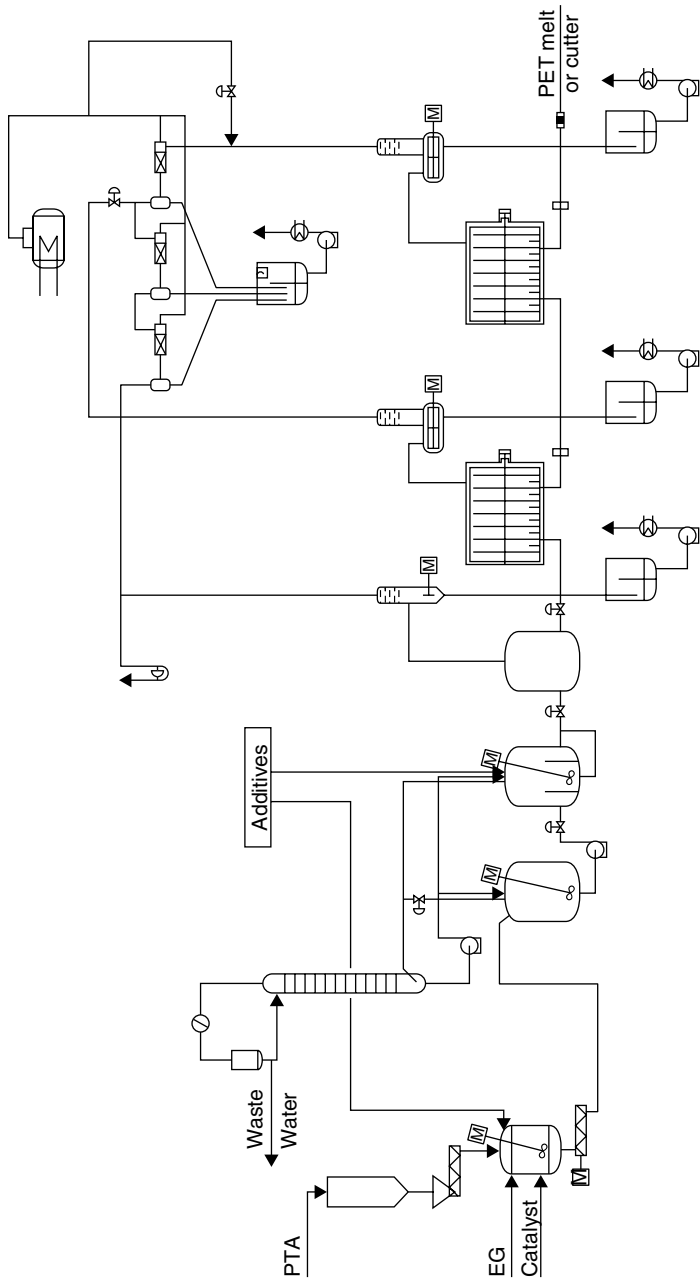


Figure 2.38 Continuous PET process based on TPA with five reactors in series [2]. From manufacturer's literature published by Zimmer AG and reproduced with permission

Table 2.13 Typical process conditions for a continuous PET process; final IV, 0.64 dL/g

Condition (unit)	Esterification	Prepolycondensation	Finisher
Product temperature(°C)	250–265	265–275	275–295
Reactor pressure (Pa)	$(1.2–1.8) \times 10^5$	2500–3000	50–150
Residence time (min)	180–360	50–70	90–150
Degree of polycondensation	4–6	15–20	100

Table 2.14 Typical evolution of PET properties during polycondensation, according to Tremblay [131]

Property (unit)	Reactor ^a				
	EI	EII	PI	PII	F
Temperature(°C)	260	260	275	280	286
Pressure(Pa)	245 000	102 000	6660	267	133
[COOH end groups](mmol kg ⁻¹)	1057	231	53.8	22.2	23.0
[OH end groups](mmol kg ⁻¹)	1620	1730	574	165	80.2
[Vinyl end groups](mmol kg ⁻¹)	0.00	0.02	0.22	0.92	2.2
IV(dL g ⁻¹)	0.049	0.057	0.14	0.38	0.61
DEG content(wt%)	0.349	0.452	0.500	0.515	0.522
P_n	4.8	5.8	17	56	99
M_n (g mol ⁻¹)	920	1110	3266	10 721	19 026

^a EI, esterification I; EII, esterification II; PI, prepolymer I; PII, prepolymer II; F, finisher.

Process vapours from the esterification reactors and EG from the EG-vapour jet, as well as from the vacuum stages of the spray condensers, are purified in the distillation unit. The distillation unit commonly consists of two or three columns and is designed for continuous operation. The purified EG is condensed at the top of the third vacuum rectification column and returned to the process via a buffer tank. Gaseous acetaldehyde and other non-condensables are vented or burned and high-boiling residues from the bottom of the third column are discharged or also burned.

5 REACTOR DESIGN FOR CONTINUOUS MELT-PHASE POLYCONDENSATION

The special requirements for esterification and polycondensation reactor design result from the understanding of kinetics and mass transport as discussed above

in Sections 2 and 3. In the esterification step, the main task is to provide sufficient heat for the evaporation of water and EG. In the polycondensation step, a large specific surface area has to be generated to increase the overall rate of the equilibrium polycondensation reaction which is diffusion-controlled.

5.1 *ESTERIFICATION REACTORS*

The design of esterification reactors is often a standard stirred-tank reactor type. With two esterification reactors in series, more heat has to be transferred to the first esterification reactor and therefore additional heating coils providing a larger heat-transfer area are installed. Both esterification reactors have heating jackets. In large reactors, the stirrer is fixed at the bottom of the reactor by means of an internal bearing housing. The diameter of the reactors often increases in the upper part. This design decreases the gas velocity and lowers carry-over of liquids by the vapour stream.

5.2 *POLYCONDENSATION REACTORS FOR LOW MELT VISCOSITY*

The design of prepolycondensation reactors meets three special requirements, i.e. (1) a large surface area for mass transfer and respectively short diffusion lengths for the low-molecular-weight by-product, (2) a sufficient heat transfer area, and (3) a design assuring low gas velocities. In stirred-tank reactors, heating coils at the reactor bottom are used for heat transfer and the reactor's jacket is heated as well. Analogous to the esterification reactors, the diameter of the prepolycondensation reactors often increases in the upper part. The ratio between diameter and height of the prepolycondensation reactor is sometimes unusually large, thus providing a large gas-liquid interface and so decreasing the gas velocity of the evaporating EG.

The design of the prepolycondensation reactors depends on the plant capacity. For higher plant capacities, a stirred-tank reactor is connected in series with a horizontal reactor. In Figure 2.39, a horizontal prepolycondensation reactor is shown, operating with rotating perforated discs to increase the specific surface area.

Kinetic experiments and rigorous modelling of the mass-transfer controlled polycondensation reaction have shown that even at low melt viscosities the diffusion of EG in the polymer melt and the mass transfer of EG into the gas phase are the rate-determining steps. Therefore, the generation of a large surface area is essential even in the prepolycondensation step.

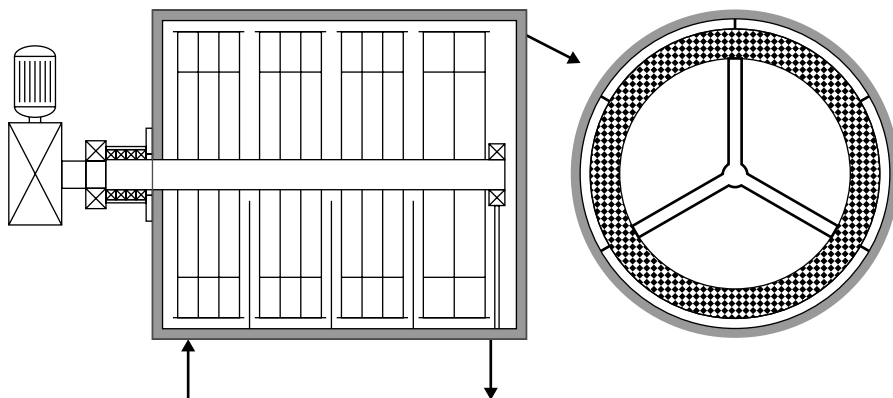


Figure 2.39 Horizontal perforated disc-ring prepolycondensation reactor [2]. From manufacturer's literature published by Zimmer AG and reproduced with permission

5.3 POLYCONDENSATION REACTORS FOR HIGH MELT VISCOSITY

In these special reactors, the product is agitated by means of a horizontal stirrer in order to generate a large polymer surface area. For a high performance at this step, disc- or cage-type reactors are common. The optimum stirrer design provides a plug flow characteristic with little back mixing. In this case, the residence time distribution is narrow and the average rate of polycondensation is high. The desired degree of polycondensation, and respectively the final melt viscosity, is set by adjusting the vacuum, the reaction temperature and the average residence time by level control. A viscometer at the outlet of the polymer discharge pump measures the actual viscosity and adjusts the process parameters. Most of the finishers are self-cleaning units and very few maintenance stops are necessary.

The cage-type finisher (Figure 2.40) is heated by means of a heat-transfer medium flowing through a jacket. This results in a higher temperature of the reactor wall than the temperature of the polymer melt. To prevent polymer from sticking to the reactor wall, a scraper is attached to the horizontal stirrer, thus reducing the gap between the stirrer and the wall. The cage-type reactor does not have a stirrer shaft, which is claimed to improve product quality due to the avoidance of polymer sticking to a shaft and thus staying in the reactor for elongated times. Very long residence times lead to thermal degradation of the sticking polymer which could cause black spots in the transparent final products.

The disc-type finisher (Figure 2.41) is heated solely by stirring through shearing of the high-viscosity melt. The temperature of the reactor walls is therefore lower than the temperature of the polymer melt, which is claimed to improve the product quality by avoiding an overheating of the polymer of the reactor wall. In Figure 2.42, a so-called double-drive disc-type finisher is shown which permits

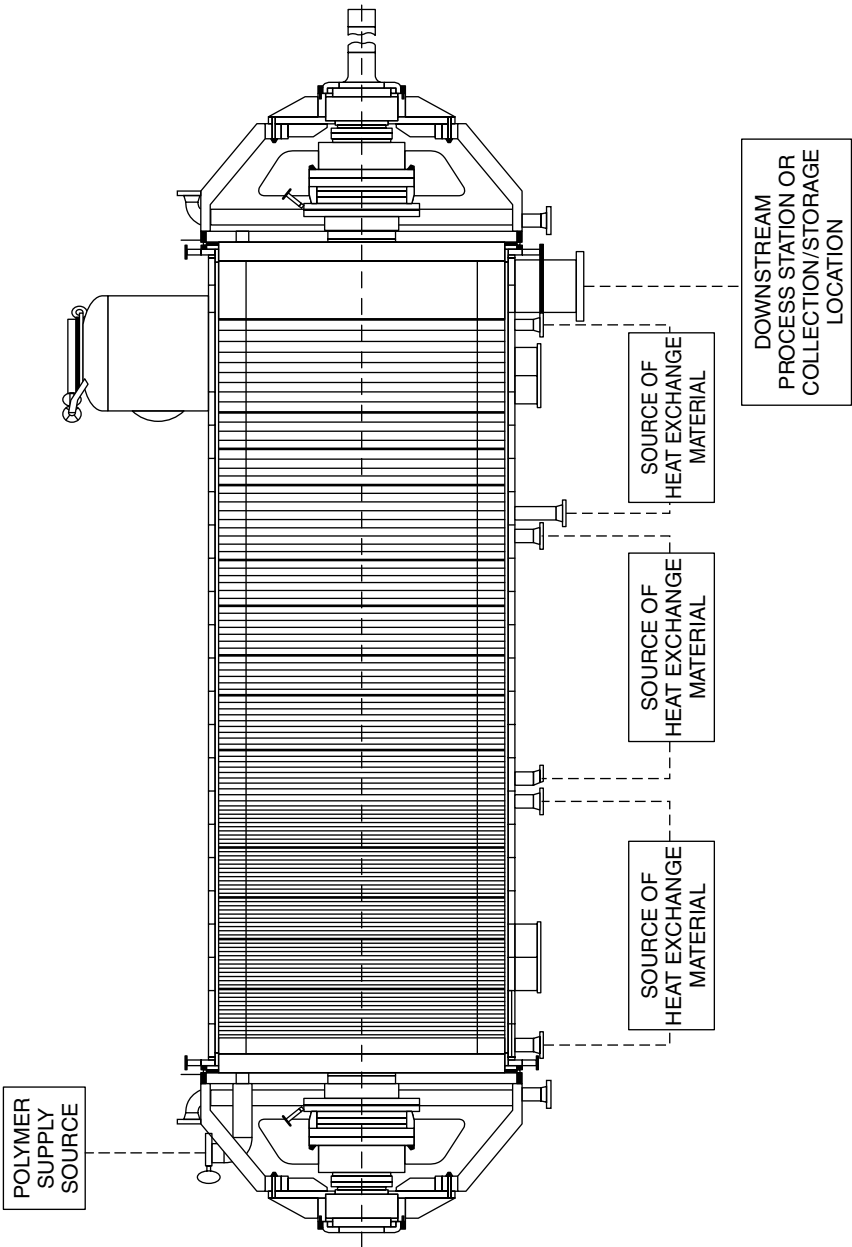


Figure 2.40 Medium-viscosity cage-type finisher [132]. From Shaw, G., Schaller, R. A., Stikeleather, W. J., Melton, M. D., Hey, H., Schmidt, R., Hartmann, R. and Lohé, H., *US Patent 5 599 507* (1997)

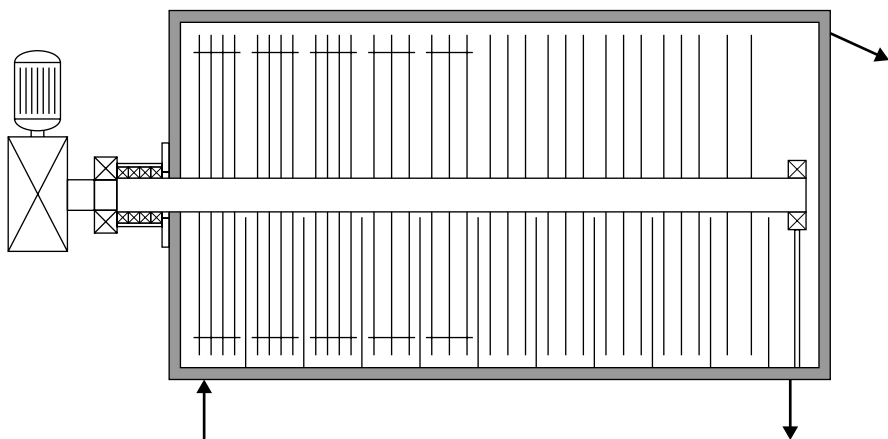


Figure 2.41 Medium-viscosity disc-type finisher [2]. From manufacturer's literature published by Zimmer AG and reproduced with permission

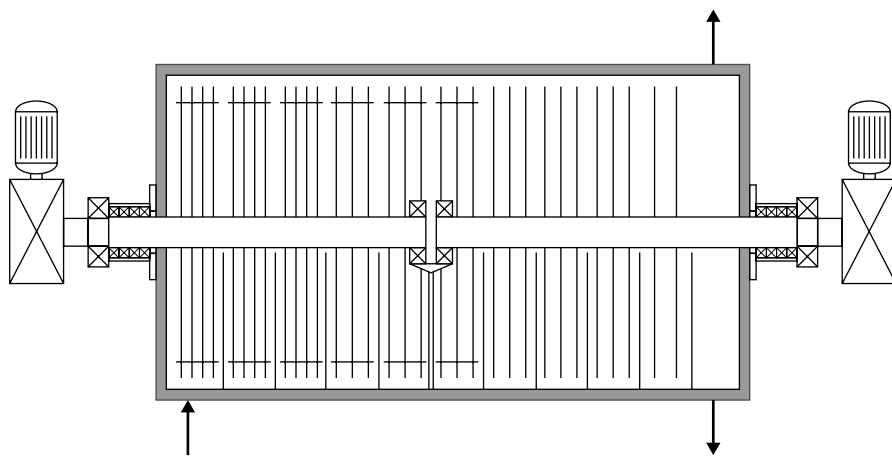


Figure 2.42 High-viscosity double-drive disc-type finisher with two different stirrer frequencies [2]. From manufacturer's literature published by Zimmer AG and reproduced with permission

the simultaneous operation at two different stirrer speeds. A higher stirrer speed is used for the first reactor part with lower melt viscosity, while a lower stirrer speed is used for the second reactor part with higher melt viscosity. This reactor type can thus be used for the production of high-viscosity PET in only one polycondensation stage.

6 FUTURE DEVELOPMENTS AND SCIENTIFIC REQUIREMENTS

The production of PET is a well-known industrial process. Early patents on PET synthesis refer to the 1940s. Esterification and transesterification reactions have been investigated since the end of the 19th century. PET production plants have been optimized over the last few decades based on well-established production 'know-how'. PET is now a commodity product with unusually rapid growth and further nearly unlimited future growth perspectives.

However, in contrast to the production 'know-how', the scientific knowledge on the details of phase equilibria, kinetics, mechanisms, catalysis and mass-transport phenomena involved in polycondensation is rather unsatisfactory. Thus, engineering calculations are based on limited scientific fundamentals. Only a few high-quality papers on the details of esterification and transesterification in PET synthesis have been published in the last 45 years. The kinetic data available in the public domain are scattered over a wide range, and for some aspects the publications even offer contradicting data.

In particular, proven reaction mechanisms are required for the catalyzed and uncatalyzed reactions concerning esterification, transesterification and etherification, together with thermal and thermo-oxidative degradation. The kinetic data for esterification/hydrolysis and transesterification/glycolysis need to be determined and the significant influences of mass transport excluded. The impact of co-monomers on reaction rates has not yet been described quantitatively. Furthermore, the reaction mechanisms responsible for yellowing are not understood and the colouring substances have not been unambiguously identified. The consecutive reaction mechanisms for the thermal and thermo-oxidative degradation are not well known, and the evolution of secondary degradation products has not been investigated under polycondensation conditions.

For the solubility of TPA in prepolymer, no data are available and the polymer-solvent interaction parameter χ_i of the Flory-Huggins relationship is not accurately known. No experimental data are available for the vapour pressures of dimer or trimer. The published values for the diffusion coefficient of EG in solid and molten PET vary by orders of magnitude. For the diffusion of water, acetaldehyde and DEG in polymer, no reliable data are available. It is not even agreed upon if the mutual diffusion coefficients depend on the polymer molecular weight or on the melt viscosity, and if they are linear or exponential functions of temperature. Molecular modelling, accompanied by the rapid growth of computer performance, will hopefully help to solve this problem in the near future. The mass-transfer mechanisms for by-products in solid PET are not established, and the dependency of the solid-state polycondensation rate on crystallinity is still a matter of assumptions.

The efforts undertaken to describe the influence of mass transport on the overall polycondensation rate should focus on the development of a polycondensation model based on model parameters being independent of the method of parameter

estimation. The common goal of future work on the details of PET synthesis should be to separate pure reaction kinetics from mass transport and mass transfer. Care has to be taken that the rate constants are valid under the operation conditions of the different reactors. With this goal achieved, it may become possible to design new reactors and to scale-up reactors while leaving undesired small scaling steps behind. Process conditions and product quality may be optimized beyond known parameter sets without parameter-fitting procedures.

Furthermore, the environmental impact of PET production should be reduced by substituting the commonly used antimony-based catalyst for an antimony-free catalyst leg, for a titanium-based catalyst. The pollution by liquid effluents could be reduced by installing a reverse-osmosis unit on top of the glycol distillation unit for the purification of water from the esterification process.

To finally conclude, it can be stated that the PET market will grow rapidly in the next few years, even without the detailed knowledge we would prefer to have for modelling purposes. However, neither an optimum plant performance nor an optimum economy will be achieved without reliable and predictive process models.

ACKNOWLEDGEMENTS

It gives us great pleasure to acknowledge the dedicated efforts of Dr Simon West, who tried hard to improve our scientific English and who's comments and suggestions on polymer chemistry and polymer engineering are always stimulating. We would also like to thank Dr Ulrich Berger from Zimmer AG for his support and permission to use graphics and flow sheets illustrating the state of the art in polycondensation technology.

REFERENCES

1. *Ullmann's Encyclopaedia of Industrial Chemistry*, Wiley-VCH, Weinheim, Germany, 1996.
2. mg Engineering, Zimmer AG, Frankfurt am Main, Germany, private communication, 2001.
3. Flory, P. J., Molecular size distribution in linear condensation polymers, *J. Am. Chem. Soc.*, **58**, 1877–1885 (1936).
4. Flory, P. J., *Principles of Polymer Chemistry*, Cornell University Press, Ithaca, New York, 1953.
5. Schulz, G. V., *Z. Phys. Chem. (Neue Folge)*, **8**, p. 284 (1956).
6. Ravindranath, K. and Mashelkar, R. A., Polyethylene terephthalate – I. Chemistry, thermodynamics and transport properties, *Chem. Eng. Sci.*, **41**, 2197–2214 (1986).

7. Kang, C.-K., Lee, B. C., Ihm, D. W. and Tremblay, D. A., A simulation study on continuous direct esterification process for poly(ethylene terephthalate) synthesis, *J. Appl. Polym. Sci.*, **63**, 163–174 (1997).
8. Rieckmann, Th. and Völker, S., Micro kinetics and mass transfer in poly(ethylene terephthalate) synthesis, *Chem. Eng. Sci.*, **56**, 945–953 (2001).
9. Fradet, A. and Maréchal, E., Kinetics and mechanisms of polyesterifications. I. Reactions of diols with diacids, *Adv. Polym. Sci.*, **43**, 51–96 (1982).
10. Schumann, H.-D., Beiträge zur Schmelzekondensation von Polyäthylenterephthalat; I. Zur Polykondensation in dünnen Schichten, *Faserforschung Textiltechnik*, **22**, 389–394 (1971).
11. Flory, P. J., Random reorganization of molecular weight distribution in linear condensation polymers, *J. Am. Chem. Soc.*, **64**, 2205–2212 (1942).
12. Schulz, G. V., *Z. Phys. Chem., A*, **182**, p. 127 (1938).
13. Flory, P. J., *J. Chem. Phys.*, **9**, p. 660 (1941).
14. Flory, P. J., *J. Chem. Phys.*, **10**, p. 51 (1942).
15. Huggins, M. L., *J. Chem. Phys.*, **9**, p. 440 (1941).
16. Huggins, M. L., Some properties of solutions of long-chain compounds, *J. Phys. Chem.*, **46**, 151–158 (1942).
17. Huggins, M. L., *Ann. N. Y. Acad. Sci.*, **41**, p. 1 (1942).
18. Otton, J. and Ratton, S., Investigation of the formation of poly(ethylene terephthalate) with model molecules. I. Carboxylic acid catalysis (mono-functional reactants), *J. Polym. Sci., Polym. Chem. Ed.*, **26**, 2187–2197 (1988).
19. Reimschuessel, H. K. and Debona, B. T., Terephthalic acid esterification kinetics: 2-(2-methoxyethoxy)ethyl terephthalates, *J. Polym. Sci., Polym. Chem. Ed.*, **17**, 3241–3254 (1979).
20. Reimschuessel, H. K., Debona, B. T. and Murthy, A. K. S., Kinetics and mechanism of the formation of glycol esters: benzoic acid – ethylene glycol system, *J. Polym. Sci., Polym. Chem. Ed.*, **17**, 3217–3239 (1979).
21. Reimschuessel, H. K., Polyethylene terephthalate formation. Mechanistic and kinetic aspects of the direct esterification process, *Ind. Eng. Prod. Res. Dev.*, **19**, 117–125 (1980).
22. Challa, G., The formation of polyethylene terephthalate by ester interchange: I. The polycondensation equilibrium, *Macromol. Chem. Phys.*, **38**, 105–122 (1960).
23. Yamada, T., Effect of diantimony trioxide on direct esterification between terephthalic acid and ethylene glycol, *J. Appl. Polym. Sci.*, **37**, 1821–1835 (1989).
24. Yamada, T. and Imamura, Y., Simulation of continuous direct esterification process between terephthalic acid and ethylene glycol, *Polym.-Plast. Technol. Eng.*, **28**, 811–876 (1989).

25. Habid, O. M. O. and Málek, J., *Collect. Czech. Chem. Commun.*, **41**, p. 2724 (1976).
26. Krumpolc, M. and Málek, J., Esterification of benzenecarboxylic acids with ethylene glycol, IV. Kinetics of the initial stage of polyesterification of terephthalic acid with ethylene glycol catalyzed by zinc oxide, *Makromol. Chem.*, **171**, 69–81 (1973).
27. Chegolya, A. S., Shevchenko, V. V. and Mikhailov, D. G., The formation of polyethylene terephthalate in the presence of dicarboxylic acids, *J. Appl. Polym. Sci.*, **17**, 889–904 (1979).
28. Yoda, K., Catalysis of trans-esterification reactions, *Makromol. Chem.*, **136**, 311–313 (1970).
29. Zimmermann, H. and Chu, D. D., Untersuchungen zur Kinetik des metallionenkatalysierten thermischen Abbaus von Polyäthylenterephthalat, *Faserforschung Textiltechnik*, **24**, 445–452 (1973).
30. Raffler, G., Reinisch, G. and Bonatz, E., Kinetics, mass transport and thoughts about the mechanism of the formation of polyethylene terephthalate by metal ion catalysis, *Acta Chim. (Budapest)*, **81**, 253–267 (1974).
31. Tomita, K., Studies on the formation of polyethylene terephthalate: 6. Catalytic activity of metal compounds in polycondensation of bis(hydroxyethyl)terephthalate, *Polymer*, **17**, 221–224 (1976).
32. Maerov, S. B., Influence of antimony catalysts with hydroxyethoxy ligands on polyester polymerization, *J. Polym. Sci., Polym. Chem. Ed.*, **17**, 4033–4040 (1979).
33. Kamatani, H., Konagaya, S., and Nakamura, Y., Effect of phosphoric acid on the polycondensation of bis(hydroxyethyl)terephthalate catalyzed by Sb(III) compounds, *Polym. J.*, **12**, 125–130 (1980).
34. Chung, J. S., Acid–base and catalytic properties of metal compounds in the preparation of poly(ethylene terephthalate), *J. Macromol. Sci., Chem.*, **A27**, 479–490 (1990).
35. Hovenkamp, S. G., Kinetic aspects of catalyzed reactions in the formation of poly(ethylene terephthalate), *J. Polym. Sci., Part A-1*, **9**, 3617–3625 (1971).
36. Otton, J., Ratton, S., Vasnev, V. A., Markova, G. D., Nametov, K. M., Bakhmutov, V. I., Komarova, L. I., Vinogradova, S. V. and Korshak, V. V., Investigation of the formation of poly(ethylene terephthalate) with model molecules: Kinetics and mechanisms of the catalytic esterification and alcoholysis reactions II. Catalysis by metallic derivatives (monofunctional reactants), *J. Polym. Sci., Polym. Chem. Ed.*, **26**, 2199–2224 (1988).
37. Otton, J., Ratton, S., Vasnev, V. A., Markova, G. D., Nametov, K. M., Bakhmutov, V. I., Vinogradova, S. V. and Korshak, V. V., Investigation of the formation of poly(ethylene terephthalate) with model molecules.

- III. Metal-catalyzed esterification and alcoholysis reactions: Influence of the structure of the reactants and of the nature of the reaction medium, *J. Polym. Sci., Polym. Chem. Ed.*, **27**, 3535–3550 (1989).
38. Otton, J. and Ratton, S., Investigation of the formation of poly(ethylene terephthalate) with model molecules. IV. Catalysis of the esterification of ethylene glycol with benzoic acid and of the condensation of ethylene glycol monobenzoate, *J. Polym. Sci., Polym. Chem. Ed.*, **29**, 377–391 (1991).
39. Weingart, F., *Titankatalysatoren bei der Herstellung von Polyethylen-terephthalat – Untersuchungen zu Wirkung und Katalysemechanismus*, Ph.D. Thesis, University of Stuttgart, 1994.
40. Siling, M. I. and Laricheva, T. N., Titanium compounds as catalysts for esterification and transesterification, *Russ. Chem. Rev.*, **65**, 279–286 (1996).
41. Challa, G., *The formation of polyethylene terephthalate by ester interchange. Equilibria kinetics and molecular weight distribution*, Ph.D. Thesis, University of Amsterdam, 1959.
42. Challa, G., The formation of polyethylene terephthalate by ester interchange: II. The kinetics of reversible melt polycondensation, *Macromol. Chem.*, **38**, 123–137 (1960).
43. Fontana, C. M., Polycondensation equilibrium and the kinetics of catalyzed transesterification in the formation of polyethylene terephthalate, *J. Polym. Sci., Part A-1*, **6**, 2343–2358 (1968).
44. Krumpolc, M. and Málek, J., Esterification of benzenecarboxylic acids with ethylene glycol, III. Kinetics of esterification of 2-hydroxyethyl hydrogen terephthalate with ethylene glycol catalyzed by zinc oxide, *Makromol. Chem.*, **168**, 119–129 (1973).
45. Hoftyzer, P. J., Kinetics of the polycondensation of ethylene glycol terephthalate, *Appl. Polym. Symp.*, **26**, 349–363 (1975).
46. Stewart, M. E., Cox, A. J., and Naylor, D. M., Reactive processing of poly(ethylene 2,5-naphthalene dicarboxylate)/poly(ethylene terephthalate) blends, *Polymer*, **34**, 4060–4067 (1993).
47. Shi, Y. and Jabarin, S. A., Transesterification reaction kinetics of poly(ethylene terephthalate)/poly(ethylene 2,6-naphthalate) blends, *J. Appl. Polym. Sci.*, **80**, 2422–2436 (2001).
48. Wang, D.-C., Chen, L.-W. and Chiu, W.-Y., Kinetic study on depolymerization by glycolysis of poly(ethylene terephthalate) with bisphenol A, *Angew. Makromol. Chem.*, **230**, 47–71 (1995).
49. Goodman, I. and Nesbitt, B. F., The structures and reversible polymerization of cyclic oligomers from PET, *J. Polym. Sci.*, **48**, 423–433 (1960).
50. Peebles, L. H., Huffmann, M. W. and Ablett, C. T., Isolation and identification of the linear and cyclic oligomers of polyethylene terephthalate

and the mechanism of cyclic oligomer formation, *J. Polym. Sci., Part A-1*, **7**, 479–496 (1969).

51. Ha, W. S. and Choun, Y. K., Kinetic studies on the formation of cyclic oligomers in poly(ethylene terephthalate), *J. Polym. Sci., Polym. Chem. Ed.*, **17**, 2103–2118 (1979).
52. Dulio, V., Po, R., Borelli, R., Guarini, A. and Santini, C., Characterization of low-molecular-weight oligomers in recycled poly(ethylene terephthalate), *Angew. Makromol. Chem.*, **225**, 109–122 (1995).
53. Goodman, I. and Nesbitt, B. F., *Polymer*, **1**, p. 384 (1960).
54. Cimecioglu, A. L., Zeronian, S. H., Alger, K. W., Collins, M. J., and East, G. C., Properties of oligomers present in poly(ethylene terephthalate), *Appl. J. Polym. Sci.*, **32**, 4719–4733 (1986).
55. West, S. M., Smallridge, A. J., Uhlherr, A. and Völker, S., Small molecules accumulated during polycondensation of poly(ethylene terephthalate), *Macromol. Chem. Phys.*, **201**, 2532–2534 (2000).
56. De A. Freire, M. T., Damant, A. P., Castle, L. and Reyes, F., Thermal stability of polyethylene terephthalate (PET): Oligomer distribution and formation of volatiles, *Packag. Technol. Sci.*, **12**, 29–39 (1999).
57. Hornof, V., Influence of metal catalysts on the formation of ether links in poly(ethylene terephthalate), *J. Macromol. Sci., Chem.*, **A15**, 503–514 (1981).
58. Renwen, H., Feng, Y., Tinszheng, H. and Shiming, G., The kinetics of formation of diethylene glycol in preparation of polyethylene terephthalate and its control in reactor design, *Angew. Makromol. Chem.*, **119**, 159–172 (1983).
59. Chen, J.-W. and Chen, L.-W., The kinetics of diethylene glycol formation in the preparation of polyethylene terephthalate, *J. Polym. Sci., Polym. Chem. Ed.*, **36**, 3073–3080 (1998).
60. Hovenkamp, S. G. and Munting, J. P., Formation of diethylene glycol as a side reaction during production of polyethylene terephthalate, *J. Polym. Sci., Part A-1*, **8**, 679–682 (1970).
61. Buxbaum, L. H., The degradation of polyethylene terephthalate, *Angew. Chem. Int. Ed. Engl.*, **7**, 182–190 (1968).
62. Chen, J.-W. and Chen, L.-W., Effect of TPA addition at the initial feed on DEG formation in the preparation of PET and the kinetics of ethylene glycol with protons in the etherification reaction, *J. Polym. Sci., Polym. Chem. Ed.*, **36**, 3081–3087 (1998).
63. Chen, J.-W. and Chen, L.-W., The kinetics of diethylene glycol formation from bishydroxyethyl terephthalate with antimony catalyst in the preparation of PET, *J. Polym. Sci., Polym. Chem. Ed.*, **37**, 1797–1803 (1999).

64. Chen, L.-W. and Chen, J.-W., Kinetics of diethylene glycol formation from bishydroxyethyl terephthalate with proton catalyst in the preparation of poly(ethylene terephthalate), *J. Appl. Polym. Sci.*, **75**, 1221–1228 (2000).
65. Chen, L.-W. and Chen, J.-W., Kinetics of diethylene glycol formation from bishydroxyethyl terephthalate with zinc catalyst in the preparation of poly(ethylene terephthalate), *J. Appl. Polym. Sci.*, **75**, 1229–1234 (2000).
66. Brückner, R., *Reaktionsmechanismen. Organische Reaktionen, Stereochemie, moderne Synthesemethoden*, Spektrum Akademischer Verlag, Heidelberg, Germany, 1996.
67. Yamada, T., Effect of titanium dioxide on direct esterification between terephthalic acid and ethylene glycol, *J. Appl. Polym. Sci.*, **45**, 765–781 (1992).
68. Zimmermann, H., Chemische Untersuchungen über faserbildende Polyester, Über die thermische Stabilisierung von Polyäthylenterephthalat, *Faserforschung Textiltechnik*, **13**, 481–494 (1962).
69. Zimmermann, H. and Leibnitz E., Chemische Untersuchungen über faserbildende Polyester. II. Modellversuche zum thermischen Abbau von Polyäthylenterephthalat, *Faserforschung Textiltechnik*, **16**, 282–290 (1965).
70. Schaaf, E. and Zimmermann, H., Thermogravimetric investigation on the thermal and thermooxydative degradation of polyethylene terephthalate, *Faserforschung Textiltechnik*, **25**, 434–440 (1974).
71. Kao, C. Y., Cheng, W. H. and Wan, B.-Z., Investigation of catalytic glycolysis of polyethylene terephthalate by differential scanning calorimetry, *Thermochim. Acta*, **292**, 95–104 (1997).
72. Kamatani, H. and Kuze, K., Formation of aromatic compounds as side reactions in the polycondensation of bishydroxyethyl terephthalate, *Polym. J.*, **11**, 787–793 (1979).
73. Goodings, E. P., Thermal degradation of PET, *Soc. Chem. Ind. (London)*, Monograph No. 13, 211–228 (1961).
74. Edge, M., Allen, N. S., Wiles, R., McDonald, W. and Mortlock, S. V., Identification of luminescent species contributing to the yellowing of poly(ethylene terephthalate), *Polymer*, **36**, 227–234 (1995).
75. Edge, M., Wiles, R., Allen, N. S., McDonald, W. A. and Mortlock, S. V., Characterisation of the species responsible for yellowing in melt degraded aromatic polyesters – I. Yellowing of poly(ethylene terephthalate), *Polym. Degrad. Stabil.*, **53**, 141–151 (1996).
76. Weingart, F., Hirt, P. and Herlinger, H., Titanium catalyst in the manufacture of poly(ethylene terephthalate), *Chem. Fibers Int.*, **46**, 96–97 (1996).
77. Datye, K. V., Raje, H. M. and Sharma, N. D., Poly(ethylene terephthalate) waste and its utilization: A Review, *Resourc. Conserv.*, **11**, 117–141 (1984).

78. Paszun, D. and Spychaj, T., Chemical recycling of poly(ethylene terephthalate), *Ind. Eng. Chem. Res.*, **36**, 1373–1383 (1997).
79. Rieckmann, Th., Recycling of PET food grade quality on a commercial scale, *Chem. Fibers Int.*, **45**, 182–185 (1995).
80. Krasnostein, P., A new process for complete PET recycling, presentation given at the *Davos Recycling Forum*, Davos, Switzerland, March 14–18, 1994.
81. Heath, R. L., *Degradation of aromatic linear polyesters*, UK Patent 610 136 (1946).
82. Heath, R. L., *Recovery of terephthalic acid from polyesters*, UK Patent 610 135 (1946).
83. Gruschke, H., Hammerschick, W. and Medem, H., *Process for depolymerizing poly(ethylen terephthalate) to terephthalic acid dimethylester*, US Patent 3 403 115 (1968).
84. Lamparter, R. A., Barna, B. A., and Johnsrud, D. R., *Process for recovering terephthalic acid from waste poly(ethylene terephthalate)*, US Patent 4 542 239 (1985).
85. Rieckmann, Th. and Völker, S., Product quality of recycled food grade PET from a bottle to bottle recycling process, presentation given at the *ECCE-3 Conference*, Nuremberg, Germany, June 26–28, 2001 (published on CD-Rom).
86. Missen, R. W., Mims, C. A. and Saville B. A., *Introduction to Chemical Reaction Engineering and Kinetics*, Wiley, New York, 1999.
87. Yoshioka, T., Motoki, T. and Okuwaki, A., Kinetics of hydrolysis of poly(ethylene terephthalate) powder in sulfuric acid by a modified shrinking-core model, *Ind. Eng. Chem. Res.*, **40**, 75–79 (2001).
88. Ravindranath, K. and Mashelkar, R. A., Modeling of poly(ethylene terephthalate) reactors: 1. A semibatch ester interchange reactor, *J. Appl. Polym. Sci.*, **26**, 3179–3204 (1981).
89. Ank, J. W. and Mellichamps, D. A., *Chem. Eng. Sci.*, **27**, p. 2219 (1972).
90. Dijkman, H. K. M. and Duvekot, C., Mathematical model of the preparation of polyethylene terephthalate, in *Proceedings of the 4th International/6th European Symposium on Chemical Reaction Engineering*, Vol. 1, Heidelberg, 1976, pp. 344–352.
91. Yokoyama, H., Sano, T., Chijiwa, T. and Kajiya, R., Degradation reactions in ethylene glycol terephthalate polycondensation process, *J. Jpn. Petrol. Inst.*, **21**, 194–198 (1978).
92. Ravindranath, K. and Mashelkar, R. A., Modeling of poly(ethylene terephthalate) reactors: 2. A continuous transesterification process, *J. Appl. Polym. Sci.*, **27**, 471–487 (1982).
93. Baronova, T. L. and Kremer, E. B., *Khim. Volokna*, **19**(4), p. 16 (1977).
94. Rieckmann, Th. and Völker, S., unpublished personal data, 2001.

95. Reid, R. C., Prausnitz, J. M. and Poling, B. E., *The Properties of Gases and Liquids*, McGraw-Hill, Singapore, 1988.
96. Vrentas, J. S., Duda, J. L. and Hsieh, S. T., Thermodynamic properties of some amorphous polymer – solvent systems, *Ind. Eng. Chem. Prod. Res. Dev.*, **22**, 326–330 (1983).
97. Jabarin, S. A., *J. Appl. Polym. Sci.*, **34**, p. 85 (1987).
98. Mallon, F. K. and Ray, W. H., Modeling of solid-state polycondensation. I. Particle models, *J. Appl. Polym. Sci.*, **69**, 1233–1250 (1998).
99. Stevenson, R. W., Polycondensation rate of poly(ethylene terephthalate) – II. Antimony trioxide catalyzed polycondensation in static thin films on metal surfaces, *J. Polym. Sci., Part A-1*, **7**, 395–407 (1969).
100. Hoftyzer, P. J. and van Krevelen, D. W., The rate of conversion in polycondensation processes as determined by combined mass transfer and chemical reaction, in *Proceedings of the 4th European Symposium on Chemical Reactions, Chem. Eng. Sci.*, 139–146 (1971).
101. Bonatz, E., Rafler, G. and Reinisch, G., Zur Kinetik der Polyethylen-terephthalat bildung im offenen System. III. Schichtdickenabhängigkeit der Polykondensationsge-Schwindigkeit in einem statischen Polykondensationssystem, *Faserforschung Textiltechnik*, **24**, 309–312 (1973).
102. Rafler, G., Bonatz, E., Gajewski, H., and Zacarias, K., Reaktion und Diffusion bei der Schmelzekondensation von Polyethylenterephthalat, *Acta Polym.*, **30**, 253–258 (1979).
103. Rafler, G., Bonatz, E., Gajewski, H. and Zacarias, K., Zur Erweiterung des Reaktions-Diffusions-Modells von Schmelzepolykondensationen, *Acta Polym.*, **31**, 732–733 (1980).
104. Rafler, G., Bonatz, E., Gajewski, H. and Zacharias, K., Zur Bestimmung der Bruttoreaktionsgeschwindigkeit des thermischen Abbaus von Polyethylenterephthalat unter Polykondensationsbedingungen, *Acta Polym.*, **31**, 684–685 (1980).
105. Rafler, G., Reinisch, G., Bonatz, E. and Versäumer, H., Kinetics of mass transfer in the melt polycondensation of poly(ethylene terephthalate), *J. Macromol. Sci., Chem.*, **A22**, 1413–1427 (1985).
106. Rafler, G., Bonatz, E., Sparing, H.-D. and Otto, B., Zur Kinetik der Polykondensation von Terephthalsäure und Ethylenglykol in dünnen Schmelzeschichten, *Acta Polym.*, **38**, 6–10 (1987).
107. Ravindranath, K. and Mashelkar, R. A., Polyethylene terephthalate – II. Engineering analysis, *Chem. Eng. Sci.*, **41**, 2969–2987 (1986).
108. Gupta, S. K. and Kumar, A., *Reaction Engineering of Step Growth Polymerization*, Plenum Press, New York, 1987.
109. Lee, K. J., Moon, D. Y., Park, O. O., and Kang, Y. S., Diffusion of ethylene glycol accompanied by reactions in poly(ethylene terephthalate) melts, *J. Polym. Sci., Polym. Phys. Ed.*, **30**, 707–716 (1992).

110. Zimmerer, W. *Thermogravimetrische Untersuchung zur Kinetik von Polykondensationsreaktionen*, Ph.D. Thesis, Swiss Federal Institute of Technology, Lausanne, 1997.
111. Laubriet, C., LeCorre, B. and Choi, K. Y., Two-phase model for continuous final stage melt polycondensation of poly(ethylene terephthalate). 1. Steady-state analysis, *Ind. Eng. Chem. Res.*, **30**, 2–12 (1991).
112. Ravindranath, K. and Mashelkar, R. A., Finishing stages of PET synthesis: a comprehensive model, *AIChE J.*, **30**, 415–422 (1984).
113. Cheong, S. I. and Choi, K. Y., Melt polycondensation of poly(ethylene terephthalate) in a rotating disk reactor, *J. Appl. Polym. Sci.*, **58**, 1473–1483 (1995).
114. Cheong, S. I. and Choi, K. Y., Modeling of a continuous rotating disk polycondensation reactor for the synthesis of thermoplastic polyesters, *J. Appl. Polym. Sci.*, **61**, 763–773 (1996).
115. Rieckmann, Th., Rösner, F. and Völker, S., Mass transfer and volatilization of small molecules from molten poly(ethylene terephthalate), presentation given at the *ECCE-2 Conference*, Montpellier, France, October 5–7, 1999 (published on CD-Rom).
116. Opfermann, J., Kinetic analysis using multivariate non-linear regression. I. Basic concepts, *J. Therm. Anal. Cal.*, **60**, 641–658 (2000).
117. Dietze, M. and Kühne, H., Development and design of commercial reactors for continuous manufacture of polyesters, *Chemiefasern*, **3**, 194–202 (1969).
118. Perry, R. H., *Perry's Chemical Reactors Handbook*, McGraw-Hill, Singapore, 1985.
119. Vijayraghvan, K. and Gupta, J. P., Thickness of the film on a vertically rotating disk partially immersed in a Newtonian fluid, *Ind. Eng. Chem. Fundam.*, **21**, 333–336 (1982).
120. Soroka, A. J. and Tallmadge, J. A., A test of the inertial theory of plate withdrawal, *AIChE J.*, **17**, 505–508 (1971).
121. Ravindranath, K. and Mashelkar, R. A., Modeling of poly(ethylene terephthalate) reactors. IX. Solid state polycondensation process, *J. Appl. Polym. Sci.*, **39**, 1325–1345 (1990).
122. Kang, C.-K., Modeling of solid-state polymerization of poly(ethylene terephthalate), *J. Appl. Polym. Sci.*, **68**, 837–846 (1998).
123. Mallon F. K. and Ray, W. H., Modeling of solid-state polycondensation. II. Reactor design issues, *J. Appl. Polym. Sci.*, **69**, 1775–1788 (1998).
124. Jürgens, Th, Kohn, J., Makonnen, G. and Rieckmann, Th., *Diol recovery process and plant*, PCT Patent WO 9 635 654, (1996).
125. Lindall, C. M., Slack, N. and Ridland, J., *Esterification catalysts*, PCT Patent WO 00/71 252 A1 (2000).

126. Cannon, K. C., Seshadri, S. R. and Dirkx, R. R., *Preparation of polyesters using lithium titanyl oxalate polycondensation catalysts*, EP Patent EP 0 970 983 A2 (2000).
127. Seidel, U. and Martl, M., *Method for producing polyesters and copolymers*, PCT Patent WO 98 56 848 A (1998).
128. Ridland, J. and Hepplewhite, I. W., *Esterification catalysts*, PCT Patent WO 99/28 033 (1999).
129. James, D. E. and Packer, L. G., Effect of reaction time on poly(ethylene terephthalate) properties, *Ind. Eng. Chem. Res.*, **34**, 4049–4057 (1995).
130. Rieckmann, Th., Polycondensation and recycling of PET fibres and other PET waste by continuous processes, presentation given at the *5th Conference on Man-Made Fibres*, Beijing, China, 1994.
131. Tremblay, D., Using simulation technology to improve profitability in the polymer industry, presentation given at the *AIChE Spring Meeting*, Houston, Texas, March 14–19, 1999.
132. Shaw, G., Schaller, R. A., Stikeleather, W. J., Melton, M. D., Hey, H., Schmidt, R., Hartmann, R. and Lohe, H., *Reactor apparatus for preparing a polymeric material*, US Patent 5 599 507 (1997).
133. Stevenson, R. W. and Nettleton, H. R., Polycondensation rate of poly(ethylene terephthalate). I. Polycondensation catalyzed by antimony trioxide in presence of reverse reaction, *J. Polym. Sci., Part A-1*, **6**, p. 889–900 (1968).
134. Tomita, K., Studies on the formation of polyethylene terephthalate: 1. Propagation and degradation reactions in the polycondensation of bis(2-hydroxyethyl)terephthalate, *Polymer*, **14**, 50–54 (1973).
135. Collins, S., Peace, S. K. and King, S. M., Transesterification in poly(ethylene terephthalate). Molecular weight and end group effects, *Macromolecules*, **33**, 2981–2988 (2000).
136. Yokoyama, H., Sano, T., Chijiwa, T. and Kajiya, R., Polycondensation rate of polyethylene terephthalate at reduced pressure, *J. Jpn. Petrol. Inst.*, **21**, 58–62 (1978).
137. Yokoyama, H., Sano, T., Chijiwa, T. and Kajiya, R., Influence of catalyst, stabilizers and temperature on the ethylene glycol terephthalate polycondensation process, *J. Jpn. Petrol. Inst.*, **21**, 208–210 (1978).
138. Mössner, W. and Vollmert, B., Eine Methode zur Untersuchung der Kinetik der Diethylenglykolbildung bei der Synthese von Polyethylenterephthalat, *Makromol. Chem., Rapid Commun.*, **6**, 527–531 (1985).
139. Marshall, I. and Todd, A., The thermal degradation of polyethylene terephthalate, *Trans. Faraday Soc.*, **49**, 67–78 (1953).
140. Jenekhe, S. A., Lin, J. W., and Sun, B., Kinetics of the thermal degradation of polyethylene terephthalate, *Thermochim. Acta*, **61**, 287–299 (1983).

141. Dollimore, D., Gamlen, G. A., Jefferies, M. and Shah, T. H., The use of the rising temperature technique to establish the kinetics of acetaldehyde evolution during atmospheric polymerization of bis(hydroxyethyl) terephthalate, *Thermochim. Acta*, **61**, 97–106 (1983).
142. Jabarin, S. A. and Lofgren, E. A., Thermal stability of polyethylene terephthalate, *Polym. Eng. Sci.*, **24**, 1056–1063 (1984).
143. Campanelli, J. R., Kamal, M. R., and Cooper, D. G., A kinetic study of the hydrolytic degradation of poly(ethylene terephthalate) at high temperatures, *J. Appl. Polym. Sci.*, **48**, 443–451 (1993).
144. Campanelli, J. R., Cooper, D. G. and Kamal, M. R., Catalyzed hydrolysis of poly(ethylene terephthalate) melts, *J. Appl. Polym. Sci.*, **53**, 985–991 (1994).
145. Campanelli, J. R., Kamal, M. R. and Cooper, D. G., Kinetics of glycolysis of poly(ethylene terephthalate) melts, *J. Appl. Polym. Sci.*, **54**, 1731–1740 (1994).
146. Kao, C.-Y., Cheng, W.-H. and Wan, B.-Z., Investigation of alkaline hydrolysis of polyethylene terephthalate by differential scanning calorimetry and thermogravimetric analysis, *J. Appl. Polym. Sci.*, **70**, 1939–1945 (1998).
147. Kao, C.-Y., Wan, B.-Z. and Cheng, W.-H., Kinetics of hydrolytic depolymerization of melt poly(ethylene terephthalate), *Ind. Eng. Chem. Res.*, **37**, 1228–1234 (1998).
148. Chen, J.-W. and Chen, L.-W., The glycolysis of poly(ethylene terephthalate), *J. Appl. Polym. Sci.*, **73**, 35–40 (1999).
149. Wan, B.-Z., Kao, C.-Y. and Cheng, W.-H., Kinetics of depolymerization of poly(ethylene terephthalate) in a potassium hydroxide solution, *Ind. Eng. Chem. Res.*, **40**, 509–514 (2001).
150. Ravindranath, K. and Mashelkar, R. A., Modelling of poly(ethylene terephthalate) reactors: 3. A semibatch prepolymerization process, *J. Appl. Polym. Sci.*, **27**, 2625–2652 (1982).
151. Ravindranath, K. and Mashelkar, R. A., Modeling of poly(ethylene terephthalate) reactors: 4. A continuous esterification process, *Polym. Eng. Sci.*, **22**, 610–618 (1982).
152. Ravindranath, K. and Mashelkar, R. A., Modeling of poly(ethylene terephthalate) reactors: 5. A continuous prepolymerization process, *Polym. Eng. Sci.*, **22**, 619–627 (1982).
153. Ravindranath, K. and Mashelkar, R. A., Modeling of poly(ethylene terephthalate) reactors: 7. MWD considerations, *Polym. Eng. Sci.*, **24**, 30–41 (1984).
154. Pell, T. M., Jr and Davis, T. G., Diffusion and reaction in polyester melts, *J. Polym. Sci., Polym. Phys. Ed.*, **11**, 1671–1682 (1973).

155. Gao, Q., Nan-Xun, H., Zhi-Lian, T. and Gerking, L., Modelling of solid state polycondensation of poly (ethylene terephthalate), *Chem. Eng. Sci.*, **52**, 371–376 (1997).
156. Ravindranath, K. and Mashelkar, R. A., Modeling of poly(ethylene terephthalate) reactors: 6: A continuous process for final stages of polycondensation, *Polym. Eng. Sci.*, **22**, 628–636 (1982).
157. Castres Saint Martin, H. and Choi, K. Y., Two-phase model for continuous final-stage melt polycondensation of poly(ethylene terephthalate). 2. Analysis of dynamic behavior, *Ind. Eng. Chem. Res.*, **30**, 1712–1718 (1991).
158. Kang, C.-K., Lee, B. C. and Ihm, D. W., Modeling of semibatch direct esterification reactor for poly(ethylene terephthalate) synthesis, *J. Appl. Polym. Sci.*, **60**, 2007–2015 (1996).
159. Samant, K. D. and Ng, K. M., Synthesis of prepolymerization stage in polycondensation processes, *AIChE J.*, **45**, 1808–1829 (1999).
160. Bhaskar, V., Gupta, S. K. and Ray, A. K., Multiobjective optimization of an industrial wiped-film PET reactor, *AIChE J.*, **46**, 1046–1058 (2000).

3

Synthesis and Polymerization of Cyclic Polyester Oligomers

D. J. BRUNELLE

GE Global Research Center, Schenectady, NY, USA

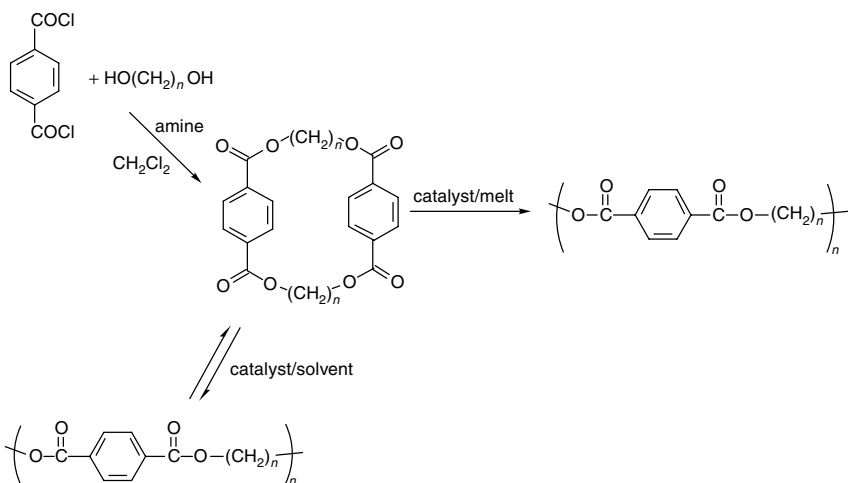
1 INTRODUCTION

Ring-opening polymerization (ROP) of cyclic oligomers of engineering thermoplastics such as poly(ethylene terephthalate) (PET) or poly(butylene terephthalate) (PBT) could be an extremely valuable technique for preparation of these materials. Typical polycondensation reactions (for example, from 1,4-butanediol and dimethyl terephthalate) require removal of reaction by-products (methanol and excess butanediol) in order to build molecular weight. As the molecular weight and melt viscosity of the polymer increases, this by-product removal can actually become a mass-transfer limitation on the rate of reaction. Polymerization of cyclic oligomers, on the other hand, does not require any by-product removal, since the cyclic oligomer has perfect stoichiometry (i.e. diol and diester components are equal). Only an entropically driven rearrangement of bonds is necessary for polymerization. For this reason, preparation of very high-molecular-weight polyesters can be achieved in a matter of minutes, thereby allowing novel processing techniques not normally associated with condensation polymers, such as casting, resin transfer molding, pultrusion, etc.

Cyclic oligomers of condensation polymers such as polycarbonates and polyesters have been known for quite some time. Early work by Carothers in the 1930s showed that preparation of aliphatic cyclic oligomers was possible via distillative depolymerization [1, 2]. However, little interest in the 'all-aliphatics' was generated, due to the low glass transition temperatures of these materials. Other small-ring, all-aliphatic cyclic ester systems, such as caprolactone, lactide

and pivalolactone have been extensively studied [3]. Hodge and co-workers have published a series of papers on a novel means for forming macrocyclic lactones, involving polymer-bound reagents [4]. This present review, however, concentrates on the cyclic oligomers of engineering thermoplastics such as PET or PBT typically formed from aromatic esters or acids. Cyclic oligomers are found in commercial grades of PBT and PET at levels of 0.5–3.0 %, being formed in their equilibrium concentration during melt polymerization reactions. The cyclic oligomers have been separated from the polymers and characterized by several groups [5–11] and synthesis of many discrete cyclics has also been reported using classical high-dilution techniques [12, 13]. Because of the limitations of extractive or high-dilution techniques, until recently, only small amounts of cyclic oligomers had been accessible.

Chemistry has been developed over the past 10 years for the facile preparation of large quantities of mixtures of cyclic oligomeric polyesters (dimer, trimer, tetramer, etc.). Through use of specific *pseudo*-high-dilution techniques in kinetically controlled reactions, cyclic oligomer mixtures have been prepared in yields as high as 90 %, and with excellent selectivity over the formation of linear oligomers [14]. These reactions were designed specifically for *high-productivity* synthesis, and have been scaled to hundreds of kilograms per batch. Additionally, development of *depolymerization* technology has demonstrated that large-scale conversion of commercial polyesters or linear polyester precursors into cyclic esters via ring–chain equilibration can be achieved. With the advent of these cyclic oligomer synthesis technologies, use of ring-opening polymerization of the cyclic oligomers for preparation of high-molecular-weight polyesters became a commercial possibility (Scheme 3.1).



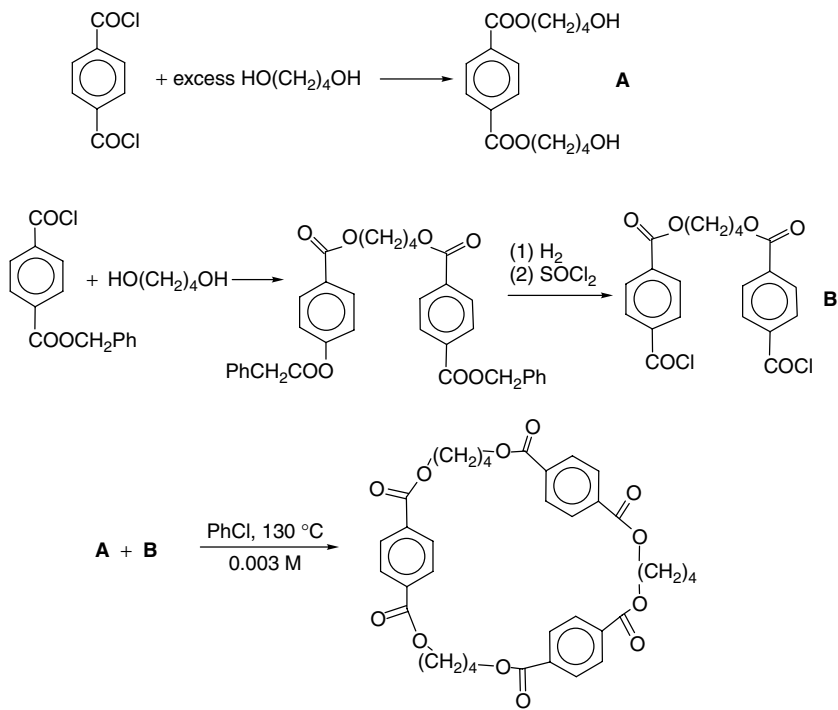
Scheme 3.1 Preparation of cyclic terephthalate esters via acid chlorides or depolymerization, and polymerization to high-molecular-weight polymer

During ring-opening preparation of polyesters from cyclic oligomers, low-molecular-weight precursors ($M_w \sim 1000$) lead to very high-molecular-weight polymers ($M_w > 100\,000$) in very fast reactions (minutes) without formation of any by-products. Thus, no diffusion-limiting removal of by-products or polymer purification were necessary. Because the molecular weight of the product polymer in an ROP reaction of a pure cyclic was controlled only by the amount of initiator, extremely high molecular weights could be attained. Additionally, the demonstration that polymerization could be achieved at temperatures well below the melting point of the final polymer meant that no thermal cycling of the molding apparatus was necessary. These attributes made use of cyclic oligomers for the preparation of composites very attractive.

2 HISTORY

Alkylene phthalate polyesters such as PET and PBT are commercial materials with a wide number of applications ranging from engineering thermoplastics to fibers. Both PET and PBT are semi-crystalline polymers with low glass transition temperatures, but with T_m s of about 265 and 225 °C, respectively. The cyclic esters based on iso- or terephthalic acid and aliphatic diols have been known for some time. The cyclic oligomers are present in commercial polymers, and have been isolated by a variety of extraction techniques, typically anti-solvent precipitation or Soxhlet extraction, followed by chromatography and recrystallization. The cyclic (3 + 3) trimer of poly(ethylene terephthalate) was first isolated in 1954 [6], and the dimer in 1969 [7]. An extensive study reporting the incidence of cyclic polyesters in 13 types of alkylene iso- and terephthalates was detailed by Wick and Zeitler in 1983 [9]. Various other authors have also studied cyclic oligomers obtained by extraction methods or melt equilibration methods [10, 11].

Macrocyclic alkylene phthalates have been prepared by various low-productivity, classical high-dilution techniques, involving multi-step reactions. Zahn and co-workers, for example, prepared macrocyclic oligomers via the reaction of oligomeric diols with oligomeric diacid chlorides, according to Scheme 3.2 [12, 13]. Very high dilution was typically necessary (<0.003 M), with an increase in concentration to 0.01 M reducing isolated yields of cyclic to only 1.5–7.9 %. The crystal structures of the macrocyclic (2 + 2) dimers of butylene terephthalate and ethylene terephthalate have been published [15, 16]. The cyclic esters of *o*-phthalates are somewhat easier to prepare, as one might expect, with the more favorable conformation for cyclization. Although numerous papers on oligomeric cyclic alkylene terephthalates have been published, no reports of *direct* formation of cyclics via reaction of monomeric terephthalate derivatives with monomeric diols could be found until the recent report of Brunelle *et al.* [14].



Scheme 3.2 Preparation of cyclic PBT oligomers via high-dilution condensation of oligomers [13]

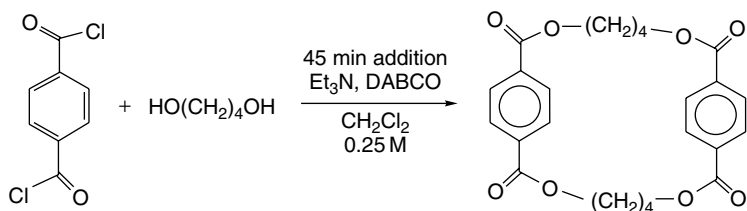
3 PREPARATION OF POLYESTER CYCLIC OLIGOMERS FROM ACID CHLORIDES

It seems reasonable that polyester cyclics could be prepared by an extension of the *pseudo*-high-dilution [17] chemistry used for the preparation of cyclic carbonate oligomers [18, 19]; however, such proved not to be the case. Brunelle *et al.* showed that the reaction of terephthaloyl chloride (TPC) with diols such as 1,4-butanediol did not occur quickly enough to prevent concentration of acid chlorides from building up during condensation [14]. Even slow addition of equimolar amounts of TPC and butanediol to an amine base (triethylamine, pyridine or dimethylaminopyridine) under anhydrous conditions did not form cyclic oligomers. (The products were identified by comparison to authentic materials isolated from commercial PBT by the method of Wick and Zeitler [9].)

Further investigation of model reactions revealed that the reaction of aromatic acid chlorides with diols such as butanediol or ethylene glycol was too slow to be useful for kinetically controlled *pseudo*-high-dilution reactions carried out

at low temperatures (0–40 °C). For example, reaction of butanediol with benzoyl chloride using stoichiometric pyridine or triethylamine as base provided only 5 or 11 % butylene dibenzoate, respectively, after one hour at ambient temperature [14]. However, additional experiments showed that less hindered amines gave significantly higher yields. In fact, very unhindered amines such as diazabicyclo[2.2.2]octane (DABCO) or quinuclidine have very fast reaction rates, forming quantitative yields of dibenzoate within 15 min at ambient temperature.

Cyclization reactions using these unhindered amines were carried out by concurrent addition of equimolar amounts of isophthaloyl chloride or TPC in CH_2Cl_2 and butanediol in dry THF to a slight stoichiometric excess of DABCO or quinuclidine in CH_2Cl_2 over one hour, with a final product concentration of 0.2 M (Equation (3.1)) [14]. HPLC analysis of the THF-soluble portion of the product indicated cyclic oligomers as the major products, with small amounts of linear oligomers (<2 %) also present. Isophthalate cyclics were isolated in 45 % yield, and PBT cyclics in 30 % yield, after filtration to remove insoluble polymer and flash chromatography to remove linear oligomers. This was the first example of the direct formation of alkylene terephthalate cyclics from reaction of monomeric diols and diacid chlorides. The major cyclic formed in both cases was the 2 + 2 dimer, which accounted for 40–65 % of the total cyclic yield, with diminishing amounts of higher cyclics. The highest oligomer observed by HPLC had a degree of polymerization (DP) of 7. Linear oligomers were present in amounts of 0.1–2 %. Cyclic dimer, trimer and tetramer were separated by column chromatography and were shown to be identical to authentic cyclics which had been isolated from commercial PBT by using literature techniques [9]. Linear oligomers were compared to oligomers prepared by reaction of dimethyl terephthalate with excess butanediol.

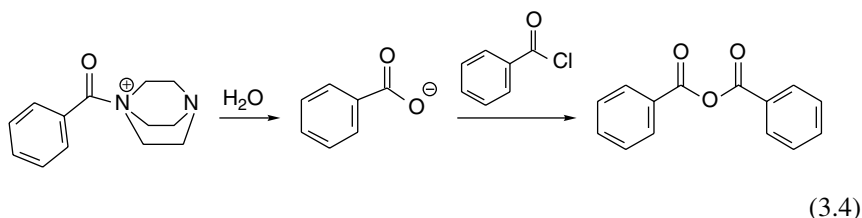
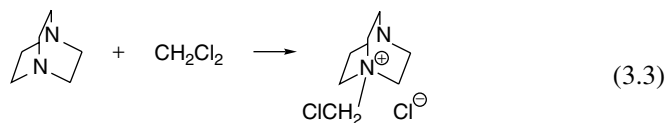
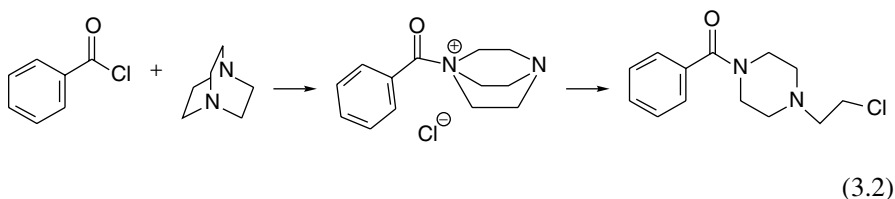


PBT cyclics: 40% with DABCO; 85% with $\text{Et}_3\text{N/DABCO}$

(3.1)

Additional work was carried out by the GE group on optimization of the reaction yield and to eliminate unwanted linear oligomers [14]. Three side reactions which interfere with synthesis of cyclics were identified: reaction of the amine with acid chloride to form an acyl ammonium salt, followed by decomposition to an amide (Equation (3.2)); reaction with CH_2Cl_2 to form a salt (Equation (3.3)); hydrolysis of the acid chloride, forming carboxylate via catalysis

with the amine via the acyl ammonium salt (Equation (3.4)). The first two reactions could be avoided by minimizing contact time between the reagents, and the third by carefully drying all reagents. When hydrolysis of acid chloride occurred, either anhydride or carboxylic-acid-containing polymers would be formed, products which would interfere with polymerization. Furthermore, hydrolysis would remove acid chloride from the reaction, thus damaging control of balanced stoichiometry.



Ultimately, only catalytic amounts (2.5–10 %) of unhindered amine were used, with Et_3N making up the remainder of the organic base, hence minimizing unwanted reactions of the very reactive unhindered amines. In addition, a means for delivering neat butanediol was devised, avoiding the need to use THF, which was also a potential source of water. Incorporating these changes into the process allowed the formation of PBT cyclics in 0.25 M reactions carried out in 1 h, with yields as high as 85 % and linear oligomer levels under 1.0 % (see Equation (3.1)). The remainder of material was higher-molecular-weight polymer, which was insoluble in the reaction medium, and could be removed directly by filtration.

Removal of the traces of linear oligomer proved to be important, since the presence of only 1 % linear oligomer limited the molecular weight achievable upon ROP. An *in situ* clean-up procedure was developed in which a slight excess of diacid chloride was added at the end of the reaction, converting any hydroxybutyl-terminated linear oligomers to acid-chloride-terminated oligomer. Upon quenching with water, hydrolysis to the carboxylic acid occurred, making the linears insoluble in CH_2Cl_2 , and easily removed by the same filtration used to remove

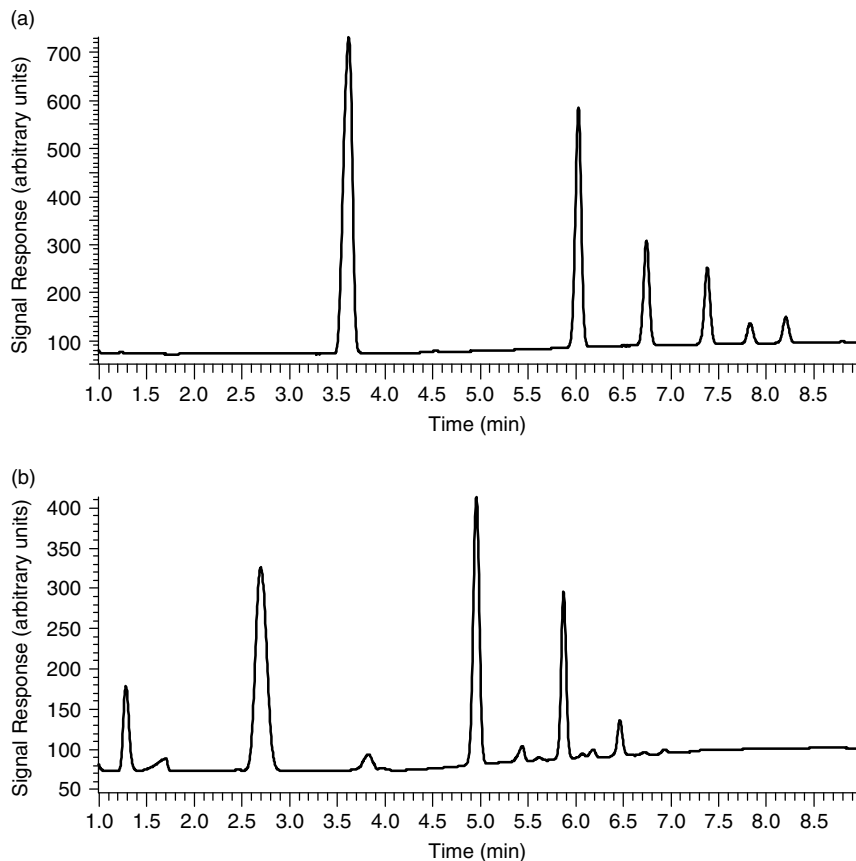
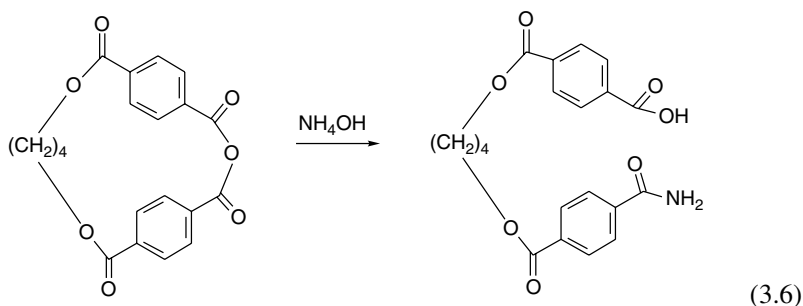
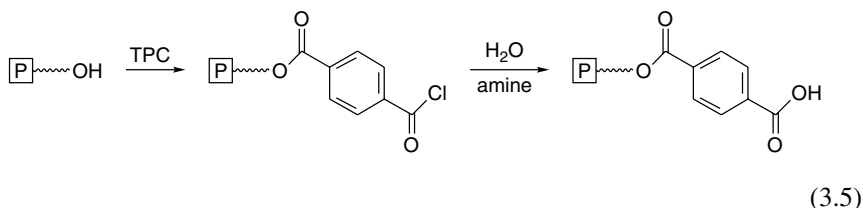


Figure 3.1 HPLC traces of (a) cyclic PBT oligomers from the reaction of butane diol with terephthaloyl chloride (cyclic dimer at 3.6 min), and (b) linear oligomers from butane diol and dimethyl terephthalate

polymer (Equation (3.5)). Traces of cyclic oligomeric anhydrides which had been formed by incidental hydrolysis of acid chlorides were removed by treatment of the crude product solution with NH_4OH , which converted them into amide-acid oligomers, which also were removed in the filtration step (Equation (3.6)). A typical HPLC trace for PBT cyclic oligomers formed by this technique is shown in Figure 3.1, along with the corresponding trace of linear oligomers made by transesterification of dimethyl terephthalate with 1,4-butanediol. The level of linear oligomer was less than 0.1 %. Once optimized, the reaction of terephthaloyl chloride with butanediol was easily scaled to several liters, and then to a 100-gal reactor, which was capable of producing 10 kg of cyclic PBT oligomers per batch in a 45 min reaction at 0.25 M. Neither long reactions times nor extremely dilute

reactions were necessary for cyclic formation.



Using similar procedures, a variety of alkylene phthalate cyclics were prepared in high yields via direct reaction of diols with diacid chlorides [14]; other than 100 % PBT and 5 % PET/PBT (molar) co-cyclic oligomers, these reactions were not optimized. The yields of cyclic oligomers from terephthaloyl chloride were somewhat lower than those from isophthaloyl chloride using either ethylene glycol or neopentylene glycol. In the former case, only a trace of cyclic (2 + 2) dimer was present, due to ring strain, and cyclic (3 + 3) trimer was the predominant species; a correspondingly higher amount of polymer was formed. It is not surprising that the isophthalates, which have a conformation more amenable toward cyclization, were formed more readily than the terephthalates.

4 POLYESTER CYCLIC OLIGOMERS VIA RING-CHAIN EQUILIBRATION (DEPOLYMERIZATION)

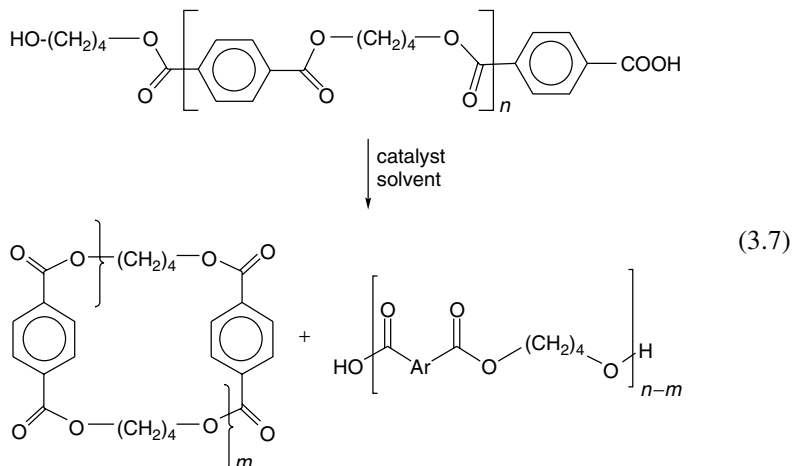
Formation of cyclic esters via ring-chain equilibration of polymers in dilute solution (depolymerization) has been known since the pioneering work of Carothers and co-workers in the 1930s [1, 2]. This procedure is particularly effective for the preparation of volatile small-ring esters such as caprolactone, which are easily distillable, thereby driving the equilibrium forward. The theory of ring-chain equilibration in polymers was first formulated in the Jacobsen-Stockmayer theory [20] and has been studied more recently [21]. According to the Jacobsen-Stockmayer theory, ring-chain equilibration of a polymer will lead to a mixture of cyclic oligomers and polymer in which a critical monomer concentration (CMC) can

be defined for each monomer structure. At concentrations below the CMC, only cyclics will be present, while above that concentration, mixtures of cyclics and polymer will be present. Kricheldorf *et al.* have recently pointed out a fact which should be obvious, namely that for condensation polymers which have *perfect* stoichiometry, and which are *completely* reacted, *only* cyclics can be formed, since the alternative is an infinite M_w polymer [22]. Of course, such conditions rarely exist outside very carefully controlled laboratory experiments. Furthermore, both PET and PBT are known to undergo β -scission reactions, forming olefin and carboxylic acid end groups. Such reactions become significant at temperatures above $\sim 250^\circ\text{C}$. Additionally, alcohol end groups on both polymers also react to form side products, back-biting to form THF and acid with PBT, and formation of ethers and diethers with PET.

With the non-volatile macrocycles required as precursors to engineering thermoplastics such as PBT (cyclic dimers are sublimable, but not higher oligomers), two limitations for commercial exploitation of depolymerization reactions have been the long reaction times necessary to reach equilibrium, and the low CMC, thus requiring large amounts of solvent. An early report of depolymerization of PET by Cooper and Semlyen suggested reaction for 96 h [23]. Similarly, a Japanese patent [24] reports the depolymerization of PET to cyclic PET oligomers, requiring reaction at $240\text{--}280^\circ\text{C}$ in α -methylnaphthalene, using 1.0 wt% of PET for 24 h, with an unspecified amount of catalyst. Attempts to depolymerize PBT polymers under such conditions afforded poor results, with mixtures of cyclics, linear oligomers and polymer being formed. It seems likely that β -scission reactions may have interfered with the chemistry at such high temperatures.

The depolymerization of polyesters has very recently been studied by several groups. An efficient preparation of alkylene phthalate cyclic oligomers via ring-chain equilibration using tin catalysts first appeared in the patent literature in 1995 (Equation (3.7)) [25]. Efficient use of titanate catalysts for the preparation of PBT cyclics via depolymerization in a continuous reactor was patented in 1997 by Brunelle *et al.* [26]. At about the same time, Bryant, Semlyen and co-workers published a series of papers on preparation of cyclics via ring-chain equilibration [27–29]. Brunelle concentrated on efficient throughput reactions to form mixtures of cyclics with careful attention paid to avoid linear oligomers, in order to utilize the cyclics for ROP reactions. Bryant and Semlyen concentrated on isolation and characterization of the oligomers by fast-atom bombardment mass spectrometry, tandem HPLC–MS and X-ray crystallography. Bryant, Semlyen and co-workers also published papers on a variety of other cyclic ester and ether ester oligomers using the same technology, including tetraethyleneglycol iso- and orthophthalates, decamethylene phthalates and poly(ethylene terephthalate)s. Hodge and co-workers have also published several papers on the depolymerization/polymerization techniques, including all-aliphatic systems [30], olefin-containing polyesters (using olefin metathesis) [31] and naphthalene dicarboxylate

systems [32]. Hodge and co-workers have also published reviews on depolymerization/polymerization technology [33, 34]. Recently, Burch *et al.* have reported novel depolymerization methods for the preparation of PET cyclic oligomers, and their polymerization to high molecular weight [35].



Laboratory studies by the GE team [25, 26] were carried out in glassware in *o*-dichlorobenzene, since PBT is quite soluble at its reflux temperature, and reaction rates were also reasonable at that temperature. Surprisingly, extremely dilute solutions were not necessary to form reasonable yields of cyclic oligomers. Using Valox® 315 (which has a weight-average molecular weight (M_w) of about 100 000 relative to polystyrene standards) as the starting material, about 50 % cyclics were detected by GPC in reactions carried out at 0.10 M (1.68 wt%) in *o*-DCB. Decreasing the concentration to 0.050 M gave an increase to about 90 %, and increasing the concentration to 0.15 M gave a decrease to 33 % yield of cyclics (see Table 3.1). Larger-scale work was carried out in either 1-L or 8-L stainless steel autoclaves, using *o*-xylene as the solvent, since use of non-chlorinated solvents was preferred. Most of the early work was carried out by using tin

Table 3.1 Effect of depolymerization concentration on cyclics and polymer

Concentration (M)	Cyclics (%) ^a	Linears (%) ^b	Polymer M_w	Polymer M_n
0.20	26	—	14 700	10 200
0.10	50	1.3	10 500	7 000
0.75	65	1.4	6 100	2 600
0.05	89	1.1	3 800	2 040

^a Using GPC.^b Using HPLC.

catalysts of various types. Early results indicated that tin catalysts were far more effective than titanates for the ring-chain equilibration reaction. Cyclic stannoxanes **1** or **2**, prepared from Bu_2SnO and ethylene glycol or 2,2-dimethyl-1,3-propanediol were used in most of the early reactions, while scoping the conditions necessary for depolymerization. Equilibration in refluxing *o*-dichlorobenzene took about 30 min to 2 h, depending on reactant and catalyst concentrations.

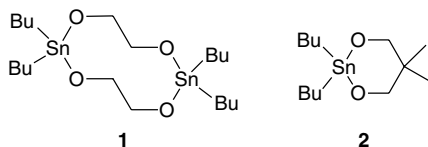


Figure 3.2 compares the level of cyclics on a molar, wt%, or yield basis as a function of reaction concentration. Note that as the reaction concentration dropped, the yield increased to near 100 %, as predicted from theory. However, the amount of cyclic PBT on a molar or wt% in solution remained constant at the critical monomer concentration, which is about 0.050 M, regardless of the concentration of polymer in solution. In fact, if one calculates the amount of cyclic present in an equilibrated melt (1–2 %), it is also about 0.05 M cyclic. *The same amount of cyclic was generated via the ring-chain equilibration process, regardless of the reaction concentration*; only the amount of polymer which remains as a by-product

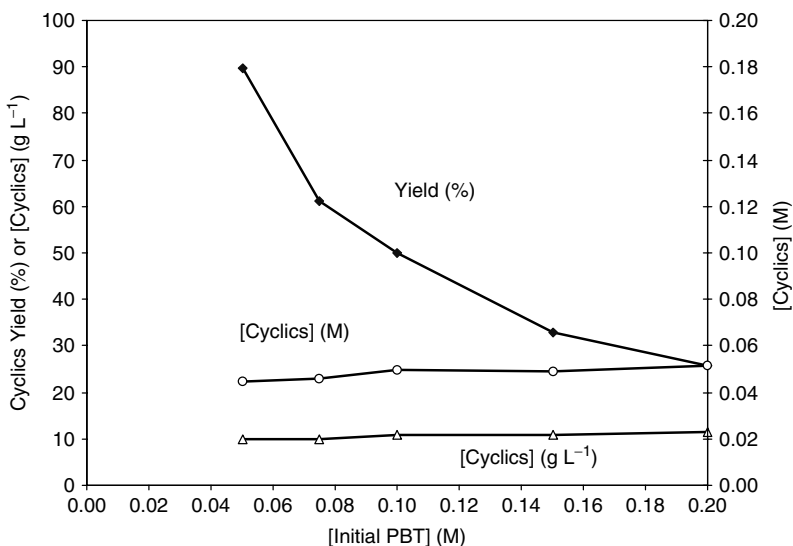


Figure 3.2 Amount of cyclics formed as a function of reaction concentration during the depolymerization of Valox® 315

differed, and hence the overall yield (i.e. cyclics divided by (cyclics + polymer)). Unfortunately, the theory breaks down at extremely low reaction concentrations, since some 'polymer' must always be formed, because the starting material has end groups (i.e. Kricheldorf's 'perfect stoichiometry' conditions [22] cannot be met); thus a 100 % yield of cyclic can never be achieved.

Figure 3.3 shows the progress of reactions carried out at various concentrations at reflux in *o*-DCB using 2 mol% of cyclic stannoxane **1** as catalyst. Most reactions, except the most dilute, reached equilibrium surprisingly quickly, in about 1 h at that temperature. Although previous reports suggested that much longer reaction times and higher temperatures were necessary, the effect may have been due to inefficient catalysis in the earlier work [23, 24]. The stannoxanes are particularly effective catalysts, since they are completely soluble in the reaction solvent. The fact that equilibrium is achieved in 30 min–1 h regardless of concentration suggests that the depolymerization reaction is first-order, as one would expect for back-biting. If so, then the reaction of catalyst with the polymer must occur faster than the rate of depolymerization. The reaction temperature seemed to have only a slight effect on the equilibrium position, with

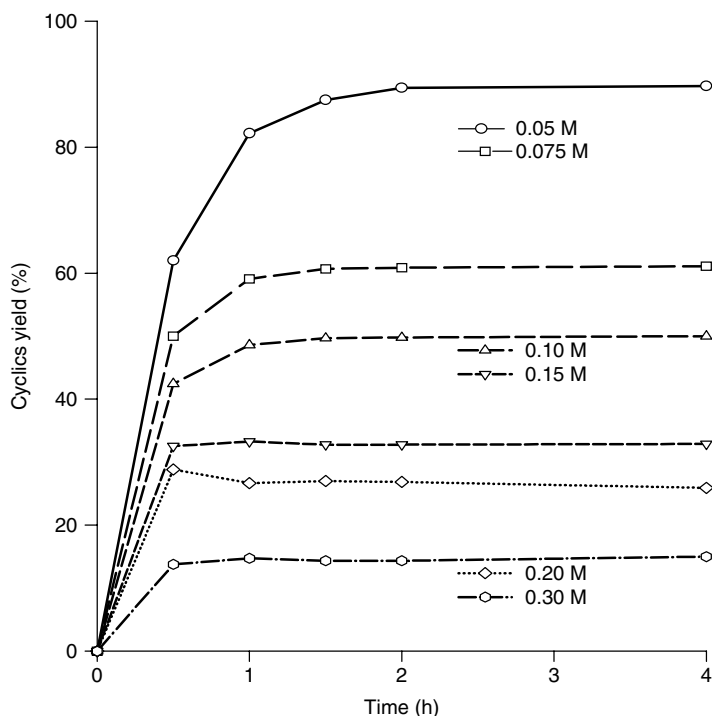
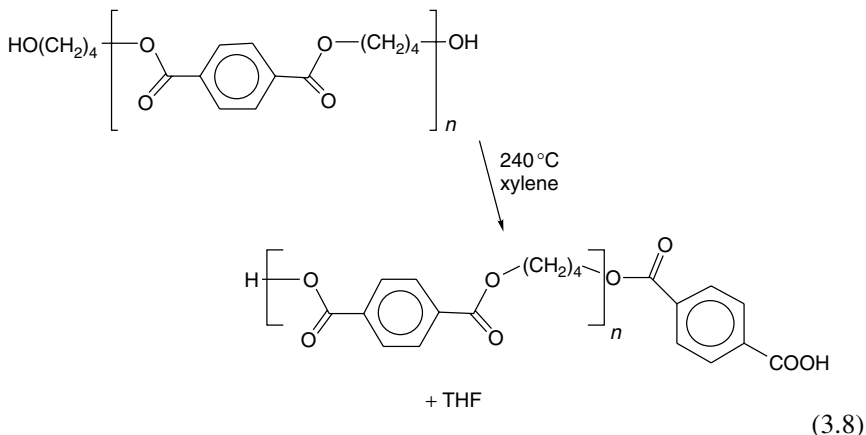


Figure 3.3 Progress of reactions carried out at various concentrations during the depolymerization of Valox® 315

similar yields being obtained from reaction in dichlorotoluene at 180 or 200 °C, or in trichlorobenzene at 214 °C; the equilibrium was achieved more rapidly at the higher temperatures, as expected. Solubility of the starting polymer in the chosen solvent was very important. Reaction rates were depressed whenever the polymer was not completely dissolved at the reaction temperature (see work by Burch *et al.* [35] described below, which also gave lower yields).

The tin catalysts are robust and relatively insensitive to water; reaction with water to form dibutyltin oxide is reversible. However, removal of traces of tin catalyst before isolation of the cyclic was necessary, in order to prevent premature polymerization, and so the easily quenchable titanates became the catalysts of choice. In the case of such catalysts, the use of absolutely dry solvents was necessary to prevent their hydrolysis [26]. Brunelle *et al.* have also reported the preparation and use of specific chelated titanates (made by reaction of diethylene glycol with tetraisopropyl titanate), which are more resistant to hydrolysis [36]. The GE group also reported that hydroxybutyl-terminated oligomers could be eliminated from the reaction products by carrying out the depolymerization reaction at elevated temperatures [26]. Elimination of tetrahydrofuran from hydroxybutyl end groups on PBT is known to occur during condensation polymerization. Use of higher temperatures encourages such reactions, forming carboxylic-acid-terminated oligomers, which were easily removed from the product solution by filtration (Equation (3.8)). Using these techniques, complete depolymerization of PBT was carried out in *o*-xylene in less than 30 min, followed by quenching with water, and isolation of the cyclic material. The PBT cyclic oligomers obtained via depolymerization had a different distribution of oligomers than those prepared via acid chlorides. Whereas the kinetically controlled cyclization (via acid chloride) produces mainly cyclic dimer (50 %), the distribution from depolymerization is broader, with the following approximate proportions: dimer – 32 %, trimer – 34 %, tetramer – 17 %, pentamer – 11 %, hexamer – 2 %, and heptamer – 4 % (Figure 3.4).



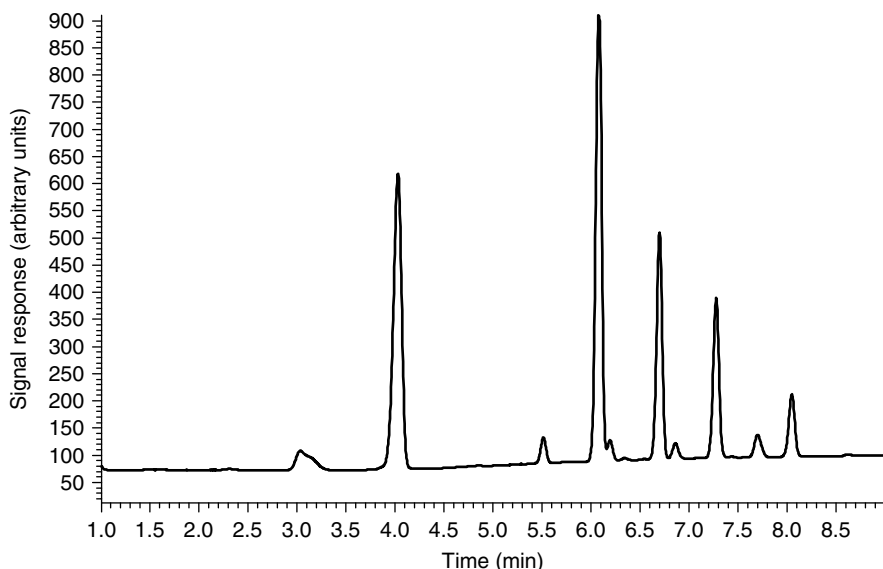


Figure 3.4 HPLC trace showing the formation of 5% PET/PBT cyclic oligomers from the depolymerization of 5% PET/PBT. Cyclic dimers are indicated at 3.0 and 4.0 min, with trimers appearing at 5.0 and 6.0 min, etc.; the small peaks represent mixed co-cyclics

Reports of depolymerization studies carried out by Semlyen and co-workers at the University of York, UK, typically used much longer reaction times (24–72 h) for the depolymerization of PET [27]. This group also reported that the titanates were ineffective catalysts for depolymerization, but it is not known whether measures to prevent titanate hydrolysis were taken. The York group also reported that the relative proportions of cyclic oligomers (trimer, tetramer, etc.) altered as the dilution ratio was changed. Similar results were seen with PBT. They have also reported fast-atom bombardment mass spectrometry (FAB-MS), LC-MS, GPC and X-ray crystallography data. The most recent work reports characterization of the cyclic oligomers from six ester and ether ester systems [29].

Burch *et al.* have recently published work on the depolymerization of PET to cyclic oligomers using either suspension or solution reactions [35]. Solution polymerizations were carried out in 1-methylnaphthalene or diphenyl ether using either high-molecular-weight PET or bis-(2-hydroxyethyl)terephthalate (BHET) (in the latter case, ethylene glycol was removed during the reaction). The distribution and yield of cyclic oligomers was essentially the same with both starting materials, since equilibrium was achieved; reaction times varied from 1 to 4 h. Reporting of yields was somewhat puzzling: the body of the paper reported 90 % yield at 2 % solids and 65 % yield at 5 % solids. However, the experimental section reported 92 % yield at 0.6 % solids, 74 % at 1.7 % solids (both from

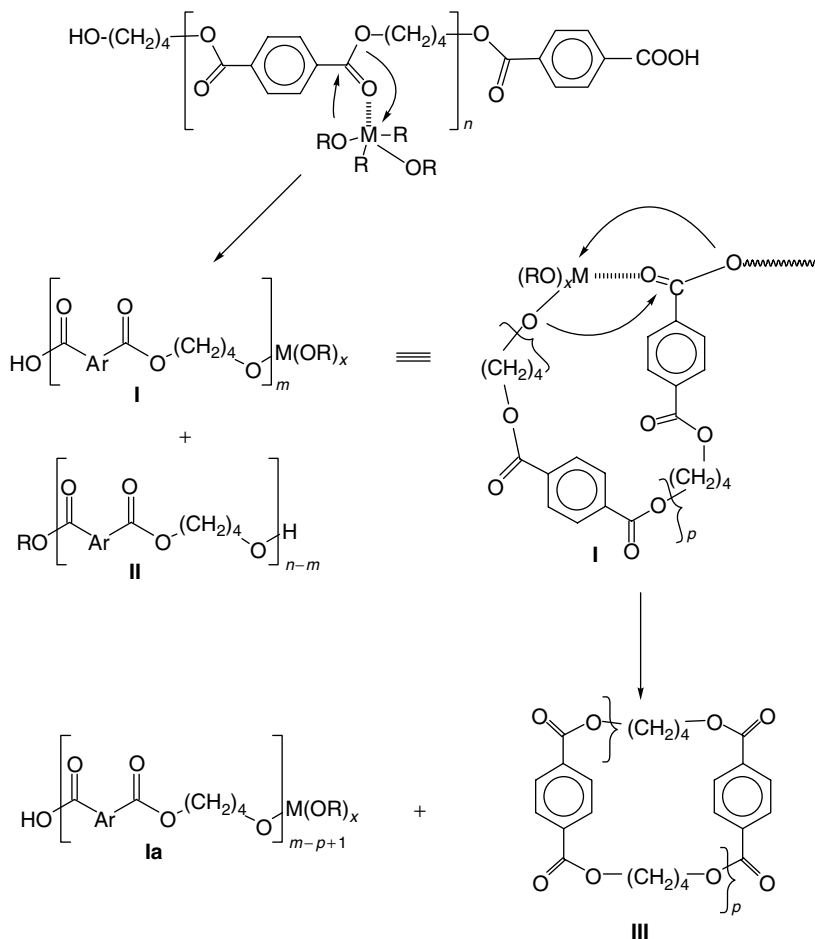
BHET), and only 11 % at 2.7 % solids from PET for reactions run in diphenyl ether, and 29 % yield for a reaction at 2.4 % solids in 1-methylnaphthalene. Otherwise, the reactions appear similar to those reported by Brunelle and co-workers [25, 26], except with longer reaction times and higher temperatures.

The suspension depolymerizations reported by Burch *et al.* are quite interesting [35]. They report that 'clean' cyclic oligomers can be obtained by carrying out depolymerization in solvents such as hexadecane, in which PET or its oligomers are *not* soluble. Thus, refluxing PET for 240 min or BHET for 20–240 min in hexadecane at 287 °C, followed by filtration to remove the polymer, provided cyclics with no detectable linear material. However, the yields were significantly lower than when using the solution technique, for example, 4 g of PET provided 0.82 g of cyclic oligomer (21 % yield) after 4 h reflux at 1.0 % solids. The yield from BHET was even lower, affording 0.80 g of cyclics from 40 g of BHET (2.6 % yield) after reflux for 20 min at 9 % solids.

Analyses for cyclics can also be carried out by using a standard size exclusion chromatography (SEC) column (e.g. Varian TSK), integrating the high vs. low M_w sections. However, clean separation of polymer from cyclics was not possible, and this method does not distinguish between oligomeric linear and cyclic materials. An HPLC method has been developed, using internal standards, which gives good quantitation of cyclics [25]. This technique also allowed quantification of the level of linear oligomers formed in the process, but required separation of the by-product polymer before analysis. A faster method utilized SEC analysis, using a special low-molecular-weight column (Polymer Laboratories Mixed E) which afforded near baseline separation of cyclics from polymer. Crude samples could simply be dissolved in HFIP/ CHCl_3 and injected directly. Semlyen and co-workers have used the same SEC columns, but in a bank of three, to obtain clean separation of dimer through octamer oligomers [27, 28]. Resolution of linear oligomers is much 'cleaner' when using HPLC rather than SEC, but it was found not to be necessary in the GE work, since production of linears was essentially eliminated at high temperatures. As the concentration of polymer in the depolymerization reaction was increased, the yield of product decreased, as mentioned above. The nature of the remaining polymer also changed, with higher-molecular-weight polymer being recovered at higher concentrations. The amount of linear *oligomer* did not seem to vary in reactions carried out in *o*-DCB (see Table 3.1).

5 MECHANISM FOR FORMATION OF CYCLICS VIA DEPOLYMERIZATION

The mechanism for cyclic formation via depolymerization is the same type of transesterification which occurs on polymerization, as outlined in Scheme 3.3. Metal alkoxides such as tetraalkyl titanates or dibutyl tin alkoxides have proven



Scheme 3.3 Mechanism for the metal alkoxide catalyzed formation of cyclics via depolymerization

to be the most efficient catalysts for such reactions. The metal alkoxides function by activating a carbonyl via complexation, and then transferring an alkoxide ligand. Thus, a linear polymer will interact with a metal alkoxide catalyst to transfer an alkoxide onto the polymer chain, forming a species such as **I**, and releasing a linear alkoxide which is terminated with the transferred ligand (**II**). The original polymer chain length (n) will be decreased by m units in such a reaction. The metal terminated polymer **I** can then react either by chain-transfer (polymerization reaction), or by a back-biting reaction to form cyclics. The degree of cyclization vs. polymerization is controlled by the concentration of species **I** in solution. Dilute solutions favor *intra*- rather than *intermolecular* reactions.

Cyclization to oligomers with a degree of polymerization $p + 1$ releases another linear polymer chain terminated with a metal (**Ia**), which is shorter in length by $p + 1$ units, and which can continue to react to form cyclics. Eventually, equilibrium is reached, and the linear chains (**I**, **Ia**, and **II**) react degenerately at the same rate as they form cyclics. The active intermediate **I** could also be formed by direct reaction of an alcohol-terminated polymer with the metal alkoxide, with loss of free alcohol, but this event is far less likely than reaction at the interior of a chain, because the number of end groups is small by comparison. In this regard, metal alkoxides have the advantage over Brønsted acids, which can only catalyze reactions of chain ends (i.e. attack of RCH_2OH at a chain end on an ester via back-biting, using acid catalysis).

Figure 3.5 shows the distribution of cyclics formed typically as a function of time in a PBT depolymerization reaction. It can be seen that initially the levels

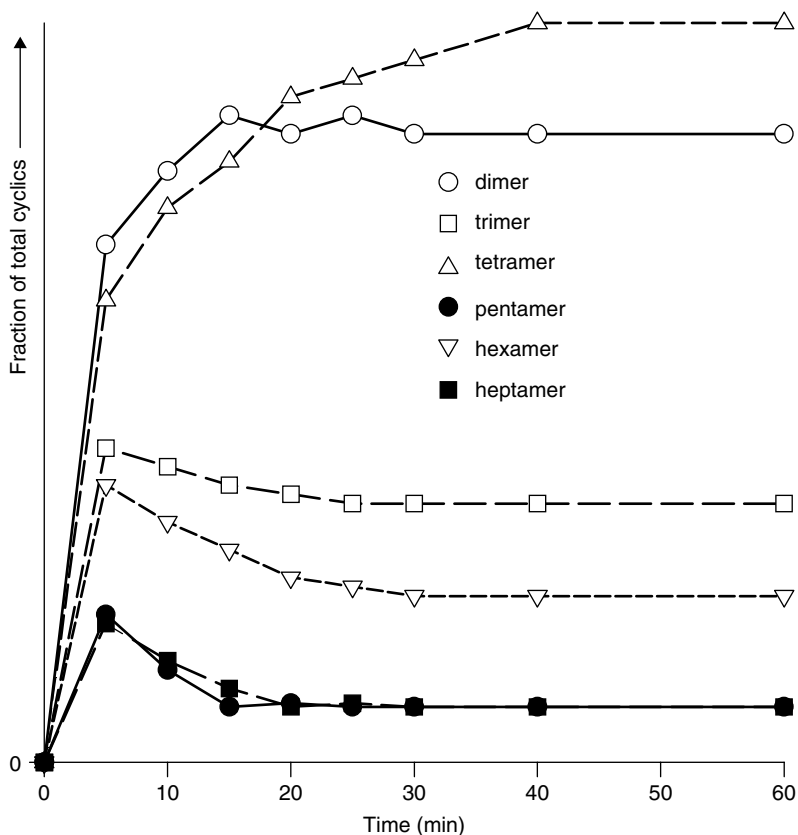


Figure 3.5 Distribution of cyclics formed as a function of time in a typical PBT depolymerization reaction

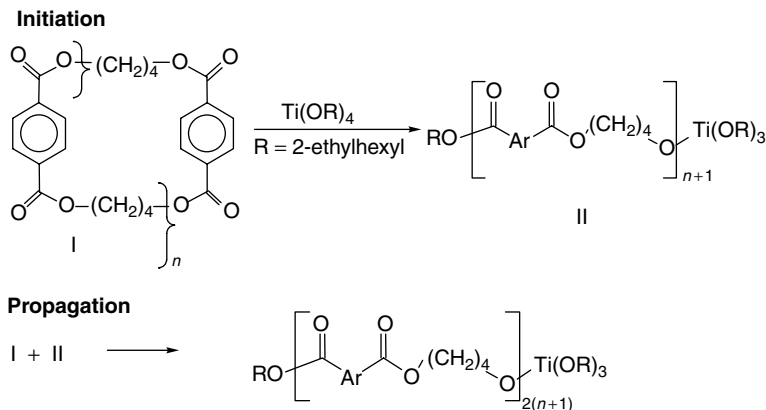
of longer chains are higher than at the end of the reaction. At this early stage, many long polymer chains are present in solution from which cyclics can form. As the reaction proceeds, not only are the linear chains reduced in size, but also the cyclics themselves can be attacked by the metal alkoxide. Such an attack forms a short polymer chain such as **I** or **Ia**, which can then react to produce a smaller cyclic. Entropy favors the formation of the smallest cyclics, as long as ring-strain is not involved. An attempt at correlation of the experimental results with theory has been presented by Hubbard *et al.* [21].

6 POLYMERIZATION OF OLIGOMERIC ESTER CYCLICS

With a supply of oligomeric cyclic phthalates readily available from two routes, the study of bulk ring-opening polymerization became feasible. Because reactive processing applications were most appealing, and because PBT or PET cyclics led to crystalline, insoluble polymers, melt polymerizations have been the methods of choice by most investigators. Additionally, the extremely low melt viscosity of PBT cyclics (about 30 cP at 190 °C) [37] made melt processing extremely attractive. Visually, the mixture of PBT cyclic oligomers began to melt at about 140 °C, and was completely molten at 160–190 °C. DSC showed a broad melting range (100–175 °C), with peaks at 130 and 160 °C; the total melting endotherm was 68 J/g [14]. It appears that the nature and amount of crystallinity in the cyclics can be a function of the isolation technique (melt vs. anti-solvent). The Burch group has carried out very careful work on the types of crystallization which occur in PET cyclics of various compositions, finding that the m.pt. of the cyclic mixture can vary from ~290 to 320 °C. Several different crystal forms were identified by scanning electron microscopy (SEM) [35].

The ROP mechanism involves initiation to form an active chain end, followed by propagation reactions continuing until all of the cyclic oligomers are depleted and the ring–chain equilibration becomes degenerate (Scheme 3.4). In this case, the initiator becomes built into the polymer, and it is not terminated unless quenched. Due to their size and flexibility, the cyclic oligomers (other than the PET dimer) are nearly strain-free, and the polymerization is almost thermoneutral, leading to complete equilibration of ester groups (i.e. initiation, propagation and chain transfer have nearly the same rates). Polydispersivities therefore approach 2.0, and were typically in the range of 2.0–3.0, as in conventional polycondensation of polyesters (commercial Valox[®] 315 has $M_w/M_n \sim 2.3$). GPC traces are typically monomodal, with a small amount (1–3 %) of cyclics remaining, presumably the equilibrium amount.

Many reports on the polymerization of PET cyclic oligomers, with various results, have appeared. Polymerization in the melt at 275–310 °C has been reported by Goodman and Nesbitt [8]. The latter claimed that a linear polyester was formed when the macrocycles are heated with a catalyst, neat, or in 2-methylnaphthalene at 240 °C. They also stated that scrupulously dried material



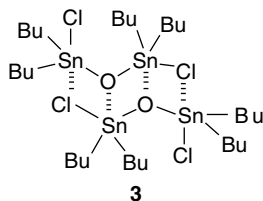
Scheme 3.4 Ring-opening polymerization of oligomeric PBT cyclics

does not polymerize in the presence of antimony oxide under dry nitrogen, suggesting that a second initiating substance (presumably water) was necessary. Polymerization was also reported with tetramethyl titanate, lead oxide or calcium oxide, but not with *p*-toluene sulfonic acid. Burch *et al.* report that low-molecular-weight linear species affect the polymerization rates [35]. Polymerization in the presence of linear oligomers occurred in two separate kinetic regimes, with one being the fast ring-opening, and the second, the slower transesterification of the linear materials. On the other hand, Burch *et al.* report that polymerization of rigorously purified cyclic trimer is extremely slow at 300 °C in the absence of linear oligomers. However, they also point out that the cyclic trimer melts only at 321 °C. Polymerization at slightly lower temperatures (280 °C) was achievable if the cyclic was heated with an equal weight of PET linear polymer ($M_w = 32\,000$) within times of 1 to 30 min. In all cases reported by these workers, only low- M_w material was obtained ($M_w = 24\,000$ – $39\,000$). These low molecular weights may reflect the presence of low-molecular-weight linear materials, which upon equilibration into the polymer, will limit the final M_w .

MacKnight and co-workers reported the preparation and polymerization of PET cyclics at about the same time [38, 39]. Polymerization to high M_w ($M_n = 20\,000$ – $27\,000$) was achieved within 10–25 min at temperatures of 270–293 °C, using antimony oxide as the catalyst at 0.3–1.0 %. Other catalysts were also investigated, including the cyclic stannoxanes reported earlier by Brunelle *et al.* [14]. However, at the high temperatures required for PET polymerization, the tin catalysts proved to be unstable.

Finally, Nagahata *et al.* have reported polymerization of PET cyclic dimer [16]. The latter is a minor component in PET cyclics, normally present at less than 10 % of the total cyclics made either from acid chlorides or via depolymerization. Nagahata *et al.* report melt polymerization at 250–325 °C, leading to an $M_w \sim$

25 000 in ~ 300 min, with optimum results obtained at 275°C . Use of catalysis was subsequently reported, with a chlorostannoxane catalyst (**3**) giving the best results (conventional catalysts like Bu_2SnO or titanates were not investigated). The authors also suggest that solid-state polymerization may have occurred [40], although in cases where the polymerization was carried out below the melting point of the dimer (225°C), such a high level of catalyst was used (4%) that dissolution in the catalyst might be a possibility. In any event, again, only low-molecular-weight polymers ($M_w < 36\,000$) were obtained.



Polymerization of oligomeric PBT cyclics is much more readily achieved, due to the low melting point of the oligomeric mixture. The polymerization is also novel for polyesters, in that melt polymerization can be achieved well below the melting point of the final polymer. Thus, although high- M_w PBT has a melting point of about 220 – 225°C , melt polymerization can be carried out at 180 – 190°C . Although many types of compounds can initiate polymerization of oligomeric cyclic esters, certain tin and titanium initiators have proven most effective (Table 3.2). Both commercially available titanates (tetrakis-(2-ethylhexyl)-titanate (TOT) or $\text{Ti}(\text{Oi-Pr})_4$) and cyclic stannoxanes such as **1** were effective initiators for polymerization at levels of 0.05–1.0 mol% based on monomer units [14]. These initiators operate via the same Lewis acid activation–insertion mechanism described above for depolymerization (Section 5). Furthermore, polymerizations reported by the GE group result in extremely high molecular weights ($M_w > 100\,000$), attesting to the ‘clean’ nature of their cyclic oligomers.

DSC analysis of a mixture of PBT cyclic oligomers containing the stannoxane **3** showed only the melting endotherm ($\Delta H = 68\text{ J/g}$), with no exotherm evident. Apparently, polymerization starts as the cyclics melt. Cooling showed the crystallization of the polymer, while the second heating stage displayed only the melting point of the PBT polymer at 213°C ($\Delta H = 54\text{ J/g}$); the polymer had an M_w of 117 000, and was 97% polymerized (from GPC analysis).

Data for examples of polymerization of PBT cyclic oligomers are shown in Table 3.2 [14]. Polymerization under mild conditions (0.2–0.3 mol% titanate initiator at 190°C) for 6 min led to M_w s of 95 000–115 000 (entries 2, 4 and 5). These results indicate that either the PBT cyclic polymerization is far more facile than observed for PET cyclics, or that the cyclics had higher purity, since the rates were faster and the final molecular weights significantly higher. As

Table 3.2 Polymerization of PET/PBT (5 % molar ratio) co-cyclic oligomers^a

Entry	Initiator (mol%) ^b	<i>T</i> (°C)	<i>t</i> (min)	Polymerization (%)	<i>M_w</i> ^c	<i>M_n</i> ^c	<i>M_w</i> / <i>M_n</i>
1	Bu ₂ Sn–O (0.5)	275	10	97	58.9	–	–
2	Ti(Oi-Pr) ₄ (0.2)	190	6	98	115	55	2.1
3	TOT (0.1)	190	20	99	352	167	2.1
4	TOT (0.2)	190	20	98	117.1	52	2.25
5	TOT (0.3)	190	6	95	95	39.7	2.4
6	TOT (0.3) + 0.5 % linear ^d	190	6	96	75.6	26.7	2.8
7	TOT (0.3) + 1.0 % linear ^d	190	6	95	61.2	22.1	2.8
8	TOT (0.3) + 2.0 % linear ^d	190	10	98	25.4	11.4	2.2
9	TOT (0.4)	190	20	97	62.1	19.6	3.2
10	TOT (0.5)	190	6	99	53.2	22.7	2.3
11	Stannoxane 1 (0.05)	190	20	91	401	303	1.3
12	Stannoxane 1 (0.1)	190	20	95	344	177	1.9
13	Stannoxane 1 (0.2)	190	20	95	445	286	1.55
14	Stannoxane 1 (0.4)	190	20	98	330	171	1.9
15	Stannoxane 1 (0.2)	*d ^e	10	97	117	51.9	2.25
16	NaOEt (1.0)	225	10	41	5.3	–	–
17	Sn(OMe) ₂ (1.0)	250	10	54	36	–	–
18	Commercial (Valox® 315)	NA ^f	NA ^f	–	111	48.7	2.3

^a Polymerizations were carried out neat by adding catalyst in a minimum amount of solvent to molten cyclic oligomers at the temperatures shown.

^b Relative to monomer units.

^c $\times 10^{-3}$, relative to polystyrene standards.

^d bis-(4-hydroxybutyl)terephthalate added at level shown.

^e Polymerization carried out in DSC pan with temperature programming from 50 to 250 °C at a rate of 20 °C/min.

^f NA, not applicable; no catalyst level for commercial Valox 315.

in living ring-opening polymerizations, the molecular weight of the polymer was controlled by the molar ratio of cyclic esters to linear functionalities. Low-molecular-weight linear oligomers, such as 1,4-bis-(4-hydroxybutyl) terephthalate or its oligomers, limited the ultimate molecular weight achieved (entries 6, 7 and 8), and hence the precautions taken for their removal during synthesis. Furthermore, some initiators (such as TOT) introduced monomers (2-ethylhexanol) which also limited the molecular weight. Thus, as the level of titanate initiator (which contains four alcohol groups) was decreased, higher molecular weights were observed (entries 3, 4, 5, 9 and 10). Unlike the titanates, when the cyclic stannoxane **3** was used as the initiator, no decrease in molecular weight was observed with increasing catalyst level, because no end groups were introduced; the tin should be built into a macrocyclic polymer which is more stable to GPC conditions than the titanate esters (entries 11–14). The GPC characteristics of the stannoxane-initiated polymerizations were quite different from those of the titanate-initiated systems (much higher *M_w*s and lower apparent dispersivities). Basic catalysis proved ineffective (entry 16).

The polymerization reaction was typically carried out at 180–200 °C, well below the PBT melting point of ~225 °C. Regardless, complete polymerization with only 1–3 % cyclics remaining (by GPC) could be achieved. Three factors controlled the completeness of polymerizations, i.e. (1) purity of the monomers, (2) complete mixing of initiator before the polymerization process caused the viscosity to increase to the point where mixing stopped (the initiator needs to be intimately mixed with the molten cyclic), and (3) polymerization at a high enough rate that it was essentially complete before crystallization occurred. For most fast initiators, polymerization at 190 °C by using mechanical stirring at 300–500 rpm was ideal for effecting complete conversion to polymer. In some cases, premature crystallization (at temperatures below 185 °C) or inefficient mixing of the initiator led to incomplete polymerization and recovery of cyclics along with polymer. Although the molten PBT cyclics are easily stirred in the absence of initiator, when using titanate initiators for polymerization at 190 °C, solidification of the polymer occurs within seconds.

Work on the kinetics of the ring-opening polymerization of PBT cyclic oligomers has also been reported [41]. By using sublimed and recrystallized PBT cyclic dimer and carrying out solution polymerizations, Brunelle and Serth-Guzzo have shown that rapid polymerization occurs at temperatures as low as 150 °C, *in the absence of linear oligomers*, when using titanate catalysis. In fact, the rate of ROP is significantly faster than the condensation rates normally reported for PBT synthesis reactions. Further work has shown that the presence of chelating groups (such as butanediol or ethylene glycol) will slow the reaction, that linear oligomers have no effect on the rate of reaction, but that aromatic carboxylic acids completely inhibit titanate-catalyzed ring-opening at 180 °C. These facts may explain the differences noted by other authors, whose polymerizations may have been contaminated by acidic impurities (Burch mentions the presence of acidic end groups [35]).

Polymers prepared from cyclic oligomers showed higher levels of crystallinity than conventionally prepared polyester (60–80 J/g vs. 35–50 J/g for commercial materials of similar molecular weights [14]). The cause of such excess crystallinity is still under investigation [42]. One possibility is that more order exists in the polymer since polymerization only requires breaking and making ester bonds, rather than removal of condensation by-products such as methanol or butanediol and the vigorous mixing which this process requires. The crystallinity of the polymer could be controlled by incorporation of low levels of another monomer (such as ethylene glycol) into the cyclics [43]. A co-cyclic prepared by mixing reactants melted at a significantly lower temperature than a physical mixture of PET and PBT cyclics which had been prepared separately. Much of the polymerization [14] and depolymerization [25, 26] work carried out at GE used a 5 % (molar) PET/PBT co-cyclic composition.

Conversion of cyclic oligomers to composite structures via Resin Transfer Molding (RTM) and Reaction Injection Molding (RIM) techniques has been demonstrated, and will be the subject of subsequent publications. Glass loadings

as high as 70% and composite tensile moduli of 3×10^6 psi are routinely achieved [44].

7 CONCLUSIONS

Recent chemistry has been developed for the efficient preparation of oligomeric cyclic terephthalate esters. The current techniques have made it possible to prepare hundreds of kilograms of the cyclic oligomers per batch, and have made these materials readily available for study. Two different methods for synthesis were developed, i.e. kinetically controlled condensation from acid chlorides, and depolymerization of linear polymers or oligomers. Both methods of synthesis have been studied mechanistically. Purification to polymerization quality has been simply achieved in both cases, with successful development of selective reactions for removal of linear oligomers. The cyclic oligomers of PBT melt at 130–180°C, and those from PET at 280–320°C, and have melt viscosities about four orders of magnitude lower than the parent high-molecular-weight polymers. Polymerization of the cyclic oligomers has been achieved with a variety of initiators, and by using various techniques. Polymerization can be complete within minutes, and can lead to very high-molecular-weight polyesters without formation of by-products, and with essentially no exotherms. The ring-opening chemistry facilitates a variety of new copolymer reactions, and has made possible the fabrication of composite structures with very high fiber loadings.

REFERENCES

1. Hill, J. W. and Carothers, W. H., Many-membered cyclic esters, *J. Am. Chem. Soc.*, **57**, 5031 (1933).
2. Spanagel, E. W. and Carothers, W. H., Macrocyclic esters, *J. Am. Chem. Soc.*, **57**, 929 (1935).
3. For example, see Slomkowski, S. and Duda, A. Anionic ring-opening polymerization, In *Ring-Opening Polymerization, Mechanisms, Catalysis, Structure, and Utility*, Brunelle, D. J. (Ed.), Hanser-Verlag, New York, pp. 87–128, 1993.
4. Hodge, P., Ji-Long, J., Owen, G. J. and Houghton, M. P., Reactions of polymer-supported ω -bromoalkylcarboxylates: formation of lactones versus oligomerization, *Polymer*, **37**, 5059 (1996).
5. Peebles, L. H., Huffman, M. W. and Ablett, C. T., Isolation and identification of the linear and cyclic oligomers of poly(ethylene terephthalate) and the mechanism of cyclic oligomer formation, *J. Polym. Sci., Part A-1*, **7**, 479 (1969).

6. Ross, S. D., Coburn, E. R., Leach, W. A. and Robinson, W. B., Isolation of a cyclic trimer from polyethylene terephthalate film, *J. Polym. Sci.*, **13**, 406 (1954).
7. Repin, E. and Papanikolaou, E., Synthesis and properties of cyclic di(ethylene terephthalate), *J. Polym. Sci., Part A-1*, **7**, 3426 (1969).
8. Goodman, I. and Nesbitt, B. F., The structures of cyclic dimers of poly(butylene terephthalate), *Polymer*, **1**, 384 (1960).
9. Wick, G. and Zeitler, H., Cyclic oligomers in polyesters from diols and aromatic dicarboxylic acids, *Angew. Makromol. Chem.*, **112**, 59 (1983).
10. East, G. C. and Girshab, A. M., Cyclic oligomers in poly(1,4-butylene terephthalate), *Polymer*, **23**, 323 (1982).
11. Montaudo, G., Puglisi, C. and Samperi, F., Primary thermal degradation mechanisms of PET and PBT, *Polym. Degrad. Stabil.*, **42**, 13 (1993).
12. Meraskentis, E. and Zahn, H., Darstellung cyclischer ester aus terephthal-saure and diolen, *Chem. Ber.*, **103**, 3034 (1970).
13. Zahn, H. and Repin, J. F., Synthese einer homologen reihe von cyclischen athylenterephthalaten, *Chem. Ber.*, **103**, 3041 (1970).
14. Brunelle, D. J., Bradt, J. E., Serth-Guzzo, J., Takekoshi, T., Evans, T. L. and Pearce, E. J., Semicrystalline polymers via ring-opening polymerization: preparation and polymerization of alkylene phthalate cyclic oligomers, *Macromolecules*, **31**, 4782 (1998).
15. Kitano, A., Ishitani, A. and Ashida, A., Crystal structure of cyclic dimer of poly(butylene terephthalate), *Polym. J.*, **23**, 949 (1991).
16. Nagahata, R., Sugiyama, J. J., Goyal, M., Goto, M., Honda, K., Asai, M., Ueda, M. and Takeuchi, K. Thermal polymerization of uniform macrocyclic ethylene terephthalate dimer, *Polymer*, **42**, 1275 (2001).
17. Rossa, L. and Vogtle, F., Synthesis of medio- and macrocyclic compounds by high dilution principle techniques, *Top. Curr. Chem.*, **113**, 1 (1983).
18. Brunelle, D. J., Boden, E. P. and Shannon, T. G., Remarkably selective formation of macrocyclic aromatic carbonates: versatile new intermediates for the synthesis of aromatic polycarbonates, *J. Am. Chem. Soc.*, **112**, 569 (1990).
19. Brunelle, D. J. and Shannon, T. G., Preparation and polymerization of bis-phenol A cyclic oligomeric carbonates, *Macromolecules*, **24**, 3053 (1991).
20. Jacobson, H. and Stockmayer, W. H., Intramolecular reaction in polycondensations. I. The theory of linear systems, *J. Chem. Phys.*, **18**, 1600 (1950).
21. Hubbard, P. A., Brittain, W. J., Mattice, W. L. and Brunelle, D. J., Ring-size distribution in the depolymerization of poly(butylene Terephthalate), *Macromolecules*, **31**, 1518 (1998).
22. Kricheldorf, H. R., Rabenstein, M., Maskos, M. and Schmidt, M., Macro-cycles 15. The role of cyclization in kinetically controlled polycondensations. 1. Polyester synthesis, *Macromolecules*, **34**, 713 (2001).

23. Cooper, D. R. and Semlyen, J. A., Equilibrium ring concentrations and the statistical conformations of polymer chains: part 11. Cyclics in poly(ethylene terephthalate), *Polymer*, **14**, 185 (1973).
24. Nippon Gijutsu Boeki Co., Jpn Patent 21 873 (1971).
25. Brunelle, D. J. and Takekoshi, T., US Patent 5 407 984 (1995, to GE).
26. Brunelle, D. J., Kailasam, G., Serth-Guzzo, J. and Wilson, P., US Patent 5 668 186 (1997, to GE).
27. Bryant, J. J. L., and Semlyen, J. A., Cyclic polyesters: 6. Preparation and characterization of two series of cyclic oligomers from solution ring-chain reactions of poly(ethylene terephthalate), *Polymer*, **38**, 2475 (1997).
28. Bryant, J. J. L., and Semlyen, J. A., Cyclic polyesters: 7. Preparation and characterization of cyclic oligomers from solution ring-chain reactions of poly(butylene terephthalate), *Polymer*, **38**, 4531 (1997).
29. Hamilton, S. C., Semlyen, J. A. and Haddleton, D. M., Cyclic polyesters: 8. Preparation and characterization of cyclic oligomers in six aromatic ester and ether-ester systems, *Polymer*, **39**, 3241 (1998).
30. Ruddick, C. L., Hodge, P., Zhuo, Y., Beddoes, R. L., and Helliwell, M., Cyclo-depolymerization of polyundecanoate and related polyesters: characterisation of cyclic oligoundecanoates and related cyclic oligoesters, *J. Mater. Chem.*, **9**, 2399 (1999).
31. Dad, S., Hall, A. J. and Hodge, P., Preparation and cyclo-depolymerization of some olefin-containing polyesters via olefin metathesis, *Polym. Prepr.* **41**(1), 466 (2000).
32. Hodge, P., Yang, Z., Abderrazak, B.-H. A., and McGrail, C. S., Cyclo-depolymerization of poly(ethylene naphthalene-2,6-dicarboxylate) and ring-opening polymerizations of the cyclic oligomers obtained, *J. Mater. Chem.*, **10**, 1533 (2000).
33. Hall, A. and Hodge, P., Recent research on the synthesis and applications of cyclic oligomers, *React. Funct. Polym.*, **41**, 133 (1999).
34. Hodge, P., Colquhoun, H. M. and Williams, D. J., From macrocycles to macromolecules and back again, *Chem. Ind.* 162 (1998).
35. Burch, R. R., Lustig, S. R. and Spinu, M., Synthesis of cyclic oligoesters and their rapid polymerization to high molecular weight, *Macromolecules*, **33**, 5053 (2000).
36. Brunelle, D. J., Takekoshi, T. and Serth-Guzzo, J., US Patent 5 710 086 (1998, to GE).
37. Measurement taken using a Brookfield viscometer: Carbone, J. and Pearce, E. J., personal communication.
38. Youk, J. H., Boulares, A., Kambour, R. P. and MacKnight, W. J., Polymerization of ethylene terephthalate cyclic oligomers with a cyclic dibutyltin initiator, *Macromolecules*, **33**, 3600 (2000).

39. Youk, J. H., Kambour, R. P., and MacKnight, W. J. Polymerization of ethylene terephthalate cyclic oligomers with antimony trioxide, *Macromolecules*, **33**, 3594 (2000).
40. Nagahata, R., Sugiyama, J.-I., Goyal, M., Asai, M., Ueda, M. and Takeuchi, K., Solid-phase thermal polymerization of macrocyclic ethylene terephthalate dimer using various transesterification catalysts, *J. Polym. Sci., Polym. Chem.*, **38**, 3360 (2000).
41. Brunelle, D. J. and Serth-Guzzo, J. Titanate-catalyzed ring-opening polymerization of cyclic phthalate ester oligomers, *Polym. Prep.*, **40**(1), 566 (1999).
42. Kambour, R. P., personal communication.
43. Brunelle, D. J., US Patent 5 648 454 (1997, to GE).
44. Evans, T. L., Brunelle D. J., Bradt J. E., Pearce E. J. and Wilson P. R., US Patent 5 466 744 (1995, to GE).

4

Continuous Solid-State Polycondensation of Polyesters

B. CULBERT AND A. CHRISTEL
Bühler AG, Uzwil, Switzerland

1 INTRODUCTION

After polymerization in the melt phase the molecular weight of a polyester can be further increased in the solid-state. This process is known as solid-state polycondensation (SSP). The processing chain for poly(ethylene terephthalate) (PET), the most commercially significant polyester, is shown in Figure 4.1. In the melt phase, a molecular weight (number average) of typically between 16 000 and 19 000 (intrinsic viscosity (IV), 0.58–0.68) is reached before the melt is cooled and granulated into amorphous pellets. After first undergoing crystallization, the molecular weight of these pellets is then increased in the solid state. Values of up to 27 000 (IV, 0.90) for bottle grade (BG), and as high as 38 000 (IV, 1.20) for technical fibre applications such as tyre cord, seat belts and air bags are attained [1]. Other polyesters that undergo a molecular weight increase in the solid state include poly(butylene terephthalate) (PBT) and poly(ethylene naphthalate) (PEN).

The SSP process enables higher molecular weights to be reached which are either technically or commercially not feasible in the melt phase. The main advantages of further increasing the molecular weight in the solid state compared to the melt phase are as follows:

- Problems associated with the stirring of the viscous melt are eliminated in the solid state. These problems become increasingly troublesome in the melt phase as the capacity increases and as the molecular weight increases above ca. 19 000.

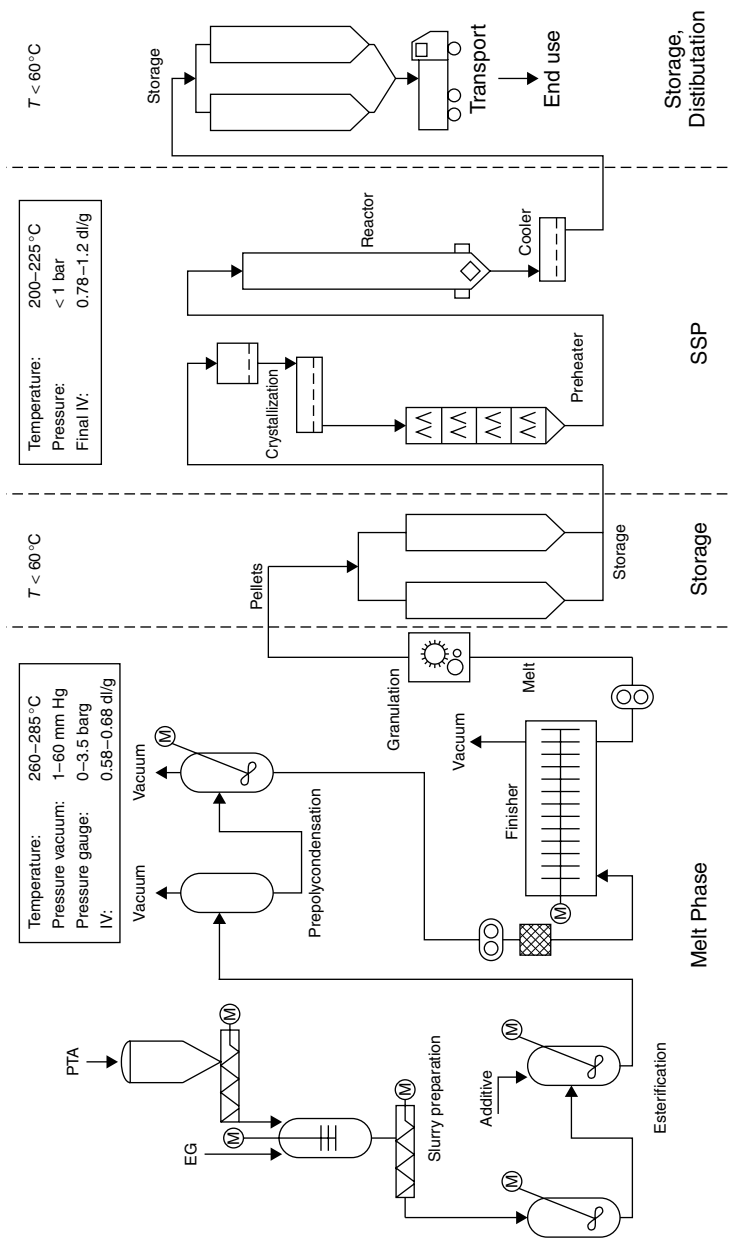


Figure 4.1 Schematic of a PET manufacturing chain

- The lower investment and running costs of the continuous SSP process, which does not require the high temperatures and vacuums associated with the melt phase. The cost splits for a 600 t/d continuous PET bottle grade plant are shown in Figures 4.2 and 4.3. The investment costs are some five times lower and the process costs approximately half for the SSP process when compared to the melt phase.
- Degradation and side reactions are limited in the solid state due to the lower processing temperatures used. PET, for use in bottle applications, is a notable example. Small concentrations of acetaldehyde (AA), a by-product of degradation and side reactions in PET, can affect the taste of carbonated soft drinks and mineral water. The SSP process is the best means of achieving PET bottles with acceptable levels of AA.

Indeed, the increasing industrial significance of the SSP process can be directly related to the success of the PET bottle. PET was introduced for use in drinking bottle applications in the mid 1970s and the SSP process was required to reduce the AA level below that achievable in the melt phase while increasing

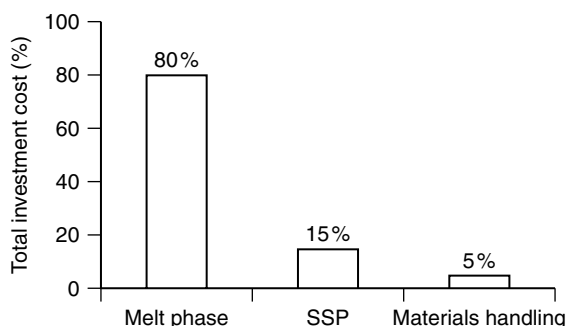


Figure 4.2 Investment costs for a 600 t/d BG resin installation [2]

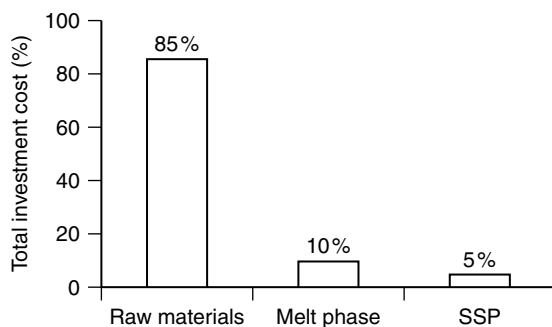


Figure 4.3 Production costs for a 600 t/d PET BG resin installation [2]

the molecular weight. Initially, SSP process development was concerned with the changeover from batch to continuous processing and the problems associated with pellets sintering or sticking in the process equipment [3–8]. In light of the double digit growth rate in the use of PET bottles since the late 1980s, reflected in Figure 4.4, the main role of SSP technology has been to keep pace with the constant demand for higher production capacities. The latter have increased some tenfold over the last 15 years in step with melt-phase capacities. Whereas back in 1985 the typical capacity was 30–60 t/d in one line, today the most typical single-line capacity is 300 t/d with the first 450 t/d plant coming into operation in 2000. In the future, the capacity is expected to increase up to 600 t/d, and possibly even higher [9].

Today, the SSP process has not only established itself as a key segment in the PET bottle manufacturing chain, but is becoming increasingly important for the attainment of high molecular weights in other PET applications such as technical fibres, strapping and upgrading in the area of recycling [10]. This also applies to PBT for high-molecular-weight applications involving engineering plastics.

The aim of this chapter is to give the reader a general overview of the thermal processing of polyesters in the solid state and in particular the SSP of PET for bottle applications. First the solid-state reactions of PET, involving molecular weight build-up, degradation and AA formation, are summarized and the mechanisms and the factors affecting SSP are discussed. In the second section, the crystallization of PET, including nucleation, crystal growth and annealing, is reviewed as it inevitably occurs during the SSP process. In the third section, the practical aspects of continuous SSP processing of PET for bottles are addressed,

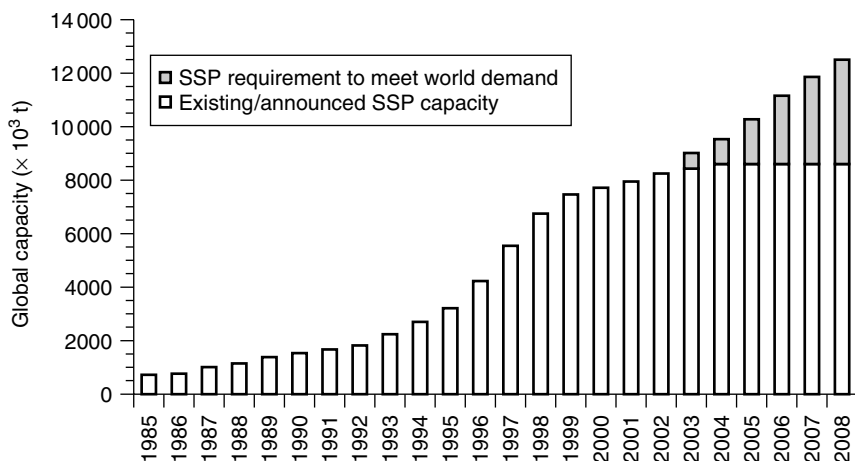


Figure 4.4 PET global solid-state capacity (source – PCI: PET Packaging, Resin and Recycling Ltd, 30 March 2001)

and the processing requirements for fibre-grade materials are compared to bottle-grade materials, as are the processing requirements of PBT and PEN. Finally, recycling will be considered by looking at a process for the closed-loop recycling of PET bottles involving SSP.

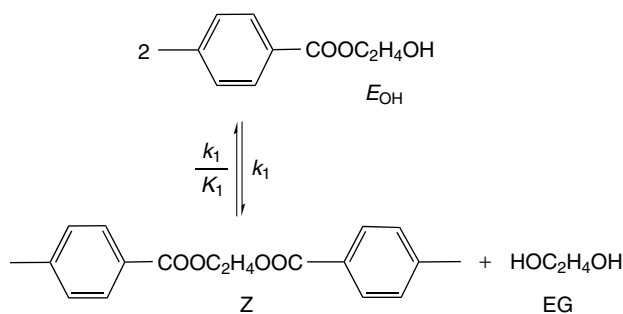
2 THE CHEMICAL REACTIONS OF PET IN THE SOLID STATE

The polycondensation of PET in the solid state is complex and still not fully understood. The reason for this is the influence of the physical processes of diffusion and crystallization on the reaction kinetics. Not only do the end groups of the polymer chains need to diffuse toward one another before they can react, but also the reaction by-products, water and ethylene glycol (EG) must be removed from the solid in order to drive the reaction forward. The reaction rate is therefore affected by the mobility of the end groups, the diffusion of the by-products through the semi-crystalline solid phase, and the removal of the by-products from the solid surface to the gas phase. Furthermore, this is occurring in a solid polymer matrix that is undergoing transformation through crystallization processes, thereby further restricting end group and by-product mobilities.

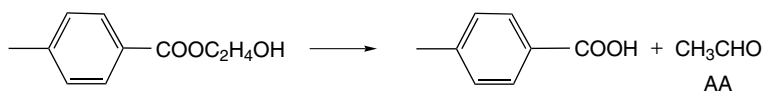
2.1 BASIC CHEMISTRY

It is generally accepted that the reaction chemistry is the same as in the melt and that the chemical reactions take place in the amorphous phase. This, by definition, implies that the polymer end groups, monomers, catalyst and by-products are present only in the amorphous phase [11]. The most important reactions occurring in the melt have been identified as follows [12]:

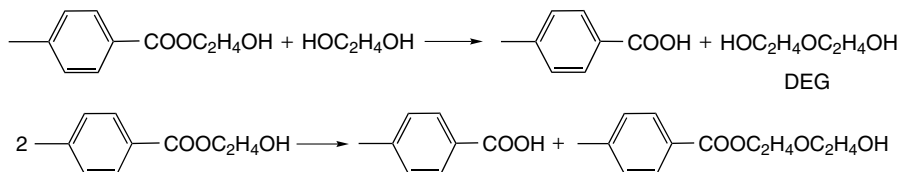
Reaction 1: Transesterification



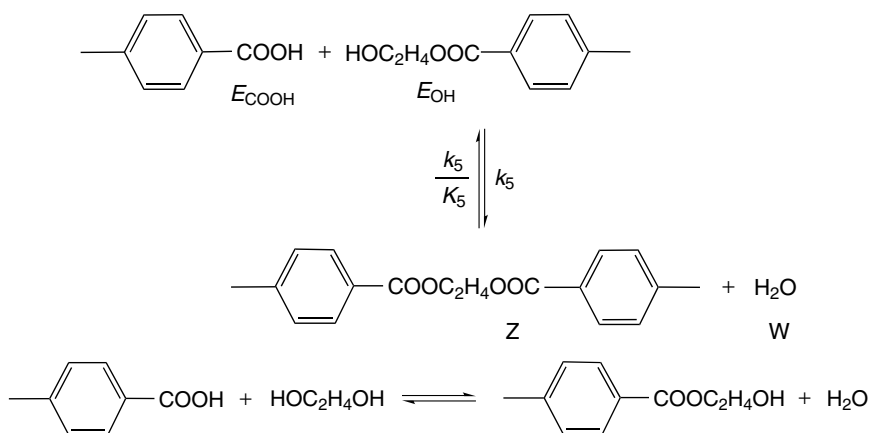
Reaction 2: Acetaldehyde Formation



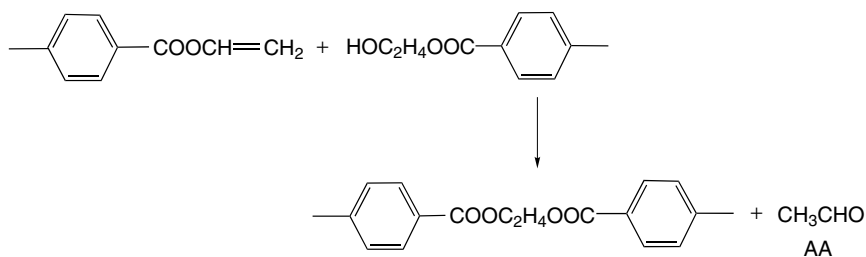
Reactions 3 and 4: Diethyleneglycol (DEG) Formation



Reactions 5 and 6: Esterification (Water Formation)



Reaction 7: Polycondensation of Vinyl End Groups



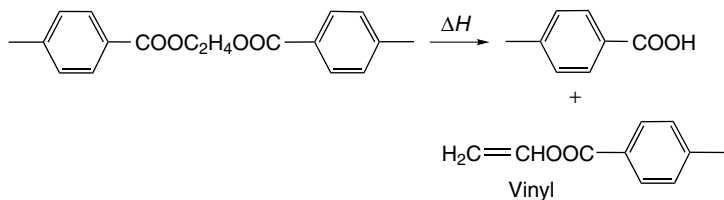
Reactions (1), (5) and (7) result in the increase in molecular weight. However, only transesterification (1) and esterification (5) are considered to contribute significantly to the molecular weight build-up. The contribution of the polycondensation of vinyl end groups (7) is considered to be insignificant because of the low formation of vinyl ester groups by the degradation of the diester linkage (reaction 8 shown below) at SSP temperatures [11, 13].

Reaction (7), although not important for the molecular weight increase, does lead to the removal of the vinyl ester groups, which along with AA is undesirable in applications for carbonated soft drink (CSD) and mineral water bottles. Vinyl groups, among other things, lead to the generation of AA during melt processing and increase the AA content of bottle preforms above that of the original material (residual AA) before melt processing [14]. Although both reactions (2) and (7) result in the formation of additional AA, the SSP treatment of material before melt processing reduces both the residual AA and the AA generation rate; both are generally reduced as the processing time and temperature in the solid state are increased [15].

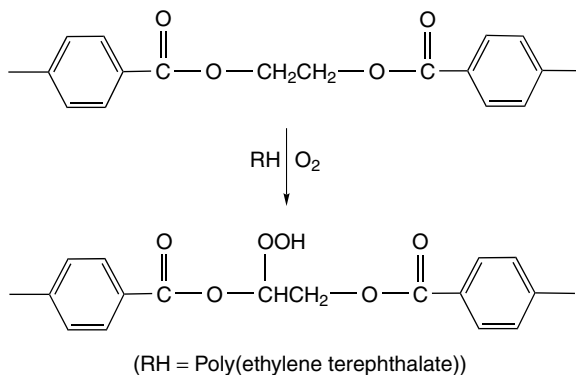
The other reactions do not change the molecular weight but are important for other reasons. Reactions (2), (3) and (5) cause a change in the OH/COOH end group balance, while reactions (3) and (4) lead to DEG formation although their significance at SSP conditions is questioned [16].

The degradation reactions of PET are complex and it is beyond the scope of this chapter to cover them fully. Therefore, the reader is referred to other literature sources for a more detailed description of the mechanisms involved [17–19]. However, the main reactions can be briefly summarized as follows:

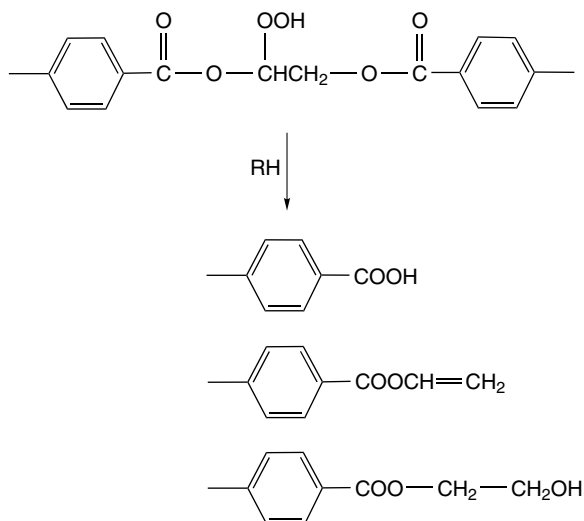
Reaction 8: Thermal Degradation



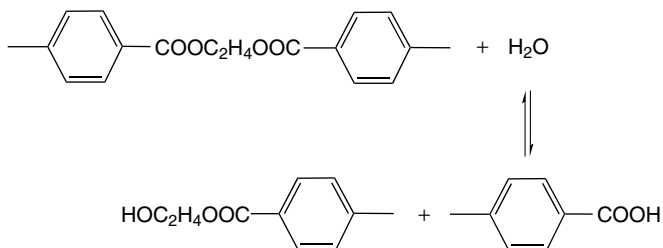
Reaction 9: Thermal Oxidative Degradation – Hydroperoxide Formation [105]



Thermal Oxidative Degradation – Degradation products from Hydroperoxide [19]



Reaction 10: Hydrolytic Degradation (Reverse of Reaction 5)



In general, the degradation of PET is characterized by a loss in molecular weight, a loss in weight in the case of thermal and thermal oxidative degradation, and an increase in the carboxyl end groups. This is usually accompanied by the material first turning yellow, then brown and finally black [17].

Thermal degradation is degradation induced by elevated temperatures in the absence of oxygen. The initial step of thermal degradation (8) is a random scission of the chain at an ester linkage to form vinyl ester and carboxyl end groups. This is accelerated to various extents by different catalyst systems [18]. It occurs principally at the higher temperatures in the melt phase, while in the solid state it is less significant. Even at the extreme SSP conditions of 10 h at 230 °C it is estimated to contribute only about 1 % of the end groups [11].

The thermal oxidative degradation of PET (9) involves the reaction of oxygen at elevated temperatures. This starts with the formation of a hydroperoxide at the methylene group in the diester linkage of the PET chain [17–19, 105]. The degradation mechanism is not completely understood but is believed to follow a free radical mechanism leading to chain cleavage and the formation of carbon and oxygen radicals, carboxyl, hydroxyl and vinyl ester end groups. Secondary reactions of the radicals can also lead to the formation of branched chains [19]. The presence of DEG in the link further decreases the thermal oxidative stability of PET [18]. In industrial applications, PET is generally treated in air at temperatures up to about 180 °C. Tests involving the treatment of PET with various catalyst and stabilizer types, at 130 °C for 200 h in air did not lead to any evidence of thermal oxidation, while a carboxyl end group increase was seen after 30 h at 180 °C and 5 h at 200 °C [13]. However, even if no evidence in the form of carboxyl group increase is seen during thermal treatment, the formation of hydroperoxides in air at temperatures below 200 °C is to be expected and can lead to higher AA generation rates and chain cleavage during melt processing [19]. Even so, the hydroperoxides formed during processing in air can be destroyed by further processing in nitrogen at temperatures as low as 60 °C [20]. Therefore, the crystallizing of PET in air is not expected to lead to higher AA generation rates if it afterwards undergoes processing under nitrogen during SSP. On the other hand, the drying of PET in air can be expected to lead to higher AA generation rates during processing in the melt.

The hydrolytic degradation of PET (10) is an autocatalytic reaction, being catalysed by the resulting carboxyl end groups. It is also accompanied by an increase in hydroxyl end groups and there is no discoloration of the product or evolution of volatile products [19]. This process is known to begin at temperatures of around 100 °C [18]. The relative rate of hydrolysis is some 10 000 times faster than that of thermal degradation in the temperature range 100–120 °C [17]. In the solid state, it is prevalent during the heating-up and crystallizing of the amorphous precursor, due to moisture being absorbed during pelletizing and storage. It can also occur at the higher SSP processing temperatures if the moisture content of the process gas is too high.

2.2 MECHANISM AND KINETICS

As mentioned above, esterification and transesterification are the two main reactions responsible for the molecular weight increase in PET. Both reactions are considered to be second-order and their rates are given as follows [12]:

$$\text{Transesterification: } \text{Rate}_1 = \frac{\partial[z]}{\partial t} = k_1 \left([\text{E}_{\text{OH}}]^2 - \frac{4[z][\text{EG}]}{K_1} \right);$$

$$K_1 = \frac{4[z][\text{EG}]}{[\text{E}_{\text{OH}}][\text{E}_{\text{OH}}]}$$

$$\text{Esterification:} \quad \text{Rate}_5 = \frac{\partial [z]}{\partial t} = k_5 \left([\text{E}_{\text{COOH}}][\text{E}_{\text{OH}}] - \frac{2[z][w]}{K_5} \right);$$

$$K_5 = \frac{2[z][w]}{[\text{E}_{\text{COOH}}][\text{E}_{\text{OH}}]}$$

where k_1 and k_5 and K_1 and K_5 are second-order rate constants and equilibrium constants, respectively; $[\text{E}_{\text{OH}}]$, and $[\text{E}_{\text{COOH}}]$ are respectively the concentrations of hydroxyl and carboxyl end groups, and $[z]$, $[\text{EG}]$ and $[w]$ are the concentrations of diester linkages ($\text{COOC}_2\text{H}_4\text{OOC}$), ethylene glycol and water, respectively. Note that a constant k_1 implies a constant catalyst concentration [1].

At equilibrium, the rates of the forward and the reverse reactions are equal. Therefore, to drive the reaction rate forward in the direction of the ester linkages, represented by z , then reaction by-products, EG and water must be removed.

Both reactions are affected by one or more of the following:

- the rate of the reversible chemical reaction;
- the rate of diffusion of the reaction by-products, water and EG, through the polymer matrix to the pellet surface;
- the rate of diffusion of the reaction by-products from the pellet surface to the gas.

These rate-controlling mechanisms are characterized as follows:

Chemical Reaction Rate Controlled Process: If the diffusion is very rapid compared to the rate of chemical reaction, then the concentration of water and EG can be considered to be nearly zero throughout the pellet and the rate of the reverse reaction can be neglected [21]. This represents the maximum possible reaction rate. It is characterized by a linear molecular weight increase with respect to time and is also dependent on the starting molecular weight and the reaction rate constants k_1 and k_2 .

Diffusion Rate Controlled Process: If the rate of chemical reaction is much faster than the diffusion of water and EG through the solid amorphous phase, then the reaction can be considered to be at equilibrium throughout the pellet [21]. The reaction rate is dependent upon the pellet size, the diffusivity of both water and EG, the starting molecular weight, and the equilibrium constants K_1 and K_5 . In addition, the pellet can be expected to have a radial viscosity profile due to a by-product concentration profile through the pellet with the molecular weight increasing as the by-product concentrations decreases in the direction of the pellet surface [22–24].

Surface Diffusion Rate Controlled: At high gas velocities, the pellet surface by-product concentration is maintained at an equilibrium value determined by the by-product concentration in the gas. In this condition, the mass transfer from the surface is balanced by the diffusion within the pellet to the surface. However

if the gas velocity is reduced the gas-side mass-transfer coefficient will also decrease [25] until eventually the mass transfer from the surface is less than the diffusion to the surface. At this point, the surface by-product concentration increases and the overall diffusion rate of the by-products is reduced. This leads to a decrease in the rate of reaction and the reaction rate becomes surface diffusion rate controlled.

The reduction in reaction rate due to surface diffusion has been shown to occur at gas velocities below 1.5 m/min [26]. However, most production plants operate at higher gas velocities and diffusion from the surface does not normally limit the reaction rate.

Many studies investigating one or more of these potential rate-determining steps have been carried out over the years. These studies have shown that the rate of reaction depends upon many factors such as temperature [15, 27–29], pellet size [27–29], crystallinity [28], additive types and concentrations [30], process gas type and quantity [31, 32], molecular weight [22, 31] and end group concentrations [16, 33] – all of which will be addressed individually later in this section. Various models have also been proposed involving kinetics [33] and/or by-product diffusion [11, 16, 21, 27–29, 34, 35] through to empirical Equations [15]. The variety of models used and the wide range of kinetic and physical data published demonstrate the complexity of the mechanisms involved.

Most recently, kinetic data from the melt have been applied to the amorphous solid phase. This is based on the well-accepted assumptions that the chemistry in the melt is the same as in the latter phase and that all of the end group reactions take place in the latter phase [11, 21, 35]. The activation energy ΔE , and the frequency factor A , defined in the following equation:

$$\text{Rate constant } (k) = A \exp(-\Delta E/RT)$$

are given as 18.5 kcal/mol and 1.36×10^6 l/(mol min) for transesterification, and 17.6 kcal/mol and 2.08×10^6 l/(mol min) for esterification, respectively [12]. The equilibrium constants are given as 0.5 and 1.25, respectively.

The molecular weight is normally measured, for convenience sake, by solution viscosity and is often given as the *intrinsic* viscosity. There is a wide range of solutions used, with the average molecular weight related to the intrinsic viscosity by the Mark-Houwink equation:

$$[\eta] = K \overline{M}^a$$

where K and a are empirical constants specific to the polymer–solvent system and are based on known standards.

Many number- and weight-average molecular weight correlations are available in the literature [106]; however, the K -values are greatly influenced by the molecular weight distribution (MWD) of the sample and therefore caution should

be taken when using these relationships. A correct interpretation of the molecular weight based on intrinsic viscosity can only be made if the polydispersity (M_w/M_n) of the sample is known.

The polydispersity of melt-phase samples is generally lower than that of solid-state samples. Gel permeation chromatography (GPC) analysis of samples prepared from the solid-state showed polydispersity values in the range of 2.57 to 2.84 compared to 2.27 to 2.49 for melt samples [107]. The higher polydispersity of solid-state samples can largely be explained by the non-uniformity in the average molecular weight across the pellet radius caused by a SSP reaction rate that is diffusion controlled [11].

2.3 PARAMETERS AFFECTING SSP

In general, no two PET materials have exactly the same SSP behaviour despite the similarities in bottle grade recipes and standard pellet sizes. The reasons for this are the numerous factors that influence the SSP reaction rate, many of which are still not fully understood. The main factors and their qualitative influence are discussed briefly below:

2.3.1 Temperature

In principle, the reaction can take place at temperatures between the glass transition and the melting temperature of the polymer. However, sufficient mobility of the end groups is required to ensure reaction. It has been shown that the reaction doesn't begin until temperatures of 150 °C [36] although it doesn't become industrially significant until temperatures above about 200 °C. As a rule of thumb, the reaction rate doubles every 12–13 °C. This is based on the data shown in Figures 4.5 and 4.6 and has been confirmed by others [37].

2.3.2 Time

When chemical reaction is the rate controlling mechanism, then the increase in molecular weight is linear with time. This was shown to be the case at 160 °C with a pellet size <2.1 mm [29]. However, under normal industrial SSP conditions, where the standard pellet diameter is between 2 and 3 mm and temperatures are >200 °C, the reaction rate decays over time. Typically, the molecular weight increase is proportional to the square root of time, as shown in Figure 4.6. This has been confirmed in other studies [15, 36–38]. Such behaviour is said to be typical for a reaction involving both chemical reaction and diffusion within the material [29].

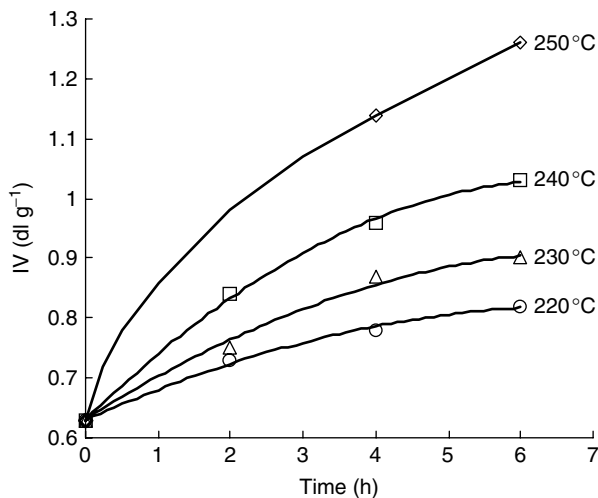


Figure 4.5 Intrinsic viscosity (IV) as a function of time at various SSP temperatures [15]. From Jabarin, S. A. and Lofgren, E. A., *J. Appl. Polym. Sci.*, **32**, 5315–5355 (1986), Copyright © John Wiley & Sons, Inc., 1986. Reprinted by permission of John Wiley & Sons, Inc

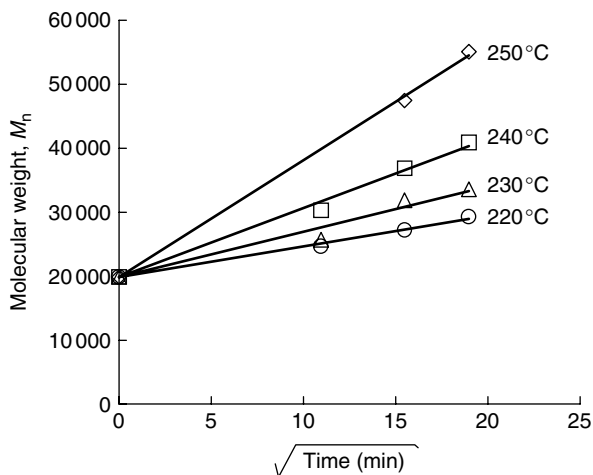


Figure 4.6 Number-average molecular weight (M_n) as a function of the square root of time at various SSP temperatures [15]. From Jabarin, S. A. and Lofgren, E. A., *J. Appl. Polym. Sci.*, **32**, 5315–5355 (1986), Copyright © John Wiley & Sons, Inc., 1986. Reprinted by permission of John Wiley & Sons, Inc

2.3.3 Particle Size

The influence of pellet size has been generally used to identify the rate controlling mechanism of the overall reaction rate. If the rate controlling mechanism is chemical-reaction limited then the pellet size will have no effect on the reaction rate. If the diffusion of by-products to the pellet surface is the rate controlling mechanism, then the reaction rate will decrease as the pellet size increases, due to the increase in the length of the diffusion path.

At 250 °C, the reaction rate was shown to be affected by pellet sizes as small as 0.2 mm [31]. At 210 °C, the reaction rate was found to be by-product diffusion limited at a particle size >16–18 mesh (ca. 1.3 mm) [27], while at 160 °C no effect of pellet size was seen for particle sizes <2.1 mm [29]. Therefore, it can be seen that the influence of the pellet size on reaction rate becomes more pronounced as the temperature increases. Under normal industrial SSP conditions, where the pellet size is between 2 and 3 mm and temperatures are >200 °C, decreasing the pellet size will lead to an increasing of the reaction rate.

2.3.4 End Group Concentration

The reaction rate is very sensitive to the ratio of hydroxyl to carboxyl end groups, as shown by Figures 4.7 and 4.8. At low carboxyl concentrations, the transesterification reaction will be favoured, while at high carboxyl concentrations the esterification route will be favoured. If the transesterification and esterifications were equal, which they are generally not, then the consumption ratio of end

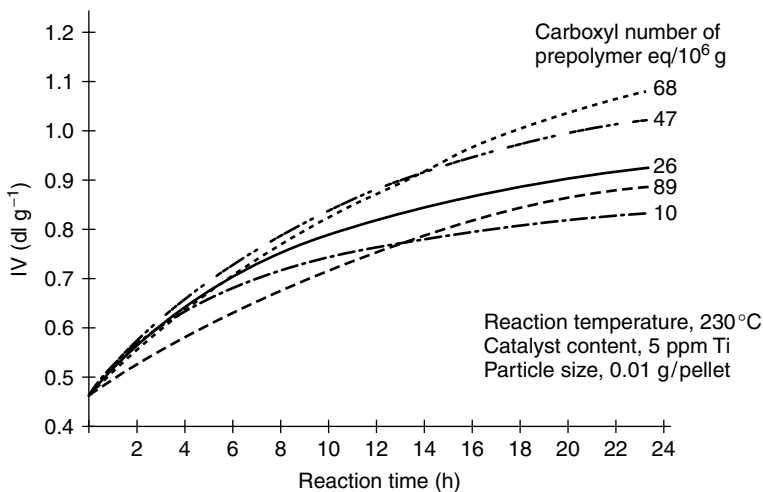


Figure 4.7 Static-bed solid polymerization rates of 0.45 dl/g IV PET prepolymers [39]. From Duh, B., US Patent, 4 238 593 (1980)

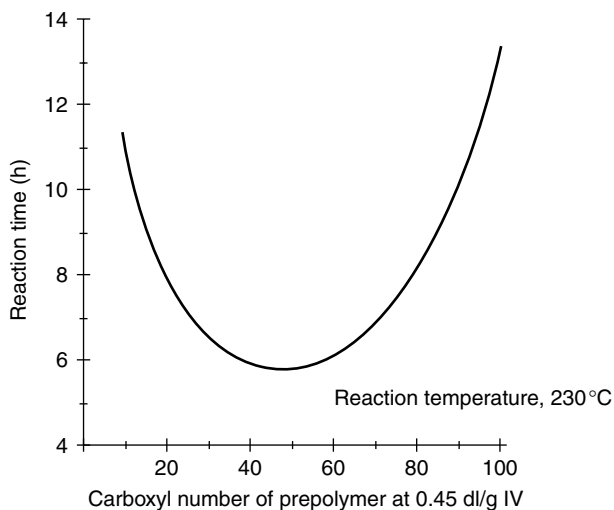


Figure 4.8 Effect of carboxyl number on reaction time required to polymerize from 0.45 to 0.72 dl/g IV [39]. From Duh, B., US Patent, 4 238 593 (1980)

groups would be three hydroxyl for every carboxyl end group. In Figure 4.8, the optimum molar ratio is about 2.7, although this will depend upon not only the starting and the final IV, as evident in Figure 4.7, but also other factors such as temperature, catalyst type, catalyst quantity and pellet size. In another study, the optimum molar ratio was found to be around 2 [33]. However, often a maximum carboxyl group concentration in the final product should not be exceeded for product quality purposes, and in particular, hydrolytic stability. This can be more important in determining the starting end group concentration rather than maximizing the reaction rate.

2.3.5 Crystallinity

Crystallization plays an important role in SSP plants for two reasons. First, the tendency of PET to sinter during crystallization requires special product handling to prevent pellet agglomeration before SSP can be carried out and it also limits the maximum SSP operating temperature. Both of these subjects are covered in more detail in the following sections on crystallization and continuous SSP. Secondly, crystallization reduces the SSP reaction rate by reducing chain mobility and by increasing the diffusion path length of the by-products. This has been demonstrated in various ways, i.e. the rate of molecular weight increase is shown to decrease with increasing polymer starting crystallinity at 230 °C [28], the reaction rate of material having undergone SSP treatment was shown to increase after

remelting [16, 40], and diffusivity was shown to be linearly proportional to the mass fraction of the amorphous phase [28].

2.3.6 Gas Type

Recently, the gas types nitrogen, carbon dioxide and helium were shown to have no influence on the reaction rate at 226 °C over 6 h [32]. Similarly, no difference between nitrogen and carbon dioxide at 210 °C over 24 h was observed [41]. An early study [31] did show that the gas type influenced the reaction rate, but it has since been suggested that the different heat capacities and thermal conductivities of the gases affected the experimental temperatures [32].

2.3.7 Gas Purity

The driving force for mass transfer from the pellet surface is reduced as the EG and water concentrations in the gas are increased. Therefore, gas having practically no EG and moisture is used for SSP in order to maximize the reaction rate.

2.3.8 Catalyst

It is known that transesterification does not proceed without the presence of a catalyst [42]. Kokkolas *et al.* [30] showed that in the solid state the transesterification rate constant increases linearly with antimony trioxide (Sb_2O_3) concentration up to levels of 1000 ppm. In the same study, they also showed that the esterification proceeds independently of Sb_2O_3 concentration.

2.3.9 Molecular Weight

It has been shown that higher starting molecular weights enable higher final molecular weights to be achieved [16, 43]. This is attributed to the tendency for lower starting molecular weights to lead to higher crystallinity build-up during SSP as well as the other reasons already mentioned in the corresponding section on crystallinity.

It should also be mentioned that as the starting molecular weight increases so too does the corresponding molecular weight increase for a given reaction rate.

3 CRYSTALLIZATION OF PET

Crystallization is an integral part of the SSP process. It begins as soon as amorphous pellets are heated above their glass transition temperature of ca. 75 °C, and continues throughout the heating up to SSP temperatures and during SSP

processing. If crystallization is not carried out correctly then the pellets tend to agglomerate, which can seriously compromise the operability of an SSP plant. Furthermore, the build-up of crystallinity can adversely affect the SSP reaction rate, as mentioned in the previous section.

PET crystallizes in a triclinic crystal structure with unit cell dimensions as follows [44]:

$$a = 4.56 \text{ nm}, b = 5.94 \text{ nm and } c = 10.75 \text{ nm}$$

$$\alpha = 98.5^\circ, \beta = 118^\circ \text{ and } \gamma = 112^\circ$$

This gives a crystalline density of 1.455 g/cm^3 , while the amorphous density is 1.335 g/cm^3 . However, the crystalline density value may be too low. Other values for the crystalline density in the literature range from 1.472 up to 1.58 g/cm^3 [45]. The dependence of the unit cell dimensions on the thermomechanical history may explain the higher values and the large range [46]. Indeed, the crystalline density of PET increases continuously with annealing temperature up to 240°C . The heat of fusion values reported for crystalline PET are generally in the range 22.6 to 27.8 kJ/mol [45].

Whether cooling from the melt or heating of amorphous material from the glassy state, the crystallization of PET, and polymers in general, first involves the formation of nuclei and then their subsequent growth. The latter is in the form of lamellae radiating outward from the nucleus by chain folding normal to the direction of growth, as shown in Figure 4.9. These structures, or *spherulites*,

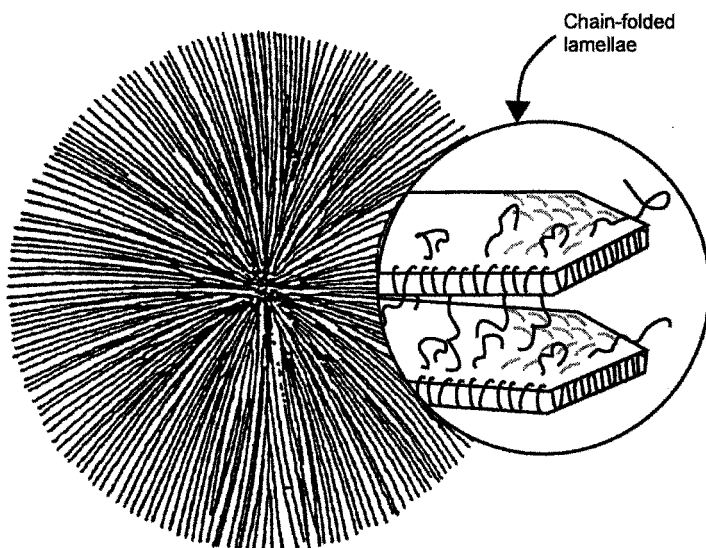


Figure 4.9 Illustration of a spherulite growing into a melt

spread at the expense of amorphous material until surface impingement with other spherulites occurs, thereby limiting further growth. This first stage of crystallization, often referred to as *primary* crystallization, is then followed by a much slower *secondary* crystallization process involving both the improvement and growth of existing crystals and the growth of new crystals in the amorphous regions between the lamellae.

The crystallization kinetics of PET have been studied both from the melt and from the glassy state by using various methods, including techniques such as density measurements [47, 48] differential scanning calorimetry (DSC) [49–56], small- and wide-angle X-ray scattering [57–60] and infrared spectroscopy [60–62]. In Figure 4.10, the crystallization behaviour, characterized by density, is shown as a function of temperature and annealing time for a PET film. The main features evident in these plots are as follows:

- The induction times to the beginning of crystallization at lower temperatures of 90 – 120 °C.
- The very fast initial density increase due to nucleation and rapid spherulite growth as shown by the dotted lines, referred to as primary crystallization.

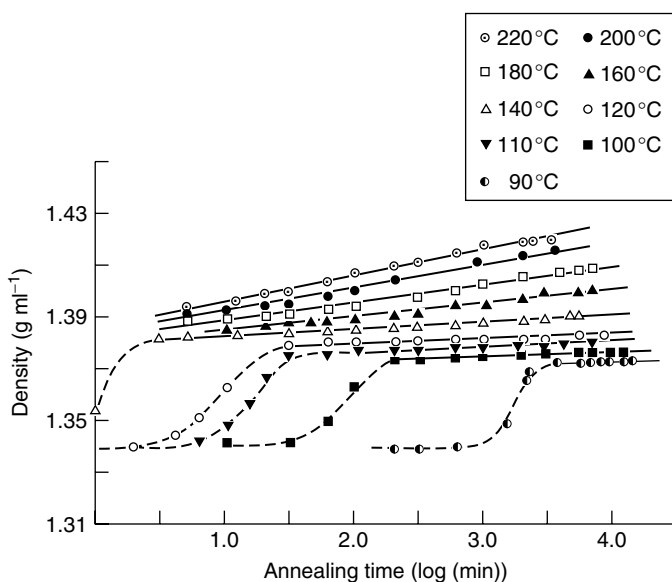


Figure 4.10 Dependence of the density of PET films on annealing time and temperature: film thickness, 0.25 mm; M_v , 24 600 g/mol; initial density, 1.34 g/ml [47]. From Lin, S. and Koenig, J., *J. Polym. Sci., Polym. Symp. Ed.*, **71**, 121–135 (1984), Copyright © John Wiley & Sons, Inc., 1984. Reprinted by permission of John Wiley & Sons, Inc

- The much slower linear increase in density with the log of time after the primary crystallization, referred to as secondary crystallization.
- The trend to higher densities or crystallinities at higher temperatures and longer residence times. During SSP processing densities rarely exceed 1.42 g/cm^3 , equivalent to a crystallinity of 70 vol% (according to the crystalline and amorphous densities given above).

3.1 NUCLEATION AND SPHERULITE GROWTH

Primary nucleation of a polymer material undergoing supercooling from the melt can be divided into three general types, namely heterogeneous, homogeneous and self nucleation [63]. Heterogeneous nucleation occurs on foreign surfaces, such as catalyst particles, which reduce the nucleus size required for crystal growth. It can be either instantaneous (athermal) where all the crystals start growing at the same time or sporadic (thermal) where new crystals grow throughout the crystallization process. Homogeneous nucleation occurs if no preformed nuclei or foreign particles are present and the nucleation mode is sporadic. A special type of nucleation, called self-nucleation, occurs when tiny regions of high degree of order persist in the melt for a long time and act later as predetermined nuclei for recrystallization.

The growth of the nuclei then occurs in one, two or three dimensions creating rods (fibrils), discs or spheres (spherulites). The development of crystallinity (V_c) under isothermal conditions with time (t) is generally analysed according to Avrami's method:

$$V_c = 1 - \exp(-Kt^n)$$

where K and n are constants (K contains both nucleation and growth parameters). The value of n , the Avrami exponent, is generally an integer between 1 and 4 and depends on the mechanism of nucleation and on the form of crystal growth (Table 4.1). Variations of this equation have been derived to take into account such aspects as non-isothermal crystallization [64], secondary crystallization and induction period [65]. Non-integer behaviour is attributed to either

Table 4.1 Standard interpretation of Avrami coefficients [66]

Avrami coefficient, n	Nucleation mode	Growth dimensionality
4	Sporadic	3
3	Sporadic	2
3	Instantaneous	3
2	Sporadic	1
2	Instantaneous	2
1	Instantaneous	1

the diffusion of non-crystallizable molecules away from the growth surface [66] or the simplified assumptions made in the Avrami model [67].

For PET, Avrami exponents over the whole range of 1 to 4 have been measured. A value of 3 [49, 54, 55, 57, 70] has been measured over a wide temperature range, from 110 to 225 °C, and is the most commonly reported value. It is generally interpreted, according to Table 4.1, to indicate heterogeneous nucleation and three-dimensional crystal growth. A value of 4 [68, 69] is typically seen close to the melting point, with values of 2 [54, 56, 68] closer to the glass transition temperature.

To explain Avrami exponents of 2 and even 1 [55], even though the final crystal structure is known to be spherulitic, it has been proposed that PET spherulites growing at low temperatures are skeletal and composed of independently propagating fibrils that gradually fill in the spherulite [66]. Such behaviour at low temperature has been observed in a time-resolved light scattering study [70]. It was reported that at the early stage of crystallization, highly disordered crystalline domains with low crystallinity appear and, by increasing in size, they develop to yield a spherulite.

The overall rate of crystallization is determined by both the rate of nuclei formation and by the crystal growth rate. The maximum crystal growth rate lies at temperatures of between 170 and 190 °C [71, 72], as does the overall crystallization rate [51, 61, 75]. The former is measured using hot stage optical microscopy while the latter is quantified by the 'half-time' of crystallization. Both are influenced by the rate of nucleation on the crystal surface and the rate of diffusion of polymer chains to this surface. It has been shown that the spherulite growth rate decreases with increasing molecular weight due to the decrease in the rate of diffusion of molecules to this surface [46, 50, 55, 71, 74].

Comonomers, such as isophthalic acid (IPA), cyclohexanedimethanol (CHDM) and diethylene glycol, (DEG) also affect the crystallization behaviour of PET, as shown in Figure 4.11. These comonomers are introduced into PET in quantities up to 5 mol %, in order to suppress crystallization behaviour during preform injection moulding and stretch blow moulding, resulting in clear brighter bottles. Note that DEG occurs inherently in small quantities in PET due to reaction (4) shown in Section 2.1. IPA- and CHDM-modified PET show slower crystallization rates when crystallized from the glassy state [51]. This is attributed to the irregularity introduced into the polymer chains. On the other hand, DEG resulted in an actual increased crystallization rate relative to a homopolyester [51]. This is ascribed to the effect of a lowering of the glass transition temperature (not seen with IPA and CHDM) and results in a shifting of the U-shaped crystallization half-time curve towards lower temperatures. When crystallizing from the melt phase, all three comonomers resulted in slower crystallization rates. This is a result of the reduction in the melting point and the reduced driving force for crystallization.

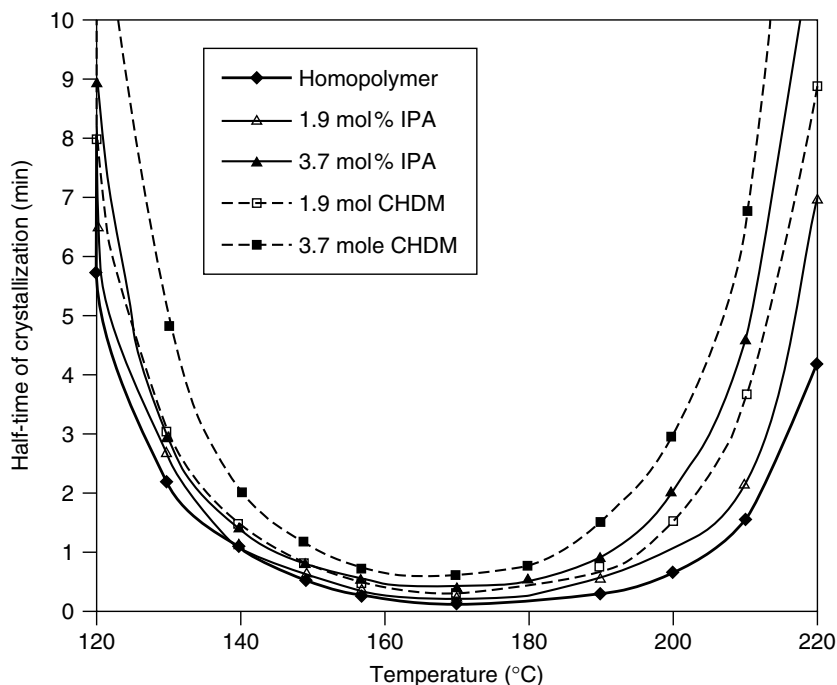


Figure 4.11 The influence of comonomer content and type on the crystallization half-time of PET [51]. Reproduced from Sakellarides, S. L., *ANTEC*, 96, 938–942 (1996), with permission from the Society of Petroleum Engineers

The nucleation rate has been shown to be increased by (a) the presence of transesterification catalysts such as Sb, Ti, Mn and Ca [54, 57, 74, 75] although the effect depends on the catalyst type [54, 74], (b) additives such as thermostabilizers [74] and nucleating agents [76], and (c) by moisture content [56, 77]. The latter is particularly important when crystallizing from the glassy state as the moisture content will vary depending on how long and at what conditions the material has been stored. Very little moisture is required to enhance nucleation. Increasing the storage humidity from 0 to 7% relative humidity was sufficient to reduce the crystallization half-time by a factor of 5 [77]. Moreover, moisture content does not affect the crystal growth rate [56].

Both the rate of nuclei formation and the crystal growth rate can also be expected to influence the spherulite size. It has been reported that, in the temperature range 130–180°C, the spherulite size increases with increasing temperature [74]. This trend can be expected to extend to higher temperatures as the nucleation rate decreases. On the other hand, the presence of nucleating

agents, such as catalysts and other additives, will obviously lead to a reduction in spherulite size.

3.2 CRYSTAL ANNEALING

The transition from primary to secondary crystallization is generally marked by the point at which a significant deviation in the Avrami kinetics occurs. The secondary crystallization is accompanied by a further densification and a shifting of the melting point of the crystals already formed to a higher temperature. It is therefore often referred to as an *annealing* of the crystals. During secondary crystallization, new single crystals are formed from amorphous material, the reorganization of existing crystals to eject imperfections occurs, and thickening of the lamellae takes place. Annealing is not as well understood as the primary crystallization process because molecular (re)alignment is driven by many different physical and chemical processes occurring simultaneously.

The influence of both time and temperature on the crystal melting are shown in Figures 4.12 and 4.13, respectively. First however, the origins of the two melting peaks seen in the diagrams must be mentioned. Their presence was long debated in the literature [78, 79]. It is now recognized that the first melting peak – the low melting peak (LMP) – is the result of melting of the crystals formed during crystallization and subsequent annealing. The high melting peak (HMP) is a result of crystals formed by simultaneous melting and recrystallization during the DSC measurement [37]. The DSC curves show that the crystal melting point increases with both annealing time and temperature. The effect of temperature on the LMP is much more pronounced than that of time. The LMP is shifted practically in tandem with the material temperature, whereby many hours residence time are required to cause a shift in the LMP to higher temperatures.

Furthermore, in the same study [47] it was shown that the maximum rate of increase in the LMP occurs between 180 and 200°C and that the percentage of the macromolecule *trans*-conformations increased in proportion to the heat of fusion or annealing. The *trans*-conformation has a torsion angle equal to 160° around the O–CH₂–CH₂–O link compared to 60° for the *gauche*-conformation [80].

Fontaine *et al.* [81] concluded that the increase in crystallinity by further heating material, crystallized at 200°C, to 215°C involves a crystal (lamellae) thickening process which is probably due to crystal perfection at the boundary layers. Further annealing of this material at temperatures above 215°C led to a melting temperature increase that was attributed to crystal perfection alone and not to crystal thickening.

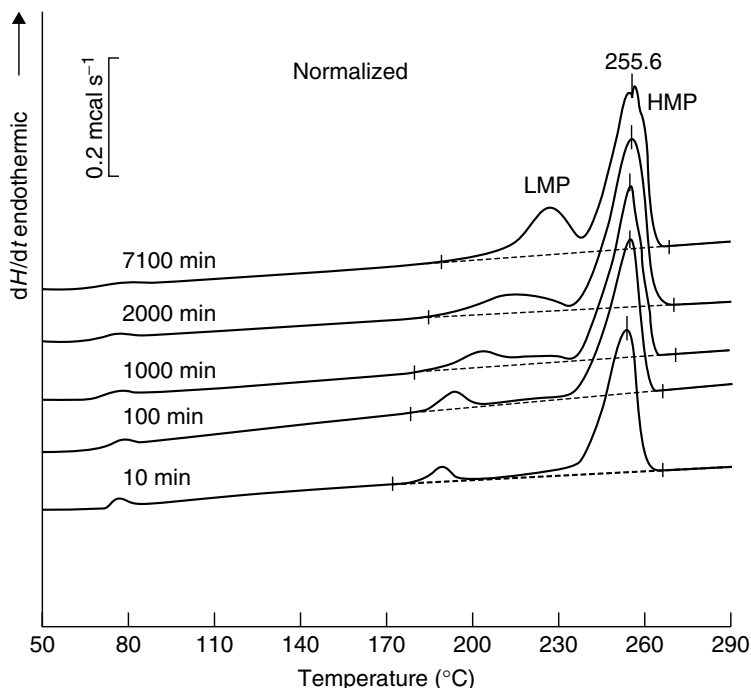


Figure 4.12 Normalized DSC thermograms of PET films annealed at 180°C for the indicated times [47]. From Lin, S. and Koenig, J., *J. Polym. Sci., Polym. Symp. Ed.*, **71**, 121–135 (1984), Copyright © John Wiley & Sons, Inc., 1984. Reprinted by permission of John Wiley & Sons, Inc

It has also been reasoned that smoothing the crystal surface and improving the chain conformations at the surface could reduce the macroscopic surface free energy and increase the melting temperature without substantially changing the crystalline perfection [82].

Elenga *et al.* [78] observed a drastic loss of drawability, together with a significant increase in strength at yield, for PET annealed for long periods of time. They attributed this to ester interchange reactions, which turn chain folds into intercrystalline tie molecules between neighbouring lamellae.

Finally, annealing studies have shown that chemical reaction at the crystal surface is possible, changing both the crystal surface and the molecular chain [82]. In addition, PET samples have been shown to undergo ester-interchange reactions at temperatures above 200°C , with the rate of reaction becoming relatively high only at temperatures above 225°C [83].

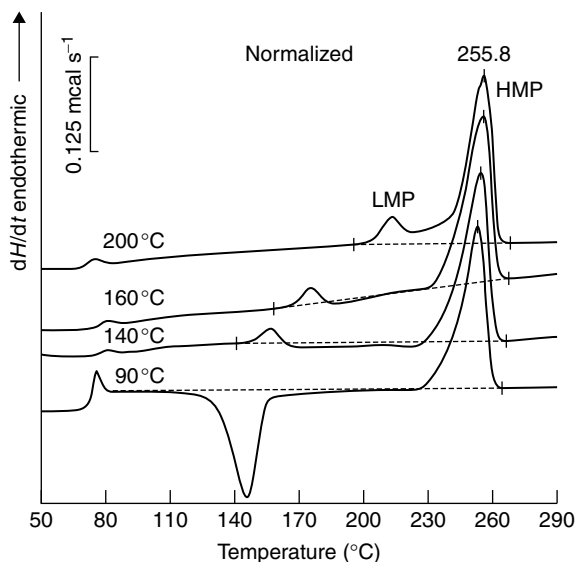


Figure 4.13 Normalized DSC thermograms of PET films annealed for 100 min at the indicated temperatures [47]. Note: the sample treated at 90°C has not crystallized. From Lin, S. and Koenig, J., *J. Polym. Sci., Polym. Symp. Ed.*, **71**, 121–135 (1984), Copyright © John Wiley & Sons, Inc., 1984. Reprinted by permission of John Wiley & Sons, Inc

4 CONTINUOUS SOLID-STATE POLYCONDENSATION PROCESSING

4.1 PET-SSP FOR BOTTLE GRADE

Continuous SSP plants are characterized by longer residence times and larger product hold-ups compared to the melt phase. This is due to the lower processing temperatures and the lower bulk density of the pellets compared to the melt. At today's standard bottle grade capacities of ca. 300 t/d, the typical plant hold-up is approximately 250 t, which equates to around 300 m³ of product volume at a bulk density of 800 kg/m³. Because the plants make use of gravity flow through the equipment they tend to be very tall – up to 50 m at 300 t/d.

At such high throughputs and large product hold-ups, these plants are required to be very robust [2]. More than one year of continuous production without maintenance is expected. In addition, the process needs to be able to be restarted after power outages of some hours without the loss of further production and with minimal 'off-spec' material.

The main functions of a PET-SSP plant for bottle-grade applications are as follows:

- To increase the molecular weight, measured by intrinsic viscosity ($IV = 2.1 \times 10^{-4} M_n^{0.82}$ using 50:50 phenol and 1,2-dichlorobenzene as solvents), of an amorphous precursor material from 0.58–0.68 dl/g up to 0.78–0.90 dl/g (M_n , 16 000–19 000 up to 22 500–27 000).
- To reduce the residual AA content from 30–150 ppm down to <1 ppm.
- To minimize the thermo-oxidative degradation of the pellets, characterized by colour or “yellowness”.
- To cool the pellets down to less than 60 °C after SSP.

The typical precursor material specification for bottle grade is as follows:

- Copolyester containing up to ca. 5 mol % of IPA, DEG or CHDM; market share: IPA > DEG 70 %; DEG > IPA 10 %; CHDM (<2.5 wt %) 10 %; DEG (>1.5 wt %) 10 % [84]
- Melting point, 248–255 °C (10 °C/min DSC rate)
- ≤ 220 ppm of antimony as transesterification catalyst [84]
- 10–50 ppm cobalt as colour additive [84]
- 10–60 ppm phosphorous as stabilizer [84]
- 30–150 ppm acetaldehyde content
- 10–40 mol/t carboxyl end group concentration

A standard pellet size and shape has established itself within the industry over recent years. The pellets tend to be cylindrical with a diameter between 2.0–3.0 mm and a length of 2–3.5 mm.

Given the SSP kinetics outlined in the previous section, it would be logical to assume that the most efficient SSP plant design would involve heating the pellets as quickly as possible to just below their melting point in order to maximize the SSP reaction rate and minimize product hold-up. However, due to PET's semi-crystalline behaviour, special equipment and product handling is required to prevent pellets from sticking or sintering together and forming agglomerates. Therefore, crystallization and annealing equipment is required to ‘prepare’ the pellets before they enter the SSP reactor column in order to prevent sintering and blockage of the pellet flow. Despite this “preparation”, the SSP temperature of continuous SSP plants is still typically limited to 200–220 °C, depending upon the plant size and the material characteristics.

4.2 BUHLER PET-SSP BOTTLE-GRADE PROCESS

A process flow diagram of a standard SSP plant design is shown in Figure 4.14. Leading PET resin producers including DuPont, Eastman, Kohap, Nan Ya, Shinkong and Wellman use this process. Some 70 plants have been installed world-wide over the last 15 years and they are responsible for approximately 4 500 000 t of bottle-grade PET. The four typical process stages are highlighted:

crystallization, annealing, SSP reaction and cooling. The accompanying DSC diagrams characterize the thermal history of the pellets through the plant.

4.2.1 Crystallization (Primary)

The amorphous feed material is crystallized in a two-stage process. In the first stage, a spouting bed, with high gas velocities, is used to achieve a vigorous pellet motion and thereby prevent agglomeration as the pellets quickly heat up and crystallize. In the second stage, a pulsed fluid bed, with lower gas velocities, is used to achieve quieter bed motion and guarantee a minimum pellet residence time. This prevents the carryover of amorphous pellets, which can be as high as 5 % after the spouting bed, and ensures an even crystallinity distribution after both crystallization stages. The crystallinity of the material is generally at least 35 vol% (determined by density measurements), depending upon the crystallization characteristic of the material.

Air is typically used as the heating medium in both beds, whereby the gas temperature generally does not exceed 185 °C. Higher temperatures can be employed, but nitrogen rather than air is used to prevent oxidation and the yellowing of pellets.

The spouting bed temperature is generally in the range of 150–170 °C, which is close to the maximum spherulite growth rate, and therefore ensures quick completion of the primary crystallization. The material temperature at the outlet of the pulsed fluid bed is usually <180 °C.

Looking at the corresponding DSC diagram of the material after crystallization in Figure 4.14, it can be seen that the exothermic peak of the raw material, due to primary crystallization, is gone. In its place is an endothermic low-melting peak due to crystals formed in the crystallization section. The beginning of melting of this low-melting peak generally corresponds to the temperature that the material has experienced in the crystallization section.

During crystallization, the bulk of the moisture and AA are removed from the pellets. In the case of moisture, this is critical before the pellets are heated to SSP temperatures above 180 °C. Moisture present at higher temperatures can lead to hydrolysis and a drop in IV, which leads to a reduction in the SSP reaction rate later in the process, as shown in Figure 4.15. The IV drop has been shown to increase significantly at temperatures over 200 °C [15]. Even at crystallization temperatures below 180 °C, a small IV drop of <0.01, depending on the initial moisture content, can be expected [86].

4.2.2 Annealing (Secondary Crystallization)

Before the crystallized material can be processed at higher SSP temperatures, the melting point of the crystals formed in the crystallization stage needs to

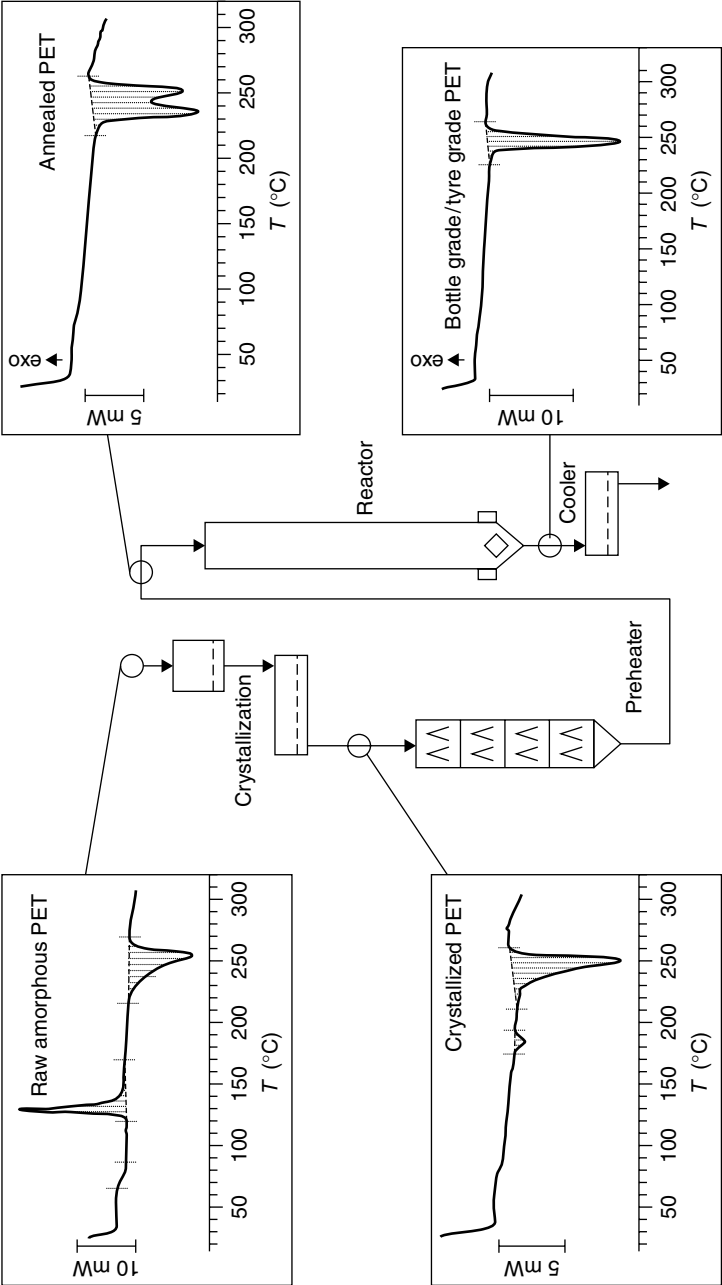


Figure 4.14 Schematic of a Buhler four-stage PET-SSP process, showing typical DSC thermograms (obtained at heating rates of 10 °C/min) at each process stage

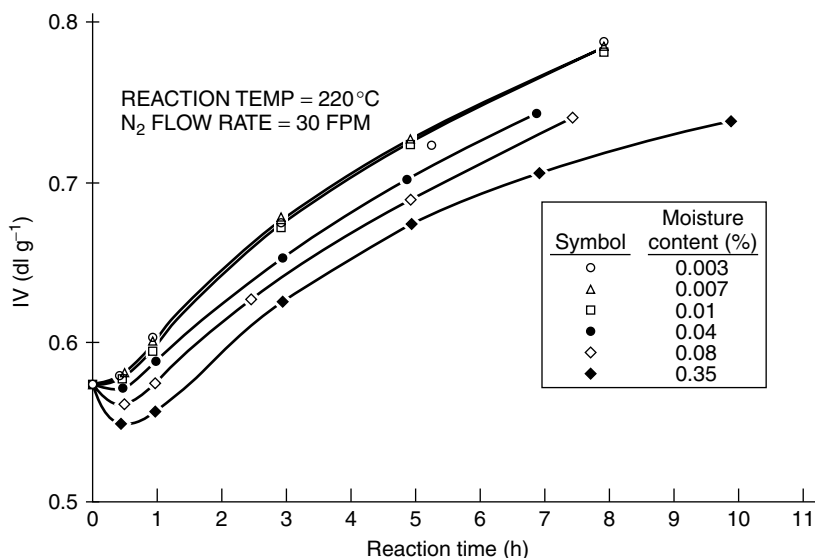


Figure 4.15 Influence of initial moisture content on PET reaction rate [85]. From Duh, B., Eur. Patent, EP 0 085 643 (1983)

be increased to above the intended SSP temperature. This shifting of the low-melting-point peak, known as *annealing*, significantly reduces the risk of sintering later on in the SSP column. A more detailed description of annealing is given in the previous section.

Because the pellets are susceptible to sintering during heat-up, the annealing takes place in a special piece of equipment known as a “roof-type” preheater, shown in Figure 4.16. In the preheater, the pellets flow by gravity between the angular roofs. This promotes relative movement between the pellets and also reduces the overall product bulk pressure in the vessel, thereby suppressing the tendency of the pellets to sinter.

The heating medium is nitrogen in order to prevent thermo-oxidative degradation of the pellets. The nitrogen flows in a cross-flow manner, entering from one side through the roofs, and then flowing through the pellets before being collected in an adjacent set of roofs and leaving the vessel on the other side. The pellets are heated in a series of two to six such preheater sections to a temperature of 210 to 220 °C.

The corresponding DSC diagram in Figure 4.14 shows that the lower-melting peak, formed after the crystallization section, has increased in size and been moved to a higher temperature, giving rise to a double melting peak. As in the crystallization section, the beginning of melting of this low-melting peak generally corresponds to the temperature that the material has experienced during annealing. The latter process takes places over residence times of up to 4 h, during

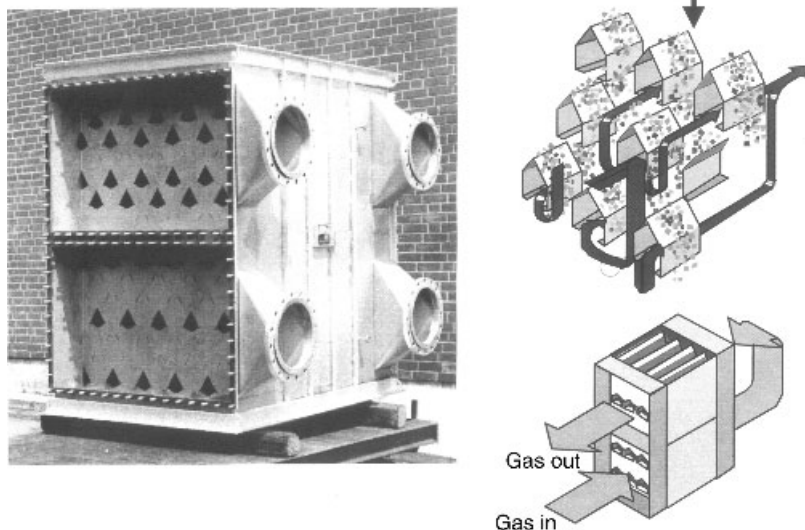


Figure 4.16 Roof-type preheater for annealing of PET pellets

which the molecular weight or IV begins to increase, the AA is significantly reduced to less than 5 ppm, and the crystallinity increases to ca. 50 vol%.

Having shifted the beginning of the low-melting-point peak above the SSP reaction temperature, the pellets are now ready for processing in the SSP column. The material can be pneumatically conveyed from the preheater to the reactor under nitrogen, thus allowing considerable capital cost saving by reducing the plant building height.

4.2.3 SSP Reaction

The reactor column is designed to provide the necessary residence time to achieve the material final IV specification. The residence times of materials vary significantly despite the apparent similarity of bottle-grade resins, and therefore laboratory testing is a very important part of sizing the reactor. Typical residence times in the range of 10–20 h at temperatures of 210 °C are required to reach the desired IV. This equates to a material hold-up of between 125 and 200 t at plant throughputs of 300 t/d. The reactor column has a diameter between 2 and 4 m and a height of up to 30 m. The current highest operating throughput is 450 t/d with product hold-ups of 300 t.

Nitrogen enters at the bottom of the reactor and flows countercurrently up through the pellets in order to remove the reaction by-products, ethylene glycol

and water. The gas-to-solid mass ratio is typically kept below 1.0. The nitrogen flow rate is generally not low enough to influence the mass transfer of the by-products from the pellet to the gas. However, the by-product concentration increases as the gas moves through the product and needs to be taken into consideration when designing the reactor residence time.

The final material viscosity is controlled by either the residence time or the reaction temperature. By adjusting the weight of material in the reactor, which is mounted on load cells, the residence time can be changed. Such a change is suitable for fine IV corrections but not for large step changes as the movement of large quantities of material can require many hours so as not to upset the whole process. The adjustment of the temperature is easily carried out at the outlet of the annealing vessel by adjusting either the gas flow rate or the gas inlet temperature. Such a change results in a sharp temperature front that follows the material down through the reactor with little or no 'off-spec' material resulting.

The temperature in the reactor is limited by the tendency of the pellets to sinter. This is a function of the material characteristics, the pre-treatment in the annealing section, the column dimensions and design, the pellet shape and the pellet sink velocity through the column. In general, the sticking tendency tends to increase with increasing temperature, increasing column diameter, and decreasing pellet velocity. This sticking tendency is measured by using empirical laboratory techniques, although experience is required in sizing the reactor column. Typically, the reactor design temperature is between 205 and 215 °C.

The sintering in the reactor is attributed to the chemical healing process that is known to occur in semi-crystalline polycondensates [87]. A combination of ester interchange or transreactions (TR), solid-state polymerization or additional condensation (AC), and mutual diffusion (D), as shown in Figure 4.17, is responsible for the joining or healing at the pellet interface which leads to the formation of agglomerates and the blocking of reactor outlets.

During the SSP processing in the reactor, the pellets continue annealing. The DSC diagram in Figure 4.14 shows a single melting peak although a double peak can also be visible depending on the SSP processing conditions. The crystallinity increases a further 2–3 % to 55 vol%, and the AA constant is less than 1 ppm. The carboxyl end group concentration decreases by approximately 6 mol/t. Theoretically, this equates to one third of the IV increase occurring through esterification and two thirds through transesterification if side reactions are neglected.

4.2.4 Cooling

Cooling of the pellets begins at the outlet of the reactor. Nitrogen enters the reactor cold and the pellets are cooled in the reactor discharge section to ca. 180 °C. The pellets then pass into a fluid bed cooler, where they are cooled within 5 min to typically less than 60 °C by fresh air.

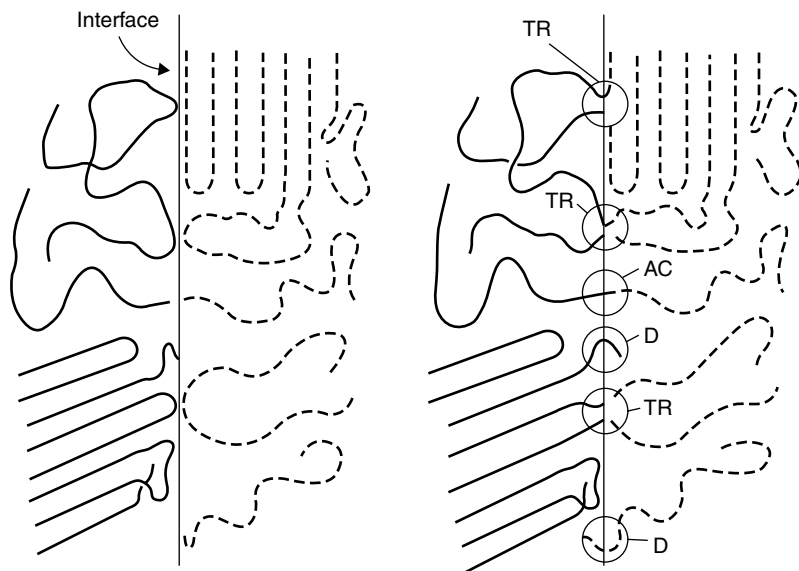


Figure 4.17 Schematic view of the chemical healing process in semi-crystalline linear polycondensates: TR, transreactions; AC, additional (post)condensation; D, diffusion [87]. From Fakirov, S., *J. Polym. Sci., Polym. Phys. Ed.*, **22**, 2095–2104 (1984), Copyright © John Wiley & Sons, Inc., 1984. Reprinted by permission of John Wiley & Sons, Inc

4.2.5 Nitrogen Cleaning Loop

The nitrogen cleaning loop consists of a filter to remove any dust, a platinum catalyst bed to remove ethylene glycol, acetaldehyde and oligomers by combustion at quasi-stoichiometric oxygen ratios, and a gas dryer for the removal of moisture down to dew points below -40°C . The oxygen content of the nitrogen is typically <10 ppm.

4.3 PROCESS COMPARISON

A simplified schematic of various available SSP systems is shown in Figure 4.18. The four main process stages of crystallization, annealing, reaction and cooling are present in all of the plant types. The processes differ from one another by the way in which the pellets are agitated in order to prevent agglomeration during heat-up.

Of the SSP processes available today only System 1, the process described above, does not use mechanical agitation to prevent the agglomeration of pellets. All other processes use some form of mechanical agitation during either

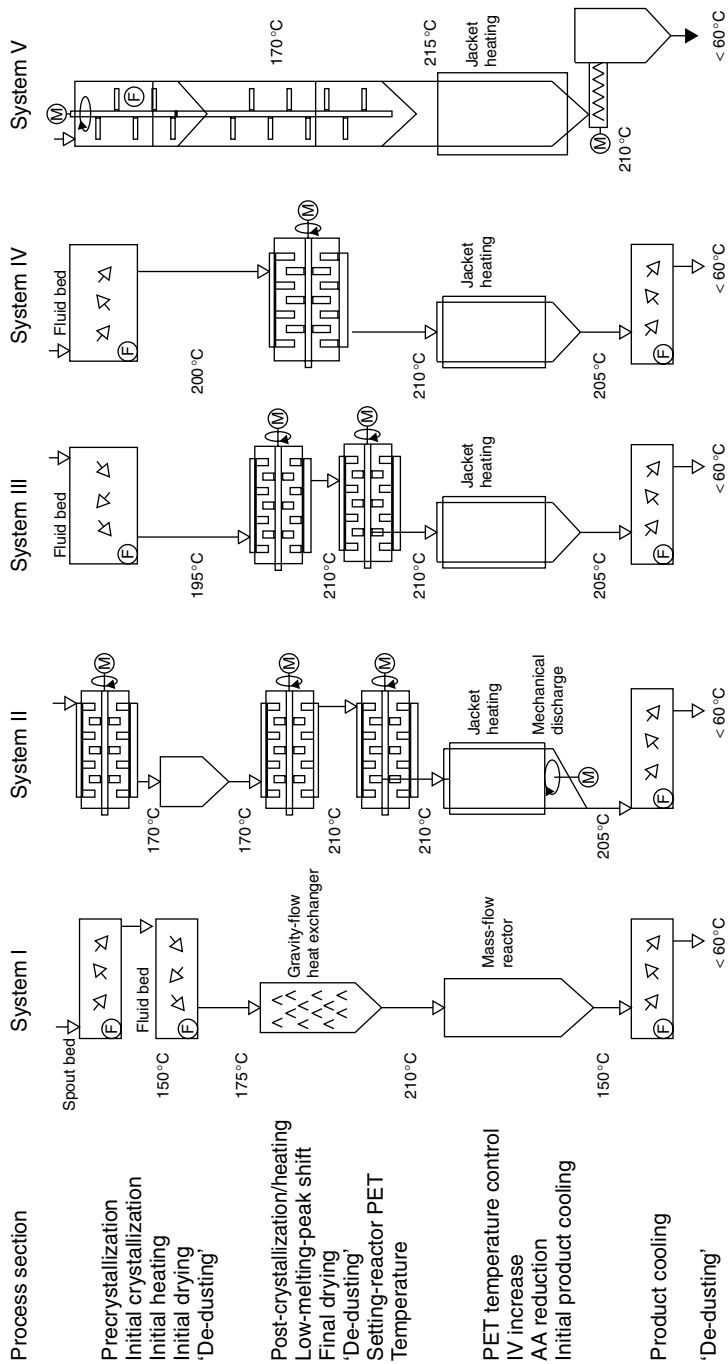


Figure 4.18 Comparison of the various PET-SSP processes: (F), fluidization; (M), mechanical agitation

primary or secondary crystallization to keep the pellets from agglomerating. This mechanical agitation is particularly prevalent in the annealing section, where the temperatures are highest. Mechanical agitation is also used in some cases to break up agglomerates at the reactor outlet in order to maintain material flow from the reactor. Dust can be generated through mechanical agitation.

The fluid bed has generally established itself as the preferred equipment for the crystallization and for the cooling section of the SSP plant. High heat-transfer coefficients enable the pellets to be heated and cooled very quickly, pellet agitation can be achieved without dust generation, and the direct contact between gas and solid enables a 'de-dusting' effect.

In the gas-cleaning loop, a catalyst bed system for the removal of hydrocarbons and a molecular sieve dryer for removing moisture is generally preferred to an ethylene glycol scrubber.

4.4 PET-SSP FOR TYRE CORD

The processing requirements for a PET-SSP plant for tyre cord are very different to those for a bottle-grade plant: First, the raw material is typically a homopolyester with a melting point of 260 °C or higher, secondly the final viscosity of 1.0 to 1.2 is much higher, and thirdly the plant throughputs, typically between 30 and 90 t/d, are much smaller. These three differences result in a rather simplified process, as shown in Figure 4.19.

Homopolyesters are less sticky and easier to handle during crystallization because they crystallize faster than copolyesters, as shown above in Figure 4.11 [51]. Therefore, single-stage crystallization, using the pulsed fluid bed with gas velocities between 1–2 m/s, is sufficient to crystallize a homopolyester without agglomeration. The gas and material temperatures are the same as for bottle-grade material; however, the crystallinity of the pellets after crystallization is higher, generally at least 40 vol%.

The very high final viscosity requirement demands either a significantly longer residence time or higher temperatures when compared to bottle grade. By applying the following rules of thumb (provided in Section 2 above) to an intrinsic viscosity change from 0.6–0.8 dl/g ($\Delta M_n = 6887$) to 0.6–1.0 dl/g ($\Delta M_n = 14\,200$) whereby:

- the molecular weight increase is proportional to the square root of residence time – then the residence time needs to be increased by a factor of 4 at constant temperature;
- the reaction rate doubles every 13 °C – then the reaction temperature needs to be increased by 14 °C at constant residence time;

In the process shown in Figure 4.19, residence times of less than 20 h are achieved by increasing the processing temperature to upwards of 230 °C. However, in order

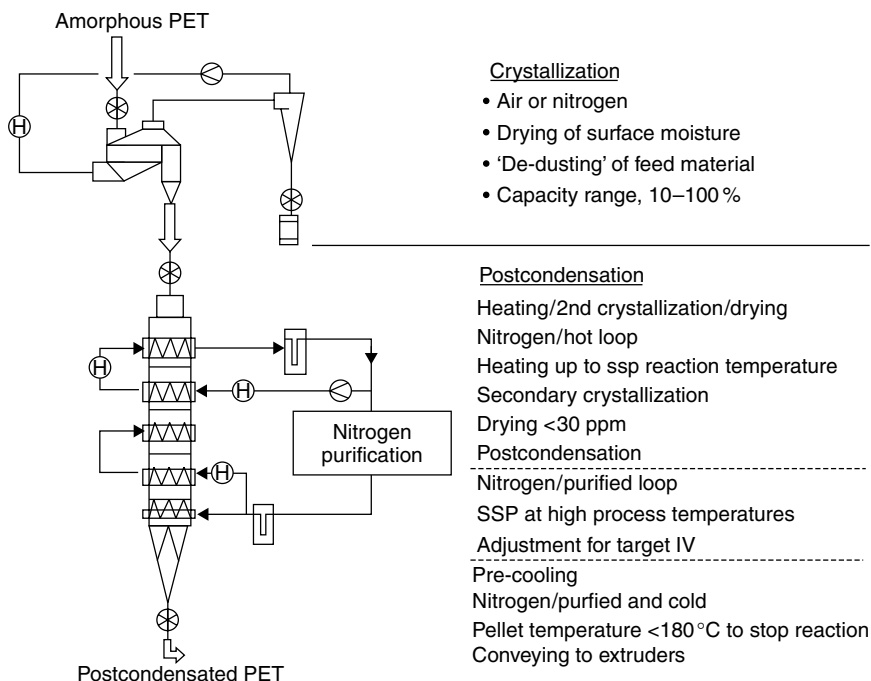


Figure 4.19 Schematic of the Buhler PET-SSP process for technical fibres:
 (H), heater

to produce material without sticking and agglomeration of the pellets, the pellet heat-up and SSP processing is carried out in the roof-type preheater. The roofs reduce the risk of sintering by relieving the product bulk pressure which is present in a column reactor and by encouraging relative movement between the pellets.

Generally, two to three preheater sections are used for the product heat-up by using nitrogen, and two to three sections are required to reach the final viscosity. Cooling is carried out either in an additional compartment or with a fluid bed. Typically, for a viscosity increase from 0.60 up to 1.0, the crystallinity increases to ca. 62 vol%, and the carboxyl end group concentration decreases by approximately 10–15 mol/t. This equates to both esterification and transesterification contributing half of the IV increase if side reactions are neglected.

4.5 OTHER POLYESTERS

4.5.1 SSP of Poly(Butylene Terephthalate)

Poly(butylene terephthalate) (PBT) closely resembles PET, the difference being that 1,4 butandiol (BD) is used instead of ethylene glycol in its manufacture. PBT

is produced both from dimethyl terephthalate (DMT) and terephthalic acid (PTA). The DMT process produces approximately 6 mol % of the by-product tetrahydrofuran, a ring molecule formed by the irreversible acid-catalyzed dehydration of BD, compared to 13 mol % for the PTA process [42]. However, the PTA process has lower raw material, energy and investment costs [42].

Molecular weights (number average) in the range of 20 000 to 35 000 [88] are achieved in the melt phase and are used for fibre and engineering plastics applications. For some injection moulding and extrusion applications, molecular weights above 40 000 [88] are required. Such high values are best achieved by SSP.

PBT has a glass transition temperature of 28 °C, extending to 49 °C [89]. The SSP processing requirements for PBT are different to that needed for PET. The PBT precursor resin is opaque and already crystalline due to the higher crystallization rates of PBT, and therefore the primary crystallization step in a fluid bed is not required. However, PBT does display a low melting point (LMP) [90]. This needs to be shifted above the reaction temperature in an annealing stage in order to reduce the risk of sintering before SSP treatment in a reactor is performed.

PBT has two crystal modifications [91]. The α -form is stable, while the β -form is reversibly formed by stretching [92]. The amorphous density is given as 1.26 g/cm³ [88] and that of 100 % crystalline in the range from 1.394 to 1.406 g/cm³ [93]. The melting point is 225 °C [43] and the heat of fusion values for crystalline PBT reported are generally in the range of 31 to 32 kJ/mol [93].

Due to the lower melting point, the SSP processing temperature is correspondingly lower – typically 180 to 200 °C. Although PBT is less oxidation-sensitive than PET [43], processing still takes place under nitrogen. The reaction rate of PBT is faster than that of PET and is attributed to a difference in the reactivity of the glycols and in the morphology [43]. Typically, the intrinsic viscosity can be increased from a value of 0.8 dl/g up to 1.2 in less than 12 h [94].

The reaction mechanisms of PBT are similar to that of PET. Both transesterification and esterification reactions are involved in the viscosity increase, although BD is the reaction by-product of transesterification rather than EG. The OH/COOH end group ratio [43, 95, 96], pellet size [43, 96, 97] and temperature all influence the reaction rate. The side reaction involving the formation of tetrahydrofuran is important in that it changes the hydroxyl into carboxyl end groups, although it does not affect the molecular weight. The concentration of the slower reacting methyl ester end groups in the SSP precursor material produced from DMT should be kept to a minimum [42].

4.5.2 SSP of Poly(Ethylene Naphthalate)

The manufacture of poly(ethylene naphthalate) (PEN) is carried out using dimethyl 2,6-naphthalene dicarboxylate (NDC) and EG and is similar to the manufacture of PET from DMT. The IV after the melt is typically in the range of 0.5

to 0.55 dl/g [98]. To achieve higher molecular weights, PEN can be solid-state polymerized.

PEN has two crystal modifications [99]. Both forms have a triclinic structure and can be obtained under crystallization conditions. Their densities are 1.407 and 1.439 g/cm³, compared to 1.326 g/cm³ for amorphous material.

The SSP processing requirements for PEN are very similar to PET. Crystallization and annealing stages are required before processing in an SSP column. However, the crystallization is more complicated than for PET. PEN has a glass transition temperature of 121 °C [99], and begins to stick at a temperature of ca. 140 °C, while the crystallization rate of PEN does not become significant until temperatures above 180 °C with the maximum crystallization rate being at ca. 200 °C [100, 101]. However, at crystallization temperatures of above ca. 195 to 200 °C PEN has a tendency to stick very strongly and in the presence of high moisture contents to expand and burst – known as “popcorning” [102]. Therefore, there is only a small crystallization window in which to crystallize PEN.

The melting point of PEN is 267 °C [103]. To achieve significant SSP reaction rates, temperatures above 220 °C and preferably 230–240 °C are required. Approximately 22 h are required to increase the intrinsic viscosity from 0.55 up to 0.75 at a temperature of 235 °C [104]. The annealing stage is required before SSP to shift the beginning of melting and to reduce the risk of sintering. The reaction kinetics of PEN are similar to that of PET. Both transesterification and esterification reactions are involved in the viscosity increase. As with PET, parameters such as OH/COOH end group ratio and pellet size influence the reaction rate.

5 PET RECYCLING

5.1 PET RECYCLING MARKET

PET is an ideal material for recycling. It can be reprocessed multiple times and the source material is available in large quantities, mostly as a ‘mono-material’. The main focus today is on PET bottles which are collected in dedicated collection systems [108] or separated from other waste streams. Around the world, countries are planning to or have already adopted legislation to reduce packaging waste by the following approaches:

- Banning the disposal of packaging waste
- Mandating collection rates
- Introducing reuse or reprocessing quotas [109, 110]

Accordingly, PET bottle recycling is increasing steadily, an effect which is compounded by an overall increase in consumption amounts and collection rates in some markets. On a world-wide basis, doubling of the PET bottle collection

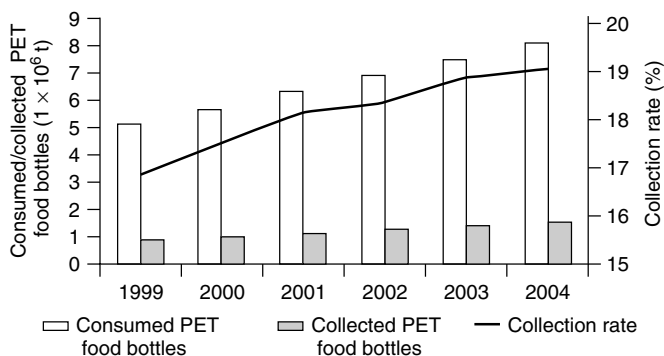


Figure 4.20 World-wide consumption and collection of PET food bottles, excluding Africa and the Middle East (source – PCI; Packaging, Resin and Recycling Ltd, 30 March 2001)

amount is expected within five to six years. At the same time, values for Europe and the Asia-Pacific rim are expected to triple (Figure 4.20).

5.2 MATERIAL FLOW

After polymerization, PET is processed to final products, distributed to consumers and eventually ends up in a waste treatment system. Manual sorting or various automated methods can be applied to separate the PET fraction from a waste stream [111].

Collected post-consumer PET bottles first undergo a reclaiming process. There, they are sorted from non-PET bottles, if necessary also by colour, ground to an average flake size typically between 6 mm and 14 mm, and washed. Labels, label adhesives, lids, base cups, some foreign plastic layers and coatings, as well as dirt and residual content, are then removed from the bottle material [112]. The washed PET flakes are recycled either through direct reprocessing (mechanical bottle recycling) or through depolymerization into monomers, which are used as an alternative source in PET manufacturing (chemical bottle recycling) (Figure 4.21).

The majority of the early mechanical recycling solutions for PET bottles were based on open-loop systems for use in applications such as fibre, fibre fill, strapping or sheet. More recently, solutions were developed which create closed-loop bottle-to-bottle recycling [113, 114, 115].

5.3 SOLID-STATE POLYCONDENSATION IN PET RECYCLING

Similar to virgin PET, solid-state polycondensation (SSP) is the method of choice to increase the molecular weight in mechanical recycling processes.

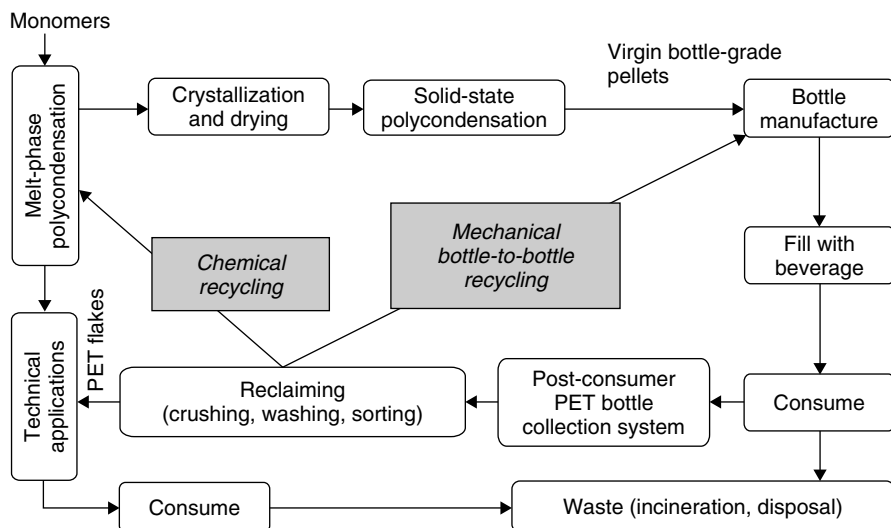


Figure 4.21 Typical scheme for PET material flow

For many recycling applications, the molecular weight or IV of the reclaimed PET needs to be increased above the level of the initial product. Even for closed-loop recycling, an increase in the molecular weight is necessary. This is required to make up for the loss in molecular weight during melt processing of PET caused by hydrolysis, thermal and thermal-oxidative degradation [19].

While an IV increase of 0.06 dl/g may be sufficient for most bottle-to-bottle applications, an IV increase of up to 0.4 dl/g might be necessary for technical yarns or foam applications. This increase can be achieved through reactive extrusion [116], by melt-phase polymerization or by solid-state polycondensation. While any process in the melt phase adds to the generation of degradation products, solid-state polycondensation not only increases the molecular weight of the PET but it also promotes the re-polymerization of degradation products from previous heat histories. For the production of PET bottle-grade qualities, the reduction of acetaldehyde during the solid-state process is of major importance.

SSP of recycled PET (RPET) can be performed as either a continuous or a batch process. A continuous SSP offers a constant and overall higher productivity, as well as a more consistent product treatment, lower operating costs [117] and better process integration with a downstream manufacturing process. A batch SSP offers a larger degree of flexibility for small-scale operations with a large variation of raw material and final product specifications.

Reclaimed PET material is either directly upgraded by solid-state polycondensation [118] or repelletized before SSP [119]. In either case, the energy consumption can be reduced by eliminating an additional drying step if the downstream

manufacturing process is continuously in line with the SSP. Some process energy from the repelletizing step before SSP can be saved if pellets are only partially cooled and then directly introduced into the SSP system [120]. The best way of processing has to be selected according to the requirements of the final product.

5.3.1 PET Bottle Recycling: Flake SSP

The advantage of direct solid-state treatment of PET bottle flakes is the faster IV increase rate when compared to pellets. This is due to the lower average thickness and therefore shorter diffusion distance (see parameters affecting SSP in Section 2.3 above). However, several aspects have to be considered, as follows:

- PET bottle flakes are not uniform in thickness. Flakes from the neck and bottom of the bottle are thicker and have a much lower IV increase rate than flakes from the bottle wall. The solid-state treatment of such a mixed product yields a final product with a wide IV spectrum [121] (Figure 4.22).
- The bulk density of the flakes is typically between 250 and 450 kg/m³. Compared to pellets, with a typical bulk density of between 750 and 850 kg/m³, this has a negative effect on equipment sizing and product handling. Further comminuting the PET flakes increases the bulk density and improves product uniformity, but also creates additional product loss to dust.

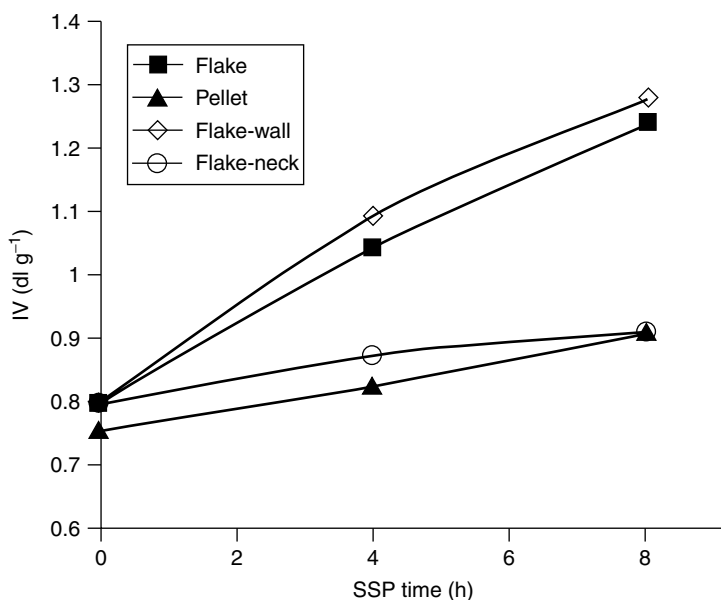


Figure 4.22 Reaction rates of various PET flakes versus that of pellets

- PET flakes have different crystallinities. The wall particles are oriented and crystallized, while the flakes from the neck and bottom of non-heat-set bottles are amorphous and require crystallization to prevent sintering before they can be subjected to SSP. Separating the thick amorphous PET flakes before SSP to circumvent the sticking risk and to improve the uniformity of the product has also been suggested [122]. However, this may only be commercially acceptable if the separated flakes can be used in a final application.
- Special attention needs to be put on the possibility of contamination with PVC. The latter decomposes under SSP conditions and produces hydrochloric acid, which has to be eliminated from the process gas stream to protect the processing equipment [123]. The PVC residues will manifest themselves as black non-melting particles in the downstream process. There is an option to eliminate the decomposed PVC residue by colour sorting after the SSP process.

The use of a flake SSP is especially advantageous if a high final IV has to be reached and if the downstream manufacturing process is set up to directly accept PET flakes.

If flakes are not acceptable, an intermediate repelletizing step will be necessary. There are several issues which have to be considered in this case, as follows:

- The IV loss in extrusion has to be anticipated in the target for the SSP.
- The starting IV for repelletizing after SSP is higher than before SSP and accordingly results in a higher IV loss during extrusion.
- The repelletizing step adds a heat history after the SSP. In particular when food applications are being considered, this adds an undesirable amount of acetaldehyde.
- An additional crystallization step becomes necessary after repelletizing to allow drying before melt processing.
- A melt filter should be introduced in the downstream process to eliminate solid contaminants such as residual glass, metal, sand, paper or wood, as well as decomposed or cross-linked polymers.

5.3.2 PET Bottle Recycling: SSP after Repelletizing

Repelletizing the PET flakes before solid-state polycondensation is a common way of processing in a recycling system. This mirrors the path of virgin PET manufacturing by applying the melt-phase process before the solid-phase process. With a correctly designed recycling loop, the final RPET quality is comparable to that of virgin PET.

During repelletizing, the PET is melted, homogenized and solidified in a uniform shape. Repelletizing is carried out after a pre-drying step or directly with undried flakes, depending on the ability to remove moisture inside the extruder and the intended final IV. Although IV retention is usually a major concern,

there are patented processes where it is desirable to reduce the IV of a recycled product to match the IV of virgin PET product resulting from melt-phase polymerization [124]. The consistency of the pellet dimensions is important for an even treatment in the SSP process. One or multiple degassing sections can be added to remove moisture and other volatile contaminants. Melt filtration should be included in the repelletizing step. Contaminants, residual adhesives and washing detergents and foreign polymers, in particular PVC, have a negative influence on the crystallization behaviour, the molecular weight and the colour of the repelletized PET [125].

The SSP plant for repelletized PET is similar to a virgin SSP plant. It is usually smaller, because of smaller feed stock availability, and should provide the flexibility to adapt to changing product requirements. Another difference results from the IV increase rate of recycled PET, which tends to be lower. This is attributed to a lower activity of the transesterification catalyst in recycled PET.

5.3.3 Closed-Loop Bottle-to-Bottle Recycling

Closed-loop bottle-to-bottle recycling is an ideal way of utilizing the material value of a used PET bottle and at the same time deal with the increasing volume of collected PET bottles on a regional scale. The energy consumption values for mechanically reprocessed bottle-grade PET, including transportation, is significantly lower than that for virgin PET, i.e. about 9.7 MJ/kg [126] compared to about 77.5 MJ/kg [127].

For a comprehensive bottle-to-bottle recycling process, several stringent requirements have to be fulfilled [128], including the following:

1. The cost for recycled PET has to be lower than virgin PET bottle material, even at low virgin prices.
2. Undesirable solid particles and organic components such as soft-drink aromas or migrated chemicals, which may result from misuse of PET bottles, must be removed.
3. The process has to limit degradation during reprocessing and reverse degradation effects from previous processing heat histories.
4. The IV increase capabilities have to be in accord with changing requirements for input and final product viscosities. Manufacturing, consumption and collection patterns are constantly changing. A recycler has to be able to adapt to these changes.
5. Uniform product quality must be achieved to ensure trouble-free bottle manufacturing
6. The upgraded product has to be compatible for use on existing injection moulding and auxiliary equipment.
7. The acetaldehyde content must be reduced to the requirements for food bottles.

Table 4.2 Processing options and their influence on PET recycling requirements: c, critical aspect, where requirement is not or only partially fulfilled

Process		Requirement						
		1	2	3	4	5	6	7
A	Solid treatment before melt treatment	–	–	c	–	–	–	c
B	Solid treatment only	–	–	–	–	c	c	–
C	Melt treatment only	–	c	c	c	–	–	c
D	Melt treatment before solid treatment	–	–	–	–	–	–	–

Several bottle-to-bottle recycling technologies have been developed to convert washed PET flakes to food-grade PET pellets [129, 130]. They can be categorized by four different ways of processing. The succession of process steps has an influence on the final result. To see the implications, each process option has to be evaluated with respect to the requirements discussed before. Some of these critical aspects are indicated in Table 4.2.

5.3.4 Buhler Bottle-to-Bottle Process

As an example for process succession D, the Buhler bottle-to-bottle process fulfils all of the requirements listed above. Acetaldehyde levels are even below those of virgin PET (Figure 4.23).

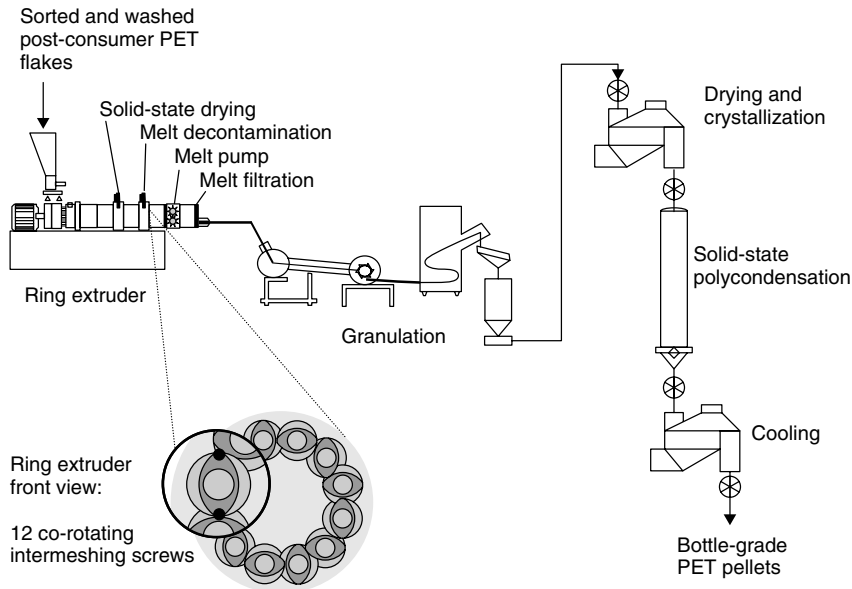


Figure 4.23 Schematic of the Buhler PET bottle-to-bottle recycling process

In this process, a vacuum extrusion step (melt treatment) is followed by a continuous SSP (solid treatment). The process starts with PET flakes which are introduced without pre-drying into a ring extruder. The flakes are dried, melted and degassed inside the extruder. A gear pump builds the necessary pressure for melt filtration, where solid particles are removed. After granulation the pellets are fed to a continuous three-step SSP unit [10].

The advantages of the ring extruder when compared to other extrusion technologies are a much higher surface-to-volume ratio and a higher surface building rate (which is equal to the regeneration rate of the devolatilized surface [131]). Both are reasons for a higher degassing efficiency which allows the running of higher throughputs and therefore yield a shorter residence time. The result is a more cost-efficient process and better product quality.

In the continuous SSP process, the product is preheated and homogeneously crystallized in a spouting bed crystallizer. This allows materials with high sintering potential to be processed without agglomeration. Inside the solid-state reactor the product reaches its final temperature and is upgraded to the desired IV. A homogeneous product quality is guaranteed through an even heat-up and a narrow residence time distribution. Maximum IV flexibility is obtained by the reactor design which allows a wide range of process temperatures. For quick cool-down, a fluid bed cooler is used. Crystallization and cooling are performed under air, while polycondensation is carried out under nitrogen.

The nitrogen is constantly cleaned in a gas purification loop. All reaction products and contaminants are burnt in a catalytic combustion system.

Some typical specifications for a product originating from a curb-side collection are shown in Table 4.3.

Table 4.3 Typical specifications for reclaimed flakes, recycled PET pellets and virgin PET pellets

Specification	Washed Flake	Upgraded pellets	Virgin (typical)
IV (dl/g) [Buhler method 22320] ^a	0.80	0.86	0.86
Colour b ^b [Buhler method 22701] ^c	1.6	1.4	<2
Acetaldehyde (ppm) [Buhler method 30810]	13	0.7	<1
Crystallinity (%) [Buhler method 22111]	–	49	54 ^d

^a Based on DIN 53728 with 50:50 phenol/1,2-dichlorobenzene.

^b Colour b* values are influenced by sample crystallinity and are not directly comparable between flakes and pellets.

^c Based on DIN 5033 and DIN 6174.

^d Approximate value.

5.3.5 Food Safety Aspects

Individual national regulations for recycled PET in direct food contact have to be followed, where these regulations have already been established. On the European level, the International Life Science Institute (ILSI) [132] has proposed specific guidelines. In the US, the Food and Drug Administration (FDA) [133] has published guidelines which require a challenge test to determine the cleaning efficiency of the recycling process [134]. A list of submissions to the FDA with favourable opinion has been published by the FDA [135].

The dual treatment in the Bühler bottle-to-bottle process is an important aspect in food safety considerations. The bulk of the contaminants are removed in the extruder. However, the SSP process provides a back-up to remove any residual contaminants, which are now homogeneously distributed in the PET pellets. The cleaning becomes a well-defined and predictable diffusion controlled process, which is defined by pellet diameter, treatment temperature and time. The same parameters also regulate the SSP process. For products with similar reactivity, a known increase in molecular weight during the solid-state process will also provide a known cleaning efficiency.

The extractable contamination concentration from 100 % recycled PET bottles into all kinds of foodstuffs (aqueous, alcoholic and fatty) was shown to be several orders of magnitude below the FDA threshold of regulation, even if the initial contaminant concentration was significantly above the values found in the waste stream [136].

REFERENCES

1. Mueller, M., PET SSP technical fibres, presentation given at the *Bühler Forum Asia*, Bühler A. G, Uzwil, Switzerland, 16–17 November, 2000.
2. Mueller, M., SSP processes for capacities up to 600 t/d, presentation given at the *Bühler Forum Protech*, Bühler A. G, Uzwil, Switzerland, 10–11 June, 1999.
3. Kibler, C., Process for solid phase polymerization of poly(ethylene terephthalate), *Can. Patent 849 098*, 1970.
4. Maxion, E. J., Polycondensation of solid polyesters with anticaking agents, *US Patent 3 544 523*, 1970.
5. Maxion, E. J., Progressive heating in polyester condensations, *US Patent 3 728 309*, 1973.
6. Rothe, H. J., Heinze, H., Whitehead, B. D. and Priepke, G., Process for the continuous production of high molecular weight poly(ethylene terephthalate), *US Patent 4 064 112*, 1977.
7. Gey, W., Langhauser, W., Heinze, H. Rothe, H. J. and Freund, P., Process for the solid state polycondensation of linear polyesters, *US Patent 4 069 194*, 1978.

8. Halek, G. W., Freed, W. T., Schaul, J. S., Rupp, R. W. and Pauls, S. L., Process for preparing poly(ethylene terephthalate) useful for beverage containers, *US Patent 4 223 128*, 1980.
9. Mueller, M., PET bottle grade resin advancements in SSP technology, presentation given at the *Polyester 2000 5th World Congress*, Maack Business Services, 8804 Au/near Zurich, Switzerland, 28 November–1 December, 2000.
10. Christel, A., Advanced PET bottle-to-bottle recycling, presentation given at the *Polyester 2000 5th World Congress*, Maack Business Services, 8804 Au/near Zurich, Switzerland, 28 November–1 December, 2000.
11. Mallon, F. K. and Ray, W. H., Modelling of solid-state polycondensation. I. Particle models, *J. of Appl. Polym. Sci.*, **69**, 1233–1250 (1998).
12. Ravindranath, K. and Mashelkar, R. A., Finishing stages of PET synthesis: a comprehensive model, *AIChE J.*, **30**, 415–423 (1984).
13. Becker, D., Zimmermann, H. and Kolbig, C., Polymeranalytische Untersuchungen zum Abbau von Polyäthylenterephthalat in fester Phase, *Faserforschung Textiltechnik*, **27**, 229–235 (1976).
14. Roth, H. and Freund P., process for the production of polyester Polymer for food packaging, *US Patent 4 263 425* (1981).
15. Jabarin, S. A. and Lofgren, E. A., Solid state polymerization of poly(ethylene terephthalate): kinetic and property parameters, *J. Appl. Polym. Sci.*, 5315–5335 (1986).
16. Wu, D., Chen, F. and Li, R., Reaction kinetics and simulations for solid-state polymerization of poly(ethylene terephthalate), *Macromolecules*, **30**, 6737–6742 (1997).
17. Buxbaum, L. H., Der Abbau von Polyäthylenterephthalat, *Angew. Chem*, **6**, 225–232 (1968).
18. Zimmermann, H., Developments in polymer degradation, *Applied Science*, Vol. 5, London, 1984, Ch. 3, pp. 79–119.
19. Jabarin, S. A., Poly(ethylene terephthalate) chemistry and kinetics, in *The Polymeric Encyclopedia*, (on CD-Rom), Salomone, J. C. (Ed.), CRC Press, Boca Raton, FL, 1996.
20. Allen, N. S., Edge, M., Mohammadian, M. and Jones, K., UV and thermal hydrolytic degradation of poly(ethylene terephthalate): importance of hydroperoxides and benzophenone end groups, *Polym. Degrad. Stabil.*, **41**, 191–196 (1993).
21. Ravindranath, K. and Mashelkar, R. A., Poly(ethylene terephthalate) reactors. IX. Solid state polycondensation process, *J. Appl. Polym. Sci.*, **39**, 1325–1345 (1990).
22. Buxbaum, L. H., Solid-state polycondensation of poly(butylene terephthalate), *J. Appl. Polym. Sci.*, **35**, 59–66 (1979).

23. Schumacher, M., Kristallisation and Festphasennachkondensation von PET in grossen Mengen, *Diplomarbeit an der Institut für Polymere der ETH Zurich*, Zurich, p. 31, 1994.
24. Mallon, F. K. and Ray, W. H., Modeling of solid-state polycondensation. II. Reactor design issues, *J. Appl. Polym. Sci.*, **69**, 1175–1788 (1998).
25. Schluender, E. U. and Tsotsas, E., *Wärmeübertragung in Festbetten, durchmischten Schuettguetern und Wirbelschichten*, Georg Thieme Verlag, Stuttgart, 1988, p. 40.
26. Huang, B. and Walsch, J. J., Solid-phase polymerization mechanism of poly(ethylene terephthalate) affected by gas flow and particle size, *Polymer*, **39**, 6991–6999 (1998).
27. Chen, S. and Chen, F., Kinetics of polyesterification III: Solid-state polymerization of poly(ethylene terephthalate), *J. Polym. Sci., Polym. Chem. Ed.*, **25**, 533–549 (1987).
28. Chang, T. M., Kinetics of thermally induced solid state polycondensation of poly(ethylene terephthalate), *Polym. Eng. Sci.* **10**, 364–368 (1970).
29. Chen, F. C., Griskey, R. G. and Beyer, G. H., Thermally induced solid state polycondensation of nylon 66, nylon 6–10 and poly(ethylene terephthalate), *AIChE J.*, **15**, 680–685 (1969).
30. Kokkolas, D., Bikiaris, D. N. and Karayannidis, G. P., Effect of the Sb_2O_3 Catalyst on the solid-state postcondensation of poly(ethylene terephthalate), *J. Appl. Polym. Sci.*, **55**, 787–791 (1995).
31. Hsu, L., Synthesis of ultrahigh molecular weight poly(ethylene terephthalate), *J. Macromol. Sci., Phys.*, **B14**, 801–813 (1967).
32. Mallon, F., Beers, K., Ives, A. and Ray, W. H., The effect of the type of purge gas on the solid-state polymerization of polyethylene terephthalate, *J. Appl. Polym. Sci.*, **69**, 1789–1791 (1998).
33. Schaaf, E., Zimmermann, H., Dietzel, W. and Lohmann, P., Nachpolykondensation von Polyethylenterephthalat in fester Phase, *Acta Polym.*, **32**, 250–256 (1981).
34. Tang, Z., Goa, Q., Huang, N. and Sironi, C., Solid-state polycondensation of poly(ethylene terephthalate): kinetics and Mechanism, *J. Appl. Polym. Sci.*, **57**, 473–485 (1995).
35. Devotta, I. and Mashelkar, R. A., Modelling of polyethylene terephthalate reactors – X. A comprehensive model for a solid-state polycondensation process, *Chem. Eng. Sci.*, **48**, 1859–1867 (1993).
36. Bamford, C. H. and Wayne, R. P., Polymerization in the solid phase: a polycondensation reaction, *Polymer*, **10**, 661–681 (1969).
37. Culbert, B., Der Einfluss der Granulatgrösse auf die PET-SSP, *Internal Buhler Report*, DS 513 222 (1991).
38. Dröscher, M. and Wegner, G., Poly(ethylene terephthalate): a solid state condensation process, *Polymer*, **19**, 43–47 (1978).

39. Duh, B., Method for production of a high molecular weight polyester prepared from a prepolymer polyester having an optimal carboxyl content, *US Patent 4 238 593*, 1980.
40. Moore, L. D., Rule, M. and Wicker, H., Process for preparing high molecular weight polyesters, *US Patent 4 446 303*, 1984.
41. Culbert, B., Influence of CO₂ on PET-SSP, *Internal Buhler Report, No. 9790* (1992).
42. Schumann, H. D., Stand der Technologie zur Herstellung von Polyester-polymer, *Chemiefasern/Textilindustrie*, **40**, 1058–1062 (November 1990).
43. Buxbaum, L. H., Solid-state polycondensation of poly(butylene terephthalate), *J. Appl. Polym. Sci., Appl. Polym. Symp.*, **35**, 59–66 (1979).
44. Daubeney, R. de P., Bunn, C. W. and Brown, C. J., *Proc. R. Soc. London*, **A, 226**, 531 (1954).
45. Miller, R. L., Crystallographic data and melting points for various polymers, In *Polymer Handbook, 4th Edn*, Wiley-Interscience, New York, pp. VI42–VI43, 1999.
46. Schultz, J. M. and Fakirov, S., *Solid State Behaviour of Polyesters and Polyamides*, Prentice Hall, New Jersey, 1990, pp. 78–79.
47. Lin, S. and Koenig, J., The transitions and melting behaviour of thermally crystallized poly(ethylene terephthalate) and their correlations with FTIR and density measurements, *J. Polym. Sci., Polym. Symp. Ed.*, **71**, 121–135 (1984).
48. Alfonso, G. C., Pedemonte, E. and Ponzetti, L., Mechanism of densification and crystal perfection of poly(ethylene terephthalate), *Polymer*, **20**, 104–111 (1979).
49. Patkar, M. and Jabarin, S. A., Effect of diethylene glycol (DEG) on the crystallization behaviour of poly(ethylene terephthalate) (PET), *J. Appl. Polym. Sci.*, **47**, 1749–1763 (1993).
50. Takeda, H., Ehara, M., Sakai, Y. and Choi., Thermal crystallization of poly(ethylene terephthalate) and its copolyesters: effect of degree of polymerization and copolymerized components, *Textile Res. J.*, **61**, 429–432 (1991).
51. Sakellarides, S. L., The effect of isophthalic acid modification on the thermal crystallization of PET, *ANTEC*, **96**, 938–942 (1996).
52. Chan, T. W. and Isayev, A. I. Quiescent polymer crystallization: modelling and measurements, *Polym. Eng. Sci.*, **34**, 461–471 (1994).
53. Kim, S. P. and Kim, S. C., Crystallization kinetics of poly(ethylene terephthalate): memory effect of shear history, *Polym. Eng. Sci.*, **33**, 83–91 (1993).
54. Jabarin, S. A., Crystallization kinetics of polyethylene terephthalate. I. Isothermal crystallization from the melt, *J. Appl. Polym. Sci.*, **34**, 85–96 (1987).
55. Jabarin, S. A., Crystallization kinetics of polyethylene terephthalate. II. Dynamic crystallization of PET, *J. of Appl. Polym. Sci.*, **34**, 97–102 (1987).

56. Jabarin, S. A., Crystallization kinetics of polyethylene terephthalate. III. Effect of moisture content on the crystallization behaviour of PET from the glassy state, *J. Appl. Polym. Sci.*, **34**, 103–108 (1987).
57. Asano, T., Dzeick-Pickuth, A. and Zachman, H. G., Influence of catalysts on the rate of crystallization and on the crystal distortions in poly(ethylene terephthalate), *J. Mater. Sci.*, **24**, 1967–1973 (1989).
58. Tant, M. R. and Culberson, W. T., Effect of molecular weight on spherulite growth rate of poly(ethylene terephthalate) via real-time small angle light scattering, *Polym. Eng. Sci.*, **33**, 1152–1156 (1993).
59. Imai, M., Kaji, K. and Kanaya, T., Structural formation of poly(ethylene terephthalate) during the induction period of crystallization. 3. Evolution of density fluctuations to lamellar crystal, *Macromolecules*, **27**, 7103–7108 (1994).
60. Rao, M. V. S. and Dweltz, N. E., Influence of molecular weight on the ordered state in poly(ethylene terephthalate), *J. of Appl. Polym. Sci.*, **31**, 1239–1249 (1986).
61. Cobbs, W. H. and Burton, R. L., Crystallization of polyethylene Terephthalate, *J. Polym. Sci.*, **10**, 275–290 (1953).
62. Richard, D. P., Weitz, E., Ouderkirk, A. J. and Dunn, D. S., Infrared depth profiling studies of recrystallization in laser-amorphized poly(ethylene terephthalate), *J. Phys. Chem.*, **97**, 12061–12066 (1993).
63. Wunderlich, B., *Macromolecular Physics, Crystal Nucleation, Growth, Annealing*, Academic Press, New York, 1976, pp. 1–70.
64. Nakamura, K., Wantanabe, T., Katayama, K. and Amano, T., *J. Appl. Polym. Sci.*, **16**, 1077 (1972).
65. Verhoyen, O., Dupret, F. and Legras, R., Isothermal and non-isothermal crystallization kinetics of polyethylene terephthalate: mathematical modeling and experimental measurement, *Polym. Eng. Sci.*, **38**, 1592–1610 (1998).
66. Schultz, J. M. and Fakirov, S., *Solid State Behaviour of Polyesters and Polyamides*, Prentice Hall, New Jersey, 1990, pp. 95–97.
67. Jog, J. P., Crystallization of polyethyleneterephthalate, *Rev. Macromol. Chem. Phys.*, **C35** 531–553 (1995).
68. Wunderlich, B., *Macromolecular Physics*, Vol. 2, Crystal Nucleation, Growth, Annealing, Academic Press, New York, 1976, p. 243.
69. Magill, J. H., Rates of crystallization of polymers In *Polymer Handbook*, 4th Edn, Wiley-Interscience, New York, 1999, VI373–VI375.
70. Lee, C. H., Saito, H. and Inoue, T., Time-resolved light scattering studies on the early stages of crystallization in poly(ethylene terephthalate), *Macromolecules*, **26**, 6566–6569 (1993).
71. Van Antwerpen, F., *J. Polym. Sci., Polym. Phys. Ed.*, **10**, 2423 (1972).
72. Magill, J. H., Rates of crystallization of polymers, In *Polymer Handbook*, 4th Edn, Wiley-Interscience, New York, 1999, pp. VI327–VI328.

73. Zachman, H. G. and Stuart, H. A., Haupt – und Nachkristallisation von Terylen aus dem Glaszustand, *Makromol. Chem.*, **41**, 131–147 (1960).
74. Guenther, B., *Einfluss der Molmassenverteilung und der Katalystaren auf die Kristallisation und Orientierbarkeit von Polyethylenterephthalat*, *Doctoral Thesis, University of Hamburg* (1983).
75. Di Fiore, C., Leone, C., De Rosa, G., Petraccone, V., Dino, G., Bianchi, R. and Vosa, R., Influence of the antimony catalyst remnants on the melt crystallization of PET, *J. Appl. Polym. Sci.*, **48**, 1997–2001 (1993).
76. Gächter, R. and Mueller, H., *Taschenbuch der Kunststoff-Additive*, Carl Hanser VERLAG, Muenchen, 1989, p. 900.
77. Weinhold, S., The Effect of absorbed water on the crystallization rate of PET from the glass, presentation given at the *Polyester 97 World Congress*, Maack Business Services, 8804 Au/near Zurich, 3–5 November, 1997.
78. Elenga, R., Seguela, R. and Rietsch, F., Thermal and mechanical behaviour of crystalline poly(ethylene terephthalate): effects of high temperature annealing and tensile drawing, *Polymer*, **32**, 11, 1975–1981 (1991).
79. Leu, S. H. and McCarthy, S., The effect of crystallization conditions on the multiple melting peaks of melt-crystallized PET, *ANTEC*, **90**, 1000–1007 (1990).
80. Boulanger, P., Pireaux, J. J., Verbist, J. J. and Delhalle, J., XPS study of polymer chain conformation in amorphous and crystalline poly(ethylene terephthalate) samples, *J. Electron Spectrosc. Rel. Phenom.*, **63**, 53–73 (1993).
81. Fontaine, F., Ledent, J., Groeninckx, G. and Reynaers, H., Morphology and melting behaviour of semi-crystalline poly(ethylene terephthalate): 3. Quantification of crystal perfection and crystallinity, *Polymer*, **23**, 185–191 (1982).
82. Wunderlich, B., *Macromolecular Physics*, Vol. 3, *Crystal Melting*, Academic Press, New York, 1980, p. 183.
83. Dröschner, M. and Schmidt, F. G., The kinetics of the ester-interchange reaction of polyethylene terephthalate, *Polym. Bull.*, **4**, 261–266 (1981).
84. Thiele, U., PET–resin production experience: constant quality for bottle making, presentation given at the *Polyester 98 World Congress*, Maack Business Services, 8804 Au/near Zurich, Switzerland, 2–4 December, 1998.
85. Duh, B., Process for the production of high molecular weight polyester, *Eur. Patent EP 0 085 643*, 1983.
86. Culbert, B., The influence of drying on IV loss, *Internal Buhler Laboratory Report, No. P-4364*, 1994.
87. Fakirov, S., Chemical healing in poly(ethylene terephthalate), *J. Poly. Sci., Polym. Phys. Ed.*, **22**, 2095–2104 (1984).
88. Binsack, R., *Thermoplastische polyester*, In *Technische Thermoplaste*, Hanser Verlag, Muenchen, 1992, p. 18.

89. Aleman, J. V., Thermodynamic properties of poly(butylene terephthalate), *Angew. Makromol. Chem.*, **133**, 141–146 (1985).
90. Kim, J. K., Nichols, M. E. and Robertson, R. E., The annealing and thermal analysis of poly(butylene terephthalate), *J. Polym. Sci., Polym. Phys.*, Ed., **32**, 887–899 (1994).
91. Hall, I. H. and Pass, M. G., *Polymer*, **18**, 825 (1976).
92. Takokoro, H., *Structure of Crystalline Polymers*, Wiley, New York, 1979, pp. 393–394.
93. Vieweg, R. and Goerden, L., *Kunststoff-Handbuch, Vol. VIII Polyester*, Carl Hanser Verlag, Muenchen, 1973.
94. Borer, C., PBT-SSP Laboratory Test, *Internal Buhler Report*, Uzwil, 2000.
95. Dinse, H. D. and Tucek, E., Untersuchungen zur Festphasen von Polyte-tramethylenterephthalat, *Acta Polym.*, **31**, 108–110 (1980).
96. Dekker, M., *Polym. Proc. Eng.*, **4**, 303 (1986).
97. Gostoli, C., Pilati, F., Sarti, G. C. and Di Giacomo, B., Chemical kinetics and diffusion in poly(butylene terephthalate) solid-state polycondensation: experiments and theory, *J Appl. Polym. Sci.*, **29**, 2873–2887 (1984).
98. Amoco Chemical Company, Preparation of poly(ethylene 2,6-naphthalate) PEN, Pamphlet GTSR-A, Amoco Chemical Company, Chicago, IL, May 1, 1984.
99. Buchner, S., Wiswe, D. and Zachman, H. G., Kinetics of crystallization and melting behaviour of poly(ethylene naphthalene-2,6-dicarboxylate), *Polymer*, **30**, 480–488 (1989).
100. Amoco Chemical Company, PEN properties, Pamphlet GTSR-B, Amoco Chemical Company, Chicago, IL, July 15, 1984.
101. Culbert, B., Crystallization and drying of PEN, *Internal Buhler Report*, No. 514 605, 1994.
102. Duh, B., Process for the crystallization of polyethylene naphthalate, *US Patent 4 963 644*, 1990.
103. Amoco Chemical Company, Extending the use of polyesters in packaging, Bulletin FA-13b, Amoco Chemical Company, Chicago, IL, April 1994.
104. Kaegi, W., Grundlagenversuche mit PEN Polyester, *Internal Buhler Report*, No. 513 203, 1990.
105. Gugumus, F., Autoxidation von Kunststoffen, In *Taschenbuch der Kunststoff-Additive*, 3rd Edn, Carl Hanser Verlag, Muenchen, 1989, pp. 3–25.
106. Kurata, M. and Tsunashima, Y., Molecular weight relationships and unperturbed dimensions of linear chain molecules, In *Polym. Handbook*, 4th Edn, Wiley-Interscience, New York, 1999, p. VII–35.
107. Jabarin, S. A. and Balduff, D. C., Gel permeation chromatography of polyethylene terephthalate, *J. Liq. Chromatogr.*, **5**, 1825–1845 (1982).
108. PETCORE, *Collecting and Sorting Plastic Bottles*, 2000 Edn, PPS Recovery Systems, Ltd, Peterborough, UK, 2000, Chs 9–14, 30–106.

109. Noone, A., *PET Recycling, Europe, Supply and Demand Report*, 4th Edn, PET Packaging Resin and Recycling, Ltd, PCI, Derby, UK, 1999, Section 2.
110. Noone, A., *PET Recycling, The Americas, Supply and Demand Report* 3rd Edn, PET Packaging, Resin and Recycling, Ltd, PCI, Derby, UK, 1998, Section 1.
111. Papaspyrides, C. D., Recycling plastics, *The Polymeric Encyclopedia* (on CD-Rom), Salomone J. C. (Ed.), CRC Press. Boca Raton, FL, 1996.
112. PETCORE, *Collecting and Sorting Plastic Bottles*, 2000 Edn, PPS Recovery Systems, Ltd, Peterborough, UK, 2000, Ch. 22, pp. 191–200.
113. NAPCOR, National Association for PET Container Resources, [http://www.napcor.com/learn], March 2001.
114. PETCORE, PET Recycling Europe, [http://www.petcore.org/envir-recprod-01.html], March, 2001.
115. APME, Plastics recycling in perspective, [http://www.apme.org], August, 2000.
116. Japon, S., Leterrier, Y. and Manson, J.-A., Increasing the melt viscosities of a polyester resin, *World Patent WO 00 29 470*, 1999.
117. Bärlocher, K. and Henzi, M., Systemanalyse der PET-Flaschen Bewirtschaftung, *Diplomarbeit Abt. VIII/ETH Zurich WS 98/99, Studienrichtung Umweltingenieur*, 1999, pp. E7–E18.
118. Van Erden, D., Vadnais, G. L., Enriquez, M. C., Adams, K. G. and Nelson, J. P., Solid state polymerization of PET, *Eur. Patent Application EP 0 856 537 A2*, 1997.
119. Deiringer, G., Process for reclaiming thermally strained polyester scrap material, *US Patent 5 225 130*, Claim 12, 1991.
120. Balint, L. J., Abos, R. L., and Snider, O. E., Process for crystallization, drying and solid state polymerization of polyesters, *US Patent 3 544 525*, 1968.
121. Näf, U., Labor Kristallisation und SSP von PET Flakes, *Internal Buhler Report, No. 515 590*, 1997.
122. Robinson, W. D., and Vadnais, G. L., Solid state polymerization of PET flakes, *Eur. Patent Application EP 0 994 146 A1*, 1999.
123. Kabitz, M., Solid-stating of post-consumer PET, *Internal Buhler Report, No. 516 670*, 1997.
124. Nichols, C. S., and Moore, C., Food quality polyester recycling, *US Patent 5 876 644*, 1996.
125. Torres, N., Robin, J. J. and Boutevin, B., Study of thermal and mechanical properties of virgin and recycled poly(ethylene terephthalate) before and after injection moulding, *Eur. Polym. J.*, **36**, 2075–2080 (2000).
126. Bärlocher, K. and Henzi, M., Systemanalyse der PET-Flaschen Bewirtschaftung, *Diplomarbeit Abt. VIII/ETH Zurich WS 98/99, Studienrichtung Umweltingenieur*, 1999, p. 42.

127. Boustead, I., *Eco Profiles of the European Plastics Industry: Polyethylene Terephthalate*, APME, Brussels, Revised September 2002, [<http://www.apme.org>].
128. Christel, A., Closed loop bottle-to-bottle recycling, *Nova-Pack Europe 2000 Düsseldorf/Neuss*, Schotland Business Research, Inc., Skillman, NJ, September 2000, p. 273.
129. Noone, A., *PET Recycling, Europe, Supply and Demand Report*, PET Packaging, Resin and Recycling, Ltd, PCI, Derby, UK, 1999, Section 7.
130. Flexon, F. D., Schmalbach-Lubeca's recyclable beer bottle program, *Nova-Pack Europe 1999 Düsseldorf/Neuss*, Schotland Business Research, Inc., Skillman, NJ, September 1999.
131. Latinen, G. A., Devolatilization of viscous polymer systems, *Adv. Chem. Ser.*, **34**, 238, (1962).
132. Castle, L., de Kruijf, N., Franz, R., Gilbet, J. and Rossi, L., Recycling of plastics for food contact use, Guidelines prepared under the responsibility of the International Life Science Institute (ILSI) European Packaging Material Task Force, Washington, DC, 1998.
133. Points to consider for the use of recycled plastics in food packaging: Chemistry considerations, US Food and Drug Administration, Center for Food Safety and Applied Nutrition, [<http://vm.cfsan.fda.gov/~dms/opa-cg3b.html>], December, 1992.
134. Welle, F. and Franz, R., PET recyclate for food packaging, in *Proceedings of the R 99 World Congress*, Geneva, Switzerland, February, 1999, EMPA, St Gallen, Switzerland, 1999, Vol. 3, pp. 514–517.
135. US Food and Drug Administration, Center for Food Safety and Applied Nutrition, [<http://vm.cfsan.fda.gov/~dms/opa-recy.html>], Revised February 2002.
136. Franz, R., Recycled Poly(ethylene terephthalate) for direct food contact application, FDA submission CTS 71903, Petitioner Buhler A. G, *Representative Laboratory: Fraunhofer Institute for Process Engineering and Packaging*, Freising, Germany, Petition to the FDA, 2000.

Solid-State Polycondensation of Polyester Resins: Fundamentals and Industrial Production

W. GÖLTNER

Mönchesweg 18, Bad Hersfeld, Germany

1 INTRODUCTION

Since Flory's discovery of polyamide synthesis in the solid state to obtain high molecular weights [1], the use of this technology in the manufacture of polyesters has become very popular. Most attention has been given to this class of polymers due to commercial reasons. Based on early experiences with chemical reactions in the solid state and later on with polyamides, the solid-state polycondensation (SSP) of polyesters became the method of choice to produce high-molecular-weight polymers, as required for bottles, sheets, engineering plastics or the manufacturing of industrial yarns.

Mechanical properties such as tenacity or fatigue behavior are mainly influenced by the molecular weight of the polymer. The production of conventional fibers for textile applications and films requires polymers with a degree of polymerization (DP) of ~ 100 . Polymers for these application have number-average molecular weights (M_n s) in the region of 15 kg/mol. Commonly, in the case of polyesters the intrinsic viscosity (IV) is a measure of the chain length of the polymer. Poly(ethylene terephthalate) (PET) with a DP of 100 (corresponding to an IV of ~ 0.64 dl/g) is used for conventional textile or film applications. PET for more engineered products such as bottles and engineering plastics usually has an IV of 0.80 dl/g and higher. The production of industrial yarns requires material with an IV in the range of 0.85–1.0 dl/g.

Polycondensation of highly viscous polyesters in the melt phase is limited. The removal of the volatile by-products becomes more difficult due to diffusion inhibited by the increased viscosity of higher-IV polyesters. In addition, undesirable side reactions due to thermal degradation impede the growth of the molecular chains. As a consequence, the reaction rate decreases and decomposition reactions dominate, thus resulting in a decrease in the melt viscosity [2]. As it is able to address these limitations, SSP has become the method of choice and is therefore so popular.

This development was driven additionally by the growing market for PET bottles and the demand for co-polyesters which cannot be produced in the desired IV range by melt polycondensation. In addition, certain co-monomers require more gentle reaction conditions, which are fulfilled in SSP. Therefore, this technology is the preferred route for producing high-quality polyesters of high molecular weight.

SSP can be carried out batchwise or continuously, either *in vacuo* or supported by an inert gas flow. Another variation of SSP is the so-called suspension process in the swollen state, which allows for the production of extremely high-molecular-weight polyesters [3]. This technology is more of academic interest than for commercial application since it requires complete removal of the high-boiling suspending oils.

The continuous process is appropriate for the large-scale production of polyesters used in bottle manufacture. Currently, reactors with capacities of more than 600 t/d have been employed. The discontinuous technology based on tumble dryers allows for the successful production of specialities on a smaller scale, particularly for engineering plastics and with respect to the fiber industry. This route is preferred due to its flexibility, simple process control and the excellent quality of the final product. It is, however, restricted by the volume of the reactors, which is generally limited to 44 m³.

The SSP process allows polycondensation under gentle conditions to obtain the desired high molecular weights and excellent polymer quality for various applications. It can be successfully introduced for the production of sensitive co-polyesters as well as for the recovery of polyester waste.

This present chapter will review the industrial relevance of the SSP process. In general, the representative production of PET is discussed, although the process can be used as a general example. Wherever particular differences are required for the production of other co-polyesters, these will be indicated.

2 PRINCIPLES

The method of increasing the molecular weights of polyesters via SSP was first developed in the 1950s. Numerous studies have been devoted to this process in order to provide deeper insight into its mechanism [4–8]. Many publications

deal with the effect of a simplified reaction mechanism on the influence of very specific parameters in the reaction but at present no completely satisfactory model has yet been developed for SSP and melt-phase polycondensation (MPPC). Only in a few cases are the reports based on considerations regarding a model of the reaction. Some of these models or assumptions cannot conclusively explain certain effects, for instance, the different disappearance rates of the carboxylic end groups (CEGs) and the hydroxyl (OH) groups, or the drop in molecular weight at long reaction times. A satisfactory explanation for the fact that MPPC and SSP show comparable reaction rates has not yet been found [4]. Two factors make the kinetics of polycondensation more complicated for PET, namely:

- the number of side reactions resulting in degradation
- the role of the ethylene glycol (EG) by-product

It is therefore the aim of this chapter not to dwell on theoretical considerations in any great detail. For those interested in such aspects, further details can be found in the text by Pilati [9].

2.1 ASPECTS OF MOLTEN-STATE POLYCONDENSATION

The understanding of the SSP process is based on the mechanism of polyester synthesis. Polycondensation in the molten (melt) state (MPPC) is a chemical equilibrium reaction governed by classical kinetic and thermodynamic parameters. Rapid removal of volatile side products as well as the influence of temperature, time and catalysts are of essential importance. In the later stages of polycondensation, the increase in the degree of polymerization (DP) is restricted by the diffusion of volatile reaction products. Additionally, competing reactions such as inter- and intramolecular esterification and transesterification put a limit to the DP (Figure 5.1).

Other possible side reactions, e.g. acidolysis, glycolysis or esterolysis, cause chain scission, and these can also lead to a lower DP. Only a few of these reactions, namely polyesterification and polytransesterification (I and II in Figure 5.1), accompanied by the liberation of water and EG, respectively, contribute to the growth of the chain [5]. Transesterification (III) causes no net effect on the molecular weight distribution. The importance of the redistribution steps is well known, although less attention has been paid to the second stage of MPPC where cyclization reactions affect the polydispersity and the quantity of cyclic compounds produced [10]. As a consequence of the high reaction temperature and the reversibility of the reactions, thermal degradation is often observed in the melt (Figure 5.2). Degradation is an irreversible reaction, accompanied by the generation of side products such as acetaldehyde (AA), CO₂, 2-methyloxolane, ethylene glycol and water, along with an increase of carboxylic end groups and vinyl ester groups (IV and V in Figure 5.1). Therefore, in order to minimize the

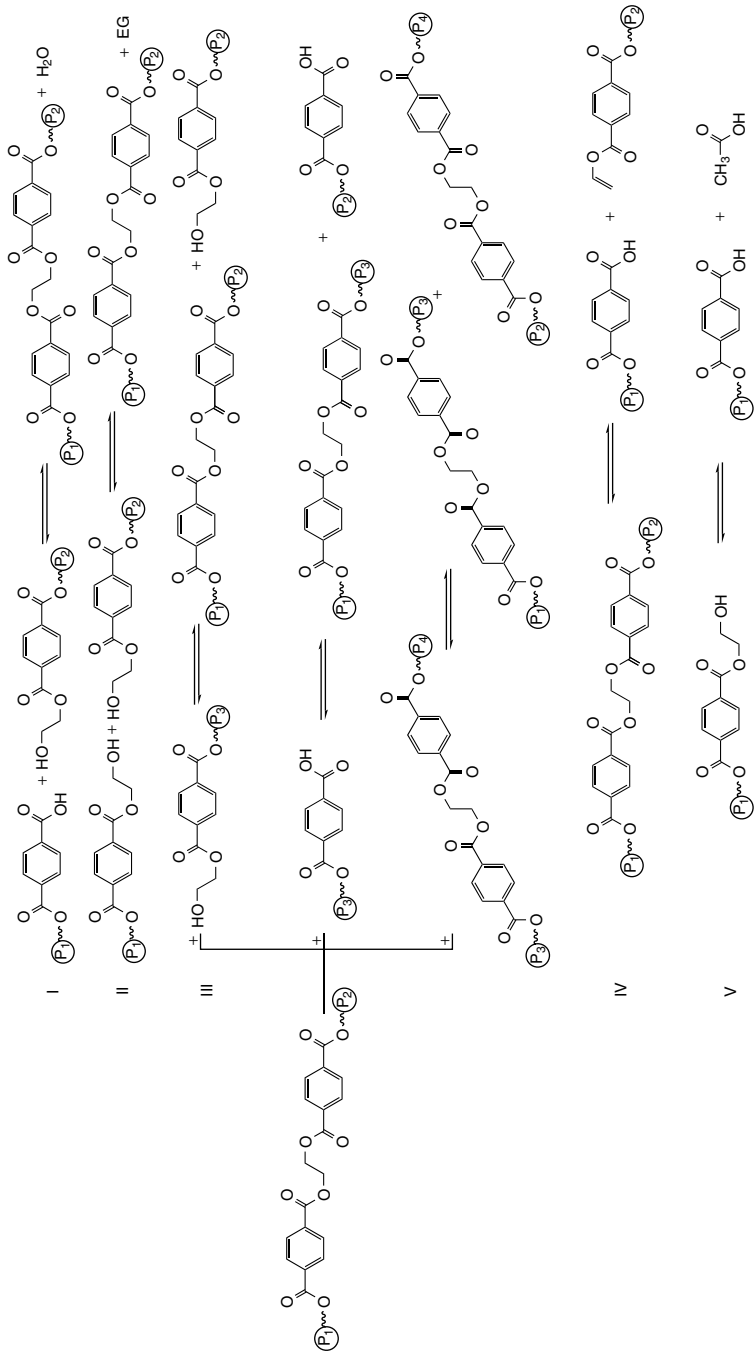


Figure 5.1 Reaction mechanism for the synthesis of polyesters (e.g. poly (ethylene terephthalate)) via molten (melt)-state polycondensation

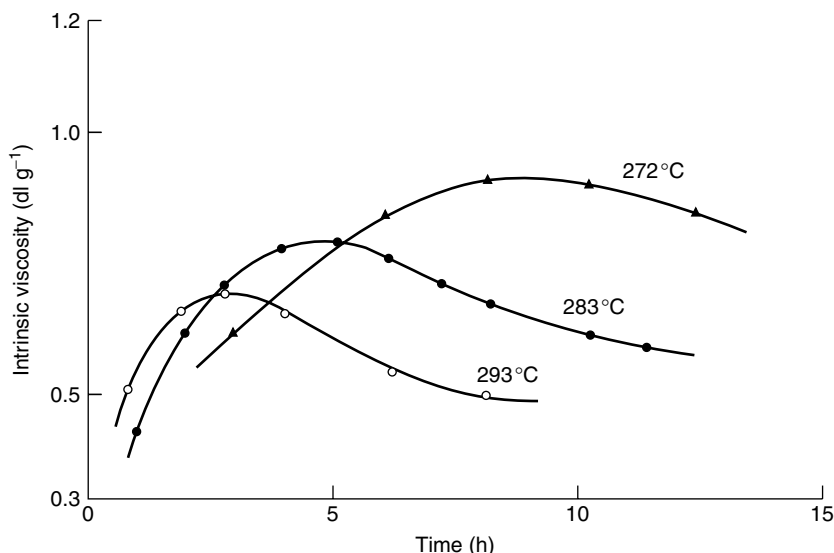


Figure 5.2 Effect of temperature on the molten (melt)-state polycondensation process for PET [15(b)]. Reprinted from *Polymer*, **14**, Tomita, K., *Polymer* **14**, 50 (1973), (see references) Copyright (1973), with permission from Elsevier Science

amount of degraded polymer, melt polycondensation should be completed before the onset of these phenomena.

Up until now, most efforts to attain high-molecular-weight and high-quality polyesters via melt-phase polycondensation have failed. Efficient agitation of the viscous melt, using the principles of thin film evaporation or highly sophisticated reactors, have not overcome the problems of thermal degradation with its negative consequences on quality. In addition, it should be noted that adhering of the viscous melt to the heated walls of the reactors diminishes the filterability of the polymer, with correspondingly severe consequences on subsequent processing.

2.2 ASPECTS OF SOLID-STATE POLYCONDENSATION

According to the principles of polycondensation, all of the above reactions will also take place during SSP. The conditions for the latter, however, are different as this process is carried out at lower temperatures in a non-homogeneous environment. In order to examine the kinetics of SSP, some assumptions have to be made to simplify the analysis. These are based on the idea that the reactive end groups and the catalyst are located in the amorphous regions. Polycondensations in the solid state are equilibrium reactions but are complicated by the two-phase character of the semicrystalline polymer.

To obtain high molecular weights, as expressed by the IV, the removal of the volatile, low-molecular-weight by-products is necessary to shift the equilibrium towards the formation of polymer. The rate of the polycondensation can be determined by measuring the level of end groups or by the amount of evaporated ethylene glycol (EG). Assuming a second-order reaction, the reaction rate is given by the following:

$$\frac{dE}{dt} = k(E_0 - E)^2 = kE^2$$

where E_0 is the concentration of initial end groups, E is the concentration of final end groups, and k is the rate constant for polycondensation (equal to the slope of a plot of E against t , which should be linear).

During the studies carried out on this process some unusual behavior has been observed. Such results have led some authors to the conclusion that SSP is a diffusion-controlled reaction. Despite this fact, the kinetics of SSP also depend on catalyst, temperature and time. In the later stages of polymerization, and particularly in the case of large particle sizes, diffusion becomes dominant, with the result that the removal of reaction products such as EG, water and acetaldehyde is controlled by the physics of mass transport in the solid state. This transport process is itself dependent on particle size, density, crystal structure, surface conditions and desorption of the reaction products.

According to various experimental studies on the solid-state reaction of PET it has been reported that at particle sizes of 80–100 mesh and SSP temperatures between 170 and 200 °C, end group diffusion is limited, whereas at 14–16 mesh particle size and 210–240 °C the ester-interchanging process is EG-diffusion controlled. The esterification depends predominantly on end group diffusion due to the increased diffusion rate of water [11]. The existing knowledge of the reaction kinetics allows an explanation of some of the factors affecting the course of the reaction, as well as a number of predictions and calculations for engineering purposes. A model has been developed based on theoretical considerations [12], and the test results for this correlate well with the rules of kinetics and thermodynamics. Based on these findings, theoretical understanding of the process can be achieved to a certain extent.

2.3 PHYSICAL ASPECTS

2.3.1 The Removal of Side Products

The removal of side products such as EG, AA, CO₂, water and oligomers is controlled by the physics of mass transport in the solid state. This mechanism correlates with particle size, density, crystallinity, crystal structure and perfection, and surface conditions, as well as the desorption of the reaction products from

the particle surfaces. Therefore, one has to distinguish between diffusion through the solid particles and evaporation assisted by vacuum or gas flow. In the case of large particles, a different reaction behavior can be observed owing to the decreased rate of diffusion. The fast removal of the volatile reaction products plays the most important role in shifting the equilibrium towards the formation of polymer. SSP can be carried out either *in vacuo* or assisted by the flow of inert gases, preferably nitrogen. The fast removal of the reaction products therefore depends on the applied pressure or the flow rate of the employed inert gas. According to Figure 5.3 [13], which shows the dependence of the number-average molecular weight (and respectively the IV) on the gas flow rate, the effect of increasing the latter is greatest at lower rates of flow. However, after a flow rate of 500 ml/min is reached, no further change is seen. No significant difference between the vacuum and gas flow methods could be observed.

However, when different gases are employed, differences in activities can then be seen [14]:



It can be assumed that this is caused by a kind of 'plasticizing' of the polymer by dissolved or finely dispersed gas or by the increased solubility of the reaction products in the gases.

Publisher's Note:

Permission to reproduce this image online was not granted by the copyright holder. Readers are kindly requested to refer to the printed version of this chapter.

Figure 5.3 Effect of nitrogen gas flow rate on the solid-state polycondensation process for PET: reaction conditions, 259 °C for 7 h: initial M_n , 16 500, with a particle size of 0.18–0.25 mm; data obtained by gas chromatographic analysis, employing a column of dimensions 8 ft × 0.75 in o.d. [5]. Reproduced from Hsu, L.-C., *J. Macromol. Sci., Phys.*, **B1**, 801 (1967), with permission from Marcel Dekker

2.3.2 Temperature

Besides the pressure (vacuum) and the flow rate of the gas, temperature is the major experimental variable in SSP and is of the highest importance for the economy of the process. Temperature dependence data for the solid-state polycondensation process are shown in Figures 5.4–5.7. According to the results

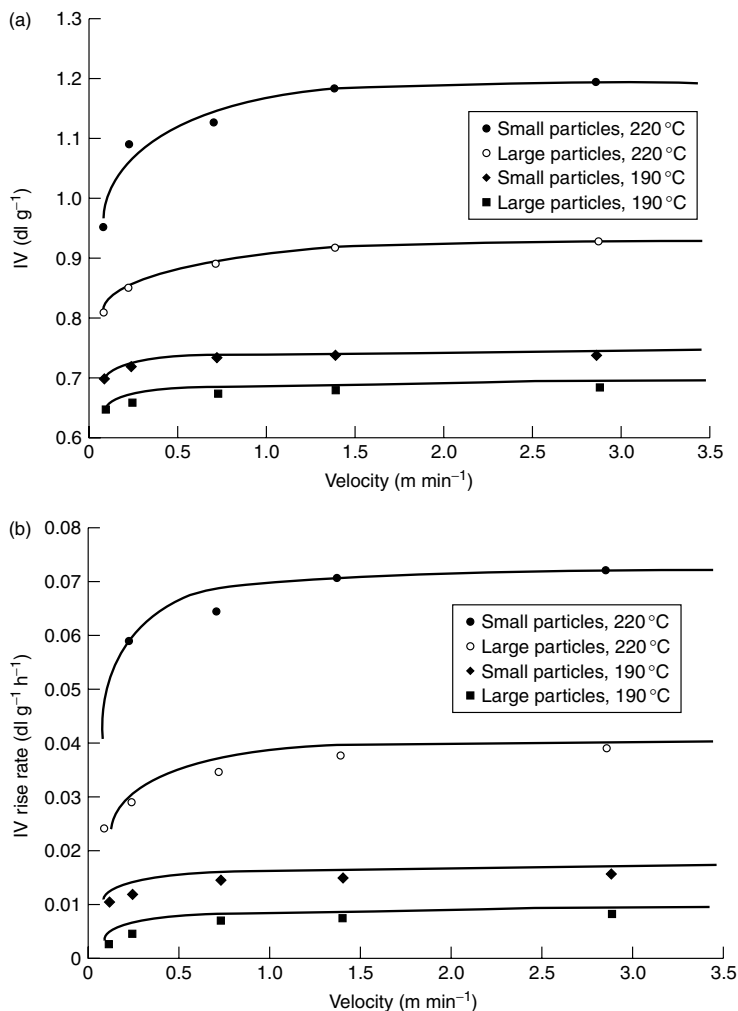


Figure 5.4 Effect of gas flow rate on (a) the SSP reaction rate of PET at temperatures of 190 and 220 °C, and (b) the rate of increase of the intrinsic viscosity of PET at various temperatures [13]. Reprinted from *Polymer*, **39**, Huang, B. and Walsh, J. J., Solid-phase polymerization mechanism of poly(ethylene terephthalate) affected by gas flow velocity and particle size, 6991–6999, Copyright (1998), with permission from Elsevier Science

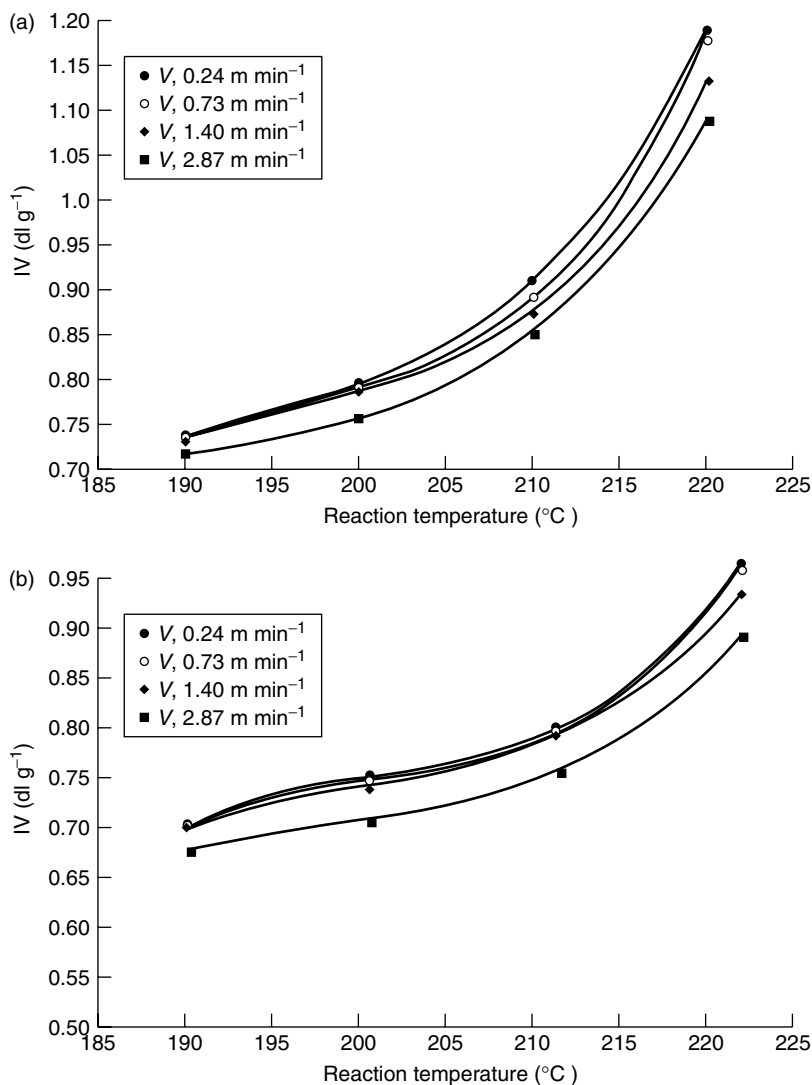


Figure 5.5 Effect of temperature on the SSP reaction rate for (a) small, and (b) large chips of PET [13]. Reprinted from *Polymer*, **39**, Huang, B. and Walsh, J. J., Solid-phase polymerization mechanism of poly(ethylene terephthalate) affected by gas flow velocity and particle size, 6991–6999, Copyright (1998), with permission from Elsevier Science

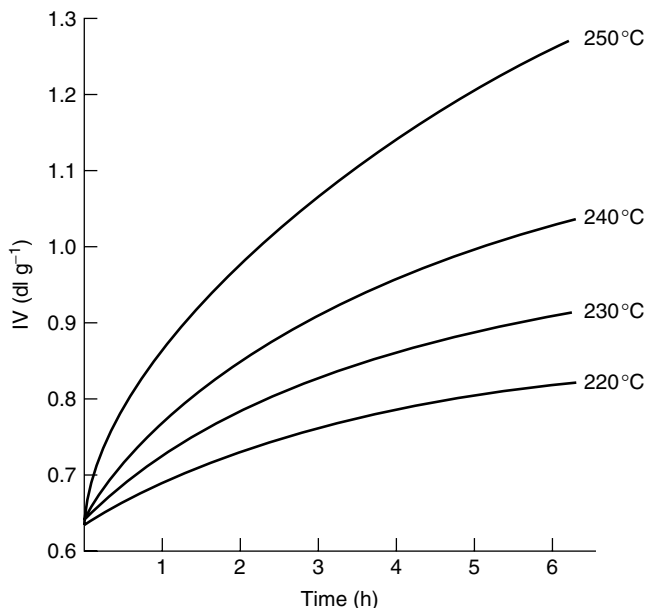


Figure 5.6 Intrinsic viscosity as a function of time at various solid-state temperatures (under a nitrogen purge at a rate of 1 l/min) [8]. From Jabarin, S. A. and Lofgren, E. A., *J. Appl. Polym. Sci.*, **28**, 5315 (1983), Copyright © John Wiley & Sons, Inc., 1983. Reprinted by permission of John Wiley & Sons, Inc.

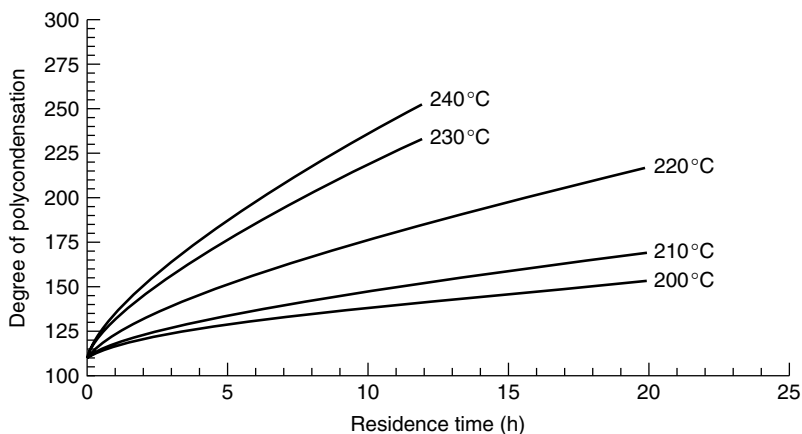


Figure 5.7 Degree of polycondensation as a function of retention time and temperature [12b]. From Weger, F., Solid-state postcondensation of polyesters and polyamides, presentation given at the *Frankl and Thomas Polymer Seminar*, 16 June, 1994, Greenville, SC, USA, and reproduced with permission of EMS Inventa-Fischer, GmbH & Co. KG

obtained under reaction conditions when the temperature is raised from 200 to 240 °C, the degree of polymerization (DP) increases by 64 %, while the residence time decreases by about 40 %. The increased reactivity is due to the reaction kinetics and the increased diffusivity caused by the elevated temperature. Little effect is seen from thermal degradation under these reaction conditions.

For those readers requiring further information on the factors effecting the kinetic versus diffusion control of the SSP process, this has been reported by several authors (for example, kinetic aspects [4, 8, 20] and diffusion-influenced aspects [5–7, 9, 11–13, 15]).

A model for the SSP of PET under typical industrial processing conditions has been developed by Ravindrath and Mashelkar [15]. Their calculations are also based on experimental data reported in the literature. The results allow the ‘rough’ conclusion that the reaction rate decreases by a factor of 6 for the temperature range between 285 and 220 °C, accompanied by a decrease of the thermal degradation by a factor of 40. The fact that suitable SSP conditions can be found to warrant a fast reaction rate and minimal degradation makes this process industrially important. These same authors also state that at an early stage of the reaction the kinetics have a predominant influence, whereas diffusivity plays a major part at a later stage of the reaction.

It has been reported that the molecular weight correlates with the square root of the reaction time for both the catalyzed (Figure 5.8 [8] and uncatalyzed SSP process [8, 16], in accordance with the theory of Flory [2a].

2.3.3 Reactivity

The use of catalysts is essential for SSP, and in particular catalysts are necessary in the SSP process for obtaining high-molecular-weight polyesters [17]. Any type of catalyst commonly used in MPPC also show reactivity in SSP as long as the reaction temperature allows chain growth. The reactivity depends on the catalyst employed for the production of the prepolymer. In addition, the catalysts influence the reaction rates more than the crystallinity. The content of carboxylic groups apparently has an accelerating effect on the SSP process, which may correlate with the presence of such groups in the diffusion-dependent later stages of the process [18].

The influence of the ratio of hydroxylic/carboxylic end groups has been studied by several research groups. In the case of PET, this varies, based on the assumed mechanism over the range of 1.5–4.5:1. For poly(butylene terephthalate) (PBT) and poly(ethylene naphthalate) (PEN), the optimum is indicated at 2.0:1 [19, 20]. Any deviation from this ratio affects the reaction rate.

2.3.4 Diffusivity

Many papers deal with the diffusivity of side products, as well as the contribution to the course of SSP. Polycondensation as the primary reaction obeys kinetic rules

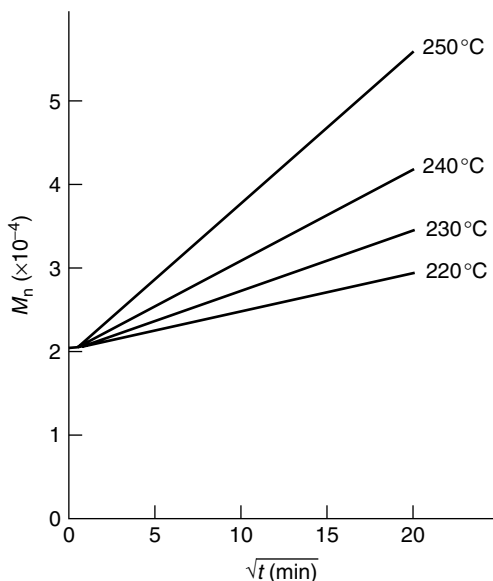


Figure 5.8 Molecular weight as a function of the square root of time at various solid-state temperatures (under a nitrogen purge at a rate of 1 l/min) [8]. From Jabarin, S. A. and Lofgren, E. A., *J. Appl. Polym. Sci.*, **28**, 5315 (1983), Copyright © John Wiley & Sons, Inc., 1983. Reprinted by permission of John Wiley & Sons, Inc.

and depends on catalysts, temperature, etc. Removal of the reaction products such as EG, acetaldehyde (AA), water and oligomers is controlled by mass transport in the solid state and is affected by diffusion. This corresponds with particle size, density, crystal structure and perfection, surface conditions, and the desorption of the reaction products. In particular for the case of large particles, a different reaction behavior can be observed owing to the effects of diffusion. The particle size, in combination with the crystallinity, is the main factor in these observations. Obviously, crystallinity and density lower the diffusion rate and correlate with the mobility of the reactive end groups which are concentrated in the amorphous regions. It should be pointed out that the crystal size and the surface structure may influence the desorption of the side products. Figure 5.9 illustrates the influence of crystallization temperature on density and molecular weight during SSP. These results have been confirmed by the work of Chang *et al.* [7].

2.3.5 Particle Size

This phenomenon can be easily investigated by ‘peeling’ the polyester chips or by casting films of specific thickness and subsequent determination of the intrinsic viscosity in such layers [9].

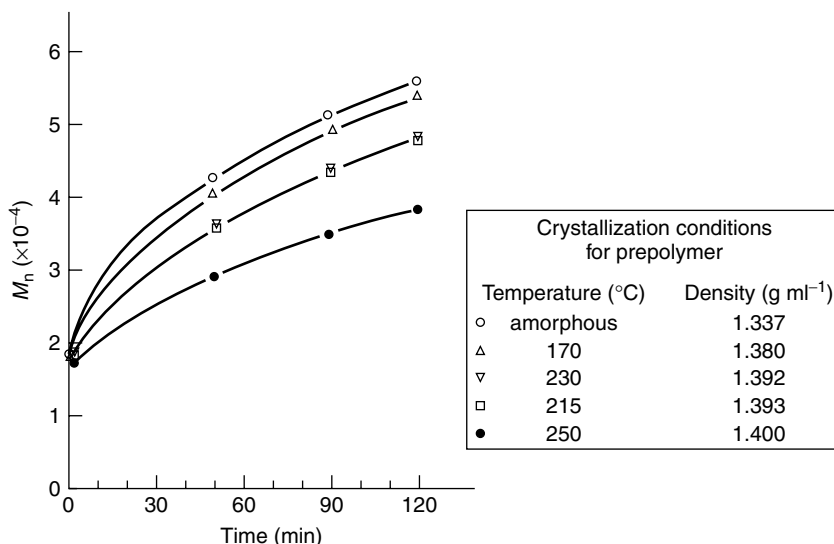


Figure 5.9 Effect of crystallinity on the solid-state polycondensation of PET, shown as the number-average molecular weight as a function of time. Conditions: fluidized bed polymerization at 230 °C; particle size, 35–48 mesh; superficial velocity of nitrogen, 43 cm/s [6]. From Chang, T. M., *Polym. Eng. Sci.*, **10**, 364 (1970), and reproduced with permission of the Society of Plastics Engineers

Figure 5.10 shows the distribution of IV across the diameter of PBT chips after peeling off consecutive layers.

In addition to these results, Hagen calculated the IV distribution across the thickness of a cylindrical particle of PET (Figure 5.11) based on the above-mentioned model [12]. The reaction takes place in the outer (10–15 %) regions of the pellet film diameter where the shortest diffusion pathways occur. The core area, in contrast, exhibits only a slightly increased and evenly distributed IV during the first 6 of SSP. This figure shows the gradient of the IV across the diameter of the chips. The results are in good agreement with the experimental data obtained for PBT and show the importance of diffusion on the progress of SSP in polyesters. This accordance also allows certain speculations regarding the polydispersity of the polymer, which can be roughly calculated based on these results.

Furthermore, the dependence of IV on the particle size confirms the (industrial) tendency to reduce the size of the chips in order to improve the manufacturing economics. This approach shortens the reaction time, and improves the quality and the cost of the process.

Huang has reported the effect of diffusion on the SSP rate as a function of particle size and reaction conditions [13]. One has to distinguish between the

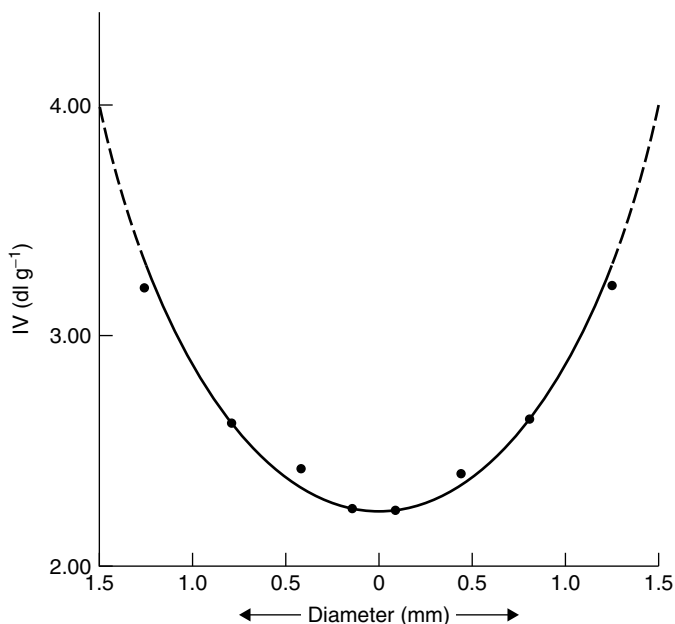


Figure 5.10 Intrinsic viscosity gradient within one PBT particle [30a]. From Buxbaum, L. H., *J. Appl. Polym. Sci., Appl. Polym. Symp.*, **35**, 59 (1979), Copyright © John Wiley & Sons, Inc., 1979. Reprinted by permission of John Wiley & Sons, Inc.

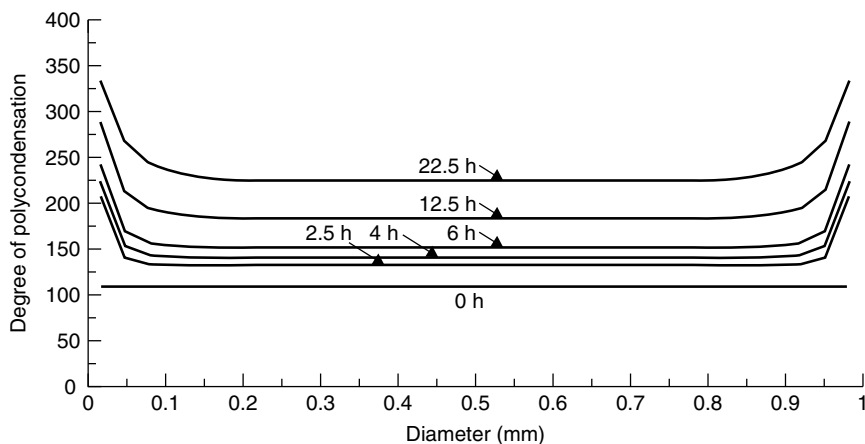


Figure 5.11 Calculated degree of polycondensation related to the axis of PET chips, shown as axial profiles for a cylindrical particle: T , 220 °C; hydraulic diameter (d_h), 2.9 mm [12b]. From Weger, F., Solid-state postcondensation of polyesters and polyamides, presentation given at the Frankl and Thomas Polymer Seminar, 16 June, 1994, Greenville, SC, USA, and reproduced with permission of EMS Inventa-Fischer, GmbH & Co. KG

internal diffusion of the volatile side products to the surfaces of the chips and the diffusion of the volatiles, and their removal, from the surface, either under gas flow or *in vacuo* conditions.

Therefore, SSP is governed by several mechanisms, including the following:

- the chemical reaction
- diffusion within the chip
- diffusion at the surface of the chip

Each step is influenced by the reaction conditions. According to the results, SSP is principally influenced by the chemical reaction; however, the size of the chips, the gas flow rate and the temperature also have strong effects on the intrinsic viscosity. In the case of temperatures $<200^{\circ}\text{C}$, SSP is controlled by the chemical reaction. At 190°C and with sufficiently high gas flow rates, surface diffusion can be neglected. The diffusivity increases with elevated temperature. Consequently, an increased side-product concentration, associated with enhanced surface diffusion, can be observed, particularly at low gas flow rates. Therefore, the internal diffusion of the volatiles to the surface becomes more important. Additionally, a smaller particle size tends to lead to increased SSP rates at higher temperatures. The required increased gas flow rate results in an increased gas-side mass-transfer coefficient as an indication of the desorption mechanism. It can be concluded that SSP of small particles at low temperatures is kinetically controlled, while at higher temperatures and low gas flow rates the reaction is diffusion controlled. This changes again in the case of a high concentration of side products at the particle surfaces. Figures 5.4 and 5.5, along with the data presented in Table 5.1, show the independence of side-product diffusion at lowered temperatures and gas flow rates with respect to the reaction rate. The latter is mostly dependent on the particle size. Increased reaction temperatures result in a raised concentration of by-products on the particle surfaces. This leads, in conjunction with a smaller particle size at a given gas flow rate, to an increased gas-side resistance. A enhanced flow rate is necessary to increase the

Table 5.1 Characterization of samples (cf. Figures 5.4 and 5.5) [13]. Reprinted from *Polymer*, **39**, Huang, B. and Walsh, J. J., Solid-phase polymerization mechanism of poly (ethylene terephthalate) affected by gas flow velocity and particle size, 6991–6999, Copyright (1998), with permission from Elsevier Science

Publisher's Note:

Permission to reproduce this image online was not granted by the copyright holder. Readers are kindly requested to refer to the printed version of this chapter.

concentration of the by-products in the gas phase, which thus results in a higher gas-side mass-transfer coefficient [13, 15]. The SSP of large particles is therefore internal-diffusion controlled and becomes surface-diffusion controlled at reduced gas flow rates [13]. Gas-side resistance will reduce the reaction rate of the SSP in the case of smaller chip sizes due to the increased concentration of sorbed reaction products at the surfaces.

2.3.6 Polydispersity

Controversial results are reported in the literature regarding the polydispersity of polyesters produced by SSP, associated with the side reactions in the later stages of the reaction. These are not only dependent on the concentrations of the reactive groups but also on their intramolecular distances [11]. Additionally, it has been found that cyclization leads to a different polydispersity. According to theoretical considerations, the polydispersity index of an SSP polymer is generally higher than that of prepolymer produced in the melt phase, which should, in an ideal case have a value of 2 [21–24, 59].

Considerations about SSP and its complex mechanism suggest an increased polydispersity index, as discussed by Pilati [9]. These expectations have been confirmed by this present author's unpublished results concerning SSP in the suspended (swollen) state to attain high-molecular-weight PET. According to these results, the polydispersity increases with the reaction time and the degree of swelling, where the latter depends on the properties of the fluid being employed.

2.3.7 Crystallinity

Much work has been devoted to the crystallization phenomena due to its great influence on the mass-transport mechanism. Due to such studies, an improved understanding of the effects related to any kind of crystallization has resulted: however, many questions regarding the influence of the surface structure on the desorption behavior of the low-molecular-weight volatile side products remain still unanswered. Crystallinity and density affect the diffusion rate and therefore the mobility of the end groups. According to recent suggestions, the reactive (mobile) chain ends are concentrated in the amorphous regions. It should be pointed out that the crystal size and the surface structure may also influence the desorption of the side products [15]. Therefore, for their removal an extremely reduced pressure or a high flow rate of nitrogen is necessary. The removal of the side products via gas flow also depends on gas-side resistance or desorption phenomena which have not yet been fully investigated. The gas-side mass-transfer coefficient increases with the flow rate but this does not explain the increased reaction rate in the case of CO₂ or helium [14].

Crystallization is a time-dependent phenomenon [25, 26]. Therefore, the increase of crystallinity during SSP reduces the reaction rate due to the hindered

mobility and diffusion of the end groups (see Figure 5.9). The increase of crystallinity, expressed by the density, as a function of time and temperature is shown in Figure 5.12. As can be seen from this figure, the curves become nearly flat after steep increases at the beginning.

The rate of crystallization, expressed by the inverse half-time of crystallization, depends on several different factors, including the temperature, the degree of modification by a co-monomer, the IV and the content of nucleants in the polymer. Any type of solid heterogeneity content functions as a nucleating agent [25, 26]. These particles can be catalyst residues or other additives, or in particular solids generated by undesirable reaction conditions during the prepolymer process, such as gels, degraded insoluble polymer from 'dead spaces' or adhered particles from the walls of the reactors or pipes. Table 5.2 shows the influence of co-monomer content, e.g. diethylene glycol (DEG), on the crystallization rate and induction time, which decrease with increased content in the polyester. In principle, these results are confirmed by the hot crystallization behavior of this kind of co-polymer (Figure 5.13). The decreased crystallization rate of co-polyesters with DEG as the modifying component can be explained by the increased content of irregularities in the structure of PET [27–29].

The crystallization is reduced by an increasing molecular weight of the intrinsic viscosity due to the decreased mobility of the polymer chains. Shorter chains

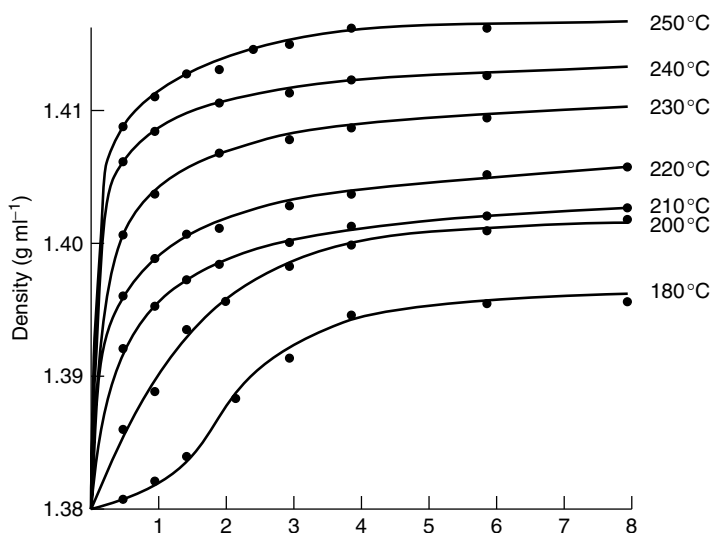


Figure 5.12 Density as a function of temperature and time during SSP [26]. From Wick, G., Characterization of PET polymer for bottle manufacturing, presentation given at the *Society of Plastics Engineers Benelux Seminar*, 20–21 May, 1980, Amsterdam, and reproduced with permission of KoSa GmbH & Co. KG

Table 5.2 Half-times and induction times (in min) for different PET samples when crystallized isothermally from the melt [26]. From Wick, G., Characterization of PET polymer for bottle manufacturing, presentation given at the *Society of Plastics Engineers Benelux Seminar*, 20–21 May, 1980, Amsterdam, and reproduced with permission of KoSa GmbH & Co. KG

Temperature (°C)	1.4 % DEG		2.08 % DEG		2.94 % DEG	
	t_{ind}	$t_{0.5}$	t_{ind}	$t_{0.5}$	t_{ind}	$t_{0.5}$
210.0	0.8	3.4	0.9	3.8	1.2	6.1
212.5	0.9	4.2	1.1	4.5	1.8	8.0
215.0	1.2	5.3	1.4	5.6	2.2	11.0
217.5	1.5	6.3	2.0	8.9	3.2	14.5
220.0	1.8	8.7	2.3	11.9	3.9	18.1
222.5	2.6	10.9	4.0	17.2	–	–

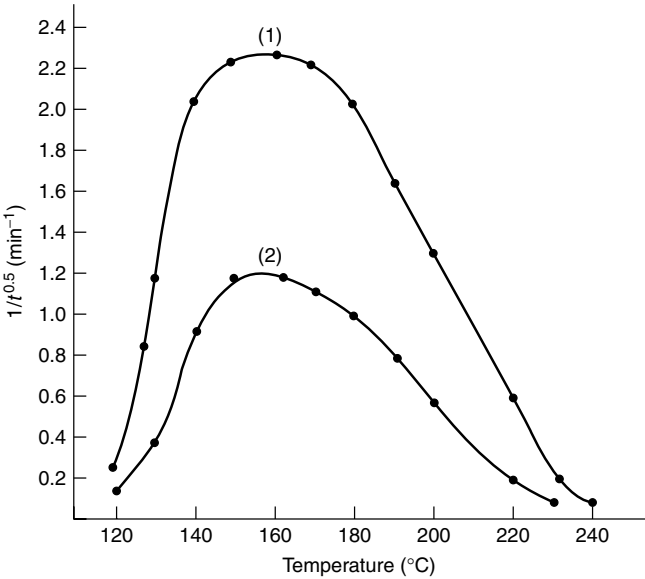


Figure 5.13 Hot crystallization rate as a function of temperature during SSP: (1) polymer with 1.28 % DEG; (2) polymer with 3.90 % DEG [26]. From Wick, G., Characterization of PET polymer for bottle manufacturing, presentation given at the *Society of Plastics Engineers Benelux Seminar*, 20–21 May, 1980, Amsterdam, and reproduced with permission of KoSa GmbH & Co. KG

result in an increased mobility and therefore in increased crystallization rates. Figure 5.14 displays the relationship between the IV and the half-time of hot crystallization.

It should be pointed out that the crystal size and the surface structure may also affect the desorption of side products. The development of crystallinity

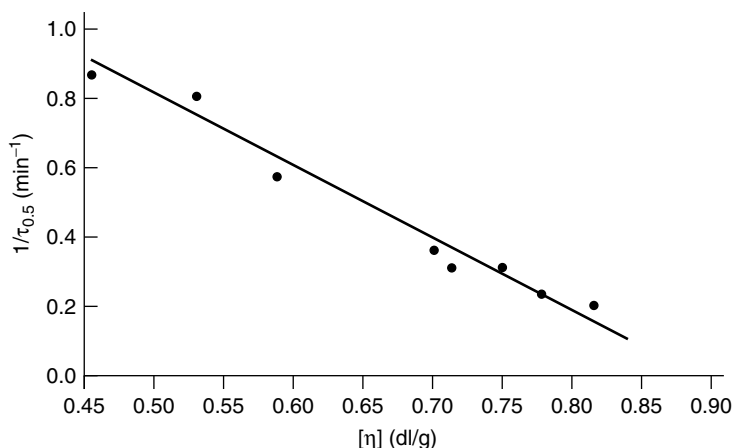


Figure 5.14 Hot crystallization rate as a function of intrinsic viscosity during SSP: T , 220 °C [26]. From Wick, G., Characterization of PET polymer for bottle manufacturing, presentation given at the *Society of Plastics Engineers Benelux Seminar*, 20–21 May, 1980, Amsterdam, and reproduced with permission of KoSa GmbH & Co. KG

during SSP affects the reaction rate, which is related to a reduced diffusivity, as can be seen in Figure 5.9. Higher crystallization temperatures lead to increased crystallinity and therefore a reduced SSP rate. Lower crystallization temperatures (<195 °C) are therefore preferred.

2.4 OTHER POLYESTERS

The above-mentioned results of the SSP of PET can be generally applied to other semicrystalline polyesters, such as poly(butylene terephthalate) (PBT), poly(trimethylene terephthalate) (PTT), poly(ethylene naphthalate) (PEN) or any other kind of semicrystalline co-polyester, as a result of their similar reaction behaviors. Most of the studies have been focused on PET and PBT due to their industrial importance. Meanwhile, the popularity of PEN is growing on account of the outstanding properties of this particular polymer.

The SSP process is obviously limited by the melting point of the prepolymer and the equilibrium temperature of the polymer process. The SSP reaction becomes too slow at temperatures below 190 °C in commercial processing. Temperatures below this level are only of scientific interest or applicable in the case of thermally sensitive polyesters. The increase in IV for the most common polyesters decreases in relation to the glycolic component, as shown in Figure 5.15; however, this figure does not show the behavior of cyclohexane dimethanol (CHDM) and PEN [30].

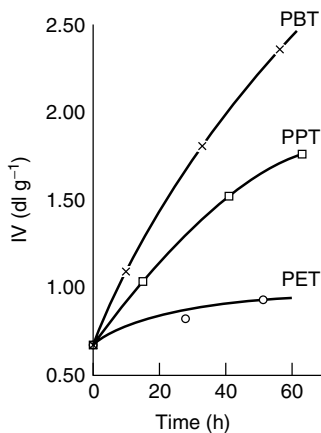
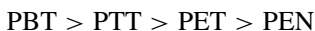


Figure 5.15 Solid-state polycondensation of various polyesters at 215 °C and 0.1 mbar: x, poly(butylene terephthalate) (PBT); □, poly(propylene terephthalate) (PPT); o, poly(ethylene terephthalate) (PET) [30a]. From Buxbaum, L. H., *J. Appl. Polym. Sci., Appl. Polym. Symp.*, **35**, 59 (1979), Copyright © John Wiley & Sons, Inc., 1979. Reprinted by permission of John Wiley & Sons, Inc.

If PEN is included in the above, the trend would be as follows:



According to reports Po' *et al.* [31] and Amoco [32], the reaction rate of PEN is lower than other polyesters. Considerations about this fact lead to the assumption that the structure-dependent reactivities of the acid and glycol components and their mobilities are responsible for the individual reaction rates of these polymers. Based on unpublished data, rigid or voluminous co-monomers result in reduced reactivities during melt polycondensation and SSP. The mobility of the component, as a result of its structure and stiffness, seems to explain this observation.

Differences in the behavior of these polymers can also be explained by the affects of reaction temperature, crystallization rate and the nature of the side products. PET and PBT behave similarly in chain-growing reactions during SSP but differently with respect to degradation. For PET, the degradation is of a more complex nature and can result in the formation of carboxylic end groups (CEGs) vinyl ester groups, and various other products such as AA, water, 2-methyloxolane, etc. This is due mainly to thermal decomposition of the ester linkage. PBT degrades, via the intramolecular cyclization of terminal 4-hydroxybutyl ester units, at an increased rate when compared to PET. Each chain scission results in the formation of two carboxylic groups and tetrahydrofuran in the case of PBT. Due to the increased rate of thermal degradation, an

autocatalytic mechanism, due to the carboxylic end groups, may be assumed. This is also the reason for keeping the ratio of hydroxylic/carboxylic groups at 2:1 in the case of PBT.

The studies of Pilati and co-workers [33] deal particularly with the SSP reaction of PBT. Their results give new and important insights into a more detailed understanding of the reaction and lead to the development of a new model, which seems to be generally valid for the SSP process. Such a model is based on various assumptions. The most important one concerns the locations of the reactive end groups and the catalyst in the amorphous regions. This model is also based on a consideration of five relevant chemical reactions and the diffusion of three side products. Calculations have been carried out by using equilibrium constant data obtained from the literature and the diffusion coefficients of butanediol, water and terephthalic acid. These calculations correlate very well with the experimental results. The model is also applicable to PET and allows predictions of the influence of certain reaction parameters, e.g. the OH/CEG ratio, particle size and temperature in the case of PBT, to the reactivity of the system. This basic knowledge of the principles of SSP is valid for many types of polyester production. Differences regarding the reactivity could be observed in the case of PEN or other special co-polyesters.

Summarizing these results, it can be concluded that for PET the SSP reaction is a rate- and diffusion-controlled process whose physical aspects change with increased particle size and reaction time. Differentiation between the reactions which occur provides a better understanding of the SSP process. Based on this knowledge, calculations and predictions for engineering purposes thus become possible.

3 EQUIPMENT

The following provides a description of the engineering principles of SSP technology and some aspects and considerations regarding processing and improving the economics of the process. The background of the technological development is characterized by a growing patent literature base. In detail, this is aimed at heat transfer, prevention of sticking and improvements of homogenous conditions, all of which lead to improved quality. The SSP process *in vacuo* is carried out mainly *discontinuously* in tumble dryers, double-cone dryers, rotary dryers or paddle dryers, whereas the *continuous* SSP of PET or PBT in a nitrogen stream can be carried out in production lines with capacities of more than 600 t/d. The discontinuous process is restricted by the reactor volumes, which normally vary between 20 and 44 m³. This process is limited to the production of smaller-scale specialities, although it is also applied to recovering waste polymer.

3.1 BATCH PROCESS

In principle, the equipment consists of a heat-jacketed reactor, a vacuum source and a heating station (Figure 5.16) [34]. The reactor contains inserts such as heating plates or pin-like tubes to improve the heat transfer and to homogenize the polymer chips during reaction. In the case of plates, these inserts have the additional function of 'chambering' the unique volume and may help to reduce sticking of the polymer. The reactor is actuated by two hollow shafts, which simultaneously circulate the heat-transfer medium and remove the vapors. These hollow shafts can be used additionally for feeding certain additives into the reactor. Heating and cooling occur via the jacket in connection with the inserts.

To shorten the residence time, the reactor should be connected to a separate intermediate tank in which the cooling of the polymer takes place after the SSP process is complete. The reactor can be equipped with a precrystallizer and a dryer. In this way, the reactor can be charged with hot, crystalline polymer, which saves energy, prevents sticking to the reactor walls and reduces the reaction time. Any type of high-efficiency dryer can be used. Fluidized bed crystallizers are preferred, although agitated crystallizers are also used in some production plants. The disadvantage of the latter devices is the increased formation of dust. Some manufacturers store the crystallized and dried chips in an intermediate hopper from which the reactor is charged. The connecting pipe between the reactor and vacuum system should be fitted with separators to protect the pumps from dust and from oligomers which evaporate during the reaction. These deposits can have a negative effect on the process due to potential blocking of the vacuum system.

To provide the vacuum, any type of conventional equipment can be used, as there are also steam jets, or preferably appropriate pumps, which are well able to attain a pressure of 0.2 mbar in the reactor. The preferred systems contain a fluid ring pump to provide the pre-vacuum and a small as well as a larger rotary pump. Mixed systems consisting of a rotary pump and a rotary vane pump are also available. Mechanical pumps should have facilities for flushing and draining. The removal of oligomers and other by-products is chiefly carried out by flushing with ethylene glycol. The pumps are assembled in stands, while the vacuum is controlled by closing with nitrogen or mechanically via the rate of pump rotation.

The heating and cooling system ensures rapid heating and cooling of the heat-transfer medium. The installation of additional intermediate silos for cooling the final polymer shortens the residence time of the polymer in the reactor and helps to increase its capacity.

The feed silo for the prepolymer, located at the top level of the plant, allows the reactor to be filled via gravity. Finally, a blending silo is needed to maintain a homogenous and constant quality with respect to the intrinsic viscosity of the product.

The new generation of vacuum reactors are linked with the docking systems via telescopic pipes to the silos. This allows automatic charging and discharging

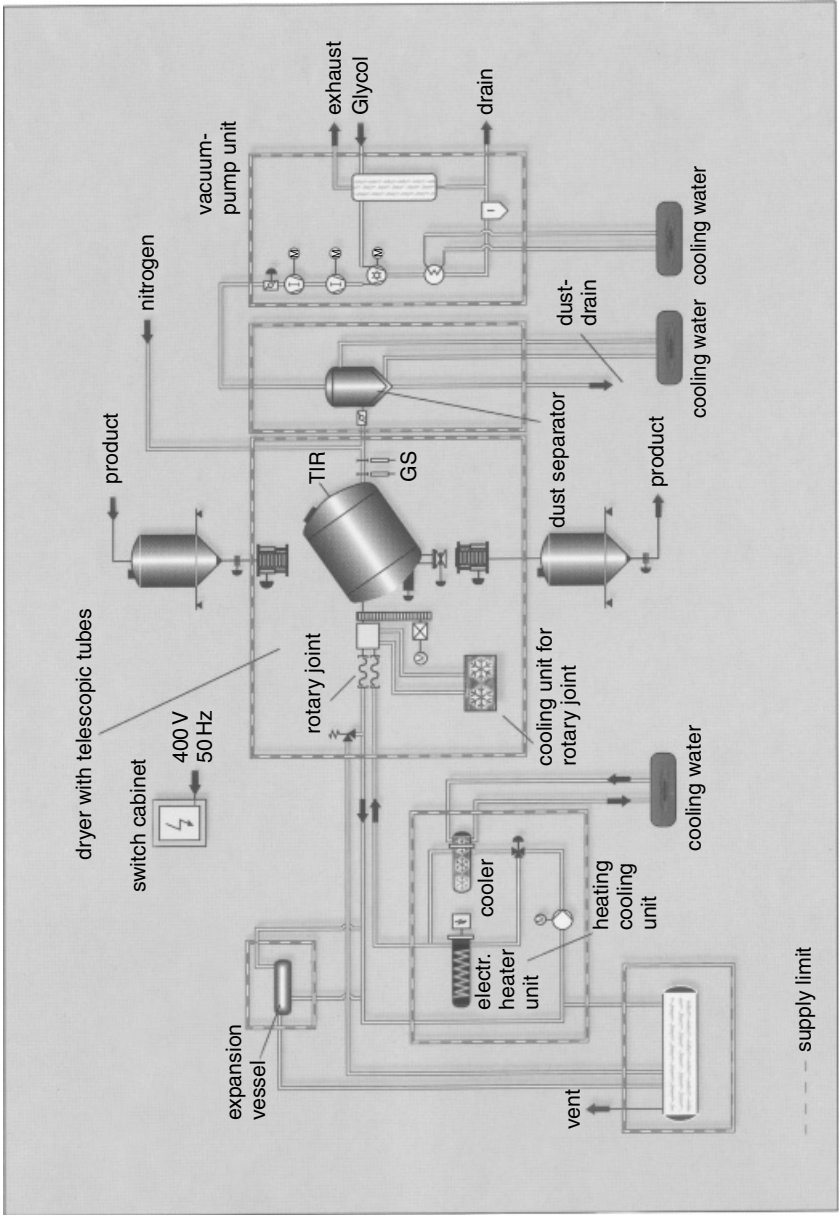


Figure 5.16 Layout of an SSP batch process reactor [34]. From manufacturer's literature published by OHL Apparatabau and Verfahrenstechnik, Limburg, Germany, and reproduced with permission

of the reactors, automatic conveying and avoids leaks, as well as reducing the extensive manual work previously required. The reactors are also equipped with samplers for process control. These systems improve the competitiveness due to the high degree of automation, as well as providing savings in energy and labor costs, thus allowing the conversion of this batch process into a continuous one.

3.2 CONTINUOUS PROCESS

The technology for this process is in principle similar to that applied in the batch process (Figure 5.17) [12, 35]. In this case, however, the devices for precrystallizing and drying have to be designed for higher throughput. The crystalline chips are conveyed into the SSP reactor and treated with a flow of hot nitrogen in counter-flow fashion. The reactor, in principle a column dryer, is heat-jacketed to prevent heat loss and a resulting temperature gradient from the center to the peripheral parts. The plug flow of the chips is a crucial feature, resulting in a narrow retention time distribution. The piston flow of the gas aims at a uniform gas distribution. There are reactors with an agitated zone in their upper levels to avoid sticking in the case of insufficient crystallization. Inserts in the reactor improve the homogeneity of the reaction conditions. The reactor can be equipped with samplers for process control. A level control in the reactor aids in reducing the pressure applied to the chips and avoids sticking, as well as improving the flexibility in situations where the throughput is changed.

Unavoidable loss of gas is compensated via a feed valve for supplying virgin nitrogen into the circulation pipe. The exhaust gas of the process has to be bypassed for purification. After the separation of dust by a filter, the gas is heated to 400°C for the catalytic combustion of the side products. The gas is then cooled down, and the excess oxygen is catalytically converted to water by using hydrogen. For economic reasons, the gas flow will recover the heat via a heat exchanger and then be cooled down by a gas cooler.

A special gas-tight air blower passes the nitrogen through a filter containing molecular sieves for drying purposes. The purified nitrogen stream (with the lowest dew point) is used to cool the final polymer to 60°C and recover a large proportion of the heat. An additional dust separator removes dust from the gas prior to feeding into the reactor. This emphasizes the importance of dust separation in the SSP process and the resulting quality of the chips.

The final dust removal takes place in the cooling hopper. Just below the outlet cone, a gas-tight discharge conveying system controls the throughput of the reactor. The cooling of chips to ca. 60°C is achieved in a hopper in counter-flowing nitrogen. The latter is fed directly to the gas circuit of the reactor from the cooling hopper. The equipment is characterized by a maximum of 'tightness', particularly for the rotary valves, air blowers and the chips-conveying system.

The heating of the gas stream is commonly carried out by using hot oil. The molecular sieves used for drying the nitrogen stream have to be changed

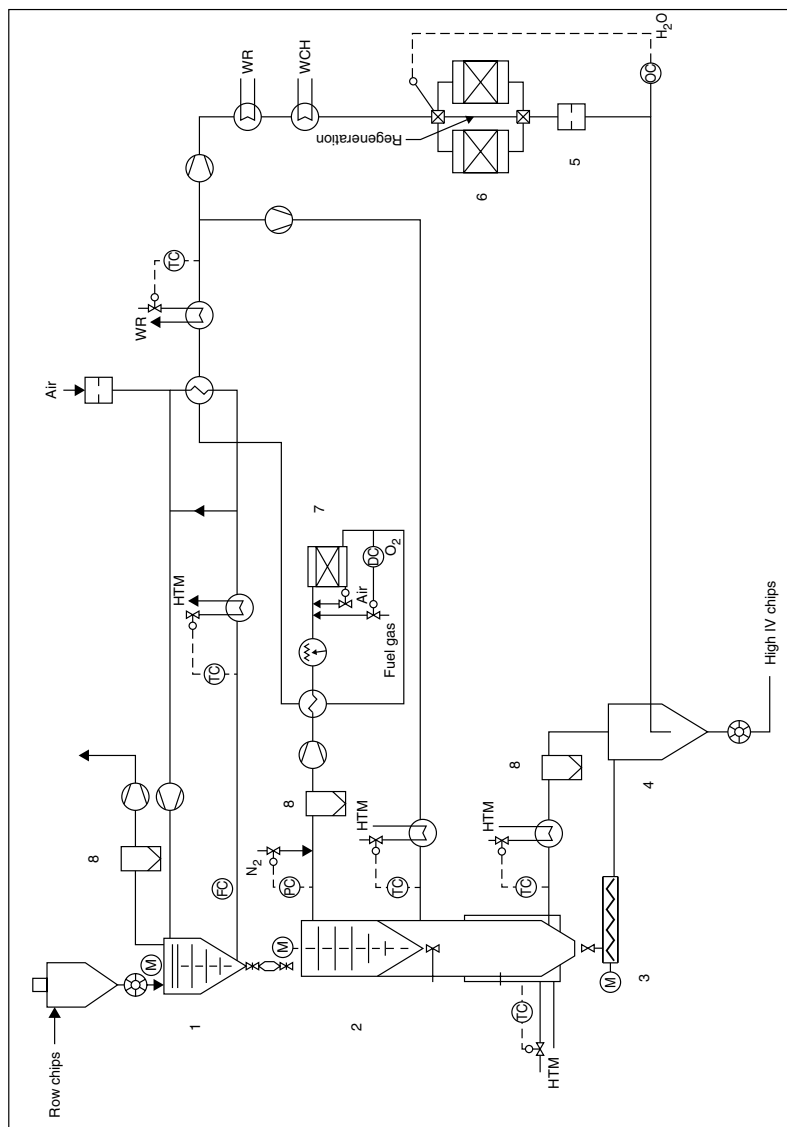


Figure 5.17 Layout of an SSP continuous process reactor: 1, dryer; 2, reactor; 3, screw feeder; 4, cooling tank; 5, filter; 6, dryer (molecular sieve); 7, combustion unit; 8, dust separator; FC, flow controller; HTM, high-temperature medium; M, motor (screw, agitator, etc.); OC, oxygen control; PC, pressure controller; TC, temperature controller; WCH, chilled water cooling; WR, cooling water [12b, 35]. From Weger, F., Solid-state postcondensation of polyesters and polyamides, presentation given at the *Frankl and Thomas Polymer Seminar*, June 16, 1994, Greenville, SC, USA, and reproduced with permission of EMS Inventa-Fischer, GmbH & Co. KG

periodically for regeneration. In principle, this same equipment can be used for the SSP of PEN and PBT. It should be emphasized, however, that in the latter case the use of a crystallizer is not necessary due to the high crystallization rate of this polymer. PBT is also relatively insensitive to oxygen. Therefore, nitrogen of a lower purity can be employed for the gas flow.

The growing demand for bottle-grade PET chips has led to engineering companies developing highly efficient equipment, allowing increased throughput without causing sticking problems. The improved 'tightness' of the blowing systems has also reduced the nitrogen loss, and therefore the manufacturing costs. The efficient separation of dust results in a better quality of product. Some novel continuous SSP lines now guarantee capacities of 600 t/d.

Additionally, it should be noted that continuous SSP can also be carried out *in vacuo*, as reported by Buxbaum [30]. Some of the previous problems regarding the 'tightness' of the bucket wheels (rotary valves) and other parts of the equipment could be solved in the meantime; however, it seems that this technology has lost its attractiveness owing to the success of the commonly preferred gas-flow method.

3.3 SSP OF SMALL PARTICLES AND POWDERS

At the early stage of development of SSP technology, ground prepolymer in the form of powders or small particles (20–40 mesh) was used. These materials were preferably produced by grinding precrystallized chips of the prepolymer. The handling of these particles after SSP, particularly in the extrusion process, became more difficult. The SSP of these small particles can be carried out batchwise *in vacuo* or continuously by gas-flow technology in fluidized-bed polymerizing systems [36], or in horizontal or vertical column reactors. The batch reactors can be equipped with agitators to keep the powder in a fluid state. The handling of the powder is more complicated because the units tend to suffer from increased blockages depending on the filling volume of the reactors. In addition, the particles 'fly off' easily at too high a flow rate of nitrogen. The separation of fine particles causes some concerns. The fluidized bed technology is favored due to an exact control of the residence time. Otherwise, the details of the technology are the same as those for the SSP of chips. In the future, more attention may be paid to this effective technology as a means of producing high-quality polymers as are required for industrial yarn applications.

3.4 SSP IN THE SUSPENDED STATE

This discontinuous process is based on a heat-jacketed reactor equipped with an agitator, an inlet for purging nitrogen and the addition of an oil, and a cooler. A cold trap condenses and separates the oil from the gas for re-use in the reactor.

The gas is heated to the reaction temperature. The reaction is preferentially carried out by blowing inert gas into the suspension to remove side products. Their removal can also be achieved *in vacuo*. Thermally stable inert oils, such as Therm S-300 (diphenyl/diphenyl oxide (26:74)), Therm-S-600 (monoethyldiphenyl, triethyldiphenyl), Therm-S700 (diethyldiphenyl), Therm-S-800 (triethyldiphenyl), Therm-S-900 (hydrogenated terphenyl, a mixture of cyclohexyldiphenyl isomers and dicyclohexylbenzene isomers, diphenylmethane, 1,2-diphenylethane and liquid paraffin), AP 500 (phenylmethylsilicone oil) and Marlican (linear alkylbenzenes, C₉–C₁₂) have all been successfully used to suspend the PET [3]. All these liquids are characterized by a high boiling point. Differences are observed due to a partial solubility of the PET, which results in swelling of the particles. Increased reaction rates (of the intrinsic viscosity) are observed by using oils with swelling properties [3].

The oil has to be removed from the SSP product by extraction or flushing with appropriate solvents such as acetone. The degree of swelling influences abrasion and the loss of fines, as well as a certain tendency to a form of sticking or adhesion. At present, this method does not appear to have been fully commercialized.

4 PRACTICAL ASPECTS OF THE REACTION STEPS

4.1 CRYSTALLIZATION AND DRYING

This very important step significantly influences the SSP process with regard to reaction time and product quality. As mentioned previously, the crystallinity and density of the chips govern the removal of the reaction products and the diffusion of the end groups. The crystallinity increases with heating time and temperature in conjunction with the content of seeds in the prepolymer, while inversely affecting their diffusivity. Generally, the crystallization of PET (as the most interesting polyester) can be carried out in the temperature range between 120 and 190 °C. The polymer has a tendency to stick at lower temperatures and so this higher range is preferred. Crystallization has been observed in the subsequent drying step and is therefore influenced in practice by additional engineering factors.

In connection with crystallization, the phenomenon of sticking of the polymer plays a very important role. Sticking occurs by agglomeration of the chips and their adhesion at the reactor walls and can block reactors and feed pipes, so causing interruptions in the production process. The level of adhered chips reduces during the SSP process and can disappear as the result of the chips grinding against each other through the revolution of the agitator or the fluidized bed. Stuck particles can remain in the reactor system, however, and can change the homogeneity of the polymer. Sticking is influenced by a number of technical factors, such as the design of the reactor and its surface conditions, by the pressure

resulting from the filling volume of the reactor, the heating program, the size of the chips and the water content of the polymer.

It is particularly influenced by the crystallization properties of the polymer and therefore of the degree of its modification. Sticking problems are generally observed at low levels of crystallinity ($< \sim 30\%$) or from slow crystallizing of highly modified co-polyesters. The pressure of the chips against each other, caused by the weight and filling volume in connection with the design of the equipment, is a significant factor. Sticking plays a very important role in the processing of PET and at the present time is still not yet sufficiently controlled.

The phenomenon of sticking is a very severe engineering problem in SSP and indeed in any drying process. It has to be viewed in connection with crystallization and in conjunction with heat release. The equipment should be designed for a balanced heating rate and a reasonable distribution of heat release, plus a sufficient movement of the chips at a minimum pressure. Sticking occurs at the beginning of crystallization and later on in connection with the appearance of a second endothermic peak in the region of ca. 230°C in the DSC thermogram. It is influenced by the following factors, i.e. crystallization rate, crystallinity, temperature and the appearance of the pre-melting peak (first endothermic peak in the DSC thermogram) which depends on the thermal history of the chips. This peak disappears after prolonged heat treatment (Figure 5.18) [8, 37].

The pressure caused by the weight of the chips in the reactors, influenced by the filling volume, is of great importance. Therefore, high column dryers are more likely to display sticking as a result of the increased pressure caused by the weight of the chips. The degree of modification of the polymer, the particle size and shape of the chips, their crystallinity and surface structure also influence the occurrence of sticking. A combination of controlled particle shape and size as well

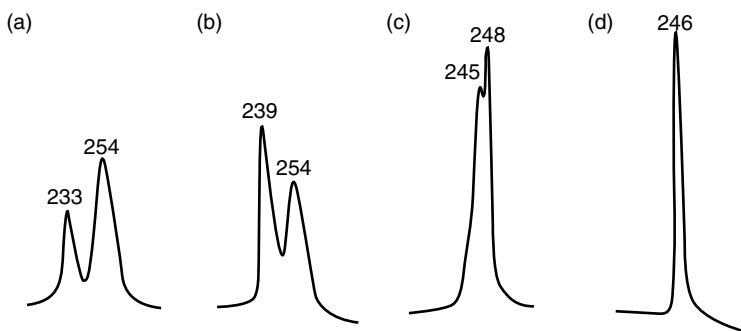


Figure 5.18 DSC endotherms obtained for samples treated in the solid state at various temperatures: (a) 200°C for 4 h; (b) 210°C for 4 h; (b) 220°C for 4 h; (d) $225\text{--}230^\circ\text{C}$ for 8 h [8]. From Jabarin, S.A. and Lofgren, E. A., *J. Appl. Polym. Sci.*, **28**, 5315 (1983), Copyright © John Wiley & Sons, Inc., 1983. Reprinted by permission of John Wiley & Sons, Inc.

as the temperature conditions, lower the tendency for sticking (Chang *et al.* [7]). These authors observed an increase in the melting point, as well as the sticking point, at increased temperatures and heating times. According to their studies, sticking depends on the premelting (first endothermic peak in the DSC trace (Figure 5.18)) in the range from 225 to 235 °C. This temperature increases with reduced oligomer content. The sticking point decreases with increasing content of co-monomer. Cubic chips tend to stick more easily due to their smooth surfaces, while cylindrical chips of short length show a lower tendency to sticking. In addition, Chang *et al.* also report on the influence of heating on the course of the SSP process, which is reduced at higher reaction temperatures [7]. A compromise has to be found regarding crystallizing conditions, reaction rate and sticking. The crystallization rate decreases with a decreased glass transition temperature (T_g) and melting point, as can be seen in Figure 5.13 above. Therefore, more care has to be taken in the case of co-polyesters, which are produced for applications such as bottles, due to their reduced crystallization rates.

Several authors have suggested various approaches for dealing with the problems associated with sticking. According to Bhatt and Filke [38], the chips have to be maintained in free-flowing conditions. The tendency to stick and the parameters influencing 'tackiness' can be analyzed by a special tester which measures the force required to break up the agglomerates. Movement of the chips by agitating in the zone of crystallization or in a fluidized bed is a very effective method for preventing sticking. A very interesting version of a crystallizer for SSP which uses a plate-shaped cutter for grinding agglomerates without the additional formation of dust has been reported [39].

Certain crystallization conditions, such as temperature, can assist in the control of sticking [18, 40]. An increase in both the melting point and sticking point in the SSP process has been observed. The heating associated with a homogenous heat flow should therefore bring the chips to the desired temperature.

It has been reported that the type of heating employed for crystallization can also have an important effect on sticking [41]. In this case, heating was carried out between 150 and 200 °C requiring (only a heating time of ca. 10 min.) A further report [42] claims that the addition of 0.5 wt% terephthalic acid to the chips also prevents sticking. The tendency to sticking can also be reduced by adding glass beads or inorganic salts such as sodium sulfate, sodium chloride or calcium nitrate to the polymer, which physically separate the chips from each other, hence reducing the likelihood of the chips becoming attached to each other [43]. Accelerated crystallization in the presence of water or ethylene glycol can also reduce the problem of sticking. This effect is not yet fully understood but can be explained by the induction of crystallization by liquids or vapors, i.e. solvent-induced crystallization [8, 16, 44]. In addition, it was found that wet chips (0.6 wt% water) crystallize nine times faster than dry material [45]. This phenomenon may be based on some kind of plasticization of the polymer. The addition of ethylene glycol has a similar effect, although this is not yet sufficiently

understood. Rapid crystallization avoids sticking under certain conditions such as low pressure on the chips resulting from their weight, in connection with the height of the equipment (crystallizer, reactor, etc.) and its diameter. Apart from optimizing the heating procedure, another way to avoid sticking is the use of a precrystallizer, which has the additional benefit of increased throughput due to the shortened heating-up phase in the reactor. This type of apparatus separates the crystallizing stage from the SSP process and shortens the residence time in the reactor. Any type of crystallizer can be used for this purpose. Fluidized-bed devices are particularly popular. Many types of tube-type crystallizers are equipped with agitators to prevent sticking. Their disadvantage is the possible formation of dust. In batch SSP processes, crystallizing and drying is commonly carried out during the heating-up phase.

The crystalline polymer must be subsequently dried in the temperature range between 150 and 200 °C, preferably 170 ± 10 °C to prevent hydrolytic degradation. Conditioned air with a dew point of at least -40 °C has been shown to produce the best results. The drying can be carried out by using either an air or nitrogen flow. The latter is more 'gentle' and minimizes the possibility of thermo-oxidative degradation. The crystallized hot chips are fed by gravity from a well-insulated storage tank into the SSP reactor. In this manner, the heat-up in the reactor can be shortened by 3–4 h. Sufficient drying requirements commonly approach 2.0–2.5 kg air/kg polymer.

4.2 SOLID-STATE POLYCONDENSATION

4.2.1 *Discontinuous Process*

The actual SSP reaction takes place in accordance with the scheme shown in Figure 5.19 in a temperature range of 15–40 °C below the melting point of the polymer and at 0.2 mbar. The procedure illustrated in this Figure represents an example of that used in commercial production. In addition, it shows the benefit of the use of precrystallized chips with respect to the shortened residence time and therefore the efficiency of the process.

Certainly, the results depend on the quality of the prepolymer, in particular its reactivity, as demonstrated in Figure 5.20.

The 'tightness' of the reactor is of the highest importance with respect to the prevention of oxidative degradation. Economic reasons cause manufacturers to optimize the filling volume, with reactors being filled up to 60 % of the nominal volume. This figure is certainly influenced by the design and the surface conditions of the reactor and its heating system. The course of the reaction can be controlled by the intrinsic viscosity of chips. After reaching the desired IV, the polymer is cooled to 100 °C or lower in a nitrogen atmosphere, either in the reactor itself or in a separate cooling tank. Blending of the batches improves the uniformity of quality for subsequent processing.

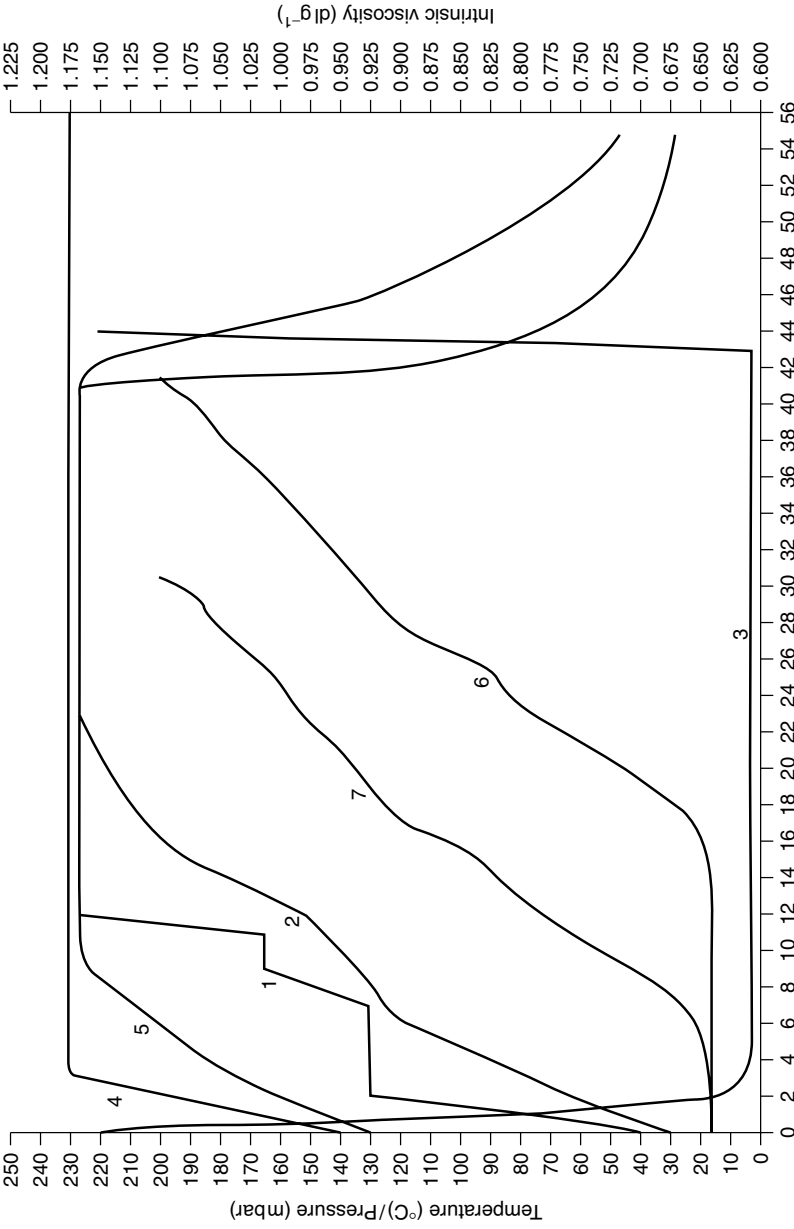


Figure 5.19 SSP discontinuous batch process for PET, showing the variation of temperature, pressure and intrinsic viscosity with batch time (reactor volume of 44 m³). Curves: 1, temperature-heating medium (amorphous material); 2, product temperature (amorphous material); 3, pressure (in mbar); 4, temperature-heating medium (crystalline chips); 5, product temperature (crystalline chips); 6, IV (amorphous material); 7, IV (crystalline chips) [34]. From manufacturer's literature published by OHL Apparatabau and Verfahrenstechnik, Limburg, Germany, and reproduced with permission

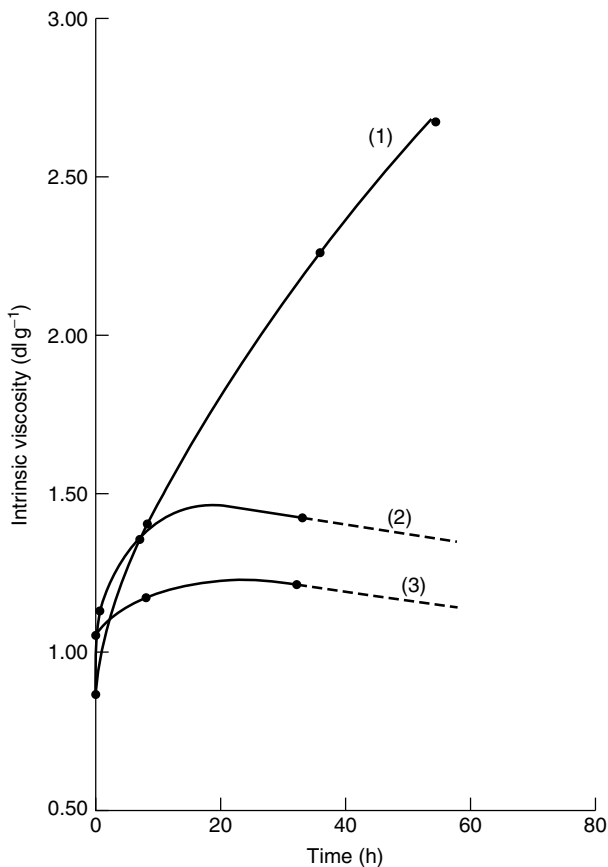


Figure 5.20 Solid-state polycondensation of poly(butylene terephthalate) with different end group concentrations: 1, [COOH], 0.67 vol/mol; 2, [COOH], 1.48 vol/mol; 3, [COOH], 1.86 vol/mol [30a]. From Buxbaum, L. H., *J. Appl. Polym. Sci., Appl. Polym. Symp.*, **35**, 59 (1979), Copyright © John Wiley & Sons, Inc., 1979. Reprinted by permission of John Wiley & Sons, Inc.

4.2.2 Continuous Process

As can be expected, continuous SSP is mainly controlled by the flow rate of the nitrogen stream and the temperature. Due to the differences in reactor designs exact comparisons regarding the conditions cannot be presented. It is easy to understand that the process depends on the individual design and special characteristics of the equipment. The reaction temperature is in the same range as in the batch process [46]. According to this patent, it should be noted that the SSP reaction is influenced additionally by the content of EG and the side products,

particularly AA in the nitrogen stream. An increased EG content reduces the CEG (carboxylic end group) content significantly.

4.3 PROCESS PARAMETERS INFLUENCING SSP

The complex nature of SSP depends on many factors, all of which can affect the course of the reaction and the quality of the final product. An optimum combination of such variables thus determines the reaction process and needs to be discussed in detail. Therefore, some of the generally known aspects are reported in the following sections.

4.3.1 Particle Size

For the solid-state process, chips are commonly preferred at the present time. The particle size and size distribution play a crucial role during the SSP process with respect to its efficiency and the quality of the product. The particle size distribution governs the molecular weight distribution, which itself determines the uniformity of quality, as indicated by spinning performance and flow properties. The particle size distribution can be controlled by the blending of different particle sizes [47]. The conditions used for re-melting, in particular the time, generally control the molecular weight distribution.

Not only quality reasons, but also economic considerations, make it necessary to reduce the particle size. Generally, the development of an economic SSP process is characterized by the trend to a reduced particle size. The commonly used cubic chips size (2–4 mm) is reduced to that of the known small nylon chips (~ 1.5 mm diameter, spherical shape). The size of the chips can be defined by the length of the cubes and is easily measured. Due to their irregular shape, however, determination of their average volume is difficult. Therefore, the definition weight (g) of 100 pieces has become popular.

Currently, the production of chips of 0.8 mm length by using special pelletizing technologies is possible [48]. The cutting of chips of this particle size requires a new pelletizing technology which may not meet the capacity of novel continuous polymer lines with 12 (and higher) t/h throughput. According to this report, the cutting of low-IV chips (below 0.40 dl/g) seems to be no problem. Pelletizing of low-IV polymer with conventional pelletizers is impossible due to the brittleness of the strands.

The grinding of crystallized chips has been well-known for about 50 years but yields problems with respect to handling and processing. Very small particle sizes can be achieved by grinding under cryogenic conditions. Lower-IV prepolymers (<0.40 dl/g) are preferred for this process. The handling of smaller particles becomes more difficult due to the increased content of ‘fines’ and their separation, particularly in continuous gas flow technology. ‘Fines’ are defined as extremely

small, highly crystallized and high-melting fine dust particles, which have a negative influence on the quality of the extrudates. Such 'fines' show a reduced solubility in common solvents. The increased melting points and the decreased solubility in these solvents depend on the undefined prolonged retention time in the SSP system.

The SSP of powdered prepolymer allows the attaining of IVs in the region of ca. 2.0 dl/g and can therefore compete with the more complicated SSP process in the swollen (suspended) state. It has been found that the SSP of powdered PET under optimum conditions provides high-grade polyesters with high IVs within relatively short reaction times. The advantage of employing powdered polymer in the production of high-quality industrial yarns has been reported by Gerking [49]. This outlines the benefits of a reduced chips size regarding reaction time and quality in commercial scale production. Additionally, it was found that the reduction of the chips size from 2.25 to 1.88 g/100 pieces results in an increase of capacity by 25 % in SSP, i.e. from 60 to 75 t/d [50]. It should be noted that the quality of smaller particles may possibly affect the extrusion process due to the content of 'fines' on account of their high melting points and lack of processability.

The use of foamed prepolymer chips is a very interesting approach to reducing the SSP process time. It has been reported [51] that these particles can be produced by passing pressurized nitrogen into the extruder prior to pelletizing. It can be rationalized that conveying and handling of these chips is less complicated. In this way, the surface/volume ratio can be optimized. Understandably, more care has to be taken with degassing this material during extrusion.

4.3.2 Catalysts

Any type of the known catalysts, which effects polycondensation in the molten state is also effective in the solid-state process, as long as the reaction temperature is sufficiently high enough to activate the reaction. SSP is commonly catalyzed by antimony, germanium and titanium compounds which are added during the prepolymer manufacture. The reaction rate depends on the type of catalyst, with the known antimony catalysts being generally preferred. The influence of the catalyst on the crystallization rate should be noted. This phenomenon, which is based on the content of nucleating catalyst particles is of importance for the production of bottle-grade polymer [25]. Germanium metal has only a small nucleating effect in the production of bottle-grade PET and reduces the content of cyclic trimer. Therefore, it is preferred with respect to optical properties. As is known, PET catalyzed by germanium compounds shows the best color and clarity [52].

Titanium- and tin-containing systems show high efficiency but tend to discolor the polymer. PET based on Ti catalysts also exhibits a lower crystallization rate in comparison with antimony. This phenomenon may be caused by the lower catalyst concentration and therefore the reduced nucleation.

The activity of Ti catalysts in SSP depends on the kind of stabilizer fed into the reactor. In the production of PET, phosphorous-containing chemicals are commonly added as stabilizers. These products improve the thermal stability, particularly in processing, which results in reduced degradation and discoloration and are therefore of importance with respect to quality. Such materials are added during the production of the prepolymer. These stabilizers are mainly based on phosphoric or phosphonic (phosphorous) acids or their esters.

Small amounts of these acids or other phosphorus compounds containing acidic OH groups inhibit the SSP process. This inhibition of Ti-catalyzed polycondensation is related to the formation of stable adducts between the acidic phosphorus compound and the catalyst [53]. Such a problem can be overcome by the use of certain compounds, for example, nonyl phosphite, in exact, equivalent amounts [54].

The addition of certain sterically hindered hydroxyphenyl phosphonates as stabilizers during production of the prepolymer accelerates the SSP reaction rate in certain specific conditions [55].

The SSP behavior of co-polyesters with rigid or voluminous comonomers, such as the flame retardant additive 9,10-dihydro[2,3-di-9-oxa-(2-hydroxyethoxy)-carbonylpropyl]-10-phosphaphenanthrene-10-oxide, or the ionic compound, sodium 5-sulfoisophthalate, is inhibited. This also occurs in the melt phase and cannot be improved by the use of catalysts [56]. The results of studies examining the influence of employed catalysts with respect to stability and quality of the polymer suggest the use of antimony catalysts. The thermal or thermo-oxidative stability is, however, reduced by the interaction of the catalyst with the carboxylic groups of the polymer [57].

4.3.3 *Intrinsic Viscosity*

The final IV after SSP at constant temperature, time and pressure depends on the initial IV of the prepolymer, i.e. PBT (Figure 5.21). For obtaining a desired high final IV at reasonable reaction times, the IV of the prepolymer should be ca. 0.60 dl/g in the case of PET. Many considerations, however, influence this choice.

An optimum compromise can be found by finalizing the reaction conditions, time, economy and quality. The quality of the prepolymer dictates that of the end product. A shorter residence time during prepolymer processing significantly improves the quality due to the detrimental effects of temperature, residence time and level of by-products. On the other hand, the pelletizing process is limited by the IV. Below an IV of 0.35 dl/g, pelletizing with conventional equipment becomes impractical due to the brittleness of the prepolymer. The variation in the final IV is influenced by that of the prepolymer, as can be seen in Figure 5.22. Remarkably, SSP cannot compensate for the deviating IV values of the prepolymer. A broader particle size distribution also broadens the IV distribution and can affect the uniformity of quality, particularly in subsequent processing.

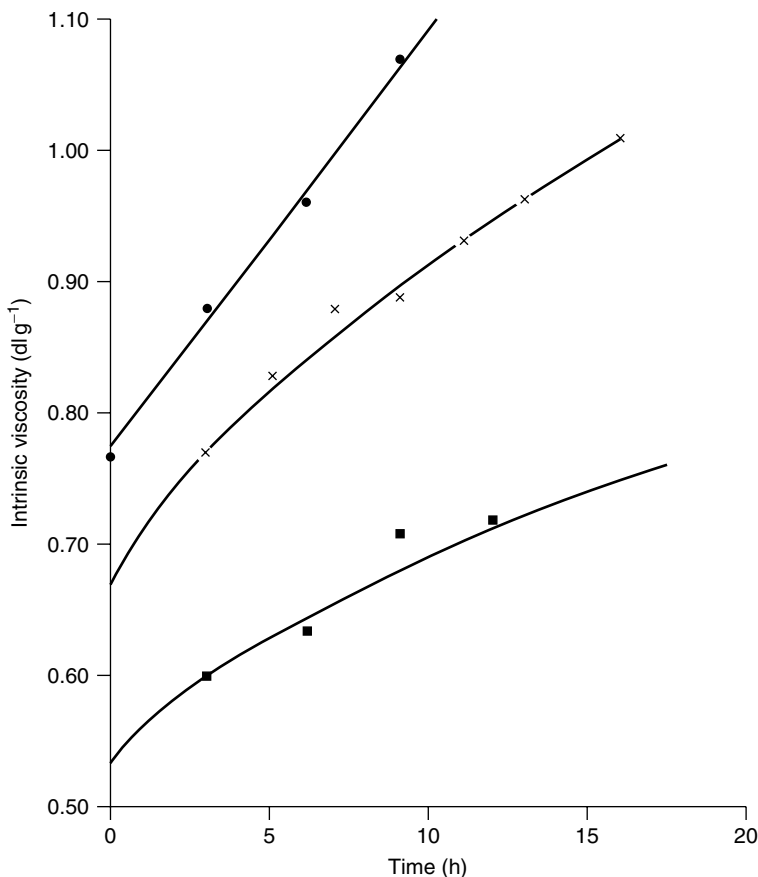


Figure 5.21 Solid-state polycondensation using different prepolymers, shown as the initial intrinsic viscosity as a function of time (at 235 °C and 0.1 mbar) [30a]. From Buxbaum, L. H., *J. Appl. Polym. Sci., Appl. Polym. Symp.*, **35**, 59 (1979), Copyright © John Wiley & Sons, Inc., 1979. Reprinted by permission of John Wiley & Sons, Inc.

4.3.4 Carboxylic End Groups

According to the principles of SSP, chain growth occurs mainly via polytransesterification and polyesterification reactions. These are accompanied by the formation of ethylene glycol (EG) and water, respectively. Due to its higher diffusion coefficient water is removed more easily. Generally, SSP needs a specific ratio of hydroxyl to carboxylic end groups (OH/CEGs). A broad range of results can be found regarding the optimum ratio reported in the literature. According to one patent disclosure [19], the ratio should be ca. 3:1, but Schaaf *et al.* [20] has

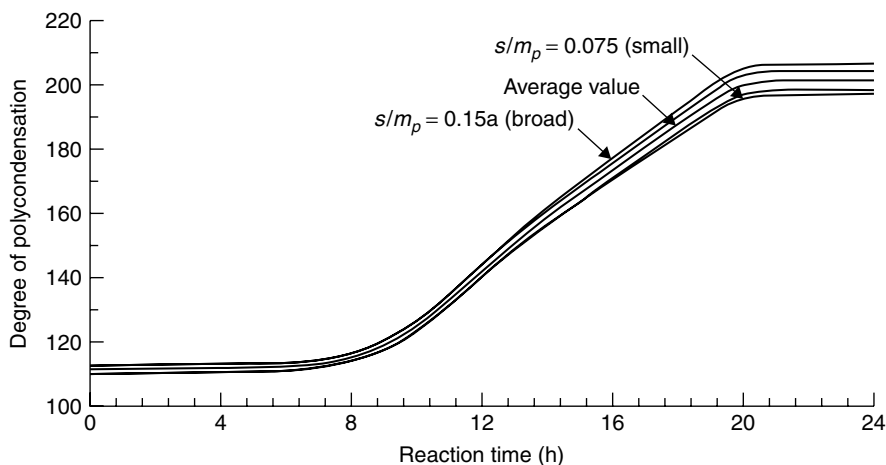


Figure 5.22 Scattering in the degree of polycondensation of the PET product, as a result of variations in the particle size and intrinsic viscosity in the virgin polymer: s/m_p , standard deviation of the particle mass [12b]. From Weger, F., Solid-state postcondensation of polyesters and polyamides, presentation given at the *Frankl and Thomas Polymer Seminar*, June 16, 1994, Greenville, SC, USA, and reproduced with permission of EMS Inventa-Fischer, GmbH & Co. KG

postulated an optimum ratio of 2:1, with the latter being based on a restricted reaction mechanism. In the cases of PBT and PEN, an OH/CEG ratio of 2:1 is required.

In practice, the concentration of CEGs in the prepolymer commonly varies between 30 and 40 meq/kg. These end groups can increase the reaction rate of SSP under certain conditions if the OH/CEG ratio is balanced with respect to the required value. In contrast, a higher degree of degradation of the prepolymer, yielding CEG groups, results in a decreased reactivity, particularly in the case of PBT [30a] (see Figure 5.20).

Prepolymer produced via the terephthalic acid (TPA) monomer route shows an increased reactivity in comparison with that produced by the dimethanol terephthalate (DMT) monomer process [49]. This behavior is possibly caused by the enhanced CEG content, which is usually higher in products from the TPA process as a result of insufficient conversion of the acid monomer in the esterification reaction (Figure 5.23). The increased reactivity may be caused by an autocatalytic influence of the carboxylic groups which seems to be disturbed by an unbalanced content of OH groups in the case of degradation.

It has been disclosed [18] that the addition of terephthalic acid after the esterification stage is complete is responsible for a high reaction rate during the SSP process. In this case, the prepolymer has commonly 30–40 meq/kg of CEGs. These observations lead to the conclusion that an increased number of CEGs are

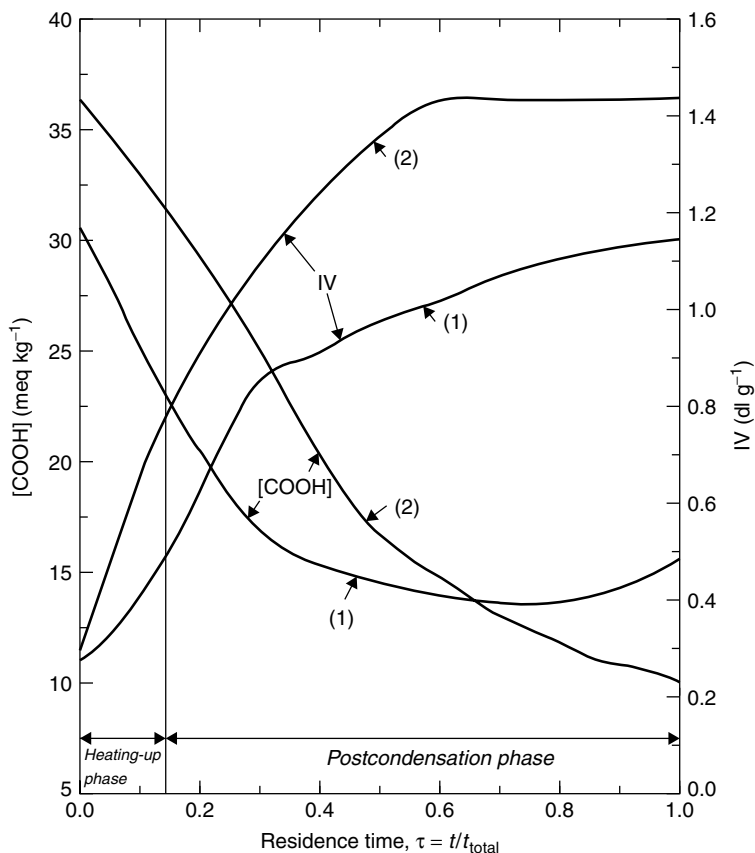


Figure 5.23 Variation in the concentration of carboxylic end groups and intrinsic viscosity during the postcondensation of PET powder produced from DMT (1) and TPA (2) prepolymers (T , 240 °C) [49]. From Gerking, L., Modifications of fiber properties by polymer and within spinning line, presentation (Paper 52b) given at the 32nd International Man-Made Fibre Congress, 22–24 September, 1993, Dornbirn, Austria, and reproduced with permission of EMS Inventa-Fischer, GmbH & Co. KG

located at the reactive sites in the SSP reaction. Therefore, they are available for reaction and do not need to diffuse to active centers.

In the case of PBT, the CEG content of the prepolymer should not exceed 40 meq/kg, or otherwise the polycondensation reaction is inhibited due to an increased formation of tetrahydrofuran (THF). The effect of the CEG content in a PBT prepolymer on the final IV is shown in Figure 5.20.

The CEG content decreases during the solid-state process for producing bottle-grade PET, under the standard conditions, by ca. 20–40 %. For the production

of tyre-cord yarns, very low CEG contents are required due to the reduced stability of the polymer to hydrolysis and aminolysis. Therefore, a minimum content of CEGs is desired for such an application. However, this is still in the region of 14 meq/kg, and even higher in the final yarn. For CEG values below 10 meq/kg, the addition of end-group-capping chemicals during the extrusion stage is required.

4.3.5 Temperature

Solid-state polycondensation is a temperature-dependent reaction, which commonly takes place at temperatures of between 10 and 40 °C below the melting point of the prepolymer. According to various experimental results, the reaction at temperatures below 150–170 °C does occur, although it is very slow [16, 28]. As shown earlier in Figure 5.7, SSP is carried out on a commercial scale at temperatures of between 220 and 245 °C. At higher temperatures, or with long reaction times, degradation becomes the dominant reaction (Figure 5.24).

Figure 5.19 displays a typical course of discontinuous SSP on the commercial scale (batch size, 22 t) with respect to the variables of temperature, time, vacuum and intrinsic viscosity. This figure shows the IV plotted as a function

Publisher's Note:
Permission to reproduce this image
online was not granted by the
copyright holder. Readers are kindly
requested to refer to the printed version
of this chapter.

Figure 5.24 Effect of reaction time on the solid-state polycondensation process for PET: reaction conditions, 250 °C: initial M_n , 16 500, with a particle size of 0.18–0.25 mm; data obtained by gas chromatographic analysis, employing a column of dimensions 8 ft \times 0.75 in o.d., with a nitrogen gas flow rate of 350 ml/min [5]. Reproduced from Hsu, L.-C., *J. Macromol. Sci., Phys.*, **B1**, 801 (1967), with permission from Marcel Dekker

of reaction time, and in addition, the benefits of a precrystallizer which shortens this time. Chang *et al.* [7] found, in the higher-temperature range, a shifting in the nature of the reaction to one of ester exchange, which was associated with an broadened molecular weight distribution. At extremely high temperatures, thermal decomposition of the polymer is observed at an early stage. This reaction is thermally initiated and not related to possible hydrolysis due to water generated by esterification. According to the different diffusion coefficients of water and diols as side products, hydrolysis plays a negligible role in degradation. This fact should be taken into account in the case of larger particle sizes.

4.3.6 Vacuum and Gas Transport

As explained earlier, efficient removal of the reaction products is extremely important in the SSP process. The lowest possible pressure in the reactor is necessary, with the reaction commonly being carried out at a pressure of 0.2 mbar. Leaks in the systems or a higher pressure range, caused by insufficient vacuum sources, lead to a lower polymer quality. Generally, the presence of oxygen deteriorates the quality and the processability of the polymer. The gas flow technology requires an optimum flow of the gas stream, as shown above in Figure 5.3. These data, obtained from laboratory experiments, are certainly not comparable with the conditions used in commercial processes but indicate the importance of such a parameter (see also Figures 5.4 and 5.5). The flow rate employed mainly depends on the particle size and the design of the reactor, where the latter influences the profile of the gas stream. Excessive flow rates in the case of smaller particle sizes and fluid bed reactors require greater effort in maintaining a possible powder build-up in the temperature range of polymerization.

The handling of smaller particles, and in particular powders in SSP, is therefore more difficult than that of chips. High flow rates are desired for larger column reactors. There is no clear-cut range of flow rates for the inert gas passing through the reactor, since the efficiency of the flow depends on the geometry of the equipment. The beginning of disappearance of the particles, which are picked up by the gas stream, determines the flow rate. By experience, this limitation may be in the region of about 0.8 m/s. Depending on the process, the nitrogen consumption varies in the range between 0.5 and 2.5 kg nitrogen per kg polymer and is influenced by the level of crystallization and drying with nitrogen or air blowing. The unavoidable loss of nitrogen and the amount of gas employed for the solid-state technique govern the economy of the process. In this context, it could be found that SSP carried out under a nitrogen flow is superior to the process conducted *in vacuo*, with respect to the acetaldehyde (AA) content of the polymer product. Removal of the absorbed AA from the surface of the chips seems to be more efficient when employing the gas-flow method [8, 16].

4.3.7 Reaction Time

The time-dependence of the SSP process has to be viewed in connection with the temperature and the factors concerning diffusion. After a certain period into the reaction, no increase in the IV is observed and thermal decomposition becomes the dominant process.

Figure 5.24 shows the molecular weight (M_n) plotted as a function of the reaction time. It can be seen from this figure that there is an optimum time for attaining the maximum IV. The slope then becomes flat and later turns downwards due to thermal degradation. The reaction is then characterized by an increasing content of CEG and vinyl ester groups, as manifested by an increasing fluorescence intensity.

The scattering of the final IV is influenced by that of the prepolymer, as can be seen from Figure 5.22. Remarkably, the reaction time employed for the SSP process cannot balance the deviating IV values of the prepolymer. Broader particle size distributions also broaden the IV distribution and can affect the uniformity of quality, particularly in subsequent processing.

4.3.8 Oligomers and Acetaldehyde

The SSP process is accompanied by a continuous loss of side products, such as acetaldehyde (AA) and oligomers. Both components can reduce the quality of the final products. Figure 5.25 displays the level of AA and the IV as a function of the reaction temperature. The concentration of AA decreases with increasing reaction temperature to a level of less than 3 ppm at 230 °C. Remelting, however, then leads to an increase in the AA content (Table 5.3).

The observed reduction in the content of oligomers during the solid-state process is shown in Figure 5.26. These contents drop during SSP upon increasing temperatures and time. However, these low levels are increased by remelting in subsequent processing.

Table 5.3 Content of acetaldehyde (ppm) during the SSP process [26]. From Wick, G., Characterization of PET polymer for bottle manufacturing, presentation given at the *Society of Plastics Engineers Benelux Seminar*, 20–21 May, 1980, Amsterdam, and reproduced with permission of KoSa GmbH & Co. KG

Material/Stage	Content
Prepolymer	25
SSP process	<3
Preform	>6
Bottles	<3

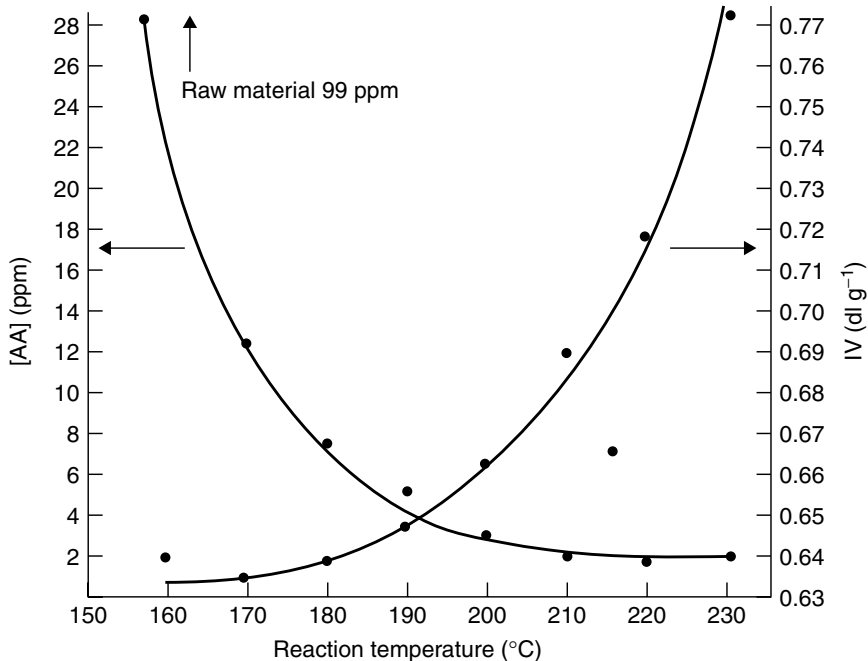


Figure 5.25 Acetaldehyde content and intrinsic viscosity as a function of the reaction temperature during the discontinuous SSP process [26]. From Wick, G., Characterization of PET polymer for bottle manufacturing, presentation given at the *Society of Plastics Engineers Benelux Seminar*, 20–21 May, 1980, Amsterdam, and reproduced with permission of KoSa GmbH & Co. KG

5 ECONOMIC CONSIDERATIONS

A comparison between the technologies of SSP employing either gas flow or *in vacuo* conditions does not reveal any differences regarding the reaction rate. Inconsistent results have been reported on the quality of the final product and comparison of the technologies with respect to this quality [3]. An unbiased assessment is indeed difficult as the different results seem to be based on various explanations. The different results are possibly influenced by the lack of detailed information concerning the parameters of SSP. Fundamental evidence is still missing due to the lack of comparable and qualified results. The capacities of the systems employed will influence the production costs. These are slightly higher for the batch process due to the more expensive equipment required. The energy costs – as a decisive factor – in particular, the nitrogen consumption of the continuous lines, only depend on the equipment being employed.

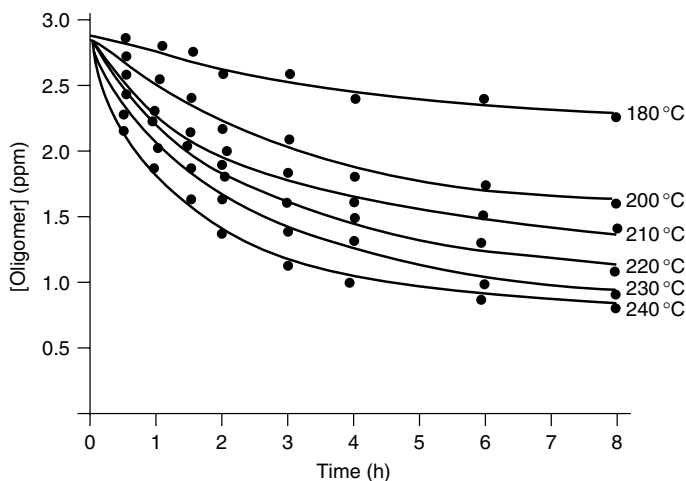


Figure 5.26 Variation of the oligomer content as a function of time and temperature during the SSP process [26]. From Wick, G., Characterization of PET polymer for bottle manufacturing, presentation given at the *Society of Plastics Engineers, Benelux Seminar*, May 20–21, 1980, Amsterdam, and reproduced with permission of KoSa GmbH & Co. KG

6 SOLID-STATE POLYCONDENSATION OF OTHER POLYESTERS

The basic knowledge of the principles of SSP usually allows a generalization concerning the production of any kind of semicrystalline polyester or co-polyester. Differences regarding the reactivities are observed which are attributed to the mobilities of the components employed, e.g. PEN, cationic dyeable polymers or flame-retardant co-polyesters.

The processing of these prepolymers differs due to the prolonged reaction times during melt-phase polycondensation and the reduced thermal stabilities of these materials. The relatively low IV values of the prepolymers has to be increased by SSP under gentle conditions with the requirement for extremely long reaction times.

PEN is of great interest as an engineering plastic because of its high T_g and excellent gas barrier behavior, as well as its thermal and chemical stability. PEN is also successfully applied in industrial yarns, which are characterized by high moduli and tenacities and low hot-air shrinkage. The IV obtainable by melt-phase polycondensation is in the region of 0.5 dl/g due to the significantly increased melt viscosity of this polyester. In the final state of the production of the prepolymer (~ 0.50 dl/g), the reaction is often accompanied by the onset of thermal degradation. The reaction temperature should therefore not exceed

300 °C. This IV region is too low for subsequent PEN processing. Therefore, SSP of the prepolymer is necessary to achieve the desired IV. A sufficiently high IV (~ 1.0 g/dl) can be obtained at reasonable but prolonged reaction times via SSP, which is conducted under similar reaction conditions as PET. The reaction is commonly conducted batchwise *in vacuo* due to the limited commercial demand.

The SSP of PEN and co-polyesters based on 2,6-naphthalene dicarboxylic acid requires prolonged reaction times, which is obviously related to the rigidity of the monomers and therefore to both the reduced mobilities of the end groups and diffusion. Only a few detailed reports exist in the literature on this subject [31, 32]. It should be noted that the analysis of PEN can become complicated due to its reduced solubility.

An additional example of applying SSP to co-polyester production has been outlined in a US patent [59]. This discloses the production of co-polyesters based on terephthalic acid and with up to 12 % bis-(hydroxy ethoxy phenyl)sulfone co-monomer content. Additional patents exist concerning the SSP of other co-polyesters [60, 61].

7 CONCLUSIONS

The SSP process is an important commercial route for producing high-molecular-weight semicrystalline polyesters with outstanding properties. The reaction follows traditional chemical kinetics and thermodynamics, as well as rates of diffusion. The latter become dominant in the case of large particles and during the later phase of the reaction where a decrease in the amount of reactive end groups is seen. The quality of the final polymer depends on that of the prepolymer, its homogeneity and the reaction conditions with respect to residence time, temperature and particle size. The chemical structure of the monomers employed influences the reactivity and therefore the attainable molecular weight.

The growing demand for high-molecular-weight polyesters for engineering plastics applications and improved economics suggest the need to develop processes to produce small particles. SSP offers opportunities for producing polymers containing thermally unstable components which would decompose under the conditions of molten-state polycondensation by adding these components during the later stage of prepolymer synthesis. The reaction can often then be continued via SSP without any adverse effect on the additive. The resulting quality makes SSP the most attractive method for producing high-molecular-weight polyesters.

REFERENCES

1. Flory, P. J., *US Patent 2 172 374* (to Du Pont), 1939.
2. (a) Flory, P. J., *Principles of Polymer Chemistry*, Cornell University Press, Ithaca, New York, 1953, Ch. 3, pp. 00–00; (b) Korshak, V. V. and Vinogradova, S. V., *Polyesters*, Pergamon Press, New York, 1964, Ch. 6, pp. 00–00.
3. (a) Tate, S., Watanabe, Y. and Chiba, A., Synthesis of ultra-high-molecular-weight PET by swollen-state polymerization, *Polymer*, **34**, 4974 (1993); (b) Toyobo, *Eur. Patent 0 207 856 B2*, 1990; (c) Toyobo, *Eur. Patent 0 251 313*, 1988; (d) Union Carbide Corporation, *US Patent 4 374 239*, 1983; (e) Toyobo, *US Patent 4 742 151*, 1988.
4. Bamford, C. H. and Wayne, R. P., Polymerization in the solid phase: a polycondensation reaction, *Polymer*, **10**, 661 (1969).
5. Hsu, L.-C., Synthesis of ultra-high-molecular-weight PET, *J. Macromol. Sci., Phys.*, **B1**, 801 (1967).
6. Chang, T. M., Kinetics of thermally induced solid state polycondensation of PET, *Polym. Eng. Sci.*, **10**, 364 (1970).
7. Chang, S., Sheu M. F. and Chen, S. M., Solid state polymerization of PET, *J. Appl. Polym. Sci.*, **28**, 3289 (1983).
8. Jabarin, S. A. and Lofgren, E. A., Solid state polymerization of PET: kinetic and property parameters, *J. Appl. Polym. Sci.*, **32**, 5315 (1986).
9. Pilati, F., Solid state polymerization, in *Comprehensive Polymer Science*, Vol. 5, Allen, G., Ledwith, A., Russo, S. and Sigwalt, P. (Eds), Pergamon Press, Oxford, UK, 1989, pp. 201–000.
10. Kumar, A., Gupta, S. K., Somu, N. and Satyanarayana Rao, M. V., Simulation of cyclics and degradation product formation in PET reactors, *Polymer*, **24**, 449 (1983).
11. Chen, S. A. and Chen, F. L., Kinetics of polyesterification. III. Solid state polymerization of PET, *J. Appl. Polym. Sci.*, **25**, 533 (1987).
12. (a) Hagen, R., Modeling and Calculations of Reaction and Transport Mechanism in Solid State Polycondensation and their Industrial Applications (in German), *Ph. D. Thesis*, Technical University of Berlin, 1993; (b) Weger, F., Solid-state postcondensation of polyesters and polyamides, presentation given at the *Frankl and Thomas Polymer Seminar*, Greenville, SC, 16 June 1994.
13. Huang, B., Research and development activities at the PolyquestSM Development Center, presentation (session III/3–8) given at the *Polyester'99 4th World Congress – The Polyester Chain*, Zurich, Switzerland, 25–28 October, 1999.
14. Chiou, J. S., Barlow, J. W. and Paul, D. R., Plasticization of glassy polymers by CO₂, *J. Appl. Polym. Sci.*, **30**, 2633 (1985).

15. (a) Ravindrath, K. and Mashelkar, R. A., Modelling of PET reactors IX. Solid state polycondensation process, *J. Appl. Polym. Sci.*, **39**, 1325 (1990).; (b) Tomita, K., *Polymer*, **14**, 50 (1973).
16. Dröscher, M. and Wegner, G., Poly(ethylene terephthalate): a solid state condensation process, *Polymer*, **19**, 43 (1978).
17. Eastman, *US Patent 3 075 952*, 1963.
18. Goodyear, *Ger. Patent DE-OS 3 022 076*, 1981.
19. Zimmer, A. G., *US Patent 4 064 112*, 1993.
20. Schaaf, E., Zimmermann, H., Dietzel, W. and Lohmann, P., Nachpolykondensation von PET in fester Phase, *Acta Polym.*, **32**, 250 (1981).
21. Paschke, E. E., Bidlingmeyer, B. A. and Bergmann, J. G., A new solvent system for gel permeation chromatography of PET, *J. Polym. Sci.*, **15**, 983 (1977).
22. Jabarin, S. A. and Balduff, D. C., Gel permeation chromatography of PET, *J. Liq. Chromatogr.*, **5**, 1825 (1982).
23. Pilati, F., Gostoli, C. and Sarti, G. C., Chemical kinetics and diffusion in PBT, *Polym. Proc. Eng.*, **4**, 403 (1986).
24. Sangla', B. and Strezielle, C., Characterisation et proprietes rheologiques en milieu dilue et a l'etat fondu des PET lineaires et ramifies, *Makromol. Chem.*, **187**, 59 (1986).
25. Jabarin, S. A., Crystallization kinetics of PET I. Isothermal crystallization from the melt, *J. Appl. Polym. Sci.*, **34**, 85 (1987).
26. Wick, G., Characteristics of PET polymer for bottle manufacturing, presentation given at the *Society of Plastics Engineers Benelux Seminar*, Amsterdam, 20– 21 May, 1980.
27. Patkar, M. and Jabarin, S. A., Effect of diethyleneglycol (DEG) on the crystallization of PET, *J. Appl. Polym. Sci.*, **47**, 1748 (1993).
28. Frank, W. P. and Zachmann, H. G., Influence of thermal treatment on crystallization of PET, *Prog. Colloid Polym. Sci.*, **62**, 88 (1977).
29. Jabarin, S. A., Optical properties of thermally crystallized PET, *Polym. Eng. Sci.*, **22**, 815 (1982).
30. (a) Buxbaum, L. H., Solid-state polycondensation of PBT, *J. Appl. Polym. Sci.*, *Appl. Polym. Symp.*, **35**, 59 (1979); (b) Sandoz, *Ger. Patent DE-OS 2 162 618*, 1972.
31. Po', R., Occhiello, E., Giannotta, G., Pelosini, P. and Abis, L., New polymeric materials for containers manufacture based on PET/PEN copolyesters and blends, *Polym. Adv. Technol.*, **7**, 365 (1996).
32. AMOCO, Extending the use of polyesters in engineering resins, Brochure GTSR-A, Amoco Chemical Company, Chicago, IL, 1 May, 1994, p. 14.
33. (a) Fortunato, P., Pilati, F. and Manaresi, F., Solid state polycondensation of PBT, *Polymer*, **22**, 655 (1981); (b) Pilati, F., Manaresi, P., Fortunato, B., Munari, A. and Passalacqua, V., Formation of PBT: secondary reactions of studied model molecules, *Polymer*, **22**, 1566 (1981); (c) Gostoli, C.,

- Pilati, F., Sarti, G. C. and Di Giacomo, B., Chemical kinetics and diffusion in PBT solid state polycondensation. Experiments and theory, *J. Appl. Polym. Sci.*, **29**, 2873 (1984); (d) Gostoli, C., Pilati, F. and Sarti G. C., presentation given at the *International Conference on Reactive Processing of Polymers*, Strasbourg, France, 1984, Preprints, p. 49; (e) Pilati, F., Gostoli, C. and Gostoli, G. L., *Polym. Proc. Eng.*, **4**, 303 (1986).
34. OHL Apparatebau und Verfahrenstechnik, Unit Concepts with System, Brochure, Limburg, Germany.
 35. EMS Inventa-Fischer, Berlin, Germany (see also reference [12]).
 36. Du Pont, *US Patent 3 031 433*, 1962.
 37. Renzi, C., Giorano, D. and Baldi, G., Solid state polycondensation of PET: mathematical model for crystallization evaluation, *Chem. Fiber Int.*, **46**, 172 (1995).
 38. Bhatt, G. M. and Filke, L., Effect of copolymer content on tackiness of PET chips during SSP, presentation given at the *Polyester' 2000 5th World Congress – The Polyester Chain*, Zurich, Switzerland, 28 November–1 December, 2000.
 39. Hoechst AG, *Eur. Patent 0 146 060 B1*, 1982.
 40. Hoechst AG, *Ger. Patent DE-OS 1 804 551*, 1982.
 41. DuPont, *US Patent 3 405 098*, 1968.
 42. Standard Oil, *US Patent 4 008 206*, 1977.
 43. Gupta, V. B., Mukherjee, A. K. and Cameotra, S. S., in *Manufactured Fibers Technology*, Gupta, V. B. and Kothari, V. K. (Eds), Chapman & Hall, London, 1997, Ch. 12, p. 295.
 44. Kambour, R. P. and Gruner, C. L., Effects of polar group incorporation on crazing of glassy polymers: styrene–acrylonitrile copolymer and a bisphenol polycarbonate, *J. Polym. Sci., Polym. Phys. Ed.*, **16**, 703 (1978).
 45. Jabarin, S. A., Crystallization kinetics of PET III. Effect of moisture on the crystallization behavior of PET from the glassy state, *J. Appl. Polym. Sci.*, **34**, 103 (1987).
 46. Mitsubishi Kasei Corporation, *Ger. Patent DE-OS 4 223 007 A1*, 1993.
 47. Kalle AG, *Ger. Patent DE-OS 1 570 844*, 1970.
 48. Ecker, A., Production concepts for high throughput rates, presentation (Session VI) given at the *Polyester'99 4th World Congress – The Polyester Chain*, Zurich, Switzerland, 25–28 October, 1999.
 49. Gerking, L., Modification of fibre properties by polymer and within spinning line, presentation (Lecture 52b) given at the *32nd International Man-Made Fibres Congress*, Dornbirn, Austria, 22–24 September, 1993.
 50. Göltner, W., unpublished data.
 51. (a) VEB Chemieanlagenbau Leipzig-Grimma, *East Ger. Patent 146 610*, 1981; (b) VEB Chemieanlagenbau Leipzig-Grimma, *East Ger. Patent 147 881*, 1981.

52. Nukui, M., PET resin development from the Mitsubishi Chemical Company: latest UV barrier polyester resin and heat resistant resin, presentation (Session IX/2–6) given at the *Polyester'2000 5th World Congress – The Polyester Chain*, Zurich, Switzerland, 28 November–1 December, 2000.
53. Fortunato, B., Munari, A. and Manaresi, P., Inhibiting effect of phosphorus compounds on model transesterification and direct esterification reactions catalysed by titanium tetrabutylate, *Polymer*, **35**, 4006 (1994).
54. Karl Fischer Industrieanlagen GmbH, *US Patent 6 013 756*, 1995.
55. (a) Ciba AG, *World Patent WO-95 EP 3037*, 1995; (b) Oertli, A., SSP acceleration, a new opportunity to increase productivity, presentation (Session XI/3–7) given at the *Polyester'98 3rd World Congress – The Polyester Chain*, Zurich, Switzerland, 2–4 December, 1998.
56. Göltner, W., unpublished data.
57. Zimmermann, H., Thermische und thermooxydative Abbauprozesse des PET, *Plast. Kautschuk*, **28**, 433 (1981).
58. Toyobo, *Eur. Patent 0 207 856 B2*, 1990.
59. Owens Illinois, *US Patent 4 330 661*, 1982.
60. General Electric Company, *Ger. Patent 2 613 649*, 1976.
61. Goodyear, *Eur. Patent Appl. 174 265 A3*, 1986.

PART III

Types of Polyesters

6

New Poly(Ethylene Terephthalate) Copolymers

D. A. SCHIRALDI

Case Western Reserve University, Cleveland, OH, USA

1 INTRODUCTION

Shortly after the development of poly(ethylene terephthalate) (PET) by Whinfield [1], and initial commercialization of this polyester by ICI and DuPont, the development of copolymers of PET began. Applications of PET in the market-place was initially focused on textiles; this was followed by films and industrial fibers (primarily for tyre reinforcement) in the 1960s, and then in soft drink and bottled water containers in the 1970s–1980s. As we start the 21st century, PET-based materials are making great inroads into the packaging of food products, such as sauces and dressings, and are taking preliminary steps into the market-place for use in beer bottles and retortable containers. As each new application for PET-based materials is added to their list of commercial uses, new performance demands are made on this polymer. These new demands can be met by changing processing conditions or molecular weight, introducing additives or fillers to the polymer matrix, or by the copolymerization of new monomers into the PET backbone which clearly changes some of the polymer's fundamental properties. Production of PET copolymers for the textile fiber industry is certainly nothing new, and has been well reviewed elsewhere [2, 3]. Typical modifications for textile fibers include introduction of monomers such as adipate and poly(ethylene glycol) (PEG) which create amorphous regions capable of holding dyestuffs, copolymerization of ionomeric groups, such as sodium 5-sulfoisophthalate, which can bind cationic dyestuffs via an ion exchange process, and introduction of phosphorous-based esters, to provide increased levels

of flammability resistance [4, 5]. Introduction of compatible molecular repeat units, such as diethylene glycol (DEG) or PEG, can be added to improve clarity in PET films. In bottles, traditional comonomers include DEG, isophthalic acid (IPA) and cyclohexanedimethanol (CHDM), all of which when added at less than 5 mol % levels, depress the crystallization rates, postponing polymer crystallization until injection molded preforms are heated above their glass transition temperatures and blow molded into the desired containers. This delay in crystallization allows for the production of aesthetically pleasing clear containers that ultimately attain crystallinity levels equivalent to that which can be obtained using PET homopolymer. One additional, well-established application of PET copolymers, the PETG copolymers pioneered by Eastman Chemical, wherein at least 35 mol % of PET's ethylene glycol is replaced with CHDM have been in commerce for a generation [6]. These copolymers, which are amorphous after normal melt processing and assembly conditions, are sold into injection molding and extrusion applications where high clarity and impact toughness are required.

The starting PET polymer sits at the crossroads of mechanical, thermal, chemical and economic properties. This polyester tends to be stronger and able to withstand higher use temperatures than commodity polyolefins, but at greater cost. The liquid crystalline polymers, polyimides, poly(phenylene oxide)s and poly(phenylene sulfides) offer greater yet physical properties, but generally at cost multiples versus PET. With its moderate rate of crystallization, PET can be injection molded, but not as rapidly or consistently as its somewhat more expensive relative, poly(butylene terephthalate) (PBT), yet with post melt orientation, PET can be formed into fibers, films and containers which possess relatively high tensile, modulus, chemical resistance and gas transport barrier properties. The ultimate goal of copolymerization of PET with modifying substances is to either accelerate or delay the onset (and ultimate) level of crystallization, to either increase or decrease tensile and modulus properties, to bring about higher or lower glass transition temperature (T_g) and melting temperature (T_m) values for the polymer, and to modify dynamic properties, such as oxygen and carbon dioxide permeation rates – all while retaining the fundamentally sound balance of properties and low manufacturing costs associated with the homopolymer. The purpose of this article then, is to answer the question 'what's new' in PET copolymers.

2 CRYSTALLINITY AND CRYSTALLIZATION RATE MODIFICATION

Random copolymerization of one or more additional monomers into the backbone of PET is a traditional approach to reducing crystallinity slightly (to increase dye uptake in textile fibers) or even to render the copolymer completely amorphous under normal processing and use conditions (to compete with polycarbonate, cellulose propionate and acrylics in clear, injection molded or extruded objects).

With the wholesale conversion of carbonated soft-drink bottles to PET from glass during the latter third of the 20th century, interest in covalent modification of the polyester to decrease the rate of thermal crystallization, without significantly limiting the ultimate level of crystallinity achievable during biaxial orientation of a blown bottles, also became of commercial importance. The objective of this modification is to retard the onset of thermal crystallization of the polyester, as it solidifies from the melt. Such retardation of crystallization rate allows for injection molding of largely amorphous bottle preforms, which then can be heated above their glass transition temperature and stretch blown to their final, desired shape and size. During this stretch blowing process, strain-induced crystallization occurs, resulting in a container which is rigid, possesses satisfactory gas-barrier properties, and the necessary dimensional stability under pressure and product filling conditions. Typical modification of PET with typically less than 5 mol % of comonomers such as diethylene glycol, poly(ethylene glycol), cyclohexanedimethanol and isophthalate have been reviewed elsewhere [2].

At this time of writing, isophthalic acid has become the most widely accepted modifier for packaging applications, due to its relatively minor effect on the PET T_g , considerable reduction in crystallization rate but not in ultimate level of crystallinity (at <5 mol% modification levels), slight enhancement in oxygen and carbon dioxide barrier properties, and relatively low monomer cost.

2.1 AMORPHOUS COPOLYESTERS OF PET

The one commercial copolymer of PET, typically amorphous under normal conditions, is the PETG copolymer of Eastman [6]. This copolymer contains approximately 35 mol % of CHDM monomer, with the CHDM being the native ~70/30 mixture of *trans/cis* obtained from catalytic hydrogenation of dimethyl terephthalate. While typically amorphous and possessing high clarity and impact strength, long periods of annealing [7] (at or above the T_g), or exposure to a variety of organic solvents [8] can cause PETG to crystallize, losing both opacity and impact toughness.

In theory, almost any comonomer diacid or dialcohol could lead to amorphous copolymers of PET. For example, incorporation of 20–80 % of 2,6-naphthalate, or greater than 30 % of isophthalate, will generate amorphous materials [9]. Amorphous copolymers of PET, produced by the wholesale substitution of other monomers into the polymeric backbone, rarely possess desirable thermo-mechanical properties, unlike the Eastman PETG compositions.

Alternative monomers for elimination of crystallinity in PET have been recently proposed. In each of these cases, cyclic monomers were employed, and in most cases, these monomers were alicyclic, and potentially possess sub- T_g molecular motions that could also be of help in dissipating impact energy through molecular motions. The four-membered ring monomer, 2,2,4,4-tetramethyl-1,3-cyclobutanediol (CBDO), first developed by the Shell Chemical Company, has

been shown to lead to amorphous copolymers when incorporated in at least 15 mol% [10]. These amorphous copolymers, much as is the case with PET/CHDM copolymers, exhibit high impact strength and glass transitions higher than that of PET homopolymer. The bicyclic monomer, norbornane 2,3-dicarboxylic acid (NBDA), has been shown by KoSa/academic workers to produce amorphous copolymers when incorporated in at least 25 and 35 mol %, for the *trans*- and *cis*-isomers, respectively [7, 11]. The T_g values for these polymers are lower than those of the analogous CHDM and CBDO, while impact properties have not been reported. An additional monomer that has been recently reported to be effective at eliminating crystallinity in PET is *t*-butyl isophthalic acid (TBIPA) [12]. The presence of the *t*-butyl group was found to restrict molecular movement, and results in lower impact properties than unsubstituted PET. This same restriction in molecular motion does lead to an increase in the T_g , but all other mechanical properties of the polymer were found to be inferior to those of unmodified PET. For commercial applications of these copolymers, simple syntheses of the modifying comonomers from inexpensive, commodity starting materials is important. Cyclohexanedimethanol is produced commercially by exhaustive hydrogenation of dimethyl terephthalate. The CBDO monomer is produced by dimerization of isobutylene, followed by oxidation, and the NBDA is produced via Diels–Alder cyclization of cyclopentadiene with maleic anhydride, followed by hydrogenation of the C–C ring bond. Unlike these relatively straightforward processes, TBIPA relies on more difficult reaction/separation schemes for its potential manufacture.

The structures of these modifiers are shown in Figure 6.1.

2.2 INCREASED CRYSTALLIZATION RATES AND CRYSTALLINITY IN PET COPOLYMERS

The traditional methods for increasing PET crystallization rates include addition of particulate nucleating agents, such as talc, chain cleavage/conversion of PET chain ends to their sodium salts, using sodium hydroxide, sodium bicarbonate or sodium benzoate, or introduction of molecular chain slip agents, such as plasticizers or linear low-density polyethylene [13–17]. The role of chain end groups in affecting the rates of crystallization are also well understood [17]. Presumably because non-PET repeat units are rejected from growing PET crystals, incorporation of comonomers generally does not enhance the crystallization rates. An exception to this general rule occurs when PET is copolymerized with less than about 15 mol% of phenolic monomers, such as hydroquinone or 4,4'-bisphenol. In these cases, the resultant polyarylate repeat units accelerate the crystallization rates to two- to four-fold that of the PET homopolymer [18, 19]. The presence of the arylene terephthalate repeat units has been proposed by Sakaguchi and co-workers to increase the nucleation densities, especially at lower temperatures, thereby accelerating the overall crystallization process.

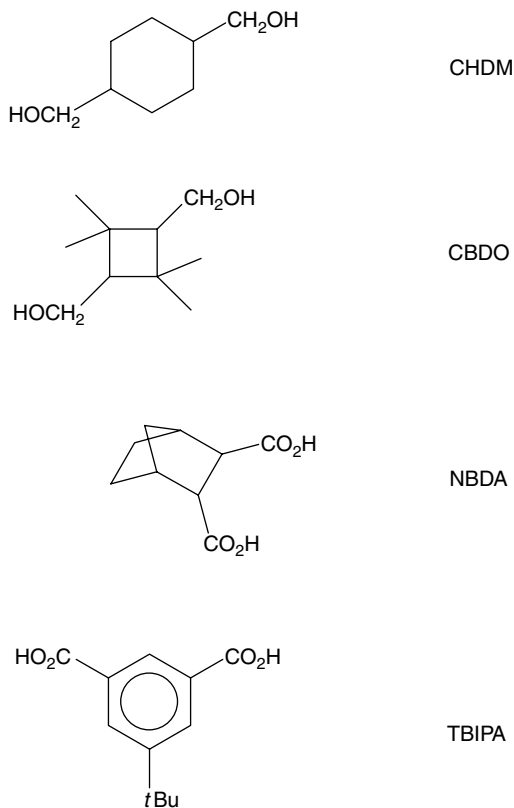


Figure 6.1 Some examples of modifiers used to produce amorphous copolymers of PET

Another exception to the generality that PET copolymers will tend to crystallize more slowly than the starting homopolymer is provided by the copolyesteramides developed by Gaymans, working in collaboration with GE Plastics [20–24]. Gaymans found that the introduction of amide linkages into PET and PBT not only resulted in increased glass transition temperatures and flexural moduli in polyesters, but that increasing levels of amide incorporation (up to 10–25 mol%) also led to increased crystallization rates. The proposed mechanism for the observed property enhancements in polyesteramide copolymers is a self-association of amide groups through hydrogen bonding (Figure 6.2). This interchain hydrogen bonding is proposed to retard segmental motion; the amide-rich regions within the copolymer are thought to serve as nucleation sites for crystallization. The crystallization rate increases, observed upon the introduction of amide groups, are not as large as those which result from introduction of heterogeneous nucleants, but this approach, free of added particulates, does not

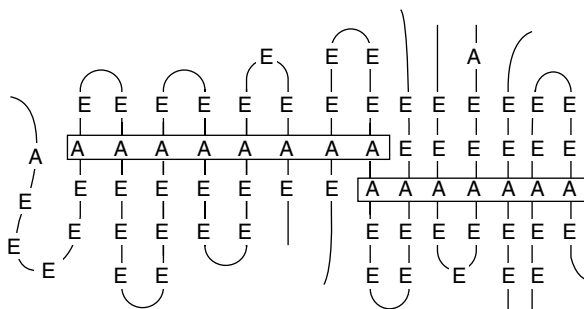


Figure 6.2 The polyesteramide structure proposed by Gaymans and co-workers: E, ester group; A, amide group [21]. Reprinted from *Polymer*, **38**, van Bennekom, A. C. M. and Gaymans, R. J., Amide-modified polybutylene terephthalate: structure and properties, 657–665, Copyright (1997), with permission from Elsevier Science

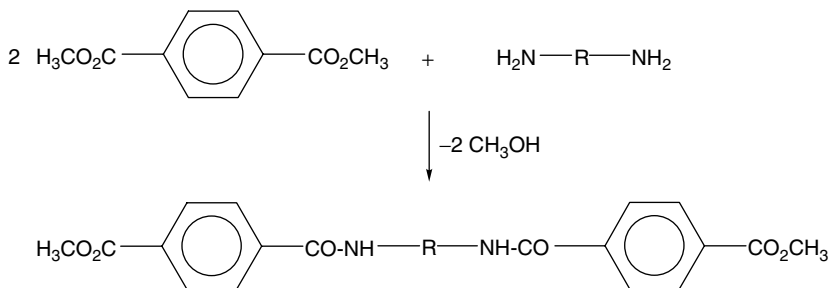


Figure 6.3 The ‘Gaymans’ approach to synthesizing polyesteramides

degrade the elongational properties (as can be seen when heterogeneous materials are added to a polymer matrix).

The idea of producing esteramides dates back almost to the days of condensation polymer pioneers Carothers and Whinfield. Early efforts relied upon processes wherein both ester and amide linkages were produced in the same reactor [25, 26]. In a limited number of cases, PET polyesteramides have been claimed to possess superior tensile and modulus properties over unmodified PET [27, 28]. The Gaymans approach (Figure 6.3), which leads to polymers of lower color (although even in this process, some yellowness, presumably derived from a nitrogenous species, is formed) relies on the synthesis of ester–amide–ester triads, which are then readily polymerized under normal polyester conditions. By judicious use of melt polymerization to relatively low molecular weight, followed by solid-state polymerization to the desired final degree of polymerization, polyesteramide polymers have been produced that are superior to those produced under conditions that require simultaneous ester- and

amide-bond formation. Despite the improvements which result from initial synthesis of ester–amide–ester triads, copolyesteramides appear to be inherently unstable, suffering considerable color degradation with additional heat history.

3 PET COPOLYMERS WITH INCREASED MODULUS AND THERMAL PROPERTIES

After its initial commercialization as a textile fiber, many subsequent applications for PET-based polymers have been in the areas of reinforcement of structures (such as tyres, hydraulic hoses and V-belts) or as a packaging material. In such applications, there is constant pressure for evolution to stronger and stiffer materials that can be ‘light weighted’, as well as interest in moving these products into increasingly higher temperature services. For these reasons, increased modulus and thermal properties are of great interest in developing PET copolymers.

3.1 SEMICRYSTALLINE MATERIALS

Neither poly(ethylene 2,6-naphthoate) (PEN), nor copolymers of PEN and PET, are new materials, but they continue to receive considerable attention, due to their relatively high T_m and T_g values, and attractive tensile, flexural and gas-barrier properties [29].

Because of interest in using PET as a lower-cost diluent to PEN, considerable attention has been given to understanding the kinetics of transesterification of the two polyesters when melt processed together, as well as their cocrystallization behaviors from the melt [30–35]. An important limitation to the approach of combining these two fairly similar polyesters is that transesterification is relatively facile at melt processing temperatures, and that compositions containing 20–80 % of PET are amorphous materials. An interesting treatment of how these two polymers progress from phase-separated mixture, through slightly copolymerized block structure, miscible mixture, and then rapid transesterification of the ethylene terephthalate and ethylene naphthalate groups, was proposed by Guo and Brittain [31], and may well exemplify the majority of transesterification processes in polyester blends (a general discussion of polyester transesterifications has been provided by Koliar [36]).

The isomeric bibenzoic acids (BBs), would appear to share similar structural features with naphthalene dicarboxylic acid. Like the PET–naphthalate copolymers, PET–bibenzoates have been demonstrated to possess moduli and glass transitions temperatures which increase with increasing levels of rigid comonomer [37–39]. Unlike the PET/PEN copolymers, when the symmetrical 4,4'-BB monomer is substituted into a PET backbone, virtually every composition of PET–BB is semicrystalline; the 2,4'- and 3,4'- isomers of BB, when

Table 6.1 Thermal properties of PET copolymers containing 10 mol% of various *x*, 4'-bibenzoic acids as comonomers

BB isomer	Polymer T_g (°C)	Polymer T_m (°C)
None ^a	78	256
2,4'	76	238
3,4'	82	230
4,4'	94	231

^a PET homopolymer.**Table 6.2** Thermal properties of PET copolymers containing high levels of various *x*, 4'-bibenzoic acids as comonomers

BB isomer	BB content (mol%)	Polymer T_g (°C)	Polymer T_m (°C)
None ^a	0	78	256
3,4'	55	91	Amorphous
3,4'	65	93	Amorphous
3,4'	100	99 (104 ^b) ^c	Amorphous
4,4'	55	106	262
4,4'	65	111 ^d	281
4,4'	100	—	343 ^c

^a PET homopolymer.^b Literature value.^c Reference [8].^d Approximate value.

copolymerized into PET, behave more like higher-temperature analogs to phthalic and isophthalic acids, respectively (Tables 6.1 and 6.2) [39].

While no direct evidence of liquid crystallinity in PET–BB copolymers has been reported, the high-BB-content copolymers have been shown to possess morphologies similar to those of liquid crystalline polyesters [40], and show major changes in both melt relaxation times and fiber tensile moduli, suggestive of structural organization in a ‘frustrated liquid crystalline polymer (LCP)’ (Table 6.3 and Figure 6.4) [41, 42].

Other, rigid-rod monomers can be incorporated into PET, to increase chain stiffness, and therefore the T_g (Figure 6.5). A prime example of such a rigid copolyester is a multi-ring poly(ethylene terephthalate–imide) [43]. As was the case with the polyesteramides of Gaymans, the imide-containing diol monomer, *N,N*-bis[p-(2-hydroxyethoxycarbonyl)phenyl]-biphenyl-3,3,4,4-tetracarboxy-diimide, was preformed prior to polycondensation, where this monomer is free

Table 6.3 Mechanical properties of injection-molded poly/copolyesters

Polymer/copolymer	Tensile strength (MPa)	Flexural modulus (GPa)
PET	67	2.9
PBT	60	2.5
PETBB-55	91	3.5

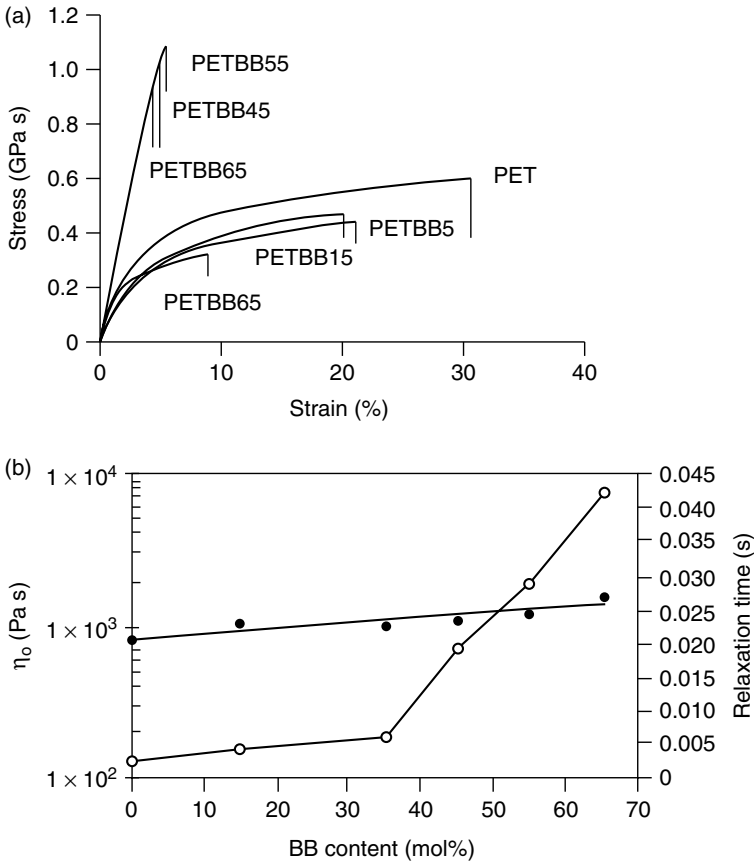


Figure 6.4 Properties of PET–BB copolymers as a function of BB content: (a) tensile properties; (b) viscosity, η_0 (●) and relaxation time (○) [42]. Reprinted with permission from Ma, H., Hibbs, H., Collard, D. M., Kumar, S. and Schiraldi, D. A., *Macromolecules*, **35**, 5123–5130 (2002). Copyright (2002) American Chemical Society

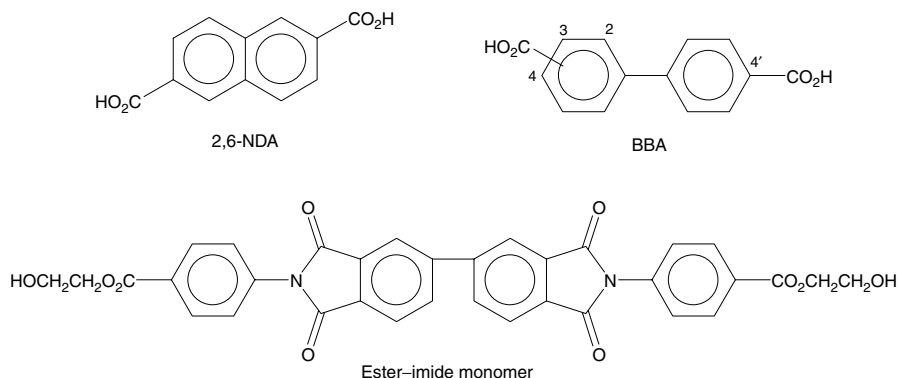


Figure 6.5 Some examples of rigid-rod comonomers that have been incorporated into PET to increase chain stiffness

to condense as a typical hydroxyethyl repeat unit. Significant in its enhancement of the T_g , introduction of this comonomer results in complete elimination of crystallinity when incorporated in as low as 5 mol% level.

3.2 LIQUID CRYSTALLINE COPOLYESTERS OF PET

Extending the PET/PEN systems to also include hydroxybenzoic acid (HBA) copolymers, PET/PEN/HBA combinations containing at least 30 % HBA, and PET/HBA combinations containing over 50 % HBA are generally found to be liquid crystalline [44–46]. While the HBA monomer used in such compositions is also typical of most commercial liquid crystalline polymers, PET modified with 70 mol% HBA is the only ethylene-glycol-containing liquid crystalline polymer (LCP) that has been commercialized to date [47]. Other LCPs have been produced from PET modified by *p*-acetoxybenzoic acid [48], hydroquinone (HQ) and HBA [49], HBA, vanillic acid, *p*-aminobenzoic acid and *m*-aminobenzoic acid [50, 51], and methylhydroquinone [52]. As could be predicted, addition of comonomers to PET/HBA or PET/PEN/HBA typically lower the temperatures of thermal transitions, the levels of observed crystallinities vary with the compositions, and the resulting LCP polymers tend to exhibit highly oriented, fibrillar structures. None of these materials have replaced the liquid crystalline polymers of commerce.

4 INCREASED FLEXIBILITY COPOLYMERS OF PET

The introduction of any flexible molecular repeat units, such as long-chain aliphatic diols or diacids, large hydrocarbon phases, such as C36 dimer acid,

or polyethers, such as poly(ethylene glycol) (PEG) and poly(tetramethylene glycol) (PTMG), would be expected to impart macroscopic flexibility to PET polymers. In many cases, the combined losses of T_m , T_g and attainable crystallinity do not represent product improvements when these flexible units are incorporated into PET; phase separation can lead to complex rheology and difficulty in processing. Unlike PBT, which forms a phase-separated thermoplastic polyester–ether elastomer when copolymerized with PTMG [53], PET is not known to produce such elastomers without incorporation of additional modification of the polymer. Two flexible comonomers, PEG and polycaprolactone (PCL), dominate recent reports of such PET-based polymers.

Workers at AlliedSignal have developed a poly(ethylene terephthalate)–polycaprolactone block copolymer, commercialized for use in ‘load-leveling’ seat belt fabrics [54]. These block copolymers were prepared by reacting caprolactone monomer with PET homopolymer, in the presence of a tin catalyst, in a twin-screw extruder. The product of this reactive extrusion is a block copolymer with domains of polycaprolactone grown from the hydroxyl end groups of the starting PET core, with minimal randomization of the monomeric units (Figure 6.6). In fiber form, this polymer has been shown to be resistant to creep under normal use, but irreversibly deforms when elongated at high strain rates, such as those encountered in an automobile accident (hopefully minimizing bodily injury to the wearer of the seat belt, who would still remain restrained by the belt).

Block copolymers of PET and PEG, produced by copolymerization of terephthalate, ethylene glycol and PEG diol, have been shown to crystallize into two phases, each with unique crystallization behaviors [55]. Shrinkage experiments demonstrated that these copolymers could be subjected to as many as 20 fatigue cycles, each time returning to its original shape upon heating; this latter brought about melting and recrystallization of the PEG blocks of the polymers. The crystallization phenomena associated with the PET–PEG copolymers are complex,

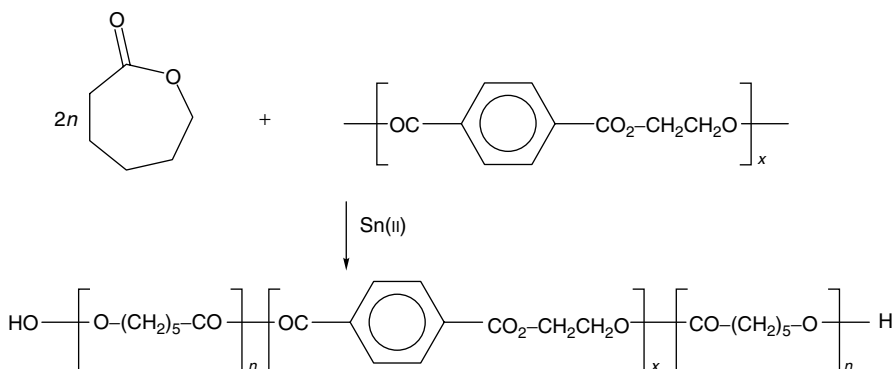


Figure 6.6 Reactive extrusion block copolymer of poly(ethylene terephthalate) and polycaprolactone

and defy simple models. Crystallization of the PEG blocks in these systems is constrained by the microstructure of the PET phases [56]. Because of the significant increase in equilibrium moisture content in the polymer as the PEG fraction is increased, it has been suggested that such PET-PEG copolymers are good candidates for biodegradation, especially in the presence of lipase enzymes [57].

While the thermo-mechanical properties of PET copolymerized with aliphatic diacids generally are unremarkable, workers at Eastman Chemical have reported that incorporation of 1–45 mol% of C3–C8 aliphatic acids, such as succinic acid or adipic acid, can lead to as much as a two-fold decrease in carbon dioxide permeability versus PET homopolymer [58]. This improvement can be explained by a decrease in the T_g , which leads to less supercooling of the polymer at room temperature (the temperature of interest in measuring loss of carbonation in soft drinks contained in polyester bottles); less supercooling leads directly to lower static free volume and lower gas solubility in the copolymer [59, 60]. Because the aliphatic diacid modifiers are highly flexible, these copolyesters exhibit enhanced intensity of their sub- T_g γ -transitions, which increase their dynamic free volumes and hence the diffusivity of gases through such aliphatic–aromatic copolyesters [60, 61]. In the case of the copolymers described by the Eastman workers, a large decrease in permeant gas solubility in the polymer is partially offset by higher diffusivity, but the overall effect is decreased permeation. With the lower T_g values and decreased gas permeation, the copolyesters of PET with aliphatic diacids are also more prone to creep under the pressure of carbonated beverages, rendering them unsatisfactory for such an application. The subject of structure–property effects upon gas solubility, diffusivity and permeation for quenched, annealed and oriented copolyesters has been intensively studied in recent years [9, 59–65], and can generally be predicted by the temperatures and intensities of the glass and gamma transitions, respectively. The permeation of water vapor [66], acetone [32] and hydrocarbons [67] through polyesters have also been investigated in recent years; not surprisingly, each of these permeations can be correlated with the free volumes existing in the polymers.

5 COPOLYMERS AS A SCAFFOLD FOR ADDITIONAL CHEMICAL REACTIONS

The incorporation of comonomers into PET and other polyesters, with the intent that these comonomers would then serve as the site for additional, post-polymerization reactions, has not been widely explored. A potential difficulty in such an approach is that the reactive comonomer cannot react under PET synthesis conditions of ca. 285 °C/2 h/Lewis acid catalyst if the modification is to be effective. Two such systems, stable under PET synthesis, and then subjected to post-polymerization reactions, have been recently reported.

Incorporation of 2,6-anthracene dicarboxylic acid (ADA), in up to 40 mol% concentration, has been shown to give materials that are higher T_g analogs to PET/naphthalate copolymers [68–72]. Diels–Alder cycloadditions across the central, 9/10 positions of anthracenes are well-established chemical reactions. Starting with PET/ADA copolymers containing 1–14 mol% ADA content, irreversible cycloadditions of a variety of maleimide dienophiles has been demonstrated as a means of grafting functional groups to the polyester chains [73]; use of bis-maleimides resulted in irreversible crosslinking of PET/ADA chains to one another (Figure 6.7) [68]. Photochemical dimerizations (assumed to be face-to-face, but potentially leading to ladder-like structures) of the random PET/ADA copolymers have been demonstrated again to be irreversible [69]. An intriguing aspect to all of these post-synthesis reactions is that these reactions can occur both in solution and in the melt, and that the equivalent reactions of the starting anthracene-based monomers are reversible. The reason for irreversibility in the polymeric systems is not well understood.

An alternative scheme for incorporating chemically reactive anthracene monomers made use of anthracene *mono*-carboxylic acid, therefore resulting in chain capping of the PET chains with anthracene units. Reaction (either in solution or via reactive extrusion) with bismaleimides resulted in chain extension, increasing polymer molecular weights from 6000–10 000 to 20 000–25 000 in as little as 3 min reaction time (Figure 6.8) [71, 72]. While such an approach could hold great promise for the rapid manufacture of polyesters, it should be pointed out that these chain-extended materials all were amorphous materials.

Another PET copolymer system that was recently demonstrated to be sufficiently stable to standard synthesis conditions, yet photochemically reactive, is that of PET–*p*-phenylene bisacrylic acid (PBA) (Figure 6.9) [74]. Upon UV irradiation, PET copolymers containing up to 15 mol% of PBA were shown to irreversibly undergo [2 + 2] cycloaddition reactions to produce lightly crosslinked, amorphous materials.

6 OTHER PET COPOLYMERS

6.1 TEXTILE-RELATED COPOLYMERS

It was previously mentioned that a large number of minor copolymers of PET have been developed over the past 50 years, with the intent of modifying textile fiber properties and processability [2, 3]. Of broader interest is that some of these textile modifications, such as PET copolymers with metal salts of 5-sulfoisophthalic acid (SIPA), have their own rich chemistries when the extent of polymer modification is increased beyond textile levels. An example of such a modification is that changing the counterions associated with SIPA can significantly effect the kinetics of polyester transesterification reactions (the

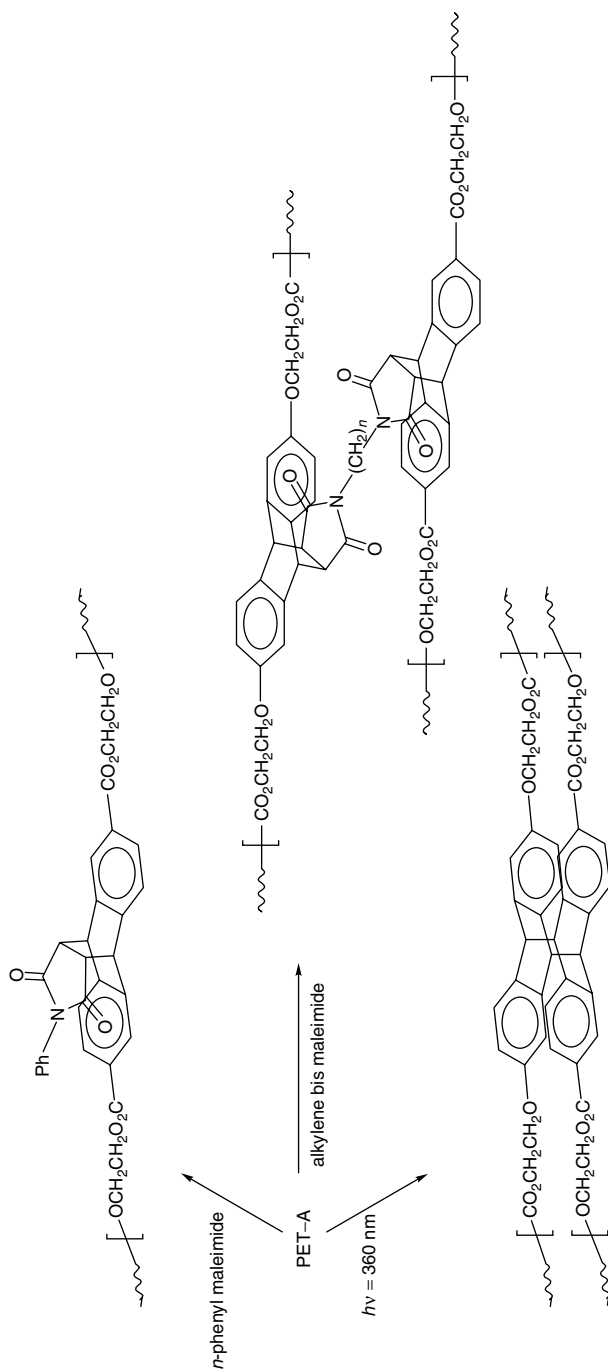


Figure 6.7 Reactions of PET-anthracene (A) copolymers

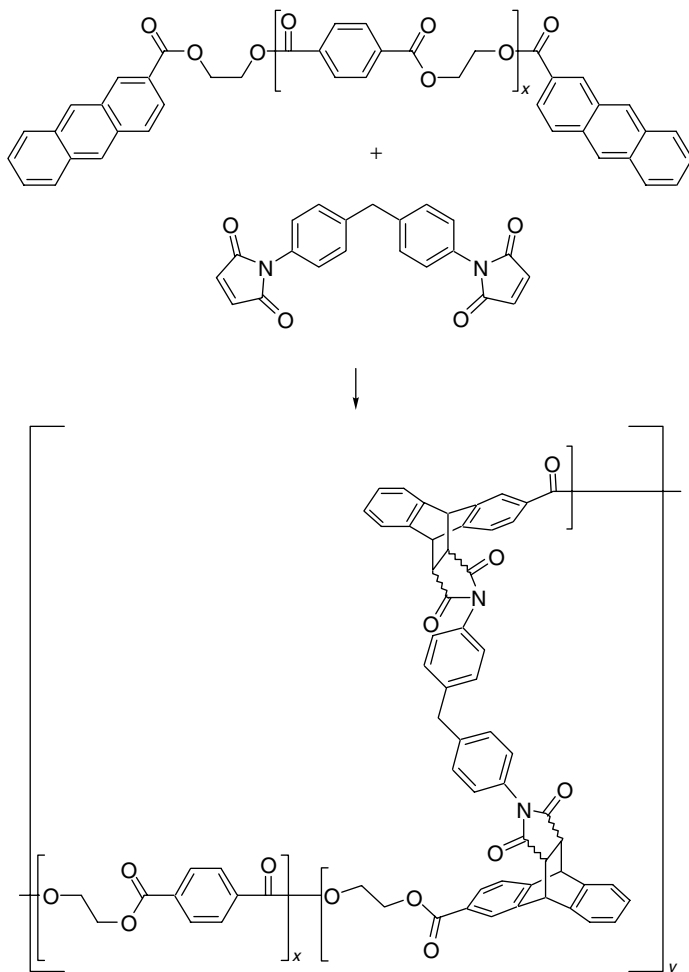


Figure 6.8 Extrusion chain extension of PET copolymers

counterions potentially serving as catalysts themselves) and of T_g , T_m , and temperature of crystallization (T_c) values for the copolymers [75]. A note of caution which should be made is that small changes in PET structure which are beneficial for fiber applications, such as light crosslinking [76] (beneficial for high-speed fiber spinning) can be highly detrimental in other applications (these same modifications limit orientation of barrier packaging materials) [60]. It is also important to note that introduction of ionic monomers, such as SIPA, generally lead to high polymer melt viscosities, thus confounding melt processing of these materials.

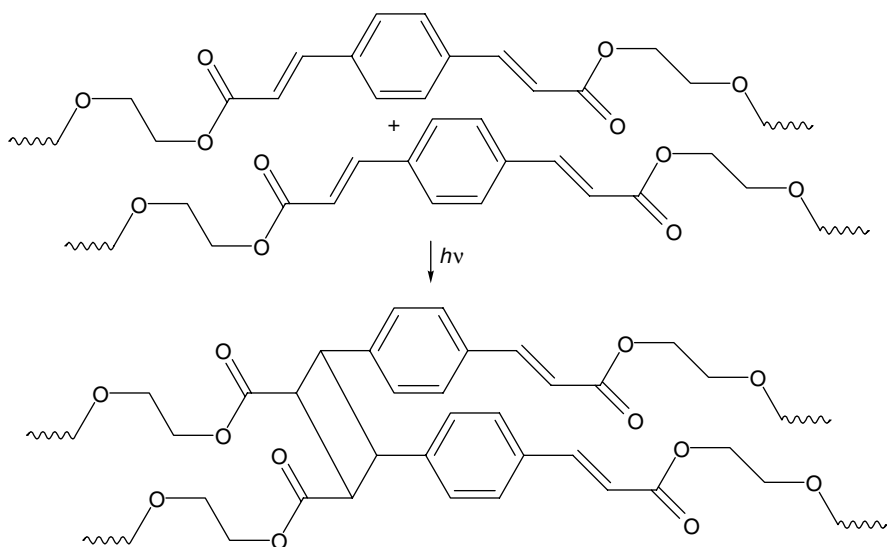


Figure 6.9 Photochemical crosslinking of a PET-*p*-phenylene bisacrylic acid (PBA) copolymer

6.2 SURFACED-MODIFIED PET

Another category of PET-based copolymers with low molar levels of modifications are the materials produced by surface modification. The reader is directed to recent papers for discussions of surface-energy modification by such processes [77, 78].

6.3 BIODEGRADABLE PET COPOLYMERS

Approaches to increasing the biodegradability of PET typically fall into the incorporation of either (i) polyethers, which increase the ambient moisture level (beyond the 0.3–0.4 wt% level of PET homopolymer [66, 79]) in addition to introducing organic radical sensitive units, and (ii) introduction of aliphatic diacid groups, such as succinate, for which catabolic pathways are widely found in nature [60, 80]. Using one or both of these substitutions into the PET backbone, various workers have demonstrated accelerated loss of mechanical integrity of PET copolymers exposed to enzymes, fungi and activated sludge [80]. A complete biodegradation of such copolymers to carbon dioxide and water, thereby actually removing the organic aromatics from an authentic ecosystem, has not yet been reported.

6.4 TEREPHTHALATE RING SUBSTITUTIONS

Copolymers of PET containing 5–75 mol% nitroterephthalic (NTA) units, were synthesized, found to be stable up to 300 °C, and demonstrated to have random distribution of the nitroaromatic groups throughout the polymer chain [81]. Introduction of the nitro groups resulted in increasing T_g values, and decreasing crystallinity as a function of substitution. Very similar results were obtained using 5-nitroisophthalate substitution levels of 5–50 mol% [82]. Prior work with methyl-substituted terephthalate [83], and with *t*-butyl isophthalate [12] again demonstrated increasing T_g levels, presumably due to hindered rotation of the substituted aromatic rings, as well as rapid loss of crystallinity as the substitution levels are increased.

6.5 FLAME-RETARDANT PET

Reduction of polymer flammability is of broad interest for applications ranging from plastics to textiles. For polyesters, given their inherent instability towards water at elevated temperatures, and the high temperatures of manufacture, many classes of flame-retardant (FR) agents, including most halogen-containing materials, are impractical. Phosphate esters, capable of incorporation into the polymer backbone, were pioneered by Hoechst AG, and continue to be the materials of choice [84, 85].

7 SUMMARY AND COMMENTS

The relatively simple chemistry of reacting diols with acids offers the availability of a rich variety of potential materials to the polymer chemist. Within those compositions that are based in part on poly(ethylene terephthalate), modifications offering practical industrial applications continue to dominate the literature. Strides have been made in the past decade towards higher modulus, higher service temperatures, impact, clarity and gas-barrier properties in PET copolymers. As global PET manufacturing capacity continues to grow, replacing older/smaller plants with large continuous commodity lines, opportunities to occupy the smaller plants with specialized copolymers would appear to represent a great opportunity for the current generation of chemists and polymer professionals. Exploitation of post-synthesis chemical reactions which further modify comonomers in a PET backbone, development of truly biodegradable PET-based materials, and continued development of higher temperature, stiffer, and tougher polyester copolymers all appear to be worthy goals.

REFERENCES

1. Whinfield, J. R., *Nature (London)*, **148**, 930 (1946).
2. Szego, L., *Adv. Polym. Sci.*, **31**, 89–131 (1979).
3. Schiraldi, D. A., Future trends in polyester polymers, in *Proceedings of the Fibres to Finished Fabrics Conference*, Prestburg, Manchester, UK, December 7–8, 1999, The Textile Institute, Manchester, UK, 1999.
4. Kleiner, H. J., Finke, M. and Bollert, U., *US Patent 3 941 752* (to Hoechst AG), 1976.
5. Bollert, U., Lohmar, E. and Ohorodnik, A., *US Patent 4 033 936* (to Hoechst AG), 1977.
6. Kibler, C. J., Bell, A. and Smith, J. G., *J. Polym. Sci., Part A*, **2**, 2115–2135 (1964).
7. Connor, D. M., Saliba, K. R., Jones, A. G., Collard, D. M., Liotta, C. L. and Schiraldi, D. A., *J. Appl. Polym. Sci.*, submitted for publication.
8. Schiraldi, D. A., unpublished data.
9. Polyakova, A., Stepanov, E. V., Sekelik, D., Schiraldi, D. A., Hiltner, A. and Baer, E., *J. Polym. Sci., Polym. Phys. Ed.*, **39**, 1911–1919 (2001).
10. Kelsey, D. R., Scardino, B. M., Grebpcwocz, J. S. and Chuah, H. H., *Macromolecules*, **33**, 5810–5818 (2000).
11. Schiraldi, D. A. and Connor, D. M., *US Patent 6 309 719* (to Artiva Specialties), 2001.
12. Fenoglio, J. and Foster, J. J., *J. Polym. Sci., Polym. Chem. Ed.*, **28**, 2753–2764 (1990).
13. Groeninckx, G., Berghmans, H., Overbergh, N. and Smets, G., *J. Polym. Sci., Part B*, **12**, 303–316 (1974).
14. Legras, R., Mercier, J. P. and Nield, E., *Nature (London)*, **304**, 432–434 (1983).
15. Jog, J. P., *Rev. Macromol. Chem. Phys.*, **C35**, 531–553 (1995).
16. Garcia, D., *J. Polym. Sci., Polym. Phys. Ed.*, **22**, 2063–2072 (1984).
17. Sakaguchi, Y., Okamoto, M. and Tanaka, I., *Macromolecules*, **28**, 6155–6160 (1995).
18. Sakaguchi, Y., *Polymer*, **38**, 2201–2207 (1997).
19. Pilati, F., Toselli, M., Messori, M., Manzoni, C., Turtutto, A. and Gattiglia, E. G., *Polymer*, **38**, 4469–4476 (1997).
20. Bouma, K., Groot, G. M. M., Feijen, J. and Gaymans, R. J., *Polymer*, **41**, 2727–2735 (2000).
21. van Bennekom, A. C. M. and Gaymans, R. J., *Polymer*, **38**, 657–665 (1997).
22. van Bennekom, A. C. M. and Gaymans, R. J., *Polymer*, **37**, 5439–5446 (1996).
23. van Bennekom, A. C. M., Willemsen, P. A. A. T. and Gaymans, R. J., *Polymer*, **37**, 5447–5459 (1996).

24. Gaymans, R. J., De Haan, J. L. and Vam Nieuwenhuize, O., *J. Polym. Sci., Polym. Chem. Ed.*, **31**, 575–580 (1993).
25. Williams, J. L. R., Laaskso, T. M. and Contois, L. E., *J. Polym. Sci.*, **61**, 353–359 (1962).
26. Williams, J. L. R. and Laaskso, T. M., *US Patent 2 851 443* (to Eastman Kodak), 1958.
27. Jackson, Jr, W. R. and Kuhfuss, H. F., *J. Appl. Polym. Sci.*, **25**, 1685–1694 (1980).
28. Nishikawa, T., Kinoshita, T. and Yotsumoto, T., *US Patent 5 391 699* (to Bridgestone Corporation), 1995.
29. Santa Cruz, C., Balta-Calleja, F. J., Zachmann, H. G. and Chen, D., *J. Mater. Sci.*, **27**, 2161–2164 (1992).
30. Aoki, Y., Li, L., Amari, T., Nishimura, K. and Arashiro, Y., *Macromolecules*, **32**, 1923–1929 (1999).
31. Guo, M. and Brittain, W. J., *Am. Chem. Soc., Div. Polym. Chem., Polym. Prepr.*, **39**(1), 385–386 (1998).
32. McDowell, C. C., Freeman, B. D., McNeely, G. W., Haider, M. I. and Hill, A. J., *J. Polym. Sci., Polym. Phys. Ed.*, **36**, 2981–3000 (1998).
33. Lu, X. and Windle, A. H., *Polymer*, **36**, 451–459 (1995).
34. Po', R., Occhiello, E., Giannotta, G., Pelosini, L. and Abis, L., *Polym. Adv. Technol.*, **7**, 365–373 (1996).
35. Collins, S., Kenwright, A. M., Pawson, C., Peace, S. K. and Richards, R. W., *Macromolecules*, **33**, 2974–2980 (2000).
36. Kotliar, A. M., *J. Polym. Sci., Macromol. Rev. Ed.*, **16**, 367–395 (1981).
37. Jackson, Jr, W. J. and Morris, J. C., Poly esters of 4,4'-biphenyl dicarboxylic acid and aliphatic glycols for high-performance plastics, in *Liquid Crystalline Polymers*, ACS Symposium Series, Vol. 453, American Chemical Society, Washington, DC, 1990, pp. 16–32.
38. Krigbaum, W. R., Asrar, J., Torkiumi, H., Ciferri, A. and Preston, J., *J. Polym. Sci., Polym. Lett. Ed.*, **20**, 109–115 (1982).
39. Schiraldi, D. A., Occelli, M. L. and Gould, S. A. C., *J. Ind. Eng. Chem.*, **7**(2), 67–71 (2001).
40. Schiraldi, D. A., Occelli, M. L. and Gould, S. A. C., *J. Appl. Polym. Sci.*, **82**, 2616–2623 (2001).
41. Jung, H.-T., Hudson, S. D. and Lenz, R. W., *Macromolecules*, **31**, 637–643 (1998).
42. Ma, H., Hibbs, H., Collard, D. M., Kumar, S. and Schiraldi, D. A., *Macromolecules*, **35**, 5123–5130 (2002).
43. Xiao, J., Wan, X., Zhang, D., Zhou, Q.-F. and Turner, S. R., *J. Polym. Sci. Polym. Chem. Ed.*, **39**, 408–415 (2001).
44. Chen, D. and Zachman, H. G., *Polymer*, **32**, 1612–1621 (1991).
45. Balta-Calleja, J. J., Santa Cruz, C., Chen, D. and Zachman, H. G., *Polymer*, **32**, 2252–2257 (1991).

46. Liu, Y., *Macromol. Chem. Phys.*, **202**, 2300–2305 (2001).
47. East, A. J. and Golder, M., Polyesters, thermoplastic, in *Kirk-Othmer Encyclopedia of Chemical Technology*, 4th Edn, Vol. 19, Wiley-Interscience, New York, 1996, pp. 641–647.
48. Kang, T.-K. and Ha, C.-S., *J Appl Polym Sci*, **73**, 1707–1719 (1999).
49. Liu, Y., Bu, H., Luise, R. R. and Bu, J., *J. Appl. Polym. Sci.*, **79**, 497–503 (2001).
50. Liu, Y., Jin, Y., Dai, L., Bu, H. and Luise, R. R., *J. Appl. Polym. Sci.*, **77**, 369–377 (1999).
51. Li, X.-G., Huang, M.-R., Guan, G.-H. and Sun, T., *J. Appl. Polym. Sci.*, **66**, 2129–2138 (1997).
52. Shaban, H. I., Al-Adwani H., Behbehani, A. and Mathew, J., *Eur. Polym. J.*, **37**, 2281–2293 (2001).
53. Cella, R. J., *J. Polym. Sci. Polym. Symp. Ed.*, **42**, 727–740 (1973).
54. Tang, W., Murthy, N. S., Mares, F., McDonnell, M. E. and Curran, S. A., *J. Appl. Polym. Sci.*, **74**, 1858–1867 (1999).
55. Ma, D., Wang, M., Wang, M., Zhang, X. and Luo, X., *J Appl Polym Sci*, **69**, 947–955 (1998).
56. Kong, X., Tan, S., Yang, X., Li, G., Zhou, E. and Ma, D., *J. Polym. Sci., Polym. Phys. Ed.*, **38**, 3230–3238 (2000).
57. Nagata, M., Kiyotsukuri, T., Minami, S., Tsutsumi, N. and Sakai, W., *Polym. Int.*, **39**, 83–89 (1996).
58. Weemes, D. A., Seymour, R. W. and Wicker, T. H., *US Patent 4401 805* (to Eastman Kodak Company), (1983).
59. Light, R. R. and Seymour, R. W., *Polym. Eng. Sci.*, **22**, 857–864 (1982).
60. Polyakova, A., *Ph.D. Dissertation*, School of Macromolecular Science, Case Western Reserve University, Cleveland, OH, 2000.
61. Qureshi, N., *M. Sc. Dissertation*, School of Macromolecular Science, Case Western Reserve University, Cleveland, OH, 2000.
62. Polyakova, A., Schiraldi, D. A., Hiltner, A. and Baer, E., *J. Polym. Sci., Polym. Phys. Ed.*, **39**, 1889–1899 (2001).
63. Polyakova, A., Connor, D. M., Collard, D. M., Schiraldi, D. A., Hiltner, A. and Baer, E., *J. Polym. Sci. Polym. Phys. Ed.*, **39**, 1900–1910 (2001).
64. Qureshi, N., Stepanov, E. V., Schiraldi, D. A., Hiltner, A. and Baer, E., *J. Polym. Sci., Polym. Phys. Ed.*, **38**, 1679–1686 (2000).
65. Liu, R. Y. F., Schiraldi, D. A., Hiltner, A. and Baer, E., *J. Polym. Sci., Polym. Phys. Ed.*, **40**, 862–877 (2002).
66. Launay, A., Thominet, F. and Verdu, J., *J. Appl. Polym. Sci.*, **73**, 1131–1137 (1999).
67. Dhoot, S. N., Freeman, B. D., Stewart, M. E. and Hill, A. J., *J. Polym. Sci., Polym. Phys. Ed.*, **39**, 1160–1172 (2001).
68. Jones, J. R., Liotta, C. L., Collard, D. M. and Schiraldi, D. A., *Macromolecules*, **32**, 5786–5792 (1999).

69. Jones, J. R., Liotta, C. L., Collard, D. M. and Schiraldi, D. A., *Macromolecules*, **33**, 1640–1645 (2000).
70. Kriegel, R. M., Collard, D. M., Liotta, C. L. and Schiraldi, D. A., *Macromol. Chem. Phys.*, **202**, 1776–1781 (2001).
71. Kriegel, R. M., *Ph.D. Dissertation*, School of Chemistry and Biochemistry, Georgia Institute of Technology, Atlanta, GA, 2001.
72. Schiraldi, D. A., Kriegel, R. M. and Collard, D. M., *Abstract, PMSE Paper 239*, 221st ACS National Meeting, San Diego, CA, April 2001.
73. Vargas, M., Kriegel, R., Collard, D. C. and Schiraldi, D. A., *J. Polym. Sci., Polym. Chem. Ed.*, **40**, 3256–3263 (2002).
74. Vargas, M., Collard, D. M., Liotta, C. L. and Schiraldi, D. A., *J. Polym. Sci., Polym. Chem. Ed.*, **38**, 2167–2176 (2000).
75. Boykin, T. L. and Moore, R. B., *Polym. Chem. Polym. Prepr.*, **39**(1), 393–394 (1998).
76. Hess, A., Hirt, P. and Oppermann, W., *J. Appl. Polym. Sci.*, **74**, 728–734 (1999).
77. Cohn, D. and Stern, T., *Macromolecules*, **33**, 137–142 (2000).
78. Yuhai, G., Jianchun, Z. and Meiwu, S., *J. Appl. Polym. Sci.*, **73**, 1161–1164 (1999).
79. Hansen, S. M. and Sargeant, P. B., *Kirk-Othmer Encyclopedia of Chemical Technology*, 4th Edn, Wiley-Interscience, New York, Vol. 10, 1996, pp 761–787.
80. Maeda, Y., Maeda, T., Yamaguchi, K., Kubota, S., Nakayama, A., Kawasaki, N. and Aiba, Y. S., *J. Polym. Sci., Polym. Chem. Ed.*, **38**, 4478–4489 (2000).
81. Kint, D. P. R., Martínez De Ilarduya A. and Muñoz-Guerra S., *J. Polym. Sci., Polym. Chem. Ed.*, **38**, 3761–3770 (2000).
82. Kint, D. P. R., Martínez De Ilarduya A. and Muñoz-Guerra S., *J. Polym. Sci., Polym. Chem. Ed.*, **38**, 1934–1942 (2000).
83. Lincoln, J., *US Patent 2 692 248* (to British Celanese Ltd.), (1951).
84. Kleiner, H.-J., Finke, M., Bollert, U. and Herwig, W., *US Patent RE 30 783* (to Hoechst AG), (1980).
85. Asrar, J., Berger, P. A. and Hurlbut, J., *J. Polym. Sci., Polym. Chem. Ed.*, **37**, 3119–3128 (1999).

7

Amorphous and Crystalline Polyesters based on 1,4-Cyclohexanedimethanol

S. R. TURNER, R. W. SEYMOUR AND J. R. DOMBROSKI
Eastman Chemical Company, Kingsport, TN, USA

NOTATION

CHDA	<i>cis/trans</i> -1,4-cyclohexanedicarboxylic acid
CHDM	<i>cis/trans</i> -1,4-cyclohexanedimethanol
DMCD	dimethyl <i>cis/trans</i> -1,4-cyclohexanedicarboxylate
EG	ethylene glycol
IPA	isophthalic acid
N	dimethyl 2,6-naphthalenedicarboxylate
NDA	2,6-naphthalenedicarboxylic acid
PCT	poly(1,4-cyclohexylenedimethylene terephthalate)
PCTA	dibasic-acid-modified PCT copolyester
PCTG	glycol-modified PCT copolyester
PET	poly(ethylene terephthalate)
PETG	CHDM-modified PET copolyester
TMCD	<i>cis/trans</i> -2,2,4,4-tetramethyl-1,3-cyclobutanediol
TPA	terephthalic acid

1 INTRODUCTION

Polyesters are highly versatile materials, which have gained increasingly important uses for packaging plastics, films, sheeting and resins for molding precision

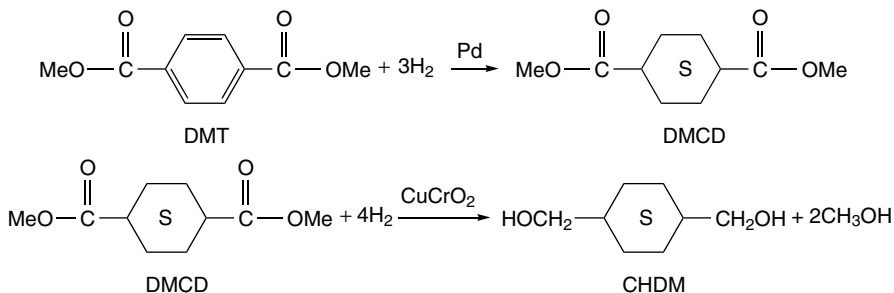
parts for medical and electronics applications. Since the first reported preparation of high-molecular-weight polyesters by Carothers and Hill in 1932 [1], many technologically important advances have been made in the synthesis, commercial development, and especially the identification of a broad array of new market applications for these materials. The scope of polyester compositions can be roughly divided into three broad categories: aliphatic, aromatic, and partly aromatic polyesters. Aliphatic-based polyesters are generally defined as polyesters prepared from an aliphatic dibasic acid and an aliphatic diol, or combinations of different aliphatic diacids and aliphatic diols. It has been well established and documented that aliphatic-based polyesters are characterized as having low melting points and poor hydrolytic stability [2–4]. Thus, the commercial utility of aliphatic-based polyesters for general plastics applications have been severely restricted by these inherent properties. Aromatic polyesters, also referred to as polyarylates, are compositions prepared from aromatic dibasic acids such as terephthalic acid (TPA) and/or isophthalic acid (IPA) and an aromatic diol, such as bisphenol-A, or diphenols [5]. Polyarylates have many desirable physical properties useful for high-performance plastics applications, but have not yet achieved large usage in the marketplace on a cost/performance basis. On the other hand, the commercial importance and application of partly aromatic-based polyesters has grown tremendously since the pioneering work reported by Whinfield and Dickson in 1946 [6]. This work is of particular importance since it led to the understanding that partly aromatic polyesters, such as poly(ethylene terephthalate) (PET), are semicrystalline, high melting and hydrolytically stable. These properties have been found to be especially desirable, and have led to the innovation and commercialization of partly aromatic polyesters and copolyesters for fibers, films and molding plastics [7]. Since the early work on PET, one of the most noteworthy variations on this composition came about with the discovery of linear polyesters prepared from terephthalic acid (TPA) and 1,4-cyclohexanedimethanol (CHDM) and revealed in the patent by Kibler *et al.* in 1959 [8]. The incorporation of CHDM in partly aromatic polyester compositions has resulted in the development of a diverse family of commercially important polyesters with properties ranging from amorphous to highly crystalline. The first major commercialization of CHDM in polyesters was the TPA/CHDM homopolyester as a textile fiber [9]. A major jump in PET consumption occurred in the mid-1970s following the commercial development of technology for stretch blow molding containers for the carbonated soft drink market [10]. Low-level incorporation of CHDM into PET was an important enabler in the development of PET for this application area in the 1980s [11, 12]. PET modified with less than about 5 mol % CHDM has experienced widespread use as a resin for this market application because of improved molding properties by widening the processing window and imparting high clarity resulting from modification of the crystallization properties of the resin. From 1982 to the present time, a family of CHDM-based polyesters has been commercially developed to meet

a diverse range of market applications, including food and medical packaging, molding resins for precision medical and electronics components, consumer applications, sheeting for signage and point-of-sale displays, and extruded tubing and profiles.

This report provides an overview of some of the newer polyester compositions based on CHDM. The basic properties and chemistries of PCT have been described in earlier reviews [9, 13]. The CHDM-based polyesters covered in this review are PCT, PCTG, PCTA, and PETG. These compositions are described in more detail in the sections that follow.

2 1,4-CYCLOHEXANEDIMETHANOL

CHDM is the major glycol used to prepare PCT, PCTG and PCTA polyesters, but is the minor glycol in the PETG composition. CHDM is manufactured by catalytic hydrogenation of dimethyl terephthalate (DMT) and was first revealed in patents issued to Eastman Kodak Company [14, 15]. A number of other CHDM synthesis patents have since been issued and describe catalysts and process technology for hydrogenation of TPA or dimethyl 1,4-cyclohexanedicarboxylate (DMCD) [16–19]. The two key steps in the reduction of DMT to CHDM are depicted as follows:



The Eastman Chemical Company is the sole producer of CHDM in the USA. CHDM is typically produced as a mixture of *cis*- and *trans*-isomers, with an equilibrium ratio of approximately 30/70 *cis/trans*. Additional patents disclose technology for affecting the CHDM isomer ratio [19] and for isomerization of *cis*-CHDM to *trans*-CHDM [14]. Most commercial CHDM polyesters are prepared from the approximately 30/70 *cis/trans* ratio, with this isomer ratio being maintained throughout the polymerization process. The effect of the *cis*- and *trans*-CHDM isomer ratio on the melting point of terephthalate-based polyester has been previously studied and reported [9, 20]. This relationship is shown in Figure 7.1.

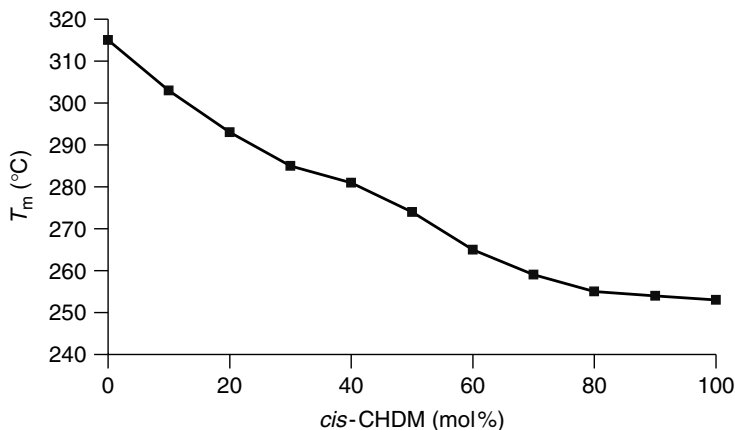


Figure 7.1 Effect of CHDM *cis/trans* ratio on the melting points of poly(1,4-cyclo-methylene terephthalate)s

A continuous increase in melting point occurs from the 100 % *cis* to the 100 % *trans* polyester. No eutectic composition in the melting or crystallization curves is observed over the entire *cis/trans* range. The investigators concluded that this trend occurs because polyester molecules containing *cis*-CHDM can fit readily into the crystalline lattice of the polyester containing the *trans*-CHDM, and vice versa [20]. Furthermore, the lower melting temperature of the *cis*-based polyester is attributed to a reduced symmetry of the repeating unit, relative to the analogous *trans*-based polyester [9].

It is well established that the physical properties of CHDM-based polyesters are influenced not only by the isomer ratio, but also by copolymerization with other common diols and diacids. This factor will be discussed in more detail below. An additional influence on the physical properties is brought about by the understanding that the cyclohexane ring of CHDM can exist as either a chair or boat conformation, and the substituents can be either in the axial or equatorial positions [9, 20]. Such structural attributes ultimately influence chain packing, sub- T_g molecular motions, gas transport properties and other important properties of CHDM-based polyesters [21]. The effect of the cyclohexylene unit on secondary relaxation and mechanical properties for a series of CHDM-based copolyesters has been studied recently by Chen *et al.* [22]. Their results support the hypothesis that dynamic fluctuations induced by motion of the cyclohexylene group makes yielding a more efficient process for these copolyesters. They point out that the decrease in yield stress may be attributed in part to conformational changes of the cyclohexylene group [23].

CHDM is thus a highly versatile monomer for producing polyesters that can be tailored to achieve a wide range of physical properties for a broad range of end-use applications.

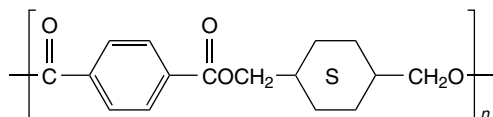
3 1,3- AND 1,2-CYCLOHEXANEDIMETHANOL: OTHER CHDM ISOMERS

1,3- and 1,2-CHDM can be prepared by hydrogenation of dimethyl isophthalate and dimethyl phthalate, respectively. Several patents have been issued revealing processes to the 1,3-derivative [24–26]. Linear, high-molecular-weight polyesters based on the 1,3 isomer of CHDM have not been commercially developed, and physical properties of polymers prepared from this monomer are only sparingly reported in the literature [27–31]. Early work with this monomer for the preparation of terephthalate-based polyesters indicates that key physical properties, especially impact strength, are generally inferior to equivalent polyester compositions prepared from 1,4-CHDM. Thus, current interest in 1,3-CHDM appears to be driven by its potential utility for the preparation of low-molecular-weight polyesters for coatings applications and as an extender for polyurethanes [32, 33]. The 1,2-isomer of CHDM appears to have even less utility for synthesis of high-molecular-weight polyesters. Attempts to incorporate 1,2-CHDM monomer in polyesters by conventional melt-phase polymerization processes result in the production of high levels of cyclic oligomers and poor conversion to linear, high-molecular-weight polymer.

3.1 DEFINITIONS: PCT, PCTG, PCTA AND PETG

The following definitions have been traditionally used in the trade to describe the range of CHDM-based polyester compositions:

- *PCT* describes a polyester composition prepared from CHDM and DMT (or TPA). The abbreviation PCT is thus derived from the technical name for the polymer, i.e. poly(1,4-cyclohexylenedimethylene terephthalate), or PCT. This material is a highly crystalline, high-melting polyester, with the following structure:

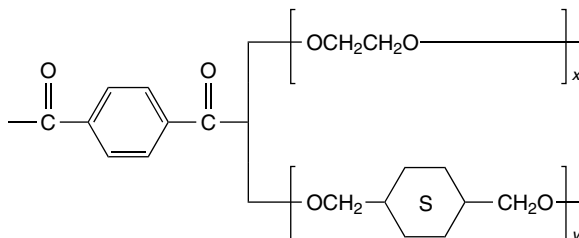


PCT: poly(1,4-cyclohexylenedimethylene terephthalate)

- *PCTG* refers to a glycol-modified PCT copolyester. Ethylene glycol (EG) has been found to be an effective and economical glycol for preparation of PCTGs having desirable processing and end-use properties. Thus, PCT polyesters with EG modification up to 50 mol% are referred to as PCTGs (see structure below). Polyesters within this compositional range have exceptional clarity

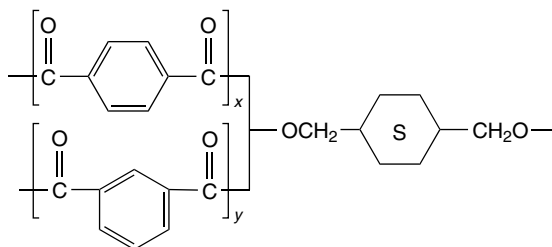
and good impact resistance. PCTG is mostly used in injection molding and is favored for its toughness and ability to precision mold thin-wall parts.

- PET modified with up to 50 mol% CHDM is referred to as *PETG*. This resin is by far the most widely used of the CHDM-based polyesters.



Structure represents PETG when x is the major glycol component
 Structure represents PCTG when y is the major glycol component

- *PCTA* likewise refers to an acid-modified PCT copolyester. Isophthalic acid (IPA), or alternatively the dimethyl ester of IPA, is the most commonly used modifying dibasic acid to prepare PCTA copolyesters. PCTA thus refers to PCT compositions modified with up to 50 mol% IPA. The PCTA structure is as follows:



Structure represents PCTA when $y \leq 50$ mol% IPA

4 SYNTHESIS OF CHDM-BASED POLYESTERS

PCT, PETG, PCTG and PCTAs can all be prepared readily via standard melt-phase polycondensation processes [34, 35]. The diacid can be delivered via transesterification of the dimethyl esters or via direct esterification of the diacids. Numerous conventional catalyst and catalyst combinations can be employed. The use of a catalyst or catalyst combination is important for the manufacture of polyesters via the melt-phase process and has been well reported in the literature [36–41]. Appropriate catalyst systems enable the production of polyesters with high processing rates and high molecular

weight, while minimizing undesirable side reactions such as color formation. Commonly used catalysts include various oxides and acetates of metal ions, particularly zinc, antimony, manganese, germanium, and the like. In addition, tetraalkyltitanates are widely used ester-interchange catalysts. Catalyst technology for the manufacture of CHDM-based polyesters has been primarily disclosed in the patent literature [42–50]. Crystalline PCT and PCTAs can be prepared to modest molecular weights in the melt phase and solid-state polymerized to useful molecular weight ranges. For amorphous copolyesters, useful molecular weight ranges must be achieved entirely in the melt phase. This can be a difficult constraint for the practical preparation on a commercial scale for some compositions where elevated low shear melt viscosities hinder achieving high molecular weight without the formation of unwanted degradation products.

Although it is well established that CHDM forms well-defined, high-molecular-weight polyesters with terephthalic acid and/or isophthalic acid by conventional melt-phase polymerization processes, the same is not true for polymerization with orthophthalic acid or phthalic anhydride. Thus, conventional melt-phase esterification procedures do not permit the production of high-molecular-weight polyesters from CHDM and *o*-phthalic acid or phthalic anhydride. However, an alternate procedure has been described for the preparation of CHDM-based polyesters from these materials by conducting the esterification/polyesterification reaction in a refluxing solvent in the presence of a catalyst and azeotroping out the water produced [51]. This process requires use of substantially equimolar amounts of CHDM and *o*-phthalic acid or phthalic anhydride and that the *o*-phthalic acid or anhydride component must be anhydrous before use. Thus, slight imbalances in the acid and glycol will limit the molecular weight of the resulting polyester. Appropriate solvents include toluene, xylene, chlorobenzene, and the like.

5 POLY(1,4-CYCLOHEXYLENEDIMETHYLENE TEREPHTHALATE)

5.1 PREPARATION AND PROPERTIES

The primary crystalline polymer based on CHDM is the terephthalate, poly(1,4-cyclohexylenedimethylene terephthalate) (PCT). This polyester was originally developed for fiber applications but has since found wider utility as a reinforced polymer for injection molding and (when copolymerized with a small amount of isophthalic acid) as a material for crystallized food packaging trays. The key property of PCT which sets it apart from other thermoplastic polyesters in these latter applications is its melting point.

When made with the normal 70/30 *trans/cis* CHDM isomer ratio, the melting point of PCT is about 290 °C. The melting point varies substantially with isomer

Table 7.1 Effect of *cis*-isomer content on the gas-barrier properties of PCT

<i>cis</i> -CHDM content (%)	Oxygen permeability (cc mil)/(100 in ² 24 h atm)
93	15
46	31
26	40

ratio, however, as mentioned previously (see Figure 7.1) [20]. For comparison, the melting point of PBT is 225 °C and that of PET is in the range of 250–260 °C. The CHDM isomer ratio also has an effect on gas-barrier properties, with a better barrier resulting from higher *cis* levels. A recent patent [52] discloses that PCT with 93/7 *cis/trans* CHDM ratio containing 50 % of 2,6-naphthalene dicarboxylic acid has an unexpectedly low permeability of 2.68 (cc mil)/(100 in² 24 h atm). This compares with an oxygen permeability of 6.51 (cc mil)/(100 in² 24 h atm) for a similar composition prepared with a nearly 50/50 *cis/trans* CHDM ratio. Because of the higher local free volume contributed by the CHDM structure, the diffusivity through PCT is generally higher than that through denser structures like PET [21]. However, the magnitude of this effect is strongly dependent on the isomer ratio, as shown in Table 7.1.

Crystallization of PCT is relatively rapid, but because of its higher T_g (90 °C) the maximum rate of crystallization occurs at a higher temperature than is typical of other crystalline polymers such as PET (T_g at about 70 °C) or PBT (T_g at about 35 °C). Figure 7.2 compares the crystallization half-times of PET and PCT from both the glass and the melt (data were obtained via DSC measurements). The effect of the higher T_g on the temperature of maximum crystallization rate (i.e. minimum half-time) is most clearly seen in the data from the melt. The basic rapid crystallization rate of PCT allows it to be used as a high-performance injection molding material.

The bulky in-chain CHDM moiety results in several other important differences between PCT and other crystallizable polyesters such as PET. The amorphous density is significantly lower, with PCT being 1.195 g/ml. compared to 1.334 g/ml for PET. PCT also exhibits a strong sub- T_g molecular relaxation, which results in a relatively low modulus at room temperature (155 MPa versus 240 MPa for PET). The downward shift in modulus and upward shift in relaxation strength are evident in the dynamic mechanical curves shown in Figures 7.3 and 7.4. In each figure, the effect of increasing CHDM at the expense of ethylene glycol is shown.

The strong sub- T_g relaxation in PCT also contributes to increased toughness of this polymer in the amorphous state. When measured on amorphous specimens, the notched Izod impact strength of PCT is greater than 1000 J/m, while that of PET is less than 100 J/m [22].

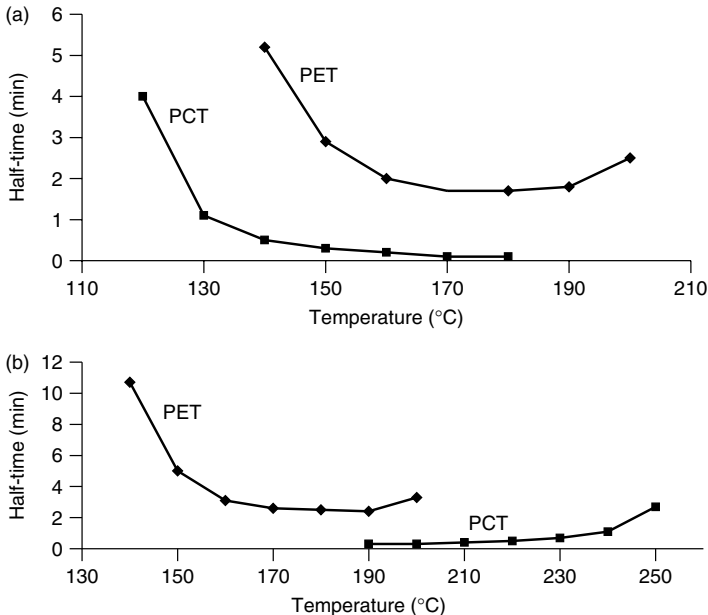


Figure 7.2 Crystallization half-times for PET and PCT from (a) the glassy state, and (b) the melt

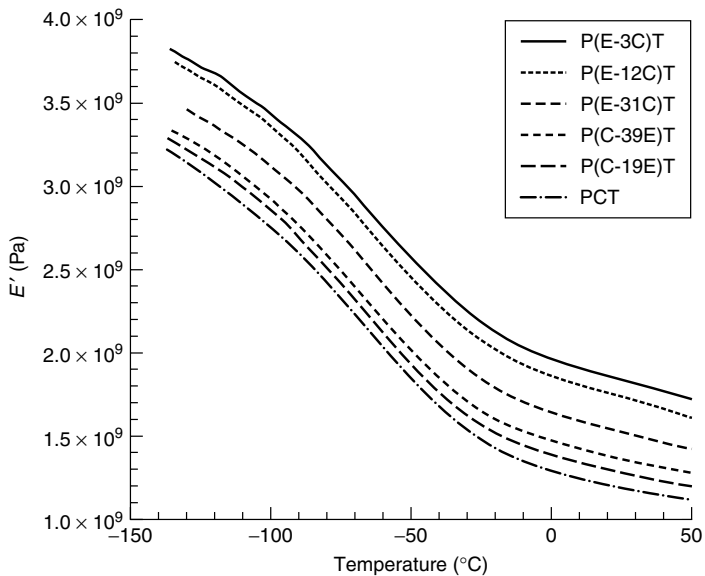


Figure 7.3 Storage moduli of polyesters prepared from PET modified with 3 mol% of CHDM (relative to PCT)

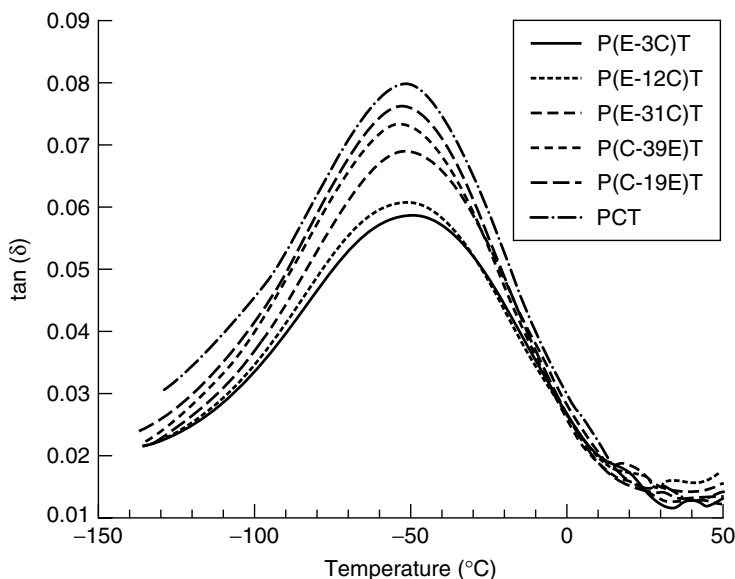


Figure 7.4 Dynamic mechanical loss curves of polyesters prepared from PET modified with 3 mol% of CHDM (relative to PCT)

Preparation of PCT is best accomplished from dimethylterephthalate (DMT) using standard transesterification catalysts such as titanium. Because of the high melting point of the polymer, final polyesterification temperatures must be high (greater than 300 °C at typical commercial *trans/cis* ratios) [27]. PCT prepared in the melt phase can be crystallized and then solid-phase polymerized to obtain even higher molecular weights. Solid-phase polymerization is generally carried out within the temperature range of 200–250 °C.

5.2 OTHER CRYSTALLINE POLYMERS BASED ON PCT OR CHDM

If PCT is modified with relatively high levels of comonomer, substantially amorphous materials result (see the following sections on PETG, PCTG and PCTA). However, it is possible to maintain crystallinity at lower levels of modification. For example, replacing up to about 10 mol% of the terephthalate units with isophthalate results in a polymer with reasonable crystallization rates and ultimate degrees of crystallinity.

One might expect that completely replacing the terephthalate unit in PCT with naphthalene dicarboxylate would make an interesting high-temperature polymer. However, such a polymer cannot be successfully prepared, because its melting point is above its degradation temperature. Reduction of the melting

point by copolymerization (for example, either with terephthalate or isophthalate) eliminates this problem.

Crystalline polyesters from CHDM and aliphatic diacids are possible, but generally of little interest because of low melting points and low glass transition temperatures. Cyclic aliphatic diacids offer some potentially attractive possibilities. For example, the polyester of CHDM with a high-*trans* isomer 1,4-cyclohexanedicarboxylate has a melting point ($\sim 225^{\circ}\text{C}$) similar to that of PBT [53].

5.3 PROCESSING OF CRYSTALLINE PCT-BASED POLYMERS

Melt processing of the high-melting PCT-type polymers must be carried out carefully, owing to a relatively small window between the melting point and the temperature at which degradation rates become significant. The degradation is both thermal and hydrolytic in nature. While it may be argued that the PCT structure is inherently more hydrolytically stable than other polyesters such as PET, the higher processing temperature compensates by accelerating the rate. Thus drying of the polymer or formulation before processing is recommended. Dessiccant drying at temperatures up to about 125°C is commonly used. Degradation results in color formation, loss of molecular weight, and deterioration of critical mechanical properties such as toughness.

5.4 APPLICATIONS FOR PCT-BASED POLYMERS

5.4.1 Injection Molding

PCT forms the basis of a family of reinforced, crystalline plastics for injection molding. As mentioned above, the high melting point of the polymer is a key property, as this results in high heat deflection temperatures (HDTs) in glass-fiber-reinforced formulations. Good toughness, flow into the mold, and rapid crystallization are also important in these applications.

Formulations for injection molding typically contain 30–40 wt % of glass fiber, or a mixture of glass fiber and mineral filler. Stabilization packages to improve processing stability and additives to enhance crystallization rate are also incorporated. As discussed previously, PCT has a reasonably high rate of crystallization, but it is often desirable to reduce the crystallization temperatures. This correspondingly reduces the mold temperature required to obtain crystallized parts, thus making processing of the formulation easier. PCT-based products may be flame-retarded or not, depending on the application area, with heat deflection temperatures (HDTs) ranging from about 250 to about 260°C . This level of heat resistance makes PCT-based plastics suitable for high-temperature applications such as electronic connectors where high soldering temperatures are encountered during the manufacturing process. (Figure 7.5). Typical competitive materials in

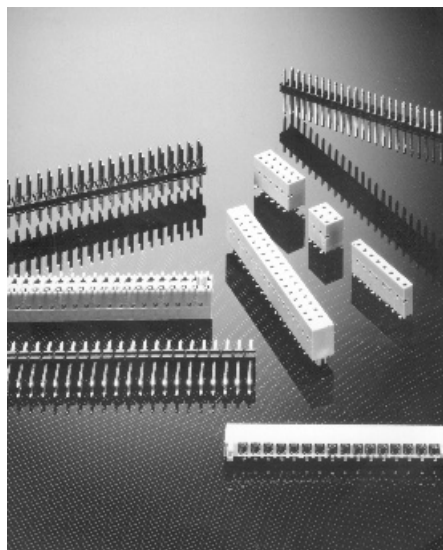


Figure 7.5 Electrical connectors molded from GFR Eastman crystalline PCT. Photograph provided by courtesy of Eastman Chemical Company

this market include poly(phenylene sulfide), with an HDT of about 260 °C, and high-temperature polyamides, with HDTs in the range of 270–280 °C. Other properties of a typical 30 % glass-reinforced, flame-retarded grade of PCT are shown in Table 7.2.

Flame-retarded grades are widely used for various computer connectors and circuit board components. Representative applications are edge card connectors, grid arrays and memory modules. Non-flame-retarded grades find use in automotive ‘under-the-hood’ applications, typically connectors and related parts. As higher temperature soldering techniques become more common in the automotive industry, the use of high-temperature plastics such as PCT is expected to increase. It is also possible to formulate unreinforced PCT with crystallization aids and

Table 7.2 Properties of 30 % glass-fiber-reinforced flame-retarded PCT

Parameter	Value
Specific gravity	1.63
Tensile strength (MPa)	120
Tensile elongation (%)	2
Flexural modulus (MPa)	9600
Notched Izod impact (J/m)	90
HDT, at 1.82 MPa (°C)	255
UL Subject 94 Flammability	V0

tougheners to provide a material similar in some respects to 'supertough' nylon. PCT provides advantages in dimensional stability and lower moisture sensitivity when compared to the polyamide-based products.

5.4.2 Extrusion

A well-established application for extruded unreinforced PCT (copolymerized with isophthalate) is crystallized, thermoformed trays for foods. Crystallized PET is widely used for this application, but where higher-temperature performance is needed the PCT-based polymer may be chosen. Such trays are formed from extruded sheet, using a hot mold to promote crystallization. Isophthalate-modified PCT polymers are approved by the Food and Drug Administration for high-temperature food contact use.

The good hydrolytic stability of PCT-based polymers leads to applications for monofilament in paper machine belts. Monofilament is extruded from high-molecular-weight polymer, drawn and crystallized, and then woven into a screen. Such belts are found in the drying sections of paper machines, where there is a combination of high moisture and high temperature. Because of their hydrolytic stability, PCT-based polymers provide much longer service life in this application than PET-based materials.

6 GLYCOL-MODIFIED PCT COPOLYESTER: PREPARATION AND PROPERTIES

Modification of PCT with up to 50 mol % of ethylene glycol (EG) results in copolyester compositions (PCTGs) with very slow crystallization rates and are therefore regarded as amorphous polyesters. The effect of increasing the EG content of PCTG copolyesters is noted by the dramatic drop-off in crystalline melting point. This effect is shown in Figure 7.6. By way of this example, it should be noted that the normally amorphous PCTG copolyester compositions were intentionally induced to crystallize by an extensive heat treatment process (i.e. extruded copolyester film was crystallized by drafting in steam, and then heatset at constant length for 1 h at 140 °C).

PCTG copolyesters can be processed by extrusion or injection molding into articles having desirable combinations of clarity and high toughness. In particular, PCTG copolyester prepared with about 40 mol % of EG has excellent clarity and toughness and has gained favorable market acceptance for injection molding thin-wall medical components. PCTG is especially well suited for molding such components since it has excellent resistance to gamma-ray sterilization and retains its high elongation to break [54]. The properties of a PCTG sample based on TPA as the diacid and with about 65 % of CHDM and 35 % of EG are shown below in Table 7.3. These properties are compared to those of a PETG and PCTA sample

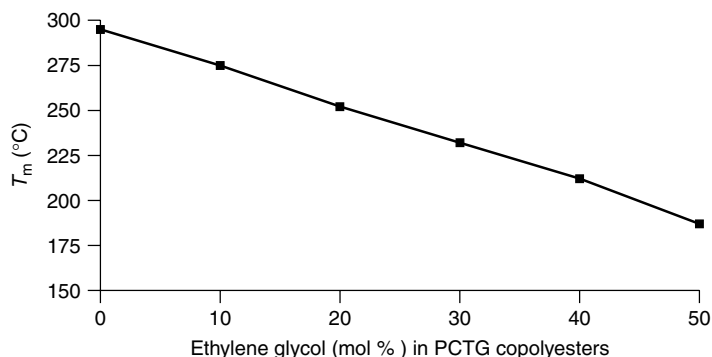


Figure 7.6 Effect of ethylene glycol concentration on the crystalline melting temperature of PCTG copolyesters

Table 7.3 Physical property comparison of amorphous PETG, PCTG and PCTA

Property	PETG	PCTG	PCTA
<i>Specific gravity</i>	1.27	1.23	1.20
<i>Thermal properties</i>			
T_g (°C)	81	84	88
HDT, at 0.455 MPa (°C)	70	74	75
HDT, at 1.82 MPa (°C)	64	65	65
<i>Tensile properties</i>			
Stress at yield (MPa)	50	45	47
Stress at break (MPa)	28	52	51
Elongation at yield (%)	4.3	5	5
Elongation at break (%)	110	330	300
<i>Flexural properties</i>			
Flexural modulus (MPa)	2100	1900	1800
Flexural yield strength (MPa)	70	66	69
<i>Izod impact strength^a</i>			
Notched at 23°C (J/m)	101	NB	80
Unnotched at 23°C (J/m)	NB	NB	NB
Notched at -40°C (J/m)	37	64	40
Unnotched at -40°C (J/m)	NB	NB	NB

^a NB, no break.

(described in the next sections) and show the enhanced toughness imparted to the structure from the CHDM moiety in the backbone.

7 CHDM-MODIFIED PET COPOLYESTER: PREPARATION AND PROPERTIES

CHDM is a very effective crystallization modifier for PET and as stated earlier low-level modification yields crystalline polyesters (PETGs) that are important

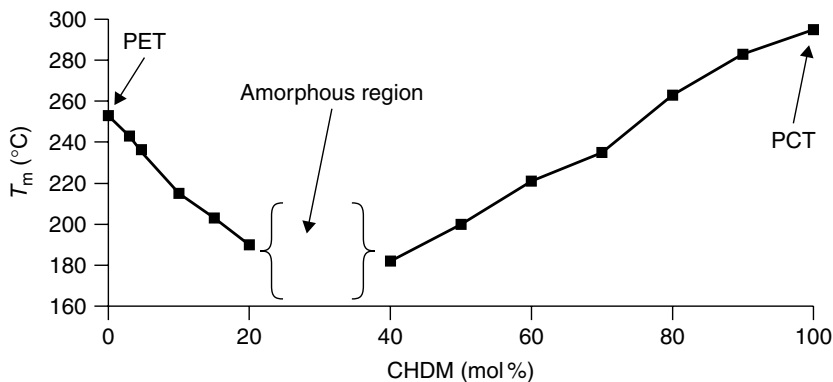


Figure 7.7 Effect of CHDM concentration on the melting point of the copolyester prepared from TPA, EG and CHDM



Figure 7.8 Refrigerator 'crisper' trays molded from Eastman Eastar® PETG 6763. Photograph provided by courtesy of Eastman Chemical Company

resins for stretch-blow molded container applications. The composition range from approximately 20–30 mol% of CHDM results in copolyesters which do not show crystallization peaks when scanned by DSC and are thus considered to be amorphous. This relationship of composition and copolyester melting point is shown in Figure 7.7.

PETG is a clear, tough, amorphous polyester that has found wide acceptance in specialty packaging applications due to its high clarity and strength over PET and other resins such as polycarbonate and polymethyl methacrylate (Figure 7.8). The largest single application for PETG is the heavy gauge sheet market. Recently,



Figure 7.9 Point-of-purchase displays fabricated from Eastman Spectar® copolyester extruded sheet. Photograph provided by courtesy of Eastman Chemical Company

Eastman Chemical Company introduced its Spectar™ brand based on proprietary manufacturing technology. Heavy gauge sheeting cast from Spectar™ copolyester has excellent combined physical and optical properties and is used widely for signage and point-of-purchase displays (Figure 7.9). The physical properties of a PETG sample based on TPA with about 70 % of EG and 30 % of CHDM are given in Table 7.3. The flexural modulus is somewhat higher than PCTG, but the toughness properties, as seen in elongation to break and notched Izod, are diminished when compared to the higher CHDM-containing PCTG sample.

8 DIBASIC-ACID-MODIFIED PCT COPOLYESTER: PREPARATION AND PROPERTIES

The crystallinity of PCT can be modified with diacids as well as with diols and these modified polyesters are often called acid-modified PCTs, or abbreviated as PCTAs. The most common diacid modifier is isophthalic acid (IPA), which can be incorporated in relatively low levels to lower the melting point of PCT to enhance processability while still maintaining crystallinity. The high T_m of PCT (295 °C) requires that the homopolymer be processed at temperatures greater than 300 °C, which is near the decomposition temperature [13].



Figure 7.10 Transparent toy kaleidoscopes molded from Eastman Durastar™ 1010 PCTA copolyester. Photograph provided by courtesy of Eastman Chemical Company

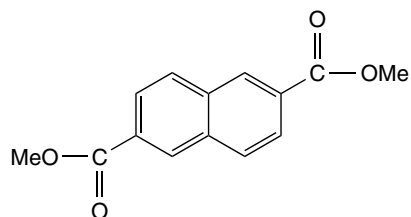
Low-level incorporation of IPA (5–10 mol %) widens the processing window by lowering the melting point of the polyester while also retaining the crystallinity, T_g and toughness of the PCT homopolymer. At higher IPA incorporation levels, chain crystallization is severely restricted so that at 35 mol % of IPA and higher, the amorphous copolyesters do not crystallize without the addition of an added nucleator [55–59].

Amorphous PCTA compositions are tough, transparent resins with good hydrolysis and chemical resistance. PCTA finds applications for precision molded parts and can be extruded into clear sheeting, pipe and profiles or shaped products (Figure 7.10). An attractive feature of PCTA is that it can be melt processed without the need for extensive pre-drying [60]. The typical properties of a PCTA formulation consisting of about 70 % of TPA and 30 % of IPA are given in Table 7.3, where the results can be compared to PETG and PCTG samples.

9 MODIFICATION OF CHDM-BASED POLYESTERS WITH OTHER GLYCOLS AND ACIDS

Although the scope of this review mainly covers CHDM-based polyesters modified with isophthalic acid or ethylene glycol (i.e. PCTA or PCTG, and PETG, respectively), many other copolyesters with interesting properties have been prepared with a variety of other comonomers.

9.1 CHDM-BASED COPOLYESTERS WITH DIMETHYL 2,6-NAPHTHALENEDICARBOXYLATE



dimethyl 2,6-naphthalenedicarboxylate (N)

Modification of PCT with increasing levels of the 2,6-naphthalenedicarboxylate moiety (N) has been reported. The effects of increasing levels of N on the thermal properties of PCT are shown in Figures 7.11 and 7.12 [61].

As indicated, the T_g of the copolyesters gradually increases with increasing levels of N. However, the crystalline melting temperature (T_m) of the N-modified PCT copolyesters initially decreases until an eutectic point is reached at about 40 mol % of N, and then begins to increase with increasing N levels. Further analytical studies using wide-angle X-ray scattering indicate that at the eutectic point, crystal structures for both poly(1,4-cyclohexanedimethylene terephthalate) (PCT) and poly(1,4-cyclohexanedimethylene 2,6-naphthalenedicarboxylate) (PCN) were observed [61]. It is of interest to note from the above figures that PCT modified with greater than 80 mol % of N cannot be successfully polymerized to high molecular weight by conventional melt-phase polymerization because the polymer crystallizes prematurely during polymerization to a high-melting solid,

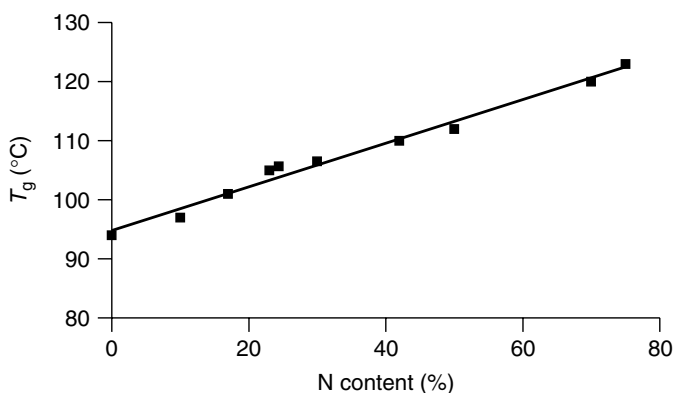


Figure 7.11 Effect of 2,6-naphthalenedicarboxylate (N) content on the T_g of PCT copolyesters [61]

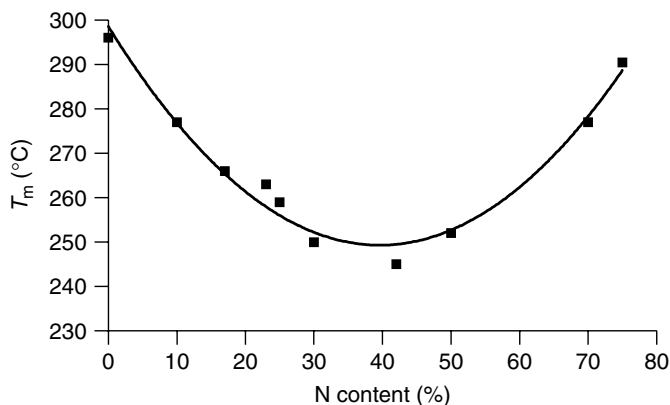


Figure 7.12 Effect of 2,6-naphthalenedicarboxylate (N) content on the T_m of PCT copolyesters [61]

so only low-molecular-weight polymer results. Solid-state polymerization must be used to increase the molecular weight of these polyester compositions. In fact, highly crystalline PCN is believed to have a T_m of 355 °C. As a general rule for PCT copolyesters, increasing the amount of N imparts higher tensile yield, increased hardness and higher heat distortion temperature. However, the use of N leads to slightly lower impact strength with no increase in stiffness. The preparation of various CHDM-based copolyester compositions containing N has also been revealed in the patent literature [62–65]. Several patents claim unexpectedly high heat resistance for selected copolyester compositions prepared from CHDM and N [66–68]. However, much of the recent interest with incorporating N in polyester compositions is associated with the ability of N to improve the oxygen-barrier properties, particularly for applications involving food and beverage packaging. A recent patent disclosed that PCT prepared with CHDM having a 93/7 *cis/trans* ratio and modified with 50 mol % of N has an unexpectedly low oxygen permeability of 2.68 (cc mil)/(100 in² 24 h atm). [52]. By comparison, the oxygen permeability of oriented PET has an oxygen permeability of 6.61 (cc mil)/(100 in² 24 h atm).

9.2 POLYESTERS PREPARED WITH 1,4-CYCLOHEXANEDICARBOXYLIC ACID

All cycloaliphatic polyesters have been prepared from CHDM and 1,4-cyclohexanedicarboxylic acid (CHDA). Dimethyl 1,4-cyclohexanedicarboxylate (DMCD) is the ester intermediate in the synthesis of CHDM and is the precursor to CHDA. 1,4-cyclohexanedicarboxylic acid is a commercially produced monomer that has

found utility as a polyester resins intermediate for a variety of industrial coatings [69]. By analogy to CHDM, the structure of the cyclohexane ring of CHDA (or DMCD) can exist in the *cis*- and *trans*-conformations. However, for most high-molecular-weight thermoplastic end uses the CHDA moiety with high *trans* content (>90 %) is preferred because of the elevated T_g and T_m that result with the increasing *trans* content. This '*trans* effect' on polyester thermal properties is shown in Table 7.4. The series of cycloaliphatic polyester compositions shown in this table was prepared by melt-phase polymerization of CHDA (having the indicated *trans*-isomer content shown in Table 7.4) and CHDM (having the indicated *trans*-content as in Table 7.4). Unlike CHDM, however, CHDA can undergo isomerization in the presence of certain catalysts and at high melt polycondensation temperatures [70] and revert to the equilibrium mixture which is about 68 % *trans* and 32 % *cis* contents.

The properties of PCTA-type structures where the modifying acid is 1,4-cyclohexanedicarboxylic acid (CHDA) have also been studied [53]. The incorporation of this diacid (95 % *trans*) as a polyester modifier maintains the toughness, but is accompanied with significant lowering of the T_g . This is contrasted to NDA modification where the T_g is enhanced but toughness is decreased. A comparison of the properties of various PCTAs versus an amorphous PCT sample, prepared by quenching, are shown in Table 7.5.

Table 7.4 Effect of CHDA and CHDM isomer content on selected polyester properties

CHDA (% <i>trans</i>)	CHDM (% <i>trans</i>)	T_g (°C)	T_m (°C) ^a	HDT (°C at 264 psi) ^b
15	3	35	ND	NA
35	70	42	125	50
95	70	66	225	59
95	100	82	246	NA

^a ND, not detected.

^b NA, not available.

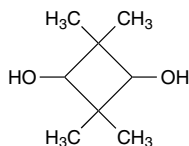
Table 7.5 Comparison of selected properties for various PCTA copolyesters [53]

Polyester composition ^a	Intrinsic viscosity (dl g ⁻¹)	Break elongation (%)	Notched Izod (ft lb) ^b	T_g (°C)
PCT	0.95	250	NB	95
PCTA ¹	0.64	165	14.2	103
PCTA ²	0.66	201	2.43	86
PCTA ³	0.75	225	NB	78

^a A¹, 30 % NDA; A², 30 % PA; A³, 48 % CHDA.

^b Measured at 23 °C; NB, no break.

9.3 CHDM-BASED COPOLYESTERS WITH 2,2,4,4-TETRAMETHYL-1,3-CYCLOBUTANEDIOL



cis/trans-2,2,4,4-tetramethyl-1,3-cyclobutanediol (TMCD)

Copolymer compositions containing CHDM and *cis/trans*-2,2,4,4-tetramethyl-1,3-cyclobutanediol (TMCD) have been reported to exhibit high heat distortion temperatures ($>95^{\circ}\text{C}$ at 264 psi stress) and high impact strengths [71]. Copolymer compositions with TMCD have also been reported to provide improved melt strength suitable for extrusion blow molding containers and blends for molding [72, 73]. Copolyesters from CHDM and TMCD have also been explored in blends with polycarbonate and found to exhibit desirable properties, including high impact strengths, enhanced heat distortion temperatures and good UV resistance [74, 75]. The rigid character of TMCD thus lends itself well to the preparation of a variety of amorphous and semicrystalline polyesters having enhanced glass transition temperatures, good thermal properties, high impact strengths, and ultraviolet light stability [76–78]. The properties of terephthalate-based copolyesters of 2,2,4,4-tetramethyl-1,3-cyclobutanediol and selected diols (albeit, not including CHDM) have been studied and reported [78].

Although TMCD is not commercially available, technology for its preparation from isobutyric acid or isobutyric anhydride has been reported [79–83]. A process for separation of the individual *cis*- and *trans*-isomers of TMCD has also been reported [84]. TMCD is usually prepared with an approximate 50/50 *cis/trans* ratio, and this is the usual equilibrium isomer ratio used for polyester preparation, although polyesters prepared from other isomer ratios and from the pure *cis*-isomer have been reported [77, 78].

9.4 CHDM-BASED COPOLYESTERS WITH OTHER SELECTED MONOMERS

The selection of monomers for preparation of copolyesters is based on applying established structure/property principles and is usually driven by new market needs and applications with specific end-use properties in mind. Thus, attempts to develop amorphous or semicrystalline CHDM-based polyester compositions for applications requiring greater heat resistance or higher heat deflection temperatures have generally followed the theme of incorporating bulky or rigid constituents to further enhance the desirable thermal properties of CHDM-based

copolyesters. By example, *trans*-4,4'-stilbenedicarboxylic acid has been incorporated in various CHDM-based copolyester compositions. This rigid diacid is claimed to enhance melt stability, tensile strength, heat resistance and hydrolytic stability of injection-molded objects [85, 86]. Specific CHDM copolyesters prepared with 4,4'-biphenyldicarboxylic acid are claimed to provide molded objects with unusually high tensile strengths [87–90].

CHDM copolyesters containing residues of 2,6-naphthalenedicarboxylate, 4,4'-biphenyldicarboxylic acid and CHDM are reported to exhibit high heat resistance [91].

Furthermore, copolymerization of CHDM with *p,p'*-isopropylidene dibenzoic acid, or other like dicarboxylic acid ring structures, has been reported to produce amorphous polymers having high heat distortion temperatures and high impact strengths [92]. Amorphous copolyesters with low melt viscosities and enhanced glass transition temperatures are claimed for compositions which comprise residues of 2,2'-(sulfonylbis(4,1-phenyleneoxy))-bisethanol and mixtures of other glycols, including CHDM [93]. Copolyesters prepared from CHDM and 3-methyl-2,2'-norbornanedimethanol and selected diacids are claimed as having high T_g s, excellent heat resistance and hydrolytic stability [94]. In a similar manner, CHDM copolyester containing 2–10 mol % of bis(2-(2-hydroxyethoxy)phenyl)fluorene is reported to exhibit high T_g values and have excellent heat resistance properties [95]. Cost, monomer availability and polymer performance are all key issues in commercialization of new copolyesters. Generally it is necessary to add a significant amount of the modifying comonomer to achieve significant property improvements. Therefore, economic barriers have limited the commercialization of many of the CHDM-based copolyesters where speciality diols or diacids are needed.

ACKNOWLEDGMENTS

The authors acknowledge Drs James Scanlan and Peter Shang of Eastman Chemical Company for providing unpublished dynamic mechanical analyses data and DSC data, respectively

REFERENCES

1. Carothers, W. H. and Hill, J. W. *J. Am. Chem. Soc.*, **54**, 1579–1587 (1932).
2. Mark, H. and Whitby, G. S. (Eds), *Collected Papers of Wallace H. Carothers on Polymerization*, Interscience Publishers, Inc., New York, 1940.
3. Brandrup, J. and Immergut, E. H., *Polymer Handbook*, 2nd Edn., Wiley, New York, 1975, p. III–159.
4. Ludewig, H., *Polyester Fibers Chemistry and Technology*, Wiley, New York, 1971, p. 4.
5. Bier, G., *Polymer* **15**, 527–535 (1974).

6. Whinfield, J. R. and Dickson, J. T., *Br. Patent 578 079* (to Imperial Chemical Industries, Ltd), 1946.
7. Whinfield, J. R. and Dickson, J. T., *US Patent 2 465 319* Inc., (1949), (to E. I. du Pont de Nemours & Co.).
8. Kibler, C. J., Bell, A. and Smith, J. G., *US Patent 2 901 466* (to Eastman Kodak Company), 1959.
9. Martin, E. V. and Kibler, C. J., Polyesters of 1,4-cyclohexane dimethanol, in *Man-Made Fiber Science and Technology*, Mark, H. F., Atlas, S. M., and Cernia, E. (Eds), Vol. 3, Wiley-Interscience, New York, 1968, 83–134.
10. Robertson, G. L., *Food Packaging*, Marcel Dekker, New York, 1993, pp. 606–608.
11. Anon, *Chem. Week*, No. 20, 32 (1994).
12. Anon, *Mod. Plast. Int.*, No. 4, 32–34 (1982).
13. Caldwell, J. R., Jackson, Jr, W. J. and Gray, Jr, T. F., Polyesters, thermoplastic, in *Encyclopedia of Polymer Science and Technology*, Mark, H. F. and Bikales, N. M. (Eds), Wiley-interscience, New York, 1967, pp. 444–467.
14. Hasek, R. H. and Knowles, M. B. *US Patent 2 917 549* (to Eastman Kodak Company), 1959.
15. Aiken, G. A., Lewis, H. J. and Reid, T. F., *Br. Patent 879 264* (to Eastman Kodak Company), 1961.
16. Heise, R., *Ger. Patent 1 099 527*, 1961.
17. Tateno, Y., *US patent 4 999 090* (to Towa Chemical Company, Ltd), 1990.
18. Hara, Y., *Jpn Patent JP 2000 007 596*, 2000.
19. Scarlett, J., Wood, M. A. and Rathwell, C. *US Patent 5 387 752* (to Eastman Chemical Company), 1995.
20. Kibler, C. J., Bell, A. and Smith, J. G., *J. Polym. Sci., Part A*, **2**, 2115–2125 (1964).
21. Light, R. R. and Seymour, R. W., *Polym. Eng. Sci.*, **22**, 857–864 (1982).
22. Chen, L. P., Yee, A. F. and Moskala, E. J., *Macromolecules*, **32**, 5944–5955 (1999).
23. Chen, L. P., Yee, A. F., Goetz, J. M. and Schaefer, J., *Macromolecules*, **31**, 5371–5382 (1998).
24. *Jpn Patent JP 06 321 823* (to Towa Kasei Kogyo KK), 1994.
25. *Jpn Patent, JP2000 212 109* (to Daicel Chemical Industries), 2000.
26. *Jpn Patent, JP2000 007 595* (to New Japan Chemical Company), 2000.
27. Kibler, C. J., Bell, A. and Smith, J. G., *US Patent 2 901 466* (to Eastman Kodak Company), 1959.
28. Jackson, W. J. and Watkins, J. J., *US Patent 4 578 453* (to Eastman Kodak Company), 1986.
29. Eckart M. D. and Goodson, R. L. *World Patent WO99 10 173* (to Eastman Chemical Company), 1999.

30. Haile, W. A., Dean, L. R. and McConnell, R. L. *World Patent WO00 12 792* (to Eastman Chemical Company), 2000.
31. *Jpn Patent, JP 55 094 929* (to Toray Industries), 1980.
32. *Br. Patent 1 240 327* (to Japan Gas-Chemical Company), 1971.
33. *Ger. Patent 2 934 416* (to Chemische Werke Huels), 1981.
34. Akin, G. A., Rush, S. J. and Russin, N. C., *US Patent 3 271 370* (to Eastman Kodak Company), 1966.
35. Yau, C. C. and Cherry, C., *US Patent 5 340 907* (to Eastman Chemical Company), 1994.
36. Chen, J.-W. and Chen, I.-W., *J. Polym. Sci., Polym. Chem. Ed.*, **37**, 1797–803 (1999).
37. Anon, *Chem. Eng.*, **108**, 15 (2001).
38. Kokkalas, D. E., Bikiaris, D. E. and Karayannidis, G. P., *J. Appl. Polym. Sci.*, **55**, 787–791 (1995).
39. Apicella, B., DiSerio, M., Fiocca, L., Po, R. and Santacesaria, E., *J. Appl. Polym., Sci.*, **69**, 2423–2433 (1988).
40. Bacaloglu, R., Fisch, M. and Biesiada, K., *Polym. Eng. Sci.*, **38**, 1014–1022 (1988).
41. Hovnof, V., *J. Macromol. Sci.*, **A15**, 503–514 (1981).
42. Jernigan, M. T., Green, C. J., Murdaugh, P., White, A. W. and Yau, C. C., *World Patent WO01 14 452* (to Eastman Chemical Company), 2001.
43. Yau, C. C. and Moody, L. S., *US Patent 5 608 031* (to Eastman Chemical Company), 1997.
44. George, S. E. and Hoffman, D. C., *US Patent 5 378 796* (to Eastman Chemical Company), 1995.
45. Yau, C. C. and Cherry, C. *World Patent WO94 25 502* (to Eastman Chemical Company), 1994.
46. Sublett, B. J., *US Patent 5 017 680* (to Eastman Chemical Company), 1991.
47. Jong, S.-Y. and Hong, Y.-H., *Jpn Patent 3 209 336* (to SK Chemicals), 2001.
48. Ito, H., Yoshida, Y. and Nakazawa, M., *Jpn Patent 10 045 646* (to New Japan Chemical Company), 1998.
49. Mori, H., Yamamoto, N. and Taziri, N., *US Patent 5 124 435* (to Mitsubishi Rayon Company), 1992.
50. Martl, M., Mezger, T., Kuhn, B., Oberlein, G., Haferland, K., Boehringer, B. and Berger, U., *US Patent 5 789 528* (to Akzo Nobel NV), 1988.
51. Jackson, W. J. and Watkins, J. J., *US Patent 4 578 453* (to Eastman Chemical Company), 1986.
52. Sublett, B. J., *US Patent 5 552 512* (to Eastman Chemical Company), 1996.
53. Hoffman, D. C., unpublished data (Eastman Chemical Company), 1994.
54. Yang, H., Moskala, E. and Jones, M., *J. Appl. Med. Polym.*, **3**(2), 50–54 (1999).
55. Li, B., Yu, J., Lee, S. and Ree, M., *Polymer*, **40**, 5371–5375 (1999).

56. Radhakrishnan, S. and Nadkarni, V. M., *Eur. Polym. J.*, **22**, 67–70 (1986).
57. Legras, R., Bailly, C., Daumerie, M., Dekoninck, J. M., Mercier, J. P., Zichy, V. and Nield, E., *Polymer*, **25**, 835–844 (1984).
58. Aharoni, S. M., *J. Appl. Polym. Sci.*, **29**, 853–865 (1984).
59. Yu, Y., Yu, Y., Jin, M. and Haishan, B., *Macromol. Chem. Phys.*, **201**, 1894–1900 (2000).
60. Dickerson, J. P., Brink, A. E., Oshinski, A. J. and Seo, K. S., *US Patent 5 656 715* (to Eastman Chemical Company), 1997.
61. Hoffman, D. C. and Pecorini, T. J., *Am. Chem. Soc., Div. Polym. Chem., Polym. Prepr.*, **40**(1), 572–573 (1999).
62. Anon, *US Patent Office, Research Disclosure 294 081* (October 1988).
63. Seymour, R. W. and Light, R. R., *US Patent 4 474 918* (to Eastman Chemical Company), 1984.
64. *Jpn Patent JP 1 201 324* (to Teijin Ltd), 1989.
65. Duling, N., *US Patent 3 293 223* (to Sun Oil Company), 1966.
66. Sublett, B. J., *US Patent 5 616 404* (to Eastman Chemical Company), 1997.
67. *Jpn Patent JP 1 201 325* (to Teijin Ltd), 1989.
68. *Jpn Patent JP 5 209 044* (to NKK Corporation), 1993.
69. Chong, C. T., *Surf. Coat. Aust.*, **35**(7), 14–20 (1998).
70. Vanhaecht, B., Teerenstra, M. N., Suwier, D. R., Willem, R., Biesemans, M. and Konig, C. E., *J. Polym. Sci., Polym. Chem. Ed.*, **39**, 833–840 (2001).
71. Coover, Jr, H. W., Shearer, N. H. and Wicker, Jr, T. H., *US Defensive Publication T875 010* (to Eastman Kodak Company), 1970.
72. Morris, J. C., Bradley, J. R. and Seo, K. S., *US Patent 5 989 663* (to Eastman Chemical Company), 1999.
73. Morris, J. C. and Bradley, J. R., *US Patent 5 955 565* (to Eastman Chemical Company), 1999.
74. Scott, C. E., Morris, J. C. and Bradley, J. R., *US Patent 6 043 322* (to Eastman Chemical Company), 2000.
75. Scott, C. E., Stewart, M. E., Wilmoth, D. S., Morris, J. C. and Bradley, J. R., *US Patent 5 942 585* (to Eastman Chemical Company), 1999.
76. Caldwell, J. R., Gilkey, R. and Kuhfuss, H. F., *Br. Patent 1 044 015* (to Eastman Kodak Company), 1966.
77. Elam, E. U., Martin, J. C. and Gilkey, R., *US Patent 3 313 777* (to Eastman Kodak Company), 1967.
78. Kelsey, D. R., Scardino, B. M., Grebowicz, J. S. and Chuah, H. H., *Macromolecules*, **33**, 5810–5818 (2000).
79. Hasek, R. H. and Elam, E. U., *US Patent 2 936 324* (to Eastman Kodak Company), 1960.
80. Mugno, M. and Bornego, M., *Chim. Ind. (Milan)*, **45**, 1216–1218 (1963).
81. Hasek, R. H. and Elam, E. U., *Br. Patent 965 762* (to Eastman Kodak Company), 1964.

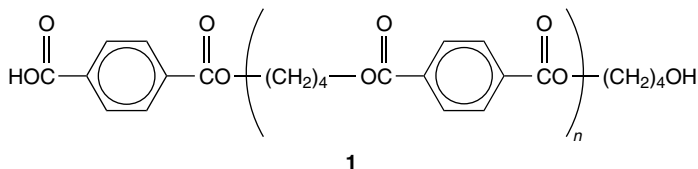
82. Sumner, Jr, C. E., Gustafson, B. L. and Knight, J. R., *US Patent 5 169 994* (to Eastman Kodak Company), 1992.
83. Sumner, Jr, C. E., Gustafson, B. L. and Knight, J. R., *US Patent 5 258 556* (to Eastman Kodak Company), 1993.
84. Martin, J. C. and Elam, E. U., *US Patent 3 227 764* (to Eastman Kodak Company), 1966.
85. Morris, J. C. and Jackson, W. J., *US Patent 4 728 717* (to Eastman Kodak Company), 1988.
86. Morris, J. C. and Jackson, W. J., *US Patent 4 728 718* (to Eastman Kodak Company), 1988.
87. Morris, J. C. and Jackson, W. J., *US Patent 4 914 179* (to Eastman Kodak Company), 1990.
88. Morris, J. C. and Jackson, W. J., *US Patent 4 956 448* (to Eastman Kodak Company), 1990.
89. Morris, J. C. and Jackson, W. J., *US Patent 4 959 450* (to Eastman Kodak Company), 1990.
90. Morris, J. C. and Jackson, W. J., *US Patent 5 011 877* (to Eastman Kodak Company), 1991.
91. Nakane, T., Konuma, H., Shiwaku, T. and Hijikata, K., *Eur. Patent 520 612* (to Polyplastics Company Ltd), 1992.
92. Sardessai, K. S., *US Patent 3 522 215* (to Mobil Oil Corporation), 1970.
93. Turner, S. R. and Sublett, B. J., *US Patent 6 120 889* (to Eastman Chemical Company), 2000.
94. *Jpn Patent JP 11 035 665* (to Showa Denko), 1999.
95. *Jpn Patent JP 8 269 178* (to Nippon Ester Company), 1996.

Poly(Butylene Terephthalate)

R. R. GALLUCCI AND B. R. PATEL
General Electric Plastics, Mt. Vernon, IN, USA

1 INTRODUCTION

Poly(butylene terephthalate) (PBT) (**1**) resins are semicrystalline thermoplastics used in a wide variety of applications, most commonly in durable goods that are formed by injection molding. Applications include electronic and communications equipment, computers, televisions, kitchen and household appliances, industrial equipment, lighting systems, gardening and agricultural equipment, pumps, medical devices, food handling systems, handles, power and hand tools, bobbins and spindles, and automotive parts in both 'under-the-hood' and exterior applications. Additionally, PBT is very widely used to form electrical connectors. PBT, through its many blended products, can be tailored to suit numerous applications.



PBT resin has been reviewed in many articles, often as part of a larger review of polyesters [1–3]. A recent article provides an historic account of polyester development as an alternative to nylon fibers [4], while the review of Kirsch and Williams in 1994 gives a business perspective on polyesters [5]. However, an understanding of PBT in the context of the more common polyester poly(ethylene terephthalate) (PET) is often overlooked. PET dominates the large volume arenas

of fiber, film, and bottle molding applications, whereas PBT is the polyester of choice for injection-molding applications.

The commercial application of PBT is at first glance very improbable. PBT is made of a more expensive raw material (1,4-butanediol vs. ethylene glycol for PET), is manufactured on a smaller scale than PET, has a lower melting point, and has slightly poorer mechanical properties than PET.

The commercial success of PBT *vis-à-vis* the lower-cost PET can be attributed principally to its ability to crystallize very rapidly. Fast crystallization allows injection-molding with fast cycle times and higher productivity for molders. Complete crystallization during molding leads to better dimensional stability of the molded part and, therefore, higher production yields. In most injection-molding applications, the commercial benefit of rapid, high yield part production outweighs the drawbacks.

For other methods of shaping plastics, such as fiber spinning, film extrusion, or blow molding of bottles, the slower-crystallizing PET is preferred. The slightly slower crystallization of PET allows for orientation during processing. Even though PET is used for injection-molding applications, PBT is more often the material of choice.

Although PBT is the fastest crystallizing polyester, it is not the only engineering polymer which exhibits fast crystallization. Like PBT, nylon 6 polyamide resin shows rapid crystallization, has a similar melting point to PBT, has good solvent resistance, and good mechanical properties. The key difference between these two materials is the low moisture absorption of PBT vs. nylon. Nylon properties will change depending on humidity; impact is improved while modulus and strength decrease. In some cases, nylon may show excessive part growth. While nylon is used successfully in many injection-molding applications, the part designer must deal with the challenge of compensating for a wider range of material variation as a function of environmental factors. PBT, by comparison, absorbs very little moisture and, therefore, provides a more consistent material which shows little change in part dimensions or mechanical properties as a function of environmental factors.

Table 8.1 shows a summary of important properties for various semicrystalline resins.

2 POLYMERIZATION OF PBT

PET and PBT are commercially produced by reacting an aliphatic glycol (diol) with an aromatic diester or diacid in the presence of a polyesterification catalyst. Although polycondensation theory calls for careful stoichiometric balance, industrial processes for manufacturing polyesters such as PBT involve initial use of excess glycol, which is later removed and recycled in the process. The advantageous, self-balancing nature of industrial PBT processes is discussed in the following Sections [6].

Table 8.1 Properties of poly(butylene terephthalate) compared with other semicrystalline resins

Property ^a	Resin (approximate composition) ^b					
	PBT (no GF)	PBT (15 % GF)	PBT (30 % GF)	Nylon 6 (no GF); dry/wet	Nylon 6 (30 % GF); dry/wet	PET (30 % GF)
Specific gravity	1.31	1.41	1.53	1.14	1.36	1.60
Water absorption after 24 h %	0.08	0.07	0.06	1.6 ^e	1.0 ^f	0.10
Mold shrink (in/in × 10 ⁻³) ^c	15–23	7–9	6–7	12	3	1–2
Mold shrink (in/in × 10 ⁻³) ^d	16–24	9–11	8–10	11	9	6 to 8
Tensile strength at yield (kpsi)	7.5	13.5	17.3	11.6/5.8	26.1/14.5	24.0
Tensile elongation at break %	300	5	3	35/≥ 200	3/6	3
Flexural modulus (kpsi)	340	700	1100	392/102	1200/725	1200
Flexural strength (kpsi)	12.0	21.0	27.5	—	40.6/24.6	34
Izod impact, notched (ft lbs/in)	1.0	1.0	1.6	1.1/14.0	2.2/2.8	1.7
HDT, at 66 psi °C	154	210	216	180/ —	215	249
HDT, at 264 psi °C	54	191	207	60/ —	200	227
CTE × 10 ⁵ (mm/mm °C), –40 to 60 °C	8.1	2.2	2.5	—	—	1.8
CTE × 10 ⁵ (mm/mm °C), 60 to 138 °C	13.9	2.2	2.5	—	—	1.6
Melting point (°C)	220	220	220	223	223	245

^a HDT, heat distortion temperature; CTE, coefficient of thermal expansion.

^b GF, glass-fiber filled.

^c Shrinkage measured 'with the flow'.

^d Shrinkage measured 'across the flow'.

^e Equilibrium in air at 50 % RH = 3.0 %; immersion = 10 %.

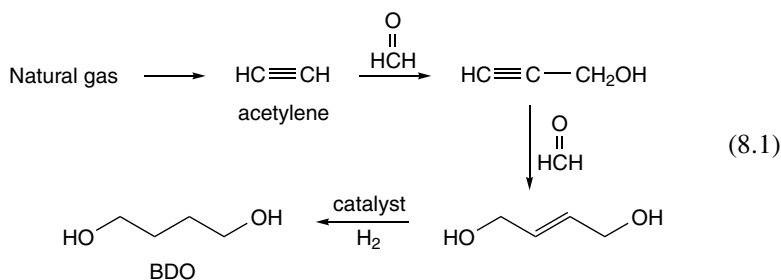
^f Equilibrium in air at 50 % RH = 2.1 %; immersion = 7 %.

2.1 MONOMERS

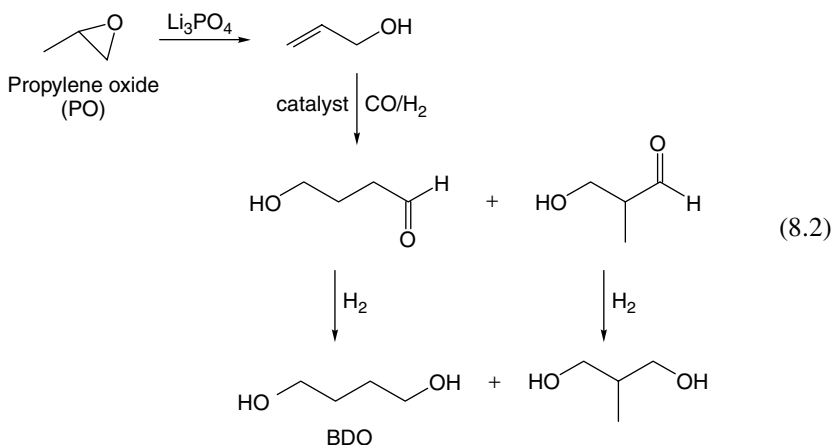
PBT is made by reacting 1,4-butanediol (BDO) with terephthalic acid (TPA) or dimethyl terephthalate (DMT) in the presence of a transesterification catalyst. A number of different commercial routes are used for producing the monomers, as discussed below.

2.1.1 1,4-Butanediol

1,4-Butanediol is commercially produced by several different processes [7]. The most prevalent process for making BDO is known as the Reppe process. This process uses acetylene, generated from natural gas, as its primary feedstock, according to the following:



Other feedstocks are also utilized for making BDO. An alternative route to BDO involves the use of propylene oxide (PO) as its primary feedstock:

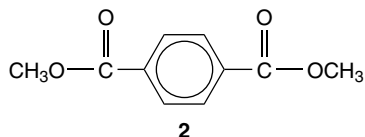


In East Asia, the predominant process for making BDO is the butadiene-acetoxylation process. The lower cost of the primary feedstock for the process, i.e. 1,3-butadiene, allows this process to be cost effective for that region.

More recent processes involving the oxidation of butane to a maleic anhydride intermediate, using both fixed-bed and fluidized-bed processes, have been commercialized. The maleic anhydride is subsequently hydrolyzed to maleic acid or esterified in the presence of methanol to dimethyl maleate, which can be reduced to BDO in the presence of hydrogen and catalyst. These processes are attractive due to the low cost of the butane feedstock. The method of choice to make BDO is often dictated by the local availability of the desired chemical feedstock.

2.1.2 Dimethyl Terephthalate and Terephthalic Acid

The large volumes of PET produced for fibers, films, blow-molding and injection-molding grades have led to large-scale, low-cost processes for making terephthalic acid, and to a lesser degree, dimethyl terephthalate (DMT) (**2**).



The diester/diacid component of PBT is made by oxidizing *para*-xylene. Oxidation followed by esterification leads to dimethyl terephthalate.

2.2 CATALYSTS

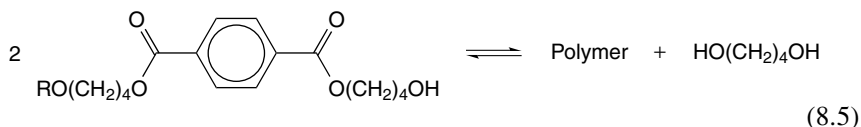
Tetraalkyl titanates are the most commonly used catalysts for PBT polymerization [8]. The varieties of titanates include tetraisopropyl titanate (TPT), tetrabutyl titanate (TBT) and tetra(2-ethylhexyl) titanate (TOT). Titanates effectively speed the reaction rate with few detrimental effects on the resin. Alkoxy zirconium and tin compounds, as well as other metal alkoxides, may also be used in PBT polymerization.

As opposed to the PET process, where a different catalyst is used in each of the two polymerization phases, the PBT process typically uses a single catalyst. In PBT resins, the catalyst is not typically quenched (deactivated) at the end of the polymerization process. An active catalyst in the resin can sometimes lead to further reaction of the PBT in subsequent processing.

2.3 PROCESS CHEMISTRY

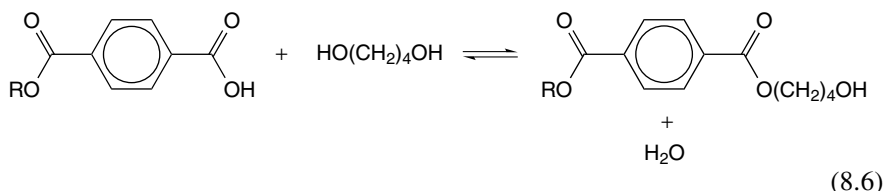
PBT can be made by using both batch and continuous processes. Early commercial processes were DMT-based batch processes that involved two distinct

butanediol:



As the polymer melt builds molecular weight, it becomes more viscous. Toward the end of the reaction where the final molecular weight is achieved, stirring of the polymer requires specially designed reactor systems. Many large scale, commercial PBT plants currently employ a continuous DMT-based process.

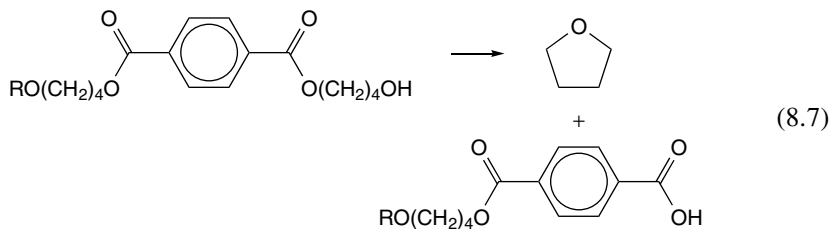
During PBT polymerization, carboxylic acid (COOH) end groups can react with BDO to regenerate hydroxybutyl endgroups and water, by a direct esterification reaction:



In a DMT-based polymerization, there are only a few carboxylic acid (COOH) end groups arising from ester hydrolyzed by the small amount of water in the system. Water is generated primarily as a result of THF formation. In a TPA-based reaction, there is a large amount of water generated in the first-stage reaction of acid with diol. TPA, acting as an acid catalyst, also gives more conversion of BDO to THF, generating about twice the THF as seen in a comparable DMT-based reaction.

Water generation during PBT polymerization is undesirable in that it can hydrolyze ester groups in the polymer backbone as well as irreversibly hydrolyze the titanate catalyst. Partially hydrolyzed titanates will have lower catalytic activity than the pure catalyst.

A complicating feature of PBT chemistry is the degradation of hydroxybutyl end groups via a reaction which results in the formation of THF and carboxylic acid end groups. This reversion is often called a 'backbiting' reaction:



This backbiting reaction is acid-catalyzed and can occur during all stages of the polymerization. It is also possible to generate THF during the subsequent processing (extrusion and molding) of PBT by conversion of hydroxybutyl end groups to carboxylic end groups. Almost all polyesters have an analogous version of this hydroxy end group reaction but with different consequences in different resins. As mentioned, PBT produces THF. In PET, dehydration of ethylene glycol and hydroxyethyl end groups gives acetaldehyde as a byproduct. In poly(propylene terephthalate) (PPT), the analogous byproduct is acrolein.

Although PBT chemistry is complex, the overall result is a robust process. PBT chemistry tends to be self-balancing; excess BDO is used to help drive the equilibrium and yet can be recycled back into the process. Any backbiting degradation that occurs results in acid end groups which can react with BDO to regenerate hydroxybutyl end groups. The only price is the generation of THF which cannot be recycled into the process. A consequence of THF generation is that the end group chemistry of the final PBT product can vary. Typical acid end group levels in PBT can range from 10 meq/kg to 80 meq/kg, depending upon the process conditions and molecular weight. The remaining end groups are primarily hydroxy with a barely detectable amount of olefin. As opposed to other condensation polymers, for example polycarbonates, polyesters are not usually end-capped with a monofunctional species.

2.4 COMMERCIAL PROCESSES

As mentioned earlier, both batch and continuous processes can be used to make PBT. Some manufacturers also incorporate solid-state or solid-phase polymerization (SSP or SPP, respectively) processes to increase molecular weight.

The commercial batch processes are typically run in multiple reactors. Usually, at least two reactors are involved: an EI reactor designed to distill methanol at atmospheric pressure, and a polycondensation reactor designed to drive the polymerization and build molecular weight by removing excess glycol as well as volatile byproducts. The reaction times in the EI stage tend to be shorter (typically about 1 h) than the polycondensation reaction times (typically 1–2 h, depending on the desired degree of polymerization).

Continuous process trains involve a series of continuous stirred-tank reactors (CSTRs) followed by finishing reactors. The series of CSTRs are used to gradually distill volatile byproducts such as methanol, THF and water. Pressure is also gradually reduced as the reagents travel through the reactor train. The bulk of the polymerization is carried out in finishing reactors that are capable of generating high surface area under vacuum to help remove excess glycol and volatile byproducts.

The SSP reactors can also be continuous or batch in nature and can be run under nitrogen or vacuum. SSP involves heating pellets or chips at a temperature

close to, but below, the melting point to drive off BDO, thereby increasing the molecular weight. A consequence of this process is to further increase the crystallinity of the resin pellet. When melted and cooled, the SSP resin will regain its normal level of crystallinity.

Commercial PBT melt polymerization can be used to make a variety of molecular weight resins, ranging from 17 000 to 40 000 M_n (melt viscosity, at 250 °C, ranging from 300 to 9000 Poise). The higher-molecular weight resins are generally made by using special mixing devices designed for agitation of the high-viscosity polymer melt, or are produced through SSP processes.

Some resin manufacturers make a variety of different molecular weight resins by stopping polymerization as various viscosities are achieved (generally by simply pumping the resin out of the reactor and cooling it to stop the reaction). Other suppliers, especially those with continuous plants, make one or two high- and low-molecular weight resins and, during subsequent melt compounding, combine different ratios of these PBT resins to make a broad range of intermediate-viscosity materials. Resins made either in the reactor or through a two-step blending process are, for all practical purposes, indistinguishable.

3 PROPERTIES OF PBT

While PBT has been fabricated into fibers [11, 12] and film [13], it is primarily used in injection-molding applications. PBT displays good solvent resistance, high heat resistance, good elongation, high strength and modulus. PBT also has low melt viscosity and very fast crystallization, hence allowing for easy molding. PBT has good cold-water resistance, excellent electrical properties [14], high gloss, good inherent lubricity and wear resistance. PBT is used in some food-contact applications.

Although PBT has many desirable properties, its rapid crystallization almost always renders it opaque. While transparent PET products are quite common, PBT crystallization can rarely be quenched to the extent necessary for the formation of transparent articles. Thin films of PBT are translucent, allowing some light to penetrate, but are almost never clear.

PBT is easily made into fiber and monofilament and has been used in some fiber applications. For example, PBT fibers are used commercially as toothbrush bristles. Compared to PET, PBT fiber is more resistant to permanent deformation. Compared to nylon, PBT shows almost no change when exposed to moisture. PBT shows much more resistance to staining than nylon and can be colored by the use of pigments. However, PBT is more difficult to color by solution dyeing than nylon. PBT is not typically used in textile applications due to its perceived high price.

Compared to amorphous resins such as ABS, polycarbonate and polystyrene, a semicrystalline resin like PBT will show much better solvent resistance, higher

strength and higher stiffness due to the presence of crystalline spherulites in the resin. In the solid phase, crystalline resins are a mixture of regularly ordered spherulites and amorphous, uncrystallized regions. In general, the crystalline PBT regions account for about 35 % of the material [15]. The crystals have a regular melting point that can be measured by a variety of techniques including differential scanning calorimetry (DSC). These crystals give the resin its resistance to solvents and mechanical strength. The amorphous region has a glass transition temperature (T_g) of about 45 °C and gives the material much of its elongation properties. The dual-phase nature of PBT leads to some interesting behavioral aspects. The spherulites which begin melting at ~215 °C give a rigid material that has high heat resistance at low loads. The heat distortion temperature (HDT) at 66 psi (154 °C) reflects this heat capability. If higher loads are used, the T_g of the amorphous region (in neat, unblended PBT) dominates load bearing capability (HDT at 264 psi = 54 °C) [16, 17].

Crystalline resins will undergo a sharp change in viscosity when the crystallites are fully melted; the melt is essentially amorphous at this point. The low-viscosity, molten polymer is easily molded prior to cooling. At its crystallization temperature (T_c), PBT crystals begin to reform. As the material cools further and the chains become less mobile, crystallization stops and the part is solid enough to be removed from the mold. PBT gives fairly reproducible crystal structure under these conditions, especially when compared to the slower-crystallizing PET. Even so, there can be some slight variation in the mechanical properties of PBT due to differences in how it was processed [18, 19].

To obtain consistent processing, the PBT resin must be dried according to manufacturer recommendations before molding. PBT does absorb a small amount of water. If PBT is melted in the presence of water, the condensation polymer will hydrolyze and begin to lose molecular weight and viscosity. Polyesters will ultimately lose mechanical properties with sufficient chain cleavage. Improper drying of PBT before melt processing, with resultant loss of melt viscosity/molecular weight, is the single most common problem encountered in molding PBT.

It is interesting to note that even pure PBT, like most other semicrystalline resins, may show a double melting point in the DSC trace. This effect is due to the formation of different distributions of crystals [20, 21]. Differences in crystal structure are the underlying cause of slight variations in the mechanical properties of PBT. If a part made of crystalline resin is only partially crystallized during molding, it may undergo further crystallization during secondary operations, storage, shipment or in final use, leading to changes in dimension as well as physical properties. Significant differences in the crystal content and structure in 'as-molded' parts can lead to similar changes in properties. Poor control of crystallization during molding may lead to widely varying part-to-part dimensions and properties. The fast, reproducible crystallization of PBT minimizes (but does not completely eliminate) these problems.

The crystallization of PBT resin will result in a rather large volume change when it transitions from the melt to a solid. This phenomenon results in a higher shrinkage than a glassy, amorphous resin. Other additives will also affect shrinkage [22]. The latter must be taken into account when designing parts and tooling, and it must be properly managed during processing.

PBT resin is used in many applications where its solvent resistance, lubricity, strength and rigidity are needed. For example, most keyboard key caps are made from PBT. Unmodified PBT is also used in optical fiber buffer tubes and some electrical connectors. However, the vast majority of PBT resins are blended with many other ingredients to give a balance of properties for different injection-molding applications. In some cases, only a small amount of additive may be combined with the PBT. In other cases, high loadings of a variety of ingredients can push the PBT content to below 30 %. In all cases, the PBT is still the continuous phase. Like many crystalline resins, the low melt viscosity of PBT and its ability to 'wet-out' many fillers and resins make it very amenable to the formation of blends.

In the remaining sections of this chapter, various additives useful in making PBT blends will be discussed. In almost all cases, these additives are compounded with PBT in a single or twin-screw extruder after polymerization. The extrusion process is carried out independently of the resin polymerization process. Depending on the specific manufacturing operation, a number of methods of adding ingredients may be utilized. The ingredients may be added in a single blend, sequentially, as pre-compounded concentrates, or any combination thereof. The reader should understand that many of these additives can be combined with each other and with PBT resins of different molecular weights and slightly different structures. With all of the various additive 'building blocks' available to the PBT product formulator, and with the various levels of additives that can be combined with PBT, the existence of many, many different commercial PBT resin products should come as no surprise. Each of these products provides a unique set of properties and was developed to solve real-world problems that existed in some application.

3.1 UNFILLED PBT

Some PBT resins are sold in pelletized form directly from the resin polymerization reactor. These grades are produced as white, opaque pellets due to the presence of spherulites. Since all of the commercial methods for resin polymerization involve melt processes, PBT powder is only available by grinding the pellets.

PBT has both hydroxy and carboxylic acid end groups, and it often contains active residual catalyst (usually titanium based). The resin is still capable of reacting, and molecular weight may be increased by solid-state polymerization.

The concentration of end groups is reduced as the polymer molecular weight builds. PBT is a fairly reactive resin that can undergo reaction during processing and molding. The importance of drying the resin to prevent hydrolysis during melt processing was noted earlier.

Due to its crystallinity, PBT is very difficult to dissolve. Very aggressive solvents are required, including a 60:40 phenol:tetrachloroethane (TCE) mixture, cresol or hexafluoroisopropanol (HFIP). In almost all cases, PBT and its blends are processed and characterized via the polymer melt rather than in solution. A most critical property of a PBT resin is its melt viscosity. The melt viscosity (MV) is measured in a number of ways, usually at the nominal processing temperature of 250°C. Melt viscosity is proportional to the PBT molecular weight [23] but can vary greatly depending on the type and amounts of ingredients mixed in formulated products. Changes in melt viscosity of closely related materials can be used for comparing these materials and is a very useful practical test. The melt viscosity can be used to measure the extent of degradation of PBT resins. Comparing the MV of pellets to molded parts to regrind parts, or to parts with several melt histories, is a quick way to measure how much degradation has occurred. As a rule of thumb, up to about a 30 % drop in initial (pellet) MV is still acceptable for good part performance. Of course, the least possible MV drop on processing usually gives the best part performance. It should be noted that the use of MV alone is only an indicator to performance and is not to be taken as a substitute for full part testing.

Addition of low levels of certain additives to PBT can be a desirable way to enhance properties. The most common additives are colorants. Both pigments and dyes can be used to color PBT. Carbon black and titanium dioxide are most widely used. Carbon black and other pigments, for example, phthalocyanines, can also act as a nucleant for speeding crystallization.

Even though PBT does not generally stick to tooling, a low level of mold release added to the polymer has been shown to improve molding performance in some instances. High-molecular-weight aliphatic esters, amides or polyolefins are commonly used to enhance mold-release properties.

In some cases, antioxidants are added to PBT to improve thermal ageing or prevent yellowing. Hindered phenols and aryl phosphites are often used for thermal stabilization. In general, PBT (even without thermal stabilizers) yields much better color retention on high-temperature ageing in air than polyamides. The latter will develop a brown color during air-drying or very early in a thermal-ageing cycle. PBT, by comparison, shows little yellowing. Proper stabilization of PBT blends containing other resins, especially impact modifiers, can be very important to performance. The *Plastics Additives Handbook* is a good general reference to these types of stabilizers [24]. For improved stability to ultraviolet radiation, stabilizers such as benzotriazoles can be added to PBT. Although UV stabilizers can improve the photoageing performance of PBT, selection of colorants can be a greater factor in determining the overall UV resistance of PBT products.

3.2 FIBERGLASS-FILLED PBT

The single most important additive used in PBT resin blends is chopped fiberglass [25]. The use of from 5 to 50 wt% of fiberglass gives PBT blends with improved flexural modulus, higher tensile and flexural strength, and slightly better Izod impact performance. The flexural modulus of glass-filled PBT ranges from 400 000 to 1 200 000 psi. Another key benefit of adding fiberglass to a blend is that, at a given temperature, the load-bearing capacity of the material is increased. When fiberglass is added to PBT, the differences in HDT measured at 66 and 264 psi for an unfilled resin essentially disappear. In an unfilled PBT at high load levels, such as 264 psi, the HDT is close to the PBT glass transition. However, in glass-filled compositions, the HDT at 264 psi is greatly increased over the unfilled resin as both the glass fibers and the melting of PBT spherulites control deflection rather than the amorphous part of the resin (see Table 8.1).

Figure 8.1 shows dynamic mechanical analysis (DMA) data for an unfilled and 30 % glass-filled PBT. Note the sharply higher modulus (E') in the glass-filled blend at all temperatures.

A disadvantage of adding fiberglass is that it increases density. Part weight is often a cost factor. Since most resin is sold by the pound, while most molded articles are sold by the piece/unit, high density is usually undesirable. Addition of fiberglass also reduces flow and adds some part anisotropy. The orientation of the fiberglass and the difference in shrinkage between the resin and glass leads to warpage – the biggest potential drawback of glass-filled parts [26]. The presence of fiberglass will decrease overall shrinkage. However, it can also result in differences when comparing shrinkage in the flow direction to shrinkage perpendicular to flow. Unfilled PBT shows high but uniform shrinkage.

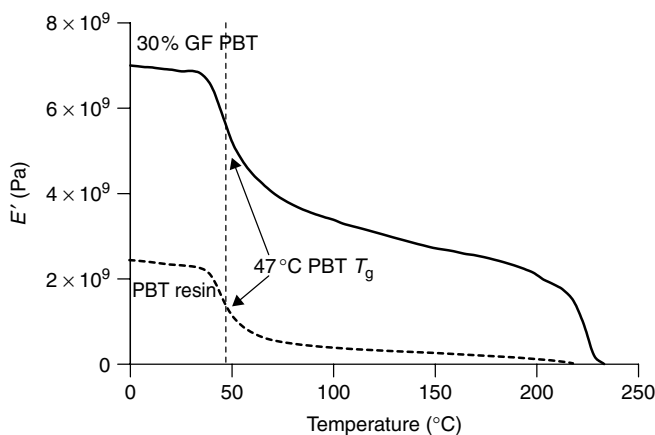


Figure 8.1 Comparison of DMA data obtained for 30 % glass-filled and unfilled PBT samples

High glass content improves overall properties more than lower content. In general, at least 5–7 wt% glass is needed to see reinforcing properties due to the need to have some fiber stress field overlap. At glass concentrations of >35 wt%, the benefit of additional glass in normal compounded products begins to decline due to issues with fiber mixing and breakage [27, 28].

Some work has been carried out with long fiber PBT composites where the glass fiber is the length of the PBT pellet (usually 0.5 in). In these systems, the glass is dispersed during molding. There is fiber mixing and breakage during molding. Properties will vary considerably depending on molding conditions and specific part design. In general, the long fiberglass-filled PBT will give the highest mechanical properties from an injection-molding grade [29].

Almost all of the glass fibers used in PBT products are made from borosilicate 'E' glass. The fiberglass is produced with a variety of surface treatments. These coatings are usually less than 1 % of the glass weight. The key purpose of the coating is to help bond the glass fiber to the resin matrix. The coating also helps to hold the fiberglass bundles together prior to compounding. Good fiber-to-resin bonding is key to getting optimal strength and impact from the composite [30].

Fiber length is also very important in achieving optimal properties. Fiber length distribution in a molded part is mainly a function of how the fibers and resin were compounded and under what conditions the part was molded. In general, the more mixing and shearing the fibers experience the more fiber breakage that is observed. Shorter fibers give poorer mechanical properties than longer fibers. A given quantity of glass powder does not give the same improvement in mechanical properties as an equivalent amount of glass fibers. Fiberglass is commonly added downstream from the throat of an extruder during mixing to give the best retention of fiber length while still achieving adequate dispersive mixing of the fibers. Fiber breakage also occurs during molding [31], especially when very small gates are used to mold parts.

Glass fiber diameter can also affect the physical properties. In general, fiber diameters from 6–17 μm have been used in PBT, with the narrower fibers giving slightly better properties. However, fiber length distribution and fiber content may play a more important role than diameter [32]. Fiber content in a PBT composite is often measured by specific gravity and by ash content. Both of these measurements need to be corrected in cases where the blend is pigmented or combined with other materials.

In addition to glass fibers, PBT can also be reinforced with carbon fibers. Many of the general trends seen with glass fibers are also observed with carbon fibers. One important aspect of carbon fibers is that they may bring electrical conductivity to PBT if sufficient fiber connectivity is achieved in the final part. Metal fibers and metal-coated carbon fibers have also been compounded with PBT, giving not only improved mechanical properties but also molded parts with enhanced ability to shield components from electromotive and radiofrequency interference (EMI–RFI) [33].

3.3 MINERAL-FILLED PBT

PBT grades often come in mineral-filled versions. Common mineral fillers are clay, talc, silica, wollastonite (calcium metasilicate), barite, muscovite and phlogopite mica, glass spheres, milled glass and glass flake [34, 35]. Fillers are generally added to PBT to reduce shrink, lower the coefficient of thermal expansion (CTE) and improve dimensional stability. A key aspect of fillers is particle size distribution. Addition of filler, as opposed to fiber reinforcements, will result in a loss of ductility in PBT. Large particles ($>10\text{ }\mu\text{m}$) will be more detrimental to ductility than small particles [36]. Particle aggregates must be well dispersed to yield this benefit. Talc, being naturally lipophilic, is a preferred filler. Talc is also a very effective nucleant for semicrystalline resins, aiding in the onset of crystal formation from the polymer melt.

Most minerals can be compounded into PBT after direct isolation from mining, milling and grinding operations. Surface treatment, commonly using functional silanes, such as gamma aminopropyl triethoxysilane (GAP), will increase bonding to the matrix, hence giving higher strength and better impact performance. Fillers will increase the modulus and strength of PBT, but not nearly to the extent that reinforcing fibers will. Minerals will reduce PBT shrinkage as a function of loading level and are often added to 'fine-tune' PBT dimensional stability. Combinations of fiberglass or carbon fibers and minerals are often used to balance modulus, shrink, warp and strength. Combinations of fiberglass with a plate-like filler, especially glass flake and most economically mica, give an excellent balance of high strength and modulus with very little warp [26].

Wollastonite is a preferred filler in some instances due to its fibrous form. While not as effective in improving the mechanical properties as glass fibers, it will give more strength than spherical fillers and less anisotropy than longer glass fibers.

By virtue of its high specific gravity, barite (barium sulfate)-filled PBT grades can be used to produce very dense, X-ray opaque, ceramic-like parts [37]. Recently, metal-filled PBT resins using copper or tungsten powder have been used to prepare blends with very high specific gravity.

A very wide variety of pigments are used to color PBT and can also be considered as fillers when used at high levels. The most common pigment is titanium dioxide which can be used in a variety of particle sizes and with various surface treatments [38].

4 PBT POLYMER BLENDS

Over the last 25 years, many commercial products have been made by melt blending PBT with other resins. Blending is most commonly carried out by extruding the PBT resin with a second resin component. Other additives, fillers, or reinforcements may be added to the blends as well.

4.1 PBT–PET BLENDS

One drawback of adding fiberglass to PBT is a loss of the smooth glossy surface of unfilled PBT. While the surface of glass-filled PBT (GF-PBT) is still generally smoother than the surface of glass-filled amorphous resin blends, higher gloss is desirable for GF-PBT parts, such as household appliances and handles that need an attractive appearance. Addition of PET to a GF-PBT gives a smooth glossy surface, especially when molded under the proper conditions. The PBT and PET blends show two distinct melting peaks but appear to co-crystallize. The blends show a single broad T_c . Even though mechanical properties are dominated by fiberglass content, PET will improve mechanical properties to a slight extent. PBT is still the predominant polymer which gives the blend fast crystallization and good properties as-molded. Under standard compounding and molding conditions there is little reaction between the PET and PBT. Formation of a copolymer will occur under more severe reaction conditions. Excessive copolymerization will reduce crystallinity and will slow the rate of crystallization, which is generally undesirable for injection-molding applications [39, 40].

4.2 PBT–POLYCARBONATE BLENDS

Some of the drawbacks of PBT are overcome by blending with an amorphous resin such as polycarbonate (PC). PC and PBT have a natural affinity for each other [41] and, when blended, give a fine morphology with good phase adhesion. The blends are partially miscible [42, 43]. There is a separate polyester phase composed of PBT crystals showing a normal T_m at $\sim 220^\circ\text{C}$, with a minor amount of PC dissolved into the amorphous PBT phase. The PC phase contains a minor amount of dissolved amorphous PBT and shows a T_g from 130 to 145°C . The lowering of the PC T_g from the normal 149°C indicates the extent of partial miscibility between the PC and PBT and will vary depending on the blend ratio and resin molecular weight [44]. The T_g s of the blend will change as a function of the extent that the PBT amorphous phase and the PC phase dissolve into each other. Most PBT–PC blends have a continuous phase of PBT which is composed of PBT crystals and a mixture of amorphous PBT and a minor amount of PC. The dispersed phase is predominately PC containing a small amount of dissolved amorphous PBT.

Figure 8.2 shows the DMA spectrum of a PBT–PC blend, along with that of the PBT resin. Note the improved modulus (E') between the PBT and PC T_g s.

This combination gives a very useful blend of mechanical properties. The PBT phase provides melt flow, solvent resistance and the ultimate heat performance of the blend (T_m). The PC phase provides reduced shrink, better dimensional stability, higher heat capability under low load (66 psi HDT) and improved impact strength. Interestingly, the PC also provides improved paint adhesion by being present as a very thin outer layer in molded parts. PBT, by virtue of its solvent

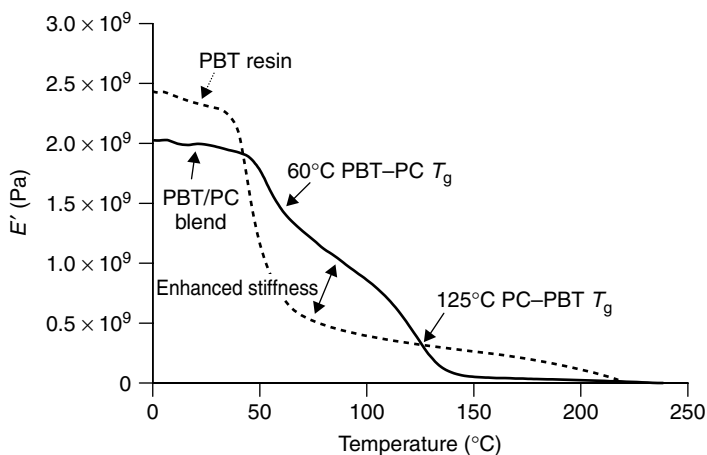


Figure 8.2 Comparison of DMA data obtained for a PBT–PC blend and a PBT resin

resistance, is not easily painted unless surface treatments or aggressive solvents are used.

The extent of the benefits of adding PC to the blend will depend on the PC/PBT ratio. Very low levels (<5 %) of PC or PBT may be totally miscible in the other resin and act like a slightly modified PC or PBT resin. Most PBT blend products use from 10–60 % PC. High PC content will improve impact and lower shrink but reduce flow and solvent resistance. More PBT gives better flow and solvent resistance with more shrink and loss of some impact. A range of PBT–PC blends covering the spread of properties is commercially available.

Initial development of PBT–PC blends was difficult due to highly variable results. It became apparent that considerable reaction could occur between the PBT and PC during normal compounding and molding. Each heat history would give more reaction between the polymers, leading to formation of a copolymer, generating gas, lowering heat performance, slowing crystallization, but improving impact. In titanium-containing PBT blends, the PBT–PC reaction is accompanied by formation of a distinctive golden yellow color, indicative of the presence of titanium phenolate species.

Studies have shown that this reaction is a result of transesterification between PBT and PC. Transesterification is influenced by many factors, including PBT end groups and catalyst residues. While a little copolymer formation is not a bad thing for the performance of the blend, uncontrolled reaction is unacceptable since the same material could never be made twice. Fortunately, methods to control this chemistry were developed. Generally, addition of certain phosphites is used to quench the transesterification and related reactions [45, 46]. Since phosphites are also used as antioxidants and color stabilizers, the ‘quencher’ was often

added to the blends without the formulator being aware of its dual function. PET blends with PC show much less melt reaction than PBT blends since most PET resins are made containing a phosphorus-based catalyst quencher not generally added to PBT.

Overall, the PC blends improve the HDT and impact, especially in the absence of fillers such as glass fiber. The PC reduces shrink and, in glass-filled blends, reduces warp (the amorphous PC resin shrinking less than the PBT). The PC also improves PBT paint adhesion and other secondary operations such as gluing.

PBT-PC blends show increased melt strength allowing them to be easily processed by blow molding and profile extrusion. The PBT-PC blends have been extruded into sheet and thermoformed into parts. Enhanced melt strength allows PBT-PC blends to be foamed. Structural foam grades for injection molding (10–30 % density reduction) are commercially available.

Similar PET-PC and PBT-PET-PC blends have been developed in unfilled, glass-filled and mineral-filled versions. One can begin to see how all of the building blocks of PBT formulation can be used interchangeably to tailor product performance.

4.3 IMPACT-MODIFIED PBT AND PBT-PC BLENDS

While PBT shows high tensile elongation, its Izod and biaxial impact strength provide only modest practical toughness. Various rubbery impact modifiers have been combined with PBT to improve impact. Most unfunctionalized rubbery materials do not show any affinity for PBT and give gross phase separation and poor mechanical properties. Although low levels ($\sim 3\%$) of polyethylene can be added to PBT, higher levels produce delaminated parts with poor properties. However, if ethylene is copolymerized with more polar comonomers, adhesion to PBT is improved along with mechanical properties of the blend. Ethylene vinyl acetate and ethylene alkylacrylate copolymers have been used in this regard. Acrylic acid olefin copolymers, and especially their metal salts (ionomer resins), have been used as PBT modifiers. Some of the carboxylic acid alkali metal salts also function as nucleants. Chemical bonding to PBT can be achieved with epoxy-functionalized olefin copolymers such as ethylene glycidyl methacrylate copolymers. Covalent bonding between the polymers gives good phase adhesion and good impact. However, care must be taken to make sure that there is not excessive reaction of the epoxy with itself during mixing.

Block copolymers such as styrene-butadiene-styrene (SBS) and its hydrogenated versions (SEBS), along with polyester-polyether block copolymers, can also be used to improve PBT impact. The SEBS and SBS copolymers [47], and especially their functionalized, grafted derivatives [48], show surprisingly good affinity for the polyester.

Styrene-acrylonitrile (SAN) copolymers have a high natural affinity for PBT, giving blends with good mechanical properties. If the SAN copolymer is grafted

to a butadiene rubber to make an acrylonitrile–butadiene–styrene (ABS) copolymer, which is in turn blended with PBT, very good impact can be achieved. The lower T_g of the butadiene rubber makes it a more effective impact modifier than the polyolefins or the block copolymers discussed previously. With sufficient rubber of the proper structure, PBT–ABS blends that are ductile at -40°C can be prepared [49].

Of course, there is a trade-off for the improved impact. Generally, it takes from 15–40 wt% of rubber to significantly improve impact. This high level of a low-modulus rubber will lower the modulus of the blend. In addition, some of the graft rubbers, like ABS, will reduce melt flow, thus making these materials more difficult to mold. When temperature is increased to fill injection-molded parts, rubber degradation often occurs, leading to splay, loss of impact, and even less flow. Judicious use of antioxidant packages is important to improving the melt stability of these rubber-modified blends. Butadiene-based rubbers are prone to degradation in the melt or by air oxidation in final use if not correctly stabilized.

One could be tempted to overcome the modulus loss in PBT–rubber blends by adding glass or mineral to the rubber-modified blends. While this works to some extent, the effect of the filler or reinforcement is to limit the ductility of the blend.

Another way to deal with the modulus versus ductility trade-off is through impact modification of PBT–PC blends [50, 51]. The latter blends have good room temperature ductility by virtue of the ductility of PC. Being a high-modulus material, the PC does not lower the blend modulus. However, low-temperature impact of these PBT–PC blends is not exceptional. Blends with an excellent balance of properties are formed by the addition of rubbery modifiers in the form of core–shell rubbers, especially methyl methacrylate–styrene shells around butadiene (MBS) or butyl acrylate rubber cores, or by use of high-rubber-content ABS graft copolymers. For the graft-butadiene-rubber-based blends, -40°C ductility is achieved. In these PBT–PC blends, about half (7–20 wt%) of the rubber loading required in PBT–rubber blends is needed to get equivalent impact, giving compositions higher flexural moduli at equivalent or better ductility. Furthermore, the PC gives less shrinkage and better dimensional stability than standard PBT–rubber blends (Table 8.2). PBT–PC–MBS blends are so tough that they have been used for over 15 years as car bumpers.

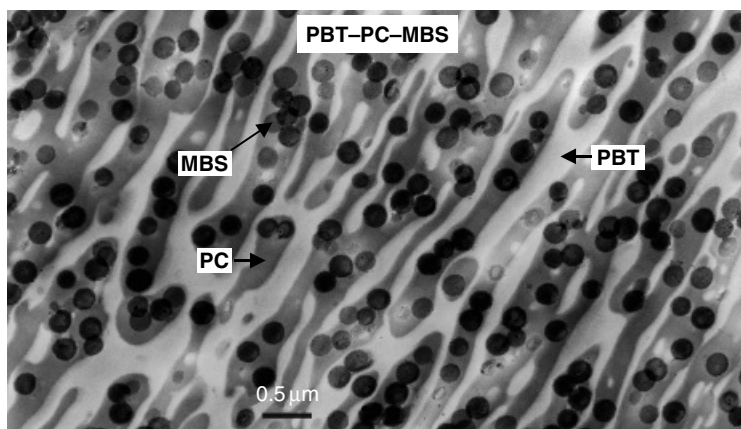
Figure 8.3 shows the morphology of a PBT–PC–MBS blend. The PC phase has been stained and shows as dark regions, while PBT is white. The MBS rubber appears as dark spheres.

4.4 PBT BLENDS WITH STYRENIC COPOLYMERS

As noted above, PBT forms well-compatible blends with SAN. Usually an ABS resin is used to improve practical impact. ABS resins impart to the blend less shrink and better dimensional stability. The ABS is present as a separate

Table 8.2 Properties of impact-modified PBT blends

Property ^a	PBT-PC-MBS ^b	PBT-ABS ^c
Specific gravity	1.21	1.22
Water absorption after 24 h %	0.12	0.10
Mold shrink (in/in $\times 10^{-3}$) ^d	8–10	24–27
Mold shrink (in/in $\times 10^{-3}$) ^e	8–10	24–27
Tensile strength at yield (kpsi)	7.7	5.7
Tensile elongation at break (%)	120	100
Flexural modulus (kpsi)	300	260
Flexural strength (kpsi)	12.3	8.2
Izod impact, notched (ft pdl/in)	13.3	16.3
HDT at 66 psi (°C)	106	99
HDT at 264 psi (°C)	99	47
Melting point (°C)	220	220

^a HDT, heat distortion temperature.^b Approximate composition, 45/45/10.^c Approximate composition, 80/20.^d Shrinkage measured 'with the flow'.^e Shrinkage measured 'across the flow'.**Figure 8.3** Morphology of a PBT-PC-MBS blend. Micrograph provided by courtesy of General Electric Plastics

phase and, by virtue of its T_g ($\sim 110^\circ\text{C}$), will improve the blend 66 psi HDT up to temperatures approaching the dispersed phase (ABS) T_g (Table 8.2).

PBT has also been blended with styrene–maleic anhydride (SMA) copolymers giving materials similar to the ABS blends. Impact modification appears to be more difficult, and one must always be attentive to possible melt reaction with the anhydride, or its ring-opened acid forms, and the PBT resin.

5 FLAME-RETARDANT ADDITIVES

PBT has very good electrical properties, acting as an insulator which is resistant to high voltage [14]. However, PBT is fairly combustible. The four-carbon linkage provides a good source of fuel. To the extent that PBT is replaced in a formulation with less combustible materials, such as fiberglass, minerals, polycarbonate resin and even PET (which is slightly less flammable than PBT), it is rendered less flammable. Addition of more combustible rubbery additives makes PBT easier to ignite. However, simple substitution of less flammable ingredients is usually not enough to achieve a flame-retardant (FR) PBT blend.

FR-PBT is usually achieved by compounding a ‘flame poison’, or materials that will generate a flame poison on burning, into the blend. During burning, these additives generate active species that may interfere with combustion, thus reducing the heat released by burning. These additives are usually organo-bromine- or organo-chlorine-based materials. It is widely known that addition of antimony compounds, almost always antimony trioxide, gives a strong synergy when used with organo-halogen species, resulting in self-extinguishing blends. It is thought that the active flame poison is antimony tribromide formed during the pyrolysis of the organo-bromine species during combustion.

Usually, a significant loading of organo-bromine or organo-chlorine compounds is necessary to achieve flame retardance: loadings as high as 4–5 wt% halogen with 1–3 wt% Sb_2O_3 may be necessary. The exact levels will depend on the fuel present in the formulation and the degree of flame retardancy desired.

Bromine is often preferred as a FR source and, considering that most organo-bromine compounds are only 40–70 wt% bromine and that antimony trioxide is used in blends, FR-PBT blends may contain from 10 to 25 wt% FR additives. This high level of additives will have an effect on the melt processability, density and mechanical properties of the blend.

In most commercial references to ‘FR’-PBT blends, what is really meant by ‘FR’ is that the materials are *ignition resistant* – not impervious to fire. With limited heat sources, such as in the UL-94 test [52] or the glow wire test [53], the FR blends will resist ignition or self-extinguish a small flame. However, in a large fire, these resins will burn, usually with a smoky flame.

Most FR-PBT blends have a V-0 performance rating at 1/16 or 1/32 inch under the UL-94 protocol. Good FR performance is usually more difficult to achieve

at thinner sections as the heat energy is applied to less material and a higher proportion of the sample is exposed directly to the flame. However, thin-walled electrical connector applications often require the V-0 rating. In any case, where plastics are used in flame-resistant applications, it is very critical to test the resin in an actual device to determine its fitness for use. No manufacturer can warranty performance of a resin in actual fire conditions.

Halogenated FR additives are usually of two broad classes, i.e. small-molecule and polymeric flame retardants. Examples of small-molecule flame retardants are polybrominated aryl compounds, such as decabromo diphenyl ether or bromo phthalimides. These compounds are efficient sources of halogen but may result in 'plate-out' issues during molding processes. They may also embrittle unfilled blends. The small-molecule FRs usually are very high-melting compounds and act as a filler during PBT molding and compounding. In GF-PBT, they have little effect on mechanical properties other than to increase density. These small-molecule flame retardants are complemented by polymeric brominated flame retardants that, due to their very high molecular weight, are held in the PBT resin matrix. These polymers usually melt during PBT processing and may be a little easier to mold. Examples of polymeric bromo materials are brominated phenoxy resins (also called bromo epoxy resins) [54], bromo aryl acrylate resins, tetrabromo bisphenol-A polycarbonates and brominated polystyrenes.

For a given level of fuel at a given thickness with the same halogen content, most halogenated compounds show more or less the same flame retardancy. The key differences among these FR additives are effects on flow, melt stability, mechanical properties and long-term ageing of the FR-PBT blend. Different end-use requirements may call for the addition of different FR additives.

Poor choice of FR additives can lead to excessive loss of PBT molecular weight upon processing, hence leading to impaired mechanical properties (usually seen as part melt-viscosity (MV) drop and, if severe, part breakage). In some cases, generation of acidic halide species can cause mold or electrical contact corrosion.

Another aspect of the burning of PBT blends is dripping. When a thermoplastic part is burned, it will begin to melt as it burns. In some cases, the plastic resin will drip away from the sample. If these drips are burning, it can lead to a spread of the fire. The UL-94 test takes this into consideration and, depending on rating, requires little or no flaming drips.

Dripping is a complex behavior that depends on the resin matrix, viscosity and part design. However, over the years, it has been found that very low levels of some fluorinated polymers, notably polytetrafluoroethylene (PTFE), can significantly reduce dripping.

Almost all FR-PBT blends contain an organo-halogen agent, an antimony synergist and a fluoropolymer anti-drip component. These three ingredients, as well as the overall fuel content of the blend, are balanced to formulate FR-PBT products.

In recent years, there has been concern about the environmental fate of halogenated FR additives. To address these concerns, a considerable amount of investigation into non-halogen-based FR packages for PBT has been initiated. Phosphate esters have often been used as FR additives in amorphous resin blends, specifically poly(phenylene ether)–polystyrene (PPE–PS) and PC–ABS blends. Phosphorus has been invoked as acting as an FR in both the gas phase as a flame poison and the solid phase as a char-former. However, most phosphate FR additives have a very low percentage of active ingredient (phosphorus). Due to the relatively low P content in most organo-phosphate additives, high levels of the FR must be added to PBT to approach a V-0 rating. In PBT blends, so much phosphate must be used that other desirable properties may be lost. There are also issues with melt blending, molding and deposits on the mold ('juicing').

Red phosphorus has been used as an effective PBT FR, is non-halogen-based, and very high in active ingredient [55, 56]. However, red phosphorus melt blending requires some special considerations. The potential generation of phosphine gas and acidic decomposition products under incorrect melt processing conditions is a concern. Recently, encapsulated grades of red phosphorus have minimized some of these potential issues. Red P blends are also limited in color capability.

6 PBT AND WATER

The interaction of PBT with water can be complex and at first confusing unless one clearly spells out the exact conditions of moisture contact. There are two broad types of moisture exposure: one is the presence of moisture in a molten polymer during processing, and the other is exposure of a solid part during its use. It is also important to understand the difference in the response of polyamides versus polyesters to water in order to choose the best material for a specific application.

PBT will absorb very little water (0.08 %), and its mechanical properties are not affected in the short term. Polyamides, on the other hand, may absorb up to 12 % of water. In nylon resins, the water acts as a plasticizer; it lowers the T_g , decreases the flexural modulus, and may cause part growth. Based on these criteria alone, polyesters are often a better choice than nylons for many applications (less variation of properties).

With short-term, limited moisture exposure, PBT parts remain essentially unchanged. However, longer-term moisture exposure is a different situation. Under some conditions, water will attack the polyester backbone, giving loss of molecular weight [57]. With enough loss of molecular weight, the polyester will lose mechanical properties and become brittle. Nylon polymer chains are more resistant to cleavage by water and, under most conditions, the polyamide does not show much chain cleavage. When a nylon part dries out, it recovers its properties since the polymer chains retain most of their original chain length. A polyester

that has experienced extensive chain cleavage will not recover its properties when dried.

The extent of polyester chain cleavage will vary greatly depending on the exact conditions of exposure to water. Temperature, time of exposure, and pH are all important. In pH-neutral, cold water below the polyester T_g , little reaction is observed; molded parts may last for a very long time. However, in the polymer melt (during processing) at 250 °C or higher, water will react very quickly with PBT, thus lowering the molecular weight of the polymer. Undried PBT, when melted and molded, can undergo a sharp molecular weight or melt viscosity drop. If enough water is present in the PBT, properties will be lost and parts will become brittle. Usually, there is not enough water present at this high temperature to give catastrophic degradation, but by losing PBT molecular weight in processing wet resin, one is sacrificing some of the ultimate part performance.

Exposure of molded PBT parts to warm water will give varying degrees of decomposition. If the water is acidic or basic, decomposition is accelerated as both acids and bases catalyze ester hydrolysis. Since one of the reaction products of PBT hydrolysis is itself a carboxylic acid, the decomposition of PBT in water is autocatalytic. Hydrolysis of PBT in its own 'juice' or with fresh, neutral water can have a different effect on the rate of chain cleavage. Hydrolysis in a soda lime glass container (creating a basic environment) may give different results than ageing in a borosilicate glass container. The exact conditions of water exposure to polyesters are important in determining the rate of hydrolysis.

PBT's resistance to warm water can be extended through the use of various strategies to suppress hydrolysis but, at severe enough conditions, PBT will eventually break down. The question is, 'will a specific PBT part ever see those conditions?'. The 'hydrolysis-resistant' modified PBT resins will give some measure of extended life to parts exposed to moisture compared to a standard PBT [58, 59].

The situation is more complex when various other ingredients are added to PBT. Glass fibers, for instance, may lose adhesion from the resin due to the action of water on the glass-PBT interface, independent of the PBT-matrix reaction. This action will depend on specific contact conditions such as time, temperature and pH. In some instances, fiber-to-matrix adhesion can be recovered when the sample is dried, resulting in the recovery of some mechanical properties (if the PBT matrix is not too severely degraded). Other additives can introduce additional complications.

Although the relationship of PBT with water sounds complicated (and it is), PBT and its various blends have been used successfully for over 25 years in many different applications. In general, the hydrolysis of PBT is not a major concern. In some specific applications, however, it is critical. In all cases where PBT will see extensive moisture above its T_g , part testing under realistic water exposure conditions is needed to ensure adequate performance.

7 CONCLUSIONS

PBT is a very versatile resin that can be combined with a wide variety of additives to give an array of products for injection-molding applications. The key to understanding PBT is to see it as a fast-crystallizing resin, allowing for rapid cycling in injection-molding applications for the production of durable goods. PBT is also a versatile blend stock that can be combined with dozens of different ingredients, in various amounts, to easily tailor performance to individual needs.

REFERENCES

1. Binsack, R., Thermoplastic Polyesters, in *Engineering Thermoplastics: Polycarbonates, Polyacetals, Polyesters and Cellulose Esters*, Bottenbruch, L. (Ed.), Hanser Publishers, New York, 1996, pp. 6–111.
2. Jaquiss, D. B. G., Borman, W. F. H. and Campbell, R. W., Polyesters, Thermoplastic, in *Kirk-Othmer Encyclopedia of Chemical Technology*, 3rd Edn, Vol. 18, Grayson, M. (Ed.), Wiley, New York, 1982, pp. 549–574.
3. Caldwell, J. R., Jackson, W. J. and Gray, T. F., Polyesters, Thermoplastic, in *Encyclopedia of Polymer Science and Technology*, Vol. 1, Suppl. 1, Bikales, N. M. (Ed.), Wiley-Interscience, New York, 1976, pp. 444–467.
4. Kiefer, D. M., Polyesters end run ‘round nylon’, *Today’s Chemist at Work*, 71–74 (September, 2000).
5. Kirsch, M. A. and Williams, D. J., Understanding the thermoplastic polyester business, *Chemtech*, **24**, 40–49 (1994).
6. Fradet, A. and Marechal, E., Kinetics and mechanisms of polyesterifications, *Adv. Polym. Sci.*, **43**, 51–142 (1982).
7. Brownstein, A. M., 1,4-Butanediol and tetrahydrofuran: exemplary small volume commodities, *Chemtech*, **21**, 506–510 (1991).
8. Siling, M. I. and Laricheva T. N., Titanium compounds as catalysts for esterification and transesterification, *Russ. Chem. Rev.*, **65**, 279–286 (1996).
9. Hsu, J. and Choi, K. Y., Kinetics of transesterification of dimethyl terephthalate with 1,4-butanediol catalyzed by tetrabutyl titanate, *J. Appl. Polym. Sci.*, **32**, 3117–3132 (1986).
10. Yurramendi, L., Barandiaran, M. J. and Asua, J. M., Kinetics of the transesterification of dimethyl terephthalate with 1,4-butanediol, *Polymer*, **29**, 871–874 (1988).
11. Ward, I. M., Wilding, M. A. and Brody, H., The Mechanical properties and structure of poly(*m*-methylene terephthalate) fibers, *J. Polym. Sci., Polym. Phys. Ed.*, **14**, 263–274 (1976).
12. Jakeways, R., Ward, I. M., Wilding, M. A., Hall, I. H., Desborough, I. J. and Pass, M. G., Crystal deformation in aromatic polyesters, *J. Polym. Sci., Polym. Phys. Ed.*, **13**, 799–813 (1975).

13. Song, K. and White, J. L., Formation and characterization of cast and biaxially stretched polybutylene terephthalate film, *Polym. Eng. Sci.*, **38**, 505–515 (1998).
14. Sandrolini, F., Motori, A. and Saccani, A., Electrical properties of poly(Butylene Terephthalate), *J. Appl. Polym. Sci.*, **44**, 765–771 (1992).
15. Cheng, S. Z. D., Pan, R. and Wunderlich, B., Thermal analysis of polybutylene terephthalate for heat capacity, rigid-amorphous content, and transition behavior, *Makromol. Chem.*, **189**, 2443–2458 (1988).
16. Sepe, M., The materials analyst: Part 38, *Injection Molding*, **8**, 52–58 (2000).
17. Takemori, M. T., Towards an understanding of heat distortion temperature of thermoplastics, *Polym. Eng. Sci.*, **19**, 1104–1109 (1979).
18. Moginger, B., Lutz, C., Polsak, A. and Fritz, U., Influence of processing on mechanical properties and morphology of PBT, *Kunststoffe*, **81**, 251–255 (1991).
19. Hobbs, S. Y. and Pratt, C. F., The effect of skin–core morphology on the impact fracture of polybutylene terephthalate, *J. Appl. Polym. Sci.*, **19**, 1701–1722 (1975).
20. Hobbs, S. Y. and Pratt, C. F., Multiple melting in polybutylene terephthalate, *Polymer*, **16**, 462–464 (1975).
21. Nichols, M. E. and Robertson, R. E., The origin of multiple melting endotherms in the thermal analysis of polymers, *J. Polym. Sci., Polym. Phys. Ed.*, **30**, 305–307 (1992).
22. Velarde, D. A. and Yeagley, M. J., Linear shrinkage differences in injection molded parts, *Plast. Eng.*, **56**, 60–64 (2000).
23. Borman, W. F. H., Molecular weight–viscosity relationships for polybutylene terephthalate, *J. Appl. Polym. Sci.*, **22**, 2119–2126 (1978).
24. Gachter, R. and Muller, H. (Eds), *Plastics Additives Handbook*, 4th Edn, Hanser Publishers, New York, 1996.
25. Schweizer, R. A. and Winterman, A. W., Reinforcing fibers and fillers, in *Thermoplastic Polymer Additives*, Lutz, J. T. (Ed.), Marcel Dekker, New York, 1989, Ch. 11, pp. 417–436.
26. Gallucci, R. R., Naar, R., Liu, N.-I., Mordecai, W., Yates, J., Huey, L. and Schweizer, R., Use of bilobe glass fibers to reduce warp in thermoplastic blends, *Plast. Eng.*, **49**, 23–25 (1993).
27. Wolf, H. J., Shortening of fibers in processing of fiber reinforced thermoplastics, *Kunststoffe*, **83**, 69–72 (1993).
28. von Turkovich, R. and Erwin, L., Fiber fracture in reinforced thermoplastic processing, *Polym. Eng. Sci.*, **23**, 743–749 (1983).
29. Travis, J. E., Cianelli, D. A. and Gore, C. R., The long and short of fiber-reinforced thermoplastics, *Machine Des.*, 193–198 (February 1987).
30. Suzuki, N. and Ishida, H., A review on the structure and characterization techniques of silane/matrix interphases, *Macromol. Symp.*, **108**, 19–53 (1996).

31. Parkar, A., Nunn, R. E. and Orroth, S. A., Fiber length degradation in the feed zone during injection molding, in *Proceedings of the 52nd SPE ANTEC'94 Conference*, May 1–5, 1994, San Francisco, CA, Society of Plastics Engineers, Brookfield, CT, 1994, pp. 378–383.
32. Ramsteiner, F. and Theysohn, R., The influence of fiber diameter on the tensile behavior of short-glass fiber reinforced polymers, *Composites Sci. Technol.*, **24**, 231–240 (1985).
33. Liu, N.-I. and van der Meer, R., Synergistic effect of metal flake and metal or metal coated fiber on EMI shielding effectiveness of thermoplastics, *US Patent 4 566 990*, 1986, and references therein.
34. Harben, P. W., *The Industrial Minerals HandyBook*, 2nd Edn, Industrial Minerals Division, Metal Bulletin PLC, London, 1995.
35. Fillers and reinforcements, in *Plastics Compounding Redbook*, Leonard, L. (Ed.), Advanstar Communications, Cleveland, OH, 2000, pp. 47–58.
36. Simonov-Emel'yanov, I. D., Kuleznev, V. N. and Trofimicheva, L. Z., Influence of the particle size of a filler on some characteristics of polymers, *Int. Polym. Sci. Technol.*, **16**, 70–72 (1989).
37. Walsh, E. B., Gallucci, R. R. and Courson, R., High density thermoplastic polyesters, in *Proceedings of the 49th SPE ANTEC'91 Conference*, May 5–9, 1991, Montréal, QC, Canada, Society of Plastics Engineers, Brookfield, CT, 1991, pp. 1334–1339.
38. Braun, U. H., Titanium dioxide – a review, *J. Coatings Technol.*, **69**, 59–72 (1997).
39. Escala, A. and Stein, R. S., Crystallization studies of blends of PET and PBT, in *Multiphase Polymers*, Advances in Chemistry Series, No. 176, Cooper, S. L. and Estes, G. M. (Eds), American Chemical Society, Washington, DC, 1979, Ch. 24, pp. 457–487.
40. Backson, S. C. E., Kenwright, A. M. and Richards, R. W., A ^{13}C NMR study of transesterification in mixtures of PET and PBT, *Polymer*, **36**, 1991–1998 (1995).
41. Hobbs, S. Y., Watkins, V. H. and Bendler, J. T., Diffusion bonding between BPA polycarbonate and polybutylene terephthalate, *Polymer*, **31**, 1663–1668 (1990).
42. Hobbs, S. Y., Dekkers, M. E. J. and Watkins, V. H., Toughened blends of polybutylene terephthalate and BPA polycarbonate, Part 1: morphology, *J. Mater. Sci.*, **23**, 1219–1224 (1988).
43. Cheng, Y.-Y., Brillhart, M., Cebe, P. and Capel, M., X-ray scattering and thermal analysis study of the effects of molecular weight on phase structure in blends of polybutylene terephthalate with polycarbonate, *J. Poly. Sci., Polym. Phys.*, **34**, 2953–2965 (1996).
44. Hamilton, D. G. and Gallucci, R. R., The effects of molecular weight on polycarbonate–polybutylene terephthalate blends, *J. Appl. Polym. Sci.*, **48**, 2249–2252 (1993).

45. Devaux, J., Godard, P. and Mercier, J. P., The transesterification of bisphenol-A polycarbonate and polybutylene terephthalate: a new route to block copolycondensates, *Polym. Eng. Sci.*, **22**, 229–233 (1982).
46. Pellow-Jarman, M. and Hetem, M., The effect of the polybutylene terephthalate constituent on the reactions occurring in PBT–polycarbonate polymer blends below their decomposition temperature, *Plast. Rubber Composites Proc. Appl.*, **23**, 31–41 (1995).
47. Gergen, W. P. and Davison, S., Thermoplastic block copolymer blends, *US Patent 4 101 605*, 1978.
48. (a) Gergen, W. P. and Lutz, R. G., Impact resistant blends of thermoplastic polyesters and modified block copolymers, *US Patent 4 797 447*, 1989; (b) Gelles, R., Modic, M. and Kirkpatrick, J., Modification of engineering thermoplastics with functionalized styrenic block copolymers, in *Proceedings of the 46th SPE ANTEC'88 Conference*, April 18–21, 1988, Atlanta, GA, Society of Plastics Engineers, Brookfield, CT, 1988, pp. 513–515.
49. Hourston, D. J., Lane, S. and Zhang, H. X., Toughened thermoplastics: Part 2: impact properties and fracture mechanisms of rubber modified PBT, *Polymer*, **32**, 2215–2220 (1991).
50. Dekkers, M. E. J., Hobbs, S. Y. and Watkins, V. H., Toughened blends of polybutylene terephthalate and BPA polycarbonate, Part 2: toughening mechanisms, *J. Mater. Sci.*, **23**, 1225–1230 (1988).
51. Wu, J. and Mai, Y.-W., Fracture toughness and fracture mechanisms of PBT–PC–IM blend, Part 2: toughening mechanisms, *J. Mater. Sci.*, **28**, 6167–6177 (1993).
52. Tests for flammability of plastic materials, *Underwriters Laboratory Bulletin UL-94*, Underwriters Laboratory, Northbrook, IL, 1985, pp. 10–13.
53. Polymeric materials – short term property evaluations: hot wire ignition, *Underwriters Laboratory Bulletin UL-746A*, Underwriters Laboratory, Northbrook, IL, 1984, pp. 24–25 (ASTM D3874-97, American Society for Testing and Materials; Glow Wire Test (IEC 695-2-1), International Electrotechnical Commission).
54. Nir, Z., Bar-Yaacov, Y., Minke, R., Touval, I., Kourtides, D. A. and Parker, J. A., A new brominated polymeric additive for flame retardant glass-filled PBT, *J. Fire Retardant Chem.*, **9**, 181–188 (1982).
55. Peters, E. N. Red phosphorus as a flame retardant, in *Flame Retardancy of Polymeric Materials*, Vol. 5, Kuryler, W. C. and Papa, A. J. (Eds), Marcel Dekker, New York, Ch. 3, pp. 113–176.
56. Granzow, A. and Cannelongo, J. F., The effect of red phosphorus on the flammability of polyethylene terephthalate, *J. Appl. Polym. Sci.*, **20**, 689–701 (1976).
57. Borman, W. F. H., The effect of temperature and humidity on the long-term performance of polybutylene terephthalate compounds, *Polym. Eng. Sci.*, **22**, 883–887 (1982).

58. Neumann, W., Holtschmidt, H., Peter, J., and Fisher, R., Stabilization of polyesters with polycarbodiimide, *US Patent 3 193 522*, 1965.
59. Gallucci, R. R., Dellacolella, B. A. and Hamilton, D. G., Hydrolysis resistant thermoplastic polyester, *Plast. Eng.*, **50**, 51–53 (1994).

Properties and Applications of Poly(Ethylene 2,6-Naphthalene), its Copolyesters and Blends

D. D. CALLANDER

M & G Polymers USA, Sharon Center, OH, USA

1 INTRODUCTION

Poly(ethylene terephthalate) (PET) has become a major synthetic polymer during the past forty years. Significant commercial markets [1] have been developed for its application in textile and industrial fibers, films, and foamed articles, containers for carbonated beverages, water and other liquids, and thermoformed applications (e.g. dual ovenable containers).

These marketing successes take advantage of PET's excellent balance of properties, including ease of melt processing, high strength, thermal resistance, transparency, high gaseous barrier, health and environmental safety and recyclability. These desirable attributes are complemented with excellent cost-effective acceptability. Since its beginning in 1977, PET's annual growth in carbonated beverages and other foodstuffs' containers has continued to exceed 10 %, amounting to 12 billion pounds worldwide in 2000 [1]. Most of these gains were at the expense of glass containers, where PET's lighter weight, transparency, shatter resistance and processing advantages are desirable.

However, there remain numerous end-use applications which require significant improvements in the properties PET has to offer. These include higher tensile strength and modulus for tyre reinforcement yarns and monofilament applications, higher temperature resistance for hot-fill containers and films, and greater gaseous barrier for longer shelf-life requirements (e.g. fruit juice and beer markets).

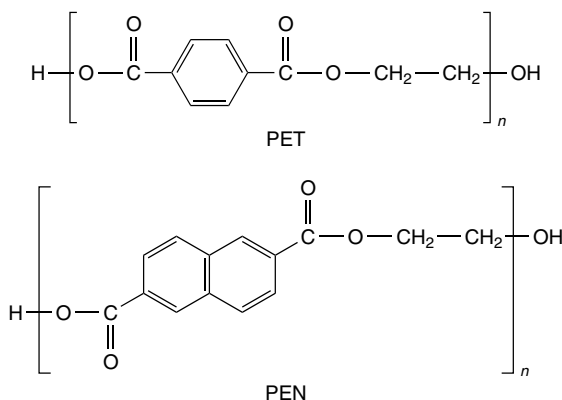


Figure 9.1 Chemical structures of PET and PEN

It is for such markets that the chemically similar polyester, poly(ethylene-2,6-naphthalate) (PEN) is being evaluated.

PEN differs from PET in that the acid component of its polymer chain is naphthalene 2,6-dicarboxylic acid, replacing the terephthalic acid of PET (Figure 9.1). In each case, the glycol monomer is ethylene glycol (EG). The two condensed aromatic rings of PEN confer on it improvements in strength and modulus, chemical and hydrolytic resistance, gaseous barrier, thermal and thermo-oxidative resistance and ultraviolet (UV) light barrier resistance compared to PET [2].

Although the superior properties of PEN have been known for many years, the unavailability of the naphthalate monomer has delayed the development of commercial markets, until relatively recently (1995) when the Amoco Chemical Company offered high purity naphthalene-2,6-dimethyl dicarboxylate (NDC) in amounts of up to 60 million pounds per year. This diester is produced by a five-step synthetic route, starting from the readily available compounds, *o*-xylene and 1,4-butadiene [3]. Prior to this, the NDC diester was obtained by extraction of 2,6-dimethylnaphthalene (DMN) from petroleum streams, where it was present in relatively low abundance. Oxidation of DMN to crude 2,6-naphthalene dicarboxylic (NDA) is conducted by a similar process to that used for conversion of *p*-xylene to purified terephthalic acid (TA), crude NDA is esterified with methanol, and is then distilled to yield high purity NDC. Other companies (e.g. the Mitsubishi Gas Chemical Company) followed Amoco's introduction with lesser amounts of NDC. Teijin [4] has manufactured PEN for many years for its own captive uses in films.

2 MANUFACTURE OF PEN

There are two major manufacturing routes for PEN and PET, i.e. (1) an ester, or (2) an acid process, named according to whether the starting monomer is

a diester or a diacid, respectively. In both cases for PEN and PET, the glycol monomer is EG. One exception to this was Toyobo's relatively short-lived process which reacted terephthalic acid with ethylene oxide [5]. Historically, as it was easier to obtain the high purity (99.5 %) needed to ensure polymerization to high-molecular-weight PET, dimethyl terephthalate (DMT) was the monomer used for the initial commercial manufacture. However, once high-purity TA became available, the acid process has been preferred, using lower catalyst and EG amounts. A similar situation exists currently for PEN manufacture, as the availability of high-purity NDA is very limited [6]. NDA is a much more intractable monomer than TA, leading to greater purification challenges and more difficult, less economic polymerization processes. Manufacturing conditions for PEN are similar to those for PET, except that the higher melting point of NDC and the greater melt viscosities of PEN necessitate higher temperatures throughout, with melt polycondensations being conducted in the range 290 to 300 °C. Solid-state polymerization (SSP) of the melt-produced resin pellets is the preferred process to upgrade the molecular weight of PEN (or PET), again at higher temperatures than those used for SSP of PET. Consequently, considerable care is taken to minimize thermal and thermo-oxidative exposure during PEN manufacture.

3 PROPERTIES OF PEN

PEN is a semicrystalline, aromatic polyester with a reduced tendency to crystallize compared to PET [7]. The intrinsic 'off-set' 2,6 disubstitution of the naphthalene ring, compared to the 1,4 linear substitution of the aromatic ring of PET, dictates the crystalline morphology. Two major crystalline forms, α and β , exist, depending on the prior thermal history of PEN [8]. The α -form is triclinic with the following unit cell dimensions: $a = 0.651$ nm; $b = 0.575$ nm; $c = 1.32$ nm; $\alpha = 81.33^\circ$, $\beta = 144^\circ$, $\gamma = 100^\circ$: its crystalline density is 1.407 g/ml. This form occurs when crystallizing at temperatures $\leq 200^\circ\text{C}$. The higher melting point β -form is also triclinic, and has the following unit cell dimensions $a = 0.926$ nm; $b = 1.559$ nm; $c = 1.217$ nm; $\alpha = 121.6^\circ$; $\beta = 95.57^\circ$; $\gamma = 122.52^\circ$: its crystalline density is 1.439 g/ml. Crystallizing at temperatures $\geq 240^\circ\text{C}$ yields this form.

In common with other EG-based polyesters, there are two major by-products of the polymerization chemistry, i.e. diethylene glycol (DEG) and acetaldehyde (AA), which influence PEN's properties and application potential. Depending on the polymerization conditions, different levels of the DEG moiety are incorporated randomly in the PEN polymer chain. The DEG content of PEN has the expected comonomer effect on its thermal transitions and performance properties. Generally, PEN manufactured from the neutral NDC diester monomer has the lowest incorporated DEG content (~ 0.4 to 0.8 wt%), although significantly higher levels are produced when higher EG/NDC molar ratios (> 2.0), higher temperatures and longer residence times, and/or acidic catalysts, are used. The balance of

higher manufacturing temperatures and reduced diffusion of AA results in similar low AA levels in PEN SSP pellets, but to ensure good final color, stagnant regions and reactor hot-spots should be eliminated.

4 THERMAL TRANSITIONS OF PEN

The typical differential scanning calorimetric (DSC) traces shown in Figure 9.2 compare the thermal transitions of similar low-DEG-content PEN and PET resins. The fact that the glass transition temperature (T_g) of PEN is 45–50 °C higher than that of PET has a major influence on the processing and performance of PEN applications. In addition, the fact that PEN's T_g is 20–25 °C above the boiling point of water has a significant effect on the thermal stability potential of many hot, aqueous exposure applications.

5 COMPARISON OF THE PROPERTIES OF PEN AND PET

The chemical and physical properties of PEN are generally superior to those of PET and have been conveniently represented in comparative ‘star diagrams’ (Figure 9.3). Typical properties of PEN are shown in this figure. PEN has greater chemical resistance than PET. This is highly desirable in most applications, but makes dissolution of PEN more difficult for analytical test methods (e.g. intrinsic viscosity (IV), carboxyl end groups, nuclear magnetic resonance (NMR), gelphase chromatography (GPC), etc. measurements). This greater ‘insolubility’ compared to PET is even greater for highly crystalline PEN. Existing test methods

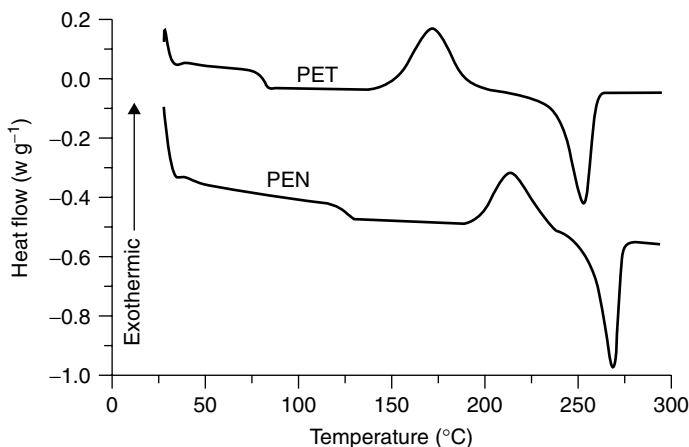


Figure 9.2 DSC transitions of PET and PEN

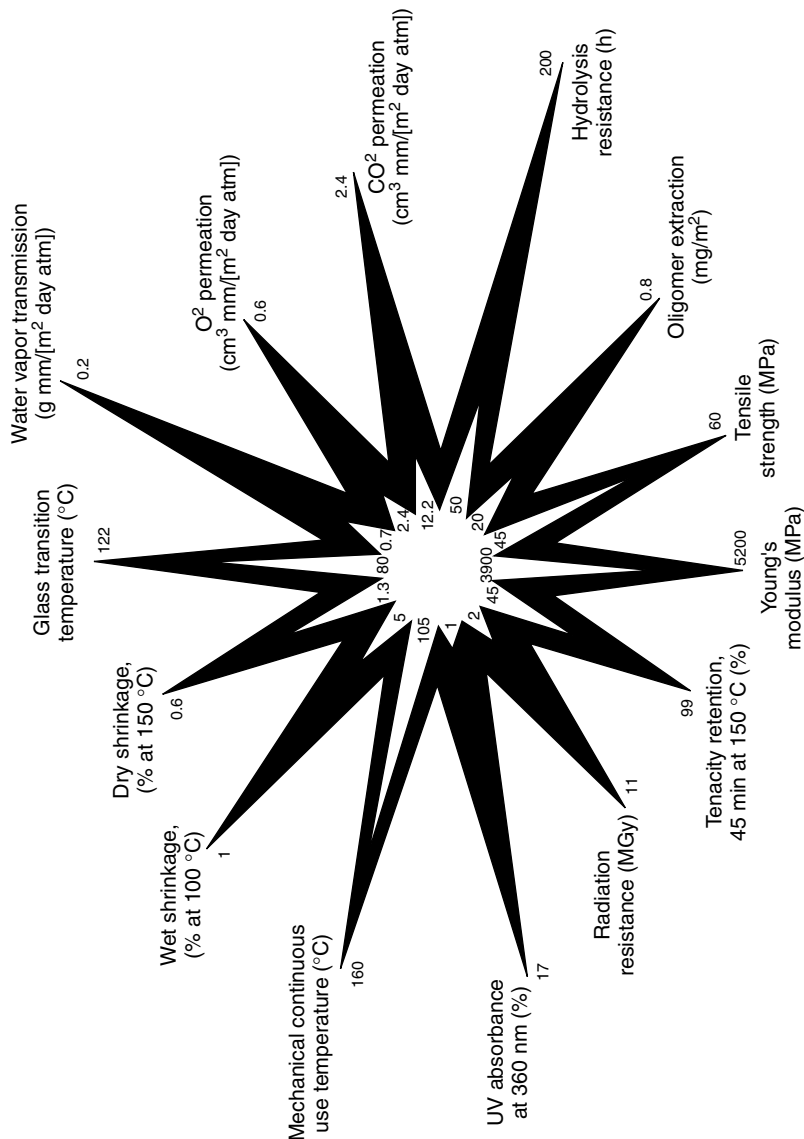


Figure 9.3 'Star diagram' illustrating the improved properties of PEN when compared to PET: PEN, 'black'; PET, 'white'. From manufacturer's literature published by BP Chemicals and reproduced with permission

for PET are often significantly modified to permit PEN characterization. For example, solution intrinsic viscosity (IV) testing of crystalline PEN may involve controlled 'melt and quenching' to the amorphous state to facilitate dissolution.

6 OPTICAL PROPERTIES OF PEN

Another intrinsic difference of PEN compared to PET is that the naphthalene ring has a more extended chromophore which absorbs UV light up to 380 nm, compared to PET's absorption up to 313 nm (Figure 9.4). This greater UV absorption has obvious application where this screening property is desirable for protection of the integrity of foodstuffs. In addition, a blue-white, visible fluorescence results when PEN is excited by black light emitting near 360 nm [9]. This permits ready identification and separation of PEN from PET containers, which has potential for recovering the more expensive PEN in post-consumer mixtures of PET and PEN containers and films.

7 SOLID-STATE POLYMERIZATION OF PEN

The higher thermal transitions and gaseous barrier of PEN compared to PET has significant implications on SSP PEN properties and processability. Whereas pre-crystallization of PET may be conducted in a dry air environment, the higher operating temperatures for PEN can oxidize the pellet surfaces, thus requiring greater process control or the use of inert atmospheres. Another phenomenon which may occur prior to crystallization of PEN pellets is 'pop-corning' or

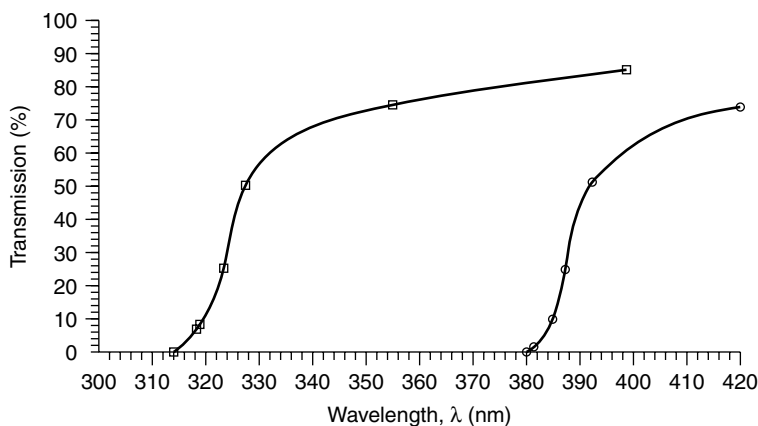


Figure 9.4 UV transmission spectra obtained for PEN and PET bottle sidewalls: ○, PEN; □, PET

volume expansion. Depending on the level of volatiles (e.g. AA, EG, water, etc.) in individual pellets, the higher barrier, modulus and temperature exposure may increase the internal pressure of the pellets, so causing significant volume expansion. Devolatilization at lower temperatures overcomes this phenomenon [10]. During the SSP process, the polymerization by-products, water and EG are removed in a diffusion-controlled manner. The higher temperatures and gaseous barrier of PEN, coupled with long SSP cycles, can create much larger differences in molecular weight and crystallinity between the core and skin of the PEN pellet compared to PET. In addition, the higher melt viscosities of the different PEN molecular weights may lead to very high melt viscosities near the skin. When these differences are too large, conventional melting extruders may be unable to achieve homogeneous melts during normal process times. In addition, if 'unmelts' and inhomogeneous melts exist, processing difficulties and properties deficiencies are likely to occur.

8 COPOLYESTERS

When the full improved property potential of PEN compared to PET is not needed for an end-use application, copolyesters may be considered. Common available comonomers which may be used include terephthalic acid and isophthalic acid (IPA), DEG and cyclohexane dimethanol glycols.

Considering the effect of TA as a typical comonomer, practicable crystallizability is achieved only up to about 15 mol% modification level. Modification of PET with naphthalate comonomer is subject to the same limitation (Figure 9.5). The T_g of T/N copolymers with EG also increases from that of PET to PEN homopolymers, according to the well-known linear relationship. The relationship of mol% modification to both T_g and T_m (melting point) measured by DSC is also shown in Figure 9.5. Enhancement of physical properties by orienting above T_g is possible for the shown crystallizable regions, but not for the more highly modified, amorphous compositions. Blends of PET and PEN, when properly controlled, can yield crystallizable compositions with enhancement of properties over the whole composition range (see Section 9 below) [11].

8.1 BENEFITS OF NAPHTHALATE-MODIFIED COPOLYESTERS

The modification of PET with low levels of naphthalate comonomer increases the T_g and enables optimally oriented articles (films, fibers, containers, etc.) to resist higher temperatures without shrinkage. Heat setting under tension may be applied to further extend thermal stability. In addition, when retention of optical transparency is required, such copolymers crystallize less readily than PET, and may readily be quenched from the melt to the transparent, amorphous state. Thus,

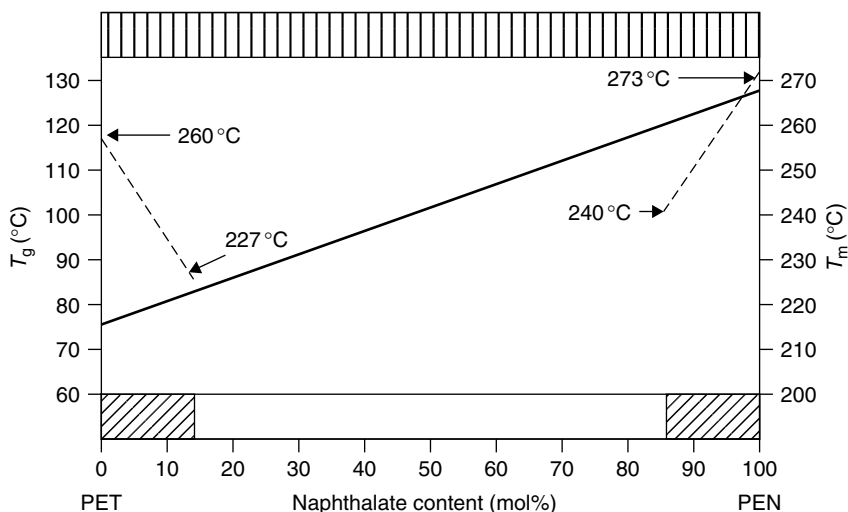


Figure 9.5 DSC transitions and crystallizability data for PET and PEN copolyesters and blends: ▨, crystallizable copolyesters; □, amorphous copolyesters; ▩, crystallizable PET/PEN blends: —, T_g ; - - - - , T_m

thicker, transparent sections are possible. Optimal strength and gaseous-barrier properties on orientation, however, require higher stretch ratios and/or higher molecular weights, for strengths equivalent to PET [12]. The beneficial absorption of UV light is still present in copolyesters of PET modified with low levels (1–5 mol%) of naphthalate [13]. This property may be utilized to protect food-stuffs in naphthalate-modified PET containers and films.

8.2 MANUFACTURE OF COPOLYESTERS

Copolyesters may be produced by conventional ester or acid processes. In addition, by utilizing the ester-exchange potential of polyesters, naphthalate-modified PET or phthalate-modified PEN may be manufactured by incorporating preformed PEN or PET, or their respective copolyesters during the melt-polymerization process [14]. The preformed resins or low-molecular-weight oligomers function as ‘masterbatch’ sources, undergoing *in-situ* ester-interchange, leading to random copolyesters at equilibrium or copolyesters with controlled levels of blockiness, depending on the time, temperature and mixing conditions being used.

9 NAPHTHALATE-BASED BLENDS

Most blends of polymers are immiscible. Solubility parameter considerations predict that miscibility may be possible when small differences (e.g. ≤ 0.5) in

these values exist [15]. Numerous evaluations have been conducted involving blending of PEN and PET or copolyesters of each [16]. Incorporation of a third tere/naphthalate copolyester has been shown to enable compatible blends [17]. PEN and PET are immiscible and usually the dispersed phase size is large enough to scatter visible light, so yielding unacceptable haze in these blends. In addition, they have an inferior balance of properties and the opacity is unacceptable in most container applications, where high transparency is required.

However, compatibility between PET and PEN homopolymers and/or copolyesters may be achieved by allowing sufficient time, temperature and mixing during melt blending to ensure that sufficient ester-interchange occurs to yield a compatible, transparent blend. The extent of ester-interchange needed for compatibilization varies depending on the blend components and the molecular weight of the component polyesters. DSC analysis has been used to determine the melt-processing conditions needed to yield a single T_g for blends [16]. NMR analysis has been used effectively to determine the extent of ester-interchange [18]. The use of such techniques has enabled conversion of PEN/PET blends to containers with significant improvements in gaseous barrier, increased hot-fill and/or pasteurization potential [19]. Thus, cost-effective small containers requiring greater gaseous-barrier performance have been demonstrated by using PEN/PET blends. Again, such improvements require properly designed preforms to provide optimal orientation in blow-molded containers [20].

10 APPLICATIONS FOR PEN, ITS COPOLYESTERS AND BLENDS

End-use applications for naphthalate-based polyester resins depend on optimizing the balance of properties desired in a specific application. Usually this involves optimizing the orientation process (uni- or bi-axial) with its accompanying crystallinity development. Subsequent heat setting may be included when additional improvements in thermal stability are needed.

10.1 FILMS

Similar to PET, PEN film is typically manufactured from resins with molecular weights lower than those needed for containers or industrial fibers. Optimal properties are achieved by considering the natural draw ratios corresponding to the molecular weight of the resin used and orienting at 20 to 40°C above its T_g . Optimal stretch ratios for PEN are usually slightly greater than those for PET (e.g. 10–12 area stretch for PET compared to 12–14 for PEN). Considerably higher stretch ratios are required for PEN copolyesters and blends for the formation of optimally stabilized morphologies, which determine the

resulting balance of properties [12]. The orientation extent should exceed the 'necking' regions to ensure that crystallites are created to stabilize the morphology in the strain-hardening process [21]. In the absence of strain-hardening, oriented regions will undergo shrinkage towards the original non-oriented state when the orientation temperature is approached. Although such considerations are also important for PET, they are especially important for PEN to ensure cost-effective performance. The use of blends of PEN with the higher- T_g amorphous polyetherimide (PEI) to overcome the low orientation necking phenomenon has been demonstrated [21].

Major PEN film applications include substrates for 'Advanced Photo System' (APS) [2] film, where PEN's higher modulus permits the thinner, curl-free films required. Capacitors capable of higher temperature performance in industrial motor windings also make use of PEN's properties.

10.2 FIBER AND MONOFILAMENT

In fiber and monofilament applications, the higher modulus and temperature stability of PEN is utilized in end-use applications. Monofilaments have been used in paper making felts, where the higher modulus, temperature and hydrolysis resistance are required [22]. PEN tyre-reinforcing yarns have also been introduced by Pirelli into high-performance motorcycle [23] tyres. Evaluations in other tyre, fan and conveyor belts application have also been conducted [24]. Stable partially oriented yarn (POY) technology is applicable to PEN as well as PET, although somewhat higher spinning speeds are required for PEN to induce the partial orientation and its associated crystallinity development [25].

10.3 CONTAINERS

Many evaluations have led to the commercial utilization of PEN, its copolyesters and blends in some commercial applications. The cost effectiveness is especially apparent in returnable-refillable applications, which take advantage of PEN's chemical resistance in commercial washing operations, so ensuring an increased number of re-fill trips [26]. Other applications benefit from PEN's increased gaseous barrier, UV absorption, thinner and lower weight potential. Considerable effort is underway to enable utilization of PEN, its copolyesters and blends for beer, higher hot-fill and heat-pasteurizable containers [27].

Again, as for films, careful consideration of the optimal stretch ratios with or without heat setting of the naphthalate composition is essential to ensure cost effectiveness in a specific container. In the absence of this optimization, performance may be inferior to properly designed containers from the much less costly PET resin.

10.4 COSMETIC AND PHARMACEUTICAL CONTAINERS

Considerable interest has been shown in the potential of PEN for cosmetic and pharmaceutical containers. Many cosmetics require the increased chemical resistance of PEN. These, generally, are small, amorphous, non-oriented containers that can resist solvent crystallization by the specific chemicals involved. Similar PET containers develop an unacceptable, solvent-induced hazy appearance. PEN has been used successfully to contain liquid anesthetics [28], while PEN blood tubes have also been demonstrated [29].

11 SUMMARY

Although PEN is still a specialty resin when compared to PET, its improved properties' potential ensures that considerable market growth will occur in the near future. This growth will stimulate increased commercial availability of the naphthalate diester and diacid monomers essential for numerous commercial applications.

REFERENCES

1. Prevost, P., BP Chemicals and the global polyester/PTA supply/demand, presentation given at the *Polyester 2000 5th World Congress*, Zurich, Switzerland, November 28–December 1, 2000, Maack Business Services [www.MBSpolymer.com].
2. Anon, Film applications: BP naphthalates, BP Chemicals [www.bpchemicals.com/naphthalates].
3. *US Patent 5 948 949* (to Mitsubishi Gas Chemical Company), 1999.
4. Anon, *Jpn Chem. Daily* (May 9, 1990).
5. *Jpn Patent 47 038 872* (to Toyobo Chemical Company), 1972.
6. Anon, HNDA specifications: BP naphthalates, BP Chemicals [www.bpchemicals.com/naphthalates].
7. Buchner, S., Wisme, D. and Zachmann, H. G., Kinetics of crystallization and melting behavior of poly(ethylenenaphthalene-2,6-dicarboxylate), *Polymer*, **30**, 480–488 (1989).
8. Liu, J., Sidoti, G., Hommema, J. A., Geil, P. H., Kim, J. C. and Cakmak, M., Crystal structure and morphology of thin film, melt-crystallized poly(ethylenenaphthalate), *J. Macromol. Sci., Phys.*, **B37**, 567–586 (1998).
9. Ouchi, I., Hosoi, M. and Matsumoto, F., Photodegradation of poly(ethylene-2,6-naphthalate) films, *J. Appl. Polym. Sci.*, **20**, 1983–1987 (1976).
10. *US Patent 4 963 644* (to Goodyear Tire and Rubber Company), 1990.
11. Callander, D. and Sisson, E., High performance PEN and naphthalate based packaging resins, presentation given at the *Bev-Pak Americas'94 Conference*, Tarpon Springs, FL, April 11–12, 1994.

12. Jenkins, S. D., PET/PEN copolymers and blends for hot-fill and high barrier packaging applications, presentation given at the *Specialty Polyesters'95 Conference*, Brussels, June 27–28, 1995, Schotland Business Research Inc., Skillman, NJ, 1995.
13. Anon, Light absorbing properties: BP naphthalates, BP Chemicals [www.bp-chemicals.com/naphthalates].
14. *US Patent 5 612 423* (to Shell Chemical Company), 1997.
15. Olabisi, O. in *Kirk-Othmer Encyclopedia of Chemical Technology*, 3rd Edition, Wiley InterScience, John Wiley & Sons, Inc., New York. Vol. 18, 1982, pp. 443–478.
16. Stewart, M. E., Cox, A. J. and Naylor, D. M., Reactive processing of poly(ethylene-2,6-naphthalene dicarboxylate)/poly(ethyleneterephthalate) blends, *Polymer*, **34**, 4060–4067 (1993).
17. *US Patent 5 006 613* (to Eastman Kodak Company), 1991.
18. Stewart, M. E., Cox, A. J. and Naylor, D. M., Transesterification of poly(ethylene-2,6-naphthalene dicarboxylate)/poly(ethyleneterephthalate) blends, in *Proceedings of the 51st SPE ANTEC'93 Conference*, May 9–13, 1993, New Orleans, LA, Society of Plastics Engineers, Brookfield, CT, 1993, Vol. 2, pp. 1222–1226.
19. *US Patent 5 888 598* (to Coca Cola Company), 1999.
20. Callander, D. D., Naphthalate-based copolyesters for containers, presentation given at the *Bev-Pak Asia Conference*, Hong Kong, September 22–23, 1994.
21. Kim, J. C., Cakmak, M. and Zhou, X., Effect of composition on orientation, optical and mechanical properties of biaxially drawn PEN and PEN/PEI blend films, *Polymer*, **39**, 4225–4234 (1998).
22. *US Patent 5 840 637* (to Albany International), 1998.
23. (a) Anon, PEN reduces road noise for Bridgestone tires, *Elements Bull. (BP Chemicals)*, **1**(1), Summer 2001 [www.bpchemicals.com/naphthalates]; (b) Pirelli Dragon Evo tyre, *Pirelli Annual Report*, Pirelli Spa., Milan, Italy, 1999, p. 34.
24. *US Patent 5 397 527* (to Allied Signal), 1995.
25. Cakmak, M. and Kim, J. C., Structure development in high speed spinning of polyethylene naphthalate (PEN) fibers, *J. Appl. Polym. Sci.*, **64**, 729–747 (1997).
26. Anon, A first for beer, *PET Planet Insider*, Issue 8/2001, Alexander B. Buchler, Heidelberg, Germany, 2001 [www.petplan.net].
27. Sisson, E. and Howell, R., PET/PEN containers recycling update, presentation given at the *Bev-Pak Americas'98 Conference*, Fort Lauderdale, FL, April 6–7, 1998.
28. Anon, PEN protects volatile anesthetic, *Elements Bull. (BP Chemicals)*, **1**(2), Winter 2002 [www.bpchemicals.com/naphthalates].
29. *US Patent 5,924,594* (to Becton Dickinson), 1999.

10

Biaxially Oriented Poly(Ethylene 2,6-Naphthalene) Films: Manufacture, Properties and Commercial Applications

B. HU AND R. M. OTTENBRITE

Virginia Commonwealth University, Richmond, VA, USA

and

J. A. SIDDIQUI

DuPont /-Technologies, Research Triangle Park, NC, USA

1 INTRODUCTION

Polyester has become a mainstay commodity material. This is one material that everyone comes in contact with daily; for example, it is used in clothing, bedding, upholstery and carpeting. The first patent to cover polyesters was filed in 1941 by Whinfield and Dickson, with the material defined as a polymer formed by the combination of a diacid and a diol [1]. Following this discovery, the first commercial polyester, poly(ethylene 1,4-terephthalate) (PET), was produced by condensation polymerization of terephthalic acid (TA) (or dimethyl terephthalate (DMT)) as the diacid moiety and ethylene glycol as the diol. PET is now a well-known and widely utilized polymer material that is used throughout the world to manufacture films and fibers.

Once the theory of combining a diacid or a diacid derivative with a diol to produce a polyester was established, many variations on the concept were investigated. One of these was to react ethylene glycol with a diacid moiety containing a naphthalene ring in place of benzene ring in PET, to produce poly(ethylene 2,6-naphthalate) (PEN). The performance of PEN fills a gap between the two traditionally used materials, i.e. the polyester (PET) and the polyimide (PI) in the world of plastics. The properties of PEN film are similar to those of PET, but PEN film offers improved performance over PET in the areas of dimensional stability, stiffness, UV weathering resistance, low monomer content, tensile strength, hydrolysis resistance and chemical resistance. When lower costs for the starting material and manufacturing are achieved, PEN could replace polyamides in many applications. Based on improved economics, PEN film has achieved additional growth through applications in areas such as advanced photo system films, flexible printed circuits, motor insulation, high temperature labels, video cassettes and capacitors [2, 3].

Although PEN is a fifty-year-old polyester product it is only now just beginning to make a major appearance into the marketplace. It was first synthesized as a laboratory curiosity in 1948 by ICI scientists [4]. Dimethyl-2,6-naphthalenedicarboxylate (NDC) is the primary starting monomer, along with glycol. The key to further development of PEN is to produce the diacid, 2,6-naphthalenedicarboxylic acid (NDA), on a commercial scale. This is a major

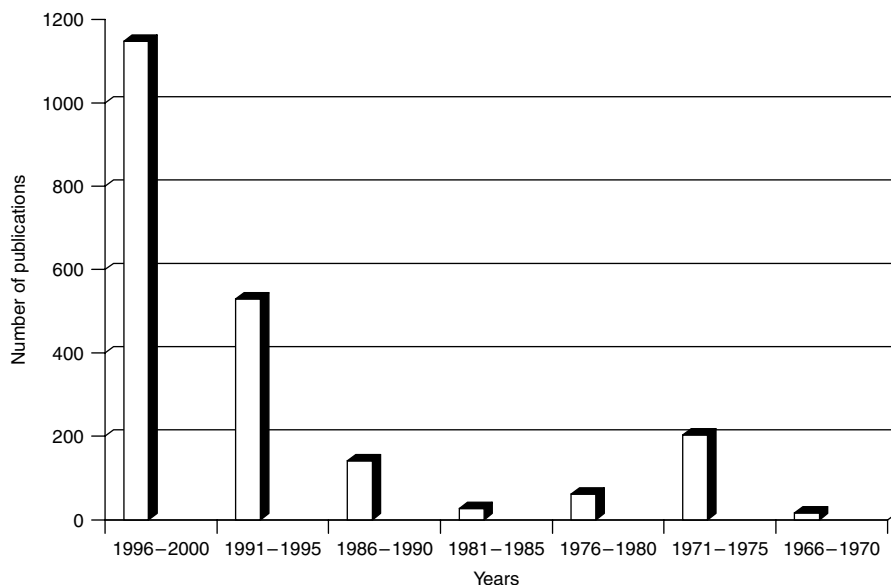


Figure 10.1 References for PEN published during the period 1967-2000 (total of 2125)

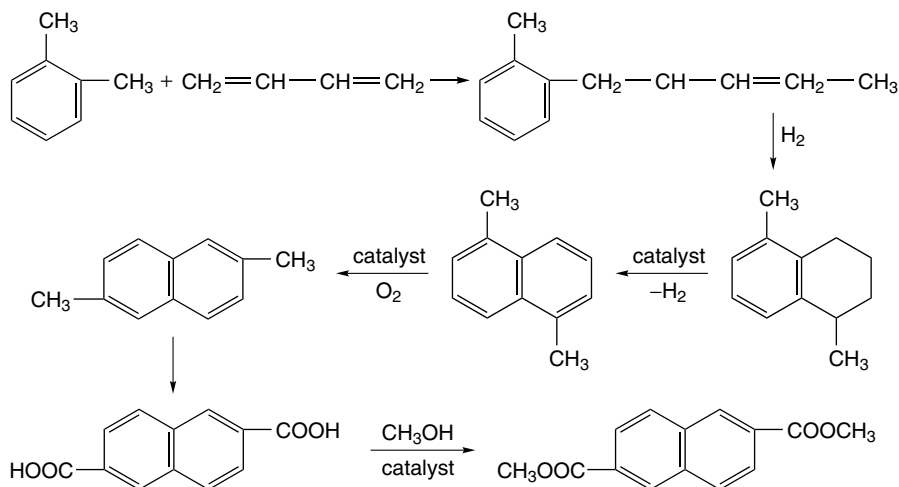
problem that has limited the wide application of PEN for a long time. This situation improved somewhat during the early 1990s, when the Amoco Chemical and Mitsubishi Gas & Chemical companies started supplying NDC on a large scale, which significantly increased raw material feed stocks and reduced the cost of PEN resin. This has, subsequently, increased PEN production and applications. The polyester market is currently taking advantage of the benefits offered by PEN in many applications. Currently, the world-wide capacity for PEN resin is 50 000 t/y. During the last five years, the number of papers and patents published on this material has almost doubled that published over the previous thirty five years (Figure 10.1).

2 THE MANUFACTURING PROCESS FOR PEN FILMS

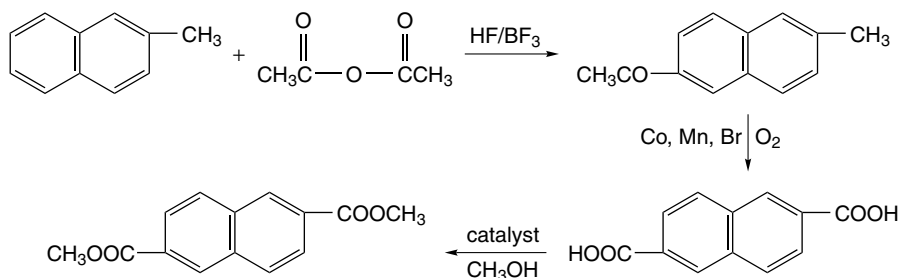
2.1 SYNTHESIS OF DIMETHYL-2,6-NAPHTHALENEDICARBOXYLATE

The monomer used for the preparation of PEN is dimethyl-2,6-naphthalenedicarboxylate (NDC) or 2,6-naphthalenedicarboxylic acid (NDA). During the long development time, several synthetic methods were developed and the manufacturing processes were improved, which finally reduced the cost for the commercialization of PEN [5–10]. The main synthesis routes are described in the following.

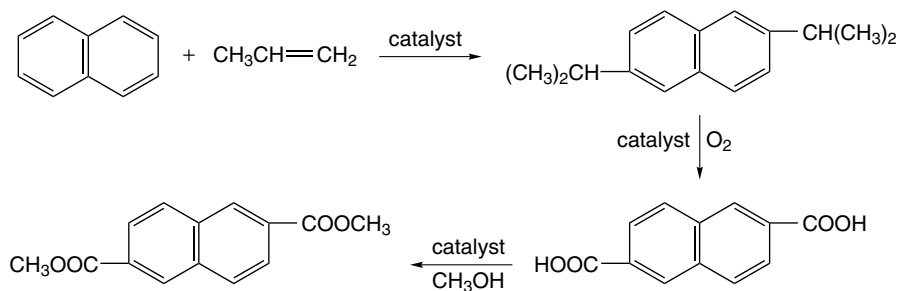
- (a) *m*-Dimethylbenzene was alkylated, cyclized, dehydrogenated and isomerized to form 2,6-dimethylnaphthalene, which then was oxidized to the diacid and esterified with methanol to obtain NDC.



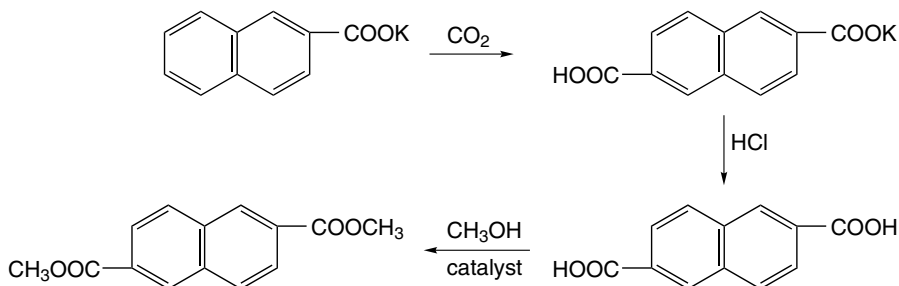
- (b) 2-Methylnaphthalene was acetylated in the 6-position, oxidized to the diacid and then esterified to form NDC.



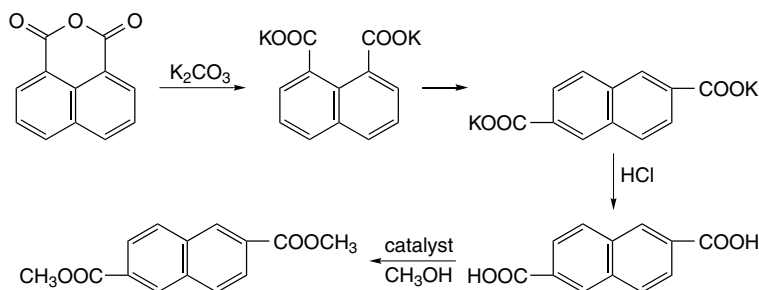
- (c) Naphthalene was reacted with 2-propylene to form 2,6-diisopropylnaphthalene, oxidized with permanganate to obtain NDA, and then esterified.



- (d) Potassium naphthalenecarbonate was carboxylated to form NDA.

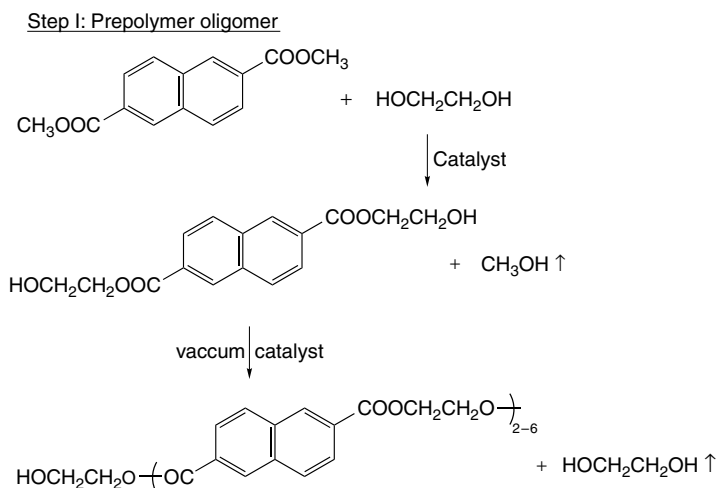


(e) Potassium 1,8-naphthalenedicarboxylate was converted to form NDA.

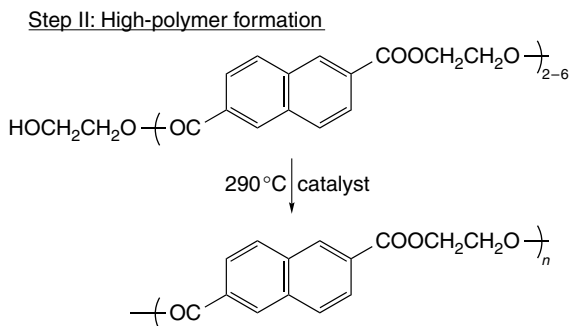


2.2 PREPARATION PROCESS OF PEN RESIN

Since it is also a polycondensation polymer, the preparation of PEN from dimethyl 2,6-naphthalenedicarboxylate (NDC) is similar to the preparation of PET from dimethyl 1,4-terephthalate (DMT) by combining a diacid ester (NDC) with ethylene glycol. In view of the fact that the commercial-scale production of PEN resin starts with 2,6-NDC, the production process is similar to that used for the production of PET from DMT. There are two main steps for the process (Scheme 10.1) [11].



Scheme 10.1 Synthesis process for producing PEN resin



Scheme 10.1 (continued)

2.2.1 Oligomer and Prepolymer Formation

The first step is an ester interchange process. During this stage, the transesterification is catalyzed by metal acetates, with the relative activities of the catalysts used being as follows: $\text{Mn} \geq \text{Zn} > \text{Co} > \text{Mg} > \text{Ni} \geq \text{Sb}$ [12]. The reaction is carried out in a reaction vessel fitted with a condenser-separating column and receiver to recover the methanol produced by the reaction. The 2,6-DNC and glycol are first heated together at atmospheric pressure and elevated temperatures to produce an oligomer with a degree of polymerization (DP) of 2–3 and methanol. The system is then evacuated to 1 mm Hg while the temperature is maintained at $\sim 195^\circ\text{C}$; under these conditions a low-molecular-weight oligomeric prepolymer with a glycol half-ester end group and a DP of 5–6 is produced.

2.2.2 High-Polymer Formation

Once the low-molecular-weight prepolymer is produced, the mixture is then heated in a melt reactor at 290°C to condense the oligomeric prepolymer. Since the reaction is reversible, the glycol side-product must be removed from the reaction vessel under reduced pressure in order to push the reaction to the polymer side of the equilibrium. The catalysts used in this step are similar to those used in the first step; however, the activity sequence is different, i.e. $\text{Ti} \geq \text{Sb} > \text{Zn} > \text{Co} > \text{Pb} > \text{Mg}$ [13]. The reaction time is $\sim 3\text{--}4.5$ h. Unlike an addition polymer reaction, the average molecular weight during the condensation process slowly increases; during the first 90 % of the reaction a DP of 9–10 is achieved and then during the final 10 % of the reaction longer polymer chains are formed. Since the polymerization process is reversible, this is a potential route for monomer reclamation. Once a predetermined average chain length has been achieved, the polymer is extruded and pelletized for future production. The overall process for producing PEN resin is summarized in Figure 10.2.

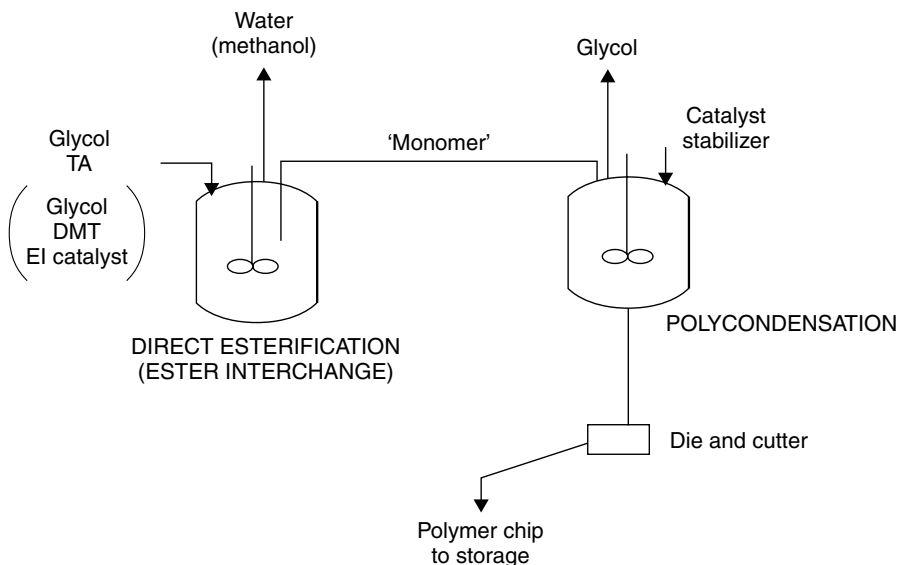


Figure 10.2 Manufacturing process used to produce PEN resin

2.3 CONTINUOUS PROCESS FOR THE MANUFACTURE OF BIAXIALLY ORIENTED PEN FILM

The amorphous PEN resin pellets are first dried at 180°C and then extruded at 290–300°C through a die, formed into a sheet, which is then followed by a two-step orientation (forward draw and sideways draw process) just above the glass transition temperature (T_g) (>120°C). After the orientation process, the PEN film is conveyed between rollers at 210–220°C to induce crystallization. At the end of the orientation and crystallization process, the film is cut and rolled into widths and lengths to suit individual customers [14–16]. Two of the process used to produce such films are shown in Figure 10.3.

3 PROPERTIES OF PEN

Since PEN and PET are polyesters with similar chemistries, it is logical to expect that they would have similar chemical and solvent resistance. However, the structural change from a benzene (a single aromatic ring) group in PET to a naphthalene (a fused aromatic double ring) group in PEN produced unique changes in the latter, such as improved chemical and physical properties. A comparison of the properties of PEN with PET and other commercial films is illustrated in Figure 10.4 and listed in Table 10.1.

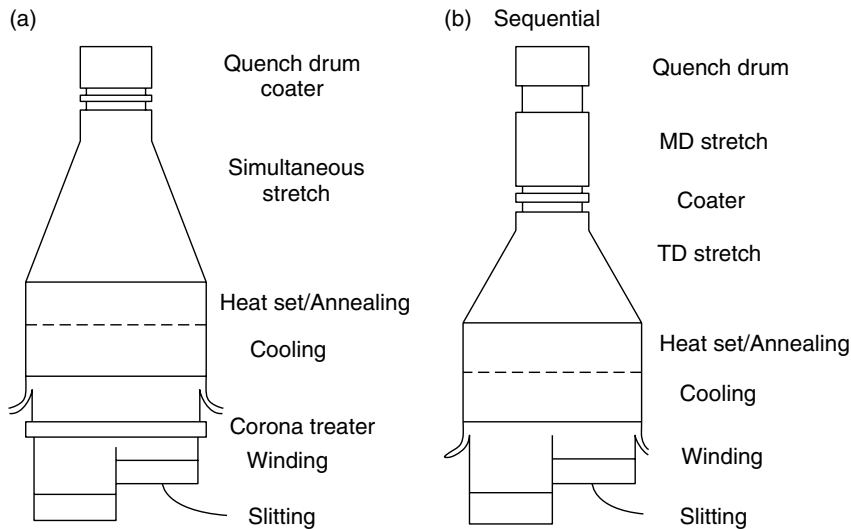


Figure 10.3 Manufacturing processes used to produce PEN films: (a) simultaneous; (b) sequential (MD, machine direction; TD, transverse direction)

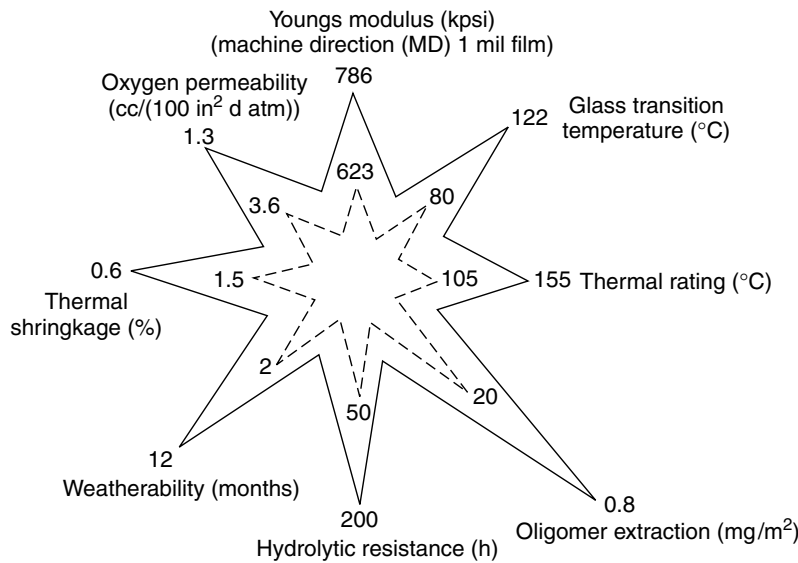


Figure 10.4 'Star diagram' showing comparison of the properties of PEN (—) and PET (---)

Table 10.1 Comparison of the properties of PEN with other commercial films

Property	Test Method	Units	PEN	Polyimide	Polyetherimide	Poly(ethylene terephthalate) film	Poly(propylene sulfide)
Tensile strength	ASTM D882-88	lb/in ²	32 000	35 000	15 000	28 000	29 000
Tensile modulus	ASTM D882-88	lb/in ²	750 000	400 000	380 000	600 000	560 000
Elongation	ASTM D882-88	%	65	75	50	150	50
Continuous use temperature	UL	°C	160	240	170	105	180
(mechanical)							
Continuous use temperature	UL	°C	180	240	180	105	180
(electrical)							
Glass transition temperature (T_g)	—	°C	120	410	212	80	90
Melt temperature (T_m)	—	°C	262	>500	365	260	285
Dielectric strength	ASTM-D150-81	V/mil	7000	7700	3500	7000	8000
Dielectric Constant (at 1.0MHz)	ASTM-D150-81	V/mil	3.16	3.5	3.2	3.3	3.0
Moisture absorption	IPC-TM-650	%	0.6	2.9	0.25	0.6	0.01
Density	—	g/cm ³	1.36	1.42	1.27	1.40	1.35
Yield (for 1 mil films)	—	ft ² /lb	1.41	136	152	142	140
Flammability	UL 94	—	VTM-2	V-0	V-0	VTM-2	VTM-0

3.1 MORPHOLOGY OF PEN

Like PET, PEN is semicrystalline with triclinic-type crystal formations. During film production, the amorphous PEN is converted into an oriented semicrystalline thin film by uniaxial or biaxial drawing. At high temperatures, the PEN modulus is considerably higher than that of PET. This difference is due to the structural and morphological differences brought about by the more rigid PEN chain. The naphthalene aromatic double-ring group in PEN induces a more planar structure which forms crystal structures more readily than PET; consequently, PEN shows a greater propensity to delaminate, at 190 °C and above, than PET. Actually, PEN has two crystal forms (α and β) and both of these are triclinic depending on the crystallization temperature [17, 18]. Crystallization at 180 °C yields the α -form as a triclinic unit with the following cell parameters: a , 0.651 nm; b , 0.575 nm; c , 1.32 nm; α , 81.33°; β , 144°; and γ , 100°. The density is 1.407 g/cm³. Crystallization above 240 °C affords the β -form. This form is also triclinic, with the following unit cell parameters: a , 0.926 nm; b , 1.559 nm; c , 1.273 nm; α , 121.6°, β , 95.57°; γ , 122.52°. The density in this case is 1.439 g/cm³. Recently, Liu *et al.* reported a number of different single-zone electron density patterns with at least one additional two-chain unit which indicates a large degree of PEN polymorphic character [19]. The morphology properties and phase behavior of PEN have been studied by NMR spectroscopy [20], FT-IR spectroscopy [22, 23], light scattering [23] and γ -radiation techniques [24].

In addition to the crystal forms, X-ray scattering studies indicate that when unoriented PEN fiber was drawn at 120 °C ($\sim T_g$), a mesophase is generated. In this form, the molecular chains are in registry with each other in the meridional direction but not fully crystallized in the equatorial direction. This conclusion was based on the presence of additional meridional peaks not accounted for by the crystal structure obtained by X-ray scattering. The mesophase is an intermediate phase and its existence is strongly dependent upon the processing conditions; consequently, it could have implications with respect to the properties of commercially produced fibers and films, since it appears to be stable and not easily converted to the crystalline form, even at elevated temperature [25, 26]. The mesophase structures of PET, PEN and poly(ethylene naphthalate bibenzoate) were compared by Carr *et al.* [27]. The phase behavior of PEN and PEN blends with other polymers has also been studied [28–32].

3.2 CHEMICAL STABILITY

A comparison of the chemical resistant properties of PEN with PET is presented in Table 10.2. PEN shows a higher resistance to most chemicals than PET [19].

Hydrolytic instability is one of the major weak points of polyesters. Both PEN and PET films are biaxially oriented and heat set, and similar filler systems and surface treatments can be used for both films. PEN, however, has better

Table 10.2 Comparison of the chemical resistance properties of PEN and PET

Reagent ^a	PEN					PET				
	Retention of tensile strength (%)	Retention of F5 ^b (%)	Retention of EB ^c (%)	Appearance	Performance	Retention of tensile strength (%)	Retention of F5 ^b (%)	Retention of EB ^c (%)	Appearance	Performance
Acetic acid	104.0	97.5	113.8	No change	Excellent	97.6	93.2	117.7	No change	Excellent
Acetone	99.0	95.2	109.1	No change	Excellent	99.3	86.8	128.3	No change	Good
Ammonium hydroxide (10 %)	103.7	97.8	121.7	No change	Excellent	97.7	93.1	126.4	No change	Good
Diethyl ether	10.3	92.2	122.4	No change	Excellent	101.1	93.0	137.3	No change	Excellent
Ethanol	101.3	94.6	101.5	No change	Excellent	97.1	92.6	121.4	No change	Excellent
Ethyl acetate	103.3	93.2	129.2	No change	Excellent	96.3	90.7	133.4	No change	Excellent
Hydrochloric Acid (SG, 1.19)	84.8	93.9	65.0	No change	Good	77.1	89.6	32.5	No change	Good
Methylene chloride	89.6	66.5	125.9	No change	Excellent	91.5	64.7	170.0	No change	Good
Methyl ethyl ketone	106.2	94.4	130.8	No change	Excellent	96.3	92.2	119.1	No change	Excellent
Phenol solution	97.2	89.3	117.4	No change	Excellent	104.8	88.4	145.7	No change	Excellent
Sodium hydroxide (30 %)	96.4	92.3	100.6	No change	Excellent	95.4	88.6	126.9	Cloudy	Excellent
Sulfuric acid (SG, 1.84)	Dissolved	Dissolved	Dissolved	No change	Poor	Dissolved	Dissolved	Dissolved	No change	Poor
Toluene	103.8	96.7	119.7	No change	Excellent	111.3	96.0	129.5	No change	Poor
Trichloroethylene	99.4	92.6	121.8	No change	Excellent	97.5	93.6	129.0	No change	Excellent

^a Tensile strips of polyester were cut, three in each direction, i.e. machine direction (MD) and transverse direction (TD). The films were then immersed in a sealed container of reagent for seven days, after which tensile and elongation measurements were then carried out.
^b F5, Modulus at 5% elongation.
^c EB, Elongation at break.

hydrolysis resistance than PET. When immersed in water at 90 °C for 70 d, PET maintained only 30 % of its tensile strength, whereas PEN retains 90 % of its tensile strength. Water reacts with the polyester bonds causing scission in the polymer chains, which reduces the average polymer chain length. It is obvious that PET does not withstand this degradation as well as PEN, which thus shows higher hydrolytic stability. Generally, the rate of polyester degradation is affected by the hydrophobicity and number of carboxylic end groups in the polymer. PEN is more hydrophobic and more crystalline than PET; therefore, it has lower water diffusivity into the solid polymer phase.

Using UV-visible and IR spectroscopies, thermal analyses and scanning electron microscopes measurements, Young and Slempe studied the performance of several polymeric materials after exposure to an 'outer-space environment'. PEN exhibited good environmental resistance to the oxygen-induced erosion, UV-induced degradation and spacecraft-induced contamination in such an environment [33].

3.3 THERMAL PROPERTIES

The enhanced thermal stability of PEN is applicable to film products, such as films for advanced photo-systems and containers for high-temperature use. Surprisingly, substitution of the aromatic benzene ring in PET by the naphthalene aromatic double ring in PEN has very little effect on the melting point (T_m), only by $\sim 10^\circ\text{C}$. However, there is a significant difference on the glass transition temperature (T_g); the T_g for PET is 78°C while that for PEN is 120°C . This greater thermal stability exhibited by PEN is manifested in many ways. For example, after being held at 190°C for 30 min, PEN film shrinks 0.8 % in the machine direction, whereas PET typically shrinks 3 % under these conditions. Consequently, heat-stabilized PEN film offers greater dimensional stability than any other polyester film.

A comparison of the mechanical relaxation behavior of PEN and PET is illustrated in Figure 10.5. PET has two typical relaxation processes α and β , i.e. a glass transition α -process and a low-temperature β -process. In addition to these α - and β -processes, also seen with PET, PEN has another stronger β^* -process above room temperature. The β -process is assigned to the local motion of the ester group while the β^* -process is typical for homologues of poly(alkylene naphthalates) [34] and is related to the motions by the naphthalene ring. Weakness of the low-temperature relaxation in PEN indicates a suppressed local segmental motion at temperatures below the β^* -process [35].

3.4 MECHANICAL PROPERTIES

PEN is considered to be a high-performance polyester material. The advantageous properties of PEN are derived from its chemical structure which contains both

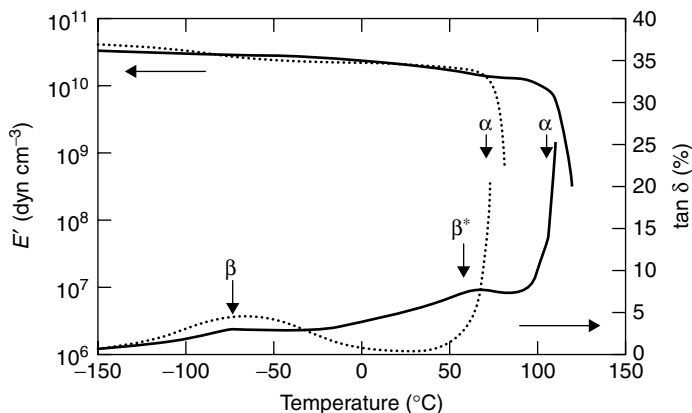


Figure 10.5 Temperature dependence of storage modulus (E') and mechanical loss ($\tan \delta$) for PEN (—) and PET (---) [35]. From Sadanobu, J. and Inata, H., *Sci. Technol. Polym. Adv. Mater.*, **4**, 141–151 (1998), and reproduced with permission of Kluwer Academic/Plenum Publishers

rigid and flexible components. The naphthalene ring in PEN provides significant rigidity and hence a higher T_g and higher modulus. However, maintaining the flexible ethylene unit in the PEN polymer chain contributes to its melt processability, unlike the wholly aromatic polyesters and aramids.

Since PEN has a relatively slow crystallization rate (Table 10.3), the polymer film obtained from the melt is highly ductile. Consequently, the film can be stretched at high draw ratios which produce highly oriented fibers and films with high Young's moduli and high tensile strengths. Compared to PET, PEN has better mechanical properties due to the ability to obtain better biaxially balanced oriented films which are attainable due to the higher draw ratio capacity of PEN. Basically, PEN film is only slightly stronger at room temperature than PET. However, at high temperatures ($>125^\circ\text{C}$), it is three to four times stiffer than PET film. This has significant benefits for packaging applications that need to be applied hot or for release liners that need to be removed from a hot substrate [36].

3.5 GAS-BARRIER PROPERTIES

PEN has excellent gas-barrier properties. The gas-permeation coefficients of unoriented cast film and biaxially oriented films for PEN and PET are given in Table 10.4.

PEN has lower gas permeation coefficients than PET for carbon dioxide, oxygen and moisture for both film types. Although the gas-barrier properties of PEN are similar to those of poly(vinyl dichloride), it is not affected by moisture in the environment. Both oriented and unoriented PEN films restrict gas diffusion more

Table 10.3 Comparison of the thermal and mechanical properties of PEN and PET

Parameter	PEN	PET
T_m (°C)	265	252
T_g (°C)	113	69
Half-crystallization time at 180 °C (min)	7	1
Density (g/cm ³)	1.41 ^a	1.46 ^a
	1.32 ^b	1.33 ^b
Young's modulus ^c (kg/mm ²)	620	540
Tensile modulus ^c (kg/mm ²)	28	23
Elongation ^c (%)	90	120

^a Crystalline.^b Amorphous.^c Biaxially stretched films; thickness, 25 μm.**Table 10.4** Gas-permeation coefficients for PEN and PET films

Polyester	As cast film		Biaxially oriented film		
	CO ₂	O ₂	CO ₂	O ₂	H ₂ O
PEN	9.0	2.8	3.7	0.8	3.4
PET	33	7.6	13	2.1	8.4

than the corresponding PET films. The orientation effects on both PET and PEN enhance the gas-barrier properties, which indicates that there is more free volume and local motion in the unoriented amorphous films. A restricted diffusive motion by small gas molecules is an important property for many applications, such as packaging. When PET was modified by blending or copolymerized with PEN, the degree of stretching, heat-set temperature and the level of crystallinity of these materials were better than those for PET alone. For example, the oxygen permeability was reduced as the naphthalate content was increased [37, 38]. The most commonly used theories for sorption and diffusion in glassy polymers is the dual-mode model [39] and the gas-polymer model [40]. By using these methods, Ward and co-workers theoretically compared the diffusion and sorption of CO₂ in PET and PEN, which correlated with experimental data [41].

3.6 ELECTRICAL PROPERTIES

As electrical insulators, PET and PEN have very similar properties. The major difference between them is the long-term thermal ageing of the respective films and the effect that such ageing has on continuous use at various temperatures. Standard PET films have a continuous-use temperature of 105 °C, as measured

Table 10.5 Comparison of the electrical and mechanical relative thermal insulation (RTI) data, under UL746 test, for PEN and PET films

Film type	RTI ^a -electrical (°C)	RTI ^a -mechanical w/o ^b impact (°C)	Reference UL file number
Standard PET	105	105	E102008(M)
Enhanced PET	140	130	E102008(M)
PEN	180	160	E151234(M)

^a RTI, relative thermal insulation.^b without.

by the Underwriters Laboratories Inc. Test UL 746B. PET is strictly a Class A material, although it is widely accepted up to Class B in the market. Some enhanced PET films, such as 'Melinex 238', which have a higher thermal rating under UL 746B, are true Class B materials (Table 10.5).

PEN films have electrical properties that are on average 25 % better than PET films; this advantage increases with increasing temperature. PEN has a significantly higher rating with an electrical continuous-use temperature of 180 °C and a mechanical rating at 160 °C. This places PEN films in the category of true Class F materials. These enhanced properties are particularly interesting when coupled to the higher continuous-use temperature [42] Guastavino *et al.* investigated the low-field ($E < 1 \text{ MV cm}^{-1}$) electrical properties of PEN and the high-field ($E > 1 \text{ MV cm}^{-1}$) regions under DC stress. They found that electrical conduction involved hot electron transport which produced polymer electroluminescence in the high-field regime while ageing under corona discharges greatly effect the conduction in the low field [43].

In addition, PEN has better resistance to moisture absorption than PET and polyurethane [44]. All of these properties endow PEN film with better electrical resistant properties than any other polymer.

3.7 OPTICAL PROPERTIES

PEN is transparent in the visible light region, but can absorb ultraviolet radiation at wavelengths below 380 nm (Figure 10.6).

PEN films have strong electrical luminescence (EL) properties (Table 10.6). Under DC stress, the emission threshold for PEN is $\sim 1.5 \text{ MV cm}^{-1}$ while for PET it is 4 MV cm^{-1} .

Compared with PET, PEN has five times more radiation resistance in air, four times more in O₂ and ten times more resistance in vacuum under continuous-use temperature [10]. Cakmak and co-workers calculated the refractive index of PEN; this parameter is highest ($n_c = 1.908$) along the chain axis and lowest ($n_n = 1.36$) normal to the naphthalene ring. Biaxially oriented PEN film has a

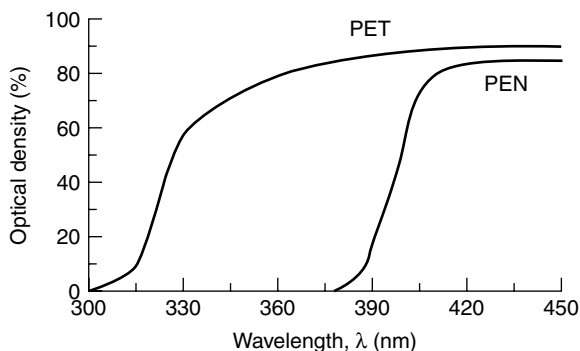


Figure 10.6 The UV absorption of PEN and PET films

bimodal orientation at the chain axis, i.e. one in the machine direction (MD) and the other in the transverse direction (TD). The refractive index in the normal direction of biaxially stretched films decreases as the orientation ratios increase. These observations are due to the orientation of naphthalene planes which orient parallel to the film surface as the expansion ratio increases [31, 45].

There are three major components in the electroluminescent spectrum of PEN. The first component, between 350 and 500 nm, is attributed to PEN excimer fluorescence excitation by hot carrier impact. The second, with a peak at 575 nm, is assigned to PEN monomer phosphorescence, which is strongly enhanced by charge recombination following impact ionization of PEN molecules. The third EL component, which peaks at 618 nm with a shoulder at 690 nm, cannot be interpreted on the basis of PEN photoluminescence. Its main contribution to the emission before breakdown is associated with the luminescence from degradation by-products of the polymer. Kinetic and spectral analyses show that electroluminescence is excited by inelastic collisions between hot electrons and the polymer molecules. Both the kinetic and spectral features are consistent with a luminescence excited by charge-carrier recombination through a tunneling mechanism. The energy level of the electron trap is directly coupled to the triplet state of the PEN molecule [46, 47].

4 APPLICATIONS FOR PEN FILMS

PEN is rapidly becoming a commodity film in the current market for high-performance materials as photographic films, motor insulators and tyre belt. PEN offers performance characteristics that exceed PET and at a cost below that of polyimide. Its thermal stability, together with its good moisture resistance, chemical and electrical properties, have earned PEN a strong position in high-temperature manufacturing. Consequently, it is becoming an important material for a number of applications, such as those described in the following sections.

Table 10.6 Assignments for the photo- and electro-induced luminescence spectra of PEN

Aspect	Wavelength range (nm)		
	350–500	550–600	600–900
<i>Photoluminescence</i> Spectral features and attribution	<ul style="list-style-type: none">• Very strong emission, peak at 425 nm• PEN excimer fluorescence	<ul style="list-style-type: none">• Very low emission, peaking at 575 nm• PEN monomer phosphorescence	<ul style="list-style-type: none">• –• –
<i>Electroluminescence</i> Attribution and characteristics	<ul style="list-style-type: none">• PEN excimer fluorescence• Red-shift attributed to polarization-mediated excimer formation• Strongly reduced due to field quenching• Impact excitation	<ul style="list-style-type: none">• PEN monomer phosphorescence• Strongly enhanced	<ul style="list-style-type: none">• Emission peaking at 618 nm, with a shoulder at 690 nm• Tentatively attributed to PEN degradation by-products• Possibility of undetected longer-wavelength components• Chemical degradation following impact excitation and/or ionization
Most likely excitation process		<ul style="list-style-type: none">• Recombination following impact ionization	

4.1 MOTORS AND MACHINE PARTS

The combination of thermal stability and dielectric performance makes PEN an attractive electrical insulator in electrical motors. Motors with high operating temperatures, such as hermetically sealed refrigerator motors and business machines, need films that are resistant to shrinking and retain nonconducting properties at high temperatures.

PEN fibers are used to make tough yarns for technical applications, such as cords for motor vehicle tyres and conveyor belts [48]. PEN was originally studied in the 1970s as tyre reinforcement cords which has since obtained wide applications with the lower cost of manufacturing PEN. Compared with the other materials used in the tyre industry, such as rayon, nylon, aramid, PET and steel, PEN can satisfy the increasing demand for high-performance tyres and provides a means for tyre manufacture to improve product quality. PEN is also used as a lightweight reinforcement material with outstanding properties, which allow tyre weight reduction and reduced rolling resistance to increase fuel efficiency. In the future, the substitution of PEN for steel would improve tyre recyclability by permitting easier shredding and combustion of tyres [49, 50].

The level of monomers and oligomers in the matrix, which can be extracted by a suitable solvent system, is an important parameter in the hermetic motor industry. Using standard industrial tests, PEN films have an almost zero level of extractable material in either traditional systems with R22 refrigerant and the mineral oil lubricant, as well as the newer R134 refrigerant and ester oil systems. The possibility of monomers and low-molecular-weight oligomers depositing on motor parts and other parts of a system can cause blockages and, consequently, early equipment failure. Therefore, the low level of oligomers extracted by the refrigerant/lubricant system in hermetic motors is a key parameter in such an application. In this area, PEN offers inherent low oligomer structures and high resistance to chemicals within these motors which adds to its appeal. The properties that PEN has thus increases design possibilities for ultimate equipment reliability to the engineer [44].

4.2 ELECTRICAL DEVICES

The Class F performance by PEN films, coupled with the many useful similarities to PET films, offers significant potential benefits in the electrical insulation industry. PEN can be used to replace Class F laminate systems with a single film layer, while offering equivalent or possibly superior performance. The outstanding dielectric properties of PEN films offer the opportunity to reduce insulation thickness for machines. Using thinner insulation can have additional beneficial effects in improving heat transfer, running the device at a higher temperature and reducing the device size. Industry has shown, that in a wide range of applications, PEN can support operating temperature 20°C higher than PET which

alone justifies the difference in cost between a PET and a PEN film. In addition, higher levels of operating safety can be achieved.

Several new trials are currently underway to evaluate PEN composite materials as laminate systems. A composite material of PEN/melamine/oxazoline can offer a system with end use up to 180–225 °C [51]. A PEN/mica system can give better thermal performance than PET/mica. PEN/PET laminates provide cost benefits, as well as enhanced performance. Applications requiring high vibration resistance are areas of considerable interest for PEN films. Power transmission products, including low- and high-voltage transformers and generators, could also benefit from using PEN as insulating materials.

PEN film has an Underwriters Laboratories (UL) continuous use rating of 180 °C for electrical and 160 °C for mechanical applications. The high-temperature dimensional stability and dielectric performance have made PEN an ideal substrate for flexible printed circuits (FPCs) [52]. Copper-clad laminates made with PEN film maintain their shape and flexibility during environmental exposure, infrared radiation and mild soldering processes, where the temperature can exceed 260 °C under a pressure of 100 psi. The low moisture retention and low oligomer content of PEN film reduce incidences of interference or signal loss in electronic devices. PEN is used for self-adhesive ‘coverlay’ to protect the copper side of a circuit. The adhesive can be roll processed, followed by a post-cure cycle or simply allowed to post-cure during the coverlay operations. Modified PEN monofilaments show good compatibility with photosensitive polymers and are useful for manufacturing printed circuit boards [53].

PEN is used in manufacturing electrochemical lithium ion batteries because it is dimensionally stable and highly resilient [54]. It could replace polyethylenimine, which is currently used at unusually high temperatures to cure special inks. PEN is also useful in membrane touch switches (MTSs) where the circuit would be exposed to a high temperature, such as the domes for switches and seat sensors in automobiles. PEN is also particularly suited to a wide range of flexible heaters and low- to intermediate-voltage heaters, such as waterbed heaters and battery heaters.

4.3 PHOTOGRAPHIC FILMS

The major features for advanced photo-systems relative to the base film are a small-size thrust cartridge and return inside the cartridge. These features require low core-set curl values and high mechanical strength. The cellulose triacetate (CTA), polycarbonate and PET materials currently used in the photographic industry are not able to satisfy these requirements. Some newly developed film materials, such as modified-PET and syndiotactic polystyrene, were also unable to satisfy such requirements. It is known that annealing films just below the T_g (BTA treatment) could reduce core-set curl tendencies. BTA treatments of

PEN films provide specifications that meet the requirements. PEN shows high mechanical properties, low fogging during manufacture and storage, and excellent thermal dimensional stability, and can be made photo-reactive with the gelatin being reactive. Consequently, it is a good support material for advanced photo-systems [55, 56].

Maehara and Fukuda have reported a PEN film modified by plasma exposure and coated the modified surface with an adhesive layer. The latter shows good adhesion to upper photosensitive layers and can be used for long-sized photographic film [57]. These workers spread an emulsion of silver halide particles on the PEN film and formed a photosensitive layer. This photographic material showed good curling resistance and gave high-contrast images [58]. Recently, several authors have described photographic PEN film production processes, PEN surface treatment and the manufacture of PEN color film, as well as comparative studies of PEN and PET [59–64].

4.4 CABLE AND WIRES INSULATION

PEN applications in the wire and cable market include printer cable and insulated wire wraps. PEN has a higher T_g and melting point, as well as higher flame resistance than PET. PEN film coated with a dispersion consisting of epoxy resin and $Al(OH_3)$ gave a semi-cured insulating film. When applied on copper wire, wound, and heated, a coil with good flame retardance and adhesion between the wire and the film was obtained [65].

4.5 TAPES AND BELTS

PEN films are excellent candidates for tape and belt applications because of the biaxially oriented processing used in the manufacturing of these films which provides uniform physical properties in the transverse direction [66]. The films are stretched in the transverse direction (TD) and relaxed in the machine direction (MD) simultaneously. This provides a high Young modulus and good dimensional stability in both directions. The Young's modulus achieved with high-molecular-weight PEN is the highest among the commercial melt-processable polymers evaluated. This feature has been utilized in the application of thin films for high-density magnetic recording media, backup tapes for computers and long-run video tapes [67–70].

PEN film is like PET film, but superior in various properties, and is finding wide application for magnetic tapes. Weick and Bhushan have compared the dynamic mechanical properties and wear/abrasion properties of PEN- and PET-based magnetic tapes. The PEN tapes have better dimensional stability, elastic moduli and coating thickness. They also have higher storage moduli

and are less susceptible to nonrecoverable deformation at higher frequencies than the PET tapes [71]. Another interesting application is in electrically and thermally conductive adhesive tape. The PEN-based tape is stable, provides shielding against electromagnetic interference due to the 'beehive-like' protuberances, prevents accumulation of static charge, and can be applied to the glass window of a monitor or microwave for directly discharging electrostatic charges [72].

Belts made with PEN film have very good mechanical properties under heat and load conditions, with low stretch and distortion under tension and heat. These belts can withstand high temperatures and show good moisture-barrier performance and find applications in industrial components, imaging units, computer printers, photoconductor belts for the 'next generation' color copiers or printers, and casting belts for both ceramic chips and for high-curing-temperature epoxy rigid circuit boards [73].

4.6 LABELS

The use of specialty substrates for labels have been driven by the market looking for materials with greater dimensional stability at higher temperature, improved mechanical performance under harsh environments, and resistance to scratching and tearing. Up until now, PET-based labels have been used where conditions are moderate, while polyimide-based labels have been employed in the most extreme environments. PEN films offer a unique performance advantage over PET and a considerable cost saving when compared to polyimide films.

PEN is a good candidate for labels where temperature tolerance is required, such as multi-layer labels for automobile bodies when being painted and dried at high temperatures. PEN is ideally suited for bar code labels where dimensional stability and registration are required at elevated temperatures. PEN labels have dimensional-excellence performance on printed circuit boards, in solvent- and aqueous-based painting operations, and in 'under-the-hood' applications. PEN labels also provide substantially improved performance over PET or vinyl labels when the label must survive in harsh chemical environments. PEN performs extremely well in applications where the label must be in contact with organic solvents, such as acetone, ethers, toluene and phenol, as well as strong bases (30 % NaOH) and moderate acids.

PEN-based labels offer superior hydrolytic stability compared to PET in applications where exposure to water and/or steam is a factor. Since the surface chemistry of PEN films is nearly identical to that of PET films, the existing coating and printing formulations can be employed. PEN films can be slit and sheeted on the same equipment used for PET films. In most applications, PEN can be substituted into coating and slitting operations used for PET without altering any processing conditions, which also reduces the cost of changing to PEN labels.

4.7 PRINTING AND EMBOSSING FILMS

Laminated PEN films have excellent adhesion to coatings and inks in ordinary conditions as well as at high temperature and humidity levels. Such films are useful as a high-strength printable media substance. These films maintain their shape during curing processes and high-pressure and high-temperature stamping, as well as displaying non-fading color and high color transmission. PEN has been used as laminatable backing substrates containing paper for simulated photographic-quality prints, creative set designing and architectural material specifics [74, 75].

Quarter-wave interference films have seen numerous uses in the field of optical security, due to the strength of reflection and the ability to select numerous colors, and in particular for their observable color shift. Decorative nanolayer quarter-wave polymeric material with more than 100 layers have been known for twenty years, but was not used in the security sector because of their weak iridescent appearance. The 3M Corporation uses PEN to manufacture reflectors with good band-edge control which are extremely efficient broadband mirrors for communication. These devices are easily noticed by the typical observer and are machine-readable. The PEN quarter-wave mirror films may be fine-line embossed and thinly layered which enhances their appearance [76].

4.8 PACKAGING MATERIALS

High-performance PEN films have excellent properties for use in various packaging applications. The clarity, strength and thermal resistance, combined with the moisture- and chemical-barrier properties of PEN, make it a leading packaging material for several emerging markets which include medical and food packaging [77]. The film, form and seal made by PEN can withstand high temperature for hot-fill food processes and corrosive high-acid foods [78]. PEN is lighter and safer with less risk of breakage than glass. The low oxygen permeability of PEN helps extend the shelf life of these products, while the 'crystal-clear' nature of PEN films makes it an attractive packaging material. It is now becoming an important container material in the beer industry.

Re-usable containers, such as bottles for carbonated soft drinks, made of PEN have high-temperature tolerance for cleaning and sterilizing [79]. The inherent UV resistance of PEN creates opportunities for colorless electronic and pharmaceutical packaging, as well as vacuum-metallized products for aerospace, industry and military applications [80, 81].

A biaxially oriented polyester film made of a copolymer consisting of 80 % ethylene 2,6-naphthalenedicarboxylate has excellent adhesion, surface hardness and wear resistance, while also providing significant transparency and antireflection properties. This material, when laminated to glass, is excellent for the prevention of shattering [82].

4.9 MEDICAL USES

PEN has a much higher gas barrier than PET and absorbs fewer active ingredients from the packaged substances, thus giving enhanced shelf life. Correlations between gas permeation and free-volume hole properties of medical-grade PEN have been studied [83]. PEN is currently being investigated as a nonpermeable membrane for transdermal drug delivery devices.

4.10 MISCELLANEOUS INDUSTRIAL APPLICATIONS

PEN has many superior properties; therefore, it can meet the needs for many further industrial applications. PEN has a high modulus-to-density ratio and so it is used for cones and domes in mobile phone speakers, stereo speakers and drum skins. Sails made of PEN are 25 % stiffer, lighter and 'loose less wind' than other materials, which hence provide more thrust from the wind to the vessel, thus enhancing its speed. Such sails have, in fact, been used in some Americas Cup competitions.

PEN has antistatic protective properties and has been used in optical devices. Compared with PET, PEN-based antistatic films show better mechanical properties, higher surface resistivity and less peeling from a polarizing plate [84].

At the present time, interest in PEN films for advanced material applications is at a high level, with a significant number of product applications currently being investigated. Not too surprisingly, however, many of these applications are being kept confidential by the end users concerned as they feel that the use of PEN can give them a key competitive advantage in the market.

REFERENCES

1. Whinfield, J. R. and Dickson, J. T., *Br. Patent* 578 079, 1941.
2. Siddiqui, J. A. and Carson, J., *Am. Chem. Soc., Div. Polym. Chem., Polym. Prepr.*, **40**(1), 582 (1999).
3. Jia, H. T. and Sheng, J., *Huaxue Gongye Gongcheng*, **16**, 347 (1999).
4. Cook, J. G., Huggle, H. P. W. and Low, A. R., *Br. Patent* 604 073, 1948.
5. Shikkenga, D. L. and Wheaton, I., *US Patent* 5 073 670, 1989.
6. Shikkenga, D. L. and Wheaton, I., *US Patent* 4 950 825, 1990.
7. Jia, H. T. and Sheng, J., *Chem. Ind. Eng. (Chin.)*, **16**, 347 (1999).
8. Motoyuki, M., Yamamoto, K., Yoshida, S., Yamamoto, S., Sapre, A. V., McWilliams, J. P., Donnelly, S. P. and Hellring, S. D., *World Patent WO 9919 281*, 1999.
9. Holzhauer, J. K. and Young, D. A., *US Patent* 5 254 719, 1993.
10. Uchida, H. and Marumo, K., *Jpn Patent JP 01 165 549*, 1989.

11. Thomsen, J. R. and Fagerburg, D. R., *US Patent 4 594 406*, 1985.
12. Wang, C. S. and Sun, Y. M., *J. Polym. Sci., Polym. Chem. Ed.*, **32**, 295 (1994).
13. Wang, C. S. and Sun, Y. M., *J. Polym. Sci., Polym. Chem. Ed.*, **33**, 406 (1995).
14. *Br. Patent Ed. 1 472 777* (to Teijen Ltd), 1977.
15. Aoki, H. and Koganei, J. A., *US Patent 3 875 119*, 1975.
16. Kanai, T. and Campbell, G. A., *Film Processing*, Hanser Publishers, Cincinnati, OH, 1999.
17. Buchner, S., Wiswe, D. and Zachmann, G., *Polymer*, **30**, 480 (1989).
18. Mencik, Z., *Chem. Prum.*, **17**, 78 (1967).
19. Liu, J., Sidoti, G., Hommema, J. A., Geil, P. H., Kim, J. C. and Cakmak, M., *J. Macromol. Sci., Phys.*, **B37**, 567 (1998).
20. Guo, M. and Zachmann, G., *Macromol. Chem. Phys.*, **199**, 1185 (1998).
21. Wang, S., Shen, D. and Qian, R., *J. Appl. Polym. Sci.*, **60**, 1358 (1996).
22. Kimura, F., Kimura, T., Sugisaki, A., Komatsu, M., Sata, H. and Ito, E., *J. Polym. Sci., Polym. Phys. Ed.*, **35**, 2741 (1997).
23. Bell, V. L. and Pezdirtz, G. F., *J. Polym. Sci., Polym. Chem. Ed.*, **21**, 3083 (1983).
24. Bang, H. J. Lee, J. K. and Lee, K. H., *J. Polym. Sci., Polym. Phys. Ed.*, **38**, 2625 (2000).
25. Jakeways, R., Klein, J. L. and Ward, I. M., *Polymer*, **37**, 3761 (1996).
26. Saw, C. K., Menczel, E. W., Choe, E. W. and Hughes, O. R., Mesophase in drawn PEN fibers. in *Proceedings of the 55th SPE ANTEC'97 Conference*, May 5–8, 1997, Toronto, ON, Canada, Society of Plastics Engineers, Brookfield, CT, 1997, Vol. 2, pp. 1610–1615.
27. Carr, P. L., Nicholson, T. M., Ward, I. M., *Polym. Adv. Technol.*, **8**, 592 (1997).
28. Bicakci, E., Zhou, X. and Cakmak, M., Phase and uniaxial deformation behavior of ternary blends of poly(ethylene naphthalate), poly(ether imide) and poly(ether ether ketone), in *Proceedings of the 55th SPE ANTEC'97 Conference*, May 5–8, 1997, Toronto, ON, Canada, Society of Plastics Engineers, Brookfield, CT, 1997, Vol. 2, pp. 1593–1599.
29. Morikawa, J. and Hashimoto, T., *Polymer*, **38**, 5397 (1997).
30. Bicakci, E. and Cakmak, M., *Polymer*, **39**, 4001 (1998).
31. Kim, J. C., Cakmak, M. and Zhou, X., Effect of composition on crystalline orientation and optical properties of biaxially stretched PEN/PEI films, in *Proceedings of the 55th SPE ANTEC'97 Conference*, May 5–8, 1997, Toronto, ON, Canada, Society of Plastics Engineers, Brookfield, CT, 1997, Vol. 2, pp. 1588–1592.
32. Galay, J. M. and Cakmak, M., Real time sensing of birefringence development in uniaxially oriented PEN and PEN/PEI films using a fast dual wavelength optical technique, in *Proceedings of the 55th SPE ANTEC'97*

- Conference*, May 5–8, 1997, Toronto, ON, Canada, Society of Plastics Engineers, Brookfield, CT, 1997, Vol. 2, pp. 1606–1609.
33. Young, P. R. and Slep, W. S., *Polym. Adv. Technol.*, **9**, 20 (1998).
 34. Sadanobu, J. and Tsukioka, M., Mechanical relaxation behaviors for homolog poly(alkylenenaphthalate)s, in *Proceedings of the 55th SPE ANTEC'97 Conference*, May 5–8, 1997, Toronto, ON, Canada, Society of Plastics Engineers, Brookfield, CT, 1997, Vol. 2, pp. 1567–1571.
 35. Sadanobu, J. and Inata, H., *Sci. Technol. Polym. Adv. Mater.*, **4**, 141 (1998).
 36. Cakmak, M. and Lee, S. W., *Polymer*, **36**, 4039 (1995).
 37. Bauer, C. W., The effects of degree of stretching on the properties of heat set biaxially stretched naphthalate-containing polyester films, in *Proceedings of the 55th SPE ANTEC'97 Conference*, May 5–8, 1997, Toronto, ON, Canada, Society of Plastics Engineers, Brookfield, CT, 1997, Vol. 2, pp. 1578–1581.
 38. Bauer, C. W., *J. Plast. Film Sheeting*, **13**, 336 (1997).
 39. Barrer, R. M., Barrie, J. A. and Slater, J., *J. Polym. Sci.*, **27**, 177 (1958).
 40. Raucher, D. and Sefcik, M. D., *ACS Symp. Ser.*, **111**, 223 (1983).
 41. Brolly, J. B., Bower, D. I. and Ward, I. M., *J. Polym. Sci., Polym. Phys. Ed.*, **34**, 769 (1996).
 42. Koji, F., Shinya, W. and Akira, K., *Jpn Patent JP 2000 343 599*, 2000.
 43. Guastavino, J., Mary, D., Krause, E., Laurent, C. and Mayoux, C., *Polym. Int.*, **46**, 72 (1998).
 44. Sharma, R., Henderson, C., Warren, G. W. and Burkett, S. L., *J. Appl. Polym. Sci.*, **68**, 553 (1998).
 45. Cakmak, M., Wang, Y. D. and Simhambhatla, M., *Polym. Eng. Sci.*, **30**, 721 (1990).
 46. Mary, D., Albertini, M. and Laurent, C., *J. Phys., D: Appl. Phys.*, **30**, 171 (1997).
 47. Teyssedre, G., Mary, D. and Laurent, C., *J. Phys., D: Appl. Phys.*, **31**, 267 (1998).
 48. Rim, P. R., *Kaut. Gummi Kunst.*, **49**, 418 (1999).
 49. Schumann, H., Wilhelm, F. and Kaempf, R., *US Patent 5 563 209*, 1996.
 50. Van den Heuvel, C. J. M. and Klop, E. A., *Polymer*, **41**, 4249 (2000).
 51. Takada, I., Kojima, S. and Mitsumura, T., *Jpn Patent JP 11 286 092*, 1999.
 52. Olson, B. D., *US Patent 5 766 740*, 1998.
 53. Katsuma, K., Hara, Y., Naruse, T., Ueda, H. and Honda, S., *Jpn Patent JP2000 336 523*, 2000.
 54. Munshi, M. and Zafar, A., *World Patent WO 2000-2000US 16 294*, 2001.
 55. Tatsuta, S., Tamaki, H., Funabashi, S., Nawano, T. and Sakai, T., *Fujifilm Res. Dev.*, **44**, 48 (1999).
 56. Shinagawa, Y., Hashimoto, K., Ikuhara, I., Sakaino, Y., Kawamoto, F., Fujikura, D. and Nawano, T., *Fujifilm Res. Dev.*, **42**, 59 (1997).
 57. Maehara, Y. and Fukuda, K., *Jpn Patent JP99 116 538*, 2000.

58. Yamagami, H., *Jpn Patent JP 07219 137*, 1995.
59. Pfeiffer, H., Bennett, C., Crass, G., Hilker, G. and Roth, W., *Eur. Patent EP 945 262*, 1999.
60. Toda, Y., Fukuda, K., Kondo, Y. and Maehara, Y., *Jpn Patent JP 11 240 968*, 1999.
61. Fleischer, C. A., McKenna, W. P. and Freeman, D. R., *Eur. Patent EP 849 628*, 1998.
62. Inoya, H. and Iwagaki, M., *Jpn Patent JP 10 003 144*, 1998.
63. Suzuki, M. and Iwamuro, M., *Jpn Patent JP 08 211 549*, 1996.
64. Anon, *UK Res. Disclosure*, **360**, 223 (1994).
65. Suzuki, S., Ikeda, K., Shimizu, T. and Izuna, T., *Jpn Patent JP 10 144 538*, 1998.
66. Tsunashima, K. and Miyakawa, K., *Jpn Patent JP2000 309 051*, 2000.
67. Matsumoto, Y., *Konbatekku*, No. 5, 55 (1991).
68. Koseki, M. and Watanabe, H., *World Patent WO99 29 488*, 1999.
69. Asakura, M., Etou, K. and Tsunekawa, T., *Eur. Patent EP 909 780*, 1999.
70. Yoshimura, Y. and Watase, S., *US Patent 5 906 885*, 1999.
71. Weick, B. L. and Bhushan, B., *Wear*, **202**, 17 (1996).
72. Lin, D., *World Patent WO00 59 715*, 2000.
73. Mimura, T., Kojima, S. and Tanaka, S., *Jpn Patent JP 9 938 470*, 2000.
74. Takata, I., Kojima, S. and Mitsumura, T., *Jpn Patent JP 10 086 303*, 1998.
75. Malhotra, S. L., *US Patent 5 795 696*, 1998.
76. Jonza, J. M., *Proc. SPIE-Int. Soc. Opt. Eng.*, **257**, 3973 (2000).
77. Wang, J., *Suliao*, **29**(5), 46 (2000).
78. Post, G., *Fluess. Obst.*, **66**, 577 (1999).
79. Katsura, T., *Nippon Hosogakkaishi*, **7**, 319 (1998).
80. Kafka, C., Thermoplastic polyesters – the new packaging materials are becoming popular. In *Proceedings of Blasformen'99 Conference*, Duesseldorf, Germany, 1999, pp. 21–44.
81. Hwo, C., Forschner, T., Lowtan, R., Gwyn, D. and Cristea, B., *J. Plast. Film Sheeting*, **15**, 219 (1999).
82. Furuya, K., Watanabe, S., Kawai, S. and Suzuki, K., *World Patent WO 99 30 905*.
83. Yang, H. E. and Jean, Y. C., *J. Appl. Med. Polym.*, **2**, 66 (1998).
84. Morimoto, Y., *Jpn Patent JP 2000 026 817*, 2000.

Synthesis, Properties and Applications of Poly(Trimethylene Terephthalate)

H. H. CHUAH

Shell Chemical Company, Houston, TX, USA

1 INTRODUCTION

Poly(trimethylene terephthalate) (PTT) is a newly commercialized aromatic polyester. Although available in commercial quantities only as recently as 1998 [1], it was one of the three high-melting-point aromatic polyesters first synthesized by Whinfield and Dickson [2] nearly 60 years ago. Two of these polyesters, poly(ethylene terephthalate) (PET) and poly(butylene terephthalate) (PBT), have become well-established high-volume polymers. PTT has remained an obscure polymer until recent times because one of its monomers, 1,3-propanediol (PDO), was not readily available. PDO was sold as a small-volume fine chemical at more than \$10/lb., and was therefore not suitable as a raw material for commercial polymers.

For a long time, the fiber industry had been aware of PTT having desirable properties for fiber applications. In a 1971 patent [3], Fiber Industries, Inc. found PTT fiber to have a lower modulus, better bending and work recoveries than PET, and was therefore more suitable than PET for making fiberfill and carpets. Ward *et al.* [4] compared the mechanical properties of the three polyester fibers, and found PTT indeed had a better tensile elastic recovery and a lower modulus than both PET and PBT. These two properties are very desirable and are valued

for making soft, stretch-fabrics with good hand and touch [5], and for resilient carpets [6]. Thus, it was a challenge for chemical and fiber companies to develop breakthrough technologies to lower PDO cost and to commercialize PTT.

In the early 1970s, the Shell Chemical Company, then a producer of PDO via the acrolein route, explored the commercial potential of PDO and PTT by sampling PDO with several fiber companies. This led to a period of active research in PTT polymerization and applications [7–10]. Despite making significant progress in lowering PDO manufacturing cost, it was still not low enough and the unfavorable polyester business atmosphere at that time stopped further development of PTT. Shell later exited the PDO business and Degussa assumed its manufacturing.

Interest in PTT revived in the late 1980s when both Shell and Degussa made breakthroughs in two different PDO manufacturing technologies. Degussa was able to lower the cost of manufacturing PDO via the acrolein route and improve its purity to levels suitable for polymerization [11]. Shell developed an alternate synthesis route by hydroformylating ethylene oxide (EO) with a combination of CO and H₂ synthesis gas [12], leveraging their core competencies in hydroformylation technology and EO feedstock. In 1995, Shell announced the commercialization of PTT, and built a 160 mm lb PDO plant in Geismar, Louisiana. This was followed by Du Pont announcing the retrofitting of an existing polyester plant in Kinston, North Carolina, to produce PTT using PDO obtained from Degussa while they and Genecore International collaborated to develop a potentially cheaper biological route for making PDO through glycerol fermentation. More than half a century after its synthesis, PTT finally joined PET and PBT, and became a commercial reality.

2 POLYMERIZATION

PTT is made by the melt polycondensation of PDO with either terephthalic acid or dimethyl terephthalate. The chemical structure is shown in Figure 11.1. It is also called 3GT in the polyester industry, with G and T standing for glycol and terephthalate, respectively. The number preceding G stands for the number of methylene units in the glycol moiety. In the literature, poly(propylene terephthalate) (PPT) is also frequently encountered; however, this nomenclature does not distinguish whether the glycol moiety is made from a branched 1,2-propanediol or a linear 1,3-propanediol. Another abbreviation sometimes used in the literature is PTMT, which could be confused with poly(tetramethylene terephthalate),

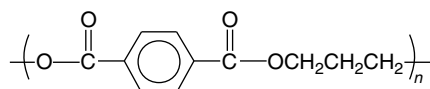


Figure 11.1 The chemical structure of poly(trimethylene terephthalate)

another name for PBT. Therefore, both PPT and PTMT abbreviations should be avoided. Shell Chemical Company's PTT is trademarked as Corterra[®] polymer, while Du Pont's trademark is Sorona[™] 3GT.

2.1 1,3-PROPANEDIOL MONOMER

PDO (CAS:504-63-2),¹ also called trimethylene glycol, is a colorless, clear liquid with a boiling point of 214 °C. There are two commercial synthesis routes. The first of these is the traditional route, via the hydration of acrolein [13] under pressure at 50 °C into 3-hydroxypropanal (3-HPA) using an acid catalyst. The 3-HPA intermediate is then hydrogenated into PDO by using Raney nickel catalyst. In the second process, Shell uses EO as a starting raw material. EO is first hydroformylated into 3-HPA by using a combination of CO and H₂ synthesis gas with cobalt catalysts [14–16]. The aqueous 3-HPA solution is then concentrated and hydrogenated to produce PDO.

A new route with the potential of further lowering PDO cost is the enzymatic fermentation [17, 18] of glycerol and alcohol. This process is still under development by Du Pont and Genecore International. With advances in biogenetic engineering, new strains of engineered bacteria have improved the yield and selectivity of the process to the point where this route is ready for pilot plant scale-up.

PDO chemistry, technology, the relative merits and the manufacturing economics of the above three routes have been reviewed by Chen *et al.* [19], Wu [20] and by SRI International in its Process Economic Progress report [21]. Therefore, PDO will not be further elaborated in this article.

2.2 THE POLYMERIZATION STAGE

PTT is melt polymerized by either the transesterification of PDO with dimethyl terephthalate (DMT) or by the direct esterification of PDO with purified terephthalic acid (PTA). The process is similar to that for PET but with major differences, as follows:

1. Because of PDO's lower reactivity, more active catalysts based on titanium and tin, which would discolor PET, are used to polymerize PTT.
2. PTT has different side reaction products. Instead of the acetaldehyde produced with PET, acrolein and allyl alcohol are the volatile byproducts of PTT production. The generation of acrolein is to be expected since it is one of the starting raw materials for making PDO. Acrolein is toxic and is a very strong lachrymator [22], and requires special handling and treatment.

¹ Chemical Abstracts Service (CAS) Registry Number.

3. Instead of cyclic trimer, PTT produces a lower-melting cyclic dimer byproduct [23].
4. Compared to 1,4-butanediol, which forms tetrahydrofuran byproduct in PBT polymerization, PDO is difficult to cyclize into oxetane because of the high ring strain. Oxetane was not found in the byproduct analysis [23].
5. PTT is polymerized at a much lower temperature between 250 and 275 °C. Because of its higher melt degradation rate and a faster crystallization rate, it requires special consideration in polymerization, pelletizing and solid-state treatment.

Direct esterification of PDO with TPA is a more economical route than transesterification with DMT. However, it is also a more difficult technology to implement. Table 11.1 summarizes the reaction conditions, catalysts and additives for both the DMT and TPA processes [24–28], while Figure 11.2 shows the direct esterification reaction scheme. Only the TPA process will be described below.

Because TPA has a melting point of >300 °C and poor solubility in PDO, direct esterification is preferably carried out in the presence of a ‘heel’ under a pressure of 70–150 kPa and at 250–270 °C for 100–140 min. A heel is an oligomeric PTT melt with a degree of polymerization (DP) of 3 to 7, purposely left in the reaction vessel from a previous batch to improve TPA solubility and to serve as a reaction medium. The esterification step is self-catalyzed by TPA.

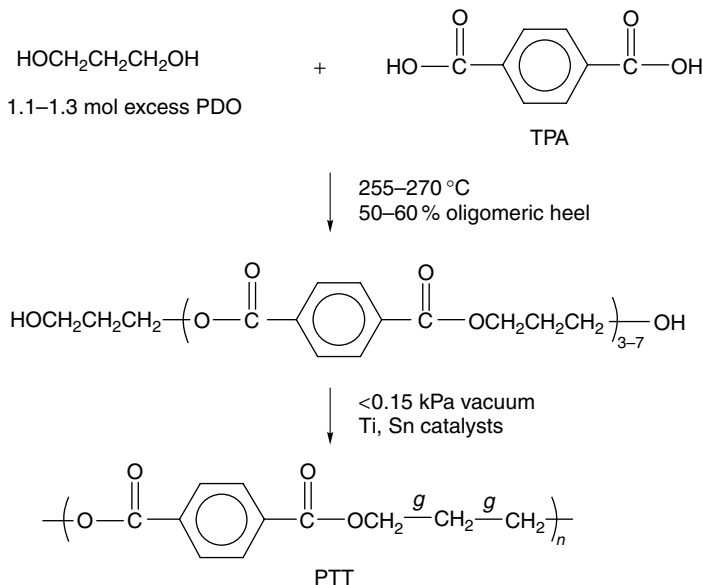


Figure 11.2 Polymerization of PTT by direct esterification of PDO with TPA using the heel process

Table 11.1 PTT polymerization conditions, catalysts and additives

PDO/DMT molar ratio	Esterification		Polymerization		Comments	Reference
	Catalyst	Reaction temperature/time /pressure	Catalyst	Polymerization temperature/time /pressure		
<i>DMT process</i>						
1.2–1.8	340 ppm titanic acid tetraethyl;	160–220 °C ^a	–	250 °C/200 min/ 0.8 mm Hg	PDO/DMT ratio > 1.8 slowed down reaction	8
1.40	50 ppm Co(OAc); 100 ppm Ti(OBu) ₄	236 °C/4.7 h ^a	450 ppm butyl stannoic acid	252 °C/4.3 h/ 0.3 mm Hg	1.5 ppm Hostaperm® CI Pigments Violet 23 or Blue 15 and 500 ppm tridecyl phosphite added to improve color values (<i>b</i> * = 2.7, <i>L</i> * = 85.9)	24, 25
1.4–2.2	2–6 × 10 ^{–4} mol Ti(OBu) ₄	140–220 °C ^a	–	260–270 °C/0.05 mbar	1–2 × 10 ^{–4} mol tributyl phosphite added to improve color (<i>L</i> * = 70, <i>b</i> * = 2) and to reduce carboxyl end groups to 7–10 mmol kg ^{–1}	26

(continued overleaf)

Table 11.1 (continued)

PDO/DMT molar ratio	Esterification		Polymerization		Reference	
	Catalyst	Reaction temperature/time /pressure	Catalyst	Polymerization temperature/time /pressure		
TPA process						
1.4	Self-catalyzed	250 °C/6 h/50 psi pressure	80 ppm Ti(OBu) ₄ , based on Ti	260 °C/3 h/2 mbar	0.05 wt% Irgafos® 168 and 3.1 mmol hindered phenolic propionic acid added to reduce acrolein and improve color	35
1.24	50 ppm Ti from co-precipitated TiO ₂ , SiO ₂	50–100 mbar pressure, degree of esterification >98.8 %	250 ppm antimony acetate	257–265 °C/ 153–162 min/ <1 mbar	40–60 ppm H ₃ PO ₄ and 40 ppm cobalt acetate added to reduce formation of acrolein and allyl alcohol to <3 ppm and <5 ppm, respectively, and the <i>b</i> * color value <–0.5	27
1.5	100–250 ppm ethylene glycol titanate	227 °C/3.3 h/3 kg cm ^{–2}	100–250 ppm antimony acetate	250 °C/5 h/1.3 torr	PTT chips have <i>b</i> * color value of <9	28

^a At atmospheric pressure.

After reaching the desired DP, 40–50 % of the oligomeric melt is transferred to the polymerization vessel. Titanium butoxide (50–150 ppm) or dibutyl tin oxide catalyst (100–250 ppm), or some combinations of the two catalysts, is added to catalyze polymerization at 260–275 °C. A vacuum of <0.15 kPa is applied to remove the condensed water so as to drive the reaction until the polymer reaches an intrinsic viscosity (IV) of 0.7–0.9 dL/g.

To obtain higher-molecular-weight PTT with an IV > 1.0 dL/g, melt-polymerized chips are solid-state polymerized [23, 29, 30] at 180–210 °C under nitrogen. The solid-state treatment prevents the polymer from becoming yellow or degraded by prolonged melt polymerization to reach the high IV. This post-condensation process also helps drive off volatile byproducts, thus reducing the amount of residual acrolein and cyclic dimer in the final polymer; however, the molecular weight distribution is broadened [23]. The reduction of cyclic dimer during post condensation is through sublimation. The chips are also more crystalline and tend to be more brittle.

2.3 SIDE REACTIONS AND PRODUCTS

PTT melt undergoes several side reactions during polymerization and melt processing. Under an inert atmosphere, PTT has a similar thermogravimetric weight loss profile to that of PET with one main decomposition step. A thermogravimetric analysis (TGA) scan of PTT does not show significant weight loss up to 280 °C [6]. Degradation in air is, however, different and involves two mechanisms [31]. At about 300 °C, degradation was decomposition-controlled. At higher temperatures, the rate increases and decomposition changes to a diffusion-controlled process.

PTT shares several similar thermo-oxidation degradation mechanisms with PET [32]. Some of the more important ones are as follows:

1. McClafferty rearrangement [32, 33] of the ester moiety (Figure 11.3). The carbonyl unit abstracts a β -methylene hydrogen through a six-member cyclic transition state, and the chains fragment with carboxyl and vinyl ester end groups. Further scission of the vinyl ester group generates allyl alcohol, which in the presence of oxygen is oxidized to acrolein.
2. 'Back-biting' of the growing polymer chain generates cyclic oligomers. Instead of cyclic trimer, PTT forms its cyclic dimer, which has a melting point of 254 °C. The amount of cyclic dimer in the final polymer is preferably below 3 wt% because it tends to sublime and deposit as needle-like crystals on the spinnerette die face, so interfering with fiber spinning process.
3. During polymerization, PDO dimerizes into dipropylene ether glycol (DPG) which incorporates into the PTT chains as a copolymer. DPG formation is more severe in the acidic TPA process. The incorporated DPG lowers the polymer's melting point and affects fiber dye uptake [34].

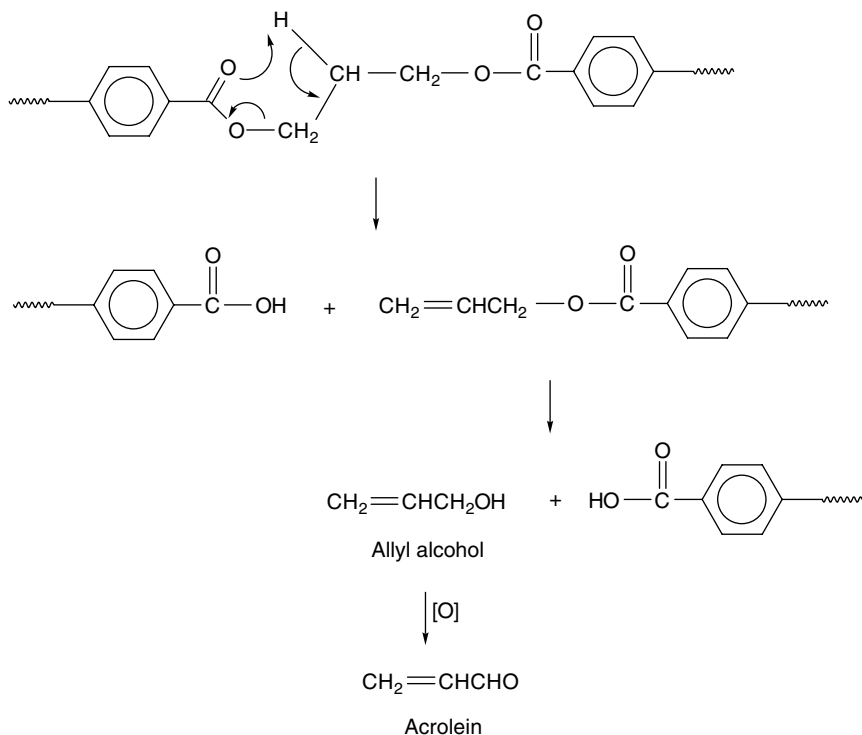


Figure 11.3 Proposed PTT thermal degradation mechanism through the Mc-Clafferty rearrangement and the formation of acrolein and allyl alcohol

The above side reactions can be suppressed to various extents by adding antioxidants and phosphites, using higher purity PDO and controlling the polymerization conditions [35].

3 PHYSICAL PROPERTIES

PTT, with three methylene units in its glycol moiety, is called an *odd-numbered* polyester. It is often compared to the *even-numbered* polyesters such as PET and PBT for the odd–even effect on their properties. Although this effect is well established for many polycondensation polymers such as polyamides, where the number of methylene units in the chemical structures determines the extent of hydrogen bonding between neighboring chains and thus their polymer properties, neighboring chain interactions in polyesters are weak dispersive, dipole interactions. We have found that many PET, PTT and PBT properties do not follow the odd–even effect. While the PTT heat of fusion and glass transition temperature have values between those of PET and PBT, properties such as modulus

and elastic recovery show an odd–even effect with values either above or below those of PBT and PET.

In general, properties that are additive and could be estimated by group contribution methods, such as density and heat of fusion, tend to follow the order of PET, PTT and PBT; properties dependent on the conformational arrangement of the methylene units, such as modulus, show an odd–even effect, at least among these three polyesters.

3.1 INTRINSIC VISCOSITY AND MOLECULAR WEIGHTS

As a norm, polyester molecular weights are reported by their intrinsic viscosities (IV), $[\eta]$. The two are related by the Mark–Houwink equation, as follows:

$$[\eta] = KM^\alpha \quad (11.1)$$

where K and α are constants unique to the polymer, the type of solvent and temperature used to measure IV. Table 11.2 summarizes the constants for PTT in various solvents and the method used to measure the molecular weight, whether it is number- or weight-average [36, 37].

PTT is a rapidly crystallizing polymer. A melt-processed PTT tends to crystallize with a crystallinity of between about 15 and 30 wt%. It is therefore more difficult to dissolve in solvents commonly used for amorphous PET. Stronger solvents, such as hexafluoroisopropanol (HFIPA) or a 1:1 mixture of trifluoroacetic acid and methylene chloride are typically used to dissolve PTT. However, HFIPA is a very expensive solvent for routine IV measurements, and methylene chloride is too volatile to maintain in a 1:1 mixture with trifluoroacetic acid at elevated temperatures or in prolonged storage. With care, a 60/40 mixture of phenol/tetrachloroethane can be used satisfactorily for IV measurement when it is heated to 110 °C to ensure complete dissolution of PTT [37].

Since IV measurements are quite laborious and time consuming, a simplified single-point method is often used by measuring the solution's specific viscosity,

Table 11.2 PTT Mark–Houwink constants in various solvents

Solvent	Temperature (°C)	Molecular weight determination method	$K \times 10^4$ (dL/g)	α	Reference
HFIPA	35	SALS ^a	5.51	0.71	37
HFIPA	35	Hydroxyl group	10.0	0.70	37
60/40 Tetrachloroethane/ phenol	30	SALS	5.36	0.69	37
50/50 Tetrachloroethane/ phenol	20	SALS	8.2	0.63	26

^a SALS, small-angle light scattering.

η_{sp} , and relative viscosity, η_{rel} , at only one low concentration. Chuah *et al.* [37] examined the application of several single-point equations for PTT. They found that when the solution concentration is <0.005 g/dL, η_{sp} can be approximated to $[\eta]$ within $\pm 3\%$. The single-point equation used in this author's laboratory is from Solomon and Ciuta [38], as follows:

$$[\eta] = \frac{\sqrt{2(\eta_{sp} - \ln \eta_{rel})}}{c} \quad (11.2)$$

3.2 CRYSTAL STRUCTURE

Like PET and PBT, PTT crystallizes into a triclinic crystal structure. Table 11.3 shows the unit cell dimensions obtained from wide-angle X-ray diffraction (WAXD) and electron diffraction (ED) crystal structure determinations [39–43], while Figure 11.4 shows the arrangement of the molecular chains viewed edge-wise. The PTT *c*-axis chain contains two repeating units, and the methylene groups are arranged in a highly contracted *gauche-gauche* conformation. The fiber identity period is only 75.3 % of the length of a fully extended PTT chain if it were to adopt an all-*trans* conformation. For PET and PBT, the fiber periods are much more extended, i.e. about 99.5 and 86.3 % of their fully extended lengths, respectively. Thus, PTT chains appear zigzag, while PET chains are fully extended, and PBT chains look buckled see Figure 11.4. The highly contracted crystalline chain gives PTT some unusual mechanical properties which are discussed in the section on 'fibers' below.

3.3 CRYSTAL DENSITY

Although the unit cell dimensions shown in Table 11.3 appear to be reasonably close to each other, the calculated cell volumes and crystal densities are divided

Table 11.3 Unit cell parameters and densities of PTT Crystal

Cell parameters and related	Method			
	WAXD [39]	WAXD [40]	ED ^a [41]	ED [42]
<i>a</i> (nm)	0.45(9)	0.458	0.4637	0.464
<i>b</i> (nm)	0.62(1)	0.622	0.6226	0.627
<i>c</i> (nm)	1.83(1)	1.812	1.864	1.864
α (°)	98.(0)	97	98.4	98
β (°)	90.(0)	89	93.0	93
γ (°)	111.(7)	111	111.1	111
Volume (nm ³)	0.4792	0.4781	0.4935	0.4983
Density (kg/m ³)	1432	1429	1387	1374

^a Supplemented with WAXD data.

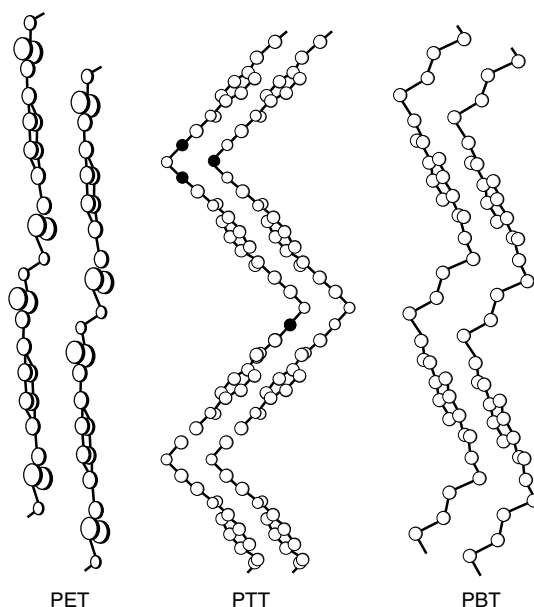


Figure 11.4 PET, PTT and PBT chains viewed edge-wise, showing the effects of methylene conformations

into two distinct groups. The WAXD density, $\sim 1430 \text{ kg/m}^3$, is much higher than the ED density of $\sim 1380 \text{ kg/m}^3$. Because of such a large difference in the literature values, the use of either WAXD or ED density values can cause confusion in crystallinity measured by the density method.

By plotting the densities of 19 PTT samples with crystallinities of between 14 and 35 wt%, determined by DSC, Ziabicki [44] extrapolated a crystal density of 1441 kg/m^3 ($R^2 = 0.984$; standard deviation) in closer agreement to those obtained by WAXD. Chuah and Chang [45] have discussed the possible reasons for the discrepancies. Until further work is done to resolve these discrepancies, this author's research group uses 1432 kg/m^3 as the crystal density based on the Desborough *et al.* crystallographic data [39]. Using van Krevelan's group contribution data [46], Chuah [47] calculated the PTT amorphous density as 1295 kg/m^3 , in good agreement with the extrapolated value of 1299 kg/m^3 obtained by Ziabicki [44].

3.4 THERMAL PROPERTIES

3.4.1 Melting and Crystallization

PTT is a semicrystalline polymer with a DSC peak melting point of 228°C (Figure 11.5). The equilibrium melting points, T_m° , obtained from the

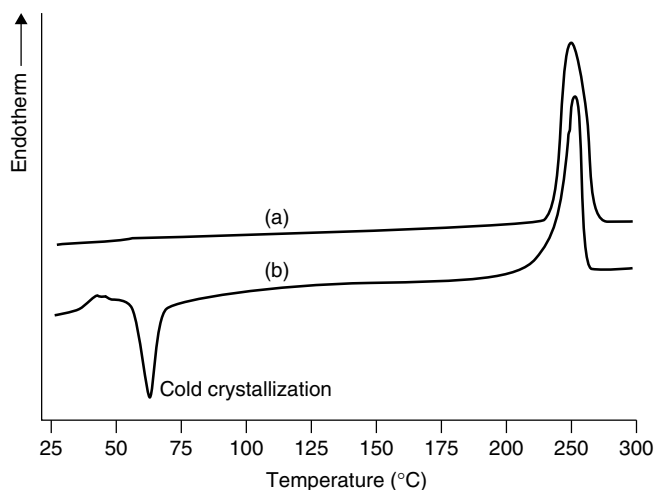


Figure 11.5 Differential scanning calorimetry scans of (a) a slowly cooled, and (b) a rapidly quenched PTT sample (heating rate, 10 °C/min)

Hoffman–Week plots, are 238 [48, 49], 244 [50] and 248 [51, 52] °C. Since the T_m° values of semicrystalline polymers are usually 15–25 °C higher than their DSC T_m values, and also because the lower-melting PBT has a T_m° of 245 °C [53], it is not unreasonable to assume that 248 °C might be a more appropriate T_m° for PTT.

Double DSC melting peaks are frequently observed in PTT, especially when scanning at a low heating rate of <5 °C/min. Huang *et al.* [52] studied the effect of crystallization temperature, time and cooling rate on these PTT double melting peaks. PTT had two melting peaks at about 222 and 228 °C when it was crystallized at 210 °C between 10 and 60 min. With prolonged crystallization to 360 min, the two peaks merged into one with a peak temperature of 225.5 °C. However, when it was crystallized at a lower temperature of 180 °C, instead of having two melting peaks, PTT had a main 228 °C endotherm with a shoulder at about 219 °C. Unlike the 210 °C crystallized samples, prolonging the crystallization time to 360 min did not change the overall shape of the DSC curves. The lower-melting shoulder persisted and moved slightly to a higher temperature. The origin of the double melting peaks was attributed to the lower-melting crystals being recrystallized and melted at a higher temperature during the heating scan, or to the polymer having two populations of crystals of substantially different sizes.

3.5 CRYSTALLIZATION KINETICS

Chuah [54, 55] compared the isothermal crystallization kinetics of PET, PTT and PBT using DSC, and found PTT to have a crystallization rate in between those

of PET and PBT. Between 175 and 195 °C, the Avrami rate constants, K , were of the order of 10^{-3} to 10^{-2} min^{-n} . This is about an order of magnitude higher than PET but an order of magnitude lower than PBT when they are compared at the same degree of undercooling. Huang and Chang [51] reported a spherulitic growth rate of 117.0–4.7 $\mu\text{m}/\text{min}$ and a 20.1 kJ/mol of work for lamellae chain-folding, in between the PET and PBT literature values. They therefore ranked the crystallization rates in the order of $\text{PBT} > \text{PTT} > \text{PET}$. Chen *et al.* [56] also reached a similar conclusion based on their crystallization activation energies.

Using secondary nucleation analysis, Huang and Chang [51] found PTT to go through a transition in the multiple nucleation mechanisms from regimes II to III at around 194 °C. However, Lee *et al.* [50] found only regime II crystallization between 180 and 200 °C.

In polymer melt processing, the crystallization half-time, $t_{1/2}$, is often a more useful parameter than the Avrami rate constant. An experienced individual can often estimate the processing conditions of a new polymer by comparing its $t_{1/2}$ value with those of known polymers. Figure 11.6 compares the $t_{1/2}$ parameters of PET, PTT and PBT, with PTT falling in between the other two polyesters.

A quenched low-crystalline PTT often cold-crystallizes when it is heated to above its T_g (see Figure 5, curve (b)). Bulkin *et al.* [57, 58] found that PTT cold-crystallizes at a much faster rate than PET by following the increase in the PTT crystalline band at 1220 cm^{-1} using rapid-scanning Raman spectroscopy.

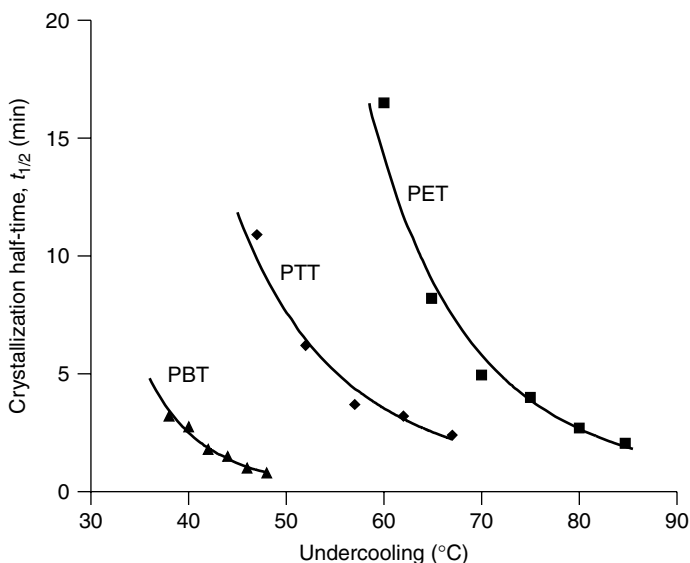


Figure 11.6 Comparison of PET, PTT and PBT crystallization half-times at the same degree of undercooling from the melts

At 71 °C, PTT crystallized and reached 80 % of its equilibrium crystallinity in <1 min, while PET, which has a higher T_g , did not cold-crystallize at all.

3.6 NON-ISOTHERMAL CRYSTALLIZATION KINETICS

Virtually all melt processing is subjected to shearing and non-isothermal crystallization conditions. For example, the melt in fiber spinning is extruded at a shear rate of 10^3 – 10^4 s⁻¹, and is rapidly quenched into solids within a short distance after leaving the spinnerettes. With high winding speed and high thread-line tension, non-isothermal stress-induced crystallization is the dominating event during solidification. Ziabicki [44] studied PTT non-isothermal crystallization by cooling the melt in a DSC system at different rates. A modified Avrami equation was used to analyze the data. As the cooling rate was increased from 2.5 to 35 °C/min, the temperature at which maximum crystallization rate occurs moved to a lower temperature, from 189 to 163 °C. A second maximum was observed between 195 and 200 °C; however, its origin was not fully understood and was thought to relate to surface crystallization. Kim *et al.* [59] also reported studies of PTT non-isothermal crystallization, and obtained an Avrami exponent of 2.7 and an activation energy of 165 kJ/mol.

3.7 HEAT CAPACITY AND HEAT OF FUSION

Pyda and co-workers [49, 60] measured the reversible and irreversible PTT heat capacity, C_p , using adiabatic calorimetry, DSC and temperature-modulated DSC (TMDSC), and compared the experimental C_p values to those calculated from the Tarasov equation by using polymer chain skeletal vibration contributions (Figure 11.7). The measured and calculated heat capacities agreed with each other to within ± 3 % standard deviation. The ΔC_p values for fully crystalline and amorphous PTT are 88.8 and 94 J/K mol, respectively.

Using the effect of diluents, González *et al.* [61] measured the heat of fusion of a 100 % crystalline PTT, ΔH_f , as 147 ± 17 J/g. Grebowicz and Chuah [48], and Pyda *et al.* [49] measured ΔC_p and the heat of fusion, ΔH , of a series of PTT samples with different thermal histories. Extrapolation to zero ΔC_p from the plot of ΔC_p versus ΔH , gave a 146 J/g ΔH_f , in good agreement with González *et al.* [61].

3.8 GLASS TRANSITION AND DYNAMIC MECHANICAL PROPERTIES

PTT has a DSC T_g of about 45 °C. At <30 % crystallinity, the T_g remains fairly constant at about 45 °C [6] (Figure 11.8). Above 30 % crystallinity, it increases rapidly to about 70 °C at 50 % crystallinity in isotropic samples.

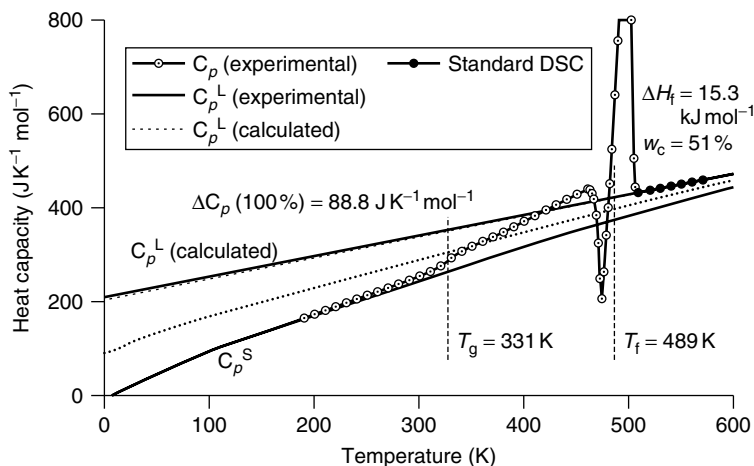


Figure 11.7 Experimental and calculated heat capacities of solid and liquid PTT [49]. From Heat capacity of poly(trimethylene terephthalate), Pyda, M., Boller, J., Grebowicz, J., Chuah, H., Lebedev, B. V. and Wunderlich, B., *J. Polym. Sci., Polym. Phys. Ed.*, **36**, 2499–2511 (1998), Copyright © (1998 John Wiley & Sons, Inc.). Reprinted by permission of John Wiley & Sons, Inc.

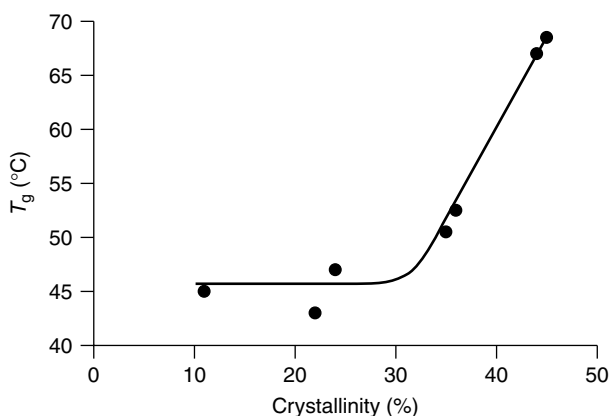


Figure 11.8 Effect of crystallinity on the PTT glass transition temperature

PTT has three dynamic mechanical viscoelastic relaxations [61, 62], α , β and γ (Figure 11.9). The $\sim 70^\circ\text{C}$ α -relaxation is the glass transition. In a study on the effect of methylene sequence length on aromatic polyester viscoelastic properties, Farrow *et al.* [63] reported a PTT α -relaxation as high as 95°C . They also found that T_g of this series of aromatic polyesters did not show any odd–even effects, which was later confirmed by Smith *et al.* [64].

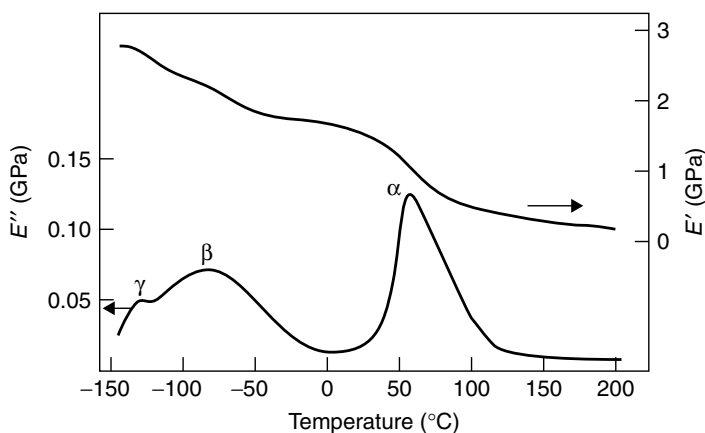


Figure 11.9 Dynamic mechanical storage (E') and loss (E'') moduli of isotropic PTT at 11 Hz showing the three relaxations [61]. From Dynamic mechanical relaxations of polyterephthalates based on trimethylene glycols, González, C. C., Pereña, J. M. and Bello, A., *J. Polym. Sci., Polym. Phys. Ed.*, **26**, 1397–1408 (1988), Copyright © (1988 John Wiley & Sons, Inc.). Reprinted by permission of John Wiley & Sons, Inc

The origin of the β -relaxation at about -70°C is a little more complex. This occurred in all poly(n -methylene terephthalate) samples studied by Farrow *et al.* [63], with n from 2 to 10. The β -relaxation loss curve was asymmetric, and the peak temperature decreased with increased methylene length. This was attributed to the re-orientation of the hydroxyl groups and local motions of the carboxyl groups in the amorphous phase [65]. In PET, the β -relaxation is very broad [66]. A third γ -relaxation, with a loss peak temperature at about -115°C appeared when poly(n -methylene terephthalate) has a longer methylene sequence. González *et al.* [61] found a γ -relaxation at about -105°C in PTT, overlapping with the β -peak, and associated the γ -relaxation with the co-operative movements of methylene chains containing at least three consecutive methylene units. The loss peak of the sub-ambient relaxation was also affected by crystallinity of the polymer. Chuah [47] found that the PTT β -relaxation shifted from -78 to -54°C after annealing.

3.9 MECHANICAL AND PHYSICAL PROPERTIES

A comparison of the mechanical and physical properties of PTT, PET and PBT [67], measured from injection molded American Society of Testing Methods (ASTM) Type II samples, is given in Table 11.4. The mechanical properties of PET and PTT are highly dependent on injection molding conditions due to

Table 11.4 Comparison of the mechanical and physical properties of PTT with those of PET and PBT [67, 68]

Property	PET	PTT	PBT
Tensile strength (MPa)	72.5	67.6	56.5
Flexural modulus (GPa)	3.11	2.76	2.34
Heat distortion temperature, at 1.8 MPa (°C)	65	59	54
Notched Izod impact (J/m)	37	48	53
Specific gravity	1.40	1.35	1.34
Mold shrinkage (m/m)	0.03	0.02	0.02
Dielectric strength (V/mil)	550	530	400
Dielectric constant, at 1 MHz	3.0	3.0	3.1
Dissipation factor, at 1 MHz	0.02	0.015	0.02
Volume resistivity (ohm cm)s	1.00×10^{15}	1.00×10^{16}	1.00×10^{16}

their slower crystallization rates, whereas PBT, which crystallizes very fast, has properties fairly independent on the molding conditions. The reported PTT tensile strength, flexural modulus and notched Izod impact data fall between those of PET and PBT. All three polyesters have similar electrical properties, except for PET with a lower volume resistivity, which is likely to be due to low sample crystallinity.

3.10 MELT RHEOLOGY

PTT exhibits melt rheological behavior similar to that of PET. At low shear rates the melt is nearly Newtonian. It shear-thins when the shear rate is $>1000 \text{ s}^{-1}$ (Figure 11.10) [68]. At the melt processing temperatures of PET, $\sim 290^\circ\text{C}$, and of PTT, $\sim 260^\circ\text{C}$, both polymers have similar viscosities of about 200 Pa s. However, PTT has a lower non-Newtonian index than PET at high shear rates. The flow behavior can be modeled by the Bueche equation, as follows:

$$\eta/\eta_0 = 1/(1 + 0.6\lambda\dot{\gamma})^{3/4} \quad (11.3)$$

where η is the melt viscosity, η_0 is the zero shear viscosity, $\dot{\gamma}$ is the shear rate and λ is the melt relaxation time. The curves presented in Figure 11.10 show that viscosities modeled from the Bueche equation agree quite well with the experimental data.

Table 11.5 shows the flow activation energies, E_a , for PET, PTT and PBT [68]. PTT has a higher E_a compared to PET but similar to that of PBT. The change in its melt viscosity is therefore less sensitive to temperatures changes than PET. However, due to the higher degradation rate, increased melt processing temperatures can have deleterious effect on the melt viscosity and IV.

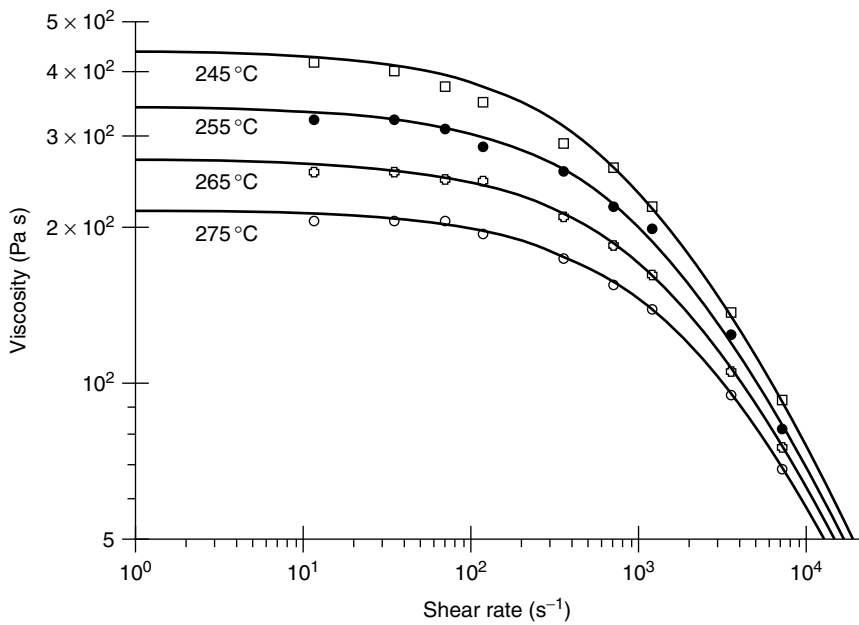


Figure 11.10 PTT viscosity as a function of the shear rate at the melt processing temperatures from 245 to 275 °C

Table 11.5 Rheological flow activation energies (E_a) of PET, PTT and PBT melts [68]

Parameter	PET	PTT	PBT
Temperature (°C) ^a	280	250	245
E_a (KJ/mol)	65.4	57.6	62.4

^a when $\eta_0 = 300$ Pa s.

4 FIBER PROPERTIES

4.1 TENSILE PROPERTIES

Figure 11.11 shows the stress–strain curves of PET, PTT and PBT fibers [4]. Both PTT and PBT have a knee or a plateau region at about 5 and 7 % strains respectively, whereas PET stress increases smoothly with strain and does not have the plateau region. Table 11.6 compares the moduli of the three polyesters before and after annealing. The modulus of PET is nearly four times higher than those of PTT and PBT. After annealing, the PET modulus decreased by nearly half due to relaxation and loss of orientation. However, the PTT modulus increased by

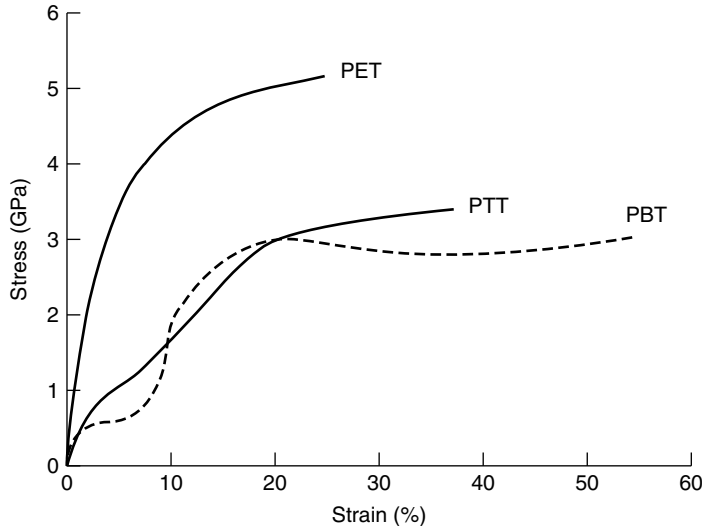


Figure 11.11 Stress–strain curves of PET, PTT and PBT fibers [69]. From Jake-ways, R., Ward, I. M., Wilding, M. A., Desborough, I. J. and Pass, M. G., *J. Polym. Sci., Polym. Phys. Ed.*, **13**, 799–813 (1975), Copyright © (1975 John Wiley & Sons, Inc.). This material is used by permission of Wiley-Liss, Inc., a subsidiary of John Wiley & Sons, Ltd

Table 11.6 Moduli (in GPa) of PTT, PET and PBT fibers before and after annealing [4]

	Annealed	Unannealed
PET	5.23	9.15
PTT	3.88	2.58
PBT	2.6	2.4

nearly 40 %, possibly due to an increase in crystallinity, while the PBT modulus remained nearly the same after annealing since the polymer is already highly crystalline with its fast crystallization rate.

4.2 ELASTIC RECOVERY

The fiber industry has long been aware of PTT’s good tensile elastic recovery [3]. Ward *et al.* [4] studied the deformation behavior of PET, PTT and PBT fibers and found the tensile elastic recoveries were ranked in the unexpected descending order of PTT > PBT > PET. Chuah [47] found that the PTT elastic recovery and permanent set nearly tracked that of nylon 66 up to 30 % strain (Figure 11.12).

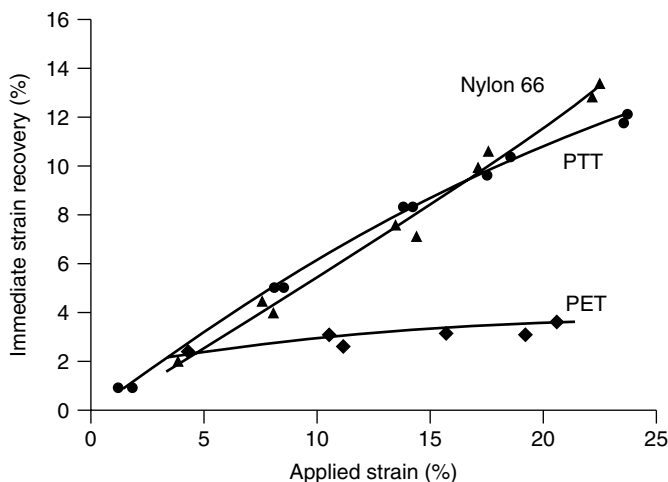


Figure 11.12 Comparison of the PTT elastic recovery with PET and nylon 66 at various strains

The unusually good PTT elastic recovery property was thought to relate to the plateau region of its stress–strain curve. Jakeways *et al.* [69] deformed PTT fiber *in situ* in a wide-angle X-ray diffractometer, and measured the changes in the fiber period d -spacing along the c -axis as a function of strain. The crystalline chain responded and deformed immediately to the applied strain. It increased in direct proportion to the applied strain up to 4% before deviating from affine deformation (Figure 11.13). Furthermore, the deformation below this critical strain was reversible. This microscopic reversible crystal deformation was tied to PTT chain conformation. The methylene units are arranged in a highly contracted and a very compliant *gauche*–*gauche* conformation [39, 41]. The contraction is even more pronounced than the *gauche*–*trans*–*gauche* PBT chains [70]. Since initial deformation involves torsional rotation of the *gauche* methylene C–C bonds, the force is only a fraction of the bond stretching force. Thus, polymer with a helical chain conformation tends to have a low crystal modulus, about 20% of the predicted modulus if the chains were in all-*trans* conformations [71].

PTT indeed has a very low X-ray crystal modulus of 2.59 GPa [72]. This value is probably too low because a highly oriented PTT fiber with about 50% crystallinity already had a 2.5 GPa modulus [4]. Using the CERRIUS II molecular simulation program, Jo [73] calculated a 12.2 GPa crystal modulus. Although considerably higher than the experimental crystal modulus of Nakamae *et al.* [72], it is still an order of magnitude lower than the 107 GPa PET crystal modulus [74]. Because of the low crystal modulus, the PTT crystalline chain responded and deformed immediately with applied macroscopic strain. The crystalline chain deformation is reversible, and is the driving force for the good elastic recovery.

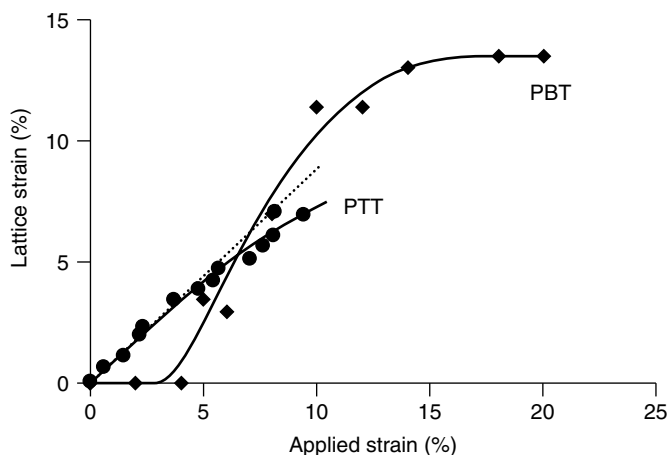


Figure 11.13 Changes of PTT (●) and PBT (◆) fibers *c*-axis lattice strains measured from X-ray diffraction spacings as a function of applied external strains; the dotted line represents affine deformation between lattice and applied strains

Jakeways *et al.* [69] addressed only the crystalline chain deformation to explain PTT's elastic recovery. The macroscopic deformation must also simultaneously involve the partially irreversible amorphous chain deformation. The higher the applied strain, then the more dominant was the irreversible amorphous deformation with deviation from affine deformation.

Although PBT fiber also has a plateau region in the stress–strain curve [4], the crystalline chains do not respond to external strain in the first few percent of deformation. They increased in length only when the strain is above 4% (see Figure 11.13). Therefore, initial macroscopic deformation involved viscous flow of the amorphous phase. Furthermore, PBT undergoes strain-induced crystal transformation at moderately low strains of 15–20% [75]. The differences in their microscopic crystalline chain deformation explained why PTT has a better elastic recovery than PBT even though both have contracted chains and knees in their stress–strain curves [4, 69].

4.3 LARGE STRAIN DEFORMATION AND CONFORMATIONAL CHANGES

Many semicrystalline polymers are polymorphic and exist in different crystal forms. When PBT fiber is uniaxially stretched [75], the contracted *gauche–trans–gauche* α -crystal chain is extended to a fully *trans* conformation of a γ -crystal. Above 20% strain, the crystal form is 100% γ -crystal with a longer *c*-axis triclinic cell dimension. Thus, it is reasonable to ask whether the

highly contracted PTT chain would undergo strain-induced crystal transformation into a fully extended *trans* crystal?

Poulin-Dandurand *et al.* [41] calculated the PTT crystalline chain conformational energy, and showed the methylene units can only deviate from the *gauche* arrangement to a small degree without a substantial increase in energy. An all-*trans* conformation would have too high a conformational energy and is unstable. Jo [73] calculated the conformation energy and reached a similar conclusion. The PTT chain could adopt an all-*trans* conformation only when it is stretched to above 30% strain accompanied by an increase in the *c*-axis cell dimension and a change in the dihedral angles. The stress required to stretch the PTT chain to a fully *trans* conformation would be very high compared to PBT where the stress remains unchanged during an α - to γ -crystal transformation. The high energy required would likely cause the PTT crystal structure to dislocate rather than transforming it into a new crystalline form. Thus, it was concluded that PTT could not adopt a new crystal structure.

However, recent *in-situ* synchrotron radiation WAXD studies of PTT fiber deformation by Wu *et al.* [76] showed that the PTT crystal 002 *d*-spacing could be stretched to a length corresponding to a fully *trans* chain. The increase in the *c*-axis dimension was accompanied by a decrease in the *b*-axis length, measured from the 010 reflection (Figure 11.14). When the strain was increased above a

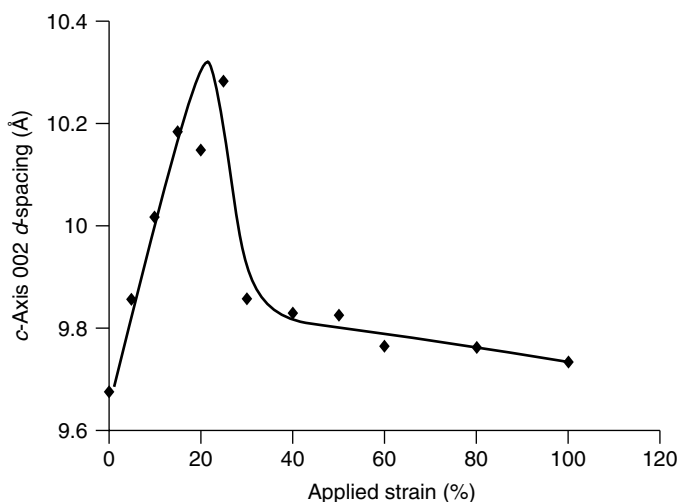


Figure 11.14 Effect of applied strain on the 002 *d*-spacing of a PTT fiber drawn at '3.3 \times ' measured by WAXD [76]. Reprinted from *Polymer*, **42**, Wu, J., Schultz, J. M., Samon, K. M., Pangelinan, A. B. and Chuah, H. H., *In situ* study of structure development in poly(trimethylene terephthalate) fibers during stretching by simultaneous synchrotron small- and wide-angle X-ray scattering, 7141–7151, Copyright (2001), with permission from Elsevier Science

threshold value, the *c*-axis dimension suddenly reverted back to near its original length. Although there was no simultaneous spectroscopic measurement of conformational changes, the simultaneous changes in the *c*- and *b*-axes dimensions indicate changes in the crystal unit cell dimensions. If this observation were indeed a strain-induced crystal transformation, the new crystal form was unstable and existed only under a critical macroscopic strain. Above that, the crystal reverted back to its original form, perhaps through dislocation or slips between planes of the crystals to relieve the stress. The question of a possible alternate PTT crystal form remains a topic for further research.

4.4 DRAWING BEHAVIOR

Figure 11.15 shows the tensile stress–strain curves of PTT at various temperatures [77]. At room temperature, PTT is ductile. It yields at 5.4 % strain, cold draws with a natural draw ratio of about 3.2, strain-hardens and breaks at 360 % strain. With increasing draw temperature, the yield stress decreases and the elongation at break increases. At 50 °C, just above the T_g , PTT becomes rubbery. The Young's modulus decreases by about two orders of magnitude from 1140 to 12.9 MPa, and the overall drawability increases with a strain at break of nearly 600 %. However, when the draw temperature was increased to 75 °C, 30 °C above the T_g , instead of becoming more rubbery and capable of higher draw, PTT became ductile again. The modulus unexpectedly increased by more than tenfold to 189 MPa. The overall drawability decreased with a drop in breaking strain to 390 %. In fact, the 75 °C stress–strain curve looked similar to that of the one

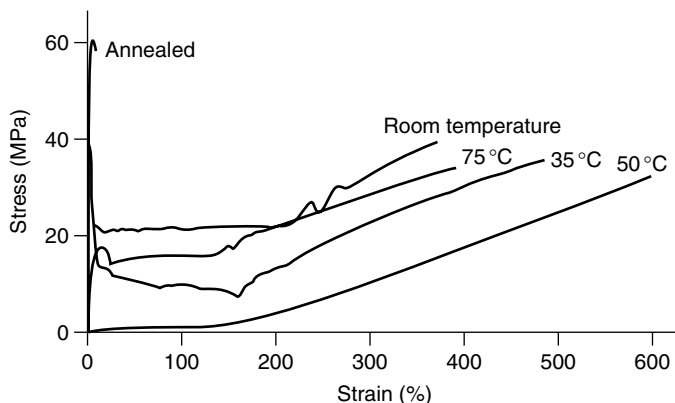


Figure 11.15 PTT stress–strain curves at draw temperatures below and above the glass transition temperature [77]. Reprinted in part with permission from Chuah, H. H., *Macromolecules*, **34**, 6985–6983 (2001). Copyright (2001) American Chemical Society

room temperature. Instead of the conventional experience of increasing drawability with increasing temperature, the PTT draw first increased, went through a maximum and decreased, all happening over a narrow range of temperature from room temperature to $T_g + 30^\circ\text{C}$.

This unexpected drawing behavior was due to the onset of cold crystallization competing with drawing. To draw a polymer, it is usually heated to temperatures above its T_g so that the polymer became soft to facilitate draw. However, when the polymer cold-crystallized during hot drawing, the increase in crystallinity increased the polymer's modulus and had an opposing effect to hot drawing, and therefore reduced the drawability. When cold-crystallization proceeded at a fast rate, PTT transitioned *in situ* from rubbery to ductile, such as the 75°C draw shown in Figure 11.15. At higher temperatures, the polymer could become brittle and cause draw failure. Thus, PTT drawability depends on its initial thermal history and morphology, and whether it can cold-crystallize or not during hot drawing. This behavior must be taken into account in PTT fiber spinning and drawing.

4.5 CRYSTAL ORIENTATION

Figure 11.16 shows the wide-angle x-ray diffraction (WAXD) pattern of an oriented PTT and indices of some of the reflections. Although PTT has a 002 reflection, the intensity is weak. It is also not a true meridional reflection, being offset from the meridian by about 3° . The offset reflections are so close to each other that they overlap and appear as one meridional reflection [39], and could not

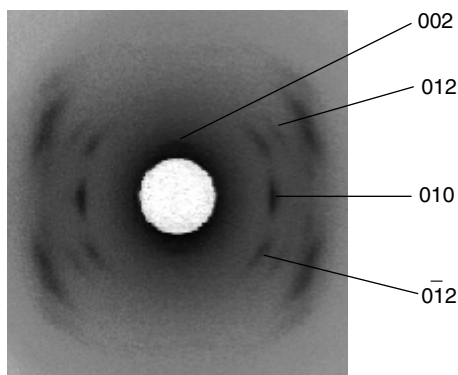


Figure 11.16 PTT WAXD pattern and indices of the reflections [45]. From *Polym. Bull.*, Crystal orientation function of poly(trimethylene terephthalate) by wide-angle X-ray diffraction, Chuah, H. H. and Chang, B. T. A., **46**, p. 310, Figure 2, Copyright © Springer-Verlag (2001). Reproduced by permission of Springer-Verlag GmbH & Co. KG

be separated easily, even at high orientation. Thus, it is better to use the more intense 010 equatorial reflection for crystal orientation function measurement. Chuah and Chang [45] derived an equation for measuring the Herman orientation function, f_c , using the 010 reflection based on Wilchinsky's treatment of uniaxial orientation. The final form of the Herman orientation function equation is expressed as follows:

$$f_c = 1 - 3\langle \cos^2 \phi_{010,z} \rangle \quad (11.4)$$

where $\langle \cos^2 \phi_{010,z} \rangle$ is the average cosine angle of the normal of the (010) plane made with the draw direction, z .

5 PROCESSING AND APPLICATIONS

5.1 APPLICATIONS

Most of the PTT application developments to date have focused on textile and carpet fibers because this polyester has a combination of several properties particularly suited for such applications.

PTT fibers and yarns have bulk, resiliency, stretch-recovery, softness, hand and drape, properties which are similar to those of nylons and much better than those of PET. Such materials are inherently resistant to most stains which are acidic in nature because they not have dye sites. They also have a lower static propensity than nylons. PTT fibers are dyed with disperse dyes but at a lower temperature than PET because of the polymer's lower T_g . The combinations of these properties are attractive to carpet and textile manufacturers in some applications where PTT could replace nylon or PET. PTT also offers the potential of creating new fiber products by using the unique combinations of these properties not found in either nylon or PET alone.

Fiber end-use applications include the following: (1) ready-to-wear, active-wear, intimate apparels, and inner linings where stretch-recovery, softness, hand and drape are the key attributes; (2) carpets where resiliency, newness retention, stain resistance and low static generation provide values over currently used materials in some market segments; (3) automotive and home upholstery, utilizing the easy dyeing, stain resistance, and stretch-recovery properties. Within a short period of time since the polymer's commercialization, PTT ready-to-wear stretch apparels [5, 78] and resilient floor coverings [79] have already appeared in the market since 1999. Figure 11.17 shows some of these commercial products.

Other potential applications of PTT are in monofilaments, non-wovens, films, engineering thermoplastics and molded goods. Hsu [80] has patented paper forming fabrics made with PTT monofilaments for use in papermaking machines because this combines the chemical resistance of a polyester and the resiliency

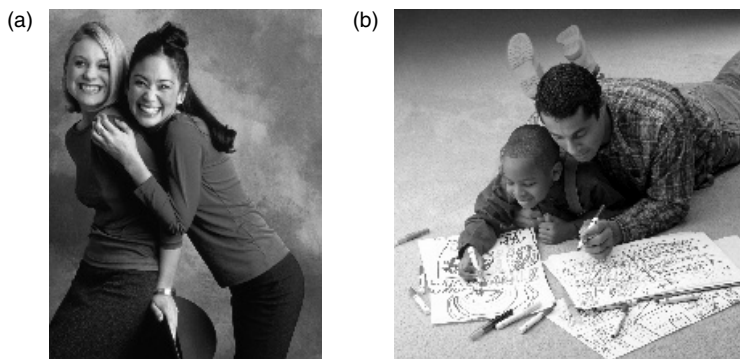


Figure 11.17 Examples of PTT applications: (a) Solo™ soft, stretch casual wear by Asahi; (b) cut-pile carpet marketed by Shaw Industries

of the less chemical resistant nylon. PTT non-woven fabric shows better dimensional stability and is softer than PP [81]. Other applications include synthetic leathers [82], flexible transparent film for packagings [83] and zip fasteners [8].

5.2 FIBER PROCESSING

Fiber grade PTT typically has an IV of 0.80–1.00 dL/g. The IV value might seem high when compared to the typical 0.64 dL/g IV fiber grade PET. Since IV is unique to each polymer, one cannot compare the IV values of two different polymers. A 0.92 dL/g IV PTT has a similar molecular weight of an 0.64 IV PET with a M_w of about 40 000.

PTT polymer pellets must be dried to a moisture level of <30 ppm, preferably in a close-loop hot air dryer, to avoid hydrolytic degradation during melt processing. Drying is carried out with 130 °C hot air with a dew point of <–40 °C for at least 4 h. Because of the faster crystallization rate, PTT pellets are already semicrystalline after pelletizing, and do not require pre-crystallization prior to drying as with PET. The dried polymer is extruded at 250–270 °C into bulk continuous filaments (BCFs), partially oriented yarn (POY), spin-draw yarn (SDY) and staple fiber.

5.2.1 Partially Oriented and Textured Yarns for Textile Applications

Brown and Chuah [84] and Oppermann *et al.* [36] studied the spinning of partially oriented yarn (POY) as a function of take-up speed from 500 to 5000 m/min. Figures 11.18 and 11.19 show, respectively, development of the tenacity and elongation as a function of spinning speed. Tenacity increases with increasing

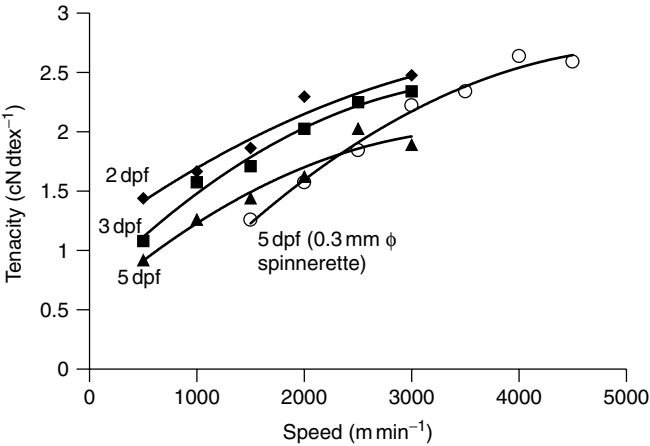


Figure 11.18 Tenacity of PTT fibers as a function of winder take-up speed, showing the effect of dpf and spinnerette diameter. Fibers indicated with 'filled symbols' were spun with 0.35 mm diameter spinnerettes, while those indicated with 'open' symbols were spun with 0.3 mm diameter spinnerettes

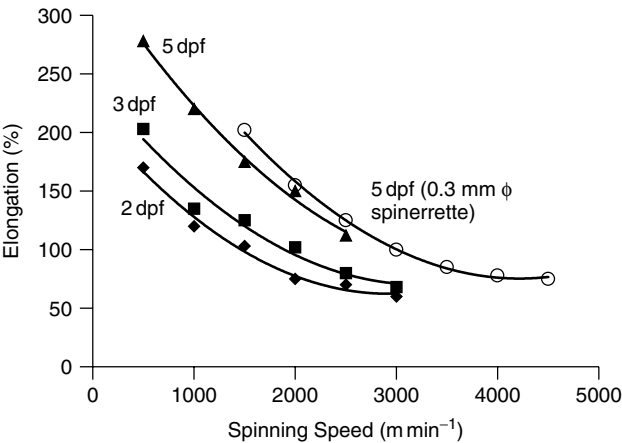


Figure 11.19 Elongation of PTT fibers as a function of winder take-up speed, showing the effect of dpf and spinnerette diameter (symbols identification as in Figure 11.18)

speed, while elongation decreases. For higher dtex per filament (dpf) fiber, the tenacity is lower at the same spinning speed due to the lower orientation. Overall, PTT has a lower tenacity and elongation than PET at equivalent spinning speeds. Another distinguishing feature is that PTT POY yarn has a tendency to shrink at ambient and elevated temperatures due to a combination of entropic relaxation

and cold-crystallization depending on the spinning speed and yarn morphology. This causes the yarn package to deform and is undesirable. This can be overcome by spinning at suitable speeds to control final yarn shrinkage, relaxation and cold-crystallization behavior [36, 85]. Alternatively, the yarn can be heat stabilized [86, 87] prior to winding, similar to the spinning of nylon fiber.

PTT POY yarns were textured by the false-twist method at 140 to 160 °C. Crimp development was almost twice as high as PET, with crimp contraction reaching about 50 %. When PTT yarns with a high level of crimp contraction are knitted into stretch fabrics, the amount of stretch achieved is equivalent to PET stretch fabrics incorporated with 6 to 8 % of Spandex [89]. In addition to stretch, PTT fabrics tend to have softer hand and better drape than PET. Since they do not absorb moisture like nylon, PTT fabrics also have a desirable dry touch and comfort.

5.2.2 Carpets

Chuah [90] has described in detail the process of making PTT carpet bulk continuous filaments (BCFs). The extruded yarn, after cooling and applying spin finish, is drawn between two sets of godets. Typically the take-up godet is not heated. The fiber is stretched at a low draw ratio of 1.01–1.3 between the take-up godet and a draw godet heated to 50–80 °C. A large draw of 2.5–3.5 is applied between the draw roll and the heated dual roll to give the final BCF an elongation at break of 40 to 70 %. The drawn yarn is textured with hot air at 160–220 °C and at a pressure of 0.6–1.0 MPa [90–93].

To make cut pile carpets, two strands of BCF yarns are twisted together and heat-set with steam using a Superba heat setting machine at 135–145 °C or at 175–195 °C when heat-set with super-heated steam in a Suessen. An experimental design experiment [94] showed the higher the heat set temperature, then the lower is the bulk of the final carpet, but there is an increase in the tip definition and walk performance. The tufted carpets are then dyed with disperse dyes at atmospheric boil [95] in a continuous or a batch process. PTT carpets showed excellent resiliency in walk test experiments, equivalent to a nylon and much better than both PET and polypropylene, had lower static charge of <3.5 kV, and were resistant to coffee, mustard, betadine, red acid dyes and other stains [96].

5.3 DYEING

Because of the low T_g , PTT fibers and fabrics are dispersed dyed at atmospheric boil without the need of a carrier [95–99]. PTT is therefore a more environmentally friendly polymer than PET in this regard, although the later is now dyed under pressure at 130 °C to avoid using carrier. Yang *et al.* [99] compared the dye uptakes of PTT and PET fibers by measuring their Kulbelka–Munk (K/S)

Table 11.7 Effect of dyeing temperature on PTT and PET fiber shade depths [99]

Disperse dye	Dyeing temperature (°C)	K/S Value	
		PTT	PET
Blue 56	100	16.4	6.0
	110	18.1	9.6
	120	17.6	13.5
	130	15.1	12.1
Blue 73	100	19.6	3.1
	110	29.3	8.3
	120	30.1	18.2
	130	27.6	20.6
Blue 79	100	11.5	2.6
	110	15.1	6.0
	120	18.2	8.8
	130	16.4	11.3

values as a function of dyeing temperature from 100 to 130 °C (Table 11.7). PTT reached a K/S value of about 16 at 100 °C while PET did not absorb as much dye at this temperature. PET dye uptake only leveled off at a >120 °C dyeing temperature with a lighter color shade K/S value of 13. PTT dyed at atmospheric boil has very good colorfastness against light, ozone and NO_x, similar to PET [95, 99].

5.4 INJECTION MOLDING

Several patents describe the injection molding of PTT for applications such as transparent heat-resistant bottles [100], impact, heat and bending resistant electrical connectors [101]. Neat PTT can be injection molded at 250–260 °C into a mold maintained at 70–80 °C under a holding pressure of 3.1–4.2 MPa and a cycle time of 40 s [68]. Colder mold temperatures tend to cause uneven crystallization with the formation of an amorphous transparent skin and a highly opaque crystalline core. The spherulites formed ranged from small and disordered at the outer edges to more perfect and larger in the core with high stress-concentration interfaces. In extreme cases, the molded part could become brittle. Glass-filled PTT crystallizes at a much faster rate and reduces the cycle time to 30 s. Table 11.8 compares the properties of a 30 % glass-filled PTT with PET and PBT [68]. The flexural modulus of glass-filled PTT is unexpectedly higher than those of PET and PBT, departing from the ranking of the unfilled polymer moduli (see Table 11.4). This anomaly could be due to unoptimized sample preparation or molding conditions between the three polymers.

Table 11.8 Properties of glass-filled polyesters [68]

Property	Units	PET	PTT	PBT
Glass content	wt%	28	30	30
Tensile strength	MPa	159	159	115
Flexural modulus	GPa	8.97	10.4	7.60
Heat distortion temperature ^a	°C	224	216	207
Notched Izod impact	J/m	101	107	85
Specific gravity	kg/m ³	1560	1550	1530
Mold shrinkage	m/m	0.002	0.002	0.002

^a At 1.8 MPa.

The heat distortion temperature (HDT) is greatly improved by the glass from 59 to 216 °C, while the notched Izod impact is similar to PET and slightly better than PBT.

6 PTT COPOLYMERS

Smith *et al.* [64] prepared a series of PET/PTT copolyesters, and found that addition of the other component suppressed the melting point of the respective homopolymer. Between 37 and 60 % PTT content, the copolymers became amorphous and did not show any melting endotherms in the differential thermal analyzer scans. A similar behavior was observed by Balakrishnan and co-workers [102] in PET/PTT copolyesters prepared by the transesterification of PET with PDO, and by the copolymerization of EG and PDO with DMT [103, 104]. The non-crystallizing behavior of copolymers with intermediate contents of the respective component is similar to that of a eutectic mixture, indicating formation of random copolyesters. The T_g and solubility temperature of the copolyesters were, however, continuous and went through minima with increasing PTT content [64].

González *et al.* [106] copolymerized PDO and DPG with DMT to modify the polymer chain stiffness between the aromatic rings. It is interesting to note that the addition of 13 % DPG suppressed the copolymer T_g and T_m to 44 and 220 °C, respectively, and the copolymer was still crystalline with 33 % DPG content and had a 172 °C melting point, whereas PET/PTT copolymers with 33 % PET content would be non-crystallizable.

Chuah *et al.* [107] prepared a series of PTT/poly(trimethylene naphthalate) (PTN) copolyesters by copolymerizing PDO with dimethyl terephthalate and dimethyl naphthalate. The PTN homopolymer has a T_g of 75 °C and a T_m of 245 °C. Despite the more rigid naphthalate moiety, the PTN T_g and T_m were much lower than the T_g of poly(ethylene naphthalate) (PEN), indicating the strong influence of the flexible trimethylene units.

Ester interchange between PEN and PTT in the melt was studied by blending the two polymers in a Brabender mixer at 300 °C [108]. PEN transesterified with PTT at a much faster rate compared to PET and PBT. After 5 min mixing, a 45/55 PEN/PTT blend showed a single T_g , whereas both PEN/PET and PEN/PBT blends still showed their respective homopolymer T_g after 5–6 min blending. After 10 min blending, the PEN/PTT copolymer had a single melting point.

When 10 % PTT is blended with PET, it suppressed the PET T_g such that it can be dyed at atmospheric boil without using a carrier [109]. A similar phenomenon was also found by Oppermann *et al.* [110]. Kelsey *et al.* [111] found that the addition of 9 % PTT to poly(cyclobutane terephthalate) (PCBDOT) improves its impact strength without too much sacrifice to the T_g . The 9/93 PTT/PCBDOT blend has a T_g of 100 °C and a notched Izod impact of 75 J/m.

7 HEALTH AND SAFETY

Since PTT is a new commercial product, the Shell Chemical Company, as the company which first introduced it to the market, took the responsibility of product stewardship [112], and registered the polymer on the chemical inventory lists in several countries. As a high-molecular-weight polymer, PTT is biologically inactive and requires safe handling like many other commercial polymers.

When PTT is exposed to high heat such as during drying and melt processing, it releases acrolein, allyl alcohol and cyclic dimer by-products. Among these, acrolein is of special concern because it is a very strong lachrymator. It can also irritate lung and respiratory tracts, and affect breathing. The effects are acute and do not have cumulative long-term effects. The US Occupational Safety and Health Agency industrial hygiene guidelines gave the time-weighted exposure limit of acrolein over a period of 8 h as 0.1 ppm, while the short-term exposure limit for 15 min is 0.3 ppm [113]. Therefore, adequate ventilation must be provided to avoid acrolein exposure.

REFERENCES

1. Semas, J. H., *Int. Fiber J.*, **12**(1), 12 (1997).
2. Whinfield, J. R. and Dickson, J. T., *Br. Patent 578 079*, 1946.
3. Fiber Industries, Inc., *Br. Patent 1 254 826*, 1971.
4. Ward, I. M., Wilding, M. A., and Brody, H., *J. Polym. Sci., Polym. Phys. Ed.*, **14**, 263 (1976).
5. Heschmeyer, C., *Int. Fiber J.*, **15**(4), 66 (2000).
6. Chuah, H. H., Brown, H. S., and Dalton, P. A., *Int. Fiber J.*, **10**(5), 50 (1995).

7. Harris, M. E., *US Patent 3 584 103*, (to E.I. du Pont de Nemours and Company), 1971.
8. Kawase, S. and Kuratsuji, T., *US Patent 3 984 600* (to Teijin Ltd), 1976.
9. Takatoshi, K., Takanori, U. and Wataru, F., *Jpn Patent JP51-140 992* (to Teijin Ltd), 1976.
10. Takatoshi, K., *Jpn Patent JP52-5320* (to Teijin Ltd), 1977.
11. Nager, P., Applications of 1,3-propanediol, presentation given at the CHEMSPEC Asia'91 conference, Tokyo, Japan, June 24-25, 1991, Specialty Chemicals Production, Marketing and Application.
12. Drent, E., *Eur. Patent 478 850 A1* (to Shell Oil Company), 1992.
13. Breitskopf, N., Dämbkes, G. and Bach, H., *US Patent 5 008 473* (to Ruhrchemie Aktiengesellschaft), 1991.
14. Weider, P. R., Powell, J. B. and Lam, K. T., *US Patent 5 684 214* (to Shell Oil Company), 1997.
15. Powell, J. P., Slaugh, L. H., Forschner, T. C., Thomason, T. B., Semple, T. C., Weider, P. R. and Arhancet, J. P., *US Patent 5 463 144* (to Shell Oil Company), 1995.
16. Powell, J. P., Slaugh, L. H., Forschner, T. C., Semple, T. C. and Weider, P. R., *US Patent 5 463 145* (to Shell Oil Company), 1995.
17. Tran-Dinh, K. and Hill, F. F., *Ger. Patent DE 3 734 764* (to Hüls AG), 1989.
18. Nair, R. V., Payne, M. S., Donald, E. and Valle, F., *World Patent WO99 28 480* (to E.I. du Pont Nemours and Company and Genecore International, Inc.), 1999.
19. Chen, G., Hwang, X. and Ku, L., *Chin. Synth. Fiber Ind.*, **21**(5), 26 (1998).
20. Wu, W.-Y., *R&D Plans and Product Design of Hi-Tech Textiles*, Taiwan Fiber Industry Association, Taipei, 52-66, 1999.
21. Moore, E. R. and Bray, R. G., *1,3-Propanediol and Polytrimethylene Terephthalate*, Process Economics Program Report 227, SRI International, Menlo Park, CA, 1999.
22. Hess, L. H., Kurtz, A. N. and Stanton, D. B., in *Acrolein and derivatives, Kirk-Othmer Encyclopedia of Chemical Technology*, 3rd Edn, Vol. 1, Grayson, M., Eckroth, D., Brickford, M., Bushey, G. J. and Klingsberg, A. (Eds), Wiley-Interscience, New York, 1978, pp. 277-297.
23. Schauhoff, S., and Schmidt, D. W., *Chem. Fibers Int.*, **46**, 263 (1996).
24. Doerr, M. L., *Eur. Patent 547 553*, (to Hoechst Celanese Corporation), 1993.
25. Doerr, M. L., Hammer, J. J. and Dees, J. R., *US Patent 5 340 909* (to Hoechst Celanese Corporation), 1994.
26. Traub, H. L., Hirt, P., Herlinger, H. and Oppermann, W., *Makromol. Chem.* **230**, 179 (1995).
27. Schimdt, W., Thieloff, U., Schauhoff, S. and Yu, D., *US Patent 5 798 433* (to Zimmer Aktiengesellschaft and Degussa Aktiengesellschaft), 1998.

28. Kuo, T.-Y., Huang, J.-C., Liao, C.-S., Tseng, I.-M., Juang, C. and Jean, L.-S., *US Patent 5 872 204* (to Industrial Technology Research Institute), 1999.
29. Chuah, H. H., Vinson, R. W. and Ulzelmeier, C. W., The Kinetics of Poly(Propylene Terephthalate) Solid-state Polymerization in *Research Awareness Bulletin*, Shell Chemical Company, July 1993, Houston, TX, pp. 101–103.
30. Stouffer, J. M., Blanchard, E. N. and Leffew, K. W., *US Patent 5 763 104* (to E.I. du Pont Nemours & Company), 1998.
31. Wang, X.-S., Li, X.-G. and Yan, D., *Polym. Degrad. Stabil.*, **69**(3), 361 (2000).
32. Zimmerman, H., Degradation and stabilisation of polyester in *Developments in Polymer Degradation –5*, Grassie, N. (Ed.), Applied Science Publishers, London, 1984, Ch. 3 79–119.
33. Luderwald, I. and Urrutia, H., *Makromol. Chem.*, **177**, 2079 (1976).
34. Kelsey, D. R., Blackbourne, R. L., Tomaskovic, R. S., Reitz, H., Seidel, E., Wilhelm, F., *US Patent 6 277 947* (to Shell Oil Company), 2001.
35. Kelsey, D. R., *US Patent 6 093 786* (to Shell Oil Company), 2000.
36. Oppermann, W., Traub, H. L., Hirt, P. and Herlinger, H., Fibres made of polytrimethylene terephthalate, presentation given at the *34th international Man-Made Fibres Congress*, Dornbirn, Austria, September 20–22, 1995.
37. Chuah, H. H., Lin-Vien, D., and Soni, U., *Polymer*, **42**, 7137 (2001).
38. Solomon, O. F. and Ciuta, I. Z., *J. Appl. Polym. Sci.*, **6**, 683 (1962).
39. Desborough, I. J., Hall, I. H., and Neisser, J. Z., *Polymer*, **20**, 545 (1979).
40. Chatani, Y., Higashibata, N., Takase, M., Tadokoro, H., and Hirahara, T., presentation given at the *Annual Meeting of the Society of Polymer Science*, Kyoto, Japan, September 14, 15, 1977.
41. Poulin-Dandurand, S., Perez, S., Revol, J.-F., and Brisse, F., *Polymer*, **20**, 419 (1979).
42. Moss, B. and Dorset, D. L., *J. Polym. Sci., Polym. Phys. Ed.*, **20**, 1789 (1982).
43. Dorset, D. L. and Moss, B., Electron crystal structure analysis of linear polymers – an appraisal, in *Polymer Characterization*, Carver, C. D. (Ed.), Advances in Chemistry Series, Vol. 203, American Chemical Society, Washington, DC, 1983, 409–416.
44. Ziabicki, A., Polish Academy of Science, private communication.
45. Chuah, H. H. and Chang, B. T. A., *Polym. Bull.*, **46**, 307 (2001).
46. Van Krevelen, D. W., *Physical Properties of Polymers*, 2nd Edn, Elsevier, Amsterdam, 1976.
47. Chuah, H. H., Shell Chemical Company, unpublished data.
48. Grebowicz, J. S. and Chuah, H. H., Thermal Properties of Poly(Propylene Terephthalate), in *Research Awareness Bulletin*, Shell Chemical Company, Houston, TX, July 1993, pp. 97–100.

49. Pyda, M., Boller, A., Grebowicz, J., Chuah, H., Lebedev, B. V. and Wunderlich, B., *J. Polym. Sci., Polym. Phys. Ed.*, **36**, 2499 (1998).
50. Lee, K. M., Kim, K. J. and Kim, Y. H., *Polymer (Korea)*, **23**, 56 (1999).
51. Huang, J. M. and Chang, F. C., *J. Polym. Sci., Polym. Phys. Ed.*, **38**, 934 (2000).
52. Huang, J.-M., Ju, M.-Y., Chu, P. P. and Chang, F.-C., *J. Polym. Res.*, **6**, 259 (1999).
53. Wunderlich, B., *Thermal Analysis*, Academic Press, New York, 1990, p. 426.
54. Chuah, H. H., *Crystallization Kinetics of Poly(Propylene Terephthalate)*, Technical Progress Report WRC-42-92, Shell Chemical Company, Houston, TX, 1992.
55. Chuah, H. H., *Polym. Eng. Sci.*, **41**, 308 (2001).
56. Chen, G., Huang, X. and Gu, L., *Sen'I Gakkaishi*, **56**(8), 396 (2000).
57. Bulkin, B. J., Lewin, M., DeBlase, F. J. and Kim, J., *Polym. Mater. Sci. Eng.*, **54**, 397 (1986).
58. Bulkin, B. J., Lewin, M. and Kim, J., *Macromolecules*, **20**, 830 (1987).
59. Kim, Y. H., Kim, K. J. and Lee, K. M., *J. Korean Fiber Soc.*, **34**, 860 (1997).
60. Pyda, M. and Wunderlich, B., *J. Polym. Sci., Polym. Phys. Ed.*, **38**, 622 (2000).
61. González, C. C., Pereña, J. M. and Bello, A., *J. Polym. Sci., Polym. Phys. Ed.*, **26**, 1397 (1988).
62. González, C. C., Pereña, J. M. and Bello, A., *Makromol. Chem., Macromol. Symp.*, **20/21**, 361 (1988).
63. Farrow, G., McIntosh, J. and Ward, I. M., *Makromol. Chem.*, **38**, 147 (1960).
64. Smith, J. G., Kibler, C. J. and Sublett, B. J., *J. Polym. Sci., Part A-1*, **4**, 1851 (1966).
65. McCrum, N. G., Read, B. E. and Williams, G., *Anelastic and Dielectric Effects in Polymeric Solids*, Wiley, London, 1967.
66. Yip, H. K. and Williams, H. L., *J. Appl. Polym. Sci.*, **20**, 1217 (1976).
67. Dangayach, K., Chuah, H., Gergen, W., Dalton, P. and Smith, F., Poly(trimethylene terephthalate) – a new opportunity in engineering thermoplastic applications, in *Proceedings of the 55th SPE ANTEC'97 Conference*, June 16–20, 1997, Chicago, IL, Society of Plastics Engineers, Brookfield, CT, 1997, pp. 2097–2101.
68. Dangayach, K., Ghosh, K., Chuah, H. H., Cristea, B. and Gergen, W. P., PTT – a new polymer for engineering applications, presentation given at the *ETP'99 Conference*, June 7–9, 1999, Zurich, Switzerland, Maack Conference, 1999.

69. Jakeways, R., Ward, I. M., Wilding, M. A., Desborough, I. J. and Pass, M. G., *J. Polym. Sci., Polym. Phys. Ed.*, **13**, 799 (1975).
70. Mencik, Z., *J. Polym. Sci., Polym. Phys. Ed.*, **3**, 2173 (1975).
71. Gedde, U. W., *Polymer Physics*, Chapman & Hall, London, 1995.
72. Nakamae, K., Nishio, T., Hata, K., Yokoyama, F. and Matsumoto, T., *Zairyo*, **35**, 1066 (1986).
73. Jo, W. H., *Polymorphism and Surface Properties of Poly(trimethylene terephthalate) (PTT)*, Final Report, Shell Chemical Company, Houston, Tx, 1999.
74. Sakurada, I. and Kaji, K., *J. Polym. Sci., Part. C*, **31**, 57 (1970).
75. Jakeways, R., Smith, T., Ward, I. M. and Wilding, M. A., *J. Polym. Sci., Polym. Lett. Ed.*, **14**, 41 (1976).
76. Wu, J., Schultz, J. M., Samon, K. M., Pangelinan, A. B. and Chuah, H. H., *Polymer*, **42**, 7141 (2001).
77. Chuah, H. H., *Macromolecules*, **34**, 6985 (2001).
78. SoronaTM 3GT's Attributes, E.I. du Pont de Nemours & Company, 2000, Website product information, [www.dupont.com/sorona/performance-attributes.html].
79. Scott, G., Oakey, D. D. and Bradford, J., *World Patent WO99 19 557* (to Interface, Inc.), 1999.
80. Hsu, C. Y. *US Patent 5 104 724* (to Wangner System Corporation), 1992.
81. Hwo, C., Forschner, T., Lowtan, R., Gwyn, D. and Cristea, B., *Poly(Tri-methylene Phthalates or Naphthalate) and Copolymers: New Opportunities in Film, Engineering Thermoplastic and Other Applications*, Technical Bulletin SC:2731-98, Shell Chemical Company, Houston, Tx, 1998.
82. Bungo, G. and Akiharu, M., *Jpn Patent JP11 222 780* (to Asahi Chemical Industry Co., Ltd), 1998.
83. Sato, T., Imamura, T. and Matsumoto, T., *Jpn Patent JP08 325 391* (to Nippon Esters, Ltd), 1996.
84. Brown, H. S. and Chuah, H. H., *Chem. Fiber Int.*, **47**, 72 (1997).
85. Grebowicz, J. S., Brown, H., Chuah, H., Olvera, J. M., Wasiak, A., Sajkiewicz, P. and Ziabicki, A., *Polymer*, **42**, 7153 (2001).
86. Polejes, J. D., Nylon and polyester production – in practice, Presentation given at the *Fundamentals of Melt Spinning and Yarn Production Conference*, Clemson University, Clemson, SC, February 26–27, 1992.
87. Fourné, F., *Synthetic Fibers, Machines and Equipment, Manufacture, Properties*, Hanser Publishers, Munich, Germany, 1999.
88. Fujimoto, K. and Kato, J., *World Patent WO99 27 168* (to Asahi Kasei), 1999.
89. Moerman, M., *Corterra® PTT Polymers: Downstream Textile Development Generation 1 Information Package*, Shell Chemical Company, Houston, TX, 2000.

90. Chuah, H. H., *Processing of Corterra® Polytrimethylene Terephthalate Polymer for Bulk Continuous Filament Carpets*, Technical Bulletin SC:2528-98, Shell Chemical Company, Houston, TX, 1998.
91. Werny, F. and Chuah, H., *Int. Fiber J.*, **11**(4), 62 (1996).
92. Howell, J. M., Tung, W. H. and Werny, F. *US Patent 5 645 782* (to E.I. du Pont de Nemours & Company), 1997.
93. Chuah, H. H., *US Patent 6 113 825* (to Shell Oil Company), 2000.
94. Polejes, J. D., Werny, F., Bass, C. and Pangelinan, A., *Int. Fiber J.*, **13**(6), 26 (1998).
95. Chuah, H. H., Werny, F. and Langley, T., Dyeing and staining of poly(trimethylene terephthalate) carpets, in *Proceedings of the Book of Paper International Conference and Exhibition*, October 8–11, 1995, Atlanta, GA, The American Association of Textile Chemists and Colorists, Research Triangle Park, NC, 1995, pp. 98–106.
96. Chuah, H. H., *Chem. Fiber Int.*, **46**, 424 (1996).
97. Traub, H. L., Hirt, P. and Herlinger, H., *Chem. Fiber Int.*, **45**, 110 (1995).
98. Traub, H. L., Hirt, P. and Herlinger, H., *Melliand Textilber*, **76**, 702 (1995).
99. Yang, Y., Li, S., Brown, H. and Casey, P., *Textile Chem. and Colorist Am. Dyestuff Rep.*, **1**(3), 50 (1999).
100. Kawaguchi, K., Nakane, T. and Hijikata, K., *Jpn Patent Application 05 031 789* (to Polyplastics Company), 1993.
101. Matsumoto, H., Yamaguchi, K., Koji and Inoue, S., *Jpn Patent 11 054 189* (to Toray Industries, Inc.), 1999.
102. Balakrishnan, T., Ponnusamy, E., Vijayakumar, C. T. and Kothandaraman, H., *Polym. Bull.*, **6**, 195 (1981).
103. Ponnusamy, E. and Balakrishnan, T., *J. Macromol. Sci., Chem.*, **A22**, 373 (1985).
104. Ponnusamy, E. and Balakrishnan, T., *Polym. J.*, **17**, 473 (1985).
105. González, C. C., Bello, A. and Pereña, J. M., *Makromol. Chem.*, **190**, 1217 (1989).
106. González, C. C., Bello, A. and Pereña, J. M., *Esp. Patent. 552 527*, 1986.
107. Chuah, H. H., Vinsan, R. W. and Maxwell, I. E., Polypropylene Naphthalene Dicarboxylate and its Copolymers in *Research Awareness Bulletin*, Shell Chemical Company, Houston, TX, November 1991, pp. 5–8.
108. Shin, D. Y., Kim, K. J. and Yoon, K. J., *J. Korean Fiber Soc.*, **35**, 731 (1998).
109. Alexander, W., *US Patent 4 167 541* (to Fiber Industries), 1979.
110. Oppermann, W., Hirt, P. and Fritz, C., Properties and morphology of polyester blends and of fibers made therefrom, Presentation given at the *37th International Man-made Fibers Congress*, Dornbirn, Austria, September 15–17, 1999.
111. Kelsey, D. R., Scardino, B. M., Grebowicz, J. S. and Chuah, H. H., *Macromolecules*, **33**, 5810 (2000).

112. Kiibler, K. S., C. A. Caico, Lin-Vien, D. and French, R. N., *Byproduct Emissions from Poly(trimethylene terephthalate): Studies on the Release of Acrolein and Allyl Alcohol During Processing, Storage, and Shipping of PTT*, Technical Information Report, WTC-3659, Shell Chemical Company, Houston, TX, 2000.
113. *Threshold Limit Values and Biological Exposure Indices for 1987–1988*, American Conference of Governmental Industrial Hygienists, Cincinnati, OH, 1987.

PART IV

Fibers and Compounds

12

Polyester Fibers: Fiber Formation and End-Use Applications

G. REESE

KoSa Corporation, Charlotte, NC, USA

1 INTRODUCTION

Of all man-made fibers, poly(ethylene terephthalate) (PET) has become the most dominant, with worldwide usage exceeding 17 000 kilotons per year [1]. It now challenges cotton as the most common textile fiber, with a steady growth rate of about 5 %. The emergence of PET as the most successful of the man-made fibers (Figure 12.1) is due to a number of factors in its favor, including the following:

- PET fiber is made from raw materials that are cheap and available, due to the large manufacturing infrastructure it shares with other common products, e.g. antifreeze and soda bottles. The polymerization byproducts are non-polluting, and the polymer can be recycled.
- The melt spinning process used for PET fibers is clean and economical.
- The thermoplastic fiber is tough, with relatively high temperature resistance. It can be processed into yarns that maintain their properties at elevated environmental temperatures, e.g. in tire reinforcement or for permanent-press fabrics.
- The basic polymer can be modified with additives or copolymers to confer specific properties for special end-use needs. A number of typical examples will be discussed in the following sections.

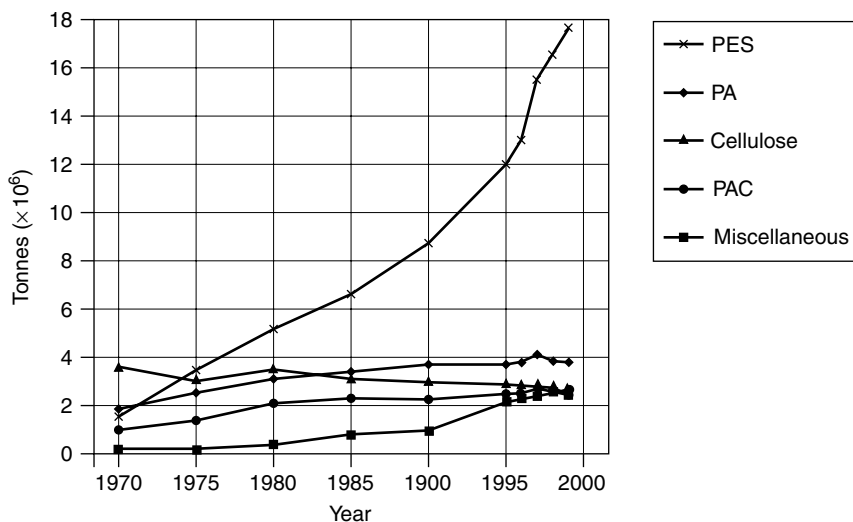


Figure 12.1 World production of man-made fibers, shown by fiber class, illustrating the historical growth of PET fibers (PES is synonymous with PET) [1]. From *Int. Fiber J.*, **15**(3), p. 8 (2000), with permission from the International Media Group, Inc.

2 GENERAL APPLICATIONS

PET fibers are produced in a variety of forms, broadly classified as staple fibers, textile filament and industrial filament. End-uses for these variants have different requirements in terms of fiber properties and physical geometry, and so different fiber manufacturing processes have evolved according to the special needs of each market segment.

Staple PET fibers are typically packaged in bales, and often blended with natural staples such as cotton or wool. They are designed with cut lengths and diameters similar to their blend partners, $\sim 30\text{--}100\text{ mm}$ long and $\sim 10\text{--}20\text{ }\mu\text{m}$ in diameter. Fiber diameter is an important parameter affecting both bending stiffness and light reflection, which affect fabric feel and appearance. Staple fibers are formed into yarns by the ancient practice of fiber spinning, where fibers are twisted together to form a continuous strand, and the number of fibers in the cross-section controls the fineness of the yarn. These yarns are formed into fabrics by the traditional methods of weaving or knitting. The protruding free ends of twisted staple yarns contribute to fuzzy fabric surfaces, which greatly impact the comfort of apparel fabrics. PET staple fibers must possess three-dimensional structure (or ‘crimp’) and surface lubricity, to allow the fibers to be processed in textile machinery and to mingle evenly with other fibers in the blend.

Staple fibers also are formed directly into nonwoven fabrics through carding, dry-lay, or wet-lay forming processes, and held together by entanglement, resin bonding or thermal bonding. Such products are typically used for filters, interliners, absorbent layers, cushioning material, etc. Special fiber types developed for nonwoven fabrics include short-cut fibers (ca. 10 mm or less in length) and thermally fusible fibers such as bicomponents (discussed below). According to the formation methods used, the structures may be fluffy or flat; lightweight blocks of foam-like structures can be made by layering and bonding such webs. Automotive applications are a growing market for PET nonwovens, preferred over traditional materials for their light weight and recyclability.

Textile filament yarns are continuous, producing woven or knitted fabric aesthetics akin to natural silk. Fiber diameter plays a strong role in fabric softness, and texturing of the yarn is used to impart three-dimensional structure and fabric bulk. In contrast to the high-volume, low-speed processes for staple fibers, continuous yarns are produced at relatively high speeds (~ 100 m/sec) and sold on bobbins; high-speed winder technology has been a crucial factor in the growth of these markets. The world's current production of polyester fibers for textiles is split roughly evenly between staple and filament yarns [2].

Nonwoven fabrics are also produced from filament spinning processes, where filaments are sprayed onto a moving belt to form a mat of randomly oriented fibers. The rate of filament production and the speed of the belt control the thickness of the mat. As in the case of staple nonwovens, structural integrity can be provided by thermal or resin bonding of the fiber mat, or by fiber entanglement. Although such fabrics may lack the aesthetics of conventional woven or knitted structures, they provide cheap and strong materials for industrial or disposable applications. It is also possible to combine nonwoven structures with yarns or loosely woven scrims that act as structural reinforcements, to obtain composite materials that are stronger and more stable.

Industrial yarns are another major market for polyester fibers. PET industrial filament yarns are used for reinforcement of rubber and for high-strength technical fabrics. Most passenger car tires produced in the USA are reinforced with yarns made from high-molecular-weight PET polymers, processed to yield high strength and low shrinkage. Neither dyeability nor appearance is important, but the physical and chemical properties of the fibers are critical.

The manufacturing processes for textile filament, staple and industrial filament yarns have become so specialized that it is not possible to make one such class of fibers on the others' equipment. Within these classes, there are production machines specialized for certain types of fibers for specific types of consumer products. Large machines designed to produce high volumes of commodity products (e.g. staple for cotton blending) at high efficiency and low cost are not well suited to the efficient production of specialty staple variants (e.g. fibers with special dyeing properties) and vice-versa.

Additives and copolymers have extended the use of PET fibers into areas where the original commodity products had deficiencies, in, for example, soil-resistance, static protection or poor dyeability. Newer members of the polyester family have found applications in markets where more stretchiness or resiliency were desired (using longer aliphatic chains) or to gain higher modulus, temperature resistance and strength (with fully aromatic polymers).

3 CHEMICAL AND PHYSICAL STRUCTURE

PET polymer (Figure 12.2) is composed of repeating units of the depicted monomer, with each unit having a physical length of about 1.09 nm and a molecular weight of about 200. Ideally, it is capped on the left by H–, and on the right by –OH when produced from ethylene glycol and terephthalic acid. Polymerization is thus accompanied by the production of water, which is removed under elevated temperature and vacuum. Accordingly, the presence of water in the molten state will rapidly depolymerize the structure, so that thorough drying of the polymer prior to melt spinning of fibers is required.

The PET polymer structure can also be generated from the reaction of ethylene glycol and dimethyl terephthalate, with methyl alcohol as the byproduct. A few producers still use this route. The aromatic rings coupled with short aliphatic chains are responsible for a relatively stiff polymer molecule, as compared with more aliphatic structures such as polyolefin or polyamide. The lack of segment mobility in the polymer chains results in relatively high thermal stability, as will be discussed later.

3.1 MELT BEHAVIOR

The degree of polymerization is adjusted to yield the desired balance of molten viscosity (for fiber extrusion) and filament strength. A textile grade polymer will have an average number of ~ 100 repeat units per molecule, so that the extended length of a typical polymer chain is about 100 nm with a molecular weight of about 20 000. Higher levels of polymerization (up to ~ 200 repeat units) produce higher-strength fibers, but the melt viscosity and stability of the melt to even tiny

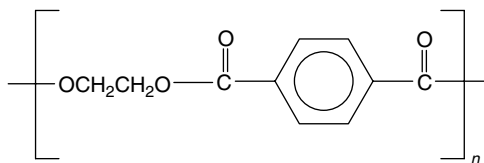


Figure 12.2 Structure of poly(ethylene terephthalate) (PET)

amounts of moisture then become extreme. Measurement of the average degree of polymerization is typically accomplished either by measurement of the molten viscosity (e.g. by measuring the pressure drop through a calibrated orifice) or of the viscosity of a dilute solution of the polymer in an appropriate solvent [3]. The latter is a measure of polymer chain length known as the 'intrinsic viscosity' (IV). A typical IV level, in *o*-chlorophenol (OCP) solvent, for the aforementioned textile grade polymer is 0.62. (Different solvents will generate different IV numbers [3].) The IV in OCP is connected to the number-averaged molecular weight (M_n) of the polymer by the Mark–Houwink formula for PET [3]:

$$IV_{\text{OCP}} = 1.7 \times 10^{-4} (M_n)^{0.83} \quad (12.1)$$

A useful formula to predict the (low shear) melt viscosity of PET from its IV is as follows:

$$\eta_0 = 0.129 (IV_{\text{OCP}})^{5.35} \exp \left(\frac{6800}{T} \right) \quad (12.2)$$

where η_0 is the Newtonian melt viscosity (poise) and T is the absolute temperature (K).

If moisture is present before the polymer is melted, hydrolytic degradation will occur upon heating. Each water molecule will break a chain, so increasing the total number of polymer chains by one. The effect on the average molecular weight will be as follows:

$$M'_n = \frac{M_n}{1 + \left(\frac{x M_n}{1800} \right)} \quad (12.3)$$

where M_n is the starting average molecular weight, M'_n is the average molecular weight after reaction with water, and x is the water content (wt%). This relationship can be used with the above formulae to determine the effect of moisture on IV and the melt viscosity.

It can be seen from these relationships that higher IVs produce rapid increases in melt viscosity and increased sensitivity of the polymer to hydrolytic degradation. The technology required to process high-IV (ca. 0.9–1.0) materials used for high-strength industrial fibers is more demanding than for lower-IV (ca. 0.6–0.7) textile materials. Pressure requirements for polymer flow, for example, are ~10 times higher.

In addition to hydrolytic degradation, random chain scissions will occur at elevated temperatures and these scissions lead to a gradual loss of average molecular weight in the polymer melt. The chemistry of thermal degradation is different from hydrolytic degradation; it results in different types of end groups on the polymer chains [4]. The chemical species that are generated during thermal

degradation reactions are deleterious to fiber properties, leading to loss of thermal stability and, in the presence of oxygen, to cross-linked gel particles.

3.2 POLYMER STRUCTURE

In the absence of any mechanism to induce preferential orientation in the polymer molecules, PET will freeze as a clear, glassy solid with a specific gravity of 1.33 [3]. The molecular structure is similar to that of a bowl of spaghetti, with the polymer chains randomly coiling about one another. The chains are attracted to each other through van der Waal forces. This attraction can be overcome with the addition of thermal energy, which induces molecular vibration and bond rotations. Some chain segments will pack together more closely than others, particularly if they are run parallel to each other for a section of their lengths. Stronger inter-chain bonds will form in these regions. If sufficient molecular alignment is present, regions of the microstructure will pack into an ordered, repetitive structure and become crystalline (Figure 12.3).

An amorphous polymer in a state of molecular alignment is not a stable structure – it is *metastable*. It can transition either to a more perfectly ordered, crystalline structure, or to a more disordered, nonoriented structure; In either case, the free energy of the system is reduced. Given enough time and/or thermal energy, an oriented amorphous polymer will transition in either or both of these directions.

Publisher's Note:
Permission to reproduce this image
online was not granted by the
copyright holder. Readers are kindly
requested to refer to the printed version
of this chapter.

Figure 12.3 Microstructure of oriented, partially crystalline polyester [13]. From Brunnschweiler, D. and Hearle, J. (Eds), *Polyester – 50 Years of Achievement*, 1993, p. 172, and reproduced by permission of The Textile Institute, Manchester, UK

The van der Waals attraction forces in the amorphous regions can be overcome at elevated temperatures. The glass transition temperature (T_g) is the characteristic temperature at which this occurs. At temperatures above the T_g , spontaneous molecular rearrangement becomes easier, allowing plastic deformation and the generation of crystalline order with the release of heat. The stronger bonding forces in the crystalline phase require higher temperatures in order to be re-broken, and this phase transition represents a true melting point, T_m . Even this transition is not sharply defined in a real polymer, however, because the melting temperatures depend on the size of the crystallites. Smaller crystallites melt more easily.

As determined from X-ray diffraction measurements, the unit cell of crystalline PET is triclinic with a repeat distance of 1.075 nm along the major axis [5, 6]. This corresponds to >98 % of the theoretical extended length of the monomer repeat unit [6]. There is very little molecular extensibility remaining in a PET crystal, resulting not only in a high modulus but also a relatively short extension range over which the crystal can be extended and still recover elastically. The density of the crystalline structure is 1.45 g/ml, or about 9 % higher than the amorphous structure [3].

A considerable amount of molecular orientation along the fiber axis is induced in the fiber manufacturing process, and crystallization will occur in regions where adjacent polymer chains are sufficiently extended and aligned so that bonds can form between adjacent chains. The rate of crystallization for oriented fibers under tension is thousands of times faster than for unoriented, quiescent melts. The length of the polymer chain entrapped within a crystalline region is typically ~20 repeat units, before entanglement with another chain terminates the process. Crystalline regions come in different sizes, and the size and distribution of these crystallites contribute to fiber properties such as dyeability and shrinkage. It is the crystalline regions that tie together the spaghetti-like polymer structure to give fibers with high strength and temperature stability.

As can be seen in Figure 12.3, the crystalline regions of PET are composed primarily of folded chain segments, so that the length of any given crystalline region is fairly small before being interrupted by an amorphous region. It has been a research goal to generate extended-chain PET structures that might provide more continuity along the fiber axis and thus generate much higher strengths, similar to the structures produced in the gel-spinning process for high-density polyethylene. This has not been attainable with high-temperature melt spinning; the rapid molecular relaxation rates quickly destroy the extended orientation. Some low-temperature solution spinning processes have been examined on a research scale, but the toxic and expensive nature of most solvents for PET (e.g. hexafluoroisopropanol) discourages serious efforts at commercialization.

The glass transition temperature of amorphous PET is in the range of 65–75 °C, and this can increase to ~125 °C after being drawn and partially crystallized, reflecting the reduced rotational mobility of the chain segments. The crystallite

melting points range from ~ 265 – 285°C . Usually, however, a single melt temperature is quoted for PET, e.g. the temperature of maximum heat absorption in differential scanning calorimetry (DSC) measurements.

Among the spectrum of melt-spinnable fibers such as polyolefins and nylons, PET stands at the upper end in terms of crystalline melt temperature and glass transition temperature. This provides superior dimensional stability for applications where moderately elevated temperatures are encountered, e.g. in automobile tires or in home laundering and drying of garments. The high thermal stability results from the aromatic rings that hinder the mobility of the polymer chain.

More elastic, less stiff polyesters can be prepared from diols with longer aliphatic chain lengths, e.g. from propylene or butylene glycols in combination with terephthalic acid (Figure 12.4). These polymers crystallize in forms with significantly less extension of the molecule; approximately 75 and 87 % of the fully extended form for the 3GT and the 4GT polymers, respectively [6]. Along with the increased softness and springiness of the polymers comes a reduction in melting points and glass transition temperatures, which is not always welcome. These polyester variants command a higher price simply because they are more rare; their raw materials are more expensive because they are not produced on the massive scale of the PET raw materials.

One alternative to PET fiber which did compete historically was poly(1,4-cyclohexylene dimethylene terephthalate) (PCT) (Figure 12.5), commercialized under the name 'Kodel II' by Eastman. This polyester gained an early footing because it was not covered by the existing patents, and was able to establish a raw material base from which it could compete both technically and economically.

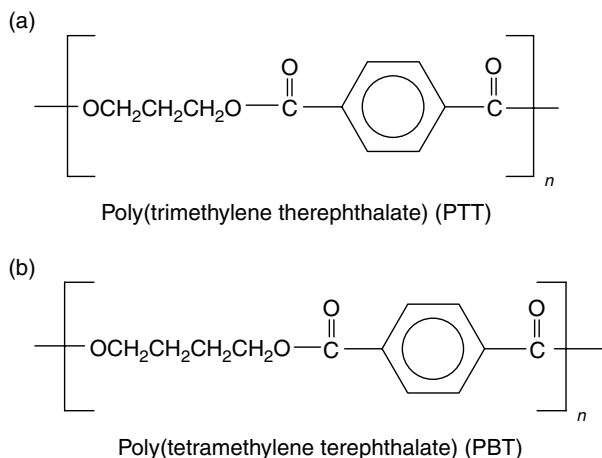


Figure 12.4 Structures of polyesters with longer aliphatic chains: (a) poly(trimethylene terephthalate) (PTT); (b) poly(tetramethylene terephthalate) (PBT)

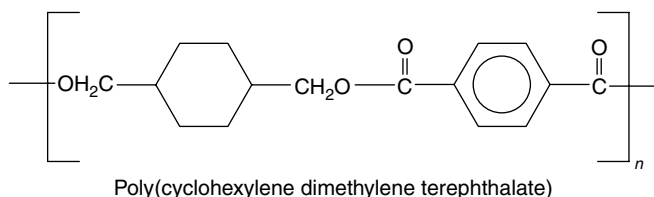


Figure 12.5 Structure of a high-temperature polyester, poly(cyclohexylene dimethylene terephthalate) (PCT)

This PCT fiber has better resiliency than PET, without compromising high-temperature resistance. It successfully competed in the carpet yarn market against nylon, where PET was limited by its relatively lower wear resistance. Recycling of PET bottles has provided a source of low-cost resins that are used for carpets in less critical markets.

A more recent entry in the polyester field is poly(lactic acid) (PLA) (Figure 12.6). This polymer is noteworthy for being made from biological raw materials (e.g. corn), rather than from petroleum. The lactic acid monomer is produced from the fermentation of dextrose, with polymerization then accomplished via ring-opening and the removal of water. By selective combination of *L* vs. *D* isomers, it is possible to make polymers with more or less crystalline content, and a range of melting points from about 150 °C to as high as 210 °C.

Although the polymer chain contains no aromatic rings, some rigidity and thermal stability is contributed by steric hindrance of the pendant methyl groups. The backbone chain is partially coiled in the crystalline form, contributing a measure of fiber elasticity and resiliency similar to that of PBT or PTT. The primary virtues of PLA fibers appear to be renewability of the raw materials and biodegradability of the polymer. Biodegradation requires exposure to an aqueous environment at >60 °C to achieve hydrolysis, after which bacterial decomposition can occur. Considerable investment in monomer production is currently being made by Cargill-Dow, with the intent of providing PLA polymer supplies at prices intermediate to PET and nylon.

Biodegradable polyesters are also made by copolymerization of aliphatic and aromatic forms, or by polyester amide structures. The molecular structures need

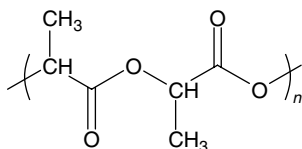


Figure 12.6 Structure of a biodegradable polyester, poly(lactic acid) (PLA), with alternating pendent groups

to be flexible in order to provide access for enzymes to the oxygen- or nitrogen-containing sites that will be hydrolyzed or oxidized. This means some sacrifice of thermal stability and rigidity. Large polymer suppliers such as Eastman, Dupont and BASF are currently active in these areas.

3.3 FIBER GEOMETRY

Solid PET polymer is relatively hard and brittle. It must be formed into very fine fibers in order to exhibit a bending stiffness that is low enough for textile materials. Most commercial PET fibers are produced in a diameter range of about 10–50 μm , considerably smaller than a human hair. Within this range lie large differences in the softness, drape and feel of fabrics formed from the fibers, since the bending stiffness of a cylindrical fiber depends on the 4th power of its diameter.

One key requirement in the commercial production of fibers is to control fiber diameters within narrow ranges of the target. Another is to control the internal structure of the fiber, particularly the orientation of the polymer molecules. It is this orientation along the fiber axis that controls the morphology, and hence the fiber properties, such as dye uptake, shrinkage and tensile strength.

The production process for fibers starts with the extrusion of molten PET through small holes at slow speeds, although the fibers will be stretched by hundreds of times their initial lengths before the production process is completed. The stretching process is responsible for diameter reduction, and for alignment of polymer molecules in the direction of stretching. As this alignment proceeds, polymer chains will pack increasingly closer, and the density of the material will rise progressively, becoming crystalline in some regions. The fiber density is a guide to the amount of orientation present in the fiber; a finished PET fiber is typically ~50 % crystalline.

4 MELT SPINNING OF PET FIBERS

A large part of the attractiveness of PET is that it is melt-spinnable into fibers, so providing a clean, pollution-free manufacturing process. The goals of melt spinning include not only the stable formation of fine fibers, but also control of the microstructure of these fibers. Ideally, this is carried out at as high a throughput rate as possible for economic reasons (Figure 12.7).

An example of typical equipment used to make PET fibers is shown in this figure. Prior to melting, the polymer chips must be thoroughly dried, typically under vacuum at elevated temperatures for several hours. The equilibrium moisture content of PET under ambient conditions is about 0.4 % [3] and this much moisture would cause unacceptable levels of degradation. The dried polymer chips are fed to an extruder which melts the chips and forwards them to a

Publisher's Note:
Permission to reproduce this image
online was not granted by the
copyright holder. Readers are kindly
requested to refer to the printed version
of this chapter.

Figure 12.7 Schematic of the melt-spinning process used to produce PET fibers

metering pump, which delivers a volumetrically controlled flow of polymer into a heated spinning pack at ca. 285–300 °C.

Modern large-scale PET fiber facilities have evolved to a continuous process of PET polymer production, and have integrated the processes of polymerization and fiber extrusion. This avoids the equipment, energy and manpower needed to freeze and pelletize the polymer, dry it, and remelt it. In large plants that operate continuously for months at a time, huge quantities (more than 200 tons per day) of fiber are produced from a single line. Such fibers may be used, for example, in commodity markets such as woven or knitted apparel, or for tire reinforcement. For more specialized markets, which require modified polymers in smaller quantities, the downtime and waste associated with changeovers of such large lines is prohibitive; smaller batch lines based on PET chips are preferred. However, whether fed by a continuous polymerization (CP) process or by remelted chips, the spinning processes are basically the same.

Under typical conditions of 290 °C spinning temperature, the molten viscosity is ca. 2000–20 000 poise, depending on the average molecular weight. This is extremely viscous – similar to hot asphalt. The pump must provide a pressure of ~100–200 bar to force the flow through the pack, which contains filtration media (e.g. a sand bed) to remove any particles larger than a few μm . Anything larger would be similar in size to the intended fibers, and will lead to filament breakage during processing.

At the bottom of the pack the polymer exits into the air via a multiplicity of small holes through a thick plate of metal (the spinneret). The number of holes can

range up to several thousand per spinneret. Each spinneret hole is ca. 0.2–0.4 mm in diameter with a typical flow rate in the range of about 1–5 g/min (less for fine fibers, more for heavy fibers). Although a round hole is most common, it is not unusual for the hole to have a complex shape intended to provide non-round fibers for special effects (discussed later). The metering pumps feeding the pack control the mass flow rate. A take-up device, typically a rotating roll system with a controlled surface speed, regulates the final speed of the extruded filaments. Assuming the same flow to every spinneret hole, the final diameter of the filaments is fixed by the metering pump and the take-up speed; the spinneret hole size does not affect fiber size.

The structure and properties of the filaments are controlled by the threadline dynamics, especially in the molten region between the exit from the spinneret and the freezing point of the fibers. After freezing, the fibers will be traveling at the take-up speed, which is typically 100–200 times faster than their exit speed from the spinneret hole. Thus, considerable acceleration (and stretching) of the threadline occurs after extrusion. The forces acting on the fibers in this transition region include gravity, surface tension, rheological drag, air drag and inertia. Because both temperature and threadline speed are rapidly changing, these force balances also change rapidly along the threadline. The dynamics of threadline formation are reasonably well understood and have been successfully modeled. References on the subject are available in the literature [7, 8]. Only an overview of the process will be presented here.

While traversing the spinneret hole (typically 1.5–5.0 times longer than its diameter), the molten fibers are in a state of viscous shear which induces molecular orientation along the fiber axis. Upon exit from the hole, the filaments slow down and bulge slightly, as the molecules relax and disorient. This is known as ‘die swell’. From the die swell region onward, the filaments accelerate, and it becomes an ongoing competition between orientation (induced by extensional flow) and thermal disorientation (due to molecular relaxation). Near the spinneret the filament is still hot, the polymer is relatively fluid, and little net orientation is present in the threadline. Further down, the filament is cooler, the polymer more viscous, and thermal disorientation less; net orientation is higher. Orientation increases progressively and reaches a maximum as the threadline ‘freezes’, i.e. stops extending, usually within ~ 1 m from the spinneret. The amount of orientation that is frozen into the spun fiber is directly related to the stress level in the fiber at the freeze point [8, p. 213].

A key parameter which controls the rate at which orientation is being generated is the rate of extension, as follows:

$$v' = \frac{dv}{dx} \quad (12.4)$$

where v is the local threadline velocity and x is the distance along the threadline.

Publisher's Note:

Permission to reproduce this image online was not granted by the copyright holder. Readers are kindly requested to refer to the printed version of this chapter.

Figure 12.8 Typical forces acting upon a spinning threadline [8]. From Ziabicki, A. and Kawai, H., *High Speed Fiber Spinning – Science and Engineering Aspects*, 1991, and reproduced by permission of Krieger, Malabar, FL

For a Newtonian polymer, the stress required to deform the polymer at extension rate v' is simply $\eta v'$, where η is the extensional viscosity of the polymer (which changes rapidly as the polymer cools). The fiber extension also corresponds to acceleration of the material at a rate equal to vv' , and the inertial resistance to this acceleration is responsible for a tension gradient along the filament. Finally, the air resistance of the fiber generates surface drag forces that increase with velocity, so that a further tension gradient appears due to air drag. These are the three dominating forces – rheological, inertial and air drag – that control spinning threadline dynamics and velocity profiles over the range of typical spinning speeds (Figure 12.8). Gravity and surface tension forces are relatively much smaller.

Starting with a more viscous polymer (whether due to higher molecular weight or lower extrusion temperature) will produce higher tension and higher final orientation. This is also the case when increasing the total amount of stretch, the 'draw-down' ratio. The primary tool for controlling the net orientation, though, is the speed of the process, i.e. the take-up speed. By increasing the velocity and extension rate of the filaments, the orientating mechanism becomes more dominant over the thermal relaxation mechanisms, and more net orientation is frozen into the fibers¹. Obviously, a higher level of v' corresponds to larger rheological and inertial forces, and higher v creates more air drag. Thus, high-speed spinning is also high-stress spinning.

¹ PET is not strictly Newtonian, or else it could not be fiber-forming. Polymers with the latter property develop increasing tension due to retraction forces as they become oriented, so that localized necks do not grow and become discontinuities. At high shear rates, molecular orientation will also reduce the resistance to shearing.

The melt spinning process for PET fibers can be divided into three regions of take-up speed, as follows:

- In low-speed spinning (<1000 m/min), spinning threadline forces are dominated by rheological deformation. Air drag may also play a role for fine filaments (with high surface–volume ratios), but drag is generally small in the fiber formation region near the spinneret where velocities are lower and diameters larger. The acceleration rate is too small for inertia to play a role. Only a small amount of residual orientation is frozen into the threadline, since thermal disorientation predominates over the orientating effects of fiber extension.
- In medium-speed spinning (ca. 1000–4000 m/min), the air speed generates higher drag and faster cooling. Inertial effects are also greater, being proportional to velocity and extensional shear rate. The resulting higher stress at the freeze point increases the orientation frozen into the spun fibers.
- At speeds beyond ~ 4000 m/min, inertial and air drag effects become the dominant contributors to fiber stress. Sufficient orientation can be induced so that significant crystallization occurs in the as-spun fiber. The structure begins to partition into either highly oriented crystalline regions, or amorphous regions of relatively low orientation. There is relatively less ‘oriented-amorphous’ structure.

The structure-partitioning effect at high speeds is believed to arise from the scaffold of oriented regions that develop within the structure and support the fiber stress. This leaves the less-ordered regions free to relax and disorient, so that a two-phase structure begins to appear where there was before a broad continuum of orientations. In this region, the highly ordered sections behave as a solid, with tensile stresses proportional to deformation, while the less-ordered regions behave more like a fluid with stresses proportional to *rate* of deformation. This is a mixture of solid and liquid phases.

It has been observed that, at speeds sufficient to induce crystallization, fiber deformation will become concentrated into a ‘neck’ region where the final amount of stretching will occur over a very short distance. The origins of this neck have been a source of speculation and research [7, 8] and efforts have been made to link necking and crystallization in a cause–effect relationship. Current evidence favors the explanation that this phenomenon is similar to necking behavior seen when cold-drawing plastic materials [9]. This means that the molten filament passes through a stage where resistance to deformation *decreases* along the threadline. The decrease in resistance is initiated by ‘shear-thinning’, where the apparent viscosity of the polymer decreases at increased shear rates. (High shear rates promote a high level of molecular orientation within the melt, which then allows the molecules to slip by each other more easily.) As the thinning process accelerates, the decrease in cross-sectional area concentrates the stress, since the overall tension does not decrease. This produces a rapidly thinning neck, where

orientation builds up quickly with little time for thermal relaxation. The necking stops when sufficient orientation has been induced such that further elongation requires additional tension, and the resistance has become *elongation*-dependent rather than *elongation-rate*-dependent. Classically, the liquid has become a solid. Coincidentally, the high levels of orientation allow crystallization to occur very quickly after stretching has stopped.

Another feature of high-speed spinning is that the fiber macro structure becomes non-uniform, with more orientation and crystallinity near the fiber surface than in the interior. This is a result of non-uniform solidification, where rapid cooling generates a lower temperature and higher viscosity at the surface. This leads to an oriented surface 'skin' which supports the spinning stress, while higher temperatures within the interior allow more relaxation and disorientation.

The skin-core structure is a macroscopic analogue of the partitioned, high/low orientation structure within the fiber. Since fiber stresses become concentrated in the oriented regions, there is a loss of participation of some of the interior molecules to support subsequent stresses. Under fiber extension, the taut molecules will break first, triggering rupture of the fiber before the unoriented molecules contribute much resistance. A loss of overall fiber strength and tenacity results. Polymer fiber strengths are only a small fraction of the theoretical breaking strengths of the combined molecules; <1 GPa versus a calculated chain strength of about 35 GPa.

Insight into the spun yarn structure can be gained by observing its behavior in hot water. The combination of elevated temperature and the plasticizing effect of the water molecules allows relaxation within the oriented regions, resulting in yarn shrinkage. As spun orientation becomes greater the spun yarn shrinkage will increase – up to a point. At sufficiently high levels of orientation, the plasticizing effect of the heat and moisture will allow crystallization to proceed very quickly within the hot water, before the oriented regions have time to relax and shrink. This rate differential will increase at higher spinning speeds. Additionally, the reduction of amorphous orientation in high-speed as-spun yarns will depress their shrinkage even further (Figure 12.9).

In summary, the strongest PET fibers are formed by *slow*-speed spinning processes, because the range of molecular orientations is more narrow. A benefit of high-speed spinning is that it generates less of the intermediate 'oriented-amorphous' structure that is prone to thermal shrinkage. The most thermally stable fibers are therefore formed by *high*-speed spinning processes. It is possible to increase spinning speeds to the point that very little extensibility remains in the fibers, but the microstructure becomes so highly partitioned that little strength remains. Nearly all commercial spinning processes target for at least ~100 % extensibility in the as-spun fibers, and further stretching is carried out at lower temperatures in order to develop the most useful fiber properties.

Publisher's Note:
Permission to reproduce this image
online was not granted by the
copyright holder. Readers are kindly
requested to refer to the printed version
of this chapter.

Figure 12.9 Effect of spinning speed on fiber orientation and shrinkage [14]. From Brunnschweiler, D. and Hearle, J. (Eds), *Polyester – 50 Years of Achievement*, 1993, p. 193, and reproduced by permission of The Textile Institute, Manchester, UK

4.1 SPINNING PROCESS CONTROL

There are a number of factors available for controlling the spinning process, to control thereby the properties of the fibers. These include melt viscosity (via temperature and/or polymerization level), hole diameter and throughput, spinning speed, and cooling rate of the filaments after extrusion. In the ideal world, each fiber would have identical history and microstructure. In reality, each filament is subjected to different thermal histories according to its position within the thread-line relative to the flow of cooling air. Uneven heat losses from the spinneret face also lead to different extrusion temperatures among the filaments. Consequently, different filaments have different average orientation levels. Additionally, any given filament will have varying levels of orientation along its length due to microscale fluctuations in cooling rate, e.g. air turbulence.

Fiber orientation uniformity is also affected by small-scale or timewise variations in polymer viscosity, related to breakage of polymer chains during the extrusion process. The degradation occurs as a result of residual moisture that immediately reacts to break chains, and by thermal degradation that occurs more gradually over time. Different residence times and temperature histories within the laminar flow streamlines lead to different viscosities, and hence different average orientation levels in the different fibers.

A primary goal of extrusion equipment and process design is to minimize the orientation variability among filaments, since such variability can have undesirable effects on product uniformity (e.g. dye uptake level) and on yarn strength and processing performance. As a rule, higher throughput rates and/or more filaments per spinneret create greater difficulties in achieving uniform cooling and fiber properties. There is a compromise between fiber uniformity and production economics, since larger-scale processes are more economical.

This tradeoff between product uniformity and production economics has affected the process design for various types of PET fibers. Products such as textile filament yarn have a strong requirement for uniform dye uptake, within and between bobbins of yarn used for weaving or knitting. No opportunity is available for 'blending out' dye differences with continuous filament (CF) yarns. Such yarns are made on spinning machines with a relatively small number and low density of holes per spinneret, and the supply of cooling air is controlled very carefully to minimize variability. These are relatively low throughput processes.

In contrast, staple fibers are always blended during the textile process, either among themselves or with other fibers. Small fiber orientation differences that might occur between various spinning machines, or over small periods of time will be blended out, so that dye uptake differences occur over such a fine scale as to be invisible to the eye in the final fabric. For this reason, tolerance for fiber non-uniformity is greater for staple than for filament products. Consequently, the spinning processes used for staple allow much higher throughput rates, with much higher numbers of holes per spinneret. This allows staple fiber to be produced at less cost than filament yarn, and the selling prices of the fibers reflect this; filament PET yarns command significantly higher prices than do commodity staples. CF products, however, do not require post-processing in order to be converted into yarns suitable for knitting and weaving. Consequently, staple and filament fabrics are similar in price.

Relative scales of the spinning processes for staple and filament products are depicted in Table 12.1. The industrial filament process is intermediate to the staple and textile filament processes, in terms of both spinning throughput and fiber orientation uniformity (here measured by spun birefringence level). Industrial yarns must be uniform enough to be drawn to much higher tenacity levels than staple yarns, but are not dyed and therefore not subject to the more demanding uniformity requirements of textile yarns.

Table 12.1 Differences in PET spinning processes

Parameter	Staple fiber	Industrial filament	Textile filament
Filaments per spinneret	6000	750	140
Pack throughput (kg/h)	240	100	12
CV ^a of orientation (%)	~15	~10	~5

^a Coefficient of variation.

While it is evident that fiber orientation level affects dye uptake, and that orientation uniformity translates to dye uniformity, it is less obvious that orientation uniformity will affect yarn strength. The breakage of fiber bundles is controlled by the 'weak link' principle, where the early breakage of a few, high-orientation fibers will initiate a catastrophic failure sequence among surviving fibers within the bundle [10]. This comes about as a result of load transfer from the broken fibers to the unbroken survivors via fiber–fiber friction, and hence stress concentration. Variable extensibility of the fibers within a yarn can thereby result in yarn strength that is much lower than the average strength of the component fibers.

5 DRAWING OF SPUN FILAMENTS

The purpose of drawing is to further align and stabilize the structure of the fibers. Additional diameter reduction occurs in this step. Drawing occurs at a much lower temperature than spinning, typically just above the T_g , so there is minimal thermal disorientation to compete with orientation induced during stretching. While fibers may have been extended by a factor of 100–200 during spinning, a draw ratio in the range of about 2–5 is typically enough to induce the maximum amount of fiber orientation short of breakage. Drawing is more efficient at orienting the structure.

The amount of drawing used depends on (1) the amount of orientation already present from spinning, and (2) the desired level of fiber properties. High levels of final orientation are desired for technical fibers where high tenacity and high initial modulus are needed. Less orientation may be needed for textile fibers, so that dye penetration is faster and the fibers are less stiff.

Figure 12.10 displays the stress–strain behavior of PET fibers that were prepared from the same spun yarn, but drawn to different ratios. The curves represent the elongation and stress in terms of initial fiber area (decitex²). The open circles represent true stress values, where stress values at break are corrected for the decreased area of the fiber after extension on the testing device.

As expected, the residual extensibility of the fiber decreases at higher draw ratios. What is not so predictable is that the true stress at failure increases as the draw ratio increases; fiber failure strength is improved by drawing the yarn. If a curve is drawn to connect the end points of the stress–strain curves, it is seen that there is an inverse relationship between tenacity and elongation to break (e_b). The form of this relationship is as follows:

$$t = \frac{K}{e_b^\alpha} \quad (12.5)$$

where t is the engineering tenacity, and K and α are constants.

² Decitex is a measure of fiber size. If 10 000 meters of fiber weigh x grams, then the decitex of the fiber = x .

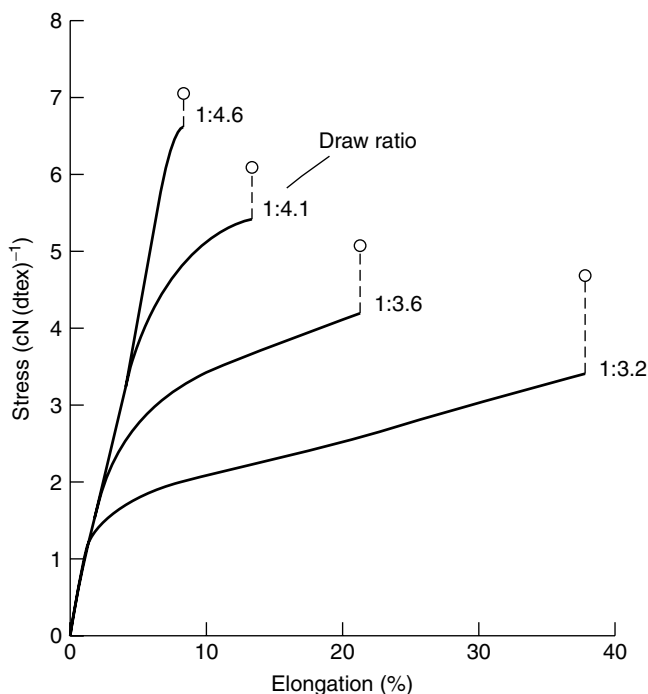


Figure 12.10 Stress-strain curves of PET filaments drawn to different draw ratios[15]. From Kagi, W., *Ullmans Encyclopedia of Industrial Chemistry*, 5th Edition, Volume A10, VCH, Weinheim, Germany, 1987, p. 527, and reproduced by permission of Wiley-VCH

Experimentally, $\alpha \sim 0.3$. The value of K is a measure of inherent fiber strength and will depend on the molecular weight of the polymer. This parameter will also increase if post-draw heatsetting is used to crystallize the oriented structure.

The presence of significant crystallinity in the fibers prior to drawing is detrimental to a smooth and continuous drawing process. Free extension of the polymer chains is inhibited by crystalline tie points, which must be disrupted for molecular extension to occur while drawing. If very high final fiber orientations are desired, then high drawing stresses may be generated, which can cause frequent breakouts of the drawing process at the sites of small fiber defects. Increasing the drawing temperature to compensate for the high tension will only hasten the crystallization process, so compounding the problem. For most PET fiber production, inhibiting spun orientation is an advantage since it will allow a higher final draw ratio, which will allow higher spinning speed and throughput. An exception is when the final fiber properties require very high levels of thermal stability that can be provided by the structures formed in high-stress spinning.

The use of a post-draw heatsetting (or annealing) step usually accompanies the drawing process. It is the purpose of this step to stabilize the structure and make it stronger. The level of yarn tension and the annealing temperature can both have significant effects on the final properties. Basically, there are two separate processes occurring during annealing, i.e. (1) crystallization in the most highly oriented regions, and (2) chain disorientation via bond rotation in amorphous regions. The relative rates of these two processes are affected differently by tension and temperature, so a significant range of different fiber properties can be achieved according to the balance of these two variables.

High-temperature ($\sim 200^\circ\text{C}$), high-tension heatsetting maintains a high level of orientation in the amorphous regions, and hence high fiber modulus and relatively lower dyeing rate. The latter can be improved by reducing the heat-setting temperature so that less crystallization occurs. If temperature is raised even higher, however, the structure can generate fewer, larger crystals as smaller ones melt and larger ones become more perfect. This will also enhance dyeability, since there are fewer crystallites to inhibit diffusion of the large dye molecules.

If the fibers are heated with low tension, then disorientation of the oriented-amorphous regions occurs and the fibers are left with low shrinkage forces (and modulus), but high dyeability. It may be desired to complete stress relaxation while the filaments are held in some particular shape, so that the memory of this shape is frozen into the microstructure. This can be done by twisting the yarn to form helical fibers, or by compressing them into random or regular modes of buckling. Such fibers retain crimp or texture, hence further enhancing their fabric aesthetics or their processability on textile machinery.

5.1 COMMERCIAL DRAWING PROCESSES

The drawing process can be continuous with spinning, or it can be carried out as a separate step. The former simplifies handling, but can require very high final roll speeds since the drawing rolls must operate at several times the spinning speed. Such spin-draw processes are commonly used for high-strength industrial yarns, at final speeds up to ca. 8000 m/min (300 mph). This speed imposes severe demands on rolls and winders that must operate at high centrifugal forces ($\sim 10\,000\text{ g}$) and must control the yarn temperatures in the few milliseconds of roll contact time that are available.

At the other extreme are discontinuous staple fiber processes that operate at relatively slow speeds ($< 500\text{ m/min}$). In order to obtain high throughput rates the spun yarns from many spinnerets are collected and drawn in parallel. A modern staple line might process up to $\sim 5 \times 10^6$ filaments at a time, producing fiber at the rate of 200–300 t/d. After crimping, such fibers are usually cut into short ($< 50\text{ mm}$) lengths and baled. Figure 12.11 depicts a modern drawing line

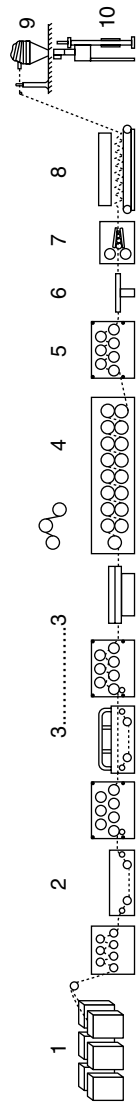


Figure 12.11 Schematic of a modern staple drawline for PET fibers: 1, spun yarn supply cans; 2, lubricating bath; 3, two-stage drawing; 4, heatsetting; 5, cooling; 6, reheating; 7, crimping; 8, dyeing; 9, cutting; 10, baling

for PET staple fibers. Such lines can be purchased as a package installation from equipment vendors, as can lines to produce the PET polymer and spin it into fibers.

Continuous filament textile yarns also use a discontinuous production process. In this case, the spun yarns are produced at speeds up to ~ 5000 m/min, precluding further in-line stretching due to exceedingly high speed requirements. The spun yarns are highly oriented (known as POY, for Partially Oriented Yarn) and are wound onto packages and then subsequently processed on a separate machine which provides the final orientation, texturing and setting in an integrated process. Most commonly, POY yarns are heatset in a highly twisted configuration and then untwisted. The memory of twist produces a fiber bundle with helical filaments, so providing bulk and stretchiness. Textured CF yarns may be knitted or woven directly into fabrics, thus eliminating the steps of blending and yarn formation used for staple fibers such as cotton or wool.

More akin to silk yarns, continuous filament POY produces lighter fabrics, typically of 100 % PET. Such yarns have provided a fertile field for imaginative engineering of cross-sectional shapes, fiber sizes and combinations of color and texture. An entire field of specialty filament yarns known as ‘Shingosen’ has been developed in Japan, providing novel and luxurious fabrics that cannot be duplicated with natural fibers.

6 SPECIALIZED APPLICATIONS

In many applications, modification of PET fiber properties is desirable in order to enhance certain features of the product or to enhance the process of converting fibers into finished goods. In these cases, most of the basic PET fiber properties are acceptable but certain enhancements are desired, even at the expense of other properties or costs that will be affected by the modification. These side effects are always present; it is the goal of fiber development personnel to engineer the best compromise.

What follows are some of the most common variations that have been applied to PET fibers; more complete information is available in the literature [11].

6.1 LIGHT REFLECTANCE

The light reflectance of yarns and fabrics can be quite sensitive to the size and shape of the fibers. Two types of light interactions occur, as follows:

- Light is reflected from the surface of the fiber, due to the change in refractive index from air into polymer (for PET, $n = 1.6$). This is specular reflection, similar to reflection from a mirror, and causes no coloration of the reflected light.

- Light that is transmitted through the fiber surface can interact with the molecular structure, e.g. dye molecules, and thereby change its spectral character before being emitted back through the surface

The mixture of these two types of light is what meets the eye, and the ratio of these two components affects the perceived depth of color. The higher the ratio of specular reflection, then the less the apparent color depth³. Additionally, any relatively large areas of specular reflection can generate visible points of light when oriented to reflect from point sources; these cause the fibers or fabrics to glitter.

Larger-diameter fibers have proportionally less surface-to-volume ratio, so proportionally less specular reflection, and thus appear darker than small fibers containing the same amount of dye. However, larger fibers also have relatively flatter surfaces and are more prone to glitter. It has long been practiced to include microscopic fragments of highly reflective material in the polymer, to opacify the fibers and to diffuse surface reflections. Powdered titanium dioxide is the common additive used for this. It gains its reflective properties by means of very high refractive index. The quantity of TiO_2 in the polymer is adjusted to produce 'clear' or 'dull', or 'semi-dull' fibers for various types of fabrics.

It is possible to microscopically roughen fiber surfaces to diffuse the surface reflections, e.g. by chemically etching the surfaces with corrosive solvents. Many of these solvents will preferentially dissolve the amorphous regions, leaving the undissolved crystalline formations standing proud at the surface. Powdered materials with refractive indices similar to PET can be incorporated into the polymer, creating rougher fiber surfaces and reduced internal reflectance at the additive/polymer interfaces. This makes transparent, but not shiny fibers. Cab-O-Sil[®], a powdered silica, is one such material. It also helps if the additive particles are small ($\leq 0.5 \mu\text{m}$); light scattering becomes negligible when the particles are smaller than the wavelength of light.

Polymer transparency also requires that the crystalline regions be smaller than the wavelength of light, since these regions also represent changes in refractive index. Larger crystallites will scatter light at their interfaces and make the PET opaque.

In addition to the aforementioned methods, fiber cross-sectional shape is used to produce differences in appearance. Surface lobes can break up smoothness and reduce glitter, and triangular or 'T' shapes can generate subtle sheen effects to fabrics and yarns. The patent literature is filled with various cross-sectional shapes which have been used to provide visual and tactile effects that are not possible with natural fibers.

³ Fine fibers of PET usually appear white, even though the polymer chips that they are made from may appear grey in color. This is a consequence of the high amount of specular reflection of ambient light, emanating from the large surface area of the fibers.

6.2 LOW PILL FIBERS

In staple yarns that do not contain high twist levels, it is relatively easy for individual fibers to work their way to the yarn surface under the influence of friction. This will cause long filaments to appear at the surface of the fabric, which then become entangled to form unsightly fuzz balls or 'pills'. With natural fibers, these pills readily break off after the attaching filament is repeatedly flexed. With PET, the attaching filaments are too tough to break, and the pills accumulate. It is difficult to prevent pills from forming, and far easier to modify the PET fiber so that it will more readily break under repeated flexing. The simplest way to do this is to reduce the molecular weight of the polymer, thereby reducing fiber strength. This also reduces the melt viscosity, however, which can create problems with the stability of the melt-spinning process.

Some anti-pill fibers are made by including a small amount of a cross-linking agent in the polymer (e.g. pentaerythritol) (Figure 12.12). This increases melt viscosity while embrittling the fiber and reducing its flex life. The penalty is a fiber that is somewhat weaker during processing, and more subject to breakage during yarn and fabric formation. An alternative is to treat fabrics with an alkaline bath that partially dissolves the PET fibers to make them weaker; this also changes the hand of the fabric. The most elegant approach is to include a chemical cross-linker that is not activated until the fabric is formed and put into an activating bath.

6.3 DEEP DYE FIBERS

The PET polymer molecule contains no chemically active species for attachment of dye molecules. Instead, 'disperse' dyes are used which diffuse into the fiber and become physically entrapped within the tangle of polymer chains in the amorphous regions. (The dye molecules are too large to fit within the more closely packed crystalline regions.) In order to encourage rapid diffusion into the structure, it is common to use pressurized dye baths, and/or 'structure-opening' chemicals that encourage swelling of the amorphous regions. The presence of large amounts of crystallinity, and/or high orientation (hence closer packing of polymer chains) in the amorphous regions, will inhibit the dye diffusion process. Differences in fiber orientation cause differences in dye depth.

A common method to increase the dyeing rate is to inhibit the formation of crystalline regions during fiber manufacture. To this end, it suffices to break up

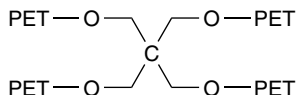


Figure 12.12 PET chains cross-linked by the reaction with pentaerythritol

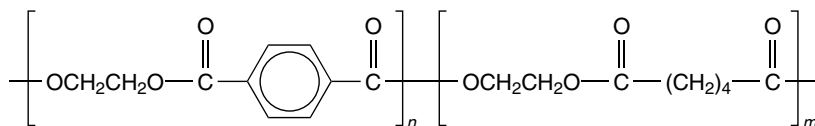


Figure 12.13 Structure of a PET copolymer with adipic acid, used for deep-dye fibers

the regularity of the repeating units of PET so that the crystalline regions are smaller and fewer. Small amounts of foreign monomers, ca. <10 %, incorporated into the chain will do this as they form copolymers.

Monomer units for this purpose include adipic acid or isophthalic acid, to substitute for some of the terephthalic acid (Figure 12.13). Similarly, propane or butane diol, or poly(ethylene glycol), can be substituted for some of the ethylene glycol.

The result is a fiber that is less crystalline and dyes more readily. The downside is an unavoidable reduction in transition temperatures, a less stable structure more prone to shrinkage, and the easier escape of dye molecules and oligomers which can deposit onto the surfaces of textile processing equipment. Depending on the level and type of comonomer used, increased problems with lightfastness or polymer degradation can also occur.

6.4 IONIC DYEABILITY

As earlier noted, PET has no dye attachment sites for chemically active dyes. It is possible to add ionic dyeability by forming copolymers of PET with monomer species that possess active sites, for example, on a pendant side chain. The most common of these has been the incorporation of a sodium salt of a dicarboxylic acid, e.g. of 5-sulfoisophthalic acid (Figure 12.14). The acidic sulfo group allows the attachment of cationic dye molecules. If both the modified and the unmodified fibers are put into a dye bath containing a mixture of disperse and cat dyes, they will emerge with two different colors. This is useful in the creation of specialty fabrics, e.g. when two different dye types are woven into fabrics with a predetermined pattern. The multicolored pattern emerges upon dyeing.

Since the basic structure of the modified fiber is a copolymer, more rapid disperse dyeing is also gained with these cat-dye fibers. Losses in fiber strength, temperature stability and increased hydrolytic degradation are the prices paid for the dyeability enhancement.

Some efforts have been made to incorporate sites into PET that accept *acid* dyes, but most of these alkaline-containing additives cause degradation and discoloration of the polymer. No acid-dye PET polymer has yet been commercially successful.

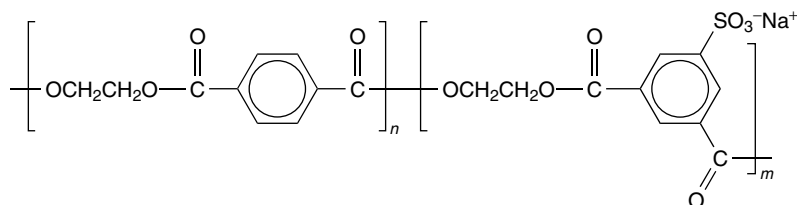


Figure 12.14 Structure of a PET copolymer with sulfoisophthalic acid, used for cat-dye fibers

6.5 ANTISTATIC/ANTISOIL FIBERS

The non-ionic character of the PET molecule makes the polymer hydrophobic and oleophilic. Without polar species, the ability to transport electrical charge along the fiber is poor. If excess static charges build up on PET fibers, as will happen unavoidably upon contact with other materials, these charges will not quickly leak away. The result can be clinging of fabrics to the skin, or discharges of static electricity. (This problem is reduced at higher humidity levels, because the small amount of water absorbed by the PET provides polar charge-carrying molecules for quicker draining of the static charge.) PET's attraction for non-polar, oily materials means that oils, which are difficult to remove, can easily stain fibers.

During the manufacture and processing of fibers, it is common to employ surface lubricants, wetting agents and antistatic treatments to assist in processing. These are temporary, however, and a longer-term solution typically requires polymer additives or copolymers. (Copolymerization typically results in greater permanence than additives which can migrate to the fiber surface and be lost.)

Poly(ethylene glycol) (PEG) is frequently added to PET to confer antistat and/or antisoil behavior. The ether groups running along the backbone of the PEG are sufficiently polar to attract moisture and to provide charge-transfer sites. This benefits both the electrical conductivity and the ability of water or detergent molecules to lift the oily stains. By using long-chain PEG additives, a block copolymer is formed (Figure 12.15). This avoids some of the thermal stability losses that occur with random copolymers.

It is also possible to add PEG at the last stages of polymerization, so that much of the additive remains agglomerated in a separate phase. In this case, subsequent scouring of the fibers removes much of the soluble PEG, leaving microscopic

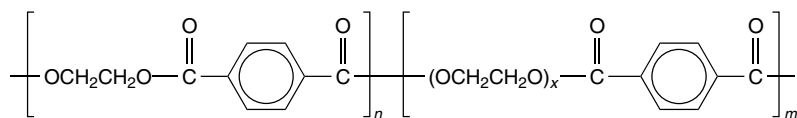


Figure 12.15 Structure of a block copolymer of PET and poly(ethylene glycol)

voids in the fibers. These voids can act as reservoirs for moisture, and will also decrease light transmission and increase the reflectance properties of the fibers.

6.6 HIGH-SHRINK FIBERS

While high fiber shrinkage is not usually desirable, benefits can occur when high- and low-shrink fibers are intimately combined. As the yarn or fabric shrinks due to the high-shrink component, the excess length in the low-shrink component forms loops at the yarn and fabric surfaces, thus providing texture. In filament yarn fabrics, these projecting loops can mimic the feel and appearance of staple yarn fabrics. Lack of crystallization in oriented fibers will allow high shrinkage, so that copolymers or non-heatset (non-crystallized) PET fibers can be used for these purposes.

6.7 LOW-MELT FIBERS

Non-crystalline polymers or copolymers can also be used to generate fibers with relatively low softening temperatures. Such fibers can be blended with regular fibers, e.g. staples, and bonded together by applying sufficient heat to melt the low-temperature component. Such fibers need not be exotic. The use of undrawn, amorphous fibers suffices for many such purposes, for example, bonded nonwoven webs formed from a mix of drawn and undrawn PET staple fibers. Without crystalline structure, the undrawn fibers will soften and become tacky at relatively low temperatures, so providing bond sites.

6.8 BICOMPONENT (BICO) FIBERS

Bico fibers are a new class of fibers, rather than a sub-set of PET fibers. Such fibers are formed from two different polymers, which are melted separately, and then combined into a single fiber at the last moment before extrusion. In some cases, the fibers are actually extruded separately, and then combined beneath the spinneret while they are still molten, so that they fuse together after spinning.

The most common cross-sectional fiber shapes are core-sheath (c/s) and side-side (s/s) configurations (Figure 12.16). By encasing a PET core in a modified sheath, it is possible to provide desirable surface characteristics (e.g. antistat/antisoil) with minimal effect on fiber strength. A popular application is to use sheath material with a lower melt point than the core. A fabric (nonwoven or conventional) can be formed from such fibers, and then heated to a temperature sufficient to melt the sheath to bond the fibers together (Figure 12.17). Since the core component is not melted, the fused fiber retains its integrity and strength.

The side-side configuration is typically used to impart crimp to the fiber. If the fiber is formed from polymers with different shrinkage characteristics, and

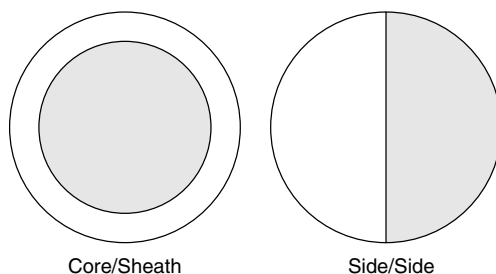


Figure 12.16 Common cross-sectional shapes for bico fibers

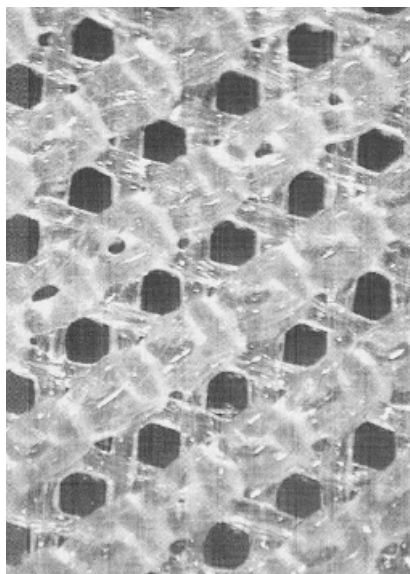


Figure 12.17 Photomicrograph of tricot knit fabric, made from core/sheath (C/S) bico filament yarn and thermally fused after knitting. Photograph reproduced by permission of KoSa Corporation

treated after fiber formation to develop the shrinkage, the differential contraction will cause the fibers to coil into a helical shape and provide three-dimensional crimp. Such self-crimping fibers provide a different type of bulk and hand than do conventionally crimped fibers.

Bico fibers have been available for at least 30 years, but only recently have they developed widespread applications. Bico production equipment is relatively more complex and expensive, and so the fibers require higher selling prices. As these fibers become more common in specialty markets, production cost is decreasing, so that they are now beginning to find uses in commodity applications.

6.9 HOLLOW FIBERS

In some applications it is desirable to generate increased bulk without adding weight, e.g. for insulation or padding. A solution is to make fibers that are larger diameter and stiffer, but with internal voids to reduce weight. By extruding hollow fibers, weight reductions of 20 % or greater can be achieved – a considerable advantage. Foaming agents in the polymer (e.g. dissolved CO₂) have also been used to generate microporous, lightweight fibers.

6.10 MICROFIBERS

A PET microfiber is loosely defined as one with a decitex (see Section 5 earlier) per filament less than one. This translates to a fiber diameter of $\sim 10\text{ }\mu\text{m}$ or less. In fabric form, such fibers provide a very soft hand and a non-shiny appearance. They can also make moisture-repellant fabrics without sacrificing comfort or air porosity, ideal for sportswear. The larger fiber surface area also can be useful for filtration applications.

Traditional melt spinning is not the best way to make microfibers. Technical problems occur with very low hole throughputs, and economics suffer. By employing bico technology, it is possible to extrude larger shapes that can be separated into smaller components after extrusion (Figure 12.18).

The ‘islands-in-the-sea’ approach uses bico technology to extrude filaments that contain a multiplicity of small fibrils encased in a soluble matrix. After fiber processing and fabric formation, the matrix is dissolved away to leave behind the microfibers. Fibers with sub-micron diameters can be produced. The process is expensive, but luxurious fabrics and nonwoven materials such as Ultrasuede[®] are made in this way.

Bico technology can also be used to form composite fibers that can be broken apart, by using polymers with poor mutual adhesion (e.g. polyolefin and PET). A fiber made with a dozen or more segments, alternating between two polymer

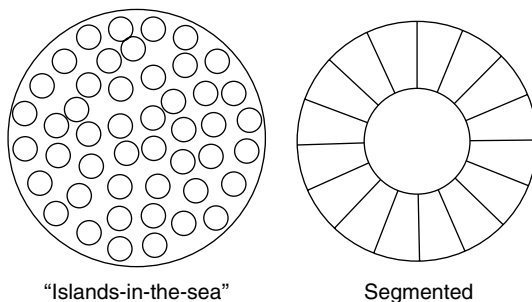


Figure 12.18 Bicomponent fibers before being separated into microfibers

types, can be post-processed to form separated fibrils of the two different materials. The shapes of the fibrils can affect the aesthetics of the fabrics, for example, sharp edges on the fibrils confer crispness and the sound of silk to fabrics.

6.11 SURFACE FRICTION AND ADHESION

Control of fiber friction is essential to the processing of fibers, and it is sometimes desirable to modify fiber surfaces for particular end-uses. Most fiber friction modifications are accomplished by coating the fibers with lubricants or finishes. In most cases, these are temporary treatments that are removed in final processing steps before sale of the finished good. In some cases, a more permanent treatment is desired, and chemical reactions are performed to attach different species to the fiber surface, e.g. siliconized slick finishes or rubber adhesion promoters. Polyester's lack of chemical bonding sites can be modified by surface treatments that generate free radicals, such as with corrosive chemicals (e.g. acrylic acid) or by ionic bombardment with plasma treatments. The broken molecular bonds produce more polar sites, thus providing increased surface wettability and reactivity.

The physical topology of the fiber surface also has a strong effect on friction. A microscopically smooth surface will generate more intermolecular attraction sites than will a roughened surface. It has been long known that including particulate additives (e.g. TiO_2 or Cab-O-Sil[®]) in the polymer reduces fiber friction, and that roughened rolls generate less friction against PET fibers than do smooth rolls.

6.12 ANTIFLAMMABILITY AND OTHER APPLICATIONS

Problems can occur with garments made from thermoplastic polymer fibers when they are exposed to flames; the molten polymer can stick to skin and cause burns. Thermal decomposition of PET also generates acetaldehyde, which is a flammable gas that feeds combustion. Additives can be used to break the combustion cycle, e.g. endothermic substances that absorb heat (inorganics), char formers that insulate the flame from the substrate, additives that react with and remove oxygen (e.g. phosphorous), or additives that promote melting and dripping to separate the molten material from the combustion area. Some of these techniques are amenable to fabric application (finishes), while proprietary polymer additives containing phosphorous and/or bromine are often used for more permanent flame-retardant PET fibers. These additives are typically expensive and/or deleterious to fiber properties. Here, bico technology is helpful, so that the additives can be incorporated into the sheath without sacrificing the strength of the core of the fiber.

their applications that have been developed for PET fibers include the incorporation of fragrances, antibacterial or absorbent additives, and also pigmented

fibers for permanent coloration. Here again, bico technology offers a route to such specialty fibers with lower raw material costs and fewer processing faults.

7 THE FUTURE OF POLYESTER FIBERS

The major properties of PET fibers are presented in Table 12.2.

Table 12.2 Properties of PET fibers

Parameter (units)	Value
Diameter (μm)	10–50
Tenacity (MPa)	
textile fiber	450–750
industrial fiber	850–1050
Elongation (%)	10–50
Initial modulus (MPa)	
textile fiber	$\leq 6\,000$
industrial fiber	$\leq 14\,500$
Shrinkage at 160 °C (%)	
textile fiber	5–15
industrial fiber	2–5
Specific gravity	
molten	1.21
amorphous	1.33
crystalline	1.44
Glass transition (°C)	
amorphous	67
oriented, crystalline	125
Crystalline melt point (°C)	265–275
Heat capacity (J/kg/K)	
at 25 °C	63
at 200 °C	105
Heat of fusion (kJ/kg)	120–140
Thermal conductivity (W/m/°C)	0.14
Thermal volumetric expansion (1/°C)	
at 30–60 °C	1.6×10^{-4}
at 90–190 °C	3.7×10^{-4}
Moisture regain (%)	
65 % RH	0.4
total immersion	0.8
Refractive index	1.58–1.64
Dielectric constant	
60 Hz	3.3
1 GHz	2.8
Electric conductivity (ohm cm)	
dry	10^{18}
0.5 % moisture	10^{12}
Solvents	<i>o</i> -chlorophenol, hexafluoroisopropanol, hot alkali
Non-solvents	alcohol, gasoline, most acids

From the proprietary developments by chemical industries in the mid-20th century, the technology for making PET fiber has become readily available to other investors. Entire plants can be purchased from machinery suppliers, for textile or industrial fibers, continuous filaments or staple. This has led to rapid expansion of PET fiber plants into developing countries by governments and/or large investment firms that supply fiber for labor-intensive fabric and apparel industries based in those countries. To an increasing degree, such apparel is imported back to the countries where the technology originated, so displacing fiber and textile businesses there. This trend will continue as the world economy becomes more global.

Standardization of the world fiber business on PET guarantees that future fiber technology efforts will remain focused on this polymer. Costs and efficiencies will get better, and other fiber types will be even less competitive. Domination of the PET commodity fiber business by Asian countries will encourage more efforts by Western and Japanese producers to further expand into niche markets with special fiber types, and to further displace natural and other synthetic fibers from their markets.

The types of products that contain PET fibers will expand, especially in areas such as nonwoven fabrics used for disposable items, e.g. industrial fabrics for diapers, disposable wipes, filters, etc. These are products that do not require much hand labor, and are relatively well protected from low labor costs in developing countries. Bicomponent fibers based on PET will become more prevalent as the production technology becomes more widespread, in areas where the bico approach can enhance properties or economics.

The domination of PET is likely to continue so long as the raw material costs remain low, and these are currently driven by the cost of oil. Although synthetic fibers use only ~1 % of the petroleum stream, they are in competition for that resource with fuels which use up to 50 times as much. Chemical producers already have efforts in place to supply raw materials for PET from renewable biological sources, so it is possible that even the increasing cost of oil will not diminish the dominance of polyester. When contrasted with increasing costs of land and resources for natural fiber production, as food for an increasing population competes for the same land, the use of PET fibers will likely become even more prevalent than today.

REFERENCES

1. Anon, *Int. Fiber J.*, **15**(3), p. 8 (2000).
2. *Paraxylene and Derivatives – World Supply and Demand Report*, PCI-Xylenes and Polyesters Ltd, Guildford, Surrey, UK.
3. Hillier, K. W., in *Man-Made Fibers, Science and Technology*, Vol. 3, Mark, H. F., Atlas, S. M. and Cernia, E. (Eds), Wiley, New York, 1968, pp. 5–14.

4. Richie, P. D., Monograph No. 13, Society of Chemical Industry, London, 1961, pp. 107–131.
5. Hansen, S. M., in *Kirk-Othmer Encyclopedia of Chemical Technology*, 4th Edn, Vol. 10, Kirk-Othmer (Eds), Wiley, New York, 1993, pp. 662–685.
6. Evans, E. F. and Pierce, N. C., *US Patent 3 671 379* (to Dupont), 1972.
7. Nakajima, T., *Advanced Fiber Spinning Technology*, Woodhead, Cambridge, UK, 1994.
8. Ziabicki, A. and Kawai, H., *High Speed Fiber Spinning – Science and Engineering Aspects*, Krieger, Malabar, FL, 1991.
9. Kim, J. and Kim, S., *J. Appl. Polym. Sci.*, **76**, 446–456 (2000).
10. Zimlicki, *MSc Thesis*, Department of Chemical Engineering, Clemson University, Clemson, SC, 1998.
11. Militky, J., Vanick, J., Krystufek, J. and Hartych, V., *Modified Polyester Fibers*, Elsevier, New York, 1991.
12. Desper, C. R., *CRC Crit. Rev. Macromol. Sci.*, 501–543 (August 1973).
13. Gupta, V. B., in *Polyester – 50 Years of Achievement*, Brunnschweiler, D. and Hearle, J. (Eds), The Textile Institute, Manchester, UK, 1993, pp. 170–173.
14. Ward, I., Cansfield, D. and Carr, P., in *Polyester – 50 Years of Achievement*, Brunnschweiler, D. and Hearle, J. (Eds), The Textile Institute, Manchester, UK, 1993, pp. 192–194.
15. Kagi, W., in *Ullman's Encyclopedia of Industrial Chemistry*, 5th Edn, Vol. A10, H-J Arpe *et al.* (Eds), VCH, Weinheim, Germany, 1987, pp. 512–566.

13

Relationship Between Polyester Quality and Processability: Hands-On Experience

W. GÖLTNER

Mönchesweg 18, Bad Hersfeld, Germany

1 INTRODUCTION

The quality of a polymer is of the highest importance for the manufacturing of commercial goods. The degree of quality of a product determines its position on the market as well as the manufacturer's economic position and competitiveness. Therefore, it is the aim of any quality management programme to improve the quality of the product and avoid adverse influences. Furthermore, any market requires constant quality of a product, and the continuous supply of a high-quality product is the aim of any production process. Attempts to achieve a compromise between the product quality and its commercial value inevitably lead to reduced care (and hence reduced cost) during production, and consequently the overall production costs will be reduced at the expense of quality. The golden rule for success in polyester production is to find the best-quality raw materials and additives. Again, the production of polyester resins is governed by the same experiences as those that occur in laboratory-scale chemical synthesis. The quality of the final product is determined by the reagents employed, the quality of the technology and process conditions and that of the supervising management.

In particular, during the course of commercial polyester development it turned out that the use of highly purified raw materials is of paramount importance. In this respect the same principles apply to laboratory-scale chemical synthesis as those that apply to industrial-scale manufacturing. Polyester syntheses, like most

organic chemical reactions that require high temperatures and prolonged reaction times, are prone to side reactions, as, for example, expressed by discoloration, the generation of degraded, insoluble solids and their deposition on the walls of the equipment. These by-products diminish the quality of the product, which result in problems during subsequent processing. Based on this simple point of view, this chapter is aimed at finding correlations between polymer quality and its final processing. It should be noted, in addition, that experiences with other plastics, particularly polyamides, can be adapted to polyesters due to the similarities of effects and their principles.

It is not the intention of this contribution to discuss phenomena that have already been expertly reported in the literature, but to create an insight into everyday polyester production that is a consequence of long years of industrial experience. For detailed mechanistic, chemical and analytical reports, readers may want to refer to a number of excellent reviews available in the literature.

Polyesters based on aromatic dicarboxylic acids and aliphatic or cycloaliphatic glycols have developed into the most important class of materials for fiber and film processing and more recently engineering plastics, owing to their unique properties, such as melting and processing behavior, crystallinity, dimensional stability and light fastness, as well as their chemical stability. Since the 1980s, poly(ethylene terephthalate) (PET) has been applied successfully as a resin for packaging materials such as sheets, flexible bottles and containers. For packaging applications, a double-figure growth rate can be expected for the next five years, while staple fiber and filament yarns will show a more sustained growth of the market. In particular, the transparency, shatter resistance and superior container performance (appropriate gas permeability, swellability, chemical stability, etc.) have made polyesters a superior class of polymer to conventional materials such as metals or glass.

Modern market trends impose a considerable pressure on the manufacturing of polymers. The evolving market and the increasing demand for new products with highly qualified properties still urge manufacturers to modify such polymers to meet modern requirements. This kind of tailoring, aimed at achieving the desired properties, has been, and still is, the real challenge for researchers. In addition, there are economic reasons that force manufacturers to enhance the performance and therefore to improve their situation on the global market. One major issue in polyester production is the tendency to increase the efficiency of polycondensation catalysts, which is commonly associated with improved quality regarding subsequent processing. On the engineering side, machine manufacturers offer equipment with the ability to increase the productivity via increased production rates. For example, the winding speed in the production of filaments has been increased by a factor of six and higher (from ~ 1000 to $\sim 6\text{--}7000$ m/min) since 1970. This development requires an increased polymer quality, as the material often has to withstand more drastic conditions during processing, and because at high production rates any interruption of the process (e.g. yarn break) becomes a

severe problem, not just with respect to quality, but also to manufacturing costs. In addition, environmental aspects lead to new developments, as there are recycling and waste recovery aspects, plus problems concerning dyeability and the removal of oligomers in textile finishing technology. Some phenomena caused by the intrinsic properties of the polymer can be accompanied by the influence of the technology and the process conditions applied. The negative effect of older equipment on the quality is known, as well as the technical measures to overcome these problems.

A considerable amount of 'non-textbook' experience has been collected by manufacturers regarding the relationship between polymer quality and processability. Most of the aspects presented here are empirical due to the gap in interest between academic research and final commercialization. The bulk of industrial knowledge regarding the relationship between polymer production conditions and quality is based on hands-on experience, regarded as internal know-how, and therefore kept more or less secret by the manufacturers. Academic research, undoubtedly extremely useful and worthy of merit, is certainly inspired by the industry to some extent, but is usually more focused on principles and mechanisms – in short, more theoretically based from an industrial point of view. As an example, the theory of fiber formation is only used as a tool to explain certain detailed phenomena in practice. However, in a few cases it was possible to create a link between fundamental results and the production of polymers, processing phenomena and their impact on the quality of the final product. The following discussion is an attempt to bridge this gap and to inspire industrial researchers to publish more of their results, although it is the fate of industrial researchers not to find sufficient time to complete solving such problems.

This review is an attempt to summarize the long-standing experiences in polyester processing according to its historical development. The base knowledge presented here is mainly focused on fiber spinning and film casting, followed by the packaging applications carried out by blow molding technology. This chapter is also an attempt to reduce the various aspects of processing to those problems that can be addressed in a modern manufacturing plant and are therefore of fundamental interest. These are extrusion, quenching, structure formation as a consequence of quenching, orientation and crystallization. The factors impairing the processing steps and the resultant quality will finally be reduced to a common denominator, namely the polymer itself.

We will also attempt to link everyday experiences with fiber and film production to the industrial engineering measures taken to improve polymer quality. The similarities based on 'non-textbook' knowledge are thus emphasized. In-depth considerations regarding special technologies would be beyond the scope of this present chapter. Therefore, the main focus is to present a modern state of knowledge regarding the relationship of polymer quality and the requirements of the processes.

2 POLYESTERS FOR FILAMENT AND STAPLE FIBER APPLICATIONS

A major aspect of polymer, in particular polyester, production is the manufacturing of fibers for textile and technical applications. This section deals with the impact of the production conditions on the fiber quality. The following discussion will be mainly based on PET fibers, but by and large the problems, phenomena and their solutions are generally relevant to the production of other polymer filaments.

2.1 SPINNABILITY

The spinnability and spinning properties of a polymer are of the highest importance in the manufacturing of staple fibers and filaments. There are many analogies to the production of films, where breaks or splits are concerned. The frequency of yarn breaks determines the economic viability of the production process, as well as the competitiveness and the reputation of the manufacturer. Today, in the age of automation, it would be theoretically possible to 'manage' the processing of the polymer with a minimum of staff if no yarn breaks disturbed the processing.

Spinnability is defined as the possibility of transforming a polymer to a shaped article such as a fiber, yarn or film via the molten or dissolved state. High degrees of spinnability are desired, as these cause little defects in the process and almost no yarn breaks. From a theoretical point of view, yarn break is a disruption of the spinning process caused by the intrinsic properties of the polymer and certain spinning parameters. High spinning speeds, as employed in the production of pre-oriented yarns (POYs) and high-modulus low-shrinkage (HMLS) yarns demand a higher degree of spinnability. In this section, the discussion of the spinning process is restricted to melt spinning technology due to its predominant position worldwide. As it is the author's intention to review phenomena occurring during the processing of polyesters, the theory of polymer spinning beyond the scope of this chapter. The interested reader may want to refer to a number of excellent textbooks on these theoretical aspects [1].

Fundamental research into the spinning process was conducted mainly in the 1960s. Many of these studies relate to rubber and polyolefins. For such polymers, the influence of molecular structure on the rheological behavior was first established. The literature dealing with plastics extrusion reports phenomena in polymer systems with quite distinctive behaviors. Ziabicki concluded the results of these studies and his own work in a fundamental theory of fiber formation [1c]. Accordingly, rheological studies were dedicated to distortion phenomena and flow instabilities of polymer (including polyester) melts at an early stage. The shear and elongational characteristics of PET have been investigated by Hill and Cuculo [2]. Due to the appearance of a slight non-Newtonian flow, pseudo-plastic behavior and a decreasing elongational viscosity with increasing temperature were

recognized. It is apparent that more studies are needed to investigate the flow properties of PET, particularly in conditions of extremely high and low shearing.

The occurrence of yarn breaks was reported early and is connected with thickness fluctuations in extruded ribbons or films, as described collectively by the phenomenon of 'draw resonance', which is characterized by oscillations of the fiber diameter, which ultimately lead to yarn break. The latter is defined as brittle fracture and is thus related to melt temperature, molecular weight, quenching conditions, and particularly to the role of viscoelasticity, as described in the following section.

The attempt to find similarities among fiber-forming polymers in order to generalize the knowledge base failed due to differences in the polymers regarding molecular weight, structure, polydispersity, flow properties and crystallinity. Surprisingly, many similarities could be found in the processing of polycondensed polymers such as polyamides and polyesters during these studies. Therefore, it seemed a valid approach to consider certain phenomena they apply to polyamides to later studies concerning polyesters.

2.1.1 Solidification, Structure Formation and Deformability

A great deal of research interest has been focused on the formation of structure and properties as well as the mechanism of deformation in the melt and the solid state as this is of utmost importance with respect to solidification in the spinning path. With the development of high-speed spinning technology, more interest has been paid to the melt strength and the phenomena accompanying solidification, as there is crystallization (including orientation-induced) as well as deformation.

The fiber- or film-forming process relies on the rheological behavior of the melt and its extensional deformation. The deformability in the molten state is mainly governed by rheological factors, such as molecular weight and viscosity. The dependence of shear and elongational viscosity as well as the viscoelasticity of polymers on temperature is a function of molecular structure, molecular weight, polydispersity and degree of branching. Viscoelasticity plays an important role regarding overall polymer properties and determines the stress profile and its evolution along the spin line. Inhomogeneous melt flow makes the spinning process vulnerable to yarn break.

The solidification as a phase transition is a function of the time-dependence of temperature and phase transformation. The rate of solidification is governed by heat and mass transfer. This phase transition is associated to a certain extent by parallelization and extension of the polymer chains along the fiber axis, hence leading to macroscopic orientation. This so-called spinning orientation is a consequence of elongational flow and depends on the degree of deformation caused by take-up speed. Spinning orientation is closely related with crystallization as well as structure and increases with the spinning speed. Many variables influence the deformability in the solid state, as there is solidification

accompanied by molecular orientation and crystallization. Competitive reactions take place between localized hardening and softening which cause deviations of the spinning stress. These effects cannot be ignored whenever the deformability of the polymer during processing is concerned. Consideration of these influences provides deeper understanding of fracture, which is one major factor of processability. The solidification of the PET fiber is accompanied by crystallization, which in turn depends on the take-up speed. The crystallinity of these fibers is a function of materials characteristics such as crystallization rate, molecular weight, melt viscosity, the presence of nucleants and the spinning conditions.

As a consequence of the low crystallization rate of PET, its fibers, spun at conventional speeds (1000–3000 m/min), show only orientational, but not positional order. Crystallization is observed at a speed of about 4000 m/min and increases dramatically with the spinning speed. In the same way, the formation of structure can be observed at high degrees of crystallinity and orientation of crystallites as well as the amorphous domains. The orientation tends to be pointing more parallel to the fiber axis than perpendicular to it. The difference in birefringence between the skin and core regions, an indicator of orientation, increases with enhanced spinning speeds at any given quenching conditions. At high speeds, birefringence of the skin region decreases due to the formation of voids. Additionally, the dye uptake is improved with increased mobility of the amorphous chains, determined by the free volume surrounding the primary crystals. The radial distribution of orientation is influenced by the quenching conditions and the heat of crystallization, but mainly by the spinning stress.

The fibers exhibit a fine structure consisting of large crystals separated by areas of poorly oriented, amorphous regions with many crystal nuclei at a pronounced skin/core character, which is a consequence of a complex structure formation mechanism. The nuclei grow into large crystals upon heating.

It can be assumed that the orientation of the amorphous regions is a result of the deformation of a rubber–elastic network. Therefore, it can be expected that crystallization during spinning occurs at the neck, where the deformation is maximal. The amorphous phase develops into a load-bearing factor which is related to its orientation, as expressed by Hermans orientation factor.

According to Jabarin [3], the crystallization behavior is a function of the catalyst system employed and can be influenced by additional aspects of the polymer process which are still largely unidentified. Particularly in high-speed spinning, increased stress and molecular orientation in the skin layers could be observed with increasing crystallization rate as well as degree of crystallinity. Consequently, different properties of the skin and core layers regarding deformation have been recognized. This phenomenon results in different stress values. Therefore, the spinning speed should not be increased infinitely due to the limitations of flow and deformation properties inherent to the polymer. Knowledge of these details is still limited, which means that the temperature-dependence of melt viscosity, strain and crystallization rate, and that of oriented crystallization during

solidification and structure formation, overshadowed by inhomogeneities of the polymer, is still only vaguely understood. The main conclusion here is that the crystallization of PET is significantly affected by molecular orientation, which is drastically increased at high spinning speeds [4].

Ziabicki and Jericki reported the crystallization characteristics of PET as well as a theory of molecular orientation and oriented crystallization [5a]. Besides these theoretical considerations, the rate of recrystallization understandably seems to play an important role, particularly in high-speed spinning. Little is known about the crystallinity gradient caused during melt spinning at high take-up speeds.

The stress-induced crystallization influences the ability to sustain the stress of deformation occurring in the spin line. Optical micrographs of 'fluffs' allow the assumption of different deformation or stress behavior of core and skin layers of spun fibers, as shown in Figure 13.1. The reason for this kind of yarn break can



Figure 13.1 Yarn break caused by skin-core differences (brittle fracture and crazes) [9]. Photograph provided by W. Göltner

be overcome only by adjusting the take-up speed or optimizing the quenching conditions according to the individual behavior of the polymer. Regarding this aspect, the crystallization properties associated with nucleation in the polymer melt are crucial factors in describing polymer quality with respect to spinnability.

The frequently used and even less precise term 'melt strength' seems to express the resistance of the melt against deformation. Practically, it relates to the phenomenon of 'die swell', which can be determined by measuring the maximum diameter of swelling below the exit of the spinneret. Melt strength can also be measured according to the method described in a patent belonging to Hoechst-Celanese [6]. Here, the addition of flexible poly(ether ester)s is reported to improve the flex crack resistance of PET films during biaxial orientation. Therefore, die swell or the melt strength are structural indicators of the polymer and can be increased by the molecular weight, expressed by the intrinsic viscosity (IV), the degree of branching, or both.

The viscoelastic behavior of the polymer plays a major part in developing the structure and the final properties. The change of molecular constitution caused by branching significantly influences the structure formation [7]. Branching, characterized by die swell as well as increased molecular weight, prolongs the retention time and improves the melt stability. Shear and extensional properties relate in the same manner to the molecular constitution or to the molecular weight distribution.

According to George [8], the freezing temperature is higher in the case of a more elastic (branched) polymer, as can be seen below in Figure 13.4. The freezing point is defined as the position in the spin line where the fiber reaches the final winding speed. Therefore, the orientation occurs in the amorphous region and later on in the semicrystalline domains at the thinning of the spun fibers. The radial distribution of structure shows differences in the skin/core layers in the case of linear PET, as assessed by the birefringence. No difference at a significantly increased level could be observed in comparison with the branched polymer. The formation of skin/core layers results in different deformation behavior and causes breaks which are increased by internal defects of the structure. In addition, particularly predominant in high-speed spinning, the high-spinning stress affects the vulnerable, brittle surface of the filaments by formation of holes, craters crazes and voids, which are the reason for breaks.

The critical state of stress-induced crystallization at high spinning speeds is governed by the viscoelasticity of the polymer in combination with its crystallization behavior. Any kind of coarse particle obviously disturbs the structure and affects the resistance against deformation. The development of stress is controlled by the rheological properties of the polymer. Shimizu *et al.* [4] found that increasing the molecular weight drastically promotes the crystallinity under stress conditions.

The different recrystallization behavior as revealed by differential scanning calorimetry (DSC) complicates the understanding of structure formation as a dependence of take-up speed and seems to particularly correspond to the

spinning of microfilaments as an important factor which influences the spinning performance [9]. At present, no explanation for this observation has been reported.

In context with the crystallization mentioned above, the different spinning behavior of bright and 'semi-dull' PET should be noted. The improved processability of semi-dull PET can be explained by the nucleating activity of TiO_2 particles added as a pigment or by surface modification of the fiber. These particles can act as a kind of 'anti-blocking agent', hence improving the performance during spinning, and in particular, drawing. In the case of hot-tube spinning (spin-crystallizing process), the increased elongation of bright yarn indicates the nucleating effect of TiO_2 particles in comparison with semi-dull material. This may explain generally the known different processing behaviors of bright filaments affected by reduced crystallization.

It has long been reported that the spinnability of a polymer is closely related to its elastic properties. In film casting, the elongational viscosity increases with the elongation rate. Therefore, this property is of essential importance for spinnability [10, 11]. An analysis of the flow behavior along a molten threadline is nearly impossible. Certainly, differences can be expected depending on the character of the individual fiber-forming polymer due to its intrinsic rheological and crystallization properties. It is well known in the fiber industry that yarn breaks occur at a critical value of take-up speed. The occurrence of such breaks depends on the molecular structure, molecular weight and molecular weight distribution [12]. However, influences of the latter have not yet been published for the processing of PET. Perez has reported the influence of rheological properties on the structure formation during high-speed spinning [13]. The influence of branching is demonstrated in Figure 13.2, where three polymers, characterized in Table 13.1, have been tested with respect to shear viscosity and shear stress.

Die-swell and draw-resonance ratio data for these polymers are presented in Table 13.2 and Table 13.3, respectively. According to these results, the influence of branching and molecular weight is significant. The extremely large increase in

Table 13.1 Intrinsic viscosity and molecular weight data for the three characterized polymers (cf. Figure 13.2) [13]. From 'Some effects of the rheological properties of PET on spinning line profile and structure developed in high-speed spinning', Perez, G., in *High-Speed Fiber Spinning*, Ziabicki, A. and Kawai, H. (Eds), 1985, pp. 333–362, copyright © (1985 John Wiley & Sons, Inc.). Reprinted by permission of John Wiley & Sons, Inc.

PET	$[\eta]$	M_w	M_n	Triol (mol%)
Linear	0.66	41 000	21 000	0.00
Linear	0.61	37 000	19 500	0.00
Branched	0.54	45 000	15 000	0.65

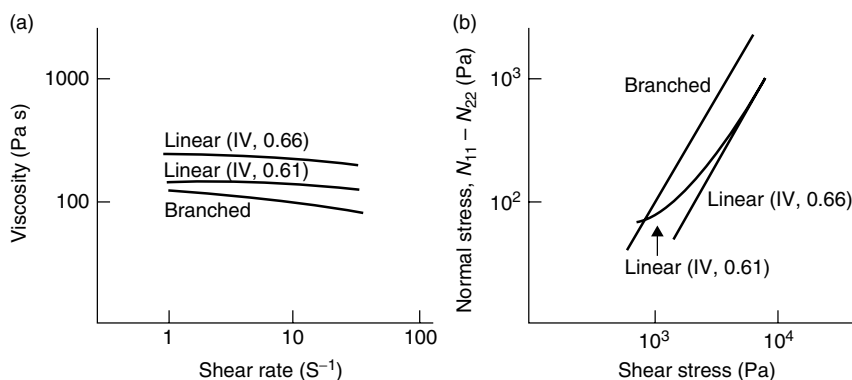


Figure 13.2 (a) Shear viscosity as a function of shear rate, and (b) normal stress difference as a function of shear stress for the three PET samples described in Table 13.1, with measurements carried out at 270 °C in a mechanical cone-and-plate viscometer [13]. From ‘Some effects of the rheological properties of PET on spinning line profile and structure developed in high-speed spinning’, Perez, G., in *High-Speed Fiber Spinning*, Ziabicki, A. and Kawai, H. (Eds), 1985, pp. 333–362, copyright © (1985 John Wiley & Sons, Inc.). Reprinted by permission of John Wiley & Sons, Inc.

Table 13.2 Die-swell ratio as a function of mean residence time in the capillary^a for the three polymers shown in Table 13.1 [13]. From ‘Some effects of the rheological properties of PET on spinning line profile and structure developed in high-speed spinning’, Perez, G., in *High-Speed Fiber Spinning*, Ziabicki, A. and Kawai, H. (Eds), 1985, pp. 333–362, copyright © (1985 John Wiley & Sons, Inc.). Reprinted by permission of John Wiley & Sons, Inc.

PET ($[\eta]$)	Residence time (ms)		
	3	10	300
Linear (0.66)	1.3	1.26	1.16
Linear (0.61)	1.28	1.26	1.15
Branched (0.54)	1.63	1.58	1.34

^a $T = 276$ °C; capillary dimensions: diameter, 0.98 mm; length, 0.98 mm.

the critical draw ratio by branching makes it mandatory to pay more attention to molecular constitution, the ratio of stored and dissipated energy and the molecular weight distribution. Viscoelastic behavior influences the spinnability but too little information has been reported on the consequences on final yarn properties, particularly the degree of order in the case of industrial fiber applications. The data shown in Figure 13.3 exhibit the different properties of linear and branched

Table 13.3 Draw-resonance ratio measured under specific experimental conditions^a for the three polymers shown in Table 13.1 [13]. From ‘Some effects of the rheological properties of PET on spinning line profile and structure developed in high-speed spinning’, Perez, G., in *High-Speed Fiber Spinning*, Ziabicki, A. and Kawai, H. (Eds), 1985, pp. 333–362, copyright © (1985 John Wiley & Sons, Inc.). Reprinted by permission of John Wiley & Sons, Inc.

PET ([η])	Critical draw ratio
Linear (0.66)	28–30
Linear (0.61)	18–20
Branched (0.54)	>76

^a $T = 285^\circ\text{C}$; capillary dimensions: diameter, 0.34 mm; length, 0.34 mm; mass through put, 0.41 g/min; water surface-to-spinneret distance, 20 mm.

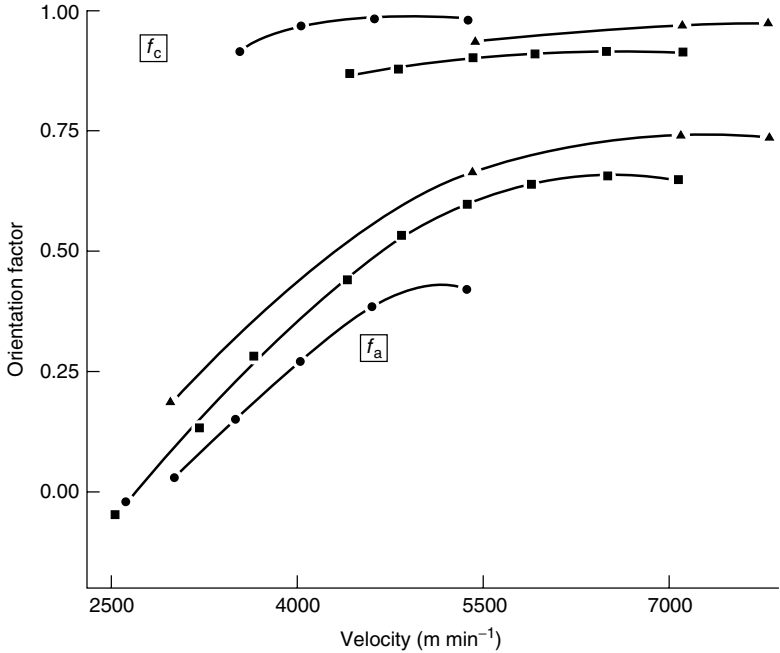


Figure 13.3 Crystalline (f_c) and amorphous (f_a) orientation factors as a function of take-up speed for the three PET samples described in Table 13.1: ●, branched; ■, linear (IV, 0.66); ▲, linear (IV, 0.61) [13]. From ‘Some effects of the rheological properties of PET on spinning line profile and structure developed in high-speed spinning’, Perez, G., in *High-Speed Fiber Spinning*, Ziabicki, A. and Kawai, H. (Eds), 1985, pp. 333–362, copyright © (1985 John Wiley & Sons, Inc.). Reprinted by permission of John Wiley & Sons, Inc.

PET. Variations in the degree of branching change the properties of the polymer in the desired and expected directions. The spinning conditions need to be adjusted via temperature or take-up speed depending on the degree of modification. The important influence of the molecular weight is also clearly demonstrated in the work of Perez [13]. Branching causes a broadened molecular weight distribution and an increased relaxation time.

Figure 13.3 also shows the orientation factors of the crystalline and amorphous regions as a function of take-up speed, which is pronounced in the case of a branched PET polymer. The shift towards increased freezing temperatures in branched polymer samples seems to be an indicator of higher elasticity (Figure 13.4).

The flow properties of polymers provide a basis for predicting processing characteristics and are usually determined by measurements which relate a shear stress to some shear rate. Any polymer is characterized by its flow curves. Even interactions between compounding ingredients and the polymer can be detected in this way.

Too little has been published about the flow properties of PET as a criterion for processing. The results of melt flow index (MFI) testing conditions do not correlate with the processing behavior in the case of PET. This may be caused by the discrepancy between the shear rates in testing and processing. MFI is defined as the amount of polymer melt (in g) extruded within 10 min through an orifice of specified diameter at a standard load and temperature. In the case of PET, this method was not very popular until recently due to the sensitivity of this material to hydrolytic degradation.

The shear viscosities of polycondensate melts depend strongly on the temperature. Polyesters exhibit a slight non-Newtonian (and therefore viscoelastic) behavior. It seems that an intensive study of the flow properties of polyesters, stimulated by the demands of bottle processing applications, will provide more information. The MFI may become a handy tool for polymer manufacturers due to its versatile applicability. For example, such a parameter seems to be suitable for investigations of the molecular weight distribution and molecular structure at low or high shear rates. A 'master curve' for PET has been presented by Shenoy *et al.* [14a]. This easy and relatively inexpensive experimental method is now gaining increasing importance in plastics engineering.

Remarkably, intense studies of the flow properties of other fiber-forming materials have revealed interesting correlations with the spinnability. However, results concerning the production of PET have not yet been published. Munari *et al.* have studied the effect of branching on flow properties in the case of poly(butylene terephthalate) (PBT) [15]. Raje *et al.* reported that the shear stress experienced with the melt flow can reach the critical limit, hence resulting in breaks in the case of a wider molecular weight distribution with a higher content of low-molecular-weight fractions. The low-viscosity fraction modifies the overall melt viscosity and causes processing instabilities [16].

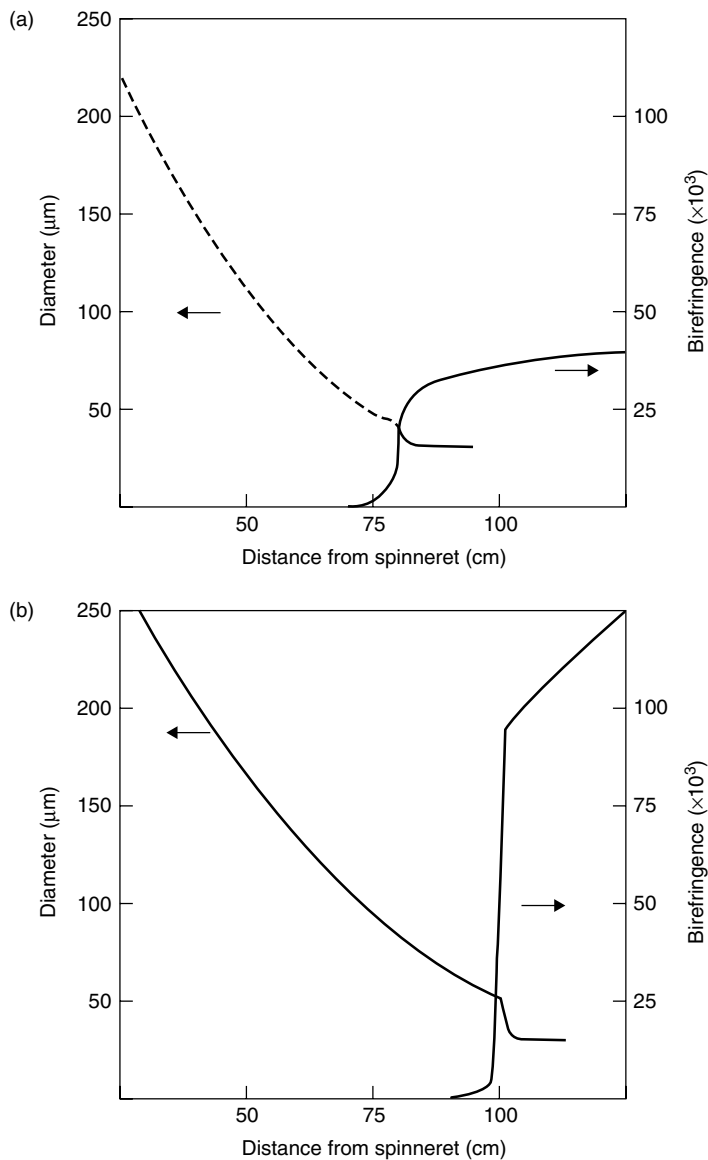


Figure 13.4 Illustration of the freezing point, as shown by the variation in diameter and birefringence with distance from the spinneret for (a) branched, and (b) linear (IV, 0.66) PET samples spun at 5400 m/min [13]. From 'Some effects of the rheological properties of PET on spinning line profile and structure developed in high-speed spinning', Perez, G., in *High-Speed Fiber Spinning*, Ziabicki, A. and Kawai, H. (Eds), 1985, pp. 333–362, copyright © (1985 John Wiley & Sons, Inc.). Reprinted by permission of John Wiley & Sons, Inc.

As has been demonstrated, the desired outstanding mechanical properties of PET filaments, particularly those for industrial applications such as tyre cord yarns, are principally based on the degree of the most highly extended crystalline structure. Materials with these properties require a high degree of linearity in the polymer. High tenacity can be obtained by using higher molecular weights. This is also the reason why the IV of industrial-yarns polymer has increased continuously from 0.78 to 1.0 dl/g within the last decade. The relationship between microstructure and spinnability is also the reason for the fact that modified polyesters for special applications, for example, flame resistance, or cationic or disperse dyeability, usually exhibit reduced mechanical fiber properties. This reduction is a result of the decreased state of microscopic order in the polymer.

Apart from this, a divergent development has been observed in the fiber industry since the end of the 1970s. As a consequence of the desire to improve the productivity of partially oriented yarn (POY) manufacturing, the production of branched PET became very popular due to the possibility of increasing the speed in spinning and drawtexturing. Further aspects to this development are high product yield and uniformity of quality. POY based on slightly branched PET withstands enhanced yarn tension in subsequent processing due to its improved drawability. Accordingly, the break rate of these yarns is significantly reduced and the yield of full bobbins subsequently increased. The improved performance guarantees more stable production conditions associated with a better quality, particularly regarding uniform dye uptake. The production of these polymers is also accompanied with slight advantages with respect to the efficiency in the polymer process due to a reduced reaction time during polymer production. It should be noted, however, that the analytical detection of the degree of branching in the polymer is difficult. The only recommendable method is nuclear magnetic resonance (NMR) spectroscopic analysis.

The addition of immiscible polymers to PET during POY spinning enhances the productivity by 40 % and higher [17]. This became the most attractive method among all of these other trends. The influence of the immiscible additive is based on the viscosity-reducing effect of polymeric additives on polypropylene (PP) observed in blow molding. Consequently, it could be found that the addition of small amounts of immiscible polymers to PET drastically suppresses the degree of orientation in POY spinning. The orientation and crystallinity of the spun yarn increase with winding speed, as indicated by the birefringence of the yarn (Figure 13.5).

The dependence of the elongation of the POY as a function of winding speed is presented in Figure 13.6(a). Melt-blending PET with small amounts of other fiber-forming polymers, such as polyolefins, nylon 6,6 and liquid crystalline polyesters (LCPs), results in a suppressed orientation, hence allowing increased production speeds. Amorphous polymethacrylates and copolymers containing maleimide moieties are also recommended. The influence of melt-blending on the

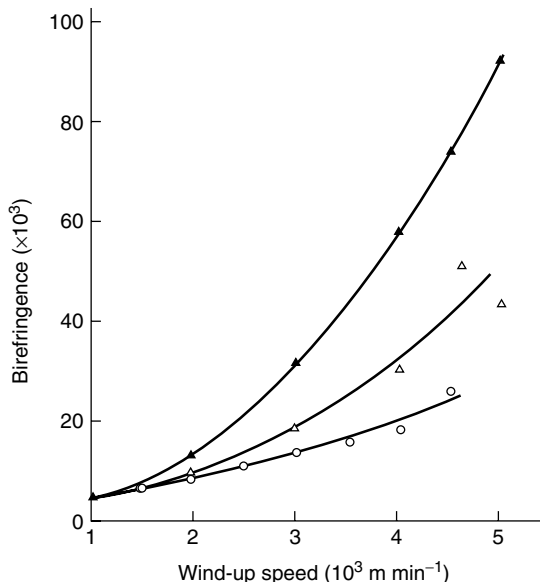


Figure 13.5 Birefringence as a function of wind-up speed: (a) ▲, PET control; (b) △, PET containing 3% copolyester of 1,4-phenyleneterephthalate and *p*-oxybenzoate; (c) ○, PET containing 3% copolymer of 6-oxy-2-naphthalene and *p*-oxybenzoate [17]. From 'Orientation suppression in fibers spun from melt blends', Brody, H., *J. Appl. Polym. Sci.*, **31**, 2753 (1986), copyright © (1986 John Wiley & Sons, Inc.). Reprinted by permission of John Wiley & Sons, Inc.

stress-strain behavior is shown in Figure 13.6(b-d), which also demonstrates the decreased orientation of the additive-containing materials when compared with the non-modified PET.

The polymeric additive should have the same (or a slightly higher) melt viscosity compared with the PET matrix, as well as good thermal stability. A sufficient dispersability of the additive in the matrix polymer is required. Therefore, a lot of effort has been dedicated to obtaining a homogeneous distribution of the additive in the matrix. The additive feed is conducted prior to extrusion. Depending on the qualification of the polymeric additive and the desired degree of suppression of orientation, the additive concentration commonly varies in the range between 0.5 and 3 wt%. Dispersing agents improve the distribution of the additive in the PET matrix. POYs modified by melt-blending require a higher draw ratio in drawtexturing to attain the desired final properties. The added polymer is dispersed in the host polymer matrix as microfibrils and so avoids the known phenomenon of necking in the spinning path. The immiscible polymer contained in the PET melt reduces the shear viscosity of the melt, increases the elongational viscosity and decreases the orientation by penetration into the host polymer. The processability is mainly influenced by the degree of homogeneous

dispersion of the admixed polymer. The latter also causes a rough filament surface with improved hand. Garments made of these products feel warmer to the touch [17].

2.2 YARN BREAK

Fracture is a complex phenomenon, and in the context of this contribution its theoretical understanding should be focused on the individual processing steps. In practice, it has been found that fracture relates to changes of deformability and directs attention to different structural features. According to this serious matter it was found that a large number of changes during polymer processing and its process conditions result in material variables and the increased probability of fracture. The latter increases with stress and the amount and particle

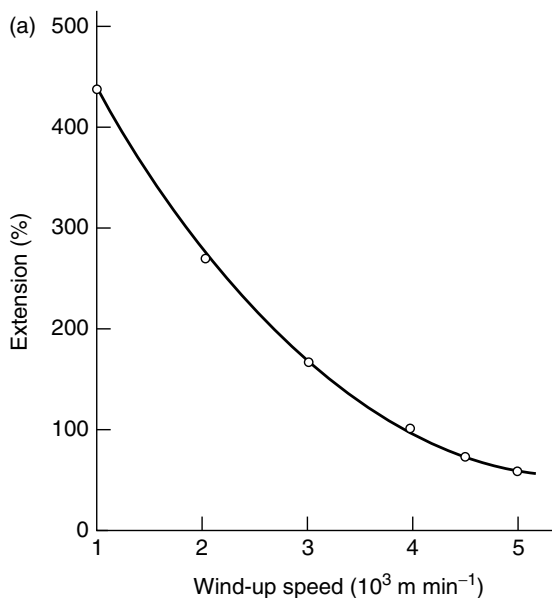


Figure 13.6 (a) Elongation as a function of wind-up speed for partially oriented yarn. (b–d) Stress–strain curves of fibers of PET blends with 3% copolyester of 1,4-phenyleneterephthalate and *p*-oxybenzoate (CLOTH) and 3% copolymer of 6-oxy-2-naphthalene and *p*-oxybenzoate (CO), spun at 3500, 4000 and 4500 m/min: (1) PET control; (2) 3% CLOTH; (3) 3% CO: the loci of the theoretical extensions of the PET control are shown as dashed curves [17]. From 'Orientation suppression in fibers spun from melt blends', Brody, H., *J. Appl. Polym. Sci.*, **31**, 2753 (1986), copyright © (1986 John Wiley & Sons, Inc.). Reprinted by permission of John Wiley & Sons, Inc.

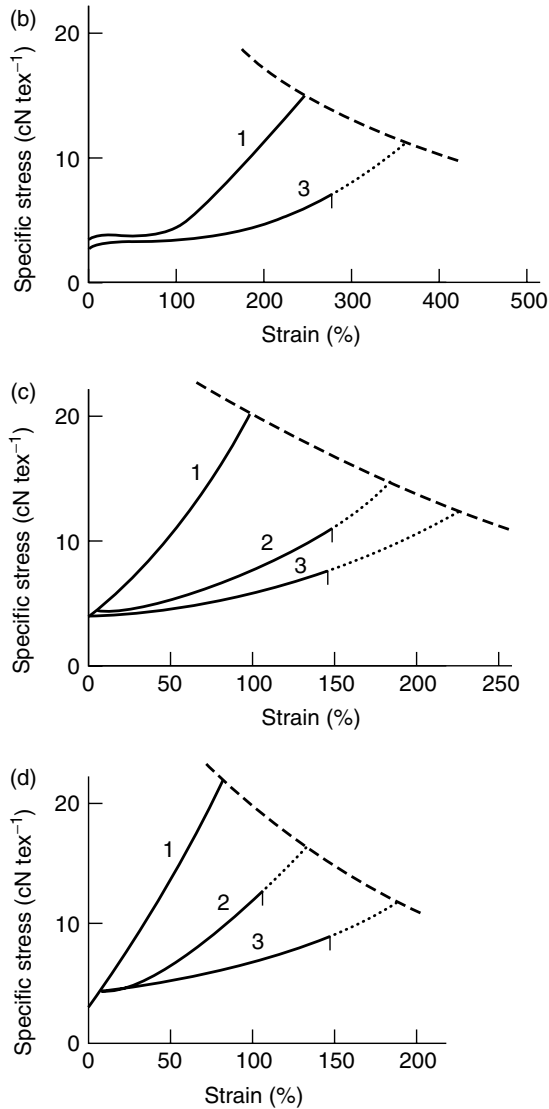


Figure 13.6 (continued)

sizes of the impurities or solid additives in the polymer which can affect the regularity of the structure. In this context, an influence of the temperature on the probability of fracture, and generally, of changes of crystallinity, preorientation and irregularities of structure with respect to deformability could be recognized.

2.2.1 *Spinning*

Spinnability and processability are defined as the ability of a yarn to withstand the conditions of spinning and drawing, particularly at high deformation rates (take-up speeds), in fiber processing in the molten and solid states. The processing of the polymer melt is influenced by rheological factors, in particular the homogeneity, melt strength and melt elasticity of the polymer. Developments in improving the processability of a polymer have to be directed towards enhancing its deformability. Some of these principles have been summarized in various reports, etc., although lack of space precludes any further discussion in this present chapter.

The rheological properties of the melt regarding extension and shear are intrinsic materials characteristics. Fiber-forming polyesters shows slight non-Newtonian and viscoelastic behavior. The shear viscosity is strongly temperature-dependent. The sensitivity of elongational flow relates to the viscoelasticity of the melt and plays an important role in melt spinning. It can be assumed that during spinning the polymer behaves as a Newtonian fluid, being temperature-dependent, but viscoelastic upon extension. Too little is known about the correlation of certain rheological properties with the spinnability. The homogeneity of the melt determines the performance of processing which can be disturbed by the molecular weight and its distribution, molecular structure, and the content of oligomers, gels or solids which influence the constancy of the melt flow. Rheological factors, which govern deformability, additionally complicate the spinning mechanism in the spinneret before solidification.

The occurrence of necking in the spin line indicates the instability of deformation and the system therefore restabilizes. Similar behavior to that shown with temperature can be observed in the presence of plasticizers. The fracture is promoted by increased stress in the case of plastic deformation. Cracks or notches at the surfaces of fibers and films are also the reason for disturbed deformation due to the more rapidly increased stress at the tips of these defect sites.

The degree of drawing, orientation and crystallinity is of the highest importance for the structure and final properties of the polymer product. These properties are influenced detrimentally by the frequency and size of defect sites along the length of the fiber or the film. Such imperfections indicate fluctuations in the molecular structure and cause flow instabilities associated with deviations of temperature and particularly stress during deformation. For polymers and multiphase systems, mainly two mechanisms are held responsible for fracture. The processing flow is more or less influenced by the elongational factor caused by the draw ratio in spinning, as well as the conditions of solidification. At an early stage of this development, the 'draw resonance', which occurs in the lower temperature range of melt spinning, was investigated. Draw resonance is the phenomenon of oscillating spinning tension which causes deviations in the yarn diameter. This phenomenon leads to the formation of crazes at the fiber surface perpendicular to

the fiber axis and finally to 'brittle' or 'cohesive' fracture in the case of high spinning speeds or low temperatures. The occurrence of crazes also has to be viewed in context with the existence of oligomers in the melt, which induce additional defects. The occurrence of brittle fracture can be observed when the local tensile stress reaches a critical range. This phenomenon is based on the theory of viscoelastic fluids (Maxwell fluids). During deformation of these fluids, a part of the energy necessary for deformation is stored in the system. Under certain external spinning conditions (speed, quenching rate, fiber diameter, etc.) and various rheological properties of the polymer, increased spinning tension above the critical range results in brittle fracture. The rheological aspects here are viscoelasticity, and temperature- and deformation-rate-dependence (elongational flow and relaxation time). These factors determine the tension and the concentration of stress. The phenomenon of brittle fracture is particularly relevant in the commercial production of fine filaments and in high-speed spinning.

The other mechanism responsible for unstable spinning is the mechanical resistance of a viscoelastic material to rapid deformation. It is a well-known fact that increased yarn breaks can be a consequence of spinning speed, which relates to prolonged relaxation time and therefore to break. The fracture can be observed at a maximum extent of deformation under distortion of the covalent bonds.

Much work has been published during the last few decades to find a suitable link between the polymer and the actual processing. Very important correlations have been found, which ultimately relate to the formation of structure. The latter seems to be of more importance than the method used to achieve it. Simplifying the complex relationship between the polymer and its processing, the phenomenon of spinnability is based on the elastic character of the polymer, which is rate-dependent on deformation. In this context, deformability denotes the property in the molten and the solid states. Elasticity usually arises from the entropic energy storage occurring during deformation of the polymer chain. The spinnability of a polymer can be measured according to the considerations of Dietrich *et al.* and other workers [18]. The spinning test is carried out at constant winding speed, temperature and IV, and with decreasing feed rate. The spinning tension then increases with enhanced draw ratio up to the point of break. In the case of high-speed-spinning conditions, the rheological equation of the law of tenacity (Newton, Trouton, etc.) can be applied and leads to process parameters such as hole diameter of the spinneret and critical fineness, and an approach towards suitable processing conditions. Test spinning is therefore necessary to obtain information on the spinnability of a polymer under defined processing conditions. The results of these test runs thus allow a judgement regarding the quality of a polymer.

In addition, the drawability of a spun yarn can be measured in a similar way by increasing the draw ratio up to yarn break at an experimental drawing position. The optimal draw ratio can also be deduced from the stress-strain curve of the spun yarn.

These results underline the importance of the structural characteristics. This relevant matter can be simplified as a consequence of distinct polymer properties in terms of strength loss or thermal-mechanical impact. The latter is relevant during heating and loading the yarn and is based on the dynamics of phase transitions during melting and solidification. Parameters, such as the surface properties of spun fibers, thermal diffusivity, heat capacity of the melt and melt viscosity, as well as molecular weight and temperature, are therefore important aspects. Defects, such as cracks on the fiber surfaces and other irregularities within the fiber adversely affect deformability due to the more rapidly increased stress at the tips or that due to inhomogeneous positions. The higher the melting point and the specific latent heat of the polymers, then the better are the properties that can be expected.

Yarn tension and the temperature applied in processing are parameters which can cause the loss of yarn strength, with the weakest link of the processed material being the break point [19]. The reduction of the mechanical properties, such as tenacity and elongation, is closely related to the coefficients of variation of tenacity and elongation and represents the stability of the polymer under given processing conditions. Improvements can be expected by achieving an optimum of balanced conditions, only indicated by such coefficients of variation.

2.2.2 Drawing

Fracture is not only a phenomenon of spinning – it also can be observed in the subsequent drawing process. In this way, the shaped article (fiber or film), characterized by a low degree of orientation and crystallinity, can be converted to the final product with the required properties. This conversion is carried out by drawing at elevated temperatures (above the glass transition temperature (T_g)). The physical parameters governing this process are viscoelastic, reversible and irreversible elongation components resulting in the formation of a maximum of molecular order. The stress-induced process of drawing leads to a change of phase structure associated with both destruction and construction of crystals, as well as an extremely high orientation of the amorphous regions. The improved mechanical properties (tenacity and elongation) achieved in such a way depend particularly on the highly oriented transition regions between lamellar crystals.

Drawing is determined by the drawing conditions and the structure of the poorly oriented spun fiber or film. Therefore, many variables influence the deformation in the solid state. The drawing tension is affected by the draw ratio, temperature, drawing speed and the degree of preorientation of the spun yarn, as well as the molecular weight. Drawing as an irreversible deformation is accompanied by a certain amount of dissipated energy, which is partly stored in the material, hence giving rise to a temperature increase. An increased drawing temperature promotes the mobility of the polymer chains and reduces the stress in the characteristic plastic flow. In the case where the critical conditions are

exceeded, the drawing process becomes unstable, as indicated by an increased break rate. Fracture expresses this instability to deformation and is caused by different factors, e.g. different molecular weights, reduced degree of orientation, localized hardening in the case of high temperatures, localized stress concentration and temperature rises and changed preorientation, as well as the inherent imperfections of the spun fiber. The localized hardening through molecular orientation competes with the softening at fracture sites and ultimately depends on the qualification of the primary structure. The probability of fracture can hence be explained as a change in deformability. In practice, the quality of the preoriented spun fiber, including the content of any kind of imperfection, determines the drawing performance. Pronounced irregularities affecting the drawability are crazes, notches, holes, oligomers, voids, holes, gels, gas bubbles, etc., produced during spinning. In addition, thermally, oxidatively or hydrolytically degraded polymers also exhibit reduced drawability. Low molecular weights further reduce the fiber strength. It can be assumed that the inhomogeneities contained in extruded polymers cause even more uneven fibers than any disturbances during production. Understandably, contaminated or damaged surfaces of the equipment (godets), which come into contact with the fiber or film, further lower the drawability.

2.2.3 Heat Setting

The drawn fiber or film is characterized by a certain degree of instability created by the viscoelastic deformation (reversible component). The material reveals internal stress and structural defects due to its frozen state. This instability towards heating causes shrinkage, which limits the final application. Subsequent relaxation treatment carried out at temperatures higher than those used in applications improves, in particular, the perfection of ordered structure, crystallinity and the dimensional stability, and also recovers the equilibrium of the primarily thermodynamically unstable system. Commercially, this relaxation, the so-called stabilization or heat setting, is carried out at elevated temperatures, either under load (tension on a fixed length) or unloaded (free state). The heat treatment in the free state causes disorder in the polymer crystals (increase of entropy). In the fixed state, the same treatment stabilizes the previous orientation of the crystals. The changes of structure as a consequence of heat setting depends on factors such as tension, temperature and time. The tenacity as a function of crystallinity and orientation decreases, which is associated with a change in the stress-strain behavior during treatment in the unloaded state. In contrast, the elongation behaves in an opposite way. The resulting shrinkage properties depend on the degree of relaxation and the temperature. The effect of free-treatment conditions results in a more efficient stabilization. High molecular weights reduce the efficiency of heat setting. This phenomenon plays an important role in the production of tyre cord yarns. It should be noted that stabilization causes severe problems in the processing of these materials. Heat setting in the unloaded state is accompanied by

shrinkage, which induces instability of the yarn tension, as indicated by undesired mobility of the threads when they pass the godets. Touching of the threads and overlapping is therefore inevitable. This leads to mechanical damage by crushing of the yarn, and in the worst cases to yarn break. The damaged material exhibits a significant deterioration of physical properties, and thus adverse consequences for subsequent processing. Therefore, thread guidance becomes problematic in the industrial heat setting process which is carried out continuously in combination with drawing. The increase of crystallinity by heat treatment in the unloaded state can be 20–30 %. Tenacity and crystallinity are constant in loaded conditions.

Heat setting in film production is mainly carried out under load. This technique is gaining more importance owing to the changes in surface properties as a consequence of changed crystallinity and crystal size, as well as the migration of oligomers (depending on the setting conditions). In this way, the formation of holes and larger crystals influence the surface properties, in particular with relation to all of the severe consequences on coating applications and abrasion resistance behavior.

It is worth noting that heat setting produces a new surface structure. The topology of the film surface can be controlled by the addition of inert inorganic solids or by surface treatment. The heat treatment assists in the agglomeration of these particles into larger aggregates, which results in protrusions on the film. The desired ‘slipperiness’ for subsequent processing is thus compromised. In this way, the abrasion and scratch resistance can be influenced significantly.

3 POLYMER CONTAMINATION

The history of man-made-fiber production provides ample evidence of the catastrophic influence of polymer contamination on the performance and quality of the final products [20]. Contamination can lead to severe problems in melt spinning and processing of filament yarns. Therefore, the ‘filterability’ of the polymer becomes an important factor in the processing of polyesters. There are many reasons for the contamination of polymers by solid or semi-solid (gel) particles. Impurities are mainly introduced as those contained in raw materials or in additives (catalysts, stabilizers, delustering agent, etc.). Polymers based on the dimethyl terephthalate (DMT) process additionally contain the ester-interchange catalysts inhibited mainly by phosphoric acid or its esters after transesterification is complete. These compounds are insoluble and distributed in the melt as particles of different size depending on the reaction condition and the way of precipitating them. Finer particles have the function of internal slipping agents and are preferred in film casting [21]. Coarse particles have to be removed by subsequent filtration in the polymer line or during processing after extrusion. The reaction of antimony-based polycondensation catalysts with phosphorous-containing stabilizers, which can provide very smooth fiber or film surfaces with

optimum conditions for subsequent drawing, is particularly interesting [22]. Usually, the content of its products of different particle size results in problems in subsequent processing. Additional contamination can be introduced via unfiltered raw materials, as, for instance, ethylene glycol (EG) solutions of antimony oxide, stabilizers or additives, and suspensions of TiO_2 , or particularly film additives in the ethylene glycol. The suspension of additives require a high degree of know-how with respect to the processing technology, qualification of the additives and the way of adding the suspension to the polymer during processing. The inappropriate causing of temperature shock or increased acidity of the reaction mixture, time and location of addition, as well as unsuitable concentration of the suspension often lead to agglomeration of the particles with adverse consequences on processing and quality. Very difficult conditions can be particularly observed during the production of cationic dyeable PET in the presence of derivatives of sodium sulfoisophthalate. These problems are mainly related to agglomeration of TiO_2 due to the acid conditions caused by the addition. A typical TiO_2 agglomerate is depicted in Figure 13.7.

Contamination can also be caused by degraded polymer particles generated through thermal decomposition of the polymer at the walls of the reactors or the melt pipes, or by dead spaces in the systems, as illustrated below in Figure 13.17.

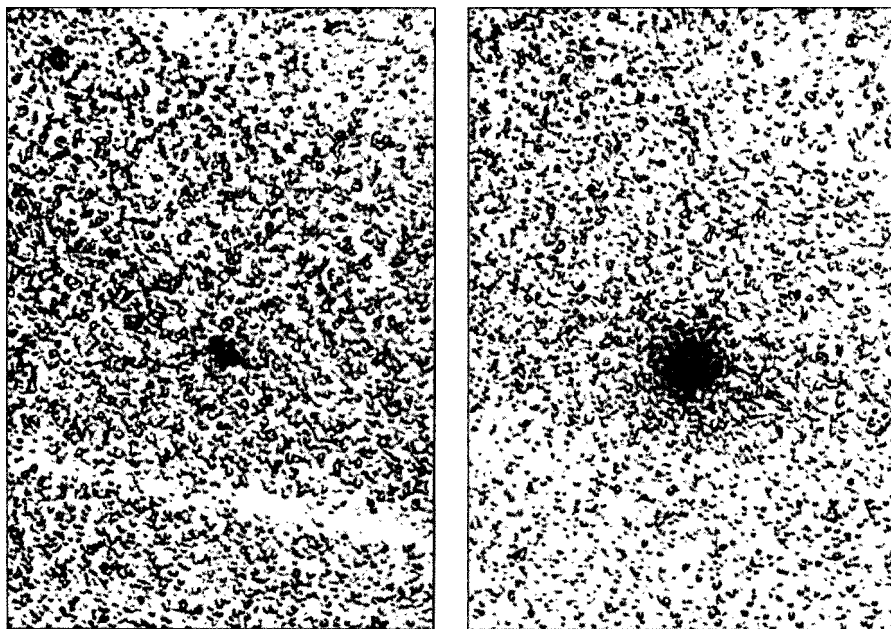


Figure 13.7 A TiO_2 agglomerate in PET polymer [9]. Optical micrographs provided by W. Göltner

The presence of oxygen caused by leaks in reactors leads to a dramatic deterioration of the product quality [23].

Finally, polymer dust is a severe source of trouble in polymer processing. The density and enhanced melting point of dust particles causes insufficient melting of this material and affects the optical clarity of bottles and films, as well as the spinning performance of fiber material. Dust is produced by abrasion of improperly cut chips or by their high-speed convection in air, as well as during storage or by mishandling. Dust builds up in layers at the pipe walls where chips are conveyed. These layers can be partially dislodged and are usually detected as highly crystalline oriented particles at the ends of broken filaments. Pollution of the polymer can additionally occur by the use of unfiltered air during conveying of chips.

Filament defects can be divided in two classes, i.e. those with or without inclusions. Defects without inclusions are due to performance reasons, while those with inclusions are a consequence of impurities. Most inclusions can be identified via polarized-light optical microscopy. Gels appear birefringent in polarized light, although they are often invisible when viewed through an ordinary light microscope. Optical microscopic analysis in plain or polarized light is a very important tool in identifying the reasons for yarn breaks. This analytical technique should be included in general production control procedures and is therefore the key to the solution of manufacturing problems. A detailed identification of inclusions can be achieved by dissolving specimens in hexafluoroisopropanol (HFIP) or concentrated sulfuric acid, or by simply heating samples on the hot stage of a microscope. The latter method provides simultaneous information on both melting point and crystallinity.

The degree of contamination governs the performance and product quality and affects the utility value of the end product. Secondary contaminants such as additive agglomerates are included in the term 'contamination'. Particularly in case of film polymers, such particles diminish the quality of audio or video tapes due to the vulnerability of films to this 'drop-out' phenomenon.

Besides optical microscopy, contamination can be detected by a variety of other analytical methods. A very popular one is the so-called 'filter test'. The polymer is extruded in a laboratory extruder equipped with a screen filter (pore size of 5 μm). The increase in the pressure is indicative of the degree of contamination. This can be quantified by the amount of polymer passing through the filter in order to increase the pressure to 100 bar. Low filter-test values indicate a high degree of contamination. Frequent control of the production by this method provides crucial information on the suitability of processing conditions and the state of the equipment. This test can also be carried out on-line, in a side-stream line of continuous polymer production lines, or in a spinpack equipped with a pressure gauge.

Other analytical methods of quantifying the degree of contamination are based on counting the contaminants in the melt, in cast films or in solution of the

dissolved polymer by optical methods. Insoluble particles of the dissolved polymer can be detected by the principle of Coulter counting or by measuring the electrical conductivity [24].

3.1 OLIGOMERIC CONTAMINANTS

For a long period of time, too little attention has been paid to the content and the role of oligomers in the spinning process. Due to the equilibrium conditions in the reaction mixture, PET contains about 1–2 % of oligomers. In certain conditions, this amount can be reduced to values below 1 % by solid-state polycondensation (SSP) processes. Figure 13.8 shows the variation of the oligomer content as a function of temperature and time during SSP processes.

Remelting of the polymer during processing causes an increase in the oligomer content, depending on the melting conditions, temperature and residence time, as illustrated in Figure 13.9.

Remelting of the polymer is additionally accompanied by a broadening of the molecular weight distribution and the formation of a low-molecular-weight fraction ($M_n = 1400\text{--}1900$). Additionally, the generation of a low-molecular-weight fraction causes problems regarding polymer quality and the formation of deposits in subsequent processes, particularly dyeing. This is of particular importance for any kind of process involving polymer recycling, especially for film and bottle waste recycling [25]. During processing, for example, spinning,

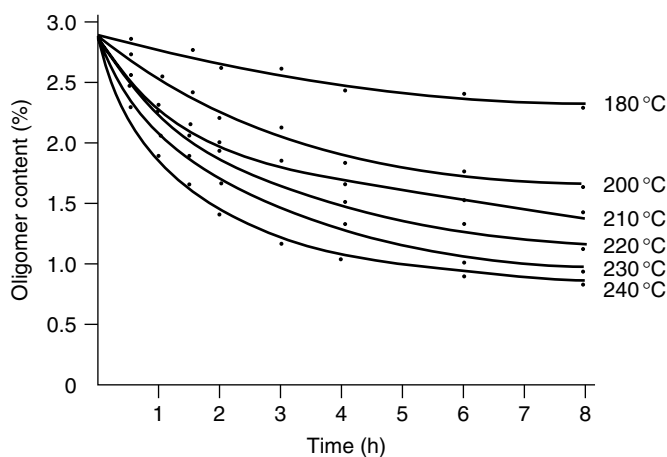


Figure 13.8 Variation of oligomer content under solid-state polymerization conditions [38]. From Wick, G., 'Characterization of PET Polymer for Bottle Manufacturing', presentation given at the *Society of Plastics Engineers, Benelux Seminar*, May 20–21, 1980, Amsterdam, and reproduced with permission of KoSa GmbH & Co. KG

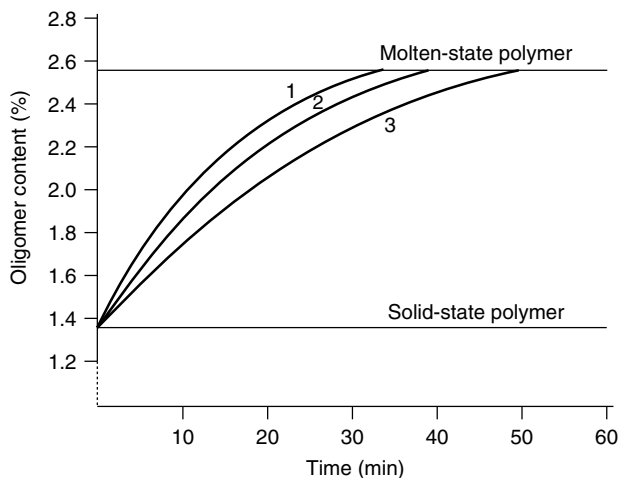


Figure 13.9 Regeneration of oligomers at different melting temperatures: 1, 300 °C; 2, 295 °C; 3, 285 °C [38]. From Wick, G., 'Characterization of PET Polymer for Bottle Manufacturing', presentation given at the *Society of Plastics Engineers, Benelux Seminar*, May 20–21, 1980, Amsterdam, and reproduced with permission of KoSa GmbH & Co. KG

a certain amount of this low-molecular-weight fraction sublimates and condenses on the surroundings of the spinneret in the form of dust. In film casting, the sublimate deposits onto the pinning devices, hence giving rise to the appearance of streaks in the film.

Studies regarding the oligomer distribution in PET processing lead to the conclusion that the cyclic trimer is one main constituent, although other linear oligoesters are observed in local concentration. The latter products have different melting points, all below that of PET. The cyclic trimer (T_m : 312 °C), commonly constituting about 70 wt % of the total amount of oligomers, has a strong tendency to diffuse to the skin layers during fiber spinning and remains there in the form of protrusions. These particles can be partly dislodged from the fiber surface, as the latter comes into contact with yarn guides or godets. As a result, crater-like holes, notches or crazes are usually observed in these fibers. Again, these defects are the reason for yarn breaks in conditions of high yarn tension, particularly in high-speed spinning or at high draw ratios in the drawing step of processing. These broken particles, together with diffusing oligomers and cracked 'spin-finish' residues, build up tough deposit layers at the surfaces of the godets, especially on the heated setting godets, which are commonly kept at 220 °C and higher for PET spinning. These layers have a detrimental effect on yarn friction. They can damage the yarn and therefore cause additional breaks. Removal of these deposits from the godets is time-consuming, and even worse, requires an interruption of the whole production process.

It is very likely that yarn break begins at the location of a defect in the fiber surface and propagates towards the core part of the fiber, which results in loss of resistance up to the final yarn break. Most of the 'normal' breaks occur according to this fatigue fracture. The mechanism of fatigue fracture is illustrated schematically in Figure 13.10 [26]. Studies of the diffusion of oligomers towards the fiber surface under the conditions of subsequent textile processing confirm this mechanism of deposition (Figure 13.11).

Dry heat treatment (Figure 13.12), hydrothermal treatment (Figure 13.13), dependent on temperature, as well as swelling the fibers in tetrachloroethane (Figure 13.14), produces a fiber morphology resembling that of known pictures of fracture. Swollen fibers show the typical shapes which cause the breaks in the manufacturing process.

In addition, the oligomers are located not only at the surface, but are also distributed inside the fiber and disturb the formation of a homogenous structure during solidification. Based on photomicroscopy studies, the formation of defects in the spun yarn can be explained. The important role of oligomeric contaminants with respect to breaks is hence underlined (Figures 13.15 and 13.16) [27]. During processing, they can break off and leave defects looking like craters or notches which are the reason for breaks. This effect is exhibited in these figures. According to the photomicrographs shown in Figure 13.17, the detrimental effect of oligomers at the fiber surface regarding yarn breaks is an expected phenomenon, as has been reported announced with respect to technological contaminants.

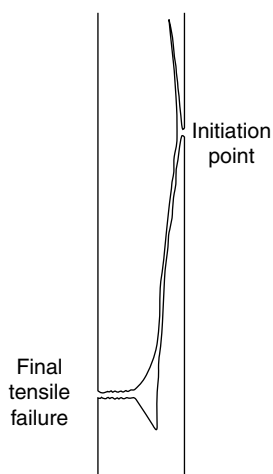


Figure 13.10 Schematic representation of the most general type of fatigue fracture of a nylon 6,6 fiber [26]. From 'The fatigue of synthetic polymeric fibers', Brunzell, A. R. and Hearle, J. W. S., *J. Appl. Polym. Sci.*, **18**, 267 (1974), copyright © (1974 John Wiley & Sons, Inc.). Reprinted by permission of John Wiley & Sons, Inc.

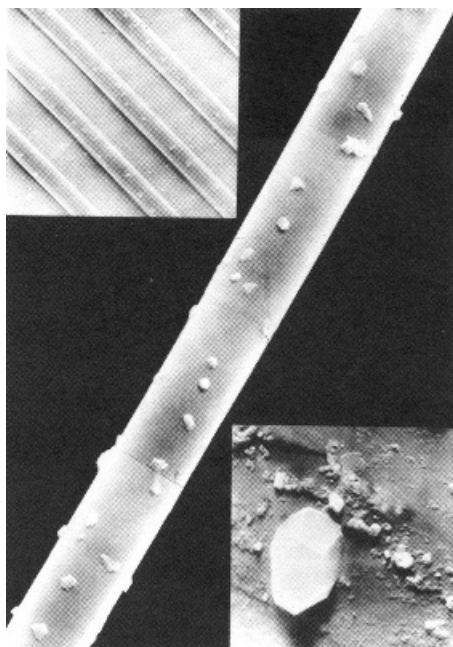


Figure 13.11 Scanning electron micrograph of a PET fiber (diameter, $22\text{ }\mu\text{m}$) after heat treatment at 215°C for 15 min showing the presence of oligomer crystals [27]. From 'Beitrag zur Kenntnis der Art und Verteilung an Oligomeren in PET', Kassenbeck, P. and Marfels, H., *Lenzinger Ber.*, **43**, 34 (1977), and reproduced with permission of Lenzing Aktiengesellschaft

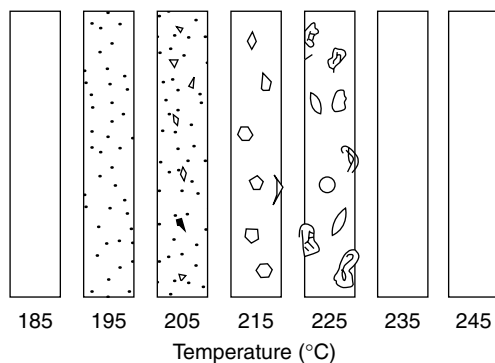


Figure 13.12 Schematic representation of the oligomer distribution at the surface of a PET fiber as a function of temperature – heat treatment [27]. From 'Beitrag zur Kenntnis der Art und Verteilung an Oligomeren in PET', Kassenbeck, P. and Marfels, H., *Lenzinger Ber.*, **43**, 34 (1977), and reproduced with permission of Lenzing Aktiengesellschaft

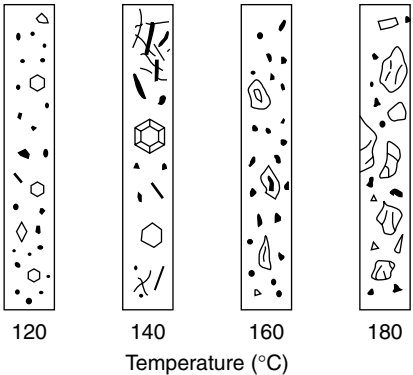


Figure 13.13 Schematic representation of the oligomer distribution at the surface of a PET fiber as a function of temperature – hydrothermal treatment [27]. From ‘Beitrag zur Kenntnis der Art und Verteilung an Oligomeren in PET’, Kassenbeck, P. and Marfels, H., *Lenzinger Ber.*, **43**, 34 (1977), and reproduced with permission of Lenzing Aktiengesellschaft

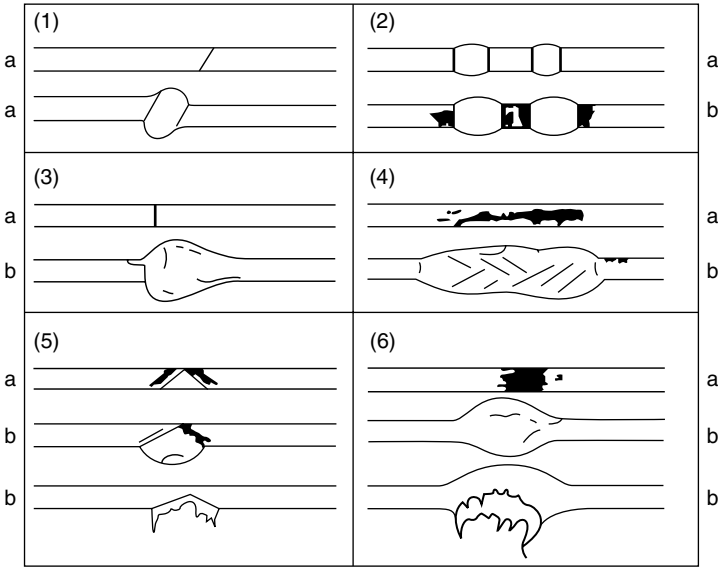


Figure 13.14 Schematic representation of defects at the surface of a PET fiber (a) before, and (b) after swelling in tetrachloroethane (at -10°C) [27]. From ‘Beitrag zur Kenntnis der Art und Verteilung an Oligomeren in PET’, Kassenbeck, P. and Marfels, H., *Lenzinger Ber.*, **43**, 34 (1977), and reproduced with permission of Lenzing Aktiengesellschaft

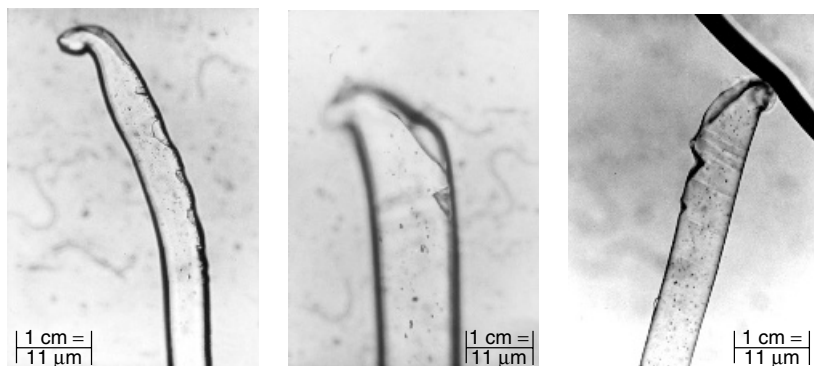


Figure 13.15 Photomicrographs of PET filaments showing surface breaks caused by oligomeric contaminants [9]. Photographs provided by W. Göltner

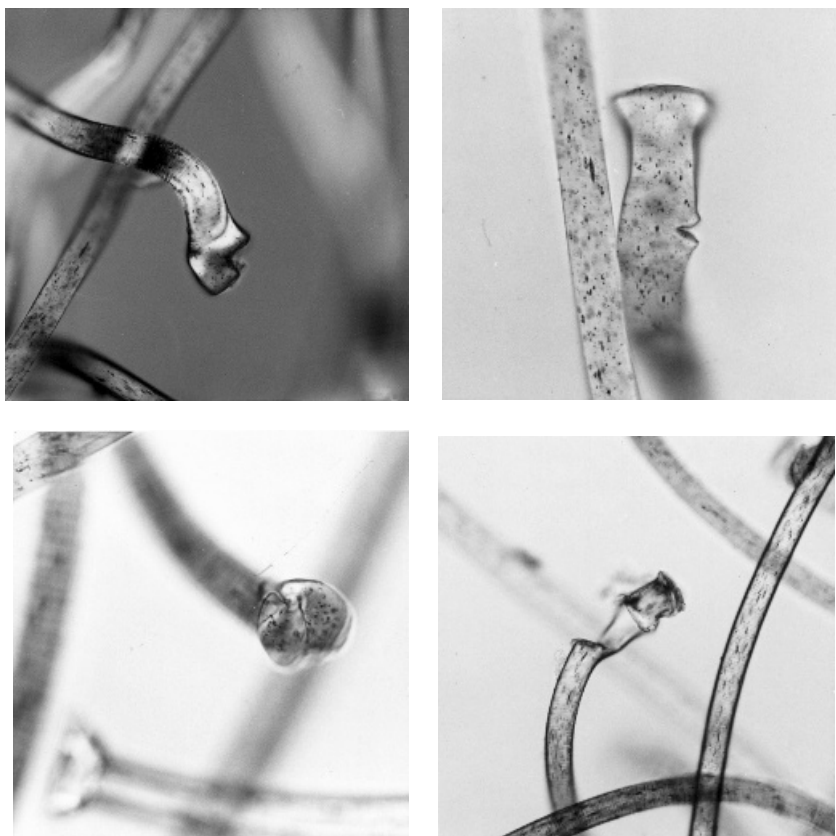


Figure 13.16 Some examples of surface breaks in PET filaments resulting from the presence of oligomeric contaminants [9]. Photographs provided by W. Göltner

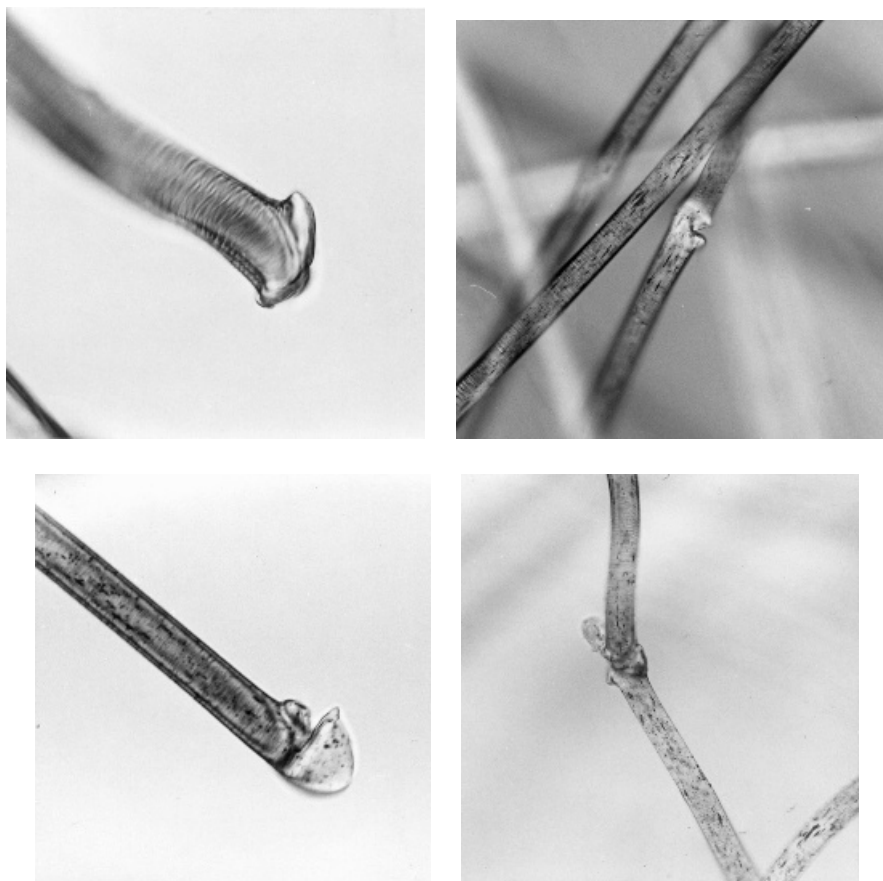


Figure 13.16 (*continued*)

Figure 13.18 shows the thin, highly oriented surface zone of a filament. Understandably, this photomicrograph explains the vulnerability of the surface zone of the fiber to contaminants. Finally, it should be noted that oligomers also cause many other severe problems by their deposition in textile finishing processes such as dyeing.

3.2 TECHNOLOGICAL ASPECTS

There are also some technological factors that influence the quality of the polymer. The design of the reactors, the flow of the molten polymer and the way of heating the systems are decisive for quality and performance [28]. Valves, tube turns, in- and out-take flanges, mixing elements and welding seams are often

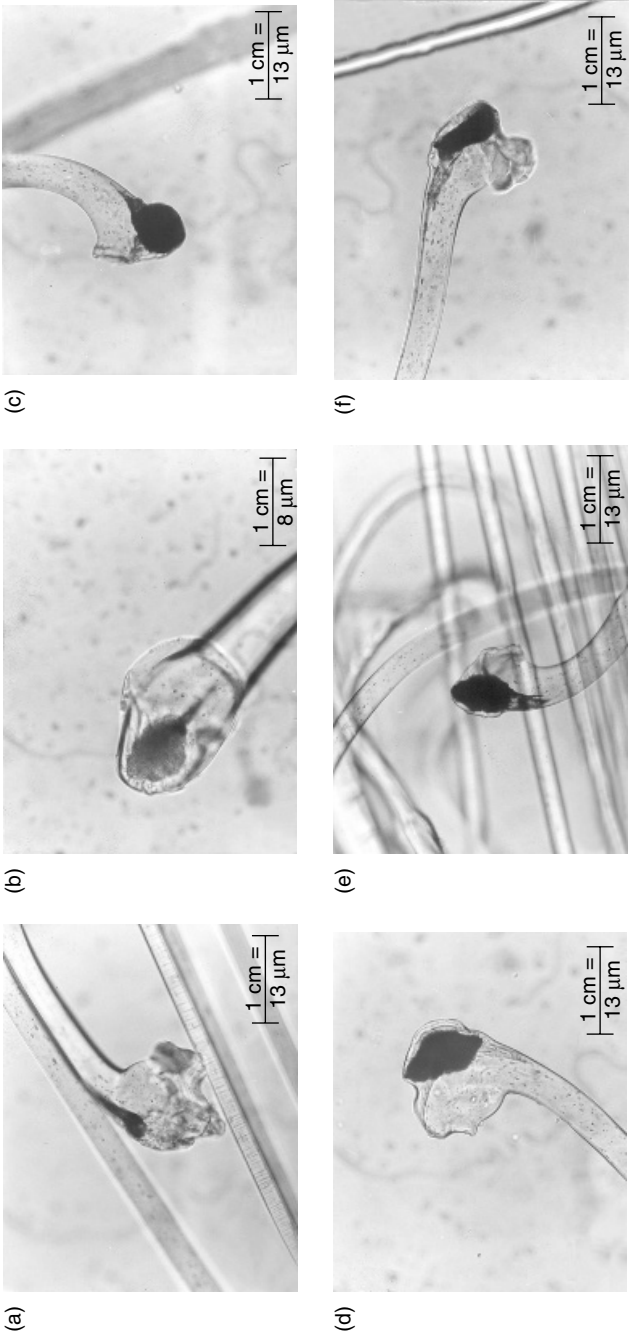
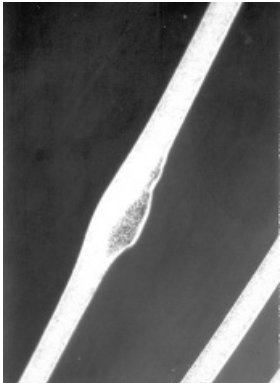
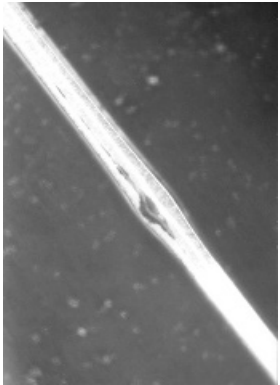


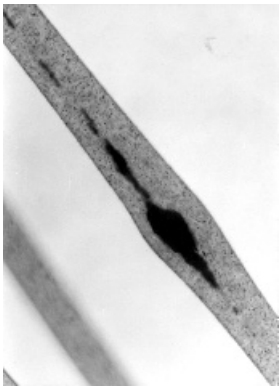
Figure 13.17 Photomicrographs of PET filaments showing breaks caused by inclusions. The image shown in (g) was obtained by using transmission illumination, with those shown in (h) and (i) obtained in reflection mode [9]. Photographs provided by W. Göltner



(i)



(h)



(g)

Figure 13.17 (continued)

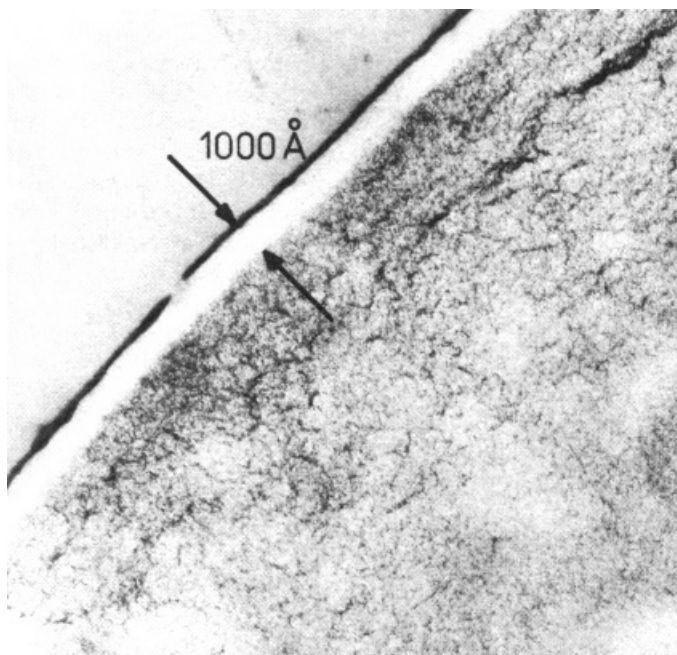


Figure 13.18 Photomicrograph of a thin, highly oriented surface zone of a PET filament [27]. From 'Beitrag zur Kenntnis der Art und Verteilung an Oligomeren in PET', Kassenbeck, P. and Marfels, H., *Lenzinger Ber.*, **43**, 34 (1977), and reproduced with permission of Lenzing Aktiengesellschaft

locations of dead spaces where all kinds of degradation can occur. The contact of the melt with the 'overheated' walls of the reactor or pipes, usually electrically heated parts of the equipment, cause increased thermal degradation. In contrast, insufficiently heated parts of the systems allow solidification of the melt and therefore the formation of highly crystalline polymer, which becomes inhomogeneously dispersed in the melt. Changes of the throughput, deviations of the liquid level in the reactors or interruptions of the process favor the deposition of the melt at the walls and the agitator and therefore promote contamination. It takes a long time to achieve steady-state conditions in a system and to remove these contaminants from the line.

3.3 THERMAL, THERMO-OXIDATIVE AND HYDROLYTIC DEGRADATION

Thermal-oxidative degradation is an additional reason for yarn breaks commonly observed during polymer processing as a consequence of leaks in the equipment. Frequent testing of tightness is therefore an important part of production

supervision. Thermal-oxidative degradation also occurs in inappropriate conditions during drying or extrusion of the polymer in the presence of air. Decreased thermal stability or enhanced temperature, particularly in the presence of oxygen during processing, results in a deterioration in polymer quality. It has been found that when chips are dried *in vacuo* and extrusion takes place in a nitrogen atmosphere then degradation is kept to a minimum level [29]. Metal derivatives used as catalysts for transesterification and polycondensation or for the synthesis of raw materials improve the rate of polymer processing and can affect the overall thermal stability. Antimony catalyst systems are more thermally stable in comparison to those containing manganese, cobalt or zinc. Thermal-oxidative degradation further causes the formation of gels by cross-linking. Gelation influences the 'filterability' of the polymer melt. Depending on the degree of cross-linking, soft (weakly cross-linked) gels or hard (highly cross-linked) gels can be observed.

The decomposition of PET via the generation of volatile by-products, such as CO₂, EG or acetic aldehyde (AA), understandably causes problems in subsequent processing. Thermal stability can be assessed by the rate of degradation determined by the IV drop or the increase in carboxylic end groups (CEGs) or vinyl ester end groups, as well as by the degree of discoloration. Practically, the easiest way to measure thermal stability is the annealing of a sample under standardized conditions, accompanied by determination of the factors mentioned above. Thermal stability can also be quantified by thermogravimetric analysis (TGA).

During the early development of nylon, a relationship between the fluorescence of a polymer and its spinnability, which can result from degradation, was established. By analogy, fluorescence measurements are a good indicator for degradation in polyesters [30]. This approach is based on the emission spectrum of PET in the range of the absorption wavelength between 360 and 500 nm, with a maximum commonly being observed at around 390 nm. The appearance of fluorescence is a sensitive indicator of thermal-oxidative degradation associated with a broadening of the emission bands. This non-invasive method can be applied in the solid state or to dissolved polymer samples. A broadening of the fluorescence spectrum and a shift of the emission maximum towards longer wavelength (500 nm), accompanied with enhanced intensity, indicates thermal-oxidative degradation.

In any case, the appearance of fluorescence is accompanied by significantly reduced spinnability. Figure 13.19 shows an impressive example of the fluorescence of three PET samples with different spinnability. The term 'excellent' is here applied to the processability of polymer A, which is by far superior to that of the other two samples. Polymer A could be processed without almost any yarn breaks in POY spinning (167 dtex¹ 32,¹ winding speed 3300 m/min), polymer B showed an acceptable performance, whereas polymer C gave many yarn breaks and therefore a bad performance. The break rate is proportional to the

¹ dtexf, the yarn weight of 10.000 m consisting of the number of filaments. For example, in this case, 10.000 m of yarn (32 filaments) weigh 167 g.

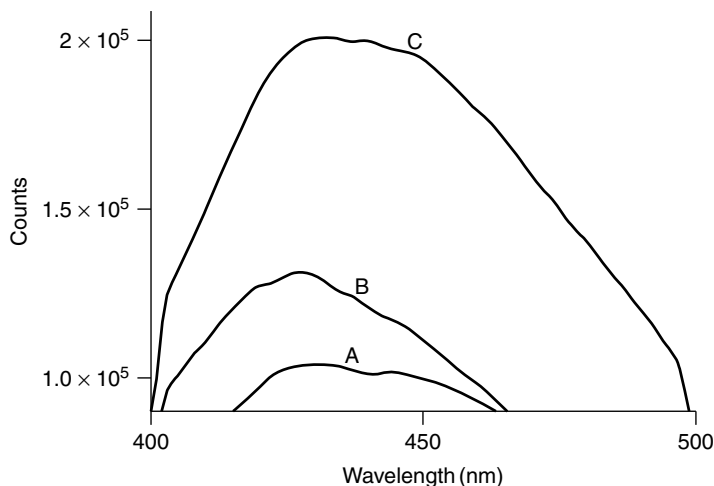


Figure 13.19 Fluorescence spectra of three PET samples with different spinnability behavior: A, excellent; B, medium; C, very poor [9]. Spectra provided by W. Göltner

fluorescence of the polymer and increases with the wavelength of the emission maximum. For the purpose of production control, the determination of fluorescence over the whole visible spectral range is of great interest. As could be seen, the wavelength of the spectral fluorescence peak shifts to a higher value (e.g. from 410 to 425 nm).

The occurrence of fluorescence is often related to inappropriate processing conditions in molten-state and solid-state polycondensation (SSP) (presence of oxygen, high temperature, long retention time, etc.), as well as the later drying of chips where prolonged residence times can occur.

Fluorescence can also be detected by using fluorescence microscopy. This method allows one to even draw conclusions about the origin of fluorescence during processing. If only the surface areas of the chips are affected, the degradation can then only have occurred during drying or SSP as a consequence of inappropriate conditions, the presence of air or prolonged residence times (indicative of dead spaces). Use of a fluorescence microscope also allows a distinction between the various reasons for fracture of broken fibers. The appearance of fluorescence should act as an 'alarm function' in production control and can therefore serve as an extremely valuable analytical tool.

Hydrolytic degradation of polymers is still the main reason for the occurrence of faults in processing. This form of degradation commonly causes a reduction of the IV, associated with a deterioration in the mechanical properties, particularly the tensile strength. Therefore, it is important to ensure sufficient drying of the raw materials. Drying is a crucial prerequisite of any polyester processing

system. In order to obtain satisfactory processing results, the water content of the polymer should be kept at values lower than 15 ppm. In the case of drying by air flow, the temperature should not exceed 180 °C in order to avoid thermal-oxidative degradation. Drying *in vacuo* usually affords an optimum in quality. In context with hydrolytic degradation, the storage conditions of the chips prior to extrusion and the humidity of the atmosphere at the inlet of the extruder are of further importance.

3.4 INSOLUBLE POLYESTERS

Up until now the exact nature of the insoluble polyester material in a polyester melt has not been sufficiently investigated. Insoluble polymer can be found after long residence times during SSP, particularly during such processing in the suspended (swollen) state. The polymer can contain up to 10 wt% insoluble content after solid-state processing. High contents of insoluble polymer fractions in the polymer shorten the lifetimes of the filters and also affect the spinning performance. Due to the unknown nature of these insoluble fractions, for this kind of contaminant the same arguments apply as for the occurrence of dust.

3.5 GAS BUBBLES AND VOIDS

The appearance of air bubbles in the polymer melt may occur under certain circumstances during processing. This phenomenon is rarely related to obvious faults in the polymer, but sometimes gas bubbles can be observed in cases of decreased thermal stability. Gas bubbles appear due to a certain amount of dispersed gas in the polymer matrix. Insufficient removal of gas from the extruder, particularly from the compression zone, can also cause the problem of air bubbles in the melt. An influence of the extruder screw could be established, because gas bubbles can be removed to some extent by using special screws or changing the extrusion conditions, along with the application of a vacuum.

Voids often look similar to air bubbles. The appearance of voids in filaments or films, however, results for different reasons. Voids can be produced during stretching in the area of necking by a kind of folding mechanism. The formation of voids may also depend on the generation of a radial gradient structure during solidification of the threads.

3.6 DYEABILITY

Different degrees of dyeability of staple fibers and filaments for textile applications seriously affect the constancy of product quality. This phenomenon has become more or less a matter of industrial production experience. Only a few

publications deal with dye uptake from a theoretical or mechanistic point of view. It is therefore surprising that this subject has not attracted more interest in the academic community. Varying dye uptake is usually an indicator of irregular production conditions and represents a severe problem in manufacturing. Dye uptake can be considered to be influenced by various structural factors, such as orientation, crystallinity and surface morphology – in short, the conditions of manufacturing. The modifying effect of diethylene glycol (DEG) on dyeability is well known. According to the results of Kanide and Kuriki [31], the penetration of the dyestuff occurs preferentially within the amorphous regions of the filaments. The dyeability is closely related to the mechanical loss tangent ($\tan \delta$) attainable from the variation of the dynamic viscoelasticity with temperature. Dyeability is therefore mainly influenced by the amorphous domains and the degree of their arrangement, as well as the free-volume fraction. In addition, dyeability depends on the molecular weight and structure of the dyestuff as well as the dyeing conditions. From the polymer aspect, the contributions to dye uptake are crystallization behavior and DEG content. To what extent the latter affects the above mentioned features is unknown and seems to depend on the conditions of the fiber process. In practice, differences of 0.1 wt% can significantly change the dye uptake. It should be noted that even small deviations of the IV can also cause irregular dyeability.

4 FILMS

Since the introduction of polyesters in film manufacturing at the end of the 1950s, the quality requirements of polyester films have become increasingly rigorous. The superiority of polyester films is based on the outstanding property profiles of most polyesters. Apart from a few similarities to fiber production, the production of films has completely different aims. Film production is mainly based on the tubular technology or 'stenter' process. This technique is the most popular one owing to its excellent quality and economic viability. The stretching of quenched films occurs in the so-called stenter frame in either the longitudinal direction, followed by stretching in the transverse direction, in reverse order, or simultaneously. Heat treatment after the stretching step is necessary to obtain the desired dimensional stability. Heat setting is carried out in low-stress conditions at enhanced temperatures (above the required usage temperature) to obtain the desired shrinkage properties. Thanks to a substantial increase in the dimensions, e.g. width up to 8 m, of the machinery, and the development of simultaneous-stretching systems, the economic production situation has been improved immensely.

Apart from a certain influence of mechanical properties, the manufacturing of films is mainly focused on the transparency and brilliancy (gloss) of the film. Agglomerations or other imperfections caused by the polymer, including solid

additives, diminish the film quality and can become very severe problems in film manufacturing. The optical properties of films depend on the crystallinity, the content of contaminants and the presence of solid particles. The particle size of the latter, as well as their size distribution, contributes the film's desired 'slipperiness'. A proportion of these particles originate from the catalyst system in the case of the dimethylene terephthalate (DMT) process. The development of films is concerned with special applications associated with the machinery in the subsequent process steps according to the customers' particular requirements. The polymer properties can be tailor-made to meet the requirements of numerous applications, such as packaging materials, carrier (for photographic, video and audio tapes, etc.) and engineering materials (capacitors and insulators). The particular manufacturing process will require the achievement of some bulk properties characterized by the molecular structure, molecular weight, crystallinity and surface properties of the polymer. This fact complicates the definition of polymer quality, which is undoubtedly related to individual applications and to the thickness of the film, which can vary between 1 and 200 μm . In addition, many individual surface properties are required in the application, which have to be viewed regarding processability and the various kinds of coatings that may be needed.

In contrast to fiber-forming technologies, the film process requires a comparatively reduced IV due to processing reasons, for example, the pressure along the die and therefore the evenness of thickness as well as the generation of structure, particularly with respect to crystallinity, will need to be considered. As usual, a compromise between intrinsic physical properties and processing has to be found.

The homogenous distribution of the melt improves the smoothness of the film owing to the uniform formation of structure and is therefore the aim of any film-casting process. The assumed distribution functions available in the literature do not explain satisfactorily the orientation phenomena of biaxially oriented films. The mechanism of structure formation and orientation of biaxial processing is very complicated and completely different in comparison to that of fiber spinning. From a theoretical point of view, six types of orientation during stretching are possible, which underlines the complexity of this processing step. Three main factors govern the resultant structure of the film, namely the kind and perfection of oriented crystallites, the overall degree of crystallinity and the ratio of *trans/gauche* conformations in the amorphous regions. In analogy to fiber processing experiences, a strong influence of highly oriented amorphous regions, caused by extreme extension, could be observed.

The ratio of *trans/gauche* structures, as determined by infrared (IR) spectroscopy is increasingly gaining importance. The amorphous, cast film commonly contains about 13 % *trans* and 87 % *gauche* conformer. The *gauche* structure is converted to the *trans* conformer by uniaxial stretching, while the *trans* content increases with increasing stretching ratio. The amount of *trans* conformer at a certain degree of crystallinity determines the mechanical properties of the

film. Transverse stretching induces movement of the crystallites from the longitudinal to the transverse direction, which is associated by a more balanced orientation [32].

A higher molecular weight improves the mechanical properties of the film, but reduces the control of the film thickness. Therefore, the drawability of the longitudinally oriented film in the transverse direction is one of the most important requirements of the polymer. Branched and more flexible polymers tend to show improved biaxial stretchability and therefore reduce the tendency to splitting or breaking during processing. Plasticizers have a similar effect, but they may influence the surface properties and have an effect on the later coating processes.

During stretching in one direction, about 20 % crystallinity can be reached depending on the draw ratio. Subsequent transverse stretching causes an increase of crystallinity by 5 %. The degree of crystallinity increases to 45–50 % during heat setting, which is a consequence of a crystallite melting–reorganization mechanism and crystal growth.

The structure of films has been studied by several methods, such as X-ray diffraction, IR spectroscopy and nuclear magnetic resonance (NMR) spectroscopy, although the simplest and least expensive technique is that of optical diffraction measurements.

4.1 SURFACE PROPERTIES

The necessity to make articles such as video or magnetic tapes more compact, urges manufacturers to reduce the thickness of the base film with all the problems of compromising the advantageous surface properties of thin films. Apart from the basic requirements of mechanical and optical properties, the variety of applications requires more custom-made products regarding smoothness, roughness, abrasion resistance of the additives at the surface, and generally improved processability in the different conditions of subsequent processing. Poor smoothness of the base film leads to the appearance of ‘drop-out’, which is caused by the phenomenon of inhomogeneities of the back surface of the base film being transferred to the coating layer, thus resulting in poor recording of information by the magnetic coating. Any kind of uneven film surface, including that caused by polymer, dust or debris of abraded material, etc., induces such drop-out. Compromises have to be found between surface smoothness (roughness) and ‘slipiness’. Polyester films have to satisfy two principal requirements, which in practice, are often counterproductive. The films should have a good slip, thus enabling handling in processing, particularly in rolling up, *and* a smooth surface as a prerequisite for coating. Slip of the film, as determined by the coefficient of friction, can be controlled by adding fillers during polymer processing. Their particle size and particle size distribution, as well as their hardness (Mohs scale of hardness) influence the surface properties. Highly sophisticated applications,

such as video or magnetic tapes, require perfect surface properties, most notably a low degree of roughness as well as abrasion and scratch resistance of the filler particles. The coefficient of dynamic friction is therefore the main indicator of the roll-up properties. Its value provides information on the slip behavior and therefore allows predictions regarding the roll-up properties. Another property related to the surfaces of the films is the height and distribution of protrusions. This can be measured via interferometry, which is based on counting the amount and the height of the particles, as well as defects at the surface. The presence of defects in connection with the height of the incorporated particles diminishes the quality of magnetic tapes by deteriorating the magnetic properties.

Roughness can be promoted by heat treatment during setting, which causes different growth rates of the spherulites and additionally agglomeration of filler particles. Many small spherulites can be found at lower temperature, while fewer, but bigger particles occur at high temperatures (Ostwald ripening). The maximum growth rate is commonly observed at 180 °C. In addition, the formation of porous surfaces also can be caused by the migration of oligomers. It should be noted that the migration of additives affects the surface properties, in particular due to the different thermal histories, for example, quenching or contact with cold rolls.

Commonly, roughness can be tailored by using additives. These are mainly based on combinations of inert, inorganic particles of different sizes and the weight ratio of large to small particle sizes. These particles should be well dispersed in the base film to prevent abrasion, which is influenced by the particle shape and the kind of embedding in the polymer matrix. The affinity of these particles to the solid polymer seems to be based on adhesion of the melt to the solids and to cohesive forces in the solid state. This phenomenon, however, has not yet been explored in sufficient detail.

Scratch resistance depends on the hardness of the added particles. The problem of a lack of this property can be addressed by adding chemically identical particles of different crystal modification and Mohs hardness. The preferred additives are silica, alumina, layered silicates such as kaolin, titania, barium sulfate and calcium carbonate. The latter is only suitable for the DMT process owing to side reaction caused by acidity during the terephthalic acid (TPA) route.

Insufficient abrasion resistance can become a severe problem in film manufacturing. This problem has to be viewed to a certain extent in relation to 'slipperiness' or roughness of the film. Slipperiness is commonly improved by the addition of solid particles. In this way, the formation of protrusions and depressions in the film surface reduces the contact between the latter and the guide rollers. Large particles in the raw polymer cause a more significant slipperiness-improving effect than smaller ones. In precision applications such as video or magnetic tapes, large particles induce a higher degree of drop-out due to increasing abrasion. The smoothest possible surface consisting of fine particles is required for such applications. It has been recognized that the incorporated filler particles of the film can be surrounded by voids. Peeling of the particles

occurs during biaxial stretching at elevated temperatures. The fine particles resist the stress of deformation to a greater extent than the coarser ones owing to their state of fixing, and therefore the surrounding voids of the large particles are relatively larger. The extent of the protrusions becomes smaller during stretching with increasing size of the voids, which is accompanied by increased friction. Consequently, damage to the surface is likely to occur. The requirement for a suitable and uniform size of the protrusions at the surface becomes understandable in view of these aspects. Frictional abrasion occurs during passing of the film over rolls rotating at different speeds, and more seriously, by passing the film over stationary guides, rolls and the like. The fixing of the embedded filler particles in the film is therefore of great importance and seems to be related to viscosity and/or the content of carboxylic end groups (CEGs) in the starting polymer. In the case of lower-viscosity polymers and a higher CEG content, the abrasion is significantly reduced [33].

4.2 STREAKS

The performance of films and their subsequent processing are determined by the homogeneity of the film thickness. Uniform thickness across the width of the film is a fundamental requirement for film production. The problem of thickness variations can be caused by an increased width of the machinery up to 6 m (and higher), as well as a decreasing thickness of the product. Therefore, a homogeneous melt flow is the main prerequisite of any film manufacturing process. This is also the reason for reducing the IV for film production, because this stabilizes the distribution of the melt along the die. Any deviation of melt viscosity diminishes the uniformity of thickness and favors the appearance of streaks. The flow properties, and therefore the melt viscosity, have to be kept constant. Deviations of the IV cause visible streaks in the manufacturing direction, due to a varying flow behavior of the melt, which is dependent on its viscosity. Besides this, variations of the IV can also influence the shrinkage behavior and crystallization in processing.

All factors affecting the constancy of the IV – as there are non-uniform IVs of the heated chips or non-constant heating conditions during extrusion, and inappropriate conditions regarding residence time, temperature and particularly the variable water content of the dried chips – are additional reasons for streaks. Hydrolytic degradation caused by insufficient drying is still a problem of film manufacturing, usually manifested in the formation of streaks. Streaks can also be observed in cases of particle separation during extrusion. In the molten state, the solid additive often tends to aggregate and forms streaks via separation after quenching. Streaks can also appear by insufficient ‘pinning’. This latter term means pressing the molten film against the chill roll by electrostatic forces to improve the efficiency of quenching. The functioning of pinning equipment can

be drastically reduced by a high content of oligomers in the polymer. Layers of oligomers are built up at the pinning wire, which is accompanied by a loss of efficiency. This leads to non-uniform cooling and therefore to heterogeneous degrees of crystallinity, associated with the appearance of streaks. The formation of droplets at the lip of the die, mostly consisting of degraded polymer and oligomers, is also responsible for the formation of streaks.

4.3 PROCESSABILITY

Interruptions of the film process are mainly caused by breaks, particularly by splitting during transverse stretching. Restarting of the process takes time and leads to tremendous losses. Polymers characterized by an increased melt strength exhibit a lower tendency to splitting and therefore improve the processability. Inhomogenous distribution of additives, plus their shape and hardness, agglomeration and contamination impair quality, performance and the utility value of the final products. The structure of the film and the conditions of its production determine its qualification for subsequent processing. Therefore, high standards are demanded regarding the suspending technology of the additives and the conditions, kind and location, as well as the time of adding during the polymer process.

The influence of oligomers on the surface properties and processing is very similar to that mentioned above for the case of fiber spinning. The deposition of oligomers at the surface of the film diminishes the homogeneity of surface properties and causes crater-like holes with different coating behavior and roughness. Certainly, the formation of a homogenous structure and the drawability of the film, particularly with thinning diameter, becomes more and more problematic.

The recovery of the separated, as-made (not drawn) film from the stenter influences the quality and economy as well. About 30 % of the employed polymer has to be recovered in modern film manufacturing. These strips are chopped and refed into the extruder, together with the raw polymer. The purity, water content and IV of this waste control the quality of the resultant film to a certain extent. The degree of blending between raw polymer and waste polymer depends on the final application and can vary. In practice, the addition of more waste is allowable in the manufacturing of packaging film. The importance of appropriate drying, in context with waste recovery, has to be underlined again.

5 BOTTLES

The demand of PET for packaging applications is growing fast. This fact is based on the outstanding and versatile properties of PET, such as tensile strength, toughness, dimensional stability, transparency and chemical resistance. The need

to reduce the crystallinity of PET bottle polymer by chemical modification was revealed at an early stage of the development. In this way, the advantage of the crystallinity of PET could be combined with an improved processability in blow molding. The polymer becomes more flexible and mobile, while still maintaining a necessary toughness. Chemical modification of PET is focused on a reduction of the cycle time at lower temperatures and the reduction of AA formation as a consequence of thermal decomposition. In addition, good physical properties, such as high tensile strength, low creep at low weight/volume ratios, high impact resistance (toughness) and good barrier properties, as well as transparency and color, are required. For bottle manufacturing, the crystallization rate of the polymer should be suppressed.

These desired mechanical properties of bottle material mainly depend on molecular weight, crystallinity and orientation and can be achieved by using a modified polymer in combination with biaxial orientation and a maximum degree of crystallinity. The necessary increased molecular weight responsible for the tensile stress can commonly be obtained by solid-state polycondensation (SSP) processes. In addition, the procedure requires careful drying of the polymer before processing to prevent hydrolytic degradation. The higher the crystallinity, then the better will be the mechanical properties of the product. This application needs therefore a tough and more flexible polymer to resist 'top-loading'.

Thermoplastic polyester resins for the manufacturing of bottles are commonly based on at least 97 % PET modified by components, which suppress crystallization. Useful modifying chemicals are isophthalic acid (IPA), diethylene glycol (DEG), cyclohexane dimethanol (CHDM) and other comonomers that can be expected to modify the polymer chains to a certain extent, hence hindering the packing into a crystalline lattice. The degree of modification represents a compromise between melting point, flow behavior and crystallization rate. The limiting factor of modification is the T_g of the final modified polymer, which should be high enough to withstand higher temperatures than required for the ultimate application, i.e. the bottle.

The flow behavior of the polymer preferentially influences the uniform shell thickness and is related directly to the molecular structure of the modifying comonomer. Modifications of PET, particularly with CHDM, improve the flow behavior during injection molding and significantly reduce the melting point of the polymer. The decreased melting point of the copolymer allows reduced processing temperatures and therefore correlates with a reduced formation of unwanted AA at shortened cycle times.

The optical properties of bottles are a matter of crystallinity affected by nucleation, depending on the content and size of light-scattering polymer solids. The purity of the raw materials and the cleanness of the reactors are prerequisites for satisfactory quality. Bottle polymer should display as little contaminations as possible. The detection of impurities is carried out by the same methods as mentioned above. Thorough filtration of the polymer is therefore mandatory. It should

be noted that the quality of TPA has a significant influence on the quality of the polymer. The size and hardness of the TPA particles affects the conversion during the esterification reaction due to its poor solubility in the monomer. Chemical impurities in the raw materials, such as heavy metals, carboxybenzaldehyde, toluenic acid and other aldehydes, and the quality of the recovered EG, influence the color of the polymer, as well as its thermal stability.

Apart from the physical properties mentioned above, some special properties are desired with respect to gas permeation of oxygen, carbon dioxide and water, as well as a minimum content of AA. The high processing temperatures (exceeding 270 °C) give rise to the formation of AA, which, even in very low concentrations, imparts a disagreeable aftertaste to food and drinks. The AA content can be lowered significantly by the use of appropriate conditions for the melt-phase and SSP reactions, in connection with careful drying and gentle processing. The residual AA levels can be reduced to less than 0.5 ppm via efficient drying. When PET degrades and the preform is cooled, the AA is trapped in the molten matrix and will later diffuse slowly into the liquid contained in the bottle. This low AA level increases during blow molding. The amount generated in the preform increases with temperature, residence time in the molten state, and the shear rate, as well as the injection pressure, and decreases with efficient cooling of the preform. The optimum of these conditions keeps the AA in the preform in the range of less than 6 ppm. Methods of suppressing the formation of AA will be discussed below.

One impediment of universally applying PET in the area of packaging is its gas-barrier properties. These can be slightly improved by measures to increase the density (crystallinity) during blow molding, for example, by treatment with ultrasound. Ultrasonic treatment during injection reduces the gas permeability to a certain extent [34].

The modification of PET with naphthalene-2,6-dicarboxylic acid and other additional comonomers is a common measure in bottle manufacturing. Copolyesters based on this compound show excellent barrier properties. Such materials can be produced by addition of the desired amount of comonomer during polymer processing or by blending PET with poly(ethylene naphthalate) (PEN). Additionally, PEN can also be modified by other comonomers such as isophthalic acid (IPA) to improve the flow properties and reduce the melting point. The high price of naphthalene dicarboxylic acid is the reason for its limited application. The overall cost may be reduced by using TPA or IPA as comonomers.

The other severe problem in the application of PET regarding food containers or bottles is that these products cannot be hot-filled. This limitation is caused by the low T_g of PET, which causes shrinkage during hot-filling. Alternatively, multilayer containers can overcome the problems, but, however, at higher manufacturing costs. PET in combination with an intermediate layer of poly(ethylene-*co*-vinyl alcohol) (PEVOH) or polybutylene has been used in such

applications. The manufacturing of these bottles, preferentially by co-injection, and their recycling is, however, complicated and expensive.

Again, polyesters based on naphthalene-2,6-dicarboxylic acid can meet the desired properties, plus have other additional advantages. Food components containing double bonds or conjugated double bonds are extremely sensitive to light-induced reactions, such as photo-oxidation. The addition of UV stabilizers is therefore necessary to protect the content of PET bottles against UV irradiation. PET, in contrast to PEN, does not show intrinsic UV protection properties.

The production of bottles are based on a two-step process. Preforms are produced by injection molding, followed by blowing, which results in orientation and the desired final properties. The latter process is carried out under infrared (IR) heating. Due to economic reasons, the cycle time should be reduced by accelerated heating, which can be achieved by enhanced IR absorption properties of the polymeric material.

The addition of finely dispersed solid particles improves the IR absorption of the polymer and positively influences blowing of the preforms. Such solid particles can be obtained by the reduction of Sb^{3+} to metallic antimony during polycondensation by the addition of trivalent phosphorous compounds such as phosphonic acid or its esters (phosphites). However, only a slight improvement in properties could be achieved by this approach [35].

IR absorption can also be achieved by the addition of fine carbon particles (3–60 ppm) to the polymer. These particles have to be small enough to be invisible to the naked eye [36].

5.1 PROCESSING

Generally, the processing conditions in blow molding seem to have more influence on the final product quality when compared with other technologies of polyester processing. The effects of many types of unsuitable processing conditions, such as temperature and humidity caused by insufficient drying, can be attributed to the more sensitive state of bottle polymer material. Insufficient drying of the polymer prior to processing impairs the tensile strength. In addition, fine voids can be observed at the fracture surface. These voids are caused by hydrolytic degradation. Mold temperature promotes crystallization but also affects color, surface gloss and thermal stability. Depending on the shell thickness, low mold temperatures afford a more pronounced difference of the crystallinities in the skin and the core regions. The kind and the degree of modification of the polymer influences the crystallinity of the bottles in relation to shell thickness. The interplay between shell thickness and mold temperature, as well as the cooling rate, is responsible for the properties of the final parts. A decreased shell thickness requires an increased mold temperature to achieve high crystallinity. Due to the importance of crystallinity with respect to the physical properties, differential scanning calorimetry (DSC) provides vital information on the degree of

crystallization. The ratio, $\Delta H_{cc}/\Delta H_f$, calculated from DSC data is a good indicator of crystallinity (ΔH_{cc} = heat of cold crystallization; ΔH_f = heat of fusion). The parameter, the temperature of cold crystallization (T_{cc}) is easy to measure, and its value characterizes the crystallization rate very well. The higher the value of the ratio $\Delta H_{cc}/\Delta H_f$, then the lower is the crystallinity of the analyzed polymer. High temperatures cause increased crystallinities, dense packing of the molecules in the crystalline lattice, bigger crystallites and a higher degree of disorder in the amorphous domains.

The production of bottle polymer is commonly based on the SSP process. Due to the sensitivity of the blow molding process, the bottle polymer is characterized by a constant IV, which should not deviate by more than 0.02 dL/g. Like film polymer, the chips should have a good gloss and a high degree of transparency. The required good color of the polymer is influenced by the catalyst system, its content and the conditions of polymer processing. The use of the extremely expensive GeO_2 provides by far the best color, as well as gloss. So-called 'blue toners' are added to the process of prepolymer production to reduce the yellowish tinge. The most preferential additive is cobalt acetate, although thermally stable, blue organic dyestuffs dispersed as pigment or soluble in the polymer, can also be used. Their content significantly reduces the transparency, depending on the molecular structure and concentration of the added dye.

Bottle polymer should have a minimum of contaminants, the determination of which is carried out by the same methods as mentioned above for fiber polymers. It should be noted that the quality of the TPA as a starting material has a significant influence on that of the polymer. The color is affected by the content of chemical impurities in the raw material, such as heavy metals, carboxybenzaldehyde and toluenic acid.

A very important factor of bottle polymer is its thermal stability, which depends on the conditions of its manufacture and the thermal history of the polymer. The amount of carboxylic end groups (CEGs) is a good indicator of the qualification of the chips. Continuously produced polymer should contain no more than 25 eq/kg CEG. Little differences between the TPA and DMT routes towards bottle polymers are observed. Chips from batch processes show higher CEG values (30 meq/kg and more). The thermal stability depends on the use and efficiency, i.e. mainly the concentration, of stabilizers.

Oligomers influence the optical properties of the final bottle material and the efficiency of the blow molding process. Like in film production, oligomers affect the surface and therefore the clarity (haze) of the bottle. They additionally contaminate the equipment used for bottle processing. Interruptions of the process for cleaning operations are the undesired, but unavoidable consequence [37]. According to this patent, the content of the cyclic trimer should not exceed 0.40 wt%. The formation of oligomers is controlled by the concentration of the different end groups. The higher the content of hydroxyl groups, then the lower will be the tendency to form oligomers. The content of oligomers in the prepolymer is

Table 13.4 Variation of the acetaldehyde content in PET depending on the processing stage

Polymer material (IV ^a)	Content (ppm)
Prepolymer (0.662)	>25
SSP polymer (>0.80)	<3
Preform (>0.80)	<6
Bottle (~0.80)	<8

^a In units of dL/g.

usually in the range between 1.0 and 2.0 wt% and can be reduced to 0.5–1.0 wt% and less via SSP. The reduction of the CEG content assists in reducing the formation of oligomers. It should be noted that remelting of the polymer during processing induces the regeneration of oligomers, depending on temperature and residence time in the molten state, as can be seen above in Figure 13.9 [38]. In addition, remelting of the chips in bottle processing influences the formation of AA, which increases from a level of <3 ppm to values up to ~8 ppm in the final bottle material (Table 13.4). The deterioration of quality by remelting is illustrated above in Figures 13.8 and 13.9. The extent of degradation can be minimized by employing gentle processing temperatures.

5.2 THE QUALITY OF POLYESTER BOTTLE POLYMER

Some additional aspects regarding the quality of polyester for bottle application are reviewed at this stage, as the polymer quality is of utmost importance to bottle manufacturing.

5.2.1 Definitions of Color, Haze and Clarity

The optical behavior of a polymer indicates the purity of its ingredients, such as the raw materials, the kind of additives and the conditions of production. Therefore, the optical properties are of importance, in particular for judging bottle grade polymer.

Color is determined by reflectance and can be determined by using a colorimeter based on the CIE color system. This method expresses the brightness as Color L^* , the absorption at the green–red axis as Color a^* and the yellowness as Color b^* along the blue–yellow axis of this color coordination system.

Haze is generally caused by the scattering of light in crystalline polymers. Optical inhomogenities with dimensions in the wavelength range of visible light cause haze. The latter often corresponds to the spherulite volume fraction, spherulite size and crystallinity. An increased size of spherulites results in

enhanced haze owing to the light scattering of these crystalline 'particles'. Optical *clarity* is extremely important for film, bottle or container applications, as mentioned above. The polymer begins to crystallize by the formation of spherulites in the case of insufficient cooling, associated with the appearance of haze or opacity. Just small concentrations of spherulites can cause a high degree of haze, even at low crystallinity. Thus, quantification of the contributions from spherulites and crystallinity is very difficult.

In the context of crystallinity as a crucial factor with respect to haze, it has to be pointed out that PET and PBT as the most industrially used polyesters are both crystallizable depending on the conditions of subsequent processing. The amorphous state can be obtained by a rapid quenching of the melt below the T_g . Heating above the T_g induces fast crystallization. PBT exhibits a significantly increased crystallization rate when compared with PET.

The content of heterogenous particles, including contaminants determines the crystallization rate via a nucleating mechanism. Every type of solid, such as catalyst residues, additives, gels or degraded polymer, can function as a nucleant [38]. Therefore, haze or transparency depends largely on the concentration of these particles. As a result, all of the known parameters influencing crystallinity, such as a modification of the polymer, molecular weight, presence of nucleants, cooling rate and stress, affect the transparency.

5.2.2 Color

The color of the final product primarily depends on the qualification of the raw materials, TPA, DMT and EG. The content of heavy metals in TPA, residues of catalysts employed during oxidation of *p*-xylene, and polymer processing affect the final color of the polymer. The tendency of certain catalysts, such as titanium or tin derivatives, to make the polyester yellowish in color is well established. The conversion during esterification is prolonged due to larger TPA particles or their hardness. Color can be influenced by these factors, as well as by chemical impurities in the raw materials, such as water, aldehydes or the quality of insufficiently recovered EG. Similar effects on color can be observed as a result of impurities caused by additives, particularly from less purified Sb_2O_3 . The quality of the latter can be assessed simply by the color of its solution in EG.

The color of the polymer can also be affected by inappropriate reaction conditions in the polymerization process, such as temperature, residence time, deposits of degraded polymer or the presence of oxygen. Degradation of polyesters and the generation of chromophores are thermally effected [29b, 29c, 39]. The mechanism of thermal decomposition is based on the pyrolysis of esters and the formation of unsaturated compounds, which can then polymerize into colored products. It can be assumed that the discoloration takes place via polymerization of the vinyl ester end groups or by further reaction of AA to polyene aldehydes.

The use of so-called 'toners' to improve the color has been described above. It should be remarked that all measures to overcome defects of a polymer caused by disregarding the 'basic principles of chemistry' are rarely of durable success, because any additive will complicate or affect the polymeric system in an undesired way.

5.2.3 Stability

The thermal stability and lightfastness of polyesters is particularly necessary for technical and high-performance applications. The modification of the polymer causes disorder and affects the stability as well as some other properties. PET modified by DEG suffers particularly from photo-oxidative reactions due to the presence of the sensitive ether bonds. These copolymers need special stabilization depending on the kind and degree of modification. The UV stability can also be influenced by the technology of the process, whereby slight improvements of DMT-based polymer are observed [29].

Polymer degradation can be investigated by detecting the degree of decomposition via (a) the rate of change of IV, (b) melt viscosity, or (c) the rate of changed end groups, as CEG or vinyl ester groups. The rate constants and activation energies for the thermal degradation of PET are presented in Table 13.5. The temperature dependence of this degradation reaction is illustrated in Figure 13.20 [29b, 29c, 39]. This methodology is additionally recommended for stability tests. The reaction is accompanied by the generation of volatile products such as aldehydes, CO₂, water, etc. The rate of degradation is accelerated in the presence of oxygen.

Table 13.5 Reaction rate constant^a and activation energy data for the thermal degradation of PET [29b, 29c, 39]. From 'Thermal degradation of PET. A kinetic analysis of gravimetric data', Covney, J. D., Day, M. and Wiles, D. M., *J. Appl. Polym. Sci.*, **28**, 2887 (1983), copyright © (1983 John Wiley & Sons, Inc.). Reprinted by permission of John Wiley & Sons, Inc.

Source of calculation	k (10^3 h ⁻¹)			E_a (kcal mol ⁻¹)			
	Reference			Reference			
	[7]	[12]	[14]	[7]	[12]	[14]	[17]
Intrinsic viscosity	1.3	2.3	1.4	62.3	—	—	—
Melt viscosity	1.7 ^b	—	—	—	32.0	48.0	—
Total gas	—	—	—	—	—	—	38.0
—COOH	3.5	—	—	41.7	—	—	—
—OH	2.4	—	—	—	—	—	—
—CHO	0.2	—	—	—	—	—	—
Total end groups	1.2	—	—	58.7	—	—	—

^a Measurements carried out at 282 °C.

^b Determined at 290 °C.

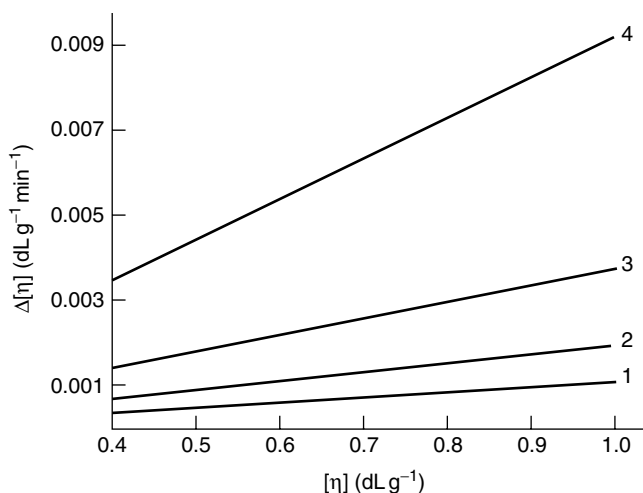


Figure 13.20 The rate of thermal degradation of PET as a function of the intrinsic viscosity measured at different temperatures: 1, 280 °C; 2, 290 °C; 3, 300 °C; 4, 310 °C [29b, 29c, 39]. From 'Thermal degradation of PET. A kinetic analysis of gravimetric data', Covney, J. D., Day, M. and Wiles, D. M., *J. Appl. Polym. Sci.*, **28**, 2887 (1983), copyright © (1983 John Wiley & Sons, Inc.). Reprinted by permission of John Wiley & Sons, Inc.

An easy method for investigating the thermal-oxidative degradation of PET is differential thermal analysis (DTA), which indicates thermal degradation by the appearance of an exothermic peak in the range of the melting temperature. This approach also can be used to assess the efficiency of stabilizers [40].

5.2.4 Acetaldehyde

The generation of acetaldehyde (AA) as a decomposition product in PET processing plays an important role in bottle manufacturing. This depends on the 'vicious circle' of the polymer stability, the AA content of the chips prior to processing, and the processing conditions. The basis of stability is a qualified polymer produced under appropriate conditions. This argument also includes the SSP process which can drastically reduce the AA content of the chips, as shown in Figure 13.21.

Decreased chips sizes favor the removal of AA due to improved diffusion conditions during the SSP process. Nowadays, solid-state produced polymers contain less than 2 ppm of AA. Formation of the latter is more pronounced with increasing temperature and prolonged residence time in the molten state during processing. The presence of water due to insufficient drying of the polymer reduces the generation of AA but enhances hydrolytic degradation. The generation of AA during

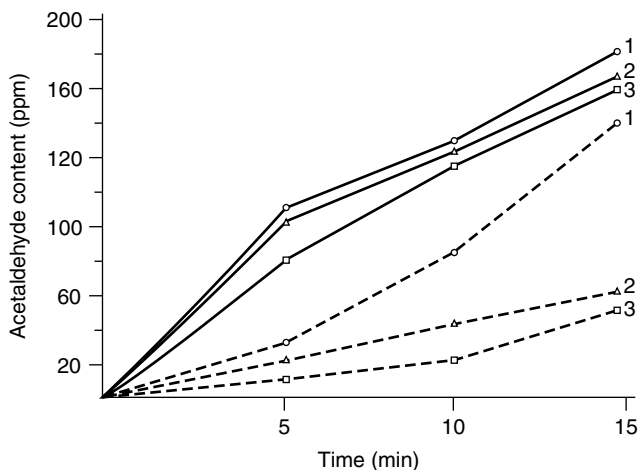


Figure 13.21 Regeneration of acetaldehyde in a closed system at different melting temperatures: 1, 290 °C; 2, 280 °C; 3, 270 °C: (—) in air; (----) in helium [38]. From Wick, G., 'Characterization of PET Polymer for Bottle Manufacturing', presentation given at the *Society of Plastics Engineers, Benelux Seminar*, May 20–21, 1980, Amsterdam, and reproduced with permission of KoSa GmbH & Co. KG

processing can be suppressed by certain additives. The latter are selected from the groups of polyamides or polyesteramides, although ethylenediamine tetraacetic acid, zeolites and protonic acids are also effective [41]. The addition of these components is preferentially conducted during extrusion.

5.2.5 Barrier Properties

The barrier properties are of the highest importance in the packaging of food and beverages. The loss of aroma, water and carbon dioxide, and the diffusion of oxygen into the bottle, by migration depends on the barrier properties, which is therefore a decisive factor in bottle manufacturing. The mechanism of migration is based on the absorption of the gas in the shell on the inside of the bottle, as well as the diffusion of the primarily absorbed gas to the surrounding polymer matrix (bottle material). This type of migration therefore follows the laws of diffusion. The barrier properties are therefore influenced by the crystallinity, the degree of orientation after stretching, and the content of amorphous regions. The latter is the main reason for increased permeability. All attempts to increase the density (i.e. increase the crystallinity) in bottle manufacturing are therefore aimed at improving the barrier properties. It can be assumed that the crystallinity of a conventional bottle is in the range of 15 to 20 %. This value can be increased under certain conditions to values of up to 35 %, which is accompanied with

a significant reduction of the permeability. Blending of PET with PEN results in additional improvement and seems to be the optimum solution of the problem at present. In addition, it is known that an increase of the isophthalic acid (IPA) content of the polymer up to 10 % enhances the gas barrier properties for oxygen by 25 % without adversely affecting the processability. The crystallinity achievable for these modified polymers lies in the range of standard bottle polymer [42]. There may also be other possibilities for improving the barrier behavior of polyester bottles via the modification of PET with suitable components. The cost of these components and other aspects of consideration, particularly the recycling of bottles, plus health and environmental reasons, will restrict such development to a minimum effort.

6 OTHER POLYESTERS

It should be taken into account that all of the aspects described above are of a general nature and therefore more or less valid for any kind of industrially relevant polyester resin. Upon closer examination, the experiences gained with PET are particularly applicable to poly(butylene terephthalate) (PBT), poly(trimethylene terephthalate) (PTT) and poly(ethylene naphthalate) (PEN). These polymers have gained major industrial importance as a result of a number of different properties in comparison with PET.

PBT is used for textile applications due to its stretchability, increased crystallinity and improved dyeability. It is introduced in the production of carpets and stretchable fabrics, where a certain degree of elasticity is desired. PBT is used preferably for the production of engineering plastics due to its combination of dimensional stability, tensile strength, increased flexibility and fast crystallization rate.

PTT has been the basis for textile purposes such as elastic, well dyeable fabrics, and particularly carpets, for many years. Both PBT and PTT are used unmodified due to their low T_g s ($<45^\circ\text{C}$).

The production of these three polyesters and their processing can be carried out principally in the same equipment as that used for PET processing. It is easy to understand that the methods considering the quality and processability of PET are directly applicable to these materials, with the exception of PEN. Only this polymer causes analytical problems due to its poor solubility in common organic solvents. Much attention has been paid to PEN. This polyester exhibits very interesting properties, which make it applicable for high-performance filaments and packaging materials. Tyrecord yarns based on PEN are characterized by high mechanical strength, associated with a high modulus, low shrinkage and significantly increased stability. In addition, this material is currently being introduced as a polymer for bottles and medical instruments, which require hot-filling and hot-sterilizing, respectively. PEN bottles have extremely reduced gas permeation

properties due to the excellent barrier properties of this polymer. Its stiffness can be reduced by modification with PET. PEN fluoresces strongly and tends to yellow upon exposure to UV light. This behavior can become a limiting factor with respect to film and fiber applications. Developments in its use in food packaging is therefore focused on fluorescence quenching. The high cost of naphthalene dicarboxylic acid as a starting material is the reason for focusing activities towards finding copolymers of similar quality and acceptable cost. PEN shows outstanding properties with respect to tensile strength, gas barrier properties, a high T_g and the capability of absorbing UV radiation. The high thermal stability has upgraded this material for high-performance applications. The drawbacks of PEN are its relatively high melt viscosity and its overall performance. Compromises could be found to improve the processability in connection with economic considerations. Po' *et al.* have reported the possibilities of these materials in an excellent article [43].

The synthesis of copolyesters containing PET is difficult due to the problems arising from the different melting temperatures of the homopolymers and their mutual incompatibilities. Reactive blending of homopolymers seems therefore to be the best way to obtain copolymers of the desired composition. The polycondensation of PEN is carried out at higher temperatures than that of PET. Reactive blending can be carried out during extrusion, before the SSP stage. The structure of the resulting materials is determined by the degree of 'randomness' (RD) and is related to the sequence length of the PEN and PET blocks, which can be determined by ^1H NMR spectroscopy.

According to these authors [43], the RD is influenced by temperature and mixing time and is limited by the length of the extruder in commercial-scale production. Long mixing times result in thermal degradation and discoloration. Each melting or cooling step of these copolymers increases the RD by about 0.05 of its value. The degree of randomness can be expressed by the following equations:

$$RD = 1/L_T + 1/L_N \quad (13.1)$$

$$L_T = 1/(1 - X_T)RD \quad (13.2)$$

$$L_N = 1/(1 - X_N)RD \quad (13.3)$$

where L_T and L_N are the lengths of the PET and the PEN segment, respectively, and X_T and X_N the molar monomer fractions. The RD influences the crystallization kinetics of a given copolymer composition. At high values of the RD , slower cooling rates are required to obtain an optimum of transparency. The crystallization of random copolymers ($RD(1)$) is only possible at a PET unit content of less than 20 % and more than 80 % with a monomer sequence length of 5–6.

The admixing of additional catalysts during blending increases the transesterification reaction but seems to affect the color of the final product. Conventional

catalysts such as the oxides of antimony and germanium are used in this application. The randomization of the blends requires long reaction times. The SSP process seems to increase the *RD* to a certain extent.

Because of the widespread use of plastic films in packaging applications, a need for films with different combinations of properties has been recognized. For example, films are required to exhibit the combination of good flexibility and a relatively high melting point. To achieve this, TPA is partly replaced by a certain amount of cyclohexane dicarboxylic acid or other aromatic or aliphatic diacids [44]. The replacement of ethylene glycol by CHDM leads to interesting products for engineering plastics. At a degree of modification of 25–30 mol%, amorphous copolyesters can be produced that are suitable for sheet applications. It should be noted that the processing of these materials is problematic owing to the lack of drying. It is well known that the type and amount of comonomer influence the T_g and the crystallinity of the polymer and increase the tendency to sticking in the drying process. Therefore, amorphous polyesters cannot be dried via conventional methods.

Finally, the use of low-melting polyesters for low-melt fibers (melting point, 110–180 °C) should be pointed out, where TPA is replaced partly by IPA or adipic acid for bond fiber application.

Copoly(ether ester)s consisting of short-chain crystalline segments of PBT and amorphous poly(ether ester) of poly(tetramethylene terephthalate) exhibit a two-phase structure and can be used for the production of high-impact-strength engineering plastics. These very interesting materials with their outstanding properties understandably require stabilization to heat and UV exposure [45].

7 CONCLUSIONS

The rapid development of polyester resins, beginning with those for textile and film, and later for packaging purposes, is based on the variety of potential applications resulting from the outstanding properties of this class of polymer. The adjustment to special applications can be achieved via chemical modification by copolycondensation or by adding additives to the polyester during processing. Considerable advances could be achieved by technological improvements and the use of more qualified ingredients, particularly with respect to the raw materials.

This review is based on the principles of structure formation and tries to bridge the gaps between polymer quality, industrial processing and the resultant properties. The formation of an optimum structure is commonly the decisive step in processing. It can be significantly influenced by disruptive factors, such as imperfect polymer quality and inappropriate processing conditions or technology. A knowledge of these correlations is the key to progress and recalls the experiences gained from laboratory-scale chemical syntheses. Success is ruled by the use of highly qualified chemicals, gentle reaction conditions and appropriate

equipment. This chapter also touches on practically applicable analytical methods of industrial production control and the importance of quality management.

Finally, it needs to be noted that the final answers to questions concerning the processability and the qualification of a polymer reflect its behavior only in the individual circumstances of the commercial processing. The analytical methods described are only a tool for understanding special sectors of materials properties and how to solve problems in industrial polymer processing.

REFERENCES

1. (a) Ludewig, H., *Polyester Fibers* (English Edition), Wiley-Interscience, New York, 1971; (b) Mark, H., Atlas, S. M. and Cernia, E., *Man-Made Fibers*, Wiley-Interscience, New York, 1967; (c) Ziabicki, A., *Fundamentals of Fibre Formation*, Wiley, New York, 1976.
2. Hill, J. W. and Cuculo, J. A., Isothermal elongational rheology of PET, *J. Appl. Polym. Sci.*, **33**, 3 (1978).
3. Jabarin, S. A., Crystallization kinetics of PET I. Isothermal crystallization from the melt, *J. Appl. Polym. Sci.*, **34**, 85 (1987).
4. Shimizu, J., Okui, N. and Kikutani, T., Simulation of dynamics and structure formation, in *High-Speed Fiber Spinning*, Ziabicki, A. and Kawai, H. (Eds), Wiley, New York, 1985, pp. 173–201.
5. (a) Ziabicki, A. and Jerecki, L., The theory of molecular orientation and oriented crystallization in 'high speed spinning', in *High-Speed Fiber Spinning*, Ziabicki, A. and Kawai, H. (Eds), Wiley, New York, 1985, pp. 225–269; (b) Davis, G. W., Everage, A. E. and Talbot, J. R., Polyester fibers: high speed melt spinning, *Fiber Producer*, 22 (February 1984).
6. Hoechst-Celanese, *US Patent 4 918 136*, 1990.
7. Monsanto, *US Patent 4 092 219*, 1978.
8. George, H. H., Model of steady state melt spinning at intermediate take-up speeds, presentation given at the *Joint Meeting of the US and Japanese Rheological Societies*, Kona, HI, 6–9 April, 1979.
9. Göltner, W., unpublished data.
10. (a) Ziabicki, A. and Kedzierska, K., Mechanical aspects of fiber spinning process in molten polymers, Part III. tensile force and stress, *Kolloid Z.*, **175**, 14 (1961); (b) Ziabicki, A. and Kedzierska, K., Mechanical aspects of fibre spinning process in molten polymers, Part II. Stream broadening after the exit from the channel of the spinneret *Kolloid Z.*, **171**, 111 (1961).
11. (a) Cogswell, F. N., Polymer melt rheology during elongational flow, *Appl. Polym. Symp.*, **27**, 1 (1975); (b) Gagon, D. K. and Denn, M. M., Computer simulation of steady polymer melt spinning, *Polym. Eng. Sci.*, **21**, 13 (1981).
12. Han, C. D. and Lamonte, R. R. Studies on melt spinning I. Effect of molecular structure and molecular weight distribution on elongational viscosity, *Trans. Soc. Rheol.*, **16**, 447 (1972).

13. Perez, G., Some effects of the rheological properties of PET on spinning line profile and structure developed in high-speed spinning, in *High-Speed Fiber Spinning*, Ziabicki, A., and Kawai, H. Wiley, New York, 1985, pp. 333–362.
14. (a) Shenoy, A. V., Saini, D. R. and Nadkarni, V. M., Rheograms for engineering thermoplastics from melt flow index, *Rheol. Acta*, **22**, 210 (1983); (b) Braun, H., Eckstein, A., Fuchs, K. and Friedrich, C., Rheological methods for determining molecular weight and molecular weight distribution, *Appl. Rheol.*, 116, (June 1996); (c) Weese, J. and Friedrich, C., Relaxation time spectra in rheology: calculation and examples, *Appl. Rheol.*, **94** (June 1994).
15. Munari, R., Pilati, F. and Pezzini, G., A study on the melt viscosity of linear and branched PBT, *Rheol. Acta*, **23**, 14 (1984).
16. Raje, S. S., Shah, W. D., Desai, V. M. and Sankhe, M. D., Molecular weight distribution and its impact on melt spinning of synthetic polymers: Part II, *Man-Made Text. Ind.*, 173 (May 1996).
17. Brody, H., Orientation suppression in fibers spun from melt blends, *J. Appl. Polym. Sci.*, **31**, 2753 (1986).
18. (a) Dietrich, W., Reichelt, G. and Renkert, H., Untersuchungen zum PET-Schmelzspinnprozeß bei Abzugsgeschwindigkeiten von 5000–10 000 m/min, *Chemiefasern/Textilindustrie*, **38**, 612 (1982); (b) Kase, S. and Matsuo, T., *J. Polym. Sci., Part A*, 3, 2841 (1965); (c) Samuels, R. J., Quantitative structural characterization of the mechanical properties of PET *J. Polym. Sci., Part A-2*, **10**, 781 (1972).
19. Bayreuther, R. and Schöne, A., Zum Problem des Fadenbruches beim Schmelzspinnprozeß organischer Hochpolymere unter Berücksichtigung von makroskopischen Störstellen im Elementarfaden, *Acta Polym.*, **34**, 68 (1963).
20. (a) Broughion, A., The detection and analysis of particulate contamination in PET filament yarns, *Text. Res. J.*, 135 (March 1976); (b) Hoffrichter, S., Untersuchungen an Fasern aus PET-Seide, *Faserforsch. Textiltech.*, **19**, 304 (1968); (c) Hoffrichter, S. and Tomoschat, K. D., Über fehlerhafte Fasern im Polyesterfaserstoffen, *Faserforsch. Textiltech.*, **20**, 578 (1969).
21. (a) Toray, *US patent 4 138 386*, 1979; (b) Toray, *US patent 4 067 855*, 1978; (c) Teijin, *Eur. Patent EP-0261 430 A-2*, 1988.
22. Toray, *US Patent 3 951 905*, 1976.
23. (a) Healey, D. H. and Adams, L., Oxidative crosslinking of PET at elevated temperatures, *J. Polym. Sci., Part A-1*, **9**, 2063 (1971); (b) Spanninger, P., Thermo-oxidative degradation leading to gels in PET, *J. Polym. Sci., Polym. Chem. Ed.*, **12**, 709 (1974); (c) Yoda, K., Tsubi, A., Wada, M. and Yamadera, R., Network formation in PET by thermo-oxidative degradation, *J. Appl. Polym. Sci.*, **14**, 2357 (1974).

24. Teichgräbe, M., Gerät zum Nachweis von Gelteilchen in der Spinnmasse, *Faserforsch. Textiltech.*, **12**, 489 (1961).
25. Dulio, V., Po', R., Borrelli, R., Guarini, A. and Santini, C., Characterization of low molecular weight oligomers in recycled PET, *Angew. Makromol. Chem.*, **225**, 109 (1993).
26. Brunsell, A. R. and Hearle, J. W. S., The fatigue of synthetic polymeric fibers, *J. Appl. Polym. Sci.*, **18**, 267 (1974).
27. Kassenbeck, P. and Marfels, H., Beitrag zur Kenntnis der Art und Verteilung an Oligomeren in PET, *Lenzinger Ber.*, **43**, 34 (1977).
28. Thiele, U., Which criteria of polymer lines of PET Production determine quality and purity of the melt (in German), presentation given at the *3rd Plastic Symposium of Gneuß* Bad Oeynhausen, Germany, 15–16 September, 1999.
29. (a) Jabarin, S. A. and Lofgren, E. A., Thermal stability of PET, *Polym. Eng. Sci.*, **24**, 1056 (1984); (b) Zimmermann, H., Thermische und thermooxydative Abbauprozesse des PET, *Plaste Kautsch.*, **28**, 433 (1981); (c) Buxbaum, L. H., The degradation of PET, *Angew. Chem. Int. Ed. Engl.*, **7**, 182 (1968).
30. (a) Kaufmann, S., Statistics regarding yarn breaks in spinning and drawtwisting, *Melliand Textilber*, **74**, 502 (1993); (b) Kaufmann, S. and Hoffrichter, S., Investigations on polyamide dust and angel hair and the phenomenon of grey melt, *Chem. Fibers Int.*, **46**, 114 (1996).
31. Kanide, K. and Kuriki, T., Structural factors governing dyeability of PET fibers, *Polym. J.*, **19**, 315 (1987).
32. (a) Heffelfinger, C. F., Survey of film processing illustrated with PET, *Polym. Eng. Sci.*, **18**, 1163 (1978); (b) Heffelfinger, C. J. and Schmidt, P. G., Structure and properties of PET films, *J. Appl. Polym. Sci.*, **9**, 2661 (1965).
33. Teijin, *US Patent 4 198 458*, 1980.
34. Ixtlan AG, *Fr. Patent 2 782 665*, 2000.
35. Jung, H., Polyester polymer production presentation given (session VI/I) at the *2nd World Congress – The Polyester Chain*, Zurich, Switzerland, 3–5 November, 1997.
36. (a) Hoechst-Celanese, *US Patent 5 925 710*, 1999; (b) Martl, M. G., Innovative technologies for polyesters, presentation given at the *5th World Congress – The Polyester Chain*, Zürich, Switzerland, 28 November–1 December 2000.
37. Mitsubishi Kasei, *Ger. patent DE-OS 4 223 007*, 1993.
38. Wick, G., Characteristics of PET polymer for bottle manufacturing, presentation given at the *Society of Plastics Engineers Benelux Seminar*, Amsterdam, 20–21 May 1980.
39. Covney, J. D., Day, M. and Wiles, D. M., Thermal degradation of PET. A kinetic analysis of gravimetric data, *J. Appl. Polym. Sci.*, **28**, 2887 (1983).

40. Angelova, A., Woinova, S. and Dimitrov, D., Differentialthermoanalytische Untersuchungen zur Effektivität einiger Stabilisatoren bei PET, *Angew. Makromol. Chem.*, **64**, 75 (1977).
41. Eastman, *World Patent W098 18 848*, 1998; (b) Eastman, *US Patent 5 258 233*, 1993; (c) Toyo Seikan Kaisha, *US patent 4 837 115*, 1989.
42. Hartwig, K., New packaging opportunities through enhanced barrier properties, presentation given at the *2nd World Congress – The Polyester Chain*, Zürich, Switzerland, 3–5 November, 1997.
43. Po', R., Occhiello, E., Giannotta, G., Pelosini, L. and Abis, L., New polymeric materials for containers manufactured based on PET/PEN copolyesters and blends, *Polym. Adv. Technol.*, **7**, 365 (1995).
44. (a) Eastman, *US Patent 4 256 860*, 1981; (b) Eastman, *US Patent 4 045 431*, 1997; (c) Dupont, *US Patent 3 856 749*, 1973; (d) GAF, *US Patent 4 195 000*, 1980.
45. Hoeschele, G. K. and Witsiepe, W. K., Polyätherester-Block-Copolymere-eine Gruppe neuartiger thermoplastischer Elastomerer, *Angew. Chem.*, **29/30**, 267 (1973).

Additives for the Modification of Poly(Ethylene Terephthalate) to Produce Engineering-Grade Polymers

J. SCHEIRS

ExcelPlas Polymer Technology, Edithvale, VIC 3196, Australia

1 INTRODUCTION

Glass-filled, toughened poly(ethylene terephthalate) (PET) resins can be readily moulded into highly impact-resistant structural parts for appliances and automotive components. The PET-based compounds are also suitable for construction (e.g. as structural members), equipment housings (e.g. printer and copier parts), agricultural applications (e.g. mower and tractor engine covers), materials handling (e.g. pallets and trays), furniture (e.g. office chair bases), as well as electrical and electronic applications.

PET may be considered a low-cost raw material for the production of engineering compounds due to its widespread availability from recycled beverage bottles. Its abundant availability and good molecular weight make it an excellent precursor for the production of toughened compounds that can in many cases compete directly with toughened and glass-filled nylons at a considerable cost advantage.

PET however, has numerous shortcomings from the perspective of an injection moulding compound. Unmodified PET is generally not useful as an injection moulding resin because of its slow crystallization rate and the tendency to embrittle upon crystallization. For these reasons, PET has not traditionally

found application in injection moulding processes. Unmodified PET can be injection moulded without difficulty only when relatively low mould temperatures (15–40 °C) are employed. Furthermore, the amorphous parts so formed tend to crystallize during heat treatment (annealing) and the resultant polymer is quite brittle. However, the abundant supply of both virgin and recycled PET has led to the development of strategies designed to overcome specific deficiencies through proper formulation. A variety of formulants can be added to PET resin to produce a formulated, engineering-grade thermoplastic. PET was not originally considered as an injection moulding material because of high moisture sensitivity, poor impact strength, excessive warpage when glass-fibre filled and slow rate of crystallization which slows the moulding cycle. However, it has a higher modulus, heat distortion temperature and gloss than poly(butylene terephthalate) (PBT). Such properties can only be fully realized if mouldings are crystalline.

As can be seen from Table 14.1, the primary drawbacks of PET apart from its hygroscopicity are its slow crystallization rate, the low glass transition temperature and relatively low impact strength. Formulation and compounding of PET can correct these shortcomings, enhance other properties, and tailor performance properties to meet specifications. The properties of PET can be modified and enhanced to such an extent that it can then be used in durable products such as appliance housings, electronics, furniture, transportation, and building and construction. Such PET resins have superior mechanical, thermal, electrical, chemical and environmental properties to conventional bottle-grade PET resins. These so-called engineering resins possess a balance of properties tailored to each durable application.

Unmodified, bottle-grade PET resin begins to soften and become rubbery at 80 °C. This makes the direct use of unmodified PET in engineered applications not feasible. For PET to be used in durable products it must be made highly crystalline and needs to be reinforced with glass fibres or mineral reinforcements.

Table 14.1 Additives used in engineering-grade PET to overcome specific shortcoming of the base resin

Property deficiency	Remedy
Hygroscopicity	Internal desiccants
Slow to crystallize	Nucleating agents, plasticizers
Uneven crystal size	Nucleating agents
Low glass transition temperature	Glass fibres
Brittle fracture behaviour	Impact modifiers
Notch sensitivity	Impact modifiers
Drop in IV during extrusion	Chain extenders
Oxidation during extrusion	Stabilizers
Hydrolysis	Hydrolysis repair additives
Autocatalytic acid-catalyzed hydrolysis	Carboxyl scavengers
Warpage	Mineral fillers

Glass-filled PET has good load-bearing characteristics and low creep, with a coefficient of thermal expansion being similar to that of brass or aluminium.

PET is a semicrystalline polymer which, depending on fabrication conditions, can have a molecular structure that is amorphous, crystalline or semicrystalline. High crystallinity is desirable in products that require high temperature stability, dimensional stability and stiffness. Crystallinity can be induced in strapping, sheet and stretch blow moulded bottles by mechanical orientation. In the case of injection mouldings, however, crystallinity needs to be induced by chemical crystallization and precisely controlled to develop certain targeted properties in the finished product. Crystallinity in PET can be induced by using nucleating agents on which crystals can grow, in combination with a crystal growth promoter or accelerator.

Unmodified PET is too slow to crystallize to allow practical moulding cycles. Relatively recent advances in nucleation chemistry have allowed the development of specific PET moulding grades such as Rynite[™] and Petra[™] (by DuPont and Honeywell, respectively). Such PET engineering resins are high molecular weight, high performance materials used for a wide range of engineering applications. Their high crystallinity and low melt viscosity means that they are ideally suited for injection moulding of complex parts which require high strength, good dimensional stability, and insulation properties.

The rheological properties of conventional PET resins are also not particularly well suited for extrusion foaming with physical blowing agents and as a result modified resins with higher melt viscosity and melt strength/‘elasticity’ are often used. In contrast to the commonly used polystyrene and low-density polyethylene (LDPE) resins, extrusion foaming of PET is quite challenging. Most commercial PET resins of relatively low molecular weight (MW) and narrow molecular weight distribution (MWD) have rheological properties at processing temperatures that are not conducive to foaming. Modified PET resins with improved rheology and melt strength for applications such as foaming, extrusion blow moulding, or simply for upgrading low-intrinsic-viscosity materials, can be produced through chain extension/branching reactions with di- or polyfunctional reagents such as chain extenders.

2 CHAIN EXTENDERS

Chain extenders (or coupling agents) can serve to reverse the MW damage caused by hydrolysis of polyesters or can modify the rheology of the polymer to increase its melt strength. Chain extenders have at least two functional groups capable of addition reactions with the terminal hydroxyl (OH) or carboxyl (COOH) groups of the polyester resin. In principle, any bifunctional (or higher functionality) chemical that reacts fast with the end groups of polycondensates may be used for chain extension or coupling. However, in practice most compounds suffer from severe side reactions or produce undesirable byproducts which limit their applicability.

Raising the molecular weight (or intrinsic viscosity or IV) of PET is usually performed by solid-state polycondensation ('solid-stating'). Conventional solid-stating is generally performed in tumble driers under high vacuum and high temperatures for extended periods of time (12–20 h). Solid-stating is characterized by very high capital costs and high production costs (since it is a time-intensive batch process). Chain extenders, on the other hand, can be simply added to the polymer during extrusion (single- or twin screw-extrusion or compounding). Furthermore, chain extenders enable the production of a whole range of viscosities, starting with only one single base resin. The chain extender couples two equal end groups in a statistical manner, in a similar process to what happens during post-condensation. However, the reaction occurs in minutes rather than hours and also chain extension does not change the MWD compared with solid-stated polyesters. Thus the main advantages of chain extension compared with a post-condensation process are lower system costs, faster reaction and more flexibility, without the need for any extra investments.

'Traditional' chain extenders for PET are compounds such as bisanhydrides, bisoxazolines, bisepoxides, etc., which react with either –OH or –COOH end groups, or both. Careful use of the correct concentrations of chain extender can allow one to tailor the IV of PET without the need for solid-stating. Chain extenders are thus very useful for building molecular weight during melt processing. Terms such as 'reactive extrusion' and 'reactive chain coupling' are used to describe the processing of polyesters such as PET with chain extenders. The latter can upgrade PET by increasing the intrinsic viscosity of bottle-grade PET, for example, from ~0.8 dL/g to greater than 1.0 dL/g. The use of chain extenders during PET compounding with modifiers and glass fibres needs to be carefully controlled since as the molecular weight of PET increases, the extent of fibre breakage and shear-induced heating during extrusion also increase.

There is a wide range of chain extenders commercially available for PET (Table 14.2). Bifunctional chain extenders promote linear chain extension while tri- and tetra-functional chain extenders promote chain branching. Such reactive compounds are also known as 'repair additives' since they can reverse the molecular weight loss of hydrolytically damaged PET.

Bifunctional molecules such as diepoxides, diisocyanates, dianhydrides or bis(oxazoline)s have been shown to increase the molecular weight of PET [1, 2] by reacting with its terminal groups. Triphenyl phosphite [3, 4], as well as diimidodiepoxides [5], have also proved to react efficiently with PET while promoting molecular weight enhancement.

The most common chain extenders are the dianhydrides (also known as tetracarboxylic dianhydrides). The most common of these is pyromellitic dianhydride (PMDA). The latter can be used in synergistic combinations with hindered phenolic aromatic phosphates such as IRGANOX 1425 manufactured by Ciba Geigy [6–8]. The hindered phenolic aromatic phosphate is used at levels of 0.1–2.5 wt%. The hindered phenolic aromatic phosphate is an advantageous co-synergist since it

Table 14.2 Chain extenders used to couple PET chains via reactive extension of end groups

Compound	Tradename	Manufacturer	Addition rate (wt%)
Pyromellitic dianhydride	PMDA	Nippon Shokubai Allco Chemical	0.05–2 % and preferably around 0.15 %–0.25 % ^a
Trimellitic anhydride	TMA	–	–
Phenylenebisoaxazoline	PBO	Mikuni (Japan)	0.4–1.5, and preferably 0.4–0.6
Carbonyl bis(1-caprolactam)	Allinco CBC	DSM	–
Diepoxide bisphenol A-diglycidyl ether	Epon 1009 ^b	Shell	0.6
Diepoxide bisphenol A-diglycidyl ether	Epon 828 ^b	Shell	0.6
Tetraepoxide tetraglycidyl diaminodiphenylmethane resins (TGDDM)	MY721	Ciba SC	0.4–0.6
Triphenylphosphite	TPP	Various	0.2–0.8

^a Note: Excess can lead to undesirable molecular branching and cross-linking. Chain branching can severely hamper the crystallization capability of PET and this may lead to a loss in performance properties.

^b Bisphenol A diglycidyl ether – prepared by a condensation reaction between epichlorohydrin and bisphenol A.

serves both as a solid-state-polymerization catalyst and a heat stabilizer to protect the PET from oxidation during solid-state polymerization.

Another highly effect chain extender is trimellitic anhydride (TMA) which gives rise to branching of the PET structure. Note that the multifunctional epoxies (see Table 14.2) react quickly with the terminal carboxylic acid groups of PET but can also react with the film former and the silane coupling agent on glass fibre reinforcements.

2.1 PYROMELLITIC DIANHYDRIDE

Pyromellitic dianhydride (PMDA) is generally used in PET at concentrations ranging from 0.05 to 2 %. Reactive extrusion of PET with PMDA has been reported by Incarnato *et al.* [9]. These authors used PMDA to increase the molecular weight of PET industrial scraps sourced from a PET processing plant. They found that concentrations of PMDA between 0.50 and 0.75 % promote chain extension reactions that lead to an increase of MW, a broadening of the MWD and branching phenomena which modify the PET scrap in such a way that makes

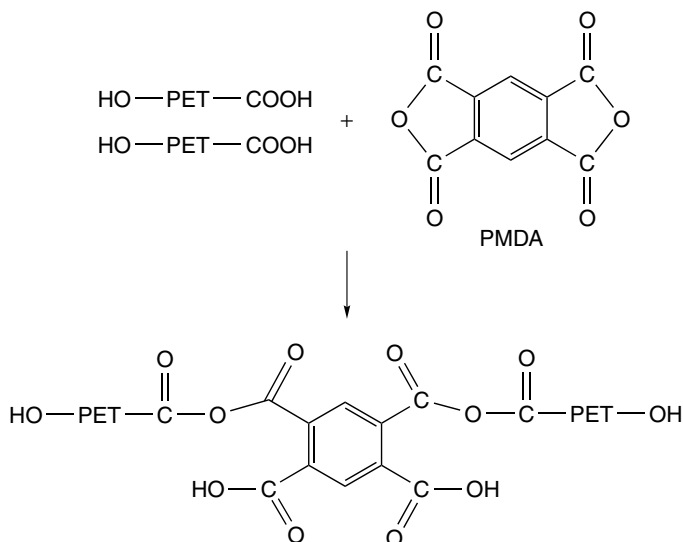


Figure 14.1 Reaction of pyromellitic dianhydride (PMDA) chain extender with PET end groups (hydroxyl and carboxylic acid groups) to give chain extension and branching of PET

it suitable for film blowing and blow moulding processes. The reaction between PMDA and PET is shown in Figure 14.1. Pentaerythritol can be added as a synergist.

A dramatic improvement in the performance of PMDA in chain extension of PET is possible if the PMDA is added to the extruder in a concentrate using a polycarbonate (PC) carrier [10]. The reason being that if PMDA is compounded in a PET carrier resin then a premature reaction results leading to ultra-high MW PET and gel problems. Alternatively, if PMDA is compounded in a polyolefin carrier then degradation of the polyolefin occurs; whereas, when PMDA is compounded in a polycarbonate carrier there is no premature reaction because PC contains no acid end groups (rather, $-\text{OH}$ end groups instead). Furthermore, PC is quite miscible with PET.

Aromatic carboxylic dianhydride chain extenders (e.g. PMDA) are a low-cost way of converting recycled PET flakes into high-IV crystalline pellets that can be used in high-value applications (e.g. bottles, strapping, foam, engineering alloys/compounds, etc.) (see Figure 14.2). PMDA is an effective chain extension additive for thermoplastic polyesters such as PET and PBT. It is suitable for the following applications:

- Enhancement of the intrinsic viscosity of PET and PBT
- Reactive extrusion of PET and PBT

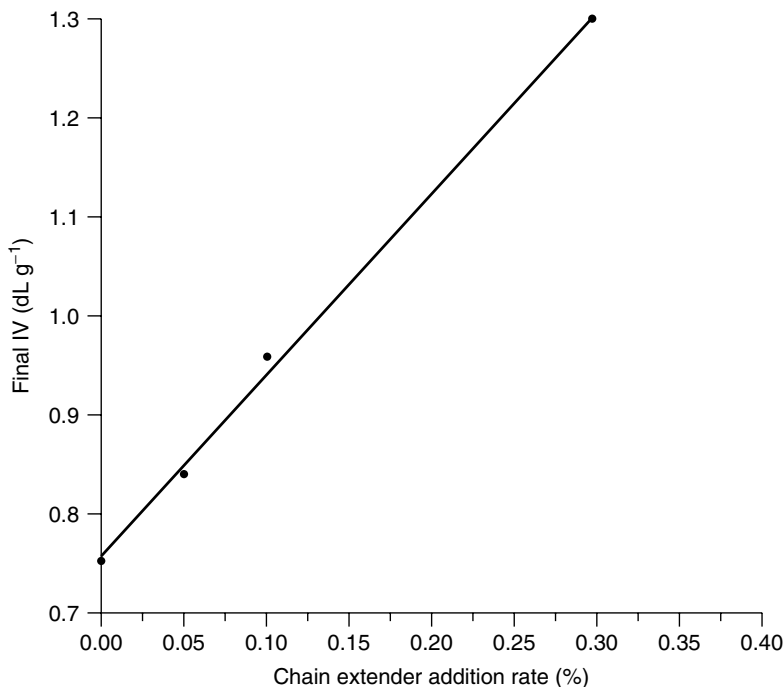


Figure 14.2 Effect of PMDA addition on the IV of PET bottle flake after extrusion at 280 °C

- Melt strength enhancement of PET and PBT for the production of blown polyester foams
- As a melt viscosity and melt-strength-enhancing additive for modifying PET for film blowing and extrusion blow moulding applications
- Tensile strength enhancement of PET and PBT for strapping applications without the need for solid-state polycondensation
- Upgrading of recycled PET flake to resin suitable for bottling applications (>0.80 dL/g)
- As an additive to reduce the time necessary for solid-phase polymerization of PET and PBT resins
- To increase the elongational viscosity of PET and PBT resins by facilitating extended and branched architectures

One of the main commercial uses of PMDA is to improve the melt strength of PET to allow it to be foamed. Unmodified PET cannot be foamed properly because its inherently low melt strength causes the cells to collapse and coalesce.

2.2 PHENYLENEBISOXAZOLINE

Both 1,3-phenylenebisoxazoline (1,3-PBO) and 1,4-phenylenebisoxazoline (1,4-PBO) are effective chain extenders for PET *via* the mechanism shown in Figure 14.3. PBO chain-extends PET by coupling together two terminal carboxylic acid groups. Effective use concentrations of PBO for PET are in the range 0.5–1.5 wt% and these can give an IV increase for PET of 0.2 IV units – that is, from 0.7 to 0.9 dL/g. The precise IV enhancement will depend on the carboxyl equivalent of the PET. Typical reaction conditions are 240 °C for 3 min. PBO also acts as a carboxyl group scavenger and in doing so increases the hydrolytic stability of the resultant PET. A concentration of 0.5 % PBO in PET can reduce the carboxyl content from 45 to 20 mmol/kg.

The product of the coupling reaction is an esteramide and no volatiles are emitted during the ring-opening reaction. The reaction is largely completed within the processing time (i.e. 3–5 min). The increase in viscosity can be adjusted by the amount of PBO. In practice, about 0.5 wt% is used. A 0.5 parts per hundred (phr) addition level of PBO in PET generally gives an intrinsic viscosity increase of about 0.2 dL/g. PBO can be used in combination with other chain extenders such as carbonyl bis(1-caprolactam) (CBC).

PBO is a very reactive compound towards PET containing carboxyl end groups but not hydroxyl end groups. Karayannidis [11] studied the effect of a PBO chain extender on the IV increase of PET during extrusion. Interestingly, these authors observed enhanced results when phthalic anhydride was added to the initial sample, before the addition of PBO. This technique succeeded in increasing the carboxyl groups by reacting phthalic anhydride with the terminal hydroxyl groups of the PET. After this initial modification of the PET sample, PBO was proved to be an even more effective chain extender. It was found that when using recycled PET with an IV of 0.78, a PET grade could be prepared having an IV

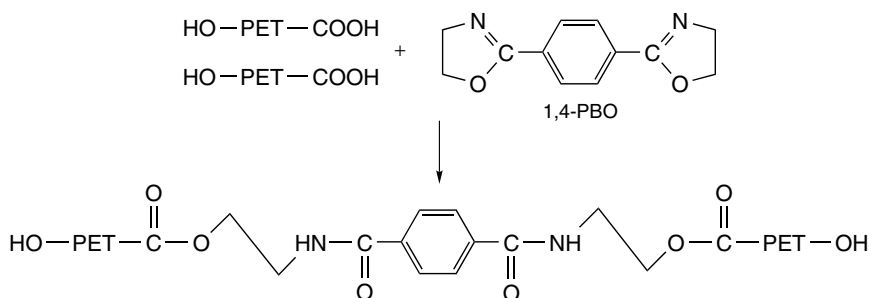


Figure 14.3 Reaction of 1,4-PBO chain extender with PET end groups (carboxylic acid groups) to give linear chain extension of PET (leading to a polyamide–polyester); 1,4-PBO, 1,4-phenylenebisoxazoline

of 0.85 (or number-average molecular weight (M_n) of 25 600) within about 5 min when using PBO as the chain extender.

2.3 DIEPOXIDE CHAIN EXTENDERS

Figure 14.4(a) shows the structure for a common diepoxide chain extender. Haralabakopoulos *et al.* [12] have reported that the molecular weight of PET increases *via* chain extension reactions with commercially available diepoxides. Low concentrations of extender and short reaction times generally favoured chain extension. In addition, purging with nitrogen resulted in chain extended polymers having the highest values of intrinsic viscosity (e.g. 0.82 dL/g).

PET chain-extended with a diepoxide as chain extender can exhibit varying degrees of branching and cross-linking depending on the level of chain extender used [13, 14]. The branched and cross-linked PETs exhibit significant improvement in tensile properties.

Bikiaris and Karayannidis [5] have investigated the use of diimidodiepoxides as chain extenders for PET resins. Starting with a PET having an IV of 0.60 dL/g and a carboxyl content (CC) of 42 eq/10⁶ g, they obtained PET with an IV of 1.16 dL/g and a CC below 5 eq/10⁶ g. The typical reaction condition for the coupling of PET was heating with the chain extender under an argon atmosphere above its melting temperature (280 °C) for several minutes.

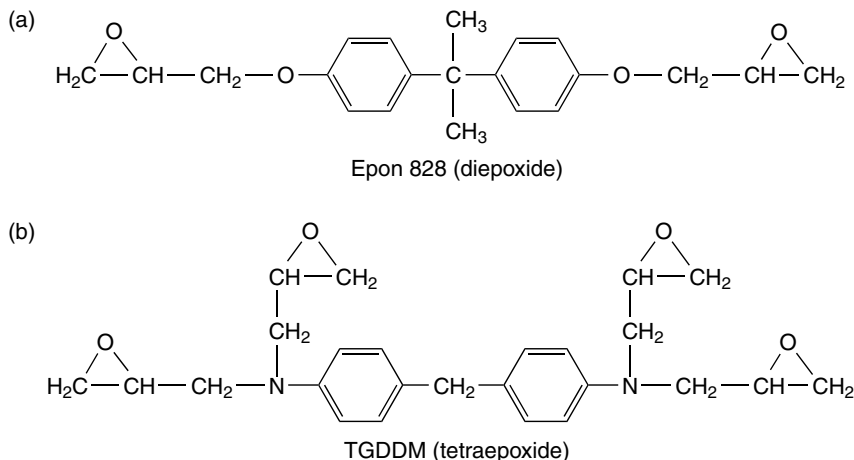


Figure 14.4 Chemical structures of two common epoxy chain extenders for PET: (a) a diepoxide, e.g. Shell Epon 828, based on bisphenol A diglycidyl ether; (b) a tetraepoxide, e.g. Ciba MY721, based on tetraglycidyl diaminodiphenyl methane (TGDDM)

2.4 TETRAEPOXIDE CHAIN EXTENDERS

Figure 14.4(b) shows the structure for a common tetraepoxide chain extender. Reactive processing of recycled PET with a tetrafunctional epoxy additive induces randomly branched molecules which gives rise to a corresponding increase in elongational melt viscosity. This enables the PET to be foamed and allows the production of closed-cell foams [15, 16]. The tetrafunctional tetraglycidyl diamino diphenyl methane (TGDDM) (CIBA SC, MY721) is particularly efficient [17].

The use of multifunctional epoxy-based modifiers to increase the melt strength of PET has been investigated in detail by Japon *et al.* [15, 16], with the aim of producing PET foams by an extrusion process. TGDDM resin was selected for the investigation of the modifier concentration effect on the reaction conversion. Using a stoichiometric concentration of TGDDM, the molecular weight distribution of modified PET, as determined by gel permeation chromatography, showed an eightfold increase of the *Z*-average molecular weight and the presence of branched molecules of very large mass. The resulting intrinsic viscosity of the modified PET was 1.13 dL/g.

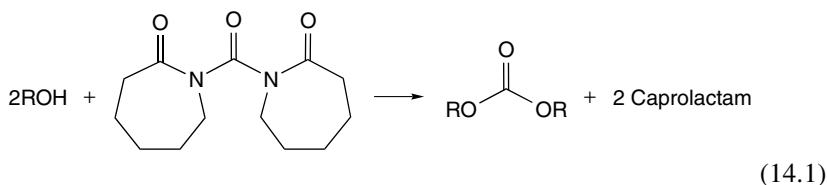
The chain extension of polyesters in the melt using a high-reactivity diepoxy, diglycidyl tetrahydrophthalate, has been studied in detail by Guo [18]. The diepoxide reacts with the hydroxyl and carboxyl end groups of polyesters such as PET at a very fast reaction rate and a relatively high temperature. The melt flow index of the chain extended polyesters dramatically decreased as the diepoxy was added to the polyester. In addition, the notched Izod impact strength and elongation-at-break of the chain extended polyesters was also found to increase. The chain extended polyesters are also more stable thermally. Compared with the conventional solid post-polycondensation method, this approach is a simpler and cheaper technique for obtaining high-molecular-weight polyester resins.

2.5 PHOSPHITES CHAIN EXTENSION PROMOTERS

The molecular weight and polydispersity of the recycled PET melt processed with organic phosphites was studied by Nascimento and Dias [19]. Some of the phosphites act as chain extending catalysts, so increasing the polymer's molecular weight. Superior chain extension results were obtained with triarylphosphites, while dialkyl- and trialkylphosphites promoted PET degradation. The study showed that triphenylphosphite was the best chain extender used in this study. The occurrence of transesterification reactions in PET/PEN blends prepared in the presence of triphenylphosphite (TPP) was investigated by Dias and Silva [20]. When PEN was processed with TPP, which is a known chain extender for PET, chain extension reactions also took place. Although transesterification inhibition was expected, this type of reaction was not suppressed by TPP.

2.6 CARBONYL BIS(1-CAPROLACTAM)

One of the newest chain extenders for PET is carbonyl bis(1-caprolactam) (CBC). The latter is a free-flowing white powder with a melting point of approximately 115°C. CBC reacts with terminal hydroxyl functional groups on the PET chains during the processing of polyesters forming carbonate, urethane and urea linkages, according to the following reaction [21]:



where R is the PET molecular chain.

During this reaction, some caprolactam is also liberated. The reaction is largely completed within the processing time (typically 3–5 min). The increase in intrinsic viscosity of PET can be adjusted by the amount of CBC. In practice, about 0.5 wt% of CBC is typically used. CBC is commercially available under the trade-name ALLINCO® (DSM, Geleen, The Netherlands). ALLINCO® is one of the most effective chain extender systems available for PET [21, 22]. CBC is often used in combination with PBO for an enhanced chain extension effect. Typically, the relative viscosity of PET is increased from 1.6 to 2.0 with a stoichiometric amount of CBC + PBO (ca. 1.2 wt%) in a single-screw extruder at 300°C.

3 SOLID-STATING ACCELERATORS

PET is a material that finds widespread use for soft drink and beverage bottle applications. For injection or blow moulding applications, high-molecular-weight PET $M_n > 30\,000$ is required. While PET with M_n of 15 000 – ~25 000 can be achieved by a standard melt-polymerization process, the high-molecular-weight PET grades require a solid-state polymerization process. Commercial solid-state polymerization process systems are usually composed of a crystallizer and a polymerization reactor. First, melt-polymerized chips are fed into the crystallizer unit and crystallized to the extent of about 40 %. In a second step, the crystallized chips are fed into a polymerization reactor vessel and then polymerized in the solid state at a temperature of around 220°C.

Solid-state polycondensation (SSP) is thus a technique applied to thermoplastic polyesters to raise their molecular weight or IV. During solid-state polycondensation, the polymer is heated above the glass transition temperature and below the melt temperature of the polymer either under an inert gas or under vacuum. Increasing the intrinsic viscosity requires a residence time of up to 12 h under vacuum or under inert gas, at temperatures from 180 to 240°C.

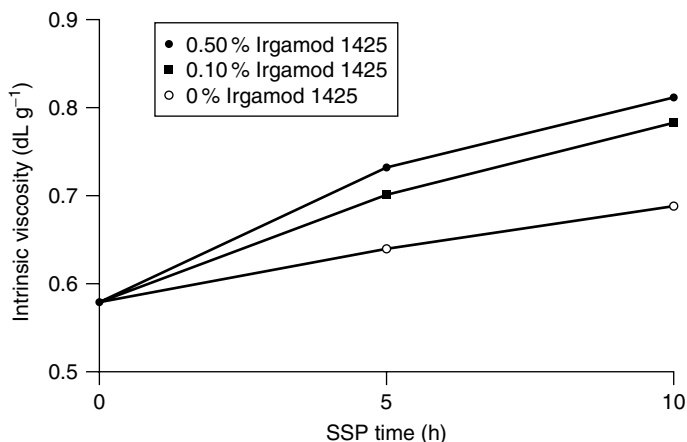


Figure 14.5 Effect of a commercial solid-stating accelerator (Irgamod 1425) on the rate of intrinsic viscosity enhancement of PET (data obtained from Ciba Specialty Chemicals)

Solid-state polycondensation of thermoplastic polyesters such as PET is therefore both time-consuming and energy-intensive. Recently, additives have been developed to accelerate this process [23, 24]. Such additives enable PET with a very high IV to be produced at reduced residence times in the solid-state reactor, with enhanced outputs and at a reduced cost. Such additives accelerate the IV enhancement of PET at low cost. One such SSP accelerator is Irgamod 1425 which when used in PET at levels of between 0.1–0.5 wt% gives an SSP acceleration of approximately 50 % (see Figure 14.5).

Typically, an IV enhancement of 0.10 dL/g requires 10 h of solid-stating. In the presence of an SSP accelerator, this time is reduced to just 5 h. Irgamod 1425 also contributes to reduced yellowing of the PET resin. For instance, 0.1 wt% can lead to a drop in *b* value (yellowness) from 1.1. to –2.9. Such SSP accelerators are based on sterically hindered hydroxyphenylalkylphosphonates such as calcium bis-ethyl-3,5-di-*t*-butyl-4-hydroxyphosphonate. Pfaendner *et al.* [24] details the use of Irganox 1425 (CAS 65140-91-2)¹ to accelerate the solid-stating of PET.

4 IMPACT MODIFIERS (TOUGHENERS)

Impact modifiers for PET are generally elastomeric compounds that increase impact strength and elongation while usually decreasing modulus. An effective way to enhance the impact strength and to induce a brittle/ductile transition of the fracture mode, is by the dispersion of a rubber phase within the PET matrix. The

¹ Chemical Abstracts Service (CAS) Registry Number.

main role of the rubber particles is to induce an overall deformation mechanism rather than a localized phenomenon, thereby strongly increasing the amount of dissipated fracture energy. The effectiveness of rubber modification is found to be highly dependent on the following:

- the rubber and compatibilizer type
- the rubber content
- the rubber particle size
- the interparticle distance

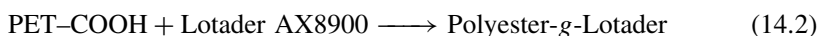
The basic mechanism of toughening is one of void formation and shear band formation (cavitation) when stress is applied.

4.1 REACTIVE IMPACT MODIFIERS

In order to obtain a finely sized dispersed phase in the PET matrix, the use of reactive compatibilization has been found to be important. Small dispersed rubber particles and a small interparticle distance are necessary to induce high toughness. For effective rubber toughening of PET, it is important that the rubber domains be less than $3\text{ }\mu\text{m}$ in diameter (and preferably less than $1\text{ }\mu\text{m}$) and that the interparticle distance be between 50–300 nm.

Reactive impact modifiers are preferred for toughening of PET since these form a stable dispersed phase by grafting to the PET matrix. Non-reactive elastomers can be dispersed into PET by intensive compounding but may coalesce downstream in the compounder. Reactive impact modifiers have functionalized end groups. Functionalization serves two purposes – first, to bond the impact modifier to the polymer matrix, and secondly to modify the interfacial energy between the polymer matrix and the impact modifier for enhanced dispersion. Some examples of commercially available reactive impact modifiers for PET are shown in Table 14.3. An example of a *non-reactive* elastomer that can be used in combination with *reactive* impact modifiers is ethylene methyl acrylate (EMA), such as the Optema™ EMA range of ethylene methyl acrylates manufactured by the Exxon-Mobil Chemical Company (see Section 4.2).

Functionalized (reactive) elastomers such as Lotader AX8900 (see Figure 14.6) are excellent toughening agents for PET as they improve interfacial adhesion and importantly, reduce interfacial tension, thus allowing the formation of smaller rubber particles (Figure 14.7). Furthermore, a grafting of the elastomer to the PET matrix occurs according to the following reaction:



The chemical reaction between glycidyl methacrylate (GMA) end groups on the reactive elastomer and the carboxylic acid end groups of PET is shown in

Table 14.3 Commercial reactive impact modifiers for PET

Elastomeric toughener ^a	Tradename	Manufacturer
E-EA-GMA (67:25:8) (ethylene-ethyl acrylate-glycidyl methacrylate terpolymer)	Lotader AX8900 ^b	Atofina
E-EA-GMA (68:24:8) (ethylene-ethyl acrylate-glycidyl methacrylate terpolymer)	Lotader 8860 Lotader 8840	Atofina
E-BA-GMA (63:31:6) (ethylene-butyl acrylate-glycidyl methacrylate terpolymer)	Elvaloy PTW	DuPont
E-VA-MA (ethylene-vinyl acetate copolymer, functionalized with maleic anhydride)	Exxelor VA1803	Exxon
SEBS-MA (styrene-ethylene butylene-styrene terpolymer, functionalized with maleic anhydride)	Tuftec M1943 Kraton G1652 Kraton FG1921X	Asahi Kasei Company Kraton

^a Note: GMA is essentially an epoxy functionality.

^b Lotader AX8900 is often used in combination with a non-reactive elastomeric toughener such as Lotryl (ethylene ethyl acrylate (EEA)). For example, a 30:70 blend of these two tougheners is a highly effective impact modifying system for PET.

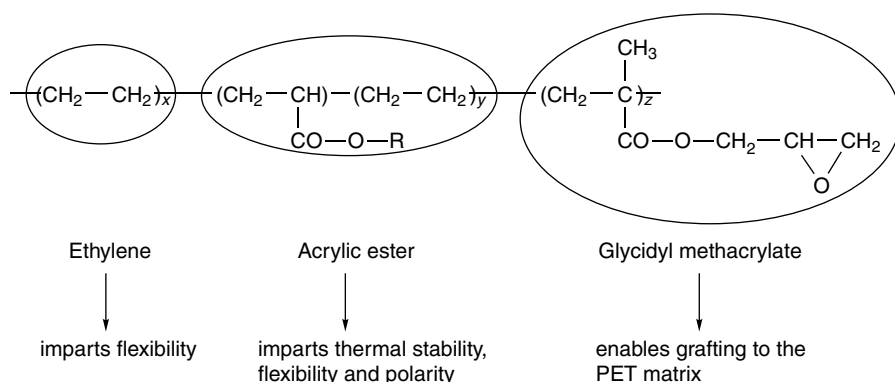


Figure 14.6 Simplified structure for random ethylene-acrylic ester-glycidyl methacrylate terpolymers which are effective rubber tougheners for PET compounds. The ethylene-acrylic ester segments provide elastomeric properties while the glycidyl methacrylate functionalities enable reactive grafting to the PET matrix via the hydroxyl and carboxyl chain ends of the latter

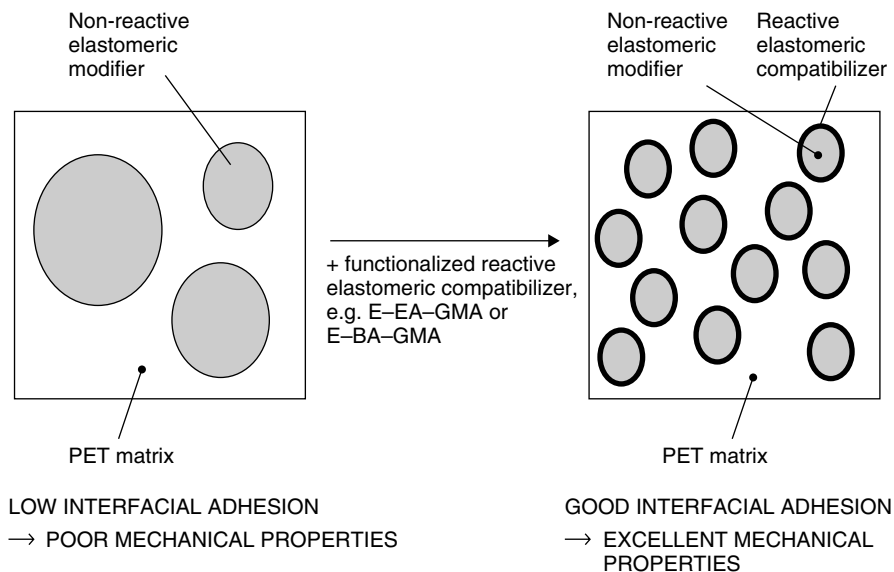


Figure 14.7 Schematic highlighting the microstructure of rubber-toughened PET and performance improvements when non-reactive elastomers are blended with reactive elastomers (adapted from Atofina literature entitled 'Lotader® and Lotryl®')

Figure 14.8. This reaction is critical in ensuring the reactive elastomeric toughener becomes grafted to the PET matrix and forms smaller, uniform domains of a rubber dispersed phase.

Reactive tougheners such as Lotader GMA AX8900, AX8920 and AX8930 exhibit high reactivity with PET and induce a fine and homogeneous dispersion of rubber domains throughout the PET matrix. Figure 14.9 clearly illustrates the superior toughening effect afforded by reactive tougheners as opposed to non-reactive tougheners.

Figure 14.10 shows the microstructure of PET containing 20 % of a reactive toughener (Lotader AX8900). The rubber domains have been selectively removed by solvent to provide contrast enhancement. Note that the scale bar is 5 μm long and that the rubber domains are consistently smaller than 1 μm . This fine morphology enables the production of 'supertough' PET with notched Izod impact strengths exceeding 700 J/m.

Elastomers with reactive end groups such as maleic anhydride (MA) or glycidyl methacrylate (GMA) are preferred for toughening PET. The reason that they are so effective is that they form a graft copolymer by reaction with the PET hydroxyl and carboxyl end groups (as shown below). The graft copolymer then acts as an emulsifier to decrease the interfacial tension and reduce the tendency

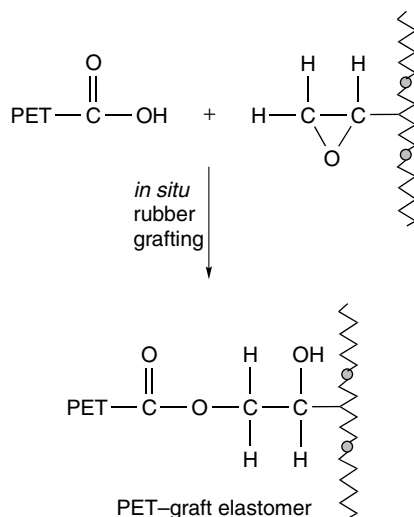


Figure 14.8 Grafting reactions between PET end groups and glycidyl-methacrylate-containing rubber tougheners. This reaction is critical in ensuring that the reactive elastomeric toughener becomes grafted to the PET matrix and forms smaller, uniform domains of a rubber dispersed phase

of the dispersed rubber particles to coalesce during processing. Furthermore in the solid state the graft copolymer promotes adhesion between the phases and facilitates cavitation in a triaxial stress state.

The use of maleic-anhydride-functionalized styrene-ethylene butylene-styrene (SEBS) elastomers (e.g. Kraton G1652 and Kraton FG1921X) to toughen PET has been reported by Tanrattanakul *et al.* [25]. Interestingly, particles of functionalized SEBS were primarily spherical in injection moulded blends, while in the unfunctionalized SBS blends the particles were highly elongated. The functionalized SEBS-PET blends exhibit far superior impact strengths compared to the unfunctionalized blends. It was found that the improvement in impact strength with the functionalized elastomers was related to a decrease in the rubber domain particle size. As little as 1 % SEBS-g-MA in PET can increase the fracture strain by more than ten times. The graft copolymer acts as an emulsifier to decrease interfacial tension and reduce the tendency of dispersed particles to coalesce, and also importantly promotes adhesion between the phases in the blend.

4.2 NON-REACTIVE IMPACT MODIFIERS (CO-MODIFIERS)

Most non-reactive (unfunctionalized) elastomeric impact modifiers such as general purpose rubbers, are not highly effective at toughening polyesters because they are unable to adequately interact with the polyester matrix so as to achieve

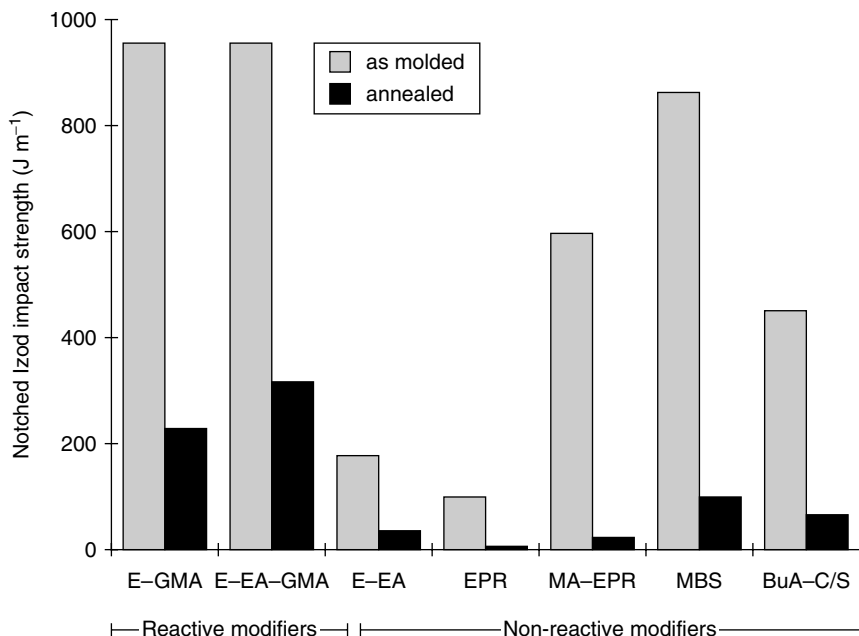


Figure 14.9 Effect of various impact modifiers (25 wt%) on the notched Izod impact strength of recycled PET (as moulded and annealed at 150 °C for 16 h): E-GMA, glycidyl-methacrylate-functionalized ethylene copolymer; E-EA-GMA, ethylene-ethyl acrylate-glycidyl methacrylate (72/20/8) terpolymer; E-EA, ethylene-ethyl acrylate; EPR, ethylene propylene rubber; MA-GPR, maleic anhydride grafted ethylene propylene rubber; MBS, poly(methyl methacrylate)-*g*-poly(butadiene/styrene); BuA-C/S, poly(butyl acrylate-*g*-poly(methyl methacrylate) core/shell rubber. Data taken from Akkapeddi *et al.* [26]

optimally sized dispersed phases and strong interfacial bonding. Non-reactive elastomeric tougheners based on random ethylene-acrylic ester copolymers are effective impact modifiers for PET compounds however, if appropriate compatibilizing polymers are used. Some examples of these systems are shown in Table 14.4. Figure 14.11 shows the effect of blending a mixture of reactive and non-reactive ethylene copolymers (E-EA-GMA + EEA = 20 %) on the notched Izod impact strength of PET.

4.2.1 Core-Shell Elastomers

MBS (methyl methacrylate-butadiene-styrene) graft copolymers are known as one of the most efficient non-reactive impact modifiers for PET and also poly(vinyl chloride) (PVC). MBS is used commercially as an effective impact modifier for PET recycle [27]. Typical MBS rubber particles contain an elastomeric core of

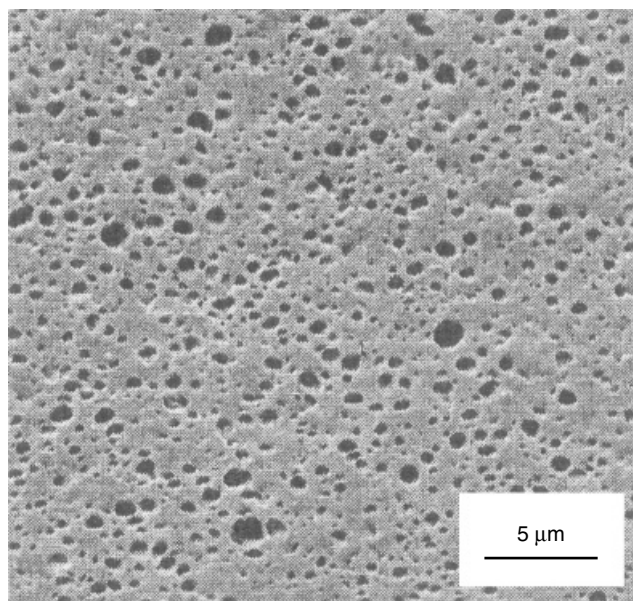


Figure 14.10 Electron micrograph of PET + 20 % E-EA-GMA (reactive toughener – Lotader AX8900) showing the size and distribution of the rubber particles (note the 5 μm scale bar). The rubber domains have been selectively etched out by solvent to provide contrast enhancement

Table 14.4 Commercial non-reactive impact modifiers for PET

Compound	Tradename	Supplier
EMA (ethylene–methyl acrylate copolymer)	Optema™ EMA	Atofina Exxon-Mobil
EEA (ethylene–ethyl acrylate copolymer) ^a	Lotryl EEA	Union Carbide
EBA (ethylene–butyl acrylate copolymer)	Lotryl	Atofina
MBS (poly(methyl methacrylate)-g-poly(butadiene/styrene) graft copolymer)	Paraloid EXL	Rohm & Haas
Core/shell acrylate	Durastrength 400	Atofina

^a E-EA-GMA (see Table 14.3) and EEA are often used in combination as a toughening system. The optimum blend ratio of reactive elastomers:non-reactive elastomers (e.g. Lotader:Lotryl) is 30/70. Since the E-EA-GMA terpolymer and EEA copolymer are mutually miscible, when blended together with PET the mixture acts as a single elastomeric phase, which is interfacially grafted to the PET continuous phase.

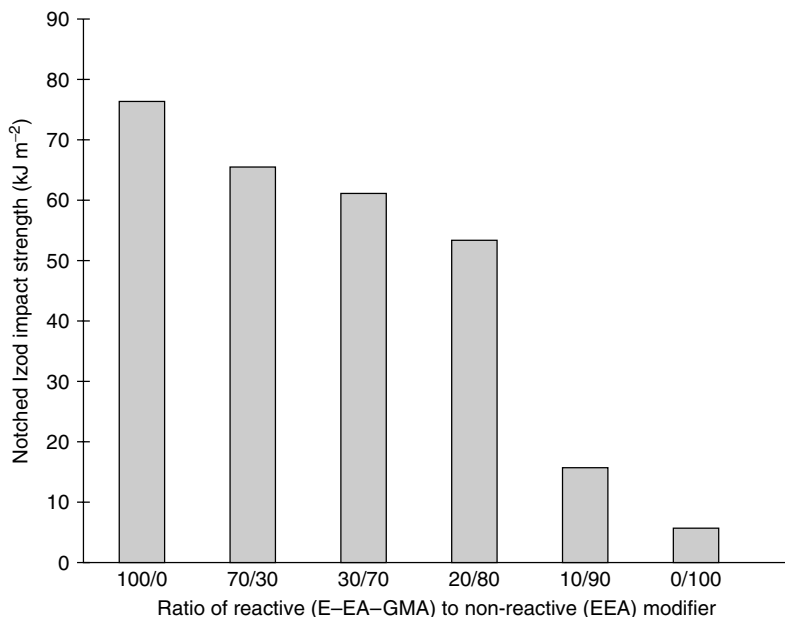


Figure 14.11 Variation of the notched Izod impact strength of PET containing 20% of an elastomeric toughening system as a function of the ratio of reactive to non-reactive modifier. It can be seen that the 30:70 reactive:non-reactive mixture provides the optimum balance. The reactive modifier acts more as a compatibilizer in this system. Note: units for impact strength (kJ m^{-2}) can be converted to J m^{-1} by multiplying by 10

styrene-*co*-butadiene random copolymer and a glassy shell composed of styrene and methyl methacrylate. MBS impact modifiers such as Paraloid EXL (Rohm & Haas) are effective tougheners for PET resins, especially those used for crystalline PET (CPET) applications which require low-temperature impact. The dispersion of small rubber 'core-shell' particles afforded by MBS tougheners provides PET with an excellent level of toughness, without strongly affecting other mechanical or thermal properties. The unique core-shell structure is obtained by copolymerization of a hard shell around a soft rubber core. This structure provides excellent impact properties to the PET due to the presence of the soft rubber core, without strongly affecting the matrix rigidity by virtue of the hard outer shell. In addition, since the core-shell structure is produced by emulsion copolymerization it provides a well-defined particle size which in turn leads to a well-controlled blend morphology. Grades of Paraloid EXL intended for PET modification include EXL 3300 and EXL 5375. Another impact modifier for PET is the core-shell modifier marketed under the trademark EXL 2330. Such impact modifiers are generally added at levels of around 10 wt%.

The PARALOID EXL range also includes PARALOID EXL 2314, an acrylic impact modifier with reactive functionality for PET impact modification.

4.3 THEORY OF IMPACT MODIFICATION OF PET

The following equation relates the interparticle distance (ID) to the volume fraction of the impact modifier (ϕ) and the weight-average particle size (dW) [28]:

$$\bullet ID = [(\pi/6\phi)1/3 - 1] dW \quad (14.2)$$

Figure 14.12 shows that the impact strength increases sharply as the interparticle distance is reduced. The toughness increases as the interparticle distance decreases to a critical size, but becomes lower again as the distance becomes too small. It can be seen that the critical interparticle distance for PET is 50 nm.

Pecorini and Calvert [28] attribute the role of small particles and a small interparticle distance to inducing high toughness in PET by promoting massive shear yielding in the matrix. Their study showed that the non-reactive impact modifier gives a system in which the rubber phase is not well dispersed. It was shown that this is not effective in toughening PET at levels of either 10 or 20 %. The

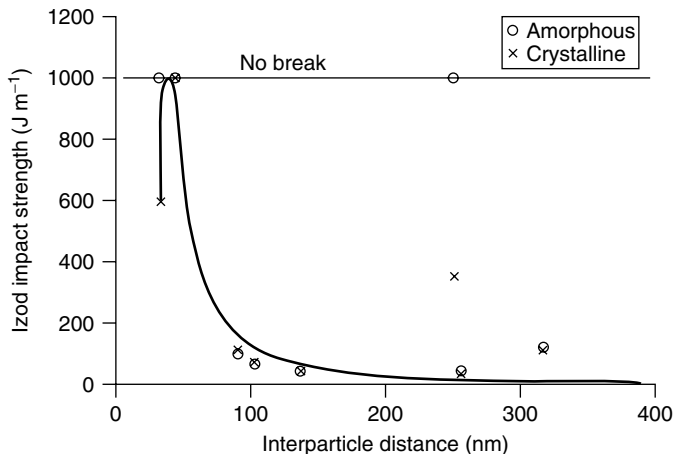


Figure 14.12 Notched Izod impact strength data (on crystallized PET) for samples of toughened polymer as a function of the ratio of interparticle distance: O, amorphous; x, crystalline [28]. Reprinted with permission from Pecorini, T. J. and Calvert, D., in *Toughening of Plastics – Advances in Modelling and Experiments*, Pearson, R. A., Sue, H.-J. and Yee, A. F. (Eds), ACS Symposium Series, 759, American Chemical Society, Washington, DC, 2000, Ch. 9, pp. 141–158. Copyright (2000) American Chemical Society

Table 14.5 Effect of impact modifier type, particle size and interparticle distance on the impact strength and elongation of PET

Property	Non-reactive modifier ^a	Non-reactive modifier ^a	Reactive modifier ^b	Reactive modifier ^b
Content (wt%)	10	20	10	20
Particle size (μm)	0.45	0.53	0.16	0.13
ID ^c (μm)	0.25	0.14	0.09	0.03
Izod impact strength (J/m)	35	45	118	659
Elongation at break (%)	8	7	16	65

^a Non-reactive impact modifier (copolymer of ethylene and methyl acrylate).

^b Reactive impact modifier (terpolymer of ethylene, methyl acrylate and glycidyl methacrylate).

^c Interparticle distance, i.e. the average distance between particles of impact modifier in the PET matrix.

reactive impact modifier, on the other hand, gives far superior impact strengths and can produce a material with 'supertoughness' (Table 14.5).

5 NUCLEATING AGENTS

One of the primary limitations of PET is related to its slow rate of crystallization from the melt. A consequence of this is that relatively long cycle times are required to provide crystallinity in PET. When this is achieved, it is often accompanied by opacity and brittleness, due to the relatively large size of crystallites formed by thermal crystallization. Crystallinity itself is often desirable in moulded parts, due to the higher thermal and mechanical stability associated with it. Crystallinity is especially desirable when parts are intended to be subjected to elevated temperatures since if the PET components are amorphous they will anneal at temperatures above 80 °C.

It is well known that PBT crystallizes much faster than PET and hence PBT is the preferred polyester resin for injection moulding. Unmodified PET cannot be injection moulded to give crystalline parts with economical cycle times. Because PET is an intrinsically slow-crystallizing polymer, nucleating agents are often used to increase the rate of crystallization. In fact, in order to use PET in injection moulding applications, nucleating agents are essential.

Quick cooling of the PET melt results in the formation of small spherulites but the crystallinity, however, remains low because the polymer is practically 'frozen' in its amorphous state. Slow cooling of the PET, on the other hand, leads to a high degree of crystallinity; however, the spherulites grow to a large size at which optimum mechanical properties are not attained. In addition, an uneven spherulite size distribution results. Achieving a high degree of crystallinity and small spherulites in PET simultaneously requires the use of nucleating agents and crystallization promoters. While inorganic nucleating agents such as talc are

somewhat effective in nucleating PET, it has been found that alkali metal salts of high-molecular-weight carboxylic acids are far more effective. The reason for this is that compared to inorganic nucleating agents which reside in the PET as discrete particles, the organic salts can be distributed throughout the PET matrix at a smaller scale and more homogeneously.

Nucleating agents in PET serve two main functions, as follows:

- To induce a small and regular crystalline structure (Figure 14.13).
- To suppress large crystal growth which causes brittleness.

Additional functions of the nucleating system include the following:

- To decrease demoulding time (i.e. decrease cycle time for the part).
- To allow the material to crystallize at a uniform rate in the mould which tends to result in lower moulded-in stresses.

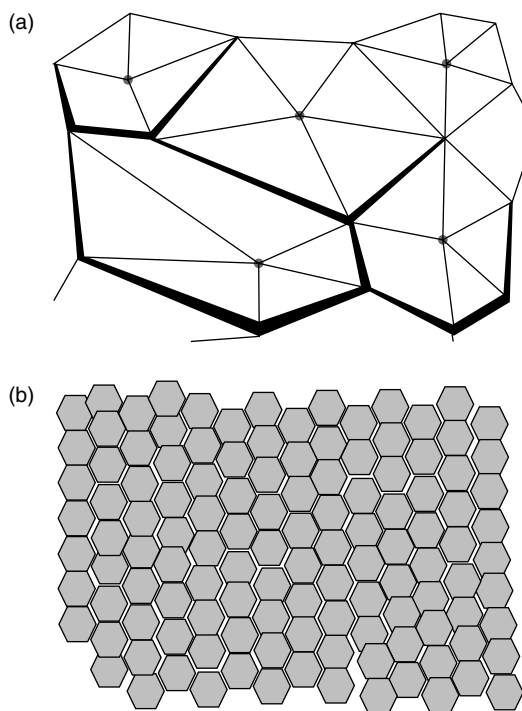


Figure 14.13 Effect of a nucleating agent on the spherulitic morphology of PET. (a) Without a nucleator, PET forms large and irregular crystallites. Mouldings are brittle since low-molecular-weight material are concentrated at the crystal boundaries. (b) With a chemical nucleating agent, PET gives a much more regular spherulitic microstructure and this translates to improved mechanical properties

- To override any effect that particulate impurities or polyolefin contamination would have in modifying the crystallization behaviour of recycled PET.

As mentioned above, PET can be nucleated physically (by heterogeneous particulates, e.g. talc particles) and chemically (by a chemical reaction). PET grades for injection moulding are usually chemically nucleated – that is, nucleating agents take part in a chemical reaction with the polymer which leads to the formation of an *in situ* nucleating species. PET is generally chemically nucleated by certain sodium salts such as sodium stearate. The high nucleation efficiency of sodium stearate is not due to the additive itself, but to the products created by reaction with PET. The precise mechanism of this type of nucleation in PET has been identified by Legras *et al.* [29–31]. Sodium stearate reacts with the ester linkages of the PET, creating sodium carboxylate chain ends (Figure 14.14). These have been shown to be effective nucleating species.

While this is an effective nucleation mechanism for PET, the efficiency of this system is not stable and decreases significantly with melt mixing (compounding) time. This instability is due to a disproportionation reaction in which the sodium chain ends react with each other to give disodium terephthalate. The subsequent decrease in ionic chain end concentration is directly linked to the loss in nucleation efficiency.

The main factors determining the efficiency of sodium salts of organic acids as nucleating agents for PET are alkalinity, solubility and thermal stability. These are widely varying for different families of products and a compromise has to be made between these properties. The more soluble and the more stable, then the

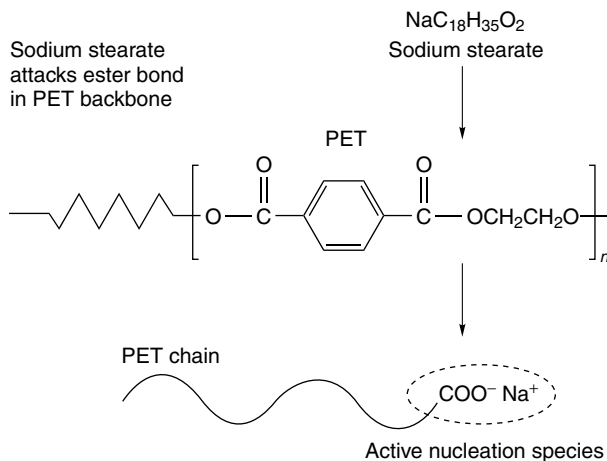


Figure 14.14 Sodium stearate is an efficient nucleating agent for PET since it scissions an ester bond and creates an ionic chain end which acts as the primary nucleation site. The disadvantage of this form of nucleation is that it leads to a reduction in the molecular weight of the polymer

more salt will react with PET. The counterion also has an influence but sodium usually offers the best compromise between reactivity for the nucleophilic attack of PET and thermal stability of the nucleating agent. The active nuclei are the platelet-like ionic chain ends. The size (and probably the crystal habit) of the nucleating molecules may also be considered as there seems to be an optimum corresponding to an optimal size of the platelet-like ionic chain ends aggregates which are thought to be the active nuclei [32].

It is not only sodium salts of monocarboxylic acids that are effective nucleating agents for PET; lithium, calcium and barium salts of monocarboxylic acids have also been found to impart nucleation ability [33].

Since chemical nucleating agents actively scission PET chains as part of their action, a drop in PET intrinsic viscosity can result. One strategy to offset this accompanying molecular weight reduction is to use both a nucleating agent and a chain extender in combination.

Due to both the limited thermal stability of sodium stearate during melt mixing and the molecular weight reduction accompanying chemical nucleation, another type of nucleating action is also employed. This is based on incorporating into the polymer a small percentage of melt-compatible resin which already contains sodium carboxylate chain ends rather than creating them *in situ*. Such ionomers have negatively charged acid groups which have been partially neutralized with sodium ions (see Figure 14.15). The nucleating system for commercial PET injection moulding compounds is thus typically based on a three-component package comprising the following:

- (i) sodium stearate (chemical nucleating agent)
- (ii) sodium ionomer (melt-miscible nucleating agent)
- (iii) poly(ether ester) (plasticizer to facilitate chain folding)

The use of nucleating agents in PET is not only intended for increasing the rate of crystallization and the crystallization temperature but also for forming a more homogeneous morphology, that is, a more uniform spherulite distribution.

Nucleating agents in PET also allow faster demoulding times, that is, the injection moulded part can be ejected from the mould more quickly or at a higher temperature.

Sodium ionomers are commercially recognized as the most effective nucleating agents for PET compounds. The typical use rate of sodium ionomer-based nucleating agents is 3–4 wt%. The sodium salt of poly(ethylene-*co*-methacrylic acid) is a particularly effective nucleating agent for PET.

Some examples of common nucleating agents used for PET are shown in Table 14.6. Aclyn ionomers (by Honeywell – formally Allied Signal) have proven to be highly efficient nucleating agents for PET and do not cause loss of MW. Use levels as low as 0.25 % promote rapid crystallization of PET. Such nucleators are particularly suited to thermoforming of PET trays where increased production rates can be achieved. Specifically, Aclyn 285 is particularly effective for lowering the crystallization onset temperature for PET, as shown in Table 14.7.

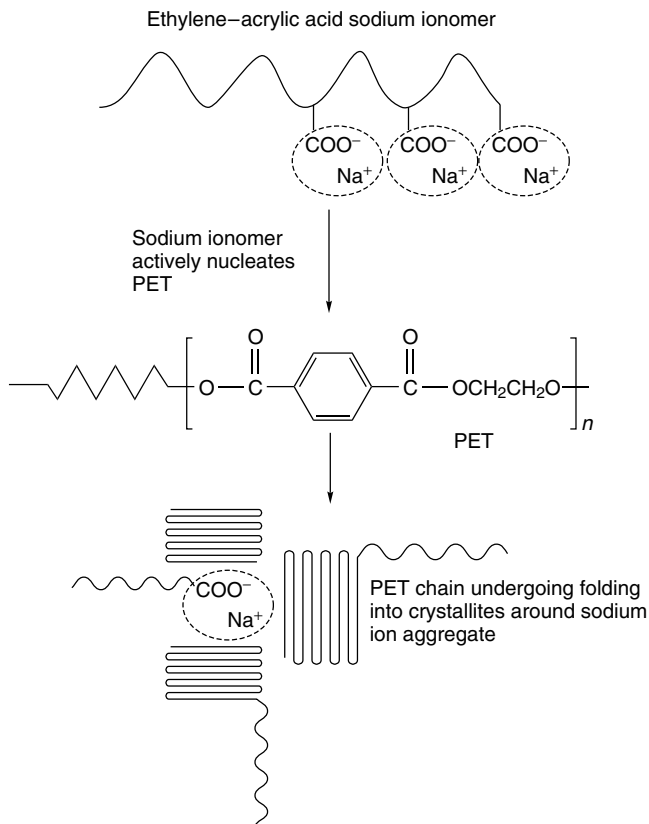


Figure 14.15 Mechanism of PET nucleation by sodium ionomers. A particular advantage of such compounds is that they provide active nucleation sites without molecular chain scission

Sodium-neutralized salts of montanic acid (e.g. Licomont NaV) are also effective nucleators for PET. Montanic wax consists of a mixture of straight-chain, saturated carboxylic acids with chain lengths in the range of 26 to 34 carbon atoms. The low volatility and high thermal stability of montanic acid waxes makes them a suitable nucleating agent for engineering plastics such as PET and PBT.

Phyllosilicates are clay-related compounds with a sheet structure such as talc, mica, kaolin, etc. for which the nucleation mechanism of PET is known to be heterogeneous, although still uncertain.

Nanoclay particles by virtue of their particulate nature are emerging as effective heterogeneous nucleating agents for polyesters. The nanoclay particles in PET/montmorillonite nanocomposites impart to PET a higher crystallization rate without the need for expensive nucleating agents.

Table 14.6 Commercial nucleating agents for PET

Nucleating agent	Tradename	Manufacturer
E-AA-Na ⁺ (ethylene-acrylic acid sodium ionomer)	Aclyn 285	Honeywell
E-MAA-Na ⁺ (ethylene-methacrylic acid sodium ionomer)	Surlyn 8920 ^a	DuPont
Sodium-neutralized salt of montanic acid wax	Licomont NaV101	Clariant
Sodium carboxylate salts (e.g. sodium stearate) ^b	—	SunAce
Sodium benzoate	—	Various
Sodium chlorobenzoate ^c	—	Aldrich

^a Copolymer of ethylene and 15 wt% of methacrylic acid neutralized with 60 % sodium cations.

^b Typical use rate is 1.2 % (can cause chain scission of PET chains).

^c Sodium chlorobenzoate reacts with PET and leads to a loss of molecular weight. Furthermore, the effectiveness of sodium chlorobenzoate is time-dependent, i.e. the effectiveness of a given amount of sodium chlorobenzoate is dependent on the processing time in the polymer melt.

Table 14.7 PET crystallization data (after 10 s exposure at 177 °C)

Nucleating agent	Nucleating agent concentration (%)	T_{ch}^a (°C)	T_{cc}^b (°C)	Crystallinity (%)
None	0	144	179	9
Aclyn 285	0.25	132	201	33
Aclyn 285	0.50	130	204	33
Aclyn 285	1.00	129	204	30

^a Temperature of hot crystallization.

^b Temperature of cold crystallization.

Newer nucleators include pyrrole-based salts which seem to produce chemical nucleation with a minimal molecular weight reduction.

6 NUCLEATION/CRYSTALLIZATION PROMOTERS

To facilitate and accelerate folding and crystallization of polymer chains, internal plasticizers are often added to PET to serve as crystallation promoters. Such additives are usually based on poly(ether ester)s. These plasticizers are liquids that are typically added at levels of 2–4 wt%. They reduce cycle time in injection moulding operations by increasing the rate of crystalline formation. They also plasticize the resin and act as processing aids by virtue of their lubricating action in the melt. On a molecular level, these plasticizers reduce the intermolecular

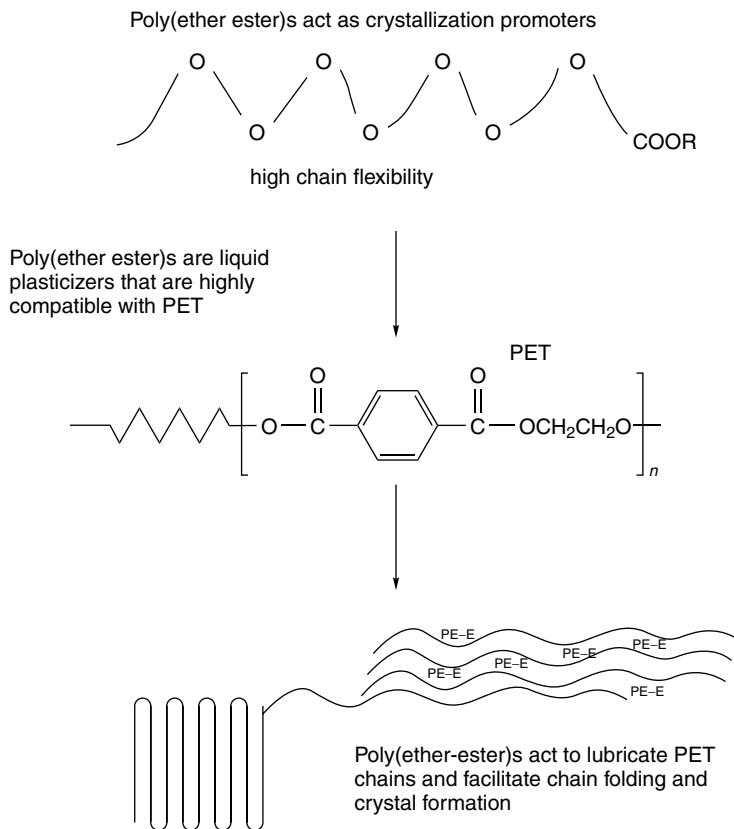


Figure 14.16 Mechanism by which poly(ether ester)s function as crystallization promoters. Such materials internally lubricate and plasticize the PET molecular chains, thus allowing reptation (i.e. chain folding) to occur more quickly

forces between the PET chains and allow the latter to slip past one another more easily (Figure 14.16).

Nucleation promoters are essentially plasticizers that have a high MW and low volatility which are compatible with polyesters and internally lubricate the polymer chains. They act by increasing the rate of crystallite formation once the nucleation agent has provided a nucleation site. Generally, these nucleation promoters/plasticizers belong to the poly(ether ester) family. These compounds provide the free volume in the PET molecules for essentially complete crystallization during the short mould-dwell time and at acceptably low mould temperatures. Such compounds reside between adjacent polymer chains and thereby aid crystal growth during nucleation. Some examples of common nucleation promoters/plasticizers for PET are shown in Table 14.8.

Table 14.8 Commercial nucleation promoters/plasticizers for PET

Promoter Plasticizer	Tradename	Manufacturer
PEG-400-diethylhexanoate	Tegmer 809	CP Hall
PEG-4-dilaurate	Uniplex 810	Unitex Chemical
Neopentyl glycol dibenzoate	Uniplex 512	Unitex Chemical
Triethylene glycol dibenzoate ^a	Benzoflex S-358	Velsicol Chemical Corporation

^a Further details given in Iida *et al.* [33].

Other less common nucleation promoters/plasticizers for PET include *N*-ethyl-toluenesulfonamide and trioctyl trimellitate.

An important requirement for liquid plasticizers intended for use in PET is that they have good high temperature stability and low volatility on account of PET's relatively high processing temperature (i.e. 280–300 °C). Furthermore, temperature stability is important since some additives that are stable during the processing of PBT may degrade in PET. Another important characteristic for additives for PET is that they have low acid and hydroxyl values since PET is susceptible to both acid- and alkali-catalyzed degradation.

7 ANTI-HYDROLYSIS ADDITIVES

PET resin contains ester bonds which are susceptible to hydrolysis at elevated temperatures in the presence of moisture. The hydrolysis reaction leads to molecular chain scission at the ester bond. As the polymer chains shorten, the molecular weight decreases such that the melt viscosity and intrinsic viscosity also drop. The concentration of carboxyl end groups also increases. The hydrolysis reaction rate begins to become significant at temperatures of 160 °C and above. Since PET is generally processed at temperatures of between 270 and 300 °C, it is apparent that the rate of hydrolysis can become appreciable. At 250 °C the rate of hydrolysis of PET is some 10,000 × that which occurs at 115 °C. Suppressing hydrolysis is especially critical for reprocessing of recycled PET. The effect of residual moisture on the notched Izod impact strengths of PET compounds is shown in Figure 14.17.

Anti-hydrolysis additives for PET are moisture scavengers that sacrificially react with moisture during melt processing or in service, thereby minimizing hydrolysis of the polyester. Anti-hydrolysis additives for PET and PBT chemically react with free moisture during extrusion. These additives can be based on carbodiimide (HN–C–NH). Commercially available polycarbodiimide additives include StabaxolTM P (Rhein Chemie Rheinau GmbH, Mannheim, Germany) and CarbodiliteTM (Nisshinbo Industries, Inc., Chiba-Shi Chiba, Japan).

Hydrolysis during melt processing can be suppressed significantly by the addition of such anti-hydrolysis additives. This enables the IV to be maintained across

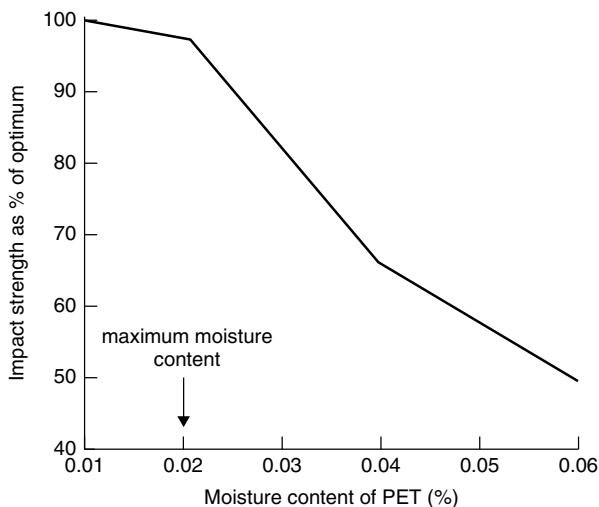


Figure 14.17 Relationship between notched impact strength of PET compounds and their moisture content. The plot emphasizes the need for proper drying of PET resin to reduce the moisture content to below 200 ppm before melt processing. Intensive drying procedures are time-consuming and costly and therefore internal desiccants are often used

melt processing operations. Improvements in tensile strength and impact strength have also been reported with the carbodiimide-mediated coupling of PET.

Such hydrolysis stabilizers act as acid- and water-scavengers, converting and neutralizing both water and acids into non-reactive urea structures. Addition rates of 0.5 wt% polycarbodiimide to PET can maintain its IV across melt processing even with only partial pre-drying of the PET. Polycarbodiimides also react with the terminal acid groups of PET and decrease the initial acid value of the polyester resin. Imashiro *et al.* [34] have described adding a carbodiimide compound to recycled PET such that the intrinsic viscosity and strength of the polyester resin during processing is maintained.

Stabaxol KE 7646 is a grade claimed for maintaining the intrinsic viscosity of recycled PET during melt processing. Such additives expand the possibilities for applications of recycled PET resin into new fields.

Polycarbodiimides are also used as additives to provide long-term hydrolytic stability to polyester components in service in moist and humid environments (e.g. glass-filled PET in dishwasher applications).

Heitz *et al.* [35] (BASF) describe the use of polycarbodiimide as an additive to produce hydrolysis-resistant PBT. Further patents describe glass-fiber-reinforced mixtures of PBT with an aromatic polycarbodiimide having improved impact strength [36], and mixtures of PBT with an aromatic polycarbodiimide having improved melt strength and intrinsic viscosity [37].

Stabaxol™ P is used normally as a hydrolysis stabilizer in non-food polyester applications. One of the main applications is the stabilization of monofilament. An additional advantage of Stabaxol™ P is that it also works as a viscosity modifier. Stabaxol™ P has no FDA approval, and this means that it can be used only for technical applications.

Some examples of common anti-hydrolysis agents for PET are presented in Table 14.9. Desiccant additives can be used in PET and PBT to control moisture evolution during melt processing of polyesters. Such additives are generally based on a treated calcium oxide which reacts chemically with any moisture present in the polymer during extrusion. The moisture scavenging process results in a calcium hydroxide residue that remains as uniformly distributed, inert particles (5 µm diameter) in the polymer (essentially it becomes a chalk filler). These additives are available as a masterbatch (e.g. Colloids Ltd, Merseyside, UK). This masterbatch is based on a selected grade of calcium oxide (60 wt%) in a low-density polyethylene carrier (melt flow index (MFI) of 5 g/10 min).

The addition rate of the Dessicante® masterbatch is typically 1.0–3.0 %. Approximately 1 % addition of the PE 48/10/96 masterbatch will remove 0.1 % of water from the polymer during the extrusion or compounding process.

8 REINFORCEMENTS

The reinforcing nature of inorganic fillers is dependant on both their aspect ratio (length to thickness ratio) and the interfacial shear strength that they develop in the PET matrix (a function of the type of surface treatment) (Table 14.10). Glass fibre reinforcement increases the flexural modulus, tensile strength and heat distortion temperature (HDT), while reducing the elongation at break. Bottle-grade recycled PET can be upgraded into engineering-grade PET for injection moulding through the addition of glass fibre reinforcement. The addition of glass fibre is used to upgrade the properties of PET recyclate from soft-drink bottles into injection moulding applications [38].

Table 14.9 Commercial anti-hydrolysis agents for PET

Compound	Tradename	Manufacturer
Polycarbodiimide	Stabaxol KE 7646 ^a	Rhein Chemie
Carbodiimide	Carbodilite E ^b	Nisshinbo Industries
Treated calcium oxide (Caloxol®)	Dessicante® PE 48/10/96	Colloids Ltd

^a Stabaxol KE 7646 (Rhein Chemie, Mannheim, Germany) is a masterbatch based on PET plus an aromatic polycarbodiimide.

^b Carbodilite E is a masterbatch of 10 wt% carbodiimide in a PET carrier resin.

Table 14.10 Commercial reinforcing agents for PET

Reinforcement	Aspect ratio	Tradenames
Glass fibre (chopped strand)	300:1 (typical dimensions, 10 μm \times 3 mm)	PPG 3540 ^a Vetrotex 952 Saint Gobain Owens Corning 183F
Wollastonite (calcium silicate)	16:1	Nyco
Montmorillonite ^b (layered silicate nanoclay)	1000:1	Cloisite 93A Cloisite 30B (Southern Clay Products)
Mica	30:1	Muscovite-type mica (supplied by KMG); phlogopite-type mica (supplied by Suzorite, Inc.)
Talc	30:1	Various

^a The glass fibre, PPG 3540, is a polyurethane-sized glass fibre manufactured by PPG Industries, Inc. The surface treatment on the glass fibre promotes good adhesion between the fibre and the polymer.

^b Note: montmorillonite is surface treated with octadecylammonium or dioctadecyldimethylammonium ions.

Wollastonite is a relatively inexpensive reinforcing filler and extending agent for thermoplastic polyesters. This material can be used to give PET some 'body' in profile extrusion and to prevent sagging. Certain grades of wollastonite (such as that supplied by Wolkem India Limited from the Wolkem's mines in Rajasthan, India) have an aspect ratio of up to 20:1. Wollastonite reinforcing agents are an ideal partial replacement for glass fibres for the reinforcement of polyesters such as PBT. With a loading of 30 % wollastonite, PBT attains a HDT (at 18.5 kg/cm²) of 180 °C. Improvements in other mechanical properties, such as tensile strength, flexural strength, flexural modulus, and notched and un-notched impact strengths, are also achieved.

Nanoclays (nanophase layered silicates) give improvements in tensile modulus and tensile strength of PET at levels of only 1 wt% compared with say 10 % conventional fillers or analogously at loadings of 3 wt% compared with 30 % glass fibre (Table 14.11). The major benefit of nanoclay reinforcements is mechanical property improvement with minimal density (i.e. weight) increase. This is particularly advantageous for plastic components for automotive applications. Another benefit conferred by nanoclays is flame retardancy due to the tortuous path that hot combustion gases evolving from the polymer must take to reach the flame zone. Nanoclay particles in PET also increase the onset temperature for thermal degradation, decrease the heat output during burning, form protective char layers, and overall, impart self-extinguishing characteristics.

Table 14.11 Property improvements of PET that are observed after the addition of 3 % nanoclay

Property	Improvement with nanoclay (%)
Elastic modulus	90 % higher
Tensile strength	55 % higher
Impact strength	22 % higher
Thermal expansion coefficient	52 % lower
Heat distortion temperature	123 % higher
Water uptake	41 % lower

9 FLAME RETARDANTS

Approximately 40 % of the thermoplastic polyester resin that is sold (excluding PET packaging resins) is flame-retarded. PET used for switches, sockets and other applications where the material is in direct contact with live parts of electronic and electrical appliances are required to be flame retardant.

PET can be made flame retardant (FR-PET) by halogenated additives in combination with synergists such as antimony compounds (which impart no flame inhibition by themselves). During combustion, volatile antimony trihalide is formed in the condensed phase and transported to the gas phase. Failure of this flame retardant in PET compounds can occur, however, due to the formation of stable metal halides such as the following:

- in the presence of calcium carbonate—stable calcium bromide forms
- in the presence of fumed silica—stable silicon bromide forms

This renders the halogen unavailable for reaction with the antimony compound, and therefore neither the halogen nor the antimony are transported into the flame zone during combustion.

The following examples demonstrate common pitfalls encountered when flame-retarding PET compounds:

- An antagonism can occur between phosphorus flame retardants and antimony compounds when used in combination.
- Phosphate esters hydrolyze easily, thus precluding their use in PET.
- Aluminium trihydrate (ATH) decomposes, absorbing energy from the flame and evolving water vapour which blankets and smothers the flame. The resulting water vapour at 230 °C can cause ‘massive’ hydrolysis of PET.
- Antimony oxide flame retardants act as depolymerization agents for PET. Instead, sodium antimonate is the synergist of choice.
- Brominated flame retardants can induce degradation namely, acid-catalyzed hydrolysis of PET.

- Magnesium hydroxide is very basic (high pH) and will degrade PET and PBT if it is used as a flame retardant [39].

Generally, flame retardants for engineering PET compositions are based on bromine-containing compounds (such as brominated polycarbonate, decabromodiphenyl oxide, brominated acrylic, brominated polystyrene, etc.). Such compounds are available commercially (such as from the Ethyl Chemical Corporation, Great Lakes Chemical Corporation, Dead Sea Bromine Company, etc.) In addition, the flame-retardant package generally contains a synergist, typically sodium antimonate. PET may also be flame-retarded with diarylphosphonate, melamine cyanurate or red phosphorus.

The two main brominated flame retardants used commercially in PET are PyroChek 68PB (see Figure 14.18) and Saytex HP-7010 (Albemarle). Both of these flame retardants are based on brominated polystyrene. While there are similarities between these flame retardants, they are not equivalents. There are quality and performance differences between these two products as they use different raw materials (i.e. polystyrenes) and the process for bromination is different. Saytex HP-7010 has better thermal stability and colour control than does PyroCheck 68PB. However, if higher flow characteristics are a necessary property of the FR-PET, then Pyrocheck 68PB would be the product of choice. Sodium antimonate is the appropriate synergist in PET since it is more stable at the higher processing temperatures required of PET and does not cause depolymerization of this polyesters.

The loading level required of these flame retardants for a 30 % glass-filled PET is in the range of 12 to 13 % for a 94V-0 rating. The antimony synergist should be used at the 4 to 6 % range. The quality differences of Saytex 7010 and Pyrocheck 68PB are such that an acid neutralizer should also be a part of the formulation, e.g. an inorganic-type stabilizer (e.g. talcite or DHT-4C). Saytex 7010 would require about 300 ppm, while Pyrocheck 68PB would need about

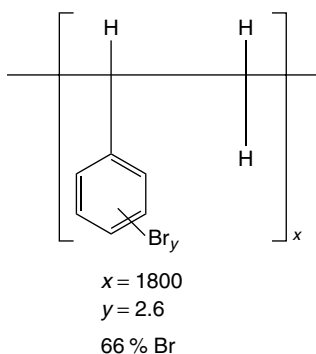


Figure 14.18 The chemical structure of PyroChek 68PB (Albemarle Corporation), a highly effective flame retardant for PET

Table 14.12 Commercial flame retardants for PET

Flame retardant	Tradename	Manufacturer
Brominated polystyrene	PyroChek 68PB	Albemarle Corporation
Brominated polystyrene	Saytex HP-7010	Albemarle Corporation
Sodium antimonate	Thermoguard FR sodium antimonate	OxyChem
Melamine polyphosphate	Melapur 200	DSM
Antidripping PTFE	Teflon 60 Hostaflon 9202	DuPont Hoechst

2000 ppm of such a stabilizer. The acid neutralizer helps with colour control, melt viscosity control and reduced equipment corrosion [40].

PET requires special flame-retardant chemistry since the antimony oxide synergist that is normally used in combination with brominated flame retardants causes de-esterification of the PET chain and concomitant molecular weight loss. In place of antimony oxide, PET requires a sodium antimonate synergist. Another problem with antimony trioxide is that it decreases the thermal stability of the brominated flame retardant which then produces hydrobromic acid which degrades the PET.

PET can achieve a UL94 V-0 rating at 0.8 mm when using 13–15 % Pyrocheck 68PB and 4–7 % sodium antimonate. For example, Pyrocheck 68PB is used in Rynite by DuPont. Sodium antimonate (NaSbO_3) (Thermoguard FR) is a fine white powder used as the antimony source to flame-retard selected polymers as well as for pigment applications. Since Thermoguard FR has a basic pH, it is the antimony synergist recommended to flame-retard acid-sensitive polymers and polyesters such as PET and PBT.

As the glass content of PET goes down, the polymer content goes up and therefore the requirement will be for additional flame retardant. In addition to the required flame-retardant loading with reduced filler, there will generally be an increase in the dripping during the burn test, such as UL94. This generally is controlled by the addition of an anti-drip agent such as Teflon at loadings of 0.5 to 1.0 wt%. The addition of 1 % of anti-drip Teflon 60, or Hostaflon 9202 or 1665, is usually used. Control of dripping will be necessary to obtain the 94V-0 rating.

Some examples of common flame retardants used for PET are shown in Table 14.12.

10 POLYMERIC MODIFIERS FOR PET

PET can be blended with PBT or polycarbonate (PC) to make blends or alloys. Polycarbonate is a high T_g (150 °C) ductile, high-impact-strength polymer but has rather poor solvent resistance because of its amorphous nature. PET/PC blends have therefore proved advantageous because they combine the solvent-resistance

Table 14.13 Common polymeric modifiers for PET

Polymer	Effect on PET properties
PC	Better impact strength
PBT	Better crystallization
Phenoxy resin	Improve impact strength and heat distortion temperature

advantages of PET with the high T_g and toughness advantages of PC. Blends of PET and PC are phase-separated systems that exhibit partial miscibility in the absence of significant ester interchange. In blends containing >40 % PET, the continuous phase (matrix) is PET-rich, while the dispersed phase (domains) is PC-rich. This partial miscibility is responsible for the self-compatibilizing nature of the blend, hence resulting in good delaminating resistance and tensile strength. However, despite the good ductility of this blend and drop-weight impact strength, the notched Izod impact strength of this blend is still quite low (<60 J/m). For this reason, an elastomeric toughener is invariably needed to improve the notch sensitivity of PET/PC blends [26].

Phenoxy resins can also be used for the modification of PET and PBT. Phenoxy resins such as PaphenTM PKFE (Inchem Corporation) are polyhydroxyether materials with pendant hydroxyl groups that can react with the PET. PaphenTM phenoxy resins are reactive modifiers that can modify and upgrade brittle polymers. Such resins contain 6 % of secondary hydroxyl groups. The latter serve as reactive sites for reaction with polyesters, polyamides, polycarbonates, epoxies and phenolics.

PET undergoes transesterification with the phenoxy polymer (actually it is an oligomer). The transesterification is a bonding reaction between the pendant hydroxyl (OH) groups on the phenoxy resin repeat unit and the terminal acid (COOH) groups on the polyester chains. The result is that individual PET polymer chains become coupled together (thus increasing the molecular weight) and also that the thermally stable phenoxy backbone is inserted into the PET structure. This is claimed to upgrade the mechanical properties of polyesters and to enhance their structural integrity.

The effects that the most commonly used polymeric modifiers have on the properties of PET are shown in Table 14.13.

11 SPECIALTY ADDITIVES

11.1 MELT STRENGTH ENHANCERS

Polycondensation polymers such as PET are characterized by low melt viscosities and low melt strengths. Furthermore, with PET there is a marked shear liquefaction

during the processing of the polymer melt – accordingly, PET exhibits low melt elasticity. These attributes are the opposite of those required for good foamability of polymers. Therefore, the production of foam from PET can only be achieved by structural modification of the polymer to improve its melt strength and melt elasticity. Melt strength enhancers are generally based on chain extenders (see Section 2).

The Eastman Chemical Company (Kingsport, TN) produces a reactive additive masterbatch, Eastolite[®] E3031-92AA, which increases the melt strength of PET to help facilitate foaming. The pyromellitic dianhydride additive attaches itself to the ends of the PET molecules, forming ‘pseudo-star molecules’ by adding chain length and branches. Starting with PET resin with an intrinsic viscosity of 0.80 dl/g, the addition of the melt-strength-enhancing additive raises the intrinsic viscosity to 1.2 dl/g and significantly increases the melt strength so that stable PET foaming can occur. Another melt strength enhancer is Eastapak MSE 14438 which is based on a PETG copolyester.

11.2 CARBOXYL ACID SCAVENGERS

The carboxyl end group (CEG) content of PET is an indicator of the number of acid groups on the ends of the PET chain. The CEG content of the PET has an influence on the hydrolysis resistance of the polymer. The lower the value, then the higher the hydrolysis resistance. Phenylenebisoxazoline (PBO) is an effective carboxyl acid scavenger for PET where it reacts with acid end groups and in doing so couples the PET chains, thus increasing the polymer molecular weight. Polycarbodiimides also react with terminal acid groups of PBT and lowers its acid value.

11.3 TRANSESTERIFICATION INHIBITORS

Transesterification of PET/PC blends can lead to copious gas evolution (carbon dioxide). To suppress transesterification of binary polyesters, inhibitors such as inorganic phosphates can be added.

11.4 GLOSS ENHANCERS

Gloss enhancers are additives that when added to PET or PBT produce a glossy surface finish that is similar to that of acrylonitrile–butadiene–styrene (ABS) terpolymer. Such additives include AC wax, such as AC316 (Honeywell).¹ These waxes have limited compatibility with PET and ‘bloom’ to the surface to give a

¹ AC[®] waxes are a range of low-molecular-weight polyethylene performance products available from Honeywell (formerly from Allied Chemicals). Further details are available on the web site: [<http://www.acperformanceproducts.com/index.html>].

high gloss surface. These wax-based additives also function as a mould release and external lubricant. AC316 can also nucleate PET in applications such as thermoformed PET trays where they enable faster processing speeds. AC400A wax, based on an ethylene–vinyl acetate copolymer, is effective as a gloss enhancer for PET resins at dosages of 0.3–1.0 %. The vinyl acetate portion gives some compatibility with PET while still providing external lubrication.

11.5 ALLOYING (COUPLING) AGENTS

Alloying agents can compatibilize polyester blends, thus producing alloys with enhanced mechanical properties. Such alloying agents can be based on titanate or zirconate compounds (e.g. Kenreact Lica-12 by Kenrich). For example, a titanate alloying agent can compatibilize an unusual mix of 80 % continuous-phase recycled PET with 20 % recycled polycarbonate (see Table 14.14). Such an organotitanate (manufactured by Kenrich Petrochemicals Inc.) at a concentration of 1 % can improve the elongation to break and impact strength of polyesters.

11.6 PROCESSING STABILIZERS

Phosphite processing stabilizers are used in PET to maintain the IV, suppress yellowing and overall to reduce thermo-oxidative degradation.

For processing and thermal stabilization of PET the following stabilizers are recommended – Irganox HP 2215, Irganox B 561, Irganox 1425, and in selected cases, Irganox 1222 (Irganox is a trademark of Ciba Specialty Chemicals).

Certain organophosphorus compounds can be used to melt-stabilize PET. Stabilizers such as 3,5-di-*t*-butyl-4-hydroxybenzyl diethyl phosphate (Irganox 1222) and triphenylphosphate lead to a reduction in the concentration of terminal carboxyl groups of PET, thus giving improved hydrolytic stability.

Table 14.14 Effect of a titanate alloying agent (Kenrich Lica-12) on a 80/20 PET/PC blend (data obtained from Kenrich Petrochemicals Ltd)

Property	Unmodified PET/PC	PET/PC +0.2 % alloying agent	PET/PC +0.5 % alloying agent
Notched Izod impact (lb ft/in)	0.832	0.819	0.80
Deflection temperature (°C)	151	165	172
Melt flow rate (285 °C, 2.16 kg) (g/10 min)	37	48	84
Tensile strength (psi)	7 085	8 137	8 405
Elongation (%)	10	93	68
Tensile modulus (psi)	189 140	348 800	330 449

12 TECHNOLOGY OF COMMERCIAL PET ENGINEERING POLYMERS

Engineering-grade PET finds widespread use in numerous load-bearing applications, as demonstrated in Table 14.15.

The principal commercial grades of engineering-grade PET are shown in Table 14.16.

12.1 RYNITE™

Rynite by DuPont is a toughened PET based on Elvaloy PTW as the impact modifier [42]. Elvaloy PTW is an ethylene terpolymer containing epoxy functional groups based on glycidyl methacrylate (GMA). This terpolymer exhibits excellent adhesion to the PET matrix because of its epoxy functionality. In addition, it confers excellent low-temperature properties due to its low glass transition temperature which is a function of the *n*-butyl acrylate component. While Elvaloy PTW markedly improves the notched impact strength of PET it does detract from PET's flexural modulus (i.e. stiffness), tensile strength and extruder residence time (due to the higher viscosity).

The formulation for Rynite™ from DuPont is described in United States Patent 4 753 980 [41]. This disclosure discusses the use of an ethylene terpolymer such

Table 14.15 Typical applications for engineering-grade PET

Sector	Specific applications
Automotive	Distributor housings, coil housings, rotors, ignition system components, electrical system components, grill opening retainers, mirror housings, windshield wiper components, headlight bezels, HVAC ^a vent doors, cowl vents
Consumer electronics and appliances	Motor housings and internal components, corn poppers, coffee makers, hair curlers and dryers
Furniture	Arm rests, seat shells and bases

^a Heating, ventilating and air-conditioning.

Table 14.16 Commercially available engineering-grade PET resins

Tradename	Manufacturer
Rynite	DuPont
Petra	Honeywell
Impet	Ticona GmbH
Eco Vylopet	Toyoda Gosei Company

as ethylene–methacrylate–glycidyl methacrylate to toughen PET. The critical point highlighted in this patent is that the dispersed elastomeric phase must have an average particle size of less than $3\text{ }\mu\text{m}$ to confer effective toughening. A typical toughened PET composition claimed in this DuPont patent is as follows:

- (a) 20 % of E–BA–GMA (Elvaloy with 63 % of ethylene, 31 % of *n*-butyl acrylate (BA) and 6 % of glycidyl methacrylate (GMA)) was first compounded with 80 % of PET.
- (b) 60 % of this compounded blend was then mixed with 30 % of coupled glass fibre, 3.8 % of Surlyn 8920 (sodium-neutralized ethylene–methacrylic acid copolymer), 0.6 % of an epoxy compound (e.g. Epon 1009 by Shell – a condensation product of epichlorohydrin and bisphenol A), 4 % of Uniplex 512 (by Unitex Chemical – the dibenzoate of neopentyl glycol) and 0.4 % of a phenolic antioxidant. This blend is then extruded through a single screw extruder.

12.2 PETRA™

The formulation for Petra™ from Honeywell (formerly Allied Signal) is described in United States Patent 5 723 520 [42]. This disclosure concerns the preparation of toughened PET composites by first pre-reacting the PET with a copolymer of ethylene and a glycidyl acrylate or methacrylate and then subsequently blending with a nucleating agent (such as the sodium salt of a carboxylic acid, e.g. sodium stearate) to increase the crystallization rate of the polyester. Glass fibers or reinforcing fillers are then added to provide rigidity and heat distortion resistance. The compositions exhibit a good balance of toughness, rigidity and gasoline resistance, and are particularly useful for automotive structural parts such as inner door frames, panels, reinforcements, bumper beams, window surrounds, and other metal-replacement applications. These glass-filled PET (GF-PET) compounds possess flexural modulus values from about 1000 to about 15 000 MPa (in accordance with ASTM D-790) and a notched Izod impact strength of at least about 70 J/m (in accordance with ASTM D-256).

12.3 IMPET™

The formulation for Impet from Ticona (a Division of the Hoechst Celanese Corporation) is described in United States Patent 6 020 414 [43]. The latter discloses toughened PET formulations based on an ethylene–alkyl acrylate copolymer and an ethylene–alkyl methacrylate copolymer. The crux of this patent is to use a combination of an elastomeric terpolymer functionalized with glycidyl acrylate or glycidyl methacrylate and an alkyl acrylate or alkyl methacrylate (the latter forming the major part of the combination – up to 40 wt%). For instance,

a typical formulation is based on PET plus 4wt% of the terpolymer ethylene–methyl acrylate–glycidyl methacrylate (E–MA–GMA) plus about 16 wt% of the total composition of ethylene–methyl acrylate (EMA) and 15 % of glass fibre. Suitable commercially available terpolymers include ethylene–methyl acrylate–glycidyl methacrylate formulations sold under the tradenames of Lotader™ AX8900, AX8920, AX8660, AX8850 and AX8870 (from Atofina).

13 COMPOUNDING PRINCIPLES FOR PREPARING ENGINEERING-GRADE PET RESINS

The compounding of toughened PET formulations is generally carried out on a twin-screw extruder with down-stream glass feeding capability. Many such compounders are commercially available (such as, for example, the Werner Pfleiderer twin-screw extruder). The extruder may be fed with the resin and additives at the main hopper while the glass is fed downstream. The melt temperature is maintained in the range 260–300 °C. The material is compounded and then pelletized. Vacuum venting is generally performed at the first two vents to remove volatiles such as moisture, carbon dioxide, ethylene glycol, etc. The compounder should be configured with at least two sets of kneading blocks and reverse bushings to give adequate high-shear regions for effective dispersion of the rubber toughener. The geometry of the screws should be set up to give the best combination of dispersive and distributive mixing. The reason for this being that for effective rubber toughening of PET, the rubber domains must have a particle size of less than 3 µm.

A twin-screw extruder is generally preferred for producing rubber-toughened, glass-filled PET compounds for injection moulding applications. The PET and impact modifier are added at the throat while the glass reinforcement is added downstream. The size of the rubber domains will depend on the amount of energy and the capability of the equipment used for dispersion.

It is important to avoid a potential interaction between the reactive impact modifiers (i.e. those with GMA end group functionalities) and the coupling agent on the glass fibre reinforcement. For this reason, it is important to add the glass fibre to the compounder downstream, by which time the reactive toughener will have grafted to the PET matrix. It is believed that the reactive toughener can inhibit the silane reaction with the PET.

14 COMMERCIAL GLASS-FILLED AND TOUGHENED PET GRADES

Literature citations report that untoughened, crystallized PET mouldings are quite brittle, particularly under conditions of stress concentration such as when sharply

Table 14.17 Commercial grades of glass-filled PET

Grade	Izod impact strength (J/m)	Comments
Petra 110 BK-112	55	15 % GF
Petra 110	70	15 % GF
Rynite 520	70	20 % GF
Rynite 530	85	30 % GF
Petra 140 BK-112	90	45 % GF
Petra 130	95	30 % GF
Petra 130 BK-112	95	30 % GF
Petra 7030	95	30 % GF
Rynite 545	106	45 % GF
Petra 140	110	45 % GF
Petra 132 BK-112	120	Impact-modified; 30 % GF
Rynite 408	120	Impact-modified; 30 % GF
Rynite 415HP	130	Impact-modified; 15 % GF

notched. Such mouldings have low notched Izod impact strengths (30–50 J/m) [26]; whereas toughened PET has Izod values of 70–120 J/m, while ‘supertoughened’ PET exhibits Izod impact values of 300–1000 J/m. Indeed, PET with 20 % reactive impact modifier can give NB (no break) results in the ASTM D-256 Izod impact test.

Table 14.17 summarizes the impact strength of commercial GF-PET resins for comparative purposes.

15 ‘SUPERTOUGH’ PET

The notched Izod impact strength of PET at room temperature is only 45 J/m. ‘Supertough’ PET with notched impact strengths up to 1000 J/m can be prepared by melt blending PET with 20 wt% of a reactive elastomeric terpolymer (e.g. E–MA–GMA). Pecorini and Calvert [28] have attributed this supertoughness phenomenon to two distinct toughening mechanisms, as follows:

- Massive shear yielding in the matrix when the dispersed particles are less than 200 μm in size.
- Multiple crazing in the matrix when the particle size of the dispersed particles is larger.

These authors found that to achieve supertoughness in PET by shear yielding, a reactive modifier is superior to a non-reactive rubber modifier and that a dispersed particle size and interparticle distance of 200 and 50 nm, respectively, are

required. Alternatively, supertoughness can also be achieved through a mechanism of multiple crazing when a dispersed particle size of $1\text{ }\mu\text{m}$ is achieved.

16 AUTOMOTIVE APPLICATIONS FOR MODIFIED PET

Some typical automotive applications for reinforced and toughened PET are illustrated in Figure 14.19.

Recently, Mitsubishi Motors have produced a 1900 cm^2 engine cover injection moulded from glass-fibre-reinforced recycled PET. This polymer material is said to have properties similar to the polyamide normally used for engine covers. Recycled PET in its conventional form has low impact strength, and so a 'strength-enhancing additive' (a rubber toughener) is employed in a design that is 10 to 30 % thicker in cross-section than conventional polyamide. The resulting component has an Izod impact strength superior to polyamide. The material, called ECO VYLOPET is based on recycled PET and was developed jointly by the Toyoda Gosei Company, Ltd and the Mitsubishi Motors Corporation. Both

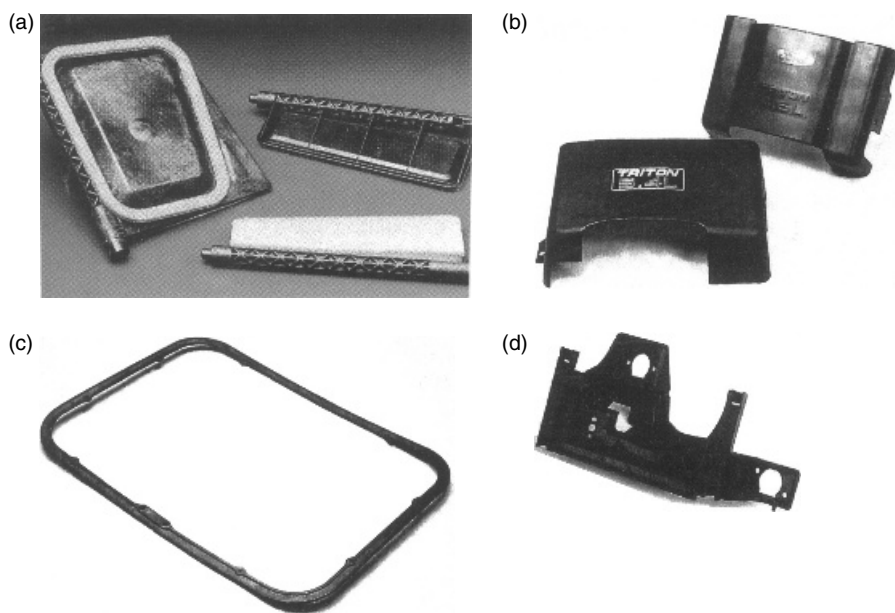


Figure 14.19 Typical automotive applications made from glass-filled recycled PET compounds: (a) heating and air conditioning door duct vents for Ford's Taurus, Mercury Sable and Lincoln Continental models; (b) engine covers for Ford vehicles; (c) fixed window surround for the Ford Excursion model; (d) headlamp retainer for GM's Montana, Yukon and Sierra trucks

the latter and the Toyota Motors Corporation use this material to produce their automobile engine covers.

A variant of the Impet Hi 430 PET grade (Ticona, USA) is being used in the Chrysler Corporation Composite Concept Vehicle (CCV). The polyester parts for the CCV body are the largest components ever moulded in an engineering thermoplastic. The new Plymouth Pronto Spyder concept sports car uses another variant of the new PET formulation in its moulded car body. Impet Hi 430 PET resin contains only 15 % glass and is easy to injection mould. At -20°C , for example, the material exhibits a 40 % higher notched impact strength (8.8 kJ/m^2) than conventional glass-reinforced PET resins. Ticona's compounding technology has given traditionally brittle PET more ductile failure modes and greater impact strength for these demanding structural applications.

REFERENCES

1. Smith, V. and Trevitt, E. W., *World patent WO 90/10 667*, 1990.
2. Hirai, T. and Amano, N., in *Proceedings of the 51st SPE ANTEC'93 Conference*, New Orleans, LA, 9–13 May, 1993, Society of Plastics Engineers, Brookfield, CT, 1993, pp. 1256.
3. Aharoni, S. M., Forbes, C. E., Hammond, W. B., Hindenlang, D. M., Mares, F., O'Brien, K. and Sedgwick, R. D., *J. Polym. Sci., Polym. Chem. Ed.*, **24**, 1281 (1986).
4. Jacques, B., Devaux, J. and Legras, R., Effectiveness of nucleating agent in PET, *Polymer*, **17**, 1189 (1996).
5. Bikiaris, D. N. and Karayannidis, G. P., Chain extension of polyesters PET and PBT with two new diimidodiepoxides, *J. Polym. Sci., Polym. Chem. Ed.*, **34**, 1337 (1996).
6. Pfaendner, R., Herbst, H. and Hoffmann, K., Increasing the molecular weight of polyesters, *US Patent 5 693 681* (to Ciba Specialty Chemicals), 1997.
7. Kao, H.-C., Chen, L.-H., Wu, C.-L., Wong, J.-J., Chan, S.-Y. and Yang, S.-T., Composition and process for preparing high molecular weight polyester, *US Patent 6 239 200* (to Industrial Technology Research Institute, Hsinchu, Taiwan), 2001.
8. Simon, D., Pfaendner, R. and Herbst, H., Molecular weight increase and modification of polycondensates, *US Patent 6 469 078* (to Ciba Specialty Chemicals GmbH, Lampertheim, Germany), 2002.
9. Incarnato, L., Scarfato, P., Di Maio, L. and Acierno D., Structure and rheology of recycled PET modified by reactive extrusion, *Polymer*, **41**, 6825 (2000).
10. Al Ghatta, H. and Cobror, S., Polyester resins having improved rheological properties, *US Patent 5 776 994* (to Sinco Engineering SpA, Italy), 1998.

11. Karayannidis, G. P. and Psalida, E. A., Chain extension of recycled poly(ethylene terephthalate) with 2,2'-(1,4-phenylene)bis(2-oxazoline), *J. Appl. Polym. Sci.*, **77**, 2206 (2000).
12. Haralabakopoulos, A. A., Tsiourvas, D. and Paleos C. M., Chain extension of poly(ethylene terephthalate) by reactive blending using diepoxides, *J. Appl. Polym. Sci.*, **71**, 2121 (1999).
13. Bikiaris, D. N. and Karayannidis, G. P., Calorimetric study of diepoxide chain-extended poly(ethylene terephthalate), *J. Therm. Anal. Calorim.*, **54**, 721 (1998).
14. Bikiaris, D. N. and Karayannidis, G. P., Dynamic thermomechanical and tensile properties of chain-extended PET, *J. Appl. Polym. Sci.*, **70**, 797 (1998).
15. Japon, S., Boogh, L., Leterrier, Y. and Manson J. A. E., Reactive processing of poly(ethylene terephthalate) modified with multifunctional epoxy-based additives, *Polymer*, **41**, 5809 (2000).
16. Japon, S., Leterrier, Y. and Manson, J.-A. E., Recycling of poly(ethylene terephthalate) into closed-cell foams, *Polym. Eng. Sci.*, **40**, 1942 (2000).
17. Leterrier, Y., Laboratoire de Technologie des Composites et Polymères (LTC), Ecole Polytechnique Fédérale de Lausanne (EPFL), CH-1015 Lausanne, Switzerland, personal communication, 2001.
18. Guo, B. H. and Chan, C. M., Chain extension of poly(butylene terephthalate) by reactive extrusion, *J. Appl. Polym. Sci.*, **71**, 1827 (1999).
19. Nascimento, C. R. and Dias, M. L., Poly(ethylene terephthalate) recycling with organic phosphites – I. Increase in molecular weight, *J. Polym. Eng.*, **20**, 143 (2000).
20. Dias, M. L. and Silva, A. P. F., Transesterification reactions in triphenyl phosphite additivated-poly(ethylene terephthalate)/poly(ethylene naphthalate) blends, *Polym. Eng. Sci.*, **40**, 1777 (2000).
21. Loontjens, T., Pauwels, K., Derks, F., Neilen, M., Sham, C. K. and Serné, M., The action of chain extender in Nylon 6, PET and model compounds, *J. Appl. Polym. Sci.*, **65**, 1813 (1997).
22. (a) Loontjens, T., Stanssens, D., Belt, W. and Weerts, P., Synthesis of bisoxazolines and their application as chain extenders for PET, *Makromol. Chem., Makromol. Symp.*, **75**, 211 (1993); (b) Loontjens, T., Stanssens, D., Belt, W. and Weerts, P., Synthesis of 1,2-bis(2-oxazolinyl)ethane and its application as a chain extender for PET, *Polym. Bull.*, **30**, 13 (1993).
23. Steiner, U. B., Borer, C., Oertli, A. and Pfaendner, R., presentation given at the *R'97 Congress*, Geneva, Switzerland, 4–7 February, 1997.
24. Pfaendner, R., Herbst, H. and Hoffman, K., Increasing the molecular weight of polycondensates, *US Patent 5 807 932* (to Ciba Specialty Chemicals GmbH, Lampertheim, Germany), 1998.

25. Tanrattanakul, V., Hiltner, A., Baer, E., Perkins, W. G., Massey, F. L. and Moet, A., Effect of elastomer functionality on toughened PET, *Polymer*, **38**, 4117 (1997).
26. Akkapeddi, M. K., Van Buskirk, B., Mason, C. D., Chung, S. S. and Swamikannu, X., Performance blends based on re cycled polymers, *Polym. Eng. Sci.*, **35**, 72 (1995).
27. Chrien, K., Reyes, J. and Freed, W., *Eng. Plast.*, **6**, 262 (1993).
28. Pecorini, T. J. and Calvert, D., The role of impact modifier particle size and adhesion on the toughness of PET, in *Toughening of Plastics – Advances in Modelling and Experiments*, Pearson, R. A., Sue, H.-J. and Yee, A. F. (Eds), ACS Symposium Series, 759, American Chemical Society, Washington, DC, 2000, Ch. 9, pp. 141–158.
29. Legras, R., Mercier, J. P. and Nield, E., *Nature (London)*, **304**, 5925 (1983).
30. Legras, R., Bailey, C., Daumerie, M., Dekoninck, J., Mercier, J., Zichy, V. and Nield, E., *Polymer*, **25**, 835 (1984).
31. Legras, R., Dekoninck, J. M., Vanzieleghem, A., Mercier, J. P. and Nield, E., *Polymer*, **27**, 1098 (1986).
32. Haubruge, H., Université Catholique de Louvain, Belgium, personal communication, 2001.
33. Iida, H., Kometani, K. and Yanagi, M., Polyethylene terephthalate moulding compositions, *US Patent 4 284 540* (to Toray Industries, Tokyo, Japan), 1981.
34. Imashiro, Y., Takahashi, I., Horie, N. and Suzuki, S., Method for obtaining polyester resin products having desired strength, and mixture used in said method, *US Patent 6 333 363* (to Nisshinbo Industries, Inc., Tokyo, Japan), 2001.
35. Heitz, T., Heym, M., Muhlbach, K. and Plachetta, C., Stabilized polyester moulding compositions, *US Patent 5 733 959* (to BASF, Ludwigshafen, Germany), 1998.
36. Thomas, N. W., Berardinelli, F. M. and Edelman, R., Reinforced polycarbodiimide modified polyalkylene terephthalate, *US Patent 4 110 302* (to Celanese Corporation, New York), 1978.
37. Thomas, N. W., Berardinelli, F. M. and Edelman, R., Polycarbodiimide modification of polyesters for extrusion applications, *US Patent 4 071 503* (to Celanese Corporation, New York), 1978.
38. Lin, C. C., *J. Polym. Sci., Macromol. Symp.*, **135**, 129 (1998).
39. Ishikawa, M., Yoshioka, T., Uchida, M. and Okuwaki, A., Hydrolysis of waste poly(ethylene terephthalate) in magnesium hydroxide slurry, presentation (ENVR 209) given at the *International Chemical Congress of Pacific Basin Societies*, Honolulu, HI, 14–19 December, 2000.
40. Glass, R., personal communication, 2001. – Albemarle Corporation USA
41. Deyrup, E. J., Toughened thermoplastic polyester compositions, *US Patent 4 753 980* (to DuPont Company, Wilmington, DA), 1988.

42. Akkapeddi, M. K., Van Buskirk, B., and Chun, S., Polyester moulding compositions and articles exhibiting good impact, heat and solvent resistance, *US Patent 5 723 520* (to Allied Signal Inc., Morristown, NJ), 1998.
43. Nelsen, S., Golder, M. and DeStio, P., Method and compositions for toughening polyester resins, *US Patent 6 020 414* (to Hoechst Celanese Corporation, Somerville, NJ), 2000.

15

Thermoplastic Polyester Composites

A. E. BRINK

Hydrosize Technologies, Inc., Raleigh, NC, USA

1 INTRODUCTION

Thermoplastic polyester composites span a wide range of properties, and are consequently utilized in a diverse array of applications including automotive, appliance, cookware, electronics, and recreation (Figure 15.1) [1]. This has been, and is predicted to be, a growth area for composites with annual growth rates of 4–7 %. This growth is driven by many factors such as weight reduction, parts consolidation and metal replacement. The largest volume thermoplastic polyester resins include poly(ethylene terephthalate) (PET), poly(butylene terephthalate) (PBT) and poly(1,4-cyclohexylenedimethylene terephthalate) (PCT), as well as several liquid crystalline compositions that will not be included in this discussion. In addition, new to the market place is poly(trimethylene terephthalate) (PTT). This product has only recently been commercialized because the monomer, 1,3-propane diol, had not been available in large quantities. In the market place, these polyesters compete against each other as well as against metal and other resins such as polypropylene, nylon, poly(phenylene sulfide) and polycarbonate. In 2000, there was an estimated 455 MM kg (1000 MM lb) of glass fiber sold for thermoplastic composites, 29 % of which was used in polyesters (Figure 15.2) [1]. There are many factors that have to be evaluated when determining which resin is best for a specific application. These include ‘fitness-for-use’ criteria such as tensile strength, impact strength, thermal stability and heat distortion temperature. Also to be considered are process variables such as drying requirements, mold temperature and cycle time. Depending on the

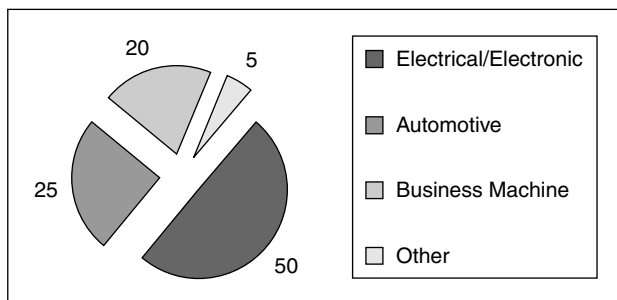


Figure 15.1 Glass-fiber-reinforced thermoplastic polyesters applications (numbers represent percentages) [1]

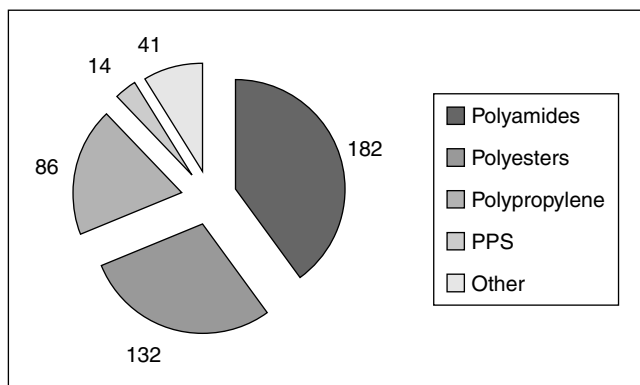


Figure 15.2 Glass-fiber-reinforced thermoplastic market data (numbers represent MM kg) [1]

particular application, cosmetic properties, such as surface appearance, are also critical. Of course, cost is always a top concern in any application. This discussion will focus on the features and benefits of the major thermoplastic polyester resins as well as what affects the mechanical properties of the final composite. Finally, some of the latest trends in thermoplastic polyester composites will be introduced.

2 POLY(ETHYLENE TEREPHTHALATE)

PET is by far the largest-volume thermoplastic polyester in production today. It was first synthesized by J. R. Winfield in the UK in the 1940s and its first commercial application was as a textile fiber. PET was also produced as a film for packaging and blow molded into bottles for beverages long before it had any

significant volume as a thermoplastic composite [2]. Even today, PET ‘takes a back seat’ to PBT in volume usage in the thermoplastic composite market, largely because of a slower crystallization rate and relative sensitivity to drying conditions. A large majority of commercial injection molding machines are equipped with water-heated molds with a maximum mold temperature of 100–110 °C. The original PET formulations that were commercialized by Akzo Chemie and Teijin would not crystallize sufficiently unless mold temperatures of at least 130 °C were utilized. In 1971, Celanese introduced PBT as a molding resin and was followed by General Electric. PBT, although more expensive than PET, crystallizes in a rapid cycle time in water-heated molds and was rapidly accepted in the market place. Since its original introduction, PET formulations enabling fast crystallization in traditional water-heated molds have been introduced and have allowed PET to make significant inroads with regard to commercial acceptance; however, it still lags behind PBT.

2.1 CRYSTALLIZATION OF POLY(ETHYLENE TEREPHTHALATE)

These newer PET formulations utilize not only a nucleating agent, but also a plasticizing agent [3–9]. The crystallization rate of polymeric materials can be broken down into two different regions, i.e. nucleation-controlled and diffusion-controlled (Figure 15.3). In the injection molding process, hot polymer is injected

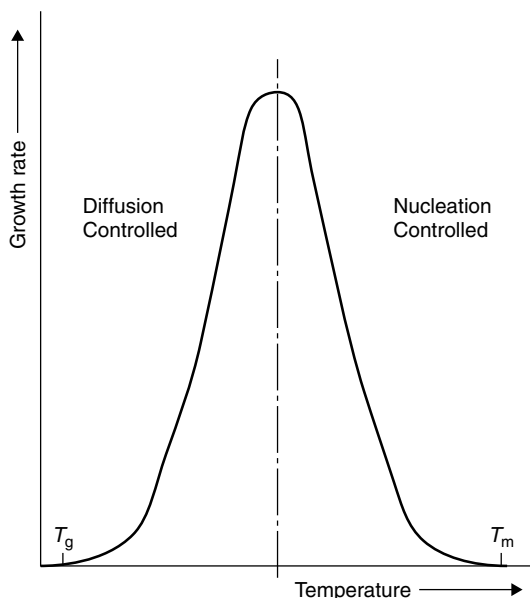


Figure 15.3 Spherulitic growth as a function of temperature

rapidly into the cooler mold. As the polymer cools from the melt, it first transitions into the nucleation-controlled regime and the crystallization process begins. The initiation of crystallization is often referred to as 'crystallization on cooling' (T_{cc}). From each nucleation site the crystal lamellae structure grows, often in a spherulitic microstructure. It is critical that as many spherulites are initiated as possible. A high level of nuclei will allow for a more rapid crystallization and will also actually improve the mechanical properties. As the spherulites grow and impinge on one another, some polymer chains will be incorporated into more than one lamellae – these are called 'tie chains'. These chains concentrate and distribute stresses throughout the material, effectively increasing the toughness of the resin [10]. The more rapidly a polymer is crystallized, then the less perfect the crystal structure – this leads to an increase in tie chains. The most effective way to increase the number of nucleation sites is to add a nucleating agent. Addition of the latter not only increases the number of nuclei, but also increases the T_{cc} . Nucleating agents can be either heterogeneous or reactive. Heterogeneous nucleating agents include non-reactive, non-melting nucleants, such as mica or talc. Chemical nucleation is performed by the reaction of the nucleating agent with the polymer chain to produce ionic end groups. Alkali metal salts of organic acids, such as sodium benzoate, have been shown to be very effective chemical nucleating agents in thermoplastic polyesters [11]. Chemical nucleating agents can also degrade the molecular weight of the polyester. Typically, the heterogeneous type, particularly talc, provides sufficient nucleation without molecular weight degradation and is widely utilized in PET.

As the polyester continues to cool in the mold, it passes through the nucleation-controlled region and into the diffusion-controlled regime. In this region, the lamellar growth rate is the slow step in crystallization, limited by polymer reptation. If the glass transition temperature of the polyester is significantly below the mold temperature, then the polymer chains never cool beyond the T_g and crystallization can occur rapidly and completely in a short cycle time. If, however, the mold temperature is below, or too close to the glass transition temperature, then the polymer chain mobility decreases and the crystallization rate slows significantly and the molded part will not be fully crystallized. In this case, a distinct skin–core morphology is formed, with the surface region of the molded part being amorphous or at least less crystalline than the center. The glass transition temperature of PBT has been reported as lying between 30 and 50 °C, while the crystallization temperature of quenched PBT can occur as low as 20 °C [12]. The glass transition temperature of completely amorphous PBT has been estimated as 15 °C by extrapolation. If the mold surface temperature is 100 °C, then this is 85 °C above the T_g and a sufficient window for rapid crystallization is achieved. The glass transition temperature of amorphous PET, in contrast, is 75–85 °C and a mold temperature of about 120–140 °C is

needed in most injection molding processes. In order to achieve the full crystallization of PET in a water-heated mold, the glass transition temperature has to be lowered. Plasticizers do exactly that. Effective plasticizers in PET need to be miscible with the resin and have a glass transition temperature significantly lower than PET. Small molecules, such as benzoate esters, or extremely flexible, low- T_g , polymers such as poly(alkylene ether)s can be effective plasticizers in thermoplastic polyesters [13]. In a patent assigned to DuPont, Deyrup [3] describes a family of effective plasticizers as low-molecular-weight organic esters produced from aliphatic carboxylic acids with 1–20 carbon atoms and 1–3 carboxyl groups and an alcohol of the formula $\text{HO}-(\text{R}''-\text{O})_y\text{R}''$ wherein R' is a hydrocarbon radical of 2–15 carbon atoms and R'' is hydrogen or a hydrocarbon radical of 2–20 carbon atoms, while y is a cardinal number between 1 and 15. An example of such a plasticizer would be an ester end-capped low-molecular-weight poly(ethylene glycol). Another patent by Bier and Binsack (assigned to Bayer [4]) describes a family of effective plasticizers for PET as aliphatic acid esters formed from an aliphatic or cycloaliphatic carboxylic acid, with between 1 and 25 carbon atoms, and an aliphatic alcohol with between 1 and 20 carbon atoms. Some of the acceptable acids and glycols that are included in this description are presented in Table 15.1 [4]. One of the early problems that was faced upon the addition of plasticizers to PET was volatilization during both the drying and molding processes. As the PET was dried, some of the plasticizer collected in the exhaust lines of the drier, causing both cleaning and safety issues as the plasticizers tend to be flammable. This problem also occurred during molding and required frequent cleaning of the molds. The newest easy crystallizing PET formulations have overcome this deficiency by utilizing plasticizers with a higher molecular weight and lower volatility. The proper choice of nucleant/plasticizer combination can allow for the injection molding of PET composites in water-heated molds in similar cycle times as PBT.

Table 15.1 Preferred aliphatic acids and glycols, as described by Bier and Binsack [4]

Acids	Glycols
Adipic acid	Ethylene glycol
Citric acid	Propanediol
Glutaric acid	Butanediol
Succinic acid	Diethylene glycol
Acetic acid	Neopentyl glycol
2-Ethylhexanoic acid	Poly(ethylene glycol) ($M_n = 400$)
Lauric acid	2-Ethylhexanol
Stearic acid	Isopropanol
Oleic acid	Tetrahydrofurfuryl alcohol
Palmitic acid	Ethyl alcohol

2.2 ADVANTAGES OF POLY(ETHYLENE TEREPHTHALATE)

The advantages of PET can be summarized as a lower raw material cost and a higher strength and temperature resistance. This is stated as a lower raw material cost because it does not always translate into a lower manufactured part cost. When processing PET it is critical to follow the supplier's guidelines for drying. If these are not strictly followed, PET will suffer hydrolytic degradation during molding and mechanical properties will suffer. This can lead to a high level of rejected parts and thus increase the average manufacturing cost. However, if proper care is taken, PET can be molded without mishap and a composite part with higher strength and temperature performance can be achieved for a lower cost than with PBT. Another advantage in the PET supply comes from the availability of recycled polymer. PET is one of the few materials that has a steady supply of recycled grades, due to the widespread recycling of beverage bottles. Bottle polymer grade PET is made to a higher molecular weight than is desirable for fiber-reinforced injection-molding grades. Thus, even after cleaning and compounding the molecular weight is more than adequate for composite applications.

3 COMPARISON OF THERMOPLASTIC POLYESTERS

3.1 POLY(BUTYLENE TEREPHTHALATE)

In addition to inherently faster crystallization kinetics in a water-heated mold, PBT offers several other benefits compared to PET. First of all, the lower processing temperatures required for PBT make it less susceptible to hydrolytic degradation and thus drying is not as critical as in the case of PET. Thermoplastic composites made from PBT also tend to have a higher % elongation to break (Table 15.2) [14, 15]. Although this attribute does not necessarily show

Table 15.2 Selected properties of 30% glass-fiber-reinforced (GFR) thermoplastic polyester composites [15–17]

Selected property	Units	GFR PBT	GFR PPT ^a	GFR PET	GFR PCT ^b
Tensile strength	MPa	138	158	155	117
Tensile elongation	%	4	2–3	2–3	2–3
Flexural strength	MPa	193	234	248	180
Flexural modulus	MPa	8275	10 335	8965	8500
Notched Izod impact strength	J/m	94	80	99	75
Deflection temperature ^c	°C	213	210	224	262

^a PTT, poly(trimethylene terephthalate).

^b PCT, poly(1,4-cyclohexylenedimethylene terephthalate).

^c At 1.82 MPa.

up in impact data such as notched Izod, it does typically translate into better 'toughness' in real-world applications.

3.2 POLY(1,4-CYCLOHEXYLENEDIMETHYLENE TEREPHTHALATE)

Poly(1,4-cyclohexylenedimethylene terephthalate) (PCT) is a high-heat thermoplastic polyester produced from 1,4-cyclohexanedimethanol and terephthalic acid. The former is produced as a combination of both the *cis*- and *trans*-isomers. The melting point of PCT is 285 °C, roughly 30 °C above PET. As shown in Table 15.2 the higher melting point translates into a heat deflection temperature HDT of 262 °C. This higher HDT has allowed PCT to carve out a niche market in surface mount components, electrical connectors, sensors and switches, especially those which require IR oven compatibility [18]. In addition, due to the higher melting temperature, a higher processing temperature is required for PCT. Typically, a melt processing temperature of 290–310 °C, with a mold temperature of 80–120 °C is recommended. The higher processing temperature has been a challenge for PCT, because it is near the limit of PCT's thermal stability. Significant effort was made by the Eastman Chemical Company regarding stabilizing formulations resulting in numerous patents [19–21]. In addition to thermal stability, initial PCT formulations also suffered from the same problems as PET regarding slow crystallization during molding. The original formulas required an oil-heated mold with a mold temperature above 120 °C. New plasticization technology has solved this deficiency and now mold temperatures as low as 80 °C can be used with excellent results [13, 22–25].

3.3 POLY(TRIMETHYLENE TEREPHTHALATE)

The newest addition to the thermoplastic polyester family is poly(trimethylene terephthalate) (PTT). This polyester falls between PBT and PET and, if it grows in volume, has the potential of being lower cost than PBT based on raw materials. Examination of Table 15.2 shows that PTT [16] has similar mechanical properties to PET, but a lower HDT (similar to PBT). Initial molding trials also indicate that PTT's crystallization kinetics are slower than PBT and will pose problems in a water-heated mold [26]. Initial marketing of this product has targeted it as an 'easier-molding PET' or a 'less-expensive PBT'. It is not exactly either and it remains to be seen if it can establish a significant market share. With the proper formulation, a faster crystallization rate can be achieved, and furthermore PTT offers improved hydrolytic stability over PET and thus the drying step is not as critical.

A relative comparison of the four main thermoplastic polyesters is shown in Table 15.3. Each resin has a different set of strengths, and depending on the application and the individual molder's requirements, the right polyester for the

Table 15.3 Performance traits of GFR thermoplastic polyesters

Property	PBT	PTT	PET	PCT
Processability	+++	++	+	++
Strength	++	+++	+++	+
Toughness	+++	++	++	++
Heat deflection	+	+	++	+++
Cost	++	++	+++	+

job can be chosen. Once the best polyester has been chosen, there are still many factors which effect the final mechanical properties that will be obtained. These factors are often interrelated and it is difficult to increase one without effecting others. The most obvious factor is fiber content. As the level of reinforcement increases, the strength and modulus of the composite also increase. This relationship is not necessarily linear, however, because other variables also effect the properties. For example, as the level of reinforcement increases the compounding process typically results in more fiber damage and a shorter average fiber length. Decreasing the fiber length results in a lower strength and a lower modulus which partially counters the benefit of increasing the fiber content. Tables 15.4 and 15.5

Table 15.4 The mechanical properties of glass-fiber-reinforced PBT [15]

Selected property	Units	PBT	15 % GFR PBT	30 % GFR PBT	40 % GFR PBT
Tensile strength	MPa	55	93	138	152
Tensile elongation	%	20	5	4	4
Flexural strength	MPa	75	145	193	220
Flexural modulus	MPa	2690	4830	8275	9655
Notched Izod impact strength	J/m	42	52	94	115
Deflection temperature ^a	°C	54	190	213	216

^a At 1.82 MPa.

Table 15.5 The mechanical properties of glass-fiber-reinforced PET [15]

Selected property	Units	PET	15 % GFR PET	30 % GFR PET	45 % GFR PET	55 % GFR PET
Tensile strength	MPa	62	80	155	190	193
Tensile elongation	%	100	6	2–3	2	1–2
Flexural strength	MPa	93	97	248	282	303
Flexural modulus	MPa	2410	3620	8965	13 790	17 240
Notched Izod impact strength	J/m	625	104	99	110	110
Deflection temperature ^a	°C	115	207	224	226	229

^a At 1.82 MPa.

provide, respectively, the mechanical properties of PBT [15] and PET [15] at several different levels of glass fiber reinforcement.

4 COMPOSITE PROPERTIES

4.1 KELLY-TYSON EQUATION

One of the best ways to thoroughly examine the variable effecting the composite properties is to examine the Kelly-Tyson equation for tensile strength, as follows [27–31]:

$$\sigma_c = \tau_i \frac{L}{d} v_f C_0 + \sigma_m v_m \quad (15.1)$$

where σ_c is the tensile strength of the composite, τ_i the interfacial shear strength, L the fiber length, d the fiber diameter, v_f the volume fraction of the fiber, C_0 the orientation function of the fiber, σ_m the tensile strength of the matrix resin and v_m the volume fraction of the matrix resin.

The interfacial shear strength can be further defined as follows:

$$\tau_i = \sigma_f \frac{d}{2L_c} \quad (15.2)$$

where σ_f is the tensile strength of the fiber and L_c the critical fiber length.

The critical fiber length (L_c) is defined as the length of fiber where the stress buildup from the two ends yields a stress exactly equal to the fiber fracture stress at the center [32]. As the interfacial shear strength increases, the critical fiber length decreases. It should be noted that Equation (15.1) only applies when the average fiber length is less than the critical fiber length, which is almost always the case in injection molded glass-fiber-reinforced polyester. If the average fiber length, or a significant portion of the fibers, are longer than the critical fiber length, then this equation should be expanded as described by Fu and Lauke [33] and Fukuda and Chou [34]. Another variable needs more attention as well, and that is the tensile strength of the matrix (σ_m). In continuous fiber composites, the tensile strength of the matrix can almost be ignored because it is small when compared to the contribution from the fiber. In short fiber composites it is significant and can account for as much as 30–40 % of the total composite strength. In most thermoplastic composite systems, once the resin is chosen, the matrix tensile strength can be considered a constant. However, thermoplastic polyesters are extremely susceptible to hydrolysis and thermal degradation and the molecular weight typically changes (decreases) with each processing step. Another important factor is that the molecular weights typically utilized in polyesters are either very close to or less than the critical molecular weight (M_c). In polyolefins, for example, it has been shown that the molecular weight does not have a significant

effect on the composite properties [35]. This is because the molecular weights are all very high, significantly above the M_c , and thus the differences are negligible. The dependence of the tensile strength on molecular weight is given as follows [36].

$$\sigma_m = \sigma_{m0} - \frac{\sigma_{m0}M_c}{M_n} \quad (15.3)$$

where σ_m is the tensile strength of the matrix, σ_{m0} the ultimate tensile strength of the matrix, M_n the number-average molecular weight and M_c the critical molecular weight.

There are numerous literature values for the ultimate tensile strength and the critical molecular weight of thermoplastic polyesters. These are dependent on the method of analysis and can also be affected by the additive package being used, especially the plasticizer. It is best to determine the ultimate tensile strength experimentally for each system. One suitable method is to injection mold and test several different-molecular-weight polyesters that have been fully formulated except for the fiber. The tensile strength can be plotted as a function of the measured molecular weight (M_n) after compounding. The intercept will be the ultimate tensile strength and the slope the product of the ultimate tensile strength and the critical molecular weight. As an example, a formulated, plasticized PET was found to have an ultimate tensile strength of 116 MPa and a critical molecular weight of 6400 Da [37]. Another method that has been performed with reasonable success is to mold one high-molecular-weight sample, again without the glass. Different-molecular-weight samples can be obtained by controlled hydrolytic degradation in boiling water. An example of such a procedure would be to place 20 tensile bars in boiling water and remove 5 bars every 5 h. Each bar can then be tested for molecular weight and tensile strength. Once again, the measured tensile strength can be plotted vs. the number-average molecular weight to estimate the σ_0 and M_c .

Once the relationship between the matrix molecular weight and the composite properties is defined, the next set of properties to consider are those of the fiber. There are numerous types of fiber reinforcements to consider, including carbon, glass, steel, aramid, and even natural fibers. The actual properties for the specific fiber to be utilized can usually be obtained from the fiber supplier. The most commonly used fiber is 'E-glass'. Because the composition of this fiber is consistent, the properties are also essentially identical, regardless of the vendor. This does not mean that the composite properties will be equal, however. The fiber manufacturers differentiate their products with the sizing formulation, which has a tremendous impact on the interfacial shear strength [38, 39]. This topic will be discussed later, as for now only the physical properties of the fiber are being considered. The ultimate tensile strength of an E-glass fiber (Table 15.6) is reported as 3448 MPa [40]. Any flaw in the fiber decreases this value considerably. Because the fiber properties are reduced by flaws, and as the fiber length

Table 15.6 Properties of E-glass fibers [40]

Property	Value
Diameter (μm) ^a	9–14
Density (g/mL)	2.58
Tensile strength (MPa)	3448
Tensile modulus (MPa)	7.24×10^{10}

^a Typical values are in this range – the actual value is dependant on the fiber grade chosen.

decreases the likelihood of a flaw decreases, the shorter the fiber length, then the closer the properties become to their ultimate values. A Weibull distribution has been used to determine the *in situ* fiber strength as a function of fiber length [41–43]. In typical short fiber composites produced by twin-screw compounding and injection molding, the fiber length is short enough that the ultimate fiber properties are a reasonable approximation to the actual.

Another important variable to consider is the fiber orientation. This is affected by many variables such as the injection molding conditions, fiber length, resin viscosity and part thickness. The fiber orientation can be determined experimentally by optical methods [44], or it can be estimated from the modulus of the molded part as follows [45–47]:

$$E_c = C_0 \eta_L E_f v_f + E_m v_m \quad (15.4)$$

where E_c is the modulus of the composite, E_f the modulus of the fiber, v_f the volume fraction of the fiber, E_m the modulus of the matrix resin and v_m the volume fraction of the matrix resin. The variable η_L is defined by the following equation:

$$\eta_L = 1 - \tanh(\frac{1}{2}\beta l) / \frac{1}{2}\beta l \quad (15.5)$$

where l is the fiber length and β is a geometric factor given by the following equation:

$$\beta = \left(\frac{2G_m}{E_f r^2 \ln(R/r)} \right)^{1/2} \quad (15.6)$$

In the above, the variable R is the radius between center to center fiber spacing, while r is the fiber radius. The shear modulus (G_m) can be approximated as $E_m/3$. The matrix modulus is effected by the level of crystallinity and it is important that the samples are fully crystallized to ensure reproducibility. The value of β for 30 wt% glass-fiber-reinforced PET has been calculated as 3.15×10^4 . Using the mathematical analysis shown above, the orientation function of the glass fiber

in standard tensile bars was calculated to be ≈ 0.7 in a 30 % GFR PET [37]. This value has been obtained by utilizing optical experimental methods as well.

The understanding of Equations (15.1) to (15.6) indicates that once the fiber type and matrix resin are chosen the most significant variables impacting the tensile strength of the composite are the following: fiber length, fiber orientation, interfacial shear strength and molecular weight. The fiber length and the resin molecular weight are interrelated. As the molecular weight increases, the melt viscosity increases, which results in more fiber breakage and a lower average fiber length. Attempting to increase the mechanical properties by increasing molecular weight can also result in molding difficulties due to the increase in viscosity. Another problem encountered by increasing the molecular weight is degradation. In one study, a higher starting-molecular-weight PCT resulted in a higher melt temperature, due to an increase in shear heating from the higher viscosity. The net result was an equal molecular weight after molding (Table 15.7). It is important to control the resin molecular weight for optimum properties, but this represents a classic case where more is not better, and in fact can be detrimental.

One unique twist in processing thermoplastic polyesters comes from understanding how PET is produced commercially. Typically, PET is made to a moderate molecular weight in the melt phase. The resin is then pelletized, crystallized and then ‘solid-stated’ [12]. The solid-state process builds molecular weight, but the temperature is below the melting point of PET, and thus the polymerization is performed in the “solid state”. The kinetics of solid-state polymerization are diffusion controlled. After solid-stating, the resin is compounded with glass fiber to produce the reinforced pellet that is supplied for injection molding. Simply changing the order of these processes can provide some very beneficial results. If the ‘un-solid-stated’, low-molecular-weight polyester is compounded with the

Table 15.7 Effect of solid-stating on the properties of 30 % GFR PCT

Property	Example 1	Example 2	Example 3	Example 4	Example 5
M_n prior to compounding	11 750	15 050	11 750	11 750	11 750
Solid State prior to compounding	No	Yes	No	No	No
Solid State after compounding	No	No	Yes	Yes	No
Compounding temperature (°C)	300	300	300	350	350
M_n prior to molding	10 730	10 150	15 300	10 600	6 260
Tensile strength (MPa)	103	104	126	114	80
Tensile elongation (%)	1.9	1.9	1.8	1.6	1.3
Flexural strength (MPa)	155	156	186	162	124
Flexural modulus (MPa)	7 630	7 840	7 370	8 260	7 870
Notched Izod impact strength (J/m)	67.2	68.2	87.9	95.1	89.7
Unnotched Izod impact strength (J/m)	488	563	650	500	280
Fiber length (μm)	403	423	413	504	503

glass fiber first and then the solid-stating is performed, several things happen. First, the lower molecular weight during compounding provides a lower melt viscosity and less fiber breakage occurs. Secondly, the molecular weight prior to injection molding is controlled by the solid-stating and can be increased by lengthening the solid-stating time. The addition of glass fiber into the pellet provides a shorter diffusion path for volatiles and the kinetics of solid-stating are actually improved. The final advantage of solid-stating after the glass addition is that it allows reactions to occur at the glass surface and can increase the interfacial shear strength if the proper glass sizing chemistry is utilized. In an example with PCT, a 22 % increase in tensile strength was achieved by implementing this process (see Table 15.7) [48]. Another interesting result is shown by Example 4. In this sample, the processing temperature was increased to 350 °C, 50 °C above normal. This resulted in severe molecular weight degradation. This sample was solid-stated until the molecular weight was equal to the sample prepared in the more conventional manner (Example 1). The net result was a longer fiber length due to the lower viscosity provided by the higher processing temperature, and the mechanical properties increased.

The contribution of the fiber length and molecular weight to the composite properties are readily characterized. The interfacial shear strength, however, is more difficult to quantify. There are numerous examples in the literature of measuring this important property. For example, single fiber pull-out, fiber debond, or microindentation studies can be performed [49–54]. One significant problem with these methods when trying to investigate short-fiber thermoplastic composites is that the interfacial shear strength is extremely dependent on the method of processing [55]. In the previously mentioned test methods, laboratory samples are generated that have no relation to commercial processing methods. One method of quantifying the critical fiber length and thus the interfacial shear strength was reported by Templeton [56]. In this method, the fracture surface of an injection molded sample broken in tension is examined by microscopy. The longest fiber length protruding from the fracture surface is taken as one half of the critical fiber length. At fracture of the composite, a fiber having lengths of X_1 and X_2 , on either side of the fracture plane, will either be pulled out of one side or the other, or break. To break, both X_1 and X_2 must exceed X_c where X_c is defined as $L_c/2$.

Another way to obtain the critical fiber length is to rearrange Equation (15.1) to give the following:

$$\tau_i = (\sigma_c - \sigma_m v_m) \left(\frac{d}{L v_f C_0} \right) \quad (15.7)$$

All of the variables except τ_i can be readily determined experimentally and thus the interfacial shear strength can be calculated. This was calculated for seven different PET formulations and the optically measured interfacial shear strength

was compared to the calculated value. In all seven cases, the measured value was within 10 % of the calculated [37].

4.2 INTERFACIAL SHEAR STRENGTH – THE IMPORTANCE OF SIZING

The interfacial shear strength in short-fiber-reinforced composites holds a unique importance. It is the only variable that can improve the composite properties without impacting other important properties in a negative way. For example, if the molecular weight is increased the mechanical properties increase but so does the melt viscosity, which can cause mold-filling problems. It has been shown that increasing the interfacial shear strength can increase viscosity as well, but only at a low shear rate. Under the high-shear-rate conditions of injection molding, the quality of the interface has no effect on flow. The maximum interfacial shear strength is achieved when it equals the matrix shear strength. This has been estimated to be 30 MPa for PET. Interfacial shear strength values obtained by utilizing three commercially available glass fibers marketed for PET ranged from a low of 20 to a high of 25, hence indicating that there is still significant room for improvement. There are several strategies that can be employed to increase this important property. Glass fiber suppliers apply a sizing to the glass surface immediately after it is formed from platinum bushing. The sizing consists of several components including a lubricant, antistatic agent, film former and coupling agent [38, 39]. The film former and coupling agent are the most significant in affecting the interfacial shear strength. The coupling agent, usually a silane, reacts with the silanol groups on the glass surface and provides a reactive moiety that can later react with the matrix resin. Typical silanes include 3-aminopropyltriethoxysilane, 3-glycidoxypolytrimethoxysilane and 3-methacryloxypropyltrimethoxysilane. The choice of the silane is controlled by the glass supplier and is often kept confidential. The other sizing component that has been shown to affect the interfacial shear strength is the film former. The primary reason for the film former is to protect the glass and improve processability. The film former, often a polyurethane, epoxy, or other water-dispersible polymer, provides a protective coating to prevent fiber–fiber contact during processing which can lead to scratches and imperfections on the glass surface and decrease the glass fiber properties. The film former also prevents fiber fuzzing and is responsible for bundle integrity. This keeps the chopped fiber in a form that is easy to feed into the extruder and aid in processing. With continuous fiber, the film former keeps the individual glass filaments together in a processable strand, easy to feed into a pultrusion machine, fiber chopper or other downstream process. In most thermoset applications, the film former is designed to readily dissolve in the matrix resin and thus does not often contribute significantly to the quality of the fiber–matrix interface, although it does effect the wet-out of the fiber. In contrast, with thermoplastic composites the film former often plays a critical role in

Table 15.8 Effect of the film former on the properties of 30 % GFR PCT [37]

Selected property	Example 1	Example 2	Example 3	Example 4	Example 5	Example 6
Glass type	A	A	B	C	D	E
Matrix tensile strength (MPa)	45.5	50.4	48.5	47.0	47.0	47.8
Fiber length (μm)	476	440	473	472	453	437
Calculated orientation function	0.63	0.63	0.67	0.63	0.59	0.61
Weight fraction of fiber	0.30	0.31	0.29	0.31	0.32	0.31
Volume fraction of fiber	0.181	0.191	0.175	0.184	0.197	0.184
Critical fiber length (μm)	755	766	783	943	785	702
Interfacial shear strength (MPa)	25.1	24.8	24.2	20.1	24.2	27.0
Composite tensile strength (MPa)	161	160	162	139	154	160

adhesion between the resin and the fiber surface. The properties can be increased with the proper selection of film former, even with the same silane coupling agent (Table 15.8) [37]. In this table, the only difference between Example 6 and Example 4 is the film former which is present on the glass fiber at only a 1 wt% loading; however, it changes the interfacial shear strength by 35 %.

Another method of improving the quality of the fiber–matrix interface is the use of additives, which can be combined with the matrix and fiber during compounding. Typical thermoplastic polyester composites are formulations consisting of the resin, nucleating agent, plasticizer, reinforcing fiber, thermal and oxidative stabilizers, coloring agents and fillers. Many of the ‘stabilizers’ are not truly stabilizers but actually reactive compounds that can chain-extend the polyester during processing, such as multifunctional epoxies [19, 57]. These additives react with the polyester; however, they can also react with the film former and the silane coupling agent. Thus to truly optimize the interfacial shear strength, the interactions between the resin, additives, film former and silane coupling agents need to be accounted for. Table 15.9 shows three different commercially available glass fibers marketed for thermoplastic polyesters evaluated in PCT [37]. The exact sizing chemistry was kept confidential; however, all three utilized an aminosilane coupling agent, but different film formers. Two different proprietary reactive additives were also evaluated. Glass sizing No. 1, without any reactive additives, provided an interfacial shear strength of 16.5 MPa. This was increased to 19.3 and 20.1 respectively when combined with reactive additives A and B. By combining glass fiber No. 2 with additive B, the interfacial shear strength can be increased to 21.4, while the maximum value was obtained with glass fiber No. 3 with additive B. Optimizing the combination of glass sizing and additive led to a 28 % increase in tensile strength at essentially no added cost.

Table 15.9 Effect of additives and film former on the properties of 30 % GFR PCT [37]

Selected property	Example 1	Example 2	Example 3	Example 4	Example 5	Example 6	Example 7
Glass type	C	C	C	B	B	A	A
Matrix tensile strength (MPa)	25.6	25.2	23.1	34.5	42.2	36.8	41.5
Fiber length (μm)	510	460	470	430	427	404	417
Calculated orientation function	0.64	0.67	0.66	0.7	0.69	0.69	0.69
Weight fraction of fiber	0.30	0.30	0.30	0.30	0.30	0.30	0.30
Volume fraction of fiber	0.83	0.83	0.83	0.83	0.83	0.83	0.83
Critical fiber length (μm)	1146	982	942	1006	887	898	844
Interfacial shear strength (MPa)	16.5	19.3	20.1	18.9	21.4	21.1	22.5
Composite tensile strength (MPa)	105	112	115	116	132	121	135

4.3 CARBON FIBER REINFORCEMENTS

Carbon fiber reinforcements are also coated with a fiber sizing; however, coupling agents have not been found to be very effective. Carbon fibers are commonly surface-treated by an electrolytic process to provide a more reactive surface in place of a coupling agent. Traditionally, the film former in carbon fiber composites has been an epoxy. The most commonly utilized matrix resin for carbon fiber composites is also epoxy. In the early years of carbon fiber development, it was found that the best interfacial shear strength between carbon fiber and an epoxy matrix resin was obtained by using unsized fiber; however, unsized fiber is very difficult to process. This led to the next best alternative, i.e. an uncured relatively low-molecular-weight epoxy sizing. This aided in processability and did not detract significantly from the mechanical properties. As the use of carbon fiber expands into non-epoxy matrix applications, the carbon fiber manufacturers and academia are researching sizings that will provide improved properties in a wide range of resins, both thermoplastic and thermoset. Currently, Fortafil Fibers [58] offers a pelletized, chopped carbon fiber, F219, for thermoplastic polyester composites. This product evolved from research evaluating the fiber surface treatment vs. composite properties in PBT (Figure 15.4). The optimization of the surface treatment provides an increase in all key mechanical properties, including tensile strength, flexural strength and notched Izod impact strength. Again, this shows the importance of the interface in the final composite properties. The fiber length is also a very critical value in determining the composite properties. In standard twin-screw compounded, injection molded composites this is a very difficult variable to improve. However, an exciting growth area in thermoplastic composites is 'long-fiber composites' [59–61]. In the production of such composites, the

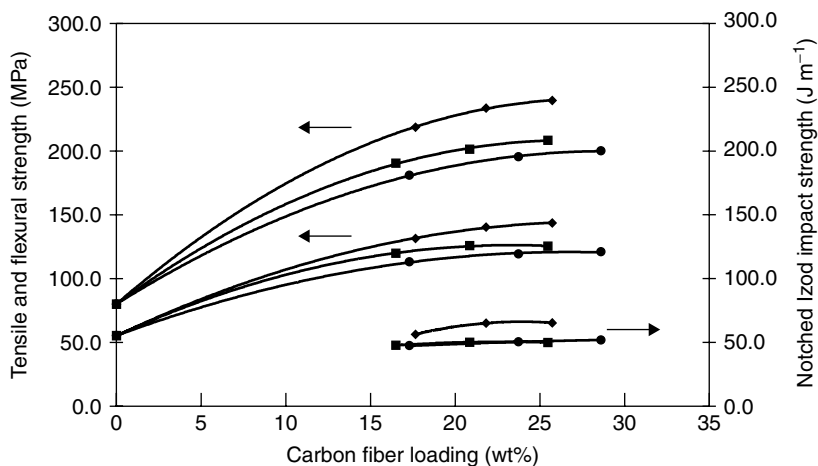


Figure 15.4 Mechanical properties as a function of loading for Fortafil fibers in PBT: ◆, F219; ■, F243; ●, F201 [58]

twin-screw compounding of the fiber and the matrix is eliminated and instead continuous fiber rovings are combined with the matrix resin in a thermoplastic pultrusion process similar to wire coating. After the fiber is combined with the resin, the strand is chopped into pellets where the fiber length is equal to the pellet length. These specialty pellets can then be injection molded. If the injection molding is modified to minimize fiber breakage, then composite parts with significantly longer fiber lengths can be achieved. This method also allows for composites with up to 60 % fiber reinforcement to be produced, significantly higher than typical compounded short-fiber composites. These materials offer significant improvements in modulus, strength and impact compared with their more conventional counterparts and the market for these is rapidly expanding, predominately as replacements for metal. Such products are readily available in polypropylene and nylon; however, PBT, PET and PCT are all still under investigation.

5 NEW COMPOSITE APPLICATIONS

Another exciting growth area for glass-fiber-reinforced thermoplastic polyesters continues to be the automotive market. Although GFR PBT and PET have been used in many 'under-the-hood' applications and smaller molded parts, Daimler-Chrysler is developing a plastic-bodied car that would result in a considerable increase in demand [62]. Currently, both GFR PET (15–20 % glass) and 35 % GFR polypropylene are being considered. Initially, traditional short-fiber composites were investigated; however, more recent efforts have also included long-fiber

composites. These materials are being molded on an 8800-t Husky injection molding machine featuring a two-stage injection unit and a 100 lb shot capability. The cycle time is currently less than 3 min. The intent of this program is to mold the vehicle structure so that only a lightweight metal frame would be required. The largest hurdle of this program is to utilize molded-in color to eliminate costly paint operations and still achieve an acceptable surface finish. This is a perfect example of how to exploit the advantages of thermoplastic polyester composites. If successful, it has the possibility of parts consolidation and weight reduction, and could even incorporate a significant amount of post-consumer resin into the automobile. All three of these are important drivers in the automobile industry.

Thermoplastic polyester composites are an extremely versatile and cost-effective solution for many applications. Since the introduction of PBT as a molding resin in 1971, there has been a tremendous increase in the body of knowledge utilizing these resins. Improvements in formulations have increased thermal stability and processability of such resins. Significant progress has also been made in understanding and improving the properties of composites made from polyesters. It has been shown that in addition to plasticizers, nucleating agents and stabilizers, the choice of glass and the quality of the fiber-matrix interface that results is extremely important in determining the mechanical performance. With every improvement to the stability, processability or mechanical properties, new applications are opened up to this important class of materials.

REFERENCES

1. Watkins, J. C., Sales and Marketing Director, TP Composites, Aston, PA, personal communication, June, 2001.
2. Deyrup, E. J., Injection moldable PET, in *High Performance Polymers: Their Origin and Development*, Seymour, R. B. and Kirshenbaum, G. S. (Eds), Elsevier, Amsterdam, 1986, pp. 81-94.
3. Deyrup, E. J., Molding compositions, *US Patent 4 486 564*, 1984.
4. Bier, P. and Binsack, R., Polyester compositions which crystallize rapidly, *US Patent 4 435 546*, 1984.
5. Vanderkooi, Jr, N. and Tuller, H. W., Polyethylene terephthalate composition containing aliphatic plasticizer and nucleating agent, *US Patent 4 327 007*, 1982.
6. Haylock, J. C., Tuller, H. W. and Bander, J. A., Polyester compositions containing ester of polyfunctional high molecular weight alcohol, *US Patent 4 731 404*, 1988.
7. Chung, J. Y., Jones, J. D. and Li, H. M., Injection moldable thermoplastic polyester composition, *US Patent 4 539 352*, 1985.
8. Chung, J. Y., Jones, J. D. and Li, H. M., Injection moldable thermoplastic polyester composition, *US Patent 4 486 561*, 1984.

9. Dege, G. J., Akkapeddi, M. K. and Vanderkooi, Jr, N., Crystallization modifier for polyester molding compositions, *US Patent 5 389 710*, 1995.
10. Van Krevelan, D. W., Crystallization of polymers and the means to influence the crystallization process, *Chimia*, **32**, 4469 (1978).
11. Pilati, F., Toselli, M., Messori, M., Manzoni, C., Turturro, A. E. and Gattiglia, E. G., On specific factors affecting the crystallization of PET: the role of carboxyl terminal groups and residual catalysts on the crystallization rate, *Polymer*, **38**, 4469 (1997).
12. Jalandar, Y., Jadhar, Y., Simon, W. and Kantor Polyesters, in *The Encyclopedia of Polymer Science and Engineering*, 2nd Edn, Vol. 12, Kroschwitz, J. I. (Ed.), Wiley, New York, 1990, pp. 216–217.
13. Brink, A. E., Turner, S. R. and Keep, G. T., Poly(alkylene ether)s as plasticizers and flow aids in poly(1,4-cyclohexanedimethylene terephthalate) resins, *US Patent 5 965 648*, 1999.
14. McNally, D. and Gall, J. S., The history of poly(butylene terephthalate) molding resins, in *High Performance Polymers: Their Origin and Development*, Seymour, R. B. and Kirshenbaum, G. S. (Eds), Elsevier, Amsterdam, 1986, pp. 71–79.
15. TP Composites, Aston, PA, Courtesy of J. C. Watkins, Sales and Marketing Director, March 2001.
16. RTP Composites Product Literature [www.RTPCompany.com].
17. Eastman Chemical Company, Kingsport, TN, Courtesy of G. Stack, Performance Plastics, March 2001.
18. Eastman Chemical Company Product Literature [www.Eastman.com].
19. Minnick, L. A. and Seymour, R. W., Poly(1,4-cyclohexylenedimethylene terephthalate) with improved melt stability, *US Patent 5 428 086*, 1995.
20. Minnick, L. A., Polyester molding composition, *US Patent 4 778 820*, 1987.
21. Auerbach, A. B. and Sell, J. W., Evaluation of poly(1,4-cyclohexylenedimethylene terephthalate) blends for improved processability, *Polym. Eng. Sci.*, **30**, 1041 (1990).
22. Minnick, L. A., Reinforced molding composition based on poly(1,4-cyclohexylenedimethylene terephthalate) having improved crystallization characteristics, *US Patent 4 859 732*, 1988.
23. Minnick, L. A., Molding compositions based on poly(1,4-cyclohexylenedimethylene terephthalate) containing an amide crystallization aid, *US Patent 4 894 404*, 1988.
24. Minnick, L. A., Reinforced molding composition based on poly(1,4-cyclohexylenedimethylene terephthalate) containing a high molecular weight aliphatic polyester, *US Patent 5 242 967*, 1992.
25. Minnick, L. A., Reinforced molding composition with improved crystallization properties, *US Patent 5 219 911*, 1992.
26. Chisholm, B. J., Fong, P. M., Zimmer, J. G. and Hendrix, R., Properties of glass-filled thermoplastic polyesters, *J. Appl. Polym. Sci.*, **74**, 889 (1999).

27. Kelly, A. and Tyson, W. R., Tensile properties of fiber reinforced metals: copper tungsten and copper/molybdenum, *J. Mech. Phys. Solids*, **13**, 329 (1965).
28. Kelly, A. and Davies, G., High strength materials, *Metall. Rev.*, **10**, 1 (1965).
29. Kelly, A., Interface effects and the work of fracture of a fibrous composite, *Proc. R. Soc. London, A.*, **319**, 95 (1970).
30. Chen, F. and Jones, F. R., Injection moulding of glass fibre reinforced phenolic composites: 1. Study of the critical fibre length and the interfacial shear strength, *Plast., Rubber Composites Proc. Appl.*, **23**, 241 (1995).
31. Termonia, Y., Structure–property relationships in short-fiber-reinforced composites, *J. Polym. Sci., Polym. Phys. Ed.*, **32**, 969 (1994).
32. Bush, S. F., Impact Strengths of injection molded long glass fiber composites. *Plast. Rubber Composites Proc. Appl.*, **24**, 139 (1995).
33. Fu, S. and Lauke, B., Effects of fiber length and fiber orientation distributions on the tensile strength of short-fiber-reinforced polymers, *Composites Sci. Technol.*, **56**, 1179 (1996).
34. Fukuda, H. and Chou, T. W., A probabilistic theory of the strength of short-fibre composites with variable fibre length and orientation, *J. Mater. Sci.*, **17**, 1003 (1982).
35. Thomason, J. L., Long fiber reinforced polypropylene composites, presentation given at the *Gordon Conference on Composites*, Ventura, CA, 10–15 January, 1997.
36. Rudin, A., *The Elements of Polymer Science and Engineering*, Academic Press, New York, 1982, pp. 41–70.
37. Brink, A. E., Glass fiber reinforced polyester composites, presentation given at the *Gordon Conference on Composites*, Ventura, CA, 10–15 January, 1997.
38. Thomason, J. L. and Schoolenberg, G. E., An investigation of glass fibre/polypropylene interface strength and its effect on composite properties, *Composites*, **25**, 197 (1994).
39. Scholtens, B. J. R. and Brackman, J. C., Influence of the film former on fibre-matrix adhesion and mechanical properties of glass-fibre reinforced thermoplastics, *J. Adhes.*, **52**, 115 (1995).
40. Owens Corning Product Literature [www.OwensCorning.com].
41. Wetherhold, R. C., Statistical distribution of strength of fiber-reinforced composite materials, *Polym. Composites*, **7**, 116 (1986).
42. Goda, K., Park, J. M. and Netravali, A. N., A new theory to obtain weibull fibre strength parameters from a single-fibre composite test, *J. Mater. Sci.*, **30**, 2722 (1995).
43. Yavin, B., Gallis, H. E., Scherf, J., Eitan, A. and Wagner, H. D., Continuous monitoring of the fragmentation phenomenon in single fiber composite materials, *Polym. Composites*, **12**, 436 (1991).

44. Fakirov, S. and Fakirova, C., Direct determination of the orientation of short glass fibers in an injection-molded poly(ethylene terephthalate) system, *Polym. Composites*, **6**, 41 (1985).
45. Agarwal, B. D., and Broutman, L. J., *Analysis and Performance of Fiber Composites*, 2nd Edn, Wiley, New York, 1989, Ch. 4, pp. 121–145.
46. Bowyer, W. H. and Bader, M. G., On the reinforcement of thermoplastics by imperfectly aligned discontinuous fibres, *J. Mater. Sci.*, **7**, 1315 (1972).
47. Hull, D., *An Introduction to Composite Materials*, Cambridge University Press, Cambridge, UK, 1981, p. 96.
48. Brink, A. E., Owens, J. T., Oshinski, A. J. and Pecorini, T. J., Process for preparing high strength fiber reinforced polymer composites, *US Patent 6 048 922*, 2000.
49. Ho, H. and Drzal, L. T., Evaluation of interfacial mechanical properties of fiber reinforced composites using the microindentation method, *Composites, A*, **27**, 961 (1996).
50. Kharrat, M., Chateauminois, A., Carpentier, L. and Kapsa, P., On the interfacial behavior of a glass/epoxy composite during a micro-indentation test: assessment of interfacial shear strength using reduced indentation curves, *Composites, A*, **28**, 39 (1997).
51. Drzal, L. T., Rich, M. J. and Ragland, W., Adhesion between fiber and matrix – its effect on composite test results, presentation given at the *42nd Annual Conference, Composites Institute*, 2–6, February, 1987, Preprint, Session 7-A/1.
52. Narkis, M., Chen, E. J. H. and Pipes, R. B., Review of methods for characterization of interfacial fiber-matrix interactions, *Polym. Composites*, **9**, 245 (1988).
53. Sauer, B. B. and Dipaolo, N. V., Development of micro-debond methods for thermoplastics including applications to liquid crystalline polymers, *J. Adhes.*, **53**, 245 (1995).
54. Heisey, C. L., Wood, P. A., McGrath, J. E. and Wightman, J. P., Measurement of adhesion between carbon fibers and bismaleimide resins, *J. Adhes.*, **53**, 117 (1995).
55. McAlea, K. P. and Besio, G. J., Adhesion kinetics of polybutylene terephthalate to E-glass fibres, *J. Mater. Sci. Lett.*, **7**, 141 (1988).
56. Templeton, P. A., Strength predictions of injection molding compounds, *J. Reinforced Plast. Composites*, **9**, 210 (1990).
57. Brink, A. E. and Owens, J. T., Thermoplastic polyurethane additives for improved polymer matrix composites and methods of making and using therefor, *US Patent 6 043 313*, 2000.
58. Cretella, M. and Secrist, D., Fortafil Fibers, Inc., Rockwood, TN, personal communication, June, 2001.
59. Montsinger, L. V., Apparatus and method for forming fiber filled thermoplastic composite materials, *US Patent 5 176 775*, 1993.

60. Hawley, R. C., Method of manufacturing a composite reinforcing structure, *US Patent 4 439 387*, 1984.
61. Hilakus, W., Resin impregnation of fiber structures, *US Patent 4 728 387*, 1986.
62. Wigotsky, V., Automotive plastics, *Plast. Eng.*, **55**, 288 (1999).

PART V

Depolymerization and Degradation

Recycling Polyesters by Chemical Depolymerization

D. D. CORNELL

D. D. Cornell Associates LLC, Kingsport, TN, USA

1 INTRODUCTION

Claims of perpetual motion create moments of mirth and consternation for those knowledgeable in the laws of thermodynamics. Yet, is it only hyperbole when a responsible journal such as the European Plastics News [1] proclaims that depolymerization of polyethylene terephthalate (PET) can be repeated indefinitely? The second law of thermodynamics brings us back to reality. The depolymerization of PET does not operate at 100 % yields, but does offer the opportunity for near-stoichiometric recovery of the monomers used to make the polyester. With high yields of potentially valuable monomers, the commercial potential for polyester depolymerization to regain feedstocks must be considered.

Recovering PET monomers has a long history – about as long as the commercial use of the resin. In 2001, the possibility of commercially successful recovery of monomers from used PET packaging prompted M & G Polymers, a major PET bottle polymer manufacturer in Europe and the United States and a unit of Gruppo Mossi & Ghisolfi of Tortona, Italy, to initiate development of a recent patented process, Renew™, for commercial application [2]. The Eastman Chemical Company announced development trials of a patented process, Optisys™, in 1999 [3]. As the mixture of collected, used PET bottles becomes more varied in color and additive composition, traditional mechanical recycling technologies find a greater proportion of collected bottles not suitable for the conventional recycled PET uses. It is the possible availability of sufficient amounts of recycled PET containers and the political need to include recycled content into

new bottles that has spurred the investigation of depolymerization commercial possibilities.

All saturated linear polyesters can theoretically be depolymerized to recover the starting monomers. The basic chemistry and processes are similar for all of the commercial saturated polyesters. Polyesters such as poly(butylene terephthalate), poly(ethylene naphthalate) and poly(cyclohexylenedimethylene terephthalate) could all be depolymerized to recover 1,4-butanediol, 2,6-naphthalenedicarboxylic acid or 2,6-dimethyl naphthalenedicarboxylate, and 1,4-cyclohexanedimethanol, respectively, along with terephthalic acid or dimethyl terephthalate and ethylene glycol. The limitation is not in the chemistry or the process technology. The limitation to practical commercial polyester depolymerization is securing a satisfactory quantity of polymer at a price that permits the economical regeneration of the monomers. The choice of technology is dependent, though, on the quality of the available feed and the desired product slate.

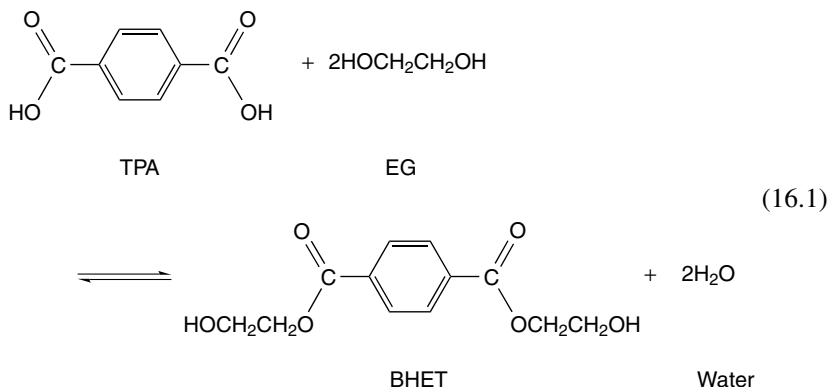
While depolymerizing poly(ethylene naphthalate) could be attractive on the small scale because of the high commercial price for the naphthalate moiety, even this candidate resin is in too little availability to permit economical depolymerization. Of polyesters, only poly(ethylene terephthalate) (PET) is available at sufficient quantities to make the commercial use of depolymerization potentially attractive.

2 CHEMISTRY

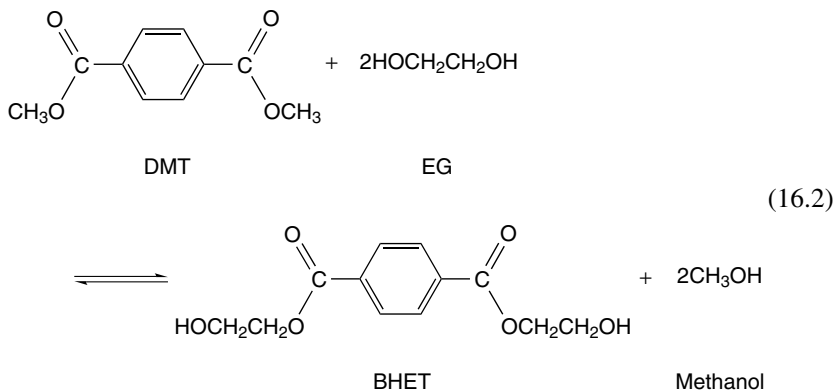
Because commercial synthetic thermoplastic polymers are either addition polymers or condensation polymers, depolymerization occurs by different routes. Addition polymers, for which the synthesis reactions are essentially not reversible, depolymerize by pyrolysis or such severe chemical attack that few useful monomers can be practically recovered. With pyrolysis, a wide spectrum of species are created, which offers little in the way of valuable reaction products without costly separation processes. The overall yield to desired products can be unattractively low.

Step-growth condensation polymers, such as polyesters and polyamides, are formed by reversible reactions. In the case of PET, the commercial synthesis is essentially carried out by two reactions. The first is the formation of bishydroxyethyl terephthalate by esterification of a diacid with a glycol or by transesterification of a diester with a glycol. The second is the formation of the polymer by a polycondensation reaction.

Bishydroxyethyl terephthalate (BHET) is the monomer used to make the PET polymer. BHET can be made either by the esterification of terephthalic acid (TPA) with ethylene glycol (EG):



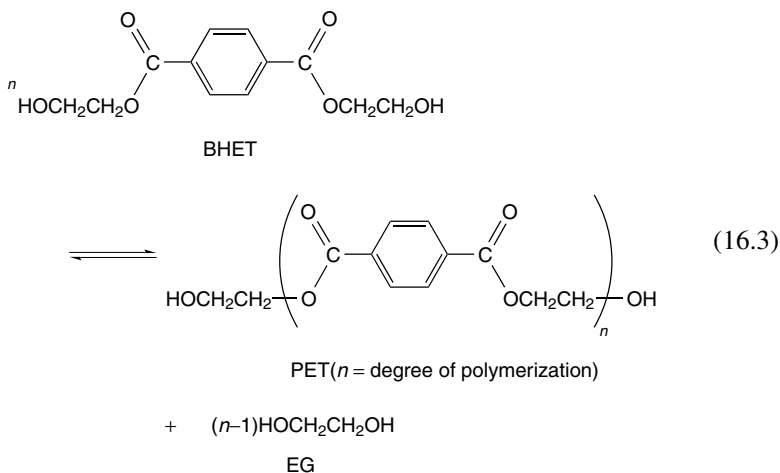
or by the transesterification of dimethyl terephthalate (DMT) with EG:



BHET formation is conducted at temperatures of 200 to 250 °C to achieve reasonable reaction rates. The activation energies of the two reactions are of the order of 25 000–30 000 cal/mol [4, 5]. The BHET formation is usually conducted under pressure to keep the ethylene glycol in the liquid state. Terephthalic acid is slurried with ethylene glycol for the esterification reaction. Dimethyl terephthalate is dissolved in ethylene glycol and BHET for a liquid-phase transesterification reaction. The synthesis of BHET is driven to this material by the removal of water or methanol. The reactions are reversible at reasonable rates if the concentrations of water or methanol reactants are held high.

The second reaction, the formation of the polyester, is commercially conducted in the bulk melt phase with the removal of ethylene glycol to drive the reaction to high molecular weight. For higher molecular weights, PET can be solid-phase polymerized by again enhancing conditions to remove ethylene

glycol. The reactions are as follows:



For the polymerization, either in the melt or solid phase, the reaction is driven to the polymer by removing ethylene glycol. The polymerization reaction is typically catalyzed by solutions consisting of antimony trioxide or germanium oxide. Both polycondensation catalysts also catalyze the reverse reaction, which is driven by an excess of ethylene glycol at melt conditions, generally above 255 °C. The polymerization reaction follows second-order kinetics with an activation energy of 22 000 cal/mol [6].

In the case of the esterification of the diacid, the reaction is self-catalyzed as the terephthalic acid acts as its own acid catalyst. The reverse reaction, the formation of TPA and EG from BHET is catalytic with regard to the usual metal oxides used to make PET, but is enhanced by either the presence of hydroxyl groups or protons. In the case of transesterification of dimethyl terephthalate with ethylene glycol, the reaction is catalytic, with a metal oxide needed to bring the reaction rate to commercial potential. The catalysts used to produce BHET are the same as those needed to depolymerize both the polymer to BHET and BHET to its simpler esters. Typically, titanium, manganese and zinc oxides are used for catalysts.

Mechanistically, three reversible reactions occur [7]. First, a rapid protonation of the carbonyl carbon in the polymer chain occurs, converting the carbonyl oxygen to a second hydroxyl group. Secondly, a slow attack by a hydroxyl oxygen from the hydroxyl-bearing added molecule occurs on the protonated carbonyl carbon atom. Thirdly, the rapid removal of the carbonyl oxygen, now a hydroxyl group, and a proton to form water or a simple alcohol and the catalytic proton takes place. Catalysts play an important role in the rate of the reactions. The slow step, the attack of, by a hydroxyl oxygen, on the carbonyl carbon atom of the carboxyl group, figures in the plan to depolymerize. The attack could be on the carbonyl carbon attached to the hydroxyethyl group on the end of the

polymer chain or on any carbonyl carbon on the chain. As such, the decomposition of PET by attack on carbonyl groups will result in a population of shorter and shorter chained species. Given enough time at temperature with enough hydroxyl material present, the PET will be reduced from a polymer to short-chained oligomers to BHET and finally to the species consistent with the nature of the hydroxyl group.

From this discussion, three different hydroxyl-containing species could be introduced in excess to drive the reactions to the initial materials for depolymerization. The first species would be ethylene glycol. Using ethylene glycol regenerates BHET and oligomers of degree of polymerization greater than 1 if the time, temperature or ethylene glycol concentration is insufficient to complete the transesterification. The polycondensation catalysts present in the PET are sufficient, if active, to form BHET from the PET. The use of the first species is referred to as glycolysis. The second species would be methanol. The latter could attack the carbonyl carbons to form ethylene glycol and dimethyl terephthalate. If the methanol is used to attack the carbonyl carbons of BHET, the reaction rate will be faster than trying to attack the carbons on the polymer chain. An economic choice must be made, or a process alternative devised, to combine the reduction of longer-chained polymers to the attack of the hydroxyl group from methanol. The use of the second species is referred to as 'methanolysis'. The third species to provide hydroxyl groups would be water. Use of water would be hydrolysis and terephthalic acid and ethylene glycol would result. Other alcohols could be used and are of ten employed. Diethylene glycol is used to make monomers for use in coatings. Use of higher-molecular-weight alcohols and diols is beneficial in making adhesives, polyols and unsaturated polyester compounds.

There are other reactions of consequence in the depolymerization of PET. The hydroxyethyl end groups can decompose to form an epoxide and carboxyl. The epoxide will react with free ethylene glycol to form diethylene glycol (DEG). This reaction is catalytically driven and is favored at high concentrations of hydroxyethyl end groups, such as when high levels of BHET are present. The consequence is the yield loss of ethylene glycol and the formation of diethylene glycol. Since some diethylene glycol is always present in PET from its formation during the esterification/transesterification step, the yield loss of ethylene glycol need not be economically serious. Patents disclose how to reduce the formation of diethylene glycol by the addition of sodium acetate [8]. More serious is the degradation of internal ethylene esters to form acetaldehyde. The latter will vaporize and represents a real yield loss of ethylene glycol.

The terephthalate moiety, either as the acid or ester, does not undergo similarly significant side-reactions with loss of commercially useful material. Terephthalic acid can sublime and dimethyl terephthalate can vaporize, and so maintenance of the vapor stream is a must.

If PET used for making bottles were just the product of combinations of terephthalate and mono- or diethylene glycol, the commercial depolymerization would

be more straightforward. In the United States, the Code of Federal Regulations permits the following modifiers to be used: isophthalic acid and dimethyl ester, azelaic acid and dimethyl ester, sebacic acid and dimethyl ester, pyromellitic anhydride, and 1,4-cyclohexane dimethanol [9]. The United States Food and Drug Administration (USFDA) also allows up to 30 % of a specific nylon, MXD6, to be mixed with PET for use in food and beverage bottles [10]. It is possible that 2,6-naphthalene dicarboxylate may also be used as a modifier for nominal PET bottles [11]. The reality is that PET is likely to be modified with levels of several percent of isophthalic acid or 1,4-cyclohexane dimethanol. The use of modifiers makes the depolymerization decision more critical. Just which monomer constituents are to be isolated, if any, must be determined based on the desired commercial product.

In addition, polyester bottles may contain colorants in the form of pigments, dyes or lakes. The colorants may be dispersed or dissolved in the polymer or may be covalently bound to the polymer backbone. Polyester packaging, which may be collected for depolymerization, may include nucleators for enhanced crystallization, anti-slip agents, branching agents, anti-blocking agents and anti-stats.

3 BACKGROUND

Although linear polyesters were probably first synthesized in the 1860s, the first polymerization of PET occurred with Whinfield in 1941 [12]. Commercial PET was formed by using dimethyl terephthalate because the dimethyl ester could be purified by distillation. Terephthalic acid purification was too inadequate to prepare acid of sufficient purity to make saleable polyester until the late 1970s. As the initial market price for dimethyl terephthalate was relatively high, converting polymer scrap back to DMT and EG was economically attractive and provided materials of needed purity for repolymerization purposes. Methanolysis processes were common and continued to exist in Eastern European countries into the 1990s. In Western countries, methanolysis plants were shut down as the market price for DMT fell with large-scale DMT production from *p*-xylene. By 1980, only the X-ray film depolymerization plant at the Eastman Kodak Company was still in regular commercial operation. This plant, built in the mid-1970s (and still operating in 2000) to recover over 50 000 000 lb of polyester annually [13], is by virtue of its continued operation thought to be economically viable in the context of the photographic business.

As the environmental movement began to focus seriously on solid waste and recycling issues, PET depolymerization received a boost. *Discover Magazine* awarded its 1992 Environmental Award to the Hoechst-Celanese Corporation and Coca Cola USA for Hoechst-Celanese's plan and Coca Cola's commitment to use methanolysis to recycle used PET beverage bottles into new bottles [14]. Ominously, likely higher costs were recognized from the beginning. E. I. DuPont

announced in 1992 its ability to recover polyester engineering resins by methanolysis. DuPont depolymerized auto fenders and soft drink bottles to DMT and EG, repolymerized the PET, spun fiber, and made sails for the recreated HMS Rose sailing ship [15]. The same company followed up the initial methanolysis development work with the investment of \$12 000 000 to convert an existing DMT facility at the company site in Cape Fear, NC, to be a methanolysis plant capable of producing 100 million lb of DMT annually by mid 1995 [16]. The process, named PetretecSM, was commercialized in 1996. The Goodyear Tire and Rubber Company commercialized its RepeteTM glycolysis process in 1992 to supply PET with post-consumer recycled content. These four companies, i.e. Eastman Kodak, Hoechst-Celanese, DuPont and Goodyear, were the United States companies which attempted to offer post-consumer recycled PET content to the beverage bottle industry. Table 16.1 presents the listing of 'letters of no objection' issued by the USFDA in response to petitions to use the product of specific company processes to make regulated food packaging. The USFDA opinion letters carry less liability limitations than do the Code of Federal Register regulations, but do indicate the agency's belief that food safety will not be jeopardized by the use of the various processes to make food packaging materials. The USFDA opinion letters pertain only to food safety, and not to aesthetics or economics. The opinion letters are specific to specified processes of named companies.

Other uses for depolymerized PET bottles have been investigated. Used bottles have been glycolized and then used to make unsaturated polyester thermosets and polyol components in rigid polyurethane foam. Evco Research announced in 1999 its EvCote[®] waterproof coatings and adhesives based on recycled PET [17, 18].

Table 16.1 USFDA 'letters of no objection' to the use of depolymerized polyester in food packaging

Issue date	Issued to	Materials included
January 9, 1991	Hoechst-Celanese Company	Regenerated DMT
August 20, 1991	Eastman Chemical Company	Regenerated DMT and EG
December 16, 1991	Goodyear Tire & Rubber Company	Glycolysis product
October 14, 1992	Dupont Company	Regenerated DMT and EG
October 12, 1995	Hoechst-Celanese Company	Glycolysis product
March 12, 1996	Wellman, Inc.	Glycolysis product
May 1, 1996	Innovations in PET Pty Ltd	Glycolysis product
October 18, 1996	Eastman Chemical Company	Regenerated dimethyl naphthalate and EG
June 6, 1997	Eastman Chemical Company	Glycolysis product
August 23, 2000	Eastman Chemical Company	Glycolysis/methanolysis product

4 TECHNOLOGY FOR POLYESTER DEPOLYMERIZATION

Because all depolymerization processes will generate waste that may be classified as hazardous waste or at least chemical waste, it will always be economically preferable to separate as much non-PET material from the PET material as is practical. Traditional bottle washing procedures can produce used bottle flake that is clean enough to be used to make more bottles or somewhat less clean and less expensive material. Technologies have been proposed to dissolve the polyester scrap in appropriate solvents to separate PET from other materials such as cotton fiber or magnetic tape components [19].

The first technology for depolymerization is glycolysis. The rate of depolymerization with ethylene glycol is faster with zinc acetate catalyst than with manganese acetate catalyst [20]. For PET made from DMT, either transesterification catalyst is likely to be present and will catalyze the formation of BHET. Glycolysis can be conducted in stirred batch reactors by adding molten PET to ethylene glycol under pressure, by melting PET in a slurry of PET flakes and EG, or dissolving PET in an oligomeric solution of partly glycolized PET. Glycolysis can also be conducted by adding ethylene glycol to an extruder for a reactive depolymerizing extrusion. A continuous glycolysis process is also possible [21]. One approach has been to use the distillation residue from ethylene glycol purification to be the dissolving media for solid PET flakes [22]. Such an approach is reasonable if the glycolysis product is to be further processed to DMT or TPA, but not particularly attractive if the glycolysis product is to be repolymerized directly. The glycolysis product can be reacted with methanol to form DMT [23]. The glycolysis product can also be used to react with other monomers to make a copolymer of PET [24].

The use of the glycolysis product, BHET and oligomers, directly for repolymerization requires either very closely controlled feed or a purification procedure. Purification operations for the glycolysis product can include filtration, crystallization, evaporation and adsorption [25, 26]. Flotation of impurities has also been envisioned [27]. Besides the conventional control of feed materials to assure glycolysis product quality, a process has been promoted and announced for commercial development utilizing PET embrittlement with boiling EG, crushing and screening, glycolysis, and purification by filtration and adsorption for glycolysis with color filtration [28]. The economic claim of equivalence with virgin PET is made for 10 000 annual tonne capacity [29]. This is the RenewTM process.

Glycolysis is also conducted to create polyols for unsaturated polyester usage. The PET can be dissolved in DEG to create polyols with ether linkages [30]. The reaction can be carried out with propylene glycol [31] or by reacting with an unsaturated dibasic acid [32] and needed additives and catalysts [33].

While glycolysis technologies can deal with non-PET components with varying degrees of success, methanolysis and hydrolysis produce discrete slates of definable molecules that can be separated and purified. Methanolysis has been

used commercially for many years. Direct hydrolysis of PET has yet to be commercialized, although hydrolysis of DMT obtained by methanolysis to produce purified TPA is commercially carried out.

The original methanolysis technology relied on pressure to keep the methanol as a liquid at reaction temperatures. Methanolysis can be performed either by conducting a glycolysis and subsequent methanol transesterification of the oligomers to form DMT and EG, or by subjecting the PET directly to methanol. Early processes focused on continuous liquid-phase methanolysis of a glycolysis product to form DMT, with purification by filtration [34]. Manganese catalysts are commonly used [35]. The DMT and EG are often purified by distillation.

Rather than keeping the methanol always as a liquid, some technologists suggested bubbling methanol vapor through crude BHET [36]. A process was described by the Eastman Kodak Company based on using vapors of methanol [37] and removing the reaction products, DMT and EG, along with excess methanol as a vapor [38]. The process was further defined to use superheated methanol and a rectifying distillation section to keep oligomers out of the product [39]. Kodak was not alone in patenting this approach. DuPont also received a process patent for methanolysis with vapor product takeoff [40].

Economically, the methanolysis reaction is less important than the purification costs to deliver purified DMT and EG. As long as catalysts are kept out of the reactants, EG can be boiled away from the DMT and subsequently purified by distillation. DMT can be crystallized and washed, or distilled, or both. Separating glycols from DMT by distillation means dealing with the DMT–EG azeotrope. Azeotropic distillation of DMT and EG has been patented [41, 42]. Patents also exist to separate other glycols, such as 1,4-cyclohexane dimethanol, from the DMT product [43]. Formation of a glycol-rich phase separate from the DMT-rich phase and then isolating the glycol has also been patented [44]. Kodak have also disclosed a process of quenching the vapors from the vapor takeoff methanolysis reactor/rectifier in order to recover the DMT [45]. Dimethyl isophthalate (DMI) from an isophthalic component in PET bottle polymer exhibits similar vapor pressure properties as DMT and is not easily separated.

With recent changes to the USFDA regulations to allow copolymers of isophthalic acid, terephthalic acid, ethylene glycol, diethylene glycol, and 1,4-cyclohexane dimethanol in food packaging [46], the regulatory need to isolate DMT, DMI, EG, DEG and 1,4-cyclohexane dimethanol was removed. However, quality issues for the containers made from repolymerized materials still remain. Methanolysis can remove valuable monomers from extraneous materials such as fillers, colors and non-volatilizing contaminants. The USFDA has recognized several times the efficacy of the methanolysis reaction and unit operations in purifying PET monomers for subsequent reuse [47]. Because the European Union and its Member Countries use a positive list and all of the utilized monomers for PET are on this list, the isolation of DMT, DMI, EG, DEG and 1,4-cyclohexane dimethanol has not been a regulatory requirement. Many countries outside of

the European Union, other than the United States, follow the EU regulatory methodology.

Another approach to methanolysis has been to marry the vapor removal of volatile PET monomers with a recombination of monomers to make a copolymer polyester. This approach produces a product of general glycolysis-like uniformity of components, but with several plates of distillation separation [48–50]. While the methanolysis reaction section shows no new economic breakthrough, the recombination of monomers to form BHET and related species inexpensively offers the potential for economic overall operation by avoiding the expensive separation equipment. In addition, the product is BHET and related monomers, fully suitable to be added to a modern PET reactor train which is based on using purified terephthalic acid. Traditional methanolysis processes produce DMT and EG. Virtually no new PET production facilities based on DMT feeds have been built since the early 1980s, hence making methanolysis an interesting but obsolete process because the DMT product is not directly useful in a TPA-based PET manufacturing operation. The Eastman Chemical Company has patented a hybrid methanolysis/BHET depolymerization process [51] and announced a process called Optisys[™] [52].

One approach to utilizing methanolysis in TPA-based PET production is to hydrolyze the DMT with water [53]. Rather than hydrolyzing DMT, technologists have proposed processes to hydrolyze PET in concentrated sulfuric acid [54], at neutral pH in water [55], at neutral pH with subsequent hydrogenation for purification [56], or via saponification with sodium hydroxide [57, 58]. The acid hydrolysis produces product of low quality. Neutral hydrolysis requires long reaction times at high temperatures and pressures, thus increasing the capital costs. Saponification reactions are quick and occur at commercially attractive rates at low temperatures and pressures. The terephthalate salt formed must be converted to the acid to be useful. Several commercial processes have been proposed to make terephthalic acid with a sodium sulfate co-product, e.g. Recopet[™] in Europe and Unpet[™] in the United States [59]. A process cited earlier, Renew[™], can be extended from producing a glycolysis product to making TPA [60]. All processes that would make terephthalic acid must deal with the difficulty of further purifying TPA and growing large crystals. As PET esterifications are conducted with a minimum of ethylene glycol, small TPA crystals mixed with ethylene glycol result in an excessively thick paste. Purification of TPA can be carried out by oxidation and hydrogenation [61], which may or may not remove the variable contaminants found in post-consumer plastics. TPA can be sublimed and recovered after neutral hydrolysis [62], or it can be recovered by a combination of vaporization of TPA with condensation and hydrogenation [63]. All of the terephthalic acid purification processes are inherently capital-intensive due to the intractable nature of TPA.

One other process has been suggested for depolymerizing PET to TPA, i.e. ammonolysis. The process proposal would react PET with ammonia, form a

water-soluble salt and filter out non-PET materials, acidify to precipitate TPA, and recovery of ammonia and EG [64]. This process has not yet been offered commercially.

Depolymerization processes have been proposed for poly(butylene terephthalate) by the glycolysis of PBT with 1,4-butanediol and a titanium catalyst [65]. Methanolysis of poly(ethylene naphthalate) to dimethyl naphthalate and ethylene glycol has also been proposed [66, 67], but not implemented. The lack of commercial depolymerization of PEN is probably due not to technical limitations, but to insufficient supplies of PEN polymer feedstock to meet the minimum quantities needed for economical operations.

5 COMMERCIAL APPLICATION

PET producers have had to deal with recovery of scrap polymer since the 1950s, particularly when raw materials were rather expensive. Glycolysis has been and is practiced within the production setting on material of known composition and acceptable purity. Methanolysis was practiced in the United States and Europe until about 1980 as most PET production was then based on DMT and EG. Methanolysis is still practiced on post-consumer and pre-consumer X-ray film by the Eastman Kodak Company which uses the DMT and EG to make more film. Other than an occasional use of glycolysis, no other large-scale, on-going commercial use of post-consumer PET is made in developed countries.

From any lack of contra-indicating legislation, depolymerization of PET has been accepted as a legitimate recycling process in the United States, and this also appears to be the case in Japan. The European Union has not fully accepted polyester depolymerization as a recycling process as legitimate as mechanical recycling. Rather, depolymerization of step-growth, condensation polymers has been categorized with pyrolysis and seen, politically, as a variant of depolymerization to produce fuel, which is akin to incineration. This will likely change as legislators and regulators more fully understand the technology. Polyester depolymerization, as we will see, must be justified economically. Either as a stand-alone investment or a necessary provision to sell polyester for packaging, depolymerization capital recovery must be recognized. The political circumstances in the United States make PET depolymerization an unsubsidized business venture. In Europe, monies can be made available via 'green dot' fees to underwrite some portion of the overall cost. Because PET trades internationally, the basic economics developed in this chapter will apply generally in all countries. What will be country-specific and may determine actual implementation are the requirements for recycled content to sell any PET for bottle packaging and the availability of additional funds to make investments attractive.

Among potential commercial processes, the RenewTM process is proposed to filter color from a glycolysis product, while the RecopetTM process creates TPA

by saponification and precipitation. The Unpet™ process etches PET with sodium hydroxide to remove stained polymer. The latter process originally was intended to produce sodium terephthalate which would be roasted for purification. The current Unpet™ process is not a complete depolymerization. The Optisys™ process apparently employs the methanolysis reaction to make a BHET-like product.

6 CRITERIA FOR COMMERCIAL SUCCESS

Simply possessing a promising technology does not guarantee commercial success. The choice of technology depends on cost, the desired products, and the quality and quantity of the feed material. Methanolysis produces DMT and EG and possession of DMT may not be useful for subsequent use without conversion to TPA. Simple glycolysis requires clean, clear PET feed as no change in composition or color will occur in the processing. Hydrolysis is capital-intensive and requires a large scale to offset capital costs. The feedstock must be available at the desired quantity with the desired minimum quality and at a stable and acceptable price long-term to allow for evaluation of risk. The capital and operating costs must be acceptable and environmental and safety hazards minimal.

One critical issue is the evaluation alternative. In the case of methanolysis, the alternatives are to make DMT and EG by depolymerization or secure materials from traditional petrochemical sources. For hydrolysis, the alternatives are TPA and EG by depolymerization or from traditional sources. For both technologies, the amount of copolymerizing isophthalate and/or 1,4-cyclohexane dimethanol is likely to be too little to justify the cost of recovery. For the various forms of glycolysis and the methanolysis/BHET hybrid, the alternative is the BHET and BHET-like materials made by the combination of a terephthalate and isophthalate plus EG and various glycols. Market prices exist for TPA and EG. BHET is not an item of commerce, and so the value must be imputed from the market price for TPA (the modern terephthaloyl) and EG, plus a conversion cost.

Other than for simple glycolysis, a substantial capital investment must be made to conduct commercial depolymerization of PET to regain PET monomers for repolymerization of PET. As the capital costs rise at roughly the 0.6 power of the relative volume [68], larger facilities are more economically attractive than smaller facilities. Besides the availability of capital to build very large depolymerization facilities, the limiting criterion has been and is likely to continue to be the sure supply of adequate PET feedstock at acceptable prices.

7 EVALUATION OF TECHNOLOGIES

This section will look at seven processes to convert post-consumer PET bottles to raw materials suitable for use to make new food and beverage bottles. The processes are as follows:

1. Liquid-phase methanolysis
2. Vapor-phase methanolysis
3. Simple glycolysis
4. Caustic hydrolysis
5. Aqueous hydrolysis
6. Methanolysis/BHET hybrid
7. Glycolysis with color filtering

All estimates are based on this author's interpretation of patent literature and similar treatment of capital and operational costs. The comparisons of processes are made for one throughput size, 22 700 tonnes annually or 50 000 000 annual pounds of feed.

7.1 FEEDSTOCK

No commercial PET depolymerization facility will feed whole, unwashed PET bottles to the process. With bottle caps, labels and occasional basecaps, about 20–22 % of a PET bottle is not actually PET and should be removed before depolymerization. The mechanical process for preparing depolymerization feed is similar to that used to render post-consumer bottles into flake for fiber, strapping, film or bottle end uses; only the intensity and costs may be different. The first economic issue in feedstock is the price of bales of PET bottles. Prices in Europe and the United States have fluctuated over the past ten years from 'lows' of \$0.04/kg in 1996 to 'highs' of \$1.05/kg in 1995. Prices of bottles are dependent on not only time and location, but on the color of the PET. Clear bottles sell for higher prices than do colored bottles. For this evaluation, we will assume that US\$ 0.132/kg is paid for mixed color bottles, FOB¹ the sorting/baling facility. The mixed color bottles are generally satisfactory for methanolysis, hydrolysis, methanolysis/BHET hybrid and glycolysis with color filtration. For simple glycolysis for which little purification of product occurs, clear bottles are required and are assumed to cost US\$ 0.264/kg. The mixed color bottles must sell for at least the cost of baling, usually taken to be about US\$ 0.100/kg, while the simple glycolysis feed bottles must compete with value-added uses such as strapping and textiles. Because no market currently exists for semi-washed flake, it is assumed that a market will develop when depolymerization can accept the less stringently clean material. As scale counts, the semi-washed flake facility

¹ FOB, 'free on board'. This is a trade term requiring the seller to deliver 'goods on board' in vessels designated by the supplier. When used in such terms, the word 'free' means that the seller has an obligation to deliver goods to a named place for transfer to a carrier. In this context, the significance is that FOB means that the buyer does not have the goods delivered at the purchase price, but must also pay a freight charge. Some goods are sold DELIVERED, meaning that the freight expenses are included in the purchase price. FOB tells the buyer where the goods can be picked up, usually at the seller's loading dock.

Table 16.2 Summary of depolymerization feed costs

Aspect	Semi-washed flake	Glycolysis-grade flake
Nominal capacity (t/year)	45 000	45 000
Fixed capital cost (US\$/kg)	0.20	0.43
Bottle purchase price, FOB ^a (US\$/kg)	0.132	0.264
Product costs (US\$/kg)	—	—
material cost	0.22	0.44
variable conversion cost	0.07	0.16
fixed conversion cost	0.09	0.14
return on capital ^b	<u>0.03</u>	<u>0.07</u>
sales price	0.42	0.81
Before tax return on investment (%)	13	13

^a FOB, 'free on board'; the purchase price does not include the transportation costs (see text for further details).

^b Profit.

envisioned is taken to be 45 000 annual tonnes in capacity, large enough to supply two depolymerization plants here presented. This is a very large mechanical reclaiming facility in an industry for which the median plant size is about 20 000 annual tonnes of capacity. For fair comparison, the size of the glycolysis-grade mechanical reclaiming facility is also taken to be 45 000 annual tonnes. For both flake-producing facilities, the before-tax return on fixed capital investment is taken to be 13 %, a value that reflects the tight profit margin of the flake making industry. The details of the flake making economics given in Table 16.2 are taken as being generally representative. The large-scale flake plants will tend to set market prices for PET flake. At 22 500 annual tonnes, the before-tax return on capital for glycolysis-grade flake sold at US\$0.811/kg drops to 5.3 %.

7.2 CAPITAL

Each process evaluated is presumed to be free-standing and supplying all of its own needed services. Tankage, distillation columns, pumps and outside battery limits (OSBLs) costs are included, in addition to reactors and melters, centrifuges, crystallizers and dryers, as needed. The simple glycolysis reaction vessel is the least expensive reactor. The vapor methanolysis and caustic hydrolysis reactors are the next most expensive, while the liquid methanolysis and glycolysis with color filtration are more expensive still. The methanolysis/BHET hybrid has the second most expensive reactor system, with the aqueous hydrolysis reactor being the most expensive due to high pressures and slow reaction rate. Both methanolysis processes require DMT crystallizers, DMT centrifuges, DMT melters and filters, along with DMT and EG vacuum distillation columns, a methanol column and a low-boilers column. Simple glycolysis requires filtration and a low-boilers distillation column. Hydrolysis processes include filters, crystallizers, centrifuges

and TPA dryers, along with EG vacuum distillation columns, water columns and low-boiler columns. Caustic hydrolysis also includes equipment to handle acid and base, and to recover salt. Methanolysis/BHET hybrid requires filters and an EG vacuum distillation column, a methanol column and a low-boilers column. Because the product of the methanolysis/BHET hybrid is molten 'monomer' which does not store well, product is processed to polymer soon after it is produced and is not shipped as monomer. Similarly, glycolysis with color filtration produces a BHET monomer product for immediate use. This second glycolysis process requires embrittlement, crushing and sorting equipment, in addition to a centrifuge, extensive filtration, an EG vacuum distillation column and a low-boilers column. A summary of the capital costs is provided in Table 16.3. In addition, installation factors are shown along with the costs of building structures. The building sizes are estimated as what is needed to house the production equipment. External storage and handling of incoming flake feeds are not explicitly included, but are part of the installed cost. The outside battery limit (OSBL) capital is given as a percentage of the direct process equipment capital to include environmental needs, access needs and plant general needs. Utility capital is included in the utility per unit costs. Table 16.3 provides the total fixed capital in US dollars and per annual kg of product. Working capital is not included here, but is included in the economics calculation.

Not surprisingly, the simple glycolysis process has the lowest capital investment. The methanolysis/BHET hybrid and glycolysis with color filtering are judged to be similar in investment cost and benefiting from not including expensive separation equipment. Full methanolysis is a step more expensive, with costly separation trains. Hydrolysis can be even more expensive, with costly separation/purification trains and costly neutral hydrolysis reaction equipment. The caustic hydrolysis process does not include an electrochemical salt breaking process, which could lower the operating purchase cost of caustic and acid.

Capital cost range from about US\$0.98/annual kg of product to US\$1.41/annual kg of product for the processes with purification, but only US\$0.39/annual kg for simple glycolysis.

8 RESULTS

Table 16.4 provides the summary of economic costs and results. The presumption throughout is that each process can be operated with environmental and human safety to produce a fully satisfactory product of sufficient quality to command market prices. The processes which produce discrete products, i.e. methanolysis and hydrolysis, will have to meet commercial specifications. The mixed-species product processes, i.e. simple glycolysis, hybrid and glycolysis with color filtration, must be able to feed adjacent polymerization facilities to make satisfactory product. Because the simple glycolysis process has little purification capability,

Table 16.3 Capital costs for 22700 annual tonne depolymerization facilities (millions of US dollars, M\$)

Equipment and related	Liquid-phase methanolysis	Vapor-phase methanolysis	Simple glycolysis	Caustic hydrolysis	Aqueous hydrolysis	Methanolysis/ BHET hybrid	Glycolysis with color filtering
Reactors, melters, filters, crystallizers, centrifuges and dryers	1.42	1.17	0.38	1.50	1.90	0.85	1.50
Tanks	1.25	1.25	0.40	1.05	0.80	1.00	0.60
Distillation columns	0.85	0.85	0.10	0.65	0.65	0.60	0.35
Pumps	0.41	0.35	0.20	0.47	0.35	0.31	0.30
Purchased equipment	3.93	3.62	1.08	3.67	3.70	2.76	2.75
Lang factor ^a	6.2	6.2	6.0	6.5	6.5	6.2	6.3
Building at \$860/M ³	0.64	0.64	0.40	0.80	0.80	0.64	0.60
ISBL ^b	25.006	23.084	6.880	24.655	24.850	17.752	17.925
OSBL/ISBL ^{b,c} (%)	25	25	30	30	25	25	30
OSBL ^c	6.252	5.771	2.064	7.397	6.213	4.438	5.378
Total fixed capital (M\$)	31.258	28.855	8.944	32.052	31.063	22.190	23.303
\$ (annual kg)	1.38	1.27	0.39	1.41	1.37	0.98	1.03

^a This is a 'multiplier', which when applied to the purchase prices of major pieces of chemical process equipment, provides an estimate of the installed cost of the chemical process.
^b ISBL, inside battery limit.
^c OSBL, outside battery limit.

Table 16.4 Summary of results for depolymerization economics

Aspect	Process						
	Liquid-phase methanolysis	Vapor-phase methanolysis	Simple glycolysis	Caustic hydrolysis	Aqueous hydrolysis	Methanolysis/ BHET hybrid	Glycolysis with color filtering
Input (t/year)	22 700	22 700	22 700	22 700	22 700	22 700	22 700
Yield to Class I (%)	91	93	97	90	90	93	93
Total fixed capital (M\$)	31.3	28.9	8.9	32.1	31.1	22.2	23.3
Total capital (M\$)	32.5	30.0	10.2	33.4	32.2	23.3	24.5
Feed cost (\$/kg feed)	0.419	0.419	0.811	0.419	0.419	0.419	0.419
Cost of goods (\$/kg feed)	1.03	0.99	1.05	1.10	0.99	0.92	0.97
Cost with 15 % BTROI ^a (\$/kg)	1.25	1.19	1.12	1.32	1.21	1.07	1.13
Value of product (\$/kg)	0.80	0.80	0.74	0.72	0.72	0.74	0.74
Premium needed for 25 % recycled content at 15 % BTROI ^a (\$/kg)	0.112	0.097	0.095	0.149	0.121	0.082	0.097

^a BTROI, before-tax return on investment.

the inexpensive process is offset by fairly expensive feeds compared to the less costly feeds useful to the other processes. The quality of product and the process robustness for the hybrid and the glycolysis with color filtration processes must be tested in actual trials and are not the subject of this study other than to say both processes do provide multiple avenues to remove contamination from the feeds.

The operating rates of each process were fixed at 22 700 annual tonnes. The yield of gross product to Class I or prime product was estimated by this author and is included in Table 16.4. Semi-washed PET flake will contain some extraneous material, by definition. All processes will lose some potential ethylene glycol due to decomposition. Hydrolysis processes are expected to lose isophthalates in the crystallization step. The methanolysis and glycolysis with filtration processes generally recover more materials for inclusion with product. Simple glycolysis recovers the most, but still loses some ethylene glycol.

The cost of goods range from US\$0.92/kg to US\$1.10/kg, with the most expensive 20 % greater than the least expensive. The hybrid process shows the lowest factory cost. Surprisingly, the glycolysis with filtration cost is higher, primarily because of loss of product in filtration and expense of disposed filtration media. Caustic hydrolysis is the most costly because of consumption of commercial acid and base. Only caustic hydrolysis produces a significant amount of useful co-product, i.e. the salt of the acid and base used. In this study, NaOH and H₂SO₄ were purchased at market prices and the resultant Na₂SO₄ was valued at market prices for chlorine-free salt.

For this study, an economic hurdle rate of 15 % before tax return on capital investment was used. This rate is higher than for the flake feed preparation facility because the depolymerization facilities cannot be as easily converted to other uses as can the flake preparation plants, which can be converted to produce mechanically cleaned PET for traditional post-consumer PET uses. Including the total capital return component, and a 12 year economic depreciation component, the total cost of the products are given in Table 16.4 as US\$1.07/kg to US\$1.32/kg.

The important question of comparative value, mentioned earlier in Section 6, now must be considered. The material output of each process per unit of feed is estimated and multiplied by the market price of the material to arrive at a value of product. The output of the methanolysis processes, DMT and EG, are shown as a methanolysis-type product value in Table 16.5. The stoichiometric ratios are adjusted with a presumed 99 % recovery of DMT and 93 % recovery of EG. The output of the hydrolysis processes, TPA and EG, have the stoichiometric ratios adjusted for a presumed 99 % recovery of TPA and 93 % recovery of EG. The glycolysis processes, including methanolysis/BHET hybrid, are valued at 99 % recovery of terephthalic acid, 95 % recovery of ethylene glycol, and a US\$0.022/kg esterification credit for making BHET. The EG recovery is higher for glycolysis-type products because of less loss of useful moieties. The three

Table 16.5 Prices of raw materials and comparative products

Materials and products	Price	
	US\$/kg	US\$/lb
Mixed-color PET bottles	0.132	0.060
Clear PET bottles	0.264	0.120
Mixed, semi-washed PET flake, purchased bottles	0.419	0.190
Mixed, semi-washed PET flake, free bottles	0.234	0.106
Clear, washed flake, purchased bottles	0.811	0.368
PTA	0.599	0.272
DMT	0.586	0.266
EG	0.579	0.263
Methanol	0.126	0.057
NaOH	0.287	0.130
H ₂ SO ₄	0.057	0.026
Na ₂ SO ₄	0.143	0.065
Glycolysis-type product	0.742	0.337
Methanolysis-type product	0.799	0.363
Hydrolysis-type Product	0.724	0.328

market values range from US\$0.72/kg to US\$0.80/kg, decidedly less than the product costs shown in Table 16.4.

Table 16.4 also shows the price premium required to offset the excessive costs to depolymerize post-consumer PET bottles in order to sell resin made from the depolymerization processes. The price premium is shown as the amount needed when 25 % recycled content is present in sales polymer by the various depolymerization processes when those processes achieve a 15 % before-tax return on investment (BTROI). The smallest required premium is needed for the methanolysis/BHET hybrid, i.e. US\$0.082/kg. The two glycolysis processes, simple glycolysis and glycolysis with color filtration, and vapor phase methanolysis require the next greater price premium, US\$0.095 to US\$0.097/kg. Hydrolysis with high capital costs or acid/base expenses requires the greatest price premium. Figure 16.1 shows the graphical presentation of the premium requirement.

The stated 25 % recycled content provision is not a limitation of the technology or regulations, but a business choice with the economic consequences shown. For processes that can use recycled PET more cheaply than those which use virgin material, the percentage-recycled content may be greater than 25 %. The 25 % content level has traditionally been seen as sufficiently high enough to represent 'substantial' content. Marketers who advertise recycled content considerably less than 25 % are frequently met with scorn and derision.

The size of the depolymerization facilities was given at 22 700 tonnes annually. As depolymerization is capital-intensive, the choice of facility size can be

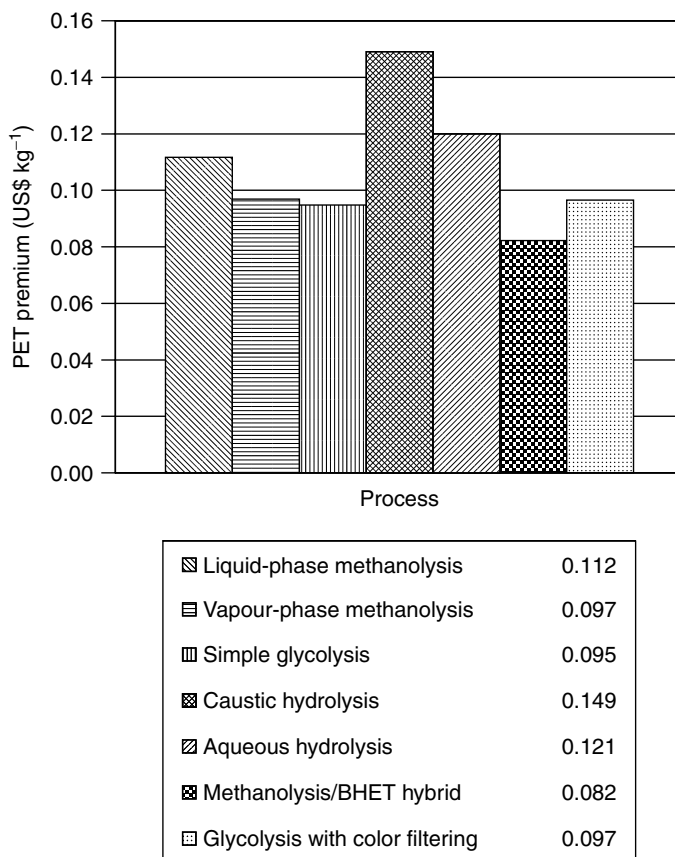


Figure 16.1 Price premium required for 25 % recycled content PET: 22 700 tonnes annual capacity; bottles purchased for US\$132/tonne

crucial to the overall economic success. For the methanolysis/BHET hybrid, the most economically attractive of the processes here examined, the effect of scale is examined in Figure 16.2. Bottles are purchased for US\$132/t and processed in the large flake preparation plant at the fixed price given in Table 16.5. The depolymerization economics provide a 15 % return on the investment and the required premium to match commercial costs of PET feedstocks is shown. Even for over 90 000 annual tonnes of production, a premium of over US\$0.04/kg PET sold is needed. Not surprisingly, the needed premium rises sharply as the depolymerization plant size decreases.

Other approaches to providing post-consumer recycled content are possible besides depolymerization. Depending on food safety regulations, recycled content in central sidewall layers and the use of especially cleaned, mechanically recycled,

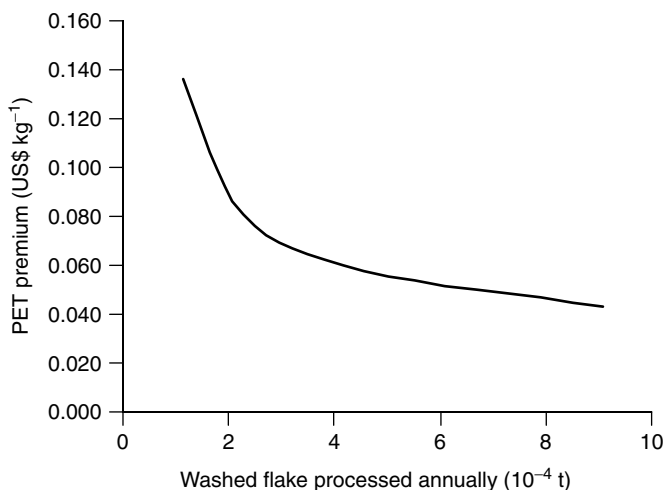


Figure 16.2 Price premium, hybrid process, for 25 % recycled content PET, with US\$ 132/tonne bottles and semi-washed flake: 15 % before-tax return on investment

post-consumer PET material can be considered. The various mechanically recycling processes do not, however, deal with unwanted colors or components.

In some jurisdictions, monies are available to underwrite the collection of used bottles. As such, authorities may consider opportunities to ship bottles at no cost to the recipient. In the 1990s, various schemes were devised in Europe not only to provide used plastic packaging for free, but also to provide a subsidy for its use. These were unsuccessful for economic and political reasons [69]. Even so, it is worth investigating what would be the economic consequence of providing bottles at no cost, FOB the baling plant. In this case, the cost of semi-washed flake delivered to the depolymerization plant falls, as shown in Table 16.5, from US\$0.419/kg flake when bottles are purchased to US\$0.234/kg flake when bottles are provided at no cost because bottle costs are paid for by means other than purchase. Figure 16.3 shows the impact on the needed premium for 25 % recycled content sales of PET when the zero-cost bottles are processed through a semi-washed flake manufacture and the methanolysis/BHET hybrid depolymerization process. At the nominal 22 700 annual tonnes, a reduced price premium is still needed. At less than approximately 75 000 annual tonnes, the price premium is no longer needed. This does not suggest that there are readily 75 000 tonnes of suitable material available for depolymerization at zero cost. It does suggest, however, that cost equivalency is possible, but not easily achieved.

While the chance of a systemic error in the modeling is always possible, the greatest variability, and uncertainty, is in raw material cost for depolymerization and the valuation of the product. Roughly speaking, the variable conversion costs,

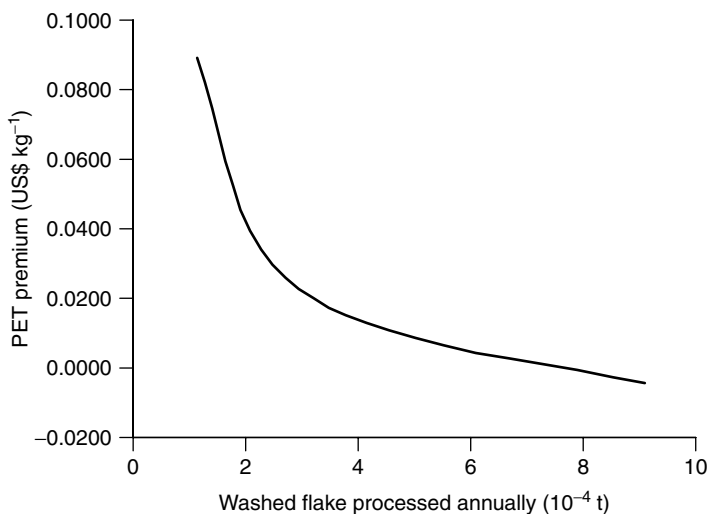


Figure 16.3 Price premium, hybrid process, for 25 % recycled content PET, with free bottles and semi-washed flake: 15 % before-tax return on investment

fixed conversion costs and financial costs are about the same and individually about 40 % of the material costs. The estimated price for mixed, colored PET bottles, i.e. US\$132/t, will likely not be much lower because of the floor price due to baling costs. A higher price depends on other, more valuable uses for mixed colored bottles. These bottles will continue to sell at prices less than clear bottles. The price for simple glycolysis feed, US\$264/t, will vary. Based on experience in the 1990s, prices for baled clear PET bottles could range from US\$120 to US\$400/t. The prices for TPA and EG, the bases for the valuation of product, will also vary. Over the seven years from 1994 through 2000 in the United States, the value of the glycolysis-type product varied from US\$0.57/kg to US\$1.06/kg compared to US\$0.742/kg used in this analysis. While used bottle prices do rise and fall in general coordination with virgin PET raw material prices, the correlation is not assured. Market forces do cause variation in the ratio of used bottle prices to the prices of TPA and EG.

9 CONCLUSIONS

The commercial potential for recycling post-consumer PET is not limited by lack of depolymerizing technology. Many options are available with varying degrees of capital intensity. The technologies most probable to provide satisfactory quality product, suitable for reuse in food packaging, are likely to cost US\$1.00/kg or more and require capacities of over 20 000 annual tonnes.

The key to commercial success is the business plan, particularly the source and cost of feedstock and the value of the depolymerization product. A range of technologies, approximating the range of patented processes for full depolymerization, have been modeled and all produce product of cost greater than value when all of the transactions are conducted in a free market. In such a free market where the raw material must be purchased away from other uses, a premium must be charged on the produced PET product with recycled content by depolymerization if the investment is to generate a return. In a free market, the break-even facility size would be very large, larger than the available supply of raw material.

In those jurisdictions where money is specifically collected from consumers to underwrite the costs of recycling plastic containers, funds may be available to offset some costs of depolymerization. If bottles are provided at no cost at the sorting/baling facility, an economically attractive venture can be contemplated, but still at a large scale. Securing the feed on a long-term basis at a favorable price will require significant co-operation.

The primary uncertainty in the estimation of commercial potential for depolymerization of PET is the value of the alternative to make polymer. For other than the simple glycolysis process, the used bottle feed material is likely not to vary substantially in dollars per tonne, although the percentage change could be sizeable. The selection of the data used to calculate the basis to value the products of depolymerization can change the overall conclusion for an investment.

Depolymerization reduces inherently valuable long-chained molecules to inherently less valuable smaller molecules. If mechanical recycling can utilize collected plastic materials profitably, it is highly unlikely that depolymerization will achieve greater profitability.

10 ACKNOWLEDGEMENT AND DISCLAIMER

The market prices used in this study represent multiple year averages for the 1990s in the United States. The capital requirements and economic estimates here presented represent the views of this present author based on interpretations of publicly available documents and are not based on any confidential information. The economic calculations follow good engineering principles and generally accepted accounting procedures, but are not guarantees of specific outcomes.

REFERENCES

1. Anon, *Eur. Plast. News*, **24**(8), 7 (September, 1997).
2. Anon, *Plast. News*, **12**(50) (February 12, 2001).
3. Anon, *Plast. News*, **12**(17) (June 26, 2000).
4. Challa, G., *Makromol. Chem.*, **38**, 138 (1960).

5. Grichl, W. and Schnock, G., *Faserforsch. Textiltechn.*, **8**, 408 (1957).
6. Lenz, R. W., *Organic Chemistry of Synthetic High Polymers*, Wiley-Interscience, New York, 1967, p. 87.
7. Yoda, K., Kimoto, K. and Toda, T., *J. Chem. Soc. Jpn.*, **67**, 907 (1964).
8. Malik, A. and Most, E. E., *US Patent 4 078 143*, 1978.
9. US Code, 21CFR1771630
10. USFDA *Premarket Notifications for Food Contact Substances*, United States Food and Drug Administration, Washington, DC, June 6, 2000.
11. US Code, 21CFR1771637
12. Lenz, R. W., *Organic Chemistry of Synthetic High Polymers*, Wiley-Interscience, New York, 1967, p. 83.
13. Website: [www.danka.com/supplies/dk 6000.html].
14. Anon, *Discover*, **13**(10), 42 (October, 1992).
15. Anon, *Automotive Ind.*, **172**, 9 (September, 1992).
16. Anon, *Chem. Eng. News*, **72**, 9 (April, 1994).
17. Seidel, S. and Salsman, R., presentation given at the *Society of Plastic Engineers Annual Recycling Conference*, Chicago, IL, 15–17 October, 1999.
18. Salsman, R. K., *US Patent 5 726 277*, 1998.
19. Everhart, W. D., Makar, K. M. and Rudolph, R. G., *US Patent 5 866 622*, 1999.
20. Yoo, D. I., Park, K. H., Kim, B. H., Shin, Y. S. and Kim, J. H., presentation given at the *4th Asian Textile Conference*, Taipei, Taiwan, 24–26 June, 1997.
21. Ostrowski, H. S., *US Patent 3 884 850*, 1975.
22. Toshihiro, M., Matsui, H. and Nagahara, M., *Jpn Patent 58 059 214 A2*, 1983.
23. Harvie, J. L., *US Patent 5 750 776*, 1998.
24. Jackson, W. J. and Kuhfuss, H. F., *US Patent 4 259 478*, 1981.
25. Ekart, M. P. and Pell, Jr, T. M., *US Patent 5 635 584*, 1997.
26. Oakley, E. O., Gorman, F. J. and Mason, J. D., *US Patent 5 236 959*, 1993.
27. Burkett, E. J. and Jenks, R. S., *US Patent 5 223 544*, 1993.
28. (a) West, S. M., *US Patent 5 504 121*, 1996; (b) West, S. M., *US Patent 5 602 187*, 1997.
29. Anon, *Chem. Eng.*, **17** (March, 2001).
30. Reck, W., *US Patent 5 948 828*, 1999.
31. Miyamoto, A., Shimizu, S., Okamura, M., Tanizake, H. and Yamamoto, K., *Jpn Patent 59 096 125 A2*, 1984.
32. Takiyama, E. and Yanagida, H., *Jpn Patent 8 151 438 A2*, 1996.
33. Yoshimura, S. and Tokutomi, K., *Jpn Patent 11 181 263 A2*, 1999.
34. Currie, R. M., Measamer, S. G. and Miller, D. N., *US Patent 3 907 868*, 1975.
35. Delattre, J., Raynaud, R. and Thomas, C., *US Patent 4 163 860*, 1979.
36. Yokoi, N., Tagami, K. and Habara, T., *Jpn Patent 53 071 035 A2*, 1978.

37. Naujokas, A. A. and Ryan, K. M., *US Patent 5 051 528*, 1991.
38. Gamble, W. J., Naujokas, A. A. and DeBruin, B. R., *US Patent 5 298 530*, 1994.
39. (a) Toot, W. E. and DeBruin, B. R., *US Patent 5 414 022*, 1995; (b) DeBruin, B. R., Naujokas, A. A. and Gamble, W. J., *US Patent 5 432 203*, 1995.
40. Gallagher, F. G., *US Patent 5 532 404*, 1996.
41. Hepner, R. R., Michel, R. E. and Trotter, R. E., *US Patent 5 391 263* 1995.
42. Hall, S. D., Hepner, R. R., Michel, R. E., Wheatcraft, Jr, D. R. and Williamson, G. M., *US Patent 5 912 275*, 1999.
43. Heise, W. H., Folk, D. P., Yau, C. C. and Sink, C. W., *US Patent 5 498 749*, 1996.
44. Smith, B. L. and Wilkins, G. E., *US Patent 5 744 503*, 1998.
45. Toot, W. E., Simpson, B. L., DeBruin, B. R., Naujokas, A. A. and Gamble, W. J., *US Patent 5 578 173*, 1996.
46. US Code, 21CFR177.1630, *USFDA Premarket Notifications for Food Contact Substances*, United States Food and Drug Administration, Washington, DC, October 5, 2000.
47. USFDA 'No objection letters' United States Food and Drugs Agency, Washington, DC.
48. Ekart, M. P., Pell, T. M., Cornell, D. D. and Shackelford, D. B., *US Patent 6 136 869*, 2000.
49. Ekart, M. P., Pell, T. M., Cornell, D. D. and Shackelford, D. B., *US Patent 6 191 177*, 2001.
50. Ekart, M. P., Pell, T. M., Cornell, D. D. and Shackelford, D. B., *World Patent (WO) 9 920 684 A1*, 1999.
51. Anon, *Chem. Market. Rep.*, **256**(2) (July 12, 1999).
52. Eastman Chemical Company, MBC-231, *Optisys Polyester Recycling Technology*, Eastman Chemical Company, Kingsport, TN, 1999.
53. Schoengen, A., Schreiber, G., Schroeder, H., *US Patent 4 302 595*, 1981.
54. Pusztaszeri, S. F., *US Patent 4 355 175*, 1982.
55. Doerr, M. L., *US Patent 4 620 032*, 1986.
56. Rosen, B. I., *US Patent 5 095 145*, 1992.
57. Tindall, G. W. and Perry, R. L., *US Patent 5 045 122*, 1991.
58. (a) Schwartz, J. A., *US Patent 5 580 905*, 1996; (b) Schwartz, J. A. and King, R. P., *US Patent 5 958 957*, 1999; (c) Schwartz, J. A. and King, R. P., *US Patent 6 197 838*, 2001.
59. Website: [petcore.com/recycfr.htm].
60. West, S. M., *US Patent 5 504 121*, 1996.
61. Broeker, J. L., Macek, J. A., Mossman, A. B., Rosen, R. I. and Bartos, T. M., *US Patent 5 414 113*, 1995.
62. Tustin, G. C., Pell, T. M., Jenkins, D. A. and Jernigan, M. T., *US Patent 5 413 681*, 1995.

63. Johnson, F., Sikkenga, D. L., Danawala, K. and Rosen, B. I., *US Patent 5 473 102*, 1995.
64. Lamparter, R. A., Barna, B. A. and Johnsrud, D. R., *US Patent 4 542 239*, 1985.
65. Hamada, S., Umeda, A., Iida, H. and Matsuki, T., *Jpn Patent 62 225 526 A2*, 1987.
66. Sato, K. and Sumitani, K., *Jpn Patent 196 578 A2*, 1995.
67. Naujokas, A. A., *Jpn Patent 10 218 983 A2*, 1998.
68. Green, D. (Ed.), *Perry's Chemical Engineers' Handbook*, 6th Edn, McGraw-Hill, New York, 1984, Sect. 25, p. 65.
69. Anon, *Chem. Week*, **157**(11), 18 (September 27, 1995).

Controlled Degradation Polyesters

F. G. GALLAGHER

DuPont Experimental Station, Wilmington, DE, USA

1 INTRODUCTION

Concerns around the environmental fate of polymers have led to increased research into the area of controlled degradation polyesters. At the present time, companies are offering many solutions to reduce the impact of polyesters in the environment. Each strategy has its supporters and critics. Techniques to compare the environmental benefit versus production cost and customer value are qualitative and also are debated, thus making it difficult to predict which solution will gain acceptance by government agencies and society. Instead of providing case studies of specific products for specific applications, this chapter presents a more holistic view of the science associated with degradable polyesters and related technologies. The reader is encouraged to contact specific producers to obtain current technical information on product offerings, application performance and degradation behavior. As environmental rules and regulations vary broadly across regions and countries in response to local socio-economic conditions, the reader is also encouraged to contact appropriate government resources in the area of interest to understand the current public view of this issue.

2 WHY DEGRADABLE POLYMERS?

Scientists created synthetic polymers to replace natural polymers in order to simplify manufacturing processes, reduce product cost and extend the useful life

of objects. These durable polymers improved the quality of life for many people by making more items affordable to the average consumer. Beginning in the 1940s, the plastic revolution has created a world where many everyday items are made from synthetic polymers.

In the late 1960s, we began to recognize that we live on a small planet with limited resources. The first Earth Day in 1970 kicked off a movement of growing concern about our use and mis-use of our limited resources. Governments and citizens vigorously attacked air and water pollution and made significant progress by establishing strict environmental regulations. As a result of stricter air pollution controls, burning refuse was abandoned to reduce air emissions, hence resulting in increased shipments of municipal solid waste to landfills.

In the mid-to-late 1980s, the US public was told that it had a landfill problem and that if something did not change quickly it would be buried in garbage. The popular press targeted plastic and single-use disposable products as a major cause of the problem. Careful technical review of the situation revealed that the primary cause of the landfill problem was a change in US solid waste regulations that required liners and leachate treatment for all active landfills after a set date. The regulations prompted the systematic closure of many older small landfills that could not economically meet the new standards. Since that time, waste management companies have responded to the need for landfill space by constructing large efficient modern landfills that can economically meet government regulations. The publicity surrounding the landfill debate has renewed society's interest in resource conservation and recycling efforts.

Initially, source reduction was encouraged to reduce the amount of material being directed to the landfill. Consumer product packaging was at the top of the list. Re-use and alternate-use initiatives challenged society to separate municipal solid waste at home for re-use or alternate-use applications. Plastic, aluminum, steel, glass, newspaper and cardboard have been systematically collected by many local communities to reduce landfill volume and extract value as recycled products. This community interest in recycling prompted the redesign of products to be 'recycling-friendly'. Rigid containers were easily identified as recyclable since a quick water rinse yielded a relatively clean, relatively pure polymer. An example is the redesign of soda bottles to eliminate the polyolefin bottom cup, thus resulting in an 'all-polyester' bottle.

However, some products could not be made recycling-friendly. Packaging films are not easily cleaned and multiple-layered products containing aluminum foils are not easily separated into relatively pure components. Other composite structures containing natural fiber products such as absorbent pads for packaged meat, diapers or personal hygiene products are not easily cleaned or separated. Municipal aerobic composting and anaerobic degradation in controlled digesters or landfills to produce methane as an energy source with eventual recovery of soil and humus were offered as solutions for these non-recyclable articles [1]. For these options to work, the synthetic polymer components were required to degrade

at a rate comparable to natural products such as lignin and cellulose. Polymer scientists were challenged to look at degradation differently and to learn how to adjust synthetic polymer degradation to match application requirements.

In order to control polyester degradation, we must understand the processes involved in how polyesters degrade. The following section presents a brief summary of degradation mechanisms that are involved.

3 POLYMER DEGRADATION

Efforts to prevent polyester degradation began the day after the first synthetic polyester was created. Polyester is one of the most diversely used synthetic polymers today because of the significant progress in halting polymer degradation during production, fabrication and use. Although degradation results from a combination of environmental factors, scientists organize degradation into a few general mechanisms, as listed below. This topic has been investigated extensively and there are many tests on the subject [2–4]. The reader is encouraged to refer to these more complete sources for details on polymer degradation mechanisms.

- Thermal degradation and heat resistance.
- Oxidative degradation – reactions with oxygen.
- Moisture sensitivity – reactions with water.
- Radiation initiated or photodegradation – free radical reactions (see Chapter 18 on photodegradation and photostabilization of poly(ethylene terephthalate)).
- Biological degradation – enzymatic catalyzed reactions [5].
- Chemical degradation – reaction with, or initiated by, specific chemicals.
- Weathering/Aging – the combined effect of cyclic exposure to varying moisture, temperature and sun exposure, or specific cyclic application conditions such as ‘under the hood’ grease, oil and temperature variations.
- Stress-induced degradation – reactions that are catalyzed by subjecting the article to mechanical stress.

The next step in developing controlled degradation polyester is to understand expectations for specific product applications. Some questions to be answered include the following:

- What are the physical property requirements for the application?
- What is the desired degradation rate?
- Are there preferred degradation products, e.g. methane, compost/humus or CO₂?
- Which degradation initiators are present in the application that may trigger degradation at the desired time?

Individual assessment of specific application factors indicate the key factors for selecting a specific polymer.

4 DEGRADABLE POLYESTER APPLICATIONS

Patents issued over the past ten years enumerate potential applications for degradable polyesters touching a broad range of everyday items. Figure 17.1 presents the applications in general groupings and the primary degradation products (methane, carbondioxide and humus). In general, degradable polymer applications address at least one of the following concerns:

- Degradation product provides benefit for application
- Reduces labor/energy required to manage solids
- Eliminates problems associated with persistent polymers

4.1 MEDICAL

Medical applications range from drug delivery to wound closure (sutures, clips, staples and surgical meshes) to aid the healing process [6]. Medisorb[®], the Alkermes' family of high-quality homo- and copolymers of glycolic (hydroxyacetic acid) and lactic acid, was approved by the United States Food and Drugs Administration (USFDA) in the early 1970s as a synthetic bioresorbable polymer. Poly (lactide-co-glycolide) has been used extensively in a variety of medical applications [7–9]. In the body, the degradation products of these aliphatic copolyesters are lactic acid and hydroxyacetic acid.

More recently, polyesters with beneficial degradation products (salicylic acid) have been produced to promote healing through enhanced regeneration of tissue [10]. Degradation mechanisms relevant to medical applications include

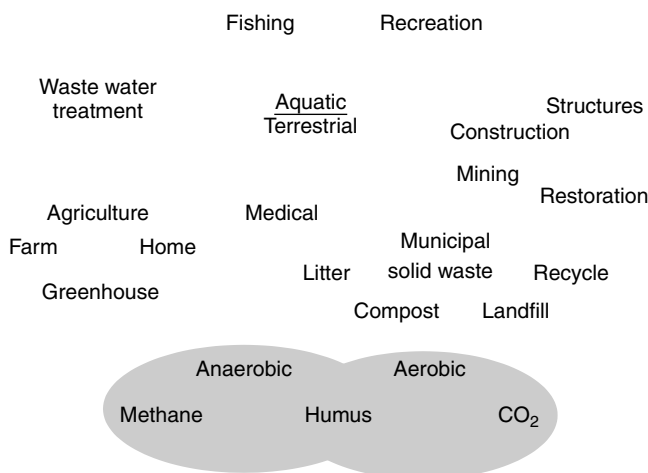


Figure 17.1 Application areas for degradable polyesters

temperature, moisture, oxygen, varying pH and microbial activity. In general, the medical applications have such a high value in use that achieving desired benefit dominates other concerns.

4.2 AQUATIC

Proposed aquaculture applications of degradable polymers include seaweed culture nets, fishing nets and lines, and temporary structures used for restoration of wet lands, beaches or other marsh areas [11–14]. Weathering and hydrolysis are the most common degradation mechanisms encountered in aquatic applications. Continually submerged articles pose special challenges since temperatures are low and photodegradation and oxidation effects are limited.

4.3 TERRESTRIAL

Agriculture products have been an active application area for degradable polyesters. Degradable polyesters are used to avoid litter problems caused by persistent plastic products and to provide beneficial degradation products (humus) to the soil. Examples include nets for crop packaging, products for ripening crops, weed barriers, crop row covers and irrigation pipes [15]. Applications have also been suggested for greenhouse or home use such as plant pots, plant root covers, peat moss substitutes and various hydroponics products [16].

The construction and mining industries offer additional applications for temporary structures, such as concrete forms and geo-textiles, as well as a wide variety of products for restoration of land including sand bags, turf covers and temporary protection for trees and plants.

As in aquatic applications, weathering and hydrolysis are the dominant degradation mechanisms for terrestrial applications. Polymer articles covered with dirt can be problematic since photodegradation is not available; however, the higher humidity levels and microbial activity in the soil when compared to the atmosphere are advantageous for degradation.

4.4 SOLID WASTE

The disposition of products after intended use, i.e. solid waste, provides the largest volume of applications for disposable polymers. Solid waste applications cited include a wide range of products. General household items for which degradable polyesters would be appropriate include crockery, cutlery, clothes hangers, toys, cigarette filters, molded articles, woven and non-woven fabrics, appliance cases, and cleaning, painting and wallpaper brushes. Generic structures are also cited such as films, sheets, fibers, filaments, injected molded parts, rigid containers

and wraps (shrink, food, pallet, crate and consumer packaging). Sanitary and health products cited include gloves, syringes, waterproof bed sheets, cushion covers, protective clothing, handkerchiefs, wipes, yarn for dental floss, comfort cushioning, absorbent articles, nappies, sanitary towels, pantliners, bandages, wound dressings, wound cleaning pads, surgical gowns, bedding items, sheets, pillowcases, foam pads and various hygiene bristles.

The four disposal options generally cited for intentional waste products are recycle, landfill, wastewater treatment facilities and composting. Unintentional solid waste is generally referred to as 'litter'.

4.4.1 Recycling

For recycling uses, degradable polyesters are desirable for relatively small mass applications, such as glues, thin coatings or labels, in order to facilitate the rapid cleaning of the primary structure for recycling. These applications may be rigid structures such as plastic containers or modifiers for paper products.

4.4.2 Landfills

As described earlier, concerns around water and air pollution have transformed landfill technology. Figure 17.4 is an illustration of a modern lined landfill with a gas recovery system, leachate collection and treatment, a cap to prevent rain water entry, and ground water monitoring to confirm the integrity of the liner. The composition of landfills have been characterized by various garbologists and

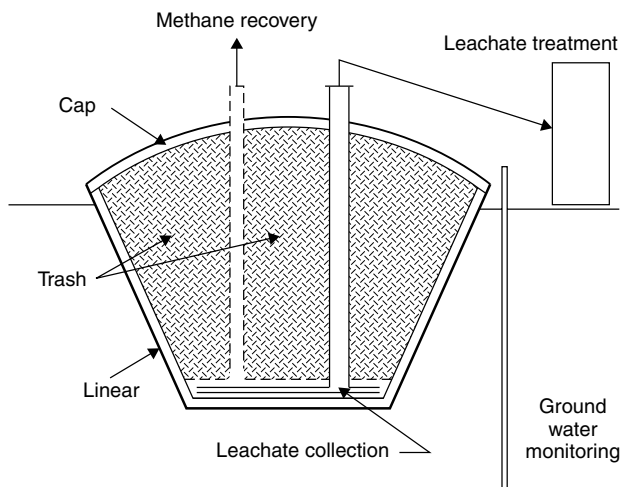


Figure 17.4 Schematic illustration of a modern lined landfill site showing the major components

varies broadly from region to region depending on local industry and the effectiveness of recycling efforts for glass, metals and plastics [17]. In general, most landfills are composed of primarily paper, cardboard, other packaging materials and 'yard-waste'.

Anaerobic microbes in the presence of water in the landfill will consume these natural products and produce methane, CO_2 and humus. One study reported the average composition of 20 year old refuse to be 33 % paper, 22 % ash and 12 % wood [18]. Thirty core samples revealed a wide range of degradation and microbial activity that were directly attributed to sample moisture content. Recovered polyethylene degradation was evaluated and determined to be as high as 54 %.

Typical landfill gas contains 50 % methane and 45 % CO_2 , with the balance composed of water and trace compounds. This landfill gas is gaining popularity as an alternative energy source. The United States Environmental Protection Agency (EPA) has a 'Landfill Methane Outreach Program' to encourage the use of landfill gas as an energy source. A visit to their web site provides facts on the benefits of using landfill gas as well as case studies of successful projects. To complement the landfill gas production, degradable polyesters need to be consumed by anaerobic microbes to produce methane at rates comparable to those generated by natural products degradation, i.e. lignin and cellulose in paper and yard-waste.

4.4.3 Wastewater Treatment Facilities

Various sanitary products such as diapers (nappies), sanitary towels, colostomy bags, pantliners and other absorbant products have been proposed for possible flushable disposal. In addition, wash water from recycling activities must be treated in wastewater facilities. A rapidly degradable or soluble polymer that will not restrict sewer systems and will degrade in the wastewater treatment facility's aerobic and anaerobic digesters is needed for these applications. The degradation byproducts from treatment are CO_2 from aerobic digestion, methane and CO_2 for anaerobic digestion and sludge (microbial solids, humus and precipitated solids).

4.4.4 Composting

Some communities have chosen municipal composting as alternative solid disposal strategies for cardboard, paper products, mixed municipal solid waste, sewage sludge, and especially, yard-waste. The technology is flexible and ranges from simple windrow piles on concrete slabs to trench composting in a building equipped with odor abatement capabilities [19–21]. The degradation mechanism is primarily hydrolysis combined with aerobic and anaerobic microbial activity.

In aerobic composting, an air blower distributes air under the pile and maintains most of the pile in aerobic conditions for faster degradation. The piles are turned daily to redistribute material and moisture and to maintain porosity of the pile. The mechanical stress imposed by turning the compost piles facilitates

the initial physical disintegration of objects to a primary dimension of about 1 in. Following a typical 21–28 day active aeration cycle, the resulting compost is held for a 3–6 month curing period prior to use. The degradation products of aerobic composting are compost and CO_2 . Anaerobic composting using thermophilic microbes to produce methane and compost has been demonstrated and is gaining support as an alternative to landfills since methane production may be faster and more predictable and methane capture is more efficient [22, 23].

Compost is added to soil to increase organic content and improve quality [24]. The organic compounds that make up compost occur naturally through the degradation of plants and animals in combination with microbial activity. The result is a complex mixture of degradation intermediates and microbial byproducts such as gums and starches. Environmental soil scientists separate the organic soil components into non-humic and humic substances [25]. The non-humic substances are relatively low-molecular-weight compounds such as fats, oils, proteins, peptides and carbohydrates. These compounds are easily consumed by microorganisms and do not persist in the soil. In general, the non-humic substances are consumed rapidly during the active stage of composting when microbial activity is high and mechanical stresses are present. The curing stage of composting continues the degradation of non-humic substances to achieve a stable compound with low levels of non-humic substances.

The dominant organic compounds in soil are humic substances, collectively referred to as humus. The latter results from the degradation of lignin, carbohydrate and proteins. Through complex microbial chemistry, lignoprotein compounds are formed. Structure analysis of humus in soil has identified hundreds of compounds [26]. These consist of around 45–60 % aliphatic carbon and 20–45 % aromatic carbon with 10–15 % of the carbon as carboxylic acid [25]. Carbon-13 studies reveal that the humus in soil can be hundreds or thousands of years old [27, 28]. Humus is typically dark brown or black, porous, friable, and spongy (not soggy) when wet. Humus is beneficial to the soil for a variety of reasons. The dark color improves springtime warming of the soil. The physical structure keeps the soil light and fluffy, which improves air penetration into the soil and root growth. The complex chemistry creates a colloidal system that provides a chelating functionality to control pH, retain necessary minerals such as Ca, Mg and K, and trap heavy metal toxins to limit availability to the plants.

4.4.5 Litter

The persistence of polymers in the environments is useful for long term durability of structures such as buildings, vehicles, docks, boats and navigation aids. Unfortunately, when the polymers are unintentional byproducts of recreational or commercial activities, collateral wildlife loss may result from entanglement in packaging materials, lost nets, lines and ropes. These wildlife losses due to litter have received significant public visibility. The critical degradation to address this



Figure 17.5 Two birds await the return of their parents in a nest partially constructed with strips of plastic film litter. Photograph reproduced by permission of F. Glenn Gallagher

public concern is degradation of structure. Once an article has been reduced in length to about 1 in or less, the collateral wildlife loss due to entanglement is significantly reduced. In Figure 17.5, two birds await the return of their parents in a nest partially constructed with strips of plastic film. This picture is an illustration of how adaptable wildlife is to available material, provided that the structure is similar to natural products.

5 SELECTING A POLYMER FOR AN APPLICATION

5.1 UNDERSTAND APPLICATION REQUIREMENT FOR A SPECIFIC LOCATION

Selection of the appropriate polymer(s) or structure for a specific application begins with an understanding of the functional requirements for the application.

What functionality is needed – strength, structure, protective coating, barrier to moisture, oxygen or CO₂, sterility, or acceptable for food contacts?

For degradable polymers, the next step is to determine when and how the polymer needs to degrade. Are there preferred degradation products? Does degradation need to be fast or slow? What environmental factors may contribute to the degradation rate – moisture, sunlight, microbes, mechanical stresses, or cyclic weathering?

As a way of illustrating this issue, consider packaging material for medical supplies to remote areas at elevations above the tree line. The first consideration is the structural and mechanical properties necessary to properly protect the medical supplies during transit to the remote area. This might be achieved with a rigid foamed polymer and some packaging tape or it might be a corrugated cardboard box covered with stretch-wrapped film and containing air-filled plastic bags for impact resistance. The packaging weight will probably be a concern with lower weights preferred provided that all of the other packaging performance criteria are met.

Once the supplies arrive and the packaging is no longer needed, how might the recipients use the packaging material? Direct re-use, as a container for storing items may be useful at first. Since they are above the tree line where fuel is scarce, burning the packaging material as fuel may be desirable. In some high-altitude locations, anaerobic manure/vegetation digesters are used to produce methane for cooking fuel [19]. In these locations, adding degradable packaging material to the anaerobic digesters may be desirable, especially if the packaging material contains compounds that would improve the performance of the digester by providing more consistent higher-quality methane.

Recreational fishing line provides another view of these issues. To be acceptable as a fishing line, the strength of the line cannot deteriorate significantly during a fishing season. A 5 lb line should hold 5 lb in the spring as well as in the fall. Many durable polyesters and polyamides meet these performance expectations. However, if the line were tangled with submerged objects and then breaks, it would be desirable for the line to degrade to avoid harming wildlife or becoming a navigation hazard. In this situation, disintegration of the structure is the primary degradation target. The line is submerged and so UV- and oxygen-induced degradation might be limited. Stress-induced degradation might be involved, especially if the line is located in an area where ice forms in the winter. Biological activity might occur, especially if the line encourages microbial or algae attachment and growth. Another strategy might be to use an inherently unstable polymer that is protected with a stabilizer, such as an antioxidant, which is rapidly degraded or extracted from the polymer when the line is submerged in water for prolonged periods. When the stabilizer protection is lost, the polymer degrades and the line disintegrates.

5.2 DEGRADATION TESTING PROTOCOL INCLUDING GOAL DEGRADATION PRODUCT

Once the application performance and degradation requirements are understood, the next step is to review available information or conduct tests to screen product options to determine the most likely products that will meet application expectations. Weathering, aging and durability testing of polymers have been used extensively for years to qualify durable polymers for specific applications. Since the mid 1980s, new standard tests have been developed for degradable polymers [2].

One group of ASTM tests addresses physical property deterioration in various environments including marine floating conditions (D5437), simulated composting (D5509 and D5512), simulated landfill (D5525) and aerobic microbial activity (D5247). A second group of ASTM tests addresses CO₂ generation in aerobic sewage sludge (D5209), aerobic activated sewage sludge (D5271) and aerobic controlled composting (D5338). A third group of ASTM tests addresses CH₄/CO₂ evolution in anaerobic environments such as anaerobic sewage sludge (D5210), anaerobic biodegradation (D5511) and accelerated landfill (D5526).

With the growing public interest in product stewardship and global warming from CO₂ and fugitive methane emissions from landfills, sequestering degradable polymers in humus is anticipated to gain support and new test methods will be needed [29]. Tests to evaluate the generation and quality of humic substances in landfills, composting or terrestrial or aquatic environments are beginning to appear. Aerobic composting with activated vermiculite provides the opportunity to recover the polymeric residues, hence allowing more complete carbon balances as well as assessments of toxic compound generation and humus quality [30–32]. This work needs to be extended to anaerobic composting to simulate landfills as well as closed systems where methane losses are reduced.

5.3 LESSONS FROM NATURAL PRODUCTS

Now that the application requirements for performance and degradation are understood, the next step is to select specific polymers and fabrication strategies. Some key insights may be gained by looking at natural products with performance similar to what is needed.

Early polymer scientists examined natural polymers to gain insight into the complex chemistry that might be possible. Advances in analytical chemistry over the past 70 years have allowed detailed characterization of the chemistry of life and have provided us with an opportunity to easily revisit these early polymer discovery days and rediscover key polymer lessons from natural polymers.

First lesson – mixtures and complex chemistry involving different chemical groups can provide unique solutions to complex problems. Examination of the

compounds present in a metabolic pathway diagram reveals extensive use of $-\text{OH}$, $-\text{COOH}$, $-\text{NH}_2$, $-\text{C}=\text{O}$, $=\text{NH}$ and ether groups [33]. Aliphatic structures dominate but aromatic rings are present in phenylalanine, tryptophan, 3-hydroxyanthranilate, homogenitise, catechol and tyrosine (see Figure 17.6 for structures). Microbes have evolved to produce a wide range of enzymes that degrade or convert complex structures. Ester bonds are used extensively in the biological world. Many plants and animals make triglycerides, the triesters of glycerol and fatty acids, to control acidity and store useful materials for future use. Microbes produce hydroxy acid esters such as polyhydroxybutyrate as a convenient storage form for future food. Aliphatic esters are often used for temporary storage as their bonds are easily hydrolyzed when needed. Aromatic structures are used to create more resilient materials.

Second lesson – subtle changes in molecular arrangement can have significant changes in physical properties. The first-year biochemistry student learns that in addition to the chemical bonds used to create a structure, the molecular arrangement can have significant impact on physical properties and susceptibility to degradation [34]. Polysaccharide chemistry demonstrates this idea well. Although all polysaccharides are constructed from repeating sugar monomers of

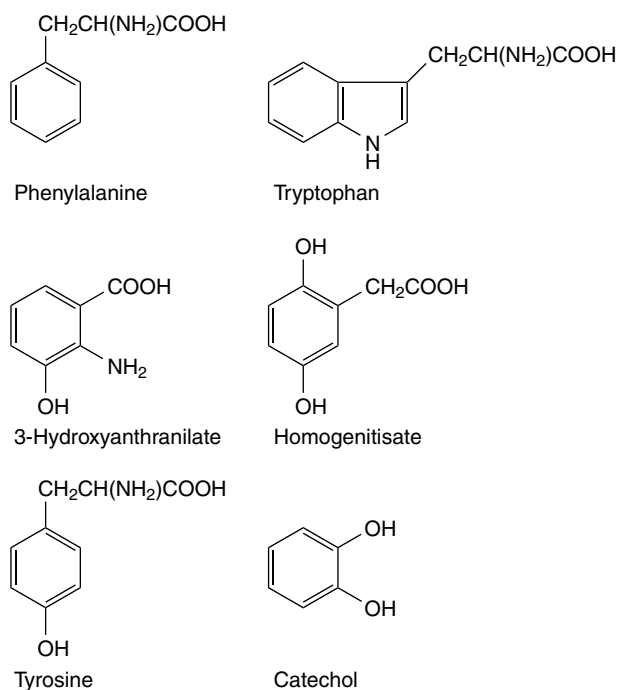


Figure 17.6 Examples of aromatic compounds found in some metabolic pathways

nominally the same chemical formula, linkage positions, branch points and chiral centers can significantly change the physical arrangement of molecules and the properties. When glucose undergoes cyclization, the presence of chiral centers creates two possible spatial arrangements, labeled 'alpha' and 'beta'. Starch is polymeric α -glucose that exist in two forms, i.e. amylose, with a linear repeating α 1–4 linkage, and amylopectin, with a linear α 1–4 linkage combined with some branched sugars containing α 1–6 branches. Dextran, another family of polysaccharides with different properties, is also composed of α -glucose; however, α 1–6 linkages predominate in this case with branch points at 1–2, 1–3 or 1–4 linkages. Cellulose is similar to starch; however, β -glucose is used in a β 1–4 linkage. The resulting polymer is most stable in a fully extended conformation.

Third lesson – substituting pendant groups change functionality. The addition of a pendant group, $-\text{NHCOCH}_3$, to replace an $-\text{OH}$ group on cellulose forms chitin and changes the hydrogen-bonding between polymer chains significantly, hence changing the strength and solubility of the polymer. The conversion of the $-\text{CH}_2\text{OH}$ group on cellulose to $-\text{COO}^-$ creates alginate, a polymeric ionomer that binds metal ions to form semi-rigid structures.

Fourth lesson – combination of different compounds in unique macrostructure provides unique performance properties. Starch is used extensively in nature to store carbon and energy. Starch is readily digested and must be protected from degradation by a resistant coating, for example, a seed (e.g. corn, wheat or rice) or a skin (e.g. potato). Woody materials such as trees, soft plants and grasses are composed of a complex combination of aliphatic and aromatic compounds (cellulose, hemicellulose and lignin).

How might these four lessons from natural products be applied to synthetic polymers to achieve performance and degradation?

6 DEGRADABLE POLYESTERS

As described previously, ester bonds and polyesters are used extensively in nature for temporary storage of carbon. The relative ease of making and breaking ester bonds makes them an ideal choice for degradable polymer backbones.

6.1 AROMATIC POLYESTERS

Poly(ethylene terephthalate) (PET) is by far the highest-volume polyester produced. PET has been used in many applications from films to fibers to rigid containers, and in numerous engineering-polymer applications. Studies on the durability of PET in geotextile applications have estimated the expected life to complete mechanical failure to be 25–50 years, depending on specific soil conditions [35]. Other studies on phthalic esters in batch anaerobic digestion of sludge report rapid degradation of diethylphthalates [36].

These results suggest that pure aromatic polyesters may function like the long-lived components in humus and may provide useful properties as a soil additive. Grass sod growing studies using municipal-waste-derived compost in combination with chopped plastic fibers demonstrated improved growing rate and root structure development to accelerate sod production.

6.2 ALIPHATIC POLYESTERS

Some aliphatic polyesters such as polyhydroxyalkanoates (PHAs), homo- and copolymers of hydroxybutyric acid and hydroxyvaleric acid, have been demonstrated to be readily biodegradable, are produced by some microbes and can accumulate intracellularly during some growth conditions [37–39]. ICI and then Monsanto offered PHA-based Biopol[®] degradable polyester at one time. Other aliphatic polyesters based on homo- and/or copolymers of lactic acid and glycolic acid have also been produced, e.g. Medisorb[®], originally from DuPont and now from Alkermes, and more recently, NatureWorks[®] (poly(lactic acid)) by Cargill Dow Polymers. The aliphatic polyesters function like starch or cellulose to produce non-humic substances such as CO₂ and methane. Applications with short usage and high mineralization rate requirements would favor the aliphatic polyesters.

6.3 COPOLYESTERS OF TEREPHTHALATE TO CONTROL DEGRADATION

There is a significant gap of degradation rates and performance properties between the aliphatic and aromatic polyesters. However, taking some hints from nature can fill this gap. Mixtures of polyesters, molecular orientation, substitution of some functional groups, and macro structures have all been proposed as a means to provide a range of application performance properties versus degradation rates.

Copolyesters of aliphatic and aromatic dicarboxylic acids have been studied as a means to vary performance properties while controlling degradation rates over a broad range from fast degradation, such as PHA and poly(lactic acid) (PLA), to very slow degradation, such as PET [40–44]. Other terephthalate copolyesters have been developed using ether and amide monomers. Others have combined the copolymers of terephthalate with degradation promoters or stabilizers to provide alternate combinations of performance properties versus degradation rates. The BIOMAX[®] hydrobiodegradable polyester, illustrated in Figures 17.2 and 17.3, from DuPont, is actually a family of terephthalate copolyester compositions developed by using combinations of these strategies [45–51].

7 CONCLUSIONS

The landfill crisis of the early 1990s stimulated renewed interest in the environmental fate of plastics and recycling. Rigid poly(ethylene terephthalate) containers emerged as the premier recyclable plastic with a recycle value second only to aluminum. However, there are geographic locations or product forms, such as thin films or composite structures, which make recycling uneconomical. In these situations, degradable polyesters provide an alternate strategy to recover value.

Consumer interest in responsible product stewardship is challenging manufacturers to consider carefully the environmental fate of their products. There is growing government and public support to extract valuable byproducts from degrading materials, such as capturing methane from landfills to reduce global warming and as an alternate energy source, as well as sequestering carbon in landfills or as humic substances. To satisfy this valuable byproduct interest, new degradation test methods are needed to evaluate the impact of degradable polymers on landfill methane production capability, as well as the quality of the resulting humic substances.

Polyesters offer multiple options to meet the complex world of degradable polymers. All polyesters degrade eventually, with hydrolysis being the dominant mechanism. Degradation rates range from weeks for aliphatic polyesters (e.g. polyhydroxyalkanoates) to decades for aromatic polyesters (e.g. PET). Specific local environmental factors such as humidity, pH and temperature significantly influence the rate of degradation.

Copolyesters (such as BIOMAX[®]) which combine aromatic esters with aliphatic esters or other polymer units (e.g. ethers and amides) provide the opportunity to adjust and control the degradation rates. These added degrees of freedom on polymer composition provide the opportunity to rebalance the polymer to more specifically match application performance in physical properties, while still maintaining the ability to adjust the copolyesters to complement the degradation of natural products for the production of methane or humic substances. Since application performance requirements and application specific environmental factors and degradation expectations vary broadly, copolyesters are, and will continue to be, an important class of degradable polyesters.

REFERENCES

1. Spencer, R., *Biocycle*, 30–33 (February 1990).
2. Hamid, S. H., *Handbook of Polymer Degradation*, 2nd Edn, Marcel Dekker, New York, 2000, pp. 473–483.
3. Kelen, T., *Polymer Degradation*, Van Nostrand Reinhold, New York, 1983.
4. Rosato, D. V. and Schwartz, R. T., *Environmental Effects on Polymeric Materials*, Vols I and II, Wiley-Interscience, New York, 1968.

5. Scott, G., *Trends Polym. Sci.*, **5**, 361–368 (1997).
6. Henry, C. M., *Chem. Eng. News*, **78**(38), 49–65 (2000).
7. Ranucci, C. S. and Moghe, P. V., *J. Biomed. Mater. Res.*, **54**, 149–161 (2000).
8. Tracy, M. A., Ward, K. L. and Jaworowicz, W. E., *World Patent WO 2000 072 830*, 2000.
9. Yamaguchi, K. and Anderson, J. M., *J. Controlled Release*, **24**, 81–93 (1993).
10. Uhrich, K. and Macedo, B., *World Patent WO 2001 041 753*, 2001.
11. Hiroshi, Y. and Kenji, C., *Jpn Patent J 11 247 060-A*, 1999.
12. Toyohiko, M., *Jpn Patent J 2 000 045 124-A*, 2000.
13. Fish, R. B., Gallagher, F. G., McKenna, J. M. and Tietz, R. F., *US Patent 5 354 616-A*, 1994.
14. Yoshihiro, S., Kimio, T., Kiyoo, I. and Tetsuya, I., *Jpn Patent JP 2 000 129 646-A*, 2000.
15. Kimiyuki, M., Takashi, G. and Tadashi, K., *Jpn Patent JP 10 052 870-A*, 1998.
16. Tomoji, M., Masahiro, K. and Toshio, S., *Jpn Patent JP 11 089 445-A*, 1999.
17. Anon, *Kids Discover*, **6**(4) (April 1996).
18. Kinman, R. N., Nutini, D. L. and Rathje, W., Analysis of 20 year-old refuse from the Mallard North landfill in Chicago, Illinois, presentation given at the *44th Annual Purdue Industrial Waste Conference*, Purdue, Indianapolis, IN, 9 May, 1989.
19. Rodale, J. I., *The Complete Book of Composting*, Rodale Books Emmaus, PA, 1970.
20. *Compost Facility Planning Guide for Municipal Solid Waste*, No 1, The Solid Waste Composting Council, Washington, DC, 1991.
21. *Manual for Composting Sewage Sludge by the Beltsville Aerated-Pile Method*, EPA-600/8-80-022, National Technical Information Service, Springfield, VA, 1980.
22. Jewell, W. J., Cummings, R. J., Richards, B. K. and Rector, D. J., *Energy Biomass Waste*, **9**, 669–693 (1985).
23. Han, U. J., Kabrick, R. M. and Jewell, W. J., Presentation given at the *40th Annual Purdue Industrial Waste Conference*, Purdue, Indianapolis, IN, 1985.
24. Gershuny, G., *Start with the Soil*, Rodale Press, Emmaus, PA, 1993.
25. Tan, K. H., *Environmental Soil Science*, Marcel Dekker, New York, 2000.
26. Choudhry, G. G., *Humic Substances*, Gordon & Breach Science Publishers, New York, 1984.
27. MacCarthy, P., Clapp C. E., Malcolm, R. L. and Bloom, P. R., *Humic Substances in Soil and Crop Sciences: Selected Readings*, American Society of Agronomy, Madison, WI, 1990.

28. Allard, B., *Humic Substances in Aquatic and Terrestrial Environment*, Springer-Verlag, New York, 1989.
29. Gerngross, T. U. and Slater, S. C., *Sci. Am.*, **238**(2), 37–41 (August, 2000).
30. Bellia, G., Tosin, M., Floridi, G. and Degli-Innocenti, F., *Polym. Degrad. Stabil.*, **66**, 65–79 (1999).
31. Bellia, G., Tosin, M. and Degli-Innocenti, F., *Polym. Degrad. Stabil.*, **69**, 113–120 (2000).
32. Degli-Innocenti, F., Bellia, G., Tosin, M., Kapanen, A. and Itavaara, M., *Polym. Degrad. Stabil.*, **73**, 101–106 (2001).
33. *Metabolic Pathways Chart*, Product No. M3907, Sigma[®] Chemical Company St Louis, MO.
34. Garrett, R. H. and Grisham, C. M., *Biochemistry*, 2nd Edn, Harcourt Brace College, New York, 1999.
35. Mohammadian, M., Allen, N. S. and Edge, M., *Textile Res. J.*, **61**, 690–696 (1991).
36. Ziogou, K., Kirk, P. and Lester, J., *Water Res.*, **23**, 743–748 (1989).
37. Jendrossek, D., *Polym. Degrad. Stabil.*, **59**, 317–325 (1998).
38. Anderson, A. J. and Dawes, E. A., *Microbiol. Rev.*, **54**, 450–472 (1990).
39. Cooke, T. F., *J. Polym. Eng.*, **9**, 171–211 (1990).
40. Witt, U., Muller, R.-J. and Deckwer, W.-D., *J. Environ. Polym. Degrad.*, **3**, 215–223 (1995).
41. Witt, U., Einig, T., Yamamoto, M., Kleeberg, I., Deckwer, W.-D. and Muller, R.-J., *Chemosphere*, **44**, 289–299 (2001).
42. Kleeberg, I., Hetz, C., Kroppenstedt, R., Muller, R.-J. and Deckwer, W.-D., *Appl. Environ. Microbiol.*, **64**, 1731–1735 (1998).
43. Ki, H. C. and Park, O. O., *Polymer*, **42**, 1849–1861 (2001).
44. Muller, R., Kleeberg, I. and Deckwer, W.-D., *J. Biotechnol.*, **86**, 87–95 (2001).
45. Tietz, R. F., *US Patent 5 053 482*, 1991.
46. Gallagher, F. G., Hamilton, C. J. and Tietz, R. F., *US Patent 5 097 004*, 1992.
47. Tietz, R. F., *US Patent 5 097 005*, 1992.
48. Gallagher, F. G., Hamilton, C. J., Hansen, S. M., Shin, H. and Tietz, R. F., *US Patent 5 171 308*, 1992.
49. Gallagher, F. G., Hamilton, C. J., Hansen, S. M., Shin, H. and Tietz, R. F., *US Patent 5 171 309*, 1992.
50. Gallagher, F. G., Shin, H. and Tietz, R. F., *US Patent 5 219 646*, 1993.
51. Romesser, J. A., Shin, H. and Tietz, R. F., *US Patent 5 295 985*, 1994.

Photodegradation of Poly(Ethylene Terephthalate) and Poly(Ethylene/1,4- Cyclohexylenedimethylene Terephthalate)

D. R. FAGERBURG

Northeast State Technical Community College, Blountville, TN, USA

and

H. CLAUBERG

Kulicke and Soffa Industries, Inc., Willow Grove, PA, USA

1 INTRODUCTION

With the remarkable growth of polymers since about the 1940s, there has been an ever increasing desire to use plastics in many outdoor applications. Among these applications, one can distinguish between those that require crystalline, opaque polymers, such as house siding, automobile panels and lawn furniture, from those that require clear and often colorless polymers, for such items as displays, signs, plastic windows, etc. The former tend to be polyolefins, PVC, ABS or polyurethanes. The requirement for clarity and colorlessness places an extra burden on the polymers for the latter category, since these features must be retained even after extensive outdoor exposure. Polymers used for the latter applications are usually

poly(methyl methacrylate), polycarbonate and, more recently, poly(ethylene-co-1,4-cyclohexylenedimethylene terephthalate)s (PECTs). The 1,4-cyclohexanedi-methanol modification of poly(ethylene terephthalate) (PET) allows it to be more easily formed into the desired shapes and greatly enhances its clarity by reducing the crystallinity of the polymer.

In this chapter, we will examine the performance of PECT copolymer in outdoor applications and how its degradation mechanism relates to the heavily studied, but still not fully understood, degradation mechanisms in PET itself.

Fibers from PET became a commercial reality in the early 1950s. The use of the aromatic terephthalic acid enabled a higher glass transition and higher melting temperature than for an aliphatic diacid and brought both of these properties into a useful range. The aromatic ring is also a strong UV absorber, of course, and so brought with it a chromophore that allowed for UV degradation. Not long after the fiber became commercial, it was quickly recognized that PET, when exposed to UV light, degrades rather rapidly in properties and also develops an intense yellow color. It was therefore unsuitable for long-term use outdoors in most locations around the world unless specifically stabilized against weather-induced degradation. However, predicting the performance of PET, or any other polymer for that matter, in the various parts of the world has proven to be a daunting challenge. To appreciate the magnitude of the problem that one might face, one only need look at the variation of solar radiation levels and other climatic variables across the globe.

2 WEATHER-INDUCED DEGRADATION

2.1 IMPORTANT CLIMATE VARIABLES

If one examines several selected US cities, for example (see Table 18.1), substantial levels of solar radiation are noted for cities even as far north as Seattle, Washington. However, one immediately also notices that the radiation data do not directly correspond to the latitude of the exposure site as one is sometimes used to employing as a good rule of thumb for solar exposure. Rather, these data show that there must be an interplay of other factors not given simply by the latitude of the exposure location, no matter what the exposure angle of the panel in that location. Some of the more important of these factors are usually understood to be the amount of cloud cover in the average day, its variation throughout the year and, in the case of direct radiation, the amount of scattering due to relative humidity of the air mass or particulate pollutants.

In point of fact, when considering the weathering performance of plastic materials, there exists even more interplay between weathering factors than the factors noted above, such as the ambient temperature, temperature of the actual specimens under exposure and the humidity during exposure of the materials. If the

Table 18.1 Solar radiation versus location versus exposure angle^a

Locality	Latitude (°)	Average yearly radiation(kWh/m ² /d)		
		0°	Latitude	90°
Miami, FL	25.80	4.8	5.2	3.0
New Orleans, LA	29.98	4.6	5.0	2.9
San Diego, CA	32.73	5.0	5.7	3.5
Fort. Worth, TX	32.83	4.9	5.4	3.3
Phoenix, AZ	33.43	5.7	6.5	4.0
Louisville, KY	38.18	4.1	4.6	3.0
Boulder, CO	40.02	4.6	5.5	3.8
Salt Lake City, UT	40.77	4.6	5.3	3.5
New York, NY	40.78	4.0	4.6	3.1
Boston, MA	42.37	3.9	4.6	3.2
Carribou, ME	46.87	3.6	4.2	3.2
Fargo, ND	46.90	3.8	4.6	3.4
Seattle, WA	47.45	3.3	3.7	2.6

^a Source: [<http://solstice.crest.org/renewables/solrad/index.html>].

material in question, such as PET, is one capable of being hydrolyzed then one must add to these variables the amount of surface moisture present on, or just in, the surface layers of the material during solar radiation exposure. Additionally, independent of whether the material can be hydrolyzed or not, if it can absorb water, then it is well known that the presence of water will depress the polymer glass transition temperature such that chain motion is now easier than in its absence. This increased chain mobility may then allow for an increased rate of degradation. With these variables, one can begin to get an appreciation for the complexity of the process that we simply call ‘weathering’ or sometimes ‘photodegradation’.

In spite of the complex interplay of photodegradative factors in a particular climate, over the years the weathering community has come to a consensus that there are a few locations worldwide that represent the ‘worst’ conditions one might encounter. A few of these places have essentially become ‘standards’ in the world of weathering of materials. The two most widely accepted in this class as being the harshest possible climates are Miami, Florida, generally south-facing at some exposure angle from 5–45° from the horizontal, and Singapore, generally at 5° from the horizontal and north-facing. Often, the Arizona desert in the area of Phoenix is added as a third ‘worst’ exposure site (usually at an exposure angle of 45° or one corresponding to the latitude) owing to its high solar radiation levels year-around, coupled with generally very high ambient temperatures, especially in the summer months when temperatures in excess of 45°C are routinely experienced for large parts of the day along with cloudless skies.

It should be noted that in spite of the lack of fundamental understanding of the complexities of degradation during weathering exposure, the judgement of worst

weathering sites rests upon evaluation of multitudes of various types of samples over many years. Long-term exposure data for a variety of materials have been collected at these three locations in particular and can give valuable insight into how a particular material might behave under outdoor exposure conditions. It is interesting to note that only one commercial exposure site in Ottawa, Canada, exists to test the effects of cold weather and the associated frost, salt, etc., even though these factors would also be assumed to have very damaging effects for many materials. In particular, freeze-thaw cycles might be expected to place large internal stresses on samples that can absorb moisture which, when enough molecular weight degradation and/or chain branching has occurred, would be expected then to cause cracking.

Although the subject of a 'standard' weathering protocol is not within the scope of this present chapter, we wish to briefly comment that one must never look upon a year's exposure in any of these locations as reflecting a 'standard' in exposure in an absolute sense. It should be intuitively obvious that there is not a 'Florida year', for example, as conditions do vary from year to year. For this reason, one always needs to expose the particular sample material of interest along with some standard material(s) for which the long-term exposure effects are well known, so that one may have a good basis for comparison.

2.2 ARTIFICIAL WEATHERING DEVICES

The variability of exposure in outdoor conditions has long motivated those in the weathering community to use artificial exposure devices to attempt to better standardize exposures of materials and better assess, and even predict, their behavior in an outdoor environment. The lure of potential reproducibility is obvious. In all of these exposure devices, one has a controlled level of radiation from a bright source, such as a xenon arc, for example, and a means of humidity and temperature control. Without lengthy discussion about the various devices available and what their several advantages and shortcomings might be, we merely note that none of these devices has been really successful in translating its results into an actual time that a particular material will provide a certain level of property retention during real outdoor exposure in any particular location in the world. The most probable reason for this is that the various processes and their quantum yields are most likely some function of all of the variables such as the spectral distribution and intensity of the light, humidity and temperature. This function is usually only poorly understood at best. The fact that it is necessarily different for different polymers also means that the correlation between performance in an artificial device versus actual outdoor exposure depends on the material being tested. This problem is exacerbated in artificial devices that provide only a poor simulation of outdoor conditions. The authors are aware of one program in progress at present that is attempting to use an approach which takes these

factors and their complicated interplay into account [1]. Only when such a compilation of quantum yields as a function of all variables is available should one then have any confidence in being able to predict the weathering performance of any material. The difficulty of this is obvious and accounts in part for why previous efforts were so restricted in their approach.

3 RECENT RESULTS FOR DEGRADATION IN PECT

Before examining further the question of the mechanism of PET photodegradation, we wish first to summarize a number of experiments that have been recently reported for the photodegradation of a PET copolymer, specifically copoly(ethylene/ 1,4-cyclohexylenedimethylene terephthalate) (PECT) where the mole percentage of the modifying 1,4-cyclohexandimethanol is sufficient to ensure a totally amorphous material. This copolymer has been commercialized by the Eastman Chemical company (trademarked Spectar copolyester) and will be referred to by its trademark in the figures. The data from these experiments will be useful in the interpretation of the previous literature data on PET photodegradation and also some recent reports on the photodegradation of PECT itself.

3.1 COLORATION

Data concerning the xenon arc exposure of PECT have been reported [2]. Note that comparison is made to general purpose polycarbonate and impact modified acrylic for the color development. The PECT copolymer obviously changes much more rapidly in b^* value [3] than either of these materials. Flatwise impact testing (see below) showed the PECT sample to be ductile at the test start and brittle at the first exposure interval of 800 kJ/m^2 exposure.

Although we want to focus on the unmodified PECT copolymer and also PET and their mechanisms of degradation in an outdoor environment, we wish to briefly mention that a solution to the color increase problem for PECT copolymer has been disclosed [4] and consists of the simple expediency of preparation of a co-extruded A-B type of structure in which the A layer, i.e. the layer facing solar exposure, contains a relatively high concentration of a very strong UV absorber. The competitive absorption thus provides a mechanism by which UV light is simply not allowed to penetrate very far into the plastic sample and thus damage by photon absorption is greatly reduced. The effect on retardation of color development (Figure 18.1) is rather dramatic. In addition, the flatwise impact according to ASTM D6395 of this 'co-ex construction' showed the material to retain ductility even at 4000 kJ/m^2 of exposure. This solution to the color problem is, of course, analogous to what is done to solve the color increase problem in polycarbonate.

In an attempt to accelerate testing, higher irradiances were employed in the 'Weather-Ometer'. Reciprocity is a necessary condition for this acceleration to be

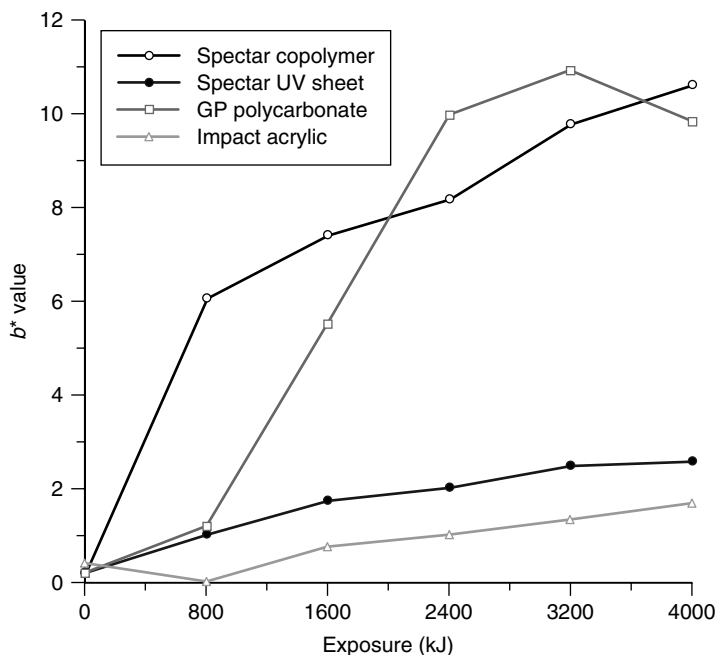


Figure 18.1 Effect of Weather-Ometer exposure ($0.35 \text{ W/m}^2/\text{nm}$) for color of materials [2]. From 'Weathering of polyester and copolymer sheeting', presentation given by D. R. Fagerburg at the *Atlas School for Natural and Accelerated Weathering* (ASNAW) course, Miami, FL, May 1999, and reproduced with permission of Atlas Electric Devices Company

valid. Reciprocity means that results are only a function of the total irradiance and not any other variable, such as the time interval over which this dose of radiation was applied. It was reported that reciprocity failure was a problem even at very low increases in irradiance by the xenon arc source [4]. The increase in irradiance employed from 0.35 to $0.70 \text{ W/m}^2/\text{nm}$ (measured at 340 nm) resulted in significant problems for tracking of the color versus exposure in kJ (Figure 18.2) for PECT and especially in haze (Figure 18.3) for both PECT and the UV-stabilized version. This haze observation, in particular, is disturbing in that it indicates that the mechanism of molecular weight degradation (gel permeation chromatography (GPC) data were reported to parallel the haze data) would seem to be dependent upon the irradiance level in the Weather-Ometer. The black panel temperature [5] of the exposure was kept at the same level. The temperature of the black panel falls off with distance into the film on the panel whereas the temperatures in these semi-transparent samples would tend to be higher slightly below the surface of the sample in the higher irradiance testing [6]. Thus, there could be higher temperatures just below the sample surface in the higher irradiance testing which

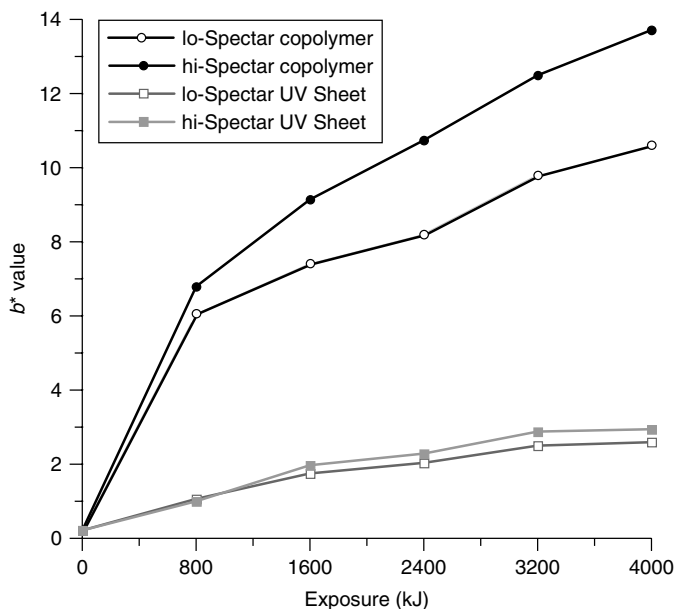


Figure 18.2 Effect of Weather-Ometer reciprocity testing at high ($0.70 \text{ W/m}^2/\text{nm}$) and low ($0.35 \text{ W/m}^2/\text{nm}$) for color of Spectar copolymer and Spectar UV sheeting [7a]. From Fagerburg, D. R. and Donelson, M. E., Effect of water spray and irradiance level on changes in copolyester sheeting with xenon arc exposure, *ANTEC'98 Conference Proceedings*, Paper 808, Atlanta, GA, April 30, 1998, and reproduced with permission of the Society of Plastics Engineers

would exacerbate degradative reactions, even though one would think from the black panel temperature that all specimens were at the same temperature.

Experiments reported where the gross effect of moisture was tested are also of interest [7]. When the water spray in the Weather-Ometer was eliminated so that samples were only exposed to ambient relative humidity in the test cabinet (55 %) and not the high surface humidity available especially during and after the spray (the light source was always on) showed color effects (Figure 18.4) that indicated that absence of moisture resulted in higher color development but lower loss (Figure 18.5) of number-average molecular weight (M_n). The conclusion reported was that a common intermediate in the photoexcitation was present and that in the presence of high moisture this intermediate went predominantly a chain scission route, while in the absence of moisture it led to color development. This indicates that photohydrolysis, which has only been hinted at in the literature, would seem to be an important effect. Quite obviously, more work needs to be done in understanding this as such behaviour is potentially a very large source of degradation in climates such as Florida where a lot of durability testing is performed.

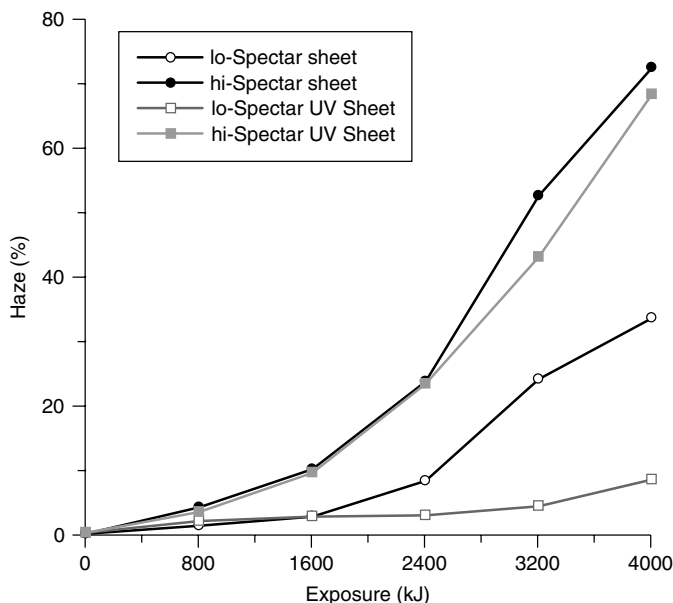


Figure 18.3 Effect of Weather-Ometer reciprocity testing at high ($0.70 \text{ W/m}^2/\text{nm}$) and low ($0.35 \text{ W/m}^2/\text{nm}$) on haze of Spectar copolymer and Spectar UV sheeting [7a]. From Fagerburg, D. R. and Donelson, M. E., Effect of water spray and irradiance level on changes in copolyester sheeting with xenon arc exposure, *ANTEC'98 Conference Proceedings*, Paper 808, Atlanta, GA, April 30, 1998, and reproduced with permission of the Society of Plastics Engineers

In examining these GPC data it should be noted that the averages and the M_z/M_n ratios are meant only to convey qualitative information about scission and branching owing to the problem of GPC calibration not being for branched molecules like those being produced [8].

When PECT copolymer was exposed outdoors, the data obtained can be related at least in some degree to that which was obtained in a xenon arc device [2, 4, 9]. The increase in color with exposure time (Figure 18.6) for PECT copolymer is quite dramatic and is initially very much higher than one sees for an unprotected polycarbonate sample. Throughout the exposure time, the color of the PECT copolymer is understandably far worse than an impact-modified acrylic sample. Interestingly, after about 6 months of exposure (see Figure 18.6) the color of the unprotected polycarbonate begins a sudden increase and at somewhere before 18 months exposure even exceeds that of the PECT copolymer. This is of no practical consequence for either material as the color values at 1 year of exposure are so far in excess of acceptable color change levels (probably, $\leq 4b^*$ units change is acceptable) as to render both materials useless in an outdoor environment.

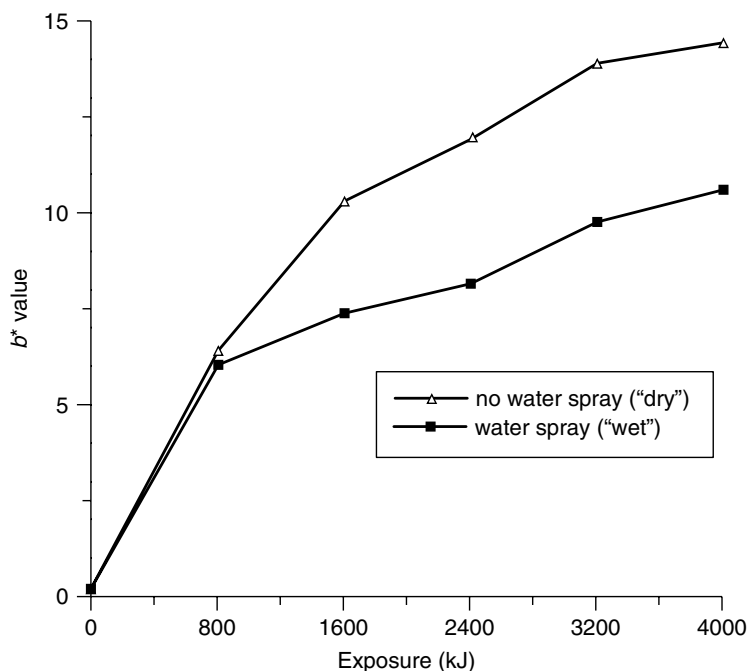


Figure 18.4 Effect on color of Weather-Ometer testing with ('wet') and without ('dry') water spray for Spectar copolymer sheeting [7a]. From Fagerburg, D. R. and Donelson, M. E., Effect of water spray and irradiance level on changes in copolyester sheeting with xenon arc exposure, *ANTEC'98 Conference Proceedings*, Paper 808, Atlanta, GA, April 30, 1998, and reproduced with permission of the Society of Plastics Engineers

3.2 LOSS OF TOUGHNESS

Another property of interest for materials exposed outdoors is the retention of toughness. Measurement of this property is often carried out by some sort of impact by a falling ball, dart or tup. One such test, instrumented impact (ASTM 3763) is particularly suited for such evaluations as it provides information corresponding to the amount of energy to begin failure, the energy to propagate the failure, the total energy overall and the mode of failure, i.e. whether ductile or brittle. The results obtained for PECT copolymer outdoors (Figure 18.7) showed that all toughness of the sample was gone at even 3 months of exposure. Polycarbonate, by comparison, retained its toughness until 12 months of exposure. It is interesting to note that both samples at their point of embrittlement exhibited an unacceptable $4.5b^*$ units or more of color change.

We note also for comparison that impact-modified acrylic polymer sheeting has a very low, but non-zero color increase upon outdoor exposure (see Figure 18.6)

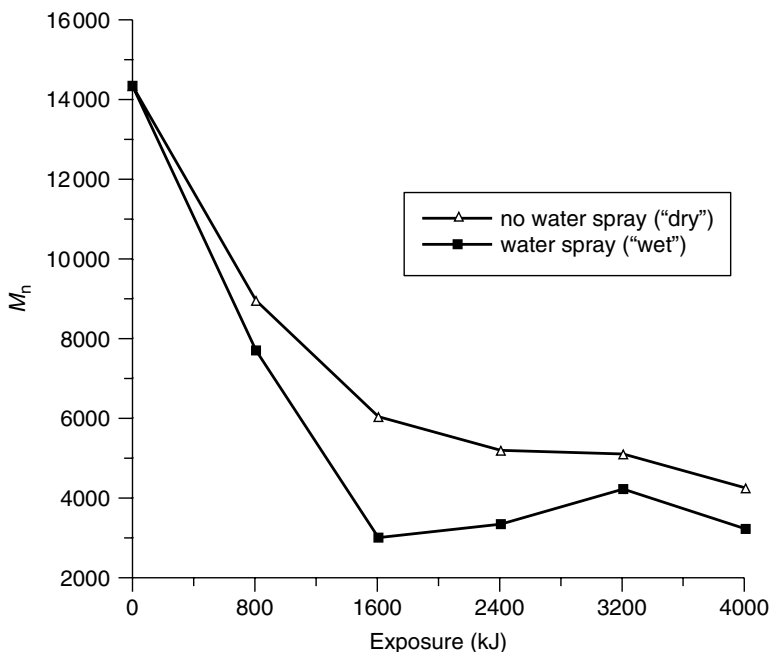


Figure 18.5 Effect on number-average molecular weight (M_n) of Weather-Ometer testing with ('wet') and without ('dry') water spray for Spectar copolymer sheeting [7]. From Fagerburg, D. R. and Donelson, M. E., Effect of water spray and irradiance level on changes in copolyester sheeting with xenon arc exposure, *ANTEC'98 Conference Proceedings*, Paper 808, Atlanta, GA, April 30, 1998, and reproduced with permission of the Society of Plastics Engineers

and although vastly superior in this respect to either PECT copolymer or polycarbonate, the change is pretty much the same as that observed for the UV-protected PECT copolymer. The latter showed excellent suppression of color development (Figure 18.6) and retention of impact (Figure 18.7).

Additionally, the instrumented impact showed that even though the acrylic is called impact-modified, it is only so relative to unmodified acrylic. Interestingly, its impact properties start off at about where unprotected PECT copolymer ends up after 3 months of exposure when it has severely embrittled.

3.3 DEPTH PROFILE OF THE DAMAGE

As somewhat of a side note on the exposure of these materials, it was also reported that there was a distinct difference in the coloration and impact properties of the UV-stabilized PECT, depending strongly on an exposure variable not often reported in the literature, that of the effect of sunlight reaching the back side of

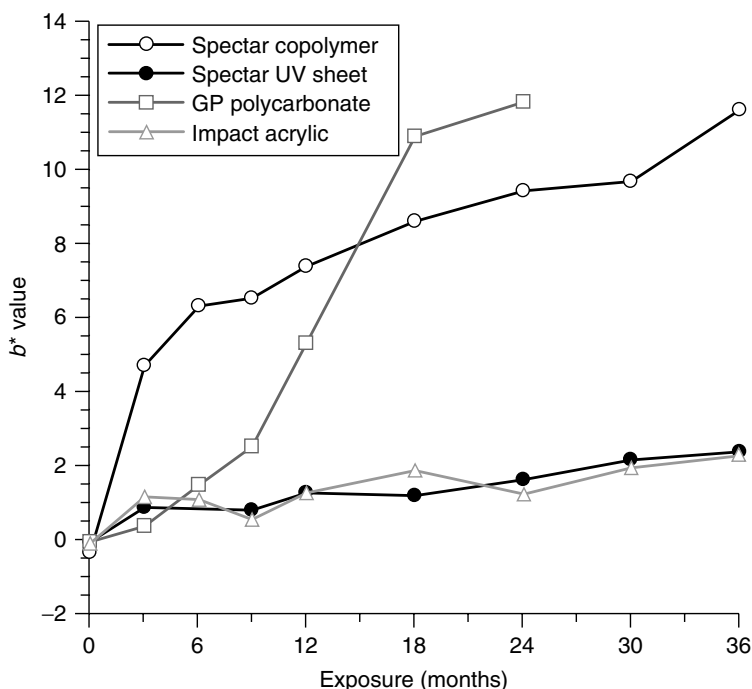


Figure 18.6 Effect of outdoor exposure, Miami, FL, on the color of selected materials [2]. From 'Weathering of polyester and copolymer sheeting', presentation given by D. R. Fagerburg at the *Atlas School for Natural and Accelerated Weathering* (ASNAW) course, Miami, FL, May 1999, and reproduced with permission of Atlas Electric Devices Company

the exposed specimens [2, 10]. When flat sheeting of the UV material with a co-extruded cap layer on one side (an A-B structure, where A is the layer containing the UV absorber and B is the bulk of the sheeting) was exposed in Miami, Florida versus ABA co-ex or AB co-ex with a sheet of the same co-ex placed several centimeters behind it, the color and impact differences versus exposure interval were dramatic (Figures 18.8 and 18.9). This is further indication of the extreme sensitivity of PECT copolyester to UV degradation.

It was reasoned that the early morning and late afternoon sun played a large role in this observation. This can be particularly so in the early morning when the surfaces of the exposed sheeting would tend to be wet with dew (yes, dew often forms on the downward facing side of samples in a Florida exposure) which would then not only have the degradant water present in high concentration for photohydrolysis, but the droplets could cause 'lensing' as well, thus further exacerbating the effect of the sunlight. It is not at all obvious, by the way, that the back side light exposure must be confined to the periods of early morning

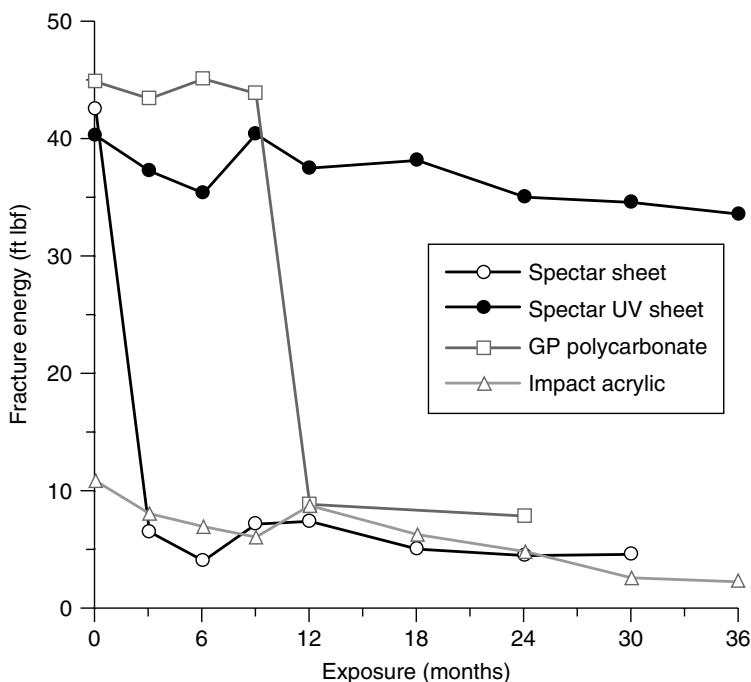


Figure 18.7 Effect of outdoor exposure, Miami, FL, on the impact energy of selected materials [2]. From 'Weathering of polyester and copolymer sheeting', presentation given by D. R. Fagerburg at the *Atlas School for Natural and Accelerated Weathering (ASNAW)* course, Miami, FL, May 1999, and reproduced with permission of Atlas Electric Devices Company

and late afternoon sun in the times of year between the spring and autumn equinox. Clearly, some radiation reaches the panel back via scattering at all times of the day as well. The magnitude of the scattered radiation has yet to be quantified.

It was also reported that color and IR data were obtained versus depth for the exposed sheet of material if one used a milling technique [9, 10]. The resultant data was interesting in that the change in IR peaks was dramatic at the surface with large changes in the hydroxylic region, both above the C–H stretch frequencies but also below them where carboxylic acid dimers generally exist. In addition, the carbonyl region had a significant broadening from the apparent addition of large numbers of other carbonyl peaks at longer wavenumbers. Some of the carbonyl broadening was even seen on the higher-wavenumber side of the main peak. Such peaks have been reported [11] to be either perester or anhydride peaks. It would seem more reasonable to ascribe these peaks to anhydride functionality given the other evidence for it (see below). This very large

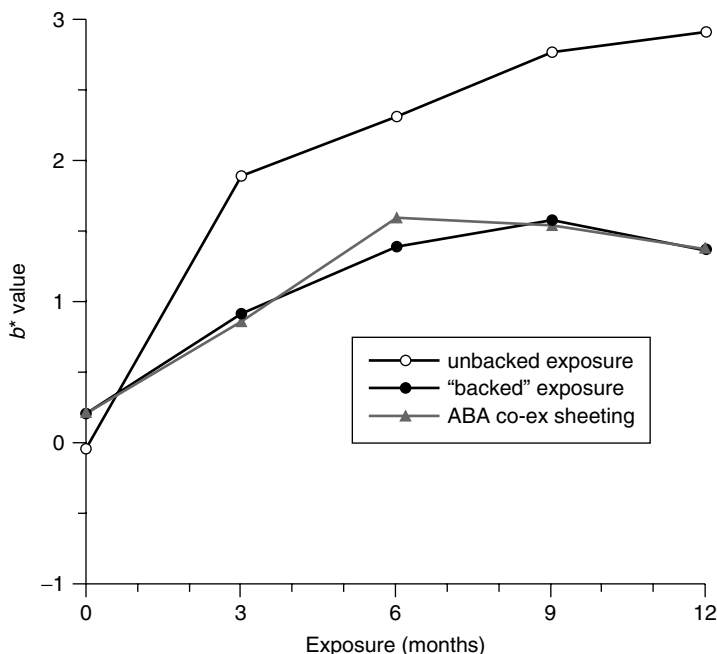


Figure 18.8 Effect on color data of 'backing' with UV-protected sheeting on Spectar UV co-ex sheeting and ABA co-ex sheeting in Miami, FL, exposure [2]. From 'Weathering of polyester and copolymer sheeting', presentation given by D. R. Fagerburg at the *Atlas School for Natural and Accelerated Weathering* (ASNAW) course, Miami, FL, May 1999, and reproduced with permission of Atlas Electric Devices Company

change at the surface of the exposed samples was, however, not seen at all in the bulk, even as shallow as $50\text{ }\mu\text{m}$ depth. Thus, changes in composition at this depth did not exceed a percent or so that is the expected sensitivity of the IR measurements.

The evolution of these peaks with very short exposure times (Figure 18.10) was also reported [9], which indicated a steady, and very large increase in carbonyl species but an apparent induction period in the addition of more $-\text{OH}$ region peaks. This induction period has yet to be adequately explained but appears connected with either ring oxidation being delayed and/or photohydrolysis being delayed. These authors favor the delay of ring oxidation given that such a process (see Scheme 18.1 discussion below) does not proceed directly from an excited state cleavage reaction but instead does require some concentration of radicals to be able to proceed at all.

When GPC analysis was employed to determine the depth profile of the damage [9], the results (Figure 18.11) showed that substantially more damage was

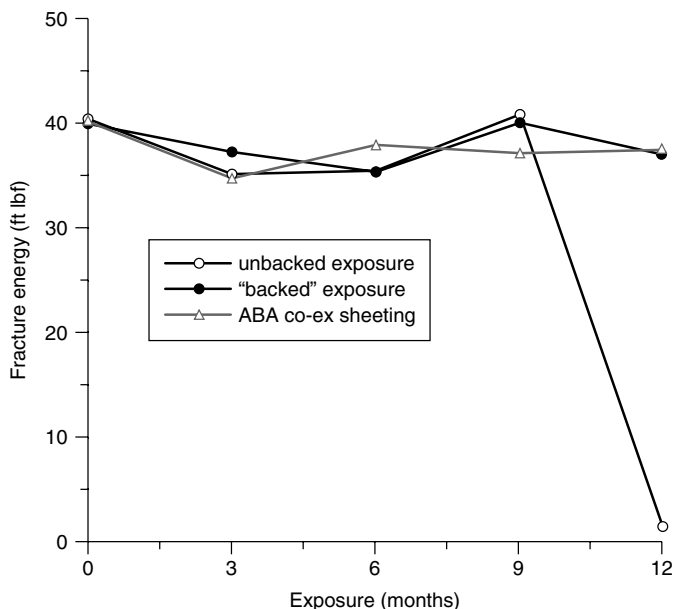


Figure 18.9 Effect on impact data of 'backing' with UV-protected sheeting on Spectar UV co-ex sheeting and ABA co-ex sheeting in Miami, FL, exposure [2]. From 'Weathering of polyester and copolymer sheeting', presentation given by D. R. Fagerburg at the *Atlas School for Natural and Accelerated Weathering* (ASNAW) course, Miami, FL, May 1999, and reproduced with permission of Atlas Electric Devices Company

detectable than by IR spectroscopy. Here it is apparent that the chain scission as measured by M_n is apparent to as deep as $250\text{ }\mu\text{m}$ (10 mil) but is quite minimal past that depth. Chain branching as measured by M_z/M_n would appear to be very similar but is slightly more evident past $250\text{ }\mu\text{m}$ depth. The profile of damage is very steep with depth of the plaque indicating that the wavelength(s) involved must be relatively short as they seem to be all but filtered out past the $250\text{ }\mu\text{m}$ depth.

Treatment of these samples with SF_4 gas to convert the carboxylic acids produced in the weathering process into carbonyl fluorides showed [2, 11] that the acids are actually a mixture of aliphatic and aromatic acids (Figure 18.12). Aromatic acid species are by far the predominant ones, however. The origin of these acids will be discussed below in conjunction with the overall mechanisms of photodegradation. Aliphatic acid species were detected by GC/MS in the artificial device exposure of PECT [11]. Note that the PECT copolymer produced more aromatic acids with the same exposure as PET but that the aliphatic acid production was several times higher for the PECT copolymer. The photo-oxidation of the co-glycol must be the reason for this difference.

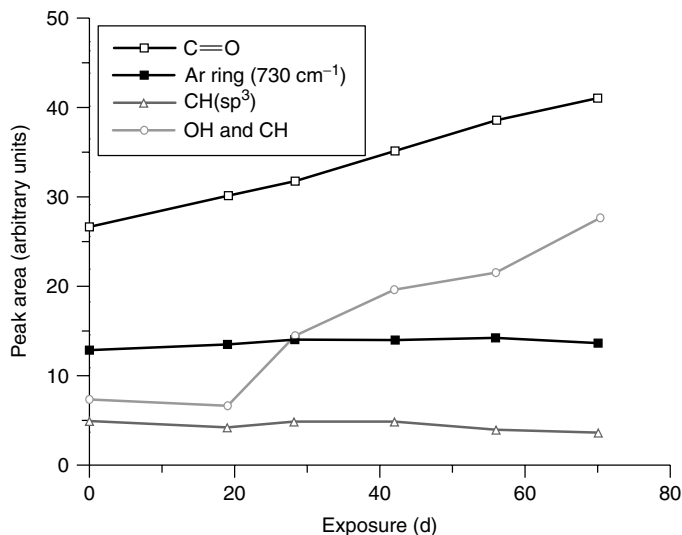


Figure 18.10 Effect of exposure in New River, AZ, on selected IR spectral peak areas for Spectar copolymer sheeting [9a]. From Fagerburg, D. R. and Donelson, M. E., Molecular weight loss and chemical changes in copolyester sheeting with outdoor exposure, *ANTEC'98 Conference Proceedings*, Paper 809, Atlanta, GA, April 30, 1998, and reproduced with permission of the Society of Plastics Engineers

Additionally, it was reported [11] that hydroperoxide production was significantly higher for the PECT copolymer than PET at equivalent radiation dosage (Figure 18.13). For both the hydroperoxide formation and the formation of aliphatic acids versus exposure it must be noted that these large differences were manifested at very short exposure times, thus leading to the conclusion that the 1,4-cyclohexandimethanol had a profound negative effect on the photo-oxidative degradation of the copolymer.

The color versus depth data [10] is quite interesting (Figure 18.14) in that there are obviously two very different regimes of color change occurring in the sample. First, there is the portion of the coloration that occurs very close to the surface of the sample which proceeds at an apparently ever-increasing slope and seems to occur in the first 250 or so μm of depth into the exposed plaque. After this depth, there appears to be an increase in coloration which is virtually linear with increasing depth, extending through to the back of the specimen. This line appears to advance pretty much steadily up to higher color at a rate that is not quite linear with exposure time.

The interpretation of this color versus depth versus exposure time data was that there are two obviously different processes having much different sensitivity to wavelength from each other. The one which represents the essentially parabolic

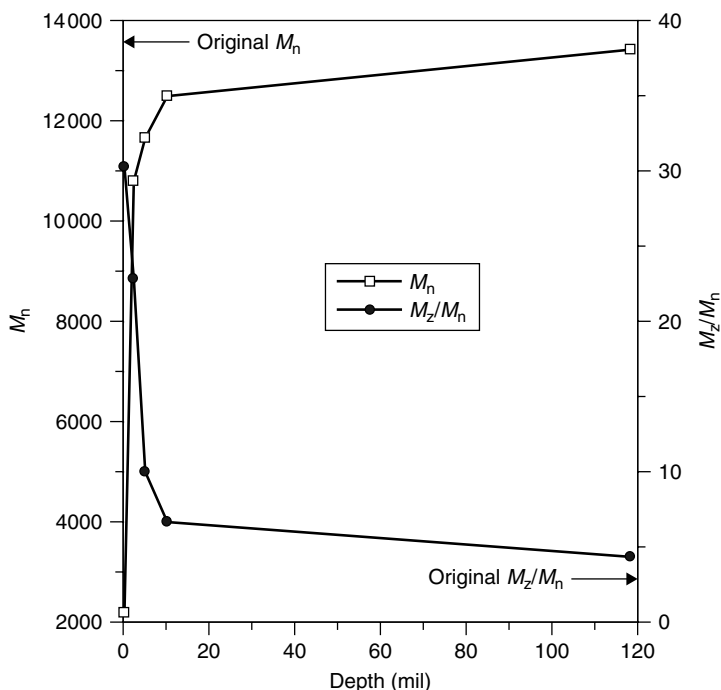


Figure 18.11 Effect of exposure in New River, AZ, on the GPC data for Spectar copolymer sheeting [10]. From 'Photodegradation in a copoly(ethylene/1,4-cyclohexylenedimethylene terephthalate) with and without UV absorber', presentation given by D. R. Fagerburg at the *37th International Symposium on Macromolecules*, IUPAC World Polymer Congress, Gold Coast, Australia, July 1998, and reproduced with permission of IUPAC

portion of the curve can be understood to be a shorter-wavelength process that in the process of exposure is progressively filtered out by the overlying yellowing layers as the exposure continues.

The second coloration process must be quite different in nature since it extends through the whole of a plaque – a full 3 mm in thickness. Only comparatively long wavelengths can still penetrate through a plaque so thick and cause yellowing in the latter stages of exposure. Thus, one concludes that color generation in this copolymer is actually two different processes, namely one operating at a relatively short wavelength, not yet quantified, and the other at a quite longer wavelength, probably greater than 340 nm. Photons of such long wavelengths are of comparatively low energy for many of the mechanistic schemes proposed below as we shall see.

It is interesting to speculate that these same processes are probably at work in PET itself although there is currently no data reported either to

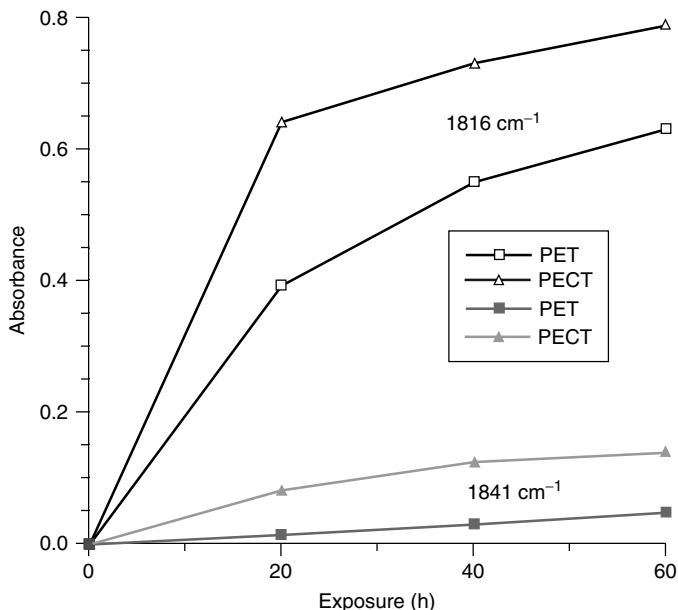


Figure 18.12 Effect of fluorescent device exposure on carboxylic acid production in Spectar copolymer as determined by SF_4 treatment: 1816 cm^{-1} , aromatic acid peak; 1841 cm^{-1} , aliphatic acid peak [11]. Reprinted from *Polymer*, **41**, Grossetete, T., Rivaton, A., Gardette, J.-L., Hoyle, C. E., Ziemer, M., Fagerburg, D. R. and Clauberg, H., Photochemical degradation of poly(ethylene terephthalate)-modified copolymer, 3541–3554, Copyright (2000), with permission from Elsevier Science

support or to refute such a suggestion. The determination of this awaits further research.

With reference back to the GPC data with depth (see above), one concludes that both sets of data are quite consistent and indicate that the short wavelength(s) capable of chain scission and branching are likely also active in color formation. The longer wavelengths responsible for the deeper coloration, however, must not be capable of very much chain scission or chain branching.

We also note data from atomic force microscopy (AFM) versus depth, carried out by using a diamond tip for scratching patterns into the surface [12]. Because of the 2° microtoming method reported, these authors were able to examine the depth profile of brittle behavior in weathered samples with excellent resolution. The data showed a very rapid decrease in the brittleness with depth into the sample which, of course, was a strong function of exposure time. The brittleness was more in line with the IR data (see above) versus depth than the molecular weight data, hence suggesting that some chain scission and branching can be tolerated in the system before it manifests brittle behavior.

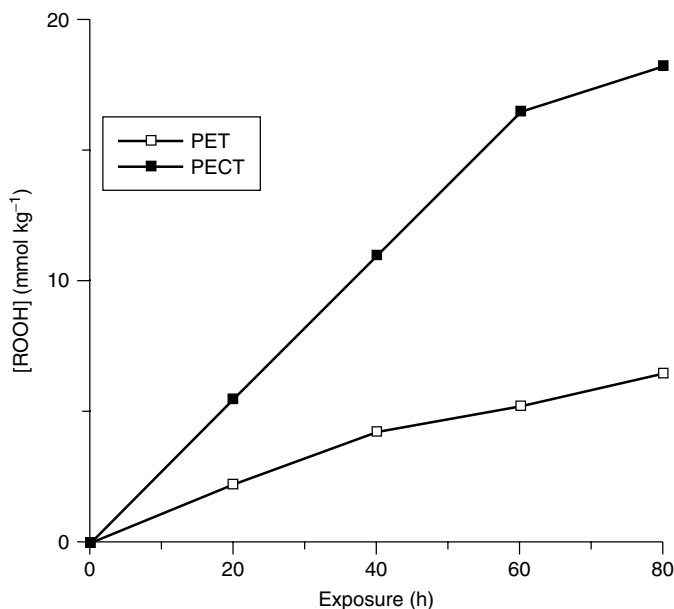


Figure 18.13 Effect of fluorescent device exposure on hydroperoxide production in Spectar copolymer [11]. Reprinted from *Polymer*, **41**, Grossetete, T., Rivaton, A., Gardette, J.-L., Hoyle, C. E., Ziemer, M., Fagerburg, D. R. and Clauberg, H., Photochemical degradation of poly(ethylene terephthalate)-modified copolymer, 3541–3554, Copyright (2000), with permission from Elsevier Science

The brittleness reported can either be a function of chain scission and/or chain branching as the AFM technique cannot distinguish between those two processes, only that the sample has become brittle as opposed to initial ductility before exposure.

4 DEGRADATION MECHANISMS IN PET AND PECT

Returning now to the specific example of PET weathering-induced property loss, we note that several early investigators began looking into the problem of PET photodegradation soon after its magnitude was appreciated. Investigations focused mainly on fiber properties and some chemical testing such as carboxyl numbers as an indication of photoreaction. There was, clearly, little mechanistic understanding at the time and the properties studied did little to advance any such understanding.

Osborn [13] reported work on 25 μm (1 mil) thick oriented PET film exposed either to a carbon arc or to fluorescent light sources using inherent viscosity measurements to track the degradation and related them to the number-average

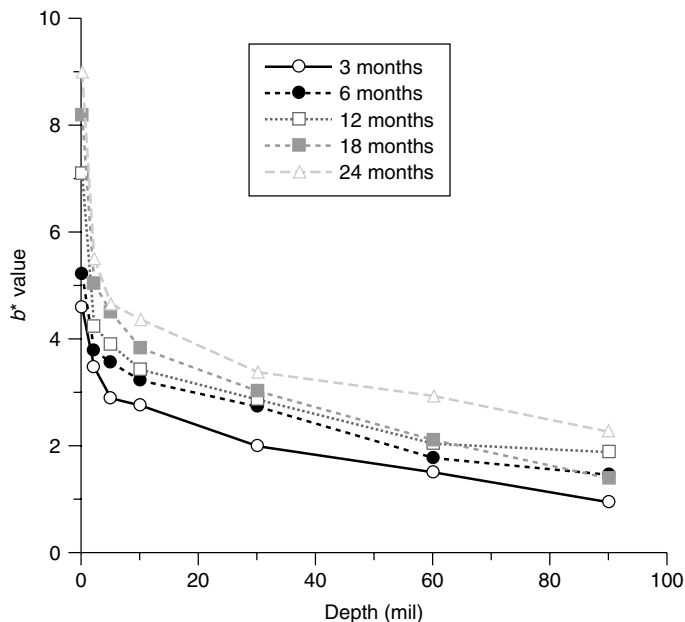


Figure 18.14 Effect of exposure time on the color versus depth profile in Spectar copolymer sheeting (3mm) exposed in New River, AZ [10]. From 'Photodegradation in a copoly(ethylene/1,4-cyclohexylenedimethylene terephthalate) with and without UV absorber', presentation given by D. R. Fagerburg at the 37th International Symposium on Macromolecules, IUPAC World Polymer Congress, Gold Coast, Australia, July 1998, and reproduced with permission of IUPAC

molecular weights obtained via osmometry from the previous literature. It was estimated that the quantum yield for the chain scission in PET was of the order of 5×10^{-4} . It was further suggested that the inefficiency of the process compared to other polymers in the same report argued that internal conversion, fluorescence or other such processes could account for the overall inefficiency of the photodegradation of PET. This low quantum yield was, of course, offset to a large degree by the fact that PET is a very strong UV absorber in and of itself.

Schultz and Leahy [14] reported the solution viscosity of stacked films of $6.2 \mu\text{m}$ (0.25 mil) thickness and saw a pronounced gradient in solution viscosity. Using a plot of inherent viscosity versus the energy of absorbed photons, they estimated the most active wavelength in the degradation to be 314 nm. This may be consistent with the shorter-wavelength yellowing process reported for PECT copolymer (see above) but certainly ignores the longer-wavelength one.

Stephenson *et al.* [15] first monitored the tensile properties and determined no damage for photon energies less than 3.2 eV (74 kcal/mol or 388 nm) by extrapolation. If this is true, then it implies that photodegradation out to quite

long wavelengths was actually known for some time. This also agrees with the PECT outdoor data cited above that showed coloration deep into exposed materials – also a very long-wavelength phenomenon. It is interesting to note that other studies into the wavelength sensitivity of the photodegradation of PET actually ignore this result and quote numbers in the range of 320 nm as the area of maximal damage, with essentially none occurring at wavelengths only tens of nm longer than this. As we shall see below, one of the already accepted pathways of degradation actually could involve 340 nm light in the chain scission.

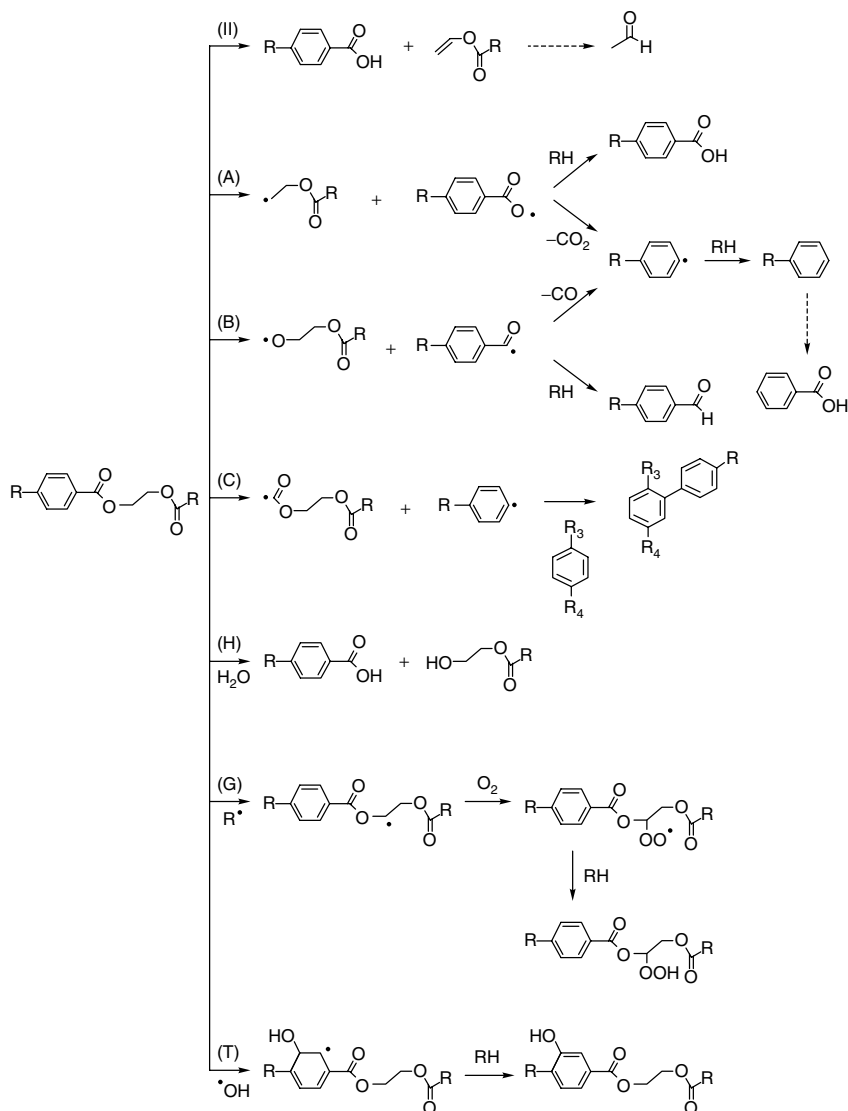
Stephenson *et al.* [16] next reported results obtained from cross-linking versus chain scission as measured by a combination of inherent viscosity and gel content measurements. Their results showed considerable cross-linking to be occurring in the photodegradation of PET. Their report of substantial gel fraction reinforces that GPC data will not provide accurate molecular weight representations (see above) of these degraded chains. The same cautions need to be applied to equations relating the inherent viscosity to the osmotically determined number-average molecular weight.

Investigation turned then to chemical and spectroscopic means to obtain the needed mechanistic understanding. Stephenson *et al.* [17] looked at gas evolution versus exposure, while Pacifici and Straley [18] used UV fluorescence spectroscopy to identify a photo-oxidation product which was later isolated by Valk *et al.* [19]. In addition, Valk and co-workers [19–21] isolated a number of additional photolysis products by a combination of hydrolysis and chromatography, Marcotte *et al.* [22] used ESR to look at radicals generated during degradation, and Day and Wiles [23–26] carried out extensive IR and fluorescence spectroscopic investigations on this subject.

The end result of these studies showed very clearly that two major processes were important, i.e. photolysis and photo-oxidation. Photolysis reactions were posited to be the result of the well-known Norrish Type 1 and Norrish Type 2 cleavage reactions. As we shall see, the Type 1 cleavage followed by several subsequent reactions can account for many of the observed degradation products.

The photo-oxidation reactions can take place either on the aromatic rings [18, 25] or the glycol units [11, 25] and lead to many of the rest of the products apparently not accounted for in the pure photolysis reactions.

Having collected much information, several investigators, notably Valk *et al.* [21] and Day and Wiles [25], were able to suggest photolysis mechanisms to account for their observations. Summaries of these have been published in review works [27]. Grossetete *et al.* [11] have also published a set of reaction schemes for the PECT copolymer. We will now present an overview set of schemes which combine all of the possible reactions they reported and some additional reactions to more fully account for products from both photolysis and photo-oxidation reactions. Evidence for each of the paths will be discussed, along with some speculation about other products that should reasonably accompany these paths but that have not yet been reported.



Scheme 18.1 The main reaction schemes for the photolysis of PET

Scheme 18.1 shows the seven main reactions that are posited to occur, with the first four being pure photodegradation, the fifth photohydrolysis and the last two photo-oxidation. Some of the main products from each of these are shown for several of the reactions but for many of the reactions they are either continued or amplified in subsequent schemes. Please note that the products that are obtained

by hydrolysis of the degraded polymer are shown following a dotted reaction arrow. Some of this could undoubtedly take place over a long period of time with exposed samples as well. Owing to hydrolysis of the polymer prior to any analyses in many of the literature reports, the amounts of these molecules existing free in the polymer matrix just after exposure has not been quantified in all cases to date. In those cases where the molecules were extracted via a simple aqueous wash of the sample, often there was only identification and not quantitation.

The first reaction in Scheme 18.1 is a Norrish Type 2 reaction. It is the only reaction where the products contain no radical species at all and hence is a 'one-time, only reaction with no possibility of any further direct reaction propagation. The evidence for this reaction was obtained by Day and Wiles [25] who reported that the production of carboxylic acids was too high in relation to CO₂ gas evolution to be accounted for by Norrish Type 1 reactions which they had previously discussed (see below).

In addition to this direct evidence, it is well accepted that there is ample literature evidence that the Norrish Type 2 reaction is commonly seen in esters [28–30].

The next three reactions of Scheme 18.1 (labeled A, B, and C respectively) are the three possible Norrish Type 1 cleavages of an ester functionality. Day and Wiles [25] suggested these three and gave estimates for the energies necessary for cleavage as obtained from the thermochemical literature. The energies of cleavage for each path are given as follows:

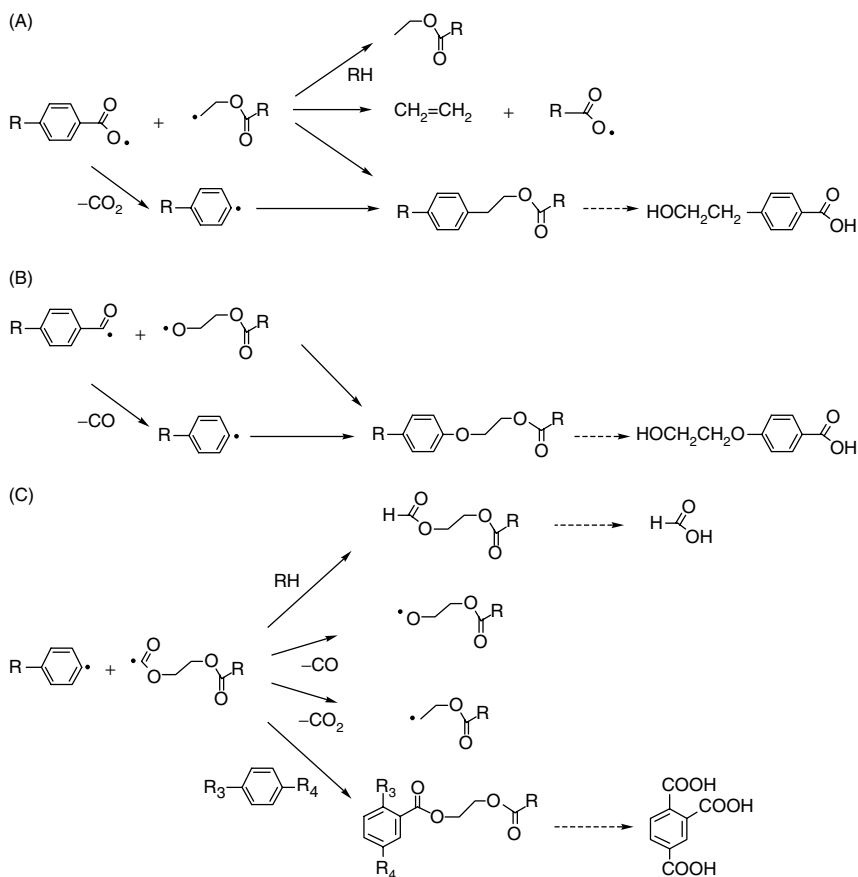
Path A	– 84 kcal/mol	340 nm
Path B	– 88 kcal/mol	326 nm
Path C	– 102 kcal/mol	281 nm

It is obvious when one examines these wavelengths that path C is apparently not likely at all given that terrestrial sunlight cuts off at about 295 nm. Please note also that it is not necessary at present to invoke path C and its 'follow-on' reactions. The CO₂ and CO evolution for which Day and Wiles reported quantum yields of production [25] and the follow-on products from this section of the scheme can be explained already by reference to paths A and B and their follow-on products, as shown in Scheme 18.1 and also in Scheme 18.2 (see below).

As shown in Scheme 18.1, probably the most important fate of the phenyl radical is in the production of cross-linking species (specifically shown in but not exclusively from path C). The literature [9] has reported this as a more reasonable alternative to the cross-linking reaction proposed long before it [22] that would rely upon two radicals combining to form a tetracarboxy species as the branching species. As was pointed out [9], the probability of two radicals at low concentration finding each other must be orders of magnitude less probable than the phenyl radical simply finding an aromatic ring in an adjacent chain with which to react. The proposed tricarboxybiphenyl species has not been isolated to date, although IR spectroscopic evidence exists [11] that would support such a species. Unfortunately, the IR peak in question at 773 cm^{–1} is not unique to a 1,2,4-trisubstituted benzene ring as the vibration is really from a *meta*-substitution pattern.

We note here that much has been made of the phenyl radical seen in an ESR study by Marcotte *et al.* [22] as an intermediate for further reactions. Although there is little doubt that they saw the radical they reported, it is usually assumed in ESR work that for the most part, radicals that are seen in such spectra are not the reactive intermediates because of the fleeting nature of such species. One usually assumes that if a radical appears in a reacting system, the radical observed is actually a 'sink', i.e. the end of a chain, and not really an intermediate in any of the reaction(s). We suggest that the sink view of the radical observed is a better interpretation as opposed to the view taken by Marcotte and co-workers and subsequent references to their work.

Some of the follow-on reactions of paths A, B and C are shown in Scheme 18.1 and also in Scheme 18.2.



Scheme 18.2 Follow-on reactions of paths A, B and C (Scheme 18.1)

Thus, the observed aromatic carboxylic acids at chain ends [11, 25] would be accounted for by the hydrogen abstraction by the carboxyl radical (Scheme 18.1, path A). This, of course, generates another radical species, R^{\cdot} , (not shown) capable of carrying on further degradative reactions.

The phenyl radical generated (or also directly produced in the path C) is an obvious precursor of the benzoic acid reported [20] which was also noted to exist free in exposed samples [11]. Also noted by investigators are IR peaks attributed to aldehyde functionalities [11, 25] which could arise via the path shown in the scheme.

In Scheme 18.2, we see that the alkyl radical produced could also account for some of the other products noted as well. Ethylene [25] was reported but not the β -hydroxyethylbenzoic acid that would be expected from the follow-on reactions of the alkyl fragment produced from path A cleavage. Note that the production of ethylene would result in more carboxylic acid being produced. That this is the case weakens but probably does not negate the argument for a Norrish Type 2 reaction in order to have a higher quantum yield of carboxylic acid with respect to that for CO_2 evolution. The fact that apparently only low levels of ethylene were observed, i.e. only one set of investigators reported it, suggests that such a path must not have a very high quantum yield.

The results of path B and its alkyl fragment are shown next in Scheme 18.2. This essentially amounts to loss of CO , with the radical fragments staying close enough to each other in the cage to allow facile recombination. The resultant product, after hydrolysis, gives the β -hydroxyethoxybenzoic acid reported [21].

Lastly, we show in Scheme 18.2 what would be two logical reaction products of the alkyl radical which is produced. The hydrogen abstraction was already proposed [11, 25] by others on the basis of spectroscopic evidence for an aldehyde but it has not been confirmed that the species was an aliphatic aldehyde being produced as opposed to an aromatic one and so is ambiguous. Hydrolysis of the top product of this section of the scheme would produce formic acid, which has been reported [11]. However, more reasonable sources of formic acid exist in Schemes 18.3 and 18.4 (see below). The other product that one would expect to see would result in trimellitic acid being observed in the hydrolysate of the degraded polyester. This has, to our knowledge, not been reported as yet.

We now return to Scheme 18.1. The fifth reaction shown is direct photohydrolysis which has not been postulated in inclusive schemes before but is included based on recent evidence [7].

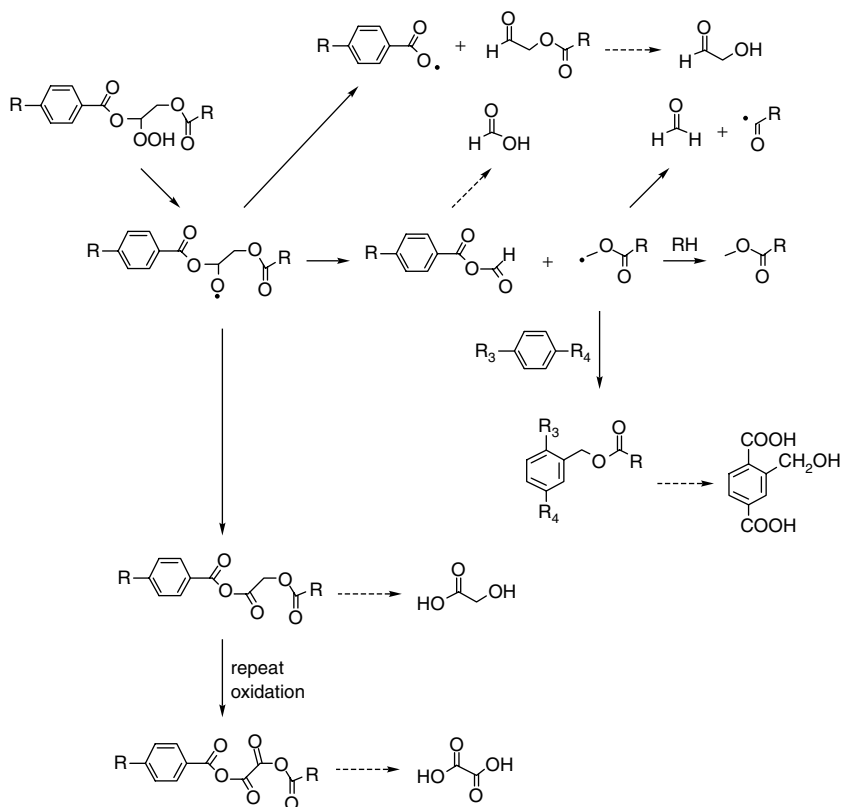
The photo-oxidation reactions are the last two in the scheme – these are listed as reactions G and T. In the former reaction, the initial radical abstraction is performed by pretty much any radical available in the polymer matrix. Reaction with oxygen to form the hydroperoxy radical followed by hydrogen abstraction to form a hydroperoxide has been suggested as a mechanism of glycol oxidation [11, 25, 31] and is, of course, a very reasonable reaction path. Note that the

hydrogen abstraction by the hydroperoxy radical regenerates a radical (not shown), although not necessarily the exact one used to initiate the photo-oxidation.

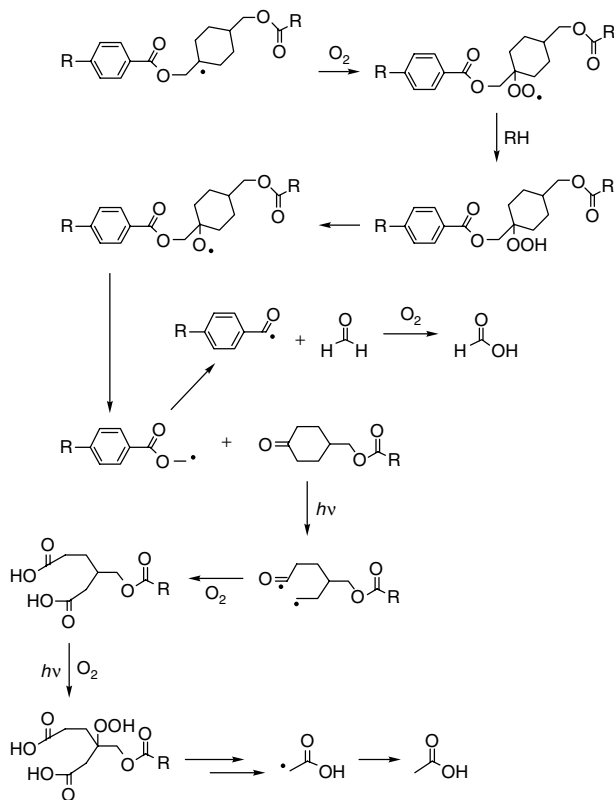
The rest of the photo-oxidation on the glycol portion is continued in Scheme 18.3. The cleavage of the O–O bond should be very facile. Both photolytic and thermal decomposition of these peroxides are possible.

Note that the step produces two radicals for every radical initiating the sequence (Scheme 18.1, path G) and thus is especially destructive in its outcome.

We next examine the possible fates of the alkoxy radical produced as a result of hydroperoxide fragmentation. It should be noted that the other fragment produced in this process, an hydroxy radical (not shown), would be an extremely reactive species. Since it is not attached to a polymer chain end, it is also capable of more readily diffusing through the polymer matrix than most of the radicals discussed to this point. This also makes the photo-oxidation of the glycol potentially more destructive.



Scheme 18.3 Photo-oxidation of the glycol portion in path G (Scheme 18.1)



Scheme 18.4 Photo-oxidation reactions of PECT [11]. Reprinted from *Polymer*, **41**, Grossetete, T., Rivaton, A., Gardette, J.-L., Hoyle, C. E., Ziemer, M., Fagerburg, D. R. and Clauberg, H., Photochemical degradation of poly(ethylene terephthalate)-modified copolymer, 3541–3554, Copyright (2000), with permission from Elsevier Science

The alkoxy radical of Scheme 18.3 (upper reaction) could scission to produce the same carboxyl radical as seen in the Norrish type 1 path (Scheme 18.1, path A) discussed above. As such, it is an additional source of CO_2 but not taken into account in the report by Day and Wiles [25]. Not reported but still obvious, the other fragment of this scission is an aliphatic aldehyde that could also have been one of the aldehyde carbonyl IR signals reported [11, 25]. Hydrolysis of this chain end would yield the reported glyoxal [21].

If the cleavage were to go in the opposite direction of the first reaction, the products produced would be an anhydride of formic acid with the terephthalic half-ester chain end. No doubt this compound would be readily hydrolyzed and should give the reported formic acid [21].

The other part of the cleaved chain would give a radical with three possible paths shown: (1) decomposition to form the reported formaldehyde [21, 25], while further oxidation of formaldehyde could give formic acid; (2) hydrogen abstraction could give a methyl ester; (3) the radical could add to a phenyl ring to give a branch point (shown reacting with the phenyl ring bearing R_3 and R_4 as substituents). This hydroxymethylterephthalate compound has not been reported as yet.

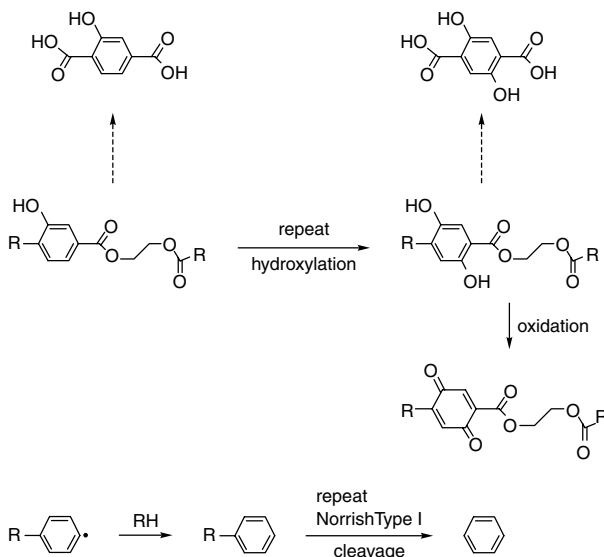
A third possible fate of the alkoxy radical is shown in Scheme 18.3 (lower reaction) and was postulated by Grossetete *et al.* [11]. In this reaction, the hydroxy radical in the cage from hydroperoxide cleavage yields an anhydride by extraction of the α -hydrogen to the radical. These workers cite IR evidence in support of this reaction which seems quite reasonable. In addition, the report by Valk *et al.* [21] of glycolic acid would seem to confirm this path as well.

Were the anhydride able to undergo a second oxidation sequence exactly analogous to what we have been currently discussing, then the product is a double-anhydride of oxalic acid – as reported by Valk *et al.* [21] – and thus this second oxidation seems likely to proceed at some non-negligible rate.

We note also that the schemes discussed until now only show the oxidation of the ethylene glycol moiety. In the PECT copolymer, the 1,4-cyclohexylenedimethylene moiety is also available for oxidation. Indeed, given that the oxidizable hydrogens are tertiary, one reasonably expects a greater ease of production of a radical from that center. Grossetete *et al.* [11] reported such to be the case with the observation that photo-oxidation reactions occurred much faster with the PECT copolymer than with PET itself. The aliphatic acids that they reported, as identified by the SF_4 treatment, could also account for previous aliphatic acid reports [25]. This is also additional support that the photo-oxidation mechanism is operating as proposed (Scheme 18.4).

The cyclohexanone postulated in this scheme should also be photoactive. The series of reactions necessary to produce the acetic acid observed [11] is indeed long but currently the only reasonable explanation of this product. Previous investigators [20, 21] had not reported acetic acid from the photolysis of PET even though they isolated acetaldehyde, although Day and Wiles [25] did report it. Thus, one may reasonably assume that the presence of 1,4-cyclohexandimethanol most likely is required to produce acetic acid, at least in significant amounts.

Returning one last time to Scheme 18.1, reaction T is a ring-oxidation reaction and requires as written the presence of a hydroxy radical. One could equally as well speculate that another radical could extract a ring hydrogen, so producing a terephthalic ester radical which then adds oxygen and undergoes the same sequence of reactions as seen for the glycol oxidation scheme. Scheme 18.5 shows the follow-on reactions expected. It is easily seen how one can produce the reported hydroxyterephthalic moiety [21]. A repeat of this oxidation would also give the reported 2,5-dihydroxyterephthalate [21].



Scheme 18.5 Follow-on reactions of path T (Scheme 18.1)

It is well to note at this point that the dihydroxy compound is the first identifiable compound from the photolysis and photo-oxidation reactions that actually has any color. The lack of other identifiable color compounds and also some preliminary experiments lead to a proposal [9] that the oxidation of the dihydroxy compound could actually continue on to give a quinone (Scheme 18.5, top). Given the ease of oxidation of hydroquinone compounds, this would seem to be a reasonable proposal. In this preliminary report where an orange-red solid was initially observed it was speculated that the color owed itself to a quinone compound as shown. This would add significantly to compounds that actually could be the color bodies formed upon weathering exposure.

The bottom part of Scheme 18.5 is intended to show another fate for the phenyl radicals produced other than those already discussed in Schemes 18.1 and 2. Simple hydrogen abstraction yields a phenyl radical as discussed above in conjunction with Scheme 18.1. Reaction with other chains yields a branch point as also discussed above. However, if after hydrogen abstraction by the phenyl radical the cleavage reaction that produced the phenyl radical originally were to be applied to the remaining ester group on the ring, then one could account for the report of benzene [25] as well.

We note that hydrogen as well as methane, ethane and toluene have been reported [25], but do not currently have good explanations in the schemes shown above. For the methane and ethane, one would have to resort to either radical displacement reactions of the methyl ester shown in Scheme 18.3 in the middle

and the ethyl ester shown in the third reaction of path C in Scheme 18.2 or to Norrish Type 1 cleavages of the respective esters to form the energetic methyl and ethyl radicals. We currently know of no precedent for a radical displacement reaction on oxygen and would be somewhat skeptical to propose such. The proposal of Norrish Type 1 cleavage is far more reasonable and is probably the way to account for the production of methane and ethane. This still leaves the hydrogen and toluene not accounted for.

We note, however, that even if methane comes from the photolysis of the methyl ester, this does not necessarily mean that all of it arises as a result of first breaking down the PET itself by photolysis. Both the PET of early reports and also the PECT were undoubtedly produced using dimethyl terephthalate (DMT) instead of terephthalic acid and so have methyl ester end groups owing to the well-known incomplete reaction of the DMT. There may be only a small level of these ester groups, but the amount of methane produced was small as well. This, at the very least, causes some potential confusion about the source of all the methane should some of it come from methyl ester photolysis. No such confusion would exist for the ethane should that be coming from photolysis of an ethyl ester.

It should additionally be noted that a number of the paths of the schemes above have received some confirmation in a number of literature reports dealing with the photolysis and photo-oxidation of other polyesters [32–35]. Because these reports investigated poly(butylene terephthalate) (PBT), poly(ethylene naphthalate) and poly(butylene naphthalate), however, they may not have direct application to understanding of the processes involved in PET and PECT and so have not been discussed in this present chapter. All do contain support for the formation of radicals leading to CO and CO₂ evolution, as well as the hydrogen abstraction at glycolic carbons to form hydroperoxides which then decompose to form alkoxy radicals and the hydroxyl radical. These species then were postulated to undergo further reaction consistent with what we have proposed above.

We also note two reports on the degradation of ‘stacked’ films of oriented PET. In the first [36], photodegradation is said to be two-step in nature with ‘weak links’ cleaving first followed by a much slower cleaving of the ‘strong links’. The chain scission process was tracked versus exposure time by measurement of solution viscosity [37]. In the second paper [38], the surface nature of the degradation was reported and the rationale elucidated for why surface degradation causes overall mechanical failure limited by that layer, much as we have discussed in the impact properties of the PECT (see above).

A particularly relevant thermo-oxidative study on PET degradation and PBT reported the degradation products observed for ethylene dibenzoate [39]. The products observed paralleled those of the photolysis and photo-oxidation reports discussed above with benzoic acid, vinyl benzoate, 2-hydroxyethylene dibenzoate, 2-carboxymethoxy benzoate and the coupling product, 1,4-butylene dibenzoate, being reported. The 2-hydroxyethylene dibenzoate and 2-carboxymethoxy

benzoate are of particular interest as they can only reasonably arise from hydrogen abstraction at the α -carbon of the glycol unit, followed by oxygen addition to give the hydroperoxy radical, followed by hydrogen abstraction to give a hydroperoxide, and then its cleavage to give an alkoxy radical. In their scheme, however, they postulated direct reaction of oxygen with the acyloxy radical produced from cleavage to give a peracid intermediate which then decomposes to the acid moiety. The parallel to the photodegradation schemes proposed is quite compelling.

5 SUMMARY

In summary, we note that almost all of the products observed by investigators for the photodegradation of PET and PECT are nicely accounted for in the summary schemes we have proposed. Additionally, there are several products that should be sought to prove or disprove additions to the previously reported pathways proposed by us and by others. It should be noted, however, that until more proof of these various schemes is obtained, then the mechanisms are still speculative even though they are very consistent with all of the available data.

There is a special need as well to discover more about the nature of the species formed as color bodies in these photo-reactions. Their identification will most likely be inherently difficult owing to their expected low concentrations – they are undoubtedly compounds with high molar absorptivities. Nevertheless, finding them could help solve the last pieces of the photodegradation puzzle for these materials and might, therefore, lead to solutions for even better weathering materials. The need for this is obvious given that thus far the only solution to the photodegradation of PECT is the simple scheme of competitive absorption currently on the market. While quite serviceable, such a scheme can never protect the sample surface and so loss of surface gloss is inevitable. This can only be remedied by a change in the actual chemistry taking place under UV exposure.

Additionally, we speculate that there needs to be research carried out utilizing absolutely pure polyester samples, i.e. ones completely free of any catalyst residues and insofar as possible, any other contaminating side products. This is, we feel, necessary owing to the fact that several of the reports cited show that damage occurs at rather much longer wavelengths than can be reasonably attributed to the absorption of the main polyester chain alone.

REFERENCES AND NOTES

1. Martin, J. W., *Progr. Org. Coatings*, **23**, 49–70 (1993).
2. Fagerburg, D. R., Weathering of polyester and copolyester sheeting, Presentation given at the *Atlas School of Natural and Accelerated Weathering (ASNAW) Course*, Miami, FL, 27–30 April, 1999, Atlas Electric Devices Company, Chicago, IL, 1999.

3. The b^* axis is the yellow–blue axis of color measurement space, with a positive b^* being yellow and a negative b^* being blue. For a more thorough explanation of the b^* value in the color measurement space, please see ASTM D2244.
4. Fagerburg, D. R. and Donelson, M. E., *J. Vinyl Additives Technol.*, **3**, 179–183 (1997).
5. The black panel temperature is measured with a thermocouple mounted on a flat black painted panel which is placed on the sample rack of the Weather-Ometer. As such, the temperature registered is meant to indicate a maximum temperature of the specimens under the same irradiation.
6. Kockett, D., Factors of weathering, Presentation given at the *Atlas School of Natural and Accelerated Weathering (ASNAW) course*, Miami, FL, 27–30 April, 1999, Atlas Electric Devices company, Chicago, IL, 1999.
7. (a) Fagerburg, D. R. and Donelson, M. E., Effects of water spray and irradiance level on changes in copolyester sheeting with xenon arc exposure, in *ANTEC'98 Conference Proceedings* (on CD-Rom), Wypych, G. (Ed.), Atlanta, GA, April. 30, 1998, Society of Plastics Engineers, Brook field, CT, 1998, Paper 808; (b) Fagerburg, D. R. and Donelson, M. E., Effects of water spray and irradiance level on changes in copolymer sheeting with xenon arc exposure, in *Weathering of Plastics: Testing to Mirror Real Life Performance*, Plastics Design Library, Norwich, NY, 1999, pp. 93–98.
8. GPC calibration curves are established based on the radius of gyration of known-molecular-weight polymers, such as well characterized, narrow-molecular-weight distribution polystyrene. Branched polymers have a lower radius of gyration for their molar mass than the corresponding linear molecule. Thus, as branching increases the GPC numbers become less and less accurate and so should only be used for trends, and *not* exact calculations as some authors have done.
9. Fagerburg, D. R. and Donelson, M. E., Molecular weight loss and chemical changes in copolyester sheeting with outdoor exposure, in *ANTEC'98 Conference Proceedings* (on CD-Rom), Wypych, G. (Ed.), Atlanta, GA, April. 30, 1998, Society of Plastics Engineers, Brookfield, CT, 1998, Paper 809; (b) Fagerburg, D. R. and Donelson, M. E., Molecular weight loss and chemical changes in copolyester sheeting with outdoor exposure, in *Weathering of Plastics: Testing to Mirror Real Life Performance*, Plastics Design Library, Norwich, NY, 1999, pp. 77–82.
10. Fagerburg, D. R., 'Photodegradation in a copoly(ethylene/1,4-cyclo hexylenedimethylene terephthalate) with and without UV absorber', Presentation given at the 37th *International Symposium on Macromolecules*, IUPAC World Polymer Congress, Gold Coast, Australia, July 14, 1998.
11. Grossetete, T., Rivaton, A., Gardette, J.-L., Hoyle, C. E., Ziemer, M., Fagerburg, D. and Clauberg, H., *Polymer*, **41**, 3541–3554 (2000).

12. Setz, S., Duran, R. S., Fagerburg, D. R. and Germinario, L. T., Nano-lithographic determination of brittleness at polymer surfaces, in *Fundamentals of Nanoindentation and Nanotribology*, Moody, N. R., Gerberich, W. W., Baker, S. P. and Burnham, N. (Eds), MRS Symposium Proceedings, Vol. 522 (MRS Spring Meeting, 1998) (on CD-Rom), Materials Research Society, Warrendale, PA, 1998.
13. Osborn, K. R., *J. Polym. Sci.*, **38**, 357–367 (1959).
14. Schultz, A. R. and Leahy, S. M., *J. Appl. Polym. Sci.*, **5**, 64–66 (1961).
15. Stephenson, C. V., Moses, B. C. and Wilcox, W. S., *J. Polym. Sci.*, **55**, 451–464 (1961).
16. Stephenson, C. V., Moses, B. C., Burks, Jr, R. E., Coburn, Jr, W. C. and Wilcox, W. S., *J. Polym. Sci.*, **55**, 465–475 (1961).
17. Stephenson, C. V., Lacey, J. C. and W. S., *J. Polym. Sci.*, **55**, 477–488 (1961).
18. Pacifici, J. G. and Straley, J. M., *J. Polym. Sci., B*, **7**, 7–9 (1969).
19. Valk, von G., Kehren, M.-L. and Daamen, I., *Angew. Makromol. Chem.*, **7**, 201–202 (1969).
20. Valk, von G. and Kehren, M.-L., *Melliand Textilber.*, **11**, 1331–1334 (1967).
21. Valk, von G., Kehren, M.-L. and Daamen, I., *Angew. Makromol. Chem.*, **13**, 97–107 (1970).
22. Marcotte, F. B., Campbell, D., Cleaveland, J. A. and Turner, D. T., *J. Polym. Sci. A1*, **5**, 481–501 (1967).
23. Day, M. and Wiles, D. M., *J. Appl. Polym. Sci.*, **16**, 175–189 (1972).
24. Day, M. and Wiles, D. M., *J. Appl. Polym. Sci.*, **16**, 191–202 (1972).
25. Day, M. and Wiles, D. M., *J. Appl. Polym. Sci.*, **16**, 203–215 (1972).
26. Day, M. and Wiles, D. M., *J. Appl. Polym. Sci.*, **17**, 1895–1907 (1973).
27. See for example: (a) Pospisil, J. and Klemchuk, P. P., *Oxidation Inhibition in Organic Materials*, Vol II, CRC Press, New York, 1990; (b) Rabek, J. F., *Polymer Photodegradation, Mechanisms and Experimental Methods*, Chapman Hall, London, 1995; (c) Wypych, G., *Handbook of Material Weathering*, 2nd Edn, ChemTec Publishing, Ontario, Canada, 1995.
28. Ausloos, P., *Can. J. Chem.*, **36**, 383–392 (1958).
29. Gano, J. E., *Tetrahedron Lett.*, 2549–2552 (1969).
30. Barltrop, J. A. and Coyle, J. D., *J. Chem. Soc. (B), Phys. Org.*, 251–255 (1970).
31. Allen, N. S., Rivalle, G., Edge, M., Corrales, T. and Catalina, F., *Polym. Degrad. Stabil.*, **75**, 237–246 (2002).
32. Casu, A. and Gardette, J.-L., *Polymer*, **36**, 4005–4009 (1995).
33. Scheirs, J. and Gardette, J.-L., *Polym. Degrad. Stabil.*, **56**, 351–356 (1997).
34. Scheirs, J. and Gardette, J.-L., *Polym. Degrad. Stabil.*, **56**, 339–350 (1997).
35. Gijsman, P., Meijers, G. and Vitarelli, G., *Polym. Degrad. Stabil.*, **65**, 433–441 (1999).

36. Wang, W., Taniguchi, A., Fukuhara, M. and Okada, T., *J. Appl. Polym. Sci.*, **74**, 306–310 (1999).
37. Solution viscosity measurements for M_n are calibrated from the flow characteristics of linear molecules of the equilibrium molecular weight distribution. Branched polymers have a lower radius of gyration for their molar mass than the corresponding linear molecule. One, therefore, expects different flow properties as branching increases, hence causing the viscosity numbers to become less and less accurate and so should only be used for trends – *not* exact calculations.
38. Wang, W., Taniguchi, A., Fukuhara, M. and Okada, T., *J. Appl. Polym. Sci.*, **67**, 705–714 (1998).
39. Botelho, G., Queiros, A., Liberal, S. and Gijsman, P., *Polym. Degrad. Stabil.*, **74**, 39–48 (2001).

PART VI

Liquid Crystal Polyesters

High-Performance Liquid Crystal Polyesters with Controlled Molecular Structure

T. INOUE AND T. YAMANAKA
Toray Industries, Inc., Tokyo, Japan

1 INTRODUCTION – CHEMICAL STRUCTURES AND LIQUID CRYSTALLINITY

The class of polyester-based liquid crystal polymers (LCPs) represent one of the most attractive materials in the field of engineering thermoplastics because of their superior mechanical properties, heat resistance, accuracy of dimensions, moldability and the excellent balance of these properties [1–5]. LCPs have been recently expanding their applications, in particular, those for precision electronic parts appropriate for surface mount technology (SMT).

Many researchers have reported the structure–thermal property correlations in LCPs from substituted hydroquinones (HQs) and dicarboxylic acids. Lenz and co-workers have investigated the liquid crystallinity of the polyarylates obtained from substituted HQs and terephthalic acid (TA) [6–10], substituted HQs and 1,10-bis(phenoxy)decane-4,4'-dicarboxylic acid [8], and substituted HQs and α,ω -bis(phenoxy)alkane-4,4'-dicarboxylic acid [11]. Kricheldorf and Schwarz [12] and Osman [13] reported the liquid crystallinity of the polyarylates obtained from substituted HQs and 1,4-cyclohexanedicarboxylic acid, while Krigbaum *et al.* [14], Heitz and co-workers [15] and Kricheldorf and Engelhardt [16] investigated the liquid crystallinity of the polyarylates synthesized from substituted HQs and substituted TAs. In addition, Jackson reported the liquid crystallinity and the moduli of fibers and injection molded specimens of the polyarylates

obtained from substituted HQs and TA [7]. However, to date there have been few reports of the influence of the factors for obtaining high moduli and high heat resistance properties in these LCPs.

We have been working on the preparation of novel LCPs from substituted HQs and substituted 1,2-bis(phenoxy)ethane-4,4'-dicarboxylic acids (PECs) [18], and substituted HQs and 4,4'-diphenyldicarboxylic acid (BB) [19–21].

Here, we would like to report some results of our investigations into the relationship between the chemical structures and the moduli and heat resistance properties of these polyesters.

2 EXPERIMENTAL

2.1 SYNTHESIS OF POLYARYLATES

The polyarylates were prepared from substituted HQ diacetates, substituted PECs and BB by melt polymerization at 250–400°C. The pressure was gradually reduced to 1 torr as the polymerization proceeded.

2.2 PREPARATION OF FIBERS

Polymers were melt-spun by using a flow tester apparatus having a capillary with a diameter of either 0.3 or 0.5 mm.

2.3 PREPARATION OF SPECIMENS

The specimens for measurements of the flexural moduli were prepared by injection molding using a Sumitomo NESTAL injection molding machine (0.5 ounce).¹

3 MEASUREMENTS

3.1 FLEXURAL MODULUS

A Toyo Baldwin Tensilon UTM-4-200 machine was used for these measurements. Determinations were performed according to ASTM D790 by using injection molded specimens with a thickness of 1/32 in.

¹ An ounce is a unit used to represent the capacity of an injection molding machine, showing the polystyrene equivalent weight of polymer for 'one shot'.

3.2 DYNAMIC STORAGE MODULUS

A Toyo Baldwin Rheovibron Viscoelastometer Rheo 2000/3000 machine was used for these determinations. Such measurements were performed at a frequency of 110 Hz, a heating rate of 2 °C/min and an 'inter-chuck' distance of 40 mm.

3.3 ANISOTROPIC MELTING TEMPERATURE AND CLEARING POINT

A hot-stage-equipped polarizing microscope was used for measurement of these parameters. The anisotropic melting temperature (T_n) was determined as the onset temperature of stir-opalescence observed on the hot-stage. The liquid crystalline–isotropic transition temperature (T_i) was also determined by the use of the hot-stage-equipped microscope.

3.4 MELTING TEMPERATURE AND GLASS TRANSITION TEMPERATURE

A Perkin-Elmer DSC-7 machine was used for these measurements. (T_m and T_g , respectively). Determinations were performed in a N₂ atmosphere at a heating rate of 20 °C/min.

3.5 ORIENTATION FUNCTION OF NEMATIC DOMAINS

The orientation functions (F -values) of as-spun fibers were calculated according to the following equation:

$$F = (3\langle \cos^2 \theta \rangle_{av} - 1)/2 \quad (19.1)$$

The θ -values were measured by wide-angle X-ray diffraction. A value of $F = 1$ indicates that the domains are perfectly aligned along the flow direction, while a value of $F = 0$ means that the domains are randomly distributed.

3.6 RELATIVE DEGREE OF CRYSTALLINITY

In order to compare the crystallinities of the polyarylates, X-ray diffraction patterns were observed in the temperature range of 25–250 °C, with the relative degree of crystallinity (I/I_0) being calculated according to the following equation:

$$I/I_0 = \frac{\text{peak intensity of polyarylates at } 2\theta = 20^\circ}{\text{peak intensity of Al}_2\text{O}_3 \text{ internal standard at } 2\theta = 43.4^\circ} \quad (19.2)$$

3.7 MORPHOLOGY

The morphologies of the tensile-fractured as-spun fibers and the flexural-fractured injection molded specimens were studied by scanning electron microscopy (SEM).

3.8 HEAT DISTORTION TEMPERATURES

The heat distortion temperatures (HDTs) of the injection molded specimens were determined under a load of 1.82 MPa according to ASTM D-648.

4 RESULTS AND DISCUSSION

4.1 MODULI OF AS-SPUN FIBERS

The liquid crystallinity and the moduli of as-spun fibers of polyarylates from substituted HQs and substituted PECs could be controlled by the substituents shown in Table 19.1. Polyarylates derived from *t*-butyl HQ (*t*Bu-HQ) and PEC (*t*Bu-HQ/PEC), and phenyl-HQ (Ph-HQ) and PEC (Ph-HQ/PEC), showed decreased liquid crystallinity when compared to chloro-HQ (Cl-HQ) and PEC (Cl-HQ/PEC), and methyl-HQ (Me-HQ) and PEC (Me-HQ/PEC), because of the bulky substituents on the HQ units.

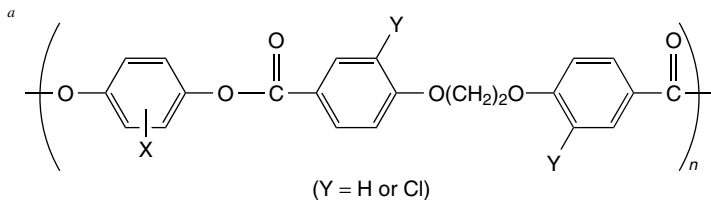
Therefore, the moduli of as-spun fibers of *t*Bu-HQ/PEC and Ph-HQ/PEC were lower than those of Cl-HQ/PEC and Me-HQ/PEC [18, 22, 23]. Tensile-fractured as-spun fibers of *t*Bu-HQ/PEC and Ph-HQ/PEC exhibited decreased orientation of fibrils when compared to Cl-HQ/PEC and Me-HQ/PEC.

Polyarylates prepared from cyclohexyl-HQ (Ch-HQ) and PEC (Ch-HQ/PEC) did not show liquid crystallinity due to the more bulky substituent on the HQ unit compared to those on *t*Bu-HQ and Ph-HQ. As-spun fibers of Ch-HQ/PEC exhibited lower moduli than those of *t*Bu-HQ/PEC and Ph-HQ/PEC. Therefore, in order to obtain high-modulus as-spun fibers, the stability of the liquid crystalline state ($T_i - T_n$) is an influential factor, as shown in Table 19.1.

On the other hand, the moduli of as-spun fibers of polyarylates from Cl-HQ and 1,2-bis(2-chlorophenoxy)ethane-4,4'-dicarboxylic acid (Cl-PEC) (Cl-HQ/Cl-PEC), and Me-HQ and Cl-PEC (Me-HQ/Cl-PEC), were higher than those of Cl-HQ/PEC and Me-HQ/PEC. The reason for the higher moduli seemed to be the increased rigidity of the polymer chain caused by the restricted rotation of the ether linkage of Cl-PEC as a result of the steric hindrance of the Cl atoms. However, the moduli of polyarylates from *t*Bu-HQ and Cl-PEC (*t*Bu-HQ/Cl-PEC), and Ph-HQ and Cl-PEC (Ph-HQ/Cl-PEC), were lower than those of *t*Bu-HQ/PEC and Ph-HQ/PEC, because the Cl atoms on the PEC units prevent

Table 19.1 Thermal properties and moduli of substituted-HQs/PEC and substituted-HQs/Cl-PEC fibers^a [23]. From Inoue, T., Yamanaka, T. and Okamoto, M., *Kobunshi Ronbunshu*, **45**, 661–665 (1988), and reproduced with permission of The Society of Polymer Science, Japan

Polymer		Thermal properties			<i>d</i> (mm) ^b	Modulus (GPa)
X	Acid	<i>T</i> _g (°C)	<i>T</i> _n (°C)	<i>T</i> _i (°C)		
Cl	PEC	87	282	>350	0.09	48
Cl	Cl-PEC	120	247	>350	0.06	68
Me	PEC	104	265	>350	0.06	42
Me	Cl-PEC	129	303	>350	0.11	72
<i>t</i> Bu	PEC	146	240	316	0.06	36
<i>t</i> Bu	Cl-PEC	141	(Isotropic)		0.06	5
Ph	PEC	124	235	265	0.07	26
Ph	Cl-PEC	115	(Isotropic)		0.08	4
Ch	PEC	139	(Isotropic)		0.07	8
Ch	Cl-PEC	133	(Isotropic)		0.11	3



^b Diameter of as-spun fibers.

the formation of liquid crystalline polyarylates only when HQ units have bulky substituents such as *t*-butyl or phenyl groups.

Tensile-fractured as-spun fibers of *t*Bu-HQ/Cl-PEC and Ph-HQ/Cl-PEC no longer exhibited fibrils, with such phenomena being different to those of the *t*Bu-HQ/PEC and Ph-HQ/PEC systems. Thus, in order to obtain high-modulus as-spun fibers, the stability of the liquid crystalline state and the rigidity of the polymer chain are both assumed to be influential factors.

Polyarylates derived from various substituted HQs and 1,2-bis(methoxyphenoxy) ethane-4,4'-dicarboxylic acid or 1,2-bis(2,6-dichlorophenoxy)ethane-4,4'-dicarboxylic acid exhibited low moduli because of the lack of liquid crystallinity resulting from the steric hindrance of the substituents on the PEC units.

Therefore, we expected that the polyarylates synthesized from substituted HQs and BB would show higher stabilities of the liquid crystalline state and higher moduli than those produced from substituted HQs and substituted PEC.

The *T*_m values of the poly(alkylene-4,4'-diphenyldicarboxylate)s are much higher than those of the poly(alkylene terephthalate)s. Therefore, as polyarylates derived from substituted HQs and BB seemed to have higher *T*_ms, the, LCPs derived from BB and alkylene glycols with higher carbon numbers have been investigated [24].

However, in spite of the higher rigidity of the polymer chains, many polyarylates derived from substituted HQs and BB exhibited liquid crystallinity and lower T_m s when compared to the polyarylates derived from substituted HQs and TA.

The 'model compound' produced from a BB unit exhibited liquid crystallinity at a lower temperature, while its liquid crystalline phase stability ($T_i - T_n$) was higher than the corresponding 'model compound' made derived from a TA unit, as shown in Table 19.2 [25].

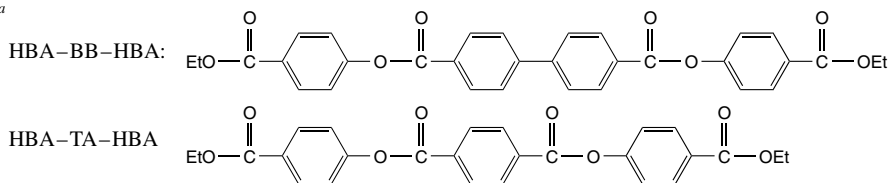
The reason for the lower liquid crystalline (LC) temperature of the BB model compound seems to be that the biphenyl unit of this compound was adopting a twisted structure in the LC state [26]. Therefore, we prepared various polyarylates containing the BB unit and determined their thermal properties and the moduli of the as-spun fibers, as shown in Table 19.3.

However, as-spun fibers of the polyarylates derived from Me-HQ and BB (Me-HQ/BB) exhibited a lower modulus than that of Me-HQ/Cl-PEC in spite

Table 19.2 Thermal properties of liquid crystalline model compounds derived from BB and TA [25]

Model compounds ^a	T_n^b (°C)	ΔH_n (cal/g)	T_i^b (°C)	ΔH_i (cal/g)	T_i/T_n (°C)
HBA-BB-HBA	189	14.8	271	0.1	82
HBA-TA-HBA	207	22.1	241	0.2	34

^a



^b T_n and T_i (isotropic melting temperature) were determined by DSC.

Table 19.3 Thermal properties and moduli of substituted-HQs/BB polyarylates [19]. From Inoue, T. and Tabata, N., *Mol. Cryst. Liq. Cryst.*, **254**, 417–428 (1994), and reproduced with permission of Gordon and Breach (Taylor and Francis) Publishers

Publisher's Note:

Permission to reproduce this image online was not granted by the copyright holder. Readers are kindly requested to refer to the printed version of this chapter.

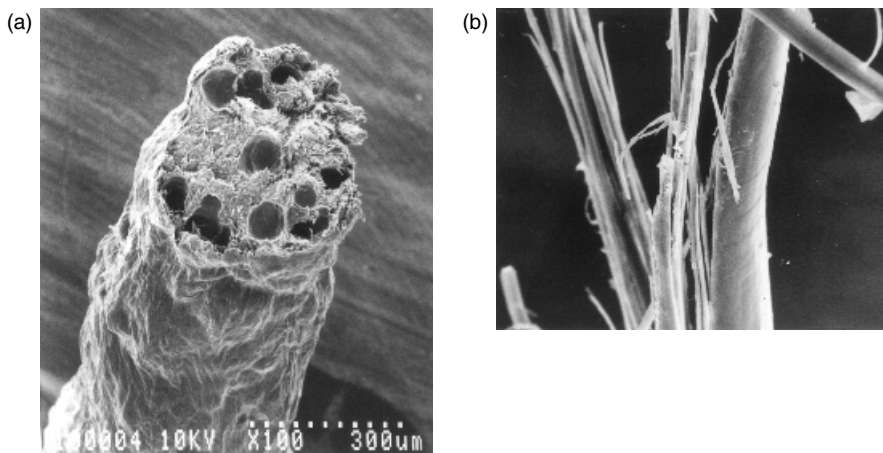


Figure 19.1 SEM images of tensile-fractured as-spun fibers of (a) Me-HQ/BB (5 GPa; F , 0.62; T_g , 175 °C) (100 \times) [19], and (b) Me-HQ/Cl-PEC (72 GPa; F , 0.90; T_g , 129 °C) (300 \times) [31]. (a) From Inoue, T. and Tabata, N., *Mol. Cryst. Liq. Cryst.*, **254**, 417–428 (1994), and reproduced with permission of Gordon and Breach (Taylor and Francis) Publishers. (b) From Inoue, T., Tabata, N. and Yamanaka, T., *Polym. J.*, **28**, 424–431 (1996), and reproduced with permission of The Society of Polymer Science, Japan

of the more rigid chemical structure. The lower modulus of Me-HQ/BB is referred to the lower F -value when compared to Me-HQ/Cl-PEC due to the lower elongational flow orientation. Tensile-fractured as-spun fibers of Me-HQ/BB exhibited a decreased orientation of fibrils when compared to Me-HQ/Cl-PEC, as shown in Figure 19.1 [19, 26]. Thus, the degree of elongational flow orientation was evaluated from the observed orientation of fibrils in the cross-sections of tensile fractured as-spun fibers.

As-spun fibers of the polyarylates derived from Ph-HQ or 2-chlorophenyl-hydroquinone (CP-HQ) and BB (CP-HQ/BB) exhibited higher moduli when compared to Me-HQ/BB in spite of the lower liquid crystallinity resulting from the bulky substituents on the HQ units. The higher modulus was referred to the higher F -values due to the higher elongational flow orientation. Tensile-fractured as-spun fibers of CP-HQ/BB exhibited many fibrils when compared to Me-HQ/BB, as shown in Figure 19.2 [19]. Thus, the elongational flow orientation (F -value) seems to be a more influential factor than the rigidity of the polymer chain and the stability of the liquid crystalline state in achieving high-modulus as-spun fibers. In order to investigate the relationship between the moduli of as-spun fibers and elongational flow orientation, samples of Cl-HQ/BB modified with TA (Cl-HQ/BB/TA) and Me-HQ/BB modified with 2,6-naphthalic dicarboxylic acid (NDA) (Me-HQ/BB/NDA) with various molar ratios were prepared [17, 18].

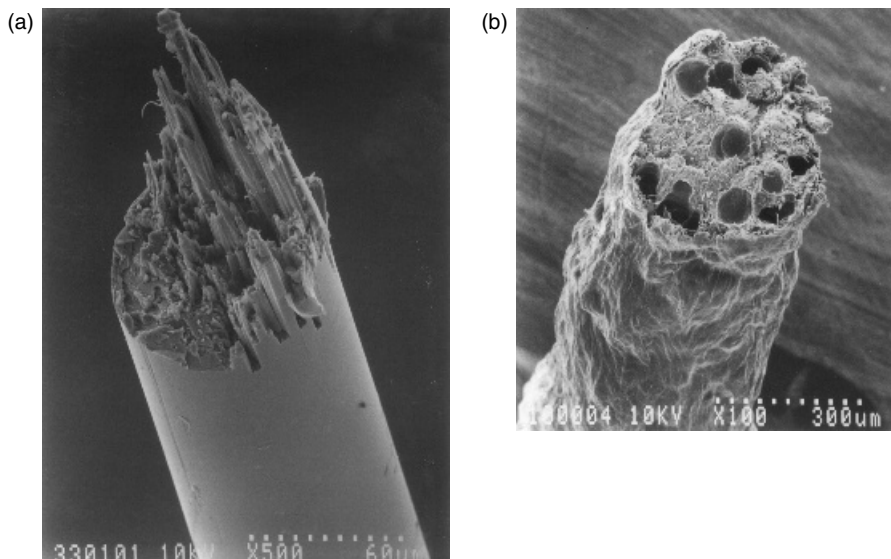


Figure 19.2 SEM images of tensile-fractured as-spun fibers of (a) CP-HQ/BB (47 GPa; F , 0.90) (500 \times), and (b) Me-HQ/BB (5 GPa; F , 0.62) (100 \times) [19]. From Inoue, T. and Tabata, N., *Mol. Cryst. Liq. Cryst.*, **254**, 417–428 (1994), and reproduced with permission of Gordon and Breach (Taylor and Francis) Publishers

Although as-spun fibers of Cl-HQ/BB/TA with $m/n = 70/30$ exhibited a modulus of 95 GPa, as-spun fibers of Cl-HQ/BB/TA with $m/n = 80/20$ exhibited a lower modulus of only 11 GPa in spite of the more rigid chemical structure due to the decreased elongational flow orientation, as shown in Figure 19.3.¹ Tensile-fractured as-spun fibers of Cl-HQ/BB/TA with $m/n = 70/30$ exhibited many fibrils when compared to those of Cl-HQ/BB/TA with $m/n = 80/20$.

In addition to this, although as-spun fibers of Me-HQ/BB/NDA with $m/n = 92.5/7.5$ exhibited a modulus of 112 GPa, as-spun fiber of Me-HQ/BB/NDA with $m/n = 95/5$ exhibited a lower modulus of only 19 GPa, as shown in Figure 19.4.

The lower modulus seemed to be referred to the lower elongational flow orientation. Tensile-fractured as-spun fiber of Me-HQ/BB/NDA with $m/n = 92.5/7.5$ exhibited many fibrils when compared to Me-HQ/BB/NDA as-spun fiber with $m/n = 95/5$, as shown in Figure 19.5.

Figure 19.6 shows the relationship between the moduli of as-spun fibers and the F -values of substituted HQs/BB and substituted HQs/BB modified with

¹ The ratio m/n represents the molar ratio of cl-HQ/BB (m) to added modifier, e.g. terephthalic acid (TA) and 2,6-naphthalic dicarboxylic acid (NDA), (n).

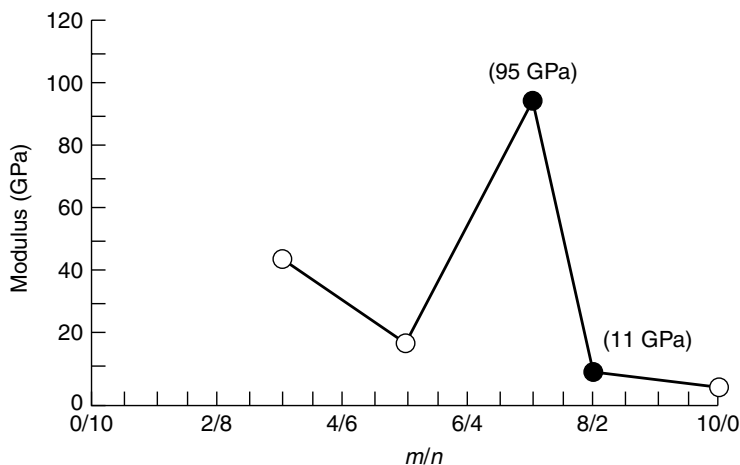


Figure 19.3 Moduli of as-spun fibers of Cl-HQ/BB/TA [18]

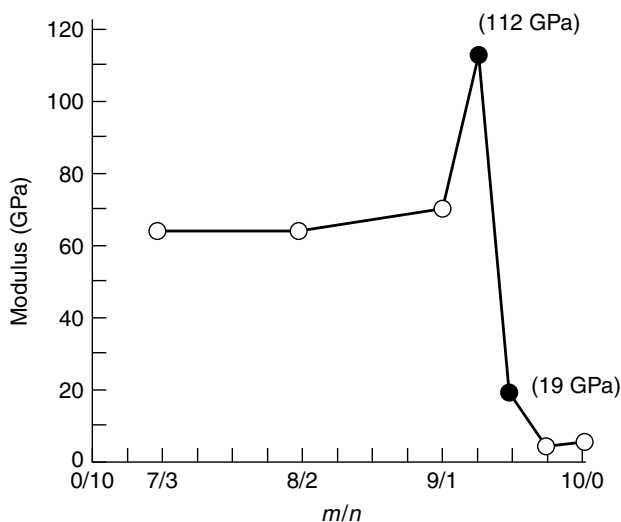


Figure 19.4 Moduli of as-spun fibers of Me-HQ/BB/NDA [20a]

4,4'-dihydroxybiphenyl (DHB), NDA, Cl-PEC and TA [20, 28–31]. We observed that the modulus increased with the increase in F -value. Thus, the influential factors in increasing the moduli of as-spun fibers are as follows: (1) the stability of the liquid crystalline state, (2) the rigidity of the polymer chain, and (3) the degree of elongational flow orientation (F -value).

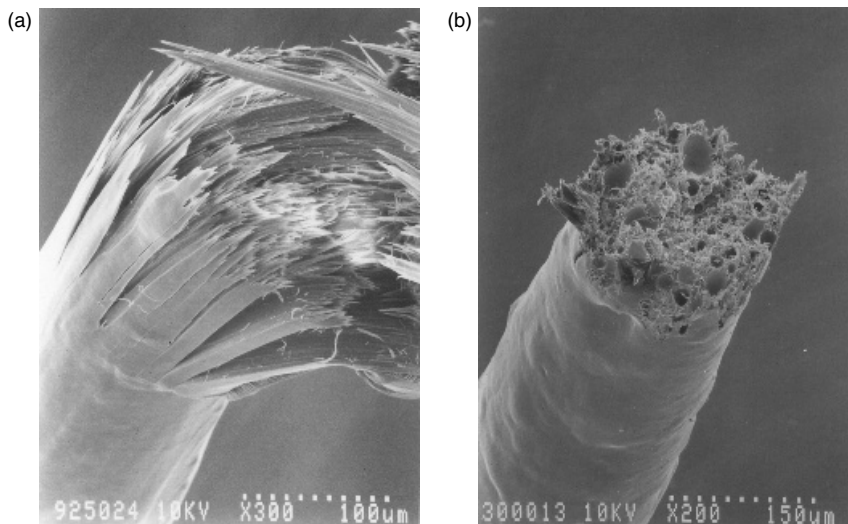


Figure 19.5 SEM images of tensile-fractured as-spun fibers of (a) Me-HQ/BB/NDA ($m/n = 92.5/7.5$) (112 GPa; F , 0.91) (300 \times), and (b) Me-HQ/BB/NDA ($m/n = 95/5$) (19 GPa; F , 0.83) (200 \times) [20a]. The latter polyarylate has the following structure:

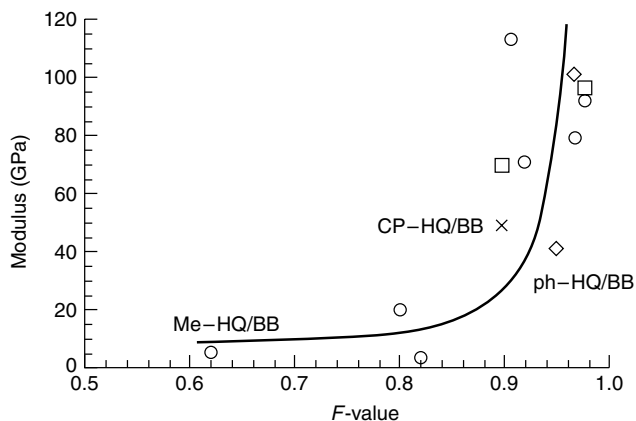
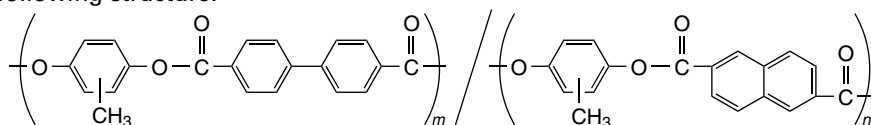


Figure 19.6 Moduli and F -values of as-spun fibers: \circ , Me-HQ/BB and copolyarylates; \square , copolyarylates of Cl-HQ/BB; \diamond , Ph-HQ/BB and copolyarylates; \times , CP-HQ/BB [31]. From Inoue, T., Tabata, N. and Yamanaka, T., *Polym. J.*, **28**, 424–431 (1996), and reproduced with permission of The Society of Polymer Science, Japan

4.2 MODULI OF INJECTION MOLDED SPECIMENS

Because as-spun fibers of Me-HQ/Cl-PEC showed a higher modulus than those of Ph-HQ/Cl-PEC, the flexural modulus of injection molded specimens of Me-HQ/Cl-PEC exhibited a higher flexural modulus than those of Ph-HQ/Cl-PEC due to the liquid crystalline state. Although flexural-fractured injection molded specimens of Me-HQ/Cl-PEC exhibited highly oriented fibrils, Ph-HQ/Cl-PEC no longer displayed fibrils because of the lack of liquid crystallinity.

Although as-spun fibers of Me-HQ/BB exhibited a lower modulus than those of Me-HQ/Cl-PEC, injection molded specimens of Me-HQ/BB exhibited a higher flexural modulus than those of Me-HQ/Cl-PEC due to the higher rigidity of the polymer chain, in spite of the lower F -value. Flexural-fractured injection molded specimens of Me-HQ/BB exhibited fewer fibrils than Me-HQ/Cl-PEC due to the lower F -value, as shown in Figure 19.7. Thus, there seemed to be no relationship between the moduli of injection molded specimens and the F -values.

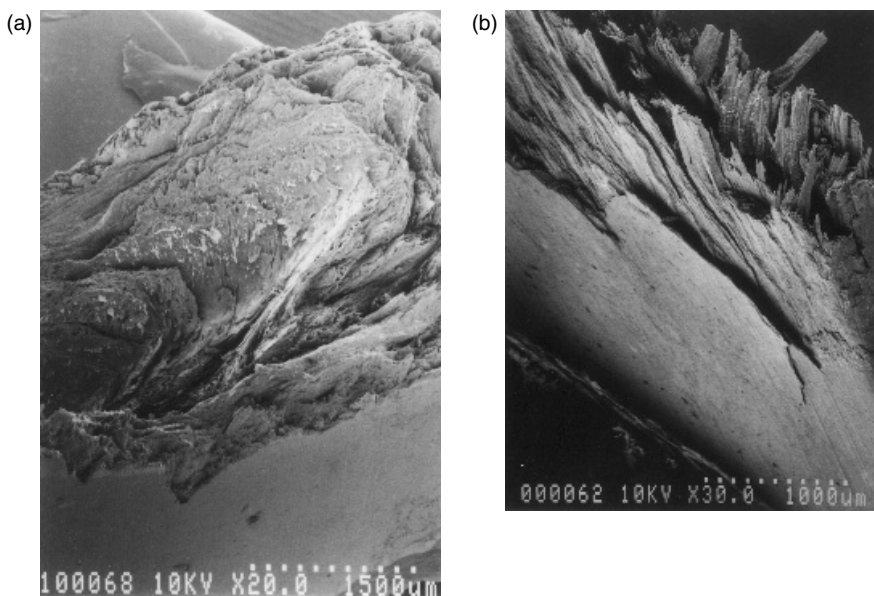


Figure 19.7 SEM images of flexural-fractured injection molded specimens of (a) Me-HQ/BB (31 GPa; T_g , 175 °C) (20 \times) [19], and (b) Me-HQ/Cl-PEC (15 GPa; T_g , 129 °C) (30 \times) [31]. (a) From Inoue, T. and Tabata, N., *Mol. Cryst. Liq. Cryst.*, **254**, 417–428 (1994), and reproduced with permission of Gordon and Breach (Taylor and Francis) Publishers. (b) From Inoue, T., Tabata, N. and Yamanaka, T., *Polym. J.*, **28**, 424–431 (1996), and reproduced with permission of The Society of Polymer Science, Japan

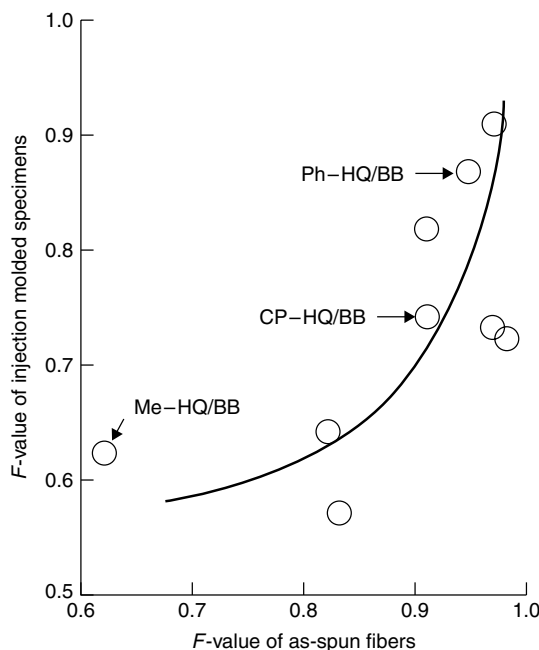


Figure 19.8 F -values of as-spun fibers and injection molded specimens [19]

As it was revealed that the F -values of both as-spun fibers and injection molded specimens had a good correlation in the case of polyarylates containing BB units (Figure 19.8), in order to investigate the relationship between the moduli of injection molded specimens and the elongational flow orientation (F -values), Me-HQ/BB/NDA samples of various molar ratios were prepared. Although as-spun fibers of Me-HQ/BB/NDA with $m/n = 95/5$ exhibited a lower modulus than Me-HQ/BB/NDA with $m/n = 92.5/7.5$, the flexural modulus of injection molded specimens of Me-HQ/BB/NDA with $m/n = 95/5$ exhibited a higher flexural modulus than Me-HQ/BB/NDA with $m/n = 92.5/7.5$, in spite of the lower F -value. Although flexural-fractured injection molded specimens of Me-HQ/BB/NDA with $m/n = 92.5/7.5$ exhibited many fibrils, those of Me-HQ/BB/NDA with $m/n = 95/5$ exhibited very few fibrils, as shown in Figure 19.9 [20]. These phenomena seemed to be due to the higher rigidity of the polymer chain.

Accordingly, we have evaluated the flexural modulus of injection molded specimens of CP-HQ/BB having higher F -values than those of Me-HQ/BB polyarylates. The flexural modulus of injection molded specimens of Me-HQ/BB

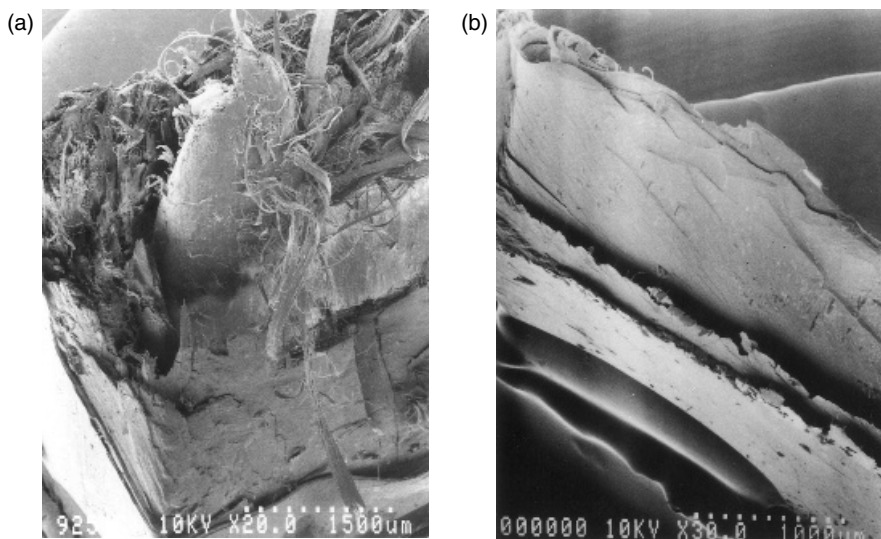


Figure 19.9 SEM images of flexural-fractured injection molded specimens of (a) Me-HQ/BB/NDA ($m/n = 92.5/7.5$) (36 GPa; F , 0.82) (20 \times), and (b) Me-HQ/BB/NDA ($m/n = 95/5$) (47 GPa; F , 0.56) (30 \times) [20a]. From Inoue, T., Yamanaka, T., Tabata, N. and Okita, S., *High Perform. Polym.*, **7**, 303–311 (1995), and reproduced with permission of Sage Publications

was higher than that of CP-HQ/BB, in spite of the lower F -value and lower rigidity of the polymer chain. In spite of the latter, the reason for the higher flexural modulus of Me-HQ/BB when compared to that of CP-HQ/BB is the higher packing density of the polymer chain due to the decrease in the size of substituents on HQ [19].

The average cross-sectional area (S) of the repeating unit can be calculated according to the following equation:

$$S = (MW/Na)/V = (MW/Na)/Ld \quad (19.3)$$

where MW is the molecular weight of the polymer repeat unit, Na the Avogadro number, V the average volume of the repeat unit, L the average length of the repeating unit, and d the density of the polymer.

According to Equation (19.3), the average cross-sectional area (S) of Me-HQ/BB was 24.9 \AA^2 , compared to the value of 32.8 \AA^2 in the case of CP-HQ/BB. Thus, to improve the packing density of Ph-HQ/BB, we have attempted to synthesize Ph-HQ/HQ/BB copolymers.

As-spun fibers of Ph-HQ/HQ/BB with $m/n = 50/50^2$ exhibited a much higher modulus (100 GPa) than Ph-HQ/BB (40 GPa) due to the increased F -value and rigidity of the polymer chain. Injection molded specimens of Ph-HQ/HQ/BB with $m/n = 50/50$ exhibited a much higher modulus than those of Ph-HQ/BB due to the increased rigidity and packing density of the polymer chain upon copolymerization with HQ. However, the F -value of injection molded specimens of Ph-HQ/HQ/BB ($m/n = 50/50$) was not much higher than those of Ph-HQ/BB, as shown in Table 19.4.

Thus, both the rigidity and packing density of the polymer chain seem to be more influential factors than the F -values in achieving a high modulus of injection molded specimens. Figure 19.10 shows the variation of the flexural moduli as a function of the F -values for various substituted-HQs/BB and substituted HQs/BB modified with DHB, HQ, 2,6-dihydroxynaphthalene (DHN), NDA, Cl-PEC and TA [31,32]. We could find no relationship between them.

Thus, the influential factors in obtaining high moduli for injection molded specimens are as follows: (1) the stability of the liquid crystalline state, (2) the rigidity of the polymer chain, and (3) the packing density of the polymer chain.

Table 19.4 Thermal properties and moduli of as-spun fibers and injection molded specimens of Ph-HQ/BB and Ph-HQ/HQ/BB ($m/n = 50/50$) polyarylates [19] From Inoue, T. and Tabata., N., *Mol. Cryst. Liq. Cryst.*, **254**, 417–428 (1994), and reproduced with permission of Gordon and Breach (Taylor and Francis) Publishers

Publisher's Note:
Permission to reproduce this image
online was not granted by the
copyright holder. Readers are kindly
requested to refer to the printed version
of this chapter.

² The ratio m/n represents the molar ratio of Ph-HQ/BB (m) to HQ/BB (n) in the Ph-HQ/HQ/BB copolymer.

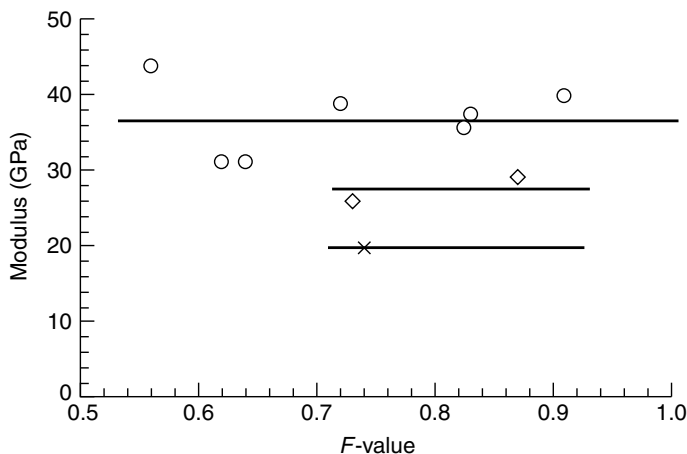


Figure 19.10 Flexural moduli and F -values of injection molded specimens: ○, Me-HQ/BB and copolyarylates; ◇, Ph-HQ and copolyarylates; ×, CP-HQ/BB [31]. From Inoue, T., Tabata, N. and Yamanaka, T., *Polym. J.*, **28**, 424–431 (1996), and reproduced with permission of The Society of Polymer Science, Japan

4.3 HEAT RESISTANCE

4.3.1 Glass Transition Temperature

The glass transition temperatures (T_g s) of polyarylates derived from substituted HQs and substituted PECs are shown above in Table 19.1. Polyarylates containing bulky substituents, such as *t*Bu, on the HQ units exhibit above high glass transitions due to the high rigidity of their molecular structures. Thus, *t*Bu-HQ/PEC shows a high T_g of 146 °C when compared to that of Me-HQ/PEC (104 °C).

In addition, as shown above in the case of Cl-PEC, the rigidity of the molecular structure increased because the chlorine substituent restricts the rotation of the ether linkage. Thus, the polyarylate Me-HQ/Cl-PEC shows a high T_g of 129 °C when compared to that of Me-HQ/PEC (104 °C).

However, the combination of HQs with bulky substituents such as *t*Bu-HQ and Cl-PEC was not suitable for formation of the liquid crystalline state and did not exhibit any improvement in the T_g .

As the aromatic dicarboxylic acid BB has a much more rigid structure than Cl-PEC, the T_g s of the LCPs derived from BB are supposed to be much higher than those derived from Cl-PEC. Although, in the case of LCPs derived from BB, it is difficult to detect the T_g values by DSC measurements, these values have good correlation with the $E''(\max)$ parameters determined by dynamic mechanical analysis (Figure 19.11). According to this study, the T_g of Me-HQ/BB was

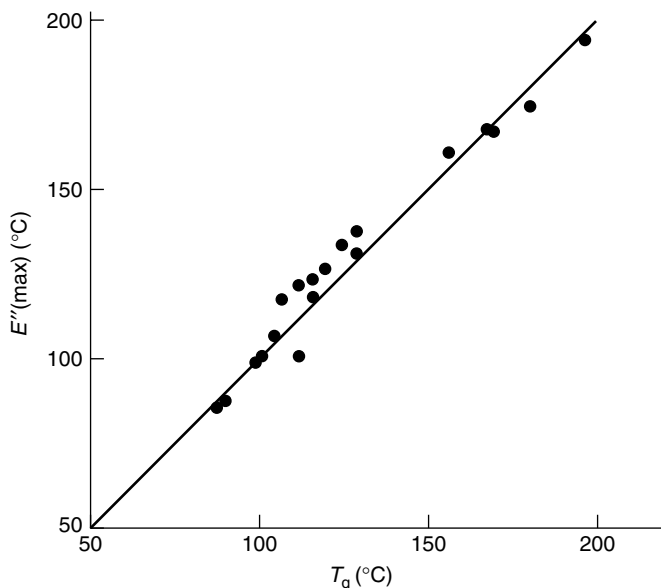


Figure 19.11 Relationship between $E''(\max)$ and T_g

175 °C, that of Ph-HQ/BB (with a bulky substituent on HQ) was 205 °C, and the T_g of CP-HQ/BB was 196 °C (see Table 19.3).

4.3.2 Heat Distortion Temperature

The heat distortion temperature (HDT), which reflects the heat resistance of injection molded specimens, has a good correlation with the T_g in the case of the polyarylates without a clear T_m , as determined by DSC measurements. For instance, Ph-HQ/BB/HBA (50/50)³ had a T_g of 178 °C ($E''(\max)$ temperature), and also an HDT of 178 °C (Figure 19.12).

On the other hand, the HDT is affected by the crystallinity of the polyarylates. Thus, polyarylates with a high crystallinity are predicted to have a high HDT.

Me-HQ/BB, having a high crystallinity, showed a higher HDT (290 °C) than CP-HQ/BB (155 °C), although the T_g of Me-HQ/BB (175 °C) is lower than that of CP-HQ/BB (196 °C) (Tables 19.3 and Table 19.5) [19]. In addition, Ph-HQ/BB having a high crystallinity exhibited a higher HDT than that estimated by the correlation between the T_g and the HDT values of amorphous LCPs, as shown in Figure 19.12 [33].

³ The ratio m/n represents the molar ratio of ph-HQ/BB (m) to Ph-HQ/HBA (where HBA = *p*-hydroxybenzoic acid) (n) in the Ph-HQ/BB/HBA copolymer.

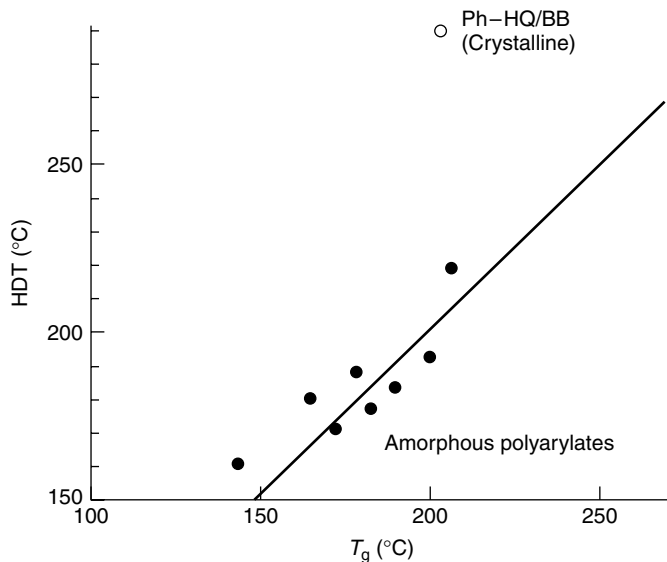


Figure 19.12 Relationship between the heat distortion temperature (HDT) (at 1.82 MPa) and T_g for the amorphous polyarylates of HBA/Ph-HQ or *t*Bu-HQ/HQ/BB and the crystalline polyarylate of Ph-HQ/BB [33]

Table 19.5 Flexural moduli and heat distortion temperature data for substituted-HQs/BB polyarylates [19]. From Inoue, T. and Tabata, N., *Mol. Cryst. Liq. Cryst.*, **254**, 417–428 (1994), and reproduced with permission of Gordon and Breach (Taylor and Francis) Publishers

Publisher's Note:
Permission to reproduce this image
online was not granted by the
copyright holder. Readers are kindly
requested to refer to the printed version
of this chapter.

Ph-HQ/HQ/BB (50/50) is a crystalline polyarylate and its HDT is 297 °C. We found that copolymerization involving small amounts of the third unit (HBA) into this system could improve its crystallinity (Figure 19.13) and HDT; finally, the HDT of the copolyarylate Ph-HQ/HQ/BB/*p*-hydroxybenzoic acid (HBA) (47.5/47.5/5) increased to above 300 °C.

The effect of the small amount of copolymerized units seems to improve the mobility of the polymer chains, and its consequent high crystallinity. We also found these same effects of small amounts in the copolymerization of HBA/PET-type LCPs [34].

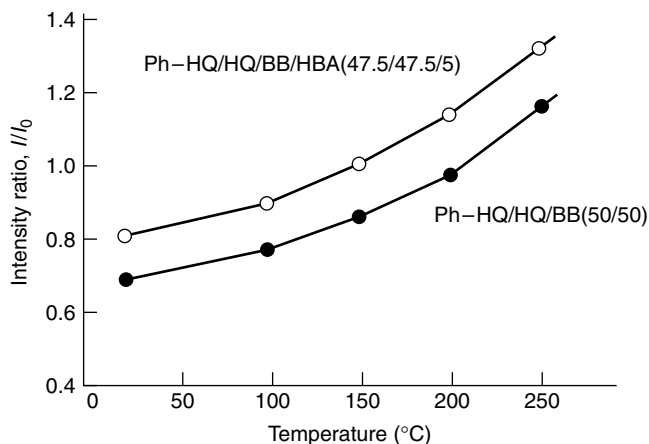


Figure 19.13 Temperature dependence of peak intensity ($2\theta = 20^\circ$); I/I_0 is the non-dimensionalized intensity, using α -alumina as the internal standard

5 CONCLUSIONS

The moduli of as-spun fibers of polyarylates depend highly upon the stability of the liquid crystalline state, the rigidity of the polymer chain, and the degree of elongational flow orientation (F -value). On the other hand, the moduli of injection molded specimens of polyarylates depend upon the stability of the liquid crystalline state, and the rigidity and packing density of the polymer chain.

Polyarylates derived from BB show a high T_g , while their HDT values depend upon both the T_g and the crystallinity.

6 ACKNOWLEDGEMENT

This work was performed under the management of the Research Association for Basic Polymer Technology as part of the R&D Program of Basic Polymer Technology for Future Industries, sponsored by the NEDO.

REFERENCES

1. Inoue, T., Liquid crystalline polymers, in *Plastics Age Encyclopedia*, Plastics Age Company Ltd, Osaka, Japan, Ch. IV-4, pp. 176–182.
2. Inoue, T., *Kagaku-Kogaku*, **58**, 374 (1994).
3. Inoue, T., *Kobunshi, High Polym., Jpn*, **43**, 730 (1994).
4. Inoue, T., *Plast. Age*, **41** 132 (1995).

5. Inoue, T. and Okita, S., in *Polymeric Materials Encyclopedia*, Salamone, J. C. (Ed.), CRC Press, Boca Raton, FL, 1996, pp. 3706.
6. Majnusz, J., Catala, J. M. and Lenz, R. W., *Eur. Polym. J.*, **19**, 1043 (1983).
7. Lenz, R. W. and Jin, J.-I., *Macromolecules*, **14**, 1405 (1981).
8. Lenz, R. W. and Jin, J.-I., *Br. Polym. J.*, **12**, 132 (1980).
9. Majnusz, J. and Lenz, R. W., *Eur. Polym. J.*, **21**, 565 (1985).
10. Dicke, H. R. and Lenz, R. W., *J. Polym. Sci., Polym. Chem. Ed.*, **21**, 2581 (1983).
11. Anton, S., Lenz, R. W. and Jin, J.-I., *J. Polym. Sci., Polym. Chem. Ed.*, **19**, 1901 (1981).
12. Kricheldorf, H. R. and Schwarz, G., *Makromol. Chem.*, **188**, 1281 (1987).
13. Osman, M. A., *Macromolecules*, **19**, 1824 (1986).
14. Krigbaum, W. R., Hakemi, H. and Kotek, R., *Macromolecules*, **18**, 965 (1985).
15. Brueggig, W., Kampschulte, U., Schmidt, H.-W. and Heitz, W., *Makromol. Chem.*, **190**, 2755 (1989).
16. Kricheldorf, H. R. and Engelhardt, J., *J. Polym. Sci., Polym. Chem. Ed.*, **28**, 2335 (1990).
17. Jackson, Jr, W. J., *Contemporary Top. Polym. Sci.*, **5**, 177 (1984).
18. Inoue, T., Thermotropic liquid crystalline polyacrylates, in *Progress in Pacific Polymer Science*, Imanishi, Y. (Ed.), Spring-Verlag, Berlin, 1992, Vol. 2, pp. 261–272.
19. Inoue, T. and Tabata, N., *Mol. Cryst. Liq. Cryst.*, **254**, 417 (1994).
20. (a) Inoue, T., Yamanaka, T., Tabata, N. and Okita, S., *High Perform. Polym.*, **7**, 303 (1995); (b) Inoue, T., Yamanaka, T., Tabata, N. and Okita, S., *J. Federation Asian Profess. Textile Assoc.*, **3**, 2 (1996).
21. Inoue, T., Okamoto, M. and Hirai, T., *Kobunshi Ronbunshu*, **43**, 253 (1986).
22. Inoue, T., Okamoto, M. and Hirai, T., *Kobunshi Ronbunshu*, **43**, 261 (1986).
23. Inoue, T., Yamanaka, T. and Okamoto, M., *Kobunshi Ronbunshu*, **45**, 661 (1988).
24. (a) Krigbaum, W. R. and Watanabe, J., *Polymer*, **24**, 1299 (1983); (b) Krigbaum, W. R., *J. Polym. Sci., Polym. Lett. Ed.*, **20**, 109 (1982).
25. Inoue, T., Tabata, N. and Yamanaka, T., *React. Functional Polym.*, **30**, 133 (1996).
26. Tashiro, K., Hou, J., Kobayashi, J. M. and Inoue, T., *J. Am. Chem. Soc.*, **112**, 8273 (1995).
27. Inoue, T., Goto, N., Tabata, N., Yamanaka, T. and Tanaka, T., *Kobunshi Ronbunshu*, **49**, 969 (1992).
28. Inoue, T. and Yamanaka, T., *Kobunshi Ronbunshu*, **45**, 783 (1988).
29. Inoue, T. and Okamoto, M., *Kobunshi Ronbunshu*, **44**, 151 (1987).
30. Inoue, T., Goto, N., Tabata, N., Yamanaka, T. and Tanaka, T., *Kobunshi Ronbunshu*, **46**, 75 (1989).
31. Inoue, T., Tabata, N. and Yamanaka T., *Polym. J.*, **28**, 424 (1996).

32. Inoue, T., Yamanaka, T., Goto, N., Tabata, N. and Tanaka, T., *Kobunshi Ronbunshu*, **48**, 765 (1991).
33. Inoue, T., Yamanaka, T., Tabata, N. and Okita, S., *High Perform. Polym.*, **7**, 1443 (1995).
34. Inoue, T., Yamanaka, T., Kurematsu, T. and Nakamura, K., *Mol. Cryst. Liq. Cryst.*, **318**, 125 (1998).

Thermotropic Liquid Crystal Polymer Reinforced Polyesters

SEONG HUN KIM

Hanyang University, Seoul, Korea

1 INTRODUCTION

Thermotropic liquid crystal polymers (TLCPs) have several advantages, such as excellent mechanical properties, good melt rheometrics for easy processing, impact absorption characteristics, chemical resistance and thermal stability. Furthermore, they have a low thermal expansion coefficient, thus providing excellent dimensional stability for injection-molded articles [1–9]. However, thermotropic LCPs have a limitation in the diversity of their applications because of their high price. Therefore, research has focused on adding minor quantities (5–30 %) of relatively expensive LCPs to commodity polymers [10–14]. These LCP blends provide some unique characteristics, such as an enhancement of the crystallization of the commodity polymers. The use of an LCP as a processing aid also acts as a compatibility enhancement, as self-reinforcement for thermoplastic composites [8, 9, 15, 16] or as fibers [17–20], and enables the utilizing of ternary blends [21, 22].

Recently, the telecommunication industry has undergone rapid expansion, and a strong consumer trend towards smaller and lighter telecommunication devices, such as cellular phones and notebook computers, is indicated. Small connection sockets and chip carriers are micro-injection-molded parts requiring the high flowability, high mechanical properties and dimensional stability of LCPs. These merits are now thought to be another application field for LCPs in the electronics industry.

This article is an overview of the novel technology of self-reinforced LCPs with polyesters, poly(ethylene terephthalate) (PET) and poly(ethylene naphthalate) (PEN) [10–13, 21, 23]. LCP/polyester blends in a polyester matrix form *in situ* fibrils which improve the mechanical properties. LCPs have an inherently low melt viscosity, and provide LCP/polyester blends that effectively lower the melt viscosity during melt spinning [24], and fast injection-molding cycles. The miscibility between the LCP and polyesters can be controlled by the degree of transesterification [25] in the reactive extrusion step, and fibril formation in LCP-reinforced polyester fibers has been studied.

2 PHB/PEN/PET MECHANICAL BLENDS

2.1 THE LIQUID CRYSTALLINE PHASE

Mechanical blending of polymers can be an effective method to improve the properties of components. However, in general, when a rigid rod polymer and a flexible polymer are simply mixed together, the blended polymers form an immiscible blend. Reactive extrusion may provide a useful way to improve the physical properties and miscibility between LCPs and thermoplastic polymers. In recent years, interest in thermoplastic liquid crystalline copolyesters has grown [23]. Binary copolyesters of poly(*p*-hydroxybenzoate) (PHB)/PET, PHB/PEN and a ternary copolyester of PHB/PEN/PET which form TLCP melts have been synthesized and studied by many researchers [21, 26–29], and the crystallization behavior and the thermal transition temperatures, including the liquid crystalline (LC) phase transition temperature, have been reported. These investigations have revealed the following:

1. Ternary copolyesters containing 30 mol % PHB are partially LC, and those containing over 50 mol % PHB are completely LC [26].
2. In copolyesters containing up to 50 mol % PHB, both PET and PEN crystals are formed. In those containing 80–90 mol % PHB, only crystals of PHB are observed [27].
3. The ternary copolyester of PHB/PEN/PET (30/35/35 (mol %)) is LC up to 160 °C, where it starts to become gradually isotropic, and becomes completely isotropic at 290 °C [28].
4. For PET/PEN copolymers, no LC phase is formed [26].

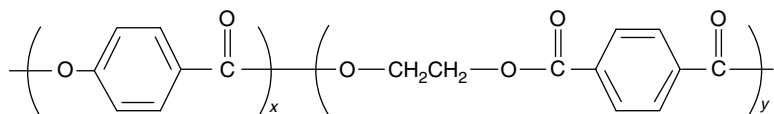
In this research, commercially available PHB/PET copolyester LCP, PEN and PET were mechanically blended to form the LC phase of the blends. The critical composition of PHB in the PEN and PET forming an LC ternary blend was investigated, and the miscibility and thermal behavior were studied using thermal analysis. The PHB content in the ternary blend was controlled by the amount of PHB/PET copolyester, as a high-molecular-weight PHB homopolyester does

not melt in the temperature range 482–538 °C, whereas the polymer rapidly decomposes in this range [26].

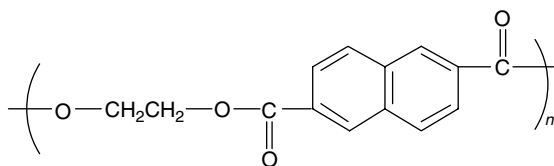
The rheological properties of the PHB/PEN/PET blends were investigated by measuring torque values during melt blending at 285 °C with a constant rotating speed of 60 rpm. The materials used in this research are shown in Figure 20.1. The torque values versus PHB content for the PHB/PEN/PET blends are shown in Figure 20.2.

Pure PEN required the highest torque (0.65 N m), because of its high melt viscosity, and pure PET also needed a high torque (0.38 N m). The torque values of the ternary blends showed similar values below 30 mol % PHB content. However, the torque values significantly decrease with increasing PHB content over 40 mol % PHB; we propose that the high PHB content allows the ternary blend to form a LC phase, as confirmed by the morphology study discussed below.

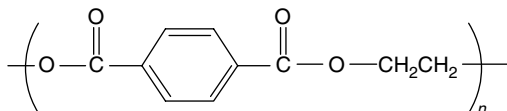
Polarized optical photographs of the blends are shown in Figure 20.3. The spherical LCP domains are irregularly dispersed in the PEN and PET phases below 20 mol % PHB content (Figure 20.3(a)). The results observed from 30 mol % PHB reveal a continuous co-existence of the PHB phase and the PEN/PET matrix in the blended polymers (Figure 20.3(b)). However, the blend with 40 mol % PHB shows a nematic LC phase. This result is similar to that found for the copolyesters synthesized by Chen and Zachmann [26], who found



Poly(*p*-hydroxybenzoate) (PHB)–poly(ethylene terephthalate) (PET), P(HB80-ET20) (Rodrun 5000) or P(HB60-ET40) (Rodrun 3000) (Unitika Company, Japan)



Poly(ethylene 2,6-naphthalate) (PEN) (IV, 0.51) (Kolon Company, Korea)



Poly(ethylene terephthalate) (PET) (IV, 0.64) (Samyang Company, Korea)

Figure 20.1 The chemical structures of the materials used in this study, i.e. the liquid crystal copolymer (PHB–PET), PEN and PET; IV, intrinsic viscosity

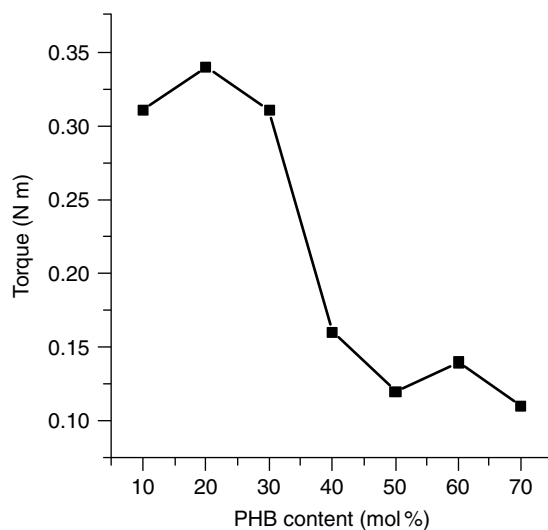


Figure 20.2 Torque value as a function of PHB content for PHB/PEN/PET ternary blends measured at 285 °C and a constant rpm of 60 using a Haake rheometer; molar ratio of PEN to PET of 1:1

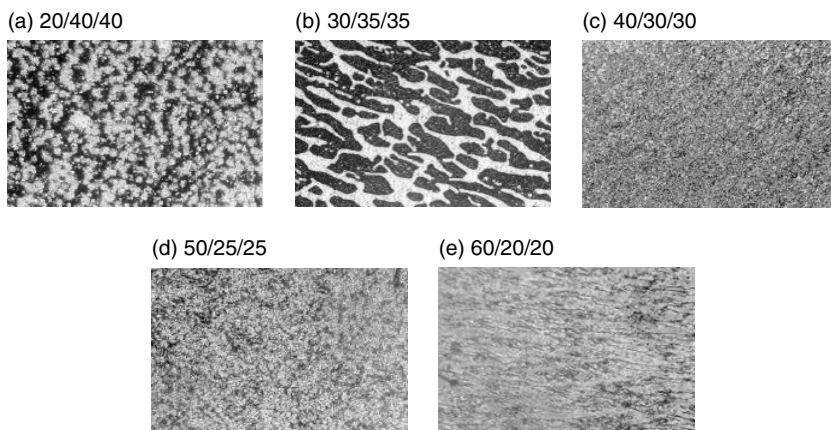


Figure 20.3 Polarized micrographs of the PHB/PEN/PET blends for various compositions (mol %)

that melts containing 30–40 mol % PHB form a LC phase. Above 50 mol % PHB content, the nematic LC phases are self-evident from the polarized micrographs. The nematic LC phase occurring above 40 mol % PHB content causes the abrupt decrease in the torque values, as shown in Figures 20.3(c)–20.3(e).

2.2 THERMAL BEHAVIOR

Differential scanning calorimetry (DSC) measurements were performed on several PEN/PET blend compositions prepared by melt blending. In the dependence of the melting behaviors on the composition, the melt temperature (T_m) and melt enthalpy (ΔH_m) appear at their lowest values at the 50/50 PEN/PET composition, as shown in Figure 20.4. This behavior indicates that at the 50/50 composition, the achievable crystallinity is the smallest possible, or that the crystalline structure formed is the least perfect. The DSC thermograms of the PHB/PEN/PET blends are shown in Figure 20.5, while the glass transition temperature (T_g) and T_m data for the blends is shown in Figure 20.6. All of the blends have a single T_g , which increases slightly with increasing PHB content. Moreover, the melting temperatures of the blends increase with increasing PHB content. The effect of a pre-heating temperature on the melting temperature of the blends is represented in Figure 20.7. The blends were pre-heated at 260, 280 and 300 °C for 2 min. At a pre-heat of 260 °C, only the PET should melt, at 280 °C, the PEN and PET portions should melt, while at 300 °C, the system should be in a completely isotropic state. As the pre-heating temperature increases, the melting temperatures decrease. The length of the 'homo-segment' in the polymer chain may be decreased, while the crystal formation is disturbed by the structural irregularity with the progress of the transesterification reaction. In other words, more randomization of the segments occurs.

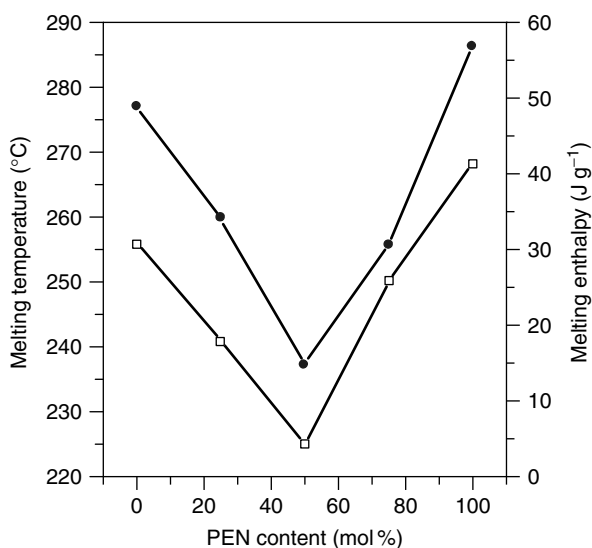


Figure 20.4 The melting temperature (□) and melting enthalpy (●) as a function of PEN content for the PEN/PET blends

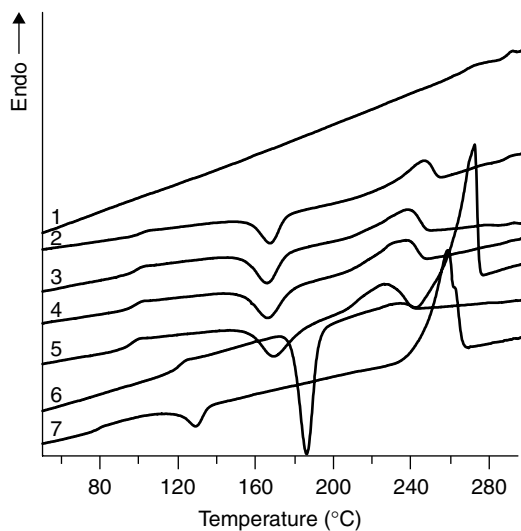


Figure 20.5 DSC thermograms of the PHB/PEN/PET blends: 1, LCP (100); 2, PHB/PEN/PET (40/30/30); 3, PHB/PEN/PET (30/35/35); 4, PHB/PEN/PET (20/40/40); 5, PHB/PEN/PET (10/45/45); 6, PEN (100); 7, PET (100) (compositions in mol %). Initial pre-heating to 280 °C at the rate of 200 °C/min, held for 2 min and then cooled to 0 °C; the second heating rate was 10 °C/min

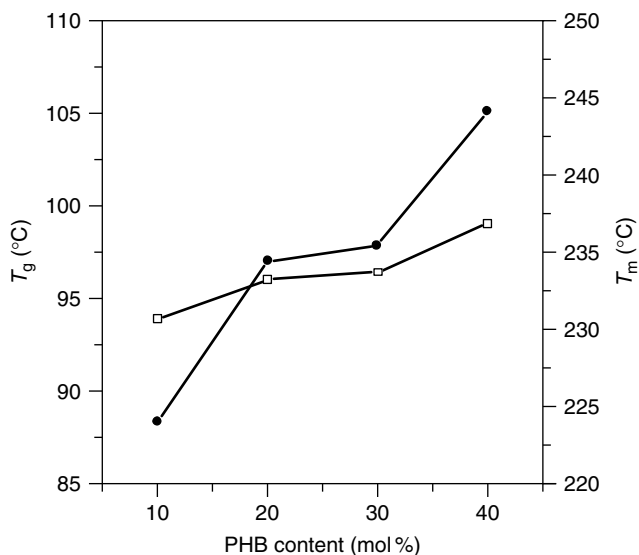


Figure 20.6 The glass transition (□) and melting (●) temperatures as a function of PHB content for the PHB/PEN/PET blends

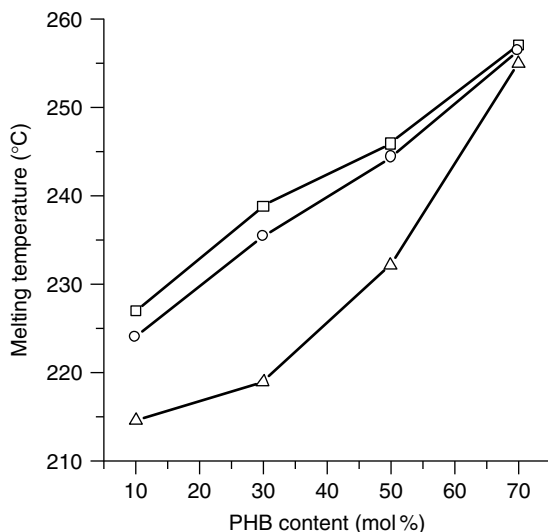


Figure 20.7 The effect of pre-heating temperatures and blend composition on the melting temperatures of the PHB/PEN/PET blends: \square , 260 °C; \circ , 280 °C; \triangle , 300 °C

2.3 MECHANICAL PROPERTIES

The mechanical properties of melt-spun monofilaments are greatly affected by the composition of the blends and the melt spinning conditions, as shown in Figure 20.8. The PHB contents are increased from 10 mol % to 40 mol % at 10 mol % increments, while the remainder of the blend, i.e. PEN/PET, is retained at a molar ratio of 1:1 for all of the blends. Both the tensile strength and the initial modulus increased with increasing PHB content and take-up speed for all compositions. This was particularly true when the take-up speed was 500 m/min, where the initial modulus of the monofilament increased significantly at 30 mol % PHB content. When the take-up speed increased to 1000 m/min, the initial modulus of the monofilament greatly increased at 40 mol % PHB content. These results are attributed to the formation of a continuous LCP fibril structure, consisting of long fibrils co-existing in the matrix polymers.

The effect of the annealing temperature on the initial modulus is also presented in Figure 20.8. The moduli of monofilaments annealed at 160 °C for 30 min are higher than those of normal monofilaments, because the matrix polymers are recrystallized with a low PHB content, and the LCP molecules in the domain are reoriented with a high PHB content. The thermal treatment of the PHB/PEN/PET fibers can be an effective way to improve the tensile properties, especially the tensile modulus, and high-speed winding may be a promising way to obtain fibers

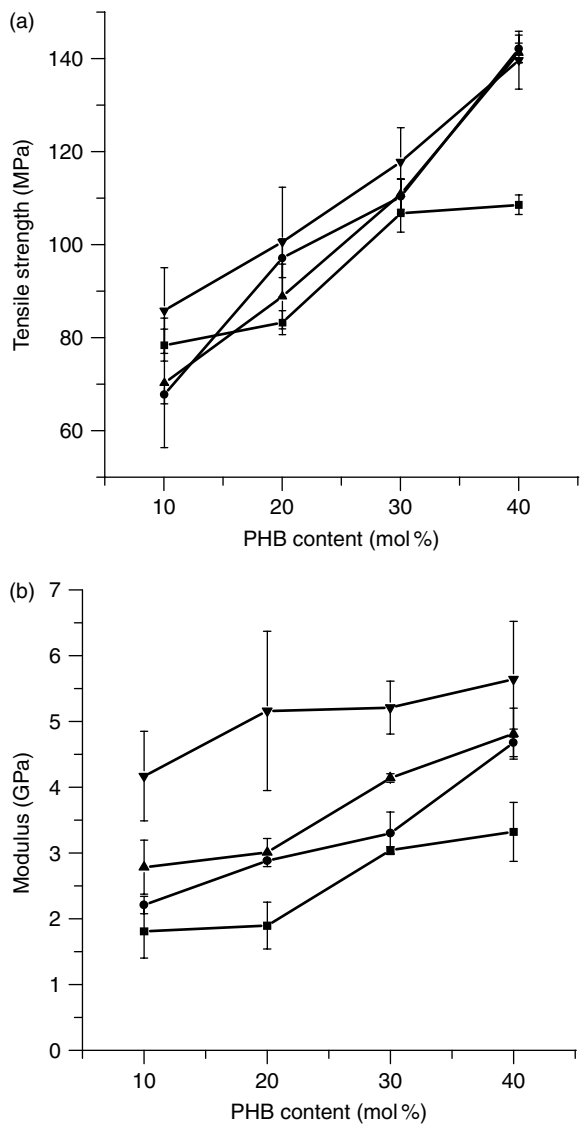


Figure 20.8 The tensile strength (a) and modulus (b) of PHB/PEN/PET as-spun and annealed monofilaments (annealed at 160 °C for 30 min); the remainder of the blend has a molar ratio of 1:1: \blacksquare , 500 m/min (quenched); \bullet , 1000 m/min (quenched); \blacktriangle , 500 m/min (160 °C); \blacktriangledown , 1000 m/min (160 °C)

with high mechanical properties fibers, caused by a high molecular orientation of the LCP in the elongational flow field.

2.4 TRANSESTERIFICATION

Transesterification, investigated by using nuclear magnetic resonance (NMR) spectroscopy, shows that the exchange reaction between PEN and PET occurs during the blending. The NMR data for the blends containing a PHB component could not be obtained because the P(HB80-ET20) (see Figure 20.1) LCP component did not dissolve in dentero(d)-trifluoroacetic acid. Therefore, the NMR spectra were only obtained for the soluble PEN and PET components. The degree of transesterification in the blends could be determined from the area that the ethylene units occupied in the NMR spectrum. The PET peak appeared at 5.11 ppm, and the PEN peak at 5.30 ppm, while a new peak also appeared at 5.25 ppm. This was attributed to the ethylene units, which exist between the terephthalic and naphthalic groups in the polymer backbone. The NMR spectra are shown in Figure 20.9 [21]. According to the theory of probabilistic analysis [30], the block length of the naphthalate unit (Ln_{PEN}) and the terephthalate unit (Ln_{PET}), as well as the probabilities (P_{NT} and P_{TN}) of finding N (or T) units next to T (or N) units, can be calculated from the integrated intensities of the resonance peaks (f_{NET} , f_{NET} and f_{TET}) as follows:

$$P_{NT} = \frac{f_{NET}}{(f_{NET} + 2f_{NEN})} = \frac{1}{Ln_{PEN}} \quad (20.1)$$

$$P_{TN} = \frac{f_{TEN}}{(f_{TEN} + 2f_{TET})} = \frac{1}{Ln_{PET}} \quad (20.2)$$

The degree of randomness (B) can be defined as the sum of the two probabilities ($P_{NT} + P_{TN}$). For random copolymers, $B = 1$, for alternative copolymers, $B = 2$, while for block copolymers or physical blends, B is close to zero.

Table 20.1 gives the various parameters of the blends as a function of blending time [21,31]. The degree of randomness is significantly influenced by the blending time, but is only negligibly influenced by the blend composition. The degree of transesterification can also be determined from the blending time. The degree of randomness changed from $B = 0$ to $B = 1$, which means that the system changed from blends of homopolymer to random copolymers. However, the blending time was only valid up to 20 min, because excess melt blending can have had an effect on the molecular weight decrement caused by excess transesterification, thermal degradation and hydrolysis. When the melt blending was kept continuous over a period of 20 min, then the degree of randomness changed from random ($B = 1$) to alternative copolymer ($B = 2$).

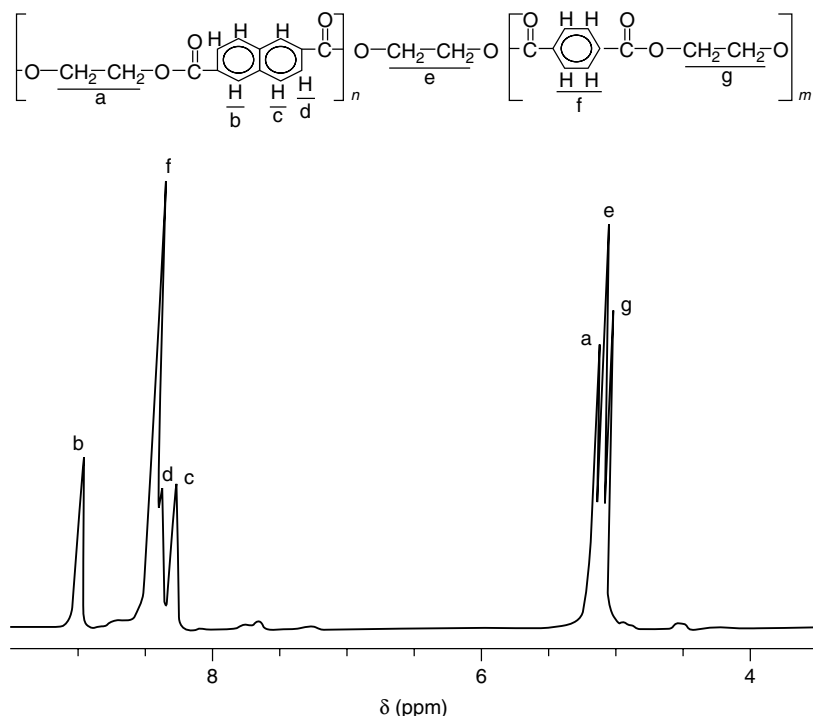


Figure 20.9 The ^1H -NMR spectrum at 300 MHz, showing the assignments of the absorptions for the PHB/PEN/PET blends dissolved in *d*-trifluoroacetic acid [21]. From Kim, S. H., Kang, S. W., Park, J. K. and Park, Y. H., *J. Appl. Polym. Sci.*, **70**, 1065–1073 (1998), Copyright © (1998, John Wiley & Sons, Inc.). This material is used by permission of John Wiley & Sons, Inc

The effect of blending time on the sequential length of the PEN and PET segments is shown in Figure 20.10 [31]. The sequential lengths of the PEN and PET segments clearly decreased from the initial blending time, but slightly decreased at blending times greater than 10 min. This is closely related to the change in chemical structure and, especially, the intermolecular chain reaction known as transesterification.

3 EFFECT OF A CATALYST ON THE COMPATIBILITY OF LCP/PEN BLENDS

3.1 MECHANICAL PROPERTY IMPROVEMENT

Since thermotropic LCPs have recently been used in applications requiring high modulus and strength, much effort has been expended to improve the processability

Table 20.1 The content of the hetero sequence (f_{TEN}), sequence lengths of the PET segment (Ln_{PET}) and PEN segment (Ln_{PEN}) and degree of randomness (B) of the PHB/PEN/PET blends [21]. From Kim, S. H., Kang, S. W., Park, J. K. and Park, Y. H., *J. Appl. Polym. Sci.*, **70**, 1065–1073 (1998), Copyright © (1998, John Wiley & Sons, Inc.). This material is used by permission of John Wiley & Sons, Inc

Composition of PHB/PEN/PET (mol %)	Blending time (min)	f_{TEN}	Ln_{PET}	Ln_{PEN}	B
13/38/49	5	0.015	80.00	53.48	0.031
	10	0.128	9.07	6.52	0.264
	15	0.209	5.63	3.95	0.431
	20	0.336	3.43	2.53	0.688
34/25/41	5	0.030	37.59	28.17	0.062
	10	0.165	6.33	5.79	0.331
	15	0.299	3.47	3.20	0.600
	20	0.399	2.66	2.42	0.789
52/16/32	5	0.010	90.91	106.38	0.020
	10	0.158	4.85	7.84	0.334
	15	0.298	2.69	4.02	0.621
	20	0.396	2.11	2.94	0.815

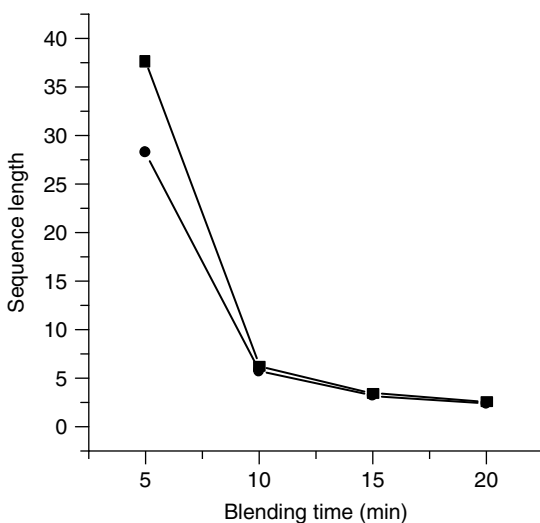


Figure 20.10 The effect of the blending time as a function of sequence length of the PET (■) and PEN (●) segments for the PHB/PEN/PET (40/30/30 (mol %)) blends [31]. From Park, J. K., Jeong, B. J. and Kim, S. H., Pseudo liquid crystallinity and characteristics of PHB/PEN/PET melt blend, *Polym. (Korea)*, **24**, 113–123 (2000). Reproduced by permission of The Polymer Society of Korea

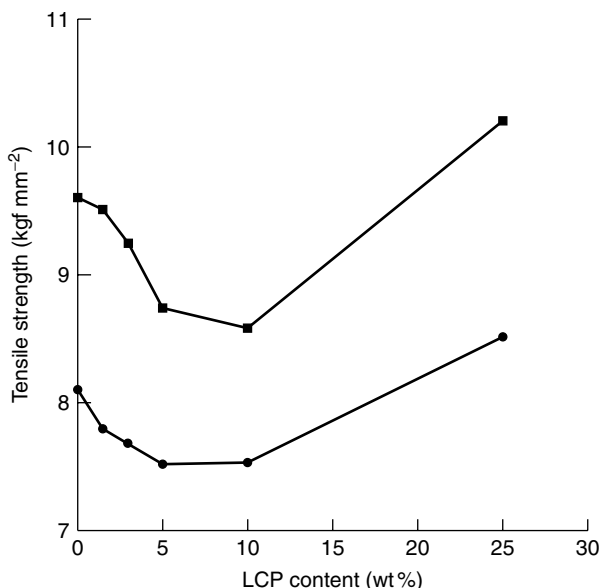


Figure 20.11 The tensile strength of the LCP/PEN blends as a function of the LCP content at draw ratios of 10 (●) and 20 (■) [13]. From Kim, S. H., Hong, S. M., Hwang, S. S. and Yoo, H. O., *J. Appl. Polym. Sci.*, **74**, 2448–2456 (1999), Copyright © (1999, John Wiley & Sons, Inc.). This material is used by permission of John Wiley & Sons, Inc

and also develop the desired mechanical properties of the semicrystalline polymers through *in situ* reinforcement technology [13]. The tensile strength and modulus for several LCP/PEN blend fibers drawn at 290 °C are plotted versus the LCP content in Figures 20.11 and 20.12 [13]. The mechanical properties of the PEN/LCP blend fibers are significantly affected by draw ratio, because of the micro-fibrillation and the orientation of the dispersed LCP domains. The abrupt drop-off in tensile strength of the as-spun fibers at a certain LCP content is indeed striking, while the modulus is enhanced by the incorporation of the liquid crystalline polymer. However, this phenomenon is not rare in blends having liquid crystalline components. Brody observed that a 3 % liquid crystalline additive in PET reduces the spin orientation, and called this phenomenon ‘windup speed suppression’ (WUSS) [32]. If the above premise is accepted, then the low tensile strengths of the blend fibers can be readily explained (at least for the 90/10 LCP/PEN blend composition). An orientation suppression would lead to low tensile strength values [32]. It is worth mentioning that LCP/PEN blend fibers display extremely low melt viscosities. Droplet deformation can be increased by any of the following factors: an increase in the medium viscosity, extension rate, dispersed LCP droplet size, or decrease in interfacial stress [33]. To overcome fiber spinning problems due to the drastic

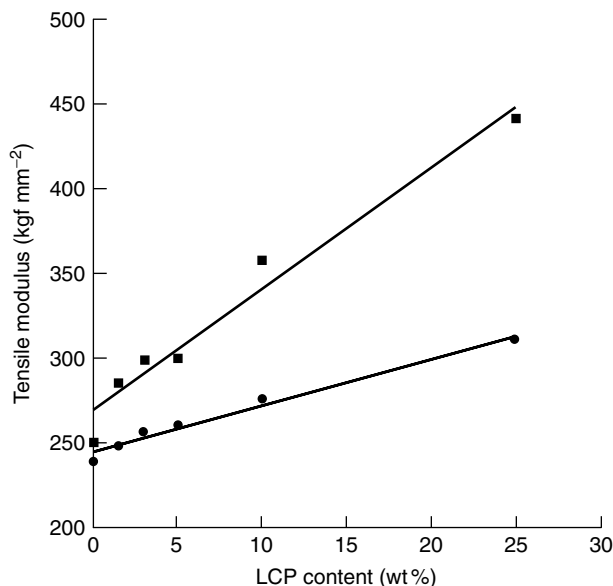


Figure 20.12 The tensile modulus of the LCP/PEN blends as a function of the LCP content at draw ratios of 10 (●) and 20 (■) [13]. From Kim, S. H., Hong, S. M., Hwang, S. S. and Yoo, H. O., *J. Appl. Polym. Sci.*, **74**, 2448–2456 (1999), Copyright © (1999, John Wiley & Sons, Inc.). This material is used by permission of John Wiley & Sons, Inc

drop-off in viscosity, it was decided to use a higher-intrinsic-viscosity (IV) PEN resin. This can be explained by the fact that the viscosity of the matrix PEN was too low to deform and break the spherical particles of the dispersed LCP phase [30]. Blends with the higher-IV (high-molecular-weight) PEN resin showed a higher melt strength and modulus during processing [34].

Figures 20.13 and 20.14 describe the effect of dibutyltin dilaurate (DBTDL) on the tensile strength and tensile modulus for the 25/75 LCP/PEN blend fibers at draw ratios of 10 and 20 [13]. As expected, the addition of DBTDL slightly enhances the mechanical properties of the blends up to ca. 500 ppm of DBTDL. The optimum quantity of DBTDL seems to be about 500 ppm at a draw ratio of 20. However, the mechanical properties deteriorate when the concentration of catalyst exceeds this optimum level. From the previous relationships between the rheological properties and the mechanical properties, it can be discerned that the interfacial adhesion and the compatibility between the two phases, PEN and LCP, were enhanced. Hence, DBTDL can be used as a catalyst to achieve reactive compatibility in this blend system. This suggests the possibility of improving the interfacial adhesion between the immiscible polymer blends containing the LCP by reactive extrusion processing with a very short residence time.

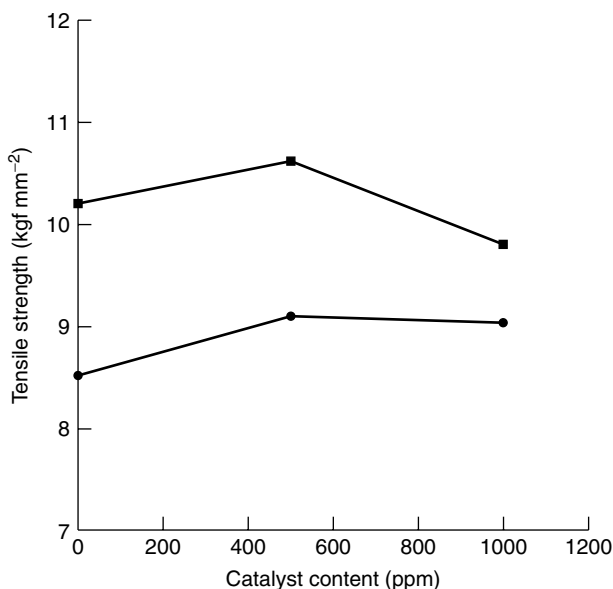


Figure 20.13 The tensile strength of 25/75 LCP/PEN blends as a function of the catalyst content at draw ratios of 10 (●) and 20 (■) [13]. From Kim, S. H., Hong, S. M., Hwang, S. S. and Yoo, H. O., *J. Appl. Polym. Sci.*, **74**, 2448–2456 (1999), Copyright © (1999, John Wiley & Sons, Inc.). This material is used by permission of John Wiley & Sons, Inc

3.2 DISPERSION OF LCP IN PEN

As a rule, the mechanical properties of the *in situ* composite are greatly influenced by the resultant morphology. First, the LCP domains must be uniformly dispersed within the matrix. Secondly, the dispersed LCP domains must be effectively deformed during the fabrication process to raise the aspect ratio to a high enough value to enable reinforcement. Thirdly, good interfacial adhesion between the two incompatible phases is essential for high-performance properties. In this respect, the addition of DBTDL as a reaction catalyst to the 25/75 LCP/PEN blend is expected to enhance the interface adhesion via reactive extrusion in the LCP/PEN blends, and such results were observed using scanning electron microscopy (SEM). Figure 20.15 shows SEM micrographs of the PEN/LCP blend fibers after an Instron tensile test at a draw ratio of 20 [13]. The LCP/PEN blend fibers consist of two phases, the structure of which is composition-dependent. At 10 wt % LCP content, the LCP is dispersed as ellipsoidal particles, while at 25 wt % LCP content, the LCP is dispersed as fibrils or rod-like structures. In all cases, the major phase forms the matrix, and the minor phase is segregated into dispersed phases.

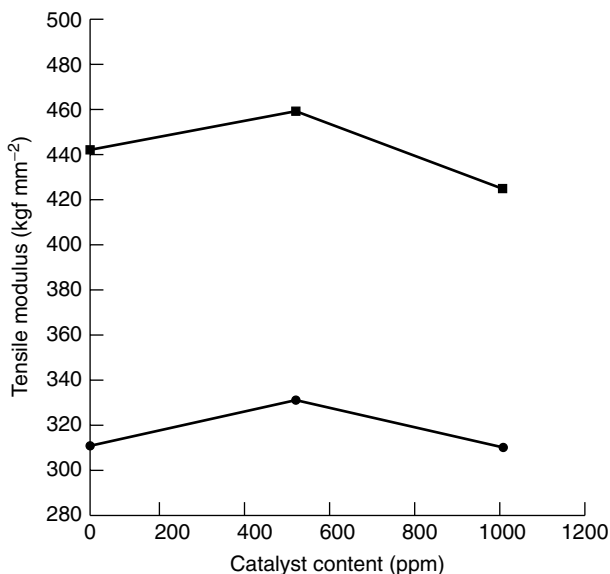


Figure 20.14 The tensile modulus of 25/75 LCP/PEN blends as a function of the catalyst content at draw ratios of 10 (●) and 20 (■) [13]. From Kim, S. H., Hong, S. M., Hwang, S. S. and Yoo, H. O., *J. Appl. Polym. Sci.*, **74**, 2448–2456 (1999), Copyright © (1999, John Wiley & Sons, Inc.). This material is used by permission of John Wiley & Sons, Inc

3.3 HETEROGENEITY OF THE BLEND

The $\log G'$ versus $\log G''$ plots of the various PHB/PEN/PET blends are presented in Figure 20.16, where the slopes of the plots are measures of the homogeneity of the system [35]. If the slope is zero, then the blend system is heterogeneous, and if it approaches 2, it means that the blend system is tending to a homogeneous system. The slopes of the plots in Figure 20.16 increase with the addition of excess PHB to the blend system.

4 THERMODYNAMIC MISCIBILITY DETERMINATION OF TLCP AND POLYESTERS

In general, the miscibility between two polymers can be predicted by thermal characterization of the blends [36]. One of the most simple and effective ways to predict miscibility between two polymers is to consider the behavior of the glass transition temperature in the blend systems, which is known as the T_g method. In miscible blend systems, only a single T_g intermediate between two components appears in the amorphous state. Therefore, we studied the change of

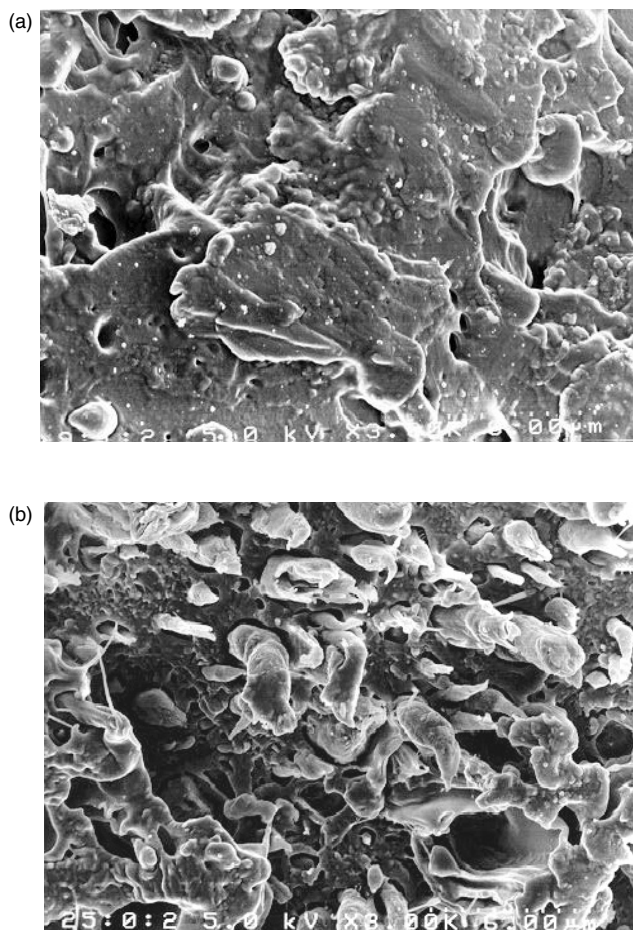


Figure 20.15 SEM fractographs of the LCP/PEN blend fibers after Instron tensile tests: (a) 10/90 (wt %); (b) 25/75 (wt %) [13]. From Kim, S. H., Hong, S. M., Hwang, S. S. and Yoo, H. O., *J. Appl. Polym. Sci.*, **74**, 2448–2456 (1999), Copyright © (1999, John Wiley & Sons, Inc.). This material is used by permission of John Wiley & Sons, Inc

the glass transition temperature in the DSC curves for the P(HB60-ET40)/PET and P(HB80-ET20)/PET blends (Figures 20.17 and 20.18).

PET ($IV = 0.64$ dl/g) was used, while the LCPs used in this study were composed of 60 mol % poly(*p*-hydroxybenzoate) and 40 mol % PET for Rodrun 3000 (P(HB60-ET40)), and 80 mol % PHB and 20 mol % PET for Rodrun 5000 (P(HB80-ET20)). A Haake Rheomix 600, with an internal mixer, was used to blend the samples according to the compositions shown in Table 20.2.

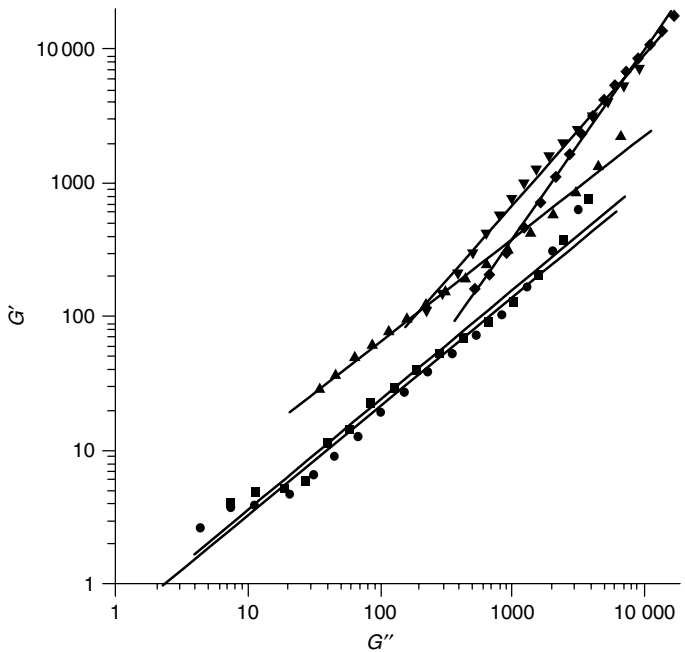


Figure 20.16 Log G' versus log G'' plots of PHB/PEN/PET blends at 290 °C: ■, 10/45/45 (slope, 0.82); ●, 20/40/40 (slope, 0.81); ▲, 30/35/35 (slope, 0.77); ▼, 40/30/30 (slope, 1.12); ◆, 50/25/25 (slope 1.41): compositions in mol %

Table 20.2 Compositions used for the P(HB60-ET40) and P(HB80-ET20) blends

Copolymer	PHB/PET composition (mol %)	LCP/PET composition (wt %)
P(HB60-ET40)	10/90	13/87
	20/80	28/72
	30/70	44/56
	40/60	61/39
	50/50	79/21
	60/40	100/0
P(HB80-ET20)	20/80	19/81
	40/60	41/59
	60/40	68/32
	80/20	100/0

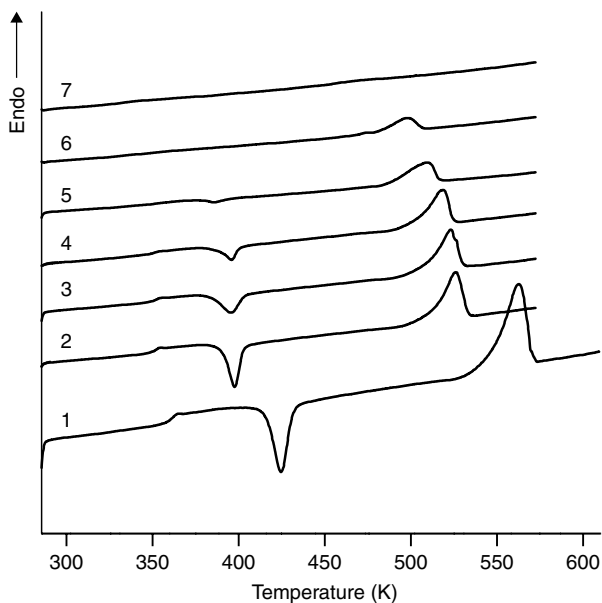


Figure 20.17 DSC curves of the P(HB60-ET40)/PET blends: 1, pure PET; 2, 13/87; 3, 28/72; 4, 44/56; 5, 61/39; 6, 79/21; 7, pure P(HB60-ET40): compositions in wt %

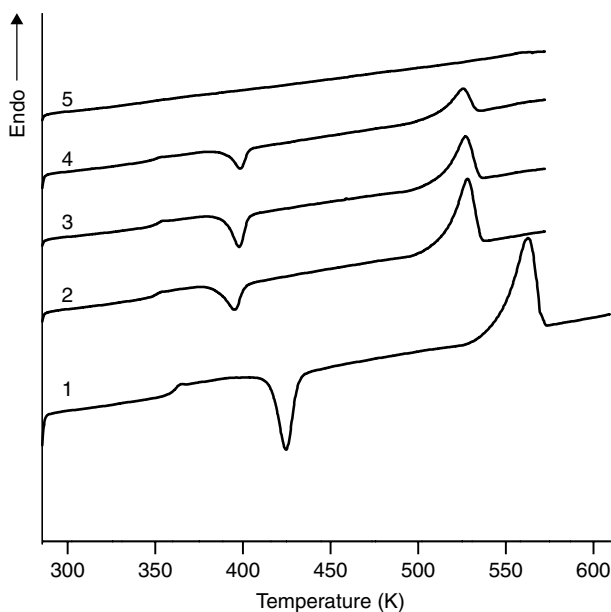


Figure 20.18 DSC curves of the P(HB80-ET20)/PET blends: 1, pure PET; 2, 19/81; 3, 41/59; 4, 68/32; 5, pure P(HB80-ET20): compositions in wt %

Melt blending was conducted for 5 min at 558 K and 60 rpm. Several thermodynamic values were obtained by employing a Perkin Elmer DSC-7 differential scanning calorimeter, which were essential to predict miscibility between the two polymers. The samples were pre-heated from 313 to 573 K using a heating rate of 200 K/min, held for 2 min, and then rapidly quenched to 313 K. They were then reheated to 573 K at a heating rate of 10 K/min. The inflection-point value in the transition was taken as the T_g . In addition, to make use of the melting temperature (T_m) as a function of the crystallization temperature (T_c), isothermal crystallization was performed. The samples were crystallized at the desired T_c directly after being melted for 2 min at 573 K and quenched. The observed T_c values were 413, 433, 453, 473 and 493 K, respectively, for each sample.

In Figure 20.17, only a single T_g was observed in the 13/87, 28/72, 44/56 and 61/39 wt % P(HB60-ET40)/PET blends. The observed T_g values were slightly lower than that of pure PET (352.2 K), where we could predict that the blends were miscible. Likewise, the DSC results presented in Figure 20.18 show that in the 19/81, 41/59 and 68/32 wt % P(HB80-ET20)/PET blends, a single T_g was observed, which was lower than that of pure PET. These three blends may be miscible. However, no T_g was detected in the 79/21 and 100/0 wt % P(HB60-ET40)/PET blends, and in the 100/0 wt % P(HB80-ET20)/PET blend. This is because of either (a) a high content of rigid rod-like liquid crystalline component, or (b) an enthalpy which was too small to detect. The dependence of T_g on the blend composition can be evaluated by using the Gordon–Taylor Equation [37], as follows:

$$T_g = \frac{w_1 T_{g1} + w_2 T_{g2}}{w_1 + k w_2} \quad (20.3)$$

where w_1 and w_2 are the weight fractions in the amorphous state of components 1 and 2, respectively. T_{g1} and T_{g2} are the respective T_g values of the pure components. The parameter k is often related to the strength of the intermolecular interactions between the components in the blends, and used as an empirical fit parameter [37]. From the Gordon–Taylor equation, the k values in both the P(HB60-ET40)/PET and P(HB80-ET20)/PET blends were in the range 0.91–0.99, except for the blends that had no detectable T_g . As it was difficult to detect T_g in pure P(HB60-ET40) and P(HB80-ET20), we used the T_g of P(HB60-ET40) as 331.6 K and the T_g of P(HB80-ET20) as 343.4 K [38]. A uniform k value is often considered to be evidence that the polymer pair is thermodynamically miscible in the amorphous state [39].

Another effective and valuable approach to assess the miscibility between the components in semicrystalline polymer blends is to use melting point depression. In miscible polymer blends, the melting point generally decreases with respect to the pure polymer due to molecular interaction. As shown in Figure 20.17, the melting points in the P(HB60-ET40)/PET blend systems decreased with increasing LCP (P(HB60-ET40)) content, but in the P(HB80-ET20)/PET systems, shown in Figure 20.18, the melting points were almost the same, or only

slightly increased. This was interesting considering the fact that different compositions of LCP copolymers, P(HB60-ET40) (60 wt % of PHB and 40 wt % of PET), and P(HB80-ET20) (80 wt % of PHB and 20 wt % of PET) showed different melting behavior. This was thought to be due to the different PHB and PET contents, and to the degree of transesterification.

The extent of the melting point depression in the blends offers a measure of the interaction parameter, as described by the Flory–Huggins theory [40, 41]. As reported by Penning and Manley, morphological parameters such as crystal thickness, as well as thermodynamic factors, affect the melting point depression [39]. The Hoffman–Weeks Equation [42] provides a convenient way to obtain the equilibrium melting temperature (T_m^0) in the polymer blends, and is represented as a plot of apparent melting temperature (T_m) as a function of the isothermal crystallization temperature, according to the following:

$$T_m = \frac{T_c}{\gamma} + \left(1 - \frac{1}{\gamma}\right) \times T_m^0 \quad (20.4)$$

where γ refers to the ratio of the initial to the final lamellar thickness. The equilibrium melting temperature (T_m^0) is obtained by intersecting this line with the line where $T_m = T_c$. The results obtained the calculated T_m^0 values are shown in Figure 20.19 and in Table 20.3.

In this study, melting point depression was used to obtain the parameter χ_{12} , known as the Flory–Huggins interaction parameter [40]:

$$\frac{1}{T_m^0} - \frac{1}{T_m^{0'}} = -\frac{RV_2}{\Delta H_2 V_1} \left[\frac{\ln \phi_2}{m_2} + \left(\frac{1}{m_2} - \frac{1}{m_1} \right) (1 - \phi_2) + \chi_{12} (1 - \phi_2)^2 \right] \quad (20.5)$$

where $T_m^{0'}$ and T_m^0 are the equilibrium melting points of the blend and PET, respectively, and ΔH_2 is the heat of fusion of 100 % crystalline PET [43]. The parameters V_1 and V_2 are respectively, the molar volumes of the repeating units

Table 20.3 Results obtained for the equilibrium melting temperatures from the Hoffman–Weeks plots of the P(HB60-ET40)/PET and P(HB80-ET20)/PET blends

Copolymer	LCP/PET (wt %)	T_m^0 (K)	T_m^0 (°C)
P(HB60-ET40)/PET	0.28/0.72	522.9	249.9
	0.44/0.56	517.4	244.4
	0.61/0.39	510.2	237.2
P(HB80-ET20)/PET	0.19/0.81	522.5	249.5
	0.41/0.59	520.7	247.7
	0.68/0.32	519.1	246.1

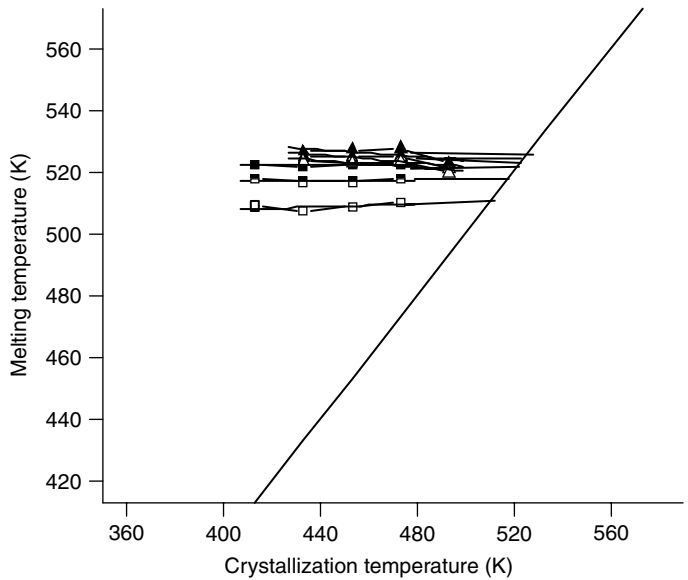


Figure 20.19 Hoffman–Weeks plots for the liquid crystallization polymer/PET blends with various compositions (in wt%): ■, P(HB60-ET40)/PET (28/72); ■, P(HB60-ET40)/PET (44/56); □, P(HB60-ET40)/PET (61/39); ▲, P(HB80-ET20) (19/81); △, P(HB80-ET20) (41/59); △, P(HB80-ET20) (68/32); the continuous line indicates $T_m = T_c$

Table 20.4 Density, molecular weight, heat of fusion, molar volume and degree of polymerization of PET, P(HB60-ET40)/PET and P(HB80-ET20)/PET blends

Polymer/blend	ρ (g/cm ³)	M_w (g/mol)	ΔH_2 (J/mol)	V_1 (cm ³ /mol)	V_2 (cm ³ /mol)	m_1	m_2
PET	1.38	12 444	117.6 ^a	—	139.1	—	64.8
P(HB60-ET40)/PET	1.40 ^b	21 500 ^b	—	106.3	—	144.5	—
P(HB80-ET20)/PET	1.41 ^b	19 500 ^b	—	95.3	—	145.1	—

^a Value taken from the literature [13].

^b Value taken from the literature [8].

of LCP and PET, while ϕ_1 and ϕ_2 are the volume fractions of LCP and PET, respectively. The degree of polymerization of LCP and PET are denoted by m_1 and m_2 , respectively. Some of the values required to calculate χ_{12} in the blends are presented in Table 20.4.

Generally, a negative χ_{12} interaction parameter means that the polymer pair is miscible, and by using the values shown in Table 20.4, we obtained negative χ_{12} values of ca. -3.5×10^{-4} to -6.7×10^{-4} for the P(HB60-ET40)/PET system

and -1.9×10^{-4} to -12.0×10^{-4} for the P(HB80-ET20)/PET system, which implies that these LCP/PET blends are miscible.

In the LCP/PET blend system, the miscibility of the polymer pair was studied. The DSC data showed that as the LCP content increased, only a single glass transition temperature appeared in both the P(HB60-ET40)/PET and P(HB80-ET20)/PET blends, which means that these blends are miscible. However, in the blends with excessive LCP contents, no glass transition temperatures were observed, owing to the high portion of rigid rod-like liquid crystalline components. The melting points decreased with increasing P(HB60-ET40) component in the P(HB60-ET40)/PET blends, and were almost unchanged in the P(HB80-ET20)/PET blends. These results indicate that the two blend systems have different melting behaviors. The Flory–Huggins interaction parameter, χ_{12} , showed negative values, which implies miscibility in the LCP/PET blend systems.

5 CRYSTALLIZATION KINETICS OF LCP WITH POLYESTERS

To understand the crystallization mechanism at a certain processing temperature, studies on the crystallization of the PHB/PEN/PET ternary blend containing 40 mol% PHB with a 1:1 ratio of PEN to PET were performed. However, this PHB/PEN/PET ternary blend did not show a distinct melt crystallization peak (T_{mc}), so the PHB/PET and PHB/PEN binary blends were studied for dynamic non-isothermal and isothermal crystallization kinetics. P(HB80-ET20) LCP (Rodrun 5000), PEN (IV, 0.51 dl/g), and PET (IV, 0.64 dl/g) were reactively blended using a HAKKW Rheomix 600 at 285 °C for 5 min. The composition ratios of the PHB/PEN and PHB/PET binary blends were matched with the ternary PHB40/PEN30/PET30 blends, as shown in Table 20.5. Thermal analysis was performed using a Perkin Elmer DSC7, and calibrated by using zinc and indium. All of the detailed experimental procedures and discussion of the results have appeared in a previous publication [44].

The non-isothermal crystallization dynamics were performed using DSC, employing cooling rates of 2.5, 5, 10, 20, 25, 30, 35 and 40 °C/min. The isothermal crystallization dynamics were studied for each sample heated to 290 °C, with a 5 min hold time, and cooled to the isothermal crystallization temperature using a cooling rate of 200 °C/min, and then holding for 40 min to obtain the crystallization exotherm.

Table 20.5 The blend ratios and weights of each component in the binary blends

Molar ratio	wt of component (g)
PHB: PEN, 4:3	LCP: PEN, 32.5:17.6
PHB: PET, 4:3	LCP: PET, 40.0:10.1

5.1 NON-ISOTHERMAL CRYSTALLIZATION DYNAMICS

The exothermic crystallization peaks using the defined cooling rates for the P(HB80-ET20)/PET (weight ratio, 4:3) and P(HB80-ET20)/PEN (weight ratio, 4:3) blends are shown in Figures 20.20 and 20.21 [44].

Generally, the spherulites had a long enough activation time at the slow cooling rate, and the spherulites had insufficient activation time at the fast cooling rate. In our own research, the crystallization spherulites formed at the slow cooling rate. The theory of isothermal crystallization dynamics uses the Ozawa Equation [45], as suggested from a modification of the Avrami Equation [46], to yield the following equation:

$$X_c(t) = 1 - \exp\left(\frac{-K(t)}{|a|^n}\right) \quad (20.6)$$

The Ozawa equation of isothermal crystallization dynamics applied to non-isothermal crystallization assumes that the crystallization proceeds under a constant cooling rate, from the valid mathematical derivation of Evans [47]. In

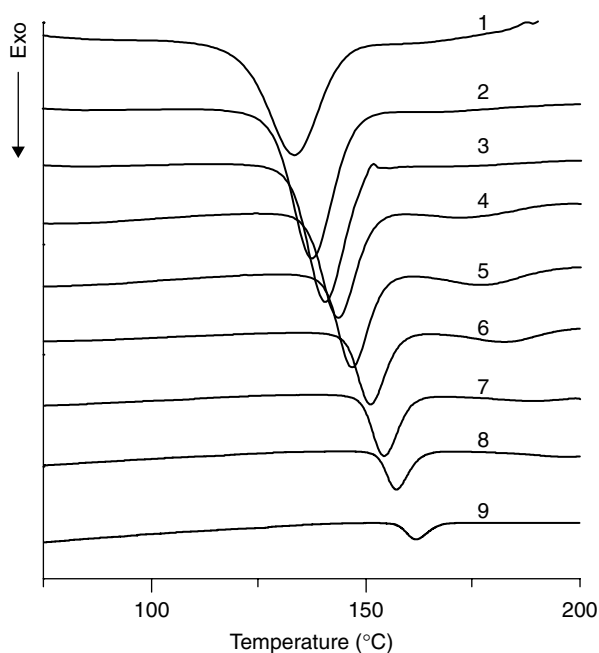


Figure 20.20 DSC thermograms of the dynamic crystallization of P(HB80-ET20)/PET (4:3 (wt%)) at various rates (°C/min): 1, 40; 2, 35; 3, 30; 4, 25; 5, 20; 6, 15; 7, 10; 8, 5; 9, 2.5 [44]. From Park, J. K., Park, Y. H., Kim, D. J. and Kim, S. H., Crystallization kinetics of TLCP with polyester blends, *J. Korean Fiber Soc.*, **37**, 69–76 (2000). Reproduced with permission of The Korean Fiber Society

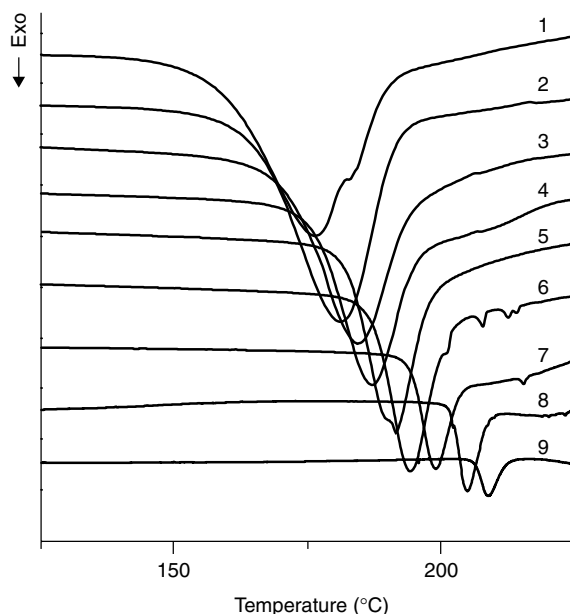


Figure 20.21 DSC thermograms of the dynamic crystallization of P(HB80-ET20)/PEN (4:3 (wt%)) at various rates ($^{\circ}\text{C}/\text{min}$): 1, 40; 2, 35; 3, 30; 4, 25; 5, 20; 6, 15; 7, 10; 8, 5; 9, 2.5 [44]. From Park, J. K., Park, Y. H., Kim, D. J. and Kim, S. H., Crystallization kinetics of TLCP with polyester blends, *J. Korean Fiber Soc.*, **37**, 69–76 (2000). Reproduced with permission of The Korean Fiber Society

Equation 20.6, $X_c(t)$ refers to the relative crystallinity at a constant temperature, t , $K(t)$ is related to the overall crystallization rate and indicates how fast crystallization occurs, a is the rate of crystallization, and n is the Avrami constant, which is dependent on the trend and shape of crystal growth. The effects of folded chain length and secondary crystallization can be ignored, because the experiment was performed under continuous temperature depression. Figures 20.22 and 20.23 show that a regression results from a plot of $\ln[-\ln(1 - X_c(t))]$ versus $\ln|a|$ at a given temperature with P(HB80-ET20)/PET (weight ratio, 4:3) and P(HB80-ET20)/PEN (weight ratio, 4:3) [44]. The Avrami constant, n , and the cooling crystallization function, $K(t)$, values are shown in Table 20.6 [44].

The P(HB80-ET20)/PET (weight ratio, 4:3) and P(HB80-ET20)/PEN (weight ratio, 4:3) blends show n values of 3.02–3.06 and 3.10–3.42, respectively. The three-dimensional spherulites grow in the blend system, as shown by the Avrami constant. The $K(t)$ values decrease with increasing crystallization temperature. The rate of crystallization growth of PEN was faster than that of PET, because the spherulite growth rate of PEN was faster, and this accelerated with the rate of crystallization growth [48].

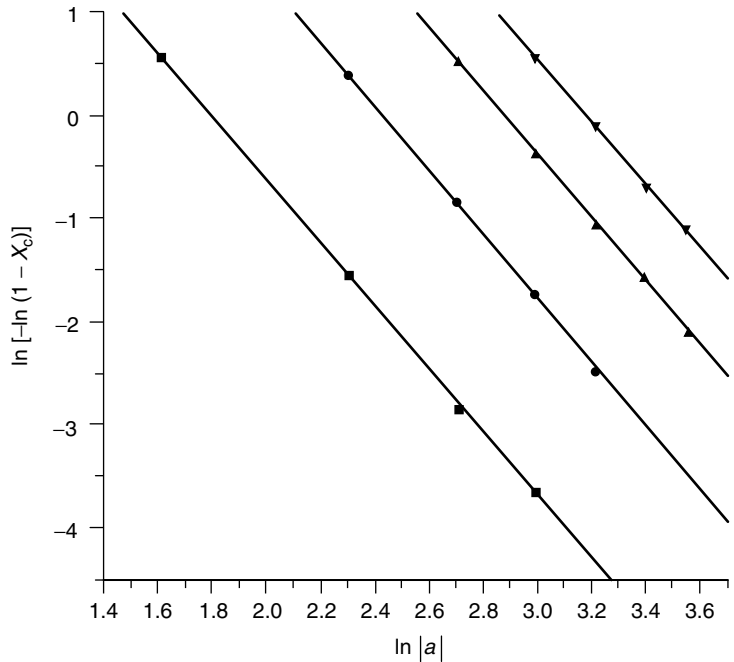


Figure 20.22 Plots of $\ln[-\ln(1 - X_c)]$ as a function of $\ln |a|$ at various temperatures for P(HB80-ET20)/PET (weight ratio, 4:3): ▼, 144 °C; ▲, 149 °C; ●, 153 °C; ■, 157 °C [44]. From Park, J. K., Park, Y. H., Kim, D. J. and Kim, S. H., Crystallization kinetics of TLCP with polyester blends, *J. Korean Fiber Soc.*, **37**, 69–76 (2000). Reproduced with permission of The Korean Fiber Society

Table 20.6 The kinetic parameters of the LCP/PET and LCP/PEN blends at each temperature [44]. From Park, J. K., Park, Y. H., Kim, D. J. and Kim, S. H., ‘Crystallization Kinetics of TLCP with polyester blends’, *J. Korean Fiber Soc.*, **37**, 69–76 (2000). Reproduced by permission of The Korean Fiber Society

Composition (weight ratio)	Temperature (°C)	Avrami exponent, n	Crystallization function, $K(t)$
P(HB80-ET20)/PET (4/3)	157	3.06	5.47
	153	3.11	7.54
	149	3.05	8.77
	145	3.02	9.61
P(HB80-ET20)/PEN (4/3)	195	3.42	8.87
	191	3.35	9.78
	187	3.27	10.29
	183	3.10	10.65

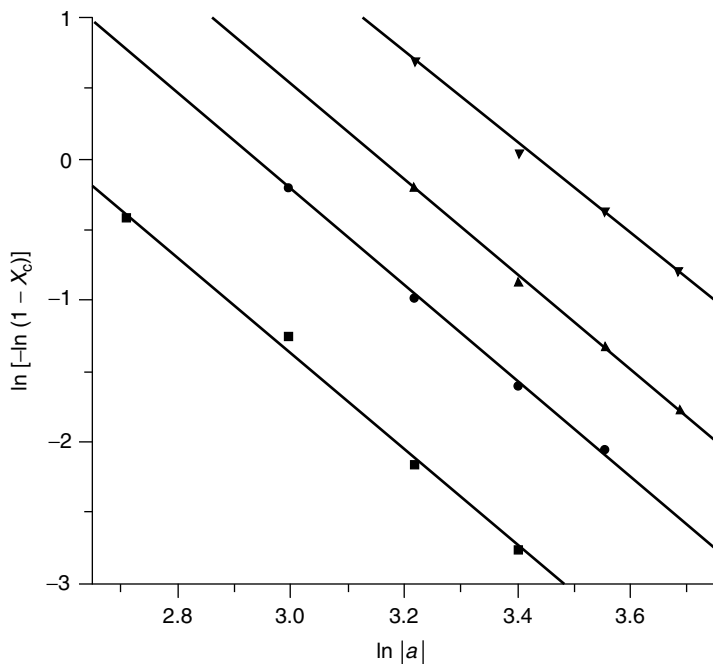


Figure 20.23 Plots of $\ln[-\ln(1 - X_c)]$ as a function of $\ln |a|$ at various temperatures for P(HB80-ET20)/PEN (weight ratio, 4:3): ▼, 183 °C; ▲, 187 °C; ●, 191 °C; ■, 195 °C [44]. From Park, J. K., Park, Y. H., Kim, D. J. and Kim, S. H., Crystallization kinetics of TLCP with polyester blends, *J. Korean Fiber Soc.*, **37**, 69–76 (2000). Reproduced with permission of The Korean Fiber Society

5.2 ISOTHERMAL CRYSTALLIZATION DYNAMICS

The isothermal crystallization study on binary blends was performed with P(HB80-ET20)/PET (weight ratio, 4:3) and P(HB80-ET20)/PEN (weight ratio, 4:3). The Avrami theory was applied, as shown in the following equation [23, 46]:

$$X_c(t) = 1 - \exp(-Kt^n) \quad (20.7)$$

The rate constant can also be calculated from the half-life for the crystallization, $t_{0.5}$, by means of the following relationship:

$$K = \frac{\ln 2}{t_{0.5}^n} \quad (20.8)$$

The term t_{\max} denotes the time needed to attain the maximum rate of crystallization. The time for this situation to occur is the t_{\max} from the isothermal DSC curves as follows:

$$t_{\max} = \left(\frac{n^* - 1}{n^* K^*} \right)^{1/n} \quad (20.9)$$

The combination of Equations 20.6 and 20.7, and a correlation with Equation 20.9, yields the following equation:

$$\frac{X_c(t_{\max})}{X_c(\infty)} = 1 - \exp \left(- \frac{n^* - 1}{n^*} \right) \quad (20.10)$$

The DSC exothermic peaks can be used to obtain $X_c(t_{\max})$ from t_{\max} . Figures 20.24 and 20.25 illustrate the linear regression analysis of the

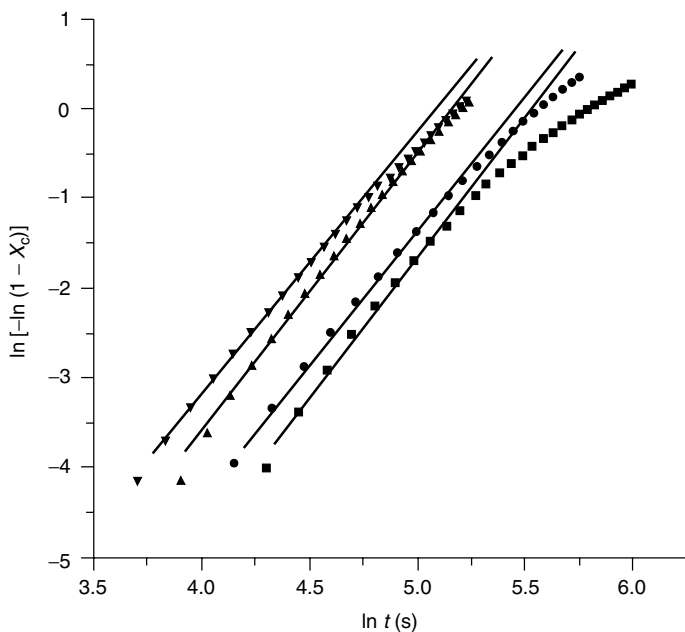


Figure 20.24 Avrami plots of P(HB60-ET20)/PET (weight ratio, 4:3): ▼, 202.5 °C; ▲, 205.0 °C; ●, 207.5 °C; ■, 210.0 °C [44]. From Park, J. K., Park, Y. H., Kim, D. J. and Kim, S. H., Crystallization kinetics of TLCP with polyester blends, *J. Korean Fiber Soc.*, **37**, 69–76 (2000). Reproduced with permission of The Korean Fiber Society

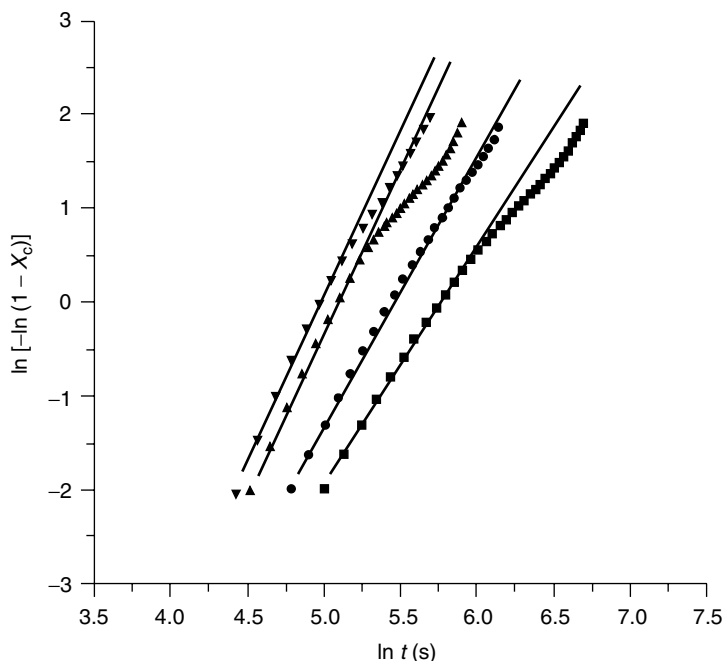


Figure 20.25 Avrami plots of P(HB60-ET20)/PEN (weight ratio, 4:3): ▼, 215 °C; ▲, 220 °C; ●, 225 °C; ■, 230 °C [44]. From Park, J. K., Park, Y. H., Kim, D. J. and Kim, S. H., Crystallization kinetics of TLCP with polyester blends, *J. Korean Fiber Soc.*, **37**, 69–76 (2000). Reproduced with permission of The Korean Fiber Society

$\ln[-\ln(1 - X_c(t))]$ versus $\ln t$ plots at various isothermal temperatures for P(HB80-ET20)/PET (weight ratio, 4:3) and P(HB80-ET20)/PEN (weight ratio, 4:3) [44].

Conclusively, the calculated Avrami exponents reveal a three-dimensional growth of the crystalline regions for each blend. The rate of crystallization of each blend increased with the decrease in crystallization temperature, and the rate of crystallization of the (PHB80-PET20)/PEN blend was faster than that of the (PHB80-PET20)/PET blend.

To confirm the shape of the spherulites described by the Avrami exponent, polarized optical micrographs of the isothermal crystallized melt blends were taken, and are shown in Figure 20.26 [44].

The morphology of the spherulites was in the form of a ‘Maltese Cross’, which was confirmed by the Avrami exponent value in the DSC study. The spherulite size of the binary blends was smaller than that of pure PET and PEN.

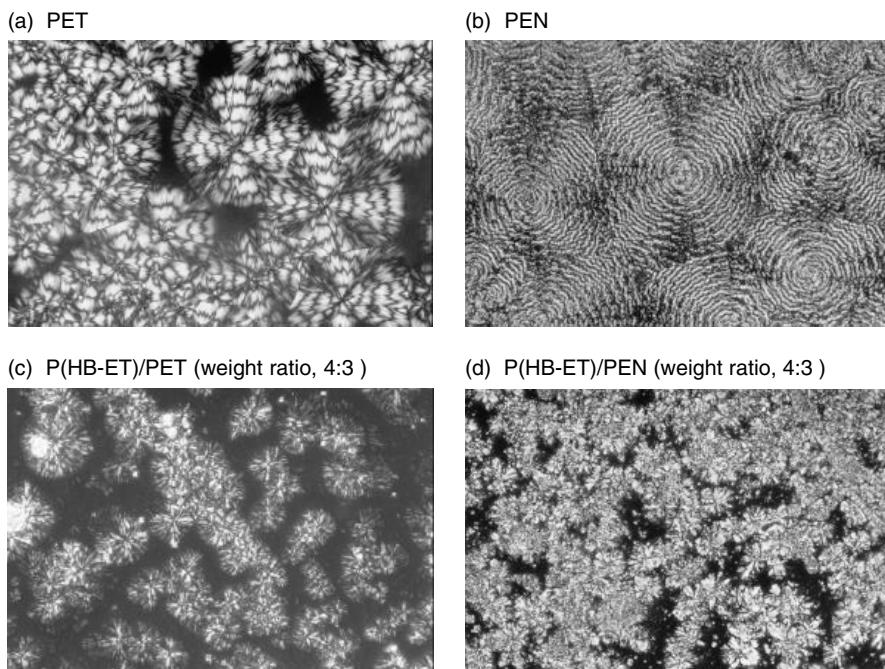


Figure 20.26 Polarized optical micrographs of isothermal crystallized (4 h) melt blends ($\times 400$): (a) 210 °C; (b) 230 °C; (c) 210 °C; (d) 230 °C [44]. From Park, J. K., Park, Y. H., Kim, D. J. and Kim, S. H., Crystallization kinetics of TLCP with polyester blends, *J. Korean Fiber Soc.*, **37**, 69–76 (2000). Reproduced with permission of The Korean Fiber Society

6 CONCLUSIONS

A liquid crystalline phase of PHB/PEN/PET ternary blend can be obtained cost-effectively, and conveniently, through reactive extrusion without using a preceding copolymer synthesis procedure. The mechanical properties of the ternary blend polyester filaments increased with increasing LCP content, winding speed, addition of a catalyst, and post-thermal treatment. A transesterification reaction among PHB, PEN and PET during reactive extrusion shows promise of controlling the miscibility and the degree of LCP fibril formation. The control of large aspect ratio and even dispersion of the LCP fibrils in the PEN/PET polymer matrix may provide greatly improved mechanical properties, even after the application of the relatively expensive LCP.

7 ACKNOWLEDGEMENTS

This study was supported by the Korea Science and Engineering Foundation directed Center for Advanced Functional Polymers, and the Brain Korea 21 program of the Ministry of Education in Korea. The author also gratefully acknowledges Mr Seong Wook Kang, Hyun Oh Yoo, Dae Soon Park, Bong Jae Jeong, Dong Jun Kim, Eun Suk Gil, Jung Gyu Lee, Sung Tack Lim, Han Sang Kim and Dong Keun Lim for experimental work carried out during their graduate studies at Hanyang University.

REFERENCES

1. Plate, N. A., *Liquid-Crystal Polymers*, Plenum Press, New York, 1992.
2. Collings, P. J. and Patel, J. S., *Handbook of Liquid Crystal Research*, Oxford University Press, New York, 1997.
3. Donald, A. M. and Windle, A. H., *Liquid Crystalline Polymers*, Cambridge University Press, Cambridge, UK, 1992.
4. Windle, A. H., in *Liquid Crystalline and Mesomorphic Polymer* Shibaev, V. P. and Lam, L., (Eds), Springer-Verlag, New York, 1993, pp. 26–76.
5. Ulcer, Y. and Cakmak, M., *Polymer*, **35**, 5651 (1994).
6. Liang, B., Pan, L. and He, X., *J. Appl. Polym. Sci.*, **66**, 217 (1997).
7. McLeod, M. A. and Baird, D. G., *Polymer*, **40**, 3743 (1999).
8. Lim, S. T., Kim, H. S. and Kim, S. H., *J. Korean Fiber Soc.*, **34**, 8 (1997).
9. Lee, J. G. and Kim, S. H., *J. Korean Fiber Soc.*, **34**, 12 (1997).
10. Bafna, S. S., Sun, T., and Baird, D. G., *Polymer*, **34**, 708 (1993).
11. Datta, A. and Baird, D. G., *Polymer*, **36**, 505 (1995).
12. Lee, W. and Dibenedetto, A. T., *Polymer*, **34**, 684 (1993).
13. Kim, S. H., Hong, S. M., Hwang, S. S. and Yoo, H. O., *J. Appl. Polym. Sci.*, **74**, 2448 (1999).
14. Kim, S. H., Lee, J. G., and Kim, H. S., *Am. Chem. Soc., Div. Polym. Chem., Polym. Prepr.*, **38**(1), 286 (1997).
15. Isayev, A. I., in *Liquid-Crystalline Polymer Systems Technological Advances*, Isayev, A. I., Kyu, T., and Chen, S. Z. D., (Eds), ACS Symposium Series, No. 632, American Chemical Society, Washington, DC, 1996, pp. 1–20.
16. Kim, S. H., Lim, D. K., Lee, S. G., and Choi, Y. Y., *Am. Chem. Soc., Polym. Mater. Sci. Eng.*, **76**, 329 (1997).
17. Kim, S. H., Lim, D. K., Yi, S. C., and Oh, K. W., *Polym. Compos.*, **21**, 806 (2000).
18. Jeong, B. J., Kim, S. H., Lee, S. G., and Jeon, H. Y., *Polym. (Korea)*, **24**, 810 (2000).

19. Kim, S. H. and Sawan, S. P., *Korea Polym. J.*, **2**, 96 (1994).
20. Kim, S. H., Jeong, B. J., Yoo, H. O., Park, J. K., Cho, H. N., Hong, S. M., and Hwang, S. S., *Am. Chem. Soc., Div. Polym. Chem., Polym. Prepr.*, **40**(1), 619 (1999).
21. Kim, S. H., Kang, S. W., Park, J. K., and Park, Y. H., *J. Appl. Polym. Sci.*, **70**, 1065 (1998).
22. Kim, S. H. and Kang, S. W., *Am. Chem. Soc., Polym. Mater. Sci. Eng.*, **78**, 162 (1998).
23. Kim, S. H., Park, S. W., and Gil, E. S., *J. Appl. Polym. Sci.*, **67**, 1383 (1998).
24. La Mantia, F. P., Roggero, A., Pedretti, U., and Magagnini, P. L., in *Liquid-Crystalline Polymer Systems Technological Advances* (Isayev, A. I., Kyu, T. and Chen, S. D. Z.(Eds), ACS Symposium series, No. 632, American Chemical Society, Washington, DC, 1996, pp. 110–117.
25. Stachowski, M. J. and DiBenedetto, A. T., in *Liquid-Crystalline Polymer Systems Technological Advances* (Isayev, A. I., Kyu, T. and Chen, S. Z. D. (Eds), ACS Symposium Series, No. 632, American Chemical Society, Washington, DC, 1996, pp. 70–83.
26. Chen, D. and Zachmann, H. G., *Polymer*, **32**, 1612 (1991).
27. Balta-Calleja, F. J., Santa-Cruz, C., Chen, D., and Zachmann, H. G., *Polymer*, **32**, 2252 (1991).
28. Spies, S. and Zachmann, H. G., *Polymer*, **35**, 3816 (1994).
29. Ahumada, O., Ezquerro, T. A., Nogales, A., Balta-Calleja, F. J., and Zachmann, H. G., *Macromolecules*, **29**, 5003 (1996).
30. Chin, H. B. and Han, C. D., *J. Rheol.*, **23**, 557 (1979).
31. Park, J. K., Jeong, B. J. and Kim, S. H., *Polym. (Korea)*, **24**, 113 (2000).
32. Brody, H., *J. Appl. Polym. Sci.*, **31**, 2753 (1986).
33. Kim, B. C., Hong, S. M., Hwang, S. S., and Kim, K. U., *Polym. Eng. Sci.*, **36**, 574 (1996).
34. Godard., P., Dekoninck., J. M., Devlesaver, V., and Devaux, J., *J. Polym. Sci., Polym. Chem. Ed.*, **24**, 3301 (1986).
35. Han, C. D. and Kim, J. K., *Macromolecules*, **22**, 4292 (1989).
36. Kim, S. H. and Park, D. S., *Am. Chem. Soc., Polym. Mat. Sci. Eng.*, **84**, 652 (2001).
37. Gordon, M., and Taylor, J. S., *J. Appl. Chem.*, **2**, 493 (1952).
38. Jung, H. C., Lee, H. S., Chun, Y. S., Kim, S. B., and Kim, W. N., *Polym. Bull.*, **41**, 387 (1998).
39. Penning, J. P. and Manley, R., *Macromolecules*, **29**, 77 (1996).
40. Flory, P. J., *Principles of Polymer Chemistry*, Cornell University Press, Ithaca, New York, 1953.
41. Nishi, T. and Wang, T. T., *Macromolecules*, **8**, 909 (1975).
42. Hoffman, J. D., and Weeks, J. J., *J. Res. Nat. Bur. Stand.*, **66**, 13 (1962).

43. Lee, S. W., Lee, B., and Ree, M., *Macromol. Chem. Phys.*, **201**, 453 (1999).
44. Park, J. K., Park, Y. H., Kim, D. J., and Kim, S. H., *J. Korean Fiber Soc.*, **37**, 69 (2000).
45. Ozawa, T., *Polymer*, **12**, 150 (1971).
46. Avrami, M., *J. Chem. Phys.*, **7**, 1104 (1939).
47. Evans, E. R., *Trans. Faraday Soc.*, **41**, 365 (1945).
48. Lopez, L. C. and Wilkes, G. L., *Polymer*, **30**, (1989).

PART VII

Unsaturated Polyesters

21

Preparation, Properties and Applications of Unsaturated Polyesters

K. G. JOHNSON

Structural Composites, Inc., Melbourne, FL, USA

and

L. S. YANG

Lyondell Chemical Company, Newtown Square, PA, USA

1 INTRODUCTION

The commercial unsaturated polyester resin industry had its beginnings in the late 1940s. With over sixty years of commercial development history, it might be expected that this class of polymer would have reached its maturity. This is far from the case. Unsaturated polyester resin applications continue to grow globally at robust rates. This growth is often in excess of many regional gross domestic product measures. This is due largely to the versatility of unsaturated polyester resins in application. Such versatility, which continues to propel unsaturated polyester resins forward into new applications, is due only in part to methods of preparation. Whereas choices of chemical constituents of unsaturated polyester resin preparations can modify resin performance, equally important are the performance attributes created through the use of additives, fillers and reinforcements.

2 PREPARATION OF UNSATURATED POLYESTER RESINS

Unsaturated polyester resin (UPR) has two main components, i.e. a polyester and a reactive diluent.

For most commercial resins, the diluent is styrene monomer, but it is possible to use other vinyl monomers such as methyl styrene and alkyl methacrylate monomers. These diluents serve two vital roles for the system. They reduce viscosity so the resins can be processed, and they cross-link with the double bonds in the polyester. The later, however, is the focus of this section. For more detailed reviews on this subject, readers are directed to the references listed at the end of this chapter [1–3].

Unsaturated polyesters are low-molecular-weight fumarate esters containing various chemical structures designed for their specific cost and performance purposes. The two most important features of unsaturated polyesters are the fumarates, which provide the active sites for radical cross-linking with the diluent monomer and the random, low molecular weight, irregular nature of the rest of the molecule, which provide the necessary solubility in the diluent monomer. The preparation of the polyester thus requires the following considerations:

- How to introduce fumarate, so that it will provide enough reactivity and cross-linking density.
- How to design the rest of the molecule, so that it will provide good solubility in styrene, as well as good mechanical integrity to the cured material.

Unsaturated polyesters are prepared through a classical esterification process. Typically, a dihydroxy compound, or mixtures of dihydroxy compounds, are treated with maleic anhydride and/or together with other dicarboxylic acids such as aromatic or aliphatic dicarboxylic acids under elevated temperature to remove the water produced during esterification process. Although various catalysts will catalyze this esterification reaction, there is enough carboxylic acid in the mixture so that it is not necessary to add extra catalyst.

The unsaturated part (the fumarates) was generated through an isomerization step of the maleate's *cis* double bond structure at high temperature during the esterification. The isomerization of maleate to fumarate usually happens rapidly at a reaction temperature (about 200 °C), and in most cases an 80 % or higher isomerization is not difficult to obtain. However, in order to produce a good long-lasting material it is necessary to improve the isomerization to over 90 %. This is achieved through careful selections of glycols and dicarboxylic acids and by careful control of the heating period.

For all purposes, polyester preparations can be grouped into either a single-stage or a two-stage process. For a single-stage process, all ingredients are added to the reactor at the beginning, and the reaction mixture is then heated to about 180 to 220 °C for a period ranging from a few hours to about 20 hours until the theoretical amount of water is removed and the product has reached:

- a low residual carboxylic acid, somewhere about 0.1–0.5 mmol/g;
- a number-average molecular weight of usually about 700 to 3000;
- a desirable viscosity, in most times measured as a styrene solution – a typical resin with 40 % styrene may have a viscosity of about 300–500 cP.

Once this is accomplished, the polyester is discharged to a blending tank and blended with cold styrene. Stabilizers such as hydroquinone and *t*-butyl hydroquinone can be added to prevent styrene polymerization.

In a chemical laboratory, setting up a glass resin reactor with a capacity from a few hundred milliliters to about 10 l is quite straightforward. The reactor should be equipped with good agitation, a nitrogen bubbling device, and a reflux condenser heated with low-pressure steam to keep glycols in the reactor, while at the same time allowing water vapor to escape to the collector. Once all of the materials are charged into the reactor, it is slowly heated to first melt the maleic anhydride at about 60 °C. As soon as the maleic anhydride goes into solution, an exothermic reaction will take place. This is the anhydride reaction with glycol to form hemi-esters. This exothermal reaction will bring the temperature to well beyond 100 °C, and sometimes closer to 150 °C. Continued heating will bring the reaction temperature to about 200 °C. The reaction is kept at this temperature until completion, while samples are withdrawn from time to time to check the acid residue and molecular weight.

In a commercial set-up, although carried out at a much larger scale, sometimes as large as 10 000 gal, and involving extensive control devices, the operation is very much identical to the laboratory operation. The raw materials are added through hoppers and pipes, while maleic anhydride is usually kept at a higher temperature, as a molten liquid, so that it can be pumped into the reactor. In a typical polyester plant, the reactor content is discharged to a blending tank, which may sit one floor below, where it is blended with cold styrene and eventually pumped to storage or tank cars for transportation.

A variation of this procedure is the so-called ‘two-stage process’. This is because some of the feed components, especially certain aromatic dicarboxylic acids, such as isophthalic acid, are very difficult to dissolve and slow to react when compared to maleic anhydride. In order to avoid excessive reaction of maleic anhydride with glycol alone, it is better to react them separately, i.e. in two steps. For a two-stage process, the glycol and aromatic acids (such as isophthalic acid) are first reacted to produce a low-molecular-weight diol ester intermediate with hydroxyl end groups. This mixture is then reacted with maleic anhydride in a second stage to give the final product.

2.1 THREE TYPES OF UNSATURATED POLYESTER RESIN PRODUCTS

As is often said, the simplest unsaturated polyester resin (UPR) is the condensation product of maleic anhydride and propylene glycol dissolved in styrene.

A product of this type will have over 50 % of its weight derived from maleic anhydride. This very high content of reactive double bonds will lead to a very brittle solid when it is cross-linked with styrene. Without further modification, this solid material will have very high tensile moduli, probably over 600 kpsi, but a very low tensile elongation, way below 1 %. Such a brittle material obviously has only very limited applications. Thus, for most general-purpose applications, it is necessary to incorporate some chemically inert components to 'soften' the polymer backbone. This will reduce the cross-linking density and improve the physical properties of the cured solid.

Since unsaturated polyesters are condensation polymers with rather low molecular weights, there are three things one can do to modify the properties of the polymer, as follows:

- Changing the components by incorporating other glycols or acids
- Changing the polymer end groups
- Changing the molecular weight

However, such an approach will quickly create an infinite number of combinations and therefore thousands of different variations. This is indeed the case in the UPR industry. There is hardly any standard type of product, plus there is hardly any identical product from two different producers. On the other hand, there are so many products available that it is almost always possible to find similar products or products with similar properties from another resin producer. It is for this reason that it is difficult to classify UPRs by their chemical structures. At its best, such an attempt will only serve its purpose as a general guideline and a starting point to understand this technology.

In modern day UPRs, there are three basic types of resins, as follows:

- The *phthalic anhydride*, *maleic anhydride* and *glycol* resins. These are generally referred to as 'general-purpose orthophthalic resins', or simply 'GP Ortho resins'.
- The *isophthalic acid*, *maleic anhydride* and *glycol* resins. These are generally referred to as 'isophthalic resins', or simply 'iso resins'.
- The *dicyclopentadiene* (DCPD)-capped resins, or simply 'DCPD resins'.

There is a fourth class, the so-called *vinyl esters*. Strictly speaking, these are not polyesters, but ester-capped polyethers and therefore will not be discussed further here.

The phthalic anhydride based resins were the first developed useful unsaturated resins. Using phthalic anhydride offers resin producers the flexibility to substitute, 'mole-for-mole', maleic anhydride out of the formulation and therefore reduce the active double-bond sites. Consequently, the product becomes less brittle. Furthermore, aromatic acid components in the polymer backbone provided much better strength for the cured products. Phthalic anhydride is not a costly material and historically it is similarly priced to maleic anhydride. By

Table 21.1 General physical properties of the three types of neat UPR casting

Property and related	Resin type		
	DCPD	GP	ISO
Styrene content (%)	40	40	45
Viscosity	Low	Medium	High
Tensile strength (psi)	7000	8000	10 000
Elongation (%)	1	1.5	2.5
Flexural strength (psi)	15 000	16 000	18 000
Flexural modulus (kpsi)	600	500	500
HDT ^a (°C)	70	80	100

^a Heat distortion temperature.

using phthalic anhydride, resin producers created the first UPR industry. These phthalic anhydride based resins are thus referred to by most as ‘General-Purpose Resins’, or GP resins.

These resins have adequate physical properties for most applications (Table 21.1), although they don’t have good resistance to wet environments. In other words, they are prone to hydrolysis by water. This is probably due to the close proximity of the two-ester groups, being *ortho* to each other.

Actually, this is not that difficult to understand. We all know that the more stable form of diesters between fumarate and maleate is the fumarate due to the *trans* configuration, which minimizes the crowdedness of the esters. In the case of phthalic esters, the aromatic esters cannot possibly rotate to any *trans* forms and are therefore in a state with a high strain energy. In order to release this energy, these esters would rather prefer to ‘kick-off’ the esters. This is why they are so prone to attack by hydrolysis, and is why GP resins will fail in any water-immersion type of test, especially under elevated temperature.

This problem was solved by the introduction of a new improved resin. This major innovation in the UPR industry came after the introduction of isophthalic acid, and especially the pioneer work of its incorporation into UPRs by the Amoco Chemical group. This very significant and extremely logic development led to the so-called *high-performance resins*.

Isophthalic acid is, of course, the oxidation product of *m*-xylene. This acid is sparsely soluble in organic systems and has a very high melting point. These two factors make it difficult to incorporate this material into a maleic anhydride and glycol reaction. Although possible, in a single-stage process, maleic anhydride and glycol will probably react to a great extent before they can react with any isophthalic acid molecules. This will lead to inhomogeneous active double bond distribution, thus causing a loss of physical properties.

To avoid this problem, isophthalic acid is reacted first with a large excess of glycol to a diol intermediate consisting mainly of the glycol–acid (2:1) adduct,

as well as the low-molecular-weight oligomers. This diol intermediate is then reacted with maleic anhydride and any make-up glycol to give the final product.

Isophthalic resins made in this way, especially those using propylene glycol or neopentyl glycol, provided polymer molecules no longer 'haunted' by the sterically crowded esters and a high strain energy. The cured product is therefore much more resistant to hydrolysis. This type of material is the 'standard bearer' for corrosion-resistant applications such as, e.g. gel coats on that part of a boat which sits under the waterline. Although there is some price penalty for the higher cost of isophthalic acid, it is worth the investment.

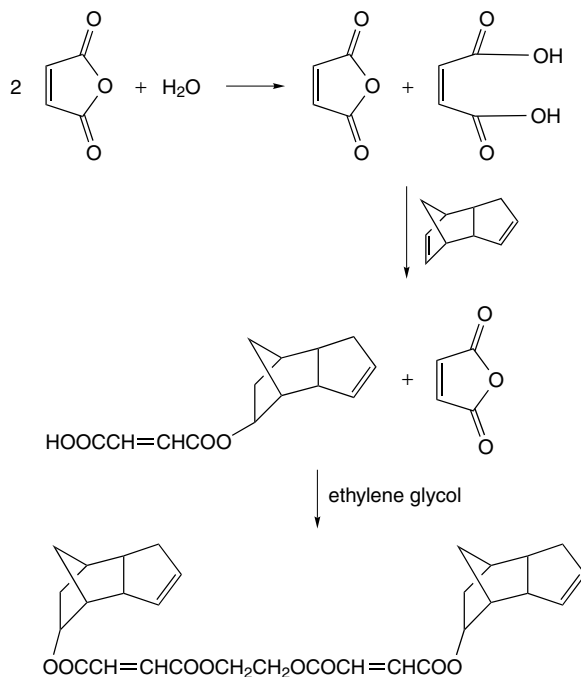
The third type of modification is end group modification. Unsaturated polyesters have rather low molecular weights. In most cases, the M_n (number-average molecular weight) is only about 1500 to 3000. If large enough groups are placed at both chain ends, this can produce significant effects, both on the performance and on the cost. The most noticeable example is the so-called DCPD (dicyclopentadiene) resin.

Dicyclopentadiene is the Diels-Alder reaction dimer of cyclopentadiene. It is the thermodynamically stable form of cyclopentadiene at room temperature, and is also a byproduct in the olefin cracking process. Industrially, it is isolated by distillation, and currently is readily available in North America.

DCPD is relatively inexpensive. This has been the motive behind an extensive effort to incorporate this material into UPRs over a long period of time. The emerged successful process is the so-called 'water process' (Scheme 21.1). First, DCPD and maleic anhydride, plus a less than equivalent amount of water, are reacted at a temperature below the decomposition temperature of DCPD. At this stage, one of the maleic carboxylic acid units will add to the strained double bond in the bridged five-member ring of the DCPD to form an ester. This DCPD-capped maleic acid is then reacted further with glycol and any extra maleic anhydride to form a very low-molecular-weight polyester, typically with an M_n of less than 1000. These polyester materials have a DCPD moiety on both ends, with DCPD accounting for up to 30–40 % of the polymer composition.

The ability to incorporate a large amount of the bulky and highly aliphatic DCPD moiety into a UPR polymer achieved two things. First, because DCPD is even less expensive than phthalic anhydride, a very cost-effective UPR is created. Secondly, the bulkiness of the DCPD moiety prevents the polymers stacking-up too closely, and consequently, reduces the shrinkage during curing. These two factors make such resins ideal for uses such as boat construction and tub and shower applications.

Although DCPD resins are very brittle due to their ultra-low molecular weights, they are apparently adequate for these 'not very demanding' applications. Furthermore, on many occasions, it is possible to improve the properties by blending a second much stronger resin into the resin solution and then co-cure the formulation.



Scheme 21.1 Outline of the conventional process used to produce DCPD resin

The blending of DCPD resins has become an important practice. Typical blended resins include combinations of DCPD resins with isophthalic, orthophthalic or vinyl ester resins. Creating blends with higher-molecular-weight phthalic anhydride, isophthalic or vinyl ester resins can toughen neat DCPD resins, which are inherently brittle. In the case of vinyl ester and isophthalic and DCPD blends, a degree of improved chemical resistance and hydrolytic stability can be gained.

3 PROPERTIES OF UNSATURATED POLYESTER RESINS

Unsaturated polyester resins are extremely versatile polymers. This versatility in meeting end-use requirements has been a significant driving force in their widespread growth. End-use physical and environmental requirements require not only the careful selection of the type of unsaturated polyester resin – which is influenced by its chemical constituents (see Table 21.1) – but also the judicious choice of additives, fillers and reinforcements. Important end-use properties are often cost, durability, dimensional stability, corrosion resistance, weight, electrical properties and physical properties, where the latter include tensile, flexural, elongation, fatigue and impact absorption. Attaining these properties requires the

Table 21.2 Constituent chemicals and resulting resin attributes

Constituent	Resulting attribute
<i>Anhydrides/Acids</i>	
Phthalic anhydride	Low cost, styrene compatibility
Malice anhydride	Chemical resistance, rigidity
Adipic acid	Flexibility, toughness
Isophthalic acid	Toughness, chemical resistance
Terephthalic acid	Higher heat resistance
<i>Glycols</i>	
Propylene glycol	Styrene compatibility
Ethylene glycol	Low cost, rigidity
Dipropylene glycol	Flexibility, toughness
Diethylene glycol	Flexibility, toughness
Methylpropane diol	Toughness, chemical resistance
Neopentyl glycol	UV and chemical resistance
<i>Other</i>	
Dicyclopentadiene	Lower cost, improved surface, lower chemical resistance

symbiotic effect of the chemical constituents, fillers, and additives used in the specified unsaturated polyester formulation.

3.1 CHEMICAL CONSTITUENTS

Table 21.2 provides a general guide to the effect that chemical constituents can have on unsaturated polyester resin end-use performance. The routes to change an unsaturated polyester resin for a particular application is normally apparent and there can be several pathways available to achieve the desired properties. As the unsaturated polyester resin markets are highly competitive, raw material cost usually reduces the number of available routes available to the formulator. As noted previously, there are three main types or families of unsaturated polyesters, namely general purpose orthophthalic, isophthalic and DCPD resins. However, within each of these families, there are hundreds of variants that incorporate these various chemical constituents in different combinations and permutations to achieve the desired results.

3.2 ADDITIVES

There are also hundreds of additives used as process aids to improve such things as air release, cure rate, thickening, viscosity reduction, mold release, wetting and dispersion of fillers, thixotropy, shrinkage and static reduction.

Low-profile additives, which control shrinkage, have emerged as a distinct science and class of additive. Unsaturated polyester resins, as do all thermosetting polymers, shrink when cured. Low-profile additives are a major class of additives used to control shrinkage, which vastly improves surface quality. This science is credited with the opening of automotive markets where surface quality is of prime importance. In exterior automotive body panels, 'Class A' surfaces are required for market acceptance.

Low-profile additives are generally materials such as poly (vinyl acetate), polystyrene, polyethylene or polycarbonate. During the unsaturated polyester cure cycle, the low-profile additives separate into a second phase, which expand to counteract the shrinkage of the curing unsaturated polyester resin. Material development and the science of low-profile additives have helped create substantial markets for unsaturated polyesters. Their use in automotive markets, where Class A 'show room' quality surfaces is a requirement, is an example of this.

3.3 FILLERS

In addition, fillers can be used for both cost reduction and property modification. Table 21.3 presents some examples of typical fillers and their effects on the unsaturated polyester resin formulation properties.

3.4 REINFORCEMENTS

Since unsaturated polyester resins alone would have insufficient strength for structural application, reinforcements are used to enhance the physical strength of such resins. Typically, tensile strength, impact strength and stiffness are the physical properties of most interest. Reinforcements can be regular particulates, as in glass microspheres, irregular particulates, as in flakes, or fibers.

By far the most common form of reinforcement is fiberglass. Products using unsaturated polyester resin as a matrix and fiberglass fiber reinforcements are commonly referred to as 'composites', 'laminates' or 'FRPs' (fiber-reinforced plastics). The latter reinforcements are sold as continuous roving, which is continuously chopped in place with a liquid resin stream, chopped roving mat, woven

Table 21.3 Common fillers and resulting resin attributes

Common filler	Resulting attribute
Calcium carbonate	Reduced cost
Clay	Improved surface
Alumina trihydrate	Fire retardant
Talc	Improved temperature resistance
Mica	Improved weathering

cloth or needle-punched 'knitted fabric'. Different fiberglass weights and fiber orientations in woven cloths and knits are used to achieve the required strength in end use. Multiple layers of fiberglass are used to achieve desired stiffness, impact strength and flexural properties. A typical boat hull, for example, could consist of a layer of chopped fiberglass, multiple layers of knit or woven fiberglass mat, and a final layer of chopped fiberglass. The multiple layer buildup is commonly referred to as the 'laminate schedule'. Usually, if the stiffness (flexibility) requirement of the laminate is achieved, the tensile and impact strength requirements are typically exceeded. A fiberglass-reinforced laminate typically contains 35–40 wt% of fiberglass reinforcements. Since unsaturated polyester resins are generally lower in cost than fiberglass, there are economic tradeoffs to consider when designing the laminate schedule.

More exotic reinforcements are also used. Carbon fiber and aramid fibers are used in the more rigorous end uses, such as in military or aerospace applications. There is also a significant cost premium for these higher-performance reinforcements.

Since the stiffness of a laminate varies as a cubic relationship with the thickness, there are alternate methods employed to achieve thickness – and hence stiffness – than by using multiple layers of fiberglass and resin. Lightweight core materials, such as end-grained balsa wood, high-density polyurethane foam, PVC foam, and honeycombed materials, are available. These materials are 'sandwiched' in between layers of unsaturated polyester resin to achieve increased laminate stiffness. The common terminology used for this technique is 'sandwich construction'.

4 APPLICATIONS OF UNSATURATED POLYESTER RESINS

The applications of unsaturated polyesters are wide-ranging and number in the thousands. Major application categories exist in the marine, construction and transportation industries. Volumes could be generated to aptly catalog the ubiquitous uses which range from buttons to bridges. What follows is a brief summary of major applications by major market segment. Table 21.4 presents a summary of the significant applications according to these market segments.

As discussed previously, there are thousands of unsaturated polyester resins based on the available chemical constituents. However, major application areas require specific performance and the unsaturated polyester resins used can be broadly categorized by the major chemical constituents that deliver the specific performance necessary. Table 21.5 contains such a categorization. This should be used as a general reference because discrete, end-product performance may dictate a departure from these general categorizations.

Gel-coat resins are a particular class of unsaturated polyester resins. Gel coats provide finish appearance to the unsaturated polyester parts and may also provide

Table 21.4 Significant applications of unsaturated polyesters

Market	Application
Marine	Powerboats, sailboats, canoes, kayaks, personal watercraft
Construction	Bathtubs, shower stalls, hot tubs, spas, cultured marble, building panels, swimming pools, floor grating, doors, electrical boxes and cabinets, countertops, sinks, tanks, pipes, pipe linings, concrete rebar, bridges, concrete forming pans
Transportation	Body panels, 'under the hood' components, truck cabs, tractor components, structural elements
General purpose	Buttons, sports equipment, medical equipment housings, computer housings, ladders, utility poles

Table 21.5 Types of unsaturated polyester resins employed in major applications

Application	Resin type
<i>Marine</i>	
General purpose	Propylene glycol/phthalic anhydride
Hull and decks	DCPD and propylene glycol/phthalic anhydride resin blends
Tooling/molds	Isophthalic
<i>Gel Coats</i>	
General use	Propylene glycol/phthalic anhydride
General purpose	Isophthalic/propylene glycol
UV performance	Neopentyl glycol/isophthalic
<i>Transportation</i>	
Bulk molding compound	Propylene glycol/dipropylene glycol/isophthalic
Body panels	Propylene glycol/phthalic anhydride
Truck body	Propylene glycol/phthalic anhydride
<i>Construction</i>	
Tubs and showers	DCPD and propylene glycol/phthalic anhydride blends
Panels	Diethylene glycol/phthalic anhydride
Faux marble	Diethylene glycol/isophthalic
Tanks and pipes	Propylene glycol/isophthalic

protection from ultraviolet or hydrolytic attack. Gel-coat formulations, aside from resin, also contain as much as 40 % of fillers and pigments. Due to their higher viscosity, gel-coat resins typically require higher styrene monomer content as a diluent processing aid.

The unsaturated polyester resins used to produce gel-coat formulations can be classified into three categories, i.e. orthophthalic-, isophthalic- and neopentyl-glycol-based. The first two types are used in perhaps two thirds of all

applications requiring gel coat. The neopentyl-glycol-based gel coats are considered to be superior for marine applications as they have higher performance with respect to fading and blistering. Other major gel-coat usage is in bath and transportation markets.

4.1 MARINE

The marine industry represents one of the largest markets for unsaturated polyester resins. First introduced to the boating industry in the mid-to-late 1950s, the use of unsaturated polyesters, coupled with their relatively low manufacturing costs, can be credited with opening boating to the mass market.

Consumption of unsaturated polyesters in the marine industry consists of broad usage for hulls, decks and numerous small parts such as hatch and engine covers. Hulls and decks are generally produced with unsaturated polyester resins and multiple layers of fiberglass cloth knits and chopped fibers. Most marine applications require the use of unsaturated polyester resin gel coats for exterior appearance and for protection from the elements.

Hulls and decks can be produced from a variety of resins depending on the intended use of the craft. High-performance – high-speed or blue-water boats – are produced from the tougher vinyl ester resins or by using blends of vinyl ester resins and dicyclopentadiene resins. General-use recreational boats are manufactured by using a lower-cost orthophthalic/dicyclopentadiene-blended resin. The dicyclopentadiene resins, which have lower shrinkage than orthophthalic resins, were originally introduced to improve the surface cosmetics of the boat hull. As an added benefit, these resins were lower in cost. However, the dicyclopentadiene resins tended to be more brittle and less hydrolytically stable. Hull blisters, which result from a pocket buildup of degraded polymer immediately behind the gel coat, became a nuisance to the industry. To reduce brittleness and enhance hydrolytic stability, dicyclopentadiene and orthophthalic, or vinyl ester or isophthalic blended resins were developed and are generally used today. Boats that will not be dry-stored on land can receive a layer of vinyl ester and chopped fiberglass immediately behind the gel coat. This commonly referred to ‘skin coat’ further enhances hydrolytic stability as an added insurance against blistering.

Although most boats are produced via the open mold spray-up process, environmental pressures are mounting due to the high styrene monomer emissions that are inherent in open molding techniques. Closed molded techniques are beginning to be commercially practiced, and it is anticipated that these processes will replace the open mold process.

4.2 CONSTRUCTION

Construction applications for unsaturated polyesters resins can be sub-divide into four significant segments, as follows:

- Bathroom components and fixtures
- Pipes, tanks and fittings
- Panels
- Miscellaneous, e.g. pultruded window frames

Unsaturated polyesters have overcome consumer acceptance issues of durability and design flexibility while providing cost-effective substitution of traditional building materials such as steel, cast iron, wood and ceramics.

Bathtubs, showers and sinks account for significant consumption of unsaturated polyester resins. Fiberglass-reinforced bathtubs and shower stalls account for as much as 90 % of the unsaturated polyester used in construction. Unsaturated polyesters have significantly replaced cast-iron bathtubs as a lower-cost material. Similarly, highly filled cast unsaturated polyesters have replaced ceramics and steel in bathroom sinks and countertops.

The driving forces for the establishment of unsaturated polyester resin pipe, tank and fittings applications were environmental regulations, on-site labor savings and corrosion resistance.

Environmental regulations related to clean air and ground water have helped build a series of markets for underground and above-ground storage of sewerage and other potential environmental contaminants. Environmental regulations generally require leak-resistant tanks and piping and mandated specific installation procedures and provide severe penalties for non-compliance. Typically, unsaturated polyester fiberglass-reinforced tanks can be installed at lower cost than steel tanks, with the added benefit of corrosion resistance. The same is true for sewer lines where *in situ* replacement with unsaturated polyesters is growing.

Typical unsaturated polyester panel applications include translucent roof panels, greenhouse panels and bathroom panels. This is generally a low-cost market where unsaturated polyesters co-exist with thermoplastics.

There are perhaps hundreds of miscellaneous unsaturated polyester resin construction applications. These would include window frames, doors, cabinet enclosures, electrical boxes, etc. In addition, recent developments bode well for unsaturated polyesters in construction markets. Concrete rebar, bridge construction and general infrastructure repair are examples of growing construction applications.

4.3 TRANSPORTATION

Transportation applications include exterior automotive body components, 'non-appearance' automotive parts, structural components, plus numerous truck, bus and rail car applications. Unsaturated polyester resins compete on the basis of weight reduction, corrosion resistance and parts consolidation. Thermoplastic resins, however, offer steep competition.

Unsaturated polyester resins have gained market share from metals because they are lightweight, corrosion resistant, and can be molded into complex shapes,

which leads to part consolidation. In addition, they can be painted and withstand the automotive paint oven temperatures without distortion.

Sheet molding compounds (SMCs) and bulk molding compounds (BMCs) are the dominant materials used in automotive applications. These composites of unsaturated polyester resin, fillers and fiberglass have advantages of high stiffness, heat resistance and low coefficient of expansion. Coupled with low creep resistance, which is a distinct advantage over thermoplastic competition, and low-profile additives, which can yield Class A surfaces, these materials are well suited for applications from exterior body panels to 'under the hood' components.

5 FUTURE DEVELOPMENTS

The growth of unsaturated polyesters will continue to be fueled by their versatility and their ability to provide cost-effective solutions to end-use requirements. Unsaturated polyester composites will continue to provide solutions to engineering demands for corrosion resistance, strength-to-weight and cost performance. Marine, transportation and construction opportunities currently identified and being developed will provide growth beyond the existing applications presented. Some examples are as follows:

1. In the marine industry, consortiums have demonstrated the viability of topside commercial ship construction using unsaturated polyester sandwich constructions and innovative joinery techniques. Large composite rudders for naval vessels have been produced and are currently completing life cycle testing.
2. In the transportation industry, there is an ever increasing use in auto, truck and bus applications. The advent of the electric vehicle, which may demand vastly improved weight reduction over today's state-of-the-art vehicles, would be a natural extension of current unsaturated polyester resin technologies.
3. New and promising composite pre-form technology which can be *in situ* molded with unsaturated polyester resins to further improve structure and performance have been demonstrated.
4. In the construction industry, composite infrastructure applications, which include bridges, housing, water and sewerage transport, and waterfront construction, abound. All composite bridges are currently under testing and long-term evaluation. Infrastructure repair and hardening of structures against earthquakes are already in commercial practice.

REFERENCES

1. Bruins, P. F. (Ed.), *Unsaturated Polyester Technology*, Gordon and Breach Science Publishers, New York, 1976.

2. Selley, J., Unsaturated polyesters, in *Encyclopedia of Polymer Science and Engineering*, 2nd Edn, Vol. 12, Mark, H. F., Bikales, N. M., Overberger, C. G., Menges, G. and Kroschwitz, J. I. (Eds), Wiley, New York, 1998, pp. 256–290.
3. Gum, W. F., Reise, W. and Ulrich, H. (Eds), *Reaction Polymers*, Hanser Publishers (Oxford University Press), New York, 1992.

PEER Polymers: New Unsaturated Polyesters for Fiber-Reinforced Composite Materials

L. S. YANG

Lyondell Chemical Company, Newtown Square, PA, USA

1 INTRODUCTION

Unsaturated polyester resins (UPRs) have been in existence since the 1940s. During the years, numerous variations and formulations designed for a great number of applications have been developed, and yet the basic chemistry for producing these thermoset resins remains relatively straightforward. The principal ingredients for these resins are an unsaturated dicarboxylic acid and a dihydroxyl compound. In its simplest form, an unsaturated polyester is the condensation reaction product of fumaric acid and ethylene glycol. However, in real practice, polyester resin formulations have become much more complicated. The fumarate moieties are actually generated from maleic anhydride. In addition, many different glycols, as well as aromatic and aliphatic diacids, are included in order to achieve different properties for the final product. These ester condensation reactions of diacids (or acids) and glycols are carried out under well-established condensation conditions, typically around 200 °C. Condensers and special devices, such as nitrogen-purge systems, are used to facilitate the removal of water until a reasonable molecular weight (or viscosity) is achieved [1–3]. The product is then blended with styrene and stabilizers and other additives to make the resin solution suitable for thermosetting applications.

In the early 1990s, at Newtown Square in Pennsylvania, Lyondell Chemical Company developed an interesting alternative to produce unsaturated polyesters. Based on this development, it became possible to produce a series of very flexible UPRs without sacrificing either mechanical or thermal properties. These products also showed good corrosion resistance when compared to conventional UPR resins.

While working on a project trying to find new uses for low-grade reclaimed poly(propylene oxide) from scrap polyurethane foams, it became apparent that a very effective chemical cleavage reaction for the aliphatic ether linkages was much desired. A literature search revealed an old cleavage reaction discovered by Knoevenagel [4] in 1914 and later further developed by Ganem and Small [5] at Cornell University in the USA. The latter reported in 1974 very good yields of acetates from dialkyl ethers by treating an aliphatic ether with acetic anhydride in the presence of ferric chloride under very mild conditions. Their results therefore suggest that if this reaction were applied to poly(propylene oxide), the ether linkages could be cleaved and the major product would be propylene glycol diacetate. Indeed, this is the case and a respectable amount of the diacetate [6] was distilled off and collected from the reactor by using this approach.

More importantly, these results also strongly imply an interesting possibility. In this reaction, if a dialkyl ether were allowed to react with a cyclic anhydride under the 'Ganem's condition', then the product would be a dialkylester of the cyclic anhydride. For example, if diethyl ether is reacted with a cyclic anhydride such as succinic anhydride, the product will be diethyl succinate. One step further, if a polyether such as a poly(propylene oxide) polyol (poly(propylene ethers) with hydroxyl end groups) is reacted with a cyclic anhydride, then a polyester is produced. Another way to picture this is to look at the oxygen atom in the polyether polymer backbone. Every time the reaction happens, the oxygen-carbon bond is attacked and the cyclic anhydride is *inserted* into the backbone. In so doing, the ether bond is now transformed into a diester. If this reaction is repeated many times, then a polyether polymer will eventually be completely converted to a polyester polymer. Furthermore, if an unsaturated cyclic anhydride such as maleic anhydride is used, then an unsaturated polyester will be produced. This possibility was quickly confirmed and the results led to a multi-year research project. Several new unsaturated polyester resins have since been developed and successfully commercialized in the past few years. This present report is an account of the work carried out on converting poly(ether polyol)s to unsaturated polyesters.

2 EXPERIMENTAL

Since this is a new technology, a few short paragraphs to briefly explain the synthetic procedures of this process are in order. The synthesis details can also be found in the patent literature listed at the end of this article.

2.1 MATERIALS

All polyols were Lyondell Chemical's ARCOL products. Maleic anhydride and phthalic anhydride are commercially available, while all catalysts were also obtained commercially.

2.2 GENERAL PROCEDURE FOR THE PREPARATION OF UNSATURATED POLYESTER RESIN FROM A POLYETHER POLYOL

A 4 l resin reactor, equipped with a condensor, a stirrer and a nitrogen inlet, is charged with a polyether polyol and maleic anhydride. The mixture is heated to 60 °C and the catalyst is added. The mixture is then heated to 185 °C for 10 h or until the acid number is reduced to 140 mg KOH/g. Some propylene glycol is added and the mixture is maintained at this temperature for another 4 h or until the acid number is lowered to about 40 mg KOH/g. The yield is about 90 %.

2.3 A TYPICAL EXAMPLE OF THE PREPARATION OF CURED POLYESTERS

The polyester product is first dissolved in styrene at a level of 60 % polyester and 40 % styrene. The initiators, either benzoyl peroxides (BPOs) or methyl ethyl ketone peroxide (MEKP), with appropriate co-catalysts, are added. The mixture is then poured into a glass mold and cured at room temperature for the MEKP system or at 100 °C for the BPO systems. A post-cure at 100 °C or 130 °C, respectively, for 5 h is then carried out. Blending experiments were carried out by using a dicyclo pentadiene (DCPD) resin, 61-AA-364, from GLS Fiberglass (Woodstock, IL, USA). This sample is 'pre-promoted', so we could only use the MEKP system.

Several more examples of specific polyester preparations and evaluations are described in the following sections.

2.4 OTHER EXAMPLES OF CURED POLYESTER PROCESSES

2.4.1 System 1

A 3000 molecular weight poly(propylene ether) triol (Arcol F3020, 90 g) was mixed with maleic anhydride (60 g) and zinc chloride (2.25 g) in a three-necked round-bottomed flask equipped with a magnetic stirrer, a condensor and a thermometer. Under a nitrogen atmosphere, the reaction mixture was heated to 190 °C

and maintained at this temperature for 6 h. A sample was withdrawn and analyzed by gel permeation chromatography, giving molecular weights of 2727 M_w and 1129 M_n . The thick mixture was cooled to 120 °C and poured into styrene (150 g) containing 40 mg of hydroquinone as a stabilizer. This mixture was stable at room temperature.

The product from this system can be cured by using a conventional radical initiator such as benzoyl peroxide (BPO). To a sample (100 g) of this product, 1.5 g of BPO in a small amount of styrene was added. The mixture was poured into a mold and heated at 50 °C overnight and then at 75 °C and 100 °C for 2 h each, and finally at 135 °C for 3 h in an air oven. The material hardened to a transparent solid with a very good surface.

2.4.2 System 2

A good catalyst for this ester insertion reaction is *P*-toluenesulfonic acid (PTSA). This example illustrates the synthesis of a PEER product using this acid as the catalyst. In a 41 resin reactor, equipped with a nitrogen inlet, condensor, and mechanical stirrer, was added 1330 g of maleic anhydride, 1755 g of a 3000 molecular weight poly(propylene oxide) triol (LG56-One, from Lyondell), 515 g of propylene glycol, and 2.5 g of *p*-toluenesulfonic acid. The reaction mixture was heated to 185 °C for about 8 h or until the acid number has dropped to 100. To this hot mixture was then added 250 g of propylene glycol and the reaction maintained at this temperature for a further 5 h. The acid number dropped to about 30 and the reaction was stopped. After brief cooling, about 300 mg of hydroquinone was added and the mixture was blended with 2400 g of cold styrene containing 600 mg of *t*-butyl hydroquinone to give about 6000 g of a yellow liquid containing about 40 % styrene and 60 % poly(ether ester). The product had molecular weights of about 1500 (M_n) and 3500 (M_w).

3 RESULTS AND DISCUSSION

3.1 ETHER CLEAVAGE REACTION LEADING TO POLY(ETHER ESTER) RESINS

Poly(propylene ether) polyol is the single most important product from propylene oxide and enjoys a predominant position in polyurethane applications. The ether linkages are very abundant in these polyols and they contribute to the physical and chemical properties in many applications such as surfactant action and hydrogen-bond formation.

One main reason for the success of these applications is because of the inertness of these ether bonds. Ethers are not usually considered active sites for

chemical modifications. Such aliphatic ether linkages are relatively stable chemically [7–9]. The carbon oxygen bond in an ether linkage is difficult to cleave. The bond energy (85 kcal/mol) is about the same as a carbon–carbon bond. Traditionally, ethers are only cleaved by using powerful reagents [4, 7] such as hydroiodic acid or boron fluoride. These reactions have only very limited applications because of the severe conditions and the costly reagents. Finding a more reasonable ether active reaction is the key to the success of the effort to chemically modify poly(ether polyol).

In their 1974 paper, Ganem and Small [5] described a new novel reaction involving reacting an aliphatic ether with an anhydride in the presence of ferric chloride. These researchers noticed that the ether bond was cleaved and two ester molecules were produced. The cleavage was carried out under very mild conditions (0°C–80°C) with catalyst dosages ranging from 0.1 to 0.55 equivalents of the ethers. Acetic anhydride was used as the acylating agent and also as the solvent. Obviously, the acetic anhydride was in large excess. Although similar reactions were reported as early as 1914 by Knoevenagel [4] and later by Karger and Mazur [10, 11], the ‘Ganem reaction’ is very significant. It is the first example of producing only esters without any acid chloride byproducts.

This reaction is truly tempting because it potentially satisfies the need in the search for a way to reclaim the chemical value of a polyurethane recycle foam project [12, 13]. When a polyurethane foam is hydrolyzed, it gives aromatic diamine and polyether polyol, both in very crude forms. The diamine can be purified by regular means, but the crude polyether polyol cannot be easily cleaned up due to its polymeric nature. If this ‘Ganem reaction’ can work well, the polyether polyol stream can be converted to a low-molecular-weight chemical, which can then be purified by conventional process such as distillation. Indeed, when this reaction was tried on a polyether triol of 3000 molecular weight as a model, the diacetate of propylene glycol was isolated by distillation. Unfortunately, the yield was too low to be of practical interest.

The major concern about applying this reaction to a polyether molecule is therefore how extensive this reaction will repeat itself randomly to all of the available ether bonds. Other questions include the necessity of excess anhydride, the rather low reported yield, and the catalyst dosage. These are crucial questions for an acceptable industrial process and failure can hamper the project seriously. On the other hand, if successful, then post-consumer foams, which represent an enormous problem for most recycling efforts, can be converted to the more valuable glycol diacetate.

Looking for a more efficient catalyst to carry out this reaction thus became the most important issue. To achieve this, a large number of common Lewis acids were screened, including the halides of aluminum, iron, zinc, titanium, zirconium, nickel, copper, tin and lead. A number of these compounds did show activities as ether cleavage catalysts. The most effective catalysts were the halides

Table 22.1 Lewis acids as ether cleavage catalysts

Catalyst	Yield of diacetate ^a
Zinc bromide	32
Zinc chloride	29
Stannous chloride	8
Ferric chloride	7
Aluminum chloride	1
Zinc acetate	0
Ferrous sulfate	0

^a Relative to aluminum chloride.

of zinc. Table 22.1 shows the activities of these Lewis acids in this ether cleavage reaction. In order to show the relative reactivities of these catalysts, the yield of propylene glycol diacetate from the AlCl_3 experiment was set as '1'. The model system experiment was carried out at 150 °C using ARCOL F3020 poly(ether polyol) and acetic anhydride.

Since the purpose of the experiment was to screen the catalyst, the yield from each individual catalyst was not optimized; rather all experiments were conducted under identical conditions so that the results can reflect the relative activities of these catalysts. Interestingly, these yields do not follow the Lewis acidity. It seems the reaction needs a very weak Lewis acid so that neither the 'catalyst and acylation agent interaction' nor the 'catalyst and ether oxygen interaction' become too strong to interfere with the catalysis cycles. This is similar to the Friedel–Crafts acylation reaction where a stoichiometric amount of a strong Lewis acid is required. In other words, while being a good Lewis acid, aluminum chloride is associated strongly to the oxygen atoms of the reactants so that it cannot dissociate itself from the reaction site for further actions. On the other hand, zinc chloride, although a weaker Lewis acid, can free itself to carry out more cleavages. Consequently, zinc chloride gives better yields as the catalyst. Based on its performance, zinc chloride was chosen as the preferred catalyst. The project to reclaim glycol diesters from recycled polyether polyol was successful and a US Patent [6] for this process was granted.

The discovery of zinc chloride as the catalyst for the ether cleavage reaction is an important step. It provided a simple method to convert a rather inert ether bond to more reactive ester linkages. When using acyclic aliphatic anhydrides the products are small diesters such as glycol diacetates. However, if the anhydride is actually a cyclic species, such as maleic anhydride or succinic anhydride, then a polyester is produced [14]. The net result of this modified 'Ganem reaction' becomes the case of replacing an ether linkage with an ester linkage and in essence has the effect of performing an *ester insertion* to the ether bonds. Thus, this reaction offers a new *non-condensational* route to make polyesters. In cases

where the amount of anhydride is less than the equivalent amount for the ether linkages in the polyether polyol, the polymer product will contain both ethers and esters. This type of material was thus named PEER™ (Poly(Ether Ester) Resin) polymer.

There are several very interesting features about this insertion reaction, as summarized in the following:

- It represents a unique method for the preparation of an otherwise difficult to make poly(ether ester).
- It offers a polyester synthesis without stoichiometry to consider or condensation water to remove. In other words, an unsaturated polyester of any degree of unsaturation up to complete ether consumption can be achieved by simply adjusting the feed of maleic anhydride.
- The molecular weight of the starting polyether polyol, to some degree, controls the molecular weight of the polymer product, in addition to the degree of condensation.
- The random distribution of the short ether chains offers very unique properties and is almost impossible to achieve by any other way.
- This is potentially a method to make complicated polyester structures such as star-shaped polyesters.
- When the cyclic anhydride is maleic anhydride, the product understandably becomes an unsaturated polyether ester somewhat similar to traditional unsaturated polyester resins (UPRs).

This last point is particularly important as the ability to produce something to compare with the commercial material (UPR) gives a unique opportunity to assess this technology, because of the following:

- Polyether polyols are commercially available in a molecular weight range similar to those of unsaturated polyesters (a few thousands).
- UPRs are a mature industry. To assess the value of this new technology against established products is relatively easy and ‘benchmarking’ is not particularly a problem.
- UPRs are a very large industry, and thus it is relatively easy to evaluate any new material at many well-established places.

Several grades of products ranging from 5 to 45 % unsaturation have since been made. The reaction process, as well the product performances, will be discussed in more detail in the following sections.

3.2 REACTION CONDITIONS AND MECHANISMS

In the early part of this project, zinc chloride was used as the catalyst. The reactions were carried out in laboratory glass reactors. The insertion was monitored

by simple titration of the unreacted anhydride (or acid) with potassium hydroxide in tetrahydrofuran (THF). The reaction conditions were as follows:

- temperature – 170–200 °C
- catalysts – 0.5–1.5 % of total weight
- anhydride – 15–45 % of total weight

When the reaction time was plotted against the logarithm of acid concentration, $\log [\text{acid}]$, a straight line was obtained, suggesting that the insertion reaction is first-order with respect to the acid (or anhydride).

The reaction time also depends on the concentration of the catalyst. At the high-concentration end (1.5 %), the reaction is completed within 7 h. At the very low level (0.5 %), it usually takes about 15 to 20 h. Using the high-catalyst level, however, is complicated by two other factors. The color of the product becomes very dark with more catalyst and also the amount of byproducts increases rapidly. Because of these considerations, the catalyst level was fixed between 0.7 and 1 % of the total weight.

The reaction temperature is limited between 170 and 200 °C. At the high-temperature end, the byproduct generation again became a concern. In addition, we have noticed a minor exotherm at around 200 °C. Since polyols can undergo depolymerization at temperatures above 230 °C, for safety reasons, it is therefore necessary to set the reaction temperature below 200 °C.

The ether cleavage reaction not only leads to the esterification reaction but also gives a mixture of low-boiling organic byproducts. Depending on the type of catalyst and the reaction conditions, this byproduct stream can amount to 3 to 20 % of the charge. The byproducts are a mixture of cyclic dimers of propylene glycol of five- and six-membered cyclic ethers. Some propyl aldehyde was also identified. Since these byproducts have very little value, it is desirable to reduce their formation. Three factors directly affect this. The most important parameter by far is the reaction temperature. Running the reaction at a temperature of around 175 °C will only produce about 3 % of the volatile byproduct. However, at this temperature, the insertion reaction will need about 15 h to complete. The next important factor is the catalyst charge. By reducing the amount of catalyst, the effect is similar. The reaction time is also increased. The amount of maleic anhydride also has an effect on byproduct generation. It was observed that the more maleic anhydride in the reaction mixture, then the more byproducts will be produced.

According to Ganem and Small [5], the reaction mechanism is an acylation at the ether oxygen followed by a dissociation step, either of an S_N1 or S_N2 nature. With carboxylate as the nucleophile, both the S_N1 and S_N2 routes are feasible. Regardless of the true mechanism, the net effect of this ‘ether-to-diester’ reaction is an ‘insertion of esters’ to ether bonds.

3.3 THE EARLY PRODUCT AND STRONG-ACID CATALYSIS DEVELOPMENT

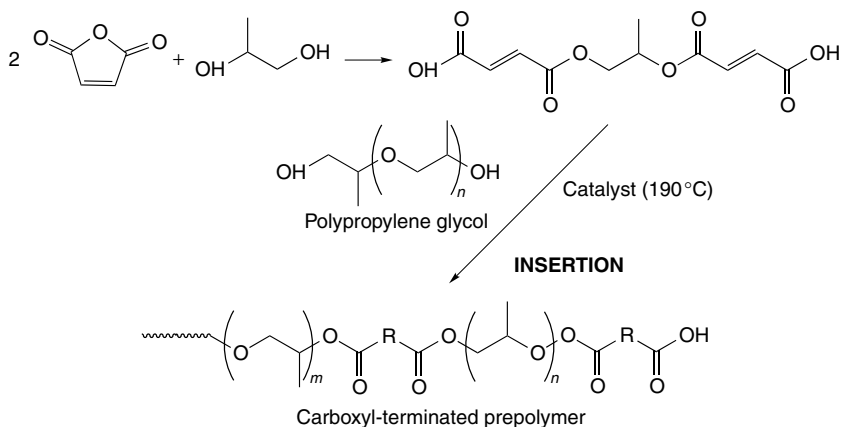
Up to this point, the zinc-chloride-catalyzed PEER polymer can be considered as a first-generation PEER polymer. The product was prepared in glass reactors in small quantities. Nevertheless, it showed very interesting properties.

PEER polymers are basically short-chain glycol ethers connected together through fumarate esters. The chain lengths of the intermittent ethers are in the range of a few units, mostly less than 10. These ether chains provided good flexibility, which in turn gives much higher tensile elongation (of the order of 4 % or higher for a polymer with 35 % of unsaturation compared to 2 % or less for most commercially available UPRs). In addition to this, there are a number of very special features about the PEER polymer.

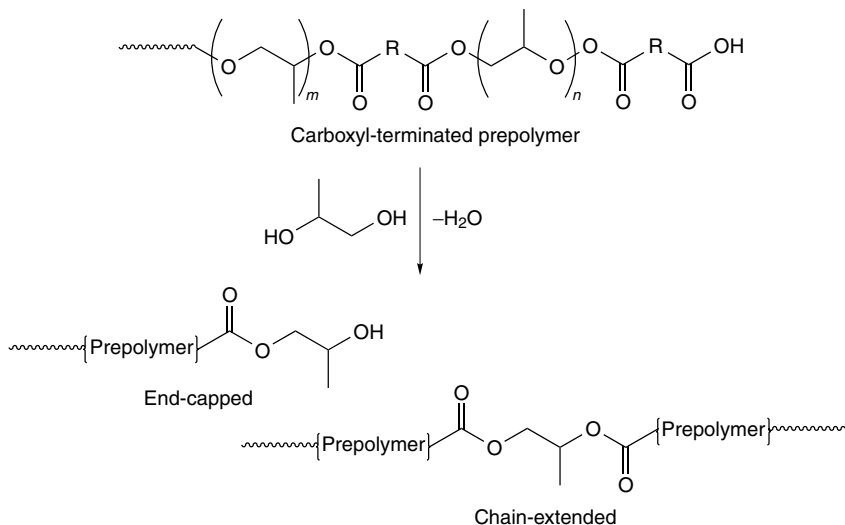
First, because of the way it is prepared, the PEER product has an extremely high fumarate content (the isomerization of maleate to fumarate is always > 95 %). This leads to a rather unusually high heat distortion temperature (HDT). Secondly, PEER polymers showed lower viscosity when compared to other UPRs of similar physical properties. This is of great importance towards lowering the overall volatile organic chemicals (VOCs) for the UPR industry. Thirdly, because of the highly lipophilic nature of the poly(propylene ether) segment, it is more water resistant than other polyesters with similar physical properties. Finally, a very intriguing synergism between PEER and dicyclopentadiene (DCPD) resins was observed. When a PEER resin is blended with a regular DCPD-based resin, especially in the 1:3 to 1:1 range, the resulting resin mixture gives superb physical strength when made into composites. This is of great importance to modern-day marine applications such as boat constructions.

These are attractive reasons to seriously consider a full scale R & D project. So, in the mid-1990s, this new PEER resin technology was scaled up to pilot-plant work. One issue that immediately came to attention was the corrosion problem caused by the chloride ions in the catalyst. To avoid this problem, a large number of zinc salts were tried, with the zinc salts of *p*-toluenesulfonic acid and trifluoromethane sulfonic acid being found to be very active. At this point, it was realized that this insertion reaction might be also strong-acid-catalyzed [15–19]. This is indeed the case – actually, *p*-toluenesulfonic acid (PTSA) was about 10 times more effective than zinc chloride, while trifluoromethane sulfonic acid was still another order of magnitude more reactive. This development was important because the catalyst level could now be reduced to about 500 ppm or less, instead of the 5000 to 10 000 ppm range. At this level of PTSA, there is no need to remove the residual catalyst in the resin. Furthermore, PTSA is relatively easy to handle and readily available. Because of this development, a successful series of pilot plant studies was carried out. This provided not only the process parameters, but it also generated enough material for application evaluations, all based on this PTSA catalyst.

The synthesis process was a two-stage process [20, 21]. In the first stage (Scheme 22.1), the polyether polyol was mixed with maleic anhydride, a small amount of a glycol, and about 500–1000 ppm of *p*-toluenesulfonic acid. The mixture was then heated to 190 °C, until the acid number had dropped to about 100 (mg of KOH per g of sample). This is followed by a second stage (Scheme 22.2) where extra glycol was added and the mixture was further reacted to a desired acid number of somewhere between 20 and 40. The synthetic process is quite fast. In most cases, the cycle time can be as short as 10 to 15 h.



Scheme 22.1 Synthesis of PEER polymer – Stage 1



Scheme 22.2 Synthesis of PEER polymer – Stage 2

3.4 LIQUID PROPERTIES OF PEER RESINS

The viscosities of PEER polymers are closely related to the amount of unsaturation in the product and the degree of chain-end modification. With 30 % unsaturation and propylene-glycol capping, the PEER polymer at reaction temperature (190 °C) is an easily pumpable liquid. When cooled to room temperature, the product becomes very thick and viscous. With higher unsaturation, it becomes a solid. However, when compared to conventional polyesters, the viscosity of the PEER polymer is still much lower. Although the PEER polymer is a very thick liquid, it is miscible with styrene and with most organic solvents. A solution containing 40 % styrene and 60 % PEER polyester gives a viscosity in the range of 50 to 150 cP, which is much lower than most conventional UPRs at this styrene content (Figure 22.1). This is highly advantageous and desirable. Since the UPR industry is facing increasing pressures to reduce volatile organic chemical (VOC) emissions, a lower-viscosity product, of course, offers opportunities for formulators to create low-styrene resins.

PEER polymers can be cured with traditional radical initiators such as methyl ethyl ketone (MEK) peroxides and benzoyl peroxide (BPO). Curing can be carried out either at room temperature or at elevated temperature. A PEER polymer containing 30 % maleic anhydride can be cured at room temperature with MEK peroxides in 10 to 60 min, depending on the type of peroxide used (Table 22.2). To cure a PEER resin with MEK peroxides at room temperature, a co-catalyst is needed. The commonly used cobalt naphthenate works very well in this case, while another co-catalyst, dimethyl aniline, is very efficient for the BPO system.

There was always the question about the effect of the different polyether polyol on the PEER polyester. Originally, it was suspected that high-ethylene-oxide-content polyethers may produce less fumarate in the polyester and thus will cure

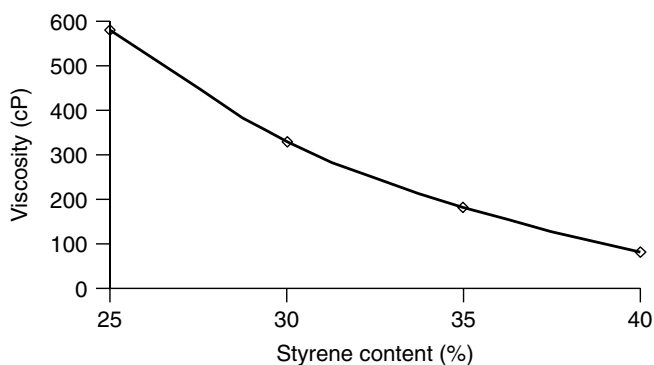


Figure 22.1 Viscosity of a PEER resin (30 % maleic anhydride) as a function of styrene content

Table 22.2 MEK peroxide as curing agent for a peer polymer containing 30 % unsaturation

MEK peroxide ^a	Gel time (min)
DDM-9	48
DHD-9	24
Delta-X-9	21
DDM-30	37

^a Various peroxides obtained from Atofina Chemical Company.

Table 22.3 Effect of starting polyol on the curing behaviors of PEER resins

Polyol	Gel time (min)	Cure time (min)	Exotherm (°F)	Inhibitor (ppm)
Polyol 1(0 % EO)	5	12	330	500
Polyol 2(8 % EO)	6	13	298	5000
Polyol 3(18 % EO)	5	11	351	100

less readily. To answer this situation, three polyesters were prepared from three different polyols. All polyols were 3000 molecular weight triols. The differences were mainly the amount of ethylene oxide content in the polyol. The gelling behaviors of these products are shown in Table 22.3. The curing characteristics, as measured by the Society of the Plastics Industry (SPI) 180°F cure behaviors, showed no meaningful trend as the lowest-content ethylene oxide sample gave 'medium' behavior with the highest-content ethylene oxide sample actually giving the most robust curing. Since the inhibitors in these polyols are mostly phenols and the amount varies greatly, it was decided to remove the inhibitors first. The different polyols were thus passed through activated alumina packed columns to remove the inhibitors. The reactivities of the PEER polymers produced from these clean polyols became almost indistinguishable from each other.

3.5 PHYSICAL PROPERTIES OF CURED PEER RESINS

The mechanical properties of PEER polymers depend greatly on the unsaturation level in the resin, and not much on the type of polyols used as the starting material. Typically, a fully cured PEER polymer containing 35 % unsaturation shows a tensile strength of about 7000 psi and a flexural strength of about 15 000 psi. Because of the ether linkages and the lack of rigid aromatic structure when compared with conventional polyesters, PEER polymers are very flexible and this

Table 22.4 Properties which can be adjusted in the 1st stage of the PEER polymer synthesis by varying the maleic anhydride content to change the cross-link density^a

Property and related	PEER 25	PEER 30	PEER 35	PEER 40	GP UPR
Maleic anhydride Wt %	25	30	35	40	20–30
Tensile strength (psi)	4500	6000	7500	9000	8000–9000
Tensile modulus (kpsi)	210	330	340	350	400–500
Elongation (%)	15	10	4	2	1–1.5
Flexural strength (psi)	8000	10 000	16 000	18 000	16 000–18 000
Flexural modulus (kpsi)	215	340	360	400	400–500
HDT (°C) ^b	60	90	100	115	60–80

^a For clear castings with 40 wt % styrene.^b Heat distortion temperature.

is shown in the percentage strain at break (elongation). With 35 % unsaturation, PEER polymers give an elongation of about 4 % at break.

One important advantage of practicing PEER technology is the freedom to adjust the degree of unsaturation and the end groups to suit the specific application. As mentioned earlier, during the first stage maleic anhydride can be added at a level of as much as 50 wt % of the reaction mixture or as little as just a few weight percent. The effect of maleic anhydride charge is shown in the Table 22.4. At the high end, a PEER product with 40 % MA behaved similarly to that of a phthalic-anhydride-based resin but with a higher heat distortion temperature (HDT) and much better corrosion resistance. With lower MA content, PEER products started to behave as ductile polymers. With less than 30 % MA, the elongation to break reached about 10 % and also showed a yield point of around 4 to 5 % elongation.

The second approach to modify the physical properties is through end-group modifications. Table 22.5 shows three different end groups with rather different properties. By using an epoxy compound or a di-primary glycol, the physical properties can be much improved.

4 APPLICATIONS

Unsaturated polyesters are generally very brittle materials. The tensile elongation for most UPRs is in the range of 1 % for dicyclopentadiene (DCPD)-based polyester resin to about 2.5 % for isophthalic acid and propylene glycol resins. This 1 % elongation posts a problem for using DCPD resin in making a

Table 22.5 Properties which can be adjusted in the 2nd stage of the PEER polymer synthesis by varying the end-capping reagent to improve the molecular weight and backbone stiffness

Property and related	Modification reagent		
	Propylene glycol	2-Methyl-1,3-propanediol	Epon 828 ^a
M _n	1300	1800	1800
Tensile strength (psi)	7500	8000	11 000
Tensile modulus (kpsi)	340	360	450
Elongation (%)	4	4	4.5
Flexural strength (psi)	16 000	17 000	20 000
Flexural modulus (kpsi)	360	380	480
HDT (°C)	100	100	110
Flexural strength after 6 days in boiling water	7000	15 000	19 000

^a A diepoxy resin from the Shell Chemical Company.^b Heat distortion temperature.

glass-fiber-reinforced composite structures such as for boats. Ideally, in a fiber-reinforced composite structure, the matrix material should have an elongation somewhat higher than the fiber to avoid matrix failure before reinforcement. Since glass-fiber material usually has an elongation of around 2 %, there is obviously a need to bring the DCPD material's elongation closer to 2 %. Although the use of DCPD resin is very cost-effective, because of its brittle nature it is necessary to blend in some stronger material to improve the toughness of this resin. In practice, this is often carried out by blending up to 30 wt % of a phthalic anhydride resin into the system.

As mentioned earlier, PEER polymers are rather flexible materials. This suggests that they should be good materials for improving the otherwise very brittle DCPD polyesters. To illustrate this point, we carried out a series of blending experiments. The base resin is a DCPD polyester (61-Aa-364 from GLS). This resin was blended with a PEER polymer containing 35 % unsaturation. However to our big surprise, the resulting material showed a remarkable synergism. The mechanical properties of these blends are shown in Figures 22.2 and 22.3, where the great improvements can be clearly seen. The 60 % or so improvement of tensile strength clearly shows the existence of a synergism between the two resins. We have since observed this synergism repeatedly on every occasion when a PEER resin and a DCPD resin has been blended [22].

This is the basis of a successful trial to build a PEER boat in 1995 in Florida. This 21 ft fishing boat is docked at a pier near Orlando in excellent shape after

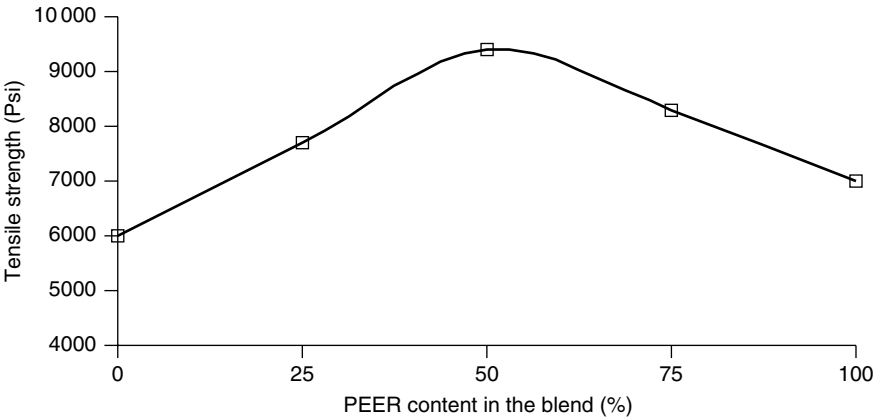


Figure 22.2 Tensile strength for blends of PEER and DCPD resins as a function of PEER content in the blend

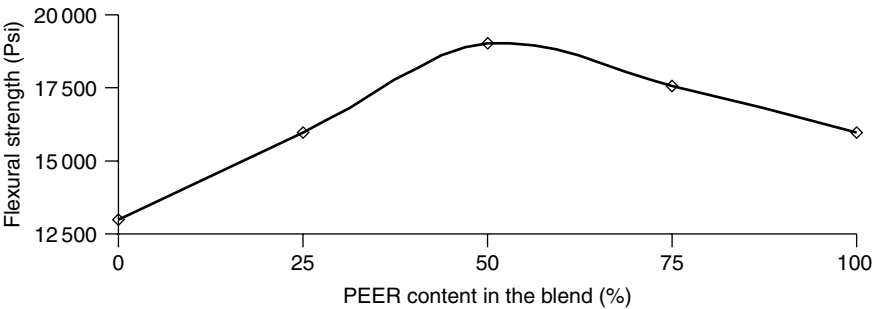


Figure 22.3 Flexural strength for blends of PEER and DCPD resins as a function of PEER content in the blend

extensive tests over the past six years. Since this development, PEER resins have been successfully formulated into several commercial resin systems by a number of resin suppliers [23, 24].

Currently, Lyondell Chemical Company is actively collaborating with several UPR resin suppliers to further develop this technology [25–31].

5 ACKNOWLEDGEMENTS

The author would like to express his appreciation to everyone involved in the PEER program, especially to Jeff Klang, Gangfeng Cai, Beth Steinmetz, Keith Johnson and Mike McGovern, for their work and support. It is indeed a challenging and exciting experience for us all.

REFERENCES

1. Bruins, P. F. (Ed.), *Unsaturated Polyester Technology*, Gordon and Breach Science Publishers, New York, 1976.
2. Selley, J., Unsaturated polyesters, in *Encyclopedia of Polymer Science and Engineering*, 2nd Edn, Vol. 12, Mark, H. F., Bikales, N. M., Overberger, C. G., Menges, G. and Kroschwitz, J. I. (Eds), Wiley, New York, 1988, pp. 256–290.
3. Gum, W. F., Riese, W. and Ulrich, H. (Eds), *Reaction Polymers*, Hanser Publishers (Oxford University Press.) New York, 1992.
4. Knoevenagel, E., *Justus Liebigs Ann. Chem.*, **402**, 133 (1914).
5. Ganem, B. and Small, V. R., Jr, *J. Org. Chem.*, **39**, 3728 (1974).
6. Yang, L. and Macarevich, D., Preparation of glycol diesters from polyethers, *US Patent 5 254 723*, 1993.
7. Burwell, R. L., *Chem. Rev.*, **54**, 615 (1954).
8. Underwood, H. W., *J. Am. Chem. Soc.*, **52**, 387 (1930).
9. Underwood, H. W., *J. Am. Chem. Soc.*, **52**, 395 (1930).
10. Karger, M. H. and Mazur, Y., *J. Org. Chem.*, **36**, 532 (1971).
11. Karger, M. H. and Mazur, Y., *J. Am. Chem. Soc.*, **90**, 3878 (1968).
12. Yang, L. and Macarevich, D., Hydrolysis of polyurethanes, *US Patent 5 208 379*, 1993.
13. Yang, L. and Kooker, D., Cured polyester plastic compositions derived from recycled polyurethanes, *US Patent 5 859 167* 1999.
14. Yang, L. and Macarevich, D., Preparation of polyesters from polyethers by an ester-insertion process, *US Patent 5 319 006*, 1994.
15. Klang, J. and Yang, L., Process for making a polyetherester, *US 5 436 313*, 1995.
16. Yang, L., Klang, J. and Cai, G., Process for making a polyetherester by insertion of a carboxylic acid into a polyether, *US 5 436 314*, 1995.
17. Yang, L. and Klang, J., Process for making a polyetherester by insertion of a carboxylic acid into a polyether, *US Patent 5 569 737*, 1996.
18. Yang, L. and Klang, J., Process for making a polyetherester by insertion of a carboxylic acid into a polyether, *US Patent 5 610 205*, 1997.
19. Yang, L., Klang, J. and Cai, G., Process for making polyetheresters with high aromatic ester content, *US Patent 5 612 444*, 1997.
20. Yang, L. and Klang, J., Polyetherester resins from diol diesters, *US Patent 5 677 396*, 1997.
21. Yang, L., Klang, J. and Cai, G., Process for making high-performance polyetherester resins and thermosets, *US Patent 5 696 225*, 1997.
22. Yang, L. and Johnson, K., Cured thermosets and glass-reinforced composites from unsaturated polyetherester resins, *US Patent 5 684 086*, 1997.
23. Hsu, C., Zhao, M. and Bergstrom, L., Aromatic polyol end-capped unsaturated polyetherester resins and resin compositions containing the same

- having improved chemical and/or water resistance, *US patent 6 211 305*, 2001.
24. Jin, L. and Nava, H., High performance polyether-polyester containing laminating resin composition, *World Patent Wo 0 116 207*, 2001.
 25. Cai, G., Yang, L. and Guo, S., Stable water-extended polyetherester emulsions, *US Patent 5 580 909*, 1996.
 26. Cai, G., Guo, S. and Yang, L., Thermosets from water-extended polyether-ester emulsions, *US Patent 5 633 315*, 1997.
 27. Cai, G., Trauth, D. and Yang, L., Process for making storage-stable epoxy-capped polyetherester resins, *US Patent 5 770 659*, 1998.
 28. Yang, L. and Klang, J., Process for making dicyclopentadiene polyether-ester resins, *US Patent 5 780 558*, 1998.
 29. Yang, L., Process for making polyetherester resins having high aromatic diester content, *US Patent 5 854 359*, 1998.
 30. Yang, L., Armstead, D. and Cai, G., Process for making polyetherester resins having high aromatic diester, *US Patent 5 880 225*, 1999.
 31. Yang, L., Armstead, D. and Cai, G., Process for making water-resistant polyetherester resins and thermosets, *US Patent 5 952 436*, 1999.

Index

Note: Page references followed by 'f' represent a figure and 't' represents a table.

- absorbable fibres 21–2
- acetaldehyde 145, 235, 235t, 236f, 325, 469, 482t, 485–6, 486f
 - aldol condensation of 62f
 - formation 58–62
 - generation as function of extruder residence time and temperature 69f
 - vapour pressure 74f
- acrolein 368f, 391
- acrylonitrile–butadiene–styrene (ABS) copolymer 311
- activation energy 153
- acyl ammonium salt 122
- addition polymers, depolymerization 566
- additives *see* under specific materials
- adipic acid 256
- Advanced Photo System (APS) film 332
- air bubbles 471
- Alcaligenes eutrophus* 23–4
- aldol condensation of acetaldehyde 62f
- aliphatic acids 256, 545t
- aliphatic polyesters 605
- alkyd
 - and related resins, historical development 4–6
 - use of term 3
- alkylene phthalate polyesters 119
- alloying agents 531, 531t
- allyl alcohol 368f
- anisotropic melting temperature 647
- 2,6-anthracene dicarboxylic acid (ADA) 257
- anti-hydrolysis additives 522–4, 524t
- AP 500 221
- aramid fibers 708
- Arnite 17
- Arnitel 20
- aromatic compounds found in metabolic pathways 603f
- aromatic polyesters 604–5
- artificial weathering devices 612–13
- as-spun fibers
 - F*-values of 656f
 - moduli of 648–58, 649t, 653f
 - tensile-fractured 651–2f, 654f
 - thermal properties and moduli 658t
- atomic force microscopy (AFM) 625
- Avrami coefficients 161–2, 161t
- Avrami equation 687
- Avrami plots 691–2f
- barrier properties in packaging 486–7
- batch processes, PET 90–3

- benzoyl peroxides (BPOs) 717–18, 725
- BHET 35, 49, 53, 72–5, 73f, 80, 92, 130, 566–9, 572–3, 576
vapour pressure 74f
- bibenzoic acids (BBs) 251, 252t
- bicomponent (bico) fibers 427–8, 428f
- biodegradable polyesters 409, 409f
- BIOMAX 596f, 605–6
- BIOS report 10
- 4,4'-biphenyldicarboxylic acid 60, 288
- 2,4',5-biphenyltricarboxylic acid 60
- 1,2-bis(4-carboxyphenyl)ethane 60
- 1,4-bis-(4-hydroxybutyl) terephthalate 137
- N,N*-bis[p-(2-hydroxyethoxycarbonyl)phenyl]-biphenyl-3,3,4,4-tetracarboxy-diimide 252
- bis(phenoxy)alkane-4,4'-dicarboxylic acid 645
- 1,10-bis(phenoxy)decane-4,4'-dicarboxylic acid 645
- 1,2-bis(phenoxy)ethane-4,4'-dicarboxylic acids (PECs) 646
- block copolymeric structures 20
- blow molding, processing conditions 480
- blow-molded containers 331
- BOPET 36
- bottle polymers
quality aspects 482–7
see also under specific materials
- Buckingham-PI theorem 84
- Buhler bottle-grade process 167–73, 169f
- Buhler bottle-to-bottle process 186
- Buhler PET bottle-to-bottle recycling process 184–5, 184f
- Buhler PET-SSP process 176f
- bulk continuous filaments (BCFs) 386, 388
- butanediol (BDO) 117, 120–1, 296–7
- t*-butyl isophthalic acid (TBIPA) 248
- cage-type finisher 100, 101f
- caprolactone 117
- carbon fiber 708
- carbon fiber reinforcements 556–7, 557f
- carbonyl bis (1-caprolactam) (CBC) 505
- carboxyl acid scavengers 530
- carboxylic acid 625f
- carboxylic end groups (CEGs) 68f, 90, 197, 214, 227, 230–3, 232f, 469, 476, 481–2, 507–9, 510f, 530
- catalysts 228–9
- chain extenders 497–505
commercially available 498, 499t
traditional 498
- CHDM 50–2, 162, 213, 246, 248, 269, 271–2, 286, 286t, 478, 489
amorphous and crystalline polyesters based on 267–92
cis/trans ratio 269, 270f
glycols 329
modification of PET 610
overview 269–70
- CHDM-based copolyesters
preparation and properties 280–2, 281f
with dimethyl 2,6-naphthalene-dicarboxylate 284
with selected monomers 287–8
with 2,2,4,4-tetramethyl-1,3-cyclobutanediol (TMCD) 287
- CHDM-based polyesters
modified with other glycols and acids 283–8
synthesis 272–3
- Chemcad* 43
- chemical healing process 172, 173f
- chemical reaction rate controlled process 152
- chromophores in PET 62
- CIELAB system 62
- clarity, definition 482–3
- class transition temperature 647
- clearing point 647
- climate variables 610–12
- color 488–9
definition 482–3
factors influencing 483–4
- composting, degradable polyesters 598–9
- condensation polymers,
depolymerization 566
- contamination
causes 456–8
degree of 458
detection 458–9
of polymers 456–72

- continuous filament textile yarns 422
- continuous processes
 - based on TPA 96–7f
 - PET 93–8
- continuous stirred-tank reactors (CSTRs) 83, 300
- controlled degradation polyesters 591–608
 - property requirements 593
- copoly(ether ester)s 489
- core-shell elastomers 511–14
- coupling agents 497–505
- critical monomer concentration (CMC) 124–5
- crystal annealing 164–5
- crystallinity, polyarylates 661, 662f
- crystallization, PHB/PEN/PET blend 686–92
- crystallization dynamics, non-isothermal 687–8
- cured polyesters
 - preparation 717
 - processes 717–18
- Cutin 23
- cyclic PBT oligomers 123f
 - preparation of 120f
- cyclic polyester oligomers 117–42
 - formation via depolymerization 131–4
 - history 119
 - overview 117–19
- cyclic terephthalate esters 118f
- cyclization reactions 121
- cyclohexane dicarboxylic acid (CHDA) 286, 286t, 489
 - polyesters prepared with 285–6
- cyclohexane dimethanol *see* CHDM
- cyclopentadiene, Diels–Alder cyclization 248
- DABCO 121
- DCPD 704–5, 705f, 717, 723, 727
 - flexural strength 729f
- DCPD-capped resins 702
- DEG 54–8, 73, 78, 80, 85, 90, 151, 162, 211, 246, 325, 329, 472, 478
 - formation 55–6f, 57t, 58f, 148
- degradable polyesters
 - application requirements 600–1
 - applications 594–600, 594f
 - aquaculture applications 595
 - landfills 597–8, 597f
 - lessons from natural products 602–4
 - litter 599–600, 600f
 - medical applications 594–5
 - recycling 597
 - selection for an application 600–4
 - solid waste applications 595–600
 - terrestrial applications 595
 - wastewater treatment facilities 598
- degradable polymers 591–3
- degradation
 - PECT 613–26
 - loss of toughness 617–18
 - weather-induced 610–13
 - see also* photodegradation
 - degradation mechanisms 593
 - PECT 626–38
 - PET 626–38
- degradation testing protocol 602
- degree of polycondensation 204f, 208f, 231f
- degree of polymerization (DP) 121, 195, 197, 205, 404
 - LCP/PET blends 685, 685t
- degree of randomness (RD) 488
- degree of transesterification 684
- depolymerization 124–31, 126t, 130f
 - cyclic polyester oligomers, formation via 131–4
 - feed costs 578t
 - metal alkoxide catalyzed formation of cyclics via 132f
 - PET *see* PET
 - technology 118
 - Valox 315 127–8f
- depolymerization/polymerization techniques 125
- dibasic-acid-modified PCT copolyesters, preparation and properties 282–3
- dibutyl tin alkoxides 131
- dibutyltin dilaurate (DBTDL) 677f
- dicarboxylic acid 645, 715
- dicyclopentadiene *see* DCPD
- Diels–Alder cyclization, cyclopentadiene 248
- Diels–Alder cycloadditions 257
- diepoxide chain extenders 503, 503f
- diester groups, thermal degradation 58–62
- diethyl succinate 716
- diethylene glycol *see* DEG

- differential thermal analysis (DTA) 485
- diffusion models 79–81
- diffusion rate controlled process 152
- dimethanol terephthalate *see* DMT
- dimethyl 1,4-cyclohexanedicarboxylate (DMCD) 269, 285
- dimethyl naphthalene (DMN) 324
- dimethyl 2,6-naphthalenedicarboxylate (NDC) 284, 336
 - synthesis 337–9
- dimethyl terephthalate *see* DMT
- Diolen 10
- dioxane 54–8, 73
 - formation 55f
 - vapor pressure 74f
- diphenyl carbonate (DPC) 22
- 4,4'-diphenyldicarboxylic acid (BB) 646
- dipropylene ether glycol (DPG) 367, 390
- disc-type finisher 100, 102f
- DMA data 308, 309f
- DMT 12, 35, 86, 117, 121, 231, 269, 276, 296–7, 335, 339, 363–4, 390, 456, 473, 481, 567, 572–4, 576, 637
- Dorlastan 19
- drawability 453
- drawing 454–5
- dry heat treatment 461
- DSC analysis 136
- DSC endotherms 222f
- dyability of staple fibers and filaments 471–2
- dynamic mechanical analysis (DMA), data for 305
- dynamic mechanical loss curves 276f
- dynamic storage modulus 647

- E-glass fiber 550–1, 551t
- Ektar 17
- elastomers, polyesters as components of 19–20
- electrical connectors 278f
- electron diffraction (ED) 370–1
- engineering-grade polymers 495–540
- equilibrium melting temperature 684t
- ester, use of term 3
- ester–amide–ester triads 251
- ester bonds, thermal degradation 59f
- ester gum 4

- esterification 90, 148, 151–2, 364, 364f
 - by-product 92
 - TPA 92
- esterification reactor 92, 98–9
- esterification temperature 92
- ether cleavage catalysts, Lewis acids as 720t
- ether cleavage reaction 718–21
- ethylene–acrylic ester copolymers 511
- ethylene glycol (EG) 35, 39, 43, 72–3, 73f, 78, 80–1, 85, 90, 92–3, 98, 120, 230, 489, 566–8, 573, 576, 716
 - vapour pressure 74f
- ethylene methyl acrylate (EMA) 507
- extruded unreinforced PCT 279

- F*-values 647, 654f, 655–8, 662
 - as-spun fibers 656f
 - injection molded specimens 656f, 659f
- fast-atom bombardment mass spectrometry (FAB-MS) 125, 130
- fatigue fracture 461, 461f
- fiber-reinforced composite materials 715–31
- fiberglass-filled PBT 305–6
- fibers
 - from partially aromatic polyesters 6–16
 - preparation 646
 - production 10–11
 - see also* specific materials
- filament defects 458
- films
 - abrasion resistance 475
 - influence of oligomers 477
 - intrinsic viscosity (IV) 473, 476
 - manufacture 472–7
 - molecular weight 474
 - packaging 489
 - processability 477
 - roughness 475
 - scratch resistance 475
 - streaks 476–7
 - structure 474
 - surface properties 474–6
 - see also* specific materials
- flame-retardant PBT 313
- flame-retardant PET 526–8, 527f, 528t
- flame-retardants 526–8, 527f, 528t

- flame-retarded grades 278
- flame-retarded PCT 278t
- flexural modulus
 - measurements 646
 - polyarylates 661t
- Flory–Huggins interaction parameter 684
- Flory–Huggins relationship 75
- Flory–Huggins theory 684
- Flory–Schulz distribution 39
- fluorescence measurements 469–71, 470f
- fluorescent device exposure 625–6f
- folded chain segments 407
- food safety 186
- Fortrel 11
- FOY (fully oriented yarn) 16
- fracture *see* yarn break
- Freidel–Crafts acylation 720
- frequency factor 153
- fumaric acid 715

- 2G10 20
- gamma aminopropyl triethoxysilane (GAP) 307
- Ganem's condition 716
- gas-barrier properties 479
- gas-bubbles 471
- gel-coat formulations 709
- gel-coat resins 708–9
- glass-fiber-reinforced (GFR)
 - flame-retarded PCT 278t
- glass-fiber-reinforced (GFR)
 - thermoplastic polyester composites, properties of 546t
- glass-fiber-reinforced (GFR)
 - thermoplastic polyesters
 - applications 542f
 - market data 542
 - performance traits 548t
- glass-reinforced polyesters (GRPs) 6
- glass transition temperature 246
 - blend systems 679
 - polyarylates 659–60, 660f
- gloss enhancers 530–1
- glow wire test 313
- glycidyl methacrylate (GMA) 507–9, 510f
- glycol-modified PCT copolyesters,
 - preparation and properties 279–80
- glycol resins 702
- glycols 545t
- glycolysis 572
- Gordon–Taylor Equation 683
- GPC analysis 130, 137, 621
- GPC data 616, 625
- grafting reactions 509, 510f
- 2GT 20

- halogenated FR additives 314
- haze, definition 482–3
- heat capacity, PTT 375f
- heat distortion temperature (HDT)
 - 277–8, 302, 310, 524, 648, 723, 727
- polyarylates 660, 661f, 661t
- heat resistance of polyarylates 659–61
- heat setting 455–6
- hexafluoroisopropanol (HFIP) 304, 369, 458
- HFIP/CHCl₃ 131
- high-dilution techniques 118
- high-modulus low-shrinkage (HMLS)
 - yarns 438
- high-performance liquid crystal
 - polyesters with controlled molecular structure 645–64
- high-performance resins 703
- high-polymer formation 340
- high-productivity synthesis 118
- Hoechst-Celanese 442
- Hoffman–Weeks equation 684
- Hoffman–Weeks plots 372, 684t
 - LCP/PET blends 685f
- HPLC analysis 121, 131
- hydrogen bonding 249
- hydrolytic degradation 476
- hydroperoxide
 - degradation products 150
 - formation 149
 - production 626f
- hydroquinones (HQs) 645
- hydrothermal treatment 461
- hydroxybenzoic acid (HBA) 254
- hydroxybutyric acid 605
- 3-hydroxypropanal (3-HPA) 363
- hydroxyvaleric acid 605
- Hytrel 20

- ignition resistance 313
- impact modifiers 506–15, 511f

- Impet 533–4
- impurities 456
- industrial yarns 403
- injection molded poly/copolyesters 253t, 471
- injection molded specimens
 - F*-values of 656f, 659f
 - moduli of 655–8, 655–7f, 659f
 - thermal properties and moduli 658t
- injection molding 277–9
- interfacial shear strength 554–5
- intrinsic viscosity (IV) 153, 156f, 195, 204f, 208f, 213, 229, 230f, 232f, 236f, 473, 476, 498, 505–6, 506f
- IRGANOX 1425 498
- isophthalic acid (IPA) 50, 162, 246, 268, 329, 478–9, 487, 702–4
- isophthaloyl chloride 121
- p,p'*-isopropylidene dibenzoic acid 288
- isothermal crystallization dynamics 690–2, 691–3f
- isothermal crystallization temperature 684

- Jacobsen–Stockmayer theory 124

- Kelly–Tyson equation 549–54
- Kodel 17
- Kodel II 408

- lactide 117
- LC–MS 130
- LCP/PEN blends
 - dispersion of LCP in PEN 678
 - effect of catalyst on compatability 674–9
 - Instron tensile tests 680f
 - kinetic parameters 689t
 - mechanical property improvement 674–7
 - tensile modulus 677f, 679f
 - tensile strength 676f, 678f
- LCP/PET blends
 - degree of polymerization 685, 685t
 - Hoffman–Weeks plots 685f
 - kinetic parameters 689t
- Lewis acids as ether cleavage catalysts 720t
- Lexan 22
- lightfastness 484

- liquid crystal polymers (LCPs) 252, 645
 - structure–thermal property correlations 645
 - see also* LCP/PET blends; thermotropic liquid crystal polymers (TLCPs)
- liquid crystalline model compounds, thermal properties of 650t
- liquid crystalline PET copolyesters 254
- liquid crystalline polyesters 18–19, 448
- litter, degradable polyesters 599–600, 600f
- low-melting fibers 489
- low-melting peak (LMP) 164
- low-melting polyesters 489
- LOY (very low orientation yarn) 15
- Lycra 19
- Lynel 19

- McClafferty rearrangement 368f
- macrocyclic alkylene phthalates 119
- magnetic tapes 475
- Makrolon 22
- maleic anhydride (MA) 248, 509–10, 701–2, 717
- Mark–Houwink constants 369t
- Mark–Houwink equation 153, 369
- mass-transfer coefficient 79
- melt-phase polycondensation (MPPC) 197
- melt strength enhancers 529–30
- melting temperature 246, 647
- Merlon 22
- metal alkoxides 131
 - catalyzed formation of cyclics via depolymerization 132f
- methyl ethyl ketone (MEK) peroxides 717, 725, 726t
- methyl methacrylate–butadiene–styrene (MBS) 511
- methyl methacrylate–styrene shells 311
- 2-methyl naphthalene 338
- 3-methyl-2,2'-norbornanedimethanol 288
- methylene conformations 371
- Milease 21
- mineral-filled PBT 307
- moduli of as-spun fibers 648–58, 649t, 653f

- moduli of injection molded specimens 655–8, 655–7f, 659f
- molecular modeling 103
- molecular weight 196, 200, 206f, 233f, 235, 497–8, 504–5
 - degradation 614
 - films 474
- molecular weight distribution (MWD) 153–4
- molten (melt)-state polycondensation 197–9, 198f
 - effect of temperature 199f
- nanoclays 525, 526t
- naphthalate-based blends 330–1
- naphthalate-modified PET copolyesters 329–30
- naphthalene 338
- naphthalene dicarboxylate 125
- 2,6-naphthalene dicarboxylate 284, 284–5f, 288
- naphthalene-2,6-dicarboxylic acid (NDA) 50, 324, 336–7, 479–80
- naphthalene-2,6-dimethyl dicarboxylate (NDC) 324, 339
- natural polyesters, occurrence 23
- nematic domains 647
- neopentyl glycol 704
- nitrogen cleaning loop 173
- nitroterephthalic (NTA) units 261
- non-reactive impact modifiers 510–14, 512t
- nonwoven fabrics 403
- norbornane 2,3-dicarboxylic acid (NBDA) 248
- nuclear magnetic resonance (NMR) spectroscopic analysis 448
- nucleating agents 515–20, 516–17f, 519f, 520t
- nucleation 161–4
- nucleation/crystallization promoters 520–2
- nucleation promoters/plasticizers 522t
- number-average molecular weight 156f
- nylon 6,6 8, 448, 461f
- nylon 9 8
- olefin-containing polyesters 125
- oligomeric contaminants 459–65, 459–60f
- oligomeric ester cyclics, polymerization of 134–9
- oligomeric PBT cyclics, ring-opening polymerization of 135f
- oligomers 235, 237f
 - formation 340
- orientation function 647
- Ozawa equation 687
- packaging, barrier properties in 486–7
- Paphen PKFE 529
- partially oriented yarn (POY) 332, 386, 448
- PBT 11, 117–19, 121–2, 124–6, 129, 134, 143, 213, 246, 293–321, 528, 541, 637
 - additives 304
 - and water 315–16
 - antioxidants 304
 - blends with styrenic copolymers 311–13
 - burning 314
 - c-axis lattice strains in fibers 381f
 - catalysts 297
 - commercial application 294
 - commercial processes 300–1
 - comparison with PCT 546–7
 - comparison with PET 487, 546–7
 - crystallization half-times 372–4, 373t
 - deformation behavior 379
 - depolymerization reaction 133f
 - dripping 314
 - elastic recovery 379–81, 379f
 - fiberglass-filled 305–6
 - flame-retardant additives 313–15
 - flow properties 446
 - glass-fiber reinforced 548
 - glass-filled properties 389–90, 390t
 - hydrolysis-resistant 523
 - impact-modified 310–13, 312t
 - mechanical properties 376–7, 377t
 - mineral-filled 307
 - moduli of fibers before and after annealing 379t
 - monomers 296–7
 - physical properties 376–7, 377t
 - polymer blends 307–13
 - polymerization 294–301, 295t
 - process chemistry 297–300
 - properties 301–7

- PBT (*continued*)
 rheological flow activation energies 378t
 SSP 176–7, 214–15, 214f, 220, 300–1
 stress–strain curves of fibers 378–9, 379f
 structure 408f
 unfilled 303–4
- PBT cyclic oligomers
 polymerization of 136
 ring-opening polymerization of 138
- PBT–PC blends, impact-modified 310–13, 312t
- PBT–PC–MBS blend 311, 312f
- PBT–PET blends 308
- PBT–polycarbonate blends 308–10, 309f
- PC–ABS 315
- PCT 269, 271, 275f, 284, 408, 541
 comparison with PET 547
 effect of film former GFR 555t
 preparation and properties 273–6
 structure 409f
- PCT-based polymers
 applications 277–9
 processing 277
- PCTA 269, 272, 280t
- PCTA copolyesters 283, 283f, 286, 286t
- PCTG copolyesters 269, 271–2, 279, 280f, 280t
- PDO 390
- Pe–Ce 8
- PECT 610
 coloration 613–16
 degradation 613–26
 loss of toughness 617–18
 mechanisms 626–38
 UV-stabilized 618–26, 618–24f
- PEER polymers 520–1, 521f, 715–31
 applications 727–9
 early product 723–4
 effect of starting polyol on curing behaviors 726t
 experimental 716–18
 liquid properties 725–6
 physical properties of cured resins 726–7
 properties 727t
 reaction conditions and mechanisms 721–2
 strong-acid catalysis 723–4
 synthesis 716–18, 724f
 tensile strength 729f
 viscosity 725f
- PEN (and PEN films) 143, 213, 323–34, 324f, 331–2, 335–60, 479, 575, 637
 applications 350–7
 cable and wires insulation 354
 chemical stability 344–6
 comparison with other commercial films 343t
 comparison with PET 326–8, 327f, 342f, 344–6, 345t, 348t, 487
 containers 332
 continuous process 341
 copolyesters 329–30
 cosmetic and pharmaceutical containers 333
 cost 353
 crystal forms 344
 DSC transitions 326f
 electrical devices 352–3
 electrical properties 348–9
 ester interchange 391
 fiber and monofilament 332
 gas-barrier properties 347–8
 gas-permeation coefficients 348–9t
 labels 355
 major appearance into the marketplace 336
 manufacture 324–5, 337–41, 342f
 mechanical properties 346–7, 347f
 medical uses 357
 membrane touch switches (MTSSs) 353
 mesophase structure 344
 miscellaneous industrial applications 357
 morphology 344
 motors and machine parts 352
 optical properties 328, 349–50
 packaging materials 356
 performance 336
 photo- and electro-induced luminescence spectra 351t
 photographic films 353–4
 printing and embossing films 356
 properties 325–6, 341–50
 references published during the period 1967–2000 336f

- SSP 177–8, 214–15, 220, 237–8, 325, 328–9
- tapes and belts 354–5
- thermal properties 346
- thermal transitions 326
- tyre-reinforcing yarns 332
- Underwriters Laboratories (UL)
 - continuous use rating 353
- use in manufacturing electrochemical lithium ion batteries 353
- UV absorption 350t
- UV transmission spectra 328f
- see also* LCP/PEN blends; PEN/PET blends; PHB/PEN/PET blends
- PEN blends, applications 331–3
- PEN copolyesters
 - applications 331–3
 - manufacture 330
- PEN fibers 352
- PEN resin 341f
 - preparation process 339–41, 339f
- PEN/PET blends 331
 - melting enthalpy 669f
 - melting temperature 669f
 - thermal behavior 669
- PEN/PTT copolymer 391
- Perkin-Elmer DSC-7 machine 647
- Perlon L 8
- PET 35, 117–19, 125, 134, 255f, 275f, 323–4, 324f, 541
 - activation energy data 484t
 - additives for modification 495–540
 - additives used in engineering-grade 496t
 - advantages 546
 - amorphous copolyesters 247–8
 - amorphous materials 251
 - anti-hydrolysis additives 522–4, 524t
 - automotive applications 536–7, 536f
 - batch processes 90–3
 - Buhler bottle-grade process 167–73, 169f
 - capacity development of continuous and discontinuous plants 90f
 - catalysts 40
 - chemical reactions in solid state 147–58
 - chemical recycling 65–7
 - chromophores in 62
 - common goal of future work 104
 - comparison with PBT 487
 - comparison with PEN 326–8, 327f, 342f, 344–6, 345t, 348t, 487
 - comparison with PTT 487
 - compounding principles 534
 - compounds and functional groups involved in synthesis 42t
 - continuous polymerisation 13
 - continuous processes 93–8, 98t
 - crystallinity 497, 515
 - crystallization 75, 158–65, 520, 543–6
 - crystallization half-times 372–4, 373t
 - crystallization kinetics 160
 - 1,4-cyclohexanedimethanol
 - modification of 610
 - decomposition via generation of volatile by-products 469
 - deformation behavior 379
 - degradation mechanism 626–38
 - in presence of oxygen 64f
 - dependence of density on annealing time and temperature 160f
 - depolymerization 566–71
 - capital costs 578–9, 581t
 - chemistry 566–70
 - commercial application 575–6
 - criteria for commercial success 576
 - economic costs and results 579–86, 581t, 583t, 584–6f
 - evaluation of technologies 576–9
 - feedstock 577–8
 - technology for 572–5
 - diffusion coefficient 81f, 82t
 - for EG and water in 86f
 - discovery of 9f
 - DSC transitions 326f
 - dyeing 388–9, 389t
 - early work leading to 6–10
 - elastic recovery 379–81, 379f
 - engineering-grade 532–7, 532t
 - environmental impact 104
 - equilibrium constants of
 - esterification/hydrolysis and transesterification/glycolysis 43, 45f
 - esterification 87–8t
 - esterification/hydrolysis 41–8, 43f
 - esterification product 77f

PET (*continued*)

- esterification rate constants 47f
- extrusion model 67
- flame-retardant 261, 526–8, 527f, 528t
- formation of chains 37
- formation of diethylene glycol and dioxane 54–8
- formation of short chain oligomers 52–4, 53f
- future production developments 103
- glass-fiber-reinforced 548
- glass-filled
 - and toughened grades 495, 534–5, 535t
 - properties 389–90, 390t
 - toughened 495
- glass-transition temperature 407
- global solid-state capacity 146f
- half-times and induction times for samples crystallized isothermally from the melt 212t
- high-speed spinning 15–16
- hydrolytic degradation 150
- impact modification 514–15, 514f, 515t
- influence of comonomer content and type 163f
- influence of initial moisture content on reaction 170f
- injection molding 495–7
- kinetic data for
 - esterification/hydrolysis reactions 46t
- kinetic data obtained for transesterification/glycolysis reactions 51t
- kinetic data used in process models 70t
- kinetics and process models for recycling 66f
- manufacture 36, 144f
- mass-transfer models 78–9
- mechanical properties 376–7, 377t
- melt behavior 404–6
- melt viscosity 405
- moduli of fibers before and after annealing 379t
- molding products 17
- monomers and co-monomers 38t

- multi-purpose discontinuous plant 91f
- normalized DSC thermograms 165–6f
- notched impact strength 511, 513–14f, 523f
- nucleating agents 515–20, 516–17f, 519f, 520t
- nucleation/crystallization promoters 520–2
- nucleation promoters/plasticizers 522t
- overview 542–3
- phase equilibria 72–5
- physical properties 376–7, 377t
- plasticizers 545
- polycondensation 75–84, 77f, 87–8t, 89–98, 98t
- polydispersity index 41f
- polymeric, modifiers 528–9, 529t
- polymerization 31–115
- processing 385–90
- processing reactions 71t
- reaction rate constant 484t
- reactions with co-monomers 50–2
- reclaimed material 180–1
- recovery of monomers 565–6
- recycling 87–8t, 178–86
 - food safety aspects 186
 - market 178–9, 179f
 - material flow 179, 180f
 - processing options 184t
 - reactions 71t
 - specifications for reclaimed flakes, recycled pellets and virgin pellets 185t
- SSP 179–86
- repolymerization 565–90
- rheological flow activation energies 378t
- rheological properties 497
- rubber-toughened 509f
- scientific requirements 103
- solid-phase polymerization 13
- solid-stating 552, 552t
- speciality additives 529–31
- spherulitic growth as function of temperature 543f
- SSP 143–215, 214f, 226f
 - for bottle grade 166–7
- static-bed solid polymerization rates 156f

- stoichiometric equations for synthesis
 - of 36f
- stress-strain curves of fibers 378-9, 379f
- structure 404-10, 404f
- supertough 535-6
- synthesis reactions 71t
- thermal degradation 58-62, 60f, 61t, 149-50, 484, 484t, 485f
- thermal oxidative degradation 61t, 149-51
- titanium-catalyzed transesterification 49f
- transesterification 87-8t
- transesterification/glycolysis 43f, 48-50
- ultra-fine fibers 16
- unmodified 497
- UV transmission spectra 328f
- world production capacity 36
- yellowing 62-5
- see also* LCP/PEN blends; PEN/PET blends; PHB/PEN/PET blends
- PET/ADA copolymers 257
- PET amorphous copolymers, modifiers 248f
- PET-anthracene copolymers 258f
- PET-BB copolymers 253f
- PET-bibenzoates 251
- PET bottle recycling
 - closed-loop bottle-to-bottle 183-4
 - flake SSP 181-2, 181f
 - SSP after repelletizing 182-3
- PET bottles 17-18, 146-7, 477-87
 - depolymerized 571
 - optical properties 478-9
 - influence of oligomer on 481
 - processing 480-2
 - special properties 479
 - UV irradiation 480
- PET/CHDM copolymers 248
- PET copolyesters 20
 - manufacture 330
 - naphthalate-modified 329-30
- PET copolymers 245-65
 - as scaffold for additional chemical reactions 256-7
 - biodegradable 260
 - crystallinity 246-51
 - crystallization rate modification 246-51
 - extrusion chain extension 259f
 - increased crystallization rates and crystallinity 248-51
 - increased flexibility 254-6
 - increased modulus 251-4
 - overview 245-6
 - surface-modified 260
 - textile-related 257-9
 - thermal properties 251-4, 252t
- PET depolymerization, technology for 572-5
- PET fibers
 - advantages 401
 - antiflammability 430
 - antistatic/antisoil 426-7
 - applications 402-4
 - bicomponent (bico) fibers 427-8, 428-9f
 - birefringence as function of wind-up speed 448-9, 499f
 - cat-dye 426f
 - commercial drawing processes 420-2, 421f
 - crystalline melt temperature 408
 - crystallinity 419
 - deep dye 424-5, 425f
 - deformability 439-50
 - die-swell ratio as function of mean residence time in capillary 444t
 - differences in spinning processes 417, 417t
 - draw-resonance ratio 445t
 - drawing of spun filaments 418-22
 - effect of spinning speed on orientation and shrinkage 416t
 - elongation as function of wind-up speed 450f
 - end-use development 14
 - flow properties 446
 - formation and end-use applications 401-33
 - freezing point 446, 447f
 - future 431-2
 - geometry 410
 - glass transition temperature 408
 - heat treatment 462f
 - high-shrink 427
 - historical growth 402f
 - hollow 429
 - hydrolytic degradation 405
 - intermediates 12
 - intrinsic viscosity 443t

- PET copolymers (*continued*)
- ionic dyeability 425, 426f
 - light reflectance 422–3
 - low-melt 427
 - low-pill 424
 - mechanical properties 448
 - melt flow index (MFI) testing 446
 - melt spinning 410–18, 411f
 - metastable 406
 - microfibers 429–30, 429f
 - microstructure 406f
 - molecular weight 443t
 - normal stress difference as function of shear stress 444f
 - oligomer distribution 462–3f
 - orientation factors as function of take-up speed 445f, 446
 - post-draw heatsetting 420
 - properties 431t
 - random chain scissions 405
 - recrystallization behavior 442–3
 - shear viscosity
 - as function of shear rate 444f
 - of polycondensate melts 446
 - skin–core structure 415
 - solidification 439–50
 - specialized applications 422–31
 - spinnability 438–50
 - spinning behavior of bright and semi-dull 443
 - spinning process control 416–18
 - stress–strain behavior 418, 419f
 - stress–strain curves 450f
 - structure 406
 - structure formation 439–50
 - structure-partitioning effect 414
 - surface breaks 464f
 - surface defects 463f
 - surface friction and adhesion 430
 - take-up speed 414
 - tricot knit fabric 428f
 - unit cell 407
 - viscoelastic behavior 444
- PET filaments
- breaks caused by inclusions 466f
 - highly oriented surface zone 468f
- PET film
- cost 353
 - gas-permeation coefficients 348–9t
 - UV absorption 350t
- PET/PBT co-cyclic oligomers, polymerization of 137t
- PET–PEG copolymers 256
- PET/PEN copolymers 251
- PET polyesteramides 250–1
- PET–naphthalate copolymers 251, 257
- PET–*p*-phenylene bisacrylic acid (PBA) 257
- photochemical crosslinking 260f
- PET/PTT copolyesters 390–1
- PETG copolymers 246–7, 269, 280t, 281–2, 281f
- Petra 533
- PHB 23–4
- PHB/PEN/PET blends 666–74
- crystal structures 667f
 - crystallization 686–92
 - DSC thermograms 670f
 - effect of pre-heating temperatures and blend composition on melting temperatures 671f
 - glass transition and melting temperatures as function of PHB content 670f
 - heterogeneity 679, 681f
 - liquid crystalline phase 666–8
 - mechanical properties 671–3, 672f
 - NMR spectra 674
 - polarized micrographs 668f
 - thermal behavior 669
 - torque value 668f
 - transesterification 673–4, 675f, 675t
- PHB/PET blends
- dynamic crystallization 687, 687–8f
 - isothermal crystallization dynamics 690–2, 691–3f
- phenylenebisisoxazoline (PBO) 502–3, 502f
- phosphite chain extension promoters 504
- phosphite processing stabilizers 531
- photodegradation 609–41
- see also* degradation
- photolysis 628, 629f
- photo-oxidation 628, 632, 633–4f
- phthalic anhydride 702, 717
- pivalolactone 118
- point-of-purchase displays 282, 282f
- poly(1,4-butylene terephthalate) *see* PBT
- polyarylates
- crystallinity 661, 662f
 - flexural moduli 661t
 - glass transition temperature 659–60, 660f

- heat distortion temperature (HDT)
 - 660, 661f, 661t
- heat resistance 659–61
- synthesis of 646
- polybutylene 479–80
- poly(butylene naphthalate) 637
- poly(butylene terephthalate) *see* PBT
- polycaprolactone 255f
- polycarbodiimides 523
- polycarbonates 22, 528–9
- polycondensation
 - batch plant 95f
 - continuous melt-phase reactor design 98–102
 - diffusion and mass transfer in melt-phase 75–84
 - PET 77f, 93, 98t
 - vinyl end groups 148
 - see also* solid-state polycondensation
- polycondensation constant 50f
- polycondensation reactors 94f
 - for high melt viscosity 100–2
 - for low melt viscosity 99
 - special requirements 99
- poly(1,4-cyclohexanedimethylene 2,6-naphthalenedicarboxylate) (PCN) 284
- poly(1,4-cyclohexylenedimethylene terephthalate) *see* PCT
- polydispersity 210, 504
 - melt-phase samples 154
- polyenes, formation from vinyl end groups 63f
- polyester, use of term 3
- polyester chain cleavage 316
- polyester cyclic oligomers
 - preparation from acid chlorides 120–4
 - via ring-chain equilibration 124–31
- polyester fibers *see* fibers and under specific materials
- polyester films *see* films and under specific materials
- polyester resins, SSP 195–242
- polyesteramide copolymers 249–50, 250f
- polyesteramides, ‘Gaymans’ approach 250f
- polyesterification 197
- polyesterification reaction between glycerol and phthalic anhydride 5
- polyesters
 - as components of elastomers 19–20
 - high molecular weight 8
 - historical development 3–28
 - solid-state polycondensation 143–94
- (poly(ether ester) resin) polymer *see* PEER polymers
- polyether polyol 717
- poly(ethylene-*co*-1,4-cyclohexylenedimethylene terephthalate) *see* PECT
- poly(ethylene glycol) (PEG) 20, 245–6, 255, 426, 426f
- poly(ethylene naphthalate) *see* PEN
- poly(ethylene naphthoate) 251
- poly(*p*-ethylene oxybenzoate) 11
- poly(ethylene terephthalate) *see* PET
- poly(ethylene-*co*-vinyl alcohol) (PEVOH) 479–80
- poly(3-hydroxybutyrate) (PHB) 23
- polyhydroxyalkanoates (PHAs) 23–4, 605
- poly(β-hydroxybutyrate) *see* PHB
- polyhydroxylic acids 23
- poly(lactic acid) (PLA) 409f, 605
- poly(β-malate) (poly(L-3-carboxy-3-hydroxypropionate)) 23
- polymer dust 458
- polymer formation 6f
- polymer melt
 - intrinsic viscosity
 - as function of extruder residence time and initial water content 68f
 - as function of extruder residence time and temperature 67f
- Polymer Plus 89
- polymerization
 - oligomeric ester cyclics 134–9
 - PBT cyclic oligomers 136
 - PET/PBT co-cyclic oligomers 137t
 - poly(ethylene terephthalate) 31–115
 - PTT 362–8, 364f, 365–6t
 - see also* degree of polymerization (DP)
- polyolefins 448
- poly(phenylene ether)–polystyrene (PPE–PS) 315
- poly(propylene ether) 716
- poly(propylene ether) polyol 718

- poly(propylene ether) triol 717
- poly(propylene oxide) 716
- poly(propylene terephthalate) (PPT) 362
 - SSP 214–15, 214f
- polytetrafluoroethylene (PTFE) 314
- poly(tetramethylene glycol) (PTMG) 255
- poly(tetramethylene terephthalate) 489
- polytransesterification 197
- poly(trimethylene terephthalate) *see* PTT
- polyurethane 716
- potassium naphthalene carbonate 338
- potassium naphthalene dicarbonate 339
- POY (pre-oriented yarn) 15, 386–8, 422, 438, 448–9, 469
- Predici 89
- pre-oriented yarn *see* POY
- prepolycondensation reactor 100f
- prepolymer formation 340
- primary crystallization 160, 164, 168
- primary nucleation 161
- processability
 - and quality relationship 435–93
 - definition 452
 - films 477
- processing stabilizers 531
- 1,3-propanediol (PDO) 361, 363
- propylene glycol 701, 704
- pseudo*-high-dilution chemistry 120
- pseudo*-high-dilution reactions 120
- pseudo*-high-dilution techniques 118
- P*-toluenesulfonic acid (PTSA) 718, 723
- PTT 213, 361–97, 382f, 541
 - applications 385–90, 386f
 - c*-axis lattice strains in fibers 381f
 - carpets 388
 - chemical structure 362f
 - comparison with PBT 547–9
 - comparison with PET 487, 547–9
 - copolymers 390–1
 - crystal density 370–1, 370t
 - crystal orientation 384–5, 384f
 - crystal structure 370, 371f
 - crystallization 371–2, 372f
 - crystallization half-times 372–4, 373t
 - crystallization kinetics 372–4
 - deformation behavior 379
 - drawing behavior 383–4, 383f
 - dyeing 388–9, 389t
 - dynamic mechanical properties 374–6, 376f
 - elastic recovery 379–81, 379f
 - elongation of fibers as function of winder take-up speed 387f
 - ester interchange 391
 - fiber end-use applications 385–6
 - fiber moduli before and after annealing 379t
 - fiber processing 386
 - glass-filled properties 389–90, 390t
 - glass transition 374–6
 - glass transition temperature 375f
 - health and safety aspects 391
 - heat capacity 374, 375f
 - heat of fusion 374
 - higher-molecular-weight 367
 - injection molding 389–90
 - intrinsic viscosity 369
 - mechanical properties 376–7, 377t
 - melt rheology 377, 378t
 - melting 371–2, 372f
 - molecular weights 369
 - non-isothermal crystallization kinetics 374
 - overview 361–2
 - partially oriented yarn (POY) 386–8
 - physical properties 368–77, 377t
 - polymerization 362–8, 364f, 365–6t
 - rheological flow activation energies 378t
 - side reactions and products 367–8
 - strain deformation and conformational changes 381–3, 382f
 - stress–strain curves at draw temperatures below and above glass transition temperature 383f
 - stress–strain curves of fibers 378–9, 379f
 - structure 408f
 - tenacity of fibers as function of winder take-up speed 387f
 - tensile properties 378–9
 - thermal degradation mechanism 368f

- thermal properties 371–2
- viscosity as function of shear rate 378f
- X-ray crystal modulus 380
- purified terephthalic acid (PTA) 12
- PyroChek 68PB 527, 527f
- pyromellitic dianhydride (PMDA) 498–501, 500–1f
- quality and processability
 - relationship 435–93
 - technological aspects 465–8
- quality requirements of polyester films 472
- quinuclidine 121
- rate constant 153
- rate-controlling mechanisms 152
- reaction injection molding (RIM) 138
- reactive extrusion block copolymer 255f
- reactive impact modifiers 507–10, 508f, 508t
- reactive toughness 509, 512f
- recycling
 - by chemical depolymerization 565–90
 - degradable polyesters 597
 - see also* specific materials and applications
- red phosphorus 315
- refrigerator crisper trays 281f
- reinforcements 524–5, 525t
- relative degree of crystallinity 647
- repolymerization, PET 565–90
- resin transfer molding (TRM) 138
- rigid-rod comonomers 254f
- rigid-rod monomers 252
- ring–chain equilibration, polyester cyclic oligomers via 124–31
- ring–chain equilibration reaction 127
- ring-opening polymerization 117–19, 122, 134, 137
 - oligomeric PBT cyclics 135f
 - PBT cyclic oligomers 138
- Riteflex 20
- roof-type preheater for annealing of PET pellets 171f
- Roult's law 75
- Rynite 17, 532–3
- scanning electron microscopy (SEM) 648
- secondary crystallization 160, 164, 168–71
- semicrystalline materials 251
- semicrystalline thermoplastics 293
- side products, removal of 200–1
- size exclusion chromatography (SEC) column 131
- sodium ionomers 518, 519f
- sodium stearate 517, 517f, 518
- sodium sulfoisophthalate 457
- solar radiation versus location versus exposure angle 611t
- solid-state polycondensation (SSP) 85, 459, 505–6
 - batch process 216–18
 - batch process reactor 217f
 - catalyst 158
 - continuous process 166–78, 218–20, 226–7
 - continuous process reactor 219f
 - cooling 172
 - crystallinity 210–13
 - crystallization 157–8, 221–4
 - density as function of temperature and time 211f
 - diffusion and mass transfer in 84–5
 - diffusivity of side products 205–6
 - discontinuous batch process 224, 225f
 - drying 221–4
 - economic considerations 236
 - effect of carboxyl number 157f
 - effect of crystallinity 207f
 - effect of diffusion 207–8
 - effect of nitrogen gas flow rate 201f
 - effect of reaction time 233f
 - end group concentration 156
 - engineering principles 215–21
 - equipment 215–21
 - foamed prepolymer chips 228
 - gas purity 158
 - gas transport 234
 - gas type 158

- solid-state polycondensation (SSP)
 (*continued*)
 hot crystallization rate
 as function of intrinsic viscosity 213f
 as function of temperature 212f
 investment costs 145f
 kinetics 199
 mechanisms 209, 209t
 molecular weight 158
 parameters affecting 154–8
 particle size effect 156, 206–10, 227–8
 PBT 176–7, 214–15, 214f, 220, 300–1
 PEN 177–8, 214–15, 220, 237–8, 325, 328–9
 PET 143–215, 214f, 226f
 PET recycling 179–86
 physical aspects 200–13
 polyesters 143–242
 powdered prepolymer 228
 PPT 214–15, 214f
 practical aspects of reaction steps 221–35
 prepolymers 230f
 process 75, 90, 481
 process comparison 173–5, 174f
 process parameters 227–35
 production costs 145f
 reaction 171–2
 reaction time 235
 small particles and powders 220
 sticking 222
 suspended state 220–1
 temperature 154, 202–5, 202–3f, 233–4
 time 154
 use of catalysts 205
 vacuum 234
 solid-stating accelerators 505–6
 speciality additives 529–31
 specific surface area 83–4
 Spectar copolyester extruded sheet 282, 282f
 spherulite growth 159f, 161–4
 spin-draw yarn (SDY) 386
 spinnability, definition 452
 spinning 452–4
 threadline dynamics 413, 413f
 Stabaxol 524
 step-growth condensation polymers 566
 4,4'-stilbenedicarboxylic acid 288
 stretch-blow molded containers 281
 styrene–acrylonitrile (SAN) 310
 styrene–butadiene–styrene (SBS) 310
 styrene–ethylene butylene–styrene (SEBS) 510
 Suberin 23
 substituted-HQs/BB polyarylates, thermal properties and moduli 650t
 succinic acid 256
 5-sulfoisophthalic acid (SIPA) 257
 Sumitomo NESTAL injection molding machine 646
 superpolyesters 8
 surface-active agents 20–1
 surface diffusion rate controlled process 152–3
 surface mount technology (SMT) 645

 t-butyl isophthalic acid (TBIPA) 248
 tandem HPLC–MS 125
 temperature-dependent equilibrium constants 44t
 terephthalate copolyesters to control degradation 605
 terephthalate ring substitutions 261
 terephthalic acid (TPA) 12, 35, 39, 43, 72–3, 73f, 90, 92–3, 231, 268, 296–7, 324, 329, 335, 364, 481, 489, 566, 568, 574
 continuous process based on 96–7f
 esterification 92
 solubility in prepolymer 103
 terephthaloyl chloride (TPC) 120–1
 Tergal 10
 Terital 10
 Terlenka 10
 Terylene 11
 Tetoron 11
 tetraalkyl titanate 131
 tetrabutyl titanate 297
 tetrachloroethane (TCE) 304
 tetraepoxide chain extenders 503f, 504
 tetra(2-ethylhexyl) titanate (TOT) 137, 297

- tetracyclidyl diaminodiphenylmethane (TGDDM) 503–4, 503f
- tetrahydrofuran (THF) 121–2, 125, 298–9
- tetraisopropyl titanate (TPT) 297
- tetrakis-(2-ethylhexyl)-titanate (TOT) 136
- 2,2,4,4-tetramethyl-1,3-cyclobutanediol (TMCD) 247, 287
- textile filament yarns 403
- Therm-S-300 221
- Therm-S-600 221
- Therm-S-800 221
- thermal stability 484
- thermodynamic miscibility 679–86, 681t, 682f
- thermogravimetric analysis (TGA) 469
- thermoplastic polyester composites 541–62
- contribution of fiber length and molecular weight 553
 - new applications 557–8
 - properties 549–57
- thermotropic liquid crystal polymers (TLCPs) 665–96
- thermodynamic miscibility determination 679–86, 681–2t
- Thermx PCT 17
- TiO₂ agglomerate 457, 457f
- TiO₂ particles 443
- titanate alloying agent 531, 531t
- titanium-catalyzed transesterification, PET 49f
- total organic carbon (TOC) 92
- Toyo Baldwin Rheobron
- Viscoelastometer Rheo 2000/3000 machine 647
- Toyo Baldwin Tensilon UTM-4–200 machine 646
- transesterification 504
- trans*-conformation 164
- transesterification 147–8, 151, 197, 251, 309, 529, 567
- PHB/PEN/PET blends 673–4, 675f, 675t
- transesterification inhibitors 530
- transesterification reaction 488–9
- trans/gauche* conformation 473
- transparent toy kaleidoscopes 283, 283f
- 9,10,16-trihydroxyhexadecanoic acid 23
- trimellitic anhydride (TMA) 499
- trimethylene glycol 363
- triphenylphosphite (TPP) 504
- tyre cord, PET-SSP plant 175–6, 176f
- UL-94 test 313
- United States Food and Drug Administration (USFDA) 570, 571t, 573, 594
- unsaturated polyesters 5, 699–713, 715–31
- additives 706–7
 - applications 708–12, 709t
 - basic types 702
 - chemical constituents 705–6, 706t
 - construction applications 710–11
 - fillers 707
 - future developments 712
 - marine application 710
 - physical properties 703t
 - preparation 700–5
 - properties 705–8
 - reinforcements 707–8
 - transportation applications 711–12
- UV degradation 610
- UV light 488
- UV-protected PECT copolymer 618
- UV radiation 488
- UV stability 484
- UV-stabilized PECT 618–26, 618–24f
- Valox 315, depolymerization of 127–8f
- van der Waals attraction forces 407
- Vectra 18
- Vectran 18
- video tapes 475
- vinyl end groups 69f
- polycondensation of 148
- vinyl esters 702
- viscoelastic behavior 442
- voids 471
- volatile organic chemicals (VOCs) 723
- Vycron 11
- Vyrene 19
- wastewater treatment facilities, degradable polyesters 598
- water, vapour pressure 74f
- Weather-Ometer 614–18f, 615

- wide-angle X-ray diffraction (WAXD)
 - 370–1, 382, 382f, 384f
- Wilke–Chang technique 79–81
- Wollastonite 525
- X-ray crystallography 125, 130
- Xydar 19
- yarn breaks 450–6
 - caused by skin–core differences 441f
 - hydrolytic degradation 470–1
 - thermal-oxidative degradation 468–71
- yellowing, PET 62–5

With kind thanks for Geoffrey Jones of Information Index for compilation of this index.